Green's functions and integral equations for the Laplace and Helmholtz operators in impedance half-spaces

Ricardo Oliver Hein Hoernig

ÉCOLE POLYTECHNIQUE

Thèse présentée pour obtenir le grade de

Docteur de l'École Polytechnique

Spécialité:

Mathématiques Appliquées

par

Ricardo Oliver HEIN HOERNIG

GREEN'S FUNCTIONS AND INTEGRAL EQUATIONS FOR THE LAPLACE AND HELMHOLTZ OPERATORS IN IMPEDANCE HALF-SPACES

Soutenue le 19 mai 2010 devant le jury composé de:

Juan Carlos DE LA LLERA MARTIN	Examinateur et rapporteur
María Cristina DEPASSIER TERAN	Examinateur et rapporteur
Mario Manuel DURÁN TORO	Co-directeur de thèse
Jean-Claude NÉDÉLEC	Directeur de thèse
Jaime Humberto ORTEGA PALMA	Examinateur et rapporteur
Cristián Guillermo VIAL EDWARDS	Président du jury

To my parents,
HANS *and* RITA,
and my brother,
ANDREAS.

NON FLVCTVS NVMERARE LICET IAM MACHINATORI,
INVENIENDA EST NAM FVNCTIO VIRIDII.

ACKNOWLEDGEMENTS

The beginning of my work and interest on the subject of this thesis can be traced back to January of the year 2004, when I undertook a *stage* (internship) of two months in the *Centre de Mathématiques Appliquées* of the *École Polytechnique* in France. The subject was afterwards further developed during my dissertation to obtain the title of engineer at the *Escuela de Ingeniería* of the *Pontificia Universidad Católica de Chile* (Hein 2006), and then continued during my master (Hein 2007) and during the current doctorate in coadvisorship that I realized between both mentioned academic institutions. A lot of effort has been spent in this thesis, and it could not have been achieved successfully without the great help and support of many people and institutions to whom I am very thankful.

First of all I want to express my special gratitude and appreciation for both of my advisors, Professor Mario Durán of the *Pontificia Universidad Católica de Chile* and Professor Jean-Claude Nédélec of the *École Polytechnique*, under whose wise and caring guidance I could accomplish this thesis. Their useful advice, excellent disposition, and close relationship made this work an enjoying and delightful research experience. It was Professor Mario Durán who first introduced me to the world of numerical methods in engineering, and who proposed me the research subject. His perseverant enthusiasm, sense of humor, and immense working energy were always available to solve any problem or doubt. An appropriate answer to even the most complicated questions was every time at hand for Professor Jean-Claude Nédélec, who generously and with formidable disposition always shared his remarkable knowledge, deep insight, and good humor. Sometimes the results of a short five-minute discussion were enough to give me work on them for more than a month.

I wish also to thank deeply the good disposition, interest, and dedication in the revision and the helpful commenting of this work by the other members of the Committee: Professor Juan Carlos De La Llera, Professor María Cristina Depassier, Professor Jaime Ortega, and Professor Cristián Vial.

I feel likewise a profound gratitude towards the organizations that funded this work. In Chile, during the first four years, it was supported by the *Conicyt* fellowship for doctorate students, which was complemented by the *Ecos/Conicyt Project #C03–E08*, to allow my stay in France. During the fifth year it was partially funded by an exceptional fellowship of the *Dirección de Investigación y Postgrado* of the *Escuela de Ingeniería* of the *Pontificia Universidad Católica de Chile*.

Many thanks also to all the people in the *Centro de Minería* of the *Pontificia Universidad Católica de Chile* and in the *Centre de Mathématiques Appliquées* of the *École Polytechnique* for their warm reception, kind support, and the opportunity to live such an enriching research and life experience. I feel most obliged to all the nice people I had the opportunity to meet there, who helped me with advice, support, and care in this magnificent adventure. To Ignacio Muga for the many advices regarding his work. To Sebastián Ossandón for his excellent reception and help in Paris. To Carlos Jerez for his comments

on photonic crystals. To Eduardo Godoy for his many advices and interesting discussions. To Carlos Pérez for so many references. To Valeria Boccardo for her joviality and encouragement. To José Miguel Morales for fixing so many computer problems. Likewise to Sylvain Ferrand, his counterpart in Paris. To Juanita Aguilera, Jeanne Bailleul, Gladys Barraza, Dominique Conne, Nathalie Gauchy, Danisa Herrera, Sébastien Jacubowicz, Audrey Lemaréchal, Aldjia Mazari, Debbie Meza, Nasséra Nacer, Francis Poirier, Sandra Schnakenbourg, María Inés Stuven, and Olivier Thuret for their help on the vast amount of administrative issues. And to all the others, who, even when they cannot be named all, will always stay in my memory with great affection.

I am also grateful to Professor Simon Chandler-Wilde for his observations on the incorrect extension of the integral equations, which led us to their correct understanding.

Especially and with all my heart I wish to thank my family, for their immeasurable love and unconditional support, always. To them I owe all and to them this thesis owes all.

And finally, infinite thanks to God Almighty for making it all possible and so marvelous, for his immense grace and help in difficult times.

VOBIS OMNIBVS GRATIAS MAXIMAS AGO!

CONTENTS

LIST OF FIGURES

LIST OF TABLES

RÉSUMÉ

Dans cette thèse on calcule la fonction de Green des équations de Laplace et Helmholtz en deux et trois dimensions dans un demi-espace avec une condition à la limite d'impédance. Pour les calculs on utilise une transformée de Fourier partielle, le principe d'absorption limite, et quelques fonctions spéciales de la physique mathématique. La fonction de Green est après utilisée pour résoudre numériquement un problème de propagation des ondes dans un demi-espace qui est perturbé de manière compacte, avec impédance, en employant des techniques des équations intégrales et la méthode d'éléments de frontière. La connaissance de son champ lointain permet d'énoncer convenablement la condition de radiation qu'on a besoin. Des expressions pour le champ proche et lointain de la solution sont données, dont l'existence et l'unicité sont discutées brièvement. Pour chaque cas un problème benchmark est résolu numériquement.

On expose étendument le fond physique et mathématique et on inclut aussi la théorie des problèmes de propagation des ondes dans l'espace plein qui est perturbé de manière compacte, avec impédance. Les techniques mathématiques développées ici sont appliquées ensuite au calcul de résonances dans un port maritime. De la même façon, ils sont appliqués au calcul de la fonction de Green pour l'équation de Laplace dans un demi-plan bidimensionnel avec une condition à la limite de dérivée oblique.

Mots Clé: Fonction de Green, équation de Laplace, équation de Helmholtz, problème direct de diffraction des ondes, condition à la limite d'impédance, condition de radiation, techniques d'équations intégrales, demi-espace avec une perturbation compacte, métode d'éléments de frontière, résonances dans un port maritime, condition à la limite de dérivée oblique.

ABSTRACT

In this thesis we compute the Green's function of the Laplace and Helmholtz equations in a two- and three-dimensional half-space with an impedance boundary condition. For the computations we use a partial Fourier transform, the limiting absorption principle, and some special functions that appear in mathematical physics. The Green's function is then used to solve a compactly perturbed impedance half-space wave propagation problem numerically by using integral equation techniques and the boundary element method. The knowledge of its far field allows stating appropriately the required radiation condition. Expressions for the near and far field of the solution are given, whose existence and uniqueness are briefly discussed. For each case a benchmark problem is solved numerically.

The physical and mathematical background is extensively exposed, and the theory of compactly perturbed impedance full-space wave propagation problems is also included. The herein developed mathematical techniques are then applied to the computation of harbor resonances in coastal engineering. Likewise, they are applied to the computation of the Green's function for the Laplace equation in a two-dimensional half-plane with an oblique-derivative boundary condition.

Keywords: Green's function, Laplace equation, Helmholtz equation, direct scattering problem, impedance boundary condition, radiation condition, integral equation techniques, compactly perturbed half-space, boundary element method, harbor resonances, oblique-derivative boundary condition.

I. INTRODUCTION

1.1 Foreword

In this thesis we are essentially interested in the mathematical modeling of wave propagation phenomena by using Green's functions and integral equation techniques. As some poet from the ancient Roman Empire inspired by the Muses might have said (Hein 2006):

> *Non fluctus numerare licet iam machinatori,*
> *Invenienda est nam functio Viridii.*

This Latin epigram can be translated more or less as "to count the waves is no longer permitted for the engineer, since to be found has the function of Green". An epigram is a short, pungent, and often satirical poem, which was very popular among the ancient Greeks and Romans. It consists commonly of one elegiac couplet, i.e., a hexameter followed by a pentameter. Two possible questions that arise from our epigram are: "why does someone want to count waves?", and even more: "what is a function of Green and for what purpose do we want to find it?" Let us hence begin with the first question.

Since the dawn of mankind have waves, specifically water waves, been a source of wonder and admiration, but also of fear and respect. Giant sea waves caused by storms have drowned thousands of ships and adventurous sailors, who blamed for their fate the wrath of the mighty gods of antiquity. On more quite days, though, it was always a delightful pleasure to watch from afar the sea waves braking against the coast. For the ancient Romans, in fact, the expression of counting sea waves (*fluctus numerare*) was used in the sense of having leisure time (*otium*), as opposed to working and doing business (*negotium*). Therefore the message is clear: the leisure time is over and the engineer has work to be done. In fact, even if it is not specifically mentioned, it is implicitly understood that this premise applies as much to the civil engineer (*machinator*) as to the military engineer (*munitor*). A straight interpretation of the hexameter is also perfectly allowed. To count the waves individually as they pass by before our eyes is usually not the best way to try to comprehend and reproduce the behavior of wave propagation phenomena, so as to be afterwards used for our convenience. Hence, to understand and treat waves, what sometimes can be quite difficult, we need powerful theoretical tools and efficient mathematical methods.

This takes us now to our second question, which is closely related to the first one. A function of Green (*functio Viridii*), usually referred to as a "Green's function", has no direct relationship with the green color as may be wrongly inferred from a straight translation that disregards the little word play lying behind. The word for Green (*Viridii*) is in the genitive singular case, i.e., it stands not for the adjective green (*viridis*), but rather as a (quite rare) singular of the plural neuter noun of the second declension for green things (*viridia*), which usually refers to green plants, herbs, and trees. Its literal translation, when we consider it as a proper noun, is then "of the Green" or "of Green", which in English is equivalent to "Green's". A Green's function is, in fact, a mathematical tool that allows us to solve wave propagation problems, as I hope should become clear throughout this thesis. The first person who used this kind of functions, and after whom they are named, was the British

mathematician and physicist George Green (1793–1841), hence the word play with the color of the same name. They were introduced by Green (1828) in his research on potential theory, where he considered a particular case of them. A Green's function helps us also to solve other kinds of physical problems, but is particularly useful when dealing with infinite exterior domains, since it achieves to synthesize the physical properties of the underlying system. It is therefore in our best interest to find (*invenienda est*) such a Green's function.

1.2 Motivation and overview

1.2.1 Wave propagation

Waves, as summarized in the insightful review by Keller (1979), are disturbances that propagate through space and time, usually by transference of energy. Propagation is the process of travel or movement from one place to another. Thus wave propagation is another name for the movement of a physical disturbance, often in an oscillatory manner. The example which has been recognized longest is that of the motion of waves on the surface of water. Another is sound, which was known to be a wave motion at least by the time of the magnificent English physicist, mathematician, astronomer, natural philosopher, alchemist, and theologian Sir Isaac Newton (1643–1727). In 1690 the Dutch mathematician, astronomer, and physicist Christiaan Huygens (1629–1695) proposed that light is also a wave motion. Gradually other types of waves were recognized. By the end of the nineteenth century elastic waves of various kinds were known, electromagnetic waves had been produced, etc. In the twentieth century matter waves governed by quantum mechanics were discovered, and an active search is still underway for gravitational waves. A discussion on the origin and development of the modern concept of wave is given by Manacorda (1991).

The laws of physics provide systems of one or more partial differential equations governing each type of wave. Any particular case of wave propagation is governed by the appropriate equations, together with certain auxiliary conditions. These may include initial conditions, boundary conditions, radiation conditions, asymptotic decaying conditions, regularity conditions, etc. The differential equations together with the auxiliary conditions constitute a mathematical problem for the determination of the wave motion. These problems are the subject matter of the mathematical theory of wave propagation. Some references on this subject that we can mention are Courant & Hilbert (1966), Elmore & Heald (1969), Felsen & Marcuwitz (2003), and Morse & Feshbach (1953).

Maxwell's equations of electromagnetic theory and Schrödinger's equation in quantum mechanics are both usually linear. They are named after the Scottish mathematician and theoretical physicist James Clerk Maxwell (1831–1879) and the Austrian physicist Erwin Rudolf Josef Alexander Schrödinger (1887–1961). Furthermore, the equations governing most waves can be linearized to describe small amplitude waves. Examples of these linearized equations are the scalar wave equation of acoustics and its time-harmonic version, the Helmholtz equation, which receives its name from the German physician and physicist Hermann Ludwig Ferdinand von Helmholtz (1821–1894). Another example is the Laplace equation in hydrodynamics, in which case it is the boundary condition which is linearized

and not the equation itself. This equation is named after the French mathematician and astronomer Pierre Simon, marquis de Laplace (1749–1827). Such linear equations with linear auxiliary conditions are the subject of the theory of linear wave propagation. It is this theory which we shall consider.

The classical researchers were concerned with obtaining exact and explicit expressions for the solutions of wave propagation problems. Because the problems were linear, they constructed these expressions by superposition, i.e., by linear combination, of particular solutions. The particular solutions had to be simple enough to be found explicitly and the problem had to be special enough for the coefficients in the linear combination to be found.

One of the devised methods is the image method (cf., e.g., Morse & Feshbach 1953), in which the particular solution is that due to a point source in the whole space. The domains to which the method applies must be bounded by one or several planes on which the field or its normal derivative vanishes. In some cases it is possible to obtain the solution due to a point source in such a domain by superposing the whole space solution due to the source and the whole space solutions due to the images of the source in the bounding planes. Unfortunately the scope of this method is very limited, but when it works it yields a great deal of insight into the solution and a simple expression for it. The image method also applies to the impedance boundary condition, in which a linear combination of the wave function and its normal derivative vanishes on a bounding plane. Then the image of a point source is a point source plus a line of sources with exponentially increasing or decreasing strengths. The line extends from the image point to infinity in a direction normal to the plane. These results can be also extended for impedance boundary conditions with an oblique derivative instead of a normal derivative (cf. Gilbarg & Trudinger 1983, Keller 1981), in which case the line of images is parallel to the direction of differentiation.

The major classical method is nonetheless that of separation of variables (cf., e.g., Evans 1998, Weinberger 1995). In this method the particular solutions are products of functions of one variable each, and the desired solution is a series or integral of these product solutions, with suitable coefficients. It follows from the partial differential equation that the functions of one variable each satisfy certain ordinary differential equations. Most of the special functions of classical analysis arose in this way, such as those of Bessel, Neumann, Hankel, Mathieu, Struve, Anger, Weber, Legendre, Hermite, Laguerre, Lamé, Lommel, etc. To determine the coefficients in the superposition of the product solutions, the method of expanding a function as a series or integral of orthogonal functions was developed. In this way the theory of Fourier series originated, and also the method of integral transforms, including those of Fourier, Laplace, Hankel, Mellin, Gauss, etc.

Despite its much broader scope than the image method, the method of separation of variables is also quite limited. Only very special partial differential equations possess enough product solutions to be useful. For example, there are only 13 coordinate systems in which the three-dimensional Laplace equation has an adequate number of such solutions, and there are only 11 coordinate systems in which the three-dimensional Helmholtz equation does. Furthermore only for very special boundaries can the expansion coefficients

be found by the use of orthogonal functions. Generally they must be complete coordinate surfaces of a coordinate system in which the equation is separable.

Another classical method is the one of eigenfunction expansions (cf. Morse & Feshbach 1953, Butkov 1968). In this case the solutions are expressed as sums or integrals of eigenfunctions, which are themselves solutions of partial differential equations. This method was developed by Lord Rayleigh and others as a consequence of partial separation of variables. They sought particular solutions which were products of a function of one variable (e.g., time) multiplied by a function of several variables (e.g., spatial coordinates). This method led to the use of eigenfunction expansions, to the introduction of adjoint problems, and to other aspects of the theory of linear operators. It also led to the use of variational principles for estimating eigenvalues and approximating eigenfunctions, such as the Rayleigh-Ritz method. These procedures are needed because there exists no way for finding eigenvalues and eigenfunctions explicitly in general. However, if the eigenfunction problem is itself separable, it can be solved by the method of separation of variables.

Finally, there is the method of converting a problem into an integral equation with the aid of a Green's function (cf., e.g., Courant & Hilbert 1966). But generally the integral equation cannot be solved explicitly. In some cases it can be solved by means of integral transforms, but then the original problem can also be solved in this way.

In more recent times several other methods have also been developed, which use, e.g., asymptotic analysis, special transforms, among other theoretical tools. A brief account on them can be found in Keller (1979).

1.2.2 Numerical methods

All the previously mentioned methods to solve wave propagation problems are analytic and they require that the involved domains have some rather specific geometries to be used satisfactorily. In the method of variable separation, e.g., the domain should be described easily in the chosen coordinate system so as to be used effectively. The advent of modern computers and their huge calculation power made it possible to develop a whole new range of methods, the so-called numerical methods. These methods are not concerned with finding an exact solution to the problem, but rather with obtaining an approximate solution that stays close enough to the exact one. The basic idea in any numerical method for differential equations is to discretize the given continuous problem with infinitely many degrees of freedom to obtain a discrete problem or system of equations with only finitely many unknowns that may be solved using a computer. At the end of the discretization procedure, a linear matrix system is obtained, which is what finally is programmed into the computer.

a) Bounded domains

Two classes of numerical methods are mainly used to solve boundary-value problems on bounded domains: the finite difference method (FDM) and the finite element method (FEM). Both yield sparse and banded linear matrix systems. In the FDM, the discrete problem is obtained by replacing the derivatives with difference quotients involving the values of the unknown at certain (finitely many) points, which conform the discrete

mesh and which are placed typically at the intersections of mutually perpendicular lines. The FDM is easy to implement, but it becomes very difficult to adapt it to more complicated geometries of the domain. A reference for the FDM is Rappaz & Picasso (1998).

The FEM, on the other hand, uses a Galerkin scheme on the variational or weak formulation of the problem. Such a scheme discretizes a boundary-value problem from its weak formulation by approximating the function space of the solution through a finite set of basis functions, and receives its name from the Russian mathematician and engineer Boris Grigoryevich Galerkin (1871–1945). The FEM is thus based on the discretization of the solution's function space rather than of the differential operator, as is the case with the FDM. The FEM is not so easy to implement as the FDM, since finite element interaction integrals have to be computed to build the linear matrix system. Nevertheless, the FEM is very flexible to be adapted to any reasonable geometry of the domain by choosing adequately the involved finite elements. It was originally introduced by engineers in the late 1950's as a method to solve numerically partial differential equations in structural engineering, but since then it was further developed into a general method for the numerical solution of all kinds of partial differential equations, having thus applications in many areas of science and engineering. Some references for this method are Ciarlet (1979), Gockenbach (2006), and Johnson (1987).

Meanwhile, several other classes of numerical methods for the treatment of differential equations have arisen, which are related to the ones above. Among them we can mention the collocation method (CM), the spectral method (SM), and the finite volume method (FVM). In the CM an approximation is sought in a finite element space by requiring the differential equation to be satisfied exactly at a finite number of collocation points, rather than by an orthogonality condition. The SM, on the other hand, uses globally defined functions, such as eigenfunctions, rather than piecewise polynomials approximating functions, and the discrete solution may be determined by either orthogonality or collocation. The FVM applies to differential equations in divergence form. This method is based on approximating the boundary integral that results from integrating over an arbitrary volume and transforming the integral of the divergence into an integral of a flux over the boundary. All these methods deal essentially with bounded domains, since infinite unbounded domains cannot be stored into a computer with a finite amount of memory. For further details on these methods we refer to Sloan et al. (2001).

b) Unbounded domains

In the case of wave propagation problems, and in particular of scattering problems, the involved domains are usually unbounded. To deal with this situation, two different approaches have been devised: domain truncation and integral equation techniques. Both approaches result in some sort of bounded domains, which can then be discretized numerically without problems.

In the first approach, i.e., the truncation of the domain, some sort of boundary condition has to be imposed on the truncated (artificial) boundary. Techniques that operate in this way are the Dirichlet-to-Neumann (DtN) or Steklov-Poincaré operator, artificial boundary

conditions (ABC), perfectly matched layers (PML), and the infinite element method (IEM). The DtN operator relates on the truncated boundary curve the Dirichlet and the Neumann data, i.e., the value of the solution and of its normal derivative. Thus, the knowledge of the problem's solution outside the truncated domain, either by a series or an integral representation, allows its use as a boundary condition for the problem inside the truncated domain. Explicit expressions for the DtN operator are usually quite difficult to obtain, except for some few specific geometries. We refer to Givoli (1999) for further details on this operator. In the case of an ABC, a condition is imposed on the truncated boundary that allows the passage only of outgoing waves and eliminates the ingoing ones. The ABC has the disadvantage that it is a global boundary condition, i.e., it specifies a coupling of the values of the solution on the whole artificial boundary by some integral expression. The same holds for the DtN operator, which can be regarded as some sort of ABC. There exist in general only approximations for an ABC, which work well when the wave incidence is nearly normal, but not so well when it is very oblique. Some references for ABC are Nataf (2006) and Tsynkov (1998). In the case of PML, an absorbing layer of finite depth is placed around the truncated boundary so as to absorb the outgoing waves and reduce as much as possible their reflections back into the truncated domain's interior. On the absorbing layer, the problem is stated using a dissipative wave equation. For further details on PML we refer to Johnson (2008). The IEM, on the other hand, avoids the need of an artificial boundary by partitioning the complement of the truncated domain into a finite amount of so-called infinite elements. These infinite elements reduce to finite elements on the coupling surface and are described in some appropriate coordinate system. References for the IEM and likewise for the other techniques are Ihlenburg (1998) and Marburg & Nolte (2008). Interesting reviews of several of these methods can be also found in Thompson (2005) and Zienkiewicz & Taylor (2000). On the whole, once the domain is truncated with any one of the mentioned techniques, the problem can be solved numerically by using the FEM, the FDM, or some other numerical method that works well with bounded domains. This approach has nonetheless the drawback that the discretization of the additional truncated boundary may produce undesired reflections of the outgoing waves back towards the interior of the truncated domain, due the involved numerical approximations.

It is in fact the second approach, i.e., the integral equation techniques, the one that is of our concern throughout this thesis. This approach takes advantage of the fact that the wave propagation problem can be converted into an integral equation with the help of a Green's function. The integral equation is built in such a way that its support lies on a bounded region, e.g., the domain's boundary. Even though we mentioned that this approach may not be so practical to find an analytic solution, it becomes very useful when it is combined with an appropriate numerical method to solve the integral equation. Typically either a collocation method or a finite element method is used for this purpose. The latter is based on a variational formulation and is thus numerically more stable and accurate than the former, particularly when the involved geometries contain corners or are otherwise complicated. At the end, the general solution of the problem is retrieved by means of an integral representation formula that requires the solution of the previously solved integral equation. Of course, integral equation techniques can be likewise used to solve wave propagation

problems in bounded domains. A big advantage of these techniques is their simplicity to represent the far field of the solution. Some references on integral equation techniques are the books of Hsiao & Wendland (2008), Nédélec (2001), and Steinbach (2008).

The drawback of integral equation techniques is their more complex mathematical treatment and the requirement of knowing the Green's function of the system. It is the Green's function that stores the information of the system's physics throughout the considered domain and which allows to collapse the problem towards an integral equation. The Green's function is usually problematic to integrate, since it corresponds to the solution of the homogeneous system subject to a singularity load, e.g., the electrical field arising from a point charge. Integrating such singular fields is not easy in general. For simple element geometries, like straight segments or planar triangles, analytical integration can be used. For more general elements it is possible to design purely numerical schemes that adapt to the singularity, but at a great computational cost. When the source point and target element where the integration is done are far apart, then the integration becomes easier due to the smooth asymptotic decay of the Green's function. It is this feature that is typically employed in schemes designed to accelerate the involved computations, e.g., in fast multipole methods (FMM). A reference for these methods is Gumerov & Duraiswami (2004).

In some particular cases the differential problem can be stated equivalently as a boundary integral equation, whose support lies on the bounded boundary. For example, this occurs in (bounded) obstacle scattering, where fields in linear homogeneous media are involved. Some kind of Green's integral theorem is typically used for this purpose. This way, to solve the wave propagation problem, only the calculation of boundary values is required rather than of values throughout the unbounded exterior domain. The technique that solves such a boundary integral equation by means of the finite element method is called the boundary element method (BEM). It is sometimes also known as the method of moments (MoM), specifically in electromagnetics, or simply as the boundary integral equation method (BIEM). The BEM is in a significant manner more efficient in terms of computational resources for problems where the surface versus volume ratio is small. The dimension of a problem expressed in the domain's volume is therefore reduced towards its boundary surface, i.e., one dimension less. The matrix resulting from the numerical discretization of the problem, though, becomes full, and to build it, as already mentioned, singular integrals have to be evaluated. The application of the BEM can be schematically described through the following steps:

1. Definition of the differential problem.
2. Calculation of the Green's function.
3. Derivation of the integral representation.
4. Development of the integral equation.
5. Rearrangement as a variational formulation.
6. Implementation of the numerical discretization.
7. Construction of the linear matrix system.
8. Computational resolution of the problem.
9. Graphical representation of the results.

The BEM is only applicable to problems for which Green's functions can be calculated, which places considerable restrictions on the range and generality of the problems to which boundary elements can be usefully applied. We remark that non-linearities and inhomogeneous media can be also included in the formulation, although they generally introduce volume integrals in the integral equation, which of course require the volume to be discretized before attempting to solve the problem, and thus removing one of the main advantages of the BEM. A good general survey on the BEM can be found in the article of Costabel (1986). Its implementation in obstacle scattering and some notions on FMM can be found in Terrasse & Abboud (2006). Other references for this method are Becker (1992), Chen & Zhou (1992), and Kirkup (2007). We note also the interesting historical remarks on boundary integral operators performed by Costabel (2007).

We mention finally that there is still an active research going on to study these numerical methods more deeply, existing also a great variety of so-called hybrid methods, where two or more of the techniques are combined together. A reference on this subject is the book of Brezzi & Fortin (1991).

1.2.3 Wave scattering and impedance half-spaces

Scattering is a general physical process whereby waves of some form, e.g., light, sound, or moving particles, are forced to deviate from a straight trajectory by one or more localized non-uniformities in the medium through which they pass. These non-uniformities are called scatterers or scattering centers. There exist many types of scatterers, ranging from microscopic particles to macroscopic targets, including bubbles, density fluctuations in fluids, surface roughness, defects in crystalline solids, among many others. In mathematics and physics, the discipline that deals with the scattering of waves and particles is called scattering theory. This theory studies basically how the solutions of partial differential equations without scatterer, i.e., freely propagating waves or particles, change when interacting with its presence, typically a boundary condition or another particle. We speak of a direct scattering problem when the scattered radiation or particle flux is to be determined, based on the known characteristics of the scatterer. In an inverse scattering problem, on the other hand, some unknown characteristic of an object is to be determined, e.g., its shape or internal constitution, from measurement data of its radiation or its scattered particles. Some references on scattering are Felsen & Marcuwitz (2003), Lax & Phillips (1989), and Pike & Sabatier (2002). For inverse scattering we refer to Potthast (2001).

Our concern throughout the thesis is specifically about direct obstacle scattering, where the scatterer (i.e., the obstacle) is given by an impenetrable macroscopic target that is modeled through a boundary condition. For a better understanding of the involved phenomena and due their inherent complexity, we consider only scalar linear wave propagation in time-harmonic regime, i.e., the partial differential equation of our model is given either by the Helmholtz or the Laplace equation. We observe that the latter equation is in fact the limit case of the former as the frequency tends towards zero. The time-harmonic regime implies that the involved system is independent of time and that only a single frequency is taken into account. If desired, time-dependent solutions of the system can be then constructed with

the help of the Fourier transform (vid. Section A.7), by combining the solutions obtained for different frequencies. Alternatively, the solutions of a time-dependent system can be directly computed by means of retarded potentials (cf. Barton 1989, Butkov 1968, Felsen & Marcuwitz 2003). Time-dependent scattering is also considered in Wilcox (1975). Once the models for these scalar linear partial differential equations are well understood, then more complex types of waves can be taken into account, e.g., electromagnetic or elastic waves. The Helmholtz and Laplace equations can be thus regarded as a more simplified case of other wave equations.

The resolution of scattering problems for bounded obstacles with arbitrary shape by means of integral equation techniques is in general well-known, particularly when dealing with Dirichlet or Neumann boundary conditions. A Dirichlet boundary condition, named after the German mathematician Johann Peter Gustav Lejeune Dirichlet (1805–1859), specifies the value of the field at the boundary. A Neumann boundary condition, on the other hand, specifies the value of the field's normal derivative at the boundary, and receives its name from the German mathematician Carl Gottfried Neumann (1832–1925), who is considered one of the initiators of the theory of integral equations. The Green's function of the system is of course also well-known, and it is obtained directly from the fundamental solution of the involved wave equation, i.e., the Helmholtz or the Laplace equation. This applies also to the radiation condition to be imposed at infinity, which is known as the Sommerfeld radiation condition in honor of the German theoretical physicist Arnold Johannes Wilhelm Sommerfeld (1868–1951), who made invaluable contributions to quantum theory and to the classical theory of electromagnetism. We remark that in particular the problem of the Laplace equation around a bounded obstacle is not strictly speaking a wave scattering problem but rather a perturbation problem, and likewise at infinity we speak of an asymptotic decaying condition rather than of a radiation condition. Some references that we can mention, among the many that exist, are Kress (2002), Nédélec (2001), and Terrasse & Abboud (2006). We mention also the interesting results about radiation conditions in a rather general framework described by Costabel & Dauge (1997).

In the case of an impedance boundary condition, the general agreement is that the theory for bounded obstacles is well-known, but it is rather scarcely discussed in the literature. An impedance boundary condition specifies a linear combination of the field's value and of its normal derivative at the boundary, i.e., it acts as a weighted combination of Dirichlet and Neumann boundary conditions. It is also known as a third type or Robin boundary condition, after the French mathematical analyst and applied mathematician Victor Gustave Robin (1855–1897). Usually the emphasis is given to Dirichlet and Neumann boundary conditions, probably because they are simpler to treat and because with an impedance boundary condition the existence and uniqueness of the problem can be only ensured almost always, but not always. Some of the references that include the impedance boundary condition are Alber & Ramm (2009), Colton & Kress (1983), Hsiao & Wendland (2008), Filippi, Bergassoli, Habault & Lefebvre (1999), and Kirsch & Grinberg (2008).

When the obstacle in a scattering problem is no longer bounded, then usually a different Green's function and a different radiation condition have to be taken into account to

find a solution by means of integral equation techniques. These work well only when the scattering problem is at most a compact perturbation of the problem for which the Green's function was originally determined, i.e., when these problems differ only on a compact portion of their involved domains. An unbounded obstacle, e.g., an infinite half-space, constitutes clearly a non-compact perturbation of the full-space.

We are particularly interested in solving scattering problems either on two- or three-dimensional half-spaces, where the former are also simply referred to as half-planes and the latter just as half-spaces. If Dirichlet or Neumann boundary conditions are considered, then the Green's function is directly found through the image method. Furthermore, the same Sommerfeld radiation condition continues to hold in this case.

For an impedance half-space, i.e., when an impedance boundary condition is used on a half-space, the story is not so straightforward. As we already pointed out, the image method can be also used in this case to compute the Green's function, but the results are far from being explicit and some of the obtained terms are only known in integral form, as so-called Sommerfeld-type integrals (cf. Casciato & Sarabandi 2000, Taraldsen 2005). The difficulties arise from the fact that an impedance boundary condition allows the propagation of surface waves along the boundary, whose relation with a point source is far from simple. Another method that we can mention and that is used to solve this kind of problems is the Wiener-Hopf technique, which yields an exact solution to complex integral equations and is based on integral transforms and analyticity properties of complex functions. Further details can be found in Davies (2002), Dettman (1984), and Wright (2005).

We remark that in scattering problems on half-spaces, or likewise on compact perturbations of them, there appear two different kinds of waves: volume and surface waves. Volume waves propagate throughout the domain and behave in the same manner as waves propagating in free-space. They are linked to the wave equation under consideration, i.e., to the Helmholtz equation, since for the Laplace equation there are no volume waves. Surface waves, on the other hand, propagate only near the boundary and are related to the considered boundary condition. They decrease exponentially towards the interior of the domain and may appear as much for the Helmholtz as for the Laplace equation. They exist only when the boundary condition is of impedance-type, but not when it is of Dirichlet- or Neumann-type, which may explain why the latter conditions are simpler in their treatment.

a) Helmholtz equation

The impedance half-space wave propagation problem for the Helmholtz equation was at first formulated by Sommerfeld (1909), who was strongly motivated by the around 1900 newly established wireless telegraphy of Maxwell, Hertz, Bose, Tesla, and Marconi, among others. Sommerfeld wanted to explain why radio waves could travel long distances across the ocean, and thus overcome the curvature of the Earth. In his work, he undertook a detailed analysis of the radiation problem for an infinitesimal vertical Hertzian dipole over a lossy medium, and as part of the solution he found explicitly a radial Zenneck surface wave, named after the German physicist and electrical engineer Jonathan Adolf Wilhelm Zenneck (1871–1959), who first described them (Zenneck 1907). Thus both Zenneck and

Sommerfeld obtained results that lent considerable credence to the view of the Italian inventor and marchese Guglielmo Marconi (1874–1937), that the electromagnetic waves were guided along the surface. Sommerfeld's solution was later criticized by the German mathematician Hermann Klaus Hugo Weyl (1885–1955), who published on the same subject (Weyl 1919) and who obtained a solution very similar to the one found by Sommerfeld, but without the surface-wave term. Sommerfeld (1926) returned later to the same problem and solved it using a different approach, where he confirmed the correctness of Weyl's solution. The apparent inclusion of a sign error in Sommerfeld's original work, which he never admitted, prompted much debate over several decades on the existence of a Zenneck-type surface wave and its significance in the fields generated by a vertical electric dipole. A more detailed account can be found in Collin (2004). The corrected formulation confirmed the existence of a surface wave for certain values of impedance and observation angles, but showed its contribution to the total field only significant within a certain range of distances, dependent on the impedance of the half-space. Thus, the concept of the surface wave as being the important factor for long-distance propagation lost favor. Further references on this historical discussion can be also found in the articles of Casciato & Sarabandi (2000), Nobile & Hayek (1985), Sarabandi, Casciato & Koh (1992), and Taraldsen (2004, 2005).

Just to finish the story, Kennelly (1902) and, independently, Heaviside (1902), had predicted before the existence of an ionized layer at considerable height above the Earth's surface. It was thought that such a layer could possibly reflect the electromagnetic waves back to Earth. Although it was not until Breit & Tuve (1926) showed experimentally that radio waves were indeed reflected from the ionosphere, that this became finally the accepted mechanism for the long-distance propagation of radio waves. We refer to Anduaga (2008) for a more detailed historical essay on the concept of the ionosphere.

Nonetheless, even if Sommerfeld's explanation proved later to be wrong, its problem remained (and still remains) of great theoretical interest. Since its first publication, it is an understatement to say that this problem has received a significant amount of attention in the literature with literally hundreds of papers published on the subject. Besides electromagnetic waves, the problem is also important for outdoor sound propagation (cf. Morse & Ingard 1961, Embleton 1996) and for water waves in shallow waters near the coast (cf. Mei, Stiassnie & Yue 2005, Herbich 1999).

Thus, as a way to state a brief account on the problem, Sommerfeld (1909), working in the field of electromagnetism, was the first to solve the spherical wave reflection problem, stated as a dipole source on a finitely conducting earth. Weyl (1919) reformulated the problem by modeling the radiation from a point source located above the earth as a superposition of an infinite number of elementary plane waves, propagating in different (complex) directions. Sommerfeld (1926) solved his problem again using integrals that were afterwards called of Sommerfeld-type. Van der Pol (1935) applied several ingenious substitutions that simplified the integrals appearing in the derivations. Norton (1936, 1937) expanded upon these and other results from Van der Pol & Niessen (1930) and, with the aid of equations by Wise (1931), generated the most useful results up to that time. Baños & Wesley (1953, 1954) and Baños (1966) obtained similar solutions by using the double

saddle point method. Further developments on the propagation of radio waves can be also found in the book of Sommerfeld (1949). We remark that in electromagnetic scattering, the impedance boundary condition describes an obstacle which is not perfectly conducting, but does not allow the electromagnetic field to penetrate deeply into the scattering domain.

The greatest interest in the problem stemmed nonetheless from the acoustics community, to describe outdoor sound propagation. The acoustical problem of spherical wave reflection was first attacked by Rudnick (1947), who relied heavily on the electromagnetic theories of Van der Pol and Norton. Subsequently, Lawhead & Rudnick (1951*a*,*b*) and Ingard (1951) obtained approximate solutions in terms of the error function. Wenzel (1974) and Chien & Soroka (1975, 1980) obtained solutions containing a surface-wave term. Exhaustive lists of references with other solutions for the problem can be found in Habault & Filippi (1981) and in Nobile & Hayek (1985). We can mention on this behalf also the articles of Briquet & Filippi (1977), Attenborough, Hayek & Lawther (1980), Li, Wu & Seybert (1994), and Attenborough (2002), and more recently also Ochmann (2004) and Ochmann & Brick (2008), among the many others that exist. For the two-dimensional case, in particular, we can refer to the articles of Chandler-Wilde & Hothersall (1995*a*,*b*) and Granat, Tahar & Ha-Duong (1999).

The purpose of these articles is essentially the same: they try to compute in one way or the other the reflection of spherical waves (in three dimensions) or cylindrical waves (in two dimensions) on an impedance boundary. This corresponds to the computation of the Green's function for the problem, since spherical and cylindrical waves are originated by a point source. Books that consider this problem and other aspects of Green's functions are the ones of Greenberg (1971), DeSanto (1992), and Duffy (2001). The great variety of results for the same problem reflects its difficulty and its interest. The expressions found for the Green's function contain typically either complicated integrals, which derive from a Fourier transform or some other kind of integral transform, or unpractical infinite series expansions, which do not hold for all conditions or everywhere. There exists no relatively simple expression in terms of known elementary or special functions. For the treatment of the integrals, special integration contours are taken into account and at the end some parts are approximated by methods of asymptotic analysis like the ones of stationary phase or of steepest descent, the latter also known as the saddle-point approximation. Some references for these asymptotic methods are Bender & Orszag (1978), Estrada & Kanwal (2002), Murray (1984), and Wong (2001).

It is notably on this behalf that using a Fourier transform yields a manageable expression for the spectral Green's function (cf. Durán, Muga & Nédélec 2005*a*,*b*, 2006, 2009). In two dimensions, we considered this expression to compute numerically the spatial Green's function with the help of a fast Fourier transform (FFT) for the regular part, whereas its singular part was treated analytically (Durán, Hein & Nédélec 2007*a*,*b*). Further details of these calculations can be found in Hein (2006, 2007). This method allows to compute effectively the Green's function, without the use of asymptotic approximations, but it can become quite burdensome when building bigger matrixes for the BEM due the multiple evaluations required for the FFT.

Outdoor sound propagation is in fact the classic application for the Helmholtz equation stated in an impedance half-space, where the acoustic waves propagate freely in the upper half-space and interact with the ground, i.e., the impenetrable lower half-space, through an impedance boundary condition on their common boundary. The Helmholtz equation is derived directly from the scalar acoustic wave equation by assuming a time-harmonic regime. The acoustic impedance in this case corresponds to a (complex) proportionality coefficient that relates the normal velocity of the fluid, where the sound propagates, to the excess pressure on the boundary. A real impedance implies that the boundary is non-dissipative, whereas a strictly complex (i.e., non-real) impedance is associated with an absorbing boundary. We remark that the limit cases of the boundary condition of impedance-type, the ones of Dirichlet- and Neumann-type, correspond respectively to sound-soft and sound-hard boundary surfaces. For more details on the physics of the problem, we refer to DeSanto (1992), Embleton (1996), Filippi et al. (1999), and Morse & Ingard (1961). The use of an impedance boundary condition is validated and discussed in the articles of Attenborough (1983) and Bermúdez, Hervella-Nieto, Prieto & Rodríguez (2007).

There exists also some literature on experimental measurements for this topic. Extensive experimental studies of sound propagation horizontally near the ground, mainly over grass, are performed by Embleton, Piercy & Olson (1976), who even suggest the presence of surface waves. Different impedance versus frequency models for various types of ground surface are compared by Attenborough (1985). Studies of acoustic wave propagation over grassland and snow are developed by Albert & Orcutt (1990). In the paper of Albert (2003), experimental evidence is given that confirms the existence of acoustic surface waves in a natural outdoor setting, which in this case is above a snow cover. For a study of sound propagation in forests we refer to Tarrero et al. (2008). Extensive measurement results and theoretical models are also discussed by Attenborough, Li & Horoshenkov (2007).

The use of some BEM to solve the problem has also received some attention in the literature. Further references can be found in De Lacerda, Wrobel & Mansur (1997), De Lacerda, Wrobel, Power & Mansur (1998), and Li et al. (1994). For some two-dimensional applications of the BEM we cite Chen & Waubke (2007), Durán, Hein & Nédélec (2007*a*,*b*), and Granat, Tahar & Ha-Duong (1999). Some integral equations for this case are also treated in Chandler-Wilde (1997) and Chandler-Wilde & Peplow (2005). Integral equations in three dimensions for Dirichlet and Neumann boundary conditions, and the low-frequency case, can be found in Dassios & Kleinman (1999). For the appropriate radiation condition of the problem, and likewise for its existence and uniqueness, we refer to Durán, Muga & Nédélec (2005*a*,*b*, 2006, 2009).

b) Laplace equation

The impedance half-space wave propagation problem for the Laplace equation is particularly of great importance in hydrodynamics, since it describes linear surface waves on water of infinite depth. The interest for this problem can be traced back to December 1813, when the French Académie des Sciences announced a mathematical prize competition on the subject of surface wave propagation on liquid of indefinite depth. The prize was

awarded in 1816 to the French mathematician and early pioneer of analysis Augustin Louis Cauchy (1789–1857), who submitted his entry in September 1815 and which was eventually published in Cauchy (1827). Another memoir, to record his independent work, was deposited in October 1815 by the French mathematician, geometer, and physicist Siméon Denis Poisson (1781–1840), one of the judges of the competition, which was published in Poisson (1818). Both memoirs are classical works in the field of hydrodynamics. For a more detailed historical account on the water-wave theory we refer to Craik (2004).

With the passage of time, the interest in the description of wave motion in the presence of submerged or floating bodies increased. The first study of wave motion caused by a submerged obstacle was carried out in the classical (and often reprinted) text of Lamb (1916), who analyzed the two-dimensional wave motion due to a submerged cylinder. Further studies dealing with simple submerged obstacles were done by Havelock (1917, 1927), for spheres and doublets, and by Dean (1945), for plane barriers.

A major breakthrough in the field arrived nonetheless with the classic works on the motion of floating bodies by John (1949, 1950), who showed how the boundary-value problem could be reduced to an integral equation over the wetted portion of the partly immersed body. John studied the problem in general form, stating necessary conditions for the uniqueness of its solution. He also gave expressions in the form of discrete eigenfunction expansions for the Green's functions of the problem, in two and three dimensions, and considering finite and infinite water depth. His work inspired (and still inspires) a vast amount of literature, particularly in the subjects of the existence and uniqueness of solutions, the computation of Green's functions, and the development of integral equation methods.

A standard reference that synthesizes the known theory up to its time is the thorough and insightful article by Wehausen & Laitone (1960). It includes also the known expressions for Green's functions. A closely related article is Wehausen (1971). More recent references on these topics are the books of Mei (1983), Linton & McIver (2001), Kuznetsov, Maz'ya & Vainberg (2002), and Mei, Stiassnie & Yue (2005). The classical representation of these Green's functions, in three dimensions, is in terms of a semi-infinite integral involving a Bessel function (vid. Subsection A.2.4) and a Cauchy principal-value singularity (vid. Subsection A.6.5). Separate expressions exist for infinite and finite (constant) depth of the fluid, but their forms are similar and the infinite-depth limit can be recovered as a special case of the finite-depth integral representation. According to Newman (1985), the principal drawback of these expressions is that they are extremely time-consuming to evaluate numerically. Some articles dealing with the finite-depth Green's function are the ones of Angell, Hsiao & Kleinman (1986), Black (1975), Chakrabarti (2001), Fenton (1978), Linton (1999), Macaskill (1979), Mei (1978), Pidcock (1985), and Xia (2001).

In the case of infinite-depth water in three dimensions, a simpler analytic representation for the source potential or Green's function exists as the sum of a finite integral, with a monotonic integrand involving elementary transcendental functions, and a wave-like term of closed form involving Bessel and Struve functions (vid. Subsection A.2.7). This expression, which was suggested by Havelock (1955), has been rederived or publicized in different forms by Kim (1965), Hearn (1977), Noblesse (1982), Newman (1984*b*, 1985),

Pidcock (1985), and Chakrabarti (2001). Other expressions for this Green's function were developed by Moran (1964), Hess & Smith (1967), Dautray & Lions (1987), and Peter & Meylan (2004). Likewise, analogous expressions for the two-dimensional Green's function are considered in the works of Thorne (1953), Kim (1965), Macaskill (1979), and Greenberg (1971). A more general two-dimensional case that takes surface tension into account was considered by Harter, Abrahams & Simon (2007), Harter, Simon & Abrahams (2008), and Motygin & McIver (2009), using potentials expressed in terms of exponential integrals (vid. Subsection A.2.3). Analogous observations to the ones of the Helmholtz equation can be made also for the case of the Laplace equation.

Water-wave motion near floating or submerged bodies is the classic application for the Laplace equation stated in an impedance half-space. The Laplace equation is obtained by considering the dynamic of an incompressible inviscid fluid, as is the case with water. The impedance boundary condition corresponds to the linearized free-surface condition, which allows the propagation of (water) surface waves. The impedance in this case can be regarded as a wave number for the surface waves, which acts in an equivalent manner as the wave number for the Helmholtz equation, but now only along the boundary surface. Again, a real impedance implies that the boundary is non-dissipative, whereas a strictly complex impedance is associated with an absorbing boundary. Further details on the physical aspects of the problem can be found in Kuznetsov, Maz'ya & Vainberg (2002) and Wehausen & Laitone (1960).

Reviews of numerical methods to solve water-wave problems and further references can be found in Mei (1978) and Yeung (1982). A review of ocean waves interacting with ice is done by Squire, Dugan, Wadhams, Rottier & Liu (1995). A computation of a Green's function for this case can be found in Squire & Dixon (2001). Boundary integral equations are developed in Angell, Hsiao & Kleinman (1986) and Sayer (1980). For the use of the BEM we refer to the articles of Hess & Smith (1967), Hochmuth (2001), Lee, Newman & Zhu (1996) and Liapis (1992, 1993). Resonances for water-wave problems are studied in Hazard & Lenoir (1993, 1998, 2002).

1.2.4 Applications

Wave propagation problems in impedance half-spaces, or in compact perturbations of them, have many applications in science and engineering. We already mentioned the applications to outdoor sound propagation (Filippi et al. 1999, Morse & Ingard 1961), to radio wave propagation above the ground (Sommerfeld 1949), and to water waves in shallow waters near the coast (Mei et al. 2005, Herbich 1999), in the case of the Helmholtz equation, and to the motion of water waves near floating or submerged bodies (Kuznetsov et al. 2002, Wehausen & Laitone 1960), in the case of the Laplace equation. Further specific applications include the scattering of light by a photonic crystal (Joannopoulos et al. 2008, Sakoda 2005, Yasumoto 2006, Durán, Guarini & Jerez-Hanckes 2009), the computation of harbor resonances in coastal engineering (Mei et al. 2005, Panchang & Demirbilek 2001), and the treatment of elliptic partial differential equations, specifically the Laplace equation,

with an oblique-derivative boundary condition (Gilbarg & Trudinger 1983, Keller 1981, Paneah 2000). This thesis is concerned with the latter two of these applications.

a) Harbor resonances in coastal engineering

A harbor (sometimes also spelled as harbour) is a partially enclosed body of water connected through one or more openings to the sea. Conventional harbors are built along a coast where a shielded area may be provided by natural indentations and/or by breakwaters protruding seaward from the coast. Harbors provide anchorage and a place of refuge for ships. Key features of all harbors include shelter from both long and short period open sea waves, easy safe access to the sea in all types of weather, adequate depth and maneuvering room within the harbor, shelter from storm winds, and minimal navigation channel dredging. A harbor can be sometimes subject to a so-called harbor oscillation or surging, which corresponds to a nontidal vertical water movement. Usually these vertical motions are low, but when oscillations are excited by a tsunami or a storm surge, they may become quite large. Variable winds, air oscillations, or surf beat may also cause oscillations. Nonetheless, the most studied excitation is caused by incident tsunamis, which have typical periods from a few minutes to an hour, and are originated from distant earthquakes. If the total duration of the tsunami is sufficiently long, oscillations excited in the harbor may persist for days, resulting in broken mooring lines, damaged fenders, hazards in berthing and loading or in navigation through the entrance, and so on. Sometimes incoming ships have to wait outside the harbor until oscillations within subside, causing costly delays. Harbor oscillations are discussed in the books of Mei (1983), Mei et al. (2005), and Herbich (1999). For a single and comprehensive technical document about coastal projects we refer to the Coastal Engineering Manual of the U.S. Army Corps of Engineers (2002).

To understand roughly the physical mechanism of these oscillations, we consider a harbor with the entrance in line with a long and straight coastline. Onshore waves are partly reflected and partly absorbed along the coast. A small portion is however diffracted through the entrance into the harbor and reflected repeatedly by the interior boundaries. Some of the reflected wave energy escapes the harbor and radiates again to the ocean, while some of it stays inside. If the wavetrain is of long duration, and the incident wave frequency is close to a standing-wave frequency in the closed basin, then a so-called resonance occurs in the basin, i.e., even a relatively weak incident wave of such characteristics can induce a large response in the harbor. When a harbor is closed and the damping is neglected, the free-wave motion is known to be the superposition of normal modes of standing waves with a discrete spectrum of characteristic frequencies. When a harbor has a small opening and is subject to incident waves we may expect a resonance whenever the frequency of the incident waves is close to a characteristic frequency of the closed harbor.

Resonances are therefore closely related to the phenomena of seiching (in lakes and harbors) and sloshing (in coffee cups and storage tanks), which correspond to standing waves in enclosed or partially enclosed bodies of water. These phenomena have been observed already since very early times. Forel (1895) quotes a vivid description of seiching in the Lake of Constance in 1549 from “Les Chroniques de Cristophe Schulthaiss”, and

Darwin (1899) refers to seiching in the Lake of Geneva in 1600 with a peak-to-peak amplitude of over one meter. Observations in cups and pots doubtless predate recorded history. Scientific studies date from Merian (1828) and Poisson (1828–1829), and especially from the observations in the Lake of Geneva by Forel (1895), which began in 1869. A thorough and historical review of the seiching phenomenon in harbors and further references can be found in Miles (1974).

A resonance of a different type is given by the so-called Helmholtz mode when the oscillatory motion inside the harbor is much slower than each of the normal modes (Burrows 1985). It corresponds to the resonant mode with the longest period, where the water appears to move up and down unison throughout the harbor, which seems to have been first studied by Miles & Munk (1961). This very long period mode appears to be particularly significant for harbors responding to the energy of a tsunami, and for several harbors on the Great Lakes that respond to long-wave energy spectra generated by storms. We remark that from the mathematical point of view, resonances correspond to poles of the scattering and radiation potentials when they are extended to the complex frequency domain (cf. Poisson & Joly 1991). Harbor resonance should be avoided or minimized in harbor planning and operation to reduce adverse effects such as hazardous navigation and mooring of vessels, deterioration of structures, and sediment deposition or erosion within the harbor.

Examples of harbor resonances are the Ciutadella inlet in the Menorca Island on the Western Mediterranean (Marcos, Monserrat, Medina & Lomónaco 2005), the Duluth-Superior Harbor in Minnesota on the Lake Superior (Jordan, Stortz & Sydor 1981), the Port Kembla Harbour on the central coast of New South Wales in Australia (Luick & Hinwood 2008), the Los Angeles Harbor Pier 400 in California (Seabergh & Thomas 1995), and the port of Ploče in Croatia on the Adriatic Sea (Vilibić & Mihanović 2005).

Considerable effort has been devoted to achieving a good understanding of the phenomena of harbor resonance. Lamb (1916) analyzed the free oscillation in closed rectangular and circular basins. His solutions then clarified the natural periods and modes of free surface oscillations related to these special configurations. As the first but important step to approach the practical situation, McNown (1952) studied the forced oscillation in a circular harbor which is connected to the open sea through a narrow mouth. He made the assumption that standing wave conditions are always formed at the harbor entrance when resonance occurs. Since the radiation effect was ruled out, he showed that a resonant harbor behaves the same as a closed basin. Similar research was also carried out by Kravtchenko & McNown (1955) on rectangular harbors.

Since the paper of Miles & Munk (1961), who first treated harbor oscillations by a scattering theory, the study of harbor resonance has been steadily progressing both theoretically and experimentally. Miles & Munk (1961) considered the wave energy radiation effect expanding offshore from the harbor entrance and applied a Green's function to analyze the harbor oscillation. They even found that the wider the harbor mouth, the smaller the amplitude of the resonant oscillation. That is, narrowing the harbor entrance does not diminish resonant oscillation, which contradicts common sense based on the conventional reasoning for a non-resonant harbor, where less wave energy is expected to be

transmitted into the harbor through a smaller opening. Miles & Munk (1961) referred to this phenomenon as the harbor paradox. Additional important contributions were made by Le Méhauté (1961), Ippen & Goda (1963), Raichlen & Ippen (1965), and Raichlen (1966). These studies considered the effect of radiation through the entrance of the harbor and the resulting frequency responses of the harbor oscillations became fairly close to the experimentally observed ones. Other rigorous solutions for the problem were presented by Lee (1969, 1971), who considered rectangular and circular harbors with openings located on a straight coastline. He discovered that the trapping of energy by the harbor leads to an amplitude of oscillation that is far greater than the one of the incident wave. Similarly, Mei & Petroni (1973) dealt with a circular harbor protruding halfway into the open sea. Theories to deal with arbitrary harbor configurations were available after Hwang & Tuck (1970) and Lee (1969, 1971), who worked with boundary integral equation methods to calculate the oscillation in harbors of constant depth with arbitrary shape. Mei & Chen (1975) developed a hybrid-boundary-element technique to also study harbors of arbitrary geometry. Harbor resonances using the FEM are likewise computed in Walker & Brebbia (1978). A comprehensive list of references can be found in Yu & Chwang (1994).

The mild-slope equation, which describes the combined effects of refraction and diffraction of linear water waves, was first suggested by Eckart (1952) and later rederived by Berkhoff (1972*a*,*b*, 1976), Smith & Sprinks (1975), and others, and is now well-accepted as the method for estimating coastal wave conditions. The underlying assumption of this equation is that evanescent modes (locally emanated waves) are not important, and that the rate of change of depth and current within a wavelength is small. The mild-slope equation is a usually expressed in an elliptic form, and it turns into the Helmholtz equation for uniform water depths. Since then, different kinds of mild-slope equations have been derived (Liu & Shi 2008). A detailed survey of the literature on the mild-slope and its related equations is provided by Hsu, Lin, Wen & Ou (2006). Some examinations on the validity of the theory are performed by Booij (1983) and Ehrenmark & Williams (2001).

Along rigid, impermeable vertical walls a Neumann boundary condition is used, since there is no flow normal to the surface. However, in general an impedance boundary condition is used along coastlines or permeable structures, to account for a partial reflection of the flow on the boundary (Demirbilek & Panchang 1998). A study of harbor resonances using an approximated DtN operator and a model based on the Helmholtz equation with an impedance boundary condition on the coast was done by Quaas (2003).

An alternative parabolic equation method to solve the problem was developed by Radder (1979) and Kirby & Dalrymple (1983), which approximates the mild-slope equation. A sea-bottom friction and absorption boundary was considered by Chen (1986) for a hybrid BEM to analyze wave-induced oscillation in a harbor with arbitrary shape and depth. Berkhoff, Booy & Radder (1982) described and compared the computational results for the models of refraction, of parabolic refraction-diffraction, and of full refraction-diffraction. Tsay, Zhu & Liu (1989) considered the effects of topographical variation and energy dissipation, and developed a finite element numerical model to investigate wave refraction, diffraction, reflection, and dissipation. Chou & Han (1993) employed a boundary element

method and under the consideration of the effect of partial reflection along boundaries to develop a numerical method for predicting wave height distribution in a harbor of arbitrary shape and variable water depth. Nardini & Brebbia (1982) proposed a DRBEM (dual reciprocity boundary element method), which was also studied by Hsiao, Lin & Fang (2001) and Hsiao, Lin & Hu (2002). The infinite element method was applied to the problem by Chen (1990). Interesting reviews of the theoretical advances on wave propagation modeling in coastal engineering can be found in Mei & Liu (1993) and Liu & Losada (2002). A review that brings together the large amount of literature on the analytical study of free-surface wave motion past porous structures is performed by Chwang & Chan (1998).

The study of harbor resonances becomes particularly important for countries with high seismicity and maritime harbors subject to tsunamis such as Chile. A tragical and recent example of the involved devastation was given by the 2010 Chilean earthquake, which occurred offshore from the Maule Region in south central Chile on February 27, 2010. Noteworthy, it had already been predicted by Ruegg et al. (2009). After the earthquake, the coast was afflicted by tsunami waves. At the port city of Talcahuano waves with amplitude up to 5 meters high were observed and the sea level rose above 2.4 meters. The tsunami caused serious damage to port facilities and lifted boats out of the water. A good harbor design should protect the waters of the harbor from such events as best as possible, and it is therefore of great interest to have a good knowledge of the appearing resonances.

b) Oblique-derivative half-plane Laplace problem

As a more theoretical application, we are interested in the study of elliptic partial differential operators, particularly the Laplace equation, with an oblique-derivative (impedance) boundary condition. This kind of operators is characterized by the inclusion of tangential derivatives in the boundary condition. We speak of a (purely) oblique-derivative boundary condition when it combines only tangential and normal derivatives, whereas a combination of tangential derivatives and an impedance boundary condition is referred to as an oblique-derivative impedance boundary condition.

The purely oblique-derivative problem for a second-order elliptic partial differential operator was first stated by the great French mathematician, theoretical physicist, and philosopher of science Jules Henri Poincaré (1854–1912) in his studies on the theory of tides (Poincaré 1910). Since then, the so-called Poincaré problem has been the subject of many publications (cf. Egorov & Kondrat'ev 1969, Paneah 2000), and it arises naturally when determining the gravitational fields of celestial bodies. Its main interest lies in the fact that it corresponds to a typical degenerate elliptic boundary-value problem where the vector field of its solution is tangent to the boundary of the domain on some subset. The Poincaré problem for harmonic functions, in particular, arises in semiconductor physics and considers constant coefficients for the oblique derivative in the boundary condition (Krutitskii & Chikilev 2000). It allows to describe the Hall effect, i.e., when the direction of an electric current and the direction of an electric field do not coincide in a semiconductor due the presence of a magnetic field (Krutitskii, Krutitskaya & Malysheva 1999). The

two-dimensional Poincaré problem for the Laplace equation is treated in Lesnic (2007), Trefethen & Williams (1986), and further references can be also found in Lions (1956).

Of special interest is the oblique-derivative impedance Laplace problem stated in a half-space, and particularly the determination of its Green's function, which describes outgoing oblique surface waves that emanate from a point source and which increase or decrease exponentially along the boundary, depending on the obliqueness of the derivative in the boundary condition. An integral representation for this Green's function in half-spaces of three and higher dimensions was developed by Gilbarg & Trudinger (1983). Using an image method, it was later generalized by Keller (1981) to a wider class of equations, including the wave equation, the heat equation, and the Laplace equation. Its use for more general linear uniformly elliptic equations with discontinuous coefficients can be found in the articles of Di Fazio & Palagachev (1996) and Palagachev, Ragusa & Softova (2000). The generalization of this image method to wedges is performed by Gautesen (1988).

For the two-dimensional case and when dealing with the Laplace equation, there exists no representation of the Green's function, except the already mentioned cases when the oblique derivative becomes a normal one.

1.3 Objectives

The main objective of this thesis is to compute the Green's function for the Laplace and Helmholtz equations in two- and three-dimensional impedance half-spaces, and to use it for solving direct wave scattering problems in compactly perturbed half-spaces by developing appropriate integral equation techniques and a corresponding boundary element method. The goal is to give a numerically effective and efficient expression for the Green's function, and to determine its far field. The developed integral equations are to be supported only on a bounded portion of the boundary, and they have to work well for arbitrary compact perturbations towards the upper half-space, as long as the considered boundary is regular enough. It is also of interest to derive expressions for the far field of the solution of the scattering problem. The developed techniques are to be programmed in Fortran, implementing benchmark problems to test these calculations and the computational subroutines. Thus the idea in this thesis is to continue and extend the preliminary work performed in Hein (2006, 2007) and in Durán, Hein & Nédélec (2007*a*,*b*).

Another objective is to use the developed expressions and techniques to solve some interesting applications in science and engineering. One of the applications to consider deals with the computation of harbor resonances in coastal engineering, enhancing the model of Quaas (2003) by working with an impedance boundary condition and solving the problem by using integral equations instead of a DtN operator. The other application considers the calculation of the Green's function for the oblique-derivative impedance half-plane Laplace problem, which generalizes the techniques used in the computation of the other Green's functions from this thesis.

The interest behind this study is to comprehend better, from the mathematical point of view, the interaction between volume and surface waves caused by a point source in

impedance half-spaces, and their application to some scattering problems in engineering. Only the linear, scalar, and time-harmonic cases are considered here, to simplify the analysis and to avoid additional complications. We include the study of the Laplace equation, where only surface waves appear, since the problem is somewhat simpler and permits a far better understanding of the treatment for the Helmholtz equation, particularly in the two-dimensional case.

To allow a better comprehension of the treated topics, this thesis is intended to be as self-contained as possible. Therefore a quick survey of the most important aspects of the mathematical and physical background and a detailed analysis of the relatively well-known full-space problems are also included. Additionally, a comprehensive list of references is given whenever possible, so as to ensure extensive further reading on the involved subjects if such an interest arises.

1.4 Contributions

Essentially, this thesis concentrates and recreates some of the most important elements of the widely dispersed knowledge on full- and half-space Green's functions for the Laplace and Helmholtz operators, and their associated integral equations, in a single document with a coherent and homogeneous notation. By doing so, new expressions are found and a better understanding of the involved techniques is achieved.

The main contribution of the thesis is the rigorous development of expressions for the Green's functions of the Helmholtz and Laplace operators in impedance half-spaces, in two and three dimensions, and their use to solve direct wave scattering problems by means of boundary integral equations. These expressions are characterized in terms of finite combinations of elementary functions, known special functions, and their primitives. In the case of the two-dimensional Laplace equation even a new explicit representation is found, based on exponential integrals and expressed in (2.94). A more general representation, based likewise on exponential integrals, is also developed for the Green's function of the oblique-derivative half-plane Laplace problem, which has not been computed before and is given explicitly in (7.41). For the other cases, effective numerical procedures are derived to evaluate the Green's functions everywhere and on all the values of interest. For the two-dimensional Helmholtz equation, we perform an improvement over our previous results in the numerical procedure (Durán et al. 2007*a*,*b*), which is now more efficient, uses a numerical quadrature formula instead of a fast Fourier transform, works better with complex impedances and wave numbers, and may be also evaluated in the complementary half-plane. The details are delineated in Section 3.5. The series-based representation for the Green's function of the three-dimensional Laplace equation (4.113), even if it is similar in a certain way to others found in the literature (cf., e.g., Noblesse 1982), it is derived in an rigorous and independent manner that sheds new light on its properties. The evaluation of the representation for the three-dimensional Helmholtz equation, specified in Section 5.5, corresponds to a direct numerical integration of the primitive-based expression of the Green's function, which can be adapted without difficulty to the other cases.

Another important contribution is the proper understanding of the limiting absorption principle and its interpretation, in the sense of distributions, as the appearance of additional Dirac masses for the spectral Green's function. This effect, which has not been particularly pointed out in the literature, allows us to treat all the involved Fourier integrals in the sense of Cauchy principal values and is expressed in (2.64), (3.59), (4.70), and (5.65). A different approach for the same topic is undertaken in Section 7.3 for the oblique-derivative case, where the additional appearing terms are interpreted as the solution of the homogeneous problem with a proper scaling, which is justified from the radiation condition, and their effect is expressed in (7.22).

The derived expressions for the Green's function yield better light on the interaction between the volume and the surface wave parts of the system's response to a point source, even in the presence of dissipation, and are coherent with results for the complex image method used to solve this problem (cf. Casciato & Sarabandi 2000, Taraldsen 2004, 2005). In particular, they retrieve the image source point on the complementary half-space and the continuous source distribution that stems from this point towards infinity along a line that is perpendicular to the half-space's boundary, increasing exponentially.

The herein treated wave scattering problems consider arbitrary compact perturbations towards the upper half-space and the associated integral representations and equations used to solve them are derived with great detail and have their support only on the perturbed portion of the boundary. In particular, a correct expression is given for the boundary integral representation on the unperturbed portion of the boundary (cf. Durán et al. 2007*a*,*b*). The integral equations are solved by using a boundary element method, and neither hybrid techniques nor domain truncation are required. Compact perturbations towards the lower half-space are not considered herein, but the thorough study of the singularities of the Green's functions (another contribution of this thesis) is the first step towards that direction to develop them in the near future.

A state of the art is developed for the full-space impedance Laplace and Helmholtz problems, since the theory for them is more or less well-known and they are closely related to the half-space problems. The main singularity of the associated Green's functions is the same, and several other aspects are analogous in both kinds of problems.

Another contribution is the development of computational subroutines to solve the considered problems, and the numerical results that are obtained by their execution. The programming is in general not easy and requires a careful treatment of the involved singular integrals (due the singularities of the Green's functions) to build the full matrixes that stem from the boundary element method. The subroutines are likewise programmed and tested for the full-space problems.

The application of the developed techniques to the computation of harbor resonances in coastal engineering is also a contribution of this thesis, which shows their use in the resolution of a practical problem in engineering.

1.5 Outline

To fulfill the objectives, this thesis is structured in eight chapters and five appendixes. Each chapter and each appendix is in his turn divided into sections and further into subsections in order to expose the contents in the hopefully most clear and accessible way for the reader. Each one starts with a short introduction that yields more light about its contents. A list of references is also included in each one of them.

Chapter I, the current chapter, presents a broad introduction to the thesis. The more general aspects are discussed and the framework that connects its different parts is described. It includes a short foreword, the motivation and overview, the objectives, the contributions, and the current outline.

In Chapters II, III, IV, and V we study the perturbed half-space impedance problems of the Laplace and Helmholtz equations in two and three dimensions respectively, using integral equation techniques and the boundary element method. These chapters include the main contributions of this thesis, particularly the computation of the Green's functions and their far-field expressions, and the development of the associated integral equations.

The following two chapters contain the applications of the developed techniques. Chapter VI deals with the computation of harbor resonances in coastal engineering, and in Chapter VII the Green's function for the oblique-derivative half-plane Laplace problem is derived and given explicitly.

Chapter VIII incorporates the conclusion of this thesis, including a short discussion on the results and some perspectives for future research. It is followed by the bibliographical references and afterwards by the appendixes.

In Appendix A we present a short survey of the mathematical and physical background of the thesis. The most important aspects are discussed and several references are given for each topic. It is intended as a quick reference guide to understand or refresh some deeper technical aspects mentioned throughout the thesis.

Appendixes B, C, D, and E, on the other hand, deal with the perturbed full-space impedance problems of the Laplace and Helmholtz equations in two and three dimensions respectively, using integral equation techniques and the boundary element method. These problems are relatively well-known (at least in theory) and the full extent of the mathematical techniques are illustrated on them.

For the not so experienced reader it is recommended to read first, after this introduction, Appendix A, and particularly the sections which contain lesser-known subjects. The references mentioned throughout should be consulted whenever some topic is not so well understood. Afterwards we recommend to read at least one of the appendixes that contain the full-space problems, i.e., Appendixes B, C, D, and E. The most detailed account of the theory is given in Appendix B, so that other chapters and appendixes may refer to it whenever necessary. Of course, if the reader is more interested in the Helmholtz equation or in the three-dimensional problems, then the corresponding appendixes should be consulted, since they contain all the important and related details. The experienced reader, on

the other hand, may prefer eventually to pass straightforwardly to Chapter II. By following this itinerary, the reading experience of this thesis should be (hopefully) more delightful and instructive.

II. HALF-PLANE IMPEDANCE LAPLACE PROBLEM

2.1 Introduction

In this chapter we study the perturbed half-plane impedance Laplace problem using integral equation techniques and the boundary element method.

We consider the problem of the Laplace equation in two dimensions on a compactly perturbed half-plane with an impedance boundary condition. The perturbed half-plane impedance Laplace problem is a surface wave scattering problem around the bounded perturbation, which is contained in the upper half-plane. In water-wave scattering the impedance boundary-value problem appears as a consequence of the linearized free-surface condition, which allows the propagation of surface waves (vid. Section A.10). This problem can be regarded as a limit case when the frequency of the volume waves, i.e., the wave number in the Helmholtz equation, tends towards zero (vid. Chapter III). The three-dimensional case is considered in Chapter IV, whereas the full-plane impedance Laplace problem with a bounded impenetrable obstacle is treated thoroughly in Appendix B. The case of an oblique-derivative boundary condition is discussed in Chapter VII.

The main application of the problem corresponds to linear water-wave propagation in a liquid of indefinite depth, which was first studied in the classical works of Cauchy (1827) and Poisson (1818). A study of wave motion caused by a submerged obstacle was carried out by Lamb (1916). The major impulse in the field came after the milestone papers on the motion of floating bodies by John (1949, 1950), who considered a Green's function and integral equations to solve the problem. Other expressions for the Green's function in two dimensions were derived by Thorne (1953), Kim (1965), and Macaskill (1979), and likewise by Greenberg (1971) and Dautray & Lions (1987). A more general problem that takes surface tension into account was considered by Harter, Abrahams & Simon (2007), Harter, Simon & Abrahams (2008), and Motygin & McIver (2009). The main references for the problem are the classical article of Wehausen & Laitone (1960) and the books of Mei (1983), Linton & McIver (2001), Kuznetsov, Maz'ya & Vainberg (2002), and Mei, Stiassnie & Yue (2005). Reviews of the numerical methods that have been used to solve water-wave problems can be found in Mei (1978) and Yeung (1982).

The Laplace equation does not allow the propagation of volume waves inside the considered domain, but the addition of an impedance boundary condition permits the propagation of surface waves along the boundary of the perturbed half-plane. The main difficulty in the numerical treatment and resolution of our problem is the fact that the exterior domain is unbounded. We solve it therefore with integral equation techniques and a boundary element method, which require the knowledge of the associated Green's function. This Green's function is computed using a Fourier transform and taking into account the limiting absorption principle, following Durán, Muga & Nédélec (2005*a*, 2006) and Durán, Hein & Nédélec (2007*a*,*b*), but here an explicit expression is found for it in terms of a finite combination of elementary and special functions.

This chapter is structured in 12 sections, including this introduction. The direct scattering problem of the Laplace equation in a two-dimensional compactly perturbed half-plane with an impedance boundary condition is presented in Section 2.2. The computation of the Green's function and its far field expression are developed respectively in Sections 2.3 and 2.4. The use of integral equation techniques to solve the direct scattering problem is discussed in Section 2.5. These techniques allow also to represent the far field of the solution, as shown in Section 2.6. The appropriate function spaces and some existence and uniqueness results for the solution of the problem are presented in Section 2.7. The dissipative problem is studied in Section 2.8. By means of the variational formulation developed in Section 2.9, the obtained integral equation is discretized using the boundary element method, which is described in Section 2.10. The boundary element calculations required to build the matrix of the linear system resulting from the numerical discretization are explained in Section 2.11. Finally, in Section 2.12 a benchmark problem based on an exterior half-circle problem is solved numerically.

2.2 Direct scattering problem

2.2.1 Problem definition

We consider the direct scattering problem of linear time-harmonic surface waves on a perturbed half-plane $\Omega_e \subset \mathbb{R}^2_+$, where $\mathbb{R}^2_+ = \{(x_1, x_2) \in \mathbb{R}^2 : x_2 > 0\}$, where the incident field u_I is known, and where the time convention $e^{-i\omega t}$ is taken. The goal is to find the scattered field u as a solution to the Laplace equation in the exterior open and connected domain Ω_e, satisfying an outgoing surface-wave radiation condition, and such that the total field u_T, which is decomposed as $u_T = u_I + u$, satisfies a homogeneous impedance boundary condition on the regular boundary $\Gamma = \Gamma_p \cup \Gamma_\infty$ (e.g., of class C^2). The exterior domain Ω_e is composed by the half-plane $\mathbb{R}^2_+$ with a compact perturbation near the origin that is contained in $\mathbb{R}^2_+$, as shown in Figure 2.1. The perturbed boundary is denoted by Γ_p, while Γ_∞ denotes the remaining unperturbed boundary of $\mathbb{R}^2_+$, which extends towards infinity on both sides. The unit normal $\boldsymbol{n}$ is taken outwardly oriented of Ω_e and the complementary domain is denoted by $\Omega_c = \mathbb{R}^2 \setminus \overline{\Omega_e}$.

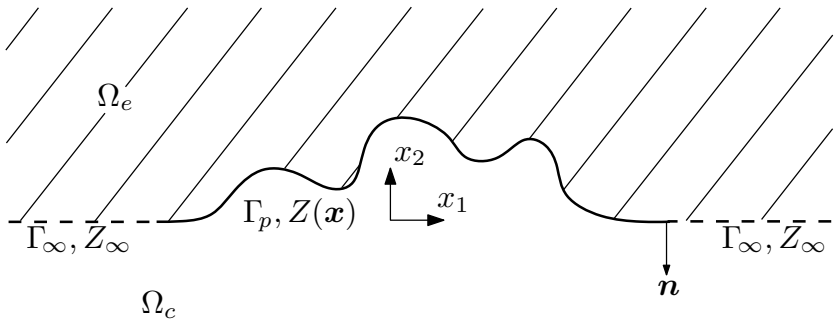

FIGURE 2.1. Perturbed half-plane impedance Laplace problem domain.

The total field u_T satisfies thus the Laplace equation

$$\Delta u_T = 0 \qquad \text{in } \Omega_e, \tag{2.1}$$

which is also satisfied by the incident field u_I and the scattered field u, due linearity. For the total field u_T we take the homogeneous impedance boundary condition

$$-\frac{\partial u_T}{\partial n} + Z u_T = 0 \qquad \text{on } \Gamma, \tag{2.2}$$

where Z is the impedance on the boundary, which is decomposed as

$$Z(\boldsymbol{x}) = Z_\infty + Z_p(\boldsymbol{x}), \qquad \boldsymbol{x} \in \Gamma, \tag{2.3}$$

being $Z_\infty > 0$ real and constant throughout Γ, and $Z_p(\boldsymbol{x})$ a possibly complex-valued impedance that depends on the position $\boldsymbol{x}$ and that has a bounded support contained in Γ_p. The case of a complex Z_∞ will be discussed later. For linear water waves, the free-surface condition considers $Z_\infty = \omega^2/g$, where ω is the radian frequency or pulsation and g denotes the acceleration caused by gravity. If $Z = 0$ or $Z = \infty$, then we retrieve respectively the classical Neumann or Dirichlet boundary conditions. The scattered field u satisfies the non-homogeneous impedance boundary condition

$$-\frac{\partial u}{\partial n} + Z u = f_z \qquad \text{on } \Gamma, \tag{2.4}$$

where the impedance data function f_z is known, has its support contained in Γ_p, and is given, because of (2.2), by

$$f_z = \frac{\partial u_I}{\partial n} - Z u_I \qquad \text{on } \Gamma. \tag{2.5}$$

An outgoing surface-wave radiation condition has to be also imposed for the scattered field u, which specifies its decaying behavior at infinity and eliminates the non-physical solutions, e.g., ingoing surface waves or exponential growth inside Ω_e. This radiation condition can be stated for $r \to \infty$ in a more adjusted way as

$$\begin{cases} |u| \le \dfrac{C}{r} \quad \text{and} \quad \left|\dfrac{\partial u}{\partial r}\right| \le \dfrac{C}{r^2} & \text{if } x_2 > \dfrac{1}{Z_\infty}\ln(1 + Z_\infty \pi r), \\[2ex] |u| \le C \quad \text{and} \quad \left|\dfrac{\partial u}{\partial r} - iZ_\infty u\right| \le \dfrac{C}{r} & \text{if } x_2 \le \dfrac{1}{Z_\infty}\ln(1 + Z_\infty \pi r), \end{cases} \tag{2.6}$$

for some constants $C > 0$, where $r = |\boldsymbol{x}|$. It implies that two different asymptotic behaviors can be established for the scattered field u, which are shown in Figure 2.2. Away from the boundary Γ and inside the domain Ω_e, the first expression in (2.6) dominates, which is related to the asymptotic decaying condition (B.7) of the Laplace equation on the exterior of a bounded obstacle. Near the boundary, on the other hand, the second part of the second expression in (2.6) resembles a Sommerfeld radiation condition like (C.8), but only along the boundary, and is therefore related to the propagation of surface waves. It is often expressed also as

$$\left|\frac{\partial u}{\partial |x_1|} - iZ_\infty u\right| \le \frac{C}{|x_1|}. \tag{2.7}$$

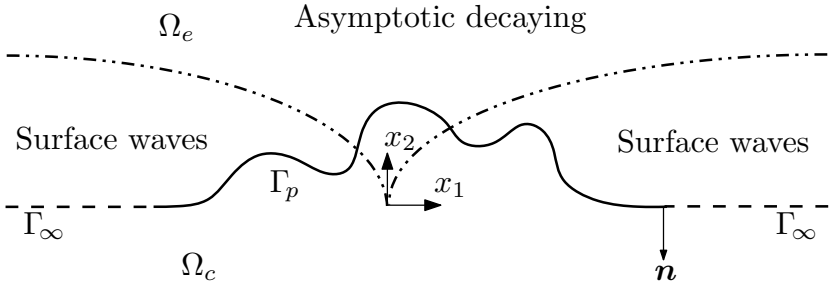

FIGURE 2.2. Asymptotic behaviors in the radiation condition.

Analogously as done by Durán, Muga & Nédélec (2005*a*, 2006) for the Helmholtz equation, the radiation condition (2.6) can be stated alternatively as

$$\begin{cases} |u| \leq \dfrac{C}{r^{1-\alpha}} \quad \text{and} \quad \left|\dfrac{\partial u}{\partial r}\right| \leq \dfrac{C}{r^{2-\alpha}} & \text{if } \; x_2 > Cr^\alpha, \\ |u| \leq C \quad \text{and} \quad \left|\dfrac{\partial u}{\partial r} - iZ_\infty u\right| \leq \dfrac{C}{r^{1-\alpha}} & \text{if } \; x_2 \leq Cr^\alpha, \end{cases} \tag{2.8}$$

for $0 < \alpha < 1$ and some constants $C > 0$, being the growth of Cr^α bigger than the logarithmic one at infinity. Equivalently, the radiation condition can be expressed in a more weaker and general formulation as

$$\begin{cases} \lim\limits_{R\to\infty} \displaystyle\int_{S_R^1} \frac{|u|^2}{R}\,\mathrm{d}\gamma = 0 \quad \text{and} \quad \lim\limits_{R\to\infty} \displaystyle\int_{S_R^1} R\left|\frac{\partial u}{\partial r}\right|^2 \mathrm{d}\gamma = 0, \\ \lim\limits_{R\to\infty} \displaystyle\int_{S_R^2} \frac{|u|^2}{\ln R}\,\mathrm{d}\gamma < \infty \quad \text{and} \quad \lim\limits_{R\to\infty} \displaystyle\int_{S_R^2} \frac{1}{\ln R}\left|\frac{\partial u}{\partial r} - iZ_\infty u\right|^2 \mathrm{d}\gamma = 0, \end{cases} \tag{2.9}$$

where

$$S_R^1 = \left\{ \boldsymbol{x} \in \mathbb{R}^2_+ : |\boldsymbol{x}| = R, \;\; x_2 > \frac{1}{Z_\infty}\ln(1 + Z_\infty \pi R) \right\}, \tag{2.10}$$

$$S_R^2 = \left\{ \boldsymbol{x} \in \mathbb{R}^2_+ : |\boldsymbol{x}| = R, \;\; x_2 < \frac{1}{Z_\infty}\ln(1 + Z_\infty \pi R) \right\}. \tag{2.11}$$

We observe that in this case

$$\int_{S_R^1} \mathrm{d}\gamma = \mathcal{O}(R) \qquad \text{and} \qquad \int_{S_R^2} \mathrm{d}\gamma = \mathcal{O}(\ln R). \tag{2.12}$$

The portions S_R^1 and S_R^2 of the half-circle and the terms depending on S_R^2 of the radiation condition (2.9) have to be modified when using instead the polynomial curves of (2.8). We refer to Stoker (1956) for a discussion on radiation conditions for surface waves.

The perturbed half-plane impedance Laplace problem can be finally stated as

$$\begin{cases} \text{Find } u : \Omega_e \to \mathbb{C} \text{ such that} \\ \Delta u = 0 & \text{in } \Omega_e, \\ -\dfrac{\partial u}{\partial n} + Zu = f_z & \text{on } \Gamma, \\ \text{+ Outgoing radiation condition as } |\boldsymbol{x}| \to \infty, \end{cases} \tag{2.13}$$

where the outgoing radiation condition is given by (2.6).

2.2.2 Incident field

To determine the incident field u_I, we study the solutions of the unperturbed and homogeneous wave propagation problem with neither a scattered field nor an associated radiation condition. The solutions are searched in particular to be physically admissible, i.e., solutions which do not explode exponentially in the propagation domain, depicted in Figure 2.3. We analyze thus the half-plane impedance Laplace problem

$$\begin{cases} \Delta u_I = 0 & \text{in } \mathbb{R}^2_+, \\ \dfrac{\partial u_I}{\partial x_2} + Z_\infty u_I = 0 & \text{on } \{x_2 = 0\}. \end{cases} \tag{2.14}$$

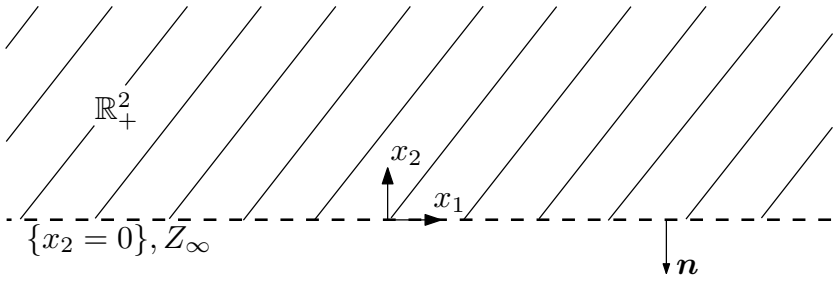

FIGURE 2.3. Positive half-plane $\mathbb{R}^2_+$.

The solutions u_I of the problem (2.14) are given, up to an arbitrary scaling factor, by the progressive plane surface waves

$$u_I(\boldsymbol{x}) = e^{ik_s x_1} e^{-Z_\infty x_2}, \qquad k_s^2 = Z_\infty^2. \tag{2.15}$$

They correspond to progressive plane volume waves of the form $e^{i\boldsymbol{k}\cdot\boldsymbol{x}}$ with a complex wave propagation vector $\boldsymbol{k} = (k_s, iZ_\infty)$. It can be observed that these surface waves are guided along the half-plane's boundary, and decrease exponentially towards its interior, hence their name. They vanish completely for classical Dirichlet ($Z_\infty = \infty$) or Neumann ($Z_\infty = 0$) boundary conditions.

2.3 Green's function

2.3.1 Problem definition

The Green's function represents the response of the unperturbed system to a Dirac mass. It corresponds to a function G, which depends on the impedance Z_∞, on a fixed source point $\boldsymbol{x} \in \mathbb{R}^2_+$, and on an observation point $\boldsymbol{y} \in \mathbb{R}^2_+$. The Green's function is computed in the sense of distributions for the variable $\boldsymbol{y}$ in the half-plane $\mathbb{R}^2_+$ by placing at the right-hand side of the Laplace equation a Dirac mass $\delta_{\boldsymbol{x}}$, centered at the point $\boldsymbol{x}$. It is therefore a solution for the radiation problem of a point source, namely

$$\left\{\begin{array}{l} \text{Find } G(\boldsymbol{x},\cdot) : \mathbb{R}^2_+ \to \mathbb{C} \text{ such that} \\ \Delta_{\boldsymbol{y}} G(\boldsymbol{x},\boldsymbol{y}) = \delta_{\boldsymbol{x}}(\boldsymbol{y}) \qquad\qquad \text{in } \mathcal{D}'(\mathbb{R}^2_+), \\ \dfrac{\partial G}{\partial y_2}(\boldsymbol{x},\boldsymbol{y}) + Z_\infty G(\boldsymbol{x},\boldsymbol{y}) = 0 \qquad \text{on } \{y_2 = 0\}, \\ \text{+ Outgoing radiation condition as } |\boldsymbol{y}| \to \infty. \end{array}\right. \tag{2.16}$$

The outgoing radiation condition, in the same way as in (2.6), is given here as $|\boldsymbol{y}| \to \infty$ by

$$\left\{\begin{array}{l} |G| \le \dfrac{C}{|\boldsymbol{y}|} \quad \text{and} \quad \left|\dfrac{\partial G}{\partial r_{\boldsymbol{y}}}\right| \le \dfrac{C}{|\boldsymbol{y}|^2} \qquad \text{if } y_2 > \dfrac{1}{Z_\infty}\ln\big(1 + Z_\infty \pi |\boldsymbol{y}|\big), \\ |G| \le C \quad \text{and} \quad \left|\dfrac{\partial G}{\partial r_{\boldsymbol{y}}} - iZ_\infty G\right| \le \dfrac{C}{|\boldsymbol{y}|} \qquad \text{if } y_2 \le \dfrac{1}{Z_\infty}\ln\big(1 + Z_\infty \pi |\boldsymbol{y}|\big), \end{array}\right. \tag{2.17}$$

for some constants $C > 0$, which are independent of $r = |\boldsymbol{y}|$.

2.3.2 Special cases

When the Green's function problem (2.16) is solved using either homogeneous Dirichlet or Neumann boundary conditions, then its solution is found straightforwardly using the method of images (cf., e.g., Morse & Feshbach 1953).

a) Homogeneous Dirichlet boundary condition

We consider in the problem (2.16) the particular case of a homogeneous Dirichlet boundary condition, namely

$$G(\boldsymbol{x},\boldsymbol{y}) = 0, \qquad \boldsymbol{y} \in \{y_2 = 0\}, \tag{2.18}$$

which corresponds to the limit case when the impedance is infinite ($Z_\infty = \infty$). In this case, the Green's function G can be explicitly calculated using the method of images, since it has to be antisymmetric with respect to the axis $\{y_2 = 0\}$. An additional image source point $\bar{\boldsymbol{x}} = (x_1, -x_2)$, located on the lower half-plane and associated with a negative Dirac mass, is placed for this purpose just opposite to the upper half-plane's source point $\boldsymbol{x} = (x_1, x_2)$. The desired solution is then obtained by evaluating the full-plane Green's function (B.23) for each Dirac mass, which yields finally

$$G(\boldsymbol{x},\boldsymbol{y}) = \frac{1}{2\pi}\ln|\boldsymbol{y} - \boldsymbol{x}| - \frac{1}{2\pi}\ln|\boldsymbol{y} - \bar{\boldsymbol{x}}|. \tag{2.19}$$

b) Homogeneous Neumann boundary condition

We consider in the problem (2.16) the particular case of a homogeneous Neumann boundary condition, namely

$$\frac{\partial G}{\partial n_{\boldsymbol{y}}}(\boldsymbol{x},\boldsymbol{y}) = 0, \qquad \boldsymbol{y} \in \{y_2 = 0\}, \tag{2.20}$$

which corresponds to the limit case when the impedance is zero ($Z_\infty = 0$). As in the previous case, the method of images is again employed, but now the half-plane Green's function G has to be symmetric with respect to the axis $\{y_2 = 0\}$. Therefore, an additional image source point $\bar{\boldsymbol{x}} = (x_1, -x_2)$, located on the lower half-plane, is placed just opposite to the upper half-plane's source point $\boldsymbol{x} = (x_1, x_2)$, but now associated with a positive Dirac mass. The desired solution is then obtained by evaluating the full-plane Green's function (B.23) for each Dirac mass, which yields

$$G(\boldsymbol{x},\boldsymbol{y}) = \frac{1}{2\pi}\ln|\boldsymbol{y}-\boldsymbol{x}| + \frac{1}{2\pi}\ln|\boldsymbol{y}-\bar{\boldsymbol{x}}|. \tag{2.21}$$

2.3.3 Spectral Green's function

a) Boundary-value problem

To solve (2.16) in the general case, we use a modified partial Fourier transform on the horizontal y_1-axis, taking advantage of the fact that there is no horizontal variation in the geometry of the problem. To obtain the corresponding spectral Green's function, we follow the same procedure as the one performed in Durán et al. (2005*a*). We define the forward Fourier transform of a function $F\big(\boldsymbol{x},(\cdot,y_2)\big) : \mathbb{R} \to \mathbb{C}$ by

$$\widehat{F}(\xi; y_2, x_2) = \frac{1}{\sqrt{2\pi}} \int_{-\infty}^{\infty} F(\boldsymbol{x},\boldsymbol{y})\, e^{-i\xi(y_1-x_1)}\, \mathrm{d}y_1, \qquad \xi \in \mathbb{R}, \tag{2.22}$$

and its inverse by

$$F(\boldsymbol{x},\boldsymbol{y}) = \frac{1}{\sqrt{2\pi}} \int_{-\infty}^{\infty} \widehat{F}(\xi; y_2, x_2)\, e^{i\xi(y_1-x_1)}\, \mathrm{d}\xi, \qquad y_1 \in \mathbb{R}. \tag{2.23}$$

To ensure a correct integration path for the Fourier transform and correct physical results, the calculations have to be performed in the framework of the limiting absorption principle, which allows to treat all the appearing integrals as Cauchy principal values. For this purpose, we take a small dissipation parameter $\varepsilon > 0$ into account and consider the problem (2.16) as the limit case when $\varepsilon \to 0$ of the dissipative problem

$$\begin{cases} \text{Find } G_\varepsilon(\boldsymbol{x},\cdot) : \mathbb{R}^2_+ \to \mathbb{C} \text{ such that} & \\ \Delta_{\boldsymbol{y}} G_\varepsilon(\boldsymbol{x},\boldsymbol{y}) = \delta_{\boldsymbol{x}}(\boldsymbol{y}) & \text{in } \mathcal{D}'(\mathbb{R}^2_+), \\ \dfrac{\partial G_\varepsilon}{\partial y_2}(\boldsymbol{x},\boldsymbol{y}) + Z_\varepsilon G_\varepsilon(\boldsymbol{x},\boldsymbol{y}) = 0 & \text{on } \{y_2 = 0\}, \end{cases} \tag{2.24}$$

where $Z_\varepsilon = Z_\infty + i\varepsilon$. This choice ensures a correct outgoing dissipative surface-wave behavior. Further references for the application of this principle can be found in Lenoir &

Martin (1981) and in Hazard & Lenoir (1998). For its application to the finite-depth case, we refer to Doppel & Hochmuth (1995).

Applying thus the Fourier transform (2.22) on the system (2.24) leads to a linear second order ordinary differential equation for the variable y_2, with prescribed boundary values, given by

$$\begin{cases} \dfrac{\partial^2 \widehat{G}_\varepsilon}{\partial y_2^2}(\xi) - \xi^2 \widehat{G}_\varepsilon(\xi) = \dfrac{\delta(y_2 - x_2)}{\sqrt{2\pi}}, & y_2 > 0, \\ \dfrac{\partial \widehat{G}_\varepsilon}{\partial y_2}(\xi) + Z_\varepsilon \widehat{G}_\varepsilon(\xi) = 0, & y_2 = 0. \end{cases} \tag{2.25}$$

We use the method of undetermined coefficients, and solve the homogeneous differential equation of the problem (2.25) respectively in the strip $\{\boldsymbol{y} \in \mathbb{R}^2_+ : 0 < y_2 < x_2\}$ and in the half-plane $\{\boldsymbol{y} \in \mathbb{R}^2_+ : y_2 > x_2\}$. This gives a solution for $\widehat{G}_\varepsilon$ in each domain, as a linear combination of two independent solutions of an ordinary differential equation, namely

$$\widehat{G}_\varepsilon(\xi) = \begin{cases} a\, e^{|\xi| y_2} + b\, e^{-|\xi| y_2} & \text{for } \ 0 < y_2 < x_2, \\ c\, e^{|\xi| y_2} + d\, e^{-|\xi| y_2} & \text{for } \ y_2 > x_2. \end{cases} \tag{2.26}$$

The unknowns a, b, c, and d, which depend on ξ and x_2, are determined through the boundary condition, by imposing continuity, and by assuming an outgoing wave behavior.

b) Spectral Green's function with dissipation

Now, thanks to (2.26), the computation of $\widehat{G}_\varepsilon$ is straightforward. From the boundary condition of (2.25) a relation for the coefficients a and b can be derived, which is given by

$$a\big(Z_\varepsilon + |\xi|\big) + b\big(Z_\varepsilon - |\xi|\big) = 0. \tag{2.27}$$

On the other hand, since the solution (2.26) has to be bounded at infinity as $y_2 \to \infty$, it follows then necessarily that

$$c = 0. \tag{2.28}$$

To ensure the continuity of the Green's function at the point $y_2 = x_2$, it is needed that

$$d = a\, e^{|\xi| 2x_2} + b. \tag{2.29}$$

Using relations (2.27), (2.28), and (2.29) in (2.26), we obtain the expression

$$\widehat{G}_\varepsilon(\xi) = a\, e^{|\xi| x_2} \left[e^{-|\xi||y_2 - x_2|} - \left(\frac{Z_\varepsilon + |\xi|}{Z_\varepsilon - |\xi|} \right) e^{-|\xi|(y_2 + x_2)} \right]. \tag{2.30}$$

The remaining unknown coefficient a is determined by replacing (2.30) in the differential equation of (2.25), taking the derivatives in the sense of distributions, particularly

$$\frac{\partial}{\partial y_2} \left\{ e^{-|\xi||y_2 - x_2|} \right\} = -|\xi| \operatorname{sign}(y_2 - x_2)\, e^{-|\xi||y_2 - x_2|}, \tag{2.31}$$

and

$$\frac{\partial}{\partial y_2} \big\{ \operatorname{sign}(y_2 - x_2) \big\} = 2\, \delta(y_2 - x_2). \tag{2.32}$$

So, the second derivative of (2.30) becomes

$$\frac{\partial^2 \widehat{G}_\varepsilon}{\partial y_2^2}(\xi) = a\, e^{|\xi| x_2} \left[\xi^2 e^{-|\xi||y_2 - x_2|} - 2|\xi| \delta(y_2 - x_2) - \left(\frac{Z_\varepsilon + |\xi|}{Z_\varepsilon - |\xi|} \right) \xi^2 e^{-|\xi|(y_2 + x_2)} \right]. \quad (2.33)$$

This way, from (2.30) and (2.33) in the first equation of (2.25), we obtain that

$$a = -\frac{e^{-|\xi| x_2}}{\sqrt{8\pi}\,|\xi|}. \quad (2.34)$$

Finally, the spectral Green's function $\widehat{G}_\varepsilon$ with dissipation ε is given by

$$\widehat{G}_\varepsilon(\xi; y_2, x_2) = -\frac{e^{-|\xi||y_2 - x_2|}}{\sqrt{8\pi}\,|\xi|} + \left(\frac{Z_\varepsilon + |\xi|}{Z_\varepsilon - |\xi|} \right) \frac{e^{-|\xi|(y_2 + x_2)}}{\sqrt{8\pi}\,|\xi|}. \quad (2.35)$$

c) Analysis of singularities

To obtain the spectral Green's function $\widehat{G}$ without dissipation, the limit $\varepsilon \to 0$ has to be taken in (2.35). This can be done directly wherever the limit is regular and continuous on ξ. Singular points, on the other hand, have to be analyzed carefully to fulfill correctly the limiting absorption principle. Thus we study first the singularities of the limit function before applying this principle, i.e., considering just $\varepsilon = 0$, in which case we have

$$\widehat{G}_0(\xi) = -\frac{e^{-|\xi||y_2 - x_2|}}{\sqrt{8\pi}\,|\xi|} + \left(\frac{Z_\infty + |\xi|}{Z_\infty - |\xi|} \right) \frac{e^{-|\xi|(y_2 + x_2)}}{\sqrt{8\pi}\,|\xi|}. \quad (2.36)$$

Possible singularities for (2.36) may only appear when $\xi = 0$ or when $|\xi| = Z_\infty$, i.e., when the denominator of the fractions is zero. Otherwise the function is regular and continuous.

For $\xi = 0$ the function (2.36) is continuous. This can be seen by writing it, analogously as in Durán, Muga & Nédélec (2006), in the form

$$\widehat{G}_0(\xi) = \frac{H\big(|\xi|\big)}{|\xi|}, \quad (2.37)$$

where

$$H(\beta) = \frac{1}{\sqrt{8\pi}} \left(-e^{-\beta\,|y_2 - x_2|} + \frac{Z_\infty + \beta}{Z_\infty - \beta}\, e^{-\beta\,(y_2 + x_2)} \right), \qquad \beta \in \mathbb{C}. \quad (2.38)$$

Since $H(\beta)$ is an analytic function in $\beta = 0$, since $H(0) = 0$, and since

$$\lim_{\xi \to 0} \widehat{G}_0(\xi) = \lim_{\xi \to 0} \frac{H\big(|\xi|\big) - H(0)}{|\xi|} = H'(0), \quad (2.39)$$

we can easily obtain that

$$\lim_{\xi \to 0} \widehat{G}_0(\xi) = \frac{1}{\sqrt{8\pi}} \left(1 + \frac{1}{Z_\infty} + |y_2 - x_2| - (y_2 + x_2) \right), \quad (2.40)$$

being thus $\widehat{G}_0$ bounded and continuous on $\xi = 0$.

For $\xi = Z_\infty$ and $\xi = -Z_\infty$, the function (2.36) presents two simple poles, whose residues are characterized by

$$\lim_{\xi \to \pm Z_\infty} (\xi \mp Z_\infty)\, \widehat{G}_0(\xi) = \mp \frac{1}{\sqrt{2\pi}}\, e^{-Z_\infty (y_2 + x_2)}. \quad (2.41)$$

To analyze the effect of these singularities, we study now the computation of the inverse Fourier transform of

$$\widehat{G}_P(\xi) = \frac{1}{\sqrt{2\pi}}\, e^{-Z_\infty(y_2+x_2)} \left(\frac{1}{\xi + Z_\infty} - \frac{1}{\xi - Z_\infty} \right), \tag{2.42}$$

which has to be done in the frame of the limiting absorption principle to obtain the correct physical results, i.e., the inverse Fourier transform has to be understood in the sense of

$$G_P(\boldsymbol{x}, \boldsymbol{y}) = \lim_{\varepsilon \to 0} \left\{ \frac{1}{2\pi}\, e^{-Z_\varepsilon(y_2+x_2)} \int_{-\infty}^{\infty} \left(\frac{1}{\xi + Z_\varepsilon} - \frac{1}{\xi - Z_\varepsilon} \right) e^{i\xi(y_1-x_1)} \mathrm{d}\xi \right\}. \tag{2.43}$$

To perform correctly the computation of (2.43), we apply the residue theorem of complex analysis (cf., e.g., Arfken & Weber 2005, Bak & Newman 1997, Dettman 1984) on the complex meromorphic mapping

$$F(\xi) = \left(\frac{1}{\xi + \xi_p} - \frac{1}{\xi - \xi_p} \right) e^{i\xi(y_1-x_1)}, \tag{2.44}$$

which admits two simple poles at ξ_p and $-\xi_p$, where $\mathfrak{Im}\{\xi_p\} > 0$. We consider also the closed complex integration contours $C^+_{R,\varepsilon}$ and $C^-_{R,\varepsilon}$, which are associated respectively with the values $(y_1 - x_1) \geq 0$ and $(y_1 - x_1) < 0$, and are depicted in Figure 2.4.

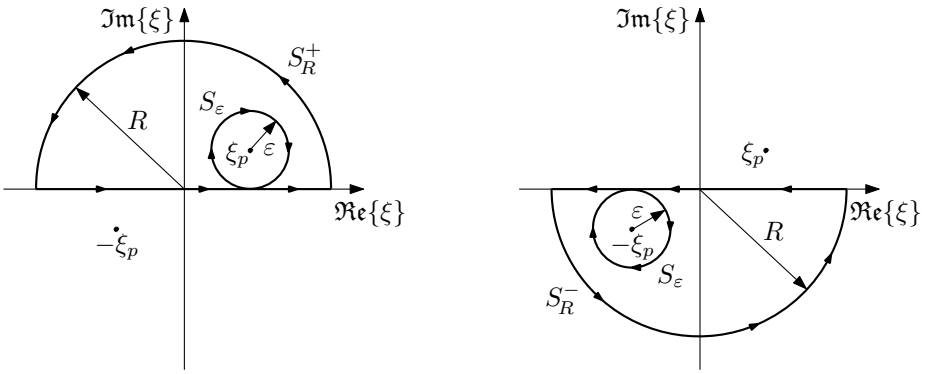

(a) Contour $C^+_{R,\varepsilon}$ (b) Contour $C^-_{R,\varepsilon}$

FIGURE 2.4. Complex integration contours using the limiting absorption principle.

Since the contours $C^+_{R,\varepsilon}$ and $C^-_{R,\varepsilon}$ enclose no singularities, the residue theorem of Cauchy implies that the respective closed path integrals are zero, i.e.,

$$\oint_{C^+_{R,\varepsilon}} F(\xi)\, \mathrm{d}\xi = 0, \tag{2.45}$$

and

$$\oint_{C^-_{R,\varepsilon}} F(\xi)\, \mathrm{d}\xi = 0. \tag{2.46}$$

By considering $(y_1 - x_1) \geq 0$ and working with the contour $C^+_{R,\varepsilon}$ in the upper complex plane, we obtain from (2.45) that

$$\int_{-R}^{\mathfrak{Re}\{\xi_p\}} F(\xi)\,\mathrm{d}\xi + \int_{S_\varepsilon} F(\xi)\,\mathrm{d}\xi + \int_{\mathfrak{Re}\{\xi_p\}}^{R} F(\xi)\,\mathrm{d}\xi + \int_{S_R^+} F(\xi)\,\mathrm{d}\xi = 0. \tag{2.47}$$

Performing the change of variable $\xi - \xi_p = \varepsilon e^{i\phi}$ for the integral on S_ε yields

$$\int_{S_\varepsilon} F(\xi)\,\mathrm{d}\xi = i\, e^{i\xi_p(y_1-x_1)} \int_{3\pi/2}^{-\pi/2} \left(\frac{\varepsilon e^{i\phi}}{\varepsilon e^{i\phi} + 2\xi_p} - 1 \right) e^{\varepsilon(i\cos\phi - \sin\phi)(y_1-x_1)}\,\mathrm{d}\phi. \tag{2.48}$$

By taking then the limit $\varepsilon \to 0$ we obtain

$$\lim_{\varepsilon\to 0} \int_{S_\varepsilon} F(\xi)\,\mathrm{d}\xi = i2\pi e^{i\xi_p(y_1-x_1)}. \tag{2.49}$$

In a similar way, taking $\xi = Re^{i\phi}$ for the integral on S_R^+ yields

$$\int_{S_R^+} F(\xi)\,\mathrm{d}\xi = \int_0^{\pi} \left(\frac{iRe^{i\phi}}{Re^{i\phi} + \xi_p} - \frac{iRe^{i\phi}}{Re^{i\phi} - \xi_p} \right) e^{R(i\cos\phi - \sin\phi)(y_1-x_1)}\,\mathrm{d}\phi. \tag{2.50}$$

Since $|e^{iR\cos\phi(y_1-x_1)}| \leq 1$ and $R\sin\phi \geq 0$ for $0 \leq \phi \leq \pi$, when taking the limit $R \to \infty$ we obtain

$$\lim_{R\to\infty} \int_{S_R^+} F(\xi)\,\mathrm{d}\xi = 0. \tag{2.51}$$

Thus, taking the limits $\varepsilon \to 0$ and $R \to \infty$ in (2.47) yields

$$\int_{-\infty}^{\infty} F(\xi)\,\mathrm{d}\xi = -i2\pi e^{i\xi_p(y_1-x_1)}, \qquad (y_1 - x_1) \geq 0. \tag{2.52}$$

By considering now $(y_1 - x_1) < 0$ and working with the contour $C^-_{R,\varepsilon}$ in the lower complex plane, we obtain from (2.46) that

$$\int_{R}^{\mathfrak{Re}\{-\xi_p\}} F(\xi)\,\mathrm{d}\xi + \int_{S_\varepsilon} F(\xi)\,\mathrm{d}\xi + \int_{\mathfrak{Re}\{-\xi_p\}}^{-R} F(\xi)\,\mathrm{d}\xi + \int_{S_R^-} F(\xi)\,\mathrm{d}\xi = 0. \tag{2.53}$$

Performing the change of variable $\xi + \xi_p = \varepsilon e^{i\phi}$ for the integral on S_ε yields

$$\int_{S_\varepsilon} F(\xi)\,\mathrm{d}\xi = i\, e^{-i\xi_p(y_1-x_1)} \int_{\pi/2}^{-3\pi/2} \left(1 - \frac{\varepsilon e^{i\phi}}{\varepsilon e^{i\phi} - 2\xi_p} \right) e^{\varepsilon(i\cos\phi - \sin\phi)(y_1-x_1)}\,\mathrm{d}\phi. \tag{2.54}$$

By taking then the limit $\varepsilon \to 0$ we obtain

$$\lim_{\varepsilon\to 0} \int_{S_\varepsilon} F(\xi)\,\mathrm{d}\xi = -i2\pi e^{-i\xi_p(y_1-x_1)}. \tag{2.55}$$

In a similar way, taking $\xi = Re^{i\phi}$ for the integral on S_R^- yields

$$\int_{S_R^-} F(\xi)\,\mathrm{d}\xi = \int_{-\pi}^{0} \left(\frac{iRe^{i\phi}}{Re^{i\phi} + \xi_p} - \frac{iRe^{i\phi}}{Re^{i\phi} - \xi_p} \right) e^{R(i\cos\phi - \sin\phi)(y_1-x_1)}\,\mathrm{d}\phi. \tag{2.56}$$

Since $|e^{iR\cos\phi(y_1-x_1)}| \leq 1$ and $R\sin\phi \leq 0$ for $-\pi \leq \phi \leq 0$, when taking the limit $R \to \infty$ we obtain

$$\lim_{R\to\infty} \int_{S_R^-} F(\xi)\,\mathrm{d}\xi = 0. \tag{2.57}$$

Thus, taking the limits $\varepsilon \to 0$ and $R \to \infty$ in (2.53) yields

$$\int_{-\infty}^{\infty} F(\xi)\,\mathrm{d}\xi = -i2\pi e^{-i\xi_p(y_1-x_1)}, \qquad (y_1 - x_1) < 0. \tag{2.58}$$

In conclusion, from (2.52) and (2.58) we obtain that

$$\int_{-\infty}^{\infty} F(\xi)\,\mathrm{d}\xi = -i2\pi e^{i\xi_p|y_1-x_1|}, \qquad (y_1 - x_1) \in \mathbb{R}. \tag{2.59}$$

Using (2.59) for $\xi_p = Z_\infty$ yields then that the inverse Fourier transform of (2.42), when considering the limiting absorption principle, is given by

$$G_P^L(\boldsymbol{x}, \boldsymbol{y}) = -i\, e^{-Z_\infty(y_2+x_2)} e^{iZ_\infty|y_1-x_1|}. \tag{2.60}$$

We observe that this expression describes the asymptotic behavior of the surface waves, which are linked to the presence of the poles in the spectral Green's function.

If the limiting absorption principle is not considered, i.e., if $\mathfrak{Im}\{\xi_p\} = 0$, then the inverse Fourier transform of (2.42) could be computed in the sense of the principal value with the residue theorem by considering, instead of $C_{R,\varepsilon}^+$ and $C_{R,\varepsilon}^-$, the contours depicted in Figure 2.5. In this case we would obtain, instead of (2.59), the quantity

$$\int_{-\infty}^{\infty} F(\xi)\,\mathrm{d}\xi = 2\pi \sin\big(\xi_p|y_1 - x_1|\big), \qquad (y_1 - x_1) \in \mathbb{R}. \tag{2.61}$$

The inverse Fourier transform of (2.42) would be in this case

$$G_P^{NL}(\boldsymbol{x}, \boldsymbol{y}) = e^{-Z_\infty(y_2+x_2)} \sin\big(Z_\infty|y_1 - x_1|\big), \tag{2.62}$$

which is correct from the mathematical point of view, but yields only a standing surface wave, and not a desired outgoing progressive surface wave as in (2.60).

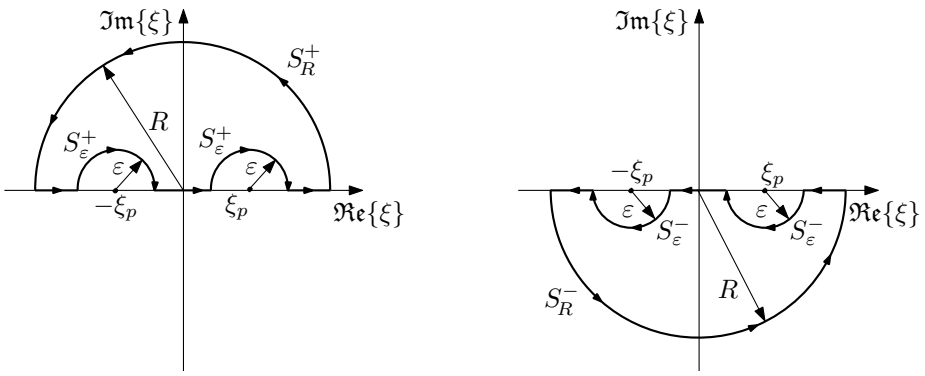

(a) Contour $C_{R,\varepsilon}^+$ (b) Contour $C_{R,\varepsilon}^-$

FIGURE 2.5. Complex integration contours without using the limiting absorption principle.

The effect of the limiting absorption principle, in the spatial dimension, is then given by the difference between (2.60) and (2.62), i.e., by

$$G_L(\boldsymbol{x},\boldsymbol{y}) = G_P^L(\boldsymbol{x},\boldsymbol{y}) - G_P^{NL}(\boldsymbol{x},\boldsymbol{y}) = -i\, e^{-Z_\infty(y_2+x_2)}\cos\big(Z_\infty(y_1-x_1)\big), \tag{2.63}$$

whose Fourier transform, and therefore the spectral effect, is given by

$$\widehat{G}_L(\xi) = \widehat{G}_P^L(\xi) - \widehat{G}_P^{NL}(\xi) = -i\sqrt{\frac{\pi}{2}}\, e^{-Z_\infty(y_2+x_2)}\big[\delta(\xi-Z_\infty)+\delta(\xi+Z_\infty)\big]. \tag{2.64}$$

d) Spectral Green's function without dissipation

The spectral Green's function $\widehat{G}$ without dissipation is therefore obtained by taking the limit $\varepsilon \to 0$ in (2.35) and considering the effect of the limiting absorption principle for the appearing singularities, summarized in (2.64). Thus we obtain in the sense of distributions

$$\begin{aligned}\widehat{G}(\xi;y_2,x_2) = &-\frac{e^{-|\xi||y_2-x_2|}}{\sqrt{8\pi}\,|\xi|} + \left(\frac{Z_\infty+|\xi|}{Z_\infty-|\xi|}\right)\frac{e^{-|\xi|(y_2+x_2)}}{\sqrt{8\pi}\,|\xi|}\\ &- i\sqrt{\frac{\pi}{2}}\, e^{-Z_\infty(y_2+x_2)}\big[\delta(\xi-Z_\infty)+\delta(\xi+Z_\infty)\big].\end{aligned} \tag{2.65}$$

For our further analysis, this spectral Green's function is decomposed into four terms according to

$$\widehat{G} = \widehat{G}_\infty + \widehat{G}_D + \widehat{G}_L + \widehat{G}_R, \tag{2.66}$$

where

$$\widehat{G}_\infty(\xi;y_2,x_2) = -\frac{e^{-|\xi||y_2-x_2|}}{\sqrt{8\pi}\,|\xi|}, \tag{2.67}$$

$$\widehat{G}_D(\xi;y_2,x_2) = \frac{e^{-|\xi|(y_2+x_2)}}{\sqrt{8\pi}\,|\xi|}, \tag{2.68}$$

$$\widehat{G}_L(\xi;y_2,x_2) = -i\sqrt{\frac{\pi}{2}}\, e^{-Z_\infty(y_2+x_2)}\big[\delta(\xi-Z_\infty)+\delta(\xi+Z_\infty)\big], \tag{2.69}$$

$$\widehat{G}_R(\xi;y_2,x_2) = \frac{e^{-|\xi|(y_2+x_2)}}{\sqrt{2\pi}\big(Z_\infty-|\xi|\big)}. \tag{2.70}$$

2.3.4 Spatial Green's function

a) Spatial Green's function as an inverse Fourier transform

The desired spatial Green's function is then given by the inverse Fourier transform of the spectral Green's function (2.65), namely by

$$\begin{aligned}G(\boldsymbol{x},\boldsymbol{y}) = &-\frac{1}{4\pi}\int_{-\infty}^{\infty}\frac{e^{-|\xi||y_2-x_2|}}{|\xi|}\, e^{i\xi(y_1-x_1)}\mathrm{d}\xi\\ &+\frac{1}{4\pi}\int_{-\infty}^{\infty}\left(\frac{Z_\infty+|\xi|}{Z_\infty-|\xi|}\right)\frac{e^{-|\xi|(y_2+x_2)}}{|\xi|}\, e^{i\xi(y_1-x_1)}\mathrm{d}\xi\\ &- i\, e^{-Z_\infty(y_2+x_2)}\cos\big(Z_\infty(y_1-x_1)\big).\end{aligned} \tag{2.71}$$

Due the linearity of the Fourier transform, the decomposition (2.66) applies also in the spatial domain, i.e., the spatial Green's function is decomposed in the same manner by

$$G = G_\infty + G_D + G_L + G_R. \tag{2.72}$$

b) Term of the full-plane Green's function

The first term in (2.71) corresponds to the inverse Fourier transform of (2.67), and can be rewritten as

$$G_\infty(\boldsymbol{x}, \boldsymbol{y}) = -\frac{1}{2\pi} \int_0^\infty \frac{e^{-\xi|y_2 - x_2|}}{\xi} \cos\big(\xi(y_1 - x_1)\big) \mathrm{d}\xi. \tag{2.73}$$

This integral is divergent in the classical sense (cf., e.g. Gradshteyn & Ryzhik 2007, equation 3.941–2) and has to be understood in the sense of homogeneous distributions (cf. Gel'fand & Shilov 1964). It can be computed as the primitive of a well-defined and known integral, e.g., with respect to the y_1-variable, namely

$$\frac{\partial G_\infty}{\partial y_1}(\boldsymbol{x}, \boldsymbol{y}) = \frac{1}{2\pi} \int_0^\infty e^{-\xi|y_2 - x_2|} \sin\big(\xi(y_1 - x_1)\big) \mathrm{d}\xi = \frac{y_1 - x_1}{2\pi|\boldsymbol{y} - \boldsymbol{x}|^2}. \tag{2.74}$$

The primitive of (2.74), and therefore the value of (2.73), is readily given by

$$G_\infty(\boldsymbol{x}, \boldsymbol{y}) = \frac{1}{2\pi} \ln|\boldsymbol{y} - \boldsymbol{x}|, \tag{2.75}$$

where the integration constant is taken as zero to fulfill the outgoing radiation condition. We observe that (2.75) is, in fact, the full-plane Green's function of the Laplace equation. Thus $G_D + G_L + G_R$ represents the perturbation of the full-plane Green's function G_∞ due the presence of the impedance half-plane.

c) Term associated with a Dirichlet boundary condition

The inverse Fourier transform of (2.68) is computed in the same manner as the term G_∞. In this case we consider in the sense of homogeneous distributions

$$G_D(\boldsymbol{x}, \boldsymbol{y}) = \frac{1}{2\pi} \int_0^\infty \frac{e^{-\xi(y_2 + x_2)}}{\xi} \cos\big(\xi(y_1 - x_1)\big) \mathrm{d}\xi, \tag{2.76}$$

which has to be again understood as the primitive of a well-defined integral, e.g., with respect to the y_1-variable, namely

$$\frac{\partial G_D}{\partial y_1}(\boldsymbol{x}, \boldsymbol{y}) = -\frac{1}{2\pi} \int_0^\infty e^{-\xi(y_2 + x_2)} \sin\big(\xi(y_1 - x_1)\big) \mathrm{d}\xi = -\frac{y_1 - x_1}{2\pi|\boldsymbol{y} - \bar{\boldsymbol{x}}|^2}, \tag{2.77}$$

where $\bar{\boldsymbol{x}} = (x_1, -x_2)$ corresponds to the image point of $\boldsymbol{x}$ in the lower half-plane. The primitive of (2.77), and therefore the value of (2.76), is given by

$$G_D(\boldsymbol{x}, \boldsymbol{y}) = -\frac{1}{2\pi} \ln|\boldsymbol{y} - \bar{\boldsymbol{x}}|, \tag{2.78}$$

which represents the additional term that appears in the Green's function due the method of images when considering a Dirichlet boundary condition, as in (2.19).

d) Term associated with the limiting absorption principle

The term G_L, the inverse Fourier transform of (2.69), is associated with the effect of the limiting absorption principle on the Green's function, and has been already calculated in (2.63). It yields the imaginary part of the Green's function, and is given by

$$G_L(\boldsymbol{x},\boldsymbol{y}) = -i\, e^{-Z_\infty(y_2+x_2)} \cos\big(Z_\infty(y_1-x_1)\big). \tag{2.79}$$

e) Remaining term

The remaining term G_R, the inverse Fourier transform of (2.70), can be computed as the integral

$$G_R(\boldsymbol{x},\boldsymbol{y}) = \frac{1}{\pi}\int_0^\infty \frac{e^{-\xi(y_2+x_2)}}{Z_\infty-\xi} \cos\big(\xi(y_1-x_1)\big)\mathrm{d}\xi. \tag{2.80}$$

We consider the change of notation

$$G_R(\boldsymbol{x},\boldsymbol{y}) = \frac{1}{\pi}\, e^{-Z_\infty(y_2+x_2)} G_B(\boldsymbol{x},\boldsymbol{y}), \tag{2.81}$$

where

$$G_B(\boldsymbol{x},\boldsymbol{y}) = \int_0^\infty \frac{e^{(Z_\infty-\xi)(y_2+x_2)}}{Z_\infty-\xi} \cos\big(\xi(y_1-x_1)\big)\mathrm{d}\xi. \tag{2.82}$$

From the derivative of (2.76) and (2.78) with respect to y_2 we obtain the relation

$$\int_0^\infty e^{-\xi(y_2+x_2)} \cos\big(\xi(y_1-x_1)\big)\mathrm{d}\xi = \frac{y_2+x_2}{|\boldsymbol{y}-\bar{\boldsymbol{x}}|^2}. \tag{2.83}$$

Consequently we have for the y_2-derivative of G_B that

$$\begin{aligned}\frac{\partial G_B}{\partial y_2}(\boldsymbol{x},\boldsymbol{y}) &= e^{Z_\infty(y_2+x_2)}\int_0^\infty e^{-\xi(y_2+x_2)} \cos\big(\xi(y_1-x_1)\big)\mathrm{d}\xi \\ &= \frac{y_2+x_2}{|\boldsymbol{y}-\bar{\boldsymbol{x}}|^2}\, e^{Z_\infty(y_2+x_2)}.\end{aligned} \tag{2.84}$$

The value of the inverse Fourier transform (2.80) can be thus obtained by means of the primitive with respect to y_2 of (2.84), i.e.,

$$G_R(\boldsymbol{x},\boldsymbol{y}) = \frac{1}{\pi}\, e^{-Z_\infty(y_2+x_2)} \int_{-\infty}^{y_2+x_2} \frac{\eta\, e^{Z_\infty\eta}}{(y_1-x_1)^2+\eta^2}\,\mathrm{d}\eta. \tag{2.85}$$

An integration by parts (or using the term associated with a Neumann instead of a Dirichlet boundary condition) would yield similar expressions for the Green's function as those derived by Greenberg (1971, page 86) and Dautray & Lions (1987, volume 2, page 745), who adapt the method of Moran (1964) and do not consider the limiting absorption principle.

It is noteworthy that the value of the primitive in (2.85) has an explicit expression. To see this, we start again with the computation by rewriting (2.80) as

$$G_R(\boldsymbol{x},\boldsymbol{y}) = \frac{1}{2\pi}\int_0^\infty \frac{e^{-\xi(y_2+x_2)}}{Z_\infty-\xi}\Big(e^{i\xi(y_1-x_1)} + e^{-i\xi(y_1-x_1)}\Big)\mathrm{d}\xi. \tag{2.86}$$

By performing the change of variable $\eta = \xi - Z_\infty$, and by defining

$$v_1 = y_1 - x_1 \qquad \text{and} \qquad v_2 = y_2 + x_2, \tag{2.87}$$

we obtain

$$G_R(\boldsymbol{x},\boldsymbol{y}) = -\frac{e^{-Z_\infty v_2}}{2\pi}\left(e^{iZ_\infty v_1}\int_{-Z_\infty}^{\infty}\frac{e^{-(v_2-iv_1)\eta}}{\eta}\,\mathrm{d}\eta + e^{-iZ_\infty v_1}\int_{-Z_\infty}^{\infty}\frac{e^{-(v_2+iv_1)\eta}}{\eta}\,\mathrm{d}\eta\right). \quad (2.88)$$

Redefining the integration limits inside the complex plane by replacing respectively in the integrals $\zeta = \eta(v_2 - iv_1)$ and $\zeta = \eta(v_2 + iv_1)$, yields

$$G_R(\boldsymbol{x},\boldsymbol{y}) = -\frac{e^{-Z_\infty v_2}}{2\pi}\left(e^{iZ_\infty v_1}\int_{L^-}\frac{e^{-\zeta}}{\zeta}\,\mathrm{d}\zeta + e^{-iZ_\infty v_1}\int_{L^+}\frac{e^{-\zeta}}{\zeta}\,\mathrm{d}\zeta\right), \quad (2.89)$$

where the integration curves L^- and L^+ are the half-lines depicted in Figure 2.6. We observe that these integrals correspond to the exponential integral function (A.57) with complex arguments. This special function is defined as a Cauchy principal value by

$$\mathrm{Ei}(z) = -\fint_{-z}^{\infty}\frac{e^{-t}}{t}\,\mathrm{d}t = \fint_{-\infty}^{z}\frac{e^{t}}{t}\,\mathrm{d}t \qquad \big(|\arg z| < \pi\big), \quad (2.90)$$

and it can be characterized in the whole complex plane by means of the series expansion

$$\mathrm{Ei}(z) = \gamma + \ln z + \sum_{n=1}^{\infty}\frac{z^n}{n\,n!} \qquad \big(|\arg z| < \pi\big), \quad (2.91)$$

where γ denotes Euler's constant (A.43) and where the principal value of the logarithm is taken. Its derivative is readily given by

$$\frac{\mathrm{d}}{\mathrm{d}z}\,\mathrm{Ei}(z) = \frac{e^z}{z}. \quad (2.92)$$

Further details on the exponential integral function can be found in Subsection A.2.3. Thus the inverse Fourier transform of the remaining term is given by

$$G_R(\boldsymbol{x},\boldsymbol{y}) = \frac{e^{-Z_\infty(y_2+x_2)}}{2\pi}\Big\{e^{iZ_\infty(y_1-x_1)}\,\mathrm{Ei}\Big(Z_\infty\big((y_2+x_2)-i(y_1-x_1)\big)\Big) + e^{-iZ_\infty(y_1-x_1)}\,\mathrm{Ei}\Big(Z_\infty\big((y_2+x_2)+i(y_1-x_1)\big)\Big)\Big\}. \quad (2.93)$$

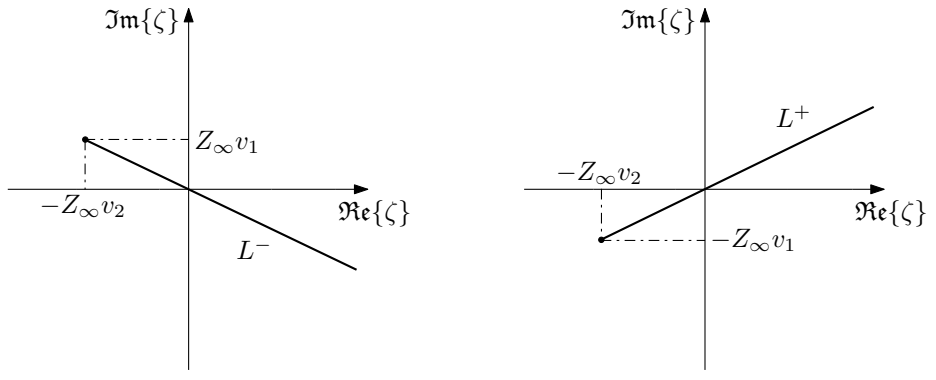

(a) Half-line L^- (b) Half-line L^+

FIGURE 2.6. Complex integration curves for the exponential integral function.

f) Complete spatial Green's function

The desired complete spatial Green's function is finally obtained, as stated in (2.72), by adding the terms (2.75), (2.78), (2.79), and (2.93). It is depicted graphically for $Z_\infty = 1$ and $\boldsymbol{x} = (0, 2)$ in Figures 2.7 & 2.8, and given explicitly by

$$G(\boldsymbol{x},\boldsymbol{y}) = \frac{1}{2\pi}\ln|\boldsymbol{y}-\boldsymbol{x}| - \frac{1}{2\pi}\ln|\boldsymbol{y}-\bar{\boldsymbol{x}}| - i\,e^{-Z_\infty(y_2+x_2)}\cos\big(Z_\infty(y_1-x_1)\big) + \frac{e^{-Z_\infty(y_2+x_2)}}{2\pi}\Big\{e^{iZ_\infty(y_1-x_1)}\,\mathrm{Ei}\Big(Z_\infty\big((y_2+x_2)-i(y_1-x_1)\big)\Big) + e^{-iZ_\infty(y_1-x_1)}\,\mathrm{Ei}\Big(Z_\infty\big((y_2+x_2)+i(y_1-x_1)\big)\Big)\Big\}. \tag{2.94}$$

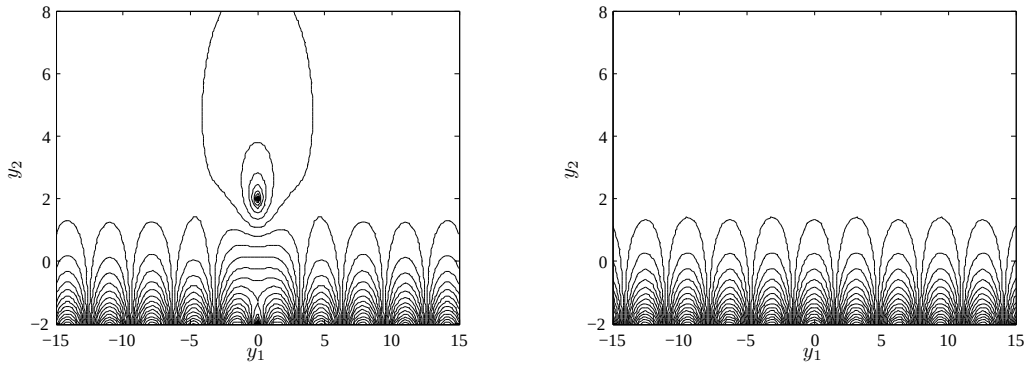

(a) Real part (b) Imaginary part

FIGURE 2.7. Contour plot of the complete spatial Green's function.

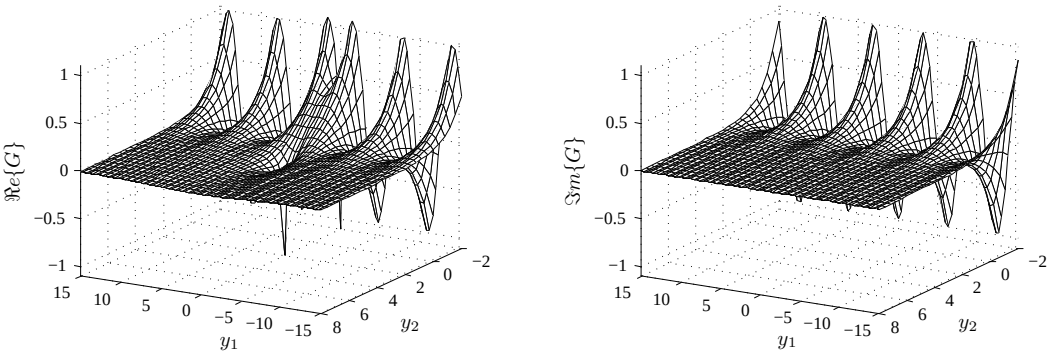

(a) Real part (b) Imaginary part

FIGURE 2.8. Oblique view of the complete spatial Green's function.

By using the notation (2.87), this can be equivalently and more compactly expressed as

$$G(\boldsymbol{x},\boldsymbol{y}) = \frac{1}{2\pi}\ln|\boldsymbol{y}-\boldsymbol{x}| - \frac{1}{2\pi}\ln|\boldsymbol{y}-\bar{\boldsymbol{x}}| - i\,e^{-Z_\infty v_2}\cos(Z_\infty v_1) + \frac{e^{-Z_\infty v_2}}{2\pi}\Big\{e^{iZ_\infty v_1}\,\mathrm{Ei}\big(Z_\infty(v_2-iv_1)\big) + e^{-iZ_\infty v_1}\,\mathrm{Ei}\big(Z_\infty(v_2+iv_1)\big)\Big\}. \quad (2.95)$$

Its gradient can be computed straightforwardly and is given by

$$\nabla_{\boldsymbol{y}} G(\boldsymbol{x},\boldsymbol{y}) = \frac{\boldsymbol{y}-\boldsymbol{x}}{2\pi|\boldsymbol{y}-\boldsymbol{x}|^2} + \frac{\boldsymbol{y}-\bar{\boldsymbol{x}}}{2\pi|\boldsymbol{y}-\bar{\boldsymbol{x}}|^2} + iZ_\infty e^{-Z_\infty v_2}\begin{bmatrix}\sin(Z_\infty v_1)\\ \cos(Z_\infty v_1)\end{bmatrix} - \frac{Z_\infty}{2\pi}e^{-Z_\infty v_2}\Big\{\begin{bmatrix}-i\\1\end{bmatrix}e^{iZ_\infty v_1}\,\mathrm{Ei}\big(Z_\infty(v_2-iv_1)\big) + \begin{bmatrix}i\\1\end{bmatrix}e^{-iZ_\infty v_1}\,\mathrm{Ei}\big(Z_\infty(v_2+iv_1)\big)\Big\}. \quad (2.96)$$

We can likewise define a gradient with respect to the $\boldsymbol{x}$ variable by

$$\nabla_{\boldsymbol{x}} G(\boldsymbol{x},\boldsymbol{y}) = \frac{\boldsymbol{x}-\boldsymbol{y}}{2\pi|\boldsymbol{x}-\boldsymbol{y}|^2} + \frac{\boldsymbol{x}-\bar{\boldsymbol{y}}}{2\pi|\boldsymbol{x}-\bar{\boldsymbol{y}}|^2} + iZ_\infty e^{-Z_\infty v_2}\begin{bmatrix}-\sin(Z_\infty v_1)\\ \cos(Z_\infty v_1)\end{bmatrix} - \frac{Z_\infty}{2\pi}e^{-Z_\infty v_2}\Big\{\begin{bmatrix}-i\\1\end{bmatrix}e^{-iZ_\infty v_1}\,\mathrm{Ei}\big(Z_\infty(v_2+iv_1)\big) + \begin{bmatrix}i\\1\end{bmatrix}e^{iZ_\infty v_1}\,\mathrm{Ei}\big(Z_\infty\big(v_2-iv_1\big)\big)\Big\}, \quad (2.97)$$

and a double-gradient matrix by

$$\begin{aligned}\nabla_{\boldsymbol{x}}\nabla_{\boldsymbol{y}} G(\boldsymbol{x},\boldsymbol{y}) = {}& -\frac{\boldsymbol{I}}{2\pi|\boldsymbol{x}-\boldsymbol{y}|^2} + \frac{(\boldsymbol{x}-\boldsymbol{y})\otimes(\boldsymbol{x}-\boldsymbol{y})}{\pi|\boldsymbol{x}-\boldsymbol{y}|^4} + \frac{(\boldsymbol{x}-\bar{\boldsymbol{y}})\otimes(\bar{\boldsymbol{x}}-\boldsymbol{y})}{\pi|\boldsymbol{x}-\bar{\boldsymbol{y}}|^4} \\ & - \frac{\bar{\boldsymbol{I}}}{2\pi|\boldsymbol{x}-\bar{\boldsymbol{y}}|^2} - iZ_\infty^2 e^{-Z_\infty v_2}\begin{bmatrix}\cos(Z_\infty v_1) & -\sin(Z_\infty v_1)\\ \sin(Z_\infty v_1) & \cos(Z_\infty v_1)\end{bmatrix} \\ & + \frac{Z_\infty^2}{2\pi}e^{-Z_\infty v_2}\Big\{\begin{bmatrix}1 & i\\ -i & 1\end{bmatrix}e^{-iZ_\infty v_1}\,\mathrm{Ei}\big(Z_\infty(v_2+iv_1)\big) \\ & + \begin{bmatrix}1 & -i\\ i & 1\end{bmatrix}e^{iZ_\infty v_1}\,\mathrm{Ei}\big(Z_\infty(v_2-iv_1)\big)\Big\} - \frac{Z_\infty}{\pi|\boldsymbol{x}-\bar{\boldsymbol{y}}|^2}\begin{bmatrix}v_2 & -v_1\\ v_1 & v_2\end{bmatrix}, \quad (2.98)\end{aligned}$$

where $\bar{\boldsymbol{y}} = (y_1, -y_2)$ and $\bar{\boldsymbol{x}} = (x_1, -x_2)$, where $\boldsymbol{I}$ denotes the 2×2 identity matrix and $\bar{\boldsymbol{I}}$ the 2×2 image identity matrix, given by

$$\bar{\boldsymbol{I}} = \begin{bmatrix}1 & 0\\ 0 & -1\end{bmatrix}, \quad (2.99)$$

and where $\otimes$ denotes the dyadic or outer product of two vectors, which results in a matrix and is defined in (A.573).

2.3.5 Extension and properties

The half-plane Green's function can be extended in a locally analytic way towards the full-plane $\mathbb{R}^2$ in a straightforward and natural manner, just by considering the expression (2.94) valid for all $\boldsymbol{x},\boldsymbol{y}\in\mathbb{R}^2$, instead of just for $\mathbb{R}^2_+$. This extension possesses two singularities of logarithmic type at the points $\boldsymbol{x}$ and $\bar{\boldsymbol{x}}$, and is continuous otherwise. The behavior of these singularities is characterized by

$$G(\boldsymbol{x},\boldsymbol{y}) \sim \frac{1}{2\pi}\ln|\boldsymbol{y}-\boldsymbol{x}|, \qquad \boldsymbol{y}\longrightarrow\boldsymbol{x}, \quad (2.100)$$

$$G(\boldsymbol{x},\boldsymbol{y}) \sim \frac{1}{2\pi}\ln|\boldsymbol{y}-\bar{\boldsymbol{x}}|, \qquad \boldsymbol{y} \longrightarrow \bar{\boldsymbol{x}}. \tag{2.101}$$

For the y_1-derivative there appears a jump across the half-line $\Upsilon = \{y_1 = x_1, y_2 < -x_2\}$, due the effect of the analytic branch cut of the exponential integral functions, shown in Figure 2.9. We denote this jump by

$$J(\boldsymbol{x},\boldsymbol{y}) = \lim_{y_1\to x_1^+}\left\{\frac{\partial G}{\partial y_1}\right\} - \lim_{y_1\to x_1^-}\left\{\frac{\partial G}{\partial y_1}\right\} = \left.\frac{\partial G}{\partial y_1^+}\right|_{y_1=x_1} - \left.\frac{\partial G}{\partial y_1^-}\right|_{y_1=x_1}. \tag{2.102}$$

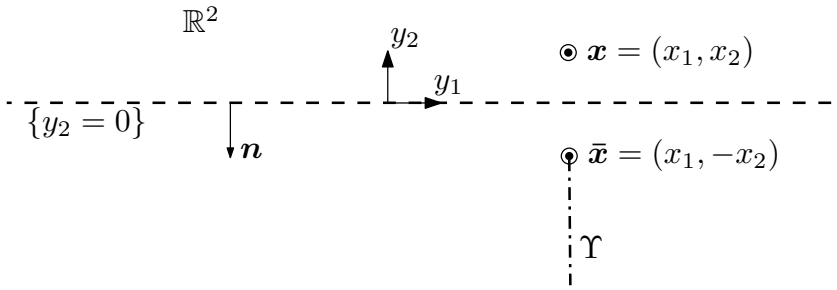

FIGURE 2.9. Domain of the extended Green's function.

Since the singularity of the exponential integral function is of logarithmic type, and since the analytic branch cuts of the logarithms fulfill, due (A.21) and for all $v_2 < 0$,

$$\lim_{\varepsilon\to 0^+}\big\{\ln(v_2+i\varepsilon)-\ln(v_2-i\varepsilon)\big\} - \lim_{\varepsilon\to 0^-}\big\{\ln(v_2+i\varepsilon)-\ln(v_2-i\varepsilon)\big\} = 4\pi i, \tag{2.103}$$

therefore we can easily derive from (2.96) that the jump has a value of

$$J(\boldsymbol{x},\boldsymbol{y}) = 2Z_\infty e^{-Z_\infty(y_2+x_2)}. \tag{2.104}$$

We remark that the Green's function (2.94) itself and its y_2-derivative are continuous across the half-line Υ, since for $v_2 < 0$ the analytic branch cuts cancel out and it holds that

$$\lim_{\varepsilon\to 0^+}\big\{\ln(v_2+i\varepsilon)+\ln(v_2-i\varepsilon)\big\} - \lim_{\varepsilon\to 0^-}\big\{\ln(v_2+i\varepsilon)+\ln(v_2-i\varepsilon)\big\} = 0. \tag{2.105}$$

As long as $x_2 \neq 0$, it is clear that the impedance boundary condition in (2.16) continues to be homogeneous. Nonetheless, if the source point $\boldsymbol{x}$ lies on the half-plane's boundary, i.e., if $x_2 = 0$, then the boundary condition ceases to be homogeneous in the sense of distributions. This can be deduced from the expression (2.71) by verifying that

$$\lim_{y_2\to 0^+}\left\{\frac{\partial G}{\partial y_2}\big((x_1,0),\boldsymbol{y}\big) + Z_\infty G\big((x_1,0),\boldsymbol{y}\big)\right\} = \delta_{x_1}(y_1). \tag{2.106}$$

Since the impedance boundary condition holds only on $\{y_2 = 0\}$, therefore the right-hand side of (2.106) can be also expressed by

$$\delta_{x_1}(y_1) = \frac{1}{2}\delta_{\boldsymbol{x}}(\boldsymbol{y}) + \frac{1}{2}\delta_{\bar{\boldsymbol{x}}}(\boldsymbol{y}), \tag{2.107}$$

which illustrates more clearly the contribution of each logarithmic singularity to the Dirac mass in the boundary condition.

It can be seen now that the Green's function extended in the abovementioned way satisfies, for $\boldsymbol{x} \in \mathbb{R}^2$, in the sense of distributions, and instead of (2.16), the problem

$$\left\{\begin{array}{l} \text{Find } G(\boldsymbol{x},\cdot) : \mathbb{R}^2 \to \mathbb{C} \text{ such that} \\ \Delta_{\boldsymbol{y}} G(\boldsymbol{x},\boldsymbol{y}) = \delta_{\boldsymbol{x}}(\boldsymbol{y}) + \delta_{\bar{\boldsymbol{x}}}(\boldsymbol{y}) + J(\boldsymbol{x},\boldsymbol{y})\delta_{\Upsilon}(\boldsymbol{y}) \qquad \text{in } \mathcal{D}'(\mathbb{R}^2), \\ \dfrac{\partial G}{\partial y_2}(\boldsymbol{x},\boldsymbol{y}) + Z_\infty G(\boldsymbol{x},\boldsymbol{y}) = \dfrac{1}{2}\delta_{\boldsymbol{x}}(\boldsymbol{y}) + \dfrac{1}{2}\delta_{\bar{\boldsymbol{x}}}(\boldsymbol{y}) \qquad \text{on } \{y_2 = 0\}, \\ \text{+ Outgoing radiation condition for } \boldsymbol{y} \in \mathbb{R}^2_+ \text{ as } |\boldsymbol{y}| \to \infty, \end{array}\right. \tag{2.108}$$

where δ_Υ denotes a Dirac mass distribution along the Υ-curve. We retrieve thus the known result that for an impedance boundary condition the image of a point source is a point source plus a half-line of sources with exponentially increasing strengths in the lower half-plane, and which extends from the image point source towards infinity along the half-plane's normal direction (cf. Keller 1979, who refers to decreasing strengths when dealing with the opposite half-plane).

We note that the half-plane Green's function (2.94) is symmetric in the sense that

$$G(\boldsymbol{x},\boldsymbol{y}) = G(\boldsymbol{y},\boldsymbol{x}) \qquad \forall \boldsymbol{x},\boldsymbol{y} \in \mathbb{R}^2, \tag{2.109}$$

and it fulfills similarly

$$\nabla_{\boldsymbol{y}} G(\boldsymbol{x},\boldsymbol{y}) = \nabla_{\boldsymbol{y}} G(\boldsymbol{y},\boldsymbol{x}) \qquad \text{and} \qquad \nabla_{\boldsymbol{x}} G(\boldsymbol{x},\boldsymbol{y}) = \nabla_{\boldsymbol{x}} G(\boldsymbol{y},\boldsymbol{x}). \tag{2.110}$$

Another property is that we retrieve the special case (2.19) of a homogenous Dirichlet boundary condition in $\mathbb{R}^2_+$ when $Z_\infty \to \infty$. Likewise, we retrieve the special case (2.21) of a homogenous Neumann boundary condition in $\mathbb{R}^2_+$ when $Z_\infty \to 0$, except for an additive constant due the extra term (2.79) that can be disregarded.

At last, we observe that the expression for the Green's function (2.94) is still valid if a complex impedance $Z_\infty \in \mathbb{C}$ such that $\mathfrak{Im}\{Z_\infty\} > 0$ and $\mathfrak{Re}\{Z_\infty\} \geq 0$ is used, which holds also for its derivatives (2.96), (2.97), and (2.98). The analytic branch cuts of the logarithms that are contained in the exponential integral functions, though, have to be treated very carefully in this case, since they have to stay on the negative v_2-axis, i.e., on the half-line Υ. A straightforward evaluation of these logarithms with a complex impedance rotates the cuts in the (v_1, v_2)-plane and generates thus two discontinuous half-lines for the Green's function in the half-plane $v_2 < 0$. This undesired behavior of the branch cuts can be avoided if the complex logarithms are taken in the sense of

$$\ln\big(Z_\infty(v_2 - iv_1)\big) = \ln(v_2 - iv_1) + \ln(Z_\infty), \tag{2.111}$$

$$\ln\big(Z_\infty(v_2 + iv_1)\big) = \ln(v_2 + iv_1) + \ln(Z_\infty), \tag{2.112}$$

where the principal value is considered for the logarithms on the right-hand side. For the remaining terms of the Green's function, the complex impedance Z_∞ can be evaluated straightforwardly without any problems.

On the account of performing the numerical evaluation of the exponential integral function for complex arguments, we mention the algorithm developed by Amos (1980, 1990*a*,*b*)

and the software based on the technical report by Morris (1993), taking care with the definition of the analytic branch cuts. Further references are listed in Lozier & Olver (1994).

2.3.6 Complementary Green's function

The complementary Green's function is the Green's function that corresponds to the lower half-plane $\mathbb{R}^2_- = \{(y_1, y_2) \in \mathbb{R}^2 \,|\, y_2 < 0\}$. We denote it by $\widetilde{G}$ and it satisfies, for $\boldsymbol{x} \in \mathbb{R}^2_-$ and instead of (2.16), the problem

$$\left\{\begin{array}{ll} \text{Find } \widetilde{G}(\boldsymbol{x},\cdot) : \mathbb{R}^2_- \to \mathbb{C} \text{ such that} & \\ \Delta_{\boldsymbol{y}} \widetilde{G}(\boldsymbol{x},\boldsymbol{y}) = \delta_{\boldsymbol{x}}(\boldsymbol{y}) & \text{in } \mathcal{D}'(\mathbb{R}^2_-), \\ -\dfrac{\partial \widetilde{G}}{\partial y_2}(\boldsymbol{x},\boldsymbol{y}) + Z_\infty \widetilde{G}(\boldsymbol{x},\boldsymbol{y}) = 0 & \text{on } \{y_2 = 0\}, \\ \text{+ Outgoing radiation condition as } |\boldsymbol{y}| \to \infty. & \end{array}\right. \tag{2.113}$$

The radiation condition, which considers outgoing surface waves and an exponential decrease towards the lower half-plane $\mathbb{R}^2_-$, is given in this case as $|\boldsymbol{y}| \to \infty$ by

$$\left\{\begin{array}{ll} |\widetilde{G}| \le \dfrac{C}{|\boldsymbol{y}|} \quad \text{and} \quad \left|\dfrac{\partial \widetilde{G}}{\partial r_{\boldsymbol{y}}}\right| \le \dfrac{C}{|\boldsymbol{y}|^2} & \text{if } y_2 < -\dfrac{1}{Z_\infty}\ln\big(1 + Z_\infty \pi |\boldsymbol{y}|\big), \\ |\widetilde{G}| \le C \quad \text{and} \quad \left|\dfrac{\partial \widetilde{G}}{\partial r_{\boldsymbol{y}}} - i Z_\infty \widetilde{G}\right| \le \dfrac{C}{|\boldsymbol{y}|} & \text{if } y_2 \ge -\dfrac{1}{Z_\infty}\ln\big(1 + Z_\infty \pi |\boldsymbol{y}|\big), \end{array}\right. \tag{2.114}$$

for some constants $C > 0$, which are independent of $r = |\boldsymbol{y}|$. This Green's function is given explicitly by

$$\begin{aligned} \widetilde{G}(\boldsymbol{x},\boldsymbol{y}) = \frac{1}{2\pi}\ln|\boldsymbol{y}-\boldsymbol{x}| - \frac{1}{2\pi}\ln|\boldsymbol{y}-\bar{\boldsymbol{x}}| - i\, e^{Z_\infty(y_2+x_2)}\cos\big(Z_\infty(y_1-x_1)\big) \\ + \frac{e^{Z_\infty(y_2+x_2)}}{2\pi}\Big\{ e^{iZ_\infty(y_1-x_1)}\,\mathrm{Ei}\Big(Z_\infty\big(-(y_2+x_2) - i(y_1-x_1)\big)\Big) \\ + e^{-iZ_\infty(y_1-x_1)}\,\mathrm{Ei}\Big(Z_\infty\big(-(y_2+x_2) + i(y_1-x_1)\big)\Big)\Big\}. \end{aligned} \tag{2.115}$$

It can be extended towards the full-plane $\mathbb{R}^2$ in the same way as done before, i.e., just by considering the expression (2.115) valid for all $\boldsymbol{x}, \boldsymbol{y} \in \mathbb{R}^2$. Since

$$|\bar{\boldsymbol{y}} - \bar{\boldsymbol{x}}| = |\boldsymbol{y} - \boldsymbol{x}| \qquad \text{and} \qquad |\bar{\boldsymbol{y}} - \boldsymbol{x}| = |\boldsymbol{y} - \bar{\boldsymbol{x}}|, \tag{2.116}$$

therefore the complementary Green's function can be characterized by

$$\widetilde{G}(\boldsymbol{x},\boldsymbol{y}) = G(\bar{\boldsymbol{x}},\bar{\boldsymbol{y}}) \qquad \forall \boldsymbol{x},\boldsymbol{y} \in \mathbb{R}^2. \tag{2.117}$$

The logarithmic singularities are the same as before, i.e., (2.100) and (2.101) continue to be true, but now the y_1-derivative has a jump along the half-line $\widetilde{\Upsilon} = \{y_1 = x_1, y_2 > x_2\}$, which instead of (2.104) adopts a value of

$$\widetilde{J}(\boldsymbol{x},\boldsymbol{y}) = J(\bar{\boldsymbol{x}},\bar{\boldsymbol{y}}) = 2Z_\infty e^{Z_\infty(y_2+x_2)}. \tag{2.118}$$

2.4 Far field of the Green's function

2.4.1 Decomposition of the far field

The far field of the Green's function, which we denote by G^{ff}, describes its asymptotic behavior at infinity, i.e., when $|\boldsymbol{x}| \to \infty$ and assuming that $\boldsymbol{y}$ is fixed. For this purpose, the terms of highest order at infinity are searched. Likewise as done for the radiation condition, the far field can be decomposed into two parts, each acting on a different region as shown in Figure 2.2. The first part, denoted by G_A^{ff}, is linked with the asymptotic decaying condition at infinity observed when dealing with bounded obstacles, and acts in the interior of the half-plane while vanishing near its boundary. The second part, denoted by G_S^{ff}, is associated with surface waves that propagate along the boundary towards infinity, which decay exponentially towards the half-plane's interior. We have thus that

$$G^{ff} = G_A^{ff} + G_S^{ff}. \tag{2.119}$$

2.4.2 Asymptotic decaying

The asymptotic decaying acts only in the interior of the half-plane and is related to the logarithmic terms in (2.94), and also to the asymptotic behavior as $x_2 \to \infty$ of the exponential integral terms. In fact, due (A.81) we have for $z \in \mathbb{C}$ that

$$\mathrm{Ei}(z) \sim \frac{e^z}{z} \qquad \text{as } \ \mathfrak{Re}\{z\} \to \infty. \tag{2.120}$$

By considering the behavior (2.120) in (2.94) and by neglecting the exponentially decreasing terms as $x_2 \to \infty$, we obtain that

$$G(\boldsymbol{x}, \boldsymbol{y}) \sim \frac{1}{2\pi} \ln|\boldsymbol{x} - \boldsymbol{y}| - \frac{1}{2\pi} \ln|\boldsymbol{x} - \bar{\boldsymbol{y}}| + \frac{x_2 + y_2}{Z_\infty \pi |\boldsymbol{x} - \bar{\boldsymbol{y}}|^2}, \tag{2.121}$$

being $\bar{\boldsymbol{y}} = (y_1, -y_2)$. The logarithm can be expanded according to

$$\ln|\boldsymbol{x}-\boldsymbol{y}| = \frac{1}{2}\ln\big(|\boldsymbol{x}|^2\big) + \frac{1}{2}\ln\left(\frac{|\boldsymbol{x}-\boldsymbol{y}|^2}{|\boldsymbol{x}|^2}\right) = \ln|\boldsymbol{x}| + \frac{1}{2}\ln\left(1 - 2\,\frac{\boldsymbol{y}\cdot\boldsymbol{x}}{|\boldsymbol{x}|^2} + \frac{|\boldsymbol{y}|^2}{|\boldsymbol{x}|^2}\right). \tag{2.122}$$

Using a Taylor expansion for the logarithm around one yields

$$\ln|\boldsymbol{x} - \boldsymbol{y}| = \ln|\boldsymbol{x}| - \frac{\boldsymbol{y}\cdot\boldsymbol{x}}{|\boldsymbol{x}|^2} + \mathcal{O}\left(\frac{1}{|\boldsymbol{x}|^2}\right). \tag{2.123}$$

Analogously, since $|\boldsymbol{x}| = |\bar{\boldsymbol{x}}|$, we have that

$$\ln|\boldsymbol{y} - \bar{\boldsymbol{x}}| = \ln|\boldsymbol{x} - \bar{\boldsymbol{y}}| = \ln|\boldsymbol{x}| - \frac{\bar{\boldsymbol{y}}\cdot\boldsymbol{x}}{|\boldsymbol{x}|^2} + \mathcal{O}\left(\frac{1}{|\boldsymbol{x}|^2}\right). \tag{2.124}$$

Therefore it holds for the two logarithmic terms that

$$\frac{1}{2\pi}\ln|\boldsymbol{y} - \boldsymbol{x}| - \frac{1}{2\pi}\ln|\boldsymbol{y} - \bar{\boldsymbol{x}}| = -\frac{(\boldsymbol{y} - \bar{\boldsymbol{y}})\cdot\boldsymbol{x}}{2\pi|\boldsymbol{x}|^2} + \mathcal{O}\left(\frac{1}{|\boldsymbol{x}|^2}\right). \tag{2.125}$$

By using another Taylor expansion, it holds that

$$\frac{1}{|\boldsymbol{x} - \bar{\boldsymbol{y}}|^2} = \frac{1}{|\boldsymbol{x}|^2}\left(1 - 2\,\frac{\boldsymbol{x}\cdot\bar{\boldsymbol{y}}}{|\boldsymbol{x}|^2} + \frac{|\bar{\boldsymbol{y}}|^2}{|\boldsymbol{x}|^2}\right)^{-1} = \frac{1}{|\boldsymbol{x}|^2} + \mathcal{O}\left(\frac{1}{|\boldsymbol{x}|^3}\right), \tag{2.126}$$

and therefore

$$\frac{x_2 + y_2}{Z_\infty \pi |\boldsymbol{x} - \bar{\boldsymbol{y}}|^2} = \frac{x_2}{Z_\infty \pi |\boldsymbol{x}|^2} + \mathcal{O}\left(\frac{1}{|\boldsymbol{x}|^2}\right). \tag{2.127}$$

We express the point $\boldsymbol{x}$ as $\boldsymbol{x} = |\boldsymbol{x}|\,\hat{\boldsymbol{x}}$, being $\hat{\boldsymbol{x}} = (\cos\theta, \sin\theta)$ a unitary vector. Hence, from (2.121) and due (2.125) and (2.127), the asymptotic decaying of the Green's function is given by

$$G_A^{ff}(\boldsymbol{x}, \boldsymbol{y}) = \frac{\sin\theta}{Z_\infty \pi |\boldsymbol{x}|}(1 - Z_\infty y_2). \tag{2.128}$$

Similarly, we have for its gradient with respect to $\boldsymbol{y}$, that

$$\nabla_{\boldsymbol{y}} G_A^{ff}(\boldsymbol{x}, \boldsymbol{y}) = -\frac{\sin\theta}{Z_\infty \pi |\boldsymbol{x}|} \begin{bmatrix} 0 \\ Z_\infty \end{bmatrix}, \tag{2.129}$$

for its gradient with respect to $\boldsymbol{x}$, that

$$\nabla_{\boldsymbol{x}} G_A^{ff}(\boldsymbol{x}, \boldsymbol{y}) = \frac{1 - Z_\infty y_2}{Z_\infty \pi |\boldsymbol{x}|^2} \begin{bmatrix} -\sin(2\theta) \\ \cos(2\theta) \end{bmatrix}, \tag{2.130}$$

and for its double-gradient matrix, that

$$\nabla_{\boldsymbol{x}} \nabla_{\boldsymbol{y}} G_A^{ff}(\boldsymbol{x}, \boldsymbol{y}) = -\frac{1}{\pi |\boldsymbol{x}|^2} \begin{bmatrix} 0 & -\sin(2\theta) \\ 0 & \cos(2\theta) \end{bmatrix}. \tag{2.131}$$

2.4.3 Surface waves in the far field

An expression for the surface waves in the far field can be obtained by studying the residues of the poles of the spectral Green's function, which determine entirely their asymptotic behavior. We already computed the inverse Fourier transform of these residues in (2.60), using the residue theorem of Cauchy and the limiting absorption principle. This implies that the Green's function behaves asymptotically, when $|x_1| \to \infty$, as

$$G(\boldsymbol{x}, \boldsymbol{y}) \sim -i\, e^{-Z_\infty (x_2 + y_2)} e^{i Z_\infty |x_1 - y_1|}. \tag{2.132}$$

Analogous computations for the Helmholtz equation, and more detailed, can be found in Durán, Muga & Nédélec (2005*a*, 2006). Similarly as in (C.36), we can use Taylor expansions to obtain the estimate

$$|x_1 - y_1| = |x_1| - y_1 \operatorname{sign} x_1 + \mathcal{O}\left(\frac{1}{|x_1|}\right). \tag{2.133}$$

Therefore, as for (C.38), we have that

$$e^{i Z_\infty |x_1 - y_1|} = e^{i Z_\infty |x_1|} e^{-i Z_\infty y_1 \operatorname{sign} x_1} \left(1 + \mathcal{O}\left(\frac{1}{|x_1|}\right)\right). \tag{2.134}$$

The surface-wave behavior of the Green's function, due (2.132) and (2.134), becomes thus

$$G_S^{ff}(\boldsymbol{x}, \boldsymbol{y}) = -i\, e^{-Z_\infty x_2} e^{i Z_\infty |x_1|} e^{-Z_\infty y_2} e^{-i Z_\infty y_1 \operatorname{sign} x_1}. \tag{2.135}$$

Similarly, we have for its gradient with respect to $\boldsymbol{y}$, that

$$\nabla_{\boldsymbol{y}} G_S^{ff}(\boldsymbol{x}, \boldsymbol{y}) = -Z_\infty e^{-Z_\infty x_2} e^{i Z_\infty |x_1|} e^{-Z_\infty y_2} e^{-i Z_\infty y_1 \operatorname{sign} x_1} \begin{bmatrix} \operatorname{sign} x_1 \\ -i \end{bmatrix}, \tag{2.136}$$

for its gradient with respect to $\boldsymbol{x}$, that

$$\nabla_{\boldsymbol{x}} G_S^{ff}(\boldsymbol{x},\boldsymbol{y}) = Z_\infty e^{-Z_\infty x_2} e^{iZ_\infty |x_1|} e^{-Z_\infty y_2} e^{-iZ_\infty y_1 \operatorname{sign} x_1} \begin{bmatrix} \operatorname{sign} x_1 \\ i \end{bmatrix}, \tag{2.137}$$

and for its double-gradient matrix, that

$$\nabla_{\boldsymbol{x}} \nabla_{\boldsymbol{y}} G_S^{ff}(\boldsymbol{x},\boldsymbol{y}) = -Z_\infty^2 e^{-Z_\infty x_2} e^{iZ_\infty |x_1|} e^{-Z_\infty y_2} e^{-iZ_\infty y_1 \operatorname{sign} x_1} \begin{bmatrix} i & \operatorname{sign} x_1 \\ -\operatorname{sign} x_1 & i \end{bmatrix}. \tag{2.138}$$

2.4.4 Complete far field of the Green's function

On the whole, the asymptotic behavior of the Green's function as $|\boldsymbol{x}| \to \infty$ can be characterized through the addition of (2.121) and (2.132), namely

$$\begin{aligned} G(\boldsymbol{x},\boldsymbol{y}) \sim \frac{1}{2\pi} \ln|\boldsymbol{x}-\boldsymbol{y}| - \frac{1}{2\pi} \ln|\boldsymbol{x}-\bar{\boldsymbol{y}}| + \frac{x_2+y_2}{Z_\infty \pi |\boldsymbol{x}-\bar{\boldsymbol{y}}|^2} \\ - i\, e^{-Z_\infty (x_2+y_2)} e^{iZ_\infty |x_1-y_1|}. \end{aligned} \tag{2.139}$$

Consequently, the complete far field of the Green's function, due (2.119), is given by the addition of (2.128) and (2.135), i.e., by

$$G^{ff}(\boldsymbol{x},\boldsymbol{y}) = \frac{\sin\theta}{Z_\infty \pi |\boldsymbol{x}|}(1 - Z_\infty y_2) - i\, e^{-Z_\infty x_2} e^{iZ_\infty |x_1|} e^{-Z_\infty y_2} e^{-iZ_\infty y_1 \operatorname{sign} x_1}. \tag{2.140}$$

The expressions for its derivatives can be obtained by considering the corresponding additions of (2.129) and (2.136), of (2.130) and (2.137), and finally of (2.131) and (2.138).

It is this far field (2.140) that justifies the radiation condition (2.17) when exchanging the roles of $\boldsymbol{x}$ and $\boldsymbol{y}$. When the first term in (2.140) dominates, i.e., the asymptotic decaying (2.128), then it is the first expression in (2.17) that matters. Conversely, when the second term in (2.140) dominates, i.e., the surface waves (2.135), then the second expression in (2.17) is the one that holds. The interface between both asymptotic behaviors can be determined by equating the amplitudes of the two terms in (2.140), i.e., by searching values of $\boldsymbol{x}$ at infinity such that

$$\frac{1}{Z_\infty \pi |\boldsymbol{x}|} = e^{-Z_\infty x_2}, \tag{2.141}$$

where the values of $\boldsymbol{y}$ can be neglected, since they remain relatively near the origin. By taking the logarithm in (2.141) and perturbing somewhat the result so as to avoid a singular behavior at the origin, we obtain finally that this interface is described by

$$x_2 = \frac{1}{Z_\infty} \ln\bigl(1 + Z_\infty \pi |\boldsymbol{x}|\bigr). \tag{2.142}$$

We remark that the asymptotic behavior (2.139) of the Green's function and the expression (2.140) of its complete far field do no longer hold if a complex impedance $Z_\infty \in \mathbb{C}$ such that $\mathfrak{Im}\{Z_\infty\} > 0$ and $\mathfrak{Re}\{Z_\infty\} \geq 0$ is used, specifically the parts (2.132) and (2.135) linked with the surface waves. A careful inspection shows that in this case the surface-wave

behavior of the Green's function, as $|x_1| \to \infty$, decreases exponentially and is given by

$$G(\boldsymbol{x},\boldsymbol{y}) \sim \begin{cases} -i\, e^{-|Z_\infty|(x_2+y_2)} e^{iZ_\infty|x_1-y_1|} & \text{if } (x_2+y_2) > 0, \\ -i\, e^{-Z_\infty(x_2+y_2)} e^{iZ_\infty|x_1-y_1|} & \text{if } (x_2+y_2) \leq 0. \end{cases} \tag{2.143}$$

Therefore the surface-wave part of the far field can be now expressed as

$$G_S^{ff}(\boldsymbol{x},\boldsymbol{y}) = \begin{cases} -i\, e^{-|Z_\infty|\, x_2} e^{iZ_\infty|x_1|} e^{-|Z_\infty|\, y_2} e^{-iZ_\infty y_1 \operatorname{sign} x_1} & \text{if } x_2 > 0, \\ -i\, e^{-Z_\infty x_2} e^{iZ_\infty|x_1|} e^{-Z_\infty y_2} e^{-iZ_\infty y_1 \operatorname{sign} x_1} & \text{if } x_2 \leq 0. \end{cases} \tag{2.144}$$

The asymptotic decaying (2.121) and its far-field expression (2.128), on the other hand, remain the same when we use a complex impedance. We remark further that if a complex impedance is taken into account, then the part of the surface waves of the outgoing radiation condition is redundant, and only the asymptotic decaying part is required, i.e., only the first two expressions in (2.17), but now holding for $y_2 > 0$.

2.5 Integral representation and equation

2.5.1 Integral representation

We are interested in expressing the solution u of the direct scattering problem (2.13) by means of an integral representation formula over the perturbed portion of the boundary Γ_p. For this purpose, we extend this solution by zero towards the complementary domain Ω_c, analogously as done in (B.124). We define by $\Omega_{R,\varepsilon}$ the domain Ω_e without the ball B_ε of radius $\varepsilon > 0$ centered at the point $\boldsymbol{x} \in \Omega_e$, and truncated at infinity by the ball B_R of radius $R > 0$ centered at the origin. We consider that the ball B_ε is entirely contained in Ω_e. Therefore, as shown in Figure 2.10, we have that

$$\Omega_{R,\varepsilon} = \big(\Omega_e \cap B_R\big) \setminus \overline{B_\varepsilon}, \tag{2.145}$$

where

$$B_R = \{\boldsymbol{y} \in \mathbb{R}^2 :\, |\boldsymbol{y}| < R\} \qquad \text{and} \qquad B_\varepsilon = \{\boldsymbol{y} \in \Omega_e :\, |\boldsymbol{y}-\boldsymbol{x}| < \varepsilon\}. \tag{2.146}$$

We consider similarly, inside Ω_e, the boundaries of the balls

$$S_R^+ = \{\boldsymbol{y} \in \mathbb{R}^2_+ :\, |\boldsymbol{y}| = R\} \qquad \text{and} \qquad S_\varepsilon = \{\boldsymbol{y} \in \Omega_e :\, |\boldsymbol{y}-\boldsymbol{x}| = \varepsilon\}. \tag{2.147}$$

We separate furthermore the boundary as $\Gamma = \Gamma_0 \cup \Gamma_+$, where

$$\Gamma_0 = \{\boldsymbol{y} \in \Gamma :\, y_2 = 0\} \qquad \text{and} \qquad \Gamma_+ = \{\boldsymbol{y} \in \Gamma :\, y_2 > 0\}. \tag{2.148}$$

The boundary Γ is likewise truncated at infinity by the ball B_R, namely

$$\Gamma_R = \Gamma \cap B_R = \Gamma_0^R \cup \Gamma_+ = \Gamma_\infty^R \cup \Gamma_p, \tag{2.149}$$

where

$$\Gamma_0^R = \Gamma_0 \cap B_R \qquad \text{and} \qquad \Gamma_\infty^R = \Gamma_\infty \cap B_R. \tag{2.150}$$

The idea is to retrieve the domain Ω_e and the boundary Γ at the end when the limits $R \to \infty$ and $\varepsilon \to 0$ are taken for the truncated domain $\Omega_{R,\varepsilon}$ and the truncated boundary Γ_R.

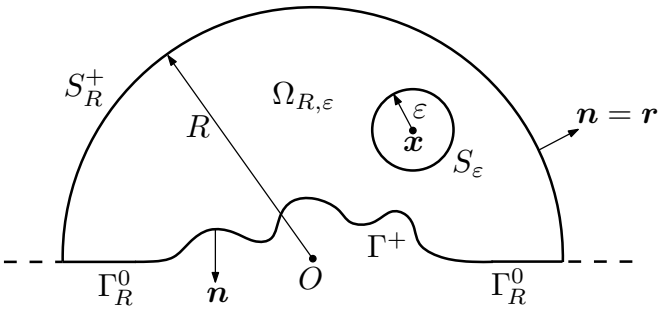

FIGURE 2.10. Truncated domain $\Omega_{R,\varepsilon}$ for $\boldsymbol{x} \in \Omega_e$.

We apply now Green's second integral theorem (A.613) to the functions u and $G(\boldsymbol{x}, \cdot)$ in the bounded domain $\Omega_{R,\varepsilon}$, yielding

$$\begin{aligned} 0 &= \int_{\Omega_{R,\varepsilon}} \big(u(\boldsymbol{y})\Delta_{\boldsymbol{y}} G(\boldsymbol{x},\boldsymbol{y}) - G(\boldsymbol{x},\boldsymbol{y})\Delta u(\boldsymbol{y})\big)\mathrm{d}\boldsymbol{y} \\ &= \int_{S_R^+} \left(u(\boldsymbol{y})\frac{\partial G}{\partial r_{\boldsymbol{y}}}(\boldsymbol{x},\boldsymbol{y}) - G(\boldsymbol{x},\boldsymbol{y})\frac{\partial u}{\partial r}(\boldsymbol{y})\right)\mathrm{d}\gamma(\boldsymbol{y}) \\ &- \int_{S_\varepsilon} \left(u(\boldsymbol{y})\frac{\partial G}{\partial r_{\boldsymbol{y}}}(\boldsymbol{x},\boldsymbol{y}) - G(\boldsymbol{x},\boldsymbol{y})\frac{\partial u}{\partial r}(\boldsymbol{y})\right)\mathrm{d}\gamma(\boldsymbol{y}) \\ &+ \int_{\Gamma_R} \left(u(\boldsymbol{y})\frac{\partial G}{\partial n_{\boldsymbol{y}}}(\boldsymbol{x},\boldsymbol{y}) - G(\boldsymbol{x},\boldsymbol{y})\frac{\partial u}{\partial n}(\boldsymbol{y})\right)\mathrm{d}\gamma(\boldsymbol{y}). \end{aligned} \tag{2.151}$$

The integral on S_R^+ can be rewritten as

$$\begin{aligned} &\int_{S_R^2} \left[u(\boldsymbol{y})\left(\frac{\partial G}{\partial r_{\boldsymbol{y}}}(\boldsymbol{x},\boldsymbol{y}) - iZ_\infty G(\boldsymbol{x},\boldsymbol{y})\right) - G(\boldsymbol{x},\boldsymbol{y})\left(\frac{\partial u}{\partial r}(\boldsymbol{y}) - iZ_\infty u(\boldsymbol{y})\right)\right]\mathrm{d}\gamma(\boldsymbol{y}) \\ &\qquad + \int_{S_R^1} \left(u(\boldsymbol{y})\frac{\partial G}{\partial r_{\boldsymbol{y}}}(\boldsymbol{x},\boldsymbol{y}) - G(\boldsymbol{x},\boldsymbol{y})\frac{\partial u}{\partial r}(\boldsymbol{y})\right)\mathrm{d}\gamma(\boldsymbol{y}), \end{aligned} \tag{2.152}$$

which for R large enough and due the radiation condition (2.6) tends to zero, since

$$\left|\int_{S_R^2} u(\boldsymbol{y})\left(\frac{\partial G}{\partial r_{\boldsymbol{y}}}(\boldsymbol{x},\boldsymbol{y}) - iZ_\infty G(\boldsymbol{x},\boldsymbol{y})\right)\mathrm{d}\gamma(\boldsymbol{y})\right| \leq \frac{C}{R}\ln R, \tag{2.153}$$

$$\left|\int_{S_R^2} G(\boldsymbol{x},\boldsymbol{y})\left(\frac{\partial u}{\partial r}(\boldsymbol{y}) - iZ_\infty u(\boldsymbol{y})\right)\mathrm{d}\gamma(\boldsymbol{y})\right| \leq \frac{C}{R}\ln R, \tag{2.154}$$

and

$$\left|\int_{S_R^1} \left(u(\boldsymbol{y})\frac{\partial G}{\partial r_{\boldsymbol{y}}}(\boldsymbol{x},\boldsymbol{y}) - G(\boldsymbol{x},\boldsymbol{y})\frac{\partial u}{\partial r}(\boldsymbol{y})\right)\mathrm{d}\gamma(\boldsymbol{y})\right| \leq \frac{C}{R^2}, \tag{2.155}$$

for some constants $C > 0$. If the function u is regular enough in the ball B_ε, then the second term of the integral on S_ε in (2.151), when $\varepsilon \to 0$ and due (2.100), is bounded by

$$\left|\int_{S_\varepsilon} G(\boldsymbol{x},\boldsymbol{y})\frac{\partial u}{\partial r}(\boldsymbol{y})\,\mathrm{d}\gamma(\boldsymbol{y})\right| \leq C\varepsilon\ln\varepsilon \sup_{\boldsymbol{y}\in B_\varepsilon}\left|\frac{\partial u}{\partial r}(\boldsymbol{y})\right|, \tag{2.156}$$

for some constant $C > 0$ and tends to zero. The regularity of u can be specified afterwards once the integral representation has been determined and generalized by means of density arguments. The first integral term on S_ε can be decomposed as

$$\int_{S_\varepsilon} u(\boldsymbol{y}) \frac{\partial G}{\partial r_{\boldsymbol{y}}}(\boldsymbol{x},\boldsymbol{y})\,\mathrm{d}\gamma(\boldsymbol{y}) = u(\boldsymbol{x}) \int_{S_\varepsilon} \frac{\partial G}{\partial r_{\boldsymbol{y}}}(\boldsymbol{x},\boldsymbol{y})\,\mathrm{d}\gamma(\boldsymbol{y}) + \int_{S_\varepsilon} \frac{\partial G}{\partial r_{\boldsymbol{y}}}(\boldsymbol{x},\boldsymbol{y})\big(u(\boldsymbol{y}) - u(\boldsymbol{x})\big)\,\mathrm{d}\gamma(\boldsymbol{y}), \tag{2.157}$$

For the first term in the right-hand side of (2.157), by considering (2.100) we have that

$$\int_{S_\varepsilon} \frac{\partial G}{\partial r_{\boldsymbol{y}}}(\boldsymbol{x},\boldsymbol{y})\,\mathrm{d}\gamma(\boldsymbol{y}) \quad \xrightarrow[\varepsilon\to 0]{} \quad 1, \tag{2.158}$$

while the second term is bounded by

$$\left| \int_{S_\varepsilon} \big(u(\boldsymbol{y}) - u(\boldsymbol{x})\big) \frac{\partial G}{\partial r_{\boldsymbol{y}}}(\boldsymbol{x},\boldsymbol{y})\,\mathrm{d}\gamma(\boldsymbol{y}) \right| \leq \sup_{\boldsymbol{y}\in B_\varepsilon} |u(\boldsymbol{y}) - u(\boldsymbol{x})|, \tag{2.159}$$

which tends towards zero when $\varepsilon \to 0$. Finally, due the impedance boundary condition (2.4) and since the support of f_z vanishes on Γ_∞, the term on Γ_R in (2.151) can be decomposed as

$$\int_{\Gamma_p} \left(\frac{\partial G}{\partial n_{\boldsymbol{y}}}(\boldsymbol{x},\boldsymbol{y}) - Z(\boldsymbol{y}) G(\boldsymbol{x},\boldsymbol{y}) \right) u(\boldsymbol{y})\,\mathrm{d}\gamma(\boldsymbol{y}) + \int_{\Gamma_p} G(\boldsymbol{x},\boldsymbol{y}) f_z(\boldsymbol{y})\,\mathrm{d}\gamma(\boldsymbol{y}) - \int_{\Gamma_\infty^R} \left(\frac{\partial G}{\partial y_2}(\boldsymbol{x},\boldsymbol{y}) + Z_\infty G(\boldsymbol{x},\boldsymbol{y}) \right) u(\boldsymbol{y})\,\mathrm{d}\gamma(\boldsymbol{y}), \tag{2.160}$$

where the integral on Γ_∞^R vanishes due the impedance boundary condition in (2.16). Therefore this term does not depend on R and has its support only on the bounded and perturbed portion Γ_p of the boundary.

In conclusion, when the limits $R \to \infty$ and $\varepsilon \to 0$ are taken in (2.151), then we obtain for $\boldsymbol{x} \in \Omega_e$ the integral representation formula

$$u(\boldsymbol{x}) = \int_{\Gamma_p} \left(\frac{\partial G}{\partial n_{\boldsymbol{y}}}(\boldsymbol{x},\boldsymbol{y}) - Z(\boldsymbol{y}) G(\boldsymbol{x},\boldsymbol{y}) \right) u(\boldsymbol{y})\,\mathrm{d}\gamma(\boldsymbol{y}) + \int_{\Gamma_p} G(\boldsymbol{x},\boldsymbol{y}) f_z(\boldsymbol{y})\,\mathrm{d}\gamma(\boldsymbol{y}), \tag{2.161}$$

which can be alternatively expressed as

$$u(\boldsymbol{x}) = \int_{\Gamma_p} \left(u(\boldsymbol{y}) \frac{\partial G}{\partial n_{\boldsymbol{y}}}(\boldsymbol{x},\boldsymbol{y}) - G(\boldsymbol{x},\boldsymbol{y}) \frac{\partial u}{\partial n}(\boldsymbol{y}) \right) \mathrm{d}\gamma(\boldsymbol{y}). \tag{2.162}$$

It is remarkable in this integral representation that the support of the integral, namely the curve Γ_p, is bounded. Let us denote the traces of the solution and of its normal derivative on Γ_p respectively by

$$\mu = u|_{\Gamma_p} \qquad \text{and} \qquad \nu = \left. \frac{\partial u}{\partial n} \right|_{\Gamma_p}. \tag{2.163}$$

We can rewrite now (2.161) and (2.162) in terms of layer potentials as

$$u = \mathcal{D}(\mu) - \mathcal{S}(Z\mu) + \mathcal{S}(f_z) \qquad \text{in } \Omega_e, \tag{2.164}$$

$$u = \mathcal{D}(\mu) - \mathcal{S}(\nu) \qquad \text{in } \Omega_e, \tag{2.165}$$

where we define for $\boldsymbol{x} \in \Omega_e$ respectively the single and double layer potentials as

$$\mathcal{S}\nu(\boldsymbol{x}) = \int_{\Gamma_p} G(\boldsymbol{x}, \boldsymbol{y})\nu(\boldsymbol{y}) \, \mathrm{d}\gamma(\boldsymbol{y}), \tag{2.166}$$

$$\mathcal{D}\mu(\boldsymbol{x}) = \int_{\Gamma_p} \frac{\partial G}{\partial n_{\boldsymbol{y}}}(\boldsymbol{x}, \boldsymbol{y})\mu(\boldsymbol{y}) \, \mathrm{d}\gamma(\boldsymbol{y}). \tag{2.167}$$

We remark that from the impedance boundary condition (2.4) it is clear that

$$\nu = Z\mu - f_z. \tag{2.168}$$

2.5.2 Integral equation

To determine entirely the solution of the direct scattering problem (2.13) by means of its integral representation, we have to find values for the traces (2.163). This requires the development of an integral equation that allows to fix these values by incorporating the boundary data. For this purpose we place the source point $\boldsymbol{x}$ on the boundary Γ, as shown in Figure 2.11, and apply the same procedure as before for the integral representation (2.161), treating differently in (2.151) only the integrals on S_ε. The integrals on S_R^+ still behave well and tend towards zero as $R \to \infty$. The Ball B_ε, though, is split in half by the boundary Γ, and the portion $\Omega_e \cap B_\varepsilon$ is asymptotically separated from its complement in B_ε by the tangent of the boundary if Γ is regular. If $\boldsymbol{x} \in \Gamma_+$, then the associated integrals on S_ε give rise to a term $-u(\boldsymbol{x})/2$ instead of just $-u(\boldsymbol{x})$ as before for the integral representation. Therefore we obtain for $\boldsymbol{x} \in \Gamma_+$ the boundary integral representation

$$\frac{u(\boldsymbol{x})}{2} = \int_{\Gamma_p} \left(\frac{\partial G}{\partial n_{\boldsymbol{y}}}(\boldsymbol{x}, \boldsymbol{y}) - Z(\boldsymbol{y})G(\boldsymbol{x}, \boldsymbol{y}) \right) u(\boldsymbol{y}) \, \mathrm{d}\gamma(\boldsymbol{y}) + \int_{\Gamma_p} G(\boldsymbol{x}, \boldsymbol{y}) f_z(\boldsymbol{y}) \, \mathrm{d}\gamma(\boldsymbol{y}). \tag{2.169}$$

On the contrary, if $\boldsymbol{x} \in \Gamma_0$, then the logarithmic behavior (2.101) contributes also to the singularity (2.100) of the Green's function and the integrals on S_ε give now rise to two terms $-u(\boldsymbol{x})/2$, i.e., on the whole to a term $-u(\boldsymbol{x})$. For $\boldsymbol{x} \in \Gamma_0$ the boundary integral representation is instead given by

$$u(\boldsymbol{x}) = \int_{\Gamma_p} \left(\frac{\partial G}{\partial n_{\boldsymbol{y}}}(\boldsymbol{x}, \boldsymbol{y}) - Z(\boldsymbol{y})G(\boldsymbol{x}, \boldsymbol{y}) \right) u(\boldsymbol{y}) \, \mathrm{d}\gamma(\boldsymbol{y}) + \int_{\Gamma_p} G(\boldsymbol{x}, \boldsymbol{y}) f_z(\boldsymbol{y}) \, \mathrm{d}\gamma(\boldsymbol{y}). \tag{2.170}$$

We must notice that in both cases, the integrands associated with the boundary Γ admit an integrable singularity at the point $\boldsymbol{x}$. In terms of boundary layer potentials, we can express these boundary integral representations as

$$\frac{u}{2} = D(\mu) - S(Z\mu) + S(f_z) \qquad \text{on } \Gamma_+, \tag{2.171}$$

$$u = D(\mu) - S(Z\mu) + S(f_z) \qquad \text{on } \Gamma_0, \tag{2.172}$$

where we consider, for $\boldsymbol{x} \in \Gamma$, the two boundary integral operators

$$S\nu(\boldsymbol{x}) = \int_{\Gamma_p} G(\boldsymbol{x}, \boldsymbol{y})\nu(\boldsymbol{y}) \, \mathrm{d}\gamma(\boldsymbol{y}), \tag{2.173}$$

$$D\mu(\boldsymbol{x}) = \int_{\Gamma_p} \frac{\partial G}{\partial n_{\boldsymbol{y}}}(\boldsymbol{x}, \boldsymbol{y})\mu(\boldsymbol{y}) \, \mathrm{d}\gamma(\boldsymbol{y}). \tag{2.174}$$

We can combine (2.171) and (2.172) into a single integral equation on Γ_p, namely

$$(1+\mathcal{I}_0)\frac{\mu}{2} + S(Z\mu) - D(\mu) = S(f_z) \qquad \text{on } \Gamma_p, \tag{2.175}$$

where $\mathcal{I}_0$ denotes the characteristic or indicator function of the set Γ_0, i.e.,

$$\mathcal{I}_0(\boldsymbol{x}) = \begin{cases} 1 & \text{if } \boldsymbol{x} \in \Gamma_0, \\ 0 & \text{if } \boldsymbol{x} \notin \Gamma_0. \end{cases} \tag{2.176}$$

It is the solution μ on Γ_p of the integral equation (2.175) which finally allows to characterize the solution u in Ω_e of the direct scattering problem (2.13) through the integral representation formula (2.164). The trace of the solution u on the boundary Γ is then found simultaneously by means of the boundary integral representations (2.171) and (2.172). In particular, when $\boldsymbol{x} \in \Gamma_\infty$ and since $\Gamma_\infty \subset \Gamma_0$, therefore it holds that

$$u = D(\mu) - S(Z\mu) + S(f_z) \qquad \text{on } \Gamma_\infty. \tag{2.177}$$

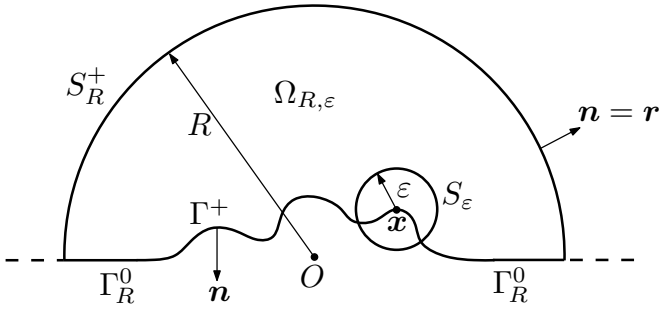

FIGURE 2.11. Truncated domain $\Omega_{R,\varepsilon}$ for $\boldsymbol{x} \in \Gamma$.

2.6 Far field of the solution

The asymptotic behavior at infinity of the solution u of (2.13) is described by the far field. It is denoted by u^{ff} and is characterized by

$$u(\boldsymbol{x}) \sim u^{ff}(\boldsymbol{x}) \qquad \text{as } |\boldsymbol{x}| \to \infty. \tag{2.178}$$

Its expression can be deduced by replacing the far field of the Green's function G^{ff} and its derivatives in the integral representation formula (2.162), which yields

$$u^{ff}(\boldsymbol{x}) = \int_{\Gamma_p} \left(\frac{\partial G^{ff}}{\partial n_{\boldsymbol{y}}}(\boldsymbol{x},\boldsymbol{y})\mu(\boldsymbol{y}) - G^{ff}(\boldsymbol{x},\boldsymbol{y})\nu(\boldsymbol{y}) \right) \mathrm{d}\gamma(\boldsymbol{y}). \tag{2.179}$$

By replacing now (2.140) and the addition of (2.129) and (2.136) in (2.179), we obtain that

$$u^{ff}(\boldsymbol{x}) = -\frac{\sin\theta}{Z_\infty \pi |\boldsymbol{x}|} \int_{\Gamma_p} \left(\begin{bmatrix} 0 \\ Z_\infty \end{bmatrix} \cdot \boldsymbol{n}_{\boldsymbol{y}}\, \mu(\boldsymbol{y}) + (1 - Z_\infty y_2)\nu(\boldsymbol{y}) \right) \mathrm{d}\gamma(\boldsymbol{y})$$
$$- e^{-Z_\infty x_2} e^{iZ_\infty |x_1|} \int_{\Gamma_p} e^{-Z_\infty y_2} e^{-iZ_\infty y_1 \operatorname{sign} x_1} \left(Z_\infty \begin{bmatrix} \operatorname{sign} x_1 \\ -i \end{bmatrix} \cdot \boldsymbol{n}_{\boldsymbol{y}}\, \mu(\boldsymbol{y}) - i\nu(\boldsymbol{y}) \right) \mathrm{d}\gamma(\boldsymbol{y}). \tag{2.180}$$

The asymptotic behavior of the solution u at infinity, as $|\boldsymbol{x}| \to \infty$, is therefore given by

$$u(\boldsymbol{x}) = \frac{1}{|\boldsymbol{x}|}\left\{u_\infty^A(\hat{\boldsymbol{x}}) + \mathcal{O}\left(\frac{1}{|\boldsymbol{x}|}\right)\right\} + e^{-Z_\infty x_2} e^{iZ_\infty |x_1|}\left\{u_\infty^S(\hat{x}_s) + \mathcal{O}\left(\frac{1}{|x_1|}\right)\right\}, \quad (2.181)$$

where $\hat{x}_s = \operatorname{sign} x_1$ and where we decompose $\boldsymbol{x} = |\boldsymbol{x}|\,\hat{\boldsymbol{x}}$, being $\hat{\boldsymbol{x}} = (\cos\theta,\, \sin\theta)$ a vector of the unit circle. The far-field pattern of the asymptotic decaying is given by

$$u_\infty^A(\hat{\boldsymbol{x}}) = -\frac{\sin\theta}{Z_\infty \pi}\int_{\Gamma_p}\left(\begin{bmatrix} 0 \\ Z_\infty \end{bmatrix}\cdot \boldsymbol{n_y}\,\mu(\boldsymbol{y}) + (1 - Z_\infty y_2)\nu(\boldsymbol{y})\right)\mathrm{d}\gamma(\boldsymbol{y}), \quad (2.182)$$

whereas the far-field pattern for the surface waves adopts the form

$$u_\infty^S(\hat{x}_s) = \int_{\Gamma_p} e^{-Z_\infty y_2} e^{-iZ_\infty y_1 \operatorname{sign} x_1}\left(Z_\infty \begin{bmatrix} -\operatorname{sign} x_1 \\ i \end{bmatrix}\cdot \boldsymbol{n_y}\,\mu(\boldsymbol{y}) + i\nu(\boldsymbol{y})\right)\mathrm{d}\gamma(\boldsymbol{y}). \quad (2.183)$$

Both far-field patterns can be expressed in decibels (dB) respectively by means of the scattering cross sections

$$Q_s^A(\hat{\boldsymbol{x}}) \;\; [\mathrm{dB}] = 20\log_{10}\left(\frac{|u_\infty^A(\hat{\boldsymbol{x}})|}{|u_0^A|}\right), \quad (2.184)$$

$$Q_s^S(\hat{x}_s) \;\; [\mathrm{dB}] = 20\log_{10}\left(\frac{|u_\infty^S(\hat{x}_s)|}{|u_0^S|}\right), \quad (2.185)$$

where the reference levels u_0^A and u_0^S are taken such that $|u_0^A| = |u_0^S| = 1$ if the incident field is given by a surface wave of the form (2.15).

We remark that the far-field behavior (2.181) of the solution is in accordance with the radiation condition (2.6), which justifies its choice.

2.7 Existence and uniqueness

2.7.1 Function spaces

To state a precise mathematical formulation of the herein treated problems, we have to define properly the involved function spaces. Since the considered domains and boundaries are unbounded, we need to work with weighted Sobolev spaces, as in Durán, Muga & Nédélec (2005*a*, 2006). We consider the classic weight functions

$$\varrho = \sqrt{1 + r^2} \qquad \text{and} \qquad \log\varrho = \ln(2 + r^2), \quad (2.186)$$

where $r = |\boldsymbol{x}|$. We define the domains

$$\Omega_e^1 = \left\{\boldsymbol{x} \in \Omega_e :\; x_2 > \frac{1}{Z_\infty}\ln(1 + Z_\infty \pi r)\right\}, \quad (2.187)$$

$$\Omega_e^2 = \left\{\boldsymbol{x} \in \Omega_e :\; x_2 < \frac{1}{Z_\infty}\ln(1 + Z_\infty \pi r)\right\}. \quad (2.188)$$

It holds that the solution of the direct scattering problem (2.13) is contained in the weighted Sobolev space

$$W^1(\Omega_e) = \left\{ v : \frac{v}{\varrho \log \varrho} \in L^2(\Omega_e),\ \nabla v \in L^2(\Omega_e)^2,\ \frac{v}{\sqrt{\varrho}} \in L^2(\Omega_e^1),\ \frac{\partial v}{\partial r} \in L^2(\Omega_e^1), \right.$$
$$\left. \frac{v}{\log \varrho} \in L^2(\Omega_e^2),\ \frac{1}{\log \varrho}\left(\frac{\partial v}{\partial r} - iZ_\infty v\right) \in L^2(\Omega_e^2) \right\}. \tag{2.189}$$

With the appropriate norm, the space $W^1(\Omega_e)$ becomes also a Hilbert space. We have likewise the inclusion $W^1(\Omega_e) \subset H^1_{\text{loc}}(\Omega_e)$, i.e., the functions of these two spaces differ only by their behavior at infinity.

Since we are dealing with Sobolev spaces, even a strong Lipschitz boundary $\Gamma \in C^{0,1}$ is admissible. The fact that this boundary Γ is also unbounded implies that we have to use weighted trace spaces like in Amrouche (2002). For this purpose, we consider the space

$$W^{1/2}(\Gamma) = \left\{ v :\ \frac{v}{\sqrt{\varrho}\log \varrho} \in H^{1/2}(\Gamma) \right\}. \tag{2.190}$$

Its dual space $W^{-1/2}(\Gamma)$ is defined via W^0-duality, i.e., considering the pivot space

$$W^0(\Gamma) = \left\{ v :\ \frac{v}{\sqrt{\varrho}\log \varrho} \in L^2(\Gamma) \right\}. \tag{2.191}$$

Analogously as for the trace theorem (A.531), if $v \in W^1(\Omega_e)$ then the trace of v fulfills

$$\gamma_0 v = v|_\Gamma \in W^{1/2}(\Gamma). \tag{2.192}$$

Moreover, the trace of the normal derivative can be also defined, and it holds that

$$\gamma_1 v = \frac{\partial v}{\partial n}|_\Gamma \in W^{-1/2}(\Gamma). \tag{2.193}$$

We remark further that the restriction of the trace of v to Γ_p is such that

$$\gamma_0 v|_{\Gamma_p} = v|_{\Gamma_p} \in H^{1/2}(\Gamma_p), \tag{2.194}$$

$$\gamma_1 v|_{\Gamma_p} = \frac{\partial v}{\partial n}|_{\Gamma_p} \in H^{-1/2}(\Gamma_p), \tag{2.195}$$

and its restriction to Γ_∞ yields

$$\gamma_0 v|_{\Gamma_\infty} = v|_{\Gamma_\infty} \in W^{1/2}(\Gamma_\infty), \tag{2.196}$$

$$\gamma_1 v|_{\Gamma_\infty} = \frac{\partial v}{\partial n}|_{\Gamma_\infty} \in W^{-1/2}(\Gamma_\infty). \tag{2.197}$$

2.7.2 Application to the integral equation

The existence and uniqueness of the solution for the direct scattering problem (2.13), due the integral representation formula (2.164), can be characterized by using the integral equation (2.175). For this purpose and in accordance with the considered function spaces, we take $\mu \in H^{1/2}(\Gamma_p)$ and $\nu \in H^{-1/2}(\Gamma_p)$. Furthermore, we consider that $Z \in L^\infty(\Gamma_p)$ and that $f_z \in H^{-1/2}(\Gamma_p)$, even though strictly speaking $f_z \in \widetilde{H}^{-1/2}(\Gamma_p)$.

It holds that the single and double layer potentials defined respectively in (2.166) and (2.167) are linear and continuous integral operators such that

$$\mathcal{S} : H^{-1/2}(\Gamma_p) \longrightarrow W^1(\Omega_e) \qquad \text{and} \qquad \mathcal{D} : H^{1/2}(\Gamma_p) \longrightarrow W^1(\Omega_e). \tag{2.198}$$

The boundary integral operators (2.173) and (2.174) are also linear and continuous applications, and they are such that

$$S : H^{-1/2}(\Gamma_p) \longrightarrow W^{1/2}(\Gamma) \qquad \text{and} \qquad D : H^{1/2}(\Gamma_p) \longrightarrow W^{1/2}(\Gamma). \tag{2.199}$$

When we restrict them to Γ_p, then it holds that

$$S|_{\Gamma_p} : H^{-1/2}(\Gamma_p) \longrightarrow H^{1/2}(\Gamma_p) \qquad \text{and} \qquad D|_{\Gamma_p} : H^{1/2}(\Gamma_p) \longrightarrow H^{1/2}(\Gamma_p). \tag{2.200}$$

Let us now study the integral equation (2.175), which is given in terms of boundary layer potentials, for $\mu \in H^{1/2}(\Gamma_p)$, by

$$(1 + \mathcal{I}_0)\frac{\mu}{2} + S(Z\mu) - D(\mu) = S(f_z) \qquad \text{in } H^{1/2}(\Gamma_p). \tag{2.201}$$

We have the following mapping properties

$$\mu \in H^{1/2}(\Gamma_p) \;\longmapsto\; (1 + \mathcal{I}_0)\frac{\mu}{2} \in H^{1/2}(\Gamma_p), \tag{2.202}$$

$$Z\mu \in L^2(\Gamma_p) \;\longmapsto\; S(Z\mu) \in H^1(\Gamma_p) \overset{c}{\hookrightarrow} H^{1/2}(\Gamma_p), \tag{2.203}$$

$$\mu \in H^{1/2}(\Gamma_p) \;\longmapsto\; D(\mu) \in H^{3/2}(\Gamma_p) \overset{c}{\hookrightarrow} H^{1/2}(\Gamma_p), \tag{2.204}$$

$$f_z \in H^{-1/2}(\Gamma_p) \;\longmapsto\; S(f_z) \in H^{1/2}(\Gamma_p). \tag{2.205}$$

We observe that (2.202) is like the identity operator, and that (2.203) and (2.204) are compact, due the imbeddings of Sobolev spaces. Thus the integral equation (2.201) has the form of (A.441) and the Fredholm alternative holds.

Since the Fredholm alternative applies to the integral equation, therefore it applies also to the direct scattering problem (2.13) due the integral representation formula. The existence of the scattering problem's solution is thus determined by its uniqueness, and the values for the impedance $Z \in \mathbb{C}$ for which the uniqueness is lost constitute a countable set, which we call the impedance spectrum of the scattering problem and denote it by σ_Z. The existence and uniqueness of the solution is therefore ensured almost everywhere. The same holds obviously for the solution of the integral equation, whose impedance spectrum we denote by ς_Z. Since the integral equation is derived from the scattering problem, it holds that $\sigma_Z \subset \varsigma_Z$. The converse, though, is not necessarily true. In any way, the set $\varsigma_Z \setminus \sigma_Z$ is at most countable. In conclusion, the scattering problem (2.13) admits a unique solution u if $Z \notin \sigma_Z$, and the integral equation (2.175) admits a unique solution μ if $Z \notin \varsigma_Z$.

2.8 Dissipative problem

The dissipative problem considers surface waves that lose their amplitude as they travel along the half-plane's boundary. These waves dissipate their energy as they propagate and

are modeled by a complex impedance $Z_\infty \in \mathbb{C}$ whose imaginary part is strictly positive, i.e., $\mathfrak{Im}\{Z_\infty\} > 0$. This choice ensures that the surface waves of the Green's function (2.94) decrease exponentially at infinity. Due the dissipative nature of the medium, it is no longer suited to take progressive plane surface waves in the form of (2.15) as the incident field u_I. Instead, we have to take a source of surface waves at a finite distance from the perturbation. For example, we can consider a point source located at $\boldsymbol{z} \in \Omega_e$, in which case the incident field is given, up to a multiplicative constant, by

$$u_I(\boldsymbol{x}) = G(\boldsymbol{x}, \boldsymbol{z}), \tag{2.206}$$

where G denotes the Green's function (2.94). This incident field u_I satisfies the Laplace equation with a source term in the right-hand side, namely

$$\Delta u_I = \delta_{\boldsymbol{z}} \qquad \text{in } \mathcal{D}'(\Omega_e), \tag{2.207}$$

which holds also for the total field u_T but not for the scattered field u, in which case the Laplace equation remains homogeneous. For a general source distribution g_s, whose support is contained in Ω_e, the incident field can be expressed by

$$u_I(\boldsymbol{x}) = G(\boldsymbol{x}, \boldsymbol{z}) * g_s(\boldsymbol{z}) = \int_{\Omega_e} G(\boldsymbol{x}, \boldsymbol{z})\, g_s(\boldsymbol{z})\, \mathrm{d}\boldsymbol{z}. \tag{2.208}$$

This incident field u_I satisfies now

$$\Delta u_I = g_s \qquad \text{in } \mathcal{D}'(\Omega_e), \tag{2.209}$$

which holds again also for the total field u_T but not for the scattered field u.

It is not difficult to see that all the performed developments for the non-dissipative case are still valid when considering dissipation. The only difference is that now a complex impedance Z_∞ such that $\mathfrak{Im}\{Z_\infty\} > 0$ has to be taken everywhere into account.

2.9 Variational formulation

To solve the integral equation we convert it to its variational or weak formulation, i.e., we solve it with respect to a certain test function in a bilinear (or sesquilinear) form. Basically, the integral equation is multiplied by the (conjugated) test function and then the equation is integrated over the boundary of the domain. The test function is taken in the same function space as the solution of the integral equation.

The variational formulation for the integral equation (2.201) searches $\mu \in H^{1/2}(\Gamma_p)$ such that $\forall \varphi \in H^{1/2}(\Gamma_p)$ we have that

$$\left\langle (1 + \mathcal{I}_0)\frac{\mu}{2} + S(Z\mu) - D(\mu), \varphi \right\rangle = \left\langle S(f_z), \varphi \right\rangle. \tag{2.210}$$

2.10 Numerical discretization

2.10.1 Discretized function space

The scattering problem (2.13) is solved numerically with the boundary element method by employing a Galerkin scheme on the variational formulation of the integral equation. We

use on the boundary curve Γ_p Lagrange finite elements of type $\mathbb{P}_1$. As shown in Figure 2.12, the curve Γ_p is approximated by the discretized curve Γ_p^h, composed by I rectilinear segments T_j, sequentially ordered from left to right for $1 \leq j \leq I$, such that their length $|T_j|$ is less or equal than h, and with their endpoints on top of Γ_p.

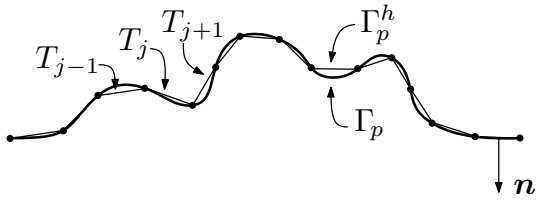

FIGURE 2.12. Curve Γ_p^h, discretization of Γ_p.

The function space $H^{1/2}(\Gamma_p)$ is approximated using the conformal space of continuous piecewise linear polynomials with complex coefficients

$$Q_h = \big\{\varphi_h \in C^0(\Gamma_p^h) \,:\, \varphi_h|_{T_j} \in \mathbb{P}_1(\mathbb{C}),\;\; 1 \leq j \leq I\big\}. \tag{2.211}$$

The space Q_h has a finite dimension $(I+1)$, and we describe it using the standard base functions for finite elements of type $\mathbb{P}_1$, denoted by $\{\chi_j\}_{j=1}^{I+1}$ and expressed as

$$\chi_j(\boldsymbol{x}) = \begin{cases} \dfrac{|\boldsymbol{x} - \boldsymbol{r}_{j-1}|}{|T_{j-1}|} & \text{if } \;\boldsymbol{x} \in T_{j-1}, \\ \dfrac{|\boldsymbol{r}_{j+1} - \boldsymbol{x}|}{|T_j|} & \text{if } \;\boldsymbol{x} \in T_j, \\ 0 & \text{if } \;\boldsymbol{x} \notin T_{j-1} \cup T_j, \end{cases} \tag{2.212}$$

where segment T_{j-1} has as endpoints $\boldsymbol{r}_{j-1}$ and $\boldsymbol{r}_j$, while the endpoints of segment T_j are given by $\boldsymbol{r}_j$ and $\boldsymbol{r}_{j+1}$.

In virtue of this discretization, any function $\varphi_h \in Q_h$ can be expressed as a linear combination of the elements of the base, namely

$$\varphi_h(\boldsymbol{x}) = \sum_{j=1}^{I+1} \varphi_j\, \chi_j(\boldsymbol{x}) \qquad \text{for } \;\boldsymbol{x} \in \Gamma_p^h, \tag{2.213}$$

where $\varphi_j \in \mathbb{C}$ for $1 \leq j \leq I+1$. The solution $\mu \in H^{1/2}(\Gamma_p)$ of the variational formulation (2.210) can be therefore approximated by

$$\mu_h(\boldsymbol{x}) = \sum_{j=1}^{I+1} \mu_j\, \chi_j(\boldsymbol{x}) \qquad \text{for } \;\boldsymbol{x} \in \Gamma_p^h, \tag{2.214}$$

where $\mu_j \in \mathbb{C}$ for $1 \leq j \leq I+1$. The function f_z can be also approximated by

$$f_z^h(\boldsymbol{x}) = \sum_{j=1}^{I+1} f_j\, \chi_j(\boldsymbol{x}) \qquad \text{for } \;\boldsymbol{x} \in \Gamma_p^h, \quad \text{with } \;f_j = f_z(\boldsymbol{r}_j). \tag{2.215}$$

2.10.2 Discretized integral equation

To see how the boundary element method operates, we apply it to the variational formulation (2.210). We characterize all the discrete approximations by the index h, including also the impedance and the boundary layer potentials. The numerical approximation of (2.210) leads to the discretized problem that searches $\mu_h \in Q_h$ such that $\forall \varphi_h \in Q_h$

$$\left\langle (1+\mathcal{I}_0^h)\frac{\mu_h}{2} + S_h(Z_h\mu_h) - D_h(\mu_h), \varphi_h \right\rangle = \left\langle S_h(f_z^h), \varphi_h \right\rangle. \tag{2.216}$$

Considering the decomposition of μ_h in terms of the base $\{\chi_j\}$ and taking as test functions the same base functions, $\varphi_h = \chi_i$ for $1 \leq i \leq I+1$, yields the discrete linear system

$$\sum_{j=1}^{I+1} \mu_j \left(\frac{1}{2}\left\langle (1+\mathcal{I}_0^h)\chi_j, \chi_i \right\rangle + \langle S_h(Z_h\chi_j), \chi_i\rangle - \langle D_h(\chi_j), \chi_i\rangle \right) = \sum_{j=1}^{I+1} f_j \langle S_h(\chi_j), \chi_i\rangle. \tag{2.217}$$

This constitutes a system of linear equations that can be expressed as a linear matrix system:

$$\begin{cases} \text{Find } \boldsymbol{\mu} \in \mathbb{C}^{I+1} \text{ such that} \\ \boldsymbol{M}\boldsymbol{\mu} = \boldsymbol{b}. \end{cases} \tag{2.218}$$

The elements m_{ij} of the matrix $\boldsymbol{M}$ are given, for $1 \leq i, j \leq I+1$, by

$$m_{ij} = \frac{1}{2}\left\langle (1+\mathcal{I}_0^h)\chi_j, \chi_i \right\rangle + \langle S_h(Z_h\chi_j), \chi_i\rangle - \langle D_h(\chi_j), \chi_i\rangle, \tag{2.219}$$

and the elements b_i of the vector $\boldsymbol{b}$ by

$$b_i = \left\langle S_h(f_z^h), \chi_i \right\rangle = \sum_{j=1}^{I+1} f_j \langle S_h(\chi_j), \chi_i\rangle \qquad \text{for } \ 1 \leq i \leq I+1. \tag{2.220}$$

The discretized solution u_h, which approximates u, is finally obtained by discretizing the integral representation formula (2.164) according to

$$u_h = \mathcal{D}_h(\mu_h) - \mathcal{S}_h(Z_h\mu_h) + \mathcal{S}_h(f_z^h), \tag{2.221}$$

which, more specifically, can be expressed as

$$u_h = \sum_{j=1}^{I+1} \mu_j \big(\mathcal{D}_h(\chi_j) - \mathcal{S}_h(Z_h\chi_j)\big) + \sum_{j=1}^{I+1} f_j\, \mathcal{S}_h(\chi_j). \tag{2.222}$$

We remark that the resulting matrix $\boldsymbol{M}$ is in general complex, full, non-symmetric, and with dimensions $(I+1) \times (I+1)$. The right-hand side vector $\boldsymbol{b}$ is complex and of size $I+1$. The boundary element calculations required to compute numerically the elements of $\boldsymbol{M}$ and $\boldsymbol{b}$ have to be performed carefully, since the integrals that appear become singular when the involved segments are adjacent or coincident, due the singularity of the Green's function at its source point. On Γ_0, the singularity of the image source point has to be taken additionally into account for these calculations.

2.11 Boundary element calculations

The boundary element calculations build the elements of the matrix $\boldsymbol{M}$ resulting from the discretization of the integral equation, i.e., from (2.218). They permit thus to compute numerically expressions like (2.219). To evaluate the appearing singular integrals, we adapt the semi-numerical methods described in the report of Bendali & Devys (1986).

We use the same notation as in Section B.12, and the required boundary element integrals, for $a, b \in \{0, 1\}$, are again

$$ZA_{a,b} = \int_K \int_L \left(\frac{s}{|K|}\right)^a \left(\frac{t}{|L|}\right)^b G(\boldsymbol{x}, \boldsymbol{y}) \, \mathrm{d}L(\boldsymbol{y}) \, \mathrm{d}K(\boldsymbol{x}), \tag{2.223}$$

$$ZB_{a,b} = \int_K \int_L \left(\frac{s}{|K|}\right)^a \left(\frac{t}{|L|}\right)^b \frac{\partial G}{\partial n_{\boldsymbol{y}}}(\boldsymbol{x}, \boldsymbol{y}) \, \mathrm{d}L(\boldsymbol{y}) \, \mathrm{d}K(\boldsymbol{x}). \tag{2.224}$$

All the integrals that stem from the numerical discretization can be expressed in terms of these two basic boundary element integrals. The impedance is again discretized as a piecewise constant function Z_h, which on each segment T_j adopts a constant value $Z_j \in \mathbb{C}$. The integrals of interest are the same as for the full-plane impedance Laplace problem and we consider furthermore that

$$\left\langle (1 + \mathcal{I}_0^h)\chi_j, \chi_i \right\rangle = \begin{cases} \langle \chi_j, \chi_i \rangle & \text{if } \boldsymbol{r}_j \in \Gamma_+, \\ 2 \langle \chi_j, \chi_i \rangle & \text{if } \boldsymbol{r}_j \in \Gamma_0. \end{cases} \tag{2.225}$$

To compute the boundary element integrals (2.223) and (2.224), we can easily isolate the singular part (2.100) of the Green's function (2.94), which corresponds in fact to the Green's function of the Laplace equation in the full-plane, and therefore the associated integrals are computed in the same way. The same applies also for its normal derivative. In the case when the segments K and L are are close enough, e.g., adjacent or coincident, and when $L \in \Gamma_0^h$ or $K \in \Gamma_0^h$, being Γ_0^h the approximation of Γ_0, we have to consider additionally the singular behavior (2.101), which is linked with the presence of the impedance half-plane. This behavior can be straightforwardly evaluated by replacing $\boldsymbol{x}$ by $\bar{\boldsymbol{x}}$ in formulae (B.340) to (B.343), i.e., by computing the quantities $ZF_b(\bar{\boldsymbol{x}})$ and $ZG_b(\bar{\boldsymbol{x}})$ with the corresponding adjustment of the notation. Otherwise, if the segments are not close enough and for the non-singular part of the Green's function, a two-point Gauss quadrature formula is used. All the other computations are performed in the same manner as in Section B.12 for the full-plane Laplace equation.

2.12 Benchmark problem

As benchmark problem we consider the particular case when the domain $\Omega_e \subset \mathbb{R}^2_+$ is taken as the exterior of a half-circle of radius $R > 0$ that is centered at the origin, as shown in Figure 2.13. We decompose the boundary of Ω_e as $\Gamma = \Gamma_p \cup \Gamma_\infty$, where Γ_p corresponds

to the upper half-circle, whereas Γ_∞ denotes the remaining unperturbed portion of the half-plane's boundary which lies outside the half-circle and which extends towards infinity on both sides. The unit normal $\boldsymbol{n}$ is taken outwardly oriented of Ω_e, e.g., $\boldsymbol{n} = -\boldsymbol{r}$ on Γ_p.

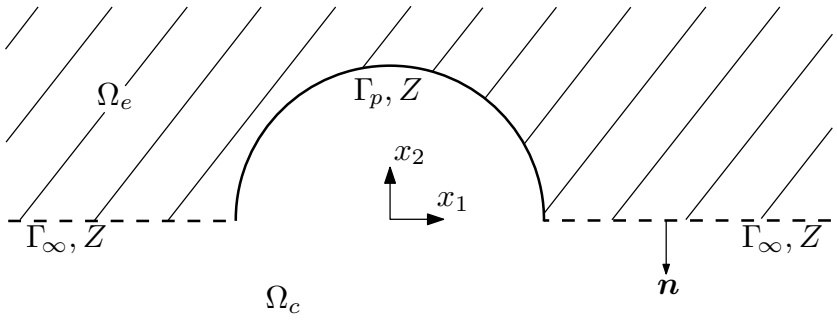

FIGURE 2.13. Exterior of the half-circle.

The benchmark problem is then stated as

$$\begin{cases} \text{Find } u : \Omega_e \to \mathbb{C} \text{ such that} \\ \Delta u = 0 \qquad\qquad \text{in } \Omega_e, \\ -\dfrac{\partial u}{\partial n} + Zu = f_z \qquad \text{on } \Gamma, \\ \text{+ Outgoing radiation condition as } |\boldsymbol{x}| \to \infty, \end{cases} \tag{2.226}$$

where we consider a constant impedance $Z \in \mathbb{C}$ throughout Γ and where the radiation condition is as usual given by (2.6). As incident field u_I we consider the same Green's function, namely

$$u_I(\boldsymbol{x}) = G(\boldsymbol{x}, \boldsymbol{z}), \tag{2.227}$$

where $\boldsymbol{z} \in \Omega_c$ denotes the source point of our incident field. The impedance data function f_z is hence given by

$$f_z(\boldsymbol{x}) = \frac{\partial G}{\partial n_{\boldsymbol{x}}}(\boldsymbol{x}, \boldsymbol{z}) - ZG(\boldsymbol{x}, \boldsymbol{z}), \tag{2.228}$$

and its support is contained in Γ_p. The analytic solution for the benchmark problem (2.226) is then clearly given by

$$u(\boldsymbol{x}) = -G(\boldsymbol{x}, \boldsymbol{z}). \tag{2.229}$$

The goal is to retrieve this solution numerically with the integral equation techniques and the boundary element method described throughout this chapter.

For the computational implementation and the numerical resolution of the benchmark problem, we consider integral equation (2.175). The linear system (2.218) resulting from the discretization (2.216) of its variational formulation (2.210) is solved computationally with finite boundary elements of type $\mathbb{P}_1$ by using subroutines programmed in Fortran 90, by generating the mesh Γ_p^h of the boundary with the free software Gmsh 2.4, and by representing graphically the results in Matlab 7.5 (R2007b).

We consider a radius $R = 1$, a constant impedance $Z = 5$, and for the incident field a source point $\boldsymbol{z} = (0, 0)$. The discretized perturbed boundary curve Γ_p^h has $I = 120$ segments and a discretization step $h = 0.02618$, being

$$h = \max_{1 \leq j \leq I} |T_j|. \tag{2.230}$$

We observe that $h \approx \pi / I$.

The numerically calculated trace of the solution μ_h of the benchmark problem, which was computed by using the boundary element method, is depicted in Figure 2.14. In the same manner, the numerical solution u_h is illustrated in Figures 2.15 and 2.16. It can be observed that the numerical solution is quite close to the exact one.

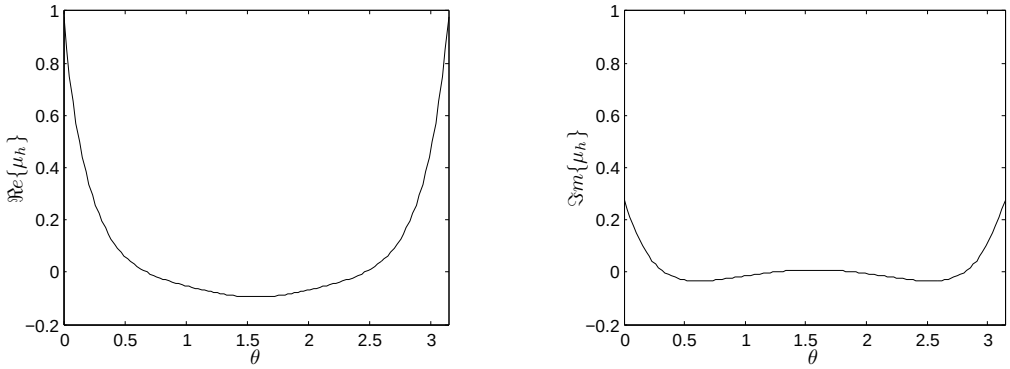

(a) Real part (b) Imaginary part

FIGURE 2.14. Numerically computed trace of the solution μ_h.

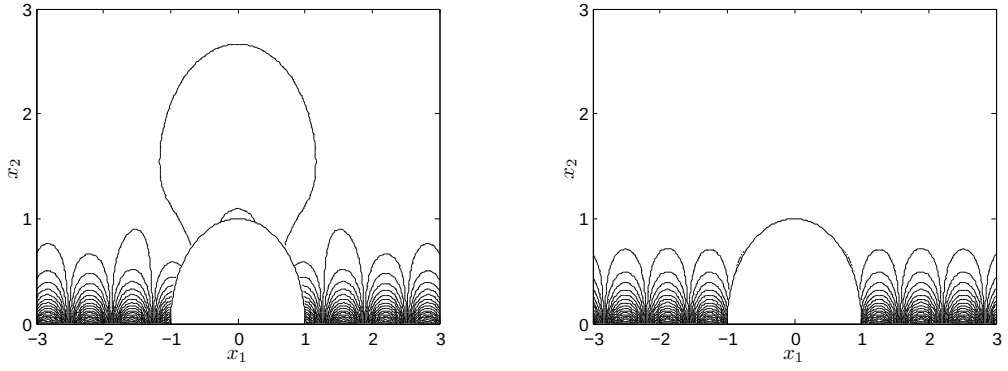

(a) Real part (b) Imaginary part

FIGURE 2.15. Contour plot of the numerically computed solution u_h.

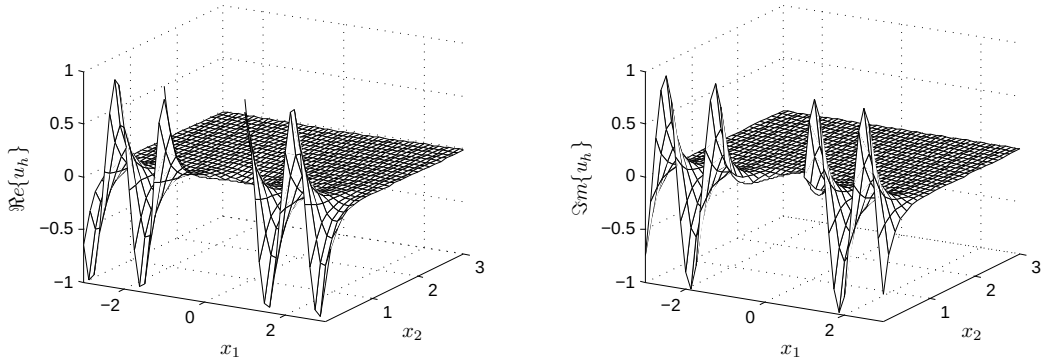

(a) Real part (b) Imaginary part

FIGURE 2.16. Oblique view of the numerically computed solution u_h.

Likewise as in (B.368), we define the relative error of the trace of the solution as

$$E_2(h, \Gamma_p^h) = \frac{\|\Pi_h \mu - \mu_h\|_{L^2(\Gamma_p^h)}}{\|\Pi_h \mu\|_{L^2(\Gamma_p^h)}}, \tag{2.231}$$

where $\Pi_h \mu$ denotes the Lagrange interpolating function of the exact solution's trace μ, i.e.,

$$\Pi_h \mu(\boldsymbol{x}) = \sum_{j=1}^{I+1} \mu(\boldsymbol{r}_j)\, \chi_j(\boldsymbol{x}) \quad \text{and} \quad \mu_h(\boldsymbol{x}) = \sum_{j=1}^{I+1} \mu_j\, \chi_j(\boldsymbol{x}) \quad \text{for } \boldsymbol{x} \in \Gamma_p^h. \tag{2.232}$$

In our case, for a step $h = 0.02618$, we obtained a relative error of $E_2(h, \Gamma_p^h) = 0.02763$.

As in (B.372), we define the relative error of the solution as

$$E_\infty(h, \Omega_L) = \frac{\|u - u_h\|_{L^\infty(\Omega_L)}}{\|u\|_{L^\infty(\Omega_L)}}, \tag{2.233}$$

being $\Omega_L = \{\boldsymbol{x} \in \Omega_e : \|\boldsymbol{x}\|_\infty < L\}$ for $L > 0$. We consider $L = 3$ and approximate Ω_L by a triangular finite element mesh of refinement h near the boundary. For $h = 0.02618$, the relative error that we obtained for the solution was $E_\infty(h, \Omega_L) = 0.01314$.

The results for different mesh refinements, i.e., for different numbers of segments I and discretization steps h, are listed in Table 2.1. These results are illustrated graphically in Figure 2.17. It can be observed that the relative errors are approximately of order h.

TABLE 2.1. Relative errors for different mesh refinements.

I	h	$E_2(h, \Gamma_p^h)$	$E_\infty(h, \Omega_L)$
12	0.2611	$2.549 \cdot 10^{-1}$	$1.610 \cdot 10^{-1}$
40	0.07852	$7.426 \cdot 10^{-2}$	$3.658 \cdot 10^{-2}$
80	0.03927	$4.014 \cdot 10^{-2}$	$1.903 \cdot 10^{-2}$
120	0.02618	$2.763 \cdot 10^{-2}$	$1.314 \cdot 10^{-2}$
240	0.01309	$1.431 \cdot 10^{-2}$	$7.455 \cdot 10^{-3}$
500	0.006283	$7.008 \cdot 10^{-3}$	$3.785 \cdot 10^{-3}$
1000	0.003142	$3.538 \cdot 10^{-3}$	$1.938 \cdot 10^{-3}$

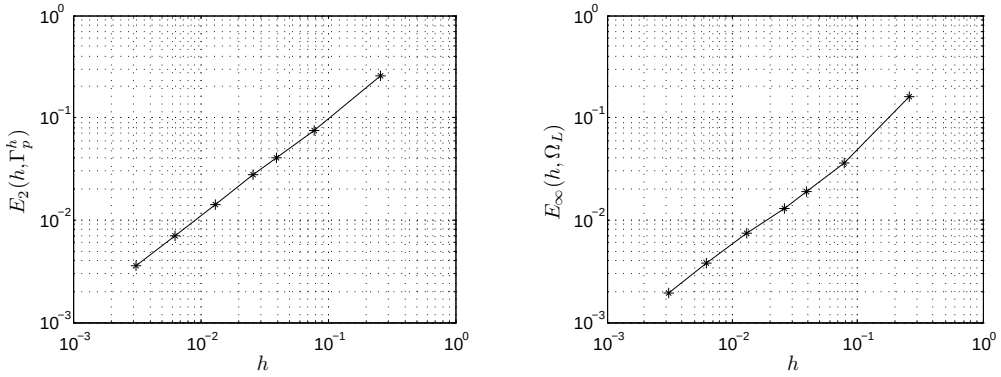

(a) Relative error $E_2(h, \Gamma_p^h)$ (b) Relative error $E_\infty(h, \Omega_L)$

FIGURE 2.17. Logarithmic plots of the relative errors versus the discretization step.

III. HALF-PLANE IMPEDANCE HELMHOLTZ PROBLEM

3.1 Introduction

In this chapter we study the perturbed half-plane impedance Helmholtz problem using integral equation techniques and the boundary element method.

We consider the problem of the Helmholtz equation in two dimensions on a compactly perturbed half-plane with an impedance boundary condition. The perturbed half-plane impedance Helmholtz problem is a wave scattering problem around the bounded perturbation, which is contained in the upper half-plane. In acoustic scattering the impedance boundary-value problem appears when we suppose that the normal velocity is proportional to the excess pressure on the boundary of the impenetrable perturbation or obstacle (vid. Section A.11). The special case of frequency zero for the volume waves has been treated already in Chapter II. The three-dimensional case is considered in Chapter V, whereas the full-plane impedance Helmholtz problem with a bounded impenetrable obstacle is treated thoroughly in Appendix C.

The main application of the problem corresponds to outdoor sound propagation, but it is also used to describe the propagation of radio waves above the ground and of water waves in shallow waters near the coast (harbor oscillations). The problem was at first considered by Sommerfeld (1909) to describe the long-distance propagation of electromagnetic waves above the earth. Different results for the electromagnetic problem were then obtained by Weyl (1919) and later again by Sommerfeld (1926). After the articles of Van der Pol & Niessen (1930), Wise (1931), and Van der Pol (1935), the most useful results up to that time were generated by Norton (1936, 1937). We can likewise mention the later works of Baños & Wesley (1953, 1954) and Baños (1966). The application of the problem to outdoor sound propagation was initiated by Rudnick (1947). Other approximate solutions to the problem were thereafter found by Lawhead & Rudnick (1951*a*,*b*) and Ingard (1951). Solutions containing surface-wave terms were obtained by Wenzel (1974) and Chien & Soroka (1975, 1980). Further references are listed in Nobile & Hayek (1985). Other articles that attempt to solve the problem are Briquet & Filippi (1977), Attenborough, Hayek & Lawther (1980), Filippi (1983), Li et al. (1994), and Attenborough (2002), and more recently also Habault (1999), Ochmann (2004), and Ochmann & Brick (2008), among others. For the two-dimensional case, in particular, we mention the articles of Chandler-Wilde & Hothersall (1995*a*,*b*) and Granat, Tahar & Ha-Duong (1999). The problem can be also found in the books of Greenberg (1971) and DeSanto (1992). The physical aspects of outdoor sound propagation can be found in Morse & Ingard (1961) and Embleton (1996). For the propagation of water waves in shallow waters near the coast (harbor oscillations) we cite the articles of Hsiao, Lin & Fang (2001) and Liu & Losada (2002), and the book of Mei, Stiassnie & Yue (2005).

The Helmholtz equation allows the propagation of volume waves inside the considered domain, and when it is supplied with an impedance boundary condition, then it allows also the propagation of surface waves along the boundary of the perturbed half-plane. The main difficulty in the numerical treatment and resolution of our problem is the fact that the

exterior domain is unbounded. We solve it therefore with integral equation techniques and a boundary element method, which require the knowledge of the associated Green's function. This Green's function is computed using a Fourier transform and taking into account the limiting absorption principle, following Durán, Muga & Nédélec (2005*a*, 2006) and Durán, Hein & Nédélec (2007*a*,*b*), but here an explicit expression is found for it in terms of a finite combination of elementary functions, special functions, and their primitives.

This chapter is structured in 13 sections, including this introduction. The direct scattering problem of the Helmholtz equation in a two-dimensional compactly perturbed half-plane with an impedance boundary condition is presented in Section 3.2. The computation of the Green's function, its far field, and its numerical evaluation are developed respectively in Sections 3.3, 3.4, and 3.5. The use of integral equation techniques to solve the direct scattering problem is discussed in Section 3.6. These techniques allow also to represent the far field of the solution, as shown in Section 3.7. The appropriate function spaces and some existence and uniqueness results for the solution of the problem are presented in Section 3.8. The dissipative problem is studied in Section 3.9. By means of the variational formulation developed in Section 3.10, the obtained integral equation is discretized using the boundary element method, which is described in Section 3.11. The boundary element calculations required to build the matrix of the linear system resulting from the numerical discretization are explained in Section 3.12. Finally, in Section 3.13 a benchmark problem based on an exterior half-circle problem is solved numerically.

3.2 Direct scattering problem

3.2.1 Problem definition

We consider the direct scattering problem of linear time-harmonic acoustic waves on a perturbed half-plane $\Omega_e \subset \mathbb{R}^2_+$, where $\mathbb{R}^2_+ = \{(x_1, x_2) \in \mathbb{R}^2 : x_2 > 0\}$, where the incident field u_I and the reflected field u_R are known, and where the time convention $e^{-i\omega t}$ is taken. The goal is to find the scattered field u as a solution to the Helmholtz equation in the exterior open and connected domain Ω_e, satisfying an outgoing radiation condition, and such that the total field u_T, decomposed as $u_T = u_I + u_R + u$, satisfies a homogeneous impedance boundary condition on the regular boundary $\Gamma = \Gamma_p \cup \Gamma_\infty$ (e.g., of class C^2). The exterior domain Ω_e is composed by the half-plane $\mathbb{R}^2_+$ with a compact perturbation near the origin that is contained in $\mathbb{R}^2_+$, as shown in Figure 3.1. The perturbed boundary is denoted by Γ_p, while Γ_∞ denotes the remaining unperturbed boundary of $\mathbb{R}^2_+$, which extends towards infinity on both sides. The unit normal $\boldsymbol{n}$ is taken outwardly oriented of Ω_e and the complementary domain is denoted by $\Omega_c = \mathbb{R}^2 \setminus \overline{\Omega_e}$. A given wave number $k > 0$ is considered, which depends on the pulsation ω and the speed of wave propagation c through the ratio $k = \omega/c$.

The total field u_T satisfies thus the Helmholtz equation

$$\Delta u_T + k^2 u_T = 0 \qquad \text{in } \Omega_e, \tag{3.1}$$

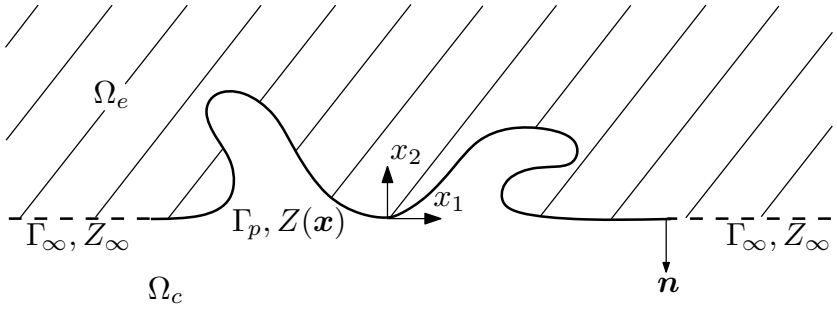

FIGURE 3.1. Perturbed half-plane impedance Helmholtz problem domain.

which is also satisfied by the incident field u_I, the reflected field u_R, and the scattered field u, due linearity. For the total field u_T we take the homogeneous impedance boundary condition

$$-\frac{\partial u_T}{\partial n} + Z u_T = 0 \qquad \text{on } \Gamma, \tag{3.2}$$

where Z is the impedance on the boundary, which is decomposed as

$$Z(\boldsymbol{x}) = Z_\infty + Z_p(\boldsymbol{x}), \qquad \boldsymbol{x} \in \Gamma, \tag{3.3}$$

being $Z_\infty > 0$ real and constant throughout Γ, and $Z_p(\boldsymbol{x})$ a possibly complex-valued impedance that depends on the position $\boldsymbol{x}$ and that has a bounded support contained in Γ_p. The case of complex Z_∞ and k will be discussed later. If $Z = 0$ or $Z = \infty$, then we retrieve respectively the classical Neumann or Dirichlet boundary conditions. The scattered field u satisfies the non-homogeneous impedance boundary condition

$$-\frac{\partial u}{\partial n} + Z u = f_z \qquad \text{on } \Gamma, \tag{3.4}$$

where the impedance data function f_z is known, has its support contained in Γ_p, and is given, because of (3.2), by

$$f_z = \frac{\partial u_I}{\partial n} - Z u_I + \frac{\partial u_R}{\partial n} - Z u_R \qquad \text{on } \Gamma. \tag{3.5}$$

An outgoing radiation condition has to be also imposed for the scattered field u, which specifies its decaying behavior at infinity and eliminates the non-physical solutions, e.g., ingoing volume or surface waves. This radiation condition can be stated for $r \to \infty$ in a more adjusted way as

$$\begin{cases} |u| \le \dfrac{C}{\sqrt{r}} \quad \text{and} \quad \left|\dfrac{\partial u}{\partial r} - iku\right| \le \dfrac{C}{r} & \text{if } x_2 > \dfrac{1}{2Z_\infty}\ln(1+\beta r), \\ |u| \le C \quad \text{and} \quad \left|\dfrac{\partial u}{\partial r} - i\sqrt{Z_\infty^2 + k^2}\,u\right| \le \dfrac{C}{r} & \text{if } x_2 \le \dfrac{1}{2Z_\infty}\ln(1+\beta r), \end{cases} \tag{3.6}$$

for some constants $C > 0$, where $r = |\boldsymbol{x}|$ and $\beta = 8\pi k Z_\infty^2/(Z_\infty^2 + k^2)$. It implies that two different asymptotic behaviors can be established for the scattered field u, which are shown in Figure 3.2. Away from the boundary Γ and inside the domain Ω_e, the first expression in (3.6) dominates, which corresponds to a classical Sommerfeld radiation condition

like (C.8) and is associated with volume waves. Near the boundary, on the other hand, the second expression in (3.6) resembles a Sommerfeld radiation condition, but only along the boundary and having a different wave number, and is therefore related to the propagation of surface waves. It is often expressed also as

$$\left| \frac{\partial u}{\partial |x_1|} - i\sqrt{Z_\infty^2 + k^2}\, u \right| \leq \frac{C}{|x_1|}. \tag{3.7}$$

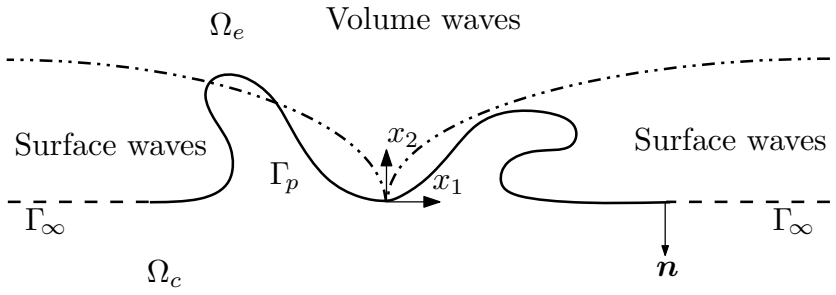

FIGURE 3.2. Asymptotic behaviors in the radiation condition.

Analogously as done by Durán, Muga & Nédélec (2005*a*, 2006), the radiation condition (3.6) can be stated alternatively as

$$\begin{cases} |u| \leq \dfrac{C}{\sqrt{r}} \quad \text{and} \quad \left| \dfrac{\partial u}{\partial r} - iku \right| \leq \dfrac{C}{r^{1-\alpha}} & \text{if } \; x_2 > Cr^\alpha, \\ |u| \leq C \quad \text{and} \quad \left| \dfrac{\partial u}{\partial r} - i\sqrt{Z_\infty^2 + k^2}\, u \right| \leq \dfrac{C}{r^{1-2\alpha}} & \text{if } \; x_2 \leq Cr^\alpha, \end{cases} \tag{3.8}$$

for $0 < \alpha < 1/2$ and some constants $C > 0$, being the growth of Cr^α bigger than the logarithmic one at infinity. Equivalently, the radiation condition can be expressed in a more weaker and general formulation as

$$\begin{cases} \lim\limits_{R\to\infty} \displaystyle\int_{S_R^1} |u|^2 \, \mathrm{d}\gamma < \infty \quad \text{and} \quad \lim\limits_{R\to\infty} \int_{S_R^1} \left| \frac{\partial u}{\partial r} - iku \right|^2 \mathrm{d}\gamma = 0, \\ \lim\limits_{R\to\infty} \displaystyle\int_{S_R^2} \frac{|u|^2}{\ln R} \, \mathrm{d}\gamma < \infty \quad \text{and} \quad \lim\limits_{R\to\infty} \int_{S_R^2} \frac{1}{\ln R} \left| \frac{\partial u}{\partial r} - i\sqrt{Z_\infty^2 + k^2}\, u \right|^2 \mathrm{d}\gamma = 0, \end{cases} \tag{3.9}$$

where

$$S_R^1 = \left\{ \boldsymbol{x} \in \mathbb{R}^2_+ : \, |\boldsymbol{x}| = R, \;\; x_2 > \frac{1}{2Z_\infty} \ln(1 + \beta R) \right\}, \tag{3.10}$$

$$S_R^2 = \left\{ \boldsymbol{x} \in \mathbb{R}^2_+ : \, |\boldsymbol{x}| = R, \;\; x_2 < \frac{1}{2Z_\infty} \ln(1 + \beta R) \right\}. \tag{3.11}$$

We observe that in this case

$$\int_{S_R^1} \mathrm{d}\gamma = \mathcal{O}(R) \qquad \text{and} \qquad \int_{S_R^2} \mathrm{d}\gamma = \mathcal{O}(\ln R). \tag{3.12}$$

The portions S_R^1 and S_R^2 of the half-circle and the terms depending on S_R^2 of the radiation condition (3.9) have to be modified when using instead the polynomial curves of (3.8). We refer to Stoker (1956) for a discussion on radiation conditions for surface waves.

The perturbed half-plane impedance Helmholtz problem can be finally stated as

$$\begin{cases} \text{Find } u : \Omega_e \to \mathbb{C} \text{ such that} \\ \Delta u + k^2 u = 0 \qquad \text{in } \Omega_e, \\ -\dfrac{\partial u}{\partial n} + Zu = f_z \qquad \text{on } \Gamma, \\ \text{+ Outgoing radiation condition as } |\boldsymbol{x}| \to \infty, \end{cases} \tag{3.13}$$

where the outgoing radiation condition is given by (3.6).

3.2.2 Incident and reflected field

To determine the incident field u_I and the reflected field u_R, we study the solutions u_T of the unperturbed and homogeneous wave propagation problem with neither a scattered field nor an associated radiation condition, being $u_T = u_I + u_R$. The solutions are searched in particular to be physically admissible, i.e., solutions which do not explode exponentially in the propagation domain, depicted in Figure 3.1. We analyze thus the half-plane impedance Helmholtz problem

$$\begin{cases} \Delta u_T + k^2 u_T = 0 \qquad \text{in } \mathbb{R}^2_+, \\ \dfrac{\partial u_T}{\partial x_2} + Z_\infty u_T = 0 \qquad \text{on } \{x_2 = 0\}. \end{cases} \tag{3.14}$$

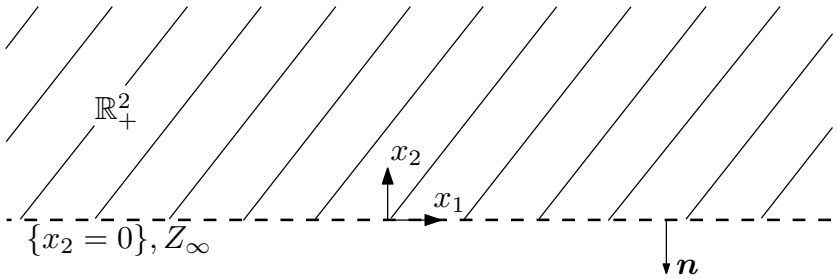

FIGURE 3.3. Positive half-plane $\mathbb{R}^2_+$.

Two different kinds of independent solutions u_T exist for the problem (3.14). They are obtained by studying the way how progressive plane waves of the form $e^{i\boldsymbol{k}\cdot\boldsymbol{x}}$ can be adjusted to satisfy the boundary condition, where the wave propagation vector $\boldsymbol{k} = (k_1, k_2)$ is such that $(\boldsymbol{k} \cdot \boldsymbol{k}) = k^2$.

The first kind of solution corresponds to a linear combination of two progressive plane volume waves and is given, up to an arbitrary multiplicative constant, by

$$u_T(\boldsymbol{x}) = e^{i\boldsymbol{k}\cdot\boldsymbol{x}} - \left(\frac{Z_\infty + ik_2}{Z_\infty - ik_2}\right) e^{i\bar{\boldsymbol{k}}\cdot\boldsymbol{x}}, \tag{3.15}$$

where $\boldsymbol{k} \in \mathbb{R}^2$ and $\bar{\boldsymbol{k}} = (k_1, -k_2)$. Due the involved physics, we consider that $k_2 \leq 0$. The first term of (3.15) can be interpreted as an incident plane volume wave, while the second term represents the reflected plane volume wave due the presence of the boundary with impedance. Thus

$$u_I(\boldsymbol{x}) = e^{i\boldsymbol{k}\cdot\boldsymbol{x}}, \tag{3.16}$$

$$u_R(\boldsymbol{x}) = -\left(\frac{Z_\infty + ik_2}{Z_\infty - ik_2}\right) e^{i\bar{\boldsymbol{k}}\cdot\boldsymbol{x}}. \tag{3.17}$$

It can be observed that the solution (3.15) vanishes when $k_2 = 0$, i.e., when the wave propagation is parallel to the half-plane's boundary. The wave propagation vector $\boldsymbol{k}$, by considering a parametrization through the angle of incidence θ_I for $0 \leq \theta_I \leq \pi$, can be expressed as $\boldsymbol{k} = (-k\cos\theta_I, -k\sin\theta_I)$. In this case the solution is described by

$$u_T(\boldsymbol{x}) = e^{-ik(x_1\cos\theta_I + x_2\sin\theta_I)} - \left(\frac{Z_\infty - ik\sin\theta_I}{Z_\infty + ik\sin\theta_I}\right) e^{-ik(x_1\cos\theta_I - x_2\sin\theta_I)}. \tag{3.18}$$

The second kind of solution, up to an arbitrary scaling factor, corresponds to a progressive plane surface wave, and is given by

$$u_T(\boldsymbol{x}) = u_I(\boldsymbol{x}) = e^{ik_s x_1} e^{-Z_\infty x_2}, \qquad k_s^2 = Z_\infty^2 + k^2. \tag{3.19}$$

It can be observed that plane surface waves correspond to plane volume waves with a complex wave propagation vector $\boldsymbol{k} = (k_s, iZ_\infty)$, are guided along the half-plane's boundary, and decrease exponentially towards its interior, hence their name. In this case there exists no reflected field, since the waves travel along the boundary. We remark that the plane surface waves vanish completely for classical Dirichlet ($Z_\infty = \infty$) or Neumann ($Z_\infty = 0$) boundary conditions.

3.3 Green's function

3.3.1 Problem definition

The Green's function represents the response of the unperturbed system to a Dirac mass. It corresponds to a function G, which depends on the wave number k, on the impedance Z_∞, on a fixed source point $\boldsymbol{x} \in \mathbb{R}^2_+$, and on an observation point $\boldsymbol{y} \in \mathbb{R}^2_+$. The Green's function is computed in the sense of distributions for the variable $\boldsymbol{y}$ in the half-plane $\mathbb{R}^2_+$ by placing at the right-hand side of the Helmholtz equation a Dirac mass $\delta_{\boldsymbol{x}}$, centered at the point $\boldsymbol{x}$. It is therefore a solution for the radiation problem of a point source,

namely

$$\left\{\begin{array}{ll} \text{Find } G(\boldsymbol{x},\cdot):\mathbb{R}^2_+\to\mathbb{C} \text{ such that} & \\ \Delta_{\boldsymbol{y}}G(\boldsymbol{x},\boldsymbol{y})+k^2G(\boldsymbol{x},\boldsymbol{y})=\delta_{\boldsymbol{x}}(\boldsymbol{y}) & \text{in } \mathcal{D}'(\mathbb{R}^2_+), \\ \dfrac{\partial G}{\partial y_2}(\boldsymbol{x},\boldsymbol{y})+Z_\infty G(\boldsymbol{x},\boldsymbol{y})=0 & \text{on } \{y_2=0\}, \\ \text{+ Outgoing radiation condition as } |\boldsymbol{y}|\to\infty. & \end{array}\right. \tag{3.20}$$

The outgoing radiation condition, in the same way as in (3.6), is given here as $|\boldsymbol{y}|\to\infty$ by

$$\left\{\begin{array}{ll} |G|\le\dfrac{C}{\sqrt{|\boldsymbol{y}|}} \quad \text{and} \quad \left|\dfrac{\partial G}{\partial r_{\boldsymbol{y}}}-ikG\right|\le\dfrac{C}{|\boldsymbol{y}|} & \text{if } y_2>\dfrac{\ln\big(1+\beta|\boldsymbol{y}|\big)}{2Z_\infty}, \\ |G|\le C \quad \text{and} \quad \left|\dfrac{\partial G}{\partial r_{\boldsymbol{y}}}-i\sqrt{Z_\infty^2+k^2}G\right|\le\dfrac{C}{|\boldsymbol{y}|} & \text{if } y_2\le\dfrac{\ln\big(1+\beta|\boldsymbol{y}|\big)}{2Z_\infty}, \end{array}\right. \tag{3.21}$$

for some constants $C>0$, independent of $r=|\boldsymbol{y}|$, where $\beta=8\pi kZ_\infty^2/(Z_\infty^2+k^2)$.

3.3.2 Special cases

When the Green's function problem (3.20) is solved using either homogeneous Dirichlet or Neumann boundary conditions, then its solution is found straightforwardly using the method of images (cf., e.g., Morse & Feshbach 1953).

a) Homogeneous Dirichlet boundary condition

We consider in the problem (3.20) the particular case of a homogeneous Dirichlet boundary condition, namely

$$G(\boldsymbol{x},\boldsymbol{y})=0, \qquad \boldsymbol{y}\in\{y_2=0\}, \tag{3.22}$$

which corresponds to the limit case when the impedance is infinite ($Z_\infty=\infty$). In this case, the Green's function G can be explicitly calculated using the method of images, since it has to be antisymmetric with respect to the axis $\{y_2=0\}$. An additional image source point $\bar{\boldsymbol{x}}=(x_1,-x_2)$, located on the lower half-plane and associated with a negative Dirac mass, is placed for this purpose just opposite to the upper half-plane's source point $\boldsymbol{x}=(x_1,x_2)$. The desired solution is then obtained by evaluating the full-plane Green's function (C.23) for each Dirac mass, which yields finally

$$G(\boldsymbol{x},\boldsymbol{y})=-\frac{i}{4}H_0^{(1)}\big(k|\boldsymbol{y}-\boldsymbol{x}|\big)+\frac{i}{4}H_0^{(1)}\big(k|\boldsymbol{y}-\bar{\boldsymbol{x}}|\big). \tag{3.23}$$

b) Homogeneous Neumann boundary condition

We consider in the problem (3.20) the particular case of a homogeneous Neumann boundary condition, namely

$$\frac{\partial G}{\partial n_{\boldsymbol{y}}}(\boldsymbol{x},\boldsymbol{y})=0, \qquad \boldsymbol{y}\in\{y_2=0\}, \tag{3.24}$$

which corresponds to the limit case when the impedance is zero ($Z_\infty=0$). As in the previous case, the method of images is again employed, but now the half-plane Green's function G has to be symmetric with respect to the axis $\{y_2=0\}$. Therefore, an additional

image source point $\bar{\boldsymbol{x}} = (x_1, -x_2)$, located on the lower half-plane, is placed just opposite to the upper half-plane's source point $\boldsymbol{x} = (x_1, x_2)$, but now associated with a positive Dirac mass. The desired solution is then obtained by evaluating the full-plane Green's function (C.23) for each Dirac mass, which yields

$$G(\boldsymbol{x}, \boldsymbol{y}) = -\frac{i}{4} H_0^{(1)}\big(k|\boldsymbol{y} - \boldsymbol{x}|\big) - \frac{i}{4} H_0^{(1)}\big(k|\boldsymbol{y} - \bar{\boldsymbol{x}}|\big). \tag{3.25}$$

3.3.3 Spectral Green's function

a) Boundary-value problem

To solve (3.20) in the general case, we use a modified partial Fourier transform on the horizontal y_1-axis, taking advantage of the fact that there is no horizontal variation in the geometry of the problem. To obtain the corresponding spectral Green's function, we follow the same procedure as the one performed in Durán et al. (2005*a*). We define the forward Fourier transform of a function $F\big(\boldsymbol{x}, (\cdot, y_2)\big) : \mathbb{R} \to \mathbb{C}$ by

$$\widehat{F}(\xi; y_2, x_2) = \frac{1}{\sqrt{2\pi}} \int_{-\infty}^{\infty} F(\boldsymbol{x}, \boldsymbol{y})\, e^{-i\xi(y_1 - x_1)}\, \mathrm{d}y_1, \qquad \xi \in \mathbb{R}, \tag{3.26}$$

and its inverse by

$$F(\boldsymbol{x}, \boldsymbol{y}) = \frac{1}{\sqrt{2\pi}} \int_{-\infty}^{\infty} \widehat{F}(\xi; y_2, x_2)\, e^{i\xi(y_1 - x_1)}\, \mathrm{d}\xi, \qquad y_1 \in \mathbb{R}. \tag{3.27}$$

To ensure a correct integration path for the Fourier transform and correct physical results, the calculations have to be performed in the framework of the limiting absorption principle, which allows to treat all the appearing integrals as Cauchy principal values. For this purpose, we take a small dissipation parameter $\varepsilon > 0$ into account and consider the problem (3.20) as the limit case when $\varepsilon \to 0$ of the dissipative problem

$$\begin{cases} \text{Find } G_\varepsilon(\boldsymbol{x}, \cdot) : \mathbb{R}^2_+ \to \mathbb{C} \text{ such that} \\ \Delta_{\boldsymbol{y}} G_\varepsilon(\boldsymbol{x}, \boldsymbol{y}) + k_\varepsilon^2 G_\varepsilon(\boldsymbol{x}, \boldsymbol{y}) = \delta_{\boldsymbol{x}}(\boldsymbol{y}) & \text{in } \mathcal{D}'(\mathbb{R}^2_+), \\ \dfrac{\partial G_\varepsilon}{\partial y_2}(\boldsymbol{x}, \boldsymbol{y}) + Z_\infty G_\varepsilon(\boldsymbol{x}, \boldsymbol{y}) = 0 & \text{on } \{y_2 = 0\}, \end{cases} \tag{3.28}$$

where $k_\varepsilon = k + i\varepsilon$. This choice ensures a correct outgoing dissipative volume-wave behavior. In the same way as for the Laplace equation, the impedance Z_∞ could be also incorporated into this dissipative framework, i.e., by considering $Z_\varepsilon = Z_\infty + i\varepsilon$, but it is not really necessary since the use of a dissipative wave number k_ε is enough to take care of all the appearing issues. Further references for the application of this principle can be found in Bonnet-BenDhia & Tillequin (2001), Hazard & Lenoir (1998), and Nosich (1994).

Applying thus the Fourier transform (3.26) on the system (3.28) leads to a linear second order ordinary differential equation for the variable y_2, with prescribed boundary values,

given by

$$\begin{cases} \dfrac{\partial^2 \widehat{G}_\varepsilon}{\partial y_2^2}(\xi) - (\xi^2 - k_\varepsilon^2)\widehat{G}_\varepsilon(\xi) = \dfrac{\delta(y_2 - x_2)}{\sqrt{2\pi}}, & y_2 > 0, \\ \dfrac{\partial \widehat{G}_\varepsilon}{\partial y_2}(\xi) + Z_\infty \widehat{G}_\varepsilon(\xi) = 0, & y_2 = 0. \end{cases} \tag{3.29}$$

We use the method of undetermined coefficients, and solve the homogeneous differential equation of the problem (3.29) respectively in the strip $\{\boldsymbol{y} \in \mathbb{R}^2_+ : 0 < y_2 < x_2\}$ and in the half-plane $\{\boldsymbol{y} \in \mathbb{R}^2_+ : y_2 > x_2\}$. This gives a solution for $\widehat{G}_\varepsilon$ in each domain, as a linear combination of two independent solutions of an ordinary differential equation, namely

$$\widehat{G}_\varepsilon(\xi) = \begin{cases} a\, e^{\sqrt{\xi^2 - k_\varepsilon^2}\, y_2} + b\, e^{-\sqrt{\xi^2 - k_\varepsilon^2}\, y_2} & \text{for } 0 < y_2 < x_2, \\ c\, e^{\sqrt{\xi^2 - k_\varepsilon^2}\, y_2} + d\, e^{-\sqrt{\xi^2 - k_\varepsilon^2}\, y_2} & \text{for } y_2 > x_2. \end{cases} \tag{3.30}$$

The unknowns a, b, c, and d, which depend on ξ and x_2, are determined through the boundary condition, by imposing continuity, and by assuming an outgoing wave behavior. The complex square root in (3.30) is defined in such a way that its real part is always positive.

b) Complex square roots

Due the application of the limiting absorption principle, the square root that appears in the general solution (3.30) has to be understood as a complex map $\xi \mapsto \sqrt{\xi^2 - k_\varepsilon^2}$, which is decomposed as the product between $\sqrt{\xi - k_\varepsilon}$ and $\sqrt{\xi + k_\varepsilon}$, and has its two analytic branch cuts on the complex ξ plane defined in such a way that they do not intersect the real axis. Further details on complex branch cuts can be found in the books of Bak & Newman (1997) and Felsen & Marcuwitz (2003). The arguments are taken in such a way that $\arg(\xi - k_\varepsilon) \in (-\frac{3\pi}{2}, \frac{\pi}{2})$ for the map $\sqrt{\xi - k_\varepsilon}$, and $\arg(\xi + k_\varepsilon) \in (-\frac{\pi}{2}, \frac{3\pi}{2})$ for the map $\sqrt{\xi + k_\varepsilon}$. These maps can be therefore defined by (Durán et al. 2005*a*)

$$\sqrt{\xi - k_\varepsilon} = -i\sqrt{|k_\varepsilon|}\, e^{\frac{i}{2}\arg(k_\varepsilon)} \exp\left(\frac{1}{2}\int_0^\xi \frac{\mathrm{d}\eta}{\eta - k_\varepsilon}\right), \tag{3.31}$$

and

$$\sqrt{\xi + k_\varepsilon} = \sqrt{|k_\varepsilon|}\, e^{\frac{i}{2}\arg(k_\varepsilon)} \exp\left(\frac{1}{2}\int_0^\xi \frac{\mathrm{d}\eta}{\eta + k_\varepsilon}\right). \tag{3.32}$$

Consequently $\sqrt{\xi^2 - k_\varepsilon^2}$ is even and analytic in the domain shown in Figure 3.4. It can be hence defined by

$$\sqrt{\xi^2 - k_\varepsilon^2} = \sqrt{\xi - k_\varepsilon}\,\sqrt{\xi + k_\varepsilon} = -ik_\varepsilon \exp\left(\int_0^\xi \frac{\eta}{\eta^2 - k_\varepsilon^2}\,\mathrm{d}\eta\right), \tag{3.33}$$

and is characterized, for $\xi, k \in \mathbb{R}$, by

$$\sqrt{\xi^2 - k^2} = \begin{cases} \sqrt{\xi^2 - k^2}, & \xi^2 \geq k^2, \\ -i\sqrt{k^2 - \xi^2}, & \xi^2 < k^2. \end{cases} \tag{3.34}$$

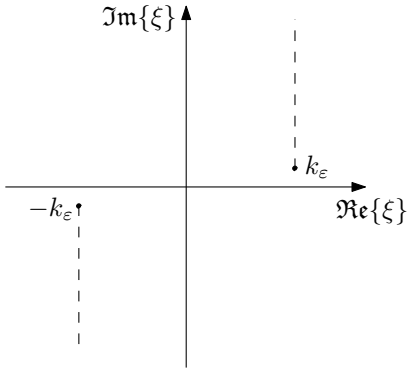

FIGURE 3.4. Analytic branch cuts of the complex map $\sqrt{\xi^2 - k_\varepsilon^2}$.

We remark that if $\xi \in \mathbb{R}$, then $\arg(\xi - k_\varepsilon) \in (-\pi, 0)$ and $\arg(\xi + k_\varepsilon) \in (0, \pi)$. This proceeds from the fact that $\arg(k_\varepsilon) \in (0, \pi)$, since by the limiting absorption principle it holds that $\mathfrak{Im}\{k_\varepsilon\} = \varepsilon > 0$. Thus $\arg\left(\sqrt{\xi - k_\varepsilon}\right) \in (-\frac{\pi}{2}, 0)$, $\arg\left(\sqrt{\xi + k_\varepsilon}\right) \in (0, \frac{\pi}{2})$, and $\arg\left(\sqrt{\xi^2 - k_\varepsilon^2}\right) \in (-\frac{\pi}{2}, \frac{\pi}{2})$. Hence, the real part of the complex map $\sqrt{\xi^2 - k_\varepsilon^2}$ for real ξ is strictly positive, i.e., $\mathfrak{Re}\left\{\sqrt{\xi^2 - k_\varepsilon^2}\right\} > 0$. Therefore the function $e^{-\sqrt{\xi^2 - k_\varepsilon^2}\, y_2}$ is even and exponentially decreasing as $y_2 \to \infty$.

c) Spectral Green's function with dissipation

Now, thanks to (3.30), the computation of $\widehat{G}_\varepsilon$ is straightforward. From the boundary condition of (3.29) a relation for the coefficients a and b can be derived, which is given by

$$a\left(Z_\infty + \sqrt{\xi^2 - k_\varepsilon^2}\right) + b\left(Z_\infty - \sqrt{\xi^2 - k_\varepsilon^2}\right) = 0. \tag{3.35}$$

On the other hand, since the solution (3.30) has to be bounded at infinity as $y_2 \to \infty$, and since $\mathfrak{Re}\left\{\sqrt{\xi^2 - k_\varepsilon^2}\right\} > 0$, it follows then necessarily that

$$c = 0. \tag{3.36}$$

To ensure the continuity of the Green's function at the point $y_2 = x_2$, it is needed that

$$d = a\, e^{\sqrt{\xi^2 - k_\varepsilon^2}\, 2x_2} + b. \tag{3.37}$$

Using relations (3.35), (3.36), and (3.37) in (3.30), we obtain the expression

$$\widehat{G}_\varepsilon(\xi) = a\, e^{\sqrt{\xi^2 - k_\varepsilon^2}\, x_2}\left[e^{-\sqrt{\xi^2 - k_\varepsilon^2}\,|y_2 - x_2|} - \left(\frac{Z_\infty + \sqrt{\xi^2 - k_\varepsilon^2}}{Z_\infty - \sqrt{\xi^2 - k_\varepsilon^2}}\right) e^{-\sqrt{\xi^2 - k_\varepsilon^2}\,(y_2 + x_2)}\right]. \tag{3.38}$$

The remaining unknown coefficient a is determined by replacing (3.38) in the differential equation of (3.29), taking the derivatives in the sense of distributions, particularly

$$\frac{\partial}{\partial y_2}\left\{e^{-\sqrt{\xi^2 - k_\varepsilon^2}\,|y_2 - x_2|}\right\} = -\sqrt{\xi^2 - k_\varepsilon^2}\, \operatorname{sign}(y_2 - x_2)\, e^{-\sqrt{\xi^2 - k_\varepsilon^2}\,|y_2 - x_2|}, \tag{3.39}$$

and

$$\frac{\partial}{\partial y_2}\big\{\operatorname{sign}(y_2 - x_2)\big\} = 2\,\delta(y_2 - x_2). \tag{3.40}$$

So, the second derivative of (3.38) becomes

$$\frac{\partial^2 \widehat{G}_\varepsilon}{\partial y_2^2}(\xi) = a\, e^{\sqrt{\xi^2-k_\varepsilon^2}\, x_2} \Bigg[(\xi^2 - k_\varepsilon^2)\, e^{-\sqrt{\xi^2-k_\varepsilon^2}\,|y_2-x_2|} - 2\sqrt{\xi^2-k_\varepsilon^2}\,\delta(y_2-x_2) \\ - \left(\frac{Z_\infty + \sqrt{\xi^2-k_\varepsilon^2}}{Z_\infty - \sqrt{\xi^2-k_\varepsilon^2}} \right) (\xi^2 - k_\varepsilon^2)\, e^{-\sqrt{\xi^2-k_\varepsilon^2}\,(y_2+x_2)} \Bigg]. \tag{3.41}$$

This way, from (3.38) and (3.41) in the first equation of (3.29), we obtain that

$$a = -\frac{e^{-\sqrt{\xi^2-k_\varepsilon^2}\, x_2}}{\sqrt{8\pi}\,\sqrt{\xi^2-k_\varepsilon^2}}. \tag{3.42}$$

Finally, the spectral Green's function $\widehat{G}_\varepsilon$ with dissipation ε is given by

$$\widehat{G}_\varepsilon(\xi; y_2, x_2) = -\frac{e^{-\sqrt{\xi^2-k_\varepsilon^2}\,|y_2-x_2|}}{\sqrt{8\pi}\sqrt{\xi^2-k_\varepsilon^2}} + \left(\frac{Z_\infty + \sqrt{\xi^2-k_\varepsilon^2}}{Z_\infty - \sqrt{\xi^2-k_\varepsilon^2}} \right) \frac{e^{-\sqrt{\xi^2-k_\varepsilon^2}\,(y_2+x_2)}}{\sqrt{8\pi}\sqrt{\xi^2-k_\varepsilon^2}}. \tag{3.43}$$

d) Analysis of singularities

To obtain the spectral Green's function $\widehat{G}$ without dissipation, the limit $\varepsilon \to 0$ has to be taken in (3.43). This can be done directly wherever the limit is regular and continuous on ξ. Singular points, on the other hand, have to be analyzed carefully to fulfill correctly the limiting absorption principle. Thus we study first the singularities of the limit function before applying this principle, i.e., considering just $\varepsilon = 0$, in which case we have

$$\widehat{G}_0(\xi) = -\frac{e^{-\sqrt{\xi^2-k^2}\,|y_2-x_2|}}{\sqrt{8\pi}\sqrt{\xi^2-k^2}} + \left(\frac{Z_\infty + \sqrt{\xi^2-k^2}}{Z_\infty - \sqrt{\xi^2-k^2}} \right) \frac{e^{-\sqrt{\xi^2-k^2}\,(y_2+x_2)}}{\sqrt{8\pi}\sqrt{\xi^2-k^2}}. \tag{3.44}$$

Possible singularities for (3.44) may only appear when $|\xi| = k$ or when $|\xi| = \xi_p$, being $\xi_p = \sqrt{Z_\infty^2 + k^2}$, i.e., when the denominator of the fractions is zero. Otherwise the function is regular and continuous.

For $\xi = k$ and $\xi = -k$ the function (3.44) is continuous. This can be seen by writing it, analogously as in Durán, Muga & Nédélec (2006), in the form

$$\widehat{G}_0(\xi) = \frac{H\big(g(\xi)\big)}{g(\xi)}, \tag{3.45}$$

where

$$g(\xi) = \sqrt{\xi^2 - k^2}, \tag{3.46}$$

and

$$H(\beta) = \frac{1}{\sqrt{8\pi}} \left(-e^{-\beta\,|y_2-x_2|} + \frac{Z_\infty + \beta}{Z_\infty - \beta}\, e^{-\beta\,(y_2+x_2)} \right), \qquad \beta \in \mathbb{C}. \tag{3.47}$$

Since $H(\beta)$ is an analytic function in $\beta = 0$, since $H(0) = 0$, and since

$$\lim_{\xi \to \pm k} \widehat{G}_0(\xi) = \lim_{\xi \to \pm k} \frac{H\big(g(\xi)\big) - H(0)}{g(\xi)} = H'(0), \tag{3.48}$$

we can easily obtain that

$$\lim_{\xi\to\pm k}\widehat{G}_0(\xi)=\frac{1}{\sqrt{8\pi}}\left(1+\frac{1}{Z_\infty}+|y_2-x_2|-(y_2+x_2)\right), \tag{3.49}$$

being thus $\widehat{G}_0$ bounded and continuous on $\xi=k$ and $\xi=-k$.

For $\xi=\xi_p$ and $\xi=-\xi_p$, where $\xi_p=\sqrt{Z_\infty^2+k^2}$, the function (3.44) presents two simple poles, whose residues are characterized by

$$\lim_{\xi\to\pm\xi_p}(\xi\mp\xi_p)\,\widehat{G}_0(\xi)=\mp\frac{Z_\infty}{\sqrt{2\pi}\,\xi_p}\,e^{-Z_\infty(y_2+x_2)}. \tag{3.50}$$

To analyze the effect of these singularities, we have to study the computation of the inverse Fourier transform of

$$\widehat{G}_P(\xi)=\frac{Z_\infty}{\sqrt{2\pi}\,\xi_p}\,e^{-Z_\infty(y_2+x_2)}\left(\frac{1}{\xi+\xi_p}-\frac{1}{\xi-\xi_p}\right), \tag{3.51}$$

which has to be done in the frame of the limiting absorption principle to obtain the correct physical results, i.e., the inverse Fourier transform has to be understood in the sense of

$$G_P(\boldsymbol{x},\boldsymbol{y})=\lim_{\varepsilon\to0}\left\{\frac{Z_\infty}{2\pi\xi_p}\,e^{-Z_\infty(y_2+x_2)}\int_{-\infty}^{\infty}\left(\frac{1}{\xi+\xi_p}-\frac{1}{\xi-\xi_p}\right)e^{i\xi(y_1-x_1)}\mathrm{d}\xi\right\}, \tag{3.52}$$

where now $\xi_p=\sqrt{Z_\infty^2+k_\varepsilon^2}$, which is such that $\mathfrak{Im}\{\xi_p\}>0$.

To perform correctly the computation of (3.52), we apply the residue theorem of complex analysis (cf., e.g., Arfken & Weber 2005, Bak & Newman 1997, Dettman 1984) on the complex meromorphic mapping

$$F(\xi)=\left(\frac{1}{\xi+\xi_p}-\frac{1}{\xi-\xi_p}\right)e^{i\xi(y_1-x_1)}, \tag{3.53}$$

which admits two simple poles at ξ_p and $-\xi_p$, where $\mathfrak{Im}\{\xi_p\}>0$. We already did this computation for the Laplace equation and obtained the expression (2.59), namely

$$\int_{-\infty}^{\infty}F(\xi)\,\mathrm{d}\xi=-i2\pi e^{i\xi_p|y_1-x_1|},\qquad(y_1-x_1)\in\mathbb{R}. \tag{3.54}$$

Using (3.54) for $\xi_p=\sqrt{Z_\infty^2+k^2}$ yields that the inverse Fourier transform of (3.51), when considering the limiting absorption principle, is given by

$$G_P^L(\boldsymbol{x},\boldsymbol{y})=-\frac{iZ_\infty}{\xi_p}\,e^{-Z_\infty(y_2+x_2)}e^{i\xi_p|y_1-x_1|}. \tag{3.55}$$

We observe that this expression describes the asymptotic behavior of the surface waves, which are linked to the presence of the poles in the spectral Green's function.

If the limiting absorption principle is not considered, i.e., if $\mathfrak{Im}\{\xi_p\}=0$, then the inverse Fourier transform of (3.51) could be again computed in the sense of the principal value with the residue theorem. In this case we would obtain, instead of (3.54) and just as the expression (2.61) for the Laplace equation, the quantity

$$\int_{-\infty}^{\infty}F(\xi)\,\mathrm{d}\xi=2\pi\sin\big(\xi_p|y_1-x_1|\big),\qquad(y_1-x_1)\in\mathbb{R}. \tag{3.56}$$

The inverse Fourier transform of (3.51) would be in this case

$$G_P^{NL}(\boldsymbol{x},\boldsymbol{y}) = \frac{Z_\infty}{\xi_p}\, e^{-Z_\infty(y_2+x_2)} \sin\big(\xi_p|y_1-x_1|\big), \tag{3.57}$$

which is correct from the mathematical point of view, but yields only a standing surface wave, and not a desired outgoing progressive surface wave as in (3.55).

The effect of the limiting absorption principle, in the spatial dimension, is then given by the difference between (3.55) and (3.57), i.e., by

$$G_L(\boldsymbol{x},\boldsymbol{y}) = G_P^{L}(\boldsymbol{x},\boldsymbol{y}) - G_P^{NL}(\boldsymbol{x},\boldsymbol{y}) = -\frac{iZ_\infty}{\xi_p}\, e^{-Z_\infty(y_2+x_2)} \cos\big(\xi_p(y_1-x_1)\big), \tag{3.58}$$

whose Fourier transform, and therefore the spectral effect, is given by

$$\widehat{G}_L(\xi) = \widehat{G}_P^{L}(\xi) - \widehat{G}_P^{NL}(\xi) = -\frac{iZ_\infty}{\xi_p}\sqrt{\frac{\pi}{2}}\, e^{-Z_\infty(y_2+x_2)} \big[\delta(\xi-\xi_p)+\delta(\xi+\xi_p)\big]. \tag{3.59}$$

e) Spectral Green's function without dissipation

The spectral Green's function $\widehat{G}$ without dissipation is therefore obtained by taking the limit $\varepsilon \to 0$ in (3.43) and considering the effect of the limiting absorption principle for the appearing singularities, summarized in (3.59). Thus we obtain in the sense of distributions

$$\begin{aligned}\widehat{G}(\xi;y_2,x_2) = &-\frac{e^{-\sqrt{\xi^2-k^2}\,|y_2-x_2|}}{\sqrt{8\pi}\sqrt{\xi^2-k^2}} + \left(\frac{Z_\infty+\sqrt{\xi^2-k^2}}{Z_\infty-\sqrt{\xi^2-k^2}}\right)\frac{e^{-\sqrt{\xi^2-k^2}\,(y_2+x_2)}}{\sqrt{8\pi}\sqrt{\xi^2-k^2}} \\ &- \frac{iZ_\infty}{\xi_p}\sqrt{\frac{\pi}{2}}\, e^{-Z_\infty(y_2+x_2)} \big[\delta(\xi-\xi_p)+\delta(\xi+\xi_p)\big].\end{aligned} \tag{3.60}$$

For our further analysis, this spectral Green's function is decomposed into four terms according to

$$\widehat{G} = \widehat{G}_\infty + \widehat{G}_D + \widehat{G}_L + \widehat{G}_R, \tag{3.61}$$

where

$$\widehat{G}_\infty(\xi;y_2,x_2) = -\frac{e^{-\sqrt{\xi^2-k^2}\,|y_2-x_2|}}{\sqrt{8\pi}\sqrt{\xi^2-k^2}}, \tag{3.62}$$

$$\widehat{G}_D(\xi;y_2,x_2) = \frac{e^{-\sqrt{\xi^2-k^2}\,(y_2+x_2)}}{\sqrt{8\pi}\sqrt{\xi^2-k^2}}, \tag{3.63}$$

$$\widehat{G}_L(\xi;y_2,x_2) = -\frac{iZ_\infty}{\xi_p}\sqrt{\frac{\pi}{2}}\, e^{-Z_\infty(y_2+x_2)} \big[\delta(\xi-\xi_p)+\delta(\xi+\xi_p)\big], \tag{3.64}$$

$$\widehat{G}_R(\xi;y_2,x_2) = \frac{e^{-\sqrt{\xi^2-k^2}\,(y_2+x_2)}}{\sqrt{2\pi}\left(Z_\infty-\sqrt{\xi^2-k^2}\right)}. \tag{3.65}$$

3.3.4 Spatial Green's function

a) Spatial Green's function as an inverse Fourier transform

The desired spatial Green's function is then given by the inverse Fourier transform of the spectral Green's function (3.60), namely by

$$\begin{aligned} G(\boldsymbol{x},\boldsymbol{y}) = &-\frac{1}{4\pi}\int_{-\infty}^{\infty}\frac{e^{-\sqrt{\xi^2-k^2}\,|y_2-x_2|}}{\sqrt{\xi^2-k^2}}\,e^{i\xi(y_1-x_1)}\mathrm{d}\xi \\ &+\frac{1}{4\pi}\int_{-\infty}^{\infty}\left(\frac{Z_\infty+\sqrt{\xi^2-k^2}}{Z_\infty-\sqrt{\xi^2-k^2}}\right)\frac{e^{-\sqrt{\xi^2-k^2}\,(y_2+x_2)}}{\sqrt{\xi^2-k^2}}\,e^{i\xi(y_1-x_1)}\mathrm{d}\xi \\ &-\frac{iZ_\infty}{\xi_p}\,e^{-Z_\infty(y_2+x_2)}\cos\big(\xi_p(y_1-x_1)\big). \end{aligned} \tag{3.66}$$

Due the linearity of the Fourier transform, the decomposition (3.61) applies also in the spatial domain, i.e., the spatial Green's function is decomposed in the same manner by

$$G = G_\infty + G_D + G_L + G_R. \tag{3.67}$$

b) Term of the full-plane Green's function

The first term in (3.66) corresponds to the inverse Fourier transform of (3.62), and is given by

$$G_\infty(\boldsymbol{x},\boldsymbol{y}) = -\frac{1}{4\pi}\int_{-\infty}^{\infty}\frac{e^{-\sqrt{\xi^2-k^2}\,|y_2-x_2|}}{\sqrt{\xi^2-k^2}}\,e^{i\xi(y_1-x_1)}\mathrm{d}\xi. \tag{3.68}$$

The value for this integral can be derived either from Magnus & Oberhettinger (1954, page 33 or 118), from Gradshteyn & Ryzhik (2007, equations 3.914–4 or 6.616–3), or from Bateman (1954, equation 1.13–59), and yields the result that

$$-\frac{1}{4\pi}\int_{-\infty}^{\infty}\frac{e^{-\sqrt{\xi^2-k^2}\,|y_2-x_2|}}{\sqrt{\xi^2-k^2}}\,e^{i\xi(y_1-x_1)}\,\mathrm{d}\xi = -\frac{i}{4}H_0^{(1)}\big(k|\boldsymbol{y}-\boldsymbol{x}|\big), \tag{3.69}$$

being $H_0^{(1)}$ the zeroth order Hankel function of the first kind (vid. Subsection A.2.4). This way, the inverse Fourier transform of (3.62) is readily given by

$$G_\infty(\boldsymbol{x},\boldsymbol{y}) = -\frac{i}{4}H_0^{(1)}\big(k|\boldsymbol{y}-\boldsymbol{x}|\big). \tag{3.70}$$

We observe that (3.70) is, in fact, the full-plane Green's function of the Helmholtz equation. Thus $G_D + G_L + G_R$ represents the perturbation of the full-plane Green's function G_∞ due the presence of the impedance half-plane.

c) Term associated with a Dirichlet boundary condition

The inverse Fourier transform of (3.63) is computed in the same manner as the term G_∞. It is given by

$$G_D(\boldsymbol{x},\boldsymbol{y}) = \frac{1}{4\pi}\int_{-\infty}^{\infty}\frac{e^{-\sqrt{\xi^2-k^2}\,(y_2+x_2)}}{\sqrt{\xi^2-k^2}}\,e^{i\xi(y_1-x_1)}\mathrm{d}\xi, \tag{3.71}$$

and in this case, instead of (3.69), we consider the relation

$$\frac{1}{4\pi}\int_{-\infty}^{\infty}\frac{e^{-\sqrt{\xi^2-k^2}\,(y_2+x_2)}}{\sqrt{\xi^2-k^2}}\,e^{i\xi(y_1-x_1)}\,\mathrm{d}\xi=\frac{i}{4}H_0^{(1)}\big(k|\boldsymbol{y}-\bar{\boldsymbol{x}}|\big),\tag{3.72}$$

where $\bar{\boldsymbol{x}}=(x_1,-x_2)$ corresponds to the image point of $\boldsymbol{x}$ in the lower half-plane. The inverse Fourier transform of (3.63) is therefore given by

$$G_D(\boldsymbol{x},\boldsymbol{y})=\frac{i}{4}H_0^{(1)}\big(k|\boldsymbol{y}-\bar{\boldsymbol{x}}|\big),\tag{3.73}$$

which represents the additional term that appears in the Green's function due the method of images when considering a Dirichlet boundary condition, as in (3.23).

d) Term associated with the limiting absorption principle

The term G_L, the inverse Fourier transform of (3.64), is associated with the effect of the limiting absorption principle on the Green's function, and has been already calculated in (3.58). It is given by

$$G_L(\boldsymbol{x},\boldsymbol{y})=-\frac{iZ_\infty}{\xi_p}\,e^{-Z_\infty(y_2+x_2)}\cos\big(\xi_p(y_1-x_1)\big).\tag{3.74}$$

e) Remaining term

The remaining term G_R, the inverse Fourier transform of (3.65), can be computed as the integral

$$G_R(\boldsymbol{x},\boldsymbol{y})=\frac{1}{2\pi}\int_{-\infty}^{\infty}\frac{e^{-\sqrt{\xi^2-k^2}\,(y_2+x_2)}}{Z_\infty-\sqrt{\xi^2-k^2}}\,e^{i\xi(y_1-x_1)}\,\mathrm{d}\xi.\tag{3.75}$$

To simplify the notation, we define

$$v_1=y_1-x_1\qquad\text{and}\qquad v_2=y_2+x_2,\tag{3.76}$$

and we consider

$$G_R(\boldsymbol{x},\boldsymbol{y})=e^{-Z_\infty v_2}G_B(v_1,v_2),\tag{3.77}$$

where

$$G_B(v_1,v_2)=\frac{e^{Z_\infty v_2}}{2\pi}\int_{-\infty}^{\infty}\frac{e^{-\sqrt{\xi^2-k^2}\,v_2}}{Z_\infty-\sqrt{\xi^2-k^2}}\,e^{i\xi v_1}\,\mathrm{d}\xi.\tag{3.78}$$

From the derivative of (3.72) with respect to y_2 we obtain that

$$\frac{1}{4\pi}\int_{-\infty}^{\infty}e^{-\sqrt{\xi^2-k^2}\,v_2}e^{i\xi v_1}\,\mathrm{d}\xi=\frac{ik}{4}H_1^{(1)}\big(k|\boldsymbol{y}-\bar{\boldsymbol{x}}|\big)\frac{v_2}{|\boldsymbol{y}-\bar{\boldsymbol{x}}|}.\tag{3.79}$$

Due (3.79), we have for the y_2-derivative of G_B that

$$\frac{\partial G_B}{\partial y_2}(v_1,v_2)=\frac{e^{Z_\infty v_2}}{2\pi}\int_{-\infty}^{\infty}e^{-\sqrt{\xi^2-k^2}\,v_2}e^{i\xi v_1}\,\mathrm{d}\xi=\frac{ik}{2}H_1^{(1)}\big(k|\boldsymbol{y}-\bar{\boldsymbol{x}}|\big)\frac{v_2\,e^{Z_\infty v_2}}{|\boldsymbol{y}-\bar{\boldsymbol{x}}|}.\tag{3.80}$$

The value of the inverse Fourier transform (3.75) can be thus obtained by means of the primitive with respect to y_2 of (3.80), i.e.,

$$G_R(\boldsymbol{x},\boldsymbol{y})=\frac{ik}{2}\,e^{-Z_\infty v_2}\int_{-\infty}^{v_2}H_1^{(1)}\Big(k\sqrt{v_1^2+\eta^2}\Big)\,\frac{\eta\,e^{Z_\infty\eta}}{\sqrt{v_1^2+\eta^2}}\,\mathrm{d}\eta.\tag{3.81}$$

The expression (3.81) contains an integral with an unbounded lower limit, but even so, due the exponential decrease of its integrand, it could be adapted to be well suited for numerical evaluation, as is done, e.g., in Chapter V. Its advantage lies in the fact that it expresses intuitively the term G_R as a primitive of known functions. We observe that further related expressions can be obtained through integration by parts, e.g.,

$$G_R(\boldsymbol{x},\boldsymbol{y}) = -\frac{i}{2}H_0^{(1)}\big(k|\boldsymbol{y}-\bar{\boldsymbol{x}}|\big) + \frac{iZ_\infty}{2}\,e^{-Z_\infty v_2}\int_{-\infty}^{v_2} H_0^{(1)}\Big(k\sqrt{v_1^2+\eta^2}\Big)\,e^{Z_\infty \eta}\,\mathrm{d}\eta. \quad (3.82)$$

Formulae of this kind seem to be absent in the literature, but they resemble in their structure the expressions described in Ochmann (2004) and Ochmann & Brick (2008) for the three-dimensional case.

In Hein (2006, 2007) and Durán, Hein & Nédélec (2007*b*), the remaining term G_R was computed numerically by using an inverse fast Fourier transform (IFFT) for the expression (3.75). In our case, due parity, we can consider the equivalent expression

$$G_R(\boldsymbol{x},\boldsymbol{y}) = \frac{1}{\pi}\int_0^\infty \frac{e^{-\sqrt{\xi^2-k^2}\,v_2}}{Z_\infty-\sqrt{\xi^2-k^2}}\cos(\xi v_1)\,\mathrm{d}\xi, \quad (3.83)$$

which can be likewise treated by using numerical integration. In both cases, the involved integrals become divergent when $v_2 < 0$. We note that the expression (3.83) has the advantage of requiring only half as many values as the one considered for the IFFT. It can be also observed that (3.75) and (3.83) are slowly decreasing when $v_2 = 0$ and decrease exponentially when $v_2 > 0$.

To obtain an expression that is practical for numerical computation and which holds for all $v_2 \in \mathbb{R}$, similarly as in Pidcock (1985), we can separate (3.81) according to

$$G_R(\boldsymbol{x},\boldsymbol{y}) = e^{-Z_\infty v_2}\left(G_B(v_1,0) + \frac{ik}{2}\int_0^{v_2} H_1^{(1)}\Big(k\sqrt{v_1^2+\eta^2}\Big)\,\frac{\eta\,e^{Z_\infty\eta}}{\sqrt{v_1^2+\eta^2}}\,\mathrm{d}\eta\right), \quad (3.84)$$

where

$$G_B(v_1,0) = \frac{1}{\pi}\int_0^\infty \frac{\cos(\xi v_1)}{Z_\infty-\sqrt{\xi^2-k^2}}\,\mathrm{d}\xi. \quad (3.85)$$

The expression (3.84) is valid for any $v_2 \in \mathbb{R}$ and it can be computed numerically without difficulty since the integration limits are bounded.

It remains to be discussed how to compute effectively (3.83) and (3.85), which requires to isolate the poles of the spectral Green's function and to treat adequately the slow decrease at infinity when $v_2 = 0$. When the impedance is comparatively bigger than the wave number, i.e., when $|Z_\infty| > |k|$, then both goals can be obtained simultaneously by considering the fact that

$$\frac{Z_\infty}{\pi\xi_p}\int_0^\infty \frac{e^{-Z_\infty\xi v_2/\xi_p}}{\xi_p-\xi}\cos(\xi v_1)\,\mathrm{d}\xi = \frac{Z_\infty}{2\pi\xi_p}\,e^{-Z_\infty v_2}\Big\{e^{i\xi_p v_1}\,\mathrm{Ei}(Z_\infty v_2 - i\xi_p v_1) + e^{-i\xi_p v_1}\,\mathrm{Ei}(Z_\infty v_2 + i\xi_p v_1)\Big\}. \quad (3.86)$$

which is computed analogously as done for the Laplace equation in (2.93). The expression in the left-hand side of (3.86) contains completely the behavior of the poles in the spectral domain and includes most of the slow decrease at infinity, which improves as $|Z_\infty| \to \infty$. As a consequence, (3.83) can be computed more effectively as

$$G_R(\boldsymbol{x},\boldsymbol{y}) = \frac{1}{\pi}\int_0^\infty \left(\frac{e^{-\sqrt{\xi^2-k^2}\,v_2}}{Z_\infty - \sqrt{\xi^2-k^2}} - \frac{Z_\infty}{\xi_p}\,\frac{e^{-Z_\infty \xi v_2/\xi_p}}{\xi_p - \xi} \right) \cos(\xi v_1)\,\mathrm{d}\xi$$
$$+ \frac{Z_\infty}{2\pi\xi_p}\,e^{-Z_\infty v_2}\Big\{ e^{i\xi_p v_1}\,\mathrm{Ei}(Z_\infty v_2 - i\xi_p v_1) + e^{-i\xi_p v_1}\,\mathrm{Ei}(Z_\infty v_2 + i\xi_p v_1)\Big\}, \quad (3.87)$$

where Ei denotes the exponential integral function (vid. Subsection A.2.3). The integral in (3.87) is computed numerically. When the impedance is smaller than the wave number, i.e., when $|Z_\infty| < |k|$, then the expression inside the integral in (3.87) does no longer behave so well numerically and it becomes more convenient to remove the poles and the slow decrease independently. For the poles, as computed in (2.59), it holds that

$$\frac{2Z_\infty}{\pi}\,e^{-Z_\infty v_2}\int_0^\infty \frac{\cos(\xi v_1)}{\xi_p^2 - \xi^2}\,\mathrm{d}\xi = -\frac{iZ_\infty}{\xi_p}\,e^{-Z_\infty v_2}e^{i\xi_p|v_1|}. \quad (3.88)$$

When k is near the real axis, then for the slow decrease at infinity it holds that

$$\frac{1}{\pi}\int_0^\infty \frac{e^{-\sqrt{\xi^2+k^2}\,v_2}}{\sqrt{\xi^2+k^2}}\cos(\xi v_1)\,\mathrm{d}\xi = \frac{i}{2}H_0^{(1)}\big(ik|\boldsymbol{y}-\bar{\boldsymbol{x}}|\big) = \frac{1}{\pi}K_0\big(k|\boldsymbol{y}-\bar{\boldsymbol{x}}|\big), \quad (3.89)$$

where K_0 denotes the modified Bessel function of the second kind of order zero (vid. Subsection A.2.5). Hence, when $|Z_\infty| < |k|$ and $\arg(k) < \pi/4$, then (3.83) can be computed more effectively as

$$G_R(\boldsymbol{x},\boldsymbol{y}) = \frac{1}{\pi}\int_0^\infty \left(\frac{e^{-\sqrt{\xi^2-k^2}\,v_2}}{Z_\infty - \sqrt{\xi^2-k^2}} - \frac{2Z_\infty e^{-Z_\infty v_2}}{\xi_p^2-\xi^2} - \frac{e^{-\sqrt{\xi^2+k^2}\,v_2}}{\sqrt{\xi^2+k^2}} \right)\cos(\xi v_1)\,\mathrm{d}\xi$$
$$- \frac{iZ_\infty}{\xi_p}\,e^{-Z_\infty v_2}e^{i\xi_p|v_1|} + \frac{i}{2}H_0^{(1)}\big(ik|\boldsymbol{y}-\bar{\boldsymbol{x}}|\big). \quad (3.90)$$

When k is near the imaginary axis, then instead of (3.89) it is better to consider for the slow decrease at infinity the expression

$$\frac{1}{\pi}\int_0^\infty \frac{e^{-\sqrt{\xi^2-k^2}\,v_2}}{\sqrt{\xi^2-k^2}}\cos(\xi v_1)\,\mathrm{d}\xi = \frac{i}{2}H_0^{(1)}\big(k|\boldsymbol{y}-\bar{\boldsymbol{x}}|\big), \quad (3.91)$$

Now, when $|Z_\infty| < |k|$ and $\arg(k) > \pi/4$, then (3.83) is computed more effectively as

$$G_R(\boldsymbol{x},\boldsymbol{y}) = \frac{1}{\pi}\int_0^\infty \left(\frac{e^{-\sqrt{\xi^2-k^2}\,v_2}}{Z_\infty - \sqrt{\xi^2-k^2}} - \frac{2Z_\infty e^{-Z_\infty v_2}}{\xi_p^2-\xi^2} - \frac{e^{-\sqrt{\xi^2-k^2}\,v_2}}{\sqrt{\xi^2-k^2}} \right)\cos(\xi v_1)\,\mathrm{d}\xi$$
$$- \frac{iZ_\infty}{\xi_p}\,e^{-Z_\infty v_2}e^{i\xi_p|v_1|} + \frac{i}{2}H_0^{(1)}\big(k|\boldsymbol{y}-\bar{\boldsymbol{x}}|\big). \quad (3.92)$$

The expressions (3.87), (3.90), and (3.92) are likewise valid when $v_2 = 0$, which allows to evaluate the term G_B in (3.85).

f) Complete spatial Green's function

The desired complete spatial Green's function is finally obtained, as stated in (3.67), by adding the terms (3.70), (3.73), (3.74), and (3.81). It can be appreciated graphically in Figures 3.5 & 3.6 for $k = 1.2$, $Z_\infty = 1$, and $\boldsymbol{x} = (0, 2)$, and it is given explicitly by

$$G(\boldsymbol{x}, \boldsymbol{y}) = -\frac{i}{4} H_0^{(1)}\big(k|\boldsymbol{y} - \boldsymbol{x}|\big) + \frac{i}{4} H_0^{(1)}\big(k|\boldsymbol{y} - \bar{\boldsymbol{x}}|\big) - \frac{iZ_\infty}{\xi_p}\, e^{-Z_\infty v_2} \cos(\xi_p v_1) + \frac{ik}{2}\, e^{-Z_\infty v_2} \int_{-\infty}^{v_2} H_1^{(1)}\Big(k\sqrt{v_1^2 + \eta^2}\Big)\, \frac{\eta\, e^{Z_\infty \eta}}{\sqrt{v_1^2 + \eta^2}}\, \mathrm{d}\eta, \tag{3.93}$$

where we use the notation (3.76). The integral in (3.93) can be computed either as (3.83) or as (3.84), depending on wether $v_2 > 0$ or $v_2 < 0$. The involved Fourier integrals of the remaining term G_R are computed according to the expressions (3.87), (3.90), and (3.92).

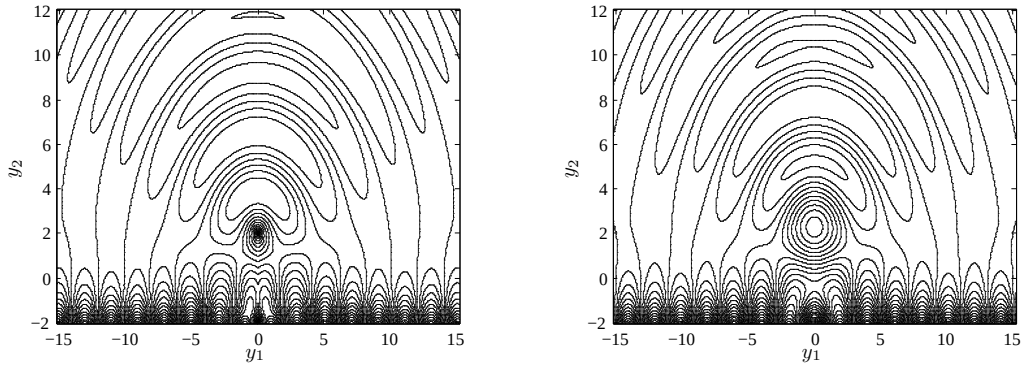

(a) Real part (b) Imaginary part

FIGURE 3.5. Contour plot of the complete spatial Green's function.

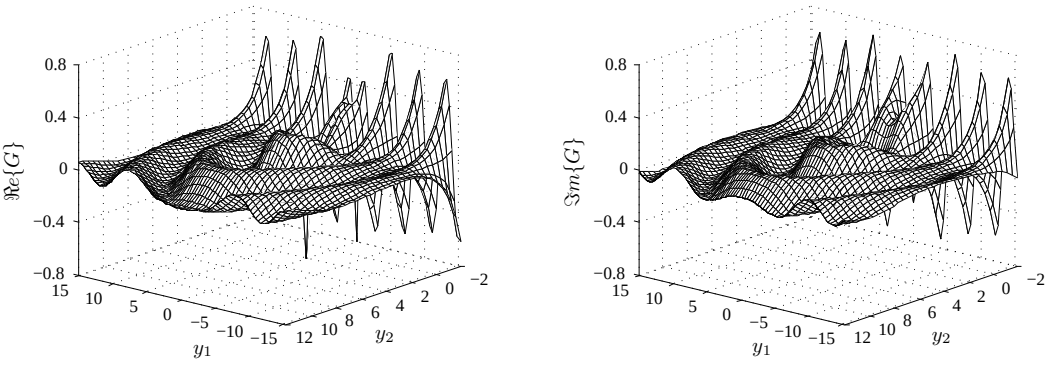

(a) Real part (b) Imaginary part

FIGURE 3.6. Oblique view of the complete spatial Green's function.

For the derivative of the Green's function with respect to the y_2-variable, it holds that

$$\frac{\partial G}{\partial y_2}(\boldsymbol{x},\boldsymbol{y}) = \frac{ik}{4}H_1^{(1)}\big(k|\boldsymbol{y}-\boldsymbol{x}|\big)\frac{y_2-x_2}{|\boldsymbol{y}-\boldsymbol{x}|} + \frac{ik}{4}H_1^{(1)}\big(k|\boldsymbol{y}-\bar{\boldsymbol{x}}|\big)\frac{v_2}{|\boldsymbol{y}-\bar{\boldsymbol{x}}|}$$
$$+ \frac{iZ_\infty^2}{\xi_p}\,e^{-Z_\infty v_2}\cos(\xi_p v_1) - \frac{ikZ_\infty}{2}\,e^{-Z_\infty v_2}\int_{-\infty}^{v_2} H_1^{(1)}\Big(k\sqrt{v_1^2+\eta^2}\Big)\,\frac{\eta\,e^{Z_\infty\eta}}{\sqrt{v_1^2+\eta^2}}\,\mathrm{d}\eta. \quad (3.94)$$

The integral in (3.94) is computed the same way as in (3.93). The derivative with respect to the y_1-variable, on the other hand, is given by

$$\frac{\partial G}{\partial y_1}(\boldsymbol{x},\boldsymbol{y}) = \frac{ik}{4}H_1^{(1)}\big(k|\boldsymbol{y}-\boldsymbol{x}|\big)\frac{v_1}{|\boldsymbol{y}-\boldsymbol{x}|} - \frac{ik}{4}H_1^{(1)}\big(k|\boldsymbol{y}-\bar{\boldsymbol{x}}|\big)\frac{v_1}{|\boldsymbol{y}-\bar{\boldsymbol{x}}|}$$
$$+ iZ_\infty e^{-Z_\infty v_2}\sin(\xi_p v_1) + \frac{ik^2}{2}\,e^{-Z_\infty v_2}\int_{-\infty}^{v_2} H_0^{(1)}\Big(k\sqrt{v_1^2+\eta^2}\Big)\,\frac{v_1^2}{v_1^2+\eta^2}\,e^{Z_\infty\eta}\,\mathrm{d}\eta$$
$$+ \frac{ik}{2}\,e^{-Z_\infty v_2}\int_{-\infty}^{v_2} H_1^{(1)}\Big(k\sqrt{v_1^2+\eta^2}\Big)\,\frac{\eta^2-v_1^2}{(v_1^2+\eta^2)^{3/2}}\,e^{Z_\infty\eta}\,\mathrm{d}\eta. \quad (3.95)$$

The integrals in (3.95) are related with the remaining term G_R and are computed respectively as the y_1-derivative of (3.84), (3.87), (3.90), and (3.92), e.g., the y_1-derivative of the Fourier integral (3.83) becomes

$$\frac{\partial G_R}{\partial y_1}(\boldsymbol{x},\boldsymbol{y}) = -\frac{1}{\pi}\int_0^\infty \frac{\xi\,e^{-\sqrt{\xi^2-k^2}\,v_2}}{Z_\infty-\sqrt{\xi^2-k^2}}\sin(\xi v_1)\,\mathrm{d}\xi. \quad (3.96)$$

The other cases are modified analogously.

3.3.5 Extension and properties

The half-plane Green's function can be extended in a locally analytic way towards the full-plane $\mathbb{R}^2$ in a straightforward and natural manner, just by considering the expression (3.93) valid for all $\boldsymbol{x},\boldsymbol{y}\in\mathbb{R}^2$, instead of just for $\mathbb{R}^2_+$. This extension possesses two singularities of logarithmic type at the points $\boldsymbol{x}$ and $\bar{\boldsymbol{x}}$, and is continuous otherwise. The behavior of these singularities is characterized by

$$G(\boldsymbol{x},\boldsymbol{y}) \sim \frac{1}{2\pi}\ln|\boldsymbol{y}-\boldsymbol{x}|, \qquad \boldsymbol{y}\longrightarrow\boldsymbol{x}, \quad (3.97)$$

$$G(\boldsymbol{x},\boldsymbol{y}) \sim \frac{1}{2\pi}\ln|\boldsymbol{y}-\bar{\boldsymbol{x}}|, \qquad \boldsymbol{y}\longrightarrow\bar{\boldsymbol{x}}. \quad (3.98)$$

For the y_1-derivative there appears a jump across the half-line $\Upsilon=\{y_1=x_1, y_2<-x_2\}$, due the effect of the analytic branch cut of the exponential integral functions, shown in Figure 3.7. We denote this jump by

$$J(\boldsymbol{x},\boldsymbol{y}) = \lim_{y_1\to x_1^+}\left\{\frac{\partial G}{\partial y_1}\right\} - \lim_{y_1\to x_1^-}\left\{\frac{\partial G}{\partial y_1}\right\} = \frac{\partial G}{\partial y_1^+}\bigg|_{y_1=x_1} - \frac{\partial G}{\partial y_1^-}\bigg|_{y_1=x_1}. \quad (3.99)$$

This jump across Υ is the same as for the Laplace equation in (2.104), since the involved singularities are the same, i.e., it has a value of

$$J(\boldsymbol{x},\boldsymbol{y}) = 2Z_\infty e^{-Z_\infty(y_2+x_2)}. \quad (3.100)$$

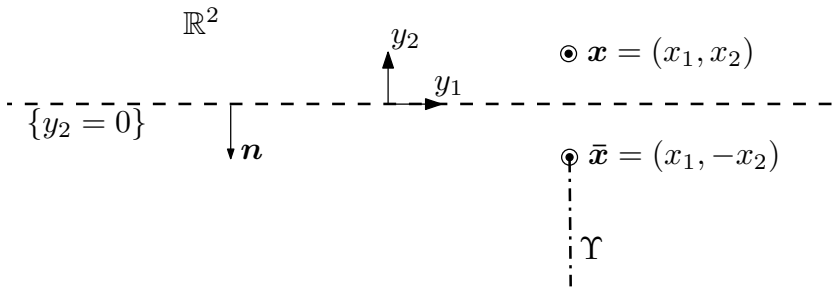

FIGURE 3.7. Domain of the extended Green's function.

We remark that the Green's function (3.93) itself and its y_2-derivative are continuous across the half-line Υ.

As long as $x_2 \neq 0$, it is clear that the impedance boundary condition in (3.20) continues to be homogeneous. Nonetheless, if the source point $\boldsymbol{x}$ lies on the half-plane's boundary, i.e., if $x_2 = 0$, then the boundary condition ceases to be homogeneous in the sense of distributions. This can be deduced from the expression (3.66) by verifying that

$$\lim_{y_2 \to 0^+} \left\{ \frac{\partial G}{\partial y_2}\big((x_1, 0), \boldsymbol{y}\big) + Z_\infty G\big((x_1, 0), \boldsymbol{y}\big) \right\} = \delta_{x_1}(y_1). \tag{3.101}$$

Since the impedance boundary condition holds only on $\{y_2 = 0\}$, therefore the right-hand side of (3.101) can be also expressed by

$$\delta_{x_1}(y_1) = \frac{1}{2}\delta_{\boldsymbol{x}}(\boldsymbol{y}) + \frac{1}{2}\delta_{\bar{\boldsymbol{x}}}(\boldsymbol{y}), \tag{3.102}$$

which illustrates more clearly the contribution of each logarithmic singularity to the Dirac mass in the boundary condition.

It can be seen now that the Green's function extended in the abovementioned way satisfies, for $\boldsymbol{x} \in \mathbb{R}^2$, in the sense of distributions, and instead of (3.20), the problem

$$\begin{cases} \text{Find } G(\boldsymbol{x}, \cdot) : \mathbb{R}^2 \to \mathbb{C} \text{ such that} \\ \Delta_{\boldsymbol{y}} G(\boldsymbol{x}, \boldsymbol{y}) + k^2 G(\boldsymbol{x}, \boldsymbol{y}) = \delta_{\boldsymbol{x}}(\boldsymbol{y}) + \delta_{\bar{\boldsymbol{x}}}(\boldsymbol{y}) + J(\boldsymbol{x}, \boldsymbol{y})\delta_\Upsilon(\boldsymbol{y}) \quad \text{in } \mathcal{D}'(\mathbb{R}^2), \\ \dfrac{\partial G}{\partial y_2}(\boldsymbol{x}, \boldsymbol{y}) + Z_\infty G(\boldsymbol{x}, \boldsymbol{y}) = \dfrac{1}{2}\delta_{\boldsymbol{x}}(\boldsymbol{y}) + \dfrac{1}{2}\delta_{\bar{\boldsymbol{x}}}(\boldsymbol{y}) \quad \text{on } \{y_2 = 0\}, \\ + \text{ Outgoing radiation condition for } \boldsymbol{y} \in \mathbb{R}^2_+ \text{ as } |\boldsymbol{y}| \to \infty, \end{cases} \tag{3.103}$$

where δ_Υ denotes a Dirac mass distribution along the Υ-curve. We retrieve thus the known result that for an impedance boundary condition the image of a point source is a point source plus a half-line of sources with exponentially increasing strengths in the lower half-plane, and which extends from the image point source towards infinity along the half-plane's normal direction (cf. Keller 1979, who refers to decreasing strengths when dealing with the opposite half-plane).

We note that the half-plane Green's function (3.93) is symmetric in the sense that

$$G(\boldsymbol{x}, \boldsymbol{y}) = G(\boldsymbol{y}, \boldsymbol{x}) \qquad \forall \boldsymbol{x}, \boldsymbol{y} \in \mathbb{R}^2, \tag{3.104}$$

and it fulfills similarly

$$\nabla_{\boldsymbol{y}} G(\boldsymbol{x},\boldsymbol{y}) = \nabla_{\boldsymbol{y}} G(\boldsymbol{y},\boldsymbol{x}) \qquad \text{and} \qquad \nabla_{\boldsymbol{x}} G(\boldsymbol{x},\boldsymbol{y}) = \nabla_{\boldsymbol{x}} G(\boldsymbol{y},\boldsymbol{x}). \tag{3.105}$$

Another property is that we retrieve the special case (3.23) of a homogenous Dirichlet boundary condition in $\mathbb{R}^2_+$ when $Z_\infty \to \infty$. Likewise, we retrieve the special case (3.25) of a homogenous Neumann boundary condition in $\mathbb{R}^2_+$ when $Z_\infty \to 0$, except for an additive constant due the extra term (3.74) that can be disregarded.

At last, we observe that the expression for the Green's function (3.93) is still valid if a complex wave number $k \in \mathbb{C}$, such that $\mathfrak{Im}\{k\} > 0$ and $\mathfrak{Re}\{k\} \geq 0$, and a complex impedance $Z_\infty \in \mathbb{C}$, such that $\mathfrak{Im}\{Z_\infty\} > 0$ and $\mathfrak{Re}\{Z_\infty\} \geq 0$, are used, which holds also for its derivatives. The logarithms, though, have to be interpreted analogously as in (2.111) and (2.112) to avoid an undesired behavior in the lower half-plane, i.e., as

$$\ln\big(Z_\infty v_2 - i\xi_p v_1\big) = \ln\big(v_2 - i v_1 \xi_p / Z_\infty\big) + \ln(Z_\infty), \tag{3.106}$$

$$\ln\big(Z_\infty v_2 + i\xi_p v_1\big) = \ln\big(v_2 + i v_1 \xi_p / Z_\infty\big) + \ln(Z_\infty), \tag{3.107}$$

where the principal value is considered for the logarithms on the right-hand side.

3.4 Far field of the Green's function

3.4.1 Decomposition of the far field

The far field of the Green's function, which we denote by G^{ff}, describes its asymptotic behavior at infinity, i.e., when $|\boldsymbol{x}| \to \infty$ and assuming that $\boldsymbol{y}$ is fixed. For this purpose, the terms of highest order at infinity are searched. Likewise as done for the radiation condition, the far field can be decomposed into two parts, each acting on a different region as shown in Figure 3.2. The first part, denoted by G^{ff}_V, is linked with the volume waves, and acts in the interior of the half-plane while vanishing near its boundary. The second part, denoted by G^{ff}_S, is associated with surface waves that propagate along the boundary towards infinity, which decay exponentially towards the half-plane's interior. We have thus that

$$G^{ff} = G^{ff}_V + G^{ff}_S. \tag{3.108}$$

3.4.2 Volume waves in the far field

The volume waves in the far field act only in the interior of the half-plane and are related to the terms of the Hankel functions in (3.93), and also to the asymptotic behavior as $x_2 \to \infty$ of the regular part. The behavior of the volume waves can be obtained by applying the stationary phase technique on the integrals in (3.66), as performed by Durán, Muga & Nédélec (2005*a*, 2006). This technique gives an expression for the leading asymptotic behavior of highly oscillating integrals in the form of

$$I(\lambda) = \int_a^b f(s) e^{i\lambda\phi(s)}\,\mathrm{d}s, \tag{3.109}$$

as $\lambda \to \infty$ along the positive real axis, where $\phi(s)$ is a regular real function, where $|f(s)|$ is integrable, and where the real integration limits a and b may be unbounded. Further

references on the stationary phase technique are Bender & Orszag (1978), Dettman (1984), Evans (1998), and Watson (1944). Integrals in the form of (3.109) are called generalized Fourier integrals. They tend towards zero very rapidly with λ, except at the so-called stationary points for which the derivative of the phase becomes zero, where the integrand vanishes less rapidly. If s_0 is such a stationary point, i.e., if $\phi'(s_0) = 0$, and if $\phi''(s_0) > 0$, then the main asymptotic contribution of the integral (3.109) is given by

$$I(\lambda) \sim e^{i\pi/4} \sqrt{\frac{2\pi}{\lambda \phi''(s_0)}}\, f(s_0) e^{i\lambda\phi(s_0)}. \tag{3.110}$$

Moreover, the residue is uniformly bounded by $C\lambda^{-3/2}$ for some constant $C > 0$ if the point s_0 is not an end-point of the integration domain.

The asymptotic behavior of the volume waves is related with the terms in (3.66) which do not decrease exponentially as $x_2 \to \infty$, i.e., with the integral terms for which $\sqrt{\xi^2 - k^2}$ is purely imaginary, which occurs when $|\xi| < k$. Hence, as $x_2 \to \infty$ it holds that

$$\begin{aligned} G(\boldsymbol{x}, \boldsymbol{y}) \sim & -\frac{1}{4\pi} \int_{|\xi|<k} \frac{e^{-\sqrt{\xi^2-k^2}\,|x_2-y_2|}}{\sqrt{\xi^2-k^2}}\, e^{-i\xi(x_1-y_1)} \mathrm{d}\xi \\ & + \frac{1}{4\pi} \int_{|\xi|<k} \left(\frac{Z_\infty + \sqrt{\xi^2-k^2}}{Z_\infty - \sqrt{\xi^2-k^2}} \right) \frac{e^{-\sqrt{\xi^2-k^2}\,(x_2+y_2)}}{\sqrt{\xi^2-k^2}}\, e^{-i\xi(x_1-y_1)} \mathrm{d}\xi. \end{aligned} \tag{3.111}$$

By using the change of variable $\xi = -k\cos\psi$, for $0 \le \psi \le \pi$, we obtain that

$$G(\boldsymbol{x}, \boldsymbol{y}) \sim \frac{i}{4\pi} \int_0^\pi \left(-1 + \frac{Z_\infty - ik\sin\psi}{Z_\infty + ik\sin\psi}\, e^{2iky_2\sin\psi} \right) e^{ik|\boldsymbol{x}-\boldsymbol{y}|\cos(\psi-\alpha)} \mathrm{d}\psi, \tag{3.112}$$

where α is such that

$$\cos\alpha = \frac{x_1 - y_1}{|\boldsymbol{x}-\boldsymbol{y}|} \qquad \text{and} \qquad \sin\alpha = \frac{x_2 - y_2}{|\boldsymbol{x}-\boldsymbol{y}|}. \tag{3.113}$$

The phase $\phi(\psi) = k\cos(\psi - \alpha)$ has only one stationary point, namely $\psi = \alpha$, which lies inside the interval $(0, \pi)$. Hence, from (3.110) we obtain that

$$G(\boldsymbol{x}, \boldsymbol{y}) \sim \frac{e^{i\pi/4}}{\sqrt{8\pi k}} \frac{e^{ik|\boldsymbol{x}-\boldsymbol{y}|}}{\sqrt{|\boldsymbol{x}-\boldsymbol{y}|}} \left(-1 + \frac{Z_\infty - ik\sin\alpha}{Z_\infty + ik\sin\alpha}\, e^{2iky_2\sin\alpha} \right), \tag{3.114}$$

Due the asymptotic behavior (A.139) of the Hankel function $H_0^{(1)}$, it holds that

$$H_0^{(1)}\big(k|\boldsymbol{x}-\boldsymbol{y}|\big) \sim e^{-i\pi/4} \sqrt{\frac{2}{\pi k}} \frac{e^{ik|\boldsymbol{x}-\boldsymbol{y}|}}{\sqrt{|\boldsymbol{x}-\boldsymbol{y}|}}, \tag{3.115}$$

$$H_0^{(1)}\big(k|\boldsymbol{x}-\bar{\boldsymbol{y}}|\big) \sim e^{-i\pi/4} \sqrt{\frac{2}{\pi k}} \frac{e^{ik|\boldsymbol{x}-\bar{\boldsymbol{y}}|}}{\sqrt{|\boldsymbol{x}-\bar{\boldsymbol{y}}|}}, \tag{3.116}$$

as $|\boldsymbol{x}| \to \infty$, where $\bar{\boldsymbol{y}} = (y_1, -y_2)$. Since $|\boldsymbol{x}-\bar{\boldsymbol{y}}| \sim |\boldsymbol{x}-\boldsymbol{y}|$ as $x_2 \to \infty$, this implies that the asymptotic behavior (3.114) can be equivalently stated as

$$G(\boldsymbol{x}, \boldsymbol{y}) \sim -\frac{i}{4} H_0^{(1)}\big(k|\boldsymbol{x}-\boldsymbol{y}|\big) + \frac{i}{4} \left(\frac{Z_\infty - ik\sin\alpha}{Z_\infty + ik\sin\alpha} \right) H_0^{(1)}\big(k|\boldsymbol{x}-\bar{\boldsymbol{y}}|\big). \tag{3.117}$$

By performing Taylor expansions, as in (C.37) and (C.38), we have that

$$\frac{e^{ik|\boldsymbol{x}-\boldsymbol{y}|}}{\sqrt{|\boldsymbol{x}-\boldsymbol{y}|}} = \frac{e^{ik|\boldsymbol{x}|}}{\sqrt{|\boldsymbol{x}|}}\, e^{-ik\boldsymbol{y}\cdot\boldsymbol{x}/|\boldsymbol{x}|} \left(1 + \mathcal{O}\Big(\frac{1}{|\boldsymbol{x}|}\Big)\right), \tag{3.118}$$

$$\frac{e^{ik|\boldsymbol{x}-\bar{\boldsymbol{y}}|}}{\sqrt{|\boldsymbol{x}-\bar{\boldsymbol{y}}|}} = \frac{e^{ik|\boldsymbol{x}|}}{\sqrt{|\boldsymbol{x}|}}\, e^{-ik\bar{\boldsymbol{y}}\cdot\boldsymbol{x}/|\boldsymbol{x}|} \left(1 + \mathcal{O}\Big(\frac{1}{|\boldsymbol{x}|}\Big)\right). \tag{3.119}$$

We express the point $\boldsymbol{x}$ as $\boldsymbol{x} = |\boldsymbol{x}|\,\hat{\boldsymbol{x}}$, being $\hat{\boldsymbol{x}} = (\cos\theta, \sin\theta)$ a unitary vector. Similar Taylor expansions as before yield that

$$\frac{Z_\infty - ik\sin\alpha}{Z_\infty + ik\sin\alpha} = \frac{Z_\infty - ik\sin\theta}{Z_\infty + ik\sin\theta} \left(1 + \mathcal{O}\Big(\frac{1}{|\boldsymbol{x}|}\Big)\right). \tag{3.120}$$

The volume-wave behavior of the Green's function, from (3.114) and due (3.118), (3.119), and (3.120), becomes thus

$$G_V^{ff}(\boldsymbol{x},\boldsymbol{y}) = \frac{e^{i\pi/4}}{\sqrt{8\pi k}} \frac{e^{ik|\boldsymbol{x}|}}{\sqrt{|\boldsymbol{x}|}}\, e^{-ik\hat{\boldsymbol{x}}\cdot\boldsymbol{y}} \left(-1 + \frac{Z_\infty - ik\sin\theta}{Z_\infty + ik\sin\theta}\, e^{2iky_2\sin\theta}\right), \tag{3.121}$$

and its gradient with respect to $\boldsymbol{y}$ is given by

$$\nabla_{\boldsymbol{y}} G_V^{ff}(\boldsymbol{x},\boldsymbol{y}) = e^{-i\pi/4}\sqrt{\frac{k}{8\pi}}\, \frac{e^{ik|\boldsymbol{x}|}}{\sqrt{|\boldsymbol{x}|}}\, e^{-ik\hat{\boldsymbol{x}}\cdot\boldsymbol{y}} \left(-\hat{\boldsymbol{x}} + \frac{Z_\infty - ik\sin\theta}{Z_\infty + ik\sin\theta}\, e^{2iky_2\sin\theta} \begin{bmatrix} \cos\theta \\ -\sin\theta \end{bmatrix}\right). \tag{3.122}$$

3.4.3 Surface waves in the far field

An expression for the surface waves in the far field can be obtained by studying the residues of the poles of the spectral Green's function, which determine entirely their asymptotic behavior. We already computed the inverse Fourier transform of these residues in (3.55), using the residue theorem of Cauchy and the limiting absorption principle. This implies that the Green's function behaves asymptotically, when $|x_1| \to \infty$, as

$$G(\boldsymbol{x},\boldsymbol{y}) \sim -\frac{iZ_\infty}{\xi_p}\, e^{-Z_\infty(x_2+y_2)} e^{i\xi_p|x_1-y_1|}, \tag{3.123}$$

where $\xi_p = \sqrt{Z_\infty^2 + k^2}$. More detailed computations can be found in Durán, Muga & Nédélec (2005*a*, 2006). Similarly as in (C.36), we can use Taylor expansions to obtain

$$|x_1 - y_1| = |x_1| - y_1 \operatorname{sign} x_1 + \mathcal{O}\Big(\frac{1}{|x_1|}\Big). \tag{3.124}$$

Therefore, as for (C.38), we have that

$$e^{i\xi_p|x_1-y_1|} = e^{i\xi_p|x_1|} e^{-i\xi_p y_1 \operatorname{sign} x_1} \left(1 + \mathcal{O}\Big(\frac{1}{|x_1|}\Big)\right). \tag{3.125}$$

The surface-wave behavior of the Green's function, due (3.123) and (3.125), becomes thus

$$G_S^{ff}(\boldsymbol{x},\boldsymbol{y}) = -\frac{iZ_\infty}{\xi_p}\, e^{-Z_\infty x_2} e^{i\xi_p|x_1|} e^{-Z_\infty y_2} e^{-i\xi_p y_1 \operatorname{sign} x_1}, \tag{3.126}$$

and its gradient with respect to $\boldsymbol{y}$ is given by

$$\nabla_{\boldsymbol{y}} G_S^{ff}(\boldsymbol{x},\boldsymbol{y}) = -\frac{Z_\infty}{\xi_p}\, e^{-Z_\infty x_2} e^{i\xi_p|x_1|} e^{-Z_\infty y_2} e^{-i\xi_p y_1 \operatorname{sign} x_1} \begin{bmatrix} \xi_p \operatorname{sign} x_1 \\ -iZ_\infty \end{bmatrix}. \tag{3.127}$$

3.4.4 Complete far field of the Green's function

On the whole, the asymptotic behavior of the Green's function as $|\boldsymbol{x}| \to \infty$ can be characterized through the addition of (3.117) and (3.123), namely

$$\begin{aligned} G(\boldsymbol{x},\boldsymbol{y}) \sim & -\frac{i}{4} H_0^{(1)}\big(k|\boldsymbol{x}-\boldsymbol{y}|\big) + \frac{i}{4}\left(\frac{Z_\infty - ik\sin\alpha}{Z_\infty + ik\sin\alpha}\right) H_0^{(1)}\big(k|\boldsymbol{x}-\bar{\boldsymbol{y}}|\big) \\ & - \frac{iZ_\infty}{\xi_p}\, e^{-Z_\infty(x_2+y_2)} e^{i\xi_p|x_1-y_1|}. \end{aligned} \tag{3.128}$$

Consequently, the complete far field of the Green's function, due (3.108), is given by the addition of (3.121) and (3.126), i.e., by

$$\begin{aligned} G^{ff}(\boldsymbol{x},\boldsymbol{y}) = & \frac{e^{i\pi/4}}{\sqrt{8\pi k}} \frac{e^{ik|\boldsymbol{x}|}}{\sqrt{|\boldsymbol{x}|}}\, e^{-ik\hat{\boldsymbol{x}}\cdot\boldsymbol{y}} \left(-1 + \frac{Z_\infty - ik\sin\theta}{Z_\infty + ik\sin\theta}\, e^{2iky_2\sin\theta}\right) \\ & - \frac{iZ_\infty}{\xi_p}\, e^{-Z_\infty x_2} e^{i\xi_p|x_1|} e^{-Z_\infty y_2} e^{-i\xi_p y_1 \operatorname{sign} x_1}. \end{aligned} \tag{3.129}$$

Its derivative with respect to $\boldsymbol{y}$ is likewise given by the addition of (3.122) and (3.127).

It is this far field (3.129) that justifies the radiation condition (3.21) when exchanging the roles of $\boldsymbol{x}$ and $\boldsymbol{y}$. When the first term in (3.129) dominates, i.e., the volume waves (3.121), then it is the first expression in (3.21) that matters. Conversely, when the second term in (3.129) dominates, i.e., the surface waves (3.126), then the second expression in (3.21) is the one that holds. The interface between both asymptotic behaviors can be determined by equating the amplitudes of the two terms in (3.129), i.e., by searching values of $\boldsymbol{x}$ at infinity such that

$$\frac{1}{\sqrt{8\pi k|\boldsymbol{x}|}} = \frac{Z_\infty}{\xi_p}\, e^{-Z_\infty x_2}, \tag{3.130}$$

where the values of $\boldsymbol{y}$ can be neglected, since they remain relatively near the origin. By taking the logarithm in (3.130) and perturbing somewhat the result so as to avoid a singular behavior at the origin, we obtain finally that this interface is described by

$$x_2 = \frac{1}{Z_\infty} \ln\left(1 + \frac{8\pi k Z_\infty^2}{Z_\infty^2 + k^2}|\boldsymbol{x}|\right). \tag{3.131}$$

We remark that the asymptotic behavior (3.128) of the Green's function and the expression (3.129) of its complete far field do no longer hold if a complex impedance $Z_\infty \in \mathbb{C}$ such that $\mathfrak{Im}\{Z_\infty\} > 0$ and $\mathfrak{Re}\{Z_\infty\} \geq 0$ is used, specifically the parts (3.123) and (3.126) linked with the surface waves. A careful inspection shows that in this case the surface-wave

behavior of the Green's function, as $|x_1| \to \infty$, decreases exponentially and is given by

$$G(\boldsymbol{x},\boldsymbol{y}) \sim \begin{cases} -\dfrac{iZ_\infty}{\xi_p}\, e^{-|Z_\infty|(x_2+y_2)} e^{i\xi_p|x_1-y_1|} & \text{if } (x_2+y_2) > 0, \\ -\dfrac{iZ_\infty}{\xi_p}\, e^{-Z_\infty(x_2+y_2)} e^{i\xi_p|x_1-y_1|} & \text{if } (x_2+y_2) \leq 0. \end{cases} \tag{3.132}$$

Therefore the surface-wave part of the far field can be now expressed as

$$G_S^{ff}(\boldsymbol{x},\boldsymbol{y}) = \begin{cases} -\dfrac{iZ_\infty}{\xi_p}\, e^{-|Z_\infty|\, x_2} e^{i\xi_p|x_1|} e^{-|Z_\infty|\, y_2} e^{-i\xi_p y_1 \operatorname{sign} x_1} & \text{if } x_2 > 0, \\ -\dfrac{iZ_\infty}{\xi_p}\, e^{-Z_\infty x_2} e^{i\xi_p|x_1|} e^{-Z_\infty y_2} e^{-i\xi_p y_1 \operatorname{sign} x_1} & \text{if } x_2 \leq 0. \end{cases} \tag{3.133}$$

The volume-waves part (3.117) and its far-field expression (3.121), on the other hand, remain the same when we use a complex impedance. We remark further that if a complex impedance or a complex wave number are taken into account, then the part of the surface waves of the outgoing radiation condition is redundant, and only the volume-waves part is required, i.e., only the first two expressions in (3.21), but now holding for $y_2 > 0$.

3.5 Numerical evaluation of the Green's function

For the numerical evaluation of the Green's function, we separate the plane $\mathbb{R}^2$ into three regions: an upper near field, a lower near field, and a far field. The near field is given by the region $|k|\,|\boldsymbol{v}| \leq 24$ and the far field encompasses $|k|\,|\boldsymbol{v}| > 24$, being $\boldsymbol{v} = \boldsymbol{y} - \bar{\boldsymbol{x}}$.

The upper near field considers $v_2 \geq 0$ and the lower near field $v_2 < 0$. In the upper near field, when $|Z_\infty| \geq |k|$ and $2|\xi_p| \geq |Z_\infty|$, the Green's function is computed by using the expression (3.87). The second condition is required, since the spectral part of (3.87) becomes slowly decreasing when $|\xi_p|$ is very small compared with $|Z_\infty|$, i.e., in the case when $Z_\infty \approx ik$. When $|Z_\infty| < |k|$ or when $2|\xi_p| < |Z_\infty|$, the Green's function is evaluated in the upper near field using (3.90) and (3.92), depending on wether $\arg(k) \leq \pi/4$ or $\arg(k) > \pi/4$, respectively. In the lower near field, on the other hand, we use the expression (3.84) to compute the Green's function, where the term G_B is computed analogously as the Green's function in the upper near field, but considering $v_2 = 0$. The numerical integration of the Fourier integrals is performed by means of a trapezoidal rule, discretizing the spectral variable ξ into $\xi_j = j\Delta\xi$ for $j = 0, \ldots, M$, where

$$\Delta\xi = \frac{2\pi|k|}{12 \cdot 24} \qquad \text{and} \qquad \xi_M = M\Delta\xi \approx |k|\Big(2 + 8\, e^{-4v_2|Z_\infty|/|k|}\Big), \tag{3.134}$$

taking thus at least 12 samples per oscillation and increasing the size of the integration interval as v_2 approaches to zero. This discretization contains all the relevant information for an accurate numerical integration.

In the far field, the Green's function can be computed either by using (3.128) or by considering the exponential integral functions for the surface-wave terms, i.e., by considering

that as $|\boldsymbol{x}| \to \infty$ it holds that

$$G(\boldsymbol{x},\boldsymbol{y}) \sim -\frac{i}{4}H_0^{(1)}\big(k|\boldsymbol{x}-\boldsymbol{y}|\big) + \frac{i}{4}\left(\frac{Z_\infty - ik\sin\alpha}{Z_\infty + ik\sin\alpha}\right)H_0^{(1)}\big(k|\boldsymbol{x}-\bar{\boldsymbol{y}}|\big)$$
$$+ \frac{Z_\infty}{2\pi\xi_p}\,e^{-Z_\infty v_2}\Big\{e^{i\xi_p v_1}\,\mathrm{Ei}(Z_\infty v_2 - i\xi_p v_1) + e^{-i\xi_p v_1}\,\mathrm{Ei}(Z_\infty v_2 + i\xi_p v_1)\Big\}$$
$$- \frac{iZ_\infty}{\xi_p}\,e^{-Z_\infty v_2}\cos(\xi_p v_1). \tag{3.135}$$

The Bessel functions can be evaluated either by using the software based on the technical report by Morris (1993) or the subroutines described in Amos (1986, 1995). The exponential integral function for complex arguments can be computed by using the algorithm developed by Amos (1980, 1990*a*,*b*) or the software based on the technical report by Morris (1993), taking care with the definition of the analytic branch cuts. Further references are listed in Lozier & Olver (1994). The biggest numerical error, excepting the singularity-distribution along the half-line Υ, is committed near the boundaries of the three described regions, and is more or less of order $6\,|k|\,/\,|Z_\infty|\cdot 10^{-3}$.

3.6 Integral representation and equation

3.6.1 Integral representation

We are interested in expressing the solution u of the direct scattering problem (3.13) by means of an integral representation formula over the perturbed portion of the boundary Γ_p. For this purpose, we extend this solution by zero towards the complementary domain Ω_c, analogously as done in (C.107). We define by $\Omega_{R,\varepsilon}$ the domain Ω_e without the ball B_ε of radius $\varepsilon > 0$ centered at the point $\boldsymbol{x} \in \Omega_e$, and truncated at infinity by the ball B_R of radius $R > 0$ centered at the origin. We consider that the ball B_ε is entirely contained in Ω_e. Therefore, as shown in Figure 3.8, we have that

$$\Omega_{R,\varepsilon} = \big(\Omega_e \cap B_R\big) \setminus \overline{B_\varepsilon}, \tag{3.136}$$

where

$$B_R = \{\boldsymbol{y} \in \mathbb{R}^2 :\, |\boldsymbol{y}| < R\} \qquad \text{and} \qquad B_\varepsilon = \{\boldsymbol{y} \in \Omega_e :\, |\boldsymbol{y}-\boldsymbol{x}| < \varepsilon\}. \tag{3.137}$$

We consider similarly, inside Ω_e, the boundaries of the balls

$$S_R^+ = \{\boldsymbol{y} \in \mathbb{R}^2_+ :\, |\boldsymbol{y}| = R\} \qquad \text{and} \qquad S_\varepsilon = \{\boldsymbol{y} \in \Omega_e :\, |\boldsymbol{y}-\boldsymbol{x}| = \varepsilon\}. \tag{3.138}$$

We separate furthermore the boundary as $\Gamma = \Gamma_0 \cup \Gamma_+$, where

$$\Gamma_0 = \{\boldsymbol{y} \in \Gamma :\, y_2 = 0\} \qquad \text{and} \qquad \Gamma_+ = \{\boldsymbol{y} \in \Gamma :\, y_2 > 0\}. \tag{3.139}$$

The boundary Γ is likewise truncated at infinity by the ball B_R, namely

$$\Gamma_R = \Gamma \cap B_R = \Gamma_0^R \cup \Gamma_+ = \Gamma_\infty^R \cup \Gamma_p, \tag{3.140}$$

where

$$\Gamma_0^R = \Gamma_0 \cap B_R \qquad \text{and} \qquad \Gamma_\infty^R = \Gamma_\infty \cap B_R. \tag{3.141}$$

The idea is to retrieve the domain Ω_e and the boundary Γ at the end when the limits $R \to \infty$ and $\varepsilon \to 0$ are taken for the truncated domain $\Omega_{R,\varepsilon}$ and the truncated boundary Γ_R.

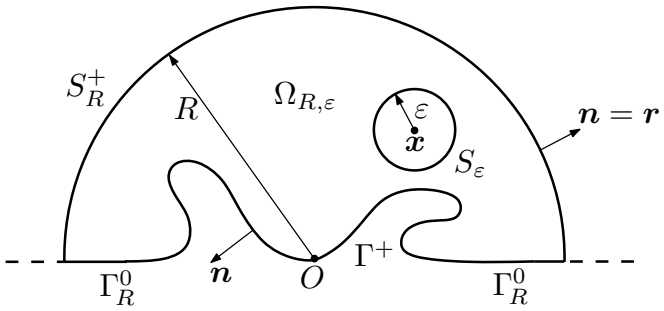

FIGURE 3.8. Truncated domain $\Omega_{R,\varepsilon}$ for $\boldsymbol{x} \in \Omega_e$.

We apply now Green's second integral theorem (A.613) to the functions u and $G(\boldsymbol{x}, \cdot)$ in the bounded domain $\Omega_{R,\varepsilon}$, by subtracting their respective Helmholtz equations, yielding

$$\begin{aligned} 0 &= \int_{\Omega_{R,\varepsilon}} \big(u(\boldsymbol{y})\Delta_{\boldsymbol{y}} G(\boldsymbol{x},\boldsymbol{y}) - G(\boldsymbol{x},\boldsymbol{y})\Delta u(\boldsymbol{y})\big)\mathrm{d}\boldsymbol{y} \\ &= \int_{S_R^+} \left(u(\boldsymbol{y})\frac{\partial G}{\partial r_{\boldsymbol{y}}}(\boldsymbol{x},\boldsymbol{y}) - G(\boldsymbol{x},\boldsymbol{y})\frac{\partial u}{\partial r}(\boldsymbol{y})\right)\mathrm{d}\gamma(\boldsymbol{y}) \\ &\quad - \int_{S_\varepsilon} \left(u(\boldsymbol{y})\frac{\partial G}{\partial r_{\boldsymbol{y}}}(\boldsymbol{x},\boldsymbol{y}) - G(\boldsymbol{x},\boldsymbol{y})\frac{\partial u}{\partial r}(\boldsymbol{y})\right)\mathrm{d}\gamma(\boldsymbol{y}) \\ &\quad + \int_{\Gamma_R} \left(u(\boldsymbol{y})\frac{\partial G}{\partial n_{\boldsymbol{y}}}(\boldsymbol{x},\boldsymbol{y}) - G(\boldsymbol{x},\boldsymbol{y})\frac{\partial u}{\partial n}(\boldsymbol{y})\right)\mathrm{d}\gamma(\boldsymbol{y}). \end{aligned} \tag{3.142}$$

The integral on S_R^+ can be rewritten as

$$\begin{aligned} &\int_{S_R^2} \left[u(\boldsymbol{y})\left(\frac{\partial G}{\partial r_{\boldsymbol{y}}}(\boldsymbol{x},\boldsymbol{y}) - iZ_\infty G(\boldsymbol{x},\boldsymbol{y})\right) - G(\boldsymbol{x},\boldsymbol{y})\left(\frac{\partial u}{\partial r}(\boldsymbol{y}) - iZ_\infty u(\boldsymbol{y})\right)\right]\mathrm{d}\gamma(\boldsymbol{y}) \\ &+ \int_{S_R^1} \left[u(\boldsymbol{y})\left(\frac{\partial G}{\partial r_{\boldsymbol{y}}}(\boldsymbol{x},\boldsymbol{y}) - ikG(\boldsymbol{x},\boldsymbol{y})\right) - G(\boldsymbol{x},\boldsymbol{y})\left(\frac{\partial u}{\partial r}(\boldsymbol{y}) - iku(\boldsymbol{y})\right)\right]\mathrm{d}\gamma(\boldsymbol{y}), \end{aligned} \tag{3.143}$$

which for R large enough and due the radiation condition (3.6) tends to zero, since

$$\left|\int_{S_R^2} u(\boldsymbol{y})\left(\frac{\partial G}{\partial r_{\boldsymbol{y}}}(\boldsymbol{x},\boldsymbol{y}) - i\sqrt{Z_\infty^2 + k^2}\, G(\boldsymbol{x},\boldsymbol{y})\right)\mathrm{d}\gamma(\boldsymbol{y})\right| \leq \frac{C}{R}\ln R, \tag{3.144}$$

$$\left|\int_{S_R^2} G(\boldsymbol{x},\boldsymbol{y})\left(\frac{\partial u}{\partial r}(\boldsymbol{y}) - i\sqrt{Z_\infty^2 + k^2}\, u(\boldsymbol{y})\right)\mathrm{d}\gamma(\boldsymbol{y})\right| \leq \frac{C}{R}\ln R, \tag{3.145}$$

and

$$\left|\int_{S_R^1} u(\boldsymbol{y})\left(\frac{\partial G}{\partial r_{\boldsymbol{y}}}(\boldsymbol{x},\boldsymbol{y}) - ikG(\boldsymbol{x},\boldsymbol{y})\right)\mathrm{d}\gamma(\boldsymbol{y})\right| \leq \frac{C}{\sqrt{R}}, \tag{3.146}$$

$$\left| \int_{S_R^1} G(\boldsymbol{x},\boldsymbol{y}) \left(\frac{\partial u}{\partial r}(\boldsymbol{y}) - iku(\boldsymbol{y}) \right) \mathrm{d}\gamma(\boldsymbol{y}) \right| \leq \frac{C}{\sqrt{R}}, \tag{3.147}$$

for some constants $C > 0$. If the function u is regular enough in the ball B_ε, then the second term of the integral on S_ε in (3.142), when $\varepsilon \to 0$ and due (3.97), is bounded by

$$\left| \int_{S_\varepsilon} G(\boldsymbol{x},\boldsymbol{y}) \frac{\partial u}{\partial r}(\boldsymbol{y}) \, \mathrm{d}\gamma(\boldsymbol{y}) \right| \leq C\varepsilon \ln \varepsilon \sup_{\boldsymbol{y}\in B_\varepsilon} \left| \frac{\partial u}{\partial r}(\boldsymbol{y}) \right|, \tag{3.148}$$

for some constant $C > 0$ and tends to zero. The regularity of u can be specified afterwards once the integral representation has been determined and generalized by means of density arguments. The first integral term on S_ε can be decomposed as

$$\begin{aligned} \int_{S_\varepsilon} u(\boldsymbol{y}) \frac{\partial G}{\partial r_{\boldsymbol{y}}}(\boldsymbol{x},\boldsymbol{y}) \, \mathrm{d}\gamma(\boldsymbol{y}) &= u(\boldsymbol{x}) \int_{S_\varepsilon} \frac{\partial G}{\partial r_{\boldsymbol{y}}}(\boldsymbol{x},\boldsymbol{y}) \, \mathrm{d}\gamma(\boldsymbol{y}) \\ &\quad + \int_{S_\varepsilon} \frac{\partial G}{\partial r_{\boldsymbol{y}}}(\boldsymbol{x},\boldsymbol{y}) \big(u(\boldsymbol{y}) - u(\boldsymbol{x}) \big) \, \mathrm{d}\gamma(\boldsymbol{y}), \end{aligned} \tag{3.149}$$

For the first term in the right-hand side of (3.149), by considering (3.97) we have that

$$\int_{S_\varepsilon} \frac{\partial G}{\partial r_{\boldsymbol{y}}}(\boldsymbol{x},\boldsymbol{y}) \, \mathrm{d}\gamma(\boldsymbol{y}) \quad \xrightarrow[\varepsilon\to 0]{} \quad 1, \tag{3.150}$$

while the second term is bounded by

$$\left| \int_{S_\varepsilon} \big(u(\boldsymbol{y}) - u(\boldsymbol{x}) \big) \frac{\partial G}{\partial r_{\boldsymbol{y}}}(\boldsymbol{x},\boldsymbol{y}) \, \mathrm{d}\gamma(\boldsymbol{y}) \right| \leq \sup_{\boldsymbol{y}\in B_\varepsilon} |u(\boldsymbol{y}) - u(\boldsymbol{x})|, \tag{3.151}$$

which tends towards zero when $\varepsilon \to 0$. Finally, due the impedance boundary condition (3.4) and since the support of f_z vanishes on Γ_∞, the term on Γ_R in (3.142) can be decomposed as

$$\begin{aligned} &\int_{\Gamma_p} \left(\frac{\partial G}{\partial n_{\boldsymbol{y}}}(\boldsymbol{x},\boldsymbol{y}) - Z(\boldsymbol{y}) G(\boldsymbol{x},\boldsymbol{y}) \right) u(\boldsymbol{y}) \, \mathrm{d}\gamma(\boldsymbol{y}) + \int_{\Gamma_p} G(\boldsymbol{x},\boldsymbol{y}) f_z(\boldsymbol{y}) \, \mathrm{d}\gamma(\boldsymbol{y}) \\ &\qquad - \int_{\Gamma_\infty^R} \left(\frac{\partial G}{\partial y_2}(\boldsymbol{x},\boldsymbol{y}) + Z_\infty G(\boldsymbol{x},\boldsymbol{y}) \right) u(\boldsymbol{y}) \, \mathrm{d}\gamma(\boldsymbol{y}), \end{aligned} \tag{3.152}$$

where the integral on Γ_∞^R vanishes due the impedance boundary condition in (3.20). Therefore this term does not depend on R and has its support only on the bounded and perturbed portion Γ_p of the boundary.

In conclusion, when the limits $R \to \infty$ and $\varepsilon \to 0$ are taken in (3.142), then we obtain for $\boldsymbol{x} \in \Omega_e$ the integral representation formula

$$u(\boldsymbol{x}) = \int_{\Gamma_p} \left(\frac{\partial G}{\partial n_{\boldsymbol{y}}}(\boldsymbol{x},\boldsymbol{y}) - Z(\boldsymbol{y}) G(\boldsymbol{x},\boldsymbol{y}) \right) u(\boldsymbol{y}) \, \mathrm{d}\gamma(\boldsymbol{y}) + \int_{\Gamma_p} G(\boldsymbol{x},\boldsymbol{y}) f_z(\boldsymbol{y}) \, \mathrm{d}\gamma(\boldsymbol{y}), \tag{3.153}$$

which can be alternatively expressed as

$$u(\boldsymbol{x}) = \int_{\Gamma_p} \left(u(\boldsymbol{y}) \frac{\partial G}{\partial n_{\boldsymbol{y}}}(\boldsymbol{x},\boldsymbol{y}) - G(\boldsymbol{x},\boldsymbol{y}) \frac{\partial u}{\partial n}(\boldsymbol{y}) \right) \mathrm{d}\gamma(\boldsymbol{y}). \tag{3.154}$$

It is remarkable in this integral representation that the support of the integral, namely the curve Γ_p, is bounded. Let us denote the traces of the solution and of its normal derivative

on Γ_p respectively by

$$\mu = u|_{\Gamma_p} \qquad \text{and} \qquad \nu = \left.\frac{\partial u}{\partial n}\right|_{\Gamma_p}. \tag{3.155}$$

We can rewrite now (3.153) and (3.154) in terms of layer potentials as

$$u = \mathcal{D}(\mu) - \mathcal{S}(Z\mu) + \mathcal{S}(f_z) \qquad \text{in } \Omega_e, \tag{3.156}$$

$$u = \mathcal{D}(\mu) - \mathcal{S}(\nu) \qquad \text{in } \Omega_e, \tag{3.157}$$

where we define for $\boldsymbol{x} \in \Omega_e$ respectively the single and double layer potentials as

$$\mathcal{S}\nu(\boldsymbol{x}) = \int_{\Gamma_p} G(\boldsymbol{x}, \boldsymbol{y})\nu(\boldsymbol{y})\,\mathrm{d}\gamma(\boldsymbol{y}), \tag{3.158}$$

$$\mathcal{D}\mu(\boldsymbol{x}) = \int_{\Gamma_p} \frac{\partial G}{\partial n_{\boldsymbol{y}}}(\boldsymbol{x}, \boldsymbol{y})\mu(\boldsymbol{y})\,\mathrm{d}\gamma(\boldsymbol{y}). \tag{3.159}$$

We remark that from the impedance boundary condition (3.4) it is clear that

$$\nu = Z\mu - f_z. \tag{3.160}$$

3.6.2 Integral equation

To determine entirely the solution of the direct scattering problem (3.13) by means of its integral representation, we have to find values for the traces (3.155). This requires the development of an integral equation that allows to fix these values by incorporating the boundary data. For this purpose we place the source point $\boldsymbol{x}$ on the boundary Γ and apply the same procedure as before for the integral representation (3.153), treating differently in (3.142) only the integrals on S_ε. The integrals on S_R^+ still behave well and tend towards zero as $R \to \infty$. The Ball B_ε, though, is split in half by the boundary Γ, and the portion $\Omega_e \cap B_\varepsilon$ is asymptotically separated from its complement in B_ε by the tangent of the boundary if Γ is regular. If $\boldsymbol{x} \in \Gamma_+$, then the associated integrals on S_ε give rise to a term $-u(\boldsymbol{x})/2$ instead of just $-u(\boldsymbol{x})$ as before for the integral representation. Therefore we obtain for $\boldsymbol{x} \in \Gamma_+$ the boundary integral representation

$$\frac{u(\boldsymbol{x})}{2} = \int_{\Gamma_p} \left(\frac{\partial G}{\partial n_{\boldsymbol{y}}}(\boldsymbol{x}, \boldsymbol{y}) - Z(\boldsymbol{y})G(\boldsymbol{x}, \boldsymbol{y}) \right) u(\boldsymbol{y})\,\mathrm{d}\gamma(\boldsymbol{y}) + \int_{\Gamma_p} G(\boldsymbol{x}, \boldsymbol{y}) f_z(\boldsymbol{y})\,\mathrm{d}\gamma(\boldsymbol{y}). \tag{3.161}$$

On the contrary, if $\boldsymbol{x} \in \Gamma_0$, then the logarithmic behavior (3.98) contributes also to the singularity (3.97) of the Green's function and the integrals on S_ε give now rise to two terms $-u(\boldsymbol{x})/2$, i.e., on the whole to a term $-u(\boldsymbol{x})$. For $\boldsymbol{x} \in \Gamma_0$ the boundary integral representation is instead given by

$$u(\boldsymbol{x}) = \int_{\Gamma_p} \left(\frac{\partial G}{\partial n_{\boldsymbol{y}}}(\boldsymbol{x}, \boldsymbol{y}) - Z(\boldsymbol{y})G(\boldsymbol{x}, \boldsymbol{y}) \right) u(\boldsymbol{y})\,\mathrm{d}\gamma(\boldsymbol{y}) + \int_{\Gamma_p} G(\boldsymbol{x}, \boldsymbol{y}) f_z(\boldsymbol{y})\,\mathrm{d}\gamma(\boldsymbol{y}). \tag{3.162}$$

We must notice that in both cases, the integrands associated with the boundary Γ admit an integrable singularity at the point $\boldsymbol{x}$. In terms of boundary layer potentials, we can express these boundary integral representations as

$$\frac{u}{2} = D(\mu) - S(Z\mu) + S(f_z) \qquad \text{on } \Gamma_+, \tag{3.163}$$

$$u = D(\mu) - S(Z\mu) + S(f_z) \qquad \text{on } \Gamma_0, \tag{3.164}$$

where we consider, for $\boldsymbol{x} \in \Gamma$, the two boundary integral operators

$$S\nu(\boldsymbol{x}) = \int_{\Gamma_p} G(\boldsymbol{x}, \boldsymbol{y})\nu(\boldsymbol{y})\, \mathrm{d}\gamma(\boldsymbol{y}), \tag{3.165}$$

$$D\mu(\boldsymbol{x}) = \int_{\Gamma_p} \frac{\partial G}{\partial n_{\boldsymbol{y}}}(\boldsymbol{x}, \boldsymbol{y})\mu(\boldsymbol{y})\, \mathrm{d}\gamma(\boldsymbol{y}). \tag{3.166}$$

We can combine (3.163) and (3.164) into a single integral equation on Γ_p, namely

$$(1 + \mathcal{I}_0)\frac{\mu}{2} + S(Z\mu) - D(\mu) = S(f_z) \qquad \text{on } \Gamma_p, \tag{3.167}$$

where $\mathcal{I}_0$ denotes the characteristic or indicator function of the set Γ_0, i.e.,

$$\mathcal{I}_0(\boldsymbol{x}) = \begin{cases} 1 & \text{if } \boldsymbol{x} \in \Gamma_0, \\ 0 & \text{if } \boldsymbol{x} \notin \Gamma_0. \end{cases} \tag{3.168}$$

It is the solution μ on Γ_p of the integral equation (3.167) which finally allows to characterize the solution u in Ω_e of the direct scattering problem (3.13) through the integral representation formula (3.156). The trace of the solution u on the boundary Γ is then found simultaneously by means of the boundary integral representations (3.163) and (3.164). In particular, when $\boldsymbol{x} \in \Gamma_\infty$ and since $\Gamma_\infty \subset \Gamma_0$, therefore it holds that

$$u = D(\mu) - S(Z\mu) + S(f_z) \qquad \text{on } \Gamma_\infty. \tag{3.169}$$

3.7 Far field of the solution

The asymptotic behavior at infinity of the solution u of (3.13) is described by the far field. It is denoted by u^{ff} and is characterized by

$$u(\boldsymbol{x}) \sim u^{ff}(\boldsymbol{x}) \qquad \text{as } |\boldsymbol{x}| \to \infty. \tag{3.170}$$

Its expression can be deduced by replacing the far field of the Green's function G^{ff} and its derivatives in the integral representation formula (3.154), which yields

$$u^{ff}(\boldsymbol{x}) = \int_{\Gamma_p} \left(\frac{\partial G^{ff}}{\partial n_{\boldsymbol{y}}}(\boldsymbol{x}, \boldsymbol{y})\mu(\boldsymbol{y}) - G^{ff}(\boldsymbol{x}, \boldsymbol{y})\nu(\boldsymbol{y}) \right) \mathrm{d}\gamma(\boldsymbol{y}). \tag{3.171}$$

By replacing now (3.129) and the addition of (3.122) and (3.127) in (3.171), we obtain that

$$\begin{aligned} u^{ff}(\boldsymbol{x}) = \frac{e^{i\pi/4}}{\sqrt{8\pi k}} \frac{e^{ik|\boldsymbol{x}|}}{\sqrt{|\boldsymbol{x}|}} \int_{\Gamma_p} e^{-ik\hat{\boldsymbol{x}}\cdot\boldsymbol{y}} \Bigg(& ik\hat{\boldsymbol{x}} \cdot \boldsymbol{n}_{\boldsymbol{y}}\, \mu(\boldsymbol{y}) + \nu(\boldsymbol{y}) \\ & - \frac{Z_\infty - ik\sin\theta}{Z_\infty + ik\sin\theta}\, e^{2iky_2\sin\theta} \left(ik \begin{bmatrix} \cos\theta \\ -\sin\theta \end{bmatrix} \cdot \boldsymbol{n}_{\boldsymbol{y}}\, \mu(\boldsymbol{y}) + \nu(\boldsymbol{y}) \right) \Bigg) \mathrm{d}\gamma(\boldsymbol{y}) \\ - \frac{Z_\infty}{\xi_p}\, e^{-Z_\infty x_2} e^{iZ_\infty |x_1|} \int_{\Gamma_p} e^{-Z_\infty y_2} e^{-iZ_\infty y_1 \operatorname{sign} x_1} & \left(\begin{bmatrix} \xi_p \operatorname{sign} x_1 \\ -iZ_\infty \end{bmatrix} \cdot \boldsymbol{n}_{\boldsymbol{y}}\, \mu(\boldsymbol{y}) - i\nu(\boldsymbol{y}) \right) \mathrm{d}\gamma(\boldsymbol{y}). \end{aligned} \tag{3.172}$$

The asymptotic behavior of the solution u at infinity, as $|\boldsymbol{x}| \to \infty$, is therefore given by

$$u(\boldsymbol{x}) = \frac{e^{ik|\boldsymbol{x}|}}{\sqrt{|\boldsymbol{x}|}} \left\{ u_\infty^V(\hat{\boldsymbol{x}}) + \mathcal{O}\left(\frac{1}{|\boldsymbol{x}|}\right) \right\} + e^{-Z_\infty x_2} e^{i\xi_p |x_1|} \left\{ u_\infty^S(\hat{x}_s) + \mathcal{O}\left(\frac{1}{|x_1|}\right) \right\}, \quad (3.173)$$

where $\hat{x}_s = \operatorname{sign} x_1$ and where we decompose $\boldsymbol{x} = |\boldsymbol{x}|\, \hat{\boldsymbol{x}}$, being $\hat{\boldsymbol{x}} = (\cos\theta,\, \sin\theta)$ a vector of the unit circle. The far-field pattern of the volume waves is given by

$$u_\infty^V(\hat{\boldsymbol{x}}) = \frac{e^{i\pi/4}}{\sqrt{8\pi k}} \int_{\Gamma_p} e^{-ik\hat{\boldsymbol{x}}\cdot\boldsymbol{y}} \Bigg(ik\hat{\boldsymbol{x}} \cdot \boldsymbol{n_y}\, \mu(\boldsymbol{y}) + \nu(\boldsymbol{y}) \\ - \frac{Z_\infty - ik\sin\theta}{Z_\infty + ik\sin\theta}\, e^{2iky_2 \sin\theta} \left(ik \begin{bmatrix} \cos\theta \\ -\sin\theta \end{bmatrix} \cdot \boldsymbol{n_y}\, \mu(\boldsymbol{y}) + \nu(\boldsymbol{y}) \right) \Bigg) \mathrm{d}\gamma(\boldsymbol{y}), \quad (3.174)$$

whereas the far-field pattern for the surface waves adopts the form

$$u_\infty^S(\hat{x}_s) = -\frac{Z_\infty}{\xi_p} \int_{\Gamma_p} e^{-Z_\infty y_2} e^{-iZ_\infty y_1 \operatorname{sign} x_1} \left(\begin{bmatrix} \xi_p \operatorname{sign} x_1 \\ -iZ_\infty \end{bmatrix} \cdot \boldsymbol{n_y}\, \mu(\boldsymbol{y}) - i\nu(\boldsymbol{y}) \right) \mathrm{d}\gamma(\boldsymbol{y}). \quad (3.175)$$

Both far-field patterns can be expressed in decibels (dB) respectively by means of the scattering cross sections

$$Q_s^V(\hat{\boldsymbol{x}}) \ \ [\mathrm{dB}] = 20 \log_{10}\left(\frac{|u_\infty^V(\hat{\boldsymbol{x}})|}{|u_0^V|} \right), \quad (3.176)$$

$$Q_s^S(\hat{x}_s) \ \ [\mathrm{dB}] = 20 \log_{10}\left(\frac{|u_\infty^S(\hat{x}_s)|}{|u_0^S|} \right), \quad (3.177)$$

where the reference levels u_0^V and u_0^S are taken such that $|u_0^V| = |u_0^S| = 1$ if the incident field is given either by a volume wave of the form (3.16) or by a surface wave of the form (3.19).

We remark that the far-field behavior (3.173) of the solution is in accordance with the radiation condition (3.6), which justifies its choice.

3.8 Existence and uniqueness

3.8.1 Function spaces

To state a precise mathematical formulation of the herein treated problems, we have to define properly the involved function spaces. Since the considered domains and boundaries are unbounded, we need to work with weighted Sobolev spaces, as in Durán, Muga & Nédélec (2005*a*, 2006). We consider the classic weight functions

$$\varrho = \sqrt{1 + r^2} \qquad \text{and} \qquad \log \varrho = \ln(2 + r^2), \quad (3.178)$$

where $r = |\boldsymbol{x}|$. We define the domains

$$\Omega_e^1 = \left\{ \boldsymbol{x} \in \Omega_e : \ x_2 > \frac{1}{2Z_\infty} \ln\left(1 + \frac{8\pi k Z_\infty^2}{Z_\infty^2 + k^2}\, r \right) \right\}, \quad (3.179)$$

$$\Omega_e^2 = \left\{ \boldsymbol{x} \in \Omega_e : \ x_2 < \frac{1}{2Z_\infty} \ln\left(1 + \frac{8\pi k Z_\infty^2}{Z_\infty^2 + k^2}\, r \right) \right\}. \quad (3.180)$$

It holds that the solution of the direct scattering problem (3.13) is contained in the weighted Sobolev space

$$W^1(\Omega_e) = \Bigg\{ v : \frac{v}{\varrho \log \varrho} \in L^2(\Omega_e),\ \frac{\nabla v}{\varrho \log \varrho} \in L^2(\Omega_e)^2,\ \frac{v}{\sqrt{\varrho}} \in L^2(\Omega_e^1),$$
$$\frac{\partial v}{\partial r} - ikv \in L^2(\Omega_e^1),\ \frac{v}{\log \varrho} \in L^2(\Omega_e^2),\ \frac{1}{\log \varrho}\left(\frac{\partial v}{\partial r} - i\xi_p v\right) \in L^2(\Omega_e^2) \Bigg\}, \quad (3.181)$$

where $\xi_p = \sqrt{Z_\infty^2 + k^2}$. With the appropriate norm, the space $W^1(\Omega_e)$ becomes also a Hilbert space. We have likewise the inclusion $W^1(\Omega_e) \subset H^1_{\text{loc}}(\Omega_e)$, i.e., the functions of these two spaces differ only by their behavior at infinity.

Since we are dealing with Sobolev spaces, even a strong Lipschitz boundary $\Gamma \in C^{0,1}$ is admissible. The fact that this boundary Γ is also unbounded implies that we have to use weighted trace spaces like in Amrouche (2002). For this purpose, we consider the space

$$W^{1/2}(\Gamma) = \left\{ v : \frac{v}{\sqrt{\varrho} \log \varrho} \in H^{1/2}(\Gamma) \right\}. \quad (3.182)$$

Its dual space $W^{-1/2}(\Gamma)$ is defined via W^0-duality, i.e., considering the pivot space

$$W^0(\Gamma) = \left\{ v : \frac{v}{\sqrt{\varrho} \log \varrho} \in L^2(\Gamma) \right\}. \quad (3.183)$$

Analogously as for the trace theorem (A.531), if $v \in W^1(\Omega_e)$ then the trace of v fulfills

$$\gamma_0 v = v|_\Gamma \in W^{1/2}(\Gamma). \quad (3.184)$$

Moreover, the trace of the normal derivative can be also defined, and it holds that

$$\gamma_1 v = \frac{\partial v}{\partial n}|_\Gamma \in W^{-1/2}(\Gamma). \quad (3.185)$$

We remark further that the restriction of the trace of v to Γ_p is such that

$$\gamma_0 v|_{\Gamma_p} = v|_{\Gamma_p} \in H^{1/2}(\Gamma_p), \quad (3.186)$$

$$\gamma_1 v|_{\Gamma_p} = \frac{\partial v}{\partial n}|_{\Gamma_p} \in H^{-1/2}(\Gamma_p), \quad (3.187)$$

and its restriction to Γ_∞ yields

$$\gamma_0 v|_{\Gamma_\infty} = v|_{\Gamma_\infty} \in W^{1/2}(\Gamma_\infty), \quad (3.188)$$

$$\gamma_1 v|_{\Gamma_\infty} = \frac{\partial v}{\partial n}|_{\Gamma_\infty} \in W^{-1/2}(\Gamma_\infty). \quad (3.189)$$

3.8.2 Application to the integral equation

The existence and uniqueness of the solution for the direct scattering problem (3.13), due the integral representation formula (3.156), can be characterized by using the integral equation (3.167). For this purpose and in accordance with the considered function spaces, we take $\mu \in H^{1/2}(\Gamma_p)$ and $\nu \in H^{-1/2}(\Gamma_p)$. Furthermore, we consider that $Z \in L^\infty(\Gamma_p)$ and that $f_z \in H^{-1/2}(\Gamma_p)$, even though strictly speaking $f_z \in \widetilde{H}^{-1/2}(\Gamma_p)$.

It holds that the single and double layer potentials defined respectively in (3.158) and (3.159) are linear and continuous integral operators such that

$$\mathcal{S} : H^{-1/2}(\Gamma_p) \longrightarrow W^1(\Omega_e) \qquad \text{and} \qquad \mathcal{D} : H^{1/2}(\Gamma_p) \longrightarrow W^1(\Omega_e). \tag{3.190}$$

The boundary integral operators (3.165) and (3.166) are also linear and continuous applications, and they are such that

$$S : H^{-1/2}(\Gamma_p) \longrightarrow W^{1/2}(\Gamma) \qquad \text{and} \qquad D : H^{1/2}(\Gamma_p) \longrightarrow W^{1/2}(\Gamma). \tag{3.191}$$

When we restrict them to Γ_p, then it holds that

$$S|_{\Gamma_p} : H^{-1/2}(\Gamma_p) \longrightarrow H^{1/2}(\Gamma_p) \qquad \text{and} \qquad D|_{\Gamma_p} : H^{1/2}(\Gamma_p) \longrightarrow H^{1/2}(\Gamma_p). \tag{3.192}$$

Let us consider the integral equation (3.167), which is given in terms of boundary layer potentials, for $\mu \in H^{1/2}(\Gamma_p)$, by

$$(1 + \mathcal{I}_0)\frac{\mu}{2} + S(Z\mu) - D(\mu) = S(f_z) \qquad \text{in } \ H^{1/2}(\Gamma_p). \tag{3.193}$$

Due the imbedding properties of Sobolev spaces and in the same way as for the half-plane impedance Laplace problem, it holds that the left-hand side of the integral equation corresponds to an identity and two compact operators, and thus Fredholm's alternative holds.

Since the Fredholm alternative applies to the integral equation, therefore it applies also to the direct scattering problem (3.13) due the integral representation formula. The existence of the scattering problem's solution is thus determined by its uniqueness, and the wave numbers $k \in \mathbb{C}$ and impedances $Z \in \mathbb{C}$ for which the uniqueness is lost constitute a countable set, which we call respectively wave number spectrum and impedance spectrum of the scattering problem and denote it by σ_k and σ_Z. The spectrum σ_k considers a fixed Z and, conversely, the spectrum σ_Z considers a fixed k. The existence and uniqueness of the solution is therefore ensured almost everywhere. The same holds obviously for the solution of the integral equation, whose wave number spectrum and impedance spectrum we denote respectively by ς_k and ς_Z. Since each integral equation is derived from the scattering problem, it holds that $\sigma_k \subset \varsigma_k$ and $\sigma_Z \subset \varsigma_Z$. The converse, though, is not necessarily true. In any way, the sets $\varsigma_k \setminus \sigma_k$ and $\varsigma_Z \setminus \sigma_Z$ are at most countable.

In conclusion, the scattering problem (3.13) admits a unique solution u if $k \notin \sigma_k$ and $Z \notin \sigma_Z$, and the integral equation (3.167) admits in the same way a unique solution μ if $k \notin \varsigma_k$ and $Z \notin \varsigma_Z$.

3.9 Dissipative problem

The dissipative problem considers waves that dissipate their energy as they propagate and are modeled by considering a complex wave number or a complex impedance. The use of a complex wave number $k \in \mathbb{C}$ whose imaginary part is strictly positive, i.e., such that $\mathfrak{Im}\{k\} > 0$, ensures an exponential decrease at infinity for both the volume and the surface waves. On the other hand, the use of a complex impedance $Z_\infty \in \mathbb{C}$ with a strictly positive imaginary part, i.e., $\mathfrak{Im}\{Z_\infty\} > 0$, ensures only an exponential decrease at infinity for the surface waves. In the first case, when considering a complex wave number k, and

due the dissipative nature of the medium, it is no longer suited to take progressive plane volume waves in the form of (3.16) and (3.17) respectively as the incident field u_I and the reflected field u_R. In both cases, likewise, it is no longer suited to take progressive plane surface waves in the form of (3.19) as the incident field u_I. Instead, we have to take a wave source at a finite distance from the perturbation. For example, we can consider a point source located at $\boldsymbol{z} \in \Omega_e$, in which case we have only an incident field, which is given, up to a multiplicative constant, by

$$u_I(\boldsymbol{x}) = G(\boldsymbol{x}, \boldsymbol{z}), \tag{3.194}$$

where G denotes the Green's function (3.93). This incident field u_I satisfies the Helmholtz equation with a source term in the right-hand side, namely

$$\Delta u_I + k^2 u_I = \delta_{\boldsymbol{z}} \qquad \text{in } \mathcal{D}'(\Omega_e), \tag{3.195}$$

which holds also for the total field u_T but not for the scattered field u, in which case the Helmholtz equation remains homogeneous. For a general source distribution g_s, whose support is contained in Ω_e, the incident field can be expressed by

$$u_I(\boldsymbol{x}) = G(\boldsymbol{x}, \boldsymbol{z}) * g_s(\boldsymbol{z}) = \int_{\Omega_e} G(\boldsymbol{x}, \boldsymbol{z})\, g_s(\boldsymbol{z})\, \mathrm{d}\boldsymbol{z}. \tag{3.196}$$

This incident field u_I satisfies now

$$\Delta u_I + k^2 u_I = g_s \qquad \text{in } \mathcal{D}'(\Omega_e), \tag{3.197}$$

which holds again also for the total field u_T but not for the scattered field u.

It is not difficult to see that all the performed developments for the non-dissipative case are still valid when considering dissipation. The only difference is that now either a complex wave number k such that $\mathfrak{Im}\{k\} > 0$, or a complex impedance Z_∞ such that $\mathfrak{Im}\{Z_\infty\} > 0$, or both, have to be taken everywhere into account.

3.10 Variational formulation

To solve the integral equation we convert it to its variational or weak formulation, i.e., we solve it with respect to a certain test function in a bilinear (or sesquilinear) form. Basically, the integral equation is multiplied by the (conjugated) test function and then the equation is integrated over the boundary of the domain. The test function is taken in the same function space as the solution of the integral equation.

The variational formulation for the integral equation (3.193) searches $\mu \in H^{1/2}(\Gamma_p)$ such that $\forall \varphi \in H^{1/2}(\Gamma_p)$ we have that

$$\Big\langle (1 + \mathcal{I}_0)\frac{\mu}{2} + S(Z\mu) - D(\mu), \varphi \Big\rangle = \big\langle S(f_z), \varphi \big\rangle. \tag{3.198}$$

3.11 Numerical discretization

3.11.1 Discretized function spaces

The scattering problem (3.13) is solved numerically with the boundary element method by employing a Galerkin scheme on the variational formulation of the integral equation. We use on the boundary curve Γ_p Lagrange finite elements of type $\mathbb{P}_1$. As shown in Figure 3.9, the curve Γ_p is approximated by the discretized curve Γ_p^h, composed by I rectilinear segments T_j, sequentially ordered from left to right for $1 \leq j \leq I$, such that their length $|T_j|$ is less or equal than h, and with their endpoints on top of Γ_p.

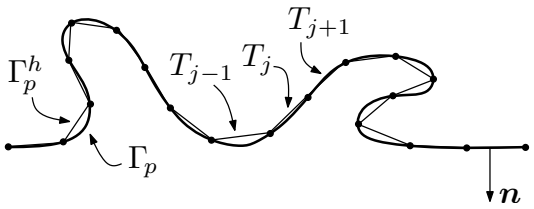

FIGURE 3.9. Curve Γ_p^h, discretization of Γ_p.

The function space $H^{1/2}(\Gamma_p)$ is approximated using the conformal space of continuous piecewise linear polynomials with complex coefficients

$$Q_h = \big\{\varphi_h \in C^0(\Gamma_p^h) \,:\, \varphi_h|_{T_j} \in \mathbb{P}_1(\mathbb{C}),\;\; 1 \leq j \leq I\big\}. \tag{3.199}$$

The space Q_h has a finite dimension $(I+1)$, and we describe it using the standard base functions for finite elements of type $\mathbb{P}_1$, denoted by $\{\chi_j\}_{j=1}^{I+1}$ and expressed as

$$\chi_j(\boldsymbol{x}) = \begin{cases} \dfrac{|\boldsymbol{x} - \boldsymbol{r}_{j-1}|}{|T_{j-1}|} & \text{if } \; \boldsymbol{x} \in T_{j-1}, \\ \dfrac{|\boldsymbol{r}_{j+1} - \boldsymbol{x}|}{|T_j|} & \text{if } \; \boldsymbol{x} \in T_j, \\ 0 & \text{if } \; \boldsymbol{x} \notin T_{j-1} \cup T_j, \end{cases} \tag{3.200}$$

where segment T_{j-1} has as endpoints $\boldsymbol{r}_{j-1}$ and $\boldsymbol{r}_j$, while the endpoints of segment T_j are given by $\boldsymbol{r}_j$ and $\boldsymbol{r}_{j+1}$.

In virtue of this discretization, any function $\varphi_h \in Q_h$ can be expressed as a linear combination of the elements of the base, namely

$$\varphi_h(\boldsymbol{x}) = \sum_{j=1}^{I+1} \varphi_j \, \chi_j(\boldsymbol{x}) \qquad \text{for } \; \boldsymbol{x} \in \Gamma_p^h, \tag{3.201}$$

where $\varphi_j \in \mathbb{C}$ for $1 \leq j \leq I+1$. The solution $\mu \in H^{1/2}(\Gamma_p)$ of the variational formulation (3.198) can be therefore approximated by

$$\mu_h(\boldsymbol{x}) = \sum_{j=1}^{I+1} \mu_j \, \chi_j(\boldsymbol{x}) \qquad \text{for } \; \boldsymbol{x} \in \Gamma_p^h, \tag{3.202}$$

where $\mu_j \in \mathbb{C}$ for $1 \leq j \leq I+1$. The function f_z can be also approximated by

$$f_z^h(\boldsymbol{x}) = \sum_{j=1}^{I+1} f_j \, \chi_j(\boldsymbol{x}) \qquad \text{for } \boldsymbol{x} \in \Gamma_p^h, \quad \text{with } f_j = f_z(\boldsymbol{r}_j). \tag{3.203}$$

3.11.2 Discretized integral equation

To see how the boundary element method operates, we apply it to the variational formulation (3.198). We characterize all the discrete approximations by the index h, including also the impedance and the boundary layer potentials. The numerical approximation of (3.198) leads to the discretized problem that searches $\mu_h \in Q_h$ such that $\forall \varphi_h \in Q_h$

$$\Big\langle (1 + \mathcal{I}_0^h)\frac{\mu_h}{2} + S_h(Z_h\mu_h) - D_h(\mu_h), \varphi_h \Big\rangle = \big\langle S_h(f_z^h), \varphi_h \big\rangle. \tag{3.204}$$

Considering the decomposition of μ_h in terms of the base $\{\chi_j\}$ and taking as test functions the same base functions, $\varphi_h = \chi_i$ for $1 \leq i \leq I+1$, yields the discrete linear system

$$\sum_{j=1}^{I+1} \mu_j \left(\frac{1}{2}\big\langle (1 + \mathcal{I}_0^h)\chi_j, \chi_i \big\rangle + \langle S_h(Z_h\chi_j), \chi_i \rangle - \langle D_h(\chi_j), \chi_i \rangle \right) = \sum_{j=1}^{I+1} f_j \, \langle S_h(\chi_j), \chi_i \rangle. \tag{3.205}$$

This constitutes a system of linear equations that can be expressed as a linear matrix system:

$$\begin{cases} \text{Find } \boldsymbol{\mu} \in \mathbb{C}^{I+1} \text{ such that} \\ \boldsymbol{M}\boldsymbol{\mu} = \boldsymbol{b}. \end{cases} \tag{3.206}$$

The elements m_{ij} of the matrix $\boldsymbol{M}$ are given, for $1 \leq i, j \leq I+1$, by

$$m_{ij} = \frac{1}{2}\big\langle (1 + \mathcal{I}_0^h)\chi_j, \chi_i \big\rangle + \langle S_h(Z_h\chi_j), \chi_i \rangle - \langle D_h(\chi_j), \chi_i \rangle, \tag{3.207}$$

and the elements b_i of the vector $\boldsymbol{b}$ by

$$b_i = \big\langle S_h(f_z^h), \chi_i \big\rangle = \sum_{j=1}^{I+1} f_j \, \langle S_h(\chi_j), \chi_i \rangle \qquad \text{for } 1 \leq i \leq I+1. \tag{3.208}$$

The discretized solution u_h, which approximates u, is finally obtained by discretizing the integral representation formula (3.156) according to

$$u_h = \mathcal{D}_h(\mu_h) - \mathcal{S}_h(Z_h\mu_h) + \mathcal{S}_h(f_z^h), \tag{3.209}$$

which, more specifically, can be expressed as

$$u_h = \sum_{j=1}^{I+1} \mu_j \big(\mathcal{D}_h(\chi_j) - \mathcal{S}_h(Z_h\chi_j) \big) + \sum_{j=1}^{I+1} f_j \, \mathcal{S}_h(\chi_j). \tag{3.210}$$

We remark that the resulting matrix $\boldsymbol{M}$ is in general complex, full, non-symmetric, and with dimensions $(I+1) \times (I+1)$. The right-hand side vector $\boldsymbol{b}$ is complex and of size $I+1$. The boundary element calculations required to compute numerically the elements of $\boldsymbol{M}$ and $\boldsymbol{b}$ have to be performed carefully, since the integrals that appear become singular when the involved segments are adjacent or coincident, due the singularity of the

Green's function at its source point. On Γ_0, the singularity of the image source point has to be taken additionally into account for these calculations.

3.12 Boundary element calculations

The boundary element calculations build the elements of the matrix $\boldsymbol{M}$ resulting from the discretization of the integral equation, i.e., from (3.206). They permit thus to compute numerically expressions like (3.207). To evaluate the appearing singular integrals, we adapt the semi-numerical methods described in the report of Bendali & Devys (1986).

We use the same notation as in Section B.12, and the required boundary element integrals, for $a, b \in \{1, 2\}$, are again

$$ZA_{a,b} = \int_K \int_L \left(\frac{s}{|K|}\right)^a \left(\frac{t}{|L|}\right)^b G(\boldsymbol{x}, \boldsymbol{y}) \, \mathrm{d}L(\boldsymbol{y}) \, \mathrm{d}K(\boldsymbol{x}), \tag{3.211}$$

$$ZB_{a,b} = \int_K \int_L \left(\frac{s}{|K|}\right)^a \left(\frac{t}{|L|}\right)^b \frac{\partial G}{\partial n_{\boldsymbol{y}}}(\boldsymbol{x}, \boldsymbol{y}) \, \mathrm{d}L(\boldsymbol{y}) \, \mathrm{d}K(\boldsymbol{x}). \tag{3.212}$$

All the integrals that stem from the numerical discretization can be expressed in terms of these two basic boundary element integrals. The impedance is again discretized as a piecewise constant function Z_h, which on each segment T_j adopts a constant value $Z_j \in \mathbb{C}$. The integrals of interest are the same as for the full-plane impedance Helmholtz problem and we consider furthermore that

$$\left\langle (1 + \mathcal{I}_0^h)\chi_j, \chi_i \right\rangle = \begin{cases} \langle \chi_j, \chi_i \rangle & \text{if } \boldsymbol{r}_j \in \Gamma_+, \\ 2 \langle \chi_j, \chi_i \rangle & \text{if } \boldsymbol{r}_j \in \Gamma_0. \end{cases} \tag{3.213}$$

To compute the boundary element integrals (3.211) and (3.212), we can easily isolate the singular part (3.97) of the Green's function (3.93), which corresponds in fact to the Green's function of the Laplace equation in the full-plane, and therefore the associated integrals are computed in the same way. The same applies also for its normal derivative. In the case when the segments K and L are are close enough, e.g., adjacent or coincident, and when $L \in \Gamma_0^h$ or $K \in \Gamma_0^h$, being Γ_0^h the approximation of Γ_0, we have to consider additionally the singular behavior (3.98), which is linked with the presence of the impedance half-plane. This behavior can be straightforwardly evaluated by replacing $\boldsymbol{x}$ by $\bar{\boldsymbol{x}}$ in formulae (B.340) to (B.343), i.e., by computing the quantities $ZF_b(\bar{\boldsymbol{x}})$ and $ZG_b(\bar{\boldsymbol{x}})$ with the corresponding adjustment of the notation. Otherwise, if the segments are not close enough and for the non-singular part of the Green's function, a two-point Gauss quadrature formula is used. All the other computations are performed in the same manner as in Section B.12 for the full-plane Laplace equation.

3.13 Benchmark problem

As benchmark problem we consider the particular case when the domain $\Omega_e \subset \mathbb{R}^2_+$ is taken as the exterior of a half-circle of radius $R > 0$ that is centered at the origin, as shown

in Figure 3.10. We decompose the boundary of Ω_e as $\Gamma = \Gamma_p \cup \Gamma_\infty$, where Γ_p corresponds to the upper half-circle, whereas Γ_∞ denotes the remaining unperturbed portion of the half-plane's boundary which lies outside the half-circle and which extends towards infinity on both sides. The unit normal $\boldsymbol{n}$ is taken outwardly oriented of Ω_e, e.g., $\boldsymbol{n} = -\boldsymbol{r}$ on Γ_p.

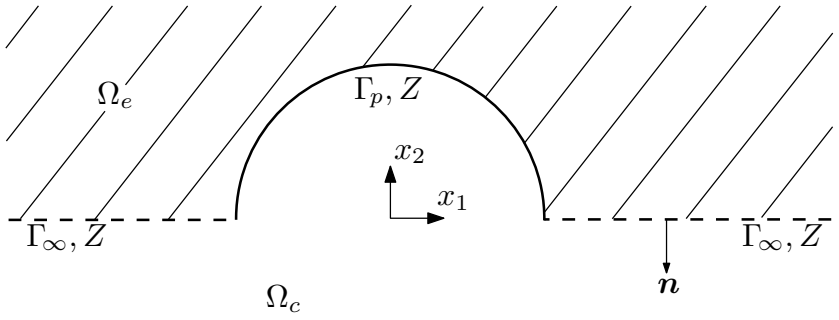

FIGURE 3.10. Exterior of the half-circle.

The benchmark problem is then stated as

$$\begin{cases} \text{Find } u : \Omega_e \to \mathbb{C} \text{ such that} \\ \Delta u + k^2 u = 0 \qquad \text{in } \Omega_e, \\ -\dfrac{\partial u}{\partial n} + Zu = f_z \qquad \text{on } \Gamma, \\ \text{+ Outgoing radiation condition as } |\boldsymbol{x}| \to \infty, \end{cases} \tag{3.214}$$

where we consider a wave number $k \in \mathbb{C}$, a constant impedance $Z \in \mathbb{C}$ throughout Γ, and where the radiation condition is as usual given by (3.6). As incident field u_I we consider the same Green's function, namely

$$u_I(\boldsymbol{x}) = G(\boldsymbol{x}, \boldsymbol{z}), \tag{3.215}$$

where $\boldsymbol{z} \in \Omega_c$ denotes the source point of our incident field. The impedance data function f_z is hence given by

$$f_z(\boldsymbol{x}) = \frac{\partial G}{\partial n_{\boldsymbol{x}}}(\boldsymbol{x}, \boldsymbol{z}) - ZG(\boldsymbol{x}, \boldsymbol{z}), \tag{3.216}$$

and its support is contained in Γ_p. The analytic solution for the benchmark problem (3.214) is then clearly given by

$$u(\boldsymbol{x}) = -G(\boldsymbol{x}, \boldsymbol{z}). \tag{3.217}$$

The goal is to retrieve this solution numerically with the integral equation techniques and the boundary element method described throughout this chapter.

For the computational implementation and the numerical resolution of the benchmark problem, we consider integral equation (3.167). The linear system (3.206) resulting from the discretization (3.204) of its variational formulation (3.198) is solved computationally with finite boundary elements of type $\mathbb{P}_1$ by using subroutines programmed in Fortran 90,

by generating the mesh Γ_p^h of the boundary with the free software Gmsh 2.4, and by representing graphically the results in Matlab 7.5 (R2007b).

We consider a radius $R = 1$, a wave number $k = 3$, a constant impedance $Z = 5$, and for the incident field a source point $\boldsymbol{z} = (0, 0)$. The discretized perturbed boundary curve Γ_p^h has $I = 120$ segments and a discretization step $h = 0.02618$, being

$$h = \max_{1 \leq j \leq I} |T_j|. \tag{3.218}$$

We observe that $h \approx \pi / I$.

The numerically calculated trace of the solution μ_h of the benchmark problem, which was computed by using the boundary element method, is depicted in Figure 3.11. In the same manner, the numerical solution u_h is illustrated in Figures 3.12 and 3.13. It can be observed that the numerical solution is quite close to the exact one.

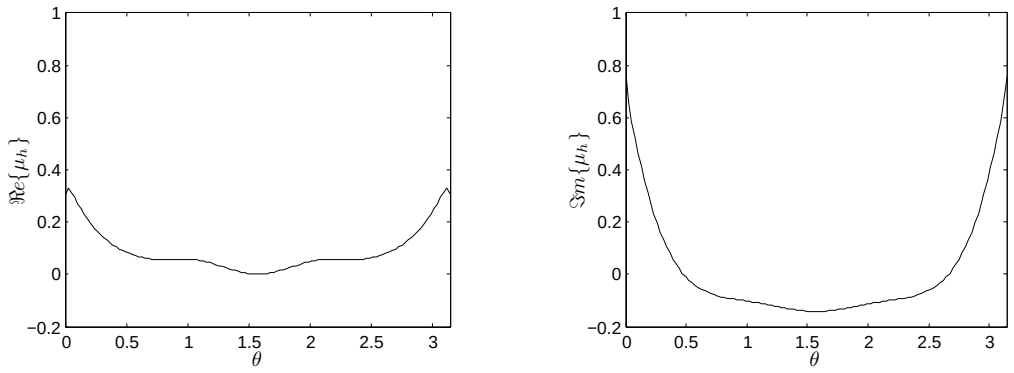

(a) Real part (b) Imaginary part

FIGURE 3.11. Numerically computed trace of the solution μ_h.

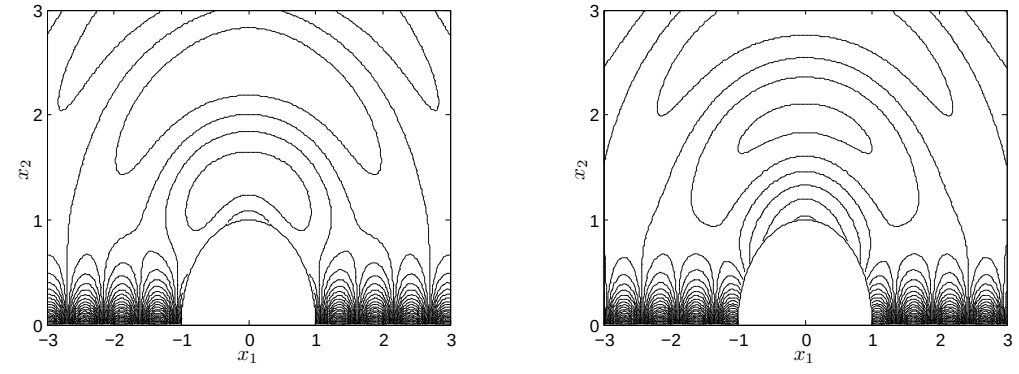

(a) Real part (b) Imaginary part

FIGURE 3.12. Contour plot of the numerically computed solution u_h.

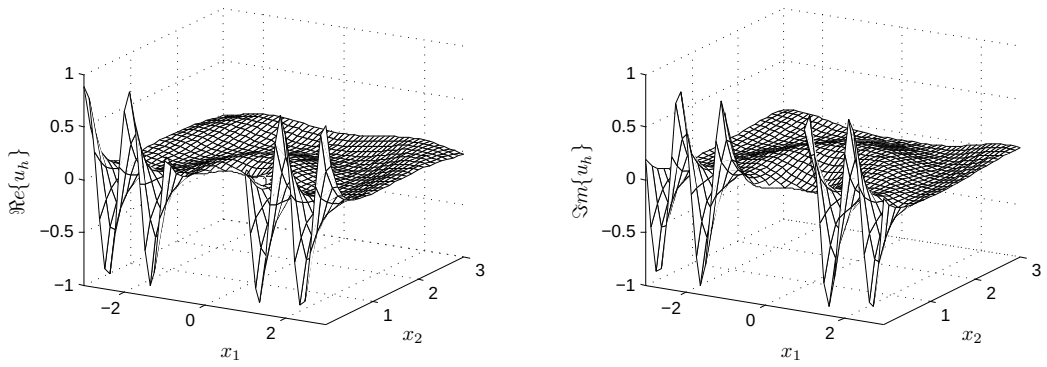

(a) Real part (b) Imaginary part

FIGURE 3.13. Oblique view of the numerically computed solution u_h.

Likewise as in (B.368), we define the relative error of the trace of the solution as

$$E_2(h, \Gamma_p^h) = \frac{\|\Pi_h \mu - \mu_h\|_{L^2(\Gamma_p^h)}}{\|\Pi_h \mu\|_{L^2(\Gamma_p^h)}}, \tag{3.219}$$

where $\Pi_h \mu$ denotes the Lagrange interpolating function of the exact solution's trace μ, i.e.,

$$\Pi_h \mu(\boldsymbol{x}) = \sum_{j=1}^{I+1} \mu(\boldsymbol{r}_j)\, \chi_j(\boldsymbol{x}) \quad \text{and} \quad \mu_h(\boldsymbol{x}) = \sum_{j=1}^{I+1} \mu_j\, \chi_j(\boldsymbol{x}) \quad \text{for } \boldsymbol{x} \in \Gamma_p^h. \tag{3.220}$$

In our case, for a step $h = 0.02618$, we obtained a relative error of $E_2(h, \Gamma_p^h) = 0.08631$.

As in (B.372), we define the relative error of the solution as

$$E_\infty(h, \Omega_L) = \frac{\|u - u_h\|_{L^\infty(\Omega_L)}}{\|u\|_{L^\infty(\Omega_L)}}, \tag{3.221}$$

being $\Omega_L = \{\boldsymbol{x} \in \Omega_e : \|\boldsymbol{x}\|_\infty < L\}$ for $L > 0$. We consider $L = 3$ and describe Ω_L by a triangular finite element mesh of refinement h near the boundary. For $h = 0.02618$, the relative error that we obtained for the solution was $E_\infty(h, \Omega_L) = 0.06178$.

The results for different mesh refinements, i.e., for different numbers of segments I and discretization steps h, are listed in Table 3.1. These results are illustrated graphically in Figure 3.14. It can be observed that the relative errors are approximately of order h for bigger values of h.

TABLE 3.1. Relative errors for different mesh refinements.

I	h	$E_2(h, \Gamma_p^h)$	$E_\infty(h, \Omega_L)$
12	0.2611	$8.483 \cdot 10^{-1}$	$7.702 \cdot 10^{-1}$
40	0.07852	$2.843 \cdot 10^{-1}$	$1.899 \cdot 10^{-1}$
80	0.03927	$1.316 \cdot 10^{-1}$	$9.362 \cdot 10^{-2}$
120	0.02618	$8.631 \cdot 10^{-2}$	$6.178 \cdot 10^{-2}$
240	0.01309	$5.076 \cdot 10^{-2}$	$3.177 \cdot 10^{-2}$
500	0.006283	$4.587 \cdot 10^{-2}$	$2.804 \cdot 10^{-2}$
1000	0.003142	$4.873 \cdot 10^{-2}$	$2.695 \cdot 10^{-2}$

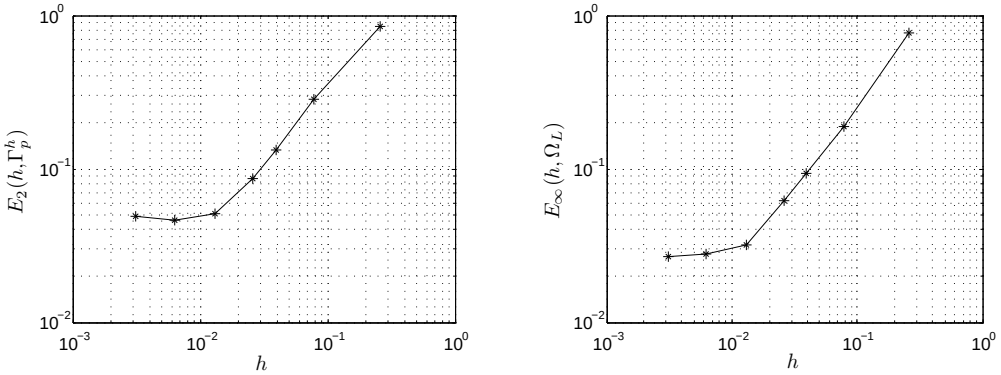

(a) Relative error $E_2(h, \Gamma_p^h)$ (b) Relative error $E_\infty(h, \Omega_L)$

FIGURE 3.14. Logarithmic plots of the relative errors versus the discretization step.

IV. HALF-SPACE IMPEDANCE LAPLACE PROBLEM

4.1 Introduction

In this chapter we study the perturbed half-space impedance Laplace problem using integral equation techniques and the boundary element method.

We consider the problem of the Laplace equation in three dimensions on a compactly perturbed half-space with an impedance boundary condition. The perturbed half-space impedance Laplace problem is a surface wave scattering problem around the bounded perturbation, which is contained in the upper half-space. In water-wave scattering the impedance boundary-value problem appears as a consequence of the linearized free-surface condition, which allows the propagation of surface waves (vid. Section A.10). This problem can be regarded as a limit case when the frequency of the volume waves, i.e., the wave number in the Helmholtz equation, tends towards zero (vid. Chapter V). The two-dimensional case is considered in Chapter II, whereas the full-space impedance Laplace problem with a bounded impenetrable obstacle is treated thoroughly in Appendix D.

The main application of the problem corresponds to linear water-wave propagation in a liquid of indefinite depth, which was first studied in the classical works of Cauchy (1827) and Poisson (1818). A study of wave motion caused by a submerged obstacle was carried out by Lamb (1916). The major impulse in the field came after the milestone papers on the motion of floating bodies by John (1949, 1950), who considered a Green's function and integral equations to solve the problem. Another expression for the Green's function was suggested by Havelock (1955), which was later rederived or publicized in different forms by Kim (1965), Hearn (1977), Noblesse (1982), and Newman (1984*b*, 1985), Pidcock (1985), and Chakrabarti (2001). Other expressions for this Green's function can be found in the articles of Moran (1964), Hess & Smith (1967), and Peter & Meylan (2004), and likewise in the books of Dautray & Lions (1987) and Duffy (2001). The main references for the problem are the classical article of Wehausen & Laitone (1960) and the books of Mei (1983), Linton & McIver (2001), Kuznetsov, Maz'ya & Vainberg (2002), and Mei, Stiassnie & Yue (2005). Reviews of the numerical methods used to solve water-wave problems can be found in Mei (1978) and Yeung (1982).

The Laplace equation does not allow the propagation of volume waves inside the considered domain, but the addition of an impedance boundary condition permits the propagation of surface waves along the boundary of the perturbed half-space. The main difficulty in the numerical treatment and resolution of our problem is the fact that the exterior domain is unbounded. We solve it therefore with integral equation techniques and a boundary element method, which require the knowledge of the associated Green's function. This Green's function is computed using a Fourier transform and taking into account the limiting absorption principle, following Durán, Muga & Nédélec (2005*b*, 2009), but here an explicit expression is found for it in terms of a finite combination of elementary functions, special functions, and their primitives.

This chapter is structured in 13 sections, including this introduction. The direct scattering problem of the Laplace equation in a three-dimensional compactly perturbed half-space with an impedance boundary condition is presented in Section 4.2. The computation of the Green's function, its far field, and its numerical evaluation are developed respectively in Sections 4.3, 4.4, and 4.5. The use of integral equation techniques to solve the direct scattering problem is discussed in Section 4.6. These techniques allow also to represent the far field of the solution, as shown in Section 4.7. The appropriate function spaces and some existence and uniqueness results for the solution of the problem are presented in Section 4.8. The dissipative problem is studied in Section 4.9. By means of the variational formulation developed in Section 4.10, the obtained integral equation is discretized using the boundary element method, which is described in Section 4.11. The boundary element calculations required to build the matrix of the linear system resulting from the numerical discretization are explained in Section 4.12. Finally, in Section 4.13 a benchmark problem based on an exterior half-sphere problem is solved numerically.

4.2 Direct scattering problem

4.2.1 Problem definition

We consider the direct scattering problem of linear time-harmonic surface waves on a perturbed half-space $\Omega_e \subset \mathbb{R}^3_+$, where $\mathbb{R}^3_+ = \{(x_1, x_2, x_3) \in \mathbb{R}^3 : x_3 > 0\}$, where the incident field u_I is known, and where the time convention $e^{-i\omega t}$ is taken. The goal is to find the scattered field u as a solution to the Laplace equation in the exterior open and connected domain Ω_e, satisfying an outgoing surface-wave radiation condition, and such that the total field u_T, which is decomposed as $u_T = u_I + u$, satisfies a homogeneous impedance boundary condition on the regular boundary $\Gamma = \Gamma_p \cup \Gamma_\infty$ (e.g., of class C^2). The exterior domain Ω_e is composed by the half-space $\mathbb{R}^3_+$ with a compact perturbation near the origin that is contained in $\mathbb{R}^3_+$, as shown in Figure 4.1. The perturbed boundary is denoted by Γ_p, while Γ_∞ denotes the remaining unperturbed boundary of $\mathbb{R}^3_+$, which extends towards infinity on every horizontal direction. The unit normal $\boldsymbol{n}$ is taken outwardly oriented of Ω_e and the complementary domain is denoted by $\Omega_c = \mathbb{R}^3 \setminus \overline{\Omega_e}$.

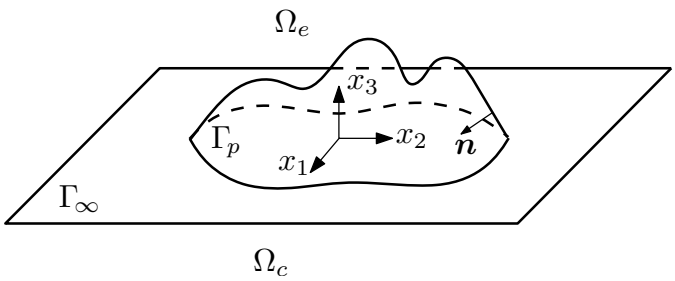

FIGURE 4.1. Perturbed half-space impedance Laplace problem domain.

The total field u_T satisfies thus the Laplace equation

$$\Delta u_T = 0 \qquad \text{in } \Omega_e, \tag{4.1}$$

which is also satisfied by the incident field u_I and the scattered field u, due linearity. For the total field u_T we take the homogeneous impedance boundary condition

$$-\frac{\partial u_T}{\partial n} + Z u_T = 0 \qquad \text{on } \Gamma, \tag{4.2}$$

where Z is the impedance on the boundary, which is decomposed as

$$Z(\boldsymbol{x}) = Z_\infty + Z_p(\boldsymbol{x}), \qquad \boldsymbol{x} \in \Gamma, \tag{4.3}$$

being $Z_\infty > 0$ real and constant throughout Γ, and $Z_p(\boldsymbol{x})$ a possibly complex-valued impedance that depends on the position $\boldsymbol{x}$ and that has a bounded support contained in Γ_p. The case of a complex Z_∞ will be discussed later. For linear water waves, the free-surface condition considers $Z_\infty = \omega^2/g$, where ω is the radian frequency or pulsation and g denotes the acceleration caused by gravity. If $Z = 0$ or $Z = \infty$, then we retrieve respectively the classical Neumann or Dirichlet boundary conditions. The scattered field u satisfies the non-homogeneous impedance boundary condition

$$-\frac{\partial u}{\partial n} + Z u = f_z \qquad \text{on } \Gamma, \tag{4.4}$$

where the impedance data function f_z is known, has its support contained in Γ_p, and is given, because of (4.2), by

$$f_z = \frac{\partial u_I}{\partial n} - Z u_I \qquad \text{on } \Gamma. \tag{4.5}$$

An outgoing surface-wave radiation condition has to be also imposed for the scattered field u, which specifies its decaying behavior at infinity and eliminates the non-physical solutions, e.g., ingoing surface waves or exponential growth inside Ω_e. This radiation condition can be stated for $r \to \infty$ in a more adjusted way as

$$\begin{cases} |u| \le \dfrac{C}{r^2} \quad \text{and} \quad \left|\dfrac{\partial u}{\partial r}\right| \le \dfrac{C}{r^3} & \text{if } x_3 > \dfrac{1}{2Z_\infty}\ln\bigl(1 + 2\pi Z_\infty r^3\bigr), \\[2ex] |u| \le \dfrac{C}{\sqrt{r}} \quad \text{and} \quad \left|\dfrac{\partial u}{\partial r} - iZ_\infty u\right| \le \dfrac{C}{r} & \text{if } x_3 \le \dfrac{1}{2Z_\infty}\ln\bigl(1 + 2\pi Z_\infty r^3\bigr), \end{cases} \tag{4.6}$$

for some constants $C > 0$, where $r = |\boldsymbol{x}|$. It implies that two different asymptotic behaviors can be established for the scattered field u. Away from the boundary Γ and inside the domain Ω_e, the first expression in (4.6) dominates, which is related to the asymptotic decaying condition (D.5) of the Laplace equation on the exterior of a bounded obstacle. Near the boundary, on the other hand, the second part of the second expression in (4.6) resembles a Sommerfeld radiation condition like (E.8), but only along the boundary, and is therefore related to the propagation of surface waves. It is often expressed also as

$$\left|\frac{\partial u}{\partial |\boldsymbol{x}_s|} - iZ_\infty u\right| \le \frac{C}{|\boldsymbol{x}_s|}, \tag{4.7}$$

where $\boldsymbol{x}_s = (x_1, x_2)$.

Analogously as done by Durán, Muga & Nédélec (2005*b*, 2009) for the Helmholtz equation, the radiation condition (4.6) can be stated alternatively as

$$\begin{cases} |u| \leq \dfrac{C}{r^{2-2\alpha}} \quad \text{and} \quad \left|\dfrac{\partial u}{\partial r}\right| \leq \dfrac{C}{r^{3-2\alpha}} & \text{if } \ x_3 > Cr^{\alpha}, \\ |u| \leq \dfrac{C}{\sqrt{r}} \quad \text{and} \quad \left|\dfrac{\partial u}{\partial r} - iZ_{\infty}u\right| \leq \dfrac{C}{r^{1-\alpha}} & \text{if } \ x_3 \leq Cr^{\alpha}, \end{cases} \tag{4.8}$$

for $0 < \alpha < 1/2$ and some constants $C > 0$, being the growth of Cr^{α} bigger than the logarithmic one at infinity. Equivalently, the radiation condition can be expressed in a more weaker and general formulation as

$$\begin{cases} \lim\limits_{R\to\infty} \displaystyle\int_{S_R^1} |u|^2 \, \mathrm{d}\gamma = 0 \quad \text{and} \quad \lim\limits_{R\to\infty} \displaystyle\int_{S_R^1} R^2 \left|\frac{\partial u}{\partial r}\right|^2 \mathrm{d}\gamma = 0, \\ \lim\limits_{R\to\infty} \displaystyle\int_{S_R^2} \frac{|u|^2}{\ln R} \, \mathrm{d}\gamma < \infty \quad \text{and} \quad \lim\limits_{R\to\infty} \displaystyle\int_{S_R^2} \frac{1}{\ln R} \left|\frac{\partial u}{\partial r} - iZ_{\infty}u\right|^2 \mathrm{d}\gamma = 0, \end{cases} \tag{4.9}$$

where

$$S_R^1 = \left\{ \boldsymbol{x} \in \mathbb{R}^3_+ : \, |\boldsymbol{x}| = R, \ \ x_3 > \frac{1}{2Z_{\infty}} \ln\bigl(1 + 2\pi Z_{\infty} R^3\bigr) \right\}, \tag{4.10}$$

$$S_R^2 = \left\{ \boldsymbol{x} \in \mathbb{R}^3_+ : \, |\boldsymbol{x}| = R, \ \ x_3 < \frac{1}{2Z_{\infty}} \ln\bigl(1 + 2\pi Z_{\infty} R^3\bigr) \right\}. \tag{4.11}$$

We observe that in this case

$$\int_{S_R^1} \mathrm{d}\gamma = \mathcal{O}(R^2) \qquad \text{and} \qquad \int_{S_R^2} \mathrm{d}\gamma = \mathcal{O}(R \ln R). \tag{4.12}$$

The portions S_R^1 and S_R^2 of the half-sphere and the terms depending on S_R^2 of the radiation condition (4.9) have to be modified when using instead the polynomial curves of (4.8). We refer to Stoker (1956) for a discussion on radiation conditions for surface waves.

The perturbed half-space impedance Laplace problem can be finally stated as

$$\begin{cases} \text{Find } u : \Omega_e \to \mathbb{C} \text{ such that} \\ \Delta u = 0 & \text{in } \ \Omega_e, \\ -\dfrac{\partial u}{\partial n} + Zu = f_z & \text{on } \ \Gamma, \\ \text{+ Outgoing radiation condition as } |\boldsymbol{x}| \to \infty, \end{cases} \tag{4.13}$$

where the outgoing radiation condition is given by (4.6).

4.2.2 Incident field

To determine the incident field u_I, we study the solutions of the unperturbed and homogeneous wave propagation problem with neither a scattered field nor an associated radiation condition. The solutions are searched in particular to be physically admissible, i.e., solutions which do not explode exponentially in the propagation domain, depicted in Figure 4.2.

We analyze thus the half-space impedance Laplace problem

$$\begin{cases} \Delta u_I = 0 & \text{in } \mathbb{R}^3_+, \\ \dfrac{\partial u_I}{\partial x_3} + Z_\infty u_I = 0 & \text{on } \{x_3 = 0\}. \end{cases} \tag{4.14}$$

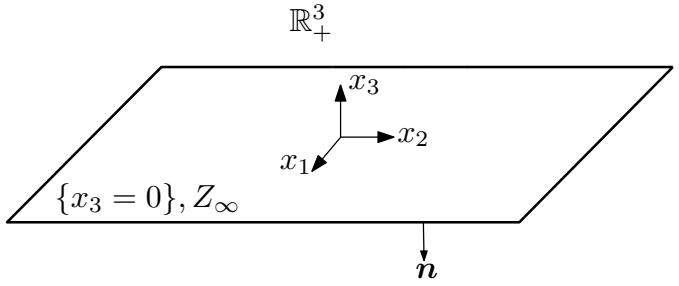

FIGURE 4.2. Positive half-space $\mathbb{R}^3_+$.

The solutions u_I of the problem (4.14) are given, up to an arbitrary scaling factor, by the progressive plane surface waves

$$u_I(\boldsymbol{x}) = e^{i\boldsymbol{k}_s \cdot \boldsymbol{x}_s} e^{-Z_\infty x_3}, \qquad (\boldsymbol{k}_s \cdot \boldsymbol{k}_s) = Z_\infty^2, \qquad \boldsymbol{x}_s = (x_1, x_2). \tag{4.15}$$

They correspond to progressive plane volume waves of the form $e^{i\boldsymbol{k}\cdot\boldsymbol{x}}$ with a complex wave propagation vector $\boldsymbol{k} = (\boldsymbol{k}_s, iZ_\infty)$, where $\boldsymbol{k}_s \in \mathbb{R}^2$. It can be observed that these surface waves are guided along the half-space's boundary, and decrease exponentially towards its interior, hence their name. They vanish completely for classical Dirichlet ($Z_\infty = \infty$) or Neumann ($Z_\infty = 0$) boundary conditions.

4.3 Green's function

4.3.1 Problem definition

The Green's function represents the response of the unperturbed system to a Dirac mass. It corresponds to a function G, which depends on the impedance Z_∞, on a fixed source point $\boldsymbol{x} \in \mathbb{R}^3_+$, and on an observation point $\boldsymbol{y} \in \mathbb{R}^3_+$. The Green's function is computed in the sense of distributions for the variable $\boldsymbol{y}$ in the half-space $\mathbb{R}^3_+$ by placing at the right-hand side of the Laplace equation a Dirac mass $\delta_{\boldsymbol{x}}$, centered at the point $\boldsymbol{x}$. It is therefore a solution for the radiation problem of a point source, namely

$$\begin{cases} \text{Find } G(\boldsymbol{x}, \cdot) : \mathbb{R}^3_+ \to \mathbb{C} \text{ such that} \\ \Delta_{\boldsymbol{y}} G(\boldsymbol{x}, \boldsymbol{y}) = \delta_{\boldsymbol{x}}(\boldsymbol{y}) & \text{in } \mathcal{D}'(\mathbb{R}^3_+), \\ \dfrac{\partial G}{\partial y_3}(\boldsymbol{x}, \boldsymbol{y}) + Z_\infty G(\boldsymbol{x}, \boldsymbol{y}) = 0 & \text{on } \{y_3 = 0\}, \\ \text{+ Outgoing radiation condition as } |\boldsymbol{y}| \to \infty. \end{cases} \tag{4.16}$$

The outgoing radiation condition, in the same way as in (4.6), is given here as $|\boldsymbol{y}| \to \infty$ by

$$\begin{cases} |G| \leq \dfrac{C}{|\boldsymbol{y}|^2} \quad \text{and} \quad \left|\dfrac{\partial G}{\partial r_{\boldsymbol{y}}}\right| \leq \dfrac{C}{|\boldsymbol{y}|^3} & \text{if } \; y_3 > \dfrac{\ln\bigl(1+2\pi Z_\infty |\boldsymbol{y}|^3\bigr)}{2Z_\infty}, \\ |G| \leq \dfrac{C}{\sqrt{|\boldsymbol{y}|}} \quad \text{and} \quad \left|\dfrac{\partial G}{\partial r_{\boldsymbol{y}}} - iZ_\infty G\right| \leq \dfrac{C}{|\boldsymbol{y}|} & \text{if } \; y_3 \leq \dfrac{\ln\bigl(1+2\pi Z_\infty |\boldsymbol{y}|^3\bigr)}{2Z_\infty}, \end{cases} \tag{4.17}$$

for some constants $C > 0$, which are independent of $r = |\boldsymbol{y}|$.

4.3.2 Special cases

When the Green's function problem (4.16) is solved using either homogeneous Dirichlet or Neumann boundary conditions, then its solution is found straightforwardly using the method of images (cf., e.g., Morse & Feshbach 1953).

a) Homogeneous Dirichlet boundary condition

We consider in the problem (4.16) the particular case of a homogeneous Dirichlet boundary condition, namely

$$G(\boldsymbol{x}, \boldsymbol{y}) = 0, \qquad \boldsymbol{y} \in \{y_3 = 0\}, \tag{4.18}$$

which corresponds to the limit case when the impedance is infinite ($Z_\infty = \infty$). In this case, the Green's function G can be explicitly calculated using the method of images, since it has to be antisymmetric with respect to the plane $\{y_3 = 0\}$. An additional image source point $\bar{\boldsymbol{x}} = (x_1, x_2, -x_3)$, located on the lower half-space and associated with a negative Dirac mass, is placed for this purpose just opposite to the upper half-space's source point $\boldsymbol{x} = (x_1, x_2, x_3)$. The desired solution is then obtained by evaluating the full-space Green's function (D.20) for each Dirac mass, which yields finally

$$G(\boldsymbol{x}, \boldsymbol{y}) = -\frac{1}{4\pi|\boldsymbol{y} - \boldsymbol{x}|} + \frac{1}{4\pi|\boldsymbol{y} - \bar{\boldsymbol{x}}|}. \tag{4.19}$$

b) Homogeneous Neumann boundary condition

We consider in the problem (4.16) the particular case of a homogeneous Neumann boundary condition, namely

$$\frac{\partial G}{\partial n_{\boldsymbol{y}}}(\boldsymbol{x}, \boldsymbol{y}) = 0, \qquad \boldsymbol{y} \in \{y_3 = 0\}, \tag{4.20}$$

which corresponds to the limit case when the impedance is zero ($Z_\infty = 0$). As in the previous case, the method of images is again employed, but now the half-space Green's function G has to be symmetric with respect to the plane $\{y_3 = 0\}$. Therefore, an additional image source point $\bar{\boldsymbol{x}} = (x_1, x_2, -x_3)$, located on the lower half-space, is placed just opposite to the upper half-space's source point $\boldsymbol{x} = (x_1, x_2, x_3)$, but now associated with a positive Dirac mass. The desired solution is then obtained by evaluating the full-space Green's function (D.20) for each Dirac mass, which yields

$$G(\boldsymbol{x}, \boldsymbol{y}) = -\frac{1}{4\pi|\boldsymbol{y} - \boldsymbol{x}|} - \frac{1}{4\pi|\boldsymbol{y} - \bar{\boldsymbol{x}}|}. \tag{4.21}$$

4.3.3 Spectral Green's function

a) Boundary-value problem

To solve (4.16) in the general case, we use a modified partial Fourier transform on the horizontal (y_1, y_2)-plane, taking advantage of the fact that there is no horizontal variation in the geometry of the problem. To obtain the corresponding spectral Green's function, we follow the same procedure as the one performed in Durán et al. (2005*b*). We define the forward Fourier transform of a function $F\big(\boldsymbol{x}, (\cdot, \cdot, y_3)\big) : \mathbb{R}^2 \to \mathbb{C}$ by

$$\widehat{F}(\boldsymbol{\xi}; y_3, x_3) = \frac{1}{2\pi} \int_{\mathbb{R}^2} F(\boldsymbol{x}, \boldsymbol{y})\, e^{-i\boldsymbol{\xi}\cdot(\boldsymbol{y}_s - \boldsymbol{x}_s)}\, \mathrm{d}\boldsymbol{y}_s, \qquad \boldsymbol{\xi} = (\xi_1, \xi_2) \in \mathbb{R}^2, \tag{4.22}$$

and its inverse by

$$F(\boldsymbol{x}, \boldsymbol{y}) = \frac{1}{2\pi} \int_{\mathbb{R}^2} \widehat{F}(\boldsymbol{\xi}; y_3, x_3)\, e^{i\boldsymbol{\xi}\cdot(\boldsymbol{y}_s - \boldsymbol{x}_s)}\, \mathrm{d}\boldsymbol{\xi}, \qquad \boldsymbol{y}_s = (y_1, y_2) \in \mathbb{R}^2, \tag{4.23}$$

where $\boldsymbol{x}_s = (x_1, x_2) \in \mathbb{R}^2$ and thus $\boldsymbol{x} = (\boldsymbol{x}_s, x_3)$.

To ensure a correct integration path for the Fourier transform and correct physical results, the calculations have to be performed in the framework of the limiting absorption principle, which allows to treat all the appearing integrals as Cauchy principal values. For this purpose, we take a small dissipation parameter $\varepsilon > 0$ into account and consider the problem (4.16) as the limit case when $\varepsilon \to 0$ of the dissipative problem

$$\begin{cases} \text{Find } G_\varepsilon(\boldsymbol{x}, \cdot) : \mathbb{R}^3_+ \to \mathbb{C} \text{ such that} & \\ \Delta_{\boldsymbol{y}} G_\varepsilon(\boldsymbol{x}, \boldsymbol{y}) = \delta_{\boldsymbol{x}}(\boldsymbol{y}) & \text{in } \mathcal{D}'(\mathbb{R}^3_+), \\ \dfrac{\partial G_\varepsilon}{\partial y_3}(\boldsymbol{x}, \boldsymbol{y}) + Z_\varepsilon G_\varepsilon(\boldsymbol{x}, \boldsymbol{y}) = 0 & \text{on } \{y_3 = 0\}, \end{cases} \tag{4.24}$$

where $Z_\varepsilon = Z_\infty + i\varepsilon$. This choice ensures a correct outgoing dissipative surface-wave behavior. Further references for the application of this principle can be found in Lenoir & Martin (1981) and in Hazard & Lenoir (1998).

Applying thus the Fourier transform (4.22) on the system (4.24) leads to a linear second order ordinary differential equation for the variable y_3, with prescribed boundary values, given by

$$\begin{cases} \dfrac{\partial^2 \widehat{G}_\varepsilon}{\partial y_3^2}(\boldsymbol{\xi}) - |\boldsymbol{\xi}|^2 \widehat{G}_\varepsilon(\boldsymbol{\xi}) = \dfrac{\delta(y_3 - x_3)}{2\pi}, & y_3 > 0, \\ \dfrac{\partial \widehat{G}_\varepsilon}{\partial y_3}(\boldsymbol{\xi}) + Z_\varepsilon \widehat{G}_\varepsilon(\boldsymbol{\xi}) = 0, & y_3 = 0. \end{cases} \tag{4.25}$$

To describe the (ξ_1, ξ_2)-plane, we use henceforth the system of signed polar coordinates

$$\xi = \begin{cases} \sqrt{\xi_1^2 + \xi_2^2} & \text{if } \xi_2 > 0, \\ \xi_1 & \text{if } \xi_2 = 0, \\ -\sqrt{\xi_1^2 + \xi_2^2} & \text{if } \xi_2 < 0, \end{cases} \qquad \text{and} \qquad \psi = \operatorname{arccot}\left(\frac{\xi_1}{\xi_2}\right), \tag{4.26}$$

where $-\infty < \xi < \infty$ and $0 \le \psi < \pi$. From (4.25) it is not difficult to see that the solution $\widehat{G}_\varepsilon$ depends only on $|\boldsymbol{\xi}|$, and therefore only on ξ, since $|\xi| = |\boldsymbol{\xi}|$. We remark that

the inverse Fourier transform (4.23) can be stated equivalently as

$$F(\boldsymbol{x},\boldsymbol{y}) = \frac{1}{2\pi}\int_{-\infty}^{\infty}\int_{0}^{\pi} \widehat{F}(\xi,\psi;y_3,x_3)|\xi|\, e^{i\xi\{(y_1-x_1)\cos\psi+(y_2-x_2)\sin\psi\}}\,\mathrm{d}\psi\,\mathrm{d}\xi. \tag{4.27}$$

We use the method of undetermined coefficients, and solve the homogeneous differential equation of the problem (4.25) respectively in the zone $\{\boldsymbol{y}\in\mathbb{R}^3_+ :\ 0<y_3<x_3\}$ and in the half-space $\{\boldsymbol{y}\in\mathbb{R}^3_+ :\ y_3>x_3\}$. This gives a solution for $\widehat{G}_\varepsilon$ in each domain, as a linear combination of two independent solutions of an ordinary differential equation, namely

$$\widehat{G}_\varepsilon(\xi) = \begin{cases} a\, e^{|\xi|y_3} + b\, e^{-|\xi|y_3} & \text{for } \ 0<y_3<x_3, \\ c\, e^{|\xi|y_3} + d\, e^{-|\xi|y_3} & \text{for } \ y_3>x_3. \end{cases} \tag{4.28}$$

The unknowns a, b, c, and d, which depend on ξ and x_3, are determined through the boundary condition, by imposing continuity, and by assuming an outgoing wave behavior.

b) Spectral Green's function with dissipation

Now, thanks to (4.28), the computation of $\widehat{G}_\varepsilon$ is straightforward. From the boundary condition of (4.25) a relation for the coefficients a and b can be derived, which is given by

$$a\big(Z_\varepsilon+|\xi|\big)+b\big(Z_\varepsilon-|\xi|\big)=0. \tag{4.29}$$

On the other hand, since the solution (4.28) has to be bounded at infinity as $y_3\to\infty$, it follows then necessarily that

$$c=0. \tag{4.30}$$

To ensure the continuity of the Green's function at the point $y_3=x_3$, it is needed that

$$d = a\, e^{|\xi|2x_3}+b. \tag{4.31}$$

Using relations (4.29), (4.30), and (4.31) in (4.28), we obtain the expression

$$\widehat{G}_\varepsilon(\xi) = a\, e^{|\xi|x_3}\left[e^{-|\xi||y_3-x_3|} - \left(\frac{Z_\varepsilon+|\xi|}{Z_\varepsilon-|\xi|}\right)e^{-|\xi|(y_3+x_3)}\right]. \tag{4.32}$$

The remaining unknown coefficient a is determined by replacing (4.32) in the differential equation of (4.25), taking the derivatives in the sense of distributions, particularly

$$\frac{\partial}{\partial y_3}\left\{e^{-|\xi||y_3-x_3|}\right\} = -|\xi|\,\mathrm{sign}(y_3-x_3)\, e^{-|\xi||y_3-x_3|}, \tag{4.33}$$

and

$$\frac{\partial}{\partial y_3}\big\{\mathrm{sign}(y_3-x_3)\big\} = 2\,\delta(y_3-x_3). \tag{4.34}$$

So, the second derivative of (4.32) becomes

$$\frac{\partial^2\widehat{G}_\varepsilon}{\partial y_3^2}(\xi) = a\, e^{|\xi|x_3}\left[|\xi|^2 e^{-|\xi||y_3-x_3|} - 2|\xi|\delta(y_3-x_3) - \left(\frac{Z_\varepsilon+|\xi|}{Z_\varepsilon-|\xi|}\right)|\xi|^2 e^{-|\xi|(y_3+x_3)}\right]. \tag{4.35}$$

This way, from (4.32) and (4.35) in the first equation of (4.25), we obtain that

$$a = -\frac{e^{-|\xi|x_3}}{4\pi|\xi|}. \tag{4.36}$$

Finally, the spectral Green's function $\widehat{G}_\varepsilon$ with dissipation ε is given by

$$\widehat{G}_\varepsilon(\xi; y_3, x_3) = -\frac{e^{-|\xi||y_3-x_3|}}{4\pi|\xi|} + \left(\frac{Z_\varepsilon + |\xi|}{Z_\varepsilon - |\xi|}\right)\frac{e^{-|\xi|(y_3+x_3)}}{4\pi|\xi|}. \tag{4.37}$$

c) Analysis of singularities

To obtain the spectral Green's function $\widehat{G}$ without dissipation, the limit $\varepsilon \to 0$ has to be taken in (4.37). This can be done directly wherever the limit is regular and continuous on ξ. Singular points, on the other hand, have to be analyzed carefully to fulfill correctly the limiting absorption principle. Thus we study first the singularities of the limit function before applying this principle, i.e., considering just $\varepsilon = 0$, in which case we have

$$\widehat{G}_0(\xi) = -\frac{e^{-|\xi||y_3-x_3|}}{4\pi|\xi|} + \left(\frac{Z_\infty + |\xi|}{Z_\infty - |\xi|}\right)\frac{e^{-|\xi|(y_3+x_3)}}{4\pi|\xi|}. \tag{4.38}$$

Possible singularities for (4.38) may only appear when $|\xi| = 0$ or when $|\xi| = Z_\infty$, i.e., when the denominator of the fractions is zero. Otherwise the function is regular and continuous.

For $|\xi| = 0$ the function (4.38) is continuous. This can be seen by writing it, analogously as in Durán, Muga & Nédélec (2005*b*), in the form

$$\widehat{G}_0(\xi) = \frac{H\big(|\xi|\big)}{|\xi|}, \tag{4.39}$$

where

$$H(\beta) = \frac{1}{4\pi}\left(-e^{-\beta\,|y_3-x_3|} + \frac{Z_\infty + \beta}{Z_\infty - \beta}\,e^{-\beta\,(y_3+x_3)}\right), \qquad \beta \in \mathbb{C}. \tag{4.40}$$

Since $H(\beta)$ is an analytic function in $\beta = 0$, since $H(0) = 0$, and since

$$\lim_{|\xi|\to 0} \widehat{G}_0(\xi) = \lim_{|\xi|\to 0} \frac{H\big(|\xi|\big) - H(0)}{|\xi|} = H'(0), \tag{4.41}$$

we can easily obtain that

$$\lim_{|\xi|\to 0} \widehat{G}_0(\xi) = \frac{1}{4\pi}\left(1 + \frac{1}{Z_\infty} + |y_3 - x_3| - (y_3 + x_3)\right), \tag{4.42}$$

being thus $\widehat{G}_0$ bounded and continuous on $|\xi| = 0$.

For $\xi = Z_\infty$ and $\xi = -Z_\infty$, the function (4.38) presents two simple poles, whose residues are characterized by

$$\lim_{\xi\to\pm Z_\infty} (\xi \mp Z_\infty)\widehat{G}_0(\xi) = \mp\frac{1}{2\pi}\,e^{-Z_\infty(y_3+x_3)}. \tag{4.43}$$

To analyze the effect of this singularity, we study now the computation of the inverse Fourier transform of

$$\widehat{G}_P(\xi) = \frac{1}{2\pi}\,e^{-Z_\infty(y_3+x_3)}\left(\frac{1}{\xi + Z_\infty} - \frac{1}{\xi - Z_\infty}\right), \tag{4.44}$$

which has to be done in the frame of the limiting absorption principle to obtain the correct physical results, i.e., the inverse Fourier transform has to be understood in the sense of

$$G_P(\boldsymbol{x},\boldsymbol{y}) = \lim_{\varepsilon\to 0}\left\{\frac{e^{-Z_\varepsilon(y_3+x_3)}}{4\pi^2}\int_0^\pi\int_{-\infty}^{\infty}\left(\frac{1}{\xi+Z_\varepsilon}-\frac{1}{\xi-Z_\varepsilon}\right)|\xi|\,e^{i\xi r\sin\theta\cos(\psi-\varphi)}\,\mathrm{d}\xi\,\mathrm{d}\psi\right\}, \tag{4.45}$$

being the spatial variables inside the integrals expressed through the spherical coordinates

$$\begin{cases} y_1-x_1 = r\sin\theta\cos\varphi, \\ y_2-x_2 = r\sin\theta\sin\varphi, \\ y_3-x_3 = r\cos\theta, \end{cases} \quad \text{for} \quad \begin{cases} 0\le r<\infty, \\ 0\le\theta\le\pi, \\ -\pi<\varphi\le\pi. \end{cases} \tag{4.46}$$

To perform correctly the computation of (4.45), we apply the residue theorem of complex analysis (cf., e.g., Arfken & Weber 2005, Bak & Newman 1997, Dettman 1984) on the complex meromorphic mapping

$$F(\xi) = \left(\frac{1}{\xi+\xi_p}-\frac{1}{\xi-\xi_p}\right)|\xi|\,e^{i\xi\tau}, \tag{4.47}$$

which admits two simple poles at ξ_p and $-\xi_p$, where $\mathfrak{Im}\{\xi_p\}>0$ and $\tau\in\mathbb{R}$. We consider also the closed complex integration contours $C^+_{R,\varepsilon}$ and $C^-_{R,\varepsilon}$, which are associated respectively with the values $\tau\ge 0$ and $\tau<0$, and are depicted in Figure 4.3.

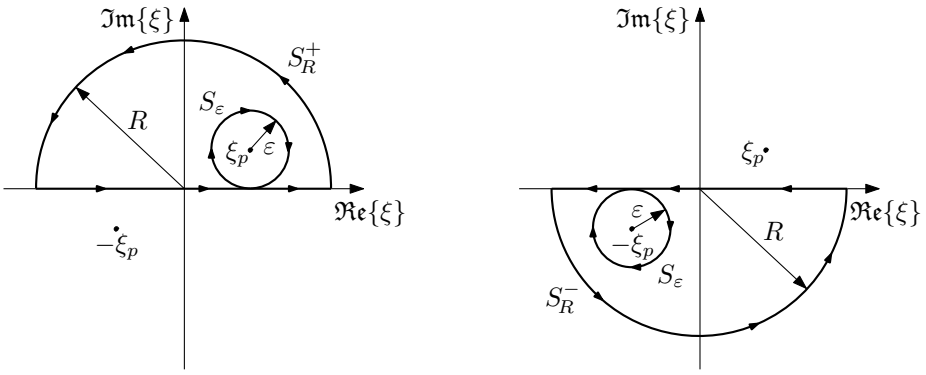

(a) Contour $C^+_{R,\varepsilon}$ (b) Contour $C^-_{R,\varepsilon}$

FIGURE 4.3. Complex integration contours using the limiting absorption principle.

Since the contours $C^+_{R,\varepsilon}$ and $C^-_{R,\varepsilon}$ enclose no singularities, the residue theorem of Cauchy implies that the respective closed path integrals are zero, i.e.,

$$\oint_{C^+_{R,\varepsilon}} F(\xi)\,\mathrm{d}\xi = 0, \tag{4.48}$$

and

$$\oint_{C^-_{R,\varepsilon}} F(\xi)\,\mathrm{d}\xi = 0. \tag{4.49}$$

By considering $\tau \geq 0$ and working with the contour $C^+_{R,\varepsilon}$ in the upper complex plane, we obtain from (4.48) that

$$\int_{-R}^{\mathfrak{Re}\{\xi_p\}} F(\xi)\,\mathrm{d}\xi + \int_{S_\varepsilon} F(\xi)\,\mathrm{d}\xi + \int_{\mathfrak{Re}\{\xi_p\}}^{R} F(\xi)\,\mathrm{d}\xi + \int_{S_R^+} F(\xi)\,\mathrm{d}\xi = 0. \tag{4.50}$$

Performing the change of variable $\xi - \xi_p = \varepsilon e^{i\phi}$ for the integral on S_ε yields

$$\int_{S_\varepsilon} F(\xi)\,\mathrm{d}\xi = i\,e^{i\xi_p\tau} \int_{3\pi/2}^{-\pi/2} \left(\frac{\varepsilon e^{i\phi}}{\varepsilon e^{i\phi} + 2\xi_p} - 1 \right) |\xi_p + \varepsilon e^{i\phi}|\, e^{\varepsilon\tau(i\cos\phi - \sin\phi)}\,\mathrm{d}\phi. \tag{4.51}$$

By taking then the limit $\varepsilon \to 0$ we obtain

$$\lim_{\varepsilon\to 0} \int_{S_\varepsilon} F(\xi)\,\mathrm{d}\xi = i2\pi|\xi_p|e^{i\xi_p\tau}. \tag{4.52}$$

In a similar way, taking $\xi = Re^{i\phi}$ for the integral on S_R^+ yields

$$\int_{S_R^+} F(\xi)\,\mathrm{d}\xi = \int_0^\pi \left(\frac{iR^2 e^{i\phi}}{Re^{i\phi} + \xi_p} - \frac{iR^2 e^{i\phi}}{Re^{i\phi} - \xi_p} \right) e^{R\tau(i\cos\phi - \sin\phi)}\,\mathrm{d}\phi. \tag{4.53}$$

Since $|e^{iR\tau\cos\phi}| \leq 1$ and $R\sin\phi \geq 0$ for $0 \leq \phi \leq \pi$, when taking the limit $R \to \infty$ we obtain

$$\lim_{R\to\infty} \int_{S_R^+} F(\xi)\,\mathrm{d}\xi = 0. \tag{4.54}$$

Thus, taking the limits $\varepsilon \to 0$ and $R \to \infty$ in (4.50) yields

$$\int_{-\infty}^{\infty} F(\xi)\,\mathrm{d}\xi = -i2\pi|\xi_p|e^{i\xi_p\tau}, \qquad \tau \geq 0. \tag{4.55}$$

By considering now $\tau < 0$ and working with the contour $C^-_{R,\varepsilon}$ in the lower complex plane, we obtain from (4.49) that

$$\int_{R}^{\mathfrak{Re}\{-\xi_p\}} F(\xi)\,\mathrm{d}\xi + \int_{S_\varepsilon} F(\xi)\,\mathrm{d}\xi + \int_{\mathfrak{Re}\{-\xi_p\}}^{-R} F(\xi)\,\mathrm{d}\xi + \int_{S_R^-} F(\xi)\,\mathrm{d}\xi = 0. \tag{4.56}$$

Performing the change of variable $\xi + \xi_p = \varepsilon e^{i\phi}$ for the integral on S_ε yields

$$\int_{S_\varepsilon} F(\xi)\,\mathrm{d}\xi = i\,e^{-i\xi_p\tau} \int_{\pi/2}^{-3\pi/2} \left(1 - \frac{\varepsilon e^{i\phi}}{\varepsilon e^{i\phi} - 2\xi_p} \right) |\xi_p - \varepsilon e^{i\phi}|\, e^{\varepsilon\tau(i\cos\phi - \sin\phi)}\,\mathrm{d}\phi. \tag{4.57}$$

By taking then the limit $\varepsilon \to 0$ we obtain

$$\lim_{\varepsilon\to 0} \int_{S_\varepsilon} F(\xi)\,\mathrm{d}\xi = -i2\pi|\xi_p|e^{-i\xi_p\tau}. \tag{4.58}$$

In a similar way, taking $\xi = Re^{i\phi}$ for the integral on S_R^- yields

$$\int_{S_R^-} F(\xi)\,\mathrm{d}\xi = \int_{-\pi}^0 \left(\frac{iR^2 e^{i\phi}}{Re^{i\phi} + \xi_p} - \frac{iR^2 e^{i\phi}}{Re^{i\phi} - \xi_p} \right) e^{R\tau(i\cos\phi - \sin\phi)}\,\mathrm{d}\phi. \tag{4.59}$$

Since $|e^{iR\tau\cos\phi}| \leq 1$ and $R\sin\phi \leq 0$ for $-\pi \leq \phi \leq 0$, when taking the limit $R \to \infty$ we obtain

$$\lim_{R\to\infty} \int_{S_R^-} F(\xi)\,\mathrm{d}\xi = 0. \tag{4.60}$$

Thus, taking the limits $\varepsilon \to 0$ and $R \to \infty$ in (4.56) yields

$$\int_{-\infty}^{\infty} F(\xi)\,\mathrm{d}\xi = -i2\pi|\xi_p|e^{-i\xi_p\tau}, \qquad \tau < 0. \tag{4.61}$$

In conclusion, from (4.55) and (4.61) we obtain that

$$\int_{-\infty}^{\infty} F(\xi)\,\mathrm{d}\xi = -i2\pi|\xi_p|e^{i\xi_p|\tau|}, \qquad \tau \in \mathbb{R}. \tag{4.62}$$

Using (4.62) for $\xi_p = Z_\infty$ and $\tau = r\sin\theta\cos(\psi-\varphi)$ yields then that the inverse Fourier transform of (4.44), when considering the limiting absorption principle, is given by

$$G_P^L(\boldsymbol{x},\boldsymbol{y}) = -\frac{iZ_\infty}{2\pi}\,e^{-Z_\infty(y_3+x_3)}\int_0^\pi e^{iZ_\infty r\sin\theta\,|\cos(\psi-\varphi)|}\,\mathrm{d}\psi. \tag{4.63}$$

It can be observed that the integral in (4.63) is independent of the angle φ, which we can choose without problems as $\varphi = \pi/2$ and therefore $|\cos(\psi-\varphi)| = \sin\psi$. Since

$$r\sin\theta = |\boldsymbol{y}_s - \boldsymbol{x}_s|, \tag{4.64}$$

we can express (4.63) as

$$G_P^L(\boldsymbol{x},\boldsymbol{y}) = -\frac{iZ_\infty}{2\pi}\,e^{-Z_\infty(y_3+x_3)}\int_0^\pi e^{iZ_\infty|\boldsymbol{y}_s-\boldsymbol{x}_s|\sin\psi}\,\mathrm{d}\psi. \tag{4.65}$$

We observe that this expression describes the asymptotic behavior of the surface waves, which are linked to the presence of the poles in the spectral Green's function. Due (A.112) and (A.244), we can rewrite (4.65) more explicitly as

$$G_P^L(\boldsymbol{x},\boldsymbol{y}) = -\frac{iZ_\infty}{2}\,e^{-Z_\infty(y_3+x_3)}\Big[J_0\big(Z_\infty|\boldsymbol{y}_s-\boldsymbol{x}_s|\big) + i\boldsymbol{H}_0\big(Z_\infty|\boldsymbol{y}_s-\boldsymbol{x}_s|\big)\Big], \tag{4.66}$$

where J_0 denotes the Bessel function of order zero (vid. Subsection A.2.4) and $\boldsymbol{H}_0$ the Struve function of order zero (vid. Subsection A.2.7).

If the limiting absorption principle is not considered, i.e., if $\mathfrak{Im}\{\xi_p\} = 0$, then the inverse Fourier transform of (4.44) could be computed in the sense of the principal value with the residue theorem by considering, instead of $C_{R,\varepsilon}^+$ and $C_{R,\varepsilon}^-$, the contours depicted in Figure 4.4. In this case we would obtain, instead of (4.62), the quantity

$$\int_{-\infty}^{\infty} F(\xi)\,\mathrm{d}\xi = 2\pi|\xi_p|\sin\big(\xi_p|\tau|\big), \qquad \tau \in \mathbb{R}. \tag{4.67}$$

The inverse Fourier transform of (4.44) would be in this case

$$G_P^{NL}(\boldsymbol{x},\boldsymbol{y}) = \frac{Z_\infty}{2}\,e^{-Z_\infty(y_3+x_3)}\boldsymbol{H}_0\big(Z_\infty|\boldsymbol{y}_s-\boldsymbol{x}_s|\big), \tag{4.68}$$

which is correct from the mathematical point of view, but yields only a standing surface wave, and not a desired outgoing progressive surface wave as in (4.66).

The effect of the limiting absorption principle, in the spatial dimension, is then given by the difference between (4.66) and (4.68), i.e., by

$$G_L(\boldsymbol{x},\boldsymbol{y}) = G_P^L(\boldsymbol{x},\boldsymbol{y}) - G_P^{NL}(\boldsymbol{x},\boldsymbol{y}) = -\frac{iZ_\infty}{2}\,e^{-Z_\infty(y_3+x_3)}J_0\big(Z_\infty|\boldsymbol{y}_s-\boldsymbol{x}_s|\big), \tag{4.69}$$

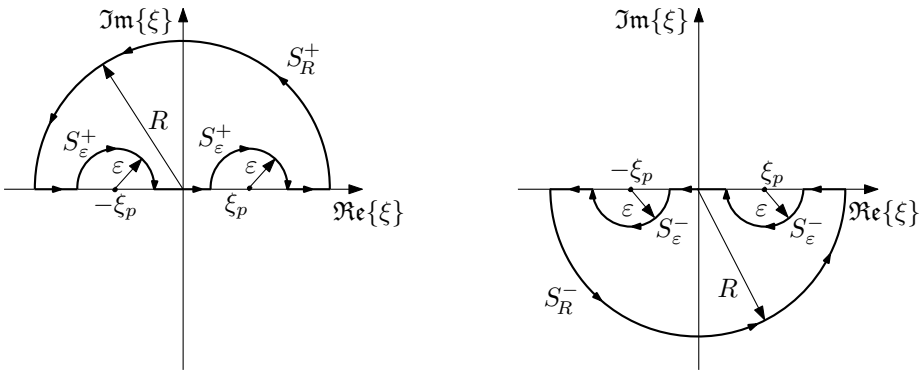

(a) Contour $C_{R,\varepsilon}^+$ (b) Contour $C_{R,\varepsilon}^-$

FIGURE 4.4. Complex integration contours without using the limiting absorption principle.

whose Fourier transform, and therefore the spectral effect, is given by

$$\widehat{G}_L(\xi) = \widehat{G}_P^L(\xi) - \widehat{G}_P^{NL}(\xi) = -\frac{iZ_\infty}{2|\xi|}\, e^{-Z_\infty(y_3+x_3)}\big[\delta(\xi - Z_\infty) + \delta(\xi + Z_\infty)\big]. \tag{4.70}$$

d) Spectral Green's function without dissipation

The spectral Green's function $\widehat{G}$ without dissipation is therefore obtained by taking the limit $\varepsilon \to 0$ in (4.37) and considering the effect of the limiting absorption principle for the appearing singularities, summarized in (4.70). Thus we obtain in the sense of distributions

$$\begin{aligned}\widehat{G}(\xi; y_3, x_3) = &- \frac{e^{-|\xi||y_3 - x_3|}}{4\pi|\xi|} + \left(\frac{Z_\infty + |\xi|}{Z_\infty - |\xi|}\right)\frac{e^{-|\xi|(y_3+x_3)}}{4\pi|\xi|} \\ &- \frac{iZ_\infty}{2|\xi|}\, e^{-Z_\infty(y_3+x_3)}\big[\delta(\xi - Z_\infty) + \delta(\xi + Z_\infty)\big].\end{aligned} \tag{4.71}$$

For our further analysis, this spectral Green's function is decomposed into four terms according to

$$\widehat{G} = \widehat{G}_\infty + \widehat{G}_N + \widehat{G}_L + \widehat{G}_R, \tag{4.72}$$

where

$$\widehat{G}_\infty(\xi; y_3, x_3) = -\frac{e^{-|\xi||y_3 - x_3|}}{4\pi|\xi|}, \tag{4.73}$$

$$\widehat{G}_N(\xi; y_3, x_3) = -\frac{e^{-|\xi|(y_3+x_3)}}{4\pi|\xi|}, \tag{4.74}$$

$$\widehat{G}_L(\xi; y_3, x_3) = -\frac{iZ_\infty}{2|\xi|}\, e^{-Z_\infty(y_3+x_3)}\big[\delta(\xi - Z_\infty) + \delta(\xi + Z_\infty)\big], \tag{4.75}$$

$$\widehat{G}_R(\xi; y_3, x_3) = \frac{Z_\infty e^{-|\xi|(y_3+x_3)}}{2\pi|\xi|\big(Z_\infty - |\xi|\big)}. \tag{4.76}$$

4.3.4 Spatial Green's function

a) Spatial Green's function as an inverse Fourier transform

The desired spatial Green's function is then given by the inverse Fourier transform of the spectral Green's function (4.71), namely by

$$\begin{aligned} G(\boldsymbol{x},\boldsymbol{y}) = &- \frac{1}{8\pi^2}\int_{-\infty}^{\infty}\int_{0}^{\pi} e^{-|\xi||y_3-x_3|}\, e^{i\xi r\sin\theta\cos(\psi-\varphi)}\,\mathrm{d}\psi\,\mathrm{d}\xi \\ &+ \frac{1}{8\pi^2}\int_{-\infty}^{\infty}\int_{0}^{\pi} \left(\frac{Z_\infty+|\xi|}{Z_\infty-|\xi|}\right) e^{-|\xi|(y_3+x_3)}\, e^{i\xi r\sin\theta\cos(\psi-\varphi)}\,\mathrm{d}\psi\,\mathrm{d}\xi \\ &- \frac{iZ_\infty}{2}\, e^{-Z_\infty(y_3+x_3)} J_0\big(Z_\infty|\boldsymbol{y}_s-\boldsymbol{x}_s|\big), \end{aligned} \tag{4.77}$$

where the spherical coordinates (4.46) are used again inside the integrals.

Due the linearity of the Fourier transform, the decomposition (4.72) applies also in the spatial domain, i.e., the spatial Green's function is decomposed in the same manner by

$$G = G_\infty + G_N + G_L + G_R. \tag{4.78}$$

b) Term of the full-space Green's function

The first term in (4.77) corresponds to the inverse Fourier transform of (4.73), and can be rewritten, due (A.794), as the Hankel transform

$$G_\infty(\boldsymbol{x},\boldsymbol{y}) = -\frac{1}{4\pi}\int_0^\infty e^{-\rho|y_3-x_3|} J_0\big(\rho|\boldsymbol{y}_s-\boldsymbol{x}_s|\big)\,\mathrm{d}\rho. \tag{4.79}$$

The value for this integral can be obtained either from Watson (1944, page 384), by using Sommerfeld's formula (Magnus & Oberhettinger 1954, page 34) for $k=0$, i.e.,

$$\int_0^\infty e^{-\rho|y_3-x_3|} J_0\big(\rho|\boldsymbol{y}_s-\boldsymbol{x}_s|\big)\,\mathrm{d}\rho = \frac{1}{|\boldsymbol{y}-\boldsymbol{x}|}, \tag{4.80}$$

from Gradshteyn & Ryzhik (2007, equation 6.611–1), or by directly computing the two integrals appearing in the first term of (4.77), beginning with the exterior one. This way, the inverse Fourier transform of (4.73) is readily given by

$$G_\infty(\boldsymbol{x},\boldsymbol{y}) = -\frac{1}{4\pi|\boldsymbol{y}-\boldsymbol{x}|}. \tag{4.81}$$

We observe that (4.81) is, in fact, the full-space Green's function of the Laplace equation. Thus $G_N+G_L+G_R$ represents the perturbation of the full-space Green's function G_∞ due the presence of the impedance half-space.

c) Term associated with a Neumann boundary condition

The inverse Fourier transform of (4.74) is computed in the same manner as the term G_∞. It is given by

$$G_N(\boldsymbol{x},\boldsymbol{y}) = -\frac{1}{4\pi}\int_0^\infty e^{-\rho(y_3+x_3)} J_0\big(\rho|\boldsymbol{y}_s-\boldsymbol{x}_s|\big)\,\mathrm{d}\rho, \tag{4.82}$$

and in this case, instead of (4.80), Sommerfeld's formula becomes

$$\int_0^\infty e^{-\rho(y_3+x_3)} J_0\big(\rho|\boldsymbol{y}_s - \boldsymbol{x}_s|\big)\,\mathrm{d}\rho = \frac{1}{|\boldsymbol{y} - \bar{\boldsymbol{x}}|}, \tag{4.83}$$

where $\bar{\boldsymbol{x}} = (x_1, x_2, -x_3)$ corresponds to the image point of $\boldsymbol{x}$ in the lower half-space. The inverse Fourier transform of (4.74) is therefore given by

$$G_N(\boldsymbol{x}, \boldsymbol{y}) = -\frac{1}{4\pi|\boldsymbol{y} - \bar{\boldsymbol{x}}|}, \tag{4.84}$$

which represents the additional term that appears in the Green's function due the method of images when considering a Neumann boundary condition, as in (4.21).

d) Term associated with the limiting absorption principle

The term G_L, the inverse Fourier transform of (4.75), is associated with the effect of the limiting absorption principle on the Green's function, and has been already calculated in (4.69). It yields the imaginary part of the Green's function, and is given by

$$G_L(\boldsymbol{x}, \boldsymbol{y}) = -\frac{iZ_\infty}{2}\, e^{-Z_\infty(y_3+x_3)} J_0\big(Z_\infty|\boldsymbol{y}_s - \boldsymbol{x}_s|\big). \tag{4.85}$$

e) Remaining term

The remaining term G_R, the inverse Fourier transform of (4.76), can be computed as the integral

$$G_R(\boldsymbol{x}, \boldsymbol{y}) = \frac{Z_\infty}{2\pi} \int_0^\infty \frac{e^{-\rho(y_3+x_3)}}{Z_\infty - \rho} J_0\big(\rho|\boldsymbol{y}_s - \boldsymbol{x}_s|\big)\,\mathrm{d}\rho. \tag{4.86}$$

We denote

$$\varrho_s = |\boldsymbol{y}_s - \boldsymbol{x}_s| \qquad \text{and} \qquad v_3 = y_3 + x_3, \tag{4.87}$$

and we consider the change of notation

$$G_R(\boldsymbol{x}, \boldsymbol{y}) = \frac{Z_\infty}{2\pi}\, e^{-Z_\infty v_3} G_B(\varrho_s, v_3), \tag{4.88}$$

being

$$G_B(\varrho_s, v_3) = \int_0^\infty \frac{e^{(Z_\infty-\rho)v_3}}{Z_\infty - \rho} J_0(\varrho_s\rho)\,\mathrm{d}\rho. \tag{4.89}$$

Consequently, by considering (4.83) we have for the y_3-derivative of G_B that

$$\frac{\partial G_B}{\partial y_3}(\varrho_s, v_3) = e^{Z_\infty v_3} \int_0^\infty e^{-\rho v_3} J_0(\varrho_s\rho)\,\mathrm{d}\rho = \frac{e^{Z_\infty v_3}}{|\boldsymbol{y} - \bar{\boldsymbol{x}}|}. \tag{4.90}$$

Following Pidcock (1985), the integral (4.86) can be thus expressed by

$$G_R(\boldsymbol{x}, \boldsymbol{y}) = \frac{Z_\infty}{2\pi}\, e^{-Z_\infty v_3} \left(G_B(\varrho_s, 0) + \int_0^{v_3} \frac{e^{Z_\infty \eta}}{\sqrt{\varrho_s^2 + \eta^2}}\,\mathrm{d}\eta \right), \tag{4.91}$$

where

$$G_B(\varrho_s, 0) = \int_0^\infty \frac{J_0(\varrho_s\rho)}{Z_\infty - \rho}\,\mathrm{d}\rho. \tag{4.92}$$

To evaluate the integral (4.92), we consider the closed complex integration contour $C_{R,\varepsilon}$ depicted in Figure 4.5 and use the fact that

$$\oint_{C_{R,\varepsilon}} \frac{H_0^{(1)}(\varrho_s \rho)}{Z_\infty - \rho} \, \mathrm{d}\rho = 0, \tag{4.93}$$

where $H_0^{(1)}$ denotes the zeroth order Hankel function of the first kind (vid. Subsection A.2.4).

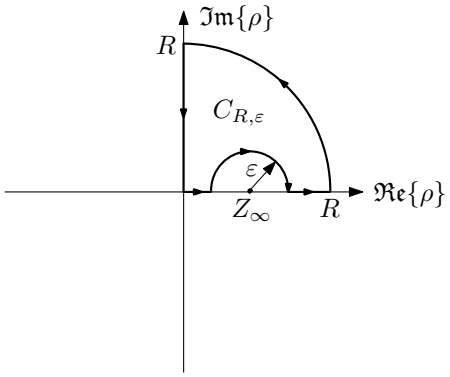

FIGURE 4.5. Complex integration contour $C_{R,\varepsilon}$.

We can express (4.93) more explicitly as

$$\begin{aligned} &\int_0^{Z_\infty - \varepsilon} \frac{H_0^{(1)}(\varrho_s \rho)}{Z_\infty - \rho} \, \mathrm{d}\rho - i \int_\pi^0 H_0^{(1)}\Big(\varrho_s\big(Z_\infty + \varepsilon e^{i\theta}\big)\Big) \, \mathrm{d}\theta + \int_{Z_\infty + \varepsilon}^R \frac{H_0^{(1)}(\varrho_s \rho)}{Z_\infty - \rho} \, \mathrm{d}\rho \\ &\quad - i \int_0^{\pi/2} \frac{H_0^{(1)}\big(\varrho_s R e^{i\theta}\big)}{Z_\infty - R e^{i\theta}} \, R e^{i\theta} \, \mathrm{d}\theta - \frac{2}{\pi} \int_0^R \frac{K_0(\varrho_s \tau)}{Z_\infty - i\tau} \, \mathrm{d}\tau = 0, \end{aligned} \tag{4.94}$$

where we use the relation (A.153) for $\nu = 0$ and where K_0 denotes the zeroth order modified Bessel function of the second kind (vid. Subsection A.2.5). By taking the limits $\varepsilon \to 0$ and $R \to \infty$ we obtain that

$$\int_0^\infty \frac{H_0^{(1)}(\varrho_s \rho)}{Z_\infty - \rho} \, \mathrm{d}\rho + i\pi H_0^{(1)}(Z_\infty \varrho_s) - \frac{2}{\pi} \int_0^\infty \left(\frac{Z_\infty + i\tau}{Z_\infty^2 + \tau^2} \right) K_0(\varrho_s \tau) \, \mathrm{d}\tau = 0, \tag{4.95}$$

where the integral on R tends to zero due the asymptotic behavior (A.139) of the Hankel function $H_0^{(1)}$. Considering the real part in (4.95) and rearranging yields

$$\int_0^\infty \frac{J_0(\varrho_s \rho)}{Z_\infty - \rho} \, \mathrm{d}\rho = \pi Y_0(Z_\infty \varrho_s) + \frac{2 Z_\infty}{\pi} \int_0^\infty \frac{K_0(\varrho_s \tau)}{Z_\infty^2 + \tau^2} \, \mathrm{d}\tau, \tag{4.96}$$

where Y_0 denotes the Neumann function of order zero. The integral on the right-hand side of (4.96) is given by (Gradshteyn & Ryzhik 2007, equation 6.566–4)

$$\frac{2 Z_\infty}{\pi} \int_0^\infty \frac{K_0(\varrho_s \tau)}{Z_\infty^2 + \tau^2} \, \mathrm{d}\tau = \frac{\pi}{2} \big[\boldsymbol{H}_0(Z_\infty \varrho_s) - Y_0(Z_\infty \varrho_s) \big]. \tag{4.97}$$

Hence, from (4.96) and (4.97) we get that

$$G_B(\varrho_s, 0) = \frac{\pi}{2} \big[\boldsymbol{H}_0(Z_\infty \varrho_s) + Y_0(Z_\infty \varrho_s) \big]. \tag{4.98}$$

By replacing in (4.91), we can express the remaining term G_R as

$$G_R(\boldsymbol{x},\boldsymbol{y}) = \frac{Z_\infty}{4}\, e^{-Z_\infty v_3}\left(Y_0(Z_\infty \varrho_s) + \boldsymbol{H}_0(Z_\infty \varrho_s) + \frac{2}{\pi}\int_0^{v_3} \frac{e^{Z_\infty \eta}}{\sqrt{\varrho_s^2+\eta^2}}\,\mathrm{d}\eta\right), \tag{4.99}$$

which corresponds to the representation derived by Kim (1965) and which was implicit in the work of Havelock (1955). For the remaining integral in (4.99), we consider the fact that

$$\int_0^{v_3} \frac{e^{Z_\infty \eta}}{\sqrt{\varrho_s^2+\eta^2}}\,\mathrm{d}\eta = \int_0^{Z_\infty v_3} \frac{e^{\alpha}}{\sqrt{Z_\infty^2\varrho_s^2+\alpha^2}}\,\mathrm{d}\alpha, \tag{4.100}$$

where we appreciate that the impedance Z_∞ appears only as a scaling factor for the variables ϱ_s and v_3. We can hence simplify the notation, by assuming temporarily that $Z_\infty = 1$ and by scaling the result at the end correspondingly by Z_∞. The power series expansion (A.8) of the exponential function implies that

$$\int_0^{v_3} \frac{e^{\eta}}{\sqrt{\varrho_s^2+\eta^2}}\,\mathrm{d}\eta = \sum_{n=0}^{\infty}\int_0^{v_3} \frac{\eta^n}{n!\sqrt{\varrho_s^2+\eta^2}}\,\mathrm{d}\eta. \tag{4.101}$$

Let us denote

$$I_n = \int_0^{v_3} \frac{\eta^n}{n!\sqrt{\varrho_s^2+\eta^2}}\,\mathrm{d}\eta, \tag{4.102}$$

in which case we can show by mathematical induction and by computing carefully (using, e.g., Gradshteyn & Ryzhik 2007, Dwight 1957, or Prudnikov et al. 1992) that

$$I_0 = \ln\Bigl(v_3 + \sqrt{\varrho_s^2+v_3^2}\Bigr), \tag{4.103}$$

$$I_1 = \sqrt{\varrho_s^2+v_3^2}\,, \tag{4.104}$$

$$\begin{aligned} I_{2n} = {}& \sqrt{\varrho_s^2+v_3^2}\,\sum_{m=0}^{n-1}(-1)^m \frac{2^{2n-2m-2}\bigl((n-m-1)!\bigr)^2}{(2n-2m-1)!\,2^{2n}(n!)^2}\, v_3^{2n-2m-1}\varrho_s^{2m} \\ & + \frac{(-1)^n}{(n!)^2}\left(\frac{\varrho_s}{2}\right)^{2n}\left(\ln\Bigl(v_3+\sqrt{\varrho_s^2+v_3^2}\Bigr) - \ln(\varrho_s)\right) \qquad (n=1,2,\ldots), \end{aligned} \tag{4.105}$$

$$\begin{aligned} I_{2n+1} = {}& \sqrt{\varrho_s^2+v_3^2}\,\sum_{m=0}^{n}(-1)^m \frac{(2n-2m)!}{2^{2n-2m}\bigl((n-m)!\bigr)^2}\left(\frac{2^n\,n!}{(2n+1)!}\right)^2 v_3^{2n-2m}\varrho_s^{2m} \\ & - (-1)^n \frac{2^{2n}(n!)^2}{\bigl((2n+1)!\bigr)^2}\,\varrho_s^{2n+1} \qquad (n=1,2,\ldots). \end{aligned} \tag{4.106}$$

We remark that (4.106) can be equivalently expressed as

$$\begin{aligned} I_{2n+1} = {}& \frac{1}{(2n+1)!}\sum_{m=0}^{n}\frac{n!}{m!\,(n-m)!}\,(-1)^m\varrho_s^{2m}\frac{\left(\sqrt{\varrho_s^2+v_3^2}\right)^{2n-2m+1}}{2n-2m+1} \\ & - (-1)^n \frac{2^{2n}(n!)^2}{\bigl((2n+1)!\bigr)^2}\,\varrho_s^{2n+1} \qquad (n=1,2,\ldots). \end{aligned} \tag{4.107}$$

We observe that the second term in (4.105) is linked with the series expansion (A.99) of the Bessel function J_0, whereas the second term in (4.106) and (4.107) is associated with

the series expansion (A.239) of the Struve function $\boldsymbol{H}_0$. Replacing these values in the right-hand side of (4.101) and rearranging yields

$$\int_0^{v_3} \frac{e^{\eta}}{\sqrt{\varrho_s^2+\eta^2}}\,\mathrm{d}\eta = J_0(\varrho_s)\Big(\ln\Big(v_3+\sqrt{\varrho_s^2+v_3^2}\Big)-\ln(\varrho_s)\Big)-\frac{\pi}{2}\boldsymbol{H}_0(\varrho_s) + \sqrt{\varrho_s^2+v_3^2}\,\Big(\mathrm{So}(\varrho_s,v_3)+\mathrm{Se}(\varrho_s,v_3)\Big), \tag{4.108}$$

where

$$\mathrm{So}(\varrho_s,v_3)=\sum_{n=0}^{\infty}\sum_{m=0}^{\infty}(-1)^m\frac{2^{2n}(n!)^2\,v_3^{2n+1}\varrho_s^{2m}}{(2n+1)!\,2^{2(m+n+1)}\big((m+n+1)!\big)^2}, \tag{4.109}$$

$$\mathrm{Se}(\varrho_s,v_3)=\sum_{n=0}^{\infty}\sum_{m=0}^{\infty}(-1)^m\frac{(2n)!}{2^{2n}(n!)^2}\left(\frac{2^{m+n}(m+n)!}{(2n+2m+1)!}\right)^2 v_3^{2n}\varrho_s^{2m}. \tag{4.110}$$

Due (4.107), we could express (4.110) alternatively as

$$\mathrm{Se}(\varrho_s,v_3)=\sum_{n=0}^{\infty}\frac{1}{(2n+1)!}\sum_{m=0}^{n}\frac{n!}{m!\,(n-m)!}\big(-\varrho_s^2\big)^m\frac{\Big(\sqrt{\varrho_s^2+v_3^2}\Big)^{2n-2m}}{2n-2m+1}. \tag{4.111}$$

Similar series expansions can be found in the article of Noblesse (1982). Scaling again the variables ϱ_s and v_3 by Z_∞ in (4.108) and replacing in (4.99) implies that

$$\begin{aligned}G_R(\boldsymbol{x},\boldsymbol{y}) = {}& \frac{Z_\infty}{2\pi}\,e^{-Z_\infty v_3}J_0(Z_\infty\varrho_s)\ln\Big(Z_\infty v_3+Z_\infty\sqrt{\varrho_s^2+v_3^2}\Big)\\ &+\frac{Z_\infty}{4}\,e^{-Z_\infty v_3}\left(Y_0(Z_\infty\varrho_s)-\frac{2}{\pi}J_0(Z_\infty\varrho_s)\ln(Z_\infty\varrho_s)\right)\\ &+\frac{Z_\infty^2}{2\pi}\sqrt{\varrho_s^2+v_3^2}\;e^{-Z_\infty v_3}\Big(\mathrm{So}\big(Z_\infty\varrho_s,Z_\infty v_3\big)+\mathrm{Se}\big(Z_\infty\varrho_s,Z_\infty v_3\big)\Big).\end{aligned} \tag{4.112}$$

f) Complete spatial Green's function

The desired complete spatial Green's function is finally obtained, as stated in (4.78), by adding the terms (4.81), (4.84), (4.85), and (4.112). It is depicted graphically for $Z_\infty=1$ and $\boldsymbol{x}=(0,0,2)$ in Figures 4.6 & 4.7, and given explicitly by

$$\begin{aligned}G(\boldsymbol{x},\boldsymbol{y}) = {}& -\frac{1}{4\pi|\boldsymbol{y}-\boldsymbol{x}|}-\frac{1}{4\pi|\boldsymbol{y}-\bar{\boldsymbol{x}}|}-\frac{iZ_\infty}{2}\,e^{-Z_\infty v_3}J_0(Z_\infty\varrho_s)\\ &+\frac{Z_\infty}{2\pi}\,e^{-Z_\infty v_3}J_0(Z_\infty\varrho_s)\ln\Big(Z_\infty v_3+Z_\infty\sqrt{\varrho_s^2+v_3^2}\Big)\\ &+\frac{Z_\infty}{4}\,e^{-Z_\infty v_3}\left(Y_0(Z_\infty\varrho_s)-\frac{2}{\pi}J_0(Z_\infty\varrho_s)\ln(Z_\infty\varrho_s)\right)\\ &+\frac{Z_\infty^2}{2\pi}\sqrt{\varrho_s^2+v_3^2}\;e^{-Z_\infty v_3}\Big(\mathrm{So}\big(Z_\infty\varrho_s,Z_\infty v_3\big)+\mathrm{Se}\big(Z_\infty\varrho_s,Z_\infty v_3\big)\Big),\end{aligned} \tag{4.113}$$

where the notation (4.87) is used and where the functions So and Se are defined respectively in (4.109) and (4.110).

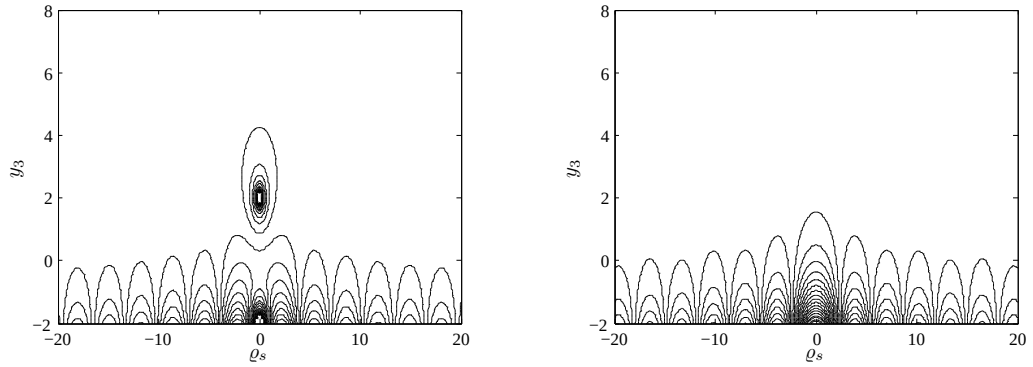

(a) Real part (b) Imaginary part

FIGURE 4.6. Contour plot of the complete spatial Green's function.

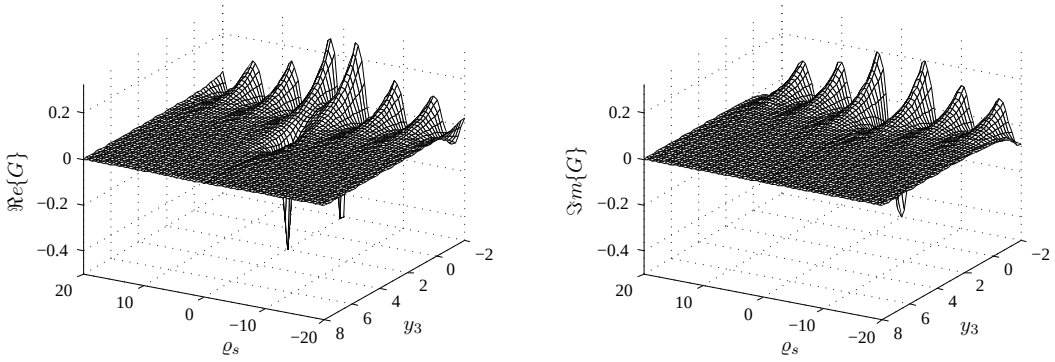

(a) Real part (b) Imaginary part

FIGURE 4.7. Oblique view of the complete spatial Green's function.

For the derivative of the Green's function with respect to the y_3-variable, it holds that

$$\frac{\partial G}{\partial y_3}(\boldsymbol{x},\boldsymbol{y}) = \frac{y_3 - x_3}{4\pi|\boldsymbol{y}-\boldsymbol{x}|^3} + \frac{v_3}{4\pi|\boldsymbol{y}-\bar{\boldsymbol{x}}|^3} + \frac{iZ_\infty^2}{2}\, e^{-Z_\infty v_3} J_0(Z_\infty \varrho_s) - Z_\infty G_R(\boldsymbol{x},\boldsymbol{y}) + \frac{Z_\infty}{2\pi|\boldsymbol{y}-\bar{\boldsymbol{x}}|}, \tag{4.114}$$

where G_R is computed according to (4.112). The derivatives for the variables y_1 and y_2 can be calculated by means of

$$\frac{\partial G}{\partial y_1} = \frac{\partial G}{\partial \varrho_s}\frac{\partial \varrho_s}{\partial y_1} = \frac{\partial G}{\partial \varrho_s}\frac{v_1}{\varrho_s} \qquad \text{and} \qquad \frac{\partial G}{\partial y_2} = \frac{\partial G}{\partial \varrho_s}\frac{\partial \varrho_s}{\partial y_2} = \frac{\partial G}{\partial \varrho_s}\frac{v_2}{\varrho_s}, \tag{4.115}$$

where

$$\begin{aligned}\frac{\partial G}{\partial \varrho_s}(\boldsymbol{x},\boldsymbol{y}) = {}& \frac{\varrho_s}{4\pi|\boldsymbol{y}-\boldsymbol{x}|^3} + \frac{\varrho_s}{4\pi|\boldsymbol{y}-\bar{\boldsymbol{x}}|^3} + \frac{iZ_\infty^2}{2}\, e^{-Z_\infty v_3} J_1(Z_\infty \varrho_s) \\ & - \frac{Z_\infty^2}{2\pi}\, e^{-Z_\infty v_3} J_1(Z_\infty \varrho_s) \ln\Big(Z_\infty v_3 + Z_\infty \sqrt{\varrho_s^2 + v_3^2} \Big) \\ & + \frac{Z_\infty}{2\pi}\, e^{-Z_\infty v_3} \frac{\varrho_s J_0(Z_\infty \varrho_s)}{\sqrt{\varrho_s^2 + v_3^2}\Big(v_3 + \sqrt{\varrho_s^2 + v_3^2} \Big)} \\ & - \frac{Z_\infty^2}{4}\, e^{-Z_\infty v_3} \left(Y_1(Z_\infty \varrho_s) - \frac{2}{\pi} J_1(Z_\infty \varrho_s) \ln(Z_\infty \varrho_s) + \frac{2}{\pi Z_\infty \varrho_s} J_0(Z_\infty \varrho_s) \right) \\ & + \frac{Z_\infty^2}{2\pi} \frac{\varrho_s}{\sqrt{\varrho_s^2 + v_3^2}}\, e^{-Z_\infty v_3} \Big(\mathrm{So}\big(Z_\infty \varrho_s, Z_\infty v_3\big) + \mathrm{Se}\big(Z_\infty \varrho_s, Z_\infty v_3\big) \Big) \\ & + \frac{Z_\infty^3}{2\pi} \sqrt{\varrho_s^2 + v_3^2}\, e^{-Z_\infty v_3} \left(\frac{\partial\, \mathrm{So}}{\partial \varrho_s}\big(Z_\infty \varrho_s, Z_\infty v_3\big) + \frac{\partial\, \mathrm{Se}}{\partial \varrho_s}\big(Z_\infty \varrho_s, Z_\infty v_3\big) \right), \end{aligned} \tag{4.116}$$

being

$$\frac{\partial\, \mathrm{So}}{\partial \varrho_s}(\varrho_s, v_3) = \sum_{n=0}^{\infty} \sum_{m=1}^{\infty} (-1)^m \frac{m\, 2^{2n+1} (n!)^2\, v_3^{2n+1} \varrho_s^{2m-1}}{(2n+1)!\, 2^{2(m+n+1)} \big((m+n+1)!\big)^2}, \tag{4.117}$$

$$\frac{\partial\, \mathrm{Se}}{\partial \varrho_s}(\varrho_s, v_3) = \sum_{n=0}^{\infty} \sum_{m=1}^{\infty} (-1)^m \frac{m\,(2n)!}{2^{2n-1}(n!)^2} \left(\frac{2^{m+n}(m+n)!}{(2n+2m+1)!} \right)^2 v_3^{2n} \varrho_s^{2m-1}. \tag{4.118}$$

4.3.5 Extension and properties

The half-space Green's function can be extended in a locally analytic way towards the full-space $\mathbb{R}^3$ in a straightforward and natural manner, just by considering the expression (4.113) valid for all $\boldsymbol{x}, \boldsymbol{y} \in \mathbb{R}^3$, instead of just for $\mathbb{R}^3_+$. As shown in Figure 4.8, this extension possesses two pole-type singularities at the points $\boldsymbol{x}$ and $\bar{\boldsymbol{x}}$, a logarithmic singularity-distribution along the half-line $\Upsilon = \{y_1 = x_1,\, y_2 = x_2,\, y_3 < -x_3\}$, and is continuous otherwise. The behavior of the pole-type singularities is characterized by

$$G(\boldsymbol{x},\boldsymbol{y}) \sim -\frac{1}{4\pi|\boldsymbol{y}-\boldsymbol{x}|}, \qquad \boldsymbol{y} \longrightarrow \boldsymbol{x}, \tag{4.119}$$

$$G(\boldsymbol{x},\boldsymbol{y}) \sim -\frac{1}{4\pi|\boldsymbol{y}-\bar{\boldsymbol{x}}|}, \qquad \boldsymbol{y} \longrightarrow \bar{\boldsymbol{x}}. \tag{4.120}$$

The logarithmic singularity-distribution stems from the fact that when $v_3 < 0$, then

$$G(\boldsymbol{x},\boldsymbol{y}) \sim -\frac{iZ_\infty}{2}\, e^{-Z_\infty v_3} H_0^{(1)}(Z_\infty \varrho_s), \tag{4.121}$$

being $H_0^{(1)}$ the zeroth order Hankel function of the first kind, whose singularity is of logarithmic type. We observe that (4.121) is related to the two-dimensional free-space Green's function of the Helmholtz equation (C.22), multiplied by the exponential weight

$$J(\boldsymbol{x},\boldsymbol{y}) = 2Z_\infty e^{-Z_\infty v_3}. \tag{4.122}$$

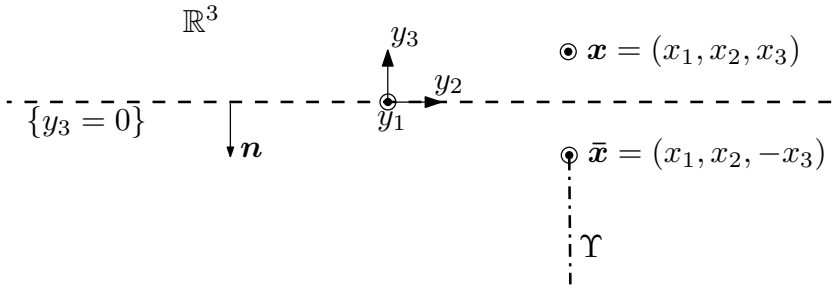

FIGURE 4.8. Domain of the extended Green's function.

As long as $x_3 \neq 0$, it is clear that the impedance boundary condition in (4.16) continues to be homogeneous. Nonetheless, if the source point $\boldsymbol{x}$ lies on the half-space's boundary, i.e., if $x_3 = 0$, then the boundary condition ceases to be homogeneous in the sense of distributions. This can be deduced from the expression (4.77) by verifying that

$$\lim_{y_3 \to 0^+} \left\{ \frac{\partial G}{\partial y_3}\big((\boldsymbol{x}_s, 0), \boldsymbol{y}\big) + Z_\infty G\big((\boldsymbol{x}_s, 0), \boldsymbol{y}\big) \right\} = \delta_{\boldsymbol{x}_s}(\boldsymbol{y}_s), \tag{4.123}$$

where $\boldsymbol{x}_s = (x_1, x_2)$ and $\boldsymbol{y}_s = (y_1, y_2)$. Since the impedance boundary condition holds only on $\{y_3 = 0\}$, therefore the right-hand side of (4.123) can be also expressed by

$$\delta_{\boldsymbol{x}_s}(\boldsymbol{y}_s) = \frac{1}{2}\delta_{\boldsymbol{x}}(\boldsymbol{y}) + \frac{1}{2}\delta_{\bar{\boldsymbol{x}}}(\boldsymbol{y}), \tag{4.124}$$

which illustrates more clearly the contribution of each pole-type singularity to the Dirac mass in the boundary condition.

It can be seen now that the Green's function extended in the abovementioned way satisfies, for $\boldsymbol{x} \in \mathbb{R}^3$, in the sense of distributions, and instead of (4.16), the problem

$$\begin{cases} \text{Find } G(\boldsymbol{x}, \cdot) : \mathbb{R}^3 \to \mathbb{C} \text{ such that} \\ \Delta_{\boldsymbol{y}} G(\boldsymbol{x}, \boldsymbol{y}) = \delta_{\boldsymbol{x}}(\boldsymbol{y}) + \delta_{\bar{\boldsymbol{x}}}(\boldsymbol{y}) + J(\boldsymbol{x}, \boldsymbol{y})\delta_\Upsilon(\boldsymbol{y}) \qquad \text{in } \mathcal{D}'(\mathbb{R}^3), \\ \dfrac{\partial G}{\partial y_3}(\boldsymbol{x}, \boldsymbol{y}) + Z_\infty G(\boldsymbol{x}, \boldsymbol{y}) = \dfrac{1}{2}\delta_{\boldsymbol{x}}(\boldsymbol{y}) + \dfrac{1}{2}\delta_{\bar{\boldsymbol{x}}}(\boldsymbol{y}) \qquad \text{on } \{y_3 = 0\}, \\ + \text{ Outgoing radiation condition for } \boldsymbol{y} \in \mathbb{R}^3_+ \text{ as } |\boldsymbol{y}| \to \infty, \end{cases} \tag{4.125}$$

where δ_Υ denotes a Dirac mass distribution along the Υ-curve. We retrieve thus the known result that for an impedance boundary condition the image of a point source is a point source plus a half-line of sources with exponentially increasing strengths in the lower half-plane, and which extends from the image point source towards infinity along the half-space's normal direction (cf. Keller 1979, who refers to decreasing strengths when dealing with the opposite half-space).

We note that the half-space Green's function (4.113) is symmetric in the sense that

$$G(\boldsymbol{x}, \boldsymbol{y}) = G(\boldsymbol{y}, \boldsymbol{x}) \qquad \forall \boldsymbol{x}, \boldsymbol{y} \in \mathbb{R}^3, \tag{4.126}$$

and it fulfills similarly

$$\nabla_{\boldsymbol{y}} G(\boldsymbol{x}, \boldsymbol{y}) = \nabla_{\boldsymbol{y}} G(\boldsymbol{y}, \boldsymbol{x}) \qquad \text{and} \qquad \nabla_{\boldsymbol{x}} G(\boldsymbol{x}, \boldsymbol{y}) = \nabla_{\boldsymbol{x}} G(\boldsymbol{y}, \boldsymbol{x}). \tag{4.127}$$

Another property is that we retrieve the special case (4.19) of a homogenous Dirichlet boundary condition in $\mathbb{R}^3_+$ when $Z_\infty \to \infty$. Likewise, we retrieve the special case (4.21) of a homogenous Neumann boundary condition in $\mathbb{R}^3_+$ when $Z_\infty \to 0$.

At last, we observe that the expression for the Green's function (4.113) is still valid if a complex impedance $Z_\infty \in \mathbb{C}$ such that $\mathfrak{Im}\{Z_\infty\} > 0$ and $\mathfrak{Re}\{Z_\infty\} \geq 0$ is used, which holds also for its derivatives (4.115), and (4.116).

4.4 Far field of the Green's function

4.4.1 Decomposition of the far field

The far field of the Green's function, which we denote by G^{ff}, describes its asymptotic behavior at infinity, i.e., when $|\boldsymbol{x}| \to \infty$ and assuming that $\boldsymbol{y}$ is fixed. For this purpose, the terms of highest order at infinity are searched. Likewise as done for the radiation condition, the far field is decomposed into two parts, each acting on a different region. The first part, denoted by G^{ff}_A, is linked with the asymptotic decaying condition at infinity observed when dealing with bounded obstacles, and acts in the interior of the half-space while vanishing near its boundary. The second part, denoted by G^{ff}_S, is associated with surface waves that propagate along the boundary towards infinity, which decay exponentially towards the half-space's interior. We have thus that

$$G^{ff} = G^{ff}_A + G^{ff}_S. \tag{4.128}$$

4.4.2 Asymptotic decaying

The asymptotic decaying acts only in the interior of the half-space and is related to the pole-type terms in (4.113), and also to the asymptotic behavior as $x_3 \to \infty$ of the remaining terms. We remember that

$$G(\boldsymbol{x},\boldsymbol{y}) = -\frac{1}{4\pi|\boldsymbol{x}-\boldsymbol{y}|} - \frac{1}{4\pi|\boldsymbol{x}-\bar{\boldsymbol{y}}|} - \frac{iZ_\infty}{2}\, e^{-Z_\infty v_3} J_0(Z_\infty \varrho_s) + G_R(\boldsymbol{x},\boldsymbol{y}), \tag{4.129}$$

being $\bar{\boldsymbol{y}} = (y_1, y_2, -y_3)$, and where different expressions for G_R were already presented in (4.86), (4.99), and (4.112). Due the axial symmetry around the axis $\{\varrho_s = 0\}$, i.e., by using the same arguments as for (4.65), we can express the inverse Fourier transform of (4.76) as

$$G_R(\boldsymbol{x},\boldsymbol{y}) = \frac{Z_\infty}{4\pi^2} \int_0^\pi \int_{-\infty}^\infty \frac{e^{-|\xi| v_3}}{Z_\infty - |\xi|}\, e^{i\xi\varrho_s \sin\psi}\, \mathrm{d}\xi\, \mathrm{d}\psi. \tag{4.130}$$

This integral can be rewritten as

$$G_R(\boldsymbol{x},\boldsymbol{y}) = \frac{Z_\infty}{\pi^2} \int_0^{\pi/2} \int_0^\infty \frac{e^{-\rho v_3}}{Z_\infty - \rho} \cos\big(\rho\varrho_s \sin\psi\big)\, \mathrm{d}\rho\, \mathrm{d}\psi. \tag{4.131}$$

The innermost integral in (4.131) is the same as the one that appears for the two-dimensional case in (2.80), and can be computed in the same way. It corresponds to exponential integral functions Ei (vid. Subsection A.2.3). By comparing (2.80) and (2.93), and by performing a change of variables on the second term to account for a sign difference, we obtain the

integral representation

$$G_R(\boldsymbol{x},\boldsymbol{y}) = \frac{Z_\infty}{2\pi^2}\, e^{-Z_\infty v_3} \int_{-\pi/2}^{\pi/2} e^{iZ_\infty \varrho_s \sin\psi}\, \mathrm{Ei}\big(Z_\infty v_3 - iZ_\infty \varrho_s \sin\psi\big)\, \mathrm{d}\psi, \tag{4.132}$$

which can be rewritten also as

$$G_R(\boldsymbol{x},\boldsymbol{y}) = \frac{Z_\infty}{2\pi^2} \int_{-1}^{1} \frac{e^{-Z_\infty(v_3 - i\varrho_s\eta)}}{\sqrt{1-\eta^2}}\, \mathrm{Ei}\big(Z_\infty(v_3 - i\varrho_s\eta)\big)\, \mathrm{d}\eta. \tag{4.133}$$

Now, as $x_3 \to \infty$, we can consider the asymptotic behavior of the exponential integral in (4.133). In fact, due (A.81) we have for $z \in \mathbb{C}$ that

$$\mathrm{Ei}(z) \sim \frac{e^z}{z} \qquad \text{as } \ \mathfrak{Re}\{z\} \to \infty. \tag{4.134}$$

Hence, as $x_3 \to \infty$ it holds that

$$G_R(\boldsymbol{x},\boldsymbol{y}) \sim \frac{1}{2\pi^2} \int_{-1}^{1} \frac{\mathrm{d}\eta}{(v_3 - i\varrho_s\eta)\sqrt{1-\eta^2}} = \frac{1}{2\pi|\boldsymbol{x}-\bar{\boldsymbol{y}}|}. \tag{4.135}$$

The Green's function (4.129) behaves thus asymptotically, when $x_3 \to \infty$, as

$$G(\boldsymbol{x},\boldsymbol{y}) \sim -\frac{1}{4\pi|\boldsymbol{x}-\boldsymbol{y}|} + \frac{1}{4\pi|\boldsymbol{x}-\bar{\boldsymbol{y}}|}. \tag{4.136}$$

By using Taylor expansions as in (D.29), we obtain that

$$-\frac{1}{4\pi|\boldsymbol{x}-\boldsymbol{y}|} + \frac{1}{4\pi|\boldsymbol{x}-\bar{\boldsymbol{y}}|} = -\frac{(\boldsymbol{y}-\bar{\boldsymbol{y}})\cdot\boldsymbol{x}}{4\pi|\boldsymbol{x}|^3} + \mathcal{O}\bigg(\frac{1}{|\boldsymbol{x}|^3}\bigg). \tag{4.137}$$

We express the point $\boldsymbol{x}$ as $\boldsymbol{x} = |\boldsymbol{x}|\,\hat{\boldsymbol{x}}$, being $\hat{\boldsymbol{x}} = (\sin\theta\cos\varphi, \sin\theta\sin\varphi, \cos\theta)$ a vector of the unit sphere. The asymptotic decaying of the Green's function is therefore given by

$$G_A^{ff}(\boldsymbol{x},\boldsymbol{y}) = -\frac{y_3\cos\theta}{2\pi|\boldsymbol{x}|^2}, \tag{4.138}$$

and its gradient with respect to $\boldsymbol{y}$ by

$$\nabla_{\boldsymbol{y}} G_A^{ff}(\boldsymbol{x},\boldsymbol{y}) = -\frac{\cos\theta}{2\pi|\boldsymbol{x}|^2} \begin{bmatrix} 0 \\ 0 \\ 1 \end{bmatrix}. \tag{4.139}$$

4.4.3 Surface waves in the far field

An expression for the surface waves in the far field can be obtained by studying the residues of the poles of the spectral Green's function, which determine entirely their asymptotic behavior. We already computed the inverse Fourier transform of these residues in (4.66), using the residue theorem of Cauchy and the limiting absorption principle. This implies that the Green's function behaves asymptotically, when $|\boldsymbol{x}_s| \to \infty$, as

$$G(\boldsymbol{x},\boldsymbol{y}) \sim -\frac{iZ_\infty}{2}\, e^{-Z_\infty v_3} \Big[J_0(Z_\infty \varrho_s) + i\boldsymbol{H}_0(Z_\infty \varrho_s)\Big] \qquad \text{for } \ v_3 > 0. \tag{4.140}$$

This expression works well in the upper half-space, but fails to retrieve the logarithmic singularity-distribution (4.121) in the lower half-space at $\varrho_s = 0$. In this case, the Struve function $\boldsymbol{H}_0$ in (4.140) has to be replaced by the Neumann function Y_0, which has the same

behavior at infinity, but additionally a logarithmic singularity at its origin. Hence in the lower half-space, the Green's function behaves asymptotically, when $|\boldsymbol{x}_s| \to \infty$, as

$$G(\boldsymbol{x},\boldsymbol{y}) \sim -\frac{iZ_\infty}{2}\, e^{-Z_\infty v_3} H_0^{(1)}(Z_\infty \varrho_s) \qquad \text{for } \; v_3 < 0. \tag{4.141}$$

In general, away from the axis $\{\varrho_s = 0\}$, the Green's function behaves, when $|\boldsymbol{x}_s| \to \infty$ and due the asymptotic expansions of the Struve and Bessel functions, as

$$G(\boldsymbol{x},\boldsymbol{y}) \sim -i\sqrt{\frac{Z_\infty}{2\pi\varrho_s}}\, e^{-Z_\infty v_3} e^{i(Z_\infty \varrho_s - \pi/4)}. \tag{4.142}$$

By performing Taylor expansions, as in (C.37) and (C.38), we have that

$$\frac{e^{iZ_\infty \varrho_s}}{\sqrt{\varrho_s}} = \frac{e^{iZ_\infty |\boldsymbol{x}_s|}}{\sqrt{|\boldsymbol{x}_s|}}\, e^{-iZ_\infty \boldsymbol{y}_s\cdot\boldsymbol{x}_s/|\boldsymbol{x}_s|} \left(1 + \mathcal{O}\Big(\frac{1}{|\boldsymbol{x}_s|}\Big)\right). \tag{4.143}$$

We express the point $\boldsymbol{x}_s$ on the surface as $\boldsymbol{x}_s = |\boldsymbol{x}_s|\,\hat{\boldsymbol{x}}_s$, being $\hat{\boldsymbol{x}}_s = (\cos\varphi, \sin\varphi)$ a unitary surface vector. The surface-wave behavior of the Green's function, due (4.142) and (4.143), becomes thus

$$G_S^{ff}(\boldsymbol{x},\boldsymbol{y}) = -i\, e^{-i\pi/4}\sqrt{\frac{Z_\infty}{2\pi|\boldsymbol{x}_s|}}\, e^{-Z_\infty x_3} e^{iZ_\infty|\boldsymbol{x}_s|} e^{-Z_\infty y_3} e^{-iZ_\infty \boldsymbol{y}_s\cdot\hat{\boldsymbol{x}}_s}, \tag{4.144}$$

and its gradient with respect to $\boldsymbol{y}$ is given by

$$\nabla_{\boldsymbol{y}} G_S^{ff}(\boldsymbol{x},\boldsymbol{y}) = -\frac{Z_\infty^{3/2}}{\sqrt{2\pi|\boldsymbol{x}_s|}}\, e^{-i\pi/4} e^{-Z_\infty x_3} e^{iZ_\infty|\boldsymbol{x}_s|} e^{-Z_\infty y_3} e^{-iZ_\infty \boldsymbol{y}_s\cdot\hat{\boldsymbol{x}}_s} \begin{bmatrix} \cos\varphi \\ \sin\varphi \\ -i \end{bmatrix}. \tag{4.145}$$

4.4.4 Complete far field of the Green's function

On the whole, the asymptotic behavior of the Green's function as $|\boldsymbol{x}| \to \infty$ can be characterized in the upper half-space through the addition of (4.136) and (4.140), and in the lower half-space by adding (4.136) and (4.141). Thus if $v_3 > 0$, then it holds that

$$G(\boldsymbol{x},\boldsymbol{y}) \sim -\frac{1}{4\pi|\boldsymbol{x}-\boldsymbol{y}|} + \frac{1}{4\pi|\boldsymbol{x}-\bar{\boldsymbol{y}}|} - \frac{iZ_\infty}{2}\, e^{-Z_\infty v_3}\Big[J_0(Z_\infty\varrho_s) + i\boldsymbol{H}_0(Z_\infty\varrho_s)\Big], \tag{4.146}$$

and if $v_3 < 0$, then

$$G(\boldsymbol{x},\boldsymbol{y}) \sim -\frac{1}{4\pi|\boldsymbol{x}-\boldsymbol{y}|} + \frac{1}{4\pi|\boldsymbol{x}-\bar{\boldsymbol{y}}|} - \frac{iZ_\infty}{2}\, e^{-Z_\infty v_3} H_0^{(1)}(Z_\infty\varrho_s). \tag{4.147}$$

Consequently, the complete far field of the Green's function, due (4.128), should be given by the addition of (4.138) and (4.144), i.e., by

$$G^{ff}(\boldsymbol{x},\boldsymbol{y}) = -\frac{y_3\cos\theta}{2\pi|\boldsymbol{x}|^2} - i\, e^{-i\pi/4}\sqrt{\frac{Z_\infty}{2\pi|\boldsymbol{x}_s|}}\, e^{-Z_\infty x_3} e^{iZ_\infty|\boldsymbol{x}_s|} e^{-Z_\infty y_3} e^{-iZ_\infty \boldsymbol{y}_s\cdot\hat{\boldsymbol{x}}_s}. \tag{4.148}$$

Its derivative with respect to $\boldsymbol{y}$ is likewise given by the addition of (4.139) and (4.145). The expression (4.148) retrieves correctly the far field of the Green's function, except in the upper half-space at the vicinity of the axis $\{\varrho_s = 0\}$, due the presence of a singularity-distribution of type $1/\sqrt{|\boldsymbol{x}_s|}$, which does not appear in the original Green's function. A

way to deal with this issue is to consider in each region only the most dominant asymptotic behavior at infinity. Since there are two different regions, we require to determine appropriately the interface between them. This can be achieved by equating the amplitudes of the two terms in (4.148), i.e., by searching values of $\boldsymbol{x}$ at infinity such that

$$\frac{1}{2\pi|\boldsymbol{x}|^2} = \sqrt{\frac{Z_\infty}{2\pi|\boldsymbol{x}|}}\, e^{-Z_\infty x_3}, \tag{4.149}$$

where we neglected the values of $\boldsymbol{y}$, since they remain relatively near the origin. Furthermore, since the interface stays relatively close to the half-space's boundary, we can also approximate $|\boldsymbol{x}_s| \approx |\boldsymbol{x}|$. By taking the logarithm in (4.149) and perturbing somewhat the result so as to avoid a singular behavior at the origin, we obtain finally that this interface is described by

$$x_3 = \frac{1}{2Z_\infty} \ln\bigl(1 + 2\pi Z_\infty |\boldsymbol{x}|^3\bigr). \tag{4.150}$$

We can say now that it is the far field (4.148) which justifies the radiation condition (4.17) when exchanging the roles of $\boldsymbol{x}$ and $\boldsymbol{y}$, and disregarding the undesired singularity around $\{\varrho_s = 0\}$. When the first term in (4.148) dominates, i.e., the asymptotic decaying (4.138), then it is the first expression in (4.17) that matters. Conversely, when the second term in (4.148) dominates, i.e., the surface waves (4.144), then the second expression in (4.17) is the one that holds. The interface between both is described by (4.150).

We remark that the asymptotic behavior (4.146) of the Green's function and the expression (4.148) of its complete far field do no longer hold if a complex impedance $Z_\infty \in \mathbb{C}$ such that $\mathfrak{Im}\{Z_\infty\} > 0$ and $\mathfrak{Re}\{Z_\infty\} \geq 0$ is used, specifically the parts (4.140) and (4.144) linked with the surface waves. A careful inspection shows that in this case the surface-wave behavior of the Green's function, as $|\boldsymbol{x}_s| \to \infty$, decreases exponentially and is given by

$$G(\boldsymbol{x}, \boldsymbol{y}) \sim -\frac{iZ_\infty}{2}\, e^{-|Z_\infty| v_3} \Bigl[J_0(Z_\infty \varrho_s) + i\boldsymbol{H}_0(Z_\infty \varrho_s) \Bigr] \qquad \text{for } \; v_3 > 0, \tag{4.151}$$

whereas (4.141) continues to hold. Likewise, the surface-wave part of the far field is expressed for $x_3 > 0$ as

$$G_S^{ff}(\boldsymbol{x}, \boldsymbol{y}) = -i\, e^{-i\pi/4} \sqrt{\frac{Z_\infty}{2\pi|\boldsymbol{x}_s|}}\, e^{-|Z_\infty| x_3} e^{iZ_\infty |\boldsymbol{x}_s|} e^{-|Z_\infty| y_3} e^{-iZ_\infty \boldsymbol{y}_s \cdot \hat{\boldsymbol{x}}_s}, \tag{4.152}$$

but for $x_3 < 0$ the expression (4.144) is still valid. The asymptotic decaying (4.136) and its far-field expression (4.138), on the other hand, remain the same when we use a complex impedance. We remark further that if a complex impedance is taken into account, then the part of the surface waves of the outgoing radiation condition is redundant, and only the asymptotic decaying part is required, i.e., only the first two expressions in (4.17), but now holding for $y_3 > 0$.

4.5 Numerical evaluation of the Green's function

For the numerical evaluation of the Green's function, we separate the space $\mathbb{R}^3$ into three regions: a near field, an upper far field, and a lower far field. In the near field,

when $|Z_\infty|\,|\boldsymbol{v}| \leq 15$, being $\boldsymbol{v} = \boldsymbol{y} - \bar{\boldsymbol{x}}$, we use the expression (4.113) to compute the Green's function, truncating the double series of the functions So and Se, in (4.109) and (4.110) respectively, after the first 30 terms for n and m. In the upper far field, when $|Z_\infty|\,|\boldsymbol{v}| > 15$ and $|Z_\infty|\,v_3 > \log\big(1 + 2\pi|Z_\infty|\varrho_s^3\big)$, we have from (4.146) that

$$G(\boldsymbol{x},\boldsymbol{y}) = -\frac{1}{4\pi|\boldsymbol{x}-\boldsymbol{y}|} + \frac{1}{4\pi|\boldsymbol{x}-\bar{\boldsymbol{y}}|} - \frac{iZ_\infty}{2}\, e^{-Z_\infty v_3}\Big[J_0(Z_\infty\varrho_s) + i\boldsymbol{H}_0(Z_\infty\varrho_s)\Big]. \quad (4.153)$$

Similarly in the lower far field, when $|Z_\infty|\,|\boldsymbol{v}| > 15$ and $|Z_\infty|\,v_3 \leq \log\big(1 + 2\pi|Z_\infty|\varrho_s^3\big)$, it holds from (4.147) that

$$G(\boldsymbol{x},\boldsymbol{y}) = -\frac{1}{4\pi|\boldsymbol{x}-\boldsymbol{y}|} + \frac{1}{4\pi|\boldsymbol{x}-\bar{\boldsymbol{y}}|} - \frac{iZ_\infty}{2}\, e^{-Z_\infty v_3} H_0^{(1)}(Z_\infty\varrho_s). \quad (4.154)$$

The Bessel functions can be evaluated either by using the software based on the technical report by Morris (1993) or the subroutines described in Amos (1986, 1995). The Struve function can be computed by means of the software described in MacLeod (1996). Further references are listed in Lozier & Olver (1994). The biggest numerical error, excepting the singularity-distribution along the half-line Υ, is committed near the boundaries of the three described regions, and amounts to less than $|Z_\infty| \cdot 10^{-3}$.

4.6 Integral representation and equation

4.6.1 Integral representation

We are interested in expressing the solution u of the direct scattering problem (4.13) by means of an integral representation formula over the perturbed portion of the boundary Γ_p. For this purpose, we extend this solution by zero towards the complementary domain Ω_c, analogously as done in (D.98). We define by $\Omega_{R,\varepsilon}$ the domain Ω_e without the ball B_ε of radius $\varepsilon > 0$ centered at the point $\boldsymbol{x} \in \Omega_e$, and truncated at infinity by the ball B_R of radius $R > 0$ centered at the origin. We consider that the ball B_ε is entirely contained in Ω_e. Therefore, as shown in Figure 4.9, we have that

$$\Omega_{R,\varepsilon} = \big(\Omega_e \cap B_R\big) \setminus \overline{B_\varepsilon}, \quad (4.155)$$

where

$$B_R = \{\boldsymbol{y} \in \mathbb{R}^3 :\, |\boldsymbol{y}| < R\} \qquad \text{and} \qquad B_\varepsilon = \{\boldsymbol{y} \in \Omega_e :\, |\boldsymbol{y}-\boldsymbol{x}| < \varepsilon\}. \quad (4.156)$$

We consider similarly, inside Ω_e, the boundaries of the balls

$$S_R^+ = \{\boldsymbol{y} \in \mathbb{R}^3_+ :\, |\boldsymbol{y}| = R\} \qquad \text{and} \qquad S_\varepsilon = \{\boldsymbol{y} \in \Omega_e :\, |\boldsymbol{y}-\boldsymbol{x}| = \varepsilon\}. \quad (4.157)$$

We separate furthermore the boundary as $\Gamma = \Gamma_0 \cup \Gamma_+$, where

$$\Gamma_0 = \{\boldsymbol{y} \in \Gamma :\, y_3 = 0\} \qquad \text{and} \qquad \Gamma_+ = \{\boldsymbol{y} \in \Gamma :\, y_3 > 0\}. \quad (4.158)$$

The boundary Γ is likewise truncated at infinity by the ball B_R, namely

$$\Gamma_R = \Gamma \cap B_R = \Gamma_0^R \cup \Gamma_+ = \Gamma_\infty^R \cup \Gamma_p, \quad (4.159)$$

where

$$\Gamma_0^R = \Gamma_0 \cap B_R \qquad \text{and} \qquad \Gamma_\infty^R = \Gamma_\infty \cap B_R. \quad (4.160)$$

The idea is to retrieve the domain Ω_e and the boundary Γ at the end when the limits $R \to \infty$ and $\varepsilon \to 0$ are taken for the truncated domain $\Omega_{R,\varepsilon}$ and the truncated boundary Γ_R.

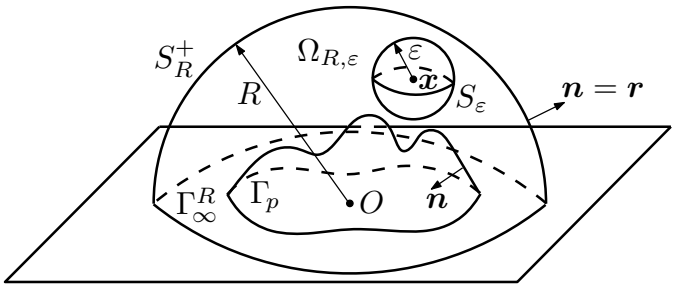

FIGURE 4.9. Truncated domain $\Omega_{R,\varepsilon}$ for $\boldsymbol{x} \in \Omega_e$.

We apply now Green's second integral theorem (A.613) to the functions u and $G(\boldsymbol{x}, \cdot)$ in the bounded domain $\Omega_{R,\varepsilon}$, yielding

$$\begin{aligned} 0 &= \int_{\Omega_{R,\varepsilon}} \big(u(\boldsymbol{y})\Delta_{\boldsymbol{y}} G(\boldsymbol{x},\boldsymbol{y}) - G(\boldsymbol{x},\boldsymbol{y})\Delta u(\boldsymbol{y})\big)\mathrm{d}\boldsymbol{y} \\ &= \int_{S_R^+} \left(u(\boldsymbol{y})\frac{\partial G}{\partial r_{\boldsymbol{y}}}(\boldsymbol{x},\boldsymbol{y}) - G(\boldsymbol{x},\boldsymbol{y})\frac{\partial u}{\partial r}(\boldsymbol{y})\right)\mathrm{d}\gamma(\boldsymbol{y}) \\ &- \int_{S_\varepsilon} \left(u(\boldsymbol{y})\frac{\partial G}{\partial r_{\boldsymbol{y}}}(\boldsymbol{x},\boldsymbol{y}) - G(\boldsymbol{x},\boldsymbol{y})\frac{\partial u}{\partial r}(\boldsymbol{y})\right)\mathrm{d}\gamma(\boldsymbol{y}) \\ &+ \int_{\Gamma_R} \left(u(\boldsymbol{y})\frac{\partial G}{\partial n_{\boldsymbol{y}}}(\boldsymbol{x},\boldsymbol{y}) - G(\boldsymbol{x},\boldsymbol{y})\frac{\partial u}{\partial n}(\boldsymbol{y})\right)\mathrm{d}\gamma(\boldsymbol{y}). \end{aligned} \tag{4.161}$$

The integral on S_R^+ can be rewritten as

$$\begin{aligned} \int_{S_R^2} \left[u(\boldsymbol{y})\left(\frac{\partial G}{\partial r_{\boldsymbol{y}}}(\boldsymbol{x},\boldsymbol{y}) - iZ_\infty G(\boldsymbol{x},\boldsymbol{y})\right) - G(\boldsymbol{x},\boldsymbol{y})\left(\frac{\partial u}{\partial r}(\boldsymbol{y}) - iZ_\infty u(\boldsymbol{y})\right)\right]\mathrm{d}\gamma(\boldsymbol{y}) \\ + \int_{S_R^1} \left(u(\boldsymbol{y})\frac{\partial G}{\partial r_{\boldsymbol{y}}}(\boldsymbol{x},\boldsymbol{y}) - G(\boldsymbol{x},\boldsymbol{y})\frac{\partial u}{\partial r}(\boldsymbol{y})\right)\mathrm{d}\gamma(\boldsymbol{y}), \end{aligned} \tag{4.162}$$

which for R large enough and due the radiation condition (4.6) tends to zero, since

$$\left|\int_{S_R^2} u(\boldsymbol{y})\left(\frac{\partial G}{\partial r_{\boldsymbol{y}}}(\boldsymbol{x},\boldsymbol{y}) - iZ_\infty G(\boldsymbol{x},\boldsymbol{y})\right)\mathrm{d}\gamma(\boldsymbol{y})\right| \leq \frac{C}{\sqrt{R}}\ln R, \tag{4.163}$$

$$\left|\int_{S_R^2} G(\boldsymbol{x},\boldsymbol{y})\left(\frac{\partial u}{\partial r}(\boldsymbol{y}) - iZ_\infty u(\boldsymbol{y})\right)\mathrm{d}\gamma(\boldsymbol{y})\right| \leq \frac{C}{\sqrt{R}}\ln R, \tag{4.164}$$

and

$$\left|\int_{S_R^1} \left(u(\boldsymbol{y})\frac{\partial G}{\partial r_{\boldsymbol{y}}}(\boldsymbol{x},\boldsymbol{y}) - G(\boldsymbol{x},\boldsymbol{y})\frac{\partial u}{\partial r}(\boldsymbol{y})\right)\mathrm{d}\gamma(\boldsymbol{y})\right| \leq \frac{C}{R^3}, \tag{4.165}$$

for some constants $C > 0$. If the function u is regular enough in the ball B_ε, then the second term of the integral on S_ε in (4.161), when $\varepsilon \to 0$ and due (4.119), is bounded by

$$\left| \int_{S_\varepsilon} G(\boldsymbol{x}, \boldsymbol{y}) \frac{\partial u}{\partial r}(\boldsymbol{y}) \, \mathrm{d}\gamma(\boldsymbol{y}) \right| \leq C\varepsilon \sup_{\boldsymbol{y} \in B_\varepsilon} \left| \frac{\partial u}{\partial r}(\boldsymbol{y}) \right|, \tag{4.166}$$

for some constant $C > 0$ and tends to zero. The regularity of u can be specified afterwards once the integral representation has been determined and generalized by means of density arguments. The first integral term on S_ε can be decomposed as

$$\begin{aligned} \int_{S_\varepsilon} u(\boldsymbol{y}) \frac{\partial G}{\partial r_{\boldsymbol{y}}}(\boldsymbol{x}, \boldsymbol{y}) \, \mathrm{d}\gamma(\boldsymbol{y}) = u(\boldsymbol{x}) \int_{S_\varepsilon} \frac{\partial G}{\partial r_{\boldsymbol{y}}}(\boldsymbol{x}, \boldsymbol{y}) \, \mathrm{d}\gamma(\boldsymbol{y}) \\ + \int_{S_\varepsilon} \frac{\partial G}{\partial r_{\boldsymbol{y}}}(\boldsymbol{x}, \boldsymbol{y}) \big(u(\boldsymbol{y}) - u(\boldsymbol{x}) \big) \, \mathrm{d}\gamma(\boldsymbol{y}), \end{aligned} \tag{4.167}$$

For the first term in the right-hand side of (4.167), by considering (4.119) we have that

$$\int_{S_\varepsilon} \frac{\partial G}{\partial r_{\boldsymbol{y}}}(\boldsymbol{x}, \boldsymbol{y}) \, \mathrm{d}\gamma(\boldsymbol{y}) \quad \xrightarrow[\varepsilon \to 0]{} \quad 1, \tag{4.168}$$

while the second term is bounded by

$$\left| \int_{S_\varepsilon} \big(u(\boldsymbol{y}) - u(\boldsymbol{x}) \big) \frac{\partial G}{\partial r_{\boldsymbol{y}}}(\boldsymbol{x}, \boldsymbol{y}) \, \mathrm{d}\gamma(\boldsymbol{y}) \right| \leq \sup_{\boldsymbol{y} \in B_\varepsilon} |u(\boldsymbol{y}) - u(\boldsymbol{x})|, \tag{4.169}$$

which tends towards zero when $\varepsilon \to 0$. Finally, due the impedance boundary condition (4.4) and since the support of f_z vanishes on Γ_∞, the term on Γ_R in (4.161) can be decomposed as

$$\begin{aligned} \int_{\Gamma_p} \left(\frac{\partial G}{\partial n_{\boldsymbol{y}}}(\boldsymbol{x}, \boldsymbol{y}) - Z(\boldsymbol{y}) G(\boldsymbol{x}, \boldsymbol{y}) \right) u(\boldsymbol{y}) \, \mathrm{d}\gamma(\boldsymbol{y}) + \int_{\Gamma_p} G(\boldsymbol{x}, \boldsymbol{y}) f_z(\boldsymbol{y}) \, \mathrm{d}\gamma(\boldsymbol{y}) \\ - \int_{\Gamma_\infty^R} \left(\frac{\partial G}{\partial y_2}(\boldsymbol{x}, \boldsymbol{y}) + Z_\infty G(\boldsymbol{x}, \boldsymbol{y}) \right) u(\boldsymbol{y}) \, \mathrm{d}\gamma(\boldsymbol{y}), \end{aligned} \tag{4.170}$$

where the integral on Γ_∞^R vanishes due the impedance boundary condition in (4.16). Therefore this term does not depend on R and has its support only on the bounded and perturbed portion Γ_p of the boundary.

In conclusion, when the limits $R \to \infty$ and $\varepsilon \to 0$ are taken in (4.161), then we obtain for $\boldsymbol{x} \in \Omega_e$ the integral representation formula

$$u(\boldsymbol{x}) = \int_{\Gamma_p} \left(\frac{\partial G}{\partial n_{\boldsymbol{y}}}(\boldsymbol{x}, \boldsymbol{y}) - Z(\boldsymbol{y}) G(\boldsymbol{x}, \boldsymbol{y}) \right) u(\boldsymbol{y}) \, \mathrm{d}\gamma(\boldsymbol{y}) + \int_{\Gamma_p} G(\boldsymbol{x}, \boldsymbol{y}) f_z(\boldsymbol{y}) \, \mathrm{d}\gamma(\boldsymbol{y}), \tag{4.171}$$

which can be alternatively expressed as

$$u(\boldsymbol{x}) = \int_{\Gamma_p} \left(u(\boldsymbol{y}) \frac{\partial G}{\partial n_{\boldsymbol{y}}}(\boldsymbol{x}, \boldsymbol{y}) - G(\boldsymbol{x}, \boldsymbol{y}) \frac{\partial u}{\partial n}(\boldsymbol{y}) \right) \mathrm{d}\gamma(\boldsymbol{y}). \tag{4.172}$$

It is remarkable in this integral representation that the support of the integral, namely the curve Γ_p, is bounded. Let us denote the traces of the solution and of its normal derivative

on Γ_p respectively by

$$\mu = u|_{\Gamma_p} \qquad \text{and} \qquad \nu = \left.\frac{\partial u}{\partial n}\right|_{\Gamma_p}. \tag{4.173}$$

We can rewrite now (4.171) and (4.172) in terms of layer potentials as

$$u = \mathcal{D}(\mu) - \mathcal{S}(Z\mu) + \mathcal{S}(f_z) \qquad \text{in } \Omega_e, \tag{4.174}$$

$$u = \mathcal{D}(\mu) - \mathcal{S}(\nu) \qquad \text{in } \Omega_e, \tag{4.175}$$

where we define for $\boldsymbol{x} \in \Omega_e$ respectively the single and double layer potentials as

$$\mathcal{S}\nu(\boldsymbol{x}) = \int_{\Gamma_p} G(\boldsymbol{x}, \boldsymbol{y})\nu(\boldsymbol{y})\,\mathrm{d}\gamma(\boldsymbol{y}), \tag{4.176}$$

$$\mathcal{D}\mu(\boldsymbol{x}) = \int_{\Gamma_p} \frac{\partial G}{\partial n_{\boldsymbol{y}}}(\boldsymbol{x}, \boldsymbol{y})\mu(\boldsymbol{y})\,\mathrm{d}\gamma(\boldsymbol{y}). \tag{4.177}$$

We remark that from the impedance boundary condition (4.4) it is clear that

$$\nu = Z\mu - f_z. \tag{4.178}$$

4.6.2 Integral equation

To determine entirely the solution of the direct scattering problem (4.13) by means of its integral representation, we have to find values for the traces (4.173). This requires the development of an integral equation that allows to fix these values by incorporating the boundary data. For this purpose we place the source point $\boldsymbol{x}$ on the boundary Γ and apply the same procedure as before for the integral representation (4.171), treating differently in (4.161) only the integrals on S_ε. The integrals on S_R^+ still behave well and tend towards zero as $R \to \infty$. The Ball B_ε, though, is split in half by the boundary Γ, and the portion $\Omega_e \cap B_\varepsilon$ is asymptotically separated from its complement in B_ε by the tangent of the boundary if Γ is regular. If $\boldsymbol{x} \in \Gamma_+$, then the associated integrals on S_ε give rise to a term $-u(\boldsymbol{x})/2$ instead of just $-u(\boldsymbol{x})$ as before for the integral representation. Therefore we obtain for $\boldsymbol{x} \in \Gamma_+$ the boundary integral representation

$$\frac{u(\boldsymbol{x})}{2} = \int_{\Gamma_p} \left(\frac{\partial G}{\partial n_{\boldsymbol{y}}}(\boldsymbol{x}, \boldsymbol{y}) - Z(\boldsymbol{y})G(\boldsymbol{x}, \boldsymbol{y}) \right) u(\boldsymbol{y})\,\mathrm{d}\gamma(\boldsymbol{y}) + \int_{\Gamma_p} G(\boldsymbol{x}, \boldsymbol{y}) f_z(\boldsymbol{y})\,\mathrm{d}\gamma(\boldsymbol{y}). \tag{4.179}$$

On the contrary, if $\boldsymbol{x} \in \Gamma_0$, then the pole-type behavior (4.120) contributes also to the singularity (4.119) of the Green's function and the integrals on S_ε give now rise to two terms $-u(\boldsymbol{x})/2$, i.e., on the whole to a term $-u(\boldsymbol{x})$. For $\boldsymbol{x} \in \Gamma_0$ the boundary integral representation is instead given by

$$u(\boldsymbol{x}) = \int_{\Gamma_p} \left(\frac{\partial G}{\partial n_{\boldsymbol{y}}}(\boldsymbol{x}, \boldsymbol{y}) - Z(\boldsymbol{y})G(\boldsymbol{x}, \boldsymbol{y}) \right) u(\boldsymbol{y})\,\mathrm{d}\gamma(\boldsymbol{y}) + \int_{\Gamma_p} G(\boldsymbol{x}, \boldsymbol{y}) f_z(\boldsymbol{y})\,\mathrm{d}\gamma(\boldsymbol{y}). \tag{4.180}$$

We must notice that in both cases, the integrands associated with the boundary Γ admit an integrable singularity at the point $\boldsymbol{x}$. In terms of boundary layer potentials, we can express these boundary integral representations as

$$\frac{u}{2} = D(\mu) - S(Z\mu) + S(f_z) \qquad \text{on } \Gamma_+, \tag{4.181}$$

$$u = D(\mu) - S(Z\mu) + S(f_z) \qquad \text{on } \Gamma_0, \tag{4.182}$$

where we consider, for $\boldsymbol{x} \in \Gamma$, the two boundary integral operators

$$S\nu(\boldsymbol{x}) = \int_{\Gamma_p} G(\boldsymbol{x}, \boldsymbol{y})\nu(\boldsymbol{y})\, \mathrm{d}\gamma(\boldsymbol{y}), \tag{4.183}$$

$$D\mu(\boldsymbol{x}) = \int_{\Gamma_p} \frac{\partial G}{\partial n_{\boldsymbol{y}}}(\boldsymbol{x}, \boldsymbol{y})\mu(\boldsymbol{y})\, \mathrm{d}\gamma(\boldsymbol{y}). \tag{4.184}$$

We can combine (4.181) and (4.182) into a single integral equation on Γ_p, namely

$$(1 + \mathcal{I}_0)\frac{\mu}{2} + S(Z\mu) - D(\mu) = S(f_z) \qquad \text{on } \Gamma_p, \tag{4.185}$$

where $\mathcal{I}_0$ denotes the characteristic or indicator function of the set Γ_0, i.e.,

$$\mathcal{I}_0(\boldsymbol{x}) = \begin{cases} 1 & \text{if } \boldsymbol{x} \in \Gamma_0, \\ 0 & \text{if } \boldsymbol{x} \notin \Gamma_0. \end{cases} \tag{4.186}$$

It is the solution μ on Γ_p of the integral equation (4.185) which finally allows to characterize the solution u in Ω_e of the direct scattering problem (4.13) through the integral representation formula (4.174). The trace of the solution u on the boundary Γ is then found simultaneously by means of the boundary integral representations (4.181) and (4.182). In particular, when $\boldsymbol{x} \in \Gamma_\infty$ and since $\Gamma_\infty \subset \Gamma_0$, therefore it holds that

$$u = D(\mu) - S(Z\mu) + S(f_z) \qquad \text{on } \Gamma_\infty. \tag{4.187}$$

4.7 Far field of the solution

The asymptotic behavior at infinity of the solution u of (4.13) is described by the far field. It is denoted by u^{ff} and is characterized by

$$u(\boldsymbol{x}) \sim u^{ff}(\boldsymbol{x}) \qquad \text{as } |\boldsymbol{x}| \to \infty. \tag{4.188}$$

Its expression can be deduced by replacing the far field of the Green's function G^{ff} and its derivatives in the integral representation formula (4.172), which yields

$$u^{ff}(\boldsymbol{x}) = \int_{\Gamma_p} \left(\frac{\partial G^{ff}}{\partial n_{\boldsymbol{y}}}(\boldsymbol{x}, \boldsymbol{y})\mu(\boldsymbol{y}) - G^{ff}(\boldsymbol{x}, \boldsymbol{y})\nu(\boldsymbol{y}) \right) \mathrm{d}\gamma(\boldsymbol{y}). \tag{4.189}$$

By replacing now (4.148) and the addition of (4.139) and (4.145) in (4.189), we obtain that

$$\begin{aligned} u^{ff}(\boldsymbol{x}) = & -\frac{\cos\theta}{2\pi|\boldsymbol{x}|^2} \int_{\Gamma_p} \left(\begin{bmatrix} 0 \\ 0 \\ 1 \end{bmatrix} \cdot \boldsymbol{n}_{\boldsymbol{y}}\, \mu(\boldsymbol{y}) - y_3 \nu(\boldsymbol{y}) \right) \mathrm{d}\gamma(\boldsymbol{y}) \\ & + i\, e^{-i\pi/4} \sqrt{\frac{Z_\infty}{2\pi|\boldsymbol{x}_s|}}\, e^{-Z_\infty x_3} e^{iZ_\infty |\boldsymbol{x}_s|} \\ & \int_{\Gamma_p} e^{-Z_\infty y_3} e^{-iZ_\infty \boldsymbol{y}_s \cdot \hat{\boldsymbol{x}}_s} \left(Z_\infty \begin{bmatrix} \cos\varphi \\ \sin\varphi \\ 1 \end{bmatrix} \cdot \boldsymbol{n}_{\boldsymbol{y}}\, \mu(\boldsymbol{y}) + \nu(\boldsymbol{y}) \right) \mathrm{d}\gamma(\boldsymbol{y}). \end{aligned} \tag{4.190}$$

The asymptotic behavior of the solution u at infinity, as $|\boldsymbol{x}| \to \infty$, is therefore given by

$$u(\boldsymbol{x}) = \frac{1}{|\boldsymbol{x}|^2}\left\{u_\infty^A(\hat{\boldsymbol{x}}) + \mathcal{O}\left(\frac{1}{|\boldsymbol{x}|}\right)\right\} + \frac{e^{-Z_\infty x_3} e^{iZ_\infty|\boldsymbol{x}_s|}}{\sqrt{|\boldsymbol{x}_s|}}\left\{u_\infty^S(\hat{\boldsymbol{x}}_s) + \mathcal{O}\left(\frac{1}{|\boldsymbol{x}_s|}\right)\right\}, \quad (4.191)$$

where we decompose $\boldsymbol{x} = |\boldsymbol{x}|\,\hat{\boldsymbol{x}}$, being $\hat{\boldsymbol{x}} = (\sin\theta\cos\varphi, \sin\theta\sin\varphi, \cos\theta)$ a vector of the unit sphere, and $\boldsymbol{x}_s = |\boldsymbol{x}_s|\,\hat{\boldsymbol{x}}_s$, being $\hat{\boldsymbol{x}}_s = (\cos\varphi, \sin\varphi)$ a vector of the unit circle. The far-field pattern of the asymptotic decaying is given by

$$u_\infty^A(\hat{\boldsymbol{x}}) = -\frac{\cos\theta}{2\pi}\int_{\Gamma_p}\left(\begin{bmatrix}0\\0\\1\end{bmatrix}\cdot\boldsymbol{n}_{\boldsymbol{y}}\,\mu(\boldsymbol{y}) - y_3\nu(\boldsymbol{y})\right)\mathrm{d}\gamma(\boldsymbol{y}), \quad (4.192)$$

whereas the far-field pattern for the surface waves adopts the form

$$u_\infty^S(\hat{\boldsymbol{x}}_s) = \frac{iZ_\infty^{1/2}}{\sqrt{2\pi}}\,e^{-i\pi/4}\int_{\Gamma_p} e^{-Z_\infty y_3} e^{-iZ_\infty \boldsymbol{y}_s\cdot\hat{\boldsymbol{x}}_s}\left(Z_\infty\begin{bmatrix}\cos\varphi\\\sin\varphi\\1\end{bmatrix}\cdot\boldsymbol{n}_{\boldsymbol{y}}\,\mu(\boldsymbol{y}) + \nu(\boldsymbol{y})\right)\mathrm{d}\gamma(\boldsymbol{y}). \quad (4.193)$$

Both far-field patterns can be expressed in decibels (dB) respectively by means of the scattering cross sections

$$Q_s^A(\hat{\boldsymbol{x}})\ \ [\text{dB}] = 20\log_{10}\left(\frac{|u_\infty^A(\hat{\boldsymbol{x}})|}{|u_0^A|}\right), \quad (4.194)$$

$$Q_s^S(\hat{\boldsymbol{x}}_s)\ \ [\text{dB}] = 20\log_{10}\left(\frac{|u_\infty^S(\hat{\boldsymbol{x}}_s)|}{|u_0^S|}\right), \quad (4.195)$$

where the reference levels u_0^A and u_0^S are taken such that $|u_0^A| = |u_0^S| = 1$ if the incident field is given by a surface wave of the form (4.15).

We remark that the far-field behavior (4.191) of the solution is in accordance with the radiation condition (4.6), which justifies its choice.

4.8 Existence and uniqueness

4.8.1 Function spaces

To state a precise mathematical formulation of the herein treated problems, we have to define properly the involved function spaces. Since the considered domains and boundaries are unbounded, we need to work with weighted Sobolev spaces, as in Durán, Muga & Nédélec (2005*b*, 2009). We consider the classic weight functions

$$\varrho = \sqrt{1+r^2} \qquad \text{and} \qquad \log\varrho = \ln(2+r^2), \quad (4.196)$$

where $r = |\boldsymbol{x}|$. We define the domains

$$\Omega_e^1 = \left\{\boldsymbol{x}\in\Omega_e :\ x_3 > \frac{1}{2Z_\infty}\ln\big(1+2\pi Z_\infty r^3\big),\right\}, \quad (4.197)$$

$$\Omega_e^2 = \left\{\boldsymbol{x}\in\Omega_e :\ x_3 < \frac{1}{2Z_\infty}\ln\big(1+2\pi Z_\infty r^3\big),\right\}. \quad (4.198)$$

It holds that the solution of the direct scattering problem (4.13) is contained in the weighted Sobolev space

$$W^1(\Omega_e) = \left\{ v : \frac{v}{\varrho} \in L^2(\Omega_e),\ \nabla v \in L^2(\Omega_e)^2,\ \frac{v}{\sqrt{\varrho}} \in L^2(\Omega_e^1),\ \frac{\partial v}{\partial r} \in L^2(\Omega_e^1), \right.$$
$$\left. \frac{v}{\log \varrho} \in L^2(\Omega_e^2),\ \frac{1}{\log \varrho}\left(\frac{\partial v}{\partial r} - iZ_\infty v\right) \in L^2(\Omega_e^2) \right\}. \tag{4.199}$$

With the appropriate norm, the space $W^1(\Omega_e)$ becomes also a Hilbert space. We have likewise the inclusion $W^1(\Omega_e) \subset H^1_{\text{loc}}(\Omega_e)$, i.e., the functions of these two spaces differ only by their behavior at infinity.

Since we are dealing with Sobolev spaces, even a strong Lipschitz boundary $\Gamma \in C^{0,1}$ is admissible. The fact that this boundary Γ is also unbounded implies that we have to use weighted trace spaces like in Amrouche (2002). For this purpose, we consider the space

$$W^{1/2}(\Gamma) = \left\{ v :\ \frac{v}{\sqrt{\varrho}\log \varrho} \in H^{1/2}(\Gamma) \right\}. \tag{4.200}$$

Its dual space $W^{-1/2}(\Gamma)$ is defined via W^0-duality, i.e., considering the pivot space

$$W^0(\Gamma) = \left\{ v :\ \frac{v}{\sqrt{\varrho}\log \varrho} \in L^2(\Gamma) \right\}. \tag{4.201}$$

Analogously as for the trace theorem (A.531), if $v \in W^1(\Omega_e)$ then the trace of v fulfills

$$\gamma_0 v = v|_\Gamma \in W^{1/2}(\Gamma). \tag{4.202}$$

Moreover, the trace of the normal derivative can be also defined, and it holds that

$$\gamma_1 v = \frac{\partial v}{\partial n}|_\Gamma \in W^{-1/2}(\Gamma). \tag{4.203}$$

We remark further that the restriction of the trace of v to Γ_p is such that

$$\gamma_0 v|_{\Gamma_p} = v|_{\Gamma_p} \in H^{1/2}(\Gamma_p), \tag{4.204}$$

$$\gamma_1 v|_{\Gamma_p} = \frac{\partial v}{\partial n}|_{\Gamma_p} \in H^{-1/2}(\Gamma_p), \tag{4.205}$$

and its restriction to Γ_∞ yields

$$\gamma_0 v|_{\Gamma_\infty} = v|_{\Gamma_\infty} \in W^{1/2}(\Gamma_\infty), \tag{4.206}$$

$$\gamma_1 v|_{\Gamma_\infty} = \frac{\partial v}{\partial n}|_{\Gamma_\infty} \in W^{-1/2}(\Gamma_\infty). \tag{4.207}$$

4.8.2 Application to the integral equation

The existence and uniqueness of the solution for the direct scattering problem (4.13), due the integral representation formula (4.174), can be characterized by using the integral equation (4.185). For this purpose and in accordance with the considered function spaces, we take $\mu \in H^{1/2}(\Gamma_p)$ and $\nu \in H^{-1/2}(\Gamma_p)$. Furthermore, we consider that $Z \in L^\infty(\Gamma_p)$ and that $f_z \in H^{-1/2}(\Gamma_p)$, even though strictly speaking $f_z \in \widetilde{H}^{-1/2}(\Gamma_p)$.

It holds that the single and double layer potentials defined respectively in (4.176) and (4.177) are linear and continuous integral operators such that

$$\mathcal{S} : H^{-1/2}(\Gamma_p) \longrightarrow W^1(\Omega_e) \qquad \text{and} \qquad \mathcal{D} : H^{1/2}(\Gamma_p) \longrightarrow W^1(\Omega_e). \tag{4.208}$$

The boundary integral operators (4.183) and (4.184) are also linear and continuous applications, and they are such that

$$S : H^{-1/2}(\Gamma_p) \longrightarrow W^{1/2}(\Gamma) \qquad \text{and} \qquad D : H^{1/2}(\Gamma_p) \longrightarrow W^{1/2}(\Gamma). \tag{4.209}$$

When we restrict them to Γ_p, then it holds that

$$S|_{\Gamma_p} : H^{-1/2}(\Gamma_p) \longrightarrow H^{1/2}(\Gamma_p) \qquad \text{and} \qquad D|_{\Gamma_p} : H^{1/2}(\Gamma_p) \longrightarrow H^{1/2}(\Gamma_p). \tag{4.210}$$

Let us consider the integral equation (4.185), which is given in terms of boundary layer potentials, for $\mu \in H^{1/2}(\Gamma_p)$, by

$$(1 + \mathcal{I}_0)\frac{\mu}{2} + S(Z\mu) - D(\mu) = S(f_z) \qquad \text{in } \ H^{1/2}(\Gamma_p). \tag{4.211}$$

Due the imbedding properties of Sobolev spaces and in the same way as for the half-plane impedance Laplace problem, it holds that the left-hand side of the integral equation corresponds to an identity and two compact operators, and thus Fredholm's alternative holds.

Since the Fredholm alternative applies to the integral equation, therefore it applies also to the direct scattering problem (4.13) due the integral representation formula. The existence of the scattering problem's solution is thus determined by its uniqueness, and the values for the impedance $Z \in \mathbb{C}$ for which the uniqueness is lost constitute a countable set, which we call the impedance spectrum of the scattering problem and denote it by σ_Z. The existence and uniqueness of the solution is therefore ensured almost everywhere. The same holds obviously for the solution of the integral equation, whose impedance spectrum we denote by ς_Z. Since the integral equation is derived from the scattering problem, it holds that $\sigma_Z \subset \varsigma_Z$. The converse, though, is not necessarily true. In any way, the set $\varsigma_Z \setminus \sigma_Z$ is at most countable. In conclusion, the scattering problem (4.13) admits a unique solution u if $Z \notin \sigma_Z$, and the integral equation (4.185) admits a unique solution μ if $Z \notin \varsigma_Z$.

4.9 Dissipative problem

The dissipative problem considers surface waves that lose their amplitude as they travel along the half-space's boundary. These waves dissipate their energy as they propagate and are modeled by a complex impedance $Z_\infty \in \mathbb{C}$ whose imaginary part is strictly positive, i.e., $\mathfrak{Im}\{Z_\infty\} > 0$. This choice ensures that the surface waves of the Green's function (4.113) decrease exponentially at infinity. Due the dissipative nature of the medium, it is no longer suited to take progressive plane surface waves in the form of (4.15) as the incident field u_I. Instead, we have to take a source of surface waves at a finite distance from the perturbation. For example, we can consider a point source located at $\boldsymbol{z} \in \Omega_e$, in which case the incident field is given, up to a multiplicative constant, by

$$u_I(\boldsymbol{x}) = G(\boldsymbol{x}, \boldsymbol{z}), \tag{4.212}$$

where G denotes the Green's function (4.113). This incident field u_I satisfies the Laplace equation with a source term in the right-hand side, namely

$$\Delta u_I = \delta_{\boldsymbol{z}} \qquad \text{in } \mathcal{D}'(\Omega_e), \tag{4.213}$$

which holds also for the total field u_T but not for the scattered field u, in which case the Laplace equation remains homogeneous. For a general source distribution g_s, whose support is contained in Ω_e, the incident field can be expressed by

$$u_I(\boldsymbol{x}) = G(\boldsymbol{x}, \boldsymbol{z}) * g_s(\boldsymbol{z}) = \int_{\Omega_e} G(\boldsymbol{x}, \boldsymbol{z})\, g_s(\boldsymbol{z})\, \mathrm{d}\boldsymbol{z}. \tag{4.214}$$

This incident field u_I satisfies now

$$\Delta u_I = g_s \qquad \text{in } \mathcal{D}'(\Omega_e), \tag{4.215}$$

which holds again also for the total field u_T but not for the scattered field u.

It is not difficult to see that all the performed developments for the non-dissipative case are still valid when considering dissipation. The only difference is that now a complex impedance Z_∞ such that $\mathfrak{Im}\{Z_\infty\} > 0$ has to be taken everywhere into account.

4.10 Variational formulation

To solve the integral equation we convert it to its variational or weak formulation, i.e., we solve it with respect to a certain test function in a bilinear (or sesquilinear) form. Basically, the integral equation is multiplied by the (conjugated) test function and then the equation is integrated over the boundary of the domain. The test function is taken in the same function space as the solution of the integral equation.

The variational formulation for the integral equation (4.211) searches $\mu \in H^{1/2}(\Gamma_p)$ such that $\forall \varphi \in H^{1/2}(\Gamma_p)$ we have that

$$\left\langle (1 + \mathcal{I}_0)\frac{\mu}{2} + S(Z\mu) - D(\mu), \varphi \right\rangle = \left\langle S(f_z), \varphi \right\rangle. \tag{4.216}$$

4.11 Numerical discretization

4.11.1 Discretized function spaces

The scattering problem (4.13) is solved numerically with the boundary element method by employing a Galerkin scheme on the variational formulation of the integral equation. We use on the boundary surface Γ_p Lagrange finite elements of type $\mathbb{P}_1$. The surface Γ_p is approximated by the triangular mesh Γ_p^h, composed by T flat triangles T_j, for $1 \leq j \leq T$, and I nodes $\boldsymbol{r}_i \in \mathbb{R}^3$, $1 \leq i \leq I$. The triangles have a diameter less or equal than h, and their vertices or corners, i.e., the nodes $\boldsymbol{r}_i$, are on top of Γ_p, as shown in Figure 4.10. The diameter of a triangle K is given by

$$\mathrm{diam}(K) = \sup_{\boldsymbol{x},\boldsymbol{y} \in K} |\boldsymbol{y} - \boldsymbol{x}|. \tag{4.217}$$

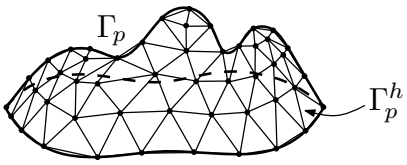

FIGURE 4.10. Mesh Γ_p^h, discretization of Γ_p.

The function space $H^{1/2}(\Gamma_p)$ is approximated using the conformal space of continuous piecewise linear polynomials with complex coefficients

$$Q_h = \big\{\varphi_h \in C^0(\Gamma_p^h) \,:\, \varphi_h|_{T_j} \in \mathbb{P}_1(\mathbb{C}),\;\; 1 \le j \le T\big\}. \tag{4.218}$$

The space Q_h has a finite dimension I, and we describe it using the standard base functions for finite elements of type $\mathbb{P}_1$, which we denote by $\{\chi_j\}_{j=1}^I$. The base function χ_j is associated with the node $\boldsymbol{r}_j$ and has its support $\operatorname{supp}\chi_j$ on the triangles that have $\boldsymbol{r}_j$ as one of their vertices. On $\boldsymbol{r}_j$ it has a value of one and on the opposed edges of the triangles its value is zero, being linearly interpolated in between and zero otherwise.

In virtue of this discretization, any function $\varphi_h \in Q_h$ can be expressed as a linear combination of the elements of the base, namely

$$\varphi_h(\boldsymbol{x}) = \sum_{j=1}^{I} \varphi_j\, \chi_j(\boldsymbol{x}) \qquad \text{for } \; \boldsymbol{x} \in \Gamma_p^h, \tag{4.219}$$

where $\varphi_j \in \mathbb{C}$ for $1 \le j \le I$. The solution $\mu \in H^{1/2}(\Gamma_p)$ of the variational formulation (4.216) can be therefore approximated by

$$\mu_h(\boldsymbol{x}) = \sum_{j=1}^{I} \mu_j\, \chi_j(\boldsymbol{x}) \qquad \text{for } \; \boldsymbol{x} \in \Gamma_p^h, \tag{4.220}$$

where $\mu_j \in \mathbb{C}$ for $1 \le j \le I$. The function f_z can be also approximated by

$$f_z^h(\boldsymbol{x}) = \sum_{j=1}^{I} f_j\, \chi_j(\boldsymbol{x}) \qquad \text{for } \; \boldsymbol{x} \in \Gamma_p^h, \quad \text{with } \; f_j = f_z(\boldsymbol{r}_j). \tag{4.221}$$

4.11.2 Discretized integral equation

To see how the boundary element method operates, we apply it to the variational formulation (4.216). We characterize all the discrete approximations by the index h, including also the impedance and the boundary layer potentials. The numerical approximation of (4.216) leads to the discretized problem that searches $\mu_h \in Q_h$ such that $\forall \varphi_h \in Q_h$

$$\Big\langle (1 + \mathcal{I}_0^h)\frac{\mu_h}{2} + S_h(Z_h\mu_h) - D_h(\mu_h), \varphi_h \Big\rangle = \big\langle S_h(f_z^h), \varphi_h \big\rangle. \tag{4.222}$$

Considering the decomposition of μ_h in terms of the base $\{\chi_j\}$ and taking as test functions the same base functions, $\varphi_h = \chi_i$ for $1 \leq i \leq I$, yields the discrete linear system

$$\sum_{j=1}^{I} \mu_j \left(\frac{1}{2} \big\langle (1 + \mathcal{I}_0^h)\chi_j, \chi_i \big\rangle + \langle S_h(Z_h\chi_j), \chi_i \rangle - \langle D_h(\chi_j), \chi_i \rangle \right) = \sum_{j=1}^{I} f_j \, \langle S_h(\chi_j), \chi_i \rangle. \tag{4.223}$$

This constitutes a system of linear equations that can be expressed as a linear matrix system:

$$\begin{cases} \text{Find } \boldsymbol{\mu} \in \mathbb{C}^I \text{ such that} \\ \boldsymbol{M}\boldsymbol{\mu} = \boldsymbol{b}. \end{cases} \tag{4.224}$$

The elements m_{ij} of the matrix $\boldsymbol{M}$ are given, for $1 \leq i, j \leq I$, by

$$m_{ij} = \frac{1}{2} \big\langle (1 + \mathcal{I}_0^h)\chi_j, \chi_i \big\rangle + \langle S_h(Z_h\chi_j), \chi_i \rangle - \langle D_h(\chi_j), \chi_i \rangle, \tag{4.225}$$

and the elements b_i of the vector $\boldsymbol{b}$ by

$$b_i = \big\langle S_h(f_z^h), \chi_i \big\rangle = \sum_{j=1}^{I} f_j \, \langle S_h(\chi_j), \chi_i \rangle \qquad \text{for } \; 1 \leq i \leq I. \tag{4.226}$$

The discretized solution u_h, which approximates u, is finally obtained by discretizing the integral representation formula (4.174) according to

$$u_h = \mathcal{D}_h(\mu_h) - \mathcal{S}_h(Z_h\mu_h) + \mathcal{S}_h(f_z^h), \tag{4.227}$$

which, more specifically, can be expressed as

$$u_h = \sum_{j=1}^{I} \mu_j \big(\mathcal{D}_h(\chi_j) - \mathcal{S}_h(Z_h\chi_j) \big) + \sum_{j=1}^{I} f_j \, \mathcal{S}_h(\chi_j). \tag{4.228}$$

We remark that the resulting matrix $\boldsymbol{M}$ is in general complex, full, non-symmetric, and with dimensions $I \times I$. The right-hand side vector $\boldsymbol{b}$ is complex and of size I. The boundary element calculations required to compute numerically the elements of $\boldsymbol{M}$ and $\boldsymbol{b}$ have to be performed carefully, since the integrals that appear become singular when the involved segments are adjacent or coincident, due the singularity of the Green's function at its source point. On Γ_0, the singularity of the image source point has to be taken additionally into account for these calculations.

4.12 Boundary element calculations

The boundary element calculations build the elements of the matrix $\boldsymbol{M}$ resulting from the discretization of the integral equation, i.e., from (4.224). They permit thus to compute numerically expressions like (4.225). To evaluate the appearing singular integrals, we adapt the semi-numerical methods described in the report of Bendali & Devys (1986).

We use the same notation as in Section D.12, and the required boundary element integrals, for $a, b \in \{0, 1\}$ and $c, d \in \{1, 2, 3\}$, are again

$$ZA_{a,b}^{c,d} = \int_K \int_L \left(\frac{s_c}{h_c^K}\right)^a \left(\frac{t_d}{h_d^L}\right)^b G(\boldsymbol{x}, \boldsymbol{y}) \, \mathrm{d}L(\boldsymbol{y}) \, \mathrm{d}K(\boldsymbol{x}), \tag{4.229}$$

$$ZB_{a,b}^{c,d} = \int_K \int_L \left(\frac{s_c}{h_c^K}\right)^a \left(\frac{t_d}{h_d^L}\right)^b \frac{\partial G}{\partial n_{\boldsymbol{y}}}(\boldsymbol{x}, \boldsymbol{y}) \, \mathrm{d}L(\boldsymbol{y}) \, \mathrm{d}K(\boldsymbol{x}). \tag{4.230}$$

All the integrals that stem from the numerical discretization can be expressed in terms of these two basic boundary element integrals. The impedance is again discretized as a piecewise constant function Z_h, which on each triangle T_j adopts a constant value $Z_j \in \mathbb{C}$. The integrals of interest are the same as for the full-space impedance Laplace problem and we consider furthermore that

$$\left\langle (1 + \mathcal{I}_0^h)\chi_j, \chi_i \right\rangle = \begin{cases} \langle \chi_j, \chi_i \rangle & \text{if } \boldsymbol{r}_j \in \Gamma_+, \\ 2 \langle \chi_j, \chi_i \rangle & \text{if } \boldsymbol{r}_j \in \Gamma_0. \end{cases} \tag{4.231}$$

To compute the boundary element integrals (4.229) and (4.230), we can easily isolate the singular part (4.119) of the Green's function (4.113), which corresponds in fact to the Green's function of the Laplace equation in the full-space, and therefore the associated integrals are computed in the same way. The same applies also for its normal derivative. In the case when the triangles K and L are are close enough, e.g., adjacent or coincident, and when $L \in \Gamma_0^h$ or $K \in \Gamma_0^h$, being Γ_0^h the approximation of Γ_0, we have to consider additionally the singular behavior (4.120), which is linked with the presence of the impedance half-space. This behavior can be straightforwardly evaluated by replacing $\boldsymbol{x}$ by $\bar{\boldsymbol{x}}$ in formulae (D.295) to (D.298), i.e., by computing the quantities $ZF_b^d(\bar{\boldsymbol{x}})$ and $ZG_b^d(\bar{\boldsymbol{x}})$ with the corresponding adjustment of the notation. Otherwise, if the triangles are not close enough and for the non-singular part of the Green's function, a three-point Gauss-Lobatto quadrature formula is used. All the other computations are performed in the same manner as in Section D.12 for the full-space Laplace equation.

4.13 Benchmark problem

As benchmark problem we consider the particular case when the domain $\Omega_e \subset \mathbb{R}^3_+$ is taken as the exterior of a half-sphere of radius $R > 0$ that is centered at the origin, as shown in Figure 4.11. We decompose the boundary of Ω_e as $\Gamma = \Gamma_p \cup \Gamma_\infty$, where Γ_p corresponds to the upper half-sphere, whereas Γ_∞ denotes the remaining unperturbed portion of the half-space's boundary which lies outside the half-sphere and which extends towards infinity. The unit normal $\boldsymbol{n}$ is taken outwardly oriented of Ω_e, e.g., $\boldsymbol{n} = -\boldsymbol{r}$ on Γ_p.

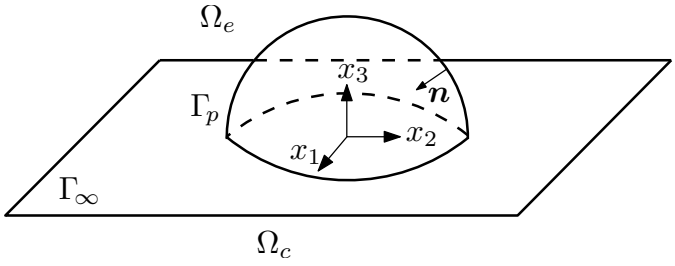

FIGURE 4.11. Exterior of the half-sphere.

The benchmark problem is then stated as

$$\begin{cases} \text{Find } u : \Omega_e \to \mathbb{C} \text{ such that} \\ \Delta u = 0 & \text{in } \Omega_e, \\ -\dfrac{\partial u}{\partial n} + Zu = f_z & \text{on } \Gamma, \\ \text{+ Outgoing radiation condition as } |\boldsymbol{x}| \to \infty, \end{cases} \tag{4.232}$$

where we consider a constant impedance $Z \in \mathbb{C}$ throughout Γ and where the radiation condition is as usual given by (4.6). As incident field u_I we consider the same Green's function, namely

$$u_I(\boldsymbol{x}) = G(\boldsymbol{x}, \boldsymbol{z}), \tag{4.233}$$

where $\boldsymbol{z} \in \Omega_c$ denotes the source point of our incident field. The impedance data function f_z is hence given by

$$f_z(\boldsymbol{x}) = \frac{\partial G}{\partial n_{\boldsymbol{x}}}(\boldsymbol{x}, \boldsymbol{z}) - ZG(\boldsymbol{x}, \boldsymbol{z}), \tag{4.234}$$

and its support is contained in Γ_p. The analytic solution for the benchmark problem (4.232) is then clearly given by

$$u(\boldsymbol{x}) = -G(\boldsymbol{x}, \boldsymbol{z}). \tag{4.235}$$

The goal is to retrieve this solution numerically with the integral equation techniques and the boundary element method described throughout this chapter.

For the computational implementation and the numerical resolution of the benchmark problem, we consider integral equation (4.185). The linear system (4.224) resulting from the discretization (4.222) of its variational formulation (4.216) is solved computationally with finite boundary elements of type $\mathbb{P}_1$ by using subroutines programmed in Fortran 90, by generating the mesh Γ_p^h of the boundary with the free software Gmsh 2.4, and by representing graphically the results in Matlab 7.5 (R2007b).

We consider a radius $R = 1$, a constant impedance $Z = 5$, and for the incident field a source point $\boldsymbol{z} = (0, 0, 0)$. The discretized perturbed boundary curve Γ_p^h has $I = 641$ nodes, $T = 1224$ triangles and a discretization step $h = 0.1676$, being

$$h = \max_{1 \le j \le T} \operatorname{diam}(T_j). \tag{4.236}$$

The numerically calculated trace of the solution μ_h of the benchmark problem, which was computed by using the boundary element method, is depicted in Figure 4.12. In the same manner, the numerical solution u_h is illustrated in Figures 4.13 and 4.14 for an angle $\varphi = 0$. It can be observed that the numerical solution is close to the exact one.

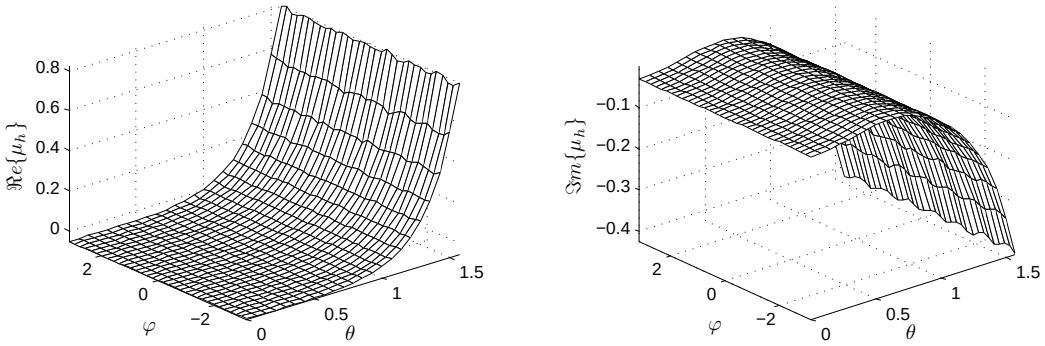

(a) Real part (b) Imaginary part

FIGURE 4.12. Numerically computed trace of the solution μ_h.

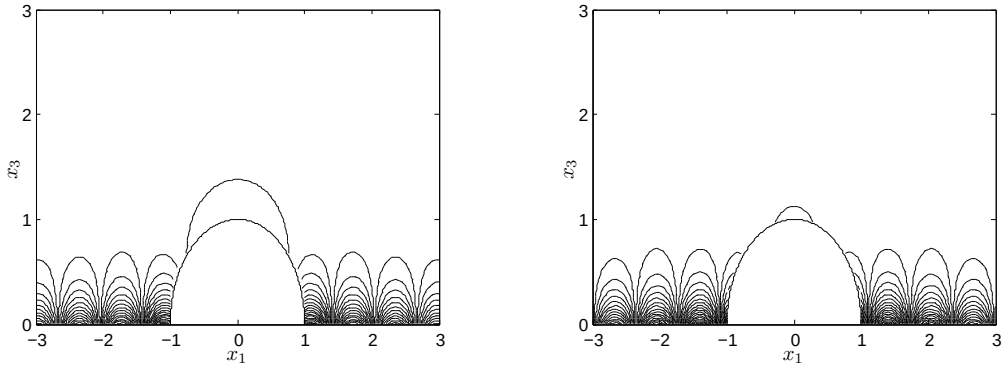

(a) Real part (b) Imaginary part

FIGURE 4.13. Contour plot of the numerically computed solution u_h for $\varphi = 0$.

Likewise as in (D.346), we define the relative error of the trace of the solution as

$$E_2(h, \Gamma_p^h) = \frac{\|\Pi_h \mu - \mu_h\|_{L^2(\Gamma_p^h)}}{\|\Pi_h \mu\|_{L^2(\Gamma_p^h)}}, \tag{4.237}$$

where $\Pi_h \mu$ denotes the Lagrange interpolating function of the exact solution's trace μ, i.e.,

$$\Pi_h \mu(\boldsymbol{x}) = \sum_{j=1}^{I} \mu(\boldsymbol{r}_j)\, \chi_j(\boldsymbol{x}) \quad \text{and} \quad \mu_h(\boldsymbol{x}) = \sum_{j=1}^{I} \mu_j\, \chi_j(\boldsymbol{x}) \quad \text{for } \boldsymbol{x} \in \Gamma_p^h. \tag{4.238}$$

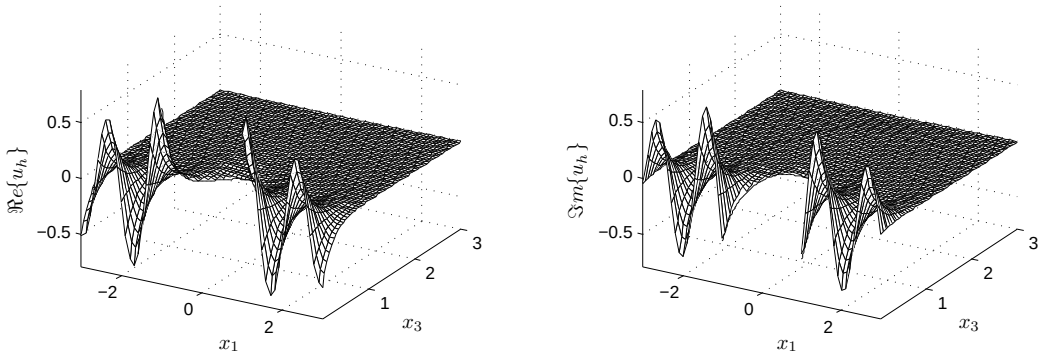

(a) Real part (b) Imaginary part

FIGURE 4.14. Oblique view of the numerically computed solution u_h for $\varphi = 0$.

In our case, for a step $h = 0.1676$, we obtained a relative error of $E_2(h, \Gamma_p^h) = 0.05359$.

As in (D.350), we define the relative error of the solution as

$$E_\infty(h, \Omega_L) = \frac{\|u - u_h\|_{L^\infty(\Omega_L)}}{\|u\|_{L^\infty(\Omega_L)}}, \tag{4.239}$$

being $\Omega_L = \{\boldsymbol{x} \in \Omega_e : \|\boldsymbol{x}\|_\infty < L\}$ for $L > 0$. We consider $L = 3$ and approximate Ω_L by a triangular finite element mesh of refinement h near the boundary. For $h = 0.1676$, the relative error that we obtained for the solution was $E_\infty(h, \Omega_L) = 0.05509$.

The results for different mesh refinements, i.e., for different numbers of triangles T, nodes I, and discretization steps h for Γ_p^h, are listed in Table 4.1. These results are illustrated graphically in Figure 4.15. It can be observed that the relative errors are approximately of order h^2.

TABLE 4.1. Relative errors for different mesh refinements.

T	I	h	$E_2(h, \Gamma_p^h)$	$E_\infty(h, \Omega_L)$
46	30	0.7071	$2.863 \cdot 10^{+1}$	$4.582 \cdot 10^{+1}$
168	95	0.4320	$3.096 \cdot 10^{-1}$	$4.131 \cdot 10^{-1}$
466	252	0.2455	$1.233 \cdot 10^{-1}$	$1.373 \cdot 10^{-1}$
700	373	0.1987	$8.414 \cdot 10^{-2}$	$9.262 \cdot 10^{-2}$
1224	641	0.1676	$5.359 \cdot 10^{-2}$	$5.509 \cdot 10^{-2}$
2100	1090	0.1286	$3.182 \cdot 10^{-2}$	$4.890 \cdot 10^{-2}$

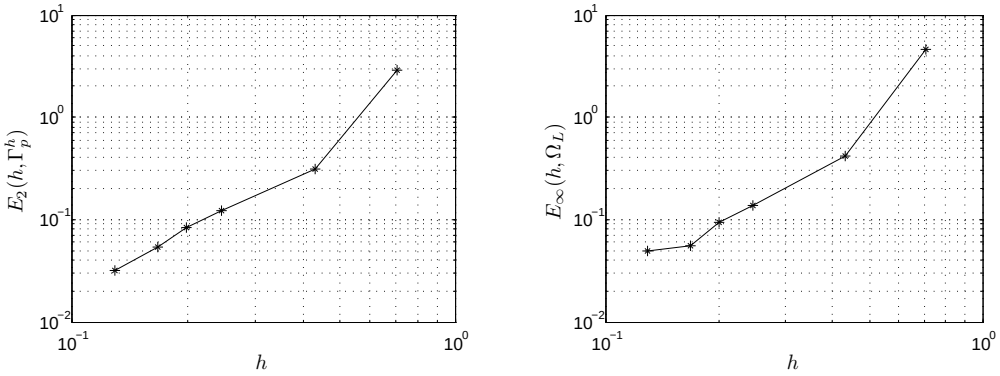

(a) Relative error $E_2(h, \Gamma_p^h)$ (b) Relative error $E_\infty(h, \Omega_L)$

FIGURE 4.15. Logarithmic plots of the relative errors versus the discretization step.

V. HALF-SPACE IMPEDANCE HELMHOLTZ PROBLEM

5.1 Introduction

In this chapter we study the perturbed half-space impedance Helmholtz problem using integral equation techniques and the boundary element method.

We consider the problem of the Helmholtz equation in three dimensions on a compactly perturbed half-space with an impedance boundary condition. The perturbed half-space impedance Helmholtz problem is a wave scattering problem around the bounded perturbation, which is contained in the upper half-space. In acoustic scattering the impedance boundary-value problem appears when we suppose that the normal velocity is proportional to the excess pressure on the boundary of the impenetrable perturbation or obstacle (vid. Section A.11). The special case of frequency zero for the volume waves has been treated already in Chapter IV. The two-dimensional case is considered in Chapter III, whereas the full-space impedance Helmholtz problem with a bounded impenetrable obstacle is treated thoroughly in Appendix E.

The main application of the problem corresponds to outdoor sound propagation, but it is also used to describe the propagation of radio waves above the ground. The problem was at first considered by Sommerfeld (1909) to describe the long-distance propagation of electromagnetic waves above the earth. Different results for the electromagnetic problem were then obtained by Weyl (1919) and later again by Sommerfeld (1926). After the articles of Van der Pol & Niessen (1930), Wise (1931), and Van der Pol (1935), the most useful results up to that time were generated by Norton (1936, 1937). We can likewise mention the later works of Baños & Wesley (1953, 1954) and Baños (1966). The application of the problem to outdoor sound propagation was initiated by Rudnick (1947). Other approximate solutions to the problem were thereafter found by Lawhead & Rudnick (1951*a*,*b*) and Ingard (1951). Solutions containing surface-wave terms were obtained by Wenzel (1974) and Chien & Soroka (1975, 1980). Further references are listed in Nobile & Hayek (1985). Other important articles that attempt to solve the problem are the ones of Briquet & Filippi (1977), Attenborough, Hayek & Lawther (1980), Filippi (1983), Li et al. (1994), and Attenborough (2002), and more recently also Habault (1999), Ochmann (2004), and Ochmann & Brick (2008), among others. The problem can be likewise found in the book of DeSanto (1992). The physical aspects of outdoor sound propagation can be found in Morse & Ingard (1961) and Embleton (1996).

The Helmholtz equation allows the propagation of volume waves inside the considered domain, and when it is supplied with an impedance boundary condition, then it allows also the propagation of surface waves along the boundary of the perturbed half-space. The main difficulty in the numerical treatment and resolution of our problem is the fact that the exterior domain is unbounded. We solve it therefore with integral equation techniques and a boundary element method, which require the knowledge of the associated Green's function. This Green's function is computed using a Fourier transform and taking into account the limiting absorption principle, following Durán, Muga & Nédélec (2005*b*, 2009), but here an

explicit expression is found for it in terms of a finite combination of elementary functions, special functions, and their primitives.

This chapter is structured in 13 sections, including this introduction. The direct scattering problem of the Helmholtz equation in a three-dimensional compactly perturbed half-space with an impedance boundary condition is presented in Section 5.2. The computation of the Green's function, its far field, and its numerical evaluation are developed respectively in Sections 5.3, 5.4, and 5.5. The use of integral equation techniques to solve the direct scattering problem is discussed in Section 5.6. These techniques allow also to represent the far field of the solution, as shown in Section 5.7. The appropriate function spaces and some existence and uniqueness results for the solution of the problem are presented in Section 5.8. The dissipative problem is studied in Section 5.9. By means of the variational formulation developed in Section 5.10, the obtained integral equation is discretized using the boundary element method, which is described in Section 5.11. The boundary element calculations required to build the matrix of the linear system resulting from the numerical discretization are explained in Section 5.12. Finally, in Section 5.13 a benchmark problem based on an exterior half-sphere problem is solved numerically.

5.2 Direct scattering problem

5.2.1 Problem definition

We consider the direct scattering problem of linear time-harmonic acoustic waves on a perturbed half-space $\Omega_e \subset \mathbb{R}^3$, where $\mathbb{R}^3_+ = \{(x_1, x_2, x_3) \in \mathbb{R}^3 : x_3 > 0\}$, where the incident field u_I and the reflected field u_R are known, and where the time convention $e^{-i\omega t}$ is taken. The goal is to find the scattered field u as a solution to the Helmholtz equation in the exterior open and connected domain Ω_e, satisfying an outgoing radiation condition, and such that the total field u_T, decomposed as $u_T = u_I + u_R + u$, satisfies a homogeneous impedance boundary condition on the regular boundary $\Gamma = \Gamma_p \cup \Gamma_\infty$ (e.g., of class C^2). The exterior domain Ω_e is composed by the half-space $\mathbb{R}^3_+$ with a compact perturbation near the origin that is contained in $\mathbb{R}^3_+$, as shown in Figure 5.1. The perturbed boundary is denoted by Γ_p, while Γ_∞ denotes the remaining unperturbed boundary of $\mathbb{R}^3_+$, which extends towards infinity on every horizontal direction. The unit normal $\boldsymbol{n}$ is taken outwardly oriented of Ω_e and the complementary domain is denoted by $\Omega_c = \mathbb{R}^3 \setminus \overline{\Omega_e}$. A given wave number $k > 0$ is considered, which depends on the pulsation ω and the speed of wave propagation c through the ratio $k = \omega/c$.

The total field u_T satisfies thus the Helmholtz equation

$$\Delta u_T + k^2 u_T = 0 \qquad \text{in } \Omega_e, \tag{5.1}$$

which is also satisfied by the incident field u_I, the reflected field u_R, and the scattered field u, due linearity. For the total field u_T we take the homogeneous impedance boundary condition

$$-\frac{\partial u_T}{\partial n} + Z u_T = 0 \qquad \text{on } \Gamma, \tag{5.2}$$

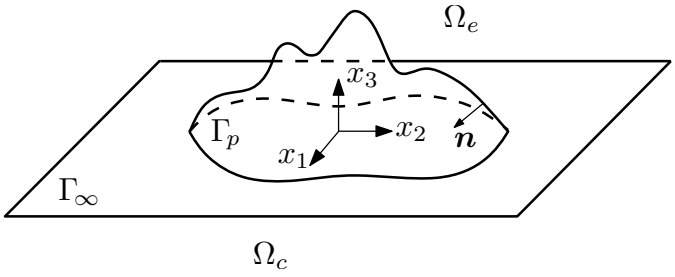

FIGURE 5.1. Perturbed half-space impedance Helmholtz problem domain.

where Z is the impedance on the boundary, which is decomposed as

$$Z(\boldsymbol{x}) = Z_\infty + Z_p(\boldsymbol{x}), \qquad \boldsymbol{x} \in \Gamma, \tag{5.3}$$

being $Z_\infty > 0$ real and constant throughout Γ, and $Z_p(\boldsymbol{x})$ a possibly complex-valued impedance that depends on the position $\boldsymbol{x}$ and that has a bounded support contained in Γ_p. The case of complex Z_∞ and k will be discussed later. If $Z = 0$ or $Z = \infty$, then we retrieve respectively the classical Neumann or Dirichlet boundary conditions. The scattered field u satisfies the non-homogeneous impedance boundary condition

$$-\frac{\partial u}{\partial n} + Zu = f_z \qquad \text{on } \Gamma, \tag{5.4}$$

where the impedance data function f_z is known, has its support contained in Γ_p, and is given, because of (5.2), by

$$f_z = \frac{\partial u_I}{\partial n} - Zu_I + \frac{\partial u_R}{\partial n} - Zu_R \qquad \text{on } \Gamma. \tag{5.5}$$

An outgoing radiation condition has to be also imposed for the scattered field u, which specifies its decaying behavior at infinity and eliminates the non-physical solutions, e.g., ingoing volume or surface waves. This radiation condition can be stated for $r \to \infty$ in a more adjusted way as

$$\begin{cases} |u| \le \dfrac{C}{r} \quad \text{and} \quad \left|\dfrac{\partial u}{\partial r} - iku\right| \le \dfrac{C}{r^2} & \text{if } x_3 > \dfrac{1}{2Z_\infty}\ln(1+\beta r), \\ |u| \le \dfrac{C}{\sqrt{r}} \quad \text{and} \quad \left|\dfrac{\partial u}{\partial r} - i\sqrt{Z_\infty^2 + k^2}u\right| \le \dfrac{C}{r} & \text{if } x_3 \le \dfrac{1}{2Z_\infty}\ln(1+\beta r), \end{cases} \tag{5.6}$$

for some constants $C > 0$, where $r = |\boldsymbol{x}|$ and $\beta = 8\pi Z_\infty^2/\sqrt{Z_\infty^2 + k^2}$. It implies that two different asymptotic behaviors can be established for the scattered field u. Away from the boundary Γ and inside the domain Ω_e, the first expression in (5.6) dominates, which corresponds to a classical Sommerfeld radiation condition like (E.8) and is associated with volume waves. Near the boundary, on the other hand, the second expression in (5.6) resembles a Sommerfeld radiation condition, but only along the boundary and having a different

wave number, and is therefore related to the propagation of surface waves. It is often expressed also as

$$\left| \frac{\partial u}{\partial |\boldsymbol{x}_s|} - i\sqrt{Z_\infty^2 + k^2}u \right| \leq \frac{C}{|\boldsymbol{x}_s|}, \tag{5.7}$$

where $\boldsymbol{x}_s = (x_1, x_2)$.

Analogously as done by Durán, Muga & Nédélec (2005*b*, 2009), the radiation condition (5.6) can be stated alternatively as

$$\begin{cases} |u| \leq \dfrac{C}{r^{1-\alpha}} \quad \text{and} \quad \left| \dfrac{\partial u}{\partial r} - iku \right| \leq \dfrac{C}{r^{2-\alpha}} & \text{if } \ x_3 > Cr^\alpha, \\ |u| \leq \dfrac{C}{\sqrt{r}} \quad \text{and} \quad \left| \dfrac{\partial u}{\partial r} - i\sqrt{Z_\infty^2 + k^2}u \right| \leq \dfrac{C}{r^{1-\alpha}} & \text{if } \ x_3 \leq Cr^\alpha, \end{cases} \tag{5.8}$$

for $0 < \alpha < 1/2$ and some constants $C > 0$, being the growth of Cr^α bigger than the logarithmic one at infinity. Equivalently, the radiation condition can be expressed in a more weaker and general formulation as

$$\begin{cases} \lim\limits_{R\to\infty} \displaystyle\int_{S_R^1} \frac{|u|^2}{R}\, \mathrm{d}\gamma = 0 \quad \text{and} \quad \lim\limits_{R\to\infty} \displaystyle\int_{S_R^1} R \left| \frac{\partial u}{\partial r} - iku \right|^2 \mathrm{d}\gamma = 0, \\ \lim\limits_{R\to\infty} \displaystyle\int_{S_R^2} \frac{|u|^2}{\ln R}\, \mathrm{d}\gamma < \infty \quad \text{and} \quad \lim\limits_{R\to\infty} \displaystyle\int_{S_R^2} \frac{1}{\ln R} \left| \frac{\partial u}{\partial r} - i\sqrt{Z_\infty^2 + k^2}u \right|^2 \mathrm{d}\gamma = 0, \end{cases} \tag{5.9}$$

where

$$S_R^1 = \left\{ \boldsymbol{x} \in \mathbb{R}^3_+ : \ |\boldsymbol{x}| = R, \ \ x_3 > \frac{1}{2Z_\infty} \ln(1 + \beta R) \right\}, \tag{5.10}$$

$$S_R^2 = \left\{ \boldsymbol{x} \in \mathbb{R}^3_+ : \ |\boldsymbol{x}| = R, \ \ x_3 < \frac{1}{2Z_\infty} \ln(1 + \beta R) \right\}. \tag{5.11}$$

We observe that in this case

$$\int_{S_R^1} \mathrm{d}\gamma = \mathcal{O}(R^2) \qquad \text{and} \qquad \int_{S_R^2} \mathrm{d}\gamma = \mathcal{O}(R \ln R). \tag{5.12}$$

The portions S_R^1 and S_R^2 of the half-sphere and the terms depending on S_R^2 of the radiation condition (5.9) have to be modified when using instead the polynomial curves of (5.8). We refer to Stoker (1956) for a discussion on radiation conditions for surface waves.

The perturbed half-space impedance Helmholtz problem can be finally stated as

$$\begin{cases} \text{Find } u : \Omega_e \to \mathbb{C} \text{ such that} \\ \Delta u + k^2 u = 0 \qquad\qquad \text{in } \ \Omega_e, \\ -\dfrac{\partial u}{\partial n} + Zu = f_z \qquad\qquad \text{on } \ \Gamma, \\ \text{+ Outgoing radiation condition as } |\boldsymbol{x}| \to \infty, \end{cases} \tag{5.13}$$

where the outgoing radiation condition is given by (5.6).

5.2.2 Incident and reflected field

To determine the incident field u_I and the reflected field u_R, we study the solutions u_T of the unperturbed and homogeneous wave propagation problem with neither a scattered field nor an associated radiation condition, being $u_T = u_I + u_R$. The solutions are searched in particular to be physically admissible, i.e., solutions which do not explode exponentially in the propagation domain, depicted in Figure 5.1. We analyze thus the half-space impedance Helmholtz problem

$$\begin{cases} \Delta u_T + k^2 u_T = 0 & \text{in } \mathbb{R}^3_+, \\ \dfrac{\partial u_T}{\partial x_3} + Z_\infty u_T = 0 & \text{on } \{x_3 = 0\}. \end{cases} \tag{5.14}$$

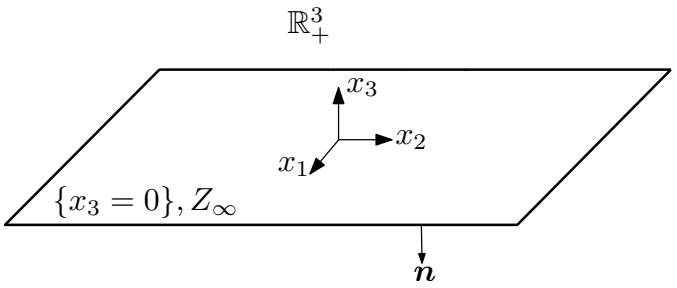

FIGURE 5.2. Positive half-space $\mathbb{R}^3_+$.

Two different kinds of independent solutions u_T exist for the problem (5.14). They are obtained by studying the way how progressive plane waves of the form $e^{i\boldsymbol{k}\cdot\boldsymbol{x}}$ can be adjusted to satisfy the boundary condition, where the wave propagation vector $\boldsymbol{k} = (k_1, k_2, k_3)$ is such that $(\boldsymbol{k} \cdot \boldsymbol{k}) = k^2$.

The first kind of solution corresponds to a linear combination of two progressive plane volume waves and is given, up to an arbitrary multiplicative constant, by

$$u_T(\boldsymbol{x}) = e^{i\boldsymbol{k}\cdot\boldsymbol{x}} - \left(\frac{Z_\infty + ik_3}{Z_\infty - ik_3}\right) e^{i\bar{\boldsymbol{k}}\cdot\boldsymbol{x}}, \tag{5.15}$$

where $\boldsymbol{k} \in \mathbb{R}^3$ and $\bar{\boldsymbol{k}} = (k_1, k_2, -k_3)$. Due the involved physics, we consider that $k_3 \leq 0$. The first term of (5.15) can be interpreted as an incident plane volume wave, while the second term represents the reflected plane volume wave due the presence of the boundary with impedance. Thus

$$u_I(\boldsymbol{x}) = e^{i\boldsymbol{k}\cdot\boldsymbol{x}}, \tag{5.16}$$

$$u_R(\boldsymbol{x}) = -\left(\frac{Z_\infty + ik_3}{Z_\infty - ik_3}\right) e^{i\bar{\boldsymbol{k}}\cdot\boldsymbol{x}}. \tag{5.17}$$

It can be observed that the solution (5.15) vanishes when $k_3 = 0$, i.e., when the wave propagation is parallel to the half-space's boundary. The wave propagation vector $\boldsymbol{k}$, by considering a parametrization through the angles of incidence θ_I and φ_I for $0 \leq \theta_I \leq \pi/2$

and $-\pi < \varphi_I \leq \pi$, can be expressed as $\boldsymbol{k} = (-k\sin\theta_I\cos\varphi_I, -k\sin\theta_I\sin\varphi_I, -k\cos\theta_I)$. In this case the solution is described by

$$u_T(\boldsymbol{x}) = e^{-ik(x_1\sin\theta_I\cos\varphi_I + x_2\sin\theta_I\sin\varphi_I + x_3\cos\theta_I)} - \left(\frac{Z_\infty - ik\cos\theta_I}{Z_\infty + ik\cos\theta_I}\right) e^{-ik(x_1\sin\theta_I\cos\varphi_I + x_2\sin\theta_I\sin\varphi_I - x_3\cos\theta_I)}. \tag{5.18}$$

The second kind of solution, up to an arbitrary scaling factor, corresponds to a progressive plane surface wave, and is given by

$$u_T(\boldsymbol{x}) = u_I(\boldsymbol{x}) = e^{i\boldsymbol{k}_s\cdot\boldsymbol{x}_s}e^{-Z_\infty x_3}, \qquad (\boldsymbol{k}_s\cdot\boldsymbol{k}_s) = Z_\infty^2 + k^2, \qquad \boldsymbol{x}_s = (x_1, x_2). \tag{5.19}$$

It can be observed that plane surface waves correspond to plane volume waves with a complex wave propagation vector $\boldsymbol{k} = (\boldsymbol{k}_s, iZ_\infty)$, where $\boldsymbol{k}_s \in \mathbb{R}^2$. They are guided along the half-space's boundary, and decrease exponentially towards its interior, hence their name. In this case there exists no reflected field, since the waves travel along the boundary. We remark that the plane surface waves vanish completely for classical Dirichlet ($Z_\infty = \infty$) or Neumann ($Z_\infty = 0$) boundary conditions.

5.3 Green's function

5.3.1 Problem definition

The Green's function represents the response of the unperturbed system to a Dirac mass. It corresponds to a function G, which depends on the wave number k, on the impedance Z_∞, on a fixed source point $\boldsymbol{x} \in \mathbb{R}^3_+$, and on an observation point $\boldsymbol{y} \in \mathbb{R}^3_+$. The Green's function is computed in the sense of distributions for the variable $\boldsymbol{y}$ in the half-space $\mathbb{R}^3_+$ by placing at the right-hand side of the Helmholtz equation a Dirac mass $\delta_{\boldsymbol{x}}$, centered at the point $\boldsymbol{x}$. It is therefore a solution for the radiation problem of a point source, namely

$$\begin{cases} \text{Find } G(\boldsymbol{x},\cdot) : \mathbb{R}^3_+ \to \mathbb{C} \text{ such that} \\ \Delta_{\boldsymbol{y}} G(\boldsymbol{x},\boldsymbol{y}) + k^2 G(\boldsymbol{x},\boldsymbol{y}) = \delta_{\boldsymbol{x}}(\boldsymbol{y}) & \text{in } \mathcal{D}'(\mathbb{R}^3_+), \\ \dfrac{\partial G}{\partial y_3}(\boldsymbol{x},\boldsymbol{y}) + Z_\infty G(\boldsymbol{x},\boldsymbol{y}) = 0 & \text{on } \{y_3 = 0\}, \\ \text{+ Outgoing radiation condition as } |\boldsymbol{y}| \to \infty. \end{cases} \tag{5.20}$$

The outgoing radiation condition, in the same way as in (5.6), is given here as $|\boldsymbol{y}| \to \infty$ by

$$\begin{cases} |G| \leq \dfrac{C}{|\boldsymbol{y}|} \quad \text{and} \quad \left|\dfrac{\partial G}{\partial r_{\boldsymbol{y}}} - ikG\right| \leq \dfrac{C}{|\boldsymbol{y}|^2} & \text{if } y_3 > \dfrac{\ln\big(1+\beta|\boldsymbol{y}|\big)}{2Z_\infty}, \\ |G| \leq \dfrac{C}{\sqrt{|\boldsymbol{y}|}} \quad \text{and} \quad \left|\dfrac{\partial G}{\partial r_{\boldsymbol{y}}} - i\sqrt{Z_\infty^2 + k^2}G\right| \leq \dfrac{C}{|\boldsymbol{y}|} & \text{if } y_3 \leq \dfrac{\ln\big(1+\beta|\boldsymbol{y}|\big)}{2Z_\infty}, \end{cases} \tag{5.21}$$

for some constants $C > 0$, independent of $r = |\boldsymbol{y}|$, where and $\beta = 8\pi Z_\infty^2/\sqrt{Z_\infty^2 + k^2}$.

5.3.2 Special cases

When the Green's function problem (5.20) is solved using either homogeneous Dirichlet or Neumann boundary conditions, then its solution is found straightforwardly using the method of images (cf., e.g., Morse & Feshbach 1953).

a) Homogeneous Dirichlet boundary condition

We consider in the problem (5.20) the particular case of a homogeneous Dirichlet boundary condition, namely

$$G(\boldsymbol{x}, \boldsymbol{y}) = 0, \qquad \boldsymbol{y} \in \{y_3 = 0\}, \tag{5.22}$$

which corresponds to the limit case when the impedance is infinite ($Z_\infty = \infty$). In this case, the Green's function G can be explicitly calculated using the method of images, since it has to be antisymmetric with respect to the plane $\{y_3 = 0\}$. An additional image source point $\bar{\boldsymbol{x}} = (x_1, x_2, -x_3)$, located on the lower half-space and associated with a negative Dirac mass, is placed for this purpose just opposite to the upper half-space's source point $\boldsymbol{x} = (x_1, x_2, x_3)$. The desired solution is then obtained by evaluating the full-space Green's function (E.22) for each Dirac mass, which yields finally

$$G(\boldsymbol{x}, \boldsymbol{y}) = -\frac{e^{ik|\boldsymbol{y}-\boldsymbol{x}|}}{4\pi|\boldsymbol{y}-\boldsymbol{x}|} + \frac{e^{ik|\boldsymbol{y}-\bar{\boldsymbol{x}}|}}{4\pi|\boldsymbol{y}-\bar{\boldsymbol{x}}|} = -\frac{ik}{4\pi} h_0^{(1)}\big(k|\boldsymbol{y}-\boldsymbol{x}|\big) + \frac{ik}{4\pi} h_0^{(1)}\big(k|\boldsymbol{y}-\bar{\boldsymbol{x}}|\big). \tag{5.23}$$

b) Homogeneous Neumann boundary condition

We consider in the problem (5.20) the particular case of a homogeneous Neumann boundary condition, namely

$$\frac{\partial G}{\partial n_{\boldsymbol{y}}}(\boldsymbol{x}, \boldsymbol{y}) = 0, \qquad \boldsymbol{y} \in \{y_3 = 0\}, \tag{5.24}$$

which corresponds to the limit case when the impedance is zero ($Z_\infty = 0$). As in the previous case, the method of images is again employed, but now the half-space Green's function G has to be symmetric with respect to the plane $\{y_3 = 0\}$. Therefore, an additional image source point $\bar{\boldsymbol{x}} = (x_1, x_2, -x_3)$, located on the lower half-space, is placed just opposite to the upper half-space's source point $\boldsymbol{x} = (x_1, x_2, x_3)$, but now associated with a positive Dirac mass. The desired solution is then obtained by evaluating the full-space Green's function (E.22) for each Dirac mass, which yields

$$G(\boldsymbol{x}, \boldsymbol{y}) = -\frac{e^{ik|\boldsymbol{y}-\boldsymbol{x}|}}{4\pi|\boldsymbol{y}-\boldsymbol{x}|} - \frac{e^{ik|\boldsymbol{y}-\bar{\boldsymbol{x}}|}}{4\pi|\boldsymbol{y}-\bar{\boldsymbol{x}}|} = -\frac{ik}{4\pi} h_0^{(1)}\big(k|\boldsymbol{y}-\boldsymbol{x}|\big) - \frac{ik}{4\pi} h_0^{(1)}\big(k|\boldsymbol{y}-\bar{\boldsymbol{x}}|\big). \tag{5.25}$$

5.3.3 Spectral Green's function

a) Boundary-value problem

To solve (5.20) in the general case, we use a modified partial Fourier transform on the horizontal (y_1, y_2)-plane, taking advantage of the fact that there is no horizontal variation in the geometry of the problem. To obtain the corresponding spectral Green's function, we follow the same procedure as the one performed in Durán et al. (2005*b*). We define the

forward Fourier transform of a function $F\big(\boldsymbol{x},(\cdot,\cdot,y_3)\big):\mathbb{R}^2\to\mathbb{C}$ by

$$\widehat{F}(\boldsymbol{\xi};y_3,x_3)=\frac{1}{2\pi}\int_{\mathbb{R}^2}F(\boldsymbol{x},\boldsymbol{y})\,e^{-i\boldsymbol{\xi}\cdot(\boldsymbol{y}_s-\boldsymbol{x}_s)}\,\mathrm{d}\boldsymbol{y}_s,\qquad \boldsymbol{\xi}=(\xi_1,\xi_2)\in\mathbb{R}^2, \tag{5.26}$$

and its inverse by

$$F(\boldsymbol{x},\boldsymbol{y})=\frac{1}{2\pi}\int_{\mathbb{R}^2}\widehat{F}(\boldsymbol{\xi};y_3,x_3)\,e^{i\boldsymbol{\xi}\cdot(\boldsymbol{y}_s-\boldsymbol{x}_s)}\,\mathrm{d}\boldsymbol{\xi},\qquad \boldsymbol{y}_s=(y_1,y_2)\in\mathbb{R}^2, \tag{5.27}$$

where $\boldsymbol{x}_s=(x_1,x_2)\in\mathbb{R}^2$ and thus $\boldsymbol{x}=(\boldsymbol{x}_s,x_3)$.

To ensure a correct integration path for the Fourier transform and correct physical results, the calculations have to be performed in the framework of the limiting absorption principle, which allows to treat all the appearing integrals as Cauchy principal values. For this purpose, we take a small dissipation parameter $\varepsilon>0$ into account and consider the problem (5.20) as the limit case when $\varepsilon\to 0$ of the dissipative problem

$$\begin{cases} \text{Find } G_\varepsilon(\boldsymbol{x},\cdot):\mathbb{R}^3_+\to\mathbb{C} \text{ such that} & \\ \Delta_{\boldsymbol{y}}G_\varepsilon(\boldsymbol{x},\boldsymbol{y})+k_\varepsilon^2G_\varepsilon(\boldsymbol{x},\boldsymbol{y})=\delta_{\boldsymbol{x}}(\boldsymbol{y}) & \text{in } \mathcal{D}'(\mathbb{R}^3_+),\\ \dfrac{\partial G_\varepsilon}{\partial y_3}(\boldsymbol{x},\boldsymbol{y})+Z_\infty G_\varepsilon(\boldsymbol{x},\boldsymbol{y})=0 & \text{on } \{y_3=0\}, \end{cases} \tag{5.28}$$

where $k_\varepsilon=k+i\varepsilon$. This choice ensures a correct outgoing dissipative volume-wave behavior. In the same way as for the Laplace equation, the impedance Z_∞ could be also incorporated into this dissipative framework, i.e., by considering $Z_\varepsilon=Z_\infty+i\varepsilon$, but it is not really necessary since the use of a dissipative wave number k_ε is enough to take care of all the appearing issues. Further references for the application of this principle can be found in Bonnet-BenDhia & Tillequin (2001), Hazard & Lenoir (1998), and Nosich (1994).

Applying thus the Fourier transform (5.26) on the system (5.28) leads to a linear second order ordinary differential equation for the variable y_3, with prescribed boundary values, given by

$$\begin{cases} \dfrac{\partial^2\widehat{G}_\varepsilon}{\partial y_3^2}(\boldsymbol{\xi})-\big(|\boldsymbol{\xi}|^2-k_\varepsilon^2\big)\widehat{G}_\varepsilon(\boldsymbol{\xi})=\dfrac{\delta(y_3-x_3)}{2\pi}, & y_3>0,\\ \dfrac{\partial\widehat{G}_\varepsilon}{\partial y_3}(\boldsymbol{\xi})+Z_\infty\widehat{G}_\varepsilon(\boldsymbol{\xi})=0, & y_3=0. \end{cases} \tag{5.29}$$

To describe the (ξ_1,ξ_2)-plane, we use henceforth the system of signed polar coordinates

$$\xi=\begin{cases} \sqrt{\xi_1^2+\xi_2^2} & \text{if } \xi_2>0,\\ \xi_1 & \text{if } \xi_2=0,\\ -\sqrt{\xi_1^2+\xi_2^2} & \text{if } \xi_2<0, \end{cases}\qquad\text{and}\qquad \psi=\operatorname{arccot}\left(\frac{\xi_1}{\xi_2}\right), \tag{5.30}$$

where $-\infty<\xi<\infty$ and $0\le\psi<\pi$. From (5.29) it is not difficult to see that the solution $\widehat{G}_\varepsilon$ depends only on $|\boldsymbol{\xi}|$, and therefore only on ξ, since $|\xi|=|\boldsymbol{\xi}|$. We remark that the inverse Fourier transform (5.27) can be stated equivalently as

$$F(\boldsymbol{x},\boldsymbol{y})=\frac{1}{2\pi}\int_{-\infty}^{\infty}\int_0^{\pi}\widehat{F}(\xi,\psi;y_3,x_3)|\xi|\,e^{i\xi\{(y_1-x_1)\cos\psi+(y_2-x_2)\sin\psi\}}\,\mathrm{d}\psi\,\mathrm{d}\xi. \tag{5.31}$$

We use the method of undetermined coefficients, and solve the homogeneous differential equation of the problem (5.29) respectively in the zone $\{\boldsymbol{y} \in \mathbb{R}^3_+ \,:\, 0 < y_3 < x_3\}$ and in the half-space $\{\boldsymbol{y} \in \mathbb{R}^3_+ \,:\, y_3 > x_3\}$. This gives a solution for $\widehat{G}_\varepsilon$ in each domain, as a linear combination of two independent solutions of an ordinary differential equation, namely

$$\widehat{G}_\varepsilon(\xi) = \begin{cases} a\, e^{\sqrt{\xi^2-k_\varepsilon^2}\, y_3} + b\, e^{-\sqrt{\xi^2-k_\varepsilon^2}\, y_3} & \text{for } \ 0 < y_3 < x_3, \\ c\, e^{\sqrt{\xi^2-k_\varepsilon^2}\, y_3} + d\, e^{-\sqrt{\xi^2-k_\varepsilon^2}\, y_3} & \text{for } \ y_3 > x_3. \end{cases} \tag{5.32}$$

The unknowns a, b, c, and d, which depend on ξ and x_3, are determined through the boundary condition, by imposing continuity, and by assuming an outgoing wave behavior.

b) Complex square roots

Due the application of the limiting absorption principle, the square root that appears in the general solution (5.32) has to be understood as a complex map $\xi \mapsto \sqrt{\xi^2 - k_\varepsilon^2}$, which is decomposed as the product between $\sqrt{\xi - k_\varepsilon}$ and $\sqrt{\xi + k_\varepsilon}$, and has its two analytic branch cuts on the complex ξ plane defined in such a way that they do not intersect the real axis. Further details on complex branch cuts can be found in the books of Bak & Newman (1997) and Felsen & Marcuwitz (2003). The arguments are taken in such a way that $\arg(\xi - k_\varepsilon) \in (-\frac{3\pi}{2}, \frac{\pi}{2})$ for the map $\sqrt{\xi - k_\varepsilon}$, and $\arg(\xi + k_\varepsilon) \in (-\frac{\pi}{2}, \frac{3\pi}{2})$ for the map $\sqrt{\xi + k_\varepsilon}$. These maps can be therefore defined by (Durán et al. 2005*b*)

$$\sqrt{\xi - k_\varepsilon} = -i\sqrt{|k_\varepsilon|}\, e^{\frac{i}{2}\arg(k_\varepsilon)} \exp\left(\frac{1}{2}\int_0^\xi \frac{\mathrm{d}\eta}{\eta - k_\varepsilon}\right), \tag{5.33}$$

and

$$\sqrt{\xi + k_\varepsilon} = \sqrt{|k_\varepsilon|}\, e^{\frac{i}{2}\arg(k_\varepsilon)} \exp\left(\frac{1}{2}\int_0^\xi \frac{\mathrm{d}\eta}{\eta + k_\varepsilon}\right). \tag{5.34}$$

Consequently $\sqrt{\xi^2 - k_\varepsilon^2}$ is even and analytic in the domain shown in Figure 5.3. It can be hence defined by

$$\sqrt{\xi^2 - k_\varepsilon^2} = \sqrt{\xi - k_\varepsilon}\,\sqrt{\xi + k_\varepsilon} = -ik_\varepsilon \exp\left(\int_0^\xi \frac{\eta}{\eta^2 - k_\varepsilon^2}\,\mathrm{d}\eta\right), \tag{5.35}$$

and is characterized, for $\xi, k \in \mathbb{R}$, by

$$\sqrt{\xi^2 - k^2} = \begin{cases} \sqrt{\xi^2 - k^2}, & \xi^2 \geq k^2, \\ -i\sqrt{k^2 - \xi^2}, & \xi^2 < k^2. \end{cases} \tag{5.36}$$

We remark that if $\xi \in \mathbb{R}$, then $\arg(\xi - k_\varepsilon) \in (-\pi, 0)$ and $\arg(\xi + k_\varepsilon) \in (0, \pi)$. This proceeds from the fact that $\arg(k_\varepsilon) \in (0, \pi)$, since by the limiting absorption principle it holds that $\mathfrak{Im}\{k_\varepsilon\} = \varepsilon > 0$. Thus $\arg\left(\sqrt{\xi - k_\varepsilon}\right) \in (-\frac{\pi}{2}, 0)$, $\arg\left(\sqrt{\xi + k_\varepsilon}\right) \in (0, \frac{\pi}{2})$, and $\arg\left(\sqrt{\xi^2 - k_\varepsilon^2}\right) \in (-\frac{\pi}{2}, \frac{\pi}{2})$. Hence, the real part of the complex map $\sqrt{\xi^2 - k_\varepsilon^2}$ for real ξ is strictly positive, i.e., $\mathfrak{Re}\left\{\sqrt{\xi^2 - k_\varepsilon^2}\right\} > 0$. Therefore the function $e^{-\sqrt{\xi^2-k_\varepsilon^2}\, y_3}$ is even and exponentially decreasing as $y_3 \to \infty$.

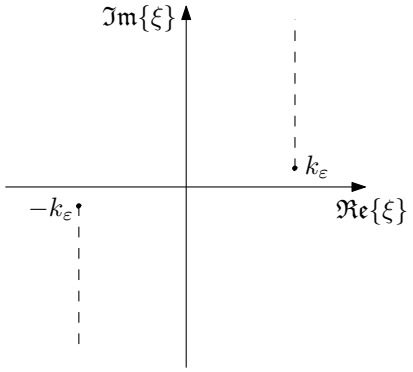

FIGURE 5.3. Analytic branch cuts of the complex map $\sqrt{\xi^2 - k_\varepsilon^2}$.

c) Spectral Green's function with dissipation

Now, thanks to (5.32), the computation of $\widehat{G}_\varepsilon$ is straightforward. From the boundary condition of (5.29) a relation for the coefficients a and b can be derived, which is given by

$$a\left(Z_\infty + \sqrt{\xi^2 - k_\varepsilon^2}\right) + b\left(Z_\infty - \sqrt{\xi^2 - k_\varepsilon^2}\right) = 0. \tag{5.37}$$

On the other hand, since the solution (5.32) has to be bounded at infinity as $y_3 \to \infty$, and since $\mathfrak{Re}\left\{\sqrt{\xi^2 - k_\varepsilon^2}\right\} > 0$, it follows then necessarily that

$$c = 0. \tag{5.38}$$

To ensure the continuity of the Green's function at the point $y_3 = x_3$, it is needed that

$$d = a\, e^{\sqrt{\xi^2 - k_\varepsilon^2}\, 2x_3} + b. \tag{5.39}$$

Using relations (5.37), (5.38), and (5.39) in (5.32), we obtain the expression

$$\widehat{G}_\varepsilon(\xi) = a\, e^{\sqrt{\xi^2 - k_\varepsilon^2}\, x_3}\left[e^{-\sqrt{\xi^2 - k_\varepsilon^2}\,|y_3 - x_3|} - \left(\frac{Z_\infty + \sqrt{\xi^2 - k_\varepsilon^2}}{Z_\infty - \sqrt{\xi^2 - k_\varepsilon^2}}\right) e^{-\sqrt{\xi^2 - k_\varepsilon^2}\,(y_3 + x_3)}\right]. \tag{5.40}$$

The remaining unknown coefficient a is determined by replacing (5.40) in the differential equation of (5.29), taking the derivatives in the sense of distributions, particularly

$$\frac{\partial}{\partial y_3}\left\{e^{-\sqrt{\xi^2 - k_\varepsilon^2}\,|y_3 - x_3|}\right\} = -\sqrt{\xi^2 - k_\varepsilon^2}\ \mathrm{sign}(y_3 - x_3)\, e^{-\sqrt{\xi^2 - k_\varepsilon^2}\,|y_3 - x_3|}, \tag{5.41}$$

and

$$\frac{\partial}{\partial y_3}\big\{\mathrm{sign}(y_3 - x_3)\big\} = 2\,\delta(y_3 - x_3). \tag{5.42}$$

So, the second derivative of (5.40) becomes

$$\begin{aligned}\frac{\partial^2 \widehat{G}_\varepsilon}{\partial y_3^2}(\xi) = a\, e^{\sqrt{\xi^2 - k_\varepsilon^2}\, x_3}\Bigg[&(\xi^2 - k_\varepsilon^2)\, e^{-\sqrt{\xi^2 - k_\varepsilon^2}\,|y_3 - x_3|} - 2\sqrt{\xi^2 - k_\varepsilon^2}\,\delta(y_3 - x_3) \\ &- \left(\frac{Z_\infty + \sqrt{\xi^2 - k_\varepsilon^2}}{Z_\infty - \sqrt{\xi^2 - k_\varepsilon^2}}\right)(\xi^2 - k_\varepsilon^2)\, e^{-\sqrt{\xi^2 - k_\varepsilon^2}\,(y_3 + x_3)}\Bigg].\end{aligned} \tag{5.43}$$

This way, from (5.40) and (5.43) in the first equation of (5.29), we obtain that

$$a = -\frac{e^{-\sqrt{\xi^2-k_\varepsilon^2}\,x_3}}{4\pi\sqrt{\xi^2-k_\varepsilon^2}}. \tag{5.44}$$

Finally, the spectral Green's function $\widehat{G}_\varepsilon$ with dissipation ε is given by

$$\widehat{G}_\varepsilon(\xi; y_3, x_3) = -\frac{e^{-\sqrt{\xi^2-k_\varepsilon^2}\,|y_3-x_3|}}{4\pi\sqrt{\xi^2-k_\varepsilon^2}} + \left(\frac{Z_\infty+\sqrt{\xi^2-k_\varepsilon^2}}{Z_\infty-\sqrt{\xi^2-k_\varepsilon^2}}\right)\frac{e^{-\sqrt{\xi^2-k_\varepsilon^2}\,(y_3+x_3)}}{4\pi\sqrt{\xi^2-k_\varepsilon^2}}. \tag{5.45}$$

d) Analysis of singularities

To obtain the spectral Green's function $\widehat{G}$ without dissipation, the limit $\varepsilon \to 0$ has to be taken in (5.45). This can be done directly wherever the limit is regular and continuous on ξ. Singular points, on the other hand, have to be analyzed carefully to fulfill correctly the limiting absorption principle. Thus we study first the singularities of the limit function before applying this principle, i.e., considering just $\varepsilon = 0$, in which case we have

$$\widehat{G}_0(\xi) = -\frac{e^{-\sqrt{\xi^2-k^2}\,|y_3-x_3|}}{4\pi\sqrt{\xi^2-k^2}} + \left(\frac{Z_\infty+\sqrt{\xi^2-k^2}}{Z_\infty-\sqrt{\xi^2-k^2}}\right)\frac{e^{-\sqrt{\xi^2-k^2}\,(y_3+x_3)}}{4\pi\sqrt{\xi^2-k^2}}. \tag{5.46}$$

Possible singularities for (5.46) may only appear when $|\xi| = k$ or when $|\xi| = \xi_p$, being $\xi_p = \sqrt{Z_\infty^2+k^2}$, i.e., when the denominator of the fractions is zero. Otherwise the function is regular and continuous.

For $\xi = k$ and $\xi = -k$ the function (5.46) is continuous. This can be seen by writing it, analogously as in Durán, Muga & Nédélec (2005*b*), in the form

$$\widehat{G}_0(\xi) = \frac{H\big(g(\xi)\big)}{g(\xi)}, \tag{5.47}$$

where

$$g(\xi) = \sqrt{\xi^2-k^2}, \tag{5.48}$$

and

$$H(\beta) = \frac{1}{4\pi}\left(-e^{-\beta\,|y_3-x_3|} + \frac{Z_\infty+\beta}{Z_\infty-\beta}\,e^{-\beta\,(y_3+x_3)}\right), \qquad \beta \in \mathbb{C}. \tag{5.49}$$

Since $H(\beta)$ is an analytic function in $\beta = 0$, since $H(0) = 0$, and since

$$\lim_{\xi\to\pm k}\widehat{G}_0(\xi) = \lim_{\xi\to\pm k}\frac{H\big(g(\xi)\big)-H(0)}{g(\xi)} = H'(0), \tag{5.50}$$

we can easily obtain that

$$\lim_{\xi\to\pm k}\widehat{G}_0(\xi) = \frac{1}{4\pi}\left(1+\frac{1}{Z_\infty}+|y_3-x_3|-(y_3+x_3)\right), \tag{5.51}$$

being thus $\widehat{G}_0$ bounded and continuous on $\xi = k$ and $\xi = -k$.

For $\xi = \xi_p$ and $\xi = -\xi_p$, where $\xi_p = \sqrt{Z_\infty^2 + k^2}$, the function (5.46) presents two simple poles, whose residues are characterized by

$$\lim_{\xi \to \pm\xi_p} (\xi \mp \xi_p)\, \widehat{G}_0(\xi) = \mp \frac{Z_\infty}{2\pi\xi_p}\, e^{-Z_\infty(y_3+x_3)}. \tag{5.52}$$

To analyze the effect of these singularities, we have to study the computation of the inverse Fourier transform of

$$\widehat{G}_P(\xi) = \frac{Z_\infty}{2\pi\xi_p}\, e^{-Z_\infty(y_3+x_3)} \left(\frac{1}{\xi + \xi_p} - \frac{1}{\xi - \xi_p} \right), \tag{5.53}$$

which has to be done in the frame of the limiting absorption principle to obtain the correct physical results, i.e., the inverse Fourier transform has to be understood in the sense of

$$G_P(\boldsymbol{x}, \boldsymbol{y}) = \lim_{\varepsilon \to 0} \left\{ \frac{Z_\infty e^{-Z_\infty(y_3+x_3)}}{4\pi^2\xi_p} \int_0^\pi \int_{-\infty}^\infty \left(\frac{1}{\xi + \xi_p} - \frac{1}{\xi - \xi_p} \right) |\xi|\, e^{i\xi r \sin\theta \cos(\psi - \varphi)}\, \mathrm{d}\xi\, \mathrm{d}\psi \right\}, \tag{5.54}$$

where now $\xi_p = \sqrt{Z_\infty^2 + k_\varepsilon^2}$, which is such that $\mathfrak{Im}\{\xi_p\} > 0$, and where the spatial variables inside the integrals are expressed through the spherical coordinates

$$\begin{cases} y_1 - x_1 = r \sin\theta \cos\varphi, \\ y_2 - x_2 = r \sin\theta \sin\varphi, \\ y_3 - x_3 = r \cos\theta, \end{cases} \quad \text{for} \quad \begin{cases} 0 \le r < \infty, \\ 0 \le \theta \le \pi, \\ -\pi < \varphi \le \pi. \end{cases} \tag{5.55}$$

To perform correctly the computation of (5.54), we apply the residue theorem of complex analysis (cf., e.g., Arfken & Weber 2005, Bak & Newman 1997, Dettman 1984) on the complex meromorphic mapping

$$F(\xi) = \left(\frac{1}{\xi + \xi_p} - \frac{1}{\xi - \xi_p} \right) |\xi|\, e^{i\xi\tau}, \tag{5.56}$$

which admits two simple poles at ξ_p and $-\xi_p$, where $\mathfrak{Im}\{\xi_p\} > 0$ and $\tau \in \mathbb{R}$. We already did this computation for the Laplace equation and obtained the expression (4.62), namely

$$\int_{-\infty}^\infty F(\xi)\, \mathrm{d}\xi = -i2\pi |\xi_p| e^{i\xi_p|\tau|}, \qquad \tau \in \mathbb{R}. \tag{5.57}$$

Using (5.57) for $\xi_p = \sqrt{Z_\infty^2 + k^2}$ and $\tau = r \sin\theta \cos(\psi - \varphi)$ yields then that the inverse Fourier transform of (5.53), when considering the limiting absorption principle, is given by

$$G_P^L(\boldsymbol{x}, \boldsymbol{y}) = -\frac{iZ_\infty}{2\pi}\, e^{-Z_\infty(y_3+x_3)} \int_0^\pi e^{i\xi_p r \sin\theta\, |\cos(\psi - \varphi)|}\, \mathrm{d}\psi. \tag{5.58}$$

It can be observed that the integral in (5.58) is independent of the angle φ, which we can choose without problems as $\varphi = \pi/2$ and therefore $|\cos(\psi - \varphi)| = \sin\psi$. Since

$$r \sin\theta = |\boldsymbol{y}_s - \boldsymbol{x}_s|, \tag{5.59}$$

we can express (5.58) as

$$G_P^L(\boldsymbol{x}, \boldsymbol{y}) = -\frac{iZ_\infty}{2\pi}\, e^{-Z_\infty(y_3+x_3)} \int_0^\pi e^{i\xi_p |\boldsymbol{y}_s - \boldsymbol{x}_s| \sin\psi}\, \mathrm{d}\psi. \tag{5.60}$$

We observe that this expression describes the asymptotic behavior of the surface waves, which are linked to the presence of the poles in the spectral Green's function. Due (A.112) and (A.244), we can rewrite (5.60) more explicitly as

$$G_P^L(\boldsymbol{x},\boldsymbol{y}) = -\frac{iZ_\infty}{2}\, e^{-Z_\infty(y_3+x_3)}\Big[J_0\big(\xi_p|\boldsymbol{y}_s-\boldsymbol{x}_s|\big) + i\boldsymbol{H}_0\big(\xi_p|\boldsymbol{y}_s-\boldsymbol{x}_s|\big)\Big], \tag{5.61}$$

where J_0 denotes the Bessel function of order zero (vid. Subsection A.2.4) and $\boldsymbol{H}_0$ the Struve function of order zero (vid. Subsection A.2.7).

If the limiting absorption principle is not considered, i.e., if $\mathfrak{Im}\{\xi_p\} = 0$, then the inverse Fourier transform of (5.53) could be again computed in the sense of the principal value with the residue theorem. In this case we would obtain, instead of (5.57) and just as the expression (4.67) for the Laplace equation, the quantity

$$\int_{-\infty}^{\infty} F(\xi)\,\mathrm{d}\xi = 2\pi|\xi_p|\sin\big(\xi_p|\tau|\big), \qquad \tau\in\mathbb{R}. \tag{5.62}$$

The inverse Fourier transform of (5.53) would be in this case

$$G_P^{NL}(\boldsymbol{x},\boldsymbol{y}) = \frac{Z_\infty}{2}\, e^{-Z_\infty(y_3+x_3)}\boldsymbol{H}_0\big(\xi_p|\boldsymbol{y}_s-\boldsymbol{x}_s|\big), \tag{5.63}$$

which is correct from the mathematical point of view, but yields only a standing surface wave, and not a desired outgoing progressive surface wave as in (5.61).

The effect of the limiting absorption principle, in the spatial dimension, is then given by the difference between (5.61) and (5.63), i.e., by

$$G_L(\boldsymbol{x},\boldsymbol{y}) = G_P^L(\boldsymbol{x},\boldsymbol{y}) - G_P^{NL}(\boldsymbol{x},\boldsymbol{y}) = -\frac{iZ_\infty}{2}\, e^{-Z_\infty(y_3+x_3)}J_0\big(\xi_p|\boldsymbol{y}_s-\boldsymbol{x}_s|\big), \tag{5.64}$$

whose Fourier transform, and therefore the spectral effect, is given by

$$\widehat{G}_L(\xi) = \widehat{G}_P^L(\xi) - \widehat{G}_P^{NL}(\xi) = -\frac{iZ_\infty}{2|\xi|}\, e^{-Z_\infty(y_3+x_3)}\big[\delta(\xi-\xi_p)+\delta(\xi+\xi_p)\big]. \tag{5.65}$$

e) Spectral Green's function without dissipation

The spectral Green's function $\widehat{G}$ without dissipation is therefore obtained by taking the limit $\varepsilon\to 0$ in (5.45) and considering the effect of the limiting absorption principle for the appearing singularities, summarized in (5.65). Thus we obtain in the sense of distributions

$$\begin{aligned}\widehat{G}(\xi;y_3,x_3) = &-\frac{e^{-\sqrt{\xi^2-k^2}\,|y_3-x_3|}}{4\pi\sqrt{\xi^2-k^2}} + \left(\frac{Z_\infty+\sqrt{\xi^2-k^2}}{Z_\infty-\sqrt{\xi^2-k^2}}\right)\frac{e^{-\sqrt{\xi^2-k^2}\,(y_3+x_3)}}{4\pi\sqrt{\xi^2-k^2}}\\ &-\frac{iZ_\infty}{2|\xi|}\, e^{-Z_\infty(y_3+x_3)}\big[\delta(\xi-\xi_p)+\delta(\xi+\xi_p)\big].\end{aligned} \tag{5.66}$$

For our further analysis, this spectral Green's function is decomposed into four terms according to

$$\widehat{G} = \widehat{G}_\infty + \widehat{G}_N + \widehat{G}_L + \widehat{G}_R, \tag{5.67}$$

where

$$\widehat{G}_\infty(\xi; y_3, x_3) = -\frac{e^{-\sqrt{\xi^2-k^2}\,|y_3-x_3|}}{4\pi\sqrt{\xi^2-k^2}}, \tag{5.68}$$

$$\widehat{G}_N(\xi; y_3, x_3) = -\frac{e^{-\sqrt{\xi^2-k^2}\,(y_3+x_3)}}{4\pi\sqrt{\xi^2-k^2}}, \tag{5.69}$$

$$\widehat{G}_L(\xi; y_3, x_3) = -\frac{iZ_\infty}{2|\xi|}\, e^{-Z_\infty(y_3+x_3)}\big[\delta(\xi-\xi_p)+\delta(\xi+\xi_p)\big], \tag{5.70}$$

$$\widehat{G}_R(\xi; y_3, x_3) = \frac{Z_\infty e^{-\sqrt{\xi^2-k^2}\,(y_3+x_3)}}{2\pi\sqrt{\xi^2-k^2}\left(Z_\infty-\sqrt{\xi^2-k^2}\right)}. \tag{5.71}$$

5.3.4 Spatial Green's function

a) Spatial Green's function as an inverse Fourier transform

The desired spatial Green's function is then given by the inverse Fourier transform of the spectral Green's function (5.66), namely by

$$\begin{aligned} G(\boldsymbol{x},\boldsymbol{y}) = &-\frac{1}{8\pi^2}\int_{-\infty}^{\infty}\int_0^{\pi}\frac{e^{-\sqrt{\xi^2-k^2}\,|y_3-x_3|}}{\sqrt{\xi^2-k^2}}|\xi|e^{i\xi r\sin\theta\cos(\psi-\varphi)}\,\mathrm{d}\psi\,\mathrm{d}\xi \\ &+\frac{1}{8\pi^2}\int_{-\infty}^{\infty}\int_0^{\pi}\left(\frac{Z_\infty+\sqrt{\xi^2-k^2}}{Z_\infty-\sqrt{\xi^2-k^2}}\right)\frac{e^{-\sqrt{\xi^2-k^2}\,(y_3+x_3)}}{\sqrt{\xi^2-k^2}}|\xi|e^{i\xi r\sin\theta\cos(\psi-\varphi)}\,\mathrm{d}\psi\,\mathrm{d}\xi \\ &-\frac{iZ_\infty}{2}\,e^{-Z_\infty(y_3+x_3)}J_0\big(\xi_p|\boldsymbol{y}_s-\boldsymbol{x}_s|\big), \end{aligned} \tag{5.72}$$

where the spherical coordinates (5.55) are used again inside the integrals.

Due the linearity of the Fourier transform, the decomposition (5.67) applies also in the spatial domain, i.e., the spatial Green's function is decomposed in the same manner by

$$G = G_\infty + G_N + G_L + G_R. \tag{5.73}$$

b) Term of the full-space Green's function

The first term in (5.72) corresponds to the inverse Fourier transform of (5.68), and can be rewritten, due (A.794), as the Hankel transform

$$G_\infty(\boldsymbol{x},\boldsymbol{y}) = -\frac{1}{4\pi}\int_0^{\infty}\frac{e^{-\sqrt{\rho^2-k^2}\,|y_3-x_3|}}{\sqrt{\rho^2-k^2}}J_0\big(\rho|\boldsymbol{y}_s-\boldsymbol{x}_s|\big)\,\rho\,\mathrm{d}\rho. \tag{5.74}$$

The value for this integral can be obtained by using Sommerfeld's formula (Magnus & Oberhettinger 1954, page 34)

$$\int_0^{\infty}\frac{e^{-\sqrt{\rho^2-k^2}\,|y_3-x_3|}}{\sqrt{\rho^2-k^2}}J_0\big(\rho|\boldsymbol{y}_s-\boldsymbol{x}_s|\big)\,\rho\,\mathrm{d}\rho = \frac{e^{ik|\boldsymbol{y}-\boldsymbol{x}|}}{|\boldsymbol{y}-\boldsymbol{x}|}. \tag{5.75}$$

This way, the inverse Fourier transform of (5.68) is readily given by

$$G_\infty(\boldsymbol{x},\boldsymbol{y}) = -\frac{e^{ik|\boldsymbol{y}-\boldsymbol{x}|}}{4\pi|\boldsymbol{y}-\boldsymbol{x}|} = -\frac{ik}{4\pi}h_0^{(1)}\big(k|\boldsymbol{y}-\boldsymbol{x}|\big), \tag{5.76}$$

where $h_0^{(1)}$ denotes the spherical Hankel function of order zero of the first kind (vid. Subsection A.2.6). We observe that (5.76) is, in fact, the full-space Green's function of the Helmholtz equation. Thus $G_N + G_L + G_R$ represents the perturbation of the full-space Green's function G_∞ due the presence of the impedance half-space.

c) Term associated with a Neumann boundary condition

The inverse Fourier transform of (5.69) is computed in the same manner as the term G_∞. It is given by

$$G_N(\boldsymbol{x},\boldsymbol{y}) = -\frac{1}{4\pi}\int_0^\infty \frac{e^{-\sqrt{\rho^2-k^2}\,(y_3+x_3)}}{\sqrt{\rho^2-k^2}} J_0\big(\rho|\boldsymbol{y}_s-\boldsymbol{x}_s|\big)\,\rho\,\mathrm{d}\rho, \tag{5.77}$$

and in this case, instead of (5.75), Sommerfeld's formula becomes

$$\int_0^\infty \frac{e^{-\sqrt{\rho^2-k^2}\,(y_3+x_3)}}{\sqrt{\rho^2-k^2}} J_0\big(\rho|\boldsymbol{y}_s-\boldsymbol{x}_s|\big)\,\rho\,\mathrm{d}\rho = \frac{e^{ik|\boldsymbol{y}-\bar{\boldsymbol{x}}|}}{|\boldsymbol{y}-\bar{\boldsymbol{x}}|}, \tag{5.78}$$

where $\bar{\boldsymbol{x}} = (x_1, x_2, -x_3)$ corresponds to the image point of $\boldsymbol{x}$ in the lower half-space. The inverse Fourier transform of (5.69) is therefore given by

$$G_N(\boldsymbol{x},\boldsymbol{y}) = -\frac{e^{ik|\boldsymbol{y}-\bar{\boldsymbol{x}}|}}{4\pi|\boldsymbol{y}-\bar{\boldsymbol{x}}|} = -\frac{ik}{4\pi}h_0^{(1)}\big(k|\boldsymbol{y}-\bar{\boldsymbol{x}}|\big), \tag{5.79}$$

which represents the additional term that appears in the Green's function due the method of images when considering a Neumann boundary condition, as in (5.25).

d) Term associated with the limiting absorption principle

The term G_L, the inverse Fourier transform of (5.70), is associated with the effect of the limiting absorption principle on the Green's function, and has been already calculated in (5.64). It is given by

$$G_L(\boldsymbol{x},\boldsymbol{y}) = -\frac{iZ_\infty}{2}\, e^{-Z_\infty(y_3+x_3)} J_0\big(\xi_p|\boldsymbol{y}_s-\boldsymbol{x}_s|\big). \tag{5.80}$$

e) Remaining term

The remaining term G_R, the inverse Fourier transform of (5.71), can be computed as the integral

$$G_R(\boldsymbol{x},\boldsymbol{y}) = \frac{Z_\infty}{2\pi}\int_0^\infty \frac{e^{-\sqrt{\rho^2-k^2}\,(y_3+x_3)}}{\sqrt{\rho^2-k^2}\left(Z_\infty-\sqrt{\rho^2-k^2}\right)} J_0\big(\rho|\boldsymbol{y}_s-\boldsymbol{x}_s|\big)\,\rho\,\mathrm{d}\rho. \tag{5.81}$$

To simplify the notation, we define

$$\varrho_s = |\boldsymbol{y}_s-\boldsymbol{x}_s| \qquad \text{and} \qquad v_3 = y_3+x_3, \tag{5.82}$$

and we consider

$$G_R(\boldsymbol{x},\boldsymbol{y}) = \frac{Z_\infty}{2\pi}\, e^{-Z_\infty v_3} G_B(\varrho_s, v_3), \tag{5.83}$$

where

$$G_B(\varrho_s, v_3) = e^{Z_\infty v_3} \int_0^\infty \frac{e^{-\sqrt{\rho^2-k^2}\,v_3}}{\sqrt{\rho^2-k^2}\left(Z_\infty - \sqrt{\rho^2-k^2}\right)} J_0(\rho\varrho_s)\,\rho\,\mathrm{d}\rho. \tag{5.84}$$

Consequently, by considering (5.78) we have for the y_3-derivative of G_B that

$$\begin{aligned}\frac{\partial G_B}{\partial y_3}(\varrho_s, v_3) &= e^{Z_\infty v_3} \int_0^\infty \frac{e^{-\sqrt{\rho^2-k^2}\,v_3}}{\sqrt{\rho^2-k^2}} J_0(\rho\varrho_s)\,\rho\,\mathrm{d}\rho \\ &= \frac{e^{ik|\boldsymbol{y}-\bar{\boldsymbol{x}}|}}{|\boldsymbol{y}-\bar{\boldsymbol{x}}|}\, e^{Z_\infty v_3}.\end{aligned} \tag{5.85}$$

The value of the inverse Fourier transform (5.81) can be thus obtained by means of the primitive with respect to y_3 of (5.85), i.e.,

$$G_R(\boldsymbol{x},\boldsymbol{y}) = \frac{Z_\infty}{2\pi}\, e^{-Z_\infty v_3} \int_{-\infty}^{v_3} \frac{e^{ik\sqrt{\varrho_s^2+\eta^2}}}{\sqrt{\varrho_s^2+\eta^2}}\, e^{Z_\infty \eta}\,\mathrm{d}\eta. \tag{5.86}$$

Formulae of this kind, but without the term linked to the limiting absorption principle, were developed in Ochmann (2004) and Ochmann & Brick (2008) by using the complex equivalent source method, a more generalized image method. The expression (5.86) contains an integral with an unbounded lower limit, but even so, due the exponential decrease of its integrand, it can be adapted to be well suited for numerical evaluation. Its advantage lies in the fact that it expresses intuitively the term G_R as a primitive of known functions. We observe that further related expressions can be obtained through integration by parts.

To compute (5.86) numerically, we can represent it in an equivalent manner as

$$G_R(\boldsymbol{x},\boldsymbol{y}) = \frac{Z_\infty}{2\pi}\, e^{-Z_\infty v_3} \left(G_B(\varrho_s, w_3) + \int_{w_3}^{v_3} \frac{e^{ik\sqrt{\varrho_s^2+\eta^2}}}{\sqrt{\varrho_s^2+\eta^2}}\, e^{Z_\infty \eta}\,\mathrm{d}\eta \right), \tag{5.87}$$

for some $w_3 \in \mathbb{R}$. If the term $G_B(\varrho_s, w_3)$ can be estimated satisfactorily in some way, then the remaining integral in (5.87) can be evaluated without difficulty by means of numerical quadrature formulae, since its integration limits are finite. One way to achieve this is to consider the asymptotic behavior of $G_B(\varrho_s, w_3)$ as $w_3 \to -\infty$, which is given by

$$G_B(\varrho_s, w_3) \sim \pi Y_0(\xi_p \varrho_s). \tag{5.88}$$

The behavior (5.88) stems from the asymptotic behavior (5.127) of the Green's function, and particularly from (5.121), which is discussed later in Section 5.4. The term G_R can be thus computed numerically as

$$G_R(\boldsymbol{x},\boldsymbol{y}) \approx \frac{Z_\infty}{2\pi}\, e^{-Z_\infty v_3} \left(\pi Y_0(\xi_p \varrho_s) + \int_{w_3}^{v_3} \frac{e^{ik\sqrt{\varrho_s^2+\eta^2}}}{\sqrt{\varrho_s^2+\eta^2}}\, e^{Z_\infty \eta}\,\mathrm{d}\eta \right), \tag{5.89}$$

which works quite well even for not so negative values of $w_3 < 0$. The expression (5.89), though, becomes unstable around $\varrho_s = 0$ and has to be modified accordingly near these

value. To deal with this issue, we consider the remaining term of the half-space Green's function for the Laplace equation, expressed in (4.99) and represented explicitly in (4.112). Due its asymptotic behavior (4.147), and particularly (4.141), we can characterize it as

$$G_{RL}(\boldsymbol{x},\boldsymbol{y}) \approx \frac{Z_\infty}{2\pi}\, e^{-Z_\infty v_3} \left(\pi Y_0(Z_\infty \varrho_s) + \int_{w_3}^{v_3} \frac{e^{Z_\infty \eta}}{\sqrt{\varrho_s^2+\eta^2}}\, \mathrm{d}\eta \right). \tag{5.90}$$

Therefore, when ϱ_s is close to zero and instead of (5.89), we consider rather the expression

$$\begin{aligned} G_R(\boldsymbol{x},\boldsymbol{y}) \approx \frac{Z_\infty}{2\pi}\, e^{-Z_\infty v_3} \left(\pi Y_0(\xi_p \varrho_s) - \pi Y_0(Z_\infty \varrho_s) + \int_{w_3}^{v_3} \frac{e^{ik\sqrt{\varrho_s^2+\eta^2}} - 1}{\sqrt{\varrho_s^2+\eta^2}}\, e^{Z_\infty \eta}\, \mathrm{d}\eta \right) \\ + G_{RL}(\boldsymbol{x},\boldsymbol{y}), \end{aligned} \tag{5.91}$$

where the term G_{RL} is computed as explained in Section 4.3, i.e., as (4.112). We remark that the expressions (5.89) and (5.91) require an exponential decrease of the integrand to work well, i.e., that $\mathfrak{Re}\{Z_\infty\} > 0$.

f) Complete spatial Green's function

The desired complete spatial Green's function is finally obtained, as stated in (5.73), by adding the terms (5.76), (5.79), (5.80), and (5.86). It is depicted graphically in Figures 5.4 & 5.5 for $k = 1.2$, $Z_\infty = 1$, and $\boldsymbol{x} = (0, 0, 2)$, and it is given explicitly by

$$\begin{aligned} G(\boldsymbol{x},\boldsymbol{y}) = &- \frac{e^{ik|\boldsymbol{y}-\boldsymbol{x}|}}{4\pi|\boldsymbol{y}-\boldsymbol{x}|} - \frac{e^{ik|\boldsymbol{y}-\bar{\boldsymbol{x}}|}}{4\pi|\boldsymbol{y}-\bar{\boldsymbol{x}}|} - \frac{iZ_\infty}{2}\, e^{-Z_\infty v_3} J_0(\xi_p \varrho_s) \\ &+ \frac{Z_\infty}{2\pi}\, e^{-Z_\infty v_3} \int_{-\infty}^{v_3} \frac{e^{ik\sqrt{\varrho_s^2+\eta^2}}}{\sqrt{\varrho_s^2+\eta^2}}\, e^{Z_\infty \eta}\, \mathrm{d}\eta, \end{aligned} \tag{5.92}$$

where the notation (5.82) is used. The integral in (5.92) is computed numerically as (5.91), when ϱ_s is close to zero, and as (5.89) elsewhere.

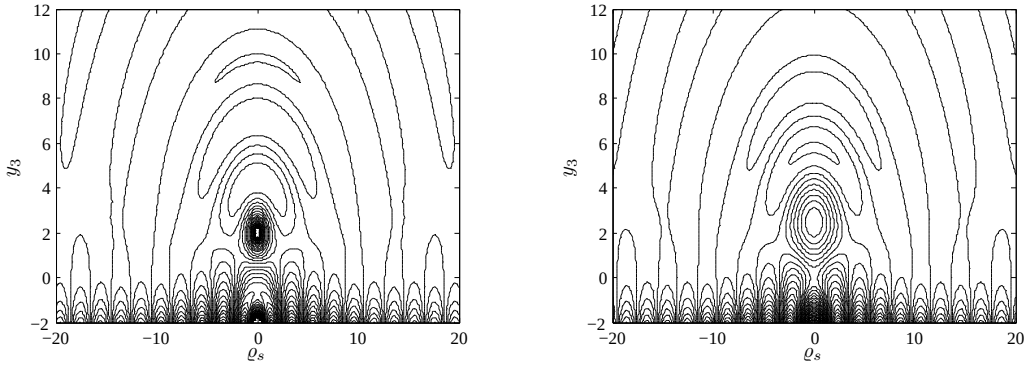

(a) Real part (b) Imaginary part

FIGURE 5.4. Contour plot of the complete spatial Green's function.

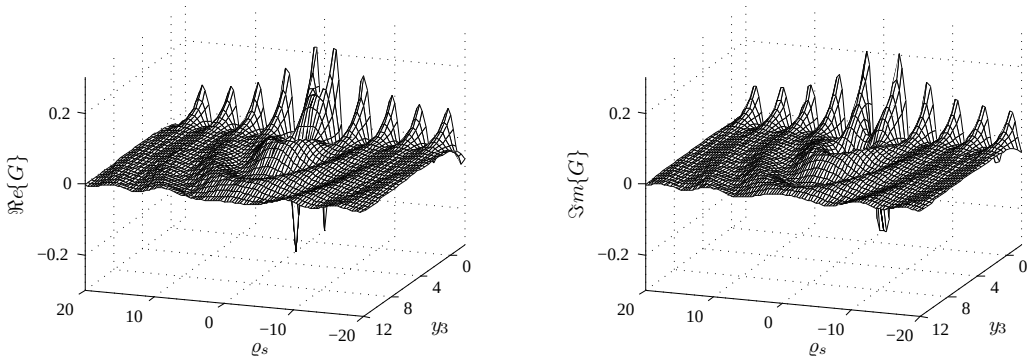

(a) Real part (b) Imaginary part

FIGURE 5.5. Oblique view of the complete spatial Green's function.

For the derivative of the Green's function with respect to the y_3-variable, it holds that

$$\frac{\partial G}{\partial y_3}(\boldsymbol{x},\boldsymbol{y}) = \frac{v_3\, e^{ik|\boldsymbol{y}-\boldsymbol{x}|}}{4\pi|\boldsymbol{y}-\boldsymbol{x}|^3}\big(1-ik|\boldsymbol{y}-\boldsymbol{x}|\big) + \frac{v_3\, e^{ik|\boldsymbol{y}-\bar{\boldsymbol{x}}|}}{4\pi|\boldsymbol{y}-\bar{\boldsymbol{x}}|^3}\big(1-ik|\boldsymbol{y}-\bar{\boldsymbol{x}}|\big) + \frac{iZ_\infty^2}{2}\, e^{-Z_\infty v_3} J_0(\xi_p\varrho_s) - Z_\infty G_R(\boldsymbol{x},\boldsymbol{y}) + \frac{Z_\infty e^{ik|\boldsymbol{y}-\bar{\boldsymbol{x}}|}}{2\pi|\boldsymbol{y}-\bar{\boldsymbol{x}}|}, \tag{5.93}$$

where G_R is given in (5.86) and computed according to (5.89) or (5.91). The derivatives for the variables y_1 and y_2 can be calculated by means of

$$\frac{\partial G}{\partial y_1} = \frac{\partial G}{\partial \varrho_s}\frac{\partial \varrho_s}{\partial y_1} = \frac{\partial G}{\partial \varrho_s}\frac{v_1}{\varrho_s} \qquad \text{and} \qquad \frac{\partial G}{\partial y_2} = \frac{\partial G}{\partial \varrho_s}\frac{\partial \varrho_s}{\partial y_2} = \frac{\partial G}{\partial \varrho_s}\frac{v_2}{\varrho_s}, \tag{5.94}$$

where

$$\frac{\partial G}{\partial \varrho_s}(\boldsymbol{x},\boldsymbol{y}) = \frac{\varrho_s\, e^{ik|\boldsymbol{y}-\boldsymbol{x}|}}{4\pi|\boldsymbol{y}-\boldsymbol{x}|^3}\big(1-ik|\boldsymbol{y}-\boldsymbol{x}|\big) + \frac{\varrho_s\, e^{ik|\boldsymbol{y}-\bar{\boldsymbol{x}}|}}{4\pi|\boldsymbol{y}-\bar{\boldsymbol{x}}|^3}\big(1-ik|\boldsymbol{y}-\bar{\boldsymbol{x}}|\big) + \frac{iZ_\infty\xi_p}{2}\, e^{-Z_\infty v_3} J_1(\xi_p\varrho_s) + \frac{Z_\infty}{2\pi}\, e^{-Z_\infty v_3}\int_{-\infty}^{v_3} \frac{\varrho_s\, e^{ik\sqrt{\varrho_s^2+\eta^2}}}{(\varrho_s^2+\eta^2)^{3/2}}\Big(ik\sqrt{\varrho_s^2+\eta^2}-1\Big)\, e^{Z_\infty\eta}\,\mathrm{d}\eta. \tag{5.95}$$

The integral in (5.95) is computed numerically in the same way as the term G_R, namely in the sense of (5.91), when ϱ_s is close to zero, and in the sense of (5.89) elsewhere.

5.3.5 Extension and properties

The half-space Green's function can be extended in a locally analytic way towards the full-space $\mathbb{R}^3$ in a straightforward and natural manner, just by considering the expression (5.92) valid for all $\boldsymbol{x},\boldsymbol{y} \in \mathbb{R}^3$, instead of just for $\mathbb{R}^3_+$. As shown in Figure 5.6, this extension possesses two pole-type singularities at the points $\boldsymbol{x}$ and $\bar{\boldsymbol{x}}$, a logarithmic singularity-distribution along the half-line $\Upsilon = \{y_1 = x_1,\, y_2 = x_2,\, y_3 < -x_3\}$, and is continuous otherwise. The behavior of the pole-type singularities is characterized by

$$G(\boldsymbol{x},\boldsymbol{y}) \sim -\frac{1}{4\pi|\boldsymbol{y}-\boldsymbol{x}|}, \qquad \boldsymbol{y} \longrightarrow \boldsymbol{x}, \tag{5.96}$$

$$G(\boldsymbol{x},\boldsymbol{y}) \sim -\frac{1}{4\pi|\boldsymbol{y}-\bar{\boldsymbol{x}}|}, \qquad \boldsymbol{y} \longrightarrow \bar{\boldsymbol{x}}. \tag{5.97}$$

The logarithmic singularity-distribution stems from the fact that when $v_3 < 0$, then

$$G(\boldsymbol{x},\boldsymbol{y}) \sim -\frac{iZ_\infty}{2}\, e^{-Z_\infty v_3} H_0^{(1)}(\xi_p \varrho_s), \tag{5.98}$$

being $H_0^{(1)}$ the zeroth order Hankel function of the first kind, whose singularity is of logarithmic type. We observe that (5.98) is related to the two-dimensional free-space Green's function of the Helmholtz equation (C.22), multiplied by the exponential weight

$$J(\boldsymbol{x},\boldsymbol{y}) = 2Z_\infty e^{-Z_\infty v_3}. \tag{5.99}$$

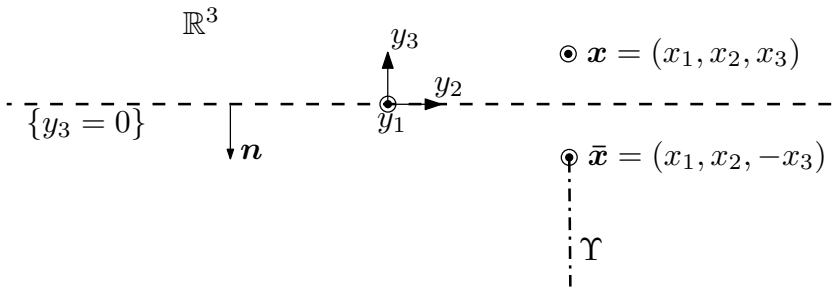

FIGURE 5.6. Domain of the extended Green's function.

As long as $x_3 \neq 0$, it is clear that the impedance boundary condition in (5.20) continues to be homogeneous. Nonetheless, if the source point $\boldsymbol{x}$ lies on the half-space's boundary, i.e., if $x_3 = 0$, then the boundary condition ceases to be homogeneous in the sense of distributions. This can be deduced from the expression (5.72) by verifying that

$$\lim_{y_3 \to 0^+} \left\{ \frac{\partial G}{\partial y_3}\big((\boldsymbol{x}_s, 0), \boldsymbol{y}\big) + Z_\infty G\big((\boldsymbol{x}_s, 0), \boldsymbol{y}\big) \right\} = \delta_{\boldsymbol{x}_s}(\boldsymbol{y}_s), \tag{5.100}$$

where $\boldsymbol{x}_s = (x_1, x_2)$ and $\boldsymbol{y}_s = (y_1, y_2)$. Since the impedance boundary condition holds only on $\{y_3 = 0\}$, therefore the right-hand side of (5.100) can be also expressed by

$$\delta_{\boldsymbol{x}_s}(\boldsymbol{y}_s) = \frac{1}{2}\delta_{\boldsymbol{x}}(\boldsymbol{y}) + \frac{1}{2}\delta_{\bar{\boldsymbol{x}}}(\boldsymbol{y}), \tag{5.101}$$

which illustrates more clearly the contribution of each pole-type singularity to the Dirac mass in the boundary condition.

It can be seen now that the Green's function extended in the abovementioned way satisfies, for $\boldsymbol{x} \in \mathbb{R}^3$, in the sense of distributions, and instead of (5.20), the problem

$$\left\{\begin{array}{l} \text{Find } G(\boldsymbol{x},\cdot) : \mathbb{R}^3 \to \mathbb{C} \text{ such that} \\ \Delta_{\boldsymbol{y}} G(\boldsymbol{x},\boldsymbol{y}) + k^2 G(\boldsymbol{x},\boldsymbol{y}) = \delta_{\boldsymbol{x}}(\boldsymbol{y}) + \delta_{\bar{\boldsymbol{x}}}(\boldsymbol{y}) + J(\boldsymbol{x},\boldsymbol{y})\delta_\Upsilon(\boldsymbol{y}) \quad \text{in } \mathcal{D}'(\mathbb{R}^3), \\ \dfrac{\partial G}{\partial y_3}(\boldsymbol{x},\boldsymbol{y}) + Z_\infty G(\boldsymbol{x},\boldsymbol{y}) = \dfrac{1}{2}\delta_{\boldsymbol{x}}(\boldsymbol{y}) + \dfrac{1}{2}\delta_{\bar{\boldsymbol{x}}}(\boldsymbol{y}) \quad \text{on } \{y_3 = 0\}, \\ \text{+ Outgoing radiation condition for } \boldsymbol{y} \in \mathbb{R}^3_+ \text{ as } |\boldsymbol{y}| \to \infty, \end{array}\right. \tag{5.102}$$

where δ_Υ denotes a Dirac mass distribution along the Υ-curve. We retrieve thus the known result that for an impedance boundary condition the image of a point source is a point source plus a half-line of sources with exponentially increasing strengths in the lower half-plane, and which extends from the image point source towards infinity along the half-space's normal direction (cf. Keller 1979, who refers to decreasing strengths when dealing with the opposite half-space).

We note that the half-space Green's function (5.92) is symmetric in the sense that

$$G(\boldsymbol{x},\boldsymbol{y}) = G(\boldsymbol{y},\boldsymbol{x}) \qquad \forall \boldsymbol{x},\boldsymbol{y} \in \mathbb{R}^3, \tag{5.103}$$

and it fulfills similarly

$$\nabla_{\boldsymbol{y}} G(\boldsymbol{x},\boldsymbol{y}) = \nabla_{\boldsymbol{y}} G(\boldsymbol{y},\boldsymbol{x}) \qquad \text{and} \qquad \nabla_{\boldsymbol{x}} G(\boldsymbol{x},\boldsymbol{y}) = \nabla_{\boldsymbol{x}} G(\boldsymbol{y},\boldsymbol{x}). \tag{5.104}$$

Another property is that we retrieve the special case (5.23) of a homogenous Dirichlet boundary condition in $\mathbb{R}^3_+$ when $Z_\infty \to \infty$. Likewise, we retrieve the special case (5.25) of a homogenous Neumann boundary condition in $\mathbb{R}^3_+$ when $Z_\infty \to 0$. A particularly interesting case occurs when $Z_\infty = ik$, in which case $\xi_p = 0$ and the primitive term of (5.92) can be characterized explicitly, namely

$$\begin{aligned} G(\boldsymbol{x},\boldsymbol{y}) = &- \frac{e^{ik|\boldsymbol{y}-\boldsymbol{x}|}}{4\pi|\boldsymbol{y}-\boldsymbol{x}|} - \frac{e^{ik|\boldsymbol{y}-\bar{\boldsymbol{x}}|}}{4\pi|\boldsymbol{y}-\bar{\boldsymbol{x}}|} + \frac{k}{2}\, e^{-ikv_3} \\ &+ \frac{ik}{2\pi}\, e^{-ikv_3}\, \mathrm{Ei}\Big(ikv_3 + ik\sqrt{\varrho_s^2 + v_3^2}\Big), \end{aligned} \tag{5.105}$$

where Ei denotes the exponential integral function (vid. Subsection A.2.3). Analogously, when $k = iZ_\infty$, we have again that $\xi_p = 0$ and that the primitive term of (5.92) can be characterized explicitly, namely

$$\begin{aligned} G(\boldsymbol{x},\boldsymbol{y}) = &- \frac{e^{-Z_\infty|\boldsymbol{y}-\boldsymbol{x}|}}{4\pi|\boldsymbol{y}-\boldsymbol{x}|} - \frac{e^{-Z_\infty|\boldsymbol{y}-\bar{\boldsymbol{x}}|}}{4\pi|\boldsymbol{y}-\bar{\boldsymbol{x}}|} - \frac{iZ_\infty}{2}\, e^{-Z_\infty v_3} \\ &- \frac{Z_\infty}{2\pi}\, e^{-Z_\infty v_3}\, \mathrm{Ei}\Big(Z_\infty v_3 - Z_\infty\sqrt{\varrho_s^2 + v_3^2}\Big). \end{aligned} \tag{5.106}$$

At last, we observe that the expression for the Green's function (5.92) is still valid if a complex wave number $k \in \mathbb{C}$, such that $\mathfrak{Im}\{k\} > 0$ and $\mathfrak{Re}\{k\} \geq 0$, and a complex impedance $Z_\infty \in \mathbb{C}$, such that $\mathfrak{Im}\{Z_\infty\} > 0$ and $\mathfrak{Re}\{Z_\infty\} \geq 0$, are used, which holds also for its derivatives.

5.4 Far field of the Green's function

5.4.1 Decomposition of the far field

The far field of the Green's function, which we denote by G^{ff}, describes its asymptotic behavior at infinity, i.e., when $|\boldsymbol{x}| \to \infty$ and assuming that $\boldsymbol{y}$ is fixed. For this purpose, the terms of highest order at infinity are searched. Likewise as done for the radiation condition, the far field can be decomposed into two parts, each acting on a different region. The first part, denoted by G_V^{ff}, is linked with the volume waves, and acts in the interior of the half-space while vanishing near its boundary. The second part, denoted by G_S^{ff}, is associated with surface waves that propagate along the boundary towards infinity, which decay exponentially towards the half-space's interior. We have thus that

$$G^{ff} = G_V^{ff} + G_S^{ff}. \tag{5.107}$$

5.4.2 Volume waves in the far field

The volume waves in the far field act only in the interior of the half-space and are related to the terms of the spherical Hankel functions in (5.92), and also to the asymptotic behavior as $x_3 \to \infty$ of the regular part. The behavior of the volume waves can be obtained by applying the stationary phase technique on the integrals in (5.72), as performed by Durán, Muga & Nédélec (2005*b*, 2009). This technique gives an expression for the leading asymptotic behavior of highly oscillating integrals in the form of

$$I(\lambda) = \int_\Omega f(\boldsymbol{s}) e^{i\lambda\phi(\boldsymbol{s})} \,\mathrm{d}\boldsymbol{s}, \tag{5.108}$$

as $\lambda \to \infty$, where $\phi(\boldsymbol{s})$ is a regular real function, where $|f(\boldsymbol{s})|$ is integrable, and where the domain $\Omega \subset \mathbb{R}^2$ may be unbounded. Further references on the stationary phase technique are Bender & Orszag (1978), Dettman (1984), Evans (1998), and Watson (1944). Integrals in the form of (5.108) are called generalized Fourier integrals. They tend towards zero very rapidly with λ, except at the so-called stationary points for which the gradient of the phase $\nabla\phi$ becomes a zero vector, where the integrand vanishes less rapidly. If $\boldsymbol{s}_0$ is such a stationary point, i.e., if $\nabla\phi(\boldsymbol{s}_0) = \boldsymbol{0}$, and if the double-gradient or Hessian matrix $\boldsymbol{H}\phi(\boldsymbol{s}_0)$ is non-singular, then the main asymptotic contribution of the integral (5.108) is given by

$$I(\lambda) \sim \frac{2\pi}{\lambda} \frac{e^{i\frac{\pi}{4}\operatorname{sign}\{\boldsymbol{H}\phi(\boldsymbol{s}_0)\}}}{\sqrt{|\det \boldsymbol{H}\phi(\boldsymbol{s}_0)|}} f(\boldsymbol{s}_0) e^{i\lambda\phi(\boldsymbol{s}_0)}, \tag{5.109}$$

where $\operatorname{sign}\{\boldsymbol{H}\phi\}$ is the signature of the Hessian matrix, which denotes the number of positive eigenvalues minus the number of negative eigenvalues. Moreover, the residue is uniformly bounded by $C\lambda^{-2}$ for some constant $C > 0$ if the point $\boldsymbol{s}_0$ is not on the boundary of the integration domain.

The asymptotic behavior of the volume waves is related with the terms in (5.72) which do not decrease exponentially as $x_3 \to \infty$, i.e., with the integral terms for which $\sqrt{\xi^2 - k^2}$

is purely imaginary, which occurs when $|\xi| < k$. Hence, as $x_3 \to \infty$ it holds that

$$G(\boldsymbol{x},\boldsymbol{y}) \sim -\frac{1}{8\pi^2}\int_{-k}^{k}\int_{0}^{\pi}\frac{e^{-\sqrt{\xi^2-k^2}\,|x_3-y_3|}}{\sqrt{\xi^2-k^2}}|\xi|e^{-i\xi r\sin\alpha\cos(\psi-\beta)}\mathrm{d}\psi\,\mathrm{d}\xi$$
$$+\frac{1}{8\pi^2}\int_{-k}^{k}\int_{0}^{\pi}\left(\frac{Z_\infty+\sqrt{\xi^2-k^2}}{Z_\infty-\sqrt{\xi^2-k^2}}\right)\frac{e^{-\sqrt{\xi^2-k^2}\,(x_3+y_3)}}{\sqrt{\xi^2-k^2}}|\xi|e^{-i\xi r\sin\alpha\cos(\psi-\beta)}\mathrm{d}\psi\,\mathrm{d}\xi, \quad (5.110)$$

where we use the notation

$$\begin{cases} x_1-y_1 = r\sin\alpha\cos\beta, \\ x_2-y_2 = r\sin\alpha\sin\beta, \\ x_3-y_3 = r\cos\alpha, \end{cases} \quad \text{for} \quad \begin{cases} 0\le r<\infty, \\ 0\le\alpha\le\pi, \\ -\pi<\beta\le\pi. \end{cases} \quad (5.111)$$

By considering the representation (5.27), we can express (5.110) equivalently as

$$G(\boldsymbol{x},\boldsymbol{y}) \sim \frac{i}{8\pi^2}\int_{|\xi|<k}\left(\frac{Z_\infty-i\sqrt{k^2-\xi^2}}{Z_\infty+i\sqrt{k^2-\xi^2}}\,e^{2i\sqrt{k^2-\xi^2}\,y_3}-1\right)\frac{e^{ir\phi(\boldsymbol{\xi})}}{\sqrt{k^2-\xi^2}}\,\mathrm{d}\boldsymbol{\xi}, \quad (5.112)$$

where

$$\phi(\boldsymbol{\xi}) = \sqrt{k^2-\xi_1^2-\xi_2^2}\,\cos\alpha-\xi_1\sin\alpha\cos\beta-\xi_2\sin\alpha\sin\beta. \quad (5.113)$$

The phase ϕ has only one stationary point, namely $\boldsymbol{\xi} = (-k\sin\alpha\cos\beta, -k\sin\alpha\sin\beta)$, which is such that $|\boldsymbol{\xi}| < k$. Hence, from (5.109) and as $x_3 \to \infty$, we obtain that

$$G(\boldsymbol{x},\boldsymbol{y}) \sim -\frac{e^{ik|\boldsymbol{x}-\boldsymbol{y}|}}{4\pi|\boldsymbol{x}-\boldsymbol{y}|}+\left(\frac{Z_\infty-ik\cos\alpha}{Z_\infty+ik\cos\alpha}\right)\frac{e^{ik|\boldsymbol{x}-\bar{\boldsymbol{y}}|}}{4\pi|\boldsymbol{x}-\bar{\boldsymbol{y}}|}, \quad (5.114)$$

where $\bar{\boldsymbol{y}} = (y_1, y_2, -y_3)$. By performing Taylor expansions, as in (E.34) and (E.35), we have that

$$\frac{e^{ik|\boldsymbol{x}-\boldsymbol{y}|}}{|\boldsymbol{x}-\boldsymbol{y}|} = \frac{e^{ik|\boldsymbol{x}|}}{|\boldsymbol{x}|}\,e^{-ik\boldsymbol{y}\cdot\boldsymbol{x}/|\boldsymbol{x}|}\left(1+\mathcal{O}\left(\frac{1}{|\boldsymbol{x}|}\right)\right), \quad (5.115)$$

$$\frac{e^{ik|\boldsymbol{x}-\bar{\boldsymbol{y}}|}}{|\boldsymbol{x}-\bar{\boldsymbol{y}}|} = \frac{e^{ik|\boldsymbol{x}|}}{|\boldsymbol{x}|}\,e^{-ik\bar{\boldsymbol{y}}\cdot\boldsymbol{x}/|\boldsymbol{x}|}\left(1+\mathcal{O}\left(\frac{1}{|\boldsymbol{x}|}\right)\right). \quad (5.116)$$

We express the point $\boldsymbol{x}$ as $\boldsymbol{x} = |\boldsymbol{x}|\,\hat{\boldsymbol{x}}$, being $\hat{\boldsymbol{x}} = (\sin\theta\cos\varphi, \sin\theta\sin\varphi, \cos\theta)$ a vector of the unit sphere. Similar Taylor expansions as before yield that

$$\frac{Z_\infty-ik\cos\alpha}{Z_\infty+ik\cos\alpha} = \frac{Z_\infty-ik\cos\theta}{Z_\infty+ik\cos\theta}\left(1+\mathcal{O}\left(\frac{1}{|\boldsymbol{x}|}\right)\right). \quad (5.117)$$

The volume-wave behavior of the Green's function, from (5.114) and due (5.115), (5.116), and (5.117), becomes thus

$$G_V^{ff}(\boldsymbol{x},\boldsymbol{y}) = \frac{e^{ik|\boldsymbol{x}|}}{4\pi|\boldsymbol{x}|}\,e^{-ik\hat{\boldsymbol{x}}\cdot\boldsymbol{y}}\left(-1+\frac{Z_\infty-ik\cos\theta}{Z_\infty+ik\cos\theta}\,e^{2iky_3\cos\theta}\right), \quad (5.118)$$

and its gradient with respect to $\boldsymbol{y}$ is given by

$$\nabla_{\boldsymbol{y}} G_V^{ff}(\boldsymbol{x},\boldsymbol{y}) = \frac{ik\, e^{ik|\boldsymbol{x}|}}{4\pi|\boldsymbol{x}|}\, e^{-ik\hat{\boldsymbol{x}}\cdot\boldsymbol{y}} \left(\hat{\boldsymbol{x}} - \frac{Z_\infty - ik\cos\theta}{Z_\infty + ik\cos\theta}\, e^{2iky_3\cos\theta} \begin{bmatrix} \sin\theta\cos\varphi \\ \sin\theta\sin\varphi \\ -\cos\theta \end{bmatrix} \right). \quad (5.119)$$

5.4.3 Surface waves in the far field

An expression for the surface waves in the far field can be obtained by studying the residues of the poles of the spectral Green's function, which determine entirely their asymptotic behavior. We already computed the inverse Fourier transform of these residues in (5.61), using the residue theorem of Cauchy and the limiting absorption principle. This implies that the Green's function behaves asymptotically, when $|\boldsymbol{x}_s| \to \infty$, as

$$G(\boldsymbol{x},\boldsymbol{y}) \sim -\frac{iZ_\infty}{2}\, e^{-Z_\infty v_3} \Big[J_0(\xi_p \varrho_s) + i\boldsymbol{H}_0(\xi_p \varrho_s) \Big] \qquad \text{for } \; v_3 > 0. \quad (5.120)$$

This expression works well in the upper half-space, but fails to retrieve the logarithmic singularity-distribution (5.98) in the lower half-space at $\varrho_s = 0$. In this case, the Struve function $\boldsymbol{H}_0$ in (5.120) has to be replaced by the Neumann function Y_0, which has the same behavior at infinity, but additionally a logarithmic singularity at its origin. Hence in the lower half-space, the Green's function behaves asymptotically, when $|\boldsymbol{x}_s| \to \infty$, as

$$G(\boldsymbol{x},\boldsymbol{y}) \sim -\frac{iZ_\infty}{2}\, e^{-Z_\infty v_3} H_0^{(1)}(\xi_p \varrho_s) \qquad \text{for } \; v_3 < 0. \quad (5.121)$$

In general, away from the axis $\{\varrho_s = 0\}$, the Green's function behaves, when $|\boldsymbol{x}_s| \to \infty$ and due the asymptotic expansions of the Struve and Bessel functions, as

$$G(\boldsymbol{x},\boldsymbol{y}) \sim -\frac{iZ_\infty}{\sqrt{2\pi\xi_p\varrho_s}}\, e^{-Z_\infty v_3} e^{i(\xi_p\varrho_s - \pi/4)}. \quad (5.122)$$

By performing Taylor expansions, as in (C.37) and (C.38), we have that

$$\frac{e^{i\xi_p\varrho_s}}{\sqrt{\varrho_s}} = \frac{e^{i\xi_p|\boldsymbol{x}_s|}}{\sqrt{|\boldsymbol{x}_s|}}\, e^{-i\xi_p \boldsymbol{y}_s\cdot\boldsymbol{x}_s/|\boldsymbol{x}_s|} \left(1 + \mathcal{O}\Big(\frac{1}{|\boldsymbol{x}_s|}\Big) \right). \quad (5.123)$$

We express the point $\boldsymbol{x}_s$ on the surface as $\boldsymbol{x}_s = |\boldsymbol{x}_s|\, \hat{\boldsymbol{x}}_s$, being $\hat{\boldsymbol{x}}_s = (\cos\varphi, \sin\varphi)$ a unitary surface vector. The surface-wave behavior of the Green's function, due (5.122) and (5.123), becomes thus

$$G_S^{ff}(\boldsymbol{x},\boldsymbol{y}) = -\frac{iZ_\infty}{\sqrt{2\pi\xi_p|\boldsymbol{x}_s|}}\, e^{-i\pi/4} e^{-Z_\infty x_3} e^{i\xi_p|\boldsymbol{x}_s|} e^{-Z_\infty y_3} e^{-i\xi_p \boldsymbol{y}_s\cdot\hat{\boldsymbol{x}}_s}, \quad (5.124)$$

and its gradient with respect to $\boldsymbol{y}$ is given by

$$\nabla_{\boldsymbol{y}} G_S^{ff}(\boldsymbol{x},\boldsymbol{y}) = -\frac{Z_\infty}{\sqrt{2\pi\xi_p|\boldsymbol{x}_s|}}\, e^{-i\pi/4} e^{-Z_\infty x_3} e^{i\xi_p|\boldsymbol{x}_s|} e^{-Z_\infty y_3} e^{-i\xi_p \boldsymbol{y}_s\cdot\hat{\boldsymbol{x}}_s} \begin{bmatrix} \xi_p\cos\varphi \\ \xi_p\sin\varphi \\ -iZ_\infty \end{bmatrix}. \quad (5.125)$$

5.4.4 Complete far field of the Green's function

On the whole, the asymptotic behavior of the Green's function as $|\boldsymbol{x}| \to \infty$ can be characterized in the upper half-space through the addition of (5.114) and (5.120), and in

the lower half-space by adding (5.114) and (5.121). Thus if $v_3 > 0$, then it holds that

$$G(\boldsymbol{x},\boldsymbol{y}) \sim -\frac{e^{ik|\boldsymbol{x}-\boldsymbol{y}|}}{4\pi|\boldsymbol{x}-\boldsymbol{y}|} + \left(\frac{Z_\infty - ik\cos\alpha}{Z_\infty + ik\cos\alpha}\right)\frac{e^{ik|\boldsymbol{x}-\bar{\boldsymbol{y}}|}}{4\pi|\boldsymbol{x}-\bar{\boldsymbol{y}}|} - \frac{iZ_\infty}{2}\, e^{-Z_\infty v_3}\Big[J_0(\xi_p\varrho_s) + i\boldsymbol{H}_0(\xi_p\varrho_s)\Big], \tag{5.126}$$

and if $v_3 < 0$, then

$$G(\boldsymbol{x},\boldsymbol{y}) \sim -\frac{e^{ik|\boldsymbol{x}-\boldsymbol{y}|}}{4\pi|\boldsymbol{x}-\boldsymbol{y}|} + \left(\frac{Z_\infty - ik\cos\alpha}{Z_\infty + ik\cos\alpha}\right)\frac{e^{ik|\boldsymbol{x}-\bar{\boldsymbol{y}}|}}{4\pi|\boldsymbol{x}-\bar{\boldsymbol{y}}|} - \frac{iZ_\infty}{2}\, e^{-Z_\infty v_3} H_0^{(1)}(\xi_p\varrho_s). \tag{5.127}$$

Consequently, the complete far field of the Green's function, due (5.107), should be given by the addition of (5.118) and (5.124), i.e., by

$$G^{ff}(\boldsymbol{x},\boldsymbol{y}) = \frac{e^{ik|\boldsymbol{x}|}}{4\pi|\boldsymbol{x}|}\, e^{-ik\hat{\boldsymbol{x}}\cdot\boldsymbol{y}}\left(-1 + \frac{Z_\infty - ik\cos\theta}{Z_\infty + ik\cos\theta}\, e^{2iky_3\cos\theta}\right) - \frac{iZ_\infty}{\sqrt{2\pi\xi_p|\boldsymbol{x}_s|}}\, e^{-i\pi/4} e^{-Z_\infty x_3} e^{i\xi_p|\boldsymbol{x}_s|} e^{-Z_\infty y_3} e^{-i\xi_p \boldsymbol{y}_s\cdot\hat{\boldsymbol{x}}_s}. \tag{5.128}$$

Its derivative with respect to $\boldsymbol{y}$ is likewise given by the addition of (5.119) and (5.125). The expression (5.128) retrieves correctly the far field of the Green's function, except in the upper half-space at the vicinity of the axis $\{\varrho_s = 0\}$, due the presence of a singularity-distribution of type $1/\sqrt{|\boldsymbol{x}_s|}$, which does not appear in the original Green's function. A way to deal with this issue is to consider in each region only the most dominant asymptotic behavior at infinity. Since there are two different regions, we require to determine appropriately the interface between them. This can be achieved by equating the amplitudes of the two terms in (5.128), i.e., by searching values of $\boldsymbol{x}$ at infinity such that

$$\frac{1}{4\pi|\boldsymbol{x}|} = \frac{Z_\infty}{\sqrt{2\pi\xi_p|\boldsymbol{x}|}}\, e^{-Z_\infty x_3}, \tag{5.129}$$

where we neglected the values of $\boldsymbol{y}$, since they remain relatively near the origin. Furthermore, since the interface stays relatively close to the half-space's boundary, we can also approximate $|\boldsymbol{x}_s| \approx |\boldsymbol{x}|$. By taking the logarithm in (5.129) and perturbing somewhat the result so as to avoid a singular behavior at the origin, we obtain finally that this interface is described by

$$x_3 = \frac{1}{2Z_\infty}\ln\left(1 + \frac{8\pi Z_\infty^2}{\xi_p}|\boldsymbol{x}|\right). \tag{5.130}$$

We can say now that it is the far field (5.128) which justifies the radiation condition (5.21) when exchanging the roles of $\boldsymbol{x}$ and $\boldsymbol{y}$, and disregarding the undesired singularity around $\{\varrho_s = 0\}$. When the first term in (5.128) dominates, i.e., the volume waves (5.118), then it is the first expression in (5.21) that matters. Conversely, when the second term in (5.128) dominates, i.e., the surface waves (5.124), then the second expression in (5.21) is the one that holds. The interface between both is described by (5.130).

We remark that the asymptotic behavior (5.126) of the Green's function and the expression (5.128) of its complete far field do no longer hold if a complex impedance $Z_\infty \in \mathbb{C}$ such that $\mathfrak{Im}\{Z_\infty\} > 0$ and $\mathfrak{Re}\{Z_\infty\} \geq 0$ is used, specifically the parts (5.120) and (5.124)

linked with the surface waves. A careful inspection shows that in this case the surface-wave behavior of the Green's function, as $|\boldsymbol{x}_s| \to \infty$, decreases exponentially and is given by

$$G(\boldsymbol{x},\boldsymbol{y}) \sim -\frac{iZ_\infty}{2}\, e^{-|Z_\infty| v_3}\Big[J_0(\xi_p \varrho_s) + i\boldsymbol{H}_0(\xi_p \varrho_s)\Big] \qquad \text{for } \; v_3 > 0, \tag{5.131}$$

whereas (5.121) continues to hold. Likewise, the surface-wave part of the far field is expressed for $x_3 > 0$ as

$$G_S^{ff}(\boldsymbol{x},\boldsymbol{y}) = -\frac{iZ_\infty}{\sqrt{2\pi\xi_p|\boldsymbol{x}_s|}}\, e^{-i\pi/4} e^{-|Z_\infty| x_3} e^{i\xi_p|\boldsymbol{x}_s|} e^{-|Z_\infty| y_3} e^{-i\xi_p \boldsymbol{y}_s\cdot\hat{\boldsymbol{x}}_s}, \tag{5.132}$$

but for $x_3 < 0$ the expression (5.124) is still valid. The volume-waves part (5.114) and its far-field expression (5.118), on the other hand, remain the same when we use a complex impedance. We remark further that if a complex impedance or a complex wave number are taken into account, then the part of the surface waves of the outgoing radiation condition is redundant, and only the volume-waves part is required, i.e., only the first two expressions in (5.21), but now holding for $y_3 > 0$.

5.5 Numerical evaluation of the Green's function

For the numerical evaluation of the Green's function, we separate the space $\mathbb{R}^3$ into four regions: a near field close to the ϱ_s-axis, a near field, an upper far field, and a lower far field. In the near field close to the ϱ_s-axis, when $|\xi_p|\,|\boldsymbol{v}| \le 24$ and $|\xi_p|\,\varrho_s \le 2/5$, being $\boldsymbol{v} = \boldsymbol{y} - \bar{\boldsymbol{x}}$, the integral in (5.92) is computed numerically according to (5.91) by using a trapezoidal rule. In the near field, when $|\xi_p|\,|\boldsymbol{v}| \le 24$ and $|\xi_p|\,\varrho_s > 2/5$, this integral is likewise computed by using a trapezoidal quadrature formula, but now according to (5.89). In both cases, satisfactory numerical results are obtained when $w_3 = -10/|Z_\infty|$ and when the integration variable η is discretized into $\eta_j = w_3 + j\Delta\eta$ for $j = 0,\ldots,M$, where $\Delta\eta = 2\pi/(50\,|\xi_p|)$, i.e., 50 samples are taken per wavelength. We remark that the term G_{RL} in (5.91) is computed as explained in Sections 4.3 & 4.5, i.e., considering (4.112) for the near field and adapting (4.153) and (4.154) for the far field by isolating the contribution of the remaining term. We remark that the integrals of the derivatives, particularly the one in (5.95), are computed following the same numerical strategy.

In the upper far field, when $|\xi_p|\,|\boldsymbol{v}| > 24$ and $|Z_\infty|\,v_3 > \log\big(1 + 8\pi\varrho_s|Z_\infty^2/\xi_p|\big)/2$, we describe the Green's function numerically by means of the expression (5.126). In the lower far field, on the other hand, when $|\xi_p|\,|\boldsymbol{v}| > 24$ and $|Z_\infty|\,v_3 < \log\big(1 + 8\pi\varrho_s|Z_\infty^2/\xi_p|\big)/2$, it is described by using (5.127).

The Bessel functions can be evaluated either by using the software based on the technical report by Morris (1993) or the subroutines described in Amos (1986, 1995). The Struve function can be computed by means of the software described in MacLeod (1996). Further references are listed in Lozier & Olver (1994).

5.6 Integral representation and equation

5.6.1 Integral representation

We are interested in expressing the solution u of the direct scattering problem (5.13) by means of an integral representation formula over the perturbed portion of the boundary Γ_p. For this purpose, we extend this solution by zero towards the complementary domain Ω_c, analogously as done in (E.104). We define by $\Omega_{R,\varepsilon}$ the domain Ω_e without the ball B_ε of radius $\varepsilon > 0$ centered at the point $\boldsymbol{x} \in \Omega_e$, and truncated at infinity by the ball B_R of radius $R > 0$ centered at the origin. We consider that the ball B_ε is entirely contained in Ω_e. Therefore, as shown in Figure 5.7, we have that

$$\Omega_{R,\varepsilon} = \big(\Omega_e \cap B_R\big) \setminus \overline{B_\varepsilon}, \tag{5.133}$$

where

$$B_R = \{\boldsymbol{y} \in \mathbb{R}^3 : |\boldsymbol{y}| < R\} \qquad \text{and} \qquad B_\varepsilon = \{\boldsymbol{y} \in \Omega_e : |\boldsymbol{y} - \boldsymbol{x}| < \varepsilon\}. \tag{5.134}$$

We consider similarly, inside Ω_e, the boundaries of the balls

$$S_R^+ = \{\boldsymbol{y} \in \mathbb{R}^3_+ : |\boldsymbol{y}| = R\} \qquad \text{and} \qquad S_\varepsilon = \{\boldsymbol{y} \in \Omega_e : |\boldsymbol{y} - \boldsymbol{x}| = \varepsilon\}. \tag{5.135}$$

We separate furthermore the boundary as $\Gamma = \Gamma_0 \cup \Gamma_+$, where

$$\Gamma_0 = \{\boldsymbol{y} \in \Gamma : y_3 = 0\} \qquad \text{and} \qquad \Gamma_+ = \{\boldsymbol{y} \in \Gamma : y_3 > 0\}. \tag{5.136}$$

The boundary Γ is likewise truncated at infinity by the ball B_R, namely

$$\Gamma_R = \Gamma \cap B_R = \Gamma_0^R \cup \Gamma_+ = \Gamma_\infty^R \cup \Gamma_p, \tag{5.137}$$

where

$$\Gamma_0^R = \Gamma_0 \cap B_R \qquad \text{and} \qquad \Gamma_\infty^R = \Gamma_\infty \cap B_R. \tag{5.138}$$

The idea is to retrieve the domain Ω_e and the boundary Γ at the end when the limits $R \to \infty$ and $\varepsilon \to 0$ are taken for the truncated domain $\Omega_{R,\varepsilon}$ and the truncated boundary Γ_R.

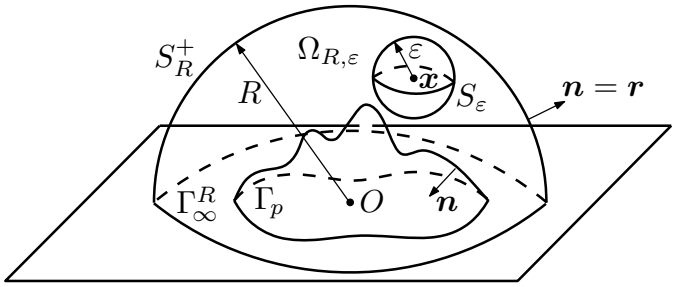

FIGURE 5.7. Truncated domain $\Omega_{R,\varepsilon}$ for $\boldsymbol{x} \in \Omega_e$.

We apply now Green's second integral theorem (A.613) to the functions u and $G(\boldsymbol{x},\cdot)$ in the bounded domain $\Omega_{R,\varepsilon}$, by subtracting their respective Helmholtz equations, yielding

$$\begin{aligned}
0 &= \int_{\Omega_{R,\varepsilon}} \big(u(\boldsymbol{y})\Delta_{\boldsymbol{y}} G(\boldsymbol{x},\boldsymbol{y}) - G(\boldsymbol{x},\boldsymbol{y})\Delta u(\boldsymbol{y})\big)\mathrm{d}\boldsymbol{y} \\
&= \int_{S_R^+} \left(u(\boldsymbol{y})\frac{\partial G}{\partial r_{\boldsymbol{y}}}(\boldsymbol{x},\boldsymbol{y}) - G(\boldsymbol{x},\boldsymbol{y})\frac{\partial u}{\partial r}(\boldsymbol{y})\right)\mathrm{d}\gamma(\boldsymbol{y}) \\
&\quad - \int_{S_\varepsilon} \left(u(\boldsymbol{y})\frac{\partial G}{\partial r_{\boldsymbol{y}}}(\boldsymbol{x},\boldsymbol{y}) - G(\boldsymbol{x},\boldsymbol{y})\frac{\partial u}{\partial r}(\boldsymbol{y})\right)\mathrm{d}\gamma(\boldsymbol{y}) \\
&\quad + \int_{\Gamma_R} \left(u(\boldsymbol{y})\frac{\partial G}{\partial n_{\boldsymbol{y}}}(\boldsymbol{x},\boldsymbol{y}) - G(\boldsymbol{x},\boldsymbol{y})\frac{\partial u}{\partial n}(\boldsymbol{y})\right)\mathrm{d}\gamma(\boldsymbol{y}). \qquad (5.139)
\end{aligned}$$

The integral on S_R^+ can be rewritten as

$$\begin{aligned}
&\int_{S_R^2} \left[u(\boldsymbol{y})\left(\frac{\partial G}{\partial r_{\boldsymbol{y}}}(\boldsymbol{x},\boldsymbol{y}) - iZ_\infty G(\boldsymbol{x},\boldsymbol{y})\right) - G(\boldsymbol{x},\boldsymbol{y})\left(\frac{\partial u}{\partial r}(\boldsymbol{y}) - iZ_\infty u(\boldsymbol{y})\right)\right]\mathrm{d}\gamma(\boldsymbol{y}) \\
&+ \int_{S_R^1} \left[u(\boldsymbol{y})\left(\frac{\partial G}{\partial r_{\boldsymbol{y}}}(\boldsymbol{x},\boldsymbol{y}) - ikG(\boldsymbol{x},\boldsymbol{y})\right) - G(\boldsymbol{x},\boldsymbol{y})\left(\frac{\partial u}{\partial r}(\boldsymbol{y}) - iku(\boldsymbol{y})\right)\right]\mathrm{d}\gamma(\boldsymbol{y}), \qquad (5.140)
\end{aligned}$$

which for R large enough and due the radiation condition (5.6) tends to zero, since

$$\left|\int_{S_R^2} u(\boldsymbol{y})\left(\frac{\partial G}{\partial r_{\boldsymbol{y}}}(\boldsymbol{x},\boldsymbol{y}) - i\sqrt{Z_\infty^2+k^2}\,G(\boldsymbol{x},\boldsymbol{y})\right)\mathrm{d}\gamma(\boldsymbol{y})\right| \leq \frac{C}{\sqrt{R}}\ln R, \qquad (5.141)$$

$$\left|\int_{S_R^2} G(\boldsymbol{x},\boldsymbol{y})\left(\frac{\partial u}{\partial r}(\boldsymbol{y}) - i\sqrt{Z_\infty^2+k^2}\,u(\boldsymbol{y})\right)\mathrm{d}\gamma(\boldsymbol{y})\right| \leq \frac{C}{\sqrt{R}}\ln R, \qquad (5.142)$$

and

$$\left|\int_{S_R^1} u(\boldsymbol{y})\left(\frac{\partial G}{\partial r_{\boldsymbol{y}}}(\boldsymbol{x},\boldsymbol{y}) - ikG(\boldsymbol{x},\boldsymbol{y})\right)\mathrm{d}\gamma(\boldsymbol{y})\right| \leq \frac{C}{R}, \qquad (5.143)$$

$$\left|\int_{S_R^1} G(\boldsymbol{x},\boldsymbol{y})\left(\frac{\partial u}{\partial r}(\boldsymbol{y}) - iku(\boldsymbol{y})\right)\mathrm{d}\gamma(\boldsymbol{y})\right| \leq \frac{C}{R}, \qquad (5.144)$$

for some constants $C > 0$. If the function u is regular enough in the ball B_ε, then the second term of the integral on S_ε in (5.139), when $\varepsilon \to 0$ and due (5.96), is bounded by

$$\left|\int_{S_\varepsilon} G(\boldsymbol{x},\boldsymbol{y})\frac{\partial u}{\partial r}(\boldsymbol{y})\,\mathrm{d}\gamma(\boldsymbol{y})\right| \leq C\varepsilon \sup_{\boldsymbol{y}\in B_\varepsilon}\left|\frac{\partial u}{\partial r}(\boldsymbol{y})\right|, \qquad (5.145)$$

for some constant $C > 0$ and tends to zero. The regularity of u can be specified afterwards once the integral representation has been determined and generalized by means of density arguments. The first integral term on S_ε can be decomposed as

$$\begin{aligned}
\int_{S_\varepsilon} u(\boldsymbol{y})\frac{\partial G}{\partial r_{\boldsymbol{y}}}(\boldsymbol{x},\boldsymbol{y})\,\mathrm{d}\gamma(\boldsymbol{y}) &= u(\boldsymbol{x})\int_{S_\varepsilon}\frac{\partial G}{\partial r_{\boldsymbol{y}}}(\boldsymbol{x},\boldsymbol{y})\,\mathrm{d}\gamma(\boldsymbol{y}) \\
&\quad + \int_{S_\varepsilon}\frac{\partial G}{\partial r_{\boldsymbol{y}}}(\boldsymbol{x},\boldsymbol{y})\big(u(\boldsymbol{y}) - u(\boldsymbol{x})\big)\,\mathrm{d}\gamma(\boldsymbol{y}), \qquad (5.146)
\end{aligned}$$

For the first term in the right-hand side of (5.146), by considering (5.96) we have that

$$\int_{S_\varepsilon} \frac{\partial G}{\partial r_{\boldsymbol{y}}}(\boldsymbol{x},\boldsymbol{y})\,\mathrm{d}\gamma(\boldsymbol{y}) \quad \xrightarrow[\varepsilon\to 0]{} \quad 1, \tag{5.147}$$

while the second term is bounded by

$$\left|\int_{S_\varepsilon} \big(u(\boldsymbol{y})-u(\boldsymbol{x})\big)\frac{\partial G}{\partial r_{\boldsymbol{y}}}(\boldsymbol{x},\boldsymbol{y})\,\mathrm{d}\gamma(\boldsymbol{y})\right| \leq \sup_{\boldsymbol{y}\in B_\varepsilon} |u(\boldsymbol{y})-u(\boldsymbol{x})|, \tag{5.148}$$

which tends towards zero when $\varepsilon \to 0$. Finally, due the impedance boundary condition (5.4) and since the support of f_z vanishes on Γ_∞, the term on Γ_R in (5.139) can be decomposed as

$$\begin{aligned}\int_{\Gamma_p} \left(\frac{\partial G}{\partial n_{\boldsymbol{y}}}(\boldsymbol{x},\boldsymbol{y}) - Z(\boldsymbol{y})G(\boldsymbol{x},\boldsymbol{y})\right) u(\boldsymbol{y})\,\mathrm{d}\gamma(\boldsymbol{y}) + \int_{\Gamma_p} G(\boldsymbol{x},\boldsymbol{y}) f_z(\boldsymbol{y})\,\mathrm{d}\gamma(\boldsymbol{y}) \\ - \int_{\Gamma_\infty^R} \left(\frac{\partial G}{\partial y_2}(\boldsymbol{x},\boldsymbol{y}) + Z_\infty G(\boldsymbol{x},\boldsymbol{y})\right) u(\boldsymbol{y})\,\mathrm{d}\gamma(\boldsymbol{y}),\end{aligned} \tag{5.149}$$

where the integral on Γ_∞^R vanishes due the impedance boundary condition in (5.20). Therefore this term does not depend on R and has its support only on the bounded and perturbed portion Γ_p of the boundary.

In conclusion, when the limits $R \to \infty$ and $\varepsilon \to 0$ are taken in (5.139), then we obtain for $\boldsymbol{x} \in \Omega_e$ the integral representation formula

$$u(\boldsymbol{x}) = \int_{\Gamma_p} \left(\frac{\partial G}{\partial n_{\boldsymbol{y}}}(\boldsymbol{x},\boldsymbol{y}) - Z(\boldsymbol{y})G(\boldsymbol{x},\boldsymbol{y})\right) u(\boldsymbol{y})\,\mathrm{d}\gamma(\boldsymbol{y}) + \int_{\Gamma_p} G(\boldsymbol{x},\boldsymbol{y}) f_z(\boldsymbol{y})\,\mathrm{d}\gamma(\boldsymbol{y}), \tag{5.150}$$

which can be alternatively expressed as

$$u(\boldsymbol{x}) = \int_{\Gamma_p} \left(u(\boldsymbol{y})\frac{\partial G}{\partial n_{\boldsymbol{y}}}(\boldsymbol{x},\boldsymbol{y}) - G(\boldsymbol{x},\boldsymbol{y})\frac{\partial u}{\partial n}(\boldsymbol{y})\right) \mathrm{d}\gamma(\boldsymbol{y}). \tag{5.151}$$

It is remarkable in this integral representation that the support of the integral, namely the curve Γ_p, is bounded. Let us denote the traces of the solution and of its normal derivative on Γ_p respectively by

$$\mu = u|_{\Gamma_p} \qquad \text{and} \qquad \nu = \left.\frac{\partial u}{\partial n}\right|_{\Gamma_p}. \tag{5.152}$$

We can rewrite now (5.150) and (5.151) in terms of layer potentials as

$$u = \mathcal{D}(\mu) - \mathcal{S}(Z\mu) + \mathcal{S}(f_z) \qquad \text{in } \Omega_e, \tag{5.153}$$

$$u = \mathcal{D}(\mu) - \mathcal{S}(\nu) \qquad \text{in } \Omega_e, \tag{5.154}$$

where we define for $\boldsymbol{x} \in \Omega_e$ respectively the single and double layer potentials as

$$\mathcal{S}\nu(\boldsymbol{x}) = \int_{\Gamma_p} G(\boldsymbol{x},\boldsymbol{y})\nu(\boldsymbol{y})\,\mathrm{d}\gamma(\boldsymbol{y}), \tag{5.155}$$

$$\mathcal{D}\mu(\boldsymbol{x}) = \int_{\Gamma_p} \frac{\partial G}{\partial n_{\boldsymbol{y}}}(\boldsymbol{x},\boldsymbol{y})\mu(\boldsymbol{y})\,\mathrm{d}\gamma(\boldsymbol{y}). \tag{5.156}$$

We remark that from the impedance boundary condition (5.4) it is clear that

$$\nu = Z\mu - f_z. \tag{5.157}$$

5.6.2 Integral equation

To determine entirely the solution of the direct scattering problem (5.13) by means of its integral representation, we have to find values for the traces (5.152). This requires the development of an integral equation that allows to fix these values by incorporating the boundary data. For this purpose we place the source point $\boldsymbol{x}$ on the boundary Γ and apply the same procedure as before for the integral representation (5.150), treating differently in (5.139) only the integrals on S_ε. The integrals on S_R^+ still behave well and tend towards zero as $R \to \infty$. The Ball B_ε, though, is split in half by the boundary Γ, and the portion $\Omega_e \cap B_\varepsilon$ is asymptotically separated from its complement in B_ε by the tangent of the boundary if Γ is regular. If $\boldsymbol{x} \in \Gamma_+$, then the associated integrals on S_ε give rise to a term $-u(\boldsymbol{x})/2$ instead of just $-u(\boldsymbol{x})$ as before for the integral representation. Therefore we obtain for $\boldsymbol{x} \in \Gamma_+$ the boundary integral representation

$$\frac{u(\boldsymbol{x})}{2} = \int_{\Gamma_p} \left(\frac{\partial G}{\partial n_{\boldsymbol{y}}}(\boldsymbol{x}, \boldsymbol{y}) - Z(\boldsymbol{y}) G(\boldsymbol{x}, \boldsymbol{y}) \right) u(\boldsymbol{y}) \, \mathrm{d}\gamma(\boldsymbol{y}) + \int_{\Gamma_p} G(\boldsymbol{x}, \boldsymbol{y}) f_z(\boldsymbol{y}) \, \mathrm{d}\gamma(\boldsymbol{y}). \tag{5.158}$$

On the contrary, if $\boldsymbol{x} \in \Gamma_0$, then the pole-type behavior (5.97) contributes also to the singularity (5.96) of the Green's function and the integrals on S_ε give now rise to two terms $-u(\boldsymbol{x})/2$, i.e., on the whole to a term $-u(\boldsymbol{x})$. For $\boldsymbol{x} \in \Gamma_0$ the boundary integral representation is instead given by

$$u(\boldsymbol{x}) = \int_{\Gamma_p} \left(\frac{\partial G}{\partial n_{\boldsymbol{y}}}(\boldsymbol{x}, \boldsymbol{y}) - Z(\boldsymbol{y}) G(\boldsymbol{x}, \boldsymbol{y}) \right) u(\boldsymbol{y}) \, \mathrm{d}\gamma(\boldsymbol{y}) + \int_{\Gamma_p} G(\boldsymbol{x}, \boldsymbol{y}) f_z(\boldsymbol{y}) \, \mathrm{d}\gamma(\boldsymbol{y}). \tag{5.159}$$

We must notice that in both cases, the integrands associated with the boundary Γ admit an integrable singularity at the point $\boldsymbol{x}$. In terms of boundary layer potentials, we can express these boundary integral representations as

$$\frac{u}{2} = D(\mu) - S(Z\mu) + S(f_z) \qquad \text{on } \Gamma_+, \tag{5.160}$$

$$u = D(\mu) - S(Z\mu) + S(f_z) \qquad \text{on } \Gamma_0, \tag{5.161}$$

where we consider, for $\boldsymbol{x} \in \Gamma$, the two boundary integral operators

$$S\nu(\boldsymbol{x}) = \int_{\Gamma_p} G(\boldsymbol{x}, \boldsymbol{y}) \nu(\boldsymbol{y}) \, \mathrm{d}\gamma(\boldsymbol{y}), \tag{5.162}$$

$$D\mu(\boldsymbol{x}) = \int_{\Gamma_p} \frac{\partial G}{\partial n_{\boldsymbol{y}}}(\boldsymbol{x}, \boldsymbol{y}) \mu(\boldsymbol{y}) \, \mathrm{d}\gamma(\boldsymbol{y}). \tag{5.163}$$

We can combine (5.160) and (5.161) into a single integral equation on Γ_p, namely

$$(1 + \mathcal{I}_0)\frac{\mu}{2} + S(Z\mu) - D(\mu) = S(f_z) \qquad \text{on } \Gamma_p, \tag{5.164}$$

where $\mathcal{I}_0$ denotes the characteristic or indicator function of the set Γ_0, i.e.,

$$\mathcal{I}_0(\boldsymbol{x}) = \begin{cases} 1 & \text{if } \boldsymbol{x} \in \Gamma_0, \\ 0 & \text{if } \boldsymbol{x} \notin \Gamma_0. \end{cases} \tag{5.165}$$

It is the solution μ on Γ_p of the integral equation (5.164) which finally allows to characterize the solution u in Ω_e of the direct scattering problem (5.13) through the integral representation formula (5.153). The trace of the solution u on the boundary Γ is then found simultaneously by means of the boundary integral representations (5.160) and (5.161). In particular, when $\boldsymbol{x} \in \Gamma_\infty$ and since $\Gamma_\infty \subset \Gamma_0$, therefore it holds that

$$u = D(\mu) - S(Z\mu) + S(f_z) \qquad \text{on } \Gamma_\infty. \tag{5.166}$$

5.7 Far field of the solution

The asymptotic behavior at infinity of the solution u of (5.13) is described by the far field. It is denoted by u^{ff} and is characterized by

$$u(\boldsymbol{x}) \sim u^{ff}(\boldsymbol{x}) \qquad \text{as } |\boldsymbol{x}| \to \infty. \tag{5.167}$$

Its expression can be deduced by replacing the far field of the Green's function G^{ff} and its derivatives in the integral representation formula (5.151), which yields

$$u^{ff}(\boldsymbol{x}) = \int_{\Gamma_p} \left(\frac{\partial G^{ff}}{\partial n_{\boldsymbol{y}}}(\boldsymbol{x}, \boldsymbol{y}) \mu(\boldsymbol{y}) - G^{ff}(\boldsymbol{x}, \boldsymbol{y}) \nu(\boldsymbol{y}) \right) \mathrm{d}\gamma(\boldsymbol{y}). \tag{5.168}$$

By replacing now (5.128) and the addition of (5.119) and (5.125) in (5.168), we obtain that

$$\begin{aligned} u^{ff}(\boldsymbol{x}) = \frac{e^{ik|\boldsymbol{x}|}}{4\pi|\boldsymbol{x}|} \int_{\Gamma_p} e^{-ik\hat{\boldsymbol{x}}\cdot\boldsymbol{y}} \Bigg\{ & ik\hat{\boldsymbol{x}} \cdot \boldsymbol{n}_{\boldsymbol{y}}\, \mu(\boldsymbol{y}) + \nu(\boldsymbol{y}) \\ & - \frac{Z_\infty - ik\cos\theta}{Z_\infty + ik\cos\theta}\, e^{2iky_3\cos\theta} \left(ik \begin{bmatrix} \sin\theta\cos\varphi \\ \sin\theta\sin\varphi \\ -\cos\theta \end{bmatrix} \cdot \boldsymbol{n}_{\boldsymbol{y}}\, \mu(\boldsymbol{y}) + \nu(\boldsymbol{y}) \right) \Bigg\} \mathrm{d}\gamma(\boldsymbol{y}) \\ - \frac{Z_\infty e^{-i\pi/4}}{\sqrt{2\pi\xi_p|\boldsymbol{x}_s|}}\, e^{-Z_\infty x_3} e^{i\xi_p|\boldsymbol{x}_s|} & \int_{\Gamma_p} e^{-Z_\infty y_3} e^{-i\xi_p \boldsymbol{y}_s\cdot\hat{\boldsymbol{x}}_s} \left(\begin{bmatrix} \xi_p\cos\varphi \\ \xi_p\sin\varphi \\ -iZ_\infty \end{bmatrix} \cdot \boldsymbol{n}_{\boldsymbol{y}}\, \mu(\boldsymbol{y}) - i\nu(\boldsymbol{y}) \right) \mathrm{d}\gamma(\boldsymbol{y}). \end{aligned} \tag{5.169}$$

The asymptotic behavior of the solution u at infinity, as $|\boldsymbol{x}| \to \infty$, is therefore given by

$$u(\boldsymbol{x}) = \frac{e^{ik|\boldsymbol{x}|}}{|\boldsymbol{x}|} \left\{ u_\infty^V(\hat{\boldsymbol{x}}) + \mathcal{O}\left(\frac{1}{|\boldsymbol{x}|}\right) \right\} + e^{-Z_\infty x_3} \frac{e^{i\xi_p|\boldsymbol{x}_s|}}{\sqrt{|\boldsymbol{x}_s|}} \left\{ u_\infty^S(\hat{\boldsymbol{x}}_s) + \mathcal{O}\left(\frac{1}{|\boldsymbol{x}_s|}\right) \right\}, \tag{5.170}$$

where we decompose $\boldsymbol{x} = |\boldsymbol{x}|\,\hat{\boldsymbol{x}}$, being $\hat{\boldsymbol{x}} = (\sin\theta\cos\varphi, \sin\theta\sin\varphi, \cos\theta)$ a vector of the unit sphere, and $\boldsymbol{x}_s = |\boldsymbol{x}_s|\,\hat{\boldsymbol{x}}_s$, being $\hat{\boldsymbol{x}}_s = (\cos\varphi, \sin\varphi)$ a vector of the unit circle. The

far-field pattern of the volume waves is given by

$$u_\infty^V(\hat{\boldsymbol{x}}) = \frac{1}{4\pi}\int_{\Gamma_p} e^{-ik\hat{\boldsymbol{x}}\cdot\boldsymbol{y}} \left\{ ik\hat{\boldsymbol{x}}\cdot\boldsymbol{n_y}\,\mu(\boldsymbol{y}) + \nu(\boldsymbol{y}) \right.$$
$$\left. -\frac{Z_\infty - ik\cos\theta}{Z_\infty + ik\cos\theta}\, e^{2iky_3\cos\theta} \left(ik \begin{bmatrix} \sin\theta\cos\varphi \\ \sin\theta\sin\varphi \\ -\cos\theta \end{bmatrix} \cdot \boldsymbol{n_y}\,\mu(\boldsymbol{y}) + \nu(\boldsymbol{y}) \right) \right\} \mathrm{d}\gamma(\boldsymbol{y}), \quad (5.171)$$

whereas the far-field pattern for the surface waves adopts the form

$$u_\infty^S(\hat{\boldsymbol{x}}_s) = -\frac{Z_\infty e^{-i\pi/4}}{\sqrt{2\pi\xi_p}} \int_{\Gamma_p} e^{-Z_\infty y_3} e^{-i\xi_p \boldsymbol{y}_s\cdot\hat{\boldsymbol{x}}_s} \left(\begin{bmatrix} \xi_p\cos\varphi \\ \xi_p\sin\varphi \\ -iZ_\infty \end{bmatrix} \cdot \boldsymbol{n_y}\,\mu(\boldsymbol{y}) - i\nu(\boldsymbol{y}) \right) \mathrm{d}\gamma(\boldsymbol{y}). \quad (5.172)$$

Both far-field patterns can be expressed in decibels (dB) respectively by means of the scattering cross sections

$$Q_s^V(\hat{\boldsymbol{x}}) \ \ [\mathrm{dB}] = 20\log_{10}\left(\frac{|u_\infty^V(\hat{\boldsymbol{x}})|}{|u_0^V|}\right), \quad (5.173)$$

$$Q_s^S(\hat{\boldsymbol{x}}_s) \ \ [\mathrm{dB}] = 20\log_{10}\left(\frac{|u_\infty^S(\hat{\boldsymbol{x}}_s)|}{|u_0^S|}\right), \quad (5.174)$$

where the reference levels u_0^V and u_0^S are taken such that $|u_0^V| = |u_0^S| = 1$ if the incident field is given either by a volume wave of the form (5.16) or by a surface wave of the form (5.19).

We remark that the far-field behavior (5.170) of the solution is in accordance with the radiation condition (5.6), which justifies its choice.

5.8 Existence and uniqueness

5.8.1 Function spaces

To state a precise mathematical formulation of the herein treated problems, we have to define properly the involved function spaces. Since the considered domains and boundaries are unbounded, we need to work with weighted Sobolev spaces, as in Durán, Muga & Nédélec (2005*b*, 2009). We consider the classic weight functions

$$\varrho = \sqrt{1+r^2} \qquad \text{and} \qquad \log\varrho = \ln(2+r^2), \quad (5.175)$$

where $r = |\boldsymbol{x}|$. We define the domains

$$\Omega_e^1 = \left\{ \boldsymbol{x}\in\Omega_e : \ x_3 > \frac{1}{2Z_\infty}\ln\left(1+\frac{8\pi Z_\infty^2}{\sqrt{Z_\infty^2+k^2}}\,r\right) \right\}, \quad (5.176)$$

$$\Omega_e^2 = \left\{ \boldsymbol{x}\in\Omega_e : \ x_3 < \frac{1}{2Z_\infty}\ln\left(1+\frac{8\pi Z_\infty^2}{\sqrt{Z_\infty^2+k^2}}\,r\right) \right\}. \quad (5.177)$$

It holds that the solution of the direct scattering problem (5.13) is contained in the weighted Sobolev space

$$W^1(\Omega_e) = \left\{ v : \frac{v}{\varrho} \in L^2(\Omega_e),\ \frac{\nabla v}{\varrho} \in L^2(\Omega_e)^2,\ \frac{v}{\sqrt{\varrho}} \in L^2(\Omega_e^1),\ \frac{\partial v}{\partial r} - ikv \in L^2(\Omega_e^1), \right.$$
$$\left. \frac{v}{\log \varrho} \in L^2(\Omega_e^2),\ \frac{1}{\log \varrho}\left(\frac{\partial v}{\partial r} - i\xi_p v\right) \in L^2(\Omega_e^2) \right\}, \tag{5.178}$$

where $\xi_p = \sqrt{Z_\infty^2 + k^2}$. With the appropriate norm, the space $W^1(\Omega_e)$ becomes also a Hilbert space. We have likewise the inclusion $W^1(\Omega_e) \subset H^1_{\text{loc}}(\Omega_e)$, i.e., the functions of these two spaces differ only by their behavior at infinity.

Since we are dealing with Sobolev spaces, even a strong Lipschitz boundary $\Gamma \in C^{0,1}$ is admissible. The fact that this boundary Γ is also unbounded implies that we have to use weighted trace spaces like in Amrouche (2002). For this purpose, we consider the space

$$W^{1/2}(\Gamma) = \left\{ v : \frac{v}{\sqrt{\varrho}\log \varrho} \in H^{1/2}(\Gamma) \right\}. \tag{5.179}$$

Its dual space $W^{-1/2}(\Gamma)$ is defined via W^0-duality, i.e., considering the pivot space

$$W^0(\Gamma) = \left\{ v : \frac{v}{\sqrt{\varrho}\log \varrho} \in L^2(\Gamma) \right\}. \tag{5.180}$$

Analogously as for the trace theorem (A.531), if $v \in W^1(\Omega_e)$ then the trace of v fulfills

$$\gamma_0 v = v|_\Gamma \in W^{1/2}(\Gamma). \tag{5.181}$$

Moreover, the trace of the normal derivative can be also defined, and it holds that

$$\gamma_1 v = \frac{\partial v}{\partial n}|_\Gamma \in W^{-1/2}(\Gamma). \tag{5.182}$$

We remark further that the restriction of the trace of v to Γ_p is such that

$$\gamma_0 v|_{\Gamma_p} = v|_{\Gamma_p} \in H^{1/2}(\Gamma_p), \tag{5.183}$$

$$\gamma_1 v|_{\Gamma_p} = \frac{\partial v}{\partial n}|_{\Gamma_p} \in H^{-1/2}(\Gamma_p), \tag{5.184}$$

and its restriction to Γ_∞ yields

$$\gamma_0 v|_{\Gamma_\infty} = v|_{\Gamma_\infty} \in W^{1/2}(\Gamma_\infty), \tag{5.185}$$

$$\gamma_1 v|_{\Gamma_\infty} = \frac{\partial v}{\partial n}|_{\Gamma_\infty} \in W^{-1/2}(\Gamma_\infty). \tag{5.186}$$

5.8.2 Application to the integral equation

The existence and uniqueness of the solution for the direct scattering problem (5.13), due the integral representation formula (5.153), can be characterized by using the integral equation (5.164). For this purpose and in accordance with the considered function spaces, we take $\mu \in H^{1/2}(\Gamma_p)$ and $\nu \in H^{-1/2}(\Gamma_p)$. Furthermore, we consider that $Z \in L^\infty(\Gamma_p)$ and that $f_z \in H^{-1/2}(\Gamma_p)$, even though strictly speaking $f_z \in \widetilde{H}^{-1/2}(\Gamma_p)$.

It holds that the single and double layer potentials defined respectively in (5.155) and (5.156) are linear and continuous integral operators such that

$$\mathcal{S} : H^{-1/2}(\Gamma_p) \longrightarrow W^1(\Omega_e) \qquad \text{and} \qquad \mathcal{D} : H^{1/2}(\Gamma_p) \longrightarrow W^1(\Omega_e). \tag{5.187}$$

The boundary integral operators (5.162) and (5.163) are also linear and continuous applications, and they are such that

$$S : H^{-1/2}(\Gamma_p) \longrightarrow W^{1/2}(\Gamma) \qquad \text{and} \qquad D : H^{1/2}(\Gamma_p) \longrightarrow W^{1/2}(\Gamma). \tag{5.188}$$

When we restrict them to Γ_p, then it holds that

$$S|_{\Gamma_p} : H^{-1/2}(\Gamma_p) \longrightarrow H^{1/2}(\Gamma_p) \qquad \text{and} \qquad D|_{\Gamma_p} : H^{1/2}(\Gamma_p) \longrightarrow H^{1/2}(\Gamma_p). \tag{5.189}$$

Let us consider the integral equation (5.164), which is given in terms of boundary layer potentials, for $\mu \in H^{1/2}(\Gamma_p)$, by

$$(1 + \mathcal{I}_0)\frac{\mu}{2} + S(Z\mu) - D(\mu) = S(f_z) \qquad \text{in } \ H^{1/2}(\Gamma_p). \tag{5.190}$$

Due the imbedding properties of Sobolev spaces and in the same way as for the half-plane impedance Laplace problem, it holds that the left-hand side of the integral equation corresponds to an identity and two compact operators, and thus Fredholm's alternative holds.

Since the Fredholm alternative applies to the integral equation, therefore it applies also to the direct scattering problem (5.13) due the integral representation formula. The existence of the scattering problem's solution is thus determined by its uniqueness, and the wave numbers $k \in \mathbb{C}$ and impedances $Z \in \mathbb{C}$ for which the uniqueness is lost constitute a countable set, which we call respectively wave number spectrum and impedance spectrum of the scattering problem and denote it by σ_k and σ_Z. The spectrum σ_k considers a fixed Z and, conversely, the spectrum σ_Z considers a fixed k. The existence and uniqueness of the solution is therefore ensured almost everywhere. The same holds obviously for the solution of the integral equation, whose wave number spectrum and impedance spectrum we denote respectively by ς_k and ς_Z. Since each integral equation is derived from the scattering problem, it holds that $\sigma_k \subset \varsigma_k$ and $\sigma_Z \subset \varsigma_Z$. The converse, though, is not necessarily true. In any way, the sets $\varsigma_k \setminus \sigma_k$ and $\varsigma_Z \setminus \sigma_Z$ are at most countable.

In conclusion, the scattering problem (5.13) admits a unique solution u if $k \notin \sigma_k$ and $Z \notin \sigma_Z$, and the integral equation (5.164) admits in the same way a unique solution μ if $k \notin \varsigma_k$ and $Z \notin \varsigma_Z$.

5.9 Dissipative problem

The dissipative problem considers waves that dissipate their energy as they propagate and are modeled by considering a complex wave number or a complex impedance. The use of a complex wave number $k \in \mathbb{C}$ whose imaginary part is strictly positive, i.e., such that $\mathfrak{Im}\{k\} > 0$, ensures an exponential decrease at infinity for both the volume and the surface waves. On the other hand, the use of a complex impedance $Z_\infty \in \mathbb{C}$ with a strictly positive imaginary part, i.e., $\mathfrak{Im}\{Z_\infty\} > 0$, ensures only an exponential decrease at infinity for the surface waves. In the first case, when considering a complex wave number k, and

due the dissipative nature of the medium, it is no longer suited to take progressive plane volume waves in the form of (5.16) and (5.17) respectively as the incident field u_I and the reflected field u_R. In both cases, likewise, it is no longer suited to take progressive plane surface waves in the form of (5.19) as the incident field u_I. Instead, we have to take a wave source at a finite distance from the perturbation. For example, we can consider a point source located at $\boldsymbol{z} \in \Omega_e$, in which case we have only an incident field, which is given, up to a multiplicative constant, by

$$u_I(\boldsymbol{x}) = G(\boldsymbol{x}, \boldsymbol{z}), \tag{5.191}$$

where G denotes the Green's function (5.92). This incident field u_I satisfies the Helmholtz equation with a source term in the right-hand side, namely

$$\Delta u_I + k^2 u_I = \delta_{\boldsymbol{z}} \qquad \text{in } \mathcal{D}'(\Omega_e), \tag{5.192}$$

which holds also for the total field u_T but not for the scattered field u, in which case the Helmholtz equation remains homogeneous. For a general source distribution g_s, whose support is contained in Ω_e, the incident field can be expressed by

$$u_I(\boldsymbol{x}) = G(\boldsymbol{x}, \boldsymbol{z}) * g_s(\boldsymbol{z}) = \int_{\Omega_e} G(\boldsymbol{x}, \boldsymbol{z})\, g_s(\boldsymbol{z})\, \mathrm{d}\boldsymbol{z}. \tag{5.193}$$

This incident field u_I satisfies now

$$\Delta u_I + k^2 u_I = g_s \qquad \text{in } \mathcal{D}'(\Omega_e), \tag{5.194}$$

which holds again also for the total field u_T but not for the scattered field u.

It is not difficult to see that all the performed developments for the non-dissipative case are still valid when considering dissipation. The only difference is that now either a complex wave number k such that $\mathfrak{Im}\{k\} > 0$, or a complex impedance Z_∞ such that $\mathfrak{Im}\{Z_\infty\} > 0$, or both, have to be taken everywhere into account.

5.10 Variational formulation

To solve the integral equation we convert it to its variational or weak formulation, i.e., we solve it with respect to a certain test function in a bilinear (or sesquilinear) form. Basically, the integral equation is multiplied by the (conjugated) test function and then the equation is integrated over the boundary of the domain. The test function is taken in the same function space as the solution of the integral equation.

The variational formulation for the integral equation (5.190) searches $\mu \in H^{1/2}(\Gamma_p)$ such that $\forall \varphi \in H^{1/2}(\Gamma_p)$ we have that

$$\Big\langle (1 + \mathcal{I}_0)\frac{\mu}{2} + S(Z\mu) - D(\mu), \varphi \Big\rangle = \big\langle S(f_z), \varphi \big\rangle. \tag{5.195}$$

5.11 Numerical discretization

5.11.1 Discretized function spaces

The scattering problem (5.13) is solved numerically with the boundary element method by employing a Galerkin scheme on the variational formulation of the integral equation. We use on the boundary surface Γ_p Lagrange finite elements of type $\mathbb{P}_1$. The surface Γ_p is approximated by the triangular mesh Γ_p^h, composed by T flat triangles T_j, for $1 \leq j \leq T$, and I nodes $\boldsymbol{r}_i \in \mathbb{R}^3$, $1 \leq i \leq I$. The triangles have a diameter less or equal than h, and their vertices or corners, i.e., the nodes $\boldsymbol{r}_i$, are on top of Γ_p, as shown in Figure 5.8. The diameter of a triangle K is given by

$$\operatorname{diam}(K) = \sup_{\boldsymbol{x},\boldsymbol{y} \in K} |\boldsymbol{y} - \boldsymbol{x}|. \tag{5.196}$$

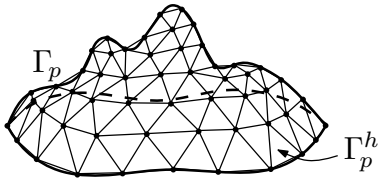

FIGURE 5.8. Mesh Γ_p^h, discretization of Γ_p.

The function space $H^{1/2}(\Gamma_p)$ is approximated using the conformal space of continuous piecewise linear polynomials with complex coefficients

$$Q_h = \big\{ \varphi_h \in C^0(\Gamma_p^h) \,:\, \varphi_h|_{T_j} \in \mathbb{P}_1(\mathbb{C}), \;\; 1 \leq j \leq T \big\}. \tag{5.197}$$

The space Q_h has a finite dimension I, and we describe it using the standard base functions for finite elements of type $\mathbb{P}_1$, which we denote by $\{\chi_j\}_{j=1}^I$. The base function χ_j is associated with the node $\boldsymbol{r}_j$ and has its support $\operatorname{supp} \chi_j$ on the triangles that have $\boldsymbol{r}_j$ as one of their vertices. On $\boldsymbol{r}_j$ it has a value of one and on the opposed edges of the triangles its value is zero, being linearly interpolated in between and zero otherwise.

In virtue of this discretization, any function $\varphi_h \in Q_h$ can be expressed as a linear combination of the elements of the base, namely

$$\varphi_h(\boldsymbol{x}) = \sum_{j=1}^{I} \varphi_j \, \chi_j(\boldsymbol{x}) \qquad \text{for } \; \boldsymbol{x} \in \Gamma_p^h, \tag{5.198}$$

where $\varphi_j \in \mathbb{C}$ for $1 \leq j \leq I$. The solution $\mu \in H^{1/2}(\Gamma_p)$ of the variational formulation (5.195) can be therefore approximated by

$$\mu_h(\boldsymbol{x}) = \sum_{j=1}^{I} \mu_j \, \chi_j(\boldsymbol{x}) \qquad \text{for } \; \boldsymbol{x} \in \Gamma_p^h, \tag{5.199}$$

where $\mu_j \in \mathbb{C}$ for $1 \leq j \leq I$. The function f_z can be also approximated by

$$f_z^h(\boldsymbol{x}) = \sum_{j=1}^{I} f_j \, \chi_j(\boldsymbol{x}) \qquad \text{for } \boldsymbol{x} \in \Gamma_p^h, \quad \text{with } f_j = f_z(\boldsymbol{r}_j). \tag{5.200}$$

5.11.2 Discretized integral equation

To see how the boundary element method operates, we apply it to the variational formulation (5.195). We characterize all the discrete approximations by the index h, including also the impedance and the boundary layer potentials. The numerical approximation of (5.195) leads to the discretized problem that searches $\mu_h \in Q_h$ such that $\forall \varphi_h \in Q_h$

$$\Big\langle (1 + \mathcal{I}_0^h)\frac{\mu_h}{2} + S_h(Z_h\mu_h) - D_h(\mu_h), \varphi_h \Big\rangle = \big\langle S_h(f_z^h), \varphi_h \big\rangle. \tag{5.201}$$

Considering the decomposition of μ_h in terms of the base $\{\chi_j\}$ and taking as test functions the same base functions, $\varphi_h = \chi_i$ for $1 \leq i \leq I$, yields the discrete linear system

$$\sum_{j=1}^{I} \mu_j \left(\frac{1}{2}\big\langle (1 + \mathcal{I}_0^h)\chi_j, \chi_i \big\rangle + \langle S_h(Z_h\chi_j), \chi_i \rangle - \langle D_h(\chi_j), \chi_i \rangle \right) = \sum_{j=1}^{I} f_j \, \langle S_h(\chi_j), \chi_i \rangle. \tag{5.202}$$

This constitutes a system of linear equations that can be expressed as a linear matrix system:

$$\begin{cases} \text{Find } \boldsymbol{\mu} \in \mathbb{C}^I \text{ such that} \\ \boldsymbol{M}\boldsymbol{\mu} = \boldsymbol{b}. \end{cases} \tag{5.203}$$

The elements m_{ij} of the matrix $\boldsymbol{M}$ are given, for $1 \leq i, j \leq I$, by

$$m_{ij} = \frac{1}{2}\big\langle (1 + \mathcal{I}_0^h)\chi_j, \chi_i \big\rangle + \langle S_h(Z_h\chi_j), \chi_i \rangle - \langle D_h(\chi_j), \chi_i \rangle, \tag{5.204}$$

and the elements b_i of the vector $\boldsymbol{b}$ by

$$b_i = \big\langle S_h(f_z^h), \chi_i \big\rangle = \sum_{j=1}^{I} f_j \, \langle S_h(\chi_j), \chi_i \rangle \qquad \text{for } 1 \leq i \leq I. \tag{5.205}$$

The discretized solution u_h, which approximates u, is finally obtained by discretizing the integral representation formula (5.153) according to

$$u_h = \mathcal{D}_h(\mu_h) - \mathcal{S}_h(Z_h\mu_h) + \mathcal{S}_h(f_z^h), \tag{5.206}$$

which, more specifically, can be expressed as

$$u_h = \sum_{j=1}^{I} \mu_j \big(\mathcal{D}_h(\chi_j) - \mathcal{S}_h(Z_h\chi_j) \big) + \sum_{j=1}^{I} f_j \, \mathcal{S}_h(\chi_j). \tag{5.207}$$

We remark that the resulting matrix $\boldsymbol{M}$ is in general complex, full, non-symmetric, and with dimensions $I \times I$. The right-hand side vector $\boldsymbol{b}$ is complex and of size I. The boundary element calculations required to compute numerically the elements of $\boldsymbol{M}$ and $\boldsymbol{b}$ have to be performed carefully, since the integrals that appear become singular when the involved segments are adjacent or coincident, due the singularity of the Green's function at

its source point. On Γ_0, the singularity of the image source point has to be taken additionally into account for these calculations.

5.12 Boundary element calculations

The boundary element calculations build the elements of the matrix $\boldsymbol{M}$ resulting from the discretization of the integral equation, i.e., from (5.203). They permit thus to compute numerically expressions like (5.204). To evaluate the appearing singular integrals, we adapt the semi-numerical methods described in the report of Bendali & Devys (1986).

We use the same notation as in Section D.12, and the required boundary element integrals, for $a, b \in \{0, 1\}$ and $c, d \in \{1, 2, 3\}$, are again

$$ZA_{a,b}^{c,d} = \int_K \int_L \left(\frac{s_c}{h_c^K}\right)^a \left(\frac{t_d}{h_d^L}\right)^b G(\boldsymbol{x}, \boldsymbol{y}) \, \mathrm{d}L(\boldsymbol{y}) \, \mathrm{d}K(\boldsymbol{x}), \tag{5.208}$$

$$ZB_{a,b}^{c,d} = \int_K \int_L \left(\frac{s_c}{h_c^K}\right)^a \left(\frac{t_d}{h_d^L}\right)^b \frac{\partial G}{\partial n_{\boldsymbol{y}}}(\boldsymbol{x}, \boldsymbol{y}) \, \mathrm{d}L(\boldsymbol{y}) \, \mathrm{d}K(\boldsymbol{x}). \tag{5.209}$$

All the integrals that stem from the numerical discretization can be expressed in terms of these two basic boundary element integrals. The impedance is again discretized as a piecewise constant function Z_h, which on each triangle T_j adopts a constant value $Z_j \in \mathbb{C}$. The integrals of interest are the same as for the full-space impedance Helmholtz problem and we consider furthermore that

$$\left\langle (1 + \mathcal{I}_0^h)\chi_j, \chi_i \right\rangle = \begin{cases} \langle \chi_j, \chi_i \rangle & \text{if } \boldsymbol{r}_j \in \Gamma_+, \\ 2 \langle \chi_j, \chi_i \rangle & \text{if } \boldsymbol{r}_j \in \Gamma_0. \end{cases} \tag{5.210}$$

To compute the boundary element integrals (5.208) and (5.209), we can easily isolate the singular part (5.96) of the Green's function (5.92), which corresponds in fact to the Green's function of the Laplace equation in the full-space, and therefore the associated integrals are computed in the same way. The same applies also for its normal derivative. In the case when the triangles K and L are are close enough, e.g., adjacent or coincident, and when $L \in \Gamma_0^h$ or $K \in \Gamma_0^h$, being Γ_0^h the approximation of Γ_0, we have to consider additionally the singular behavior (5.97), which is linked with the presence of the impedance half-space. This behavior can be straightforwardly evaluated by replacing $\boldsymbol{x}$ by $\bar{\boldsymbol{x}}$ in formulae (D.295) to (D.298), i.e., by computing the quantities $ZF_b^d(\bar{\boldsymbol{x}})$ and $ZG_b^d(\bar{\boldsymbol{x}})$ with the corresponding adjustment of the notation. Otherwise, if the triangles are not close enough and for the non-singular part of the Green's function, a three-point Gauss-Lobatto quadrature formula is used. All the other computations are performed in the same manner as in Section D.12 for the full-space Laplace equation.

5.13 Benchmark problem

As benchmark problem we consider the particular case when the domain $\Omega_e \subset \mathbb{R}_+^3$ is taken as the exterior of a half-sphere of radius $R > 0$ that is centered at the origin, as shown

in Figure 5.9. We decompose the boundary of Ω_e as $\Gamma = \Gamma_p \cup \Gamma_\infty$, where Γ_p corresponds to the upper half-sphere, whereas Γ_∞ denotes the remaining unperturbed portion of the half-space's boundary which lies outside the half-sphere and which extends towards infinity. The unit normal $\boldsymbol{n}$ is taken outwardly oriented of Ω_e, e.g., $\boldsymbol{n} = -\boldsymbol{r}$ on Γ_p.

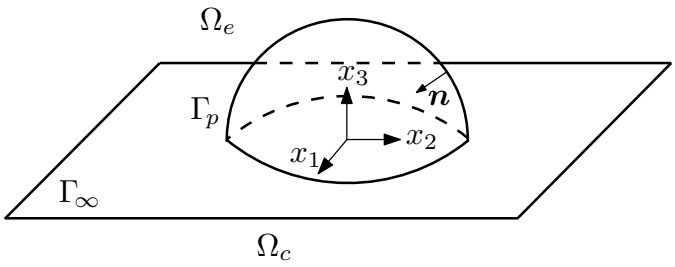

FIGURE 5.9. Exterior of the half-sphere.

The benchmark problem is then stated as

$$\begin{cases} \text{Find } u : \Omega_e \to \mathbb{C} \text{ such that} \\ \Delta u + k^2 u = 0 \qquad \text{in } \Omega_e, \\ -\dfrac{\partial u}{\partial n} + Zu = f_z \qquad \text{on } \Gamma, \\ \text{+ Outgoing radiation condition as } |\boldsymbol{x}| \to \infty, \end{cases} \tag{5.211}$$

where we consider a wave number $k \in \mathbb{C}$, a constant impedance $Z \in \mathbb{C}$ throughout Γ and where the radiation condition is as usual given by (5.6). As incident field u_I we consider the same Green's function, namely

$$u_I(\boldsymbol{x}) = G(\boldsymbol{x}, \boldsymbol{z}), \tag{5.212}$$

where $\boldsymbol{z} \in \Omega_c$ denotes the source point of our incident field. The impedance data function f_z is hence given by

$$f_z(\boldsymbol{x}) = \frac{\partial G}{\partial n_{\boldsymbol{x}}}(\boldsymbol{x}, \boldsymbol{z}) - ZG(\boldsymbol{x}, \boldsymbol{z}), \tag{5.213}$$

and its support is contained in Γ_p. The analytic solution for the benchmark problem (5.211) is then clearly given by

$$u(\boldsymbol{x}) = -G(\boldsymbol{x}, \boldsymbol{z}). \tag{5.214}$$

The goal is to retrieve this solution numerically with the integral equation techniques and the boundary element method described throughout this chapter.

For the computational implementation and the numerical resolution of the benchmark problem, we consider integral equation (5.164). The linear system (5.203) resulting from the discretization (5.201) of its variational formulation (5.195) is solved computationally with finite boundary elements of type $\mathbb{P}_1$ by using subroutines programmed in Fortran 90, by generating the mesh Γ_p^h of the boundary with the free software Gmsh 2.4, and by representing graphically the results in Matlab 7.5 (R2007b).

We consider a radius $R = 1$, a wave number $k = 3.5$, a constant impedance $Z = 3$, and for the incident field a source point $\boldsymbol{z} = (0, 0, 0)$. The discretized perturbed boundary curve Γ_p^h has $I = 641$ nodes, $T = 1224$ triangles and a discretization step $h = 0.1676$, being

$$h = \max_{1 \leq j \leq T} \operatorname{diam}(T_j). \tag{5.215}$$

The numerically calculated trace of the solution μ_h of the benchmark problem, which was computed by using the boundary element method, is depicted in Figure 5.10. In the same manner, the numerical solution u_h is illustrated in Figures 5.11 and 5.12 for an angle $\varphi = 0$. It can be observed that the numerical solution is close to the exact one.

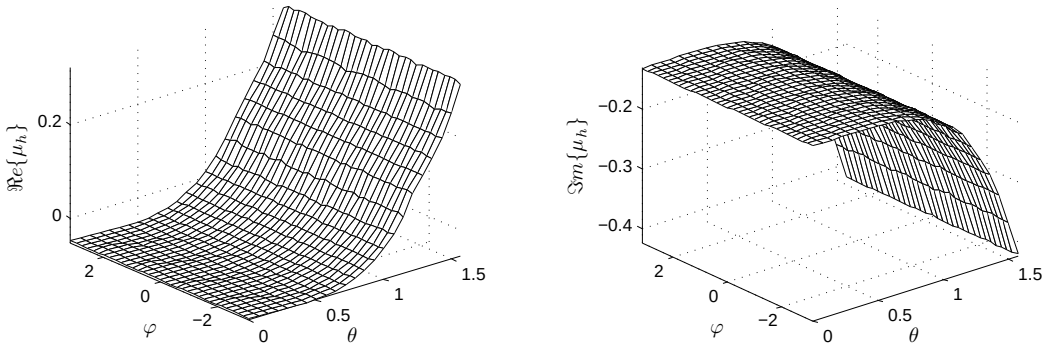

(a) Real part (b) Imaginary part

FIGURE 5.10. Numerically computed trace of the solution μ_h.

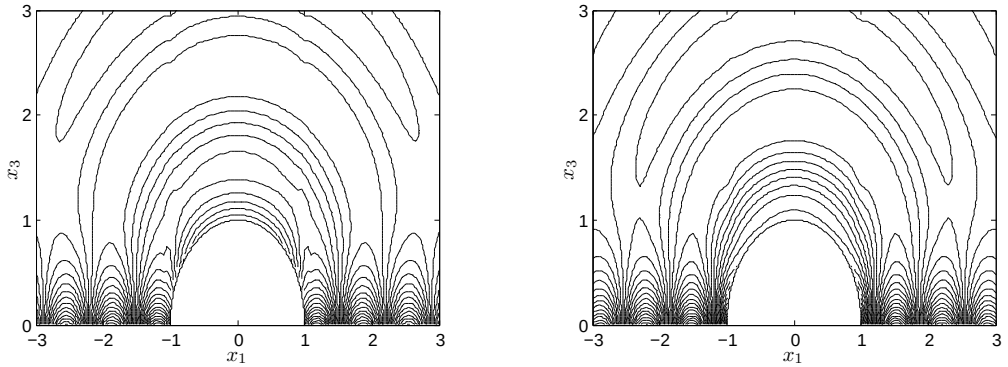

(a) Real part (b) Imaginary part

FIGURE 5.11. Contour plot of the numerically computed solution u_h for $\varphi = 0$.

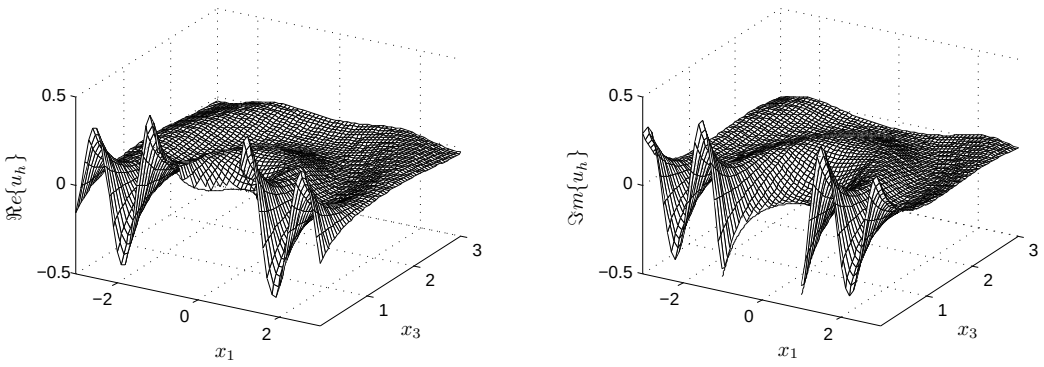

(a) Real part (b) Imaginary part

FIGURE 5.12. Oblique view of the numerically computed solution u_h for $\varphi = 0$.

Likewise as in (D.346), we define the relative error of the trace of the solution as

$$E_2(h, \Gamma_p^h) = \frac{\|\Pi_h \mu - \mu_h\|_{L^2(\Gamma_p^h)}}{\|\Pi_h \mu\|_{L^2(\Gamma_p^h)}}, \tag{5.216}$$

where $\Pi_h \mu$ denotes the Lagrange interpolating function of the exact solution's trace μ, i.e.,

$$\Pi_h \mu(\boldsymbol{x}) = \sum_{j=1}^{I} \mu(\boldsymbol{r}_j)\, \chi_j(\boldsymbol{x}) \quad \text{and} \quad \mu_h(\boldsymbol{x}) = \sum_{j=1}^{I} \mu_j\, \chi_j(\boldsymbol{x}) \quad \text{for } \boldsymbol{x} \in \Gamma_p^h. \tag{5.217}$$

In our case, for a step $h = 0.1676$, we obtained a relative error of $E_2(h, \Gamma_p^h) = 0.08726$.

As in (D.350), we define the relative error of the solution as

$$E_\infty(h, \Omega_L) = \frac{\|u - u_h\|_{L^\infty(\Omega_L)}}{\|u\|_{L^\infty(\Omega_L)}}, \tag{5.218}$$

being $\Omega_L = \{\boldsymbol{x} \in \Omega_e : \|\boldsymbol{x}\|_\infty < L\}$ for $L > 0$. We consider $L = 3$ and approximate Ω_L by a triangular finite element mesh of refinement h near the boundary. For $h = 0.1676$, the relative error that we obtained for the solution was $E_\infty(h, \Omega_L) = 0.08685$.

The results for different mesh refinements, i.e., for different numbers of triangles T, nodes I, and discretization steps h for Γ_p^h, are listed in Table 5.1. These results are illustrated graphically in Figure 5.13. It can be observed that the relative errors are more or less of order h, but they tend to stagnate due the involved accuracy of the Green's function.

TABLE 5.1. Relative errors for different mesh refinements.

T	I	h	$E_2(h, \Gamma_p^h)$	$E_\infty(h, \Omega_L)$
46	30	0.7071	$1.617 \cdot 10^{-1}$	$3.171 \cdot 10^{-1}$
168	95	0.4320	$8.714 \cdot 10^{-2}$	$1.574 \cdot 10^{-1}$
466	252	0.2455	$8.412 \cdot 10^{-2}$	$9.493 \cdot 10^{-2}$
700	373	0.1987	$8.537 \cdot 10^{-2}$	$9.071 \cdot 10^{-2}$
1224	641	0.1676	$8.726 \cdot 10^{-2}$	$8.685 \cdot 10^{-2}$
2100	1090	0.1286	$8.868 \cdot 10^{-2}$	$8.399 \cdot 10^{-2}$

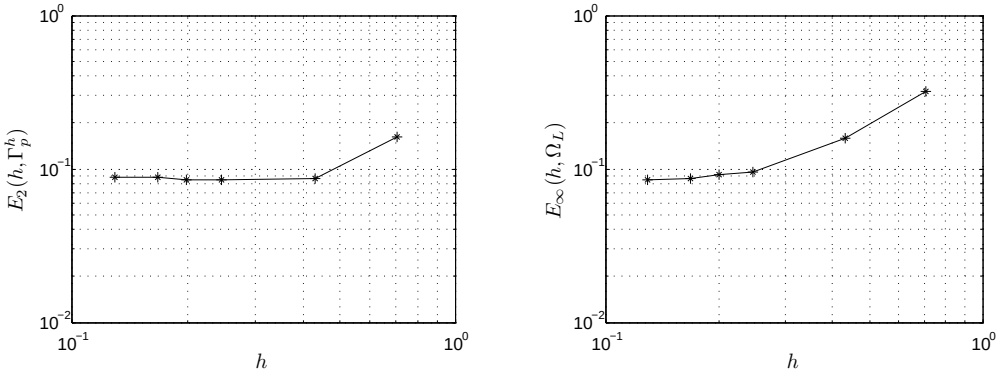

(a) Relative error $E_2(h, \Gamma_p^h)$ (b) Relative error $E_\infty(h, \Omega_L)$

FIGURE 5.13. Logarithmic plots of the relative errors versus the discretization step.

VI. HARBOR RESONANCES IN COASTAL ENGINEERING

6.1 Introduction

In this chapter we consider the application of the half-plane Helmholtz problem described in Chapter III to the computation of harbor resonances in coastal engineering.

We consider the problem of computing resonances for the Helmholtz equation in a two-dimensional compactly perturbed half-plane with an impedance boundary condition. One of its main applications corresponds to coastal engineering, acting as a simple model to determine the resonant states of a maritime harbor. In this model the sea is modeled as an infinite half-plane, which is locally perturbed by the presence of the harbor, and the coast is represented by means of an impedance boundary condition. Some references on the harbor oscillations that are responsible for these resonances are Mei (1983), Mei et al. (2005), Herbich (1999), and Panchang & Demirbilek (2001).

Resonances are closely related to the phenomena of seiching (in lakes and harbors) and sloshing (in coffee cups and storage tanks), which correspond to standing waves in enclosed or partially enclosed bodies of water. These phenomena have been observed already since very early times. Scientific studies date from Merian (1828) and Poisson (1828–1829), and especially from the observations in the Lake of Geneva by Forel (1895), which began in 1869. A thorough and historical review of the seiching phenomenon in harbors and further references can be found in Miles (1974).

Oscillations in harbors, though, were first studied for circular and rectangular closed basins by Lamb (1916). More practical approaches for the same kind of basins, but now connected to the open sea through a narrow mouth, were then implemented respectively by McNown (1952) and Kravtchenko & McNown (1955).

But it was the paper of Miles & Munk (1961), the first to treat harbor oscillations by a scattering theory, which really arose the research interest on the subject. Their work, together with the contributions of Le Méhauté (1961), Ippen & Goda (1963), Raichlen & Ippen (1965), and Raichlen (1966), made the description of harbor oscillations to become fairly close to the experimentally observed one. Theories to deal with arbitrary harbor configurations were available after Hwang & Tuck (1970) and Lee (1969, 1971), who worked with boundary integral equation methods to calculate the oscillation in harbors of constant depth with arbitrary shape. Mei & Chen (1975) developed a hybrid-boundary-element technique to also study harbors of arbitrary geometry. Harbor resonances using the finite element method are likewise computed in Walker & Brebbia (1978). A comprehensive list of references can be found in Yu & Chwang (1994).

The mild-slope equation, which describes the combined effects of refraction and diffraction of linear water waves, was first suggested by Eckart (1952) and later rederived by Berkhoff (1972*a*,*b*, 1976), Smith & Sprinks (1975), and others, and is now well-accepted as the method for estimating coastal wave conditions. It corresponds to an approximate model developed in the framework of the linear water-wave theory (vid. Section A.10), which assumes waves of small amplitude and a mild slope on the bottom of the sea, i.e., a slowly

varying bathymetry. The mild-slope equation models the propagation and transformation of water waves, as they travel through waters of varying depth and interact with lateral boundaries such as cliffs, beaches, seawalls, and breakwaters. As a result, it describes the variations in wave amplitude, or equivalently wave height. From the wave amplitude, the amplitude of the flow velocity oscillations underneath the water surface can also be computed. These quantities, wave amplitude and flow-velocity amplitude, may subsequently be used to determine the wave effects on coastal and offshore structures, ships and other floating objects, sediment transport and resulting geomorphology changes of the sea bed and coastline, mean flow fields and mass transfer of dissolved and floating materials. Most often, the mild-slope equation is solved by computers using methods from numerical analysis. The mild-slope equation is a usually expressed in an elliptic form, and it turns into the Helmholtz equation for uniform water depths. Different kinds of mild-slope equations have been derived (Liu & Shi 2008). A detailed survey of the literature on the mild-slope and its related equations is provided by Hsu, Lin, Wen & Ou (2006). Some examinations on the validity of the theory are performed by Booij (1983) and Ehrenmark & Williams (2001).

A resonance of a different type is given by the so-called Helmholtz mode when the oscillatory motion inside the harbor is much slower than each of the normal modes (Burrows 1985). It corresponds to the resonant mode with the longest period, where the water appears to move up and down unison throughout the harbor, which seems to have been first studied by Miles & Munk (1961) and which appears to be particularly significant for harbors responding to the energy of a tsunami. We remark that from the mathematical point of view, resonances correspond to poles of the scattering and radiation potentials when they are extended to the complex frequency domain (cf. Poisson & Joly 1991). Harbor resonance should be avoided or minimized in harbor planning and operation to reduce adverse effects such as hazardous navigation and mooring of vessels, deterioration of structures, and sediment deposition or erosion within the harbor.

Along rigid, impermeable vertical walls a Neumann boundary condition is used, since there is no flow normal to the surface. However, in general an impedance boundary condition is used along coastlines or permeable structures, to account for a partial reflection of the flow on the boundary (Demirbilek & Panchang 1998). A study of harbor resonances using an approximated Dirichlet-to-Neumann operator and a model based on the Helmholtz equation with an impedance boundary condition on the coast was done by Quaas (2003). In the current chapter this problem is extended to be solved with integral equation techniques, by profiting from the knowledge of the Green's function developed in Chapter III.

This chapter is structured in 4 sections, including this introduction. The harbor scattering problem is presented in Section 6.2. Section 6.3 describes the computation of resonances for the harbor scattering problem by using integral equation techniques and the boundary element method. Finally, in Section 6.4 a benchmark problem based on a rectangular harbor is presented and solved numerically.

6.2 Harbor scattering problem

We are interested in computing the resonances of a maritime harbor, as the one depicted in Figure 6.1 The sea is modeled as the compactly perturbed half-plane $\Omega_e \subset \mathbb{R}^2_+$, where $\mathbb{R}^2_+ = \{(x_1, x_2) \in \mathbb{R}^2 : x_2 > 0\}$ and where the perturbation represents the presence of the harbor. We denote its boundary by Γ, which is regular (e.g., of class C^2) and decomposed according to $\Gamma = \Gamma_p \cup \Gamma_\infty$. The perturbed boundary describing the harbor is denoted by Γ_p, while Γ_∞ denotes the remaining unperturbed boundary of $\mathbb{R}^2_+$, which represents the coast and extends towards infinity on both sides. The unit normal $\boldsymbol{n}$ is taken outwardly oriented of Ω_e and the land is represented by the complementary domain $\Omega_c = \mathbb{R}^2 \setminus \overline{\Omega_e}$.

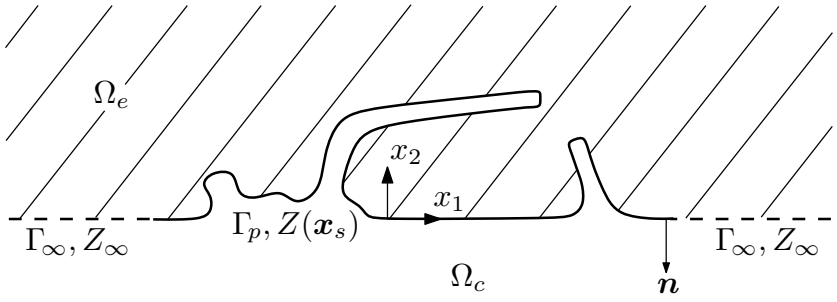

FIGURE 6.1. Harbor domain.

To describe the propagation of time-harmonic linear water waves over a slowly varying bathymetry we consider for the wave amplitude or surface elevation η the mild-slope equation (Herbich 1999)

$$\operatorname{div}(cc_g\nabla\eta) + k^2 cc_g\eta = 0 \qquad \text{in } \Omega_e, \tag{6.1}$$

where k is the wave number, where c and c_g denote respectively the local phase and group velocities of a plane progressive wave of angular frequency ω, and where the time convention $e^{-i\omega t}$ is used. The local phase and group velocities are given respectively by

$$c = \frac{\omega}{k} \qquad \text{and} \qquad c_g = \frac{\mathrm{d}\omega}{\mathrm{d}k} = \frac{c}{2}\left(1 + \frac{2kh}{\sinh(2kh)}\right), \tag{6.2}$$

where h denotes the local water depth. The wave number k and the local depth h vary slowly in the horizontal directions x_1 and x_2 according to the frequency dispersion relation

$$\omega^2 = gk\tanh(kh), \tag{6.3}$$

where g is the gravitational acceleration. We remark that the mild-slope equation (6.1) holds also for the velocity potential ϕ, since it is related to the wave height η through

$$g\eta = i\omega\phi. \tag{6.4}$$

We observe furthermore that through the transformation $\psi = \sqrt{cc_g}\,\eta$, the mild-slope equation (6.1) can be cast in the form of a Helmholtz equation, i.e.,

$$\Delta\psi + k_c^2\psi = 0, \qquad \text{where } k_c^2 = k^2 - \frac{\Delta(cc_g)^{1/2}}{(cc_g)^{1/2}}. \tag{6.5}$$

In shallow water, when $kh \ll 1$, the difference $k_c^2 - k^2$ may become appreciable. In this case $\tanh(kh) \approx kh$ and $\sinh(kh) \approx kh$, and thus we have from (6.3) that (Radder 1979)

$$k^2 \approx \frac{\omega^2}{gh}, \qquad c \approx c_g \approx \sqrt{gh}, \qquad \text{and} \qquad k_c^2 \approx \frac{\omega^2}{gh} - \frac{\Delta h}{2h} + \frac{|\nabla h|^2}{4h^2}. \tag{6.6}$$

It follows that k_c may be approximated by k if

$$|\Delta h| \ll 2\omega^2/g \qquad \text{and} \qquad |\nabla h|^2 \ll 4\omega^2 h/g, \tag{6.7}$$

implying a slowly varying depth and a small bottom slope, or high-frequency wave propagation. Hence, if (6.7) is satisfied for shallow water, then we can readily work with the Helmholtz equation

$$\Delta\psi + k^2\psi = 0 \qquad \text{in } \Omega_e. \tag{6.8}$$

On the other hand, for short waves in deep water, when $kh \gg 1$, we have that $c_g \approx c/2$ is more or less constant and thus again the Helmholtz equation (6.8) applies. We observe that the Helmholtz equation holds as well whenever the depth h is constant, i.e.,

$$\Delta\eta + k^2\eta = 0 \qquad \text{in } \Omega_e. \tag{6.9}$$

On coastline and surface-protruding structures, the following impedance or partial reflection boundary condition is used (cf., e.g., Berkhoff 1976, Tsay et al. 1989):

$$-\frac{\partial\eta}{\partial n} + Z\eta = 0 \qquad \text{on } \Gamma, \tag{6.10}$$

where the impedance Z is taken as purely imaginary and typically represented by means of a reflection coefficient K_r as (Herbich 1999)

$$Z = ik\,\frac{1 - K_r}{1 + K_r}. \tag{6.11}$$

The coefficient K_r varies between 0 and 1, and specific values for different types of reflecting surfaces have been compiled by Thompson, Chen & Hadley (1996). Values of K_r are normally chosen based on the boundary material and shape, e.g., for a natural beach $0.05 \le K_r \le 0.2$ and for a vertical wall with the crown above the water $0.7 \le K_r \le 1.0$. Effects such as slope, permeability, relative depth, wave period, breaking, and overtopping can be considered in selecting values within these fairly wide ranges. We note that Z is equal to zero for fully reflective boundaries ($K_r = 1$) and it is equal to ik for fully absorbing boundaries ($K_r = 0$). Thus the reflection characteristics of boundaries that are not fully reflective will inherently have some dependence on local wavelength through k. In practice, wave periods range from about 6 s to 20 s. For a representative water depth of 10 m, the value of k ranges from 0.03 m^{-1} to 0.13 m^{-1}. For long waves, k and Z become small, and boundaries may behave as nearly full reflectors regardless of the value of K_r. It may be verified that (6.10) is strictly valid only for fully reflecting boundaries ($K_r = 1$). For

partially reflecting boundaries, it is valid only if waves approach the boundary normally. For other conditions (6.10) is approximate and may produce distortions. More accurate boundary conditions are described in Panchang & Demirbilek (2001). In our model, we assume that the impedance can be decomposed as

$$Z(\boldsymbol{x}) = Z_\infty + Z_p(\boldsymbol{x}), \qquad \boldsymbol{x} \in \Gamma, \tag{6.12}$$

being Z_∞ constant throughout Γ, and depending $Z_p(\boldsymbol{x})$ on the position $\boldsymbol{x}$ with a bounded support contained in Γ_p.

We consider now the direct scattering problem of linear water waves around a harbor. The total field η is decomposed as $\eta = u_I + u_R + u$, where u_I and u_R are respectively the known incident and reflected fields, and where u denotes the unknown scattered field. The goal is to find u as a solution to the Helmholtz equation in Ω_e, satisfying an outgoing radiation condition, and such that the total field η satisfies a homogeneous impedance boundary condition on Γ. We have thus for the scattered field that

$$-\frac{\partial u}{\partial n} + Zu = f_z \qquad \text{on } \Gamma, \tag{6.13}$$

where f_z is known, has its support contained in Γ_p, and is given by

$$f_z = \frac{\partial u_I}{\partial n} - Zu_I + \frac{\partial u_R}{\partial n} - Zu_R \qquad \text{on } \Gamma. \tag{6.14}$$

As u_I we take an incident plane volume wave of the form (3.16), with a wave propagation vector $\boldsymbol{k} \in \mathbb{R}^2$ such that $k_2 \leq 0$. The reflected field u_R is thus of the form (3.17) and has a wave propagation vector $\bar{\boldsymbol{k}} = (k_1, -k_2)$. Hence,

$$u_I(\boldsymbol{x}) = e^{i\boldsymbol{k}\cdot\boldsymbol{x}} \qquad \text{and} \qquad u_R(\boldsymbol{x}) = -\left(\frac{Z_\infty + ik_2}{Z_\infty - ik_2}\right) e^{i\bar{\boldsymbol{k}}\cdot\boldsymbol{x}}. \tag{6.15}$$

To eliminate the non-physical solutions, we have to impose also an outgoing radiation condition in the form of (3.6) for the scattered field u, i.e., when $r \to \infty$ it is required that

$$\begin{cases} |u| \leq \dfrac{C}{\sqrt{r}} \quad \text{and} \quad \left|\dfrac{\partial u}{\partial r} - iku\right| \leq \dfrac{C}{r} \quad \text{if } x_2 > \dfrac{1}{2Z_\infty}\ln(1+\beta r), \\ |u| \leq C \quad \text{and} \quad \left|\dfrac{\partial u}{\partial r} - i\xi_p u\right| \leq \dfrac{C}{r} \quad \text{if } x_2 \leq \dfrac{1}{2Z_\infty}\ln(1+\beta r), \end{cases} \tag{6.16}$$

for some constants $C > 0$, where $r = |\boldsymbol{x}|$, $\beta = 8\pi k Z_\infty^2/\xi_p^2$, and $\xi_p = \sqrt{Z_\infty^2 + k^2}$. The harbor scattering problem is thus given by

$$\begin{cases} \text{Find } u : \Omega_e \to \mathbb{C} \text{ such that} \\ \Delta u + k^2 u = 0 \qquad \text{in } \Omega_e, \\ -\dfrac{\partial u}{\partial n} + Zu = f_z \qquad \text{on } \Gamma, \\ \text{+ Outgoing radiation condition as } |\boldsymbol{x}| \to \infty, \end{cases} \tag{6.17}$$

where the outgoing radiation condition is stated in (6.16).

The problem of finding harbor resonances amounts to search wave numbers k for which the scattering problem (6.17) without excitation, i.e., with $f_z = 0$, admits non-zero solutions u. The harbor resonance problem can be hence stated as

$$\begin{cases} \text{Find } k \in \mathbb{C} \text{ and } u : \Omega_e \to \mathbb{C},\ u \neq 0, \text{ such that} \\ \Delta u + k^2 u = 0 \qquad \text{in } \ \Omega_e, \\ -\dfrac{\partial u}{\partial n} + Zu = 0 \qquad \text{on } \ \Gamma, \\ \text{+ Outgoing radiation condition as } |\boldsymbol{x}| \to \infty. \end{cases} \tag{6.18}$$

6.3 Computation of resonances

The resonance problem (6.18) is solved in the same manner as the half-plane impedance Helmholtz problem described in Chapter III, by using integral equation techniques and the boundary element method. The required Green's function G is expressed in (3.93). If we denote the trace of the solution on Γ_p by $\mu = u|_{\Gamma_p}$, then we have from (3.156) that the solution u admits the integral representation

$$u = \mathcal{D}(\mu) - \mathcal{S}(Z\mu) \qquad \text{in } \ \Omega_e, \tag{6.19}$$

where we define for $\boldsymbol{x} \in \Omega_e$ the single and double layer potentials respectively by

$$\mathcal{S}\nu(\boldsymbol{x}) = \int_{\Gamma_p} G(\boldsymbol{x}, \boldsymbol{y})\nu(\boldsymbol{y})\, \mathrm{d}\gamma(\boldsymbol{y}) \quad \text{and} \quad \mathcal{D}\mu(\boldsymbol{x}) = \int_{\Gamma_p} \frac{\partial G}{\partial n_{\boldsymbol{y}}}(\boldsymbol{x}, \boldsymbol{y})\mu(\boldsymbol{y})\, \mathrm{d}\gamma(\boldsymbol{y}). \tag{6.20}$$

If the boundary is decomposed as $\Gamma = \Gamma_0 \cup \Gamma_+$, being

$$\Gamma_0 = \{\boldsymbol{y} \in \Gamma :\ y_2 = 0\} \qquad \text{and} \qquad \Gamma_+ = \{\boldsymbol{y} \in \Gamma :\ y_2 > 0\}, \tag{6.21}$$

then u admits also, from (3.163) and (3.164), the boundary integral representation

$$\frac{u}{2} = D(\mu) - S(Z\mu) \qquad \text{on } \ \Gamma_+, \tag{6.22}$$

$$u = D(\mu) - S(Z\mu) \qquad \text{on } \ \Gamma_0, \tag{6.23}$$

where the boundary integral operators, for $\boldsymbol{x} \in \Gamma$, are defined by

$$S\nu(\boldsymbol{x}) = \int_{\Gamma_p} G(\boldsymbol{x}, \boldsymbol{y})\nu(\boldsymbol{y})\, \mathrm{d}\gamma(\boldsymbol{y}) \quad \text{and} \quad D\mu(\boldsymbol{x}) = \int_{\Gamma_p} \frac{\partial G}{\partial n_{\boldsymbol{y}}}(\boldsymbol{x}, \boldsymbol{y})\mu(\boldsymbol{y})\, \mathrm{d}\gamma(\boldsymbol{y}). \tag{6.24}$$

It holds that (6.22) and (6.23) can be combined on Γ_p into the single integral equation

$$(1 + \mathcal{I}_0)\frac{\mu}{2} + S(Z\mu) - D(\mu) = 0 \qquad \text{on } \ \Gamma_p, \tag{6.25}$$

where $\mathcal{I}_0$ denotes the characteristic or indicator function of the set Γ_0, i.e.,

$$\mathcal{I}_0(\boldsymbol{x}) = \begin{cases} 1 & \text{if } \ \boldsymbol{x} \in \Gamma_0, \\ 0 & \text{if } \ \boldsymbol{x} \notin \Gamma_0. \end{cases} \tag{6.26}$$

The desired resonances are thus given by the wave numbers k for which the integral equation (6.25) admits non-zero solutions μ. Care has to be taken, though, with possible spurious resonances that may appear for the integral equation, which are not resonances of

the original problem (6.18) and which are related with a resonance problem in the complementary domain Ω_c. To find the resonances, we use the boundary element method on the variational formulation of (6.25). This variational formulation, as indicated in (3.198), searches $k \in \mathbb{C}$ and $\mu \in H^{1/2}(\Gamma_p)$, $\mu \neq 0$, such that $\forall \varphi \in H^{1/2}(\Gamma_p)$ we have that

$$\left\langle (1+\mathcal{I}_0)\frac{\mu}{2} + S(Z\mu) - D(\mu), \varphi \right\rangle = 0. \tag{6.27}$$

As performed in Section 3.11 and with the same notation, we discretize (6.27) employing a Galerkin scheme. We use on the boundary curve Γ_p Lagrange finite elements of type $\mathbb{P}_1$. The curve Γ_p is approximated by the discretized curve Γ_p^h, composed by I rectilinear segments T_j, sequentially ordered from left to right for $1 \leq j \leq I$, such that their length $|T_j|$ is less or equal than h, and with their endpoints on top of Γ_p. The function space $H^{1/2}(\Gamma_p)$ is approximated using the conformal space of continuous piecewise linear polynomials with complex coefficients

$$Q_h = \big\{ \varphi_h \in C^0(\Gamma_p^h) \,:\, \varphi_h|_{T_j} \in \mathbb{P}_1(\mathbb{C}), \;\; 1 \leq j \leq I \big\}. \tag{6.28}$$

The space Q_h has a finite dimension $(I+1)$, and we describe it using the standard base functions for finite elements of type $\mathbb{P}_1$, denoted by $\{\chi_j\}_{j=1}^{I+1}$. We approximate the solution $\mu \in H^{1/2}(\Gamma_p)$ by $\mu_h \in Q_h$, being

$$\mu_h(\boldsymbol{x}) = \sum_{j=1}^{I+1} \mu_j \, \chi_j(\boldsymbol{x}) \qquad \text{for } \; \boldsymbol{x} \in \Gamma_p^h, \tag{6.29}$$

where $\mu_j \in \mathbb{C}$ for $1 \leq j \leq I+1$. We characterize all the discrete approximations by the index h, including also the wave number, the impedance and the boundary layer potentials. The numerical approximation of (6.27) becomes searching $\mu_h \in Q_h$ such that $\forall \varphi_h \in Q_h$

$$\left\langle (1+\mathcal{I}_0^h)\frac{\mu_h}{2} + S_h(Z_h\mu_h) - D_h(\mu_h), \varphi_h \right\rangle = 0. \tag{6.30}$$

Considering this decomposition of μ_h in terms of the base $\{\chi_j\}$ and taking as test functions the same base functions, $\varphi_h = \chi_i$ for $1 \leq i \leq I+1$, yields the discrete linear system

$$\sum_{j=1}^{I+1} \mu_j \left(\frac{1}{2}\big\langle (1+\mathcal{I}_0^h)\chi_j, \chi_i \big\rangle + \langle S_h(Z_h\chi_j), \chi_i \rangle - \langle D_h(\chi_j), \chi_i \rangle \right) = 0. \tag{6.31}$$

This can be expressed as the linear matrix system

$$\begin{cases} \text{Find } k_h \in \mathbb{C} \text{ and } \boldsymbol{\mu} \in \mathbb{C}^{I+1}, \, \boldsymbol{\mu} \neq \mathbf{0}, \text{ such that} \\ \boldsymbol{M}(k_h)\, \boldsymbol{\mu} = \mathbf{0}. \end{cases} \tag{6.32}$$

The elements m_{ij} of the matrix $\boldsymbol{M}(k_h)$ are given, for $1 \leq i,j \leq I+1$, by

$$m_{ij} = \frac{1}{2}\big\langle (1+\mathcal{I}_0^h)\chi_j, \chi_i \big\rangle + \langle S_h(Z_h\chi_j), \chi_i \rangle - \langle D_h(\chi_j), \chi_i \rangle. \tag{6.33}$$

The desired resonances of the discretized system (6.32) are given by the values of k_h for which the matrix $\boldsymbol{M}(k_h)$ becomes singular, i.e., non-invertible. Since the dependence on k_h is highly non-linear (through the Green's function and eventually the impedance), it is in general not straightforward to find these resonances. One alternative is to consider, as

done by Durán et al. (2007*b*), the function of resonance-peaks

$$g_\lambda(k_h) = \frac{|\lambda_{\max}(k_h)|}{|\lambda_{\min}(k_h)|}, \tag{6.34}$$

where $\lambda_{\max}(k_h)$ and $\lambda_{\min}(k_h)$ denote respectively the biggest and smallest eigenvalues in modulus of the matrix $\boldsymbol{M}(k_h)$. This function possesses a countable amount of singularities in the complex plane, which correspond to the resonances. The computation of the eigenvalues can be performed by means of standard eigenvalue computation subroutines based on the QR-factorization (Anderson et al. 1999) or by means of power methods (cf., e.g., Burden & Faires 2001). Alternatively, instead of the eigenvalues we could also take into account in (6.34) the diagonal elements of the $\boldsymbol{U}$-matrix that stems from the LU-factorization of $\boldsymbol{M}(k_h)$, as done by Durán, Nédélec & Ossandón (2009).

To compute the resonant states or eigenstates associated to each resonance, we can take advantage of the knowledge of the eigenvector related with the smallest eigenvalue, e.g., obtained from some power method. If k_h^* denotes a resonance, then $\boldsymbol{M}(k_h^*)$ becomes singular and $\lambda_{\min}(k_h^*) = 0$. The corresponding eigenstate $\boldsymbol{\mu}^*$ fulfills thus

$$\boldsymbol{M}(k_h^*)\,\boldsymbol{\mu}^* = \lambda_{\min}(k_h^*)\,\boldsymbol{\mu}^* = \boldsymbol{0}, \qquad \boldsymbol{\mu}^* \neq \boldsymbol{0}. \tag{6.35}$$

Consequently, it can be seen that the desired eigenstate $\boldsymbol{\mu}^*$ corresponds to the eigenvector of $\boldsymbol{M}(k_h^*)$ that is associated to $\lambda_{\min}(k_h^*)$.

6.4 Benchmark problem

6.4.1 Characteristic frequencies of the rectangle

As benchmark problem we consider the particular case of a rectangular harbor with a small opening. Resonances for a harbor of this kind are expected whenever the frequency of an incident wave is close to a characteristic frequency of the closed rectangle. To obtain the characteristic frequencies and oscillation modes of such a closed rectangle we have to solve first the problem

$$\begin{cases} \text{Find } k \in \mathbb{C} \text{ and } u : \Omega_r \to \mathbb{C},\ u \neq 0, \text{ such that} \\ \Delta u + k^2 u = 0 \qquad \text{in } \ \Omega_r, \\ \dfrac{\partial u}{\partial n} = 0 \qquad\quad \text{on } \ \Gamma_r, \end{cases} \tag{6.36}$$

where we denote the domain encompassed by the rectangle as Ω_r and its boundary as Γ_r. The unit normal $\boldsymbol{n}$ is taken outwardly oriented of Ω_r. The rectangle is assumed to be of length a and width b. The eigenfrequencies and eigenstates of the rectangle are well-known and can be determined analytically by using the method of variable separation. For this purpose we separate

$$u(\boldsymbol{x}) = v(x_1)w(x_2), \tag{6.37}$$

placing the origin at the lower left corner of the rectangle, as shown in Figure 6.2.

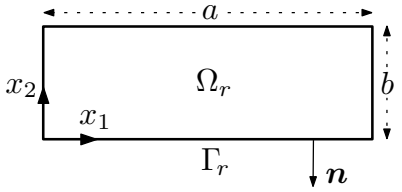

FIGURE 6.2. Closed rectangle.

Replacing now (6.37) in the Helmholtz equation, dividing by vw, and rearranging yields

$$-\frac{v''(x_1)}{v(x_1)} = \frac{w''(x_2)}{w(x_2)} + k^2. \tag{6.38}$$

Since both sides of the differential equation (6.38) depend on different variables, consequently they must be equal to a constant, denoted for convenience by κ^2, i.e.,

$$-\frac{v''(x_1)}{v(x_1)} = \frac{w''(x_2)}{w(x_2)} + k^2 = \kappa^2. \tag{6.39}$$

This way we obtain the two independent ordinary differential equations

$$v''(x_1) + \kappa^2 v(x_1) = 0, \tag{6.40}$$

$$w''(x_2) + (k^2 - \kappa^2) w(x_2) = 0. \tag{6.41}$$

The solutions of (6.40) and (6.41) are respectively of the form

$$v(x_1) = A_v \cos(\kappa x_1) + B_v \sin(\kappa x_1), \tag{6.42}$$

$$w(x_2) = A_w \cos\Big(\sqrt{k^2 - \kappa^2}\, x_2\Big) + B_w \sin\Big(\sqrt{k^2 - \kappa^2}\, x_2\Big), \tag{6.43}$$

where A_v, B_v, A_w, B_w are constants to be determined. This is performed by means of the boundary condition in (6.36), which implies that

$$v'(0) = v'(a) = w'(0) = w'(b) = 0. \tag{6.44}$$

Since $v'(0) = w'(0) = 0$, thus $B_v = B_w = 0$. From the fact that $v'(a) = 0$ we get that $\kappa a = m\pi$ for $m \in \mathbb{Z}$. Hence

$$\kappa = \frac{m\pi}{a}. \tag{6.45}$$

On the other hand, $w'(b) = 0$ implies that $\sqrt{k^2 - \kappa^2}\, b = n\pi$ for $n \in \mathbb{Z}$. By rearranging and replacing (6.45) we obtain the real eigenfrequencies

$$k = \sqrt{\Big(\frac{m\pi}{a}\Big)^2 + \Big(\frac{n\pi}{b}\Big)^2}, \qquad m, n \in \mathbb{Z}. \tag{6.46}$$

The corresponding eigenstates, up to an arbitrary multiplicative constant, are then given by

$$u(\boldsymbol{x}) = \cos\Big(\frac{m\pi}{a} x_1\Big) \cos\Big(\frac{n\pi}{b} x_2\Big), \qquad m, n \in \mathbb{Z}. \tag{6.47}$$

For the particular case of a rectangle with length $a = 800$ and width $b = 400$, the characteristic frequencies are listed in Table 6.1.

TABLE 6.1. Eigenfrequencies of the rectangle in the range from 0 to 0.02.

m \ n	0	1	2
0	0.00000	0.00785	0.01571
1	0.00393	0.00878	0.01619
2	0.00785	0.01111	0.01756
3	0.01178	0.01416	0.01963
4	0.01571	0.01756	
5	0.01963		

6.4.2 Rectangular harbor problem

We consider now the particular case when the domain $\Omega_e \subset \mathbb{R}^2_+$ is taken as a rectangular harbor with a small opening d, such as the domain depicted in Figure 6.3. We take for the rectangle a length $a = 800$, a width $b = 400$, and a small opening of size $d = 20$.

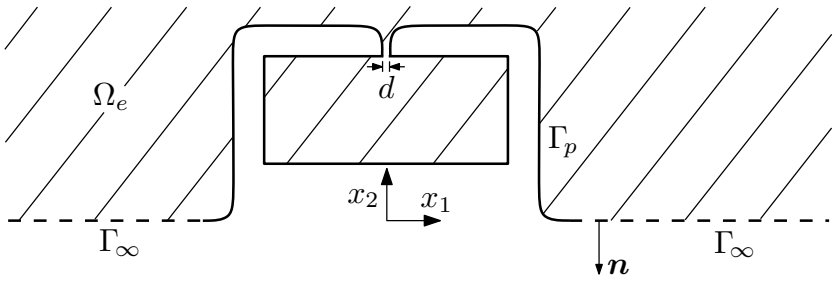

FIGURE 6.3. Rectangular harbor domain.

To simplify the problem, on Γ_∞ we consider an impedance boundary condition with a constant impedance $Z_\infty = 0.02$ and on Γ_p we take a Neumann boundary condition into account. The rectangular harbor problem can be thus stated as

$$\begin{cases} \text{Find } k \in \mathbb{C} \text{ and } u : \Omega_e \to \mathbb{C},\ u \neq 0, \text{ such that} \\ \Delta u + k^2 u = 0 & \text{in } \Omega_e, \\ \dfrac{\partial u}{\partial n} = 0 & \text{on } \Gamma_p, \\ -\dfrac{\partial u}{\partial n} + Z_\infty u = 0 & \text{on } \Gamma_\infty, \\ \text{+ Outgoing radiation condition as } |\boldsymbol{x}| \to \infty, \end{cases} \tag{6.48}$$

where the outgoing radiation condition is stated in (6.16).

The boundary curve Γ_p is discretized into $I = 135$ segments with a discretization step $h = 40.4959$, as illustrated in Figure 6.4. The problem is solved computationally with finite boundary elements of type $\mathbb{P}_1$ by using subroutines programmed in Fortran 90, by

generating the mesh Γ_p^h of the boundary with the free software Gmsh 2.4, and by representing graphically the results in Matlab 7.5 (R2007b). The eigenvalues of the matrix $\boldsymbol{M}(k_h)$, required to build the function of resonance-peaks (6.34), are computed by using the Lapack subroutines for complex nonsymmetric matrixes (cf. Anderson et al. 1999).

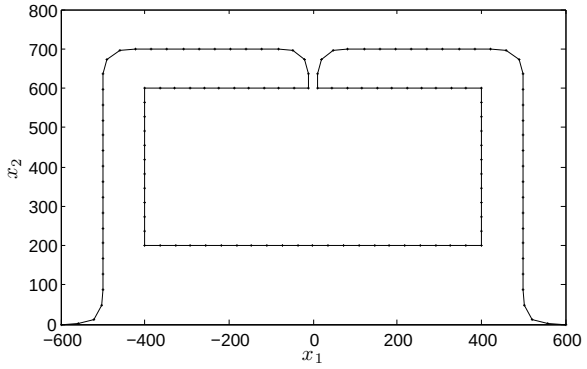

FIGURE 6.4. Mesh Γ_p^h of the rectangular harbor.

The numerical results for the resonances, considering a step $\Delta k = 5 \cdot 10^{-5}$ between wave number samples, are illustrated in Figure 6.5. It can be observed that the peaks tend to coincide with the eigenfrequencies of the rectangle, which are represented by the dashed vertical lines. The first six oscillation modes are depicted in Figures 6.6, 6.7 & 6.8. Only the real parts are displayed, since the imaginary parts are close to zero. We remark that the first observed resonance corresponds to the so-called Helmholtz mode, since its associated eigenmode is constant.

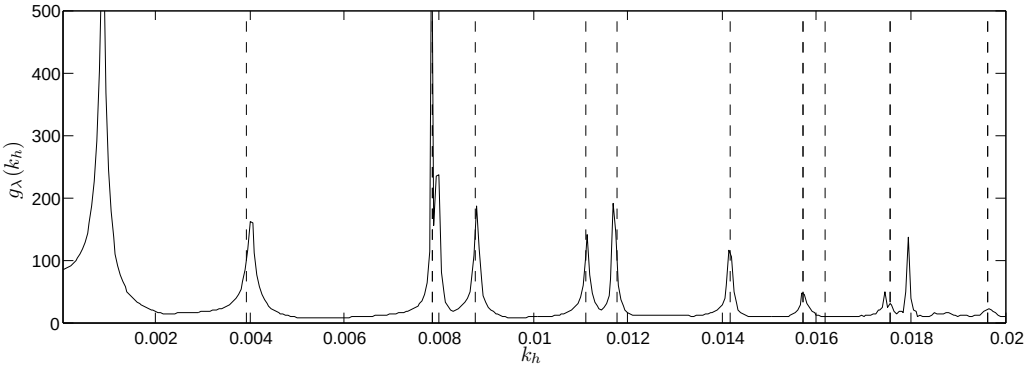

FIGURE 6.5. Resonances for the rectangular harbor.

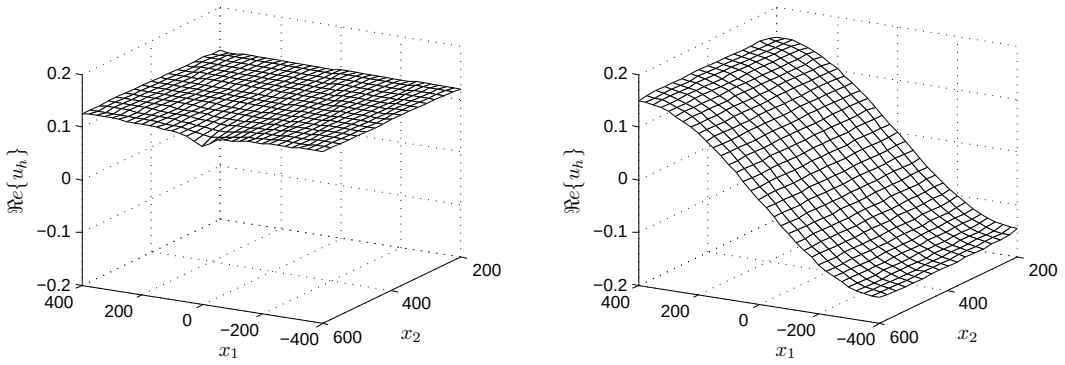

(a) $k_h = 0.000875$ (b) $k_h = 0.00393$

FIGURE 6.6. Oscillation modes: (a) Helmholtz mode; (b) Mode (1,0).

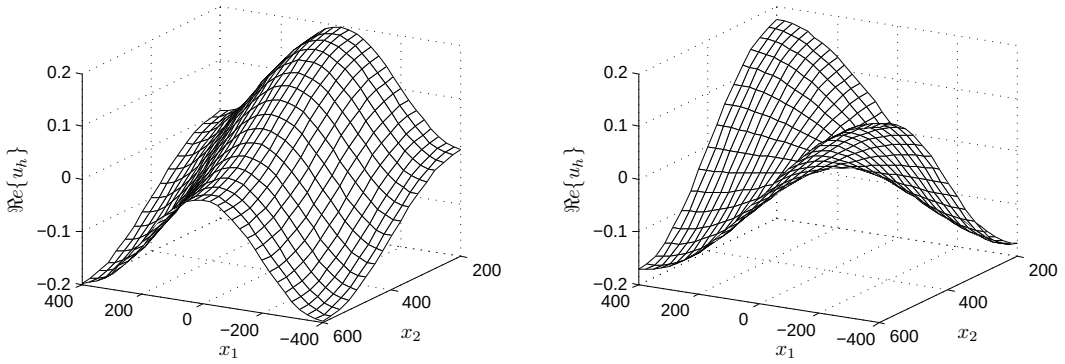

(a) $k_h = 0.00785$ (b) $k_h = 0.00878$

FIGURE 6.7. Oscillation modes: (a) Modes (0,1) and (2,0); (b) Mode (1,1).

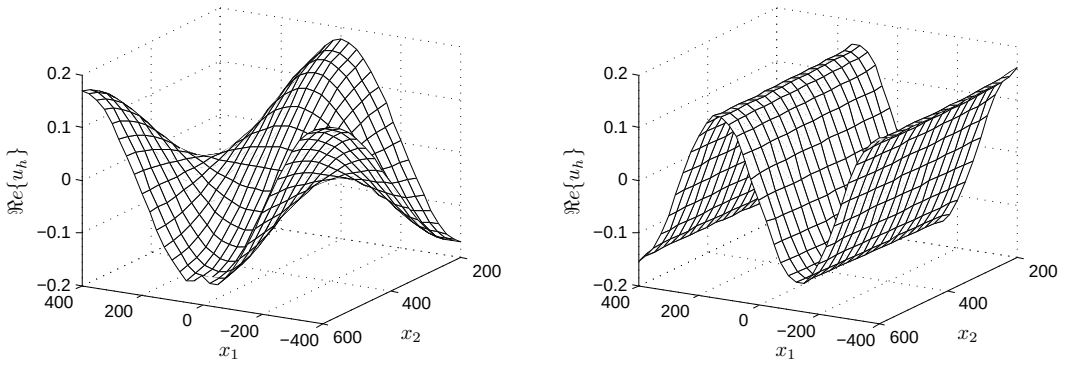

(a) $k_h = 0.01111$ (b) $k_h = 0.01178$

FIGURE 6.8. Oscillation modes: (a) Mode (2,1); (b) Mode (0,3).

VII. OBLIQUE-DERIVATIVE HALF-PLANE LAPLACE PROBLEM

7.1 Introduction

In this chapter we apply the developed techniques to the computation of the Green's function for the oblique-derivative (impedance) half-plane Laplace problem.

We consider the problem of finding the Green's function for the Laplace equation in a two-dimensional half-plane with an oblique-derivative (impedance) boundary condition. Essentially, this Green's function describes outgoing oblique surface waves that emanate from a point source and which increase or decrease exponentially along the boundary, depending on the obliqueness of the derivative in the boundary condition.

An integral representation for this Green's function in half-spaces of three and higher dimensions was developed by Gilbarg & Trudinger (1983, page 121). Using an image method, it was later generalized by Keller (1981) to a wider class of equations, including the wave equation, the heat equation, and the Laplace equation. Its use for more general linear uniformly elliptic equations with discontinuous coefficients can be found in the articles of Di Fazio & Palagachev (1996) and Palagachev, Ragusa & Softova (2000). The generalization of this image method to wedges is performed by Gautesen (1988). When dealing with time-harmonic problems, this representation of the Green's function has to be supplied with an additional term to account for an outgoing surface-wave behavior, e.g., the terms (2.63) and (3.58) associated with the limiting absorption principle.

In the particular case when the oblique derivative becomes a normal derivative, we speak of a free-surface or impedance boundary condition, and the response to the point source is referred to as an infinite-depth free-surface Green's function, which is of great importance in linear water-wave theory (vid. Section A.10). An explicit representation for this Green's function in two dimensions was derived in Chapter II and its main relevance is that it allows to solve boundary value problems stated on compactly perturbed half-planes by using boundary integral equations and the boundary element method (Durán, Hein & Nédélec 2007*b*). Boundary layer potentials constructed by using Green's functions are also important for such different topics as proving solvability theorems and computing resonant states (Kuznetsov, Maz'ya & Vainberg 2002).

Poincaré was the first to state an oblique-derivative problem for a second-order elliptic partial differential operator in his studies on the theory of tides (Poincaré 1910). Since then, the so-called Poincaré problem has been the subject of many publications (cf. Egorov & Kondrat'ev 1969, Paneah 2000), and it arises naturally when determining the gravitational fields of celestial bodies. In this problem, the impedance of the boundary condition is taken as zero. Its main interest lies in the fact that it corresponds to a typical degenerate elliptic boundary value problem where the vector field of its solution is tangent to the boundary of the domain on some subset. The Poincaré problem for harmonic functions, in particular, arises in semiconductor physics and considers constant coefficients for the oblique derivative in the boundary condition (Krutitskii & Chikilev 2000). It allows to describe the Hall effect, i.e., when the direction of an electric current and the direction

of an electric field do not coincide in a semiconductor due the presence of a magnetic field (Krutitskii, Krutitskaya & Malysheva 1999). The two-dimensional Poincaré problem for the Laplace equation is treated in Lesnic (2007), Trefethen & Williams (1986), and further references can be also found in Lions (1956).

The main goal of this chapter is to derive rigorously an explicit representation for the half-plane Green's function of the Laplace equation with an oblique-derivative impedance boundary condition by extending and adapting the results obtained in Chapter II. Excepting the particular cases mentioned before, there has been no attempt to compute it explicitly. The aim is to express the Green's function in terms of a finite combination of known special and elementary functions, so as to be practical for numerical computation. It is also of interest to extend this representation, e.g., towards the complementary half-plane or by considering a complex impedance instead of a real one. There is likewise the interest of having adjusted expressions for the far field of the Green's function and to state the involved radiation condition accordingly.

The differential problem for the Green's function is stated in the upper half-plane and is defined in Section 7.2. In Section 7.3, the spectral Green's function is determined by using a partial Fourier transform along the horizontal axis. By computing its inverse Fourier transform, the desired spatial Green's function is then obtained in Section 7.4. Some properties and extensions of the Green's function are presented in Section 7.5, particularly its extension towards the lower half-plane and its extension to consider a complex impedance. The far field of the Green's function is determined in Section 7.6.

7.2 Green's function problem

We consider the radiation problem of oblique surface waves in the upper half-plane $\mathbb{R}^2_+ = \{\boldsymbol{y} \in \mathbb{R}^2 : y_2 > 0\}$ emanating from a fixed source point $\boldsymbol{x} \in \mathbb{R}^2_+$, as shown in Figure 7.1. The Green's function G corresponds to the solution of this problem, computed in the sense of distributions for the variable $\boldsymbol{y}$ in the half-plane $\mathbb{R}^2_+$ by placing at the right-hand side of the Laplace equation a Dirac mass $\delta_{\boldsymbol{x}}$, which is located at $\boldsymbol{x}$. It is hence a solution $G(\boldsymbol{x}, \cdot) : \mathbb{R}^2_+ \to \mathbb{C}$ of

$$\Delta_{\boldsymbol{y}} G(\boldsymbol{x}, \boldsymbol{y}) = \delta_{\boldsymbol{x}}(\boldsymbol{y}) \qquad \text{in } \mathcal{D}'(\mathbb{R}^2_+), \tag{7.1a}$$

subject to the oblique-derivative impedance boundary condition

$$\frac{\partial G}{\partial s_{\boldsymbol{y}}}(\boldsymbol{x}, \boldsymbol{y}) + Z\, G(\boldsymbol{x}, \boldsymbol{y}) = 0 \qquad \text{on } \{y_2 = 0\}, \tag{7.1b}$$

where the oblique, skew, or directional derivative is given by

$$\frac{\partial G}{\partial s_{\boldsymbol{y}}}(\boldsymbol{x}, \boldsymbol{y}) = \boldsymbol{s} \cdot \nabla_{\boldsymbol{y}} G(\boldsymbol{x}, \boldsymbol{y}) = s_1 \frac{\partial G}{\partial y_1}(\boldsymbol{x}, \boldsymbol{y}) + s_2 \frac{\partial G}{\partial y_2}(\boldsymbol{x}, \boldsymbol{y}), \tag{7.1c}$$

and is taken in the direction of the vector

$$\boldsymbol{s} = (s_1, s_2) = (\cos\sigma,\, \sin\sigma), \qquad |\boldsymbol{s}| = \sqrt{s_1^2 + s_2^2} = 1. \tag{7.1d}$$

The boundary condition (7.1b) is expressed in terms of a real impedance $Z > 0$ and the unit vector $\boldsymbol{s}$ is constant and such that $s_2 > 0$, i.e., such that $0 < \sigma < \pi$. The case of complex Z is discussed later in Section 7.5.

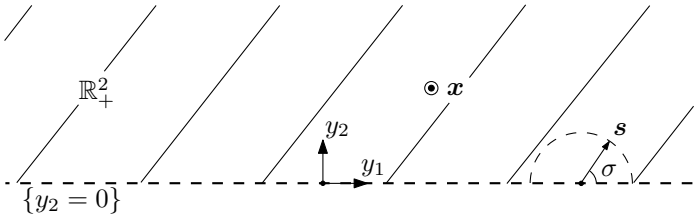

FIGURE 7.1. Domain of the Green's function problem.

To obtain outgoing oblique surface waves for the radiation problem and to ensure the uniqueness of its solution, an outgoing radiation condition has to be imposed additionally at infinity. We express it in its more adjusted form, as in (2.17), which is later justified from the far field of the Green's function, developed in Section 7.6. The outgoing radiation condition is given, as $|\boldsymbol{y}| \to \infty$, by

$$|G| \le \frac{C}{|\boldsymbol{y}|} \quad \text{and} \quad \left|\frac{\partial G}{\partial |\boldsymbol{y}|}\right| \le \frac{C}{|\boldsymbol{y}|^2} \qquad \text{if } \boldsymbol{y}\cdot\boldsymbol{s} > \frac{1}{Z}\ln\bigl(1 + Z\pi|\boldsymbol{y}|\bigr), \tag{7.1e}$$

$$|G| \le Ce^{-Z\boldsymbol{y}\cdot\boldsymbol{s}} \quad \text{and} \quad \left|\frac{\partial G}{\partial |\boldsymbol{y}\times\boldsymbol{s}|} - iZG\right| \le \frac{Ce^{-Z\boldsymbol{y}\cdot\boldsymbol{s}}}{|\boldsymbol{y}\times\boldsymbol{s}|} \qquad \text{if } \boldsymbol{y}\cdot\boldsymbol{s} < \frac{1}{Z}\ln\bigl(1 + Z\pi|\boldsymbol{y}|\bigr), \tag{7.1f}$$

for some constants $C > 0$, which are independent of $\boldsymbol{y}$, and where

$$\boldsymbol{y}\cdot\boldsymbol{s} = s_1y_1 + s_2y_2 \qquad \text{and} \qquad \boldsymbol{y}\times\boldsymbol{s} = s_2y_1 - s_1y_2. \tag{7.2}$$

This radiation condition specifies two regions of different asymptotic behaviors for the Green's function, analogously as shown in Figure 2.2. Both behaviors are separated by rotated logarithmic curves. Above and away from the line $\boldsymbol{y}\cdot\boldsymbol{s} = 0$, the behavior (7.1e) dominates, which is related to the asymptotic decaying of the fundamental solution for the Laplace equation. Below and near the line $\boldsymbol{y}\cdot\boldsymbol{s} = 0$, on the other hand, the behavior (7.1f) resembles a Sommerfeld radiation condition, and is therefore associated to surface waves propagating in an oblique direction, i.e., to oblique surface waves. Along the boundary $\{y_2 = 0\}$, these waves decrease or increase exponentially, and their real and imaginary parts have the same amplitude.

To solve the Green's function problem (7.1), we separate its solution G into a homogeneous and a particular part, namely $G = G_H + G_P$. The homogeneous solution G_H, appropriately scaled, corresponds to the additional term that is required to ensure an appropriate outgoing behavior for the oblique surface waves. In the particular case when the oblique derivative becomes normal, as in Chapter II, then a limiting absorption principle

can be used to explain its presence. The solution G_H of the homogeneous problem, i.e., of (7.1*a–b*) without the Dirac mass, can be conveniently expressed as

$$G_H(\boldsymbol{x},\boldsymbol{y}) = \alpha\, e^{-Z(s_2+is_1)(v_2-iv_1)} + \beta\, e^{-Z(s_2-is_1)(v_2+iv_1)}, \tag{7.3}$$

where the notation

$$v_1 = y_1 - x_1 \qquad \text{and} \qquad v_2 = y_2 + x_2 \tag{7.4}$$

is used. The constants $\alpha, \beta \in \mathbb{C}$ in (7.3) are arbitrary and may depend on $\boldsymbol{x}$. These constants are fixed later on by means of the radiation condition, once the particular solution G_P of (7.1) has been better determined.

7.3 Spectral Green's function

7.3.1 Spectral boundary-value problem

The particular solution G_P satisfies (7.1*a–b*) and has to remain bounded as $y_2 \to \infty$. To compute it, we use a modified partial Fourier transform on the horizontal y_1-axis, taking advantage of the fact that there is no horizontal variation in the geometry of the problem. We define the Fourier transform of a function $F\big(\boldsymbol{x},(\cdot,y_2)\big) : \mathbb{R} \to \mathbb{C}$ by

$$\widehat{F}(\xi; y_2, x_2) = \frac{1}{\sqrt{2\pi}} \int_{-\infty}^{\infty} F(\boldsymbol{x},\boldsymbol{y})\, e^{-i\xi(y_1-x_1)}\, \mathrm{d}y_1, \qquad \xi \in \mathbb{R}. \tag{7.5}$$

Applying the Fourier transform (7.5) on (7.1*a–b*) leads to a second-order boundary-value problem for the variable y_2, given by

$$\frac{\partial^2 \widehat{G}_P}{\partial y_2^2}(\xi) - \xi^2 \widehat{G}_P(\xi) = \frac{\delta(y_2 - x_2)}{\sqrt{2\pi}}, \qquad y_2 > 0, \tag{7.6a}$$

$$s_2 \frac{\partial \widehat{G}_P}{\partial y_2}(\xi) + \big(is_1\xi + Z\big)\widehat{G}_P(\xi) = 0, \qquad y_2 = 0. \tag{7.6b}$$

We use undetermined coefficients and solve the differential equation (7.6a) respectively in the strip $\{\boldsymbol{y} \in \mathbb{R}^2_+ \,:\, 0 < y_2 < x_2\}$ and in the half-plane $\{\boldsymbol{y} \in \mathbb{R}^2_+ \,:\, y_2 > x_2\}$. This gives a solution for $\widehat{G}_P$ in each domain, as a linear combination of two independent solutions of an ordinary differential equation, namely

$$\widehat{G}_P(\xi) = \begin{cases} a\, e^{|\xi| y_2} + b\, e^{-|\xi| y_2} & \text{for } \ 0 < y_2 < x_2, \\ c\, e^{|\xi| y_2} + d\, e^{-|\xi| y_2} & \text{for } \ y_2 > x_2. \end{cases} \tag{7.7}$$

The unknowns a, b, c, and d, which depend on ξ and x_2, are determined through the boundary condition and by considering continuity and the behavior at infinity.

7.3.2 Particular spectral Green's function

Now, thanks to (7.7), the computation of $\widehat{G}_P$ is straightforward. From (7.6b) a relation for the coefficients a and b can be derived, which is given by

$$a\big(Z + s_2|\xi| + is_1\xi\big) + b\big(Z - s_2|\xi| + is_1\xi\big) = 0. \tag{7.8}$$

Since the solution (7.7) has to remain bounded at infinity as $y_2 \to \infty$, it follows that

$$c = 0. \tag{7.9}$$

To ensure continuity for the Green's function at the point $y_2 = x_2$, it is needed that

$$d = a\, e^{|\xi| 2x_2} + b. \tag{7.10}$$

Using relations (7.8), (7.9), and (7.10) in (7.7), we obtain the expression

$$\widehat{G}_P(\xi) = a\, e^{|\xi| x_2} \left[e^{-|\xi||y_2 - x_2|} - \left(\frac{Z + s_2|\xi| + i s_1 \xi}{Z - s_2|\xi| + i s_1 \xi} \right) e^{-|\xi|(y_2 + x_2)} \right]. \tag{7.11}$$

By computing the second derivative of (7.11) in the sense of distributions and by replacing it in (7.6a), we obtain that

$$a = -\frac{e^{-|\xi| x_2}}{\sqrt{8\pi}\,|\xi|}. \tag{7.12}$$

Finally, the particular spectral Green's function $\widehat{G}_P$ is given by

$$\widehat{G}_P(\xi; y_2, x_2) = -\frac{e^{-|\xi||y_2 - x_2|}}{\sqrt{8\pi}\,|\xi|} + \left(\frac{Z + s_2|\xi| + i s_1 \xi}{Z - s_2|\xi| + i s_1 \xi} \right) \frac{e^{-|\xi|(y_2 + x_2)}}{\sqrt{8\pi}\,|\xi|}. \tag{7.13}$$

7.3.3 Analysis of singularities

We have to analyze now the singularities of the particular spectral Green's function $\widehat{G}_P$, so as to obtain its asymptotic behavior and thus determine the constants α, β of the homogeneous solution (7.3). For this purpose, we extend the Fourier variable towards the complex domain, i.e., $\xi \in \mathbb{C}$, in which case the absolute value $|\xi|$ has to be understood as the square root $\sqrt{\xi^2}$, where $-\pi/2 < \arg\sqrt{\xi^2} \leq \pi/2$, that is, always the root with the nonnegative real part is taken. This square root presents two branch cuts, which are located respectively on the positive and on the negative imaginary axis of ξ. The particular spectral Green's function $\widehat{G}_P$, for $\xi \in \mathbb{C}$, becomes therefore

$$\widehat{G}_P(\xi) = -\frac{e^{-\sqrt{\xi^2}\,|y_2 - x_2|}}{\sqrt{8\pi}\,\sqrt{\xi^2}} + \left(\frac{Z + s_2\sqrt{\xi^2} + i s_1 \xi}{Z - s_2\sqrt{\xi^2} + i s_1 \xi} \right) \frac{e^{-\sqrt{\xi^2}\,(y_2 + x_2)}}{\sqrt{8\pi}\,\sqrt{\xi^2}}. \tag{7.14}$$

This function is continuous on ξ along the real axis and it incorporates a removable singularity at $\xi = 0$, in the same manner as shown in Section 2.3. The function $\widehat{G}_P$ has also branch cuts on the positive and negative imaginary axis. Finally, (7.14) presents two simple poles at $\xi = Z(s_2 + i s_1)$ and $\xi = -Z(s_2 - i s_1)$, whose residues are characterized by

$$\lim_{\xi \to \pm Z(s_2 \pm i s_1)} \big(\xi \mp Z(s_2 \pm i s_1) \big)\, \widehat{G}_P(\xi) = \mp \frac{s_2}{\sqrt{2\pi}} (s_2 \pm i s_1) e^{-Z(s_2 \pm i s_1) v_2}. \tag{7.15}$$

Otherwise the function $\widehat{G}_P$ is regular and continuous. To analyze the effect of the poles, we study at first the inverse Fourier transform of

$$\widehat{P}(\xi) = -\frac{s_2}{\sqrt{2\pi}} (s_2 + i s_1) \frac{e^{-Z(s_2 + i s_1) v_2}}{\xi - Z(s_2 + i s_1)} + \frac{s_2}{\sqrt{2\pi}} (s_2 - i s_1) \frac{e^{-Z(s_2 - i s_1) v_2}}{\xi + Z(s_2 - i s_1)}. \tag{7.16}$$

This can be achieved by considering the Fourier transform of the sign function, i.e.,

$$\operatorname{sign}(v_1) \qquad \xrightarrow{\mathcal{F}} \qquad -i\sqrt{\frac{2}{\pi}}\frac{1}{\xi}, \tag{7.17}$$

whose right-hand side is to be interpreted in the sense of the principal value, and by using the translation, scaling, and linearity properties of the Fourier transform, as much in the spatial as in the spectral domain (cf., e.g., Gasquet & Witomski 1999). The inverse Fourier transform of (7.16) is then given by

$$\begin{aligned} P(\boldsymbol{x},\boldsymbol{y}) = & -i\frac{s_2}{2}(s_2+is_1)\operatorname{sign}(v_1)\, e^{-Z(s_2v_2+s_1v_1)}e^{iZ(s_2v_1-s_1v_2)} \\ & +i\frac{s_2}{2}(s_2-is_1)\operatorname{sign}(v_1)\, e^{-Z(s_2v_2+s_1v_1)}e^{-iZ(s_2v_1-s_1v_2)}. \end{aligned} \tag{7.18}$$

The exponential terms in (7.18) are compatible with the asymptotic behavior of the Green's function, as will be seen later, but the one-dimensional nature of the Fourier transform does not allow to retrieve correctly the direction of the cut that is present due the sign function. Instead of being vertical along the v_2-axis as in (7.18), the direction of this cut has to coincide with the oblique vector $\boldsymbol{s}$ in the (v_1, v_2)-plane. To account for this issue we can consider, instead of (7.16), the expression

$$\begin{aligned} \widehat{Q}(\xi) = & -\frac{s_2}{\sqrt{2\pi}}(s_2+is_1)\, e^{-i\frac{s_1}{s_2}v_2(\xi-Z(s_2+is_1))}\frac{e^{-Z(s_2+is_1)v_2}}{\xi-Z(s_2+is_1)} \\ & +\frac{s_2}{\sqrt{2\pi}}(s_2-is_1)\, e^{-i\frac{s_1}{s_2}v_2(\xi+Z(s_2-is_1))}\frac{e^{-Z(s_2-is_1)v_2}}{\xi+Z(s_2-is_1)}, \end{aligned} \tag{7.19}$$

which also describes correctly the residues of the poles, but incorporating an additional exponential behavior that treats properly the v_2-variable. We remark that this additional exponential factor becomes unity when $s_1 = 0$, i.e., when the oblique derivative becomes normal. By using again (7.17) and the same properties of the Fourier transform as before, we obtain that the inverse Fourier transform of (7.19) is readily given by

$$\begin{aligned} Q(\boldsymbol{x},\boldsymbol{y}) = & -i\frac{s_2}{2}(s_2+is_1)\operatorname{sign}(s_2v_1-s_1v_2)\, e^{-Z(s_2v_2+s_1v_1)}e^{iZ(s_2v_1-s_1v_2)} \\ & +i\frac{s_2}{2}(s_2-is_1)\operatorname{sign}(s_2v_1-s_1v_2)\, e^{-Z(s_2v_2+s_1v_1)}e^{-iZ(s_2v_1-s_1v_2)}. \end{aligned} \tag{7.20}$$

Now the cut due the sign function coincides correctly with the oblique vector $\boldsymbol{s}$ and retrieves appropriately the asymptotic behavior of the oblique surface waves.

It can be observed that (7.20) describes the asymptotic behavior of stationary oblique surface waves, since its imaginary part is zero. In order to obtain an outgoing-wave behavior, this missing imaginary part is provided by the homogeneous solution (7.3), which has to be scaled according to

$$\begin{aligned} G_H(\boldsymbol{x},\boldsymbol{y}) = & -i\frac{s_2}{2}(s_2+is_1)\, e^{-Z(s_2v_2+s_1v_1)}e^{iZ(s_2v_1-s_1v_2)} \\ & -i\frac{s_2}{2}(s_2-is_1)\, e^{-Z(s_2v_2+s_1v_1)}e^{-iZ(s_2v_1-s_1v_2)}. \end{aligned} \tag{7.21}$$

The Fourier transform of (7.21) contains two Dirac masses and is given by

$$\begin{aligned}\widehat{G}_H(\xi; y_2, x_2) = &- i\sqrt{\frac{\pi}{2}}\, s_2(s_2 + is_1)\, e^{-Z(s_2+is_1)v_2}\, \delta\big(\xi - Z(s_2 + is_1)\big) \\ &- i\sqrt{\frac{\pi}{2}}\, s_2(s_2 - is_1)\, e^{-Z(s_2-is_1)v_2}\, \delta\big(\xi + Z(s_2 - is_1)\big). \end{aligned} \tag{7.22}$$

7.3.4 Complete spectral Green's function

The complete spectral Green's function, decomposed as $\widehat{G} = \widehat{G}_P + \widehat{G}_H$, is thus obtained by adding the particular solution (7.13) and the homogeneous solution (7.22), which yields

$$\begin{aligned}\widehat{G}(\xi; y_2, x_2) = &- \frac{e^{-|\xi||y_2 - x_2|}}{\sqrt{8\pi}\,|\xi|} + \left(\frac{Z + s_2|\xi| + is_1\xi}{Z - s_2|\xi| + is_1\xi}\right) \frac{e^{-|\xi|(y_2+x_2)}}{\sqrt{8\pi}\,|\xi|} \\ &- i\sqrt{\frac{\pi}{2}}\, s_2(s_2 + is_1)\, e^{-Z(s_2+is_1)(y_2+x_2)} \delta\big(\xi - Z(s_2 + is_1)\big) \\ &- i\sqrt{\frac{\pi}{2}}\, s_2(s_2 - is_1)\, e^{-Z(s_2-is_1)(y_2+x_2)} \delta\big(\xi + Z(s_2 - is_1)\big). \end{aligned} \tag{7.23}$$

For our further analysis, we decompose the particular solution (7.13) into three terms, namely $\widehat{G}_P = \widehat{G}_\infty + \widehat{G}_D + \widehat{G}_R$, where

$$\widehat{G}_\infty(\xi; y_2, x_2) = -\frac{e^{-|\xi||y_2 - x_2|}}{\sqrt{8\pi}\,|\xi|}, \tag{7.24}$$

$$\widehat{G}_D(\xi; y_2, x_2) = \frac{e^{-|\xi|(y_2+x_2)}}{\sqrt{8\pi}\,|\xi|}, \tag{7.25}$$

$$\widehat{G}_R(\xi; y_2, x_2) = \frac{s_2\, e^{-|\xi|(y_2+x_2)}}{\sqrt{2\pi}\,\big(Z - s_2|\xi| + is_1\xi\big)}. \tag{7.26}$$

7.4 Spatial Green's function

7.4.1 Decomposition

The particular spatial Green's function G_P is given by the inverse Fourier transform of (7.13), namely by

$$\begin{aligned}G_P(\boldsymbol{x}, \boldsymbol{y}) = &- \frac{1}{4\pi}\int_{-\infty}^{\infty} \frac{e^{-|\xi||y_2 - x_2|}}{|\xi|}\, e^{i\xi(y_1 - x_1)} \mathrm{d}\xi \\ &+ \frac{1}{4\pi}\int_{-\infty}^{\infty} \left(\frac{Z + s_2|\xi| + is_1\xi}{Z - s_2|\xi| + is_1\xi}\right) \frac{e^{-|\xi|(y_2+x_2)}}{|\xi|}\, e^{i\xi(y_1 - x_1)} \mathrm{d}\xi. \end{aligned} \tag{7.27}$$

Due the linearity of the Fourier transform, the decomposition $G_P = G_\infty + G_D + G_R$ holds also in the spatial domain. We compute now each term in an independent manner and add the results at the end.

7.4.2 Term of the full-plane Green's function

The first term in (7.27) corresponds to the inverse Fourier transform of (7.24), and can be rewritten as

$$G_\infty(\boldsymbol{x},\boldsymbol{y}) = -\frac{1}{2\pi}\int_0^\infty \frac{e^{-\xi|y_2-x_2|}}{\xi}\cos\big(\xi(y_1-x_1)\big)\mathrm{d}\xi. \tag{7.28}$$

This integral is divergent in the classical sense (cf., e.g., Gradshteyn & Ryzhik 2007, equation 3.941–2) and yields, as for (2.75), the full-plane Green's function of the Laplace equation, namely

$$G_\infty(\boldsymbol{x},\boldsymbol{y}) = \frac{1}{2\pi}\ln|\boldsymbol{y}-\boldsymbol{x}|. \tag{7.29}$$

7.4.3 Term associated with a Dirichlet boundary condition

The inverse Fourier transform of (7.25) is obtained in the same manner as the term G_∞. In this case we have that

$$G_D(\boldsymbol{x},\boldsymbol{y}) = \frac{1}{2\pi}\int_0^\infty \frac{e^{-\xi(y_2+x_2)}}{\xi}\cos\big(\xi(y_1-x_1)\big)\mathrm{d}\xi, \tag{7.30}$$

which implies that

$$G_D(\boldsymbol{x},\boldsymbol{y}) = -\frac{1}{2\pi}\ln|\boldsymbol{y}-\bar{\boldsymbol{x}}|, \tag{7.31}$$

being $\bar{\boldsymbol{x}} = (x_1,-x_2)$ the image point of $\boldsymbol{x}$ in the lower half-plane. It represents the additional term that appears in the Green's function due the method of images when considering a Dirichlet boundary condition.

7.4.4 Remaining term

The remaining term G_R, the inverse Fourier transform of (7.26), can be expressed as

$$G_R(\boldsymbol{x},\boldsymbol{y}) = \frac{s_2}{2\pi}\int_{-\infty}^\infty \frac{e^{-|\xi|v_2}}{Z-s_2|\xi|+is_1\xi}\,e^{i\xi v_1}\,\mathrm{d}\xi. \tag{7.32}$$

Separating positive and negative values of ξ in the integral and rearranging, yields

$$\begin{aligned} G_R(\boldsymbol{x},\boldsymbol{y}) = {}& \frac{s_2}{2\pi}(s_2+is_1)\int_0^\infty \frac{e^{-\xi(v_2-iv_1)}}{Z(s_2+is_1)-\xi}\,\mathrm{d}\xi \\ & + \frac{s_2}{2\pi}(s_2-is_1)\int_0^\infty \frac{e^{-\xi(v_2+iv_1)}}{Z(s_2-is_1)-\xi}\,\mathrm{d}\xi. \end{aligned} \tag{7.33}$$

By performing respectively in the first and second integrals of (7.33) the change of variable $\eta = (v_2-iv_1)\big(\xi - Z(s_2+is_1)\big)$ and $\eta = (v_2+iv_1)\big(\xi - Z(s_2-is_1)\big)$, we obtain

$$\begin{aligned} G_R(\boldsymbol{x},\boldsymbol{y}) = {}& \frac{s_2}{2\pi}(s_2+is_1)\,e^{-Z\boldsymbol{v}\cdot\boldsymbol{s}+iZ\boldsymbol{v}\times\boldsymbol{s}}\,\mathrm{Ei}\big(Z\boldsymbol{v}\cdot\boldsymbol{s}-iZ\boldsymbol{v}\times\boldsymbol{s}\big) \\ & + \frac{s_2}{2\pi}(s_2-is_1)\,e^{-Z\boldsymbol{v}\cdot\boldsymbol{s}-iZ\boldsymbol{v}\times\boldsymbol{s}}\,\mathrm{Ei}\big(Z\boldsymbol{v}\cdot\boldsymbol{s}+iZ\boldsymbol{v}\times\boldsymbol{s}\big), \end{aligned} \tag{7.34}$$

where we use the notation

$$\boldsymbol{v}\cdot\boldsymbol{s} = s_2v_2+s_1v_1 \qquad \text{and} \qquad \boldsymbol{v}\times\boldsymbol{s} = s_2v_1-s_1v_2, \tag{7.35}$$

and where Ei denotes the exponential integral function (vid. Subsection A.2.3). This special function is defined as a Cauchy principal value by

$$\mathrm{Ei}(z) = -\fint_{-z}^{\infty} \frac{e^{-t}}{t}\,\mathrm{d}t = \fint_{-\infty}^{z} \frac{e^{t}}{t}\,\mathrm{d}t \qquad \big(|\arg z| < \pi\big), \tag{7.36}$$

and it can be characterized in the whole complex plane through the series expansion

$$\mathrm{Ei}(z) = \gamma + \ln z + \sum_{n=1}^{\infty} \frac{z^n}{n\,n!} \qquad \big(|\arg z| < \pi\big), \tag{7.37}$$

where γ denotes Euler's constant and where the principal value of the logarithm is taken, i.e., the branch cut runs along the negative real axis. Its derivative is

$$\frac{\mathrm{d}}{\mathrm{d}z}\,\mathrm{Ei}(z) = \frac{e^z}{z}. \tag{7.38}$$

For large arguments, as $x \to \infty$ along the real line and as $|y| \to \infty$ along the imaginary axis, the exponential integral admits the asymptotic divergent series expansions

$$\mathrm{Ei}(x) = \frac{e^x}{x} \sum_{n=0}^{\infty} \frac{n!}{x^n} \qquad (x > 0), \tag{7.39}$$

$$\mathrm{Ei}(iy) = i\pi\,\mathrm{sign}(y) + \frac{e^{iy}}{iy} \sum_{n=0}^{\infty} \frac{n!}{(iy)^n} \qquad (y \in \mathbb{R}). \tag{7.40}$$

7.4.5 Complete spatial Green's function

The complete spatial Green's function is finally obtained by adding the terms (7.22), (7.29), (7.31), and (7.34), and is thus given explicitly by

$$\begin{aligned} G(\boldsymbol{x},\boldsymbol{y}) = {} & \frac{1}{2\pi}\ln|\boldsymbol{y}-\boldsymbol{x}| - \frac{1}{2\pi}\ln|\boldsymbol{y}-\bar{\boldsymbol{x}}| \\ & + \frac{s_2}{2\pi}(s_2 + is_1)\,e^{-Z\boldsymbol{v}\cdot\boldsymbol{s}+iZ\boldsymbol{v}\times\boldsymbol{s}}\Big(\mathrm{Ei}\big(Z\boldsymbol{v}\cdot\boldsymbol{s} - iZ\boldsymbol{v}\times\boldsymbol{s}\big) - i\pi\Big) \\ & + \frac{s_2}{2\pi}(s_2 - is_1)\,e^{-Z\boldsymbol{v}\cdot\boldsymbol{s}-iZ\boldsymbol{v}\times\boldsymbol{s}}\Big(\mathrm{Ei}\big(Z\boldsymbol{v}\cdot\boldsymbol{s} + iZ\boldsymbol{v}\times\boldsymbol{s}\big) - i\pi\Big), \end{aligned} \tag{7.41}$$

where $\bar{\boldsymbol{x}} = (x_1, -x_2)$ and where the notations (7.4) and (7.35) are used.

The numerical evaluation of the Green's function (7.41) can be performed straightforwardly in Mathematica, by using the function `ExpIntegralEi`, and almost directly in Fortran, by adapting the computational subroutines described in Morris (1993) or, alternatively, the algorithm delineated in Amos (1990*a*,*b*). Great care has to be taken in the latter case, though, with the correct definition of the exponential integral, and particularly with the analytic branch cut. The case for $Z = 1$, $\sigma = 5\pi/11$, and $\boldsymbol{x} = (0, 2)$ is illustrated in Figures 7.2 & 7.3.

7.5 Extension and properties

The spatial Green's function can be extended in a locally analytic way towards the full-plane $\mathbb{R}^2$ in a straightforward and natural manner, just by considering the expression (7.41)

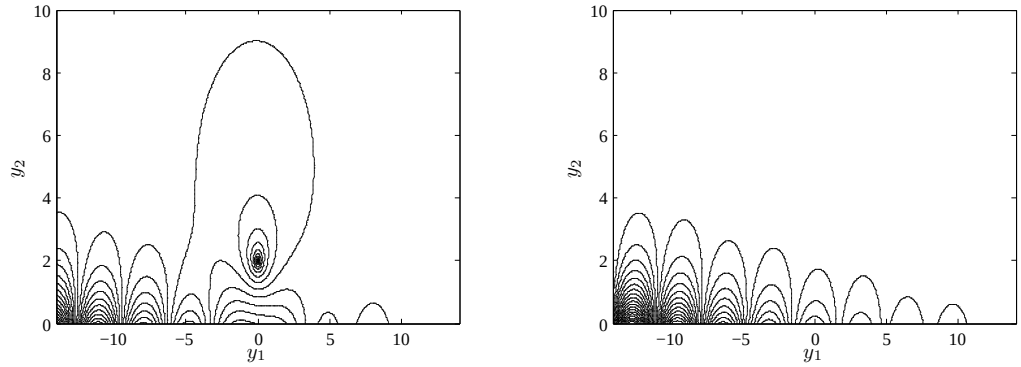

(a) Real part (b) Imaginary part

FIGURE 7.2. Contour plot of the complete spatial Green's function.

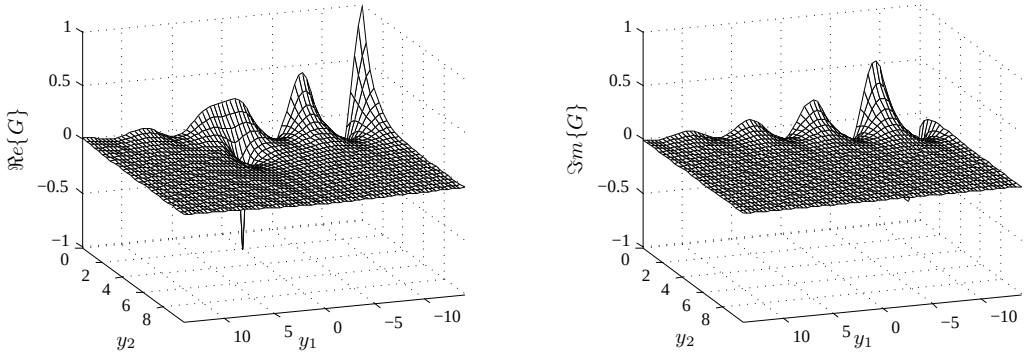

(a) Real part (b) Imaginary part

FIGURE 7.3. Oblique view of the complete spatial Green's function.

valid for all $\boldsymbol{x}, \boldsymbol{y} \in \mathbb{R}^2$, instead of just for $\mathbb{R}^2_+$. This extension has two singularities of logarithmic type at the points $\boldsymbol{x}$ and $\bar{\boldsymbol{x}}$, whose behavior is characterized by

$$G(\boldsymbol{x}, \boldsymbol{y}) \sim \frac{1}{2\pi} \ln |\boldsymbol{y} - \boldsymbol{x}|, \qquad \boldsymbol{y} \longrightarrow \boldsymbol{x}, \tag{7.42}$$

$$G(\boldsymbol{x}, \boldsymbol{y}) \sim \left(\frac{2s_2 - 1}{2\pi} \right) \ln |\boldsymbol{y} - \bar{\boldsymbol{x}}|, \qquad \boldsymbol{y} \longrightarrow \bar{\boldsymbol{x}}. \tag{7.43}$$

Across the half-line $\Upsilon = \{\boldsymbol{y} \in \mathbb{R}^2 : \boldsymbol{y} = \bar{\boldsymbol{x}} - \alpha \boldsymbol{s}, \ \alpha > 0\}$, as shown in Figure 7.4, a jump appears for the Green's function due the analytic branch cut of the exponential integral functions, which is given by

$$K(\boldsymbol{x}, \boldsymbol{y}) = G|_+ - G|_- = 2s_1 s_2 \, e^{-Z(s_2 v_2 + s_1 v_1)}. \tag{7.44}$$

For the same reason, there exists also a jump for the perpendicular oblique derivative across Υ, which is represented by

$$J(\boldsymbol{x},\boldsymbol{y}) = \left.\frac{\partial G}{\partial t_{\boldsymbol{y}}}\right|_{+} - \left.\frac{\partial G}{\partial t_{\boldsymbol{y}}}\right|_{-} = 2Z s_2^2\, e^{-Z(s_2 v_2 + s_1 v_1)}, \tag{7.45}$$

where $\partial G/\partial t_{\boldsymbol{y}} = \boldsymbol{t}\cdot\nabla_{\boldsymbol{y}} G$, being $\boldsymbol{t} = (s_2, -s_1)$.

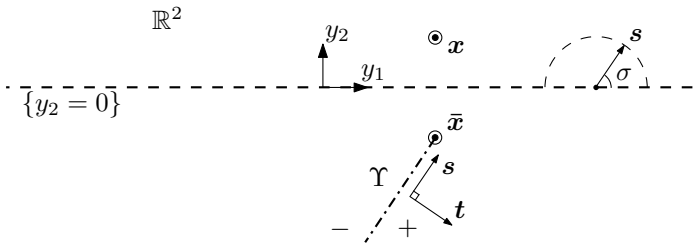

FIGURE 7.4. Domain of the extended Green's function.

As long as $x_2 \neq 0$ the boundary condition (7.1b) continues to be homogeneous. Nonetheless, if the source point $\boldsymbol{x}$ lies on the half-plane's boundary, i.e., if $x_2 = 0$, then the boundary condition ceases to be homogeneous in the sense of distributions. This can be deduced from (7.22) and (7.27) by verifying that

$$\lim_{y_2\to 0^+}\left\{\frac{\partial G}{\partial s_{\boldsymbol{y}}}\big((x_1,0),\boldsymbol{y}\big) + Z\,G\big((x_1,0),\boldsymbol{y}\big)\right\} = s_2\,\delta_{x_1}(y_1). \tag{7.46}$$

To illustrate more clearly the contribution of each logarithmic singularity to the Dirac mass in the boundary condition, which holds only on $\{y_2 = 0\}$, we express the right-hand side of (7.46) as

$$s_2\,\delta_{x_1}(y_1) = \frac{1}{2}\,\delta_{\boldsymbol{x}}(\boldsymbol{y}) + \left(s_2 - \frac{1}{2}\right)\delta_{\bar{\boldsymbol{x}}}(\boldsymbol{y}). \tag{7.47}$$

It can be seen now that the Green's function extended in the abovementioned way satisfies, for $\boldsymbol{x} \in \mathbb{R}^2$, in the sense of distributions, and instead of (7.1), the problem of finding $G(\boldsymbol{x},\cdot) : \mathbb{R}^2 \to \mathbb{C}$ such that

$$\Delta_{\boldsymbol{y}} G = \delta_{\boldsymbol{x}} + (2s_2 - 1)\,\delta_{\bar{\boldsymbol{x}}} + J\delta_{\Upsilon} + K\frac{\partial \delta_{\Upsilon}}{\partial t} \qquad \text{in } \mathcal{D}'(\mathbb{R}^2), \tag{7.48a}$$

$$\frac{\partial G}{\partial s_{\boldsymbol{y}}} + Z\,G = \frac{1}{2}\,\delta_{\boldsymbol{x}} + \left(s_2 - \frac{1}{2}\right)\delta_{\bar{\boldsymbol{x}}} \qquad \text{on } \{y_2 = 0\}, \tag{7.48b}$$

and such that the radiation condition (7.1*e–f*) is satisfied as $|\boldsymbol{y}| \to \infty$ for $\boldsymbol{y} \in \mathbb{R}^2_+$, where δ_{Υ} denotes a Dirac-mass distribution along the Υ-curve.

We note that the half-plane Green's function (7.41) is not symmetric in $\boldsymbol{x}$ and $\boldsymbol{y}$ in the general case since the differential operator is not self-adjoint, but it holds that

$$G(\boldsymbol{x},\boldsymbol{y}) = G(-\bar{\boldsymbol{y}}, -\bar{\boldsymbol{x}}) \qquad \forall \boldsymbol{x},\boldsymbol{y} \in \mathbb{R}^2, \tag{7.49}$$

where again $\bar{\boldsymbol{x}} = (x_1, -x_2)$ and $\bar{\boldsymbol{y}} = (y_1, -y_2)$.

When the oblique derivative becomes a normal derivative, i.e., when $s_2 = 1$, then the expression (7.41) effectively corresponds to the infinite-depth free-surface Green's function expressed in (2.94).

Another property is that we retrieve with (7.41) the special case of a homogenous Dirichlet boundary condition in $\mathbb{R}^2_+$ when $Z \to \infty$, namely

$$G(\boldsymbol{x}, \boldsymbol{y}) = \frac{1}{2\pi} \ln |\boldsymbol{y} - \boldsymbol{x}| - \frac{1}{2\pi} \ln |\boldsymbol{y} - \bar{\boldsymbol{x}}|. \tag{7.50}$$

The same Green's function (7.50) is also obtained when $s_2 = 0$. Likewise, we retrieve with (7.41) the special case of the Poincaré problem in $\mathbb{R}^2_+$ when $Z \to 0$, i.e.,

$$\begin{aligned} G(\boldsymbol{x}, \boldsymbol{y}) = {} & \frac{1}{2\pi} \ln |\boldsymbol{y} - \boldsymbol{x}| - \frac{1}{2\pi} \ln |\boldsymbol{y} - \bar{\boldsymbol{x}}| \\ & + \frac{s_2}{2\pi}(s_2 + is_1) \ln(\boldsymbol{v} \cdot \boldsymbol{s} - i\boldsymbol{v} \times \boldsymbol{s}) + \frac{s_2}{2\pi}(s_2 - is_1) \ln(\boldsymbol{v} \cdot \boldsymbol{s} + i\boldsymbol{v} \times \boldsymbol{s}), \end{aligned} \tag{7.51}$$

except for an additive complex constant that can be disregarded. When $s_2 = 1$, then (7.51) turns moreover into the Green's function resulting from a homogeneous Neumann boundary condition in $\mathbb{R}^2_+$ when $Z \to 0$, namely

$$G(\boldsymbol{x}, \boldsymbol{y}) = \frac{1}{2\pi} \ln |\boldsymbol{y} - \boldsymbol{x}| + \frac{1}{2\pi} \ln |\boldsymbol{y} - \bar{\boldsymbol{x}}|, \tag{7.52}$$

excepting again an additive complex constant.

At last, we observe that the expression for the Green's function (7.41) is still valid if a complex impedance $Z \in \mathbb{C}$ such that $\mathfrak{Im}\{Z\} > 0$ and $\mathfrak{Re}\{Z\} \geq 0$ is used, which is associated with dissipative wave propagation. The branch cuts of the logarithms that are contained in the exponential integral functions, though, have to be treated very carefully in this case, since they have to stay on the half-line Υ. A straightforward evaluation of these logarithms with a complex impedance rotates the branch cuts in the (v_1, v_2)-plane and generates thus two discontinuous half-lines for the Green's function in the half-plane $\boldsymbol{v} \cdot \boldsymbol{s} < 0$. This undesired behavior of the branch cuts can be avoided if the complex logarithms are taken in the sense of

$$\ln\big(Z\boldsymbol{v} \cdot \boldsymbol{s} - iZ\boldsymbol{v} \times \boldsymbol{s}\big) = \ln(\boldsymbol{v} \cdot \boldsymbol{s} - i\boldsymbol{v} \times \boldsymbol{s}) + \ln(Z), \tag{7.53a}$$

$$\ln\big(Z\boldsymbol{v} \cdot \boldsymbol{s} + iZ\boldsymbol{v} \times \boldsymbol{s}\big) = \ln(\boldsymbol{v} \cdot \boldsymbol{s} + i\boldsymbol{v} \times \boldsymbol{s}) + \ln(Z), \tag{7.53b}$$

where the principal value is considered for the logarithms on the right-hand side. For the remaining terms of the Green's function, the complex impedance Z can be evaluated directly without any problems.

7.6 Far field of the Green's function

7.6.1 Decomposition of the far field

The far field of the Green's function (7.41), denoted by G^{ff}, describes its asymptotic behavior at infinity, i.e., when $|\boldsymbol{y}| \to \infty$ and assuming that $\boldsymbol{x}$ is fixed. For this purpose, the terms of highest order at infinity are searched. Likewise as for the radiation condition, the

far field can be also decomposed into two parts, namely

$$G^{ff} = G_A^{ff} + G_S^{ff}. \tag{7.54}$$

The first part, G_A^{ff}, is linked with the asymptotic decaying of the fundamental solution for the Laplace equation, whereas the second part, G_S^{ff}, is associated with the oblique surface waves.

7.6.2 Asymptotic decaying

The asymptotic decaying acts above and away from the line $\boldsymbol{y}\cdot\boldsymbol{s}=0$, and is related to the logarithmic terms in (7.41), and also to the asymptotic behavior as $\boldsymbol{y}\cdot\boldsymbol{s}\to\infty$ of the exponential integral terms. In fact, due (7.39) we have for $z\in\mathbb{C}$ that

$$\mathrm{Ei}(z) \sim \frac{e^z}{z} \qquad \text{as } \ \mathfrak{Re}\{z\}\to\infty. \tag{7.55}$$

By considering the behavior (7.55) in (7.41), by remembering (7.1d), and by neglecting the exponentially decreasing terms as $\boldsymbol{y}\cdot\boldsymbol{s}\to\infty$, we obtain that

$$G(\boldsymbol{x},\boldsymbol{y}) \sim \frac{1}{2\pi}\ln|\boldsymbol{y}-\boldsymbol{x}| - \frac{1}{2\pi}\ln|\boldsymbol{y}-\bar{\boldsymbol{x}}| + \frac{s_2}{Z\pi}\,\frac{y_2+x_2}{|\boldsymbol{y}-\bar{\boldsymbol{x}}|^2}. \tag{7.56}$$

Using Taylor expansions as in Section 2.4, we have that

$$\frac{1}{2\pi}\ln|\boldsymbol{y}-\boldsymbol{x}| - \frac{1}{2\pi}\ln|\boldsymbol{y}-\bar{\boldsymbol{x}}| = -\frac{(\boldsymbol{x}-\bar{\boldsymbol{x}})\cdot\boldsymbol{y}}{2\pi|\boldsymbol{y}|^2} + \mathcal{O}\!\left(\frac{1}{|\boldsymbol{y}|^2}\right), \tag{7.57}$$

and likewise that

$$\frac{s_2}{Z\pi}\,\frac{y_2+x_2}{|\boldsymbol{y}-\bar{\boldsymbol{x}}|^2} = \frac{s_2}{Z\pi}\,\frac{y_2}{|\boldsymbol{y}|^2} + \mathcal{O}\!\left(\frac{1}{|\boldsymbol{y}|^2}\right). \tag{7.58}$$

We consider $\boldsymbol{y}=|\boldsymbol{y}|\,\hat{\boldsymbol{y}}$, being $\hat{\boldsymbol{y}}=(\cos\theta,\sin\theta)$ a unitary vector. Hence, from (7.56) and due (7.57) and (7.58), the asymptotic decaying of the Green's function is given by

$$G_A^{ff}(\boldsymbol{x},\boldsymbol{y}) = \frac{\sin\theta}{Z\pi|\boldsymbol{y}|}\big(s_2 - Zx_2\big). \tag{7.59}$$

7.6.3 Surface waves in the far field

The oblique surface waves present in the far field are found by studying the poles of the spectral Green's function, which determine their asymptotic behavior and which wad already done. The expression that describes them is obtained by adding (7.20) and (7.21), which implies that the Green's function behaves asymptotically, when $|\boldsymbol{y}\times\boldsymbol{s}|\to\infty$, as

$$\begin{aligned} G(\boldsymbol{x},\boldsymbol{y}) \sim\ & -i\frac{s_2}{2}(s_2+is_1)\big(1+\mathrm{sign}(\boldsymbol{v}\times\boldsymbol{s})\big)\,e^{-Z\boldsymbol{v}\cdot\boldsymbol{s}+iZ\boldsymbol{v}\times\boldsymbol{s}} \\ & -i\frac{s_2}{2}(s_2-is_1)\big(1-\mathrm{sign}(\boldsymbol{v}\times\boldsymbol{s})\big)\,e^{-Z\boldsymbol{v}\cdot\boldsymbol{s}-iZ\boldsymbol{v}\times\boldsymbol{s}}, \end{aligned} \tag{7.60}$$

or, equivalently, as

$$G(\boldsymbol{x},\boldsymbol{y}) \sim -is_2\big(s_2+is_1\,\mathrm{sign}(\boldsymbol{v}\times\boldsymbol{s})\big)\,e^{-Z\boldsymbol{v}\cdot\boldsymbol{s}+iZ|\boldsymbol{v}\times\boldsymbol{s}|}. \tag{7.61}$$

We can use again Taylor expansions to obtain the estimates

$$|\boldsymbol{v}\times\boldsymbol{s}| = |\boldsymbol{y}\times\boldsymbol{s}| - (\bar{\boldsymbol{x}}\times\boldsymbol{s})\,\mathrm{sign}(\boldsymbol{y}\times\boldsymbol{s}) + \mathcal{O}\!\left(\frac{1}{|\boldsymbol{y}\times\boldsymbol{s}|}\right), \tag{7.62}$$

$$\operatorname{sign}(\boldsymbol{v}\times\boldsymbol{s}) = \operatorname{sign}(\boldsymbol{y}\times\boldsymbol{s}) + \mathcal{O}\Big(\frac{1}{|\boldsymbol{y}\times\boldsymbol{s}|}\Big). \tag{7.63}$$

Therefore we have that

$$e^{iZ|\boldsymbol{v}\times\boldsymbol{s}|} = e^{iZ|\boldsymbol{y}\times\boldsymbol{s}|}e^{-iZ(\bar{\boldsymbol{x}}\times\boldsymbol{s})\operatorname{sign}(\boldsymbol{y}\times\boldsymbol{s})}\left(1+\mathcal{O}\Big(\frac{1}{|\boldsymbol{y}\times\boldsymbol{s}|}\Big)\right). \tag{7.64}$$

The surface-wave behavior, due (7.61), (7.63), and (7.64), is thus given by

$$G_S^{ff}(\boldsymbol{x},\boldsymbol{y}) = -is_2\big(s_2+is_1\operatorname{sign}(\boldsymbol{y}\times\boldsymbol{s})\big)\,e^{-Z\boldsymbol{y}\cdot\boldsymbol{s}+iZ|\boldsymbol{y}\times\boldsymbol{s}|}e^{Z\bar{\boldsymbol{x}}\cdot\boldsymbol{s}-iZ(\bar{\boldsymbol{x}}\times\boldsymbol{s})\operatorname{sign}(\boldsymbol{y}\times\boldsymbol{s})}. \tag{7.65}$$

7.6.4 Complete far field of the Green's function

On the whole, the asymptotic behavior of the Green's function as $|\boldsymbol{y}|\to\infty$ can be characterized through the addition of (7.56) and (7.61), namely

$$\begin{aligned} G(\boldsymbol{x},\boldsymbol{y}) \sim{}& \frac{1}{2\pi}\ln|\boldsymbol{y}-\boldsymbol{x}| - \frac{1}{2\pi}\ln|\boldsymbol{y}-\bar{\boldsymbol{x}}| + \frac{s_2}{Z\pi}\,\frac{y_2+x_2}{|\boldsymbol{y}-\bar{\boldsymbol{x}}|^2} \\ &- is_2\big(s_2+is_1\operatorname{sign}(\boldsymbol{v}\times\boldsymbol{s})\big)\,e^{-Z\boldsymbol{v}\cdot\boldsymbol{s}+iZ|\boldsymbol{v}\times\boldsymbol{s}|}. \end{aligned} \tag{7.66}$$

Consequently, the complete far field of the Green's function, due (7.54), is given by the addition of (7.59) and (7.65), i.e., by

$$\begin{aligned} G^{ff}(\boldsymbol{x},\boldsymbol{y}) = {}& \frac{\sin\theta}{Z\pi|\boldsymbol{y}|}\big(s_2-Zx_2\big) \\ &- is_2\big(s_2+is_1\operatorname{sign}(\boldsymbol{y}\times\boldsymbol{s})\big)\,e^{-Z\boldsymbol{y}\cdot\boldsymbol{s}+iZ|\boldsymbol{y}\times\boldsymbol{s}|}e^{Z\bar{\boldsymbol{x}}\cdot\boldsymbol{s}-iZ(\bar{\boldsymbol{x}}\times\boldsymbol{s})\operatorname{sign}(\boldsymbol{y}\times\boldsymbol{s})}. \end{aligned} \tag{7.67}$$

It is this far field (7.67) that justifies the radiation condition (7.1*e–f*). When the first term in (7.67) dominates, i.e., the asymptotic decaying (7.59), then it is the behavior (7.1e) that matters. Conversely, when the second term in (7.67) dominates, i.e., the oblique surface waves (7.65), then (7.1f) is the one that holds. The interface between both asymptotic behaviors can be determined by equating the amplitudes of the two terms in (7.67), i.e., by searching values of $\boldsymbol{y}$ at infinity such that

$$\frac{s_2}{Z\pi|\boldsymbol{y}|} = s_2\,e^{-Z\boldsymbol{y}\cdot\boldsymbol{s}}, \tag{7.68}$$

where the values of $\boldsymbol{x}$ can be neglected, since they remain relatively near the origin. By taking the logarithm in (7.68) and perturbing somewhat the result so as to avoid a singular behavior at the origin, we obtain finally that this interface is described by

$$\boldsymbol{y}\cdot\boldsymbol{s} = \frac{1}{Z}\ln\big(1+Z\pi|\boldsymbol{y}|\big). \tag{7.69}$$

We remark that the asymptotic behavior (7.66) of the Green's function and the expression (7.67) of its complete far field do no longer hold if a complex impedance Z such that $\mathfrak{Im}\{Z\}>0$ and $\mathfrak{Re}\{Z\}\geq 0$ is used, specifically the parts (7.61) and (7.65) linked

with the oblique surface waves. A careful inspection shows that in this case the surface-wave behavior, as $|\boldsymbol{y}\times\boldsymbol{s}|\to\infty$, decreases exponentially and is given by

$$G(\boldsymbol{x},\boldsymbol{y})\sim\begin{cases}-is_2\big(s_2+is_1\,\mathrm{sign}(\boldsymbol{v}\times\boldsymbol{s})\big)\,e^{-|Z|\boldsymbol{v}\cdot\boldsymbol{s}+iZ|\boldsymbol{v}\times\boldsymbol{s}|} & \text{if } \boldsymbol{v}\cdot\boldsymbol{s}>0,\\ -is_2\big(s_2+is_1\,\mathrm{sign}(\boldsymbol{v}\times\boldsymbol{s})\big)\,e^{-Z\boldsymbol{v}\cdot\boldsymbol{s}+iZ|\boldsymbol{v}\times\boldsymbol{s}|} & \text{if } \boldsymbol{v}\cdot\boldsymbol{s}\le 0.\end{cases}\tag{7.70}$$

Therefore the surface-wave part of the far field is now expressed, if $\boldsymbol{y}\cdot\boldsymbol{s}>0$, as

$$G_S^{ff}(\boldsymbol{x},\boldsymbol{y})=-is_2\big(s_2+is_1\,\mathrm{sign}(\boldsymbol{y}\times\boldsymbol{s})\big)\,e^{-|Z|\boldsymbol{y}\cdot\boldsymbol{s}+iZ|\boldsymbol{y}\times\boldsymbol{s}|}e^{|Z|\bar{\boldsymbol{x}}\cdot\boldsymbol{s}-iZ(\bar{\boldsymbol{x}}\times\boldsymbol{s})\,\mathrm{sign}(\boldsymbol{y}\times\boldsymbol{s})},\tag{7.71}$$

and if $\boldsymbol{y}\cdot\boldsymbol{s}\le 0$, then it becomes

$$G_S^{ff}(\boldsymbol{x},\boldsymbol{y})=-is_2\big(s_2+is_1\,\mathrm{sign}(\boldsymbol{y}\times\boldsymbol{s})\big)\,e^{-Z\boldsymbol{y}\cdot\boldsymbol{s}+iZ|\boldsymbol{y}\times\boldsymbol{s}|}e^{Z\bar{\boldsymbol{x}}\cdot\boldsymbol{s}-iZ(\bar{\boldsymbol{x}}\times\boldsymbol{s})\,\mathrm{sign}(\boldsymbol{y}\times\boldsymbol{s})}.\tag{7.72}$$

The asymptotic decaying (7.56) and its far-field expression (7.59), on the other hand, remain the same when a complex impedance is used.

VIII. CONCLUSION

8.1 Discussion

The main conclusion of this thesis is that the desired Green's functions were computed and used effectively to solve direct wave scattering problems by means of integral equation techniques and the boundary element method.

For the two-dimensional Laplace and Helmholtz equations we derived respectively the expressions (2.94) and (3.93), whereas for their three-dimensional counterparts we obtained respectively (4.113) and (5.92). Detailed procedures were implemented to evaluate these expressions numerically, everywhere, and for all values of interest. We analyzed likewise their properties and developed expressions for their far fields. These Green's functions were then used to solve direct wave scattering problems in compactly perturbed half-spaces, like (2.13), by using integral equations in the form of (2.175). The considered arbitrary compact perturbations of the domain were contained in the upper half-space. The integral equations were solved by using the boundary element method, which was programmed in Fortran. To validate the computations, appropriate benchmark problems were developed and solved numerically.

Low relative error bounds were obtained in the resolution of the benchmark problems, which decreased as the discretization step became smaller. The best results among the half-space problems were acquired for the two-dimensional Laplace equation, since its Green's function was determined explicitly and was computed with very high accuracy (vid. Figure 2.17). In the other half-space problems some sort of lower bound for the relative error could be observed, which was related to the accuracy of the corresponding Green's function (vid. Figures 3.14, 4.15 & 5.13). If the accuracy of the Green's function is increased, then this lower bound becomes smaller. The drawbacks of refining the proposed numerical procedures, to attain higher accuracy, are much higher computation times and the need of more precise expressions for the Green's function, e.g., taking more integration nodes for the quadrature formulae or increasing the far-field radius, among others.

As one of the applications for the developed expressions and techniques, we achieved to compute harbor resonances in coastal engineering. A benchmark problem based on a rectangular harbor was developed and the computed resonances coincided with the predicted eigenfrequencies, as shown in Figure 6.5. Additionally, as a more theoretical application we derived the explicit representation (7.41) for the Green's function of the oblique-derivative impedance half-plane Laplace problem, discussing some of its properties and determining its far field.

A detailed theoretical background for the involved mathematics and physics was included in the appendix, allowing thus a far deeper comprehension of the presented topics and an extensive list of references. The theory of wave scattering problems for bounded obstacles with an impedance boundary condition was also enclosed in the appendix, due its relevance in the proper understanding of the half-space problems and since, even if it is assumed to be a known topic, its literature is widespread and not always so complete as

desired for our purposes. These full-space problems were also treated by means of integral equation techniques and the boundary element method, and corresponding benchmark problems were implemented and solved. In their resolution low relative error bounds were obtained and the accuracy of the involved Green's functions, which were known explicitly, was enough so that no lower bounds could be appreciated in Figures B.18, C.9, D.18 & E.9.

In conclusion, the objectives outlined in Section 1.3 were fulfilled satisfactorily.

8.2 Perspectives for future research

The interest in the subject of this thesis began over a hundred years ago and it still remains an active field of research with an enormous potential. Based on the present work and on the obtained insight, many perspectives for future research can be established.

A first topic that can be thought of on this behalf is the need of even more accurate numerical expressions for the Green's functions of the half-space Helmholtz problems and of the three-dimensional half-space Laplace problem. In particular, it would be very useful to have polynomial approximations of high accuracy to describe them, as much in the near field as in the far field. The highest achievement would be nonetheless the development of an explicit representation formula for them.

The herein developed techniques can be adapted and extended to other interesting cases, e.g., half-space problems in linear elasticity and in electromagnetism. They can be also applied to impedance problems in infinite strips and in finite-depth infinite layers, which are of particular interest for the water-wave problem in linear water-wave theory. They can be likewise adapted to solve time-dependent problems through retarded potentials or even through time-reversal techniques.

A still pending topic is the development of appropriate integral equations in impedance half-space problems when the compact perturbation is partially or entirely contained in the complementary half-space, in which case the other appearing singularities of the Green's function, i.e., the image source point $\bar{\boldsymbol{x}}$ and the image half-line Υ, have to be also taken into account. The integral equations are supported in this case not only on the perturbed boundary but also on the portion of its image surface contained in the upper half-space and on the space between them.

The considered problems can be likewise extended to consider inhomogeneous media, which implies integral equations supported also on the volume encompassed by the inhomogeneity, i.e., so-called Lippmann-Schwinger-type equations.

Further studies can be performed on the stability of the developed method with respect to different geometrical configurations and regularities of the boundary surface. The results can be also compared with other numerical methods like perfectly matched layers, absorbing boundary conditions, and the Dirichlet-to-Neumann operator. These methods could be even combined into new hybrid methods, to exploit better certain common advantages.

The derived Green's functions and their related integral equations are of great importance for the treatment of inverse scattering problems in impedance half-spaces, where an active field of research is still in development.

On behalf of the first application, the study of harbor resonances could be extended to the case of a more variable bottom slope by considering directly the mild-slope equation. Further modeling can be performed for real maritime harbors and the results compared with experimental and real-life observations. Practical approaches to filter out spurious resonances are likewise of great interest.

For the oblique-derivative half-plane Laplace problem, corresponding integral equations can be derived and solved numerically. Further oblique-derivative problems can be considered for the three-dimensional Laplace equation, for the Helmholtz equation, etc.

As further applications to consider we may mention the scattering of light by a photonic crystal, acoustic and electromagnetic scattering above ground, and water-wave scattering for floating or submerged bodies, among many others.

The possibilities for new applications and techniques are almost infinite and therefore the perspectives for future research on the field look very promising....

REFERENCES

Abramowitz, M. & Stegun, I. A. (1972), *Handbook of Mathematical Functions with Formulas, Graphs, and Mathematical Tables*, Dover, New York.

Adams, R. A. (1975), *Sobolev Spaces*, Academic Press, London.

Ahner, J. F. (1978), 'The exterior Robin problem for the Helmholtz equation', *Journal of Mathematical Analysis and Applications* **66**, 37–54.

Ahner, J. F. & Wiener, H. W. (1991), 'On an exterior Laplace equation problem with Robin boundary condition', *Journal of Mathematical Analysis and Applications* **157**, 127–146.

Alber, H.-D. & Ramm, A. G. (2009), 'Asymptotics of the solution to Robin problem', *Journal of Mathematical Analysis and Applications* **349**, 156–164.

Albert, D. G. (2003), 'Observations of acoustic surface waves in outdoor sound propagation', *Journal of the Acoustical Society of America* **113**(5), 2495–2500.

Albert, D. G. & Orcutt, J. A. (1990), 'Acoustic pulse propagation above grassland and snow: Comparison of theoretical and experimental waveforms', *Journal of the Acoustical Society of America* **87**(1), 93–100.

Ammari, H. (2008), *An Introduction to Mathematics of Emerging Biomedical Imaging*, Springer, Berlin.

Amos, D. E. (1980), 'Computation of exponential integrals', *ACM Transactions on Mathematical Software* **6**(3), 365–377.

Amos, D. E. (1986), 'Algorithm 644: A portable package for Bessel functions of a complex argument and nonnegative order', *ACM Transactions on Mathematical Software* **12**(3), 265–273.

Amos, D. E. (1990*a*), 'Algorithm 683: A portable FORTRAN subroutine for exponential integrals of a complex argument', *ACM Transactions on Mathematical Software* **16**(2), 178–182.

Amos, D. E. (1990*b*), 'Computation of exponential integrals of a complex argument', *ACM Transactions on Mathematical Software* **16**(2), 169–177.

Amos, D. E. (1990*c*), 'Remark on algorithm 644', *ACM Transactions on Mathematical Software* **16**(4), 404–404.

Amos, D. E. (1995), 'A remark on algorithm 644: "A portable package for Bessel functions of a complex argument and nonnegative order"', *ACM Transactions on Mathematical Software* **21**(4), 388–393.

Amrouche, C. (2002), 'The Neumann problem in the half-space', *Comptes Rendus de l'Académie des Sciences de Paris, Série I* **335**, 151–156.

Anderson, E., Bai, Z., Bischof, C., Blackford, S., Demmel, J., Dongarra, J., Du Croz, J., Greenbaum, A., Hammarling, S., McKenney, A. & Sorensen, D. (1999), *LAPACK User's Guide*, SIAM, Philadelphia.

Anduaga, A. (2008), 'The realist interpretation of the atmosphere', *Studies in History and Philosophy of Modern Physics* **39**, 465–510.

Angell, T. S., Hsiao, G. C. & Kleinman, R. E. (1986), 'An integral equation for the floating-body problem', *Journal of Fluid Mechanics* **166**, 161–171.

Angell, T. S. & Kleinman, R. E. (1982), 'Boundary integral equations for the Helmholtz equation: The third boundary value problem', *Mathematical Methods in the Applied Sciences* **4**, 164–193.

Angell, T. S., Kleinman, R. E. & Hettlich, F. (1990), 'The resistive and conductive problems for the exterior Helmholtz equation', *SIAM Journal on Applied Mathematics* **50**(6), 1607–1622.

Angell, T. S. & Kress, R. (1984), 'L^2-boundary integral equations for the Robin problem', *Mathematical Methods in the Applied Sciences* **6**, 345–352.

Arfken, G. B. & Weber, H. J. (2005), *Mathematical Methods for Physicists*, 6th edn., Elsevier Academic Press, Amsterdam.

Atkinson, K. E. & Han, W. (2005), *Theoretical Numerical Analysis: A Functional Analysis Framework*, Vol. 39 of *Texts in Applied Mathematics*, 2nd edn., Springer, New York.

Attenborough, K. (1983), 'Acoustical characteristics of rigid fibrous absorbents and granular materials', *Journal of the Acoustical Society of America* **73**(3), 785–799.

Attenborough, K. (1985), 'Acoustical impedance models for outdoor ground surfaces', *Journal of Sound and Vibration* **99**(4), 521–544.

Attenborough, K. (2002), 'Sound propagation close to the ground', *Annual Review of Fluid Mechanics* **34**, 51–82.

Attenborough, K., Hayek, S. I. & Lawther, J. M. (1980), 'Propagation of sound above a porous half-space', *Journal of the Acoustical Society of America* **68**(5), 1493–1501.

Attenborough, K., Li, K. M. & Horoshenkov, K. (2007), *Predicting Outdoor Sound*, Taylor & Francis, London.

Bak, J. & Newman, D. J. (1997), *Complex Analysis*, Springer, New York.

Baños, A. (1966), *Dipole Radiation in the Presence of a Conducting Half-Space*, Pergamon, New York.

Baños, A. & Wesley, J. P. (1953), The horizontal electric dipole in a conducting half-space, Technical report SIO Reference 53-33, Marine Physical Laboratory of the Scripps Institution of Oceanography, University of California, San Diego.

Baños, A. & Wesley, J. P. (1954), The horizontal electric dipole in a conducting half-space II, Technical report SIO Reference 54-31, Marine Physical Laboratory of the Scripps Institution of Oceanography, University of California, San Diego.

Barton, G. (1989), *Elements of Green's Functions and Propagation: Potentials, Diffusion and Waves*, Oxford University Press, Oxford.

Bateman, H. (1932), *Partial Differential Equations of Mathematical Physics*, Dover, New York.

Bateman, H. (1954), *Tables of Integral Transforms*, Vol. 1–2, McGraw-Hill, New York.

Becker, A. A. (1992), *The Boundary Element Method in Engineering: A Complete Course*, McGraw-Hill, New York.

Bendali, A. & Devys, C. (1986), Calcul numérique du rayonnement de cornets électromagnétiques dont l'ouverture est partiellement remplie par un diélectrique, Technical report, Paris.

Bendali, A. & Souilah, M. (1994), 'Consistency estimates for a double-layer potential and application to the numerical analysis of the boundary-element approximation of acoustic

scattering by a penetrable object', *Mathematics of Computation* **62**(205), 65–91.
Bender, C. M. & Orszag, S. A. (1978), *Advanced Mathematical Methods for Scientists and Engineers*, McGraw-Hill, New York.
Berkhoff, J. C. W. (1972*a*), Computation of combined refraction and diffraction, *in* 'Proceedings of the 13th International Conference on Coastal Engineering', ASCE, Vancouver, 471–490. Also: Publication 119, Delft Hydraulics Laboratory, Delft (1974).
Berkhoff, J. C. W. (1972*b*), Mathematical models for simple harmonic linear water waves: wave diffraction and refraction, Publication 163, Delft Hydraulics Laboratory, Delft. Also: PhD thesis, Delft University of Technology, Delft.
Berkhoff, J. C. W. (1976), Mathematical models for simple harmonic linear water waves: wave diffraction and refraction, Publication 163, Delft Hydraulics Laboratory, Delft. Also: PhD thesis, Delft University of Technology, Delft.
Berkhoff, J. C. W., Booy, N. & Radder, A. C. (1982), 'Verification of numerical wave propagation models for simple harmonic linear water waves', *Coastal Engineering* **6**(3), 255–279.
Bermúdez, A., Hervella-Nieto, L., Prieto, A. & Rodríguez, R. (2007), 'Validation of acoustic models for time-harmonic dissipative scattering problems', *Journal of Computational Acoustics* **15**(1), 95–121.
Black, J. L. (1975), 'Wave forces on vertical axisymmetric bodies', *Journal of Fluid Mechanics* **67**(2), 369–376.
Bonnet-BenDhia, A.-S. & Tillequin, A. (2001), 'A limiting absorption principle for scattering problems with unbounded obstacles', *Mathematical Methods in the Applied Sciences* **24**, 1089–1111.
Bony, J.-M. (2001), *Cours d'Analyse*, Éditions de l'École Polytechnique, Palaiseau.
Booij, N. (1983), 'A note on the accuracy of the mild-slope equation', *Coastal Engineering* **7**(3), 191–203.
Breit, G. & Tuve, M. A. (1926), 'A test of the existence of the conducting layer', *Physical Review* **28**(3), 554–575.
Bremermann, H. (1965), *Distributions, Complex Variables, and Fourier Transforms*, Addison-Wesley, Reading, Massachusetts.
Brezis, H. (1999), *Analyse Fonctionnelle: Théorie et Applications*, Dunod, Paris.
Brezzi, F. & Fortin, M. (1991), *Mixed and Hybrid Finite Element Methods*, Springer, New York.
Briquet, M. & Filippi, P. (1977), 'Diffraction of a spherical wave by an absorbing plane', *Journal of the Acoustical Society of America* **61**(3), 640–646.
Burden, R. & Faires, J. D. (2001), *Numerical Analysis*, 7th edn., Brooks/Cole Publishing, New York.
Burrows, A. (1985), 'Waves incident on a circular harbour', *Proceedings of the Royal Society of London, Series A, Mathematical and Physical Sciences* **401**(1821), 349–371.
Butkov, E. (1968), *Mathematical Physics*, Addison Wesley, Reading.
Cakoni, F., Colton, D. & Monk, P. (2001), 'The direct and inverse scattering problems for partially coated obstacles', *Inverse Problems* **17**, 1997–2015.

Casciato, M. D. & Sarabandi, K. (2000), 'Fields of an infinitesimal dipole radiating near an impedance half-space by application of exact image theory', *IEEE Antennas and Propagation Society International Symposium* **1**, 442–445.

Cauchy, A. L. (1827), Mémoire sur la théorie de la propagation des ondes à la surface d'un fluide pesant d'une profondeur indéfinie, *in* 'Mémoires Présentés par Divers Savants à l'Académie Royale des Sciences de l'Institut de France', Vol. 1, Imprimerie Royale, Paris, 3–312.

Chakrabarti, S. K. (2001), 'Application and verification of deepwater Green function for water waves', *Journal of Ship Research* **45**(3), 187–196.

Chandler-Wilde, S. N. (1997), 'The impedance boundary value problem for the Helmholtz equation in a half-plane', *Mathematical Methods in the Applied Sciences* **20**, 813–840.

Chandler-Wilde, S. N. & Hothersall, D. C. (1995*a*), 'Efficient calculation of the Green function for acoustic propagation above a homogeneous impedance plane', *Journal of Sound and Vibration* **180**(5), 705–724.

Chandler-Wilde, S. N. & Hothersall, D. C. (1995*b*), 'A uniformly valid far field asymptotic expansion of the Green function for two-dimensional propagation above a homogeneous impedance plane', *Journal of Sound and Vibration* **182**(5), 665–675.

Chandler-Wilde, S. N. & Peplow, A. (2005), 'A boundary integral equation formulation for the Helmholtz equation in a locally perturbed half-plane', *Zeitschrift für Angewandte Mathematik und Mechanik* **85**(2), 79–88.

Chaudhry, M. A. & Zubair, S. M. (2002), *On a Class of Incomplete Gamma Functions with Applications*, Chapman & Hall/CRC, Boca Raton.

Chen, G. & Zhou, J. (1992), *Boundary Element Methods*, Academic Press, Cambridge.

Chen, H. S. (1986), 'Effects of bottom friction and boundary absorption on water wave scattering', *Applied Ocean Research* **8**(2), 99–104.

Chen, H. S. (1990), 'Infinite elements for water wave radiation and scattering', *International Journal for Numerical Methods in Fluids* **11**(5), 555–569.

Chen, Z.-S. & Waubke, H. (2007), 'A formulation of the boundary element method for acoustic radiation and scattering from two-dimensional structures', *Journal of Computational Acoustics* **15**(3), 333–352.

Chien, C. F. & Soroka, W. W. (1975), 'Sound propagation along an impedance plane', *Journal of Sound and Vibration* **43**(1), 9–20.

Chien, C. F. & Soroka, W. W. (1980), 'A note on the calculation of sound propagation along an impedance surface', *Journal of Sound and Vibration* **69**(2), 340–343.

Chou, C.-R. & Han, W.-Y. (1993), 'Wave-induced oscillations in harbours with dissipating quays', *Coastal Engineering in Japan* **36**(1), 1–23.

Chwang, A. T. & Chan, A. T. (1998), 'Interaction between porous media and wave motion', *Annual Reviews of Fluid Mechanics* **30**, 53–84.

Ciarlet, P. G. (1979), *The Finite Element Method for Elliptic Problems*, North-Holland, Amsterdam.

Collin, R. (2004), 'Hertzian dipole radiating over a lossy earth or sea: Some early and late 20th-century controversies', *IEEE Antennas and Propagation Magazine* **46**(2), 64–79.

Colton, D. & Kirsch, A. (1981), 'The determination of the surface impedance of an obstacle from measurements of the far field pattern', *SIAM Journal on Applied Mathematics* **41**(1), 8–15.

Colton, D. & Kress, R. (1983), *Integral Equation Methods in Scattering Theory*, Wiley-Interscience, New York.

Colton, D. & Kress, R. (1995), 'Eigenvalues of the far field operator for the Helmholtz equation in an absorbing medium', *SIAM Journal on Applied Mathematics* **55**(6), 1724–1735.

Costabel, M. (1986), Principles of boundary element methods, Lecture notes, Technische Hochschule Darmstadt, Lausanne.

Costabel, M. (1988), 'Boundary integral operators on Lipschitz domains: Elementary results', *SIAM Journal on Mathematical Analysis* **106**, 367–279.

Costabel, M. (2007), Some historical remarks on the positivity of boundary integral operators, *in* M. Schanz & O. Steinbach, eds., 'Boundary Element Analysis: Mathematical Aspects and Applications', Vol. 29, Lecture Notes in Applied and Computational Mechanics, Springer, Berlin, 1–27.

Costabel, M. & Dauge, M. (1997), 'On representation formulas and radiation conditions', *Mathematical Methods in the Applied Sciences* **20**, 133–150.

Costabel, M. & Stephan, E. (1985), 'A direct boundary integral equation method for transmission problems', *Journal of Mathematical Analysis and Applications* **106**, 367–279.

Courant, R. & Hilbert, D. (1966), *Methods of Mathematical Physics*, Vol. 1 & 2, Interscience, New York.

Cowper, G. R. (1973), 'Gaussian quadrature formulas for triangles', *International Journal of Numerical Methods in Engineering* **7**, 405–408.

Craik, A. D. D. (2004), 'The origins of water wave theory', *Annual Review of Fluid Mechanics* **36**, 1–28.

Darwin, G. H. (1899), *The Tides and Kindred Phenomena in the Solar System*, Riverside Press, Cambridge.

Dassios, G. & Kamvyssas, G. (1997), 'The impedance scattering problem for a point-source field. The small resistive sphere', *The Quarterly Journal of Mechanics and Applied Mathematics* **50**(2), 321–332.

Dassios, G. & Kleinman, R. (1999), 'Half space scattering problems at low frequencies', *IMA Journal of Applied Mathematics* **62**, 61–79.

Dautray, R. & Lions, J.-L. (1987), *Analyse Mathématique et Calcul Numérique pour les Sciences et les Techniques*, Vol. 1–7, Masson, Paris.

Davies, B. (2002), *Integral Transforms and Their Applications*, 3rd edn., Springer, New York.

De Lacerda, L. A., Wrobel, L. C. & Mansur, W. J. (1997), 'A dual boundary element formulation for sound propagation around barriers over an infinite plane', *Journal of Sound and Vibration* **2002**(2), 235–247.

De Lacerda, L. A., Wrobel, L. C., Power, H. & Mansur, W. J. (1998), 'A novel boundary integral formulation for three-dimensional analysis of thin acoustic barriers over an impedance plane', *Journal of the Acoustical Society of America* **104**(2), 671–678.

Dean, W. R. (1945), 'On the reflexion of surface waves by a submerged plane barrier', *Proceedings of the Cambridge Philosophical Society* **41**, 231–238.

Demirbilek, Z. & Panchang, V. (1998), CGWAVE: A coastal surface water wave model of the mild slope equation, Technical Report CHL-98-xx, Headquarters, U.S. Army Corps of Engineers, United States of America.

DeSanto, J. A. (1992), *Scalar Wave Theory: Green's Functions and Applications*, Springer, Berlin.

Dettman, J. W. (1984), *Applied Complex Variables*, Dover, New York.

Di Fazio, G. & Palagachev, D. K. (1996), 'Oblique derivative problem for elliptic equations in non-divergence form with VMO coefficients', *Commentationes Mathematicae Universitatis Carolinae* **37**(3), 537–556.

Doppel, K. & Hochmuth, R. (1995), 'An application of the limit absorption principle to a mixed boundary value problem in an infinite strip', *Mathematical Methods in the Applied Sciences* **18**, 529–548.

Duffy, D. G. (2001), *Green's Functions with Applications*, Chapman & Hall/CRC, Boca Raton.

Dunavant, D. A. (1985), 'High degree efficient symmetrical Gaussian quadrature rules for the triangle', *International Journal of Numerical Methods in Engineering* **21**, 1129–1148.

Durán, M., Guarini, M. & Jerez-Hanckes, C. F. (2009), Hybrid FEM/BEM modeling of finite-sized photonic crystals for semiconductor laser beams, Research report No. 2009-25, Eidgenössische Technische Hochschule, Zürich.

Durán, M., Hein, R. & Nédélec, J.-C. (2007*a*), Computing numerically the Green's function of the half-plane Helmholtz equation with impedance boundary conditions, *in* 'Proceedings of Waves 2007, The 8th International Conference on Mathematical and Numerical Aspects of Waves', University of Reading, Reading, 384–386.

Durán, M., Hein, R. & Nédélec, J.-C. (2007*b*), 'Computing numerically the Green's function of the half-plane Helmholtz operator with impedance boundary conditions', *Numerische Mathematik* **107**, 295–314.

Durán, M., Muga, I. & Nédélec, J.-C. (2005*a*), 'The Helmholtz equation with impedance in a half-plane', *Comptes Rendus de l'Académie des Sciences de Paris, Série I* **340**, 483–488.

Durán, M., Muga, I. & Nédélec, J.-C. (2005*b*), 'The Helmholtz equation with impedance in a half-space', *Comptes Rendus de l'Académie des Sciences de Paris, Série I* **341**, 561–566.

Durán, M., Muga, I. & Nédélec, J.-C. (2006), 'The Helmholtz equation in a locally perturbed half-plane with passive boundary', *IMA Journal of Applied Mathematics* **71**, 853–876.

Durán, M., Muga, I. & Nédélec, J.-C. (2009), 'The Helmholtz equation in a locally perturbed half-space with non-absorbing boundary', *Archive for Rational Mechanics and Analysis* **191**, 143–172.

Durán, M., Nédélec, J.-C. & Ossandón, S. (2009), 'An efficient Galerkin BEM to compute high acoustic eigenfrequencies', *Journal of Vibration and Acoustics* **131**(3), 031001.

Dwight, H. B. (1957), *Tables of Integrals and Other Mathematical Data*, 3rd edn., Macmillan, New York.

Eckart, C. (1952), The propagation of gravity waves from deep to shallow water, *in* 'Gravity Waves', National Bureau of Standards, Circular 521, 165–173.

Egorov, J. V. & Kondrat'ev, V. A. (1969), 'The oblique derivative problem', *Mathematics of the USSR Sbornik* **7**(1), 139–169.

Ehrenmark, U. T. & Williams, P. S. (2001), 'Wave parameter tuning for the application of the mild-slope equation on steep beaches and in shallow water', *Coastal Engineering* **42**(1), 17–34.

Elmore, W. C. & Heald, M. A. (1969), *Physics of Waves*, 3rd edn., McGraw-Hill, New York.

Embleton, T. F. (1996), 'Tutorial on sound propagation outdoors', *Journal of the Acoustical Society of America* **100**(1), 31–48.

Embleton, T. F., Piercy, J. E. & Olson, N. (1976), 'Outdoor sound propagation over ground of finite impedance', *Journal of the Acoustical Society of America* **59**(2), 267–277.

Erdélyi, A. (1953), *Higher Transcendental Functions*, Vol. 1–3, McGraw-Hill, New York.

Estrada, R. & Kanwal, R. P. (2002), *A Distributional Approach to Asymptotics: Theory and Applications*, Birkhäuser, Boston.

Evans, L. C. (1998), *Partial Differential Equations*, American Mathematical Society, Providence.

Fasino, D. & Inglese, G. (1999), 'An inverse Robin problem for Laplace's equation: theoretical results and numerical methods', *Inverse Problems* **15**, 41–48.

Feistauer, M., Hsiao, G. C. & Kleinman, R. E. (1996), 'Asymptotic and a posteriori error estimates for boundary element solutions of hypersingular integral equations', *SIAM Journal on Numerical Analysis* **33**(2), 666–685.

Felsen, L. B. & Marcuwitz, N. (2003), *Radiation and Scattering of Waves*, John Wiley & Sons, New York.

Fenton, J. D. (1978), 'Wave forces on vertical bodies of revolution', *Journal of Fluid Mechanics* **85**(2), 241–255.

Filippi, P. (1983), 'Extended sources radiation and Laplace type integral representation: Application to wave propagation above and within layered media', *Journal of Sound and Vibration* **91**(1), 65–84.

Filippi, P., Bergassoli, A., Habault, D. & Lefebvre, J. P. (1999), *Acoustics: Basic Physics Theory and Methods*, Academic Press, London.

Forel, F. A. (1895), *Le Léman, Monographie Limnologique*, Vol. 2, Librairie de l'Université, Lausanne.

Gasquet, C. & Witomski, P. (1999), *Fourier Analysis and Applications*, Springer, New York.

Gautesen, A. K. (1988), 'Oblique derivative boundary conditions and the image method for wedges', *SIAM Journal on Applied Mathematics* **48**(6), 1487–1492.

Gel'fand, I. M. & Shilov, G. E. (1964), *Generalized Functions*, Vol. 1, Academic Press, New York.

Gilbarg, D. & Trudinger, N. S. (1983), *Elliptic Partial Differential Equations of Second Order*, 2nd edn., Springer, Berlin.

Giroire, J. (1987), Étude de quelques Problèmes aux Limites Exterieurs et Résolution par Équations Intégrales, PhD thesis, Université Pierre et Marie Curie, Paris.

Givoli, D. (1999), 'Recent advances in the DtN FE method', *Archives of Computational Methods in Engineering* **6**(2), 71–116.

Glaisher, J. W. L. (1870), 'Tables of the numerical values of the sine-integral, cosine-integral, and exponential-integral', *Philosophical Transactions of the Royal Society of London* **160**, 367–388.

Gockenbach, M. S. (2006), *Understanding and Implementing the Finite Element Method*, SIAM, Philadelphia.

Gradshteyn, I. S. & Ryzhik, I. M. (2007), *Tables of Integrals, Series and Products*, 7th edn., Academic Press, San Diego.

Granat, C., Tahar, M. B. & Ha-Duong, T. (1999), 'Variational formulation using integral equations to solve sound scattering above an absorbing plane', *Journal of the Acoustical Society of America* **105**(5), 2557–2564.

Green, G. (1828), *An Essay on the Application of Mathematical Analysis to the Theories of Electricity and Magnetism*, Printed for the Author by T. Wheelhouse, Nottingham.

Greenberg, M. D. (1971), *Application of Green's functions in Science and Engineering*, Prentice-Hall, Englewood Cliffs.

Griffel, D. H. (1985), *Applied Functional Analysis*, Dover, New York.

Grisvard, P. (1985), *Elliptic Problems in Nonsmooth Domains*, Pitman, Boston.

Gumerov, N. A. & Duraiswami, R. (2004), *Fast Multipole Methods for the Helmholtz Equation in Three Dimensions*, Elsevier Series in Electromagnetism, Elsevier, Amsterdam.

Ha-Duong, T. (1987), Équations Intégrales pour la Résolution Numérique de Problèmes de Diffraction d'Ondes Acoustiques dans $\mathbb{R}^3$, PhD thesis, Université Pierre et Marie Curie, Paris.

Habault, D. (1999), Outdoor sound propagation, *in* P. Filippi, A. Bergassoli, D. Habault & J. P. Lefebvre, eds., 'Acoustics: Basic Physics Theory and Methods', Academic Press, London, 121–157.

Habault, D. & Filippi, P. (1981), 'Ground effect analysis: Surface wave and layer potential representations', *Journal of Sound and Vibration* **79**(4), 529–550.

Harter, R., Abrahams, I. D. & Simon, M. J. (2007), 'The effect of surface tension on trapped modes in water-wave problems', *Proceedings of the Royal Society A: Mathematical, Physical and Engineering Science* **463**(2088), 3131–3149.

Harter, R., Simon, M. J. & Abrahams, I. D. (2008), 'The effect of surface tension on localized free-surface oscillations about surface-piercing bodies', *Proceedings of the Royal Society A: Mathematical, Physical and Engineering Science* **464**(2099), 3039–3054.

Havelock, T. H. (1917), 'Some cases of wave motion due to a submerged obstacle', *Proceedings of the Royal Society of London, Series A, Containing Papers of a Mathematical and Physical Character* **93**(654), 520–532.

Havelock, T. H. (1927), 'The method of images in some problems of surface waves', *Proceedings of the Royal Society of London, Series A, Containing Papers of a Mathematical*

and Physical Character **115**(771), 268–280.

Havelock, T. H. (1955), 'Waves due to a floating sphere making periodic heaving oscillations', *Proceedings of the Royal Society of London, Series A, Mathematical and Physical Sciences* **231**(1184), 1–7.

Hazard, C. & Lenoir, M. (1993), 'Determination of scattering frequencies for an elastic floating body', *SIAM Journal on Mathematical Analysis* **24**(6), 1458–1514.

Hazard, C. & Lenoir, M. (1998), Stabilité et résonance pour le problème du mouvement sur la houle, Technical report Nr. 310, École Nationale Supérieure de Techniques Avancées, Paris.

Hazard, C. & Lenoir, M. (2002), Scattering in oceans Chapter 1.9.1: Surface water waves, *in* E. R. Pike & P. C. Sabatier, eds., 'Scattering — Scattering and Inverse Scattering in Pure and Applied Science', Academic Press, London, 618–636.

Hearn, G. E. (1977), 'Alternative methods of evaluating Green's function in three-dimensional ship-wave problems', *Journal of Ship Research* **21**, 89–93.

Heaviside, O. (1902), The theory of electric telegraphy, *in* 'Encyclopaedia Britannica', 10th edn., Vol. 33, London, 215.

Hein, R. (2006), Computing numerically the Green's function of the half-plane Helmholtz equation with impedance boundary conditions, Dissertation, Pontificia Universidad Católica de Chile, Santiago de Chile.

Hein, R. (2007), Computing numerically the Green's function of the half-plane Helmholtz equation with impedance boundary conditions, Rapport de stage, Centre de Mathématiques Appliquées, École Polytechnique, Palaiseau.

Herbich, J. B., ed. (1999), *Developments in Offshore Engineering: Wave Phenomena and Offshore Topics*, Gulf Publishing, Houston.

Hess, J. L. & Smith, A. M. O. (1967), Calculation of potential flow about arbitrary bodies, *in* D. Kuchemann, ed., 'Progress in Aeronautical Sciences', Vol. 8, Pergamon Press, New York, 1–138.

Hochmuth, R. (2001), 'A localized boundary element method for the floating body problem', *IMA Journal of Numerical Analysis* **21**, 799–816.

Howe, M. S. (2007), *Hydrodynamics and Sound*, Cambridge University Press, Cambridge.

Hsiao, G. C., Lin, M.-C. & Hu, N.-C. (2002), 'DRBEM analysis of combined wave refraction and diffraction in the presence of current', *Journal of Marine Science and Technology* **10**(1), 54–60.

Hsiao, G. C. & Wendland, W. L. (2008), *Boundary Integral Equations*, Springer, Berlin.

Hsiao, S.-S., Lin, J.-G. & Fang, H.-M. (2001), DRBEM analysis on wave oscillation due to energy dissipation, *in* 'Proceedings of the Eleventh International Offshore and Polar Engineering Conference', Stavanger, 581–586.

Hsu, T.-W., Lin, T.-Y., Wen, C.-C. & Ou, S.-H. (2006), 'A complementary mild-slope equation derived using higher-order depth function for waves obliquely propagating on sloping bottom', *Physics of Fluids* **18**, 087106.

Hwang, L. S. & Tuck, E. O. (1970), 'On the oscillations of harbours of arbitrary shape', *Journal of Fluid Mechanics* **42**(3), 447–464.

Ihlenburg, F. (1998), *Finite Element Analysis of Acoustic Scattering*, Springer, New York.

Ingard, U. (1951), 'On the reflection of a spherical sound wave from an infinite plane', *Journal of the Acoustical Society of America* **23**(3), 329–335.

Ippen, A. T. & Goda, Y. (1963), Wave-induced oscillations in harbor: The solution for a rectangular harbor connected to open-sea, Technical Report 59, Hydrodynamic Laboratory, Massachusetts Institute of Technology, Massachusetts.

Irarrázaval, P. (1999), *Análisis de Señales*, McGraw-Hill/Interamericana de Chile Ltda., Santiago de Chile.

Jackson, J. D. (1999), *Classical Electrodynamics*, 3rd edn., John Wiley & Sons, New York.

Jahnke, E. & Emde, F. (1945), *Tables of Functions with Formulae and Curves*, 4th edn., Dover, New York.

Jerry, A. J. (1977), 'The Shannon sampling theorem — its various extensions and applications: A tutorial review', *Proceedings of the IEEE* **65**(11), 1565–1596.

Jerry, A. J. (1979), 'Correction to "The Shannon sampling theorem — its various extensions and applications: A tutorial review"', *Proceedings of the IEEE* **67**(4), 695–695.

Joannopoulos, J. D., Johnson, S. G., Winn, J. N. & Meade, R. D. (2008), *Photonic Crystals*, 2nd edn., Princeton University Press, Princeton.

John, F. (1949), 'On the motion of floating bodies I', *Communications on Pure and Applied Mathematics* **2**, 13–57.

John, F. (1950), 'On the motion of floating bodies II', *Communications on Pure and Applied Mathematics* **3**, 45–101.

Johnson, C. (1987), *Numerical Solutions of Partial Differential Equations by the Finite Element Method*, Cambridge University Press, Cambridge.

Johnson, C. & Nédélec, J.-C. (1980), 'On the coupling of boundary integral and finite element methods', *Mathematics of Computation* **35**(152), 1063–1079.

Johnson, S. G. (2008), Notes on perfectly matched layers (PMLs), Lecture notes, Massachusetts Institute of Technology, Massachusetts.

Jordan, T. F., Stortz, K. R. & Sydor, M. (1981), 'Resonant oscillation in Duluth-Superior Harbor', *Limnology and Oceanography* **26**(1), 186–190.

Keller, J. B. (1979), 'Progress and prospects in the theory of linear wave propagation', *SIAM Review* **21**(2), 229–245.

Keller, J. B. (1981), 'Oblique derivative boundary conditions and the image method', *SIAM Journal on Applied Mathematics* **41**(2), 294–300.

Kellogg, O. D. (1929), *Foundations of Potential Theory*, Springer, Berlin.

Kennelly, A. E. (1902), 'On the elevation of the electrically conducting strata of the Earth's atmosphere', *Electric World and Engineering* **39**, 473.

Kim, W. D. (1965), 'On the harmonic oscillations of a rigid body on a free surface', *Journal of Fluid Mechanics* **21**(3), 427–451.

Kinsler, L. E., Frey, A. R., Coppens, A. B. & Sanders, J. V. (1999), *Fundamentals of Acoustics*, 4th edn., John Wiley & Sons, New York.

Kirby, J. T. & Dalrymple, R. A. (1983), 'A parabolic equation for the combined refrection-diffraction of Stokes waves by mildly varying topography', *Journal of Fluid Mechanics* **136**, 453–466.

Kirkup, S. (2007), *The Boundary Element Method in Acoustics*, Integrated Sound Software, West Yorkshire.

Kirsch, A. (1981), 'Optimal control of an exterior Robin problem', *Journal of Mathematical Analysis and Applications* **82**, 144–151.

Kirsch, A. & Grinberg, N. (2008), *The Factorization Method for Inverse Problems*, Oxford University Press, Oxford.

Kravtchenko, J. & McNown, J. S. (1955), 'Seiche in rectangular ports', *Quarterly of Applied Mathematics* **13**, 19–26.

Kress, R. (1989), *Linear Integral Equations*, Springer, Berlin.

Kress, R. (1995), 'On the numerical solution of a hypersingular integral equation in scattering theory', *Journal of Computational and Applied Mathematics* **61**, 345–360.

Kress, R. (2002), Acoustic scattering Chapter 1.2.1: Specific theoretical tools Chapter 1.2.2: Scattering by obstacles, *in* E. R. Pike & P. C. Sabatier, eds., 'Scattering: Scattering and Inverse Scattering in Pure and Applied Science', Vol. 1, Academic Press, London, 37–73.

Kress, R. & Lee, K.-M. (2003), 'Integral equation methods for scattering from an impedance crack', *Journal of Computational and Applied Mathematics* **161**, 161–177.

Krutitskii, P. A. (2002), 'Integral equation method for the acoustic impedance problem in interior multiply connected domain', *Journal of Mathematical Analysis and Applications* **274**, 1–15.

Krutitskii, P. A. (2003*a*), 'Hypersingular integral equations not needed in the impedance problem in scattering theory', *Computers and Mathematics with Applications* **145**(1–3), 391–399.

Krutitskii, P. A. (2003*b*), 'Method of interior boundaries for the impedance problem in scattering theory', *Applied Mathematics and Computation* **135**(1), 147–160.

Krutitskii, P. A. & Chikilev, A. O. (2000), 'The method of integral equations in the oblique derivative problem arising in semiconductor physics', *Differential Equations* **36**(9), 1196–1208.

Krutitskii, P. A., Krutitskaya, N. C. & Malysheva, G. Y. (1999), 'A problem related to the Hall effect in a semiconductor with an electrode of an arbitrary shape', *Mathematical Problems in Engineering* **5**(1), 83–95.

Kuttruff, H. (2007), *Acoustics: An Introduction*, Taylor & Francis, London.

Kuznetsov, N., Maz'ya, V. & Vainberg, B. (2002), *Linear Water Waves: A Mathematical Approach*, Cambridge University Press, Cambridge.

Lamb, H. (1916), *Hydrodynamics*, 4th edn., Cambridge University Press, Cambridge.

Lanzani, L. & Shen, Z. (2004), 'On the Robin boundary condition for Laplace's equation in Lipschitz domains', *Communications in Partial Differential Equations* **29**(1 & 2), 91–109.

Lawhead, R. B. & Rudnick, I. (1951*a*), 'Acoustic wave propagation along a constant normal impedance boundary', *Journal of the Acoustical Society of America* **23**(5), 546–549.

Lawhead, R. B. & Rudnick, I. (1951*b*), 'Measurements on an acoustic wave propagated along a boundary', *Journal of the Acoustical Society of America* **23**(5), 541–545.

Lax, P. D. & Milgram, A. N. (1954), Parabolic equations, *in* L. Bers, S. Bochner & F. John, eds., 'Contributions to the Theory of Partial Differential Equations', Vol. 33 of *Annals of Mathematical Studies*, Princeton University Press, Princeton, 167–190.

Lax, P. D. & Phillips, R. S. (1989), *Scattering Theory*, Academic Press, Boston.

Le Méhauté, B. (1961), 'Theory of wave agitation in a harbor', *Journal of the Hydraulics Division, ASCE* **87**(2), 31–50.

Lee, C. H., Newman, J. N. & Zhu, X. (1996), 'An extended boundary integral equation method for the removal of irregular frequency effects', *International Journal for Numerical Methods in Fluids* **23**(7), 637–660.

Lee, J.-J. (1969), Wave-induced oscillations in harbors of arbitrary shape, Technical Report KH-R-20, California Institute of Technology, Pasadena.

Lee, J.-J. (1971), 'Wave-induced oscillations in harbours of arbitrary geometry', *Journal of Fluid Mechanics* **45**, 372–394.

Lenoir, M. (2005), Équations intégrales et problèmes de diffraction, Lecture notes, Cours D 11-1, ENSTA, Paris.

Lenoir, M. & Martin, D. (1981), 'An application of the principle of limiting absorption to the motions of floating bodies', *Journal of Mathematical Analysis and Applications* **79**, 370–383.

Lesnic, D. (2007), 'The boundary element method for solving the Laplace equation in two-dimensions with oblique derivative boundary conditions', *Communications in Numerical Methods in Engineering* **23**, 1071–1080.

Li, W. L., Wu, T. W. & Seybert, A. F. (1994), 'A half-space boundary element method for acoustic problems with a reflecting plane of arbitrary impedance', *Journal of Sound and Vibration* **171**(2), 173–184.

Liapis, S. (1992), 'Numerical methods for water-wave radiation problems', *International Journal for Numerical Methods in Fluids* **15**(1), 83–97.

Liapis, S. (1993), 'A boundary integral equation method for water wave-structure interaction problems', *Transactions on Modelling and Simulation* **2**, 555–566.

Lin, F. & Fang, W. (2005), 'A linear integral equation approach to the Robin inverse problem', *Inverse Problems* **21**, 1757–1772.

Lin, T.-C. (1987), 'On an integral equation approach for the exterior Robin problem for the Helmholtz equation', *Journal of Mathematical Analysis and Applications* **126**, 547–555.

Linton, C. M. (1999), 'Rapidly convergent representations for Green's functions for Laplace's equation', *Proceedings of the Royal Society A: Mathematical, Physical and Engineering Sciences* **455**(1985), 1767–1797.

Linton, C. M. & McIver, P. (2001), *Handbook of Mathematical Techniques for Wave/Structure Interactions*, CRC Press, Boca Raton.

Lions, J. L. (1956), 'Sur les problèmes aux limites du type dérivée oblique', *Annals of Mathematics* **64**(2), 207–239.

Lions, J. L. & Magenes, E. (1972), *Non-Homogeneous Boundary Value Problems and Applications*, Vol. I, Springer, New York.

Liu, P. & Losada, I. (2002), 'Wave propagation modeling in coastal engineering', *Journal of Hydraulic Research, IAHR* **40**(3), 229–240.

Liu, Y.-Z. & Shi, J. Z. (2008), 'A theoretical formulation for wave propagations over uneven bottom', *Ocean Engineering* **35**(3–4), 426–432.

Lozier, D. W. & Olver, F. W. J. (1994), Numerical evaluation of special functions, *in* 'Mathematics of Computation 1943–1993: A Half-Century of Computational Mathematics', Vol. 48, Proceedings of Symposia in Applied Mathematics, American Mathematical Society, Providence, Rhode Island, 79–125.

Luick, J. L. & Hinwood, J. B. (2008), 'Water levels in a dual-basin harbour in response to infragravity and edge waves', *Progress In Oceanography* **77**(4), 367–375.

Luke, Y. L. (1962), *Integrals of Bessel functions*, McGraw-Hill, New York.

Macaskill, C. (1979), 'Reflexion of water waves by a permeable barrier', *Journal of Fluid Mechanics* **95**, 141–157.

MacLeod, A. J. (1996), 'Algorithm 757: MISCFUN, a software package to compute uncommon special functions', *ACM Transactions on Mathematical Software* **22**(3), 288–301.

Magnus, W. & Oberhettinger, F. (1954), *Formulas and Theorems for the Functions of Mathematical Physics*, Chelsea, New York.

Mallat, S. (2000), *Une Exploration des Signaux en Ondelettes*, Éditions de l'École Polytechnique, Palaiseau.

Manacorda, T. (1991), 'Origin and development of the concept of wave', *Meccanica* **26**(1), 1–5.

Marburg, S. (2008), Discretization requirements: How many elements per wavelength are necessary?, *in* S. Marburg & B. Nolte, eds., 'Computational Acoustics of Noise Propagation in Fluids: Finite and Boundary Element Methods', Springer, Berlin, 309–332.

Marburg, S. & Nolte, B., eds. (2008), *Computational Acoustics of Noise Propagation in Fluids: Finite and Boundary Element Methods*, Springer, Berlin.

Marcos, M., Monserrat, S., Medina, R. & Lomónaco, P. (2005), 'Response of a harbor with two connected basins to incoming long waves', *Applied Ocean Research* **27**(4–5), 209–215.

McNown, J. S. (1952), Waves and seiche in idealized ports, *in* 'Gravity Waves', National Bureau of Standards, Circular 521, 153–164.

Medková, D. (1998), 'Solution of the Robin problem for the Laplace equation', *Applications of Mathematics* **43**(2), 133–155.

Medková, D. & Krutitskii, P. (2005), 'Neumann and Robin problems in a cracked domain with jump conditions on cracks', *Journal of Mathematical Analysis and Applications* **301**, 99–114.

Mei, C. C. (1978), 'Numerical methods in water-wave diffraction and radiation', *Annual Reviews of Fluid Mechanics* **10**, 393–416.

Mei, C. C. (1983), *The Applied Dynamics of Ocean Surface Waves*, Wiley-Interscience, New York.

Mei, C. C. & Chen, H. S. (1975), 'Hybrid element method for water waves', *2nd Annual Symposium of the Waterways and Harbors Division, ASCE* **1**, 63–81.

Mei, C. C. & Liu, P. L.-F. (1993), 'Surface waves and coastal dynamics', *Annual Reviews of Fluid Mechanics* **25**, 215–240.

Mei, C. C. & Petroni, R. V. (1973), 'Waves in a harbor with protruding breakwaters', *Journal of the Waterways, Harbors and Coastal Engineering Division, ASCE* **99**(2), 209–229.

Mei, C. C., Stiassnie, M. & Yue, D. K.-P. (2005), *Theory and Applications of Ocean Surface Waves, Part 1: Linear Aspects*, World Scientific, New Jersey.

Merian, J. R. (1828), *Ueber die Bewegung tropfbarer Flüssigkeiten in Gefässen*, Schweighauser, Basel.

Miles, J. W. (1974), 'Harbor seiching', *Annual Reviews of Fluid Mechanics* **6**, 17–33.

Miles, J. W. & Munk, W. (1961), 'Harbor paradox', *Journal of the Waterways and Harbors Division, ASCE* **87**(3), 111–130.

Moran, J. P. (1964), 'Image solution for vertical motion of a point source towards a free surface', *Journal of Fluid Mechanics* **18**, 315–320.

Morris, A. H. (1993), NSWC Library of Mathematics Subroutines, Classics in Applied Mathematics NSWC TR 92-425, Naval Surface Warfare Center Dahlgren Division, Dahlgren.

Morse, P. M. & Feshbach, H. (1953), *Methods of Theoretical Physics*, Vol. 1 & 2, McGraw-Hill, New York.

Morse, P. M. & Ingard, K. U. (1961), Linear acoustic theory, *in* S. Flügge, ed., 'Encyclopedia of Physics', Vol. XI/1, Springer, Berlin, 1–128.

Motygin, O. V. & McIver, P. (2009), 'On uniqueness in the problem of gravity-capillary water waves above submerged bodies', *Proceedings of the Royal Society A: Mathematical, Physical and Engineering Science* **465**(2106), 1743–1761.

Murray, J. D. (1984), *Asymptotic Analysis*, Springer, New York.

Muskhelishvili, N. I. (1953), *Singular Integral Equations: Boundary Problems of Function Theory and Their Application to Mathematical Physics*, Noordhoff, Groningen.

Nardini, D. & Brebbia, C. A. (1982), A new approach to free vibration analysis using boundary elements, *in* C. A. Brebbia, ed., 'Boundary Element Method in Engineering', Springer, Berlin, 312–326.

Nataf, F. (2006), Introduction aux conditions aux limites artificielles (C.L.A.) pour l'équation des ondes, Lecture notes, Centre de Mathématiques Appliquées, École Polytechnique, Palaiseau.

Nédélec, J.-C. (1977), Approximation des équations intégrales en mécanique et en physique, Rapport interne, Centre de Mathématiques Appliquées, École Polytechnique, Palaiseau.

Nédélec, J.-C. (1979), Notions sur les équations intégrales de la physique: Théorie et approximation, Rapport interne, Centre de Mathématiques Appliquées, École Polytechnique, Palaiseau.

Nédélec, J.-C. (2001), *Acoustic and Electromagnetic Equations: Integral Representations for Harmonic Problems*, Springer, Berlin.

Newman, J. N. (1984*a*), 'Approximations for the Bessel and Struve functions', *Mathematics of Computation* **43**(168), 551–556.

Newman, J. N. (1984*b*), 'Double-precision evaluation of the oscillatory source potential', *Journal of Ship Research* **28**, 151–154.

Newman, J. N. (1985), 'Algorithms for the free-surface Green function', *Journal of Engineering Mathematics* **19**(1), 57–67.

Nobile, M. A. & Hayek, S. I. (1985), 'Acoustic propagation over an impedance plane', *Journal of the Acoustical Society of America* **78**(4), 1325–1336.

Noblesse, F. (1982), 'The Green function in the theory of radiation and diffraction of regular water waves by a body', *Journal of Engineering Mathematics* **16**(2), 137–169.

Norton, K. A. (1936), 'The propagation of radio waves over the surface of the Earth and in the upper atmosphere: Part I', *Proceedings of the Institute of Radio Engineers* **24**(10), 1367–1387.

Norton, K. A. (1937), 'The propagation of radio waves over the surface of the Earth and in the upper atmosphere: Part II', *Proceedings of the Institute of Radio Engineers* **25**(9), 1203–1236.

Nosich, A. I. (1994), 'Radiation conditions, limiting absorption principle, and general relations in open waveguide scattering', *Journal of Electromagnetic Waves and Applications* **8**(3), 329–353.

Ochmann, M. (2004), 'The complex equivalent source method for sound propagation over an impedance plane', *Journal of the Acoustical Society of America* **116**(6), 3304–3311.

Ochmann, M. & Brick, H. (2008), Acoustical radiation and scattering above an impedance plane, *in* S. Marburg & B. Nolte, eds., 'Computational Acoustics of Noise Propagation in Fluids: Finite and Boundary Element Methods', Springer, Berlin, 459–494.

Palagachev, D. K., Ragusa, M. A. & Softova, L. G. (2000), 'Regular oblique derivative problem in Morrey spaces', *Electronic Journal of Differential Equations* **39**, 1–17.

Panchang, V. & Demirbilek, Z. (2001), Simulation of waves in harbors using two-dimensional elliptic equation models, *in* P. L.-F. Liu, ed., 'Advances in Coastal and Ocean Engineering', Vol. 7, World Scientific Publishing, Singapore, 125–162.

Paneah, B. P. (2000), *The Oblique Derivative Problem: The Poincaré Problem*, Vol. 17 of *Mathematical Topics*, Wiley-VCH, Berlin.

Peter, M. A. & Meylan, M. H. (2004), 'The eigenfunction expansion of the infinite depth free surface Green function in three dimensions', *Wave Motion* **40**, 1–11.

Pidcock, M. K. (1985), 'The calculation of Green's functions in three dimensional hydrodynamic gravity wave problems', *International Journal for Numerical Methods in Fluids* **5**(10), 891–909.

Pike, E. R. & Sabatier, P. C., eds. (2002), *Scattering: Scattering and Inverse Scattering in Pure and Applied Science*, Vol. 1 & 2, Academic Press, London.

Poincaré, H. (1910), *Leçons de Mécanique Céleste*, Vol. III, Théorie des Marées, Gauthier-Villards, Paris.

Poisson, O. & Joly, P. (1991), Calculs des pôles de résonance associés à la diffraction d'ondes acoustiques et élastiques par un obstacle en dimension 2, Technical report Nr. 1430, Institut National de Recherche en Informatique et en Automatique, Le Chesnay.

Poisson, S. D. (1818), Mémoire sur la théorie des ondes, *in* F. Didot, ed., 'Mémoires de l'Académie Royale des Sciences de l'Institut de France: Année 1816', Vol. 1, Imprimerie Royale, Paris, 71–186.

Poisson, S. D. (1828–1829), 'Hydrodynamique. Mémoire sur les petites oscillations de l'eau contenue dans un cylindre', *Annales de Mathématiques Pures et Appliquées* **19**, 225–240.

Polyanin, A. D., ed. (2002), *Handbook of Linear Partial Differential Equations for Engineers and Scientists*, Chapman & Hall/CRC, Boca Raton.

Potthast, R. (2001), *Point Sources and Multipoles in Inverse Scattering Theory*, Research Notes in Mathematics Series, Chapman & Hall/CRC, Boca Raton.

Prudnikov, A. P., Brychkov, Y. A. & Marichev, O. I. (1992), *Integrals and Series*, Vol. 1–4, 3rd edn., Gordon and Breach, New York.

Quaas, C. (2003), Modelación matemática y simulación computacional de la propagación de ondas acústicas en dominios exteriores. Aplicación al cálculo de resonancias en una dársena, Dissertation, Academia Politécnica Militar, Santiago de Chile.

Radder, A. C. (1979), 'On the parabolic equation method for water-wave propagation', *Journal of Fluid Mechanics* **95**, 159–176.

Raichlen, F. (1966), Harbor resonance, interaction of structures and waves, *in* A. T. Ippen, ed., 'Estuary and Coastline Hydrodynamics', McGraw-Hill, New York, 281–315.

Raichlen, F. & Ippen, A. T. (1965), 'Wave induced oscillations in harbors', *Journal of the Hydraulics Division, ASCE* **91**(2), 1–26.

Ramm, A. G. (2001), 'A simple proof of the Fredholm alternative and a characterization of the Fredholm operators', *The American Mathematical Monthly* **108**(9), 855–860.

Ramm, A. G. (2005), *Wave Scattering by Small Bodies of Arbitrary Shapes*, World Scientific Publishing, Singapore.

Rappaz, J. & Picasso, M. (1998), *Introduction à l'Analyse Numérique*, Presses Polytechniques et Universitaires Romandes, Lausanne.

Raviart, P. A. (1991), Résolution des modèles aux dérivées partielles Chapitre VII, Lecture notes, Majeure Sciences de l'Ingénieur et Calcul Scientifique, Département de Mathématiques Appliquées, École Polytechnique, Palaiseau.

Raviart, P. A. & Thomas, J.-M. (1983), *Introduction à l'Analyse Numérique des Équations aux Dérivées Partielles*, Masson, Paris.

Reed, M. & Simon, B. (1980), *Methods of Modern Mathematical Physics*, Vol. I–IV, Academic Press, London.

Rjasanow, S. & Steinbach, O. (2007), *The Fast Solution of Boundary Integral Equations*, Springer, New York.

Royden, H. L. (1988), *Real Analysis*, Macmillan, New York.

Rudin, W. (1973), *Functional Analysis*, McGraw-Hill, New York.

Rudnick, I. (1947), 'The propagation of an acoustic wave along a boundary', *Journal of the Acoustical Society of America* **19**(2), 348–356.

Ruegg, J. C., Rudloff, A., Vigny, C., Madariaga, R., De Chabalier, J. B., Campos, J., Kausel, E., Barrientos, S. & Dimitrov, D. (2009), 'Interseismic strain accumulation measured by GPS in the seismic gap between Constitución and Concepción in Chile', *Physics of the Earth and Planetary Interiors* **175**, 78–85.

Sakoda, K. (2005), *Optical Properties of Photonic Crystals*, Vol. 80 of *Springer Series in Optical Sciences*, Springer, Berlin.

Sarabandi, K., Casciato, M. D. & Koh, I.-S. (1992), 'Efficient calculation of the fields of a dipole radiating above an impedance surface', *IEEE Transactions on Antennas and Propagation* **50**(9), 1222–1235.

Sayer, P. (1980), 'An integral-equation method for determining the fluid motion due to a cylinder heaving on water of finite depth', *Proceedings of the Royal Society of London, Series A, Mathematical and Physical Sciences* **372**(1748), 93–110.

Schwartz, L. (1978), *Théorie des Distributions*, Hermann, Paris.

Seabergh, W. C. & Thomas, L. J. (1995), Los Angeles Harbor Pier 400 harbor resonance model study, Technical Report CERC-95-8, U.S. Army Corps of Engineers, U.S. Army Engineer District, Los Angeles.

Sloan, D. M., Süli, E., Vandewalle, S., Goovaerts, M. J., Mitsui, T., Wimp, J. & Wuytack, L., eds. (2001), *Numerical Analysis 2000*, Vol. VII: Partial Differential Equations, Elsevier Science, Amsterdam.

Smith, R. T. (1985), 'An inverse acoustic scattering problem for an obstacle with an impedance boundary condition', *Journal of Mathematical Analysis and Applications* **105**, 333–356.

Smith, T. & Sprinks, R. (1975), 'Scattering of surface waves by a conical island', *Journal of Fluid Mechanics* **72**, 373–384.

Sommerfeld, A. (1909), 'Über die Ausbreitung der Wellen in der drahtlosen Telegraphie', *Annalen der Physik (Leipzig)* **333**(4), 665–736.

Sommerfeld, A. (1926), 'Über die Ausbreitung der Wellen in der drahtlosen Telegraphie', *Annalen der Physik (Leipzig)* **386**(25), 1135–1153.

Sommerfeld, A. (1949), *Partial Differential Equations in Physics*, Academic Press, New York.

Spiegel, M. R. & Liu, J. X. (1999), *Schaum's Mathematical Handbook of Formulas and Tables*, McGraw-Hill, New York.

Spurk, J. H. (1997), *Fluid Mechanics*, Springer, Berlin.

Squire, V. A. & Dixon, T. W. (2001), 'On modelling an iceberg embedded in shore-fast sea ice', *Journal of Engineering Mathematics* **40**(3), 211–226.

Squire, V. A., Dugan, J. P., Wadhams, P., Rottier, P. J. & Liu, A. K. (1995), 'Of ocean waves and sea ice', *Annual Reviews of Fluid Mechanics* **27**, 115–168.

Steinbach, O. (2008), *Numerical Approximation Methods for Elliptic Boundary Value Problems: Finite and Boundary Elements*, Springer, New York.

Stoker, J. J. (1956), 'On radiation conditions', *Communications on Pure and Applied Mathematics* **9**(3), 577–595.

Stoker, J. J. (1957), *Water Waves: The Mathematical Theory with Applications*, Interscience, New York.

Strauss, W. (1992), *Partial Differential Equations: An Introduction*, John Wiley & Sons, New York.

Strutt, J. W. (1877), *The Theory of Sound*, Vol. 1 & 2, Macmillan, London.

Taraldsen, G. (2004), 'A note on reflection of spherical waves', *Journal of the Acoustical Society of America* **117**(6), 3389–3392.

Taraldsen, G. (2005), 'The complex image method', *Wave Motion* **43**, 91–97.

Tarrero, A. I., Martín, M. A., González, J., Machimbarrena, M. & Jacobsen, F. (2008), 'Sound propagation in forests: A comparison of experimental results and values predicted by the Nord 2000 model', *Applied Acoustics* **69**(7), 662–671.

Terrasse, I. & Abboud, T. (2006), Modélisation des phénomènes de propagation d'ondes, Lecture notes, Majeure de Mathématiques Appliquées, École Polytechnique, Palaiseau.

Thompson, E. F., Chen, H. S. & Hadley, L. L. (1996), 'Validation of numerical model for wind waves and swell in harbors', *Journal of Waterway, Port, Coastal and Ocean Engineering, ASCE* **122**(5), 245–257.

Thompson, L. L. (2005), 'A review of finite-element methods for time-harmonic acoustics', *Journal of the Acoustical Society of America* **119**(3), 1315–1330.

Thorne, R. C. (1953), 'Multipole expansions in the theory of surface waves', *Proceedings of the Cambridge Philosophical Society* **49**, 707–716.

Trefethen, L. N. & Williams, R. J. (1986), 'Conformal mapping solution of Laplace's equation on a polygon with oblique derivative boundary conditions', *Journal of Computational and Applied Mathematics* **14**, 227–249.

Tsay, T.-K., Zhu, W. & Liu, P. L.-F. (1989), 'A finite element model for wave refraction, diffraction, reflection and dissipation', *Applied Ocean Research* **11**(1), 33–38.

Tsynkov, S. V. (1998), 'Numerical solution of problems on unbounded domains. A review', *Applied Numerical Mathematics* **27**, 465–532.

Unser, M. (2000), 'Sampling — 50 years after Shannon', *Proceedings of the IEEE* **88**(4), 569–587.

U.S. Army Corps of Engineers (2002), Coastal Engineering Manual, Engineer Manual 1110-2-1100, U.S. Army Corps of Engineers, Washington, D.C.

Van der Pol, B. (1935), 'Theory of the reflection of the light from a point source by a finitely conducting flat mirror with an application to radiotelegraphy', *Physica* **2**, 843–853.

Van der Pol, B. & Niessen, K. F. (1930), 'Über die Ausbreitung elektromagnetischer Wellen über eine ebene Erde', *Annalen der Physik (Leipzig)* **398**(3), 273–294.

Van Oosterom, A. & Strackee, J. (1983), 'The solid angle of a plane triangle', *IEEE Transactions on Biomedical Engineering* **30**, 125–126.

Vilibić, I. & Mihanović, H. (2005), 'Resonance in Ploče Harbor (Adriatic Sea)', *Acta Adriatica* **46**(2), 125–136.

Walker, S. & Brebbia, C. A. (1978), 'Harbour resonance problems using finite elements', *Advances in Water Resources* **1**(4), 205–211.

Watson, G. N. (1944), *Treatise on the Theory of Bessel Functions*, Cambridge University Press, Cambridge.

Wehausen, J. V. (1971), 'The motion of floating bodies', *Annual Reviews of Fluid Mechanics* **3**, 237–268.

Wehausen, J. V. & Laitone, E. V. (1960), Surface waves, *in* S. Flügge, ed., 'Encyclopedia of Physics', Vol. IX, Springer, Berlin, 446–778.

Weinberger, H. F. (1995), *A First Course in Partial Differential Equations with Complex Variables and Transform Methods*, Dover, New York.

Weisstein, E. W. (2002), *CRC Concise Encyclopedia of Mathematics*, 2nd edn., CRC Press, Boca Raton.

Wendland, W. L., Stephan, E. & Hsiao, G. C. (1979), 'On the integral equation method for the plane mixed boundary value problem of the Laplacian', *Mathematical Methods in the Applied Sciences* **1**, 265–321.

Wenzel, A. R. (1974), 'Propagation of waves along an impedance boundary', *Journal of the Acoustical Society of America* **55**(5), 956–963.

Werner, D. (1997), *Funktionalanalysis*, Springer, Berlin.

Weyl, H. (1919), 'Ausbreitung elektromagnetischer Wellen über einem ebenen Leiter', *Annalen der Physik (Leipzig)* **365**(21), 481–500.

Wilcox, C. H. (1975), *Scattering Theory for the D'Alembert Equation in Exterior Domains*, Lecture Notes in Mathematics, Springer, Berlin.

Wise, W. H. (1931), 'The grounded condenser antenna radiation formula', *Proceedings of the Institute of Radio Engineers* **19**(9), 1684–1689.

Wong, R. (2001), *Asymptotic Approximations of Integrals*, SIAM, Philadelphia.

Wright, M. C. M. (2005), The Wiener-Hopf technique, *in* M. C. M. Wright, ed., 'Lecture Notes on the Mathematics of Acoustics', Imperial College Press, London, 109–124.

Xia, J. (2001), 'Evaluation of the Green function for 3-D wave-body interactions in a channel', *Journal of Engineering Mathematics* **40**(1), 1–16.

Yasumoto, K., ed. (2006), *Electromagnetic Theory and Applications for Photonic Crystals*, CRC Press, Boca Raton.

Yeung, R. W. (1982), 'Numerical methods in free-surface flows', *Annual Reviews of Fluid Mechanics* **14**, 395–442.

Yu, X. & Chwang, A. T. (1994), 'Wave-induced oscillation in harbor with porous breakwaters', *Journal of Waterway, Port, Coastal, and Ocean Engineering, ASCE* **120**, 125–144.

Zenneck, J. (1907), 'Über die Fortpflanzung ebener elektromagnetischer Wellen längs einer ebenen Leiterfläche und ihre Beziehung zur drahtlosen Telegraphie', *Annalen der Physik (Leipzig)* **328**(10), 846–866.

Ziemer, W. P. (1989), *Weakly Differentiable Functions: Sobolev Spaces and Functions of Bounded Variation*, Springer, New York.

Zienkiewicz, O. C. & Taylor, R. L. (2000), *The Finite Element Method*, Vol. 1–3, 5th edn., Butterworth-Heinemann, Oxford.

APPENDIX

A. MATHEMATICAL AND PHYSICAL BACKGROUND

A.1 Introduction

A short survey of the mathematical and physical background of the thesis is presented in this appendix. The most important aspects are discussed and several references are given for each topic. It is thus intended as a quick reference guide to understand or refresh some deeper technical (and sometimes more obscure) aspects mentioned throughout the thesis.

This appendix is structured in 11 sections, including this introduction. In Section A.2 we present several special functions that appear in mathematical physics and which are closely related to our work. Some notions of functional analysis are introduced in Section A.3, in particular Lax-Milgram's theorem and Fredholm's alternative. The Sobolev spaces are introduced in Section A.4, which constitute the natural function spaces in which the solutions of boundary-value problems are searched. In Section A.5 we present some operators and integral theorems that appear in vector calculus and in elementary differential geometry. The powerful mathematical tool of the theory of distributions is described in Section A.6. In Section A.7 we describe multi-dimensional Fourier transforms and their properties in the framework of the theory of distributions. In Section A.8 a general outline of Green's functions and fundamental solutions is found. In section A.9 we present a brief survey of wave propagation and some related topics. Linear water-wave theory, which is one of the main applications for the Laplace equation, is shown in Section A.10. Finally, in Section A.11 we study some aspects of the linear acoustic theory, which is one of the main applications for the Helmholtz equation.

A.2 Special functions

The special functions of mathematical physics, also known as higher transcendental functions, are functions that play a fundamental role in a great variety of physical and mathematical applications. They can not be described as a composition of a finite number of elementary functions. Elementary functions are functions which are built upon a finite combination of constant functions, elementary field operations (addition, subtraction, multiplication, division, and root extraction), and algebraic, exponential, trigonometric, and logarithmic functions and their inverses under repeated compositions. Elementary functions are divided into algebraic and transcendental functions. An algebraic function is a function which can be constructed using only a finite number of the elementary field operations together with the inverses of functions capable of being so constructed. A transcendental function is a function that is not algebraic, e.g., the exponential and trigonometric functions and their inverses are transcendental. The higher transcendental functions are functions which go even beyond the transcendental functions, and can only be described by means of integral representations and infinite series expansions. Some of them, though, are widely studied due their multiple applications, and are therefore called special functions.

Definitions and some properties of several special functions, which are used throughout this thesis, are presented in this section. We begin with the complex exponential and logarithm. They are only transcendental functions, but they allow to comprehend better the other special functions, particularly their properties in the complex plane. The singularities of the Green's functions studied herein for two-dimensional problems are always of logarithmic type. Afterwards we present the gamma or generalized factorial function. The exponential integral and its related functions appear in the computation of the half-plane Green's function for the Laplace equation. Bessel and Hankel functions play an important role in problems with circular or cylindrical symmetry. They are also known as cylindrical harmonics and appear in the computation of the Green's function for the Helmholtz equation in two dimensions. Closely related to them are the modified Bessel functions. Spherical Bessel and Hankel functions appear in problems with spherical symmetry and, in particular, in the computation of the Green's function for the Helmholtz equation in three dimensions. Struve functions can be seen as some sort of perturbed Bessel and Hankel functions, and appear when taking primitives of them. They also appear in some impedance calculations. Finally we present the Legendre functions, the associated Legendre functions, and the spherical harmonics, which are all closely related, and which appear in problems with spherical symmetry.

The special functions and their properties are deeply linked with the theory of complex variables. To understand the former, some knowledge is required of the latter, which deals with the complex imaginary unit, $i = \sqrt{-1}$, and with related topics, such as complex integration contours, residue calculus, analytic continuation, etc. Some references for the complex variable theory are Arfken & Weber (2005), Bak & Newman (1997), Dettman (1984), and Morse & Feshbach (1953). Further interesting topics are the theory of asymptotic expansions (Courant & Hilbert 1966, Dettman 1984, Estrada & Kanwal 2002), and the methods of stationary phase and steepest descent (Bender & Orszag 1978, Dettman 1984, Watson 1944). Specific references for special functions are given in each subsection. In particular, some references which are useful for almost all of these special functions are Abramowitz & Stegun (1972), Erdélyi (1953), and Magnus & Oberhettinger (1954). Another somewhat older but still quite interesting reference is Jahnke & Emde (1945).

A.2.1 Complex exponential and logarithm

a) Complex exponential

The complex exponential and logarithm are trascendental functions that play a central role in the theory of complex functions. Even though they are not considered to be special functions, their intrinsic properties allow a far better comprehension of the latter, and are therefore listed herein. Some references are Abramowitz & Stegun (1972), Bak & Newman (1997), Dettman (1984), Jahnke & Emde (1945), and Weisstein (2002). The complex exponential is an analytic function in the entire complex z-plane, being thus an entire function, and it coincides with the usual exponential function for real arguments, which is shown in Figure A.1. It is defined by

$$\exp z = e^z = e^x e^{iy} = e^x \cos y + i\, e^x \sin y, \qquad z = x + iy, \tag{A.1}$$

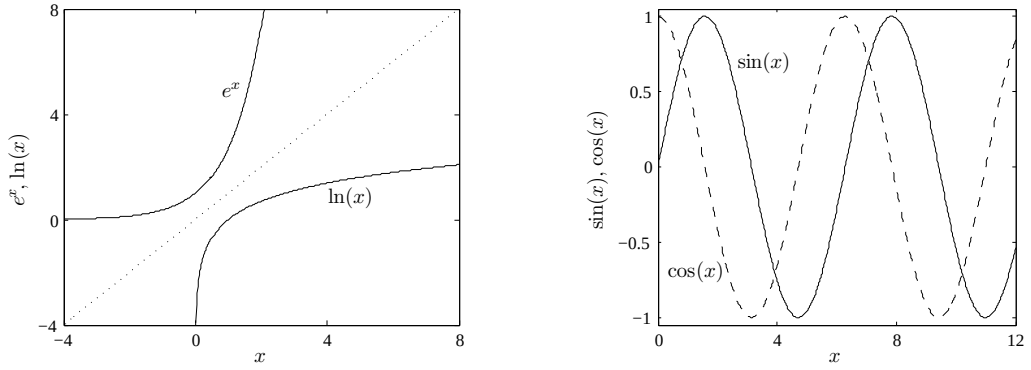

(a) Exponential and logarithm (b) Sine and cosine

FIGURE A.1. Exponential, logarithm, and trigonometric functions for real arguments.

where e denotes Euler's number

$$e = \lim_{n\to\infty} \left(1 + \frac{1}{n}\right)^n = \sum_{n=0}^{\infty} \frac{1}{n!} = 2.718281828\ldots, \tag{A.2}$$

which receives its name from the Swissborn Russian mathematician and physicist Leonhard Euler (1707–1783), who is considered one of the greatest mathematicians of all time. Some properties of the complex exponential are

$$e^{z_1} e^{z_2} = e^{z_1+z_2}, \tag{A.3}$$

$$e^{z_1} / e^{z_2} = e^{z_1-z_2}, \tag{A.4}$$

$$|e^z| = e^x, \tag{A.5}$$

$$e^{z+2\pi i} = e^z. \tag{A.6}$$

Property (A.5) implies that $\exp z$ has no zeros, and property (A.6) means that $\exp z$ is periodic with period $2\pi i$. The derivative and the primitive of the complex exponential, omitting the integration constant, is the function itself:

$$\frac{\mathrm{d}}{\mathrm{d}z}\, e^z = e^z, \qquad \int e^z \,\mathrm{d}z = e^z. \tag{A.7}$$

It has the power series expansion

$$e^z = \sum_{n=0}^{\infty} \frac{z^n}{n!}. \tag{A.8}$$

The complex exponential allows us also to define the complex trigonometric functions

$$\sin z = \frac{e^{iz} - e^{-iz}}{2i}, \tag{A.9}$$

$$\cos z = \frac{e^{iz} + e^{-iz}}{2}, \tag{A.10}$$

$$\tan z = \frac{\sin z}{\cos z} = -i\, \frac{e^{iz} - e^{-iz}}{e^{iz} + e^{-iz}}, \tag{A.11}$$

and likewise the complex hyperbolic functions

$$\sinh z = \frac{e^z - e^{-z}}{2} = -i\sin(iz), \tag{A.12}$$

$$\cosh z = \frac{e^z + e^{-z}}{2} = \cos(iz), \tag{A.13}$$

$$\tanh z = \frac{\sinh z}{\cosh z} = \frac{e^z - e^{-z}}{e^z + e^{-z}} = -i\tan(iz). \tag{A.14}$$

The sine and cosine trigonometric functions for real arguments are illustrated in Figure A.1.

b) Complex logarithm

The complex logarithm $\ln z$ is an extension of the natural logarithm function for real arguments (vid. Figure A.1) into the whole complex z-plane, and is thus the inverse function of the complex exponential $\exp z$. There is, however, a difficulty in trying to define this inverse function due the periodicity of the exponential, i.e., due the fact that

$$e^{z+i2\pi n} = e^z, \qquad n \in \mathbb{Z}. \tag{A.15}$$

The complex logarithm has to be understood thus as a multi-valued function, which can become properly single-valued when the domain of the exponential is restricted, e.g., to the strip $-\pi < \mathfrak{Im}\, z \leq \pi$. In this specific case, the function is one-to-one and an inverse does exist, called the principal value of the logarithm, which is given by

$$\ln z = \ln|z| + i\arg z, \qquad -\pi < \arg z \leq \pi, \tag{A.16}$$

or, equivalently in polar and cartesian coordinates, by

$$\ln z = \ln r + i\theta, \qquad -\pi < \theta \leq \pi, \tag{A.17}$$

$$\ln z = \ln\sqrt{x^2+y^2} + i\arctan\frac{y}{x}, \qquad -\pi < \arctan\frac{y}{x} \leq \pi, \tag{A.18}$$

where

$$z = re^{i\theta} = x + iy. \tag{A.19}$$

So defined, the logarithm $\ln z$ is holomorphic for all complex numbers which do not lie on the negative real axis including the origin, and has the property

$$e^{\ln z} = z, \qquad z \neq 0. \tag{A.20}$$

We see that it is not defined at $z = 0$ and is discontinuous on the negative real axis, which means that the function cannot be analytic at these points. In fact, the jump across the negative real axis is given by

$$\ln(x + i0) - \ln(x - i0) = i2\pi \qquad \forall x < 0. \tag{A.21}$$

Elsewhere the function is differentiable, and its derivative and primitive, omitting the integration constant, are given by

$$\frac{\mathrm{d}}{\mathrm{d}z}\ln z = \frac{1}{z}, \qquad \int \ln z\,\mathrm{d}z = z\ln z - z, \qquad z \neq 0. \tag{A.22}$$

Particularly, it holds that

$$\ln(i) = \frac{i\pi}{2}. \tag{A.23}$$

It admits also the power series expansions

$$\ln z = \sum_{n=0}^{\infty} \frac{2}{2n+1} \left(\frac{z-1}{z+1} \right)^{2n+1}, \qquad \mathfrak{Re}\, z > 0, \tag{A.24}$$

$$\ln(z+1) = \sum_{n=1}^{\infty} (-1)^{n+1} \frac{z^n}{n}, \qquad |z| < 1. \tag{A.25}$$

There exist consequently many logarithm functions depending on the restriction that is placed on the argument $\arg z$ to make the function single-valued. The complex logarithm can be conceived as having many branches, each of which is single-valued and fits the definition of a proper function. If we take the argument $\arg z$ satisfying the above restriction for the principal value, then

$$\operatorname{Ln} z = \ln|z| + i(\arg z \pm 2\pi n), \qquad -\pi < \arg z \leq \pi, \qquad n = 0, 1, 2, \ldots, \tag{A.26}$$

is a multi-valued function with infinitely many branches, each for a different integer n, and each single-valued. This general logarithmic function can be defined by

$$\operatorname{Ln} z = \int_1^z \frac{\mathrm{d}t}{t}, \tag{A.27}$$

where the integration path does not pass through the origin. Another way to work with the complex logarithm function is using a more complicated surface consisting of infinitely many planes joined together so that the function varies continuously when passing from one plane to the next. Such a surface is called Riemann surface in honor of the German mathematician Georg Friedrich Bernhard Riemann (1826–1866), who made important contributions to analysis and differential geometry. The discontinuity of the complex logarithm at the negative real axis was introduced in a rather arbitrary way as a restriction on the $\arg z$ to make the function single-valued. This line of discontinuity is called a branch cut and can be moved at will by defining different branches of the function. It does not even need to be a straight line, but it must start at $z = 0$, where the logarithm fails to be analytic. This point is called a branch point and is a more basic type of singularity than the points on a particular branch cut. The branch cut connects thus the branch point $z = 0$ with infinity, which is the other branch point. Working with Riemann surfaces avoids the use of branch cuts, but gives up the simplicity of defining a function on a set of points in a single complex plane, which is the reason why we will not use them, and deal with branch cuts instead throughout this work. For the multi-valued complex logarithm $\operatorname{Ln} z$ the usual properties of the real logarithm hold, e.g.,

$$\operatorname{Ln}(z_1 z_2) = \operatorname{Ln} z_1 + \operatorname{Ln} z_2, \tag{A.28}$$

$$\operatorname{Ln}(z_1/z_2) = \operatorname{Ln} z_1 - \operatorname{Ln} z_2, \tag{A.29}$$

which also holds for the single-valued complex logarithm $\ln z$, provided that care is exercised in selecting the branches. The complex logarithm allows also to define the function z^a, where a is any complex constant, due

$$z^a = e^{a \operatorname{Ln} z}. \tag{A.30}$$

If $a = m$, an integer, then (A.30) is single-valued due the periodicity of the complex exponential. If $a = p/q$, where p and q are integers, then (A.30) has q distinct values. And finally, if a is irrational or complex, then there are infinitely many values of z^a. We have also that, except at the branch point $z = 0$ and on a branch cut, z^a is analytic and, omitting the integration constant,

$$\frac{\mathrm{d}}{\mathrm{d}z} z^a = a z^{a-1}, \qquad \int z^a \, \mathrm{d}z = \frac{z^{a+1}}{a+1}. \tag{A.31}$$

In particular, the complex square root is defined by

$$\sqrt{z} = z^{1/2} = e^{\frac{1}{2} \operatorname{Ln} z}, \tag{A.32}$$

and we characterize its principal value as

$$\sqrt{z} = \sqrt{x+iy} = \sqrt{r}\, e^{i\theta/2} = \sqrt{\frac{r+x}{2}} + \frac{iy}{\sqrt{2(r+x)}} \qquad (-\pi < \theta \leq \pi). \tag{A.33}$$

The complex logarithm allows in the same way to define several other functions, which have branch cuts or have to be considered as multi-valued. Among these are, e.g., the inverse trigonometric functions

$$\arcsin z = -i \operatorname{Ln}\Big(iz + \sqrt{1 - z^2} \Big), \tag{A.34}$$

$$\arccos z = -i \operatorname{Ln}\Big(z + \sqrt{z^2 - 1} \Big) = \frac{\pi}{2} - \arcsin z, \tag{A.35}$$

$$\arctan z = \frac{i}{2} \big(\operatorname{Ln}(1 - iz) - \operatorname{Ln}(1 + iz) \big), \tag{A.36}$$

and the inverse hyperbolic functions

$$\operatorname{arcsinh} z = \operatorname{Ln}\Big(z + \sqrt{1 + z^2} \Big) = -i \arcsin(iz), \tag{A.37}$$

$$\operatorname{arccosh} z = \operatorname{Ln}\Big(z + \sqrt{z^2 - 1} \Big) = i \arccos z, \tag{A.38}$$

$$\operatorname{arctanh} z = \frac{1}{2} \big(\operatorname{Ln}(1 + z) - \operatorname{Ln}(1 - z) \big) = -i \arctan(iz). \tag{A.39}$$

Finally we remark that throughout this work, unless it is specifically stated otherwise, always the principal value for the complex logarithm is used, which has a branch cut along the negative real axis, and has the advantage of reducing itself to the usual natural logarithm when z is real and positive. This consideration is applied also to complex functions that are derived from the complex logarithm.

A.2.2 Gamma function

a) Definition

The gamma function is a special function that is defined to be an extension of the factorial function to complex and real number arguments. Some references on this function are the books of Abramowitz & Stegun (1972), Arfken & Weber (2005), Erdélyi (1953), Jahnke & Emde (1945), Magnus & Oberhettinger (1954), Spiegel & Liu (1999), and the one of Weisstein (2002). It is defined by

$$\Gamma(z) = \int_0^\infty t^{z-1} e^{-t}\,\mathrm{d}t \qquad (\mathfrak{Re}\, z > 0). \tag{A.40}$$

It can be also defined by Euler's formula

$$\Gamma(z) = \lim_{n\to\infty} \frac{n!\, n^z}{z(z+1)(z+2)\ldots(z+n)} \qquad (z \neq 0, -1, -2, -3, \ldots). \tag{A.41}$$

A third definition is given by Euler's infinite product formula

$$\frac{1}{\Gamma(z)} = z\, e^{\gamma z} \prod_{n=1}^{\infty} \left[\left(1 + \frac{z}{n}\right) e^{-z/n} \right], \tag{A.42}$$

where γ denotes Euler's constant (sometimes also called Euler-Mascheroni constant), which he discovered in 1735 and which is given by

$$\gamma = \lim_{n\to\infty} \left(\sum_{p=1}^{n} \frac{1}{p} - \ln(n) \right) = -\int_0^\infty e^{-t} \ln t\,\mathrm{d}t = 0.5772156649\ldots. \tag{A.43}$$

Euler's constant can be also represented as

$$\gamma = \int_0^\infty \frac{1}{t} \left(\frac{1}{t+1} - e^{-t} \right) \mathrm{d}t = \int_0^\infty \left(\frac{1}{1-e^{-t}} - \frac{1}{t} \right) e^{-t}\,\mathrm{d}t. \tag{A.44}$$

The gamma function is graphically depicted in Figure A.2.

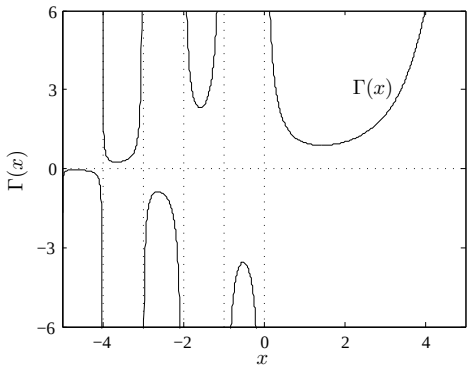

FIGURE A.2. Gamma function for real arguments.

b) Properties

The gamma function $\Gamma(z)$ is single-valued and analytic over the entire complex plane, save for the points $z = -n$ ($n = 0, 1, 2, 3, \ldots$), where it possesses simple poles with residues $(-1)^n/n!$. Its reciprocal $1/\Gamma(z)$ is an entire function possessing simple zeros at the points $z = -n$ ($n = 0, 1, 2, 3, \ldots$). There are no points z where $\Gamma(z) = 0$. The gamma function satisfies the recurrence relation

$$\Gamma(z+1) = z\Gamma(z), \tag{A.45}$$

and the reflection formula

$$\Gamma(z)\Gamma(1-z) = \frac{\pi}{\sin(\pi z)} \qquad (z \notin \mathbb{Z}). \tag{A.46}$$

The gamma function satisfies also the duplication formula

$$\Gamma(2z) = (2\pi)^{-\frac{1}{2}} 2^{2z-\frac{1}{2}} \Gamma(z)\Gamma\left(z + \frac{1}{2}\right), \tag{A.47}$$

and, in general, the Gauss' multiplication formula

$$\Gamma(nz) = (2\pi)^{\frac{1}{2}(1-n)} 2^{nz-\frac{1}{2}} \prod_{k=0}^{n-1} \Gamma\left(z + \frac{k}{n}\right), \tag{A.48}$$

which receives its name from the German mathematician and scientist of profound genius Carl Friedrich Gauss (1777–1855), who contributed significantly to many fields in mathematics and science. The gamma function is linked with the factorial function, for integer arguments, through

$$\Gamma(n+1) = n! \qquad (n = 0, 1, 2, 3, \ldots), \tag{A.49}$$

where, in particular,

$$\Gamma(1) = 0! = 1. \tag{A.50}$$

Special values for the gamma function are

$$\Gamma\left(\frac{1}{2}\right) = \sqrt{\pi}, \tag{A.51}$$

$$\Gamma\left(n + \frac{1}{2}\right) = \frac{(2n)!\sqrt{\pi}}{n!\, 2^{2n}} \qquad (n = 0, 1, 2, 3, \ldots), \tag{A.52}$$

$$\Gamma\left(-n + \frac{1}{2}\right) = \frac{(-1)^n n!\, 2^{2n}\sqrt{\pi}}{(2n)!} \qquad (n = 0, 1, 2, 3, \ldots). \tag{A.53}$$

The derivative of the gamma function is given by

$$\frac{\mathrm{d}}{\mathrm{d}z}\Gamma(z) = -\Gamma(z)\left[\gamma + \frac{1}{z} + \sum_{n=1}^{\infty}\left(\frac{1}{n+z} - \frac{1}{n}\right)\right], \tag{A.54}$$

and a power series expansion for its logarithm is

$$\ln\Gamma(z) = -\ln(z) - \gamma z - \sum_{n=1}^{\infty}\left[\ln\left(1 + \frac{z}{n}\right) - \frac{z}{n}\right]. \tag{A.55}$$

The Γ function, for large arguments as $|z| \to \infty$, has the asymptotic expansion

$$\Gamma(z) \sim \sqrt{2\pi}\, e^{-z} z^{z-\frac{1}{2}} \left[1 + \frac{1}{12z} + \frac{1}{288z^2} - \frac{139}{51840z^3} - \frac{571}{2488320z^4} + \cdots\right], \tag{A.56}$$

which is called Stirling's formula, named in honor of the Scottish mathematician James Stirling (1692–1770).

A.2.3 Exponential integral and related functions

a) Definition

The exponential integral, the cosine integral, and the sine integral functions are special functions that appear frequently in physical problems. Some references for them are Abramowitz & Stegun (1972), Arfken & Weber (2005), Chaudhry & Zubair (2002), Erdélyi (1953), Glaisher (1870), Jahnke & Emde (1945), and Weisstein (2002). The exponential integral is defined by

$$\mathrm{Ei}(z) = -\!\!\!\!\!\!\int_{-z}^{\infty} \frac{e^{-t}}{t}\,\mathrm{d}t = \!\!\!\!\!\!\int_{-\infty}^{z} \frac{e^{t}}{t}\,\mathrm{d}t \qquad \big(|\arg z| < \pi\big). \tag{A.57}$$

Analytic continuation of (A.57) yields a multi-valued function with branch points at $z = 0$ and $z = \infty$. It is a single-valued function in the complex z-plane cut along the negative real axis. Since $1/t$ diverges at $t = 0$, the integral has to be understood in terms of the Cauchy principal value (cf., e.g., Arfken & Weber 2005, or vid. Subsection A.6.5), named after the French mathematician and early pioneer of analysis Augustin Louis Cauchy (1789–1857). We introduce also the complementary exponential integral function

$$\mathrm{Ein}(z) = \int_0^z \frac{e^t - 1}{t}\,\mathrm{d}t, \tag{A.58}$$

which is an entire function and whose relation with (A.57) is given by

$$\mathrm{Ein}(z) = \mathrm{Ei}(z) - \gamma - \ln z, \tag{A.59}$$

where γ denotes Euler's constant (A.43). For the cosine integral function, there exist at least three definitions, which are

$$\mathrm{Ci}(z) = \gamma + \ln z + \int_0^z \frac{\cos t - 1}{t}\,\mathrm{d}t \qquad \big(|\arg z| < \pi\big), \tag{A.60}$$

$$\mathrm{ci}(z) = -\int_z^{\infty} \frac{\cos t}{t}\,\mathrm{d}t \qquad \big(|\arg z| < \pi\big), \tag{A.61}$$

$$\mathrm{Cin}(z) = \int_0^z \frac{\cos t - 1}{t}\,\mathrm{d}t. \tag{A.62}$$

The cosine integral $\mathrm{ci}(z)$ is the primitive of $\cos(z)/z$ which is zero for $z = \infty$. In the same manner as the exponential integral (A.57), the cosine integral functions (A.60) and (A.61) have also a branch cut along the negative real axis. They are related by

$$\mathrm{ci}(z) = \mathrm{Ci}(z) \qquad \big(|\arg z| < \pi\big), \tag{A.63}$$

$$\mathrm{Cin}(z) = \mathrm{Ci}(z) - \gamma - \ln z. \tag{A.64}$$

For the sine integral function, two different definitions exist, which are

$$\mathrm{Si}(z) = \int_0^z \frac{\sin t}{t}\,\mathrm{d}t, \tag{A.65}$$

$$\mathrm{si}(z) = -\int_z^\infty \frac{\sin t}{t}\,\mathrm{d}t. \tag{A.66}$$

The sine integral $\mathrm{Si}(z)$ is the primitive of $\sin(z)/z$ which is zero for $z = 0$, while $\mathrm{si}(z)$ is the primitive of $\sin(z)/z$ which is zero for $z = \infty$. They are both analytic in the whole complex z-plane, and are related by

$$\mathrm{si}(z) = \mathrm{Si}(z) - \frac{\pi}{2}. \tag{A.67}$$

The exponential integral and its related trigonometric integrals are illustrated in Figure A.3.

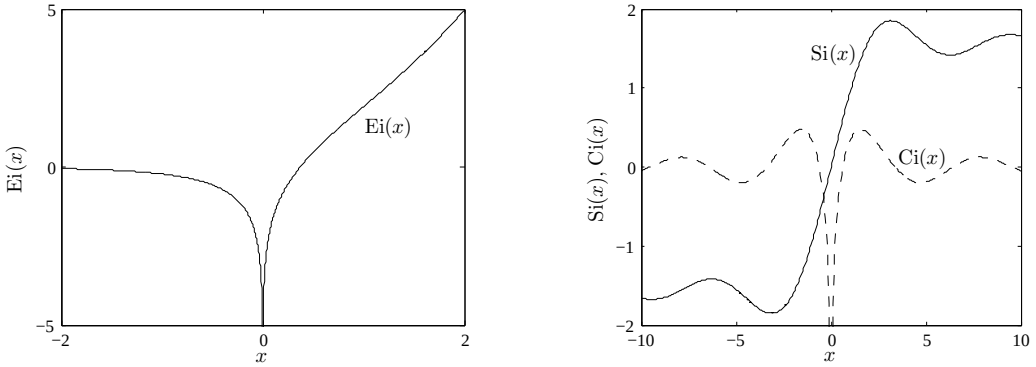

(a) Exponential integral (b) Sine integral and cosine integral

FIGURE A.3. Exponential integral and trigonometric integrals for real arguments.

b) Properties

The exponential integral, the cosine integral, and the sine integral functions satisfy the relations

$$\mathrm{Ei}(iz) = \mathrm{Ci}(z) + i\left(\mathrm{Si}(z) + \frac{\pi}{2}\right) \qquad (\mathfrak{Re}\, z > 0), \tag{A.68}$$

$$\mathrm{Ei}(-iz) = \mathrm{Ci}(z) - i\left(\mathrm{Si}(z) + \frac{\pi}{2}\right) \qquad (\mathfrak{Re}\, z > 0), \tag{A.69}$$

$$\mathrm{Ci}(z) = \frac{1}{2}\big[\,\mathrm{Ei}(iz) + \mathrm{Ei}(-iz)\,\big] \qquad (\mathfrak{Re}\, z > 0), \tag{A.70}$$

$$\mathrm{Si}(z) = \frac{1}{2i}\big[\,\mathrm{Ei}(iz) - \mathrm{Ei}(-iz)\,\big] - \frac{\pi}{2} \qquad (\mathfrak{Re}\, z > 0), \tag{A.71}$$

Their derivatives and primitives, omitting the integration constants, are given by

$$\frac{\mathrm{d}}{\mathrm{d}z}\,\mathrm{Ei}(z) = \frac{e^z}{z}, \qquad \int \mathrm{Ei}(z)\,\mathrm{d}z = z\,\mathrm{Ei}(z) - e^z, \tag{A.72}$$

$$\frac{\mathrm{d}}{\mathrm{d}z}\,\mathrm{Ci}(z)=\frac{\cos z}{z},\qquad \int \mathrm{Ci}(z)\,\mathrm{d}z=z\,\mathrm{Ci}(z)-\sin z, \tag{A.73}$$

$$\frac{\mathrm{d}}{\mathrm{d}z}\,\mathrm{Si}(z)=\frac{\sin z}{z},\qquad \int \mathrm{Si}(z)\,\mathrm{d}z=z\,\mathrm{Si}(z)+\cos z. \tag{A.74}$$

For small arguments z, the exponential, cosine, and sine integral functions have the convergent series expansions

$$\mathrm{Ei}(z)=\gamma+\ln z+\sum_{n=1}^{\infty}\frac{z^n}{n\,n!}, \tag{A.75}$$

$$\mathrm{Ci}(z)=\gamma+\ln z+\sum_{n=1}^{\infty}\frac{(-1)^n z^{2n}}{2n(2n)!}, \tag{A.76}$$

$$\mathrm{Si}(z)=\sum_{n=0}^{\infty}\frac{(-1)^n z^{2n+1}}{(2n+1)(2n+1)!}, \tag{A.77}$$

which can be alternatively used to define them. They can be derived from the integral representations. For instance, (A.75) results from considering the primitive of the first expression in (A.72), replacing the exponential function by its series expansion (A.8). Hence

$$\mathrm{Ei}(z)=C+\ln z+\sum_{n=1}^{\infty}\frac{z^n}{n\,n!}. \tag{A.78}$$

To find the remaining integration constant C we can take, in the sense of the principal value for the appearing integrals, the limit

$$\begin{aligned} C&=\lim_{\varepsilon\to 0^+}\left\{\,\mathrm{Ei}(\varepsilon)-\ln(\varepsilon)\,\right\}=\lim_{\varepsilon\to 0^+}\left\{-\int_{\varepsilon}^{\infty}\frac{e^{-t}}{t}\,\mathrm{d}t+\int_{\varepsilon}^{\infty}\frac{1}{t(t+1)}\,\mathrm{d}t-\ln(1+\varepsilon)\right\}\\ &=\int_0^{\infty}\frac{1}{t}\left(\frac{1}{t+1}-e^{-t}\right)\mathrm{d}t=\gamma, \end{aligned} \tag{A.79}$$

where we considered (A.44) and the fact that

$$\ln(z)=\ln(1+z)-\int_z^{\infty}\frac{1}{t(t+1)}\,\mathrm{d}t. \tag{A.80}$$

For large arguments, as $x\to\infty$ along the real line, these exponential and trigonometric integrals have the asymptotic divergent series expansions

$$\mathrm{Ei}(x)=\frac{e^x}{x}\sum_{n=0}^{\infty}\frac{n!}{x^n}, \tag{A.81}$$

$$\mathrm{Ci}(x)=\frac{\sin x}{x}\sum_{n=0}^{\infty}\frac{(-1)^n(2n)!}{x^{2n}}-\frac{\cos x}{x}\sum_{n=0}^{\infty}\frac{(-1)^n(2n+1)!}{x^{2n+1}}, \tag{A.82}$$

$$\mathrm{Si}(x)=\frac{\pi}{2}-\frac{\cos x}{x}\sum_{n=0}^{\infty}\frac{(-1)^n(2n)!}{x^{2n}}-\frac{\sin x}{x}\sum_{n=0}^{\infty}\frac{(-1)^n(2n+1)!}{x^{2n+1}}. \tag{A.83}$$

Therefore on the imaginary axis, as $|y| \to \infty$ for $y \in \mathbb{R}$, the exponential integral has the asymptotic divergent series expansion

$$\mathrm{Ei}(iy) = i\pi \,\mathrm{sign}(y) + \frac{e^{iy}}{iy} \sum_{n=0}^{\infty} \frac{n!}{(iy)^n}. \tag{A.84}$$

A.2.4 Bessel and Hankel functions

a) Differential equation and definition

Bessel functions, also called cylinder functions or cylindrical harmonics, are special functions that, together with the closely related Hankel functions, appear in a wide variety of physical problems. Some references on them are Abramowitz & Stegun (1972), Arfken & Weber (2005), Courant & Hilbert (1966), Erdélyi (1953), Jackson (1999), Jahnke & Emde (1945), Luke (1962), Magnus & Oberhettinger (1954), Morse & Feshbach (1953), Sommerfeld (1949), Spiegel & Liu (1999), Watson (1944), and Weisstein (2002). We consider the Bessel differential equation of order ν for a function $W : \mathbb{C} \to \mathbb{C}$, given by

$$z^2 \frac{\mathrm{d}^2 W}{\mathrm{d}z^2}(z) + z \frac{\mathrm{d}W}{\mathrm{d}z}(z) + (z^2 - \nu^2) W(z) = 0, \tag{A.85}$$

where, in general, $\nu \in \mathbb{C}$ is an unrestricted value. The Bessel differential equation is named after the German mathematician and astronomer Friedrich Wilhelm Bessel (1784–1846), who generalized and systemized thoroughly the Bessel functions, although it was the Dutch-born Swiss mathematician Daniel Bernoulli (1700–1782) who in fact first defined them. Independent solutions of this equation are the Bessel functions of the first kind $J_\nu(z)$ and of the second kind $Y_\nu(z)$, the latter also known as Neumann or Weber function, named respectively after the German mathematicians Franz Ernst Neumann (1798–1895) and Heinrich Martin Weber (1842–1913). They are depicted in Figure A.4 and related through

$$Y_\nu(z) = \frac{J_\nu(z)\cos(\nu\pi) - J_{-\nu}(z)}{\sin(\nu\pi)}, \qquad \nu \notin \mathbb{Z}, \tag{A.86}$$

$$Y_n(z) = \lim_{\nu \to n} \frac{J_\nu(z)\cos(\nu\pi) - J_{-\nu}(z)}{\sin(\nu\pi)}, \qquad n \in \mathbb{Z}. \tag{A.87}$$

It holds in particular that

$$Y_{n+1/2}(z) = (-1)^{n+1} J_{-n-1/2}(z), \qquad n \in \mathbb{Z}. \tag{A.88}$$

The Hankel functions of the first kind $H_\nu^{(1)}(z)$ and of the second kind $H_\nu^{(2)}(z)$, also known as Bessel functions of the third kind, are also linearly independent solutions of the differential equation (A.85). They receive their name from the German mathematician Hermann Hankel (1839–1873), and are related to the Bessel functions of the first and second kinds through the complex linear combinations

$$H_\nu^{(1)}(z) = J_\nu(z) + iY_\nu(z), \tag{A.89}$$

$$H_\nu^{(2)}(z) = J_\nu(z) - iY_\nu(z). \tag{A.90}$$

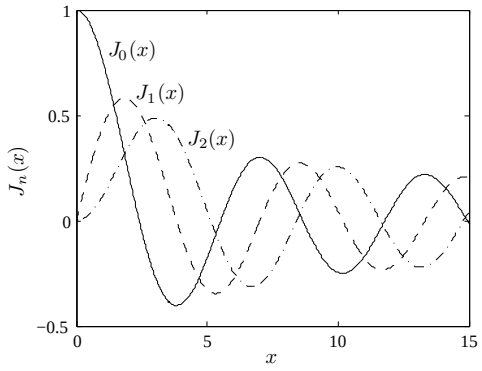

(a) Bessel function $J_n(x)$ for $n = 0, 1, 2$

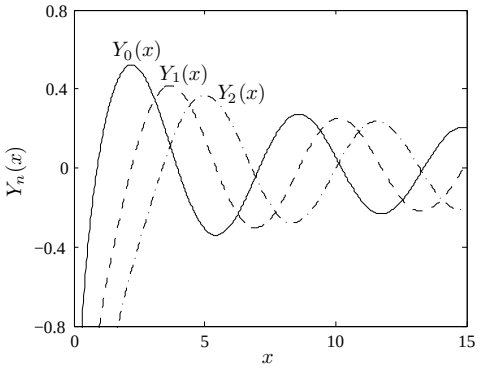

(b) Neumann function $Y_n(x)$ for $n = 0, 1, 2$

FIGURE A.4. Bessel and Neumann functions for real arguments.

The three kinds of Bessel functions are holomorphic functions of z throughout the complex z-plane cut along the negative real axis, and for fixed z ($\neq 0$) each is an entire function of ν. When $\nu = n$, for $n \in \mathbb{Z}$, then $J_\nu(z)$ has no branch point and is an entire function of z. It holds that $J_\nu(z)$, for $\mathfrak{Re}\,\nu \geq 0$, is bounded as $z \to 0$ in any bounded range of $\arg z$. The functions $J_\nu(z)$ and $J_{-\nu}(z)$ are linearly independent except when ν is an integer. The functions $J_\nu(z)$ and $Y_\nu(z)$ are linearly independent for all values of ν. The function $H_\nu^{(1)}(z)$ tends to zero as $|z| \to \infty$ in the sector $0 < \arg z < \pi$ and the function $H_\nu^{(2)}(z)$ tends to zero as $|z| \to \infty$ in the sector $-\pi < \arg z < 0$. For all values of ν, $H_\nu^{(1)}(z)$ and $H_\nu^{(2)}(z)$ are linearly independent. The Bessel functions satisfy also the relations:

$$J_{-n}(z) = (-1)^n J_n(z), \qquad Y_{-n}(z) = (-1)^n Y_n(z), \tag{A.91}$$

$$H_{-\nu}^{(1)}(z) = e^{\nu\pi i} H_\nu^{(1)}(z), \qquad H_{-\nu}^{(2)}(z) = e^{-\nu\pi i} H_\nu^{(2)}(z). \tag{A.92}$$

When using complex conjugate arguments, then for $\nu \in \mathbb{R}$ follows

$$J_\nu(\bar{z}) = \overline{J_\nu(z)}, \qquad Y_\nu(\bar{z}) = \overline{Y_\nu(z)}, \tag{A.93}$$

$$H_\nu^{(1)}(\bar{z}) = \overline{H_\nu^{(2)}(z)}, \qquad H_\nu^{(2)}(\bar{z}) = \overline{H_\nu^{(1)}(z)}. \tag{A.94}$$

b) Ascending series

The Bessel function $J_\nu(z)$ has the power series expansion

$$J_\nu(z) = \sum_{m=0}^{\infty} \frac{(-1)^m}{m!\,\Gamma(\nu + m + 1)} \left(\frac{z}{2}\right)^{2m+\nu}, \tag{A.95}$$

where Γ stands for the gamma function (A.40). For an integer order $n \geq 0$, the Bessel function $J_n(z)$ has the power series expansion

$$J_n(z) = \sum_{m=0}^{\infty} \frac{(-1)^m}{m!\,(m+n)!} \left(\frac{z}{2}\right)^{2m+n}, \tag{A.96}$$

and for the Neumann function $Y_n(z)$ it is given by

$$Y_n(z) = \frac{2}{\pi} J_n(z) \left(\ln \frac{z}{2} + \gamma \right) - \frac{1}{\pi} \sum_{m=0}^{n-1} \frac{(n-m-1)!}{m!} \left(\frac{z}{2} \right)^{2m-n} - \frac{1}{\pi} \sum_{m=0}^{\infty} (-1)^m \frac{\psi(m+n) + \psi(m)}{m!\,(m+n)!} \left(\frac{z}{2} \right)^{2m+n}, \tag{A.97}$$

where

$$\psi(0) = 0, \qquad \psi(m) = \sum_{p=1}^{m} \frac{1}{p} \qquad (m = 1, 2, \ldots), \tag{A.98}$$

and γ denotes Euler's constant (A.43). For $n = 0$ the following expansions hold

$$J_0(z) = 1 - \frac{z^2/4}{(1!)^2} + \frac{(z^2/4)^2}{(2!)^2} - \frac{(z^2/4)^3}{(3!)^2} + \ldots, \tag{A.99}$$

$$Y_0(z) = \frac{2}{\pi} J_0(z) \left(\ln \frac{z}{2} + \gamma \right) + \frac{2}{\pi} \left\{ \frac{z^2/4}{(1!)^2} - \left(1 + \frac{1}{2} \right) \frac{(z^2/4)^2}{(2!)^2} + \left(1 + \frac{1}{2} + \frac{1}{3} \right) \frac{(z^2/4)^3}{(3!)^2} - \ldots \right\}. \tag{A.100}$$

Similarly, if $n = 1$, then

$$J_1(z) = \frac{z}{2} \left\{ 1 - \frac{z^2/4}{2\,(1!)^2} + \frac{(z^2/4)^2}{3\,(2!)^2} - \frac{(z^2/4)^3}{4\,(3!)^2} + \ldots \right\}, \tag{A.101}$$

$$Y_1(z) = \frac{2}{\pi} J_1(z) \left(\ln \frac{z}{2} + \gamma \right) - \frac{2}{\pi z} + \frac{1}{\pi} \left\{ -\frac{z}{2} + \frac{2\left(1 + \frac{1}{2}\right) - \frac{1}{2}}{2\,(1!)^2} \left(\frac{z}{2} \right)^3 - \frac{2\left(1 + \frac{1}{2} + \frac{1}{3}\right) - \frac{1}{3}}{3\,(2!)^2} \left(\frac{z}{2} \right)^5 + \ldots \right\}. \tag{A.102}$$

c) Generating function and associated series

The Bessel function $J_n(z)$ has the generating function

$$e^{\frac{1}{2} z \left(t - \frac{1}{t} \right)} = \sum_{m=-\infty}^{\infty} J_m(z)\, t^m \qquad (t \neq 0). \tag{A.103}$$

This function allows, for an angle θ, the series expansions in terms of Bessel functions:

$$\cos(z \sin\theta) = J_0(z) + 2 \sum_{m=1}^{\infty} J_{2m}(z) \cos(2m\theta), \tag{A.104}$$

$$\sin(z \sin\theta) = 2 \sum_{m=0}^{\infty} J_{2m+1}(z) \sin\big((2m+1)\theta\big), \tag{A.105}$$

$$\cos(z \cos\theta) = J_0(z) + 2 \sum_{m=1}^{\infty} J_{2m}(z) \cos(2m\theta), \tag{A.106}$$

$$\sin(z\cos\theta) = 2\sum_{m=0}^{\infty}(-1)^m J_{2m+1}(z)\cos\big((2m+1)\theta\big). \tag{A.107}$$

By combining (A.106) and (A.107) we obtain the Jacobi-Anger expansion

$$e^{iz\cos\theta} = \sum_{m=-\infty}^{\infty} i^m J_m(z)\, e^{im\theta}, \tag{A.108}$$

named after the Prussian mathematician Carl Gustav Jacob Jacobi (1804–1851) and the German mathematician and astronomer Carl Theodor Anger (1803–1858). It describes the expansion of a plane wave in terms of cylindrical waves. Other related special series are

$$1 = J_0(z) + 2\sum_{m=1}^{\infty} J_{2m}(z), \tag{A.109}$$

$$\cos z = J_0(z) + 2\sum_{m=1}^{\infty}(-1)^m J_{2m}(z), \tag{A.110}$$

$$\sin z = 2\sum_{m=0}^{\infty}(-1)^m J_{2m+1}(z). \tag{A.111}$$

d) Integral representations

The Bessel functions of order zero admit the integral representations

$$J_0(z) = \frac{1}{\pi}\int_0^{\pi}\cos(z\sin\theta)\,\mathrm{d}\theta = \frac{1}{\pi}\int_0^{\pi}\cos(z\cos\theta)\,\mathrm{d}\theta, \tag{A.112}$$

$$Y_0(z) = \frac{4}{\pi^2}\int_0^{\pi/2}\cos(z\cos\theta)\big\{\gamma + \ln(2z\sin^2\theta)\big\}\,\mathrm{d}\theta. \tag{A.113}$$

For arbitrary orders and for $|\arg z| < \pi/2$ we have

$$J_\nu(z) = \frac{1}{\pi}\int_0^{\pi}\cos(z\sin\theta - \nu\theta)\,\mathrm{d}\theta - \frac{\sin(\nu\pi)}{\pi}\int_0^{\infty} e^{-z\sinh t - \nu t}\,\mathrm{d}t, \tag{A.114}$$

$$Y_\nu(z) = \frac{1}{\pi}\int_0^{\pi}\sin(z\sin\theta - \nu\theta)\,\mathrm{d}\theta - \frac{1}{\pi}\int_0^{\infty}\big\{e^{\nu t} + e^{-\nu t}\cos(\nu\pi)\big\}\, e^{-z\sinh t}\,\mathrm{d}t. \tag{A.115}$$

The Hankel functions admit the integral representations

$$H_\nu^{(1)}(z) = \frac{1}{\pi i}\int_{-\infty}^{\infty+\pi i} e^{z\sinh t - \nu t}\,\mathrm{d}t \qquad \big(|\arg z| < \pi/2\big), \tag{A.116}$$

$$H_\nu^{(2)}(z) = -\frac{1}{\pi i}\int_{-\infty}^{\infty-\pi i} e^{z\sinh t - \nu t}\,\mathrm{d}t \qquad \big(|\arg z| < \pi/2\big). \tag{A.117}$$

e) Recurrence relations

If W_ν is used to denote J_ν, Y_ν, $H_\nu^{(1)}$, $H_\nu^{(2)}$, or any linear combination of these functions whose coefficients are independent of z and ν, then the following recurrence relations hold

for all of them:

$$\frac{2\nu}{z}W_\nu(z) = W_{\nu-1}(z) + W_{\nu+1}(z), \tag{A.118}$$

$$2\,\frac{\mathrm{d}W_\nu}{\mathrm{d}z}(z) = W_{\nu-1}(z) - W_{\nu+1}(z), \tag{A.119}$$

$$\frac{\mathrm{d}W_\nu}{\mathrm{d}z}(z) = W_{\nu-1}(z) - \frac{\nu}{z}W_\nu(z), \tag{A.120}$$

$$\frac{\mathrm{d}W_\nu}{\mathrm{d}z}(z) = -W_{\nu+1}(z) + \frac{\nu}{z}W_\nu(z), \tag{A.121}$$

$$\frac{\mathrm{d}W_0}{\mathrm{d}z}(z) = -W_1(z). \tag{A.122}$$

Particular cases for the above are

$$\frac{\mathrm{d}W_1}{\mathrm{d}z}(z) = W_0(z) - \frac{1}{z}W_1(z), \tag{A.123}$$

$$W_2(z) = \frac{2}{z}W_1(z) - W_0(z), \tag{A.124}$$

$$\frac{\mathrm{d}W_2}{\mathrm{d}z}(z) = \left(1 - \frac{4}{z^2}\right)W_1(z) + \frac{2}{z}W_0(z) = W_1(z) - \frac{2}{z}W_2(z). \tag{A.125}$$

For the derivatives, considering $m = 0, 1, 2, \ldots$, it also holds that

$$\left(\frac{1}{z}\frac{\mathrm{d}}{\mathrm{d}z}\right)^m \left\{z^\nu W_\nu(z)\right\} = z^{\nu-m}W_{\nu-m}(z), \tag{A.126}$$

$$\left(\frac{1}{z}\frac{\mathrm{d}}{\mathrm{d}z}\right)^m \left\{z^{-\nu} W_\nu(z)\right\} = (-1)^m z^{-\nu-m}W_{\nu+m}(z). \tag{A.127}$$

Some primitives of Bessel functions, omitting the integration constants, are given by

$$\int W_0(z)\,\mathrm{d}z = \frac{\pi z}{2}\big\{W_0(z)\boldsymbol{H}_{-1}(z) + W_1(z)\boldsymbol{H}_0(z)\big\}, \tag{A.128}$$

$$\int W_1(z)\,\mathrm{d}z = -W_0(z), \tag{A.129}$$

where $\boldsymbol{H}_\nu$ denotes the Struve function of order ν (vid. Subsection A.2.7).

f) Asymptotic behavior

For small arguments, when ν is fixed and $z \to 0$, the Bessel functions behave like

$$J_\nu(z) \sim \frac{1}{\Gamma(\nu+1)}\left(\frac{z}{2}\right)^\nu \qquad (\nu \neq -1, -2, -3, \ldots), \tag{A.130}$$

$$Y_0(z) \sim -iH_0^{(1)}(z) \sim iH_0^{(2)}(z) \sim \frac{2}{\pi}\ln z, \tag{A.131}$$

$$Y_\nu(z) \sim -iH_\nu^{(1)}(z) \sim iH_\nu^{(2)}(z) \sim -\frac{\Gamma(\nu)}{\pi}\left(\frac{2}{z}\right)^\nu \qquad (\mathfrak{Re}\,\nu > 0). \tag{A.132}$$

The asymptotic forms of the Bessel functions, when ν is fixed and $|z| \to \infty$, are given by

$$J_\nu(z) \sim \sqrt{\frac{2}{\pi z}} \cos\Big(z - \frac{\nu\pi}{2} - \frac{\pi}{4}\Big), \qquad |\arg z| < \pi, \tag{A.133}$$

$$Y_\nu(z) \sim \sqrt{\frac{2}{\pi z}} \sin\Big(z - \frac{\nu\pi}{2} - \frac{\pi}{4}\Big), \qquad |\arg z| < \pi, \tag{A.134}$$

$$H_\nu^{(1)}(z) \sim \sqrt{\frac{2}{\pi z}}\, e^{i\left(z - \frac{\nu\pi}{2} - \frac{\pi}{4}\right)}, \qquad -\pi < \arg z < 2\pi, \tag{A.135}$$

$$H_\nu^{(2)}(z) \sim \sqrt{\frac{2}{\pi z}}\, e^{-i\left(z - \frac{\nu\pi}{2} - \frac{\pi}{4}\right)}, \qquad -2\pi < \arg z < \pi. \tag{A.136}$$

In particular, the zeroth and first order Hankel functions behave at the origin, for $z \to 0$, as

$$H_0^{(1)}(z) \sim \frac{2i}{\pi} \ln z, \qquad H_0^{(2)}(z) \sim -\frac{2i}{\pi} \ln z, \tag{A.137}$$

$$H_1^{(1)}(z) \sim -\frac{2i}{\pi z}, \qquad H_1^{(2)}(z) \sim \frac{2i}{\pi z}. \tag{A.138}$$

At infinity, for $|z| \to \infty$, they behave like

$$H_0^{(1)}(z) \sim \sqrt{\frac{2}{\pi z}}\, e^{i(z - \frac{\pi}{4})}, \qquad H_0^{(2)}(z) \sim \sqrt{\frac{2}{\pi z}}\, e^{-i(z - \frac{\pi}{4})}, \tag{A.139}$$

$$H_1^{(1)}(z) \sim \sqrt{\frac{2}{\pi z}}\, e^{i(z - \frac{3\pi}{4})}, \qquad H_1^{(2)}(z) \sim \sqrt{\frac{2}{\pi z}}\, e^{-i(z - \frac{3\pi}{4})}. \tag{A.140}$$

g) Addition theorems

If W_ν denotes any linear combination of Bessel, Neumann, or Hankel functions, then Neumann's addition theorem for $u, v \in \mathbb{C}$ asserts that

$$W_\nu(u \pm v) = \sum_{m=-\infty}^{\infty} W_{\nu \mp m}(u) J_m(v) \qquad \big(|v| < |u|\big). \tag{A.141}$$

The restriction $|v| < |u|$ is unnecessary when $W_\nu = J_\nu$ and ν is an integer or zero. We have similarly Graf's addition theorem, which states that

$$W_\nu(w) e^{i\nu\chi} = \sum_{m=-\infty}^{\infty} W_{\nu+m}(u) J_m(v) e^{im\alpha} \qquad \big(|ve^{\pm i\alpha}| < |u|\big), \tag{A.142}$$

where

$$w = \sqrt{u^2 + v^2 - 2uv\cos\alpha}, \tag{A.143}$$

and

$$u - v\cos\alpha = w\cos\chi, \qquad v\sin\alpha = w\sin\chi, \tag{A.144}$$

being the branches chosen so that $w \to u$ and $\chi \to 0$ as $v \to 0$. If u, v are real and positive, and $0 \le \alpha \le \pi$, then w, χ are real and nonnegative, and the geometrical relationship of the variables is shown in Figure A.5. Again, the restriction $|ve^{\pm i\alpha}| < |u|$ is unnecessary when $W_\nu = J_\nu$ and ν is an integer or zero.

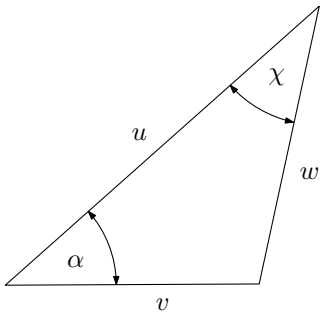

FIGURE A.5. Geometrical relationship of the variables for Graf's addition theorem.

The addition theorem of Graf allows us to establish, for $\boldsymbol{x}, \boldsymbol{y} \in \mathbb{R}^2$ and $k \in \mathbb{C}$, the addition theorem for the Hankel functions

$$H_\nu^{(1)}\big(k|\boldsymbol{x}-\boldsymbol{y}|\big)e^{i\nu\varphi} = \sum_{m=-\infty}^{\infty} H_{\nu+m}^{(1)}\big(k|\boldsymbol{x}|\big)J_m\big(k|\boldsymbol{y}|\big)e^{im\theta} \qquad \big(|\boldsymbol{y}|<|\boldsymbol{x}|\big), \quad \text{(A.145)}$$

where

$$\cos\theta = \frac{\boldsymbol{x}\cdot\boldsymbol{y}}{|\boldsymbol{x}|\,|\boldsymbol{y}|} \qquad \cos\varphi = \frac{\boldsymbol{x}\cdot(\boldsymbol{x}-\boldsymbol{y})}{|\boldsymbol{x}|\,|\boldsymbol{x}-\boldsymbol{y}|}. \quad \text{(A.146)}$$

In the particular case when $\nu = 0$, the addition theorem for $|\boldsymbol{y}| < |\boldsymbol{x}|$ becomes

$$H_0^{(1)}\big(k|\boldsymbol{x}-\boldsymbol{y}|\big) = H_0^{(1)}\big(k|\boldsymbol{x}|\big)J_0\big(k|\boldsymbol{y}|\big) + 2\sum_{m=1}^{\infty} H_m^{(1)}\big(k|\boldsymbol{x}|\big)J_m\big(k|\boldsymbol{y}|\big)\cos(m\theta). \quad \text{(A.147)}$$

A.2.5 Modified Bessel functions

a) Differential equation and definition

Modified Bessel functions are special functions that appear also in a wide variety of physical problems. Roughly speaking, they correspond to Bessel and Hankel functions (vid. Subsection A.2.4) with a purely imaginary argument and therefore they do not oscillate on the real axis as the former but rather increase or decrease exponentially. Some references for them are Abramowitz & Stegun (1972), Arfken & Weber (2005), Erdélyi (1953), Jackson (1999), Jahnke & Emde (1945), Luke (1962), Magnus & Oberhettinger (1954), Morse & Feshbach (1953), Spiegel & Liu (1999), Watson (1944), and Weisstein (2002). We consider the modified Bessel differential equation of order ν for a function $W : \mathbb{C} \to \mathbb{C}$, which is given by

$$z^2\frac{\mathrm{d}^2W}{\mathrm{d}z^2}(z) + z\frac{\mathrm{d}W}{\mathrm{d}z}(z) - (z^2+\nu^2)W(z) = 0, \quad \text{(A.148)}$$

where, in general, $\nu \in \mathbb{C}$ is an unrestricted value. Independent solutions of this equation are the modified Bessel functions of the first kind $I_\nu(z)$ and of the second kind $K_\nu(z)$. They are depicted in Figure A.6. Each is a regular function of z throughout the z-plane cut along the negative real axis, and for fixed z ($\neq 0$) each is an entire function of ν. When $\nu = n$, for $n \in \mathbb{Z}$, then $I_\nu(z)$ is an entire function of z. The function $I_\nu(z)$, for $\mathfrak{Re}\,\nu \geq 0$, is bounded as $z \to 0$ in any bounded range of $\arg z$. The functions $I_\nu(z)$ and $I_{-\nu}(z)$

are linearly independent except when ν is an integer. The function $K_\nu(z)$ tends to zero as $|z| \to \infty$ in the sector $|\arg z| < \pi/2$, and for all values of ν, $I_\nu(z)$ and $K_\nu(z)$ are linearly independent. The functions $I_\nu(z)$ and $K_\nu(z)$ are real and positive when $\nu > -1$ and $z > 0$. The function $K_\nu(z)$ is related to $I_\nu(z)$ through

$$K_\nu(z) = \frac{\pi}{2}\left(\frac{I_{-\nu}(z) - I_\nu(z)}{\sin(\nu\pi)}\right), \qquad \nu \notin \mathbb{Z}, \tag{A.149}$$

$$K_n(z) = \lim_{\nu \to n} \frac{\pi}{2}\left(\frac{I_{-\nu}(z) - I_\nu(z)}{\sin(\nu\pi)}\right), \qquad n \in \mathbb{Z}. \tag{A.150}$$

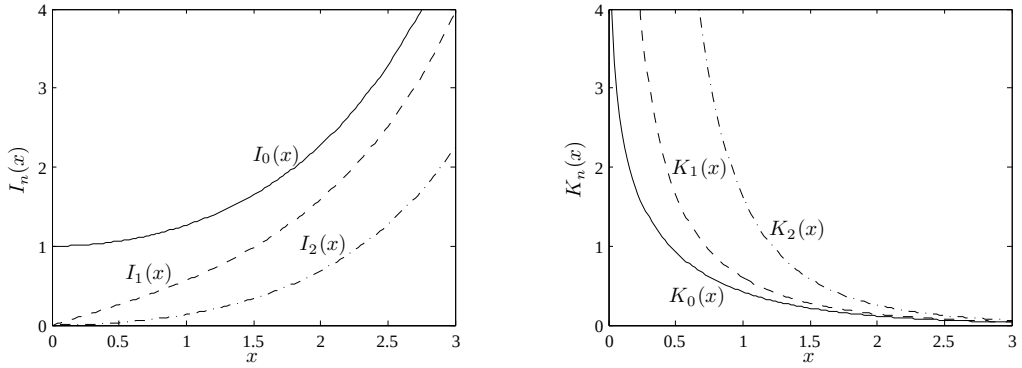

(a) Modified Bessel function $I_n(x)$, $n = 0, 1, 2$ (b) Modified Bessel function $K_n(x)$, $n = 0, 1, 2$

FIGURE A.6. Modified Bessel functions for real arguments.

The modified Bessel function $I_\nu(z)$ is related to the Bessel function $J_\nu(z)$ through

$$I_\nu(z) = e^{-i\nu\pi/2} J_\nu\big(z\, e^{i\pi/2}\big), \qquad -\pi < \arg z \le \frac{\pi}{2}, \tag{A.151}$$

$$I_\nu(z) = e^{3i\nu\pi/2} J_\nu\big(z\, e^{-3i\pi/2}\big), \qquad -\frac{\pi}{2} < \arg z \le \pi, \tag{A.152}$$

and $K_\nu(z)$ is related to the Hankel functions $H_\nu^{(1)}(z)$ and $H_\nu^{(2)}(z)$ through

$$K_\nu(z) = \frac{i\pi}{2} e^{i\nu\pi/2} H_\nu^{(1)}\big(z\, e^{i\pi/2}\big), \qquad -\pi < \arg z \le \frac{\pi}{2}, \tag{A.153}$$

$$K_\nu(z) = -\frac{i\pi}{2} e^{-i\nu\pi/2} H_\nu^{(2)}\big(z\, e^{-i\pi/2}\big), \qquad -\frac{\pi}{2} < \arg z \le \pi. \tag{A.154}$$

For the Neumann function $Y_\nu(z)$ it holds that

$$Y_\nu(z) = e^{i(\nu+1)\pi/2} I_\nu(z) - \frac{2}{\pi} e^{-i\nu\pi/2} K_\nu(z), \qquad -\pi < \arg z \le \frac{\pi}{2}. \tag{A.155}$$

For negative orders it holds also that

$$I_{-n}(z) = I_n(z), \qquad n \in \mathbb{Z}, \tag{A.156}$$

$$K_{-\nu}(z) = K_\nu(z), \qquad \nu \in \mathbb{C}. \tag{A.157}$$

When using complex conjugate arguments, then for $\nu \in \mathbb{R}$ follows

$$I_\nu(\bar{z}) = \overline{I_\nu(z)}, \qquad K_\nu(\bar{z}) = \overline{K_\nu(z)}. \tag{A.158}$$

Most of the properties of modified Bessel functions can be deduced immediately from those of ordinary Bessel functions by the application of these relations.

b) Ascending series

The modified Bessel function $I_\nu(z)$ has the power series expansion

$$I_\nu(z) = \sum_{m=0}^{\infty} \frac{1}{m!\,\Gamma(\nu+m+1)} \left(\frac{z}{2}\right)^{2m+\nu}, \tag{A.159}$$

where Γ stands for the gamma function (A.40). For an integer order $n \geq 0$, the modified Bessel function $I_n(z)$ has the power series expansion

$$I_n(z) = \sum_{m=0}^{\infty} \frac{1}{m!\,(m+n)!} \left(\frac{z}{2}\right)^{2m+n}, \tag{A.160}$$

and for the function $K_n(z)$ it is given by

$$\begin{aligned} K_n(z) = (-1)^{n+1} I_n(z) \left(\ln\frac{z}{2} + \gamma\right) + \frac{1}{2}\sum_{m=0}^{n-1} (-1)^m \frac{(n-m-1)!}{m!} \left(\frac{z}{2}\right)^{2m-n} \\ + \frac{(-1)^n}{2} \sum_{m=0}^{\infty} \frac{\psi(m+n)+\psi(m)}{m!\,(m+n)!} \left(\frac{z}{2}\right)^{2m+n}, \end{aligned} \tag{A.161}$$

where

$$\psi(0) = 0, \qquad \psi(m) = \sum_{p=1}^{m} \frac{1}{p} \qquad (m = 1, 2, \ldots), \tag{A.162}$$

and γ denotes Euler's constant (A.43). For $n = 0$ the following expansions hold

$$I_0(z) = 1 + \frac{z^2/4}{(1!)^2} + \frac{(z^2/4)^2}{(2!)^2} + \frac{(z^2/4)^3}{(3!)^2} + \ldots, \tag{A.163}$$

$$\begin{aligned} K_0(z) = -I_0(z) \left(\ln\frac{z}{2} + \gamma\right) \\ + \frac{z^2/4}{(1!)^2} + \left(1+\frac{1}{2}\right)\frac{(z^2/4)^2}{(2!)^2} + \left(1+\frac{1}{2}+\frac{1}{3}\right)\frac{(z^2/4)^3}{(3!)^2} + \ldots. \end{aligned} \tag{A.164}$$

Similarly, if $n = 1$, then

$$I_1(z) = \frac{z}{2}\left\{1 + \frac{z^2/4}{2\,(1!)^2} + \frac{(z^2/4)^2}{3\,(2!)^2} + \frac{(z^2/4)^3}{4\,(3!)^2} + \ldots\right\}, \tag{A.165}$$

$$\begin{aligned} K_1(z) = I_1(z)\left(\ln\frac{z}{2} + \gamma\right) + \frac{1}{z} \\ - \frac{1}{2}\left\{\frac{z}{2} + \frac{2\left(1+\frac{1}{2}\right)-\frac{1}{2}}{2\,(1!)^2}\left(\frac{z}{2}\right)^3 + \frac{2\left(1+\frac{1}{2}+\frac{1}{3}\right)-\frac{1}{3}}{3\,(2!)^2}\left(\frac{z}{2}\right)^5 + \ldots\right\}. \end{aligned} \tag{A.166}$$

c) Generating function and associated series

The modified Bessel function $I_n(z)$ has the generating function

$$e^{\frac{1}{2}z\left(t+\frac{1}{t}\right)} = \sum_{m=-\infty}^{\infty} I_m(z)\, t^m \qquad (t \neq 0), \tag{A.167}$$

which allows, for an angle θ, the series expansions in terms of modified Bessel functions:

$$e^{z\cos\theta} = I_0(z) + 2\sum_{m=1}^{\infty} I_m(z)\cos(m\theta), \tag{A.168}$$

$$\begin{aligned} e^{z\sin\theta} = {} & I_0(z) + 2\sum_{m=0}^{\infty}(-1)^m I_{2m+1}(z)\sin\big((2m+1)\theta\big) \\ & + 2\sum_{m=1}^{\infty}(-1)^m I_{2m}(z)\cos\big(2m\theta\big). \end{aligned} \tag{A.169}$$

Other related special series are

$$1 = I_0(z) + 2\sum_{m=1}^{\infty}(-1)^m I_{2m}(z), \tag{A.170}$$

$$e^{z} = I_0(z) + 2\sum_{m=1}^{\infty} I_m(z), \tag{A.171}$$

$$e^{-z} = I_0(z) + 2\sum_{m=1}^{\infty}(-1)^m I_m(z), \tag{A.172}$$

$$\cosh z = I_0(z) + 2\sum_{m=1}^{\infty} I_{2m}(z), \tag{A.173}$$

$$\sinh z = 2\sum_{m=0}^{\infty} I_{2m+1}(z). \tag{A.174}$$

d) Integral representations

The modified Bessel functions of order zero admit the integral representations

$$I_0(z) = \frac{1}{\pi}\int_0^{\pi} e^{\pm z\cos\theta}\,\mathrm{d}\theta = \frac{1}{\pi}\int_0^{\pi}\cosh(z\cos\theta)\,\mathrm{d}\theta, \tag{A.175}$$

$$K_0(z) = -\frac{1}{\pi}\int_0^{\pi} e^{\pm z\cos\theta}\big\{\gamma + \ln(2z\sin^2\theta)\big\}\,\mathrm{d}\theta. \tag{A.176}$$

For arbitrary orders and for $|\arg z| < \pi/2$ we have that

$$I_\nu(z) = \frac{1}{\pi}\int_0^{\pi} e^{z\cos\theta}\cos(\nu\theta)\,\mathrm{d}\theta - \frac{\sin(\nu\pi)}{\pi}\int_0^{\infty} e^{-z\cosh t-\nu t}\,\mathrm{d}t, \tag{A.177}$$

$$K_\nu(z) = \int_0^{\infty} e^{-z\cosh t}\cosh(\nu t)\,\mathrm{d}t. \tag{A.178}$$

e) Recurrence relations

If W_ν is used to denote I_ν, $e^{\nu\pi i}K_\nu$, or any linear combination of these functions whose coefficients are independent of z and ν, then the following recurrence relations hold:

$$\frac{2\nu}{z}W_\nu(z) = W_{\nu-1}(z) - W_{\nu+1}(z), \tag{A.179}$$

$$2\,\frac{\mathrm{d}W_\nu}{\mathrm{d}z}(z) = W_{\nu-1}(z) + W_{\nu+1}(z), \tag{A.180}$$

$$\frac{\mathrm{d}W_\nu}{\mathrm{d}z}(z) = W_{\nu-1}(z) - \frac{\nu}{z}W_\nu(z), \tag{A.181}$$

$$\frac{\mathrm{d}W_\nu}{\mathrm{d}z}(z) = W_{\nu+1}(z) + \frac{\nu}{z}W_\nu(z), \tag{A.182}$$

$$\frac{\mathrm{d}I_0}{\mathrm{d}z}(z) = I_1(z), \qquad \frac{\mathrm{d}K_0}{\mathrm{d}z}(z) = -K_1(z). \tag{A.183}$$

For the derivatives, considering $m = 0, 1, 2, \ldots$, it also holds that

$$\left(\frac{1}{z}\frac{\mathrm{d}}{\mathrm{d}z}\right)^m \left\{z^\nu W_\nu(z)\right\} = z^{\nu-m}W_{\nu-m}(z), \tag{A.184}$$

$$\left(\frac{1}{z}\frac{\mathrm{d}}{\mathrm{d}z}\right)^m \left\{z^{-\nu} W_\nu(z)\right\} = z^{-\nu-m}W_{\nu+m}(z). \tag{A.185}$$

f) Asymptotic behavior

Modified Bessel functions behave for small arguments, when ν is fixed and $z \to 0$, as

$$I_\nu(z) \sim \frac{1}{\Gamma(\nu+1)}\left(\frac{z}{2}\right)^\nu \qquad (\nu \neq -1, -2, -3, \ldots), \tag{A.186}$$

$$K_0(z) \sim -\ln z, \tag{A.187}$$

$$K_\nu(z) \sim \frac{\Gamma(\nu)}{2}\left(\frac{2}{z}\right)^\nu \qquad (\mathfrak{Re}\,\nu > 0). \tag{A.188}$$

The asymptotic forms of the modified Bessel functions, when ν is fixed and $|z| \to \infty$, are

$$I_\nu(z) \sim \frac{e^z}{\sqrt{2\pi z}}, \qquad |\arg z| < \frac{\pi}{2}, \tag{A.189}$$

$$K_\nu(z) \sim \sqrt{\frac{\pi}{2z}}\,e^{-z}, \qquad |\arg z| < \frac{3\pi}{2}. \tag{A.190}$$

A.2.6 Spherical Bessel and Hankel functions

a) Differential equation and definition

Spherical Bessel functions or Bessel functions of fractional order are special functions that play the role of Bessel or cylinder functions for spherical problems. Some references are Abramowitz & Stegun (1972), Arfken & Weber (2005), Erdélyi (1953), Jackson (1999),

and Weisstein (2002). They satisfy the spherical Bessel differential equation

$$z^2\frac{\mathrm{d}^2w}{\mathrm{d}z^2}(z)+2z\frac{\mathrm{d}w}{\mathrm{d}z}(z)+\big(z^2-\nu(\nu+1)\big)w(z)=0 \qquad (\nu\in\mathbb{C}), \tag{A.191}$$

which can be obtained by applying separation of spherical variables to the Helmholtz equation. Particular linearly independent solutions of this equation are the spherical Bessel functions of the first kind

$$j_\nu(z)=\sqrt{\frac{\pi}{2z}}J_{\nu+1/2}(z), \tag{A.192}$$

and the spherical Bessel functions of the second kind or spherical Neumann functions

$$y_\nu(z)=\sqrt{\frac{\pi}{2z}}Y_{\nu+1/2}(z), \tag{A.193}$$

where $J_{\nu+1/2}$ and $Y_{\nu+1/2}$ denote respectively the Bessel function of the first kind and the Bessel function of the second kind or Neumann function. They are shown in Figure A.7. Other independent solutions of (A.191) are the spherical Hankel functions of the first and second kinds, also known as spherical Bessel functions of the third kind, given by

$$h_\nu^{(1)}(z)=j_\nu(z)+iy_\nu(z)=\sqrt{\frac{\pi}{2z}}H_{\nu+1/2}^{(1)}(z), \tag{A.194}$$

$$h_\nu^{(2)}(z)=j_\nu(z)-iy_\nu(z)=\sqrt{\frac{\pi}{2z}}H_{\nu+1/2}^{(2)}(z), \tag{A.195}$$

where $H_{\nu+1/2}^{(1)}$ and $H_{\nu+1/2}^{(2)}$ denote respectively the Hankel functions of the first and second kinds. The Bessel and Hankel functions are thoroughly discussed in Subsection A.2.4. The spherical Bessel and Hankel functions are most commonly encountered in the case where $\nu=n$, being n a positive integer or zero. They satisfy for $n\in\mathbb{Z}$ the relations

$$y_n(z)=(-1)^{n+1}j_{-n-1}(z), \tag{A.196}$$

and

$$h_{-n-1}^{(1)}(z)=i(-1)^n h_n^{(1)}(z), \qquad h_{-n-1}^{(2)}(z)=-i(-1)^n h_n^{(2)}(z). \tag{A.197}$$

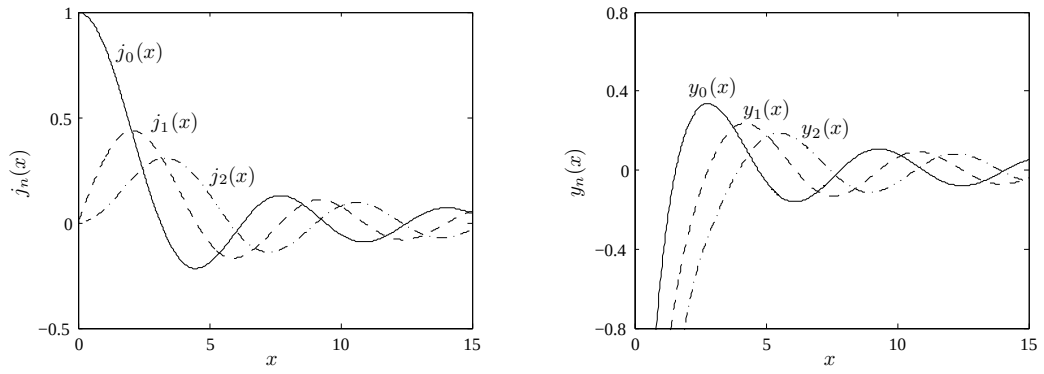

(a) Spherical Bessel function $j_n(x)$, $n=0,1,2$ (b) Spherical Neumann function $y_n(x)$, $n=0,1,2$

FIGURE A.7. Spherical Bessel and Neumann functions for real arguments.

b) Ascending series

The spherical Bessel function $j_\nu(z)$ has the ascending series expansion

$$j_\nu(z) = \frac{\sqrt{\pi}}{2} \sum_{m=0}^{\infty} \frac{(-1)^m}{m!\,\Gamma(\nu + m + 3/2)} \left(\frac{z}{2}\right)^{2m+\nu}, \tag{A.198}$$

where Γ denotes the gamma function (A.40). For the spherical Neumann function $y_\nu(z)$ it is given by

$$y_\nu(z) = \frac{(-1)^{\nu+1}}{2^\nu z^{\nu+1}} \sum_{m=0}^{\infty} \frac{(-1)^m 4^{\nu-m}\sqrt{\pi}}{m!\,\Gamma(m - \nu + 1/2)} z^{2m}. \tag{A.199}$$

For an integer order $n \geq 0$ they are given by

$$j_n(z) = 2^n z^n \sum_{m=0}^{\infty} \frac{(-1)^m (m+n)!}{m!\,(2n + 2m + 1)!} z^{2m}, \tag{A.200}$$

and

$$y_n(z) = \frac{(-1)^{n+1}}{2^n z^{n+1}} \sum_{m=0}^{\infty} \frac{(-1)^m (m-n)!}{m!\,(2m - 2n)!} z^{2m}. \tag{A.201}$$

For the spherical Hankel functions we have also the exact formulae

$$h_n^{(1)}(z) = (-i)^{n+1} \frac{e^{iz}}{z} \sum_{m=0}^{n} \frac{i^m}{m!\,(2z)^m} \frac{(n+m)!}{(n-m)!}, \tag{A.202}$$

$$h_n^{(2)}(z) = i^{n+1} \frac{e^{-iz}}{z} \sum_{m=0}^{n} \frac{(-i)^m}{m!\,(2z)^m} \frac{(n+m)!}{(n-m)!}. \tag{A.203}$$

c) Special values

The spherical Bessel function $j_n(z)$ adopts, for $n = 0, 1, 2$, the values

$$j_0(z) = \frac{\sin z}{z}, \tag{A.204}$$

$$j_1(z) = \frac{\sin z}{z^2} - \frac{\cos z}{z}, \tag{A.205}$$

$$j_2(z) = \left(\frac{3}{z^3} - \frac{1}{z}\right) \sin z - \frac{3}{z^2} \cos z. \tag{A.206}$$

For $n = 0, 1, 2$ the spherical Neumann function $y_n(z)$ adopts the values

$$y_0(z) = -j_{-1}(z) = -\frac{\cos z}{z}, \tag{A.207}$$

$$y_1(z) = -j_{-2}(z) = -\frac{\cos z}{z^2} - \frac{\sin z}{z}, \tag{A.208}$$

$$y_2(z) = -j_{-3}(z) = \left(-\frac{3}{z^3} + \frac{1}{z}\right) \cos z - \frac{3}{z^2} \sin z. \tag{A.209}$$

For the spherical Hankel functions, these values are given by

$$h_0^{(1)}(z) = -\frac{i}{z}e^{iz}, \qquad h_0^{(2)}(z) = \frac{i}{z}e^{-iz}, \tag{A.210}$$

$$h_1^{(1)}(z) = \left(-\frac{1}{z} - \frac{i}{z^2}\right)e^{iz}, \qquad h_1^{(2)}(z) = \left(-\frac{1}{z} + \frac{i}{z^2}\right)e^{-iz}, \tag{A.211}$$

$$h_2^{(1)}(z) = \left(\frac{i}{z} - \frac{3}{z^2} - \frac{3i}{z^3}\right)e^{iz}, \qquad h_2^{(2)}(z) = \left(-\frac{i}{z} - \frac{3}{z^2} + \frac{3i}{z^3}\right)e^{-iz}. \tag{A.212}$$

d) Recurrence relations

If w_n is used to denote j_n, y_n, $h_n^{(1)}$, $h_n^{(2)}$, or any linear combination of these functions whose coefficients are independent of z and n, then the following recurrence relations hold:

$$\frac{2n+1}{z}w_n(z) = w_{n-1}(z) + w_{n+1}(z), \tag{A.213}$$

$$(2n+1)\frac{\mathrm{d}w_n}{\mathrm{d}z}(z) = n\,w_{n-1}(z) - (n+1)w_{n+1}(z). \tag{A.214}$$

$$\frac{\mathrm{d}w_n}{\mathrm{d}z}(z) = w_{n-1}(z) - \frac{n+1}{z}w_n(z). \tag{A.215}$$

$$\frac{\mathrm{d}w_n}{\mathrm{d}z}(z) = \frac{n}{z}w_n(z) - w_{n+1}(z). \tag{A.216}$$

$$\frac{\mathrm{d}w_0}{\mathrm{d}z}(z) = -w_1(z). \tag{A.217}$$

Rearranging these relations yields

$$\frac{\mathrm{d}}{\mathrm{d}z}\left\{z^{n+1}w_n(z)\right\} = z^{n+1}w_{n-1}(z), \tag{A.218}$$

$$\frac{\mathrm{d}}{\mathrm{d}z}\left\{z^{-n}w_n(z)\right\} = -z^{-n}w_{n+1}(z). \tag{A.219}$$

By mathematical induction we can establish also the Rayleigh formulae

$$j_n(z) = (-1)^n z^n \left(\frac{1}{z}\frac{\mathrm{d}}{\mathrm{d}z}\right)^n \left\{\frac{\sin z}{z}\right\}, \tag{A.220}$$

$$y_n(z) = -(-1)^n z^n \left(\frac{1}{z}\frac{\mathrm{d}}{\mathrm{d}z}\right)^n \left\{\frac{\cos z}{z}\right\}, \tag{A.221}$$

$$h_n^{(1)}(z) = -i(-1)^n z^n \left(\frac{1}{z}\frac{\mathrm{d}}{\mathrm{d}z}\right)^n \left\{\frac{e^{iz}}{z}\right\}, \tag{A.222}$$

$$h_n^{(2)}(z) = i(-1)^n z^n \left(\frac{1}{z}\frac{\mathrm{d}}{\mathrm{d}z}\right)^n \left\{\frac{e^{-iz}}{z}\right\}. \tag{A.223}$$

e) Limiting values

The asymptotic limiting values of the spherical Bessel functions for small arguments, i.e., as $z \to 0$ and for fixed n, are given by

$$j_n(z) \sim \frac{2^n n!}{(2n+1)!} z^n, \tag{A.224}$$

$$y_n(z) \sim -\frac{(2n)!}{2^n n!} z^{-n-1}. \tag{A.225}$$

The asymptotic forms of the spherical Bessel and Hankel functions for large arguments, as $|z| \to \infty$ and for fixed n, are, likewise as for the Bessel and Hankel functions, given by

$$j_n(z) \sim \frac{1}{z} \sin\Big(z - \frac{n\pi}{2}\Big), \tag{A.226}$$

$$y_n(z) \sim -\frac{1}{z} \cos\Big(z - \frac{n\pi}{2}\Big), \tag{A.227}$$

$$h_n^{(1)}(z) \sim (-i)^{n+1} \frac{e^{iz}}{z} = -i \frac{e^{i(z-n\pi/2)}}{z}, \tag{A.228}$$

$$h_n^{(2)}(z) \sim i^{n+1} \frac{e^{-iz}}{z} = i \frac{e^{-i(z-n\pi/2)}}{z}. \tag{A.229}$$

f) Addition theorems

The spherical Bessel functions satisfy, for arbitrary complex u, v, λ, θ, the addition theorems

$$j_0(\lambda w) = \sum_{n=0}^{\infty} (2n+1) j_n(\lambda u) j_n(\lambda v) P_n(\cos\theta), \tag{A.230}$$

$$y_0(\lambda w) = \sum_{n=0}^{\infty} (2n+1) y_n(\lambda u) j_n(\lambda v) P_n(\cos\theta) \qquad \big(|v e^{\pm i\theta}| < |u|\big), \tag{A.231}$$

where

$$w = \sqrt{u^2 + v^2 - 2uv\cos\theta}, \tag{A.232}$$

and where $P_n(z)$ denotes the Legendre polynomial of degree n (vid. Subsection A.2.8). Similarly, for the spherical Hankel functions we have that

$$h_0^{(1)}(\lambda w) = \sum_{n=0}^{\infty} (2n+1) h_n^{(1)}(\lambda u) j_n(\lambda v) P_n(\cos\theta) \qquad \big(|v e^{\pm i\theta}| < |u|\big). \tag{A.233}$$

As for cylindrical functions, we have the Jacobi-Anger expansion

$$e^{i\lambda\cos\theta} = \sum_{n=0}^{\infty} i^n (2n+1) j_n(\lambda) P_n(\cos\theta), \tag{A.234}$$

which describes the expansion of a plane wave in terms of spherical waves.

A.2.7 Struve functions

a) Differential equation and definition

Struve functions are special functions that occur in many places in physics and applied mathematics, e.g., in optics, in fluid dynamics, and quite prominently in acoustics for impedance calculations. Some references for Struve functions are Abramowitz & Stegun (1972), Erdélyi (1953), Jahnke & Emde (1945), Magnus & Oberhettinger (1954), and Weisstein (2002). They satisfy for a function $\boldsymbol{W} : \mathbb{C} \to \mathbb{C}$ the following non-homogeneous Bessel differential equation of order ν:

$$z^2 \frac{\mathrm{d}^2 \boldsymbol{W}}{\mathrm{d}z^2}(z) + z \frac{\mathrm{d}\boldsymbol{W}}{\mathrm{d}z}(z) + (z^2 - \nu^2)\boldsymbol{W}(z) = \frac{4\,(z/2)^{\nu+1}}{\sqrt{\pi}\,\Gamma(\nu + 1/2)}, \tag{A.235}$$

where, in general, $\nu \in \mathbb{C}$ is an unrestricted value, and Γ denotes the gamma function (A.40). The general solution of (A.235) is given by

$$\boldsymbol{W}(z) = a\,J_\nu(z) + b\,Y_\nu(z) + \boldsymbol{H}_\nu(z) \qquad (a, b \in \mathbb{C}), \tag{A.236}$$

where $J_\nu(z)$ and $Y_\nu(z)$ are the Bessel and Neumann functions of order ν (cf. Subsection A.2.4), and where $z^{-\nu}\boldsymbol{H}_\nu(z)$ is an entire function of z. The function $\boldsymbol{H}_\nu(z)$ is known as the Struve function of order ν, and is named after the Russian-born German astronomer Karl Hermann Struve (1854–1920), who was part of the famous Struve family of astronomers. It is illustrated in Figure A.8 for real arguments and some integer orders.

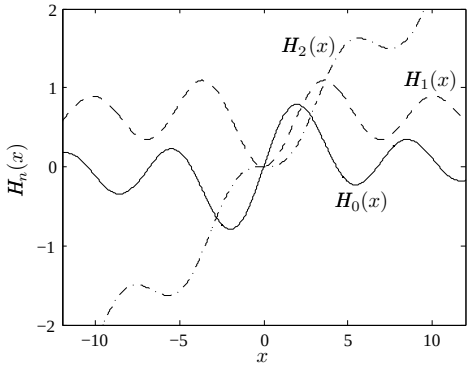

FIGURE A.8. Struve function $\boldsymbol{H}_n(x)$ for real arguments, where $n = 0, 1, 2$.

b) Power series expansion

The Struve function $\boldsymbol{H}_\nu(z)$ admits the power series expansion

$$\boldsymbol{H}_\nu(z) = \left(\frac{z}{2}\right)^{\nu+1} \sum_{m=0}^{\infty} \frac{(-1)^m (z/2)^{2m}}{\Gamma(m + 3/2)\Gamma(m + \nu + 3/2)}. \tag{A.237}$$

By considering n as a positive integer, we have for half integer orders that

$$\boldsymbol{H}_{n+1/2}(z) = Y_{n+1/2}(z) + \frac{1}{\pi} \sum_{m=0}^{n} \frac{\Gamma(m + 1/2)}{\Gamma(n - m + 1)} \left(\frac{z}{2}\right)^{-2m+n-1/2}. \tag{A.238}$$

Particular power series expansions are

$$\boldsymbol{H}_0(z) = \frac{2}{\pi}\left\{z - \frac{z^3}{1^2\cdot 3^2} + \frac{z^5}{1^2\cdot 3^2\cdot 5^2} - \dots\right\}, \tag{A.239}$$

and

$$\boldsymbol{H}_1(z) = \frac{2}{\pi}\left\{\frac{z^2}{1^2\cdot 3} - \frac{z^4}{1^2\cdot 3^2\cdot 5} + \frac{z^6}{1^2\cdot 3^2\cdot 5^2\cdot 7} - \dots\right\}. \tag{A.240}$$

c) Integral representations

If $\mathfrak{Re}\,\nu > -1/2$, then the Struve function $\boldsymbol{H}_\nu(z)$ has the integral representation

$$\boldsymbol{H}_\nu(z) = \frac{2\,(z/2)^\nu}{\sqrt{\pi}\,\Gamma(\nu+1/2)}\int_0^1 (1-t^2)^{\nu-1/2}\sin(zt)\,\mathrm{d}t. \tag{A.241}$$

Under the same condition, it admits also the integral representations

$$\boldsymbol{H}_\nu(z) = \frac{2\,(z/2)^\nu}{\sqrt{\pi}\,\Gamma(\nu+1/2)}\int_0^{\pi/2} \sin(z\cos\theta)\sin^{2\nu}\theta\,\mathrm{d}\theta, \tag{A.242}$$

and, for $|\arg z| < \pi/2$, also

$$\boldsymbol{H}_\nu(z) = Y_\nu(z) + \frac{2\,(z/2)^\nu}{\sqrt{\pi}\,\Gamma(\nu+1/2)}\int_0^\infty e^{-zt}(1+t^2)^{\nu-1/2}\,\mathrm{d}t. \tag{A.243}$$

In particular, it holds that

$$\boldsymbol{H}_0(z) = \frac{1}{\pi}\int_0^\pi \sin(z\sin\theta)\,\mathrm{d}\theta = \frac{2}{\pi}\int_0^{\pi/2}\sin(z\cos\theta)\,\mathrm{d}\theta, \tag{A.244}$$

and

$$\boldsymbol{H}_1(z) = \frac{z}{\pi}\int_0^\pi \sin(z\sin\theta)\cos^2\theta\,\mathrm{d}\theta = \frac{2z}{\pi}\int_0^{\pi/2}\sin(z\cos\theta)\sin^2\theta\,\mathrm{d}\theta. \tag{A.245}$$

d) Recurrence relations

The Struve function $\boldsymbol{H}_\nu(z)$ satisfies the recurrence relations

$$\boldsymbol{H}_{\nu-1}(z) + \boldsymbol{H}_{\nu+1}(z) = \frac{2\nu}{z}\boldsymbol{H}_\nu(z) + \frac{(z/2)^\nu}{\sqrt{\pi}\,\Gamma(\nu+3/2)}, \tag{A.246}$$

$$\boldsymbol{H}_{\nu-1}(z) - \boldsymbol{H}_{\nu+1}(z) = 2\,\frac{\mathrm{d}\boldsymbol{H}_\nu}{\mathrm{d}z}(z) - \frac{(z/2)^\nu}{\sqrt{\pi}\,\Gamma(\nu+3/2)}, \tag{A.247}$$

$$\frac{\mathrm{d}\boldsymbol{H}_0}{\mathrm{d}z}(z) = \frac{2}{\pi} - \boldsymbol{H}_1(z) = \boldsymbol{H}_{-1}(z). \tag{A.248}$$

For the derivatives it also holds that

$$\frac{\mathrm{d}}{\mathrm{d}z}\big\{z^\nu \boldsymbol{H}_\nu(z)\big\} = z^\nu \boldsymbol{H}_{\nu-1}(z), \tag{A.249}$$

$$\frac{\mathrm{d}}{\mathrm{d}z}\big\{z^{-\nu} \boldsymbol{H}_\nu(z)\big\} = \frac{1}{\sqrt{\pi}\,2^\nu\Gamma(\nu+3/2)} - z^{-\nu}\boldsymbol{H}_{\nu+1}(z). \tag{A.250}$$

e) Special properties

For an integer $n \geq 0$ holds

$$\boldsymbol{H}_{-n-1/2}(z) = (-1)^n J_{n+1/2}(z). \tag{A.251}$$

Special values are

$$\boldsymbol{H}_{1/2}(z) = \sqrt{\frac{2}{\pi z}}\,(1 - \cos z), \tag{A.252}$$

$$\boldsymbol{H}_{3/2}(z) = \sqrt{\frac{z}{2\pi}}\left(1 + \frac{2}{z^2}\right) - \sqrt{\frac{2}{\pi z}}\left(\sin z + \frac{\cos z}{z}\right). \tag{A.253}$$

Struve functions can be be also expanded in terms of Bessel functions according to

$$\boldsymbol{H}_0(z) = \frac{4}{\pi}\sum_{m=0}^{\infty}\frac{J_{2m+1}(z)}{2m+1}, \tag{A.254}$$

$$\boldsymbol{H}_1(z) = \frac{2}{\pi} - \frac{2}{\pi}J_0(z) + \frac{4}{\pi}\sum_{m=1}^{\infty}\frac{J_{2m}(z)}{4m^2-1}. \tag{A.255}$$

f) Integrals

The Struve function $\boldsymbol{H}_0(z)$ satisfies

$$\int_z^{\infty} t^{-1}\boldsymbol{H}_0(t)\,\mathrm{d}t = \frac{\pi}{2} - \frac{2}{\pi}\left\{z - \frac{z^3}{1^2\cdot 3^2\cdot 3} + \frac{z^5}{1^2\cdot 3^2\cdot 5^2\cdot 5} - \ldots\right\}, \tag{A.256}$$

and in particular

$$\int_0^{\infty} t^{-1}\boldsymbol{H}_0(t)\,\mathrm{d}t = \frac{\pi}{2}. \tag{A.257}$$

Its primitive is given by

$$\int_0^{z} \boldsymbol{H}_0(t)\,\mathrm{d}t = \frac{\pi}{2}\left\{\frac{z^2}{2} - \frac{z^4}{1^2\cdot 3^2\cdot 4} + \frac{z^6}{1^2\cdot 3^2\cdot 5^2\cdot 6} - \ldots\right\}. \tag{A.258}$$

We have also that

$$\int_z^{\infty} t^{-2}\boldsymbol{H}_1(t)\,\mathrm{d}t = \frac{1}{2z}\boldsymbol{H}_1(t) + \frac{1}{2}\int_z^{\infty} t^{-1}\boldsymbol{H}_0(t)\,\mathrm{d}t. \tag{A.259}$$

For higher orders we have

$$\int_0^{z} t^{-\nu}\boldsymbol{H}_{\nu+1}(t)\,\mathrm{d}t = \frac{z}{\sqrt{\pi}\,2^{\nu}\Gamma(\nu+3/2)} - z^{-\nu}\boldsymbol{H}_{\nu}(z). \tag{A.260}$$

If $|\mathfrak{Re}\,\mu| < 1$ and $\mathfrak{Re}\,\nu > \mathfrak{Re}\,\mu - 3/2$, then

$$\int_0^{\infty} t^{\mu-\nu-1}\boldsymbol{H}_{\nu}(t)\,\mathrm{d}t = \frac{\Gamma(\mu/2)\,2^{\mu-\nu-1}\tan(\mu\pi/2)}{\Gamma(\nu-\mu/2+1)}. \tag{A.261}$$

If $\mathfrak{Re}\,\nu > -1/2$, then we have also that

$$\int_0^z t^{\nu+1}\boldsymbol{H}_{\nu+1}(t)\,\mathrm{d}t = (2\nu+1)\int_0^z t^{\nu}\boldsymbol{H}_{\nu}(t)\,\mathrm{d}t - z^{\nu+1}\boldsymbol{H}_{\nu}(t) + \frac{z^{2\nu+2}}{(\nu+1)\,2^{\nu+1}\sqrt{\pi}\,\Gamma(\nu+3/2)}. \tag{A.262}$$

g) Asymptotic expansions for large arguments

The Struve functions behave asymptotically for large arguments, as $|z| \to \infty$ and considering $|\arg z| < \pi$, as

$$\boldsymbol{H}_{\nu}(z) - Y_{\nu}(z) = \frac{1}{\pi}\sum_{m=0}^{n-1}\frac{\Gamma(n+1/2)}{\Gamma(\nu-m+1/2)}\left(\frac{2}{z}\right)^{\nu-2m-1} + R_n, \tag{A.263}$$

where $R_n = \mathcal{O}\big(|z|^{\nu-2n-1}\big)$. If ν is real, z positive, and $n+1/2-\nu \geq 0$, then the remainder after n terms is of the same sign and numerically less than the first term neglected. In particular, for $|\arg z| < \pi$, it holds that

$$\boldsymbol{H}_0(z) - Y_0(z) \sim \frac{2}{\pi}\left\{\frac{1}{z} - \frac{1}{z^3} + \frac{1^2\cdot 3^2}{z^5} - \frac{1^2\cdot 3^2\cdot 5^2}{z^7} + \ldots\right\}, \tag{A.264}$$

and

$$\boldsymbol{H}_1(z) - Y_1(z) \sim \frac{2}{\pi}\left\{1 + \frac{1}{z^2} - \frac{1^2\cdot 3}{z^4} + \frac{1^2\cdot 3^2\cdot 5}{z^6} - \ldots\right\}. \tag{A.265}$$

For primitives of $\boldsymbol{H}_0(z)$ we have also, for $|\arg z| < \pi$, that

$$\int_0^z \big\{\boldsymbol{H}_0(t) - Y_0(t)\big\}\,\mathrm{d}t - \frac{2}{\pi}\big\{\ln(2z) + \gamma\big\} \sim \frac{2}{\pi}\sum_{m=1}^{\infty}\frac{(-1)^{m+1}(2m)!(2m-1)!}{(m!)^2(2z)^{2m}}, \tag{A.266}$$

and

$$\int_z^{\infty} t^{-1}\big\{\boldsymbol{H}_0(t) - Y_0(t)\big\}\,\mathrm{d}t \sim \frac{2}{\pi z}\sum_{m=0}^{\infty}\frac{(-1)^m\{(2m)!\}^2}{(m!)^2(2m+1)(2z)^{2m}}, \tag{A.267}$$

where γ denotes Euler's constant (A.43).

A.2.8 Legendre functions

a) Differential equation and definition

Legendre functions are special functions that appear in many mathematical and physical situations. They receive their name from the French mathematician Adrien-Marie Legendre (1752–1833). Some references for them are Abramowitz & Stegun (1972), Arfken & Weber (2005), Courant & Hilbert (1966), Erdélyi (1953), Jackson (1999), Jahnke & Emde (1945), Magnus & Oberhettinger (1954), and Morse & Feshbach (1953), and likewise Spiegel & Liu (1999), Sommerfeld (1949), and Weisstein (2002). We use the convention $z = x + iy$, where x, y are reals, and in particular, x always means a real number in the interval $-1 \leq x \leq 1$ with $\cos\theta = x$, where θ is likewise a real number. We consider also $\nu \in \mathbb{C}$ unrestricted and n a positive integer or zero.

Legendre functions of degree ν are the solutions of the Legendre differential equation

$$(1-z^2)\frac{\mathrm{d}^2P}{\mathrm{d}z^2}(z) - 2z\frac{\mathrm{d}P}{\mathrm{d}z}(z) + \nu(\nu+1)P(z) = 0, \tag{A.268}$$

which can be also rewritten as

$$\frac{\mathrm{d}}{\mathrm{d}z}\left\{(1-z^2)\frac{\mathrm{d}P}{\mathrm{d}z}(z)\right\} + \nu(\nu+1)P(z) = 0. \tag{A.269}$$

The Legendre differential equation has nonessential singularities at $z = 1$, -1, and ∞. Since the Legendre differential equation is a second-order ordinary differential equation, it has two linearly independent solutions. A solution $P_\nu(z)$, which is regular at finite points, is called a Legendre function of the first kind, while a solution $Q_\nu(z)$, which is singular at the points $z = \pm 1$, is called a Legendre function of the second kind.

For an integer degree $\nu = n$ ($n = 0, 1, 2, \ldots$), the Legendre function of the first kind reduces to a polynomial $P_n(z)$, known as the Legendre polynomial. It is a polynomial of n-th degree, and can be represented by the Rodrigues formula

$$P_n(z) = \frac{1}{2^n n!}\frac{\mathrm{d}^n}{\mathrm{d}z^n}\left\{(z^2-1)^n\right\}, \tag{A.270}$$

which is named after the French banker, mathematician, and social reformer Benjamin Olinde Rodrigues (1795–1851).

In a similar way, for an integer degree $\nu = n$ ($n \in \mathbb{N}_0$) and for all z that do not lie on the real line segment $[-1, 1]$, we can represent the Legendre function of the second kind by

$$Q_n(z) = \frac{1}{2^n n!}\frac{\mathrm{d}^n}{\mathrm{d}z^n}\left\{(z^2-1)^n \ln\left(\frac{z+1}{z-1}\right)\right\} - \frac{1}{2}P_n(z)\ln\left(\frac{z+1}{z-1}\right), \tag{A.271}$$

which can be rewritten as

$$Q_n(z) = \frac{1}{2}P_n(z)\ln\left(\frac{z+1}{z-1}\right) - W_{n-1}(z), \tag{A.272}$$

where

$$W_{n-1}(z) = \sum_{m=1}^{n}\frac{1}{m}P_{m-1}(z)P_{n-m}(z), \qquad n \geq 1, \tag{A.273}$$

$$W_{-1}(z) = 0. \tag{A.274}$$

The function $Q_n(z)$ is single-valued and has a branch cut on the real axis between the branch points -1 and $+1$. Values of $Q_n(z)$ on the cut line are customarily assigned by the relation

$$Q_n(x) = \frac{1}{2}\big\{Q_n(x+i0) + Q_n(x-i0)\big\}, \qquad -1 < x < 1, \tag{A.275}$$

where the arithmetic average approaches from both the positive imaginary side and the negative imaginary side. Thus, in formulae like (A.271) and (A.272) we have only to replace

$$\ln\left(\frac{z+1}{z-1}\right) \quad \text{by} \quad \ln\left(\frac{1+x}{1-x}\right) \tag{A.276}$$

to obtain valid expressions that hold on the cut line $-1 < x < 1$. For example, (A.272) has to be replaced in this case by

$$Q_n(x) = \frac{1}{2} P_n(x) \ln\left(\frac{1+x}{1-x}\right) - W_{n-1}(x) \qquad -1 < x < 1. \tag{A.277}$$

For a non-integer degree ν, the Legendre function of the first kind P_ν can be defined by means of the Schläfli integral

$$P_\nu(z) = \frac{1}{2\pi i} \oint_C \frac{(t^2-1)^\nu}{2^\nu (t-z)^{\nu+1}} \, \mathrm{d}t, \tag{A.278}$$

where C is a simple complex integration contour around the points $t = z$ and $t = 1$, but not crossing the cut line -1 to $-\infty$. This integral is named after the Swiss mathematician Ludwig Schläfli (1814–1895), who among other important contributions gave the integral representations of the Bessel and gamma functions.

The Legendre function of the second kind Q_ν, for a non-integer degree ν, is obtained from the Schläfli integral, and defined by

$$Q_\nu(z) = \frac{-1}{4i \sin(\nu\pi)} \oint_D \frac{(t^2-1)^\nu}{2^\nu (z-t)^{\nu+1}} \, \mathrm{d}t, \qquad \nu \notin \mathbb{Z}, \tag{A.279}$$

where the integration contour D has the form of a figure eight and it does not enclose the point $t = z$. Furthermore, we have that $\arg(t^2-1) = 0$ on the intersection of the integration contour D with the positive real axis at the right of $t = 1$. The function Q_ν thus obtained is regular and single-valued in the complex z-plane which has been cut along the real axis from $+1$ to $-\infty$. In case that the real part of $\nu + 1$ is positive, we can contract the path of integration and write (A.279) as

$$Q_\nu(z) = \frac{1}{2^{\nu+1}} \int_{-1}^{1} \frac{(1-t^2)^\nu}{(z-t)^{\nu+1}} \, \mathrm{d}t, \tag{A.280}$$

being this formula now applicable for nonnegative integral ν also.

b) Properties on the complex plane

The Legendre functions P_ν satisfy, for all $z \in \mathbb{C}$ and for unrestricted degree ν, the recurrence relations

$$(2\nu+1) z P_\nu(z) = (\nu+1) P_{\nu+1}(z) + \nu P_{\nu-1}(z), \tag{A.281}$$

$$(2\nu+1) P_\nu(z) = \frac{\mathrm{d}P_{\nu+1}}{\mathrm{d}z}(z) - \frac{\mathrm{d}P_{\nu-1}}{\mathrm{d}z}(z), \tag{A.282}$$

$$(\nu+1) P_\nu(z) = \frac{\mathrm{d}P_{\nu+1}}{\mathrm{d}z}(z) - z\frac{\mathrm{d}P_\nu}{\mathrm{d}z}(z), \tag{A.283}$$

$$\nu P_\nu(z) = z\frac{\mathrm{d}P_\nu}{\mathrm{d}z}(z) - \frac{\mathrm{d}P_{\nu-1}}{\mathrm{d}z}(z), \tag{A.284}$$

$$(z^2-1)\frac{\mathrm{d}P_\nu}{\mathrm{d}z}(z) = \nu z P_\nu(z) - \nu P_{\nu-1}(z), \tag{A.285}$$

$$(z^2-1)\frac{\mathrm{d}P_\nu}{\mathrm{d}z}(z) = (\nu+1) P_{\nu+1}(z) - (\nu-1) z P_\nu(z), \tag{A.286}$$

which hold also for Q_ν and for any linear combination of P_ν and Q_ν. In particular, they hold also on the cut line $-1 < x < 1$. With respect to the degree ν we have the identities

$$P_\nu(z) = P_{-\nu-1}(z), \tag{A.287}$$

$$Q_\nu(z) = Q_{-\nu-1}(z). \tag{A.288}$$

c) Properties on the cut line

On the cut line $-1 < x < 1$ and for an integer degree n, the Legendre polynomials P_n satisfy the recurrence relations

$$(2n+1)xP_n(x) = (n+1)P_{n+1}(x) + nP_{n-1}(x), \tag{A.289}$$

$$(2n+1)P_n(x) = \frac{\mathrm{d}P_{n+1}}{\mathrm{d}x}(x) - \frac{\mathrm{d}P_{n-1}}{\mathrm{d}x}(x), \tag{A.290}$$

$$(n+1)P_n(x) = \frac{\mathrm{d}P_{n+1}}{\mathrm{d}x}(x) - x\frac{\mathrm{d}P_n}{\mathrm{d}x}(x), \tag{A.291}$$

$$nP_n(x) = x\frac{\mathrm{d}P_n}{\mathrm{d}x}(x) - \frac{\mathrm{d}P_{n-1}}{\mathrm{d}x}(x), \tag{A.292}$$

$$(x^2-1)\frac{\mathrm{d}P_n}{\mathrm{d}x}(x) = nxP_n(x) - nP_{n-1}(x), \tag{A.293}$$

$$(x^2-1)\frac{\mathrm{d}P_n}{\mathrm{d}x}(x) = (n+1)P_{n+1}(x) - (n-1)xP_n(x), \tag{A.294}$$

which holds also for Q_n and for any linear combination of P_n and Q_n. The Legendre functions P_n and Q_n on the cut line are represented graphically in Figure A.9 for some integer orders. We have similarly for negative arguments that

$$P_n(-x) = (-1)^n P_n(x), \tag{A.295}$$

$$Q_n(-x) = (-1)^{n+1} Q_n(x). \tag{A.296}$$

With respect to the degree n we have the identities

$$P_n(x) = P_{-n-1}(x), \tag{A.297}$$

$$Q_n(x) = Q_{-n-1}(x). \tag{A.298}$$

A generating function for the Legendre polynomials is given by

$$\frac{1}{\sqrt{1-2tx+t^2}} = \sum_{n=0}^{\infty} P_n(x)t^n, \qquad |t| < 1. \tag{A.299}$$

Another generating function is given by

$$e^{tx} J_0\Big(t\sqrt{1-x^2}\Big) = \sum_{n=0}^{\infty} \frac{P_n(x)}{n!}\, t^n, \tag{A.300}$$

where $J_0(x)$ is a zeroth order Bessel function of the first kind (vid. Subsection A.2.4). Expanding the Rodrigues formula (A.270) yields the sum formula

$$P_n(z) = \frac{1}{2^n} \sum_{m=0}^{[n/2]} \frac{(-1)^m (2n-2m)!}{m!\,(n-m)!\,(n-2m)!}\, z^{n-2m}, \tag{A.301}$$

where $[r]$ denotes the floor function of r, i.e., the highest integer smaller than r. Another sum formula is

$$P_n(z) = \frac{1}{2^n} \sum_{m=0}^{n} \left(\frac{n!}{m!\,(n-m)!} \right)^2 (z-1)^{n-m}(z+1)^m. \tag{A.302}$$

The Legendre polynomials are orthogonal in the interval $[-1, 1]$, and satisfy the relation

$$\int_{-1}^{1} P_n(x) P_m(x)\,\mathrm{d}x = \frac{2}{2n+1}\,\delta_{nm}, \tag{A.303}$$

where δ_{nm} denotes the delta of Kronecker,

$$\delta_{nm} = \begin{cases} 1 & \text{if } n = m, \\ 0 & \text{if } n \neq m, \end{cases} \tag{A.304}$$

named after the German mathematician and logician Leopold Kronecker (1823–1891).

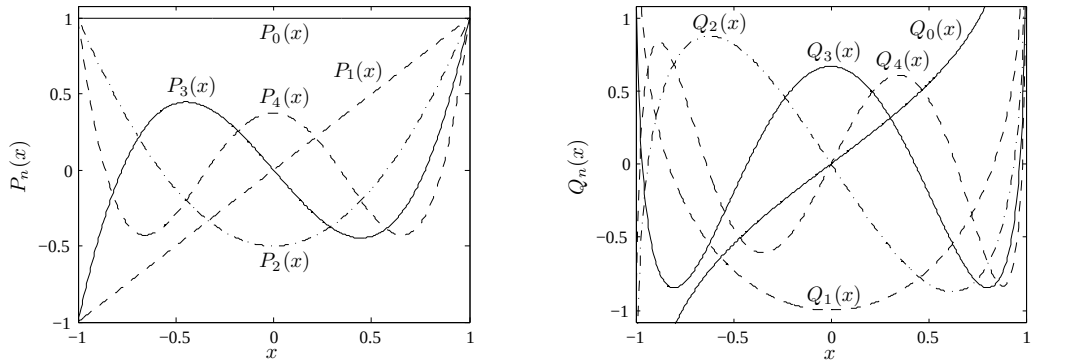

(a) Legendre polynomials $P_n(x)$, $n = 0, 1, 2, 3, 4$ (b) Legendre functions $Q_n(x)$, $n = 0, 1, 2, 3, 4$

FIGURE A.9. Legendre functions on the cut line.

Some special values of the Legendre polynomials P_n are

$$P_n(1) = 1, \tag{A.305}$$

$$P_n(-1) = (-1)^n. \tag{A.306}$$

On the origin it holds that

$$P_n(0) = \begin{cases} (-1)^{n/2}\,\dfrac{1 \cdot 3 \cdot 5 \cdots (n-1)}{2 \cdot 4 \cdot 6 \cdots n} & \text{if } n \text{ even}, \\ 0 & \text{if } n \text{ odd}. \end{cases} \tag{A.307}$$

We have also the bound

$$|P_n(x)| \leq 1, \qquad -1 < x < 1. \tag{A.308}$$

For the Legendre function of the second kind Q_n we have the special values

$$Q_n(1) = \infty, \tag{A.309}$$

$$Q_n(\infty) = 0. \tag{A.310}$$

On the origin it holds that

$$Q_n(0) = \begin{cases} (-1)^{(n+1)/2}\,\dfrac{2\cdot 4\cdot 6\cdots(n-1)}{1\cdot 3\cdot 5\cdot 7\cdots n} & \text{if } n \text{ odd}, \\ 0 & \text{if } n \text{ even}, \end{cases} \tag{A.311}$$

being, in particular, $Q_1(0) = -1$.

d) Explicit expressions

Some explicit expressions of Legendre polynomials, for $0 \leq n \leq 4$ and considering respectively $-1 \leq x \leq 1$ and $\cos\theta = x$, are

$$P_0(x) = 1, \qquad P_0(\cos\theta) = 1, \tag{A.312}$$

$$P_1(x) = x, \qquad P_1(\cos\theta) = \cos\theta, \tag{A.313}$$

$$P_2(x) = \frac{1}{2}(3x^2 - 1), \qquad P_2(\cos\theta) = \frac{1}{2}(3\cos^2\theta - 1), \tag{A.314}$$

$$P_3(x) = \frac{1}{2}(5x^3 - 3x), \qquad P_3(\cos\theta) = \frac{1}{2}\cos\theta(5\cos^2\theta - 3), \tag{A.315}$$

$$P_4(x) = \frac{1}{8}(35x^4 - 30x^2 + 3), \quad P_4(\cos\theta) = \frac{1}{8}(35\cos^4\theta - 30\cos^2\theta + 3). \tag{A.316}$$

For the Legendre functions of the second kind, when considering the values on the branch cut $-1 < x < 1$, we have the expressions

$$Q_0(x) = \frac{1}{2}\ln\left(\frac{1+x}{1-x}\right), \tag{A.317}$$

$$Q_1(x) = \frac{x}{2}\ln\left(\frac{1+x}{1-x}\right) - 1, \tag{A.318}$$

$$Q_2(x) = \frac{1}{4}(3x^2 - 1)\ln\left(\frac{1+x}{1-x}\right) - \frac{3x}{2}, \tag{A.319}$$

$$Q_3(x) = \frac{1}{4}(5x^3 - 3x)\ln\left(\frac{1+x}{1-x}\right) - \frac{5x^2}{2} + \frac{2}{3}, \tag{A.320}$$

$$Q_4(x) = \frac{1}{16}(35x^4 - 30x^2 + 3)\ln\left(\frac{1+x}{1-x}\right) - \frac{35x^3}{8} + \frac{55x}{24}. \tag{A.321}$$

We remark that formulae (A.312)–(A.316) can be extended straightforwardly from x to $z \in \mathbb{C}$. To extend formulae (A.317)–(A.321) in such a way, though, we have to consider the replacement done in (A.276).

A.2.9 Associated Legendre functions

a) Differential equation and definition

The associated Legendre functions or Legendre functions of higher order are special functions that can be regarded as a generalization of the Legendre functions (vid. Subsection A.2.8). They are also important for many mathematical and physical situations. Some

references for them are Abramowitz & Stegun (1972), Arfken & Weber (2005), Courant & Hilbert (1966), Erdélyi (1953), Jackson (1999), Jahnke & Emde (1945), Magnus & Oberhettinger (1954), Morse & Feshbach (1953), Sommerfeld (1949), Spiegel & Liu (1999), and Weisstein (2002). We use the convention $z = x + iy$, where x, y are reals, and in particular, x always means a real number in the interval $-1 \leq x \leq 1$ with $\cos\theta = x$, where θ is likewise a real number. We consider also $\nu, \mu \in \mathbb{C}$ unrestricted and n, m positive integers or zero. We follow mainly the notation of Abramowitz & Stegun (1972), Jackson (1999), and Magnus & Oberhettinger (1954).

Associated Legendre functions of degree ν and order μ are the solutions of the associated Legendre differential equation

$$(1-z^2)\frac{\mathrm{d}^2P}{\mathrm{d}z^2}(z) - 2z\frac{\mathrm{d}P}{\mathrm{d}z}(z) + \left(\nu(\nu+1) + \frac{\mu^2}{1-z^2}\right)P(z) = 0, \tag{A.322}$$

which can be rewritten as

$$\frac{\mathrm{d}}{\mathrm{d}z}\left\{(1-z^2)\frac{\mathrm{d}P}{\mathrm{d}z}(z)\right\} + \left(\nu(\nu+1) + \frac{\mu^2}{1-z^2}\right)P(z) = 0. \tag{A.323}$$

The associated Legendre differential equation has nonessential singularities at $z = 1$, -1 and ∞, which are ordinary branch points. Since the associated Legendre differential equation is a second-order ordinary differential equation, it has two linearly independent solutions. A solution $P_\nu^\mu(z)$, which is regular at finite points, is called an associated Legendre function of the first kind, while a solution $Q_\nu^\mu(z)$, which is singular at the points $z = \pm 1$, is called an associated Legendre function of the second kind.

For integer degree $\nu = n$ ($n \in \mathbb{N}_0$), integer order $\mu = m$ ($m \in \mathbb{N}_0$), and for all z that do not lie on the real line segment $[-1, 1]$, we can represent the associated Legendre functions of the first and second kind by the Rodrigues' formulae

$$P_n^m(z) = (z^2-1)^{m/2}\frac{\mathrm{d}^m}{\mathrm{d}z^m}P_n(z) = \frac{(z^2-1)^{m/2}}{2^n n!}\,\frac{\mathrm{d}^{m+n}}{\mathrm{d}z^{m+n}}\left\{(z^2-1)^n\right\}, \tag{A.324}$$

and

$$Q_n^m(z) = (z^2-1)^{m/2}\frac{\mathrm{d}^m}{\mathrm{d}z^m}Q_n(z), \tag{A.325}$$

where $P_n(z)$ and $Q_n(z)$ denote respectively the Legendre functions of the first and second kind. Both functions, $P_n^m(z)$ and $Q_n^m(z)$, are single-valued and have a branch cut on the real axis between the branch points -1 and $+1$. The appearing square roots have to be considered in such a way that

$$(z^2-1)^{m/2} = (z-1)^{m/2}(z+1)^{m/2}, \tag{A.326}$$

where

$$|\arg(z \pm 1)| < \pi, \qquad |\arg(z)| < \pi. \tag{A.327}$$

The values of $P_n^m(z)$ and $Q_n^m(z)$ on the cut line $-1 < x < 1$ are customarily assigned by the relations

$$P_n^m(x) = \frac{1}{2}\left\{e^{i\pi m/2}P_n^m(x+i0) + e^{-i\pi m/2}P_n(x-i0)\right\}, \tag{A.328}$$

and

$$Q_n^m(x) = \frac{1}{2} e^{-i\pi m} \left\{ e^{-i\pi m/2} Q_n^m(x + i0) + e^{i\pi m/2} Q_n(x - i0) \right\}. \tag{A.329}$$

These formulae are obtained through the replacement of $z - 1$ by $(1 - x)e^{\pm i\pi}$, $(z^2 - 1)$ by $(1 - x^2)e^{\pm i\pi}$, and $z + 1$ by $1 + x$, for $z = x \pm i0$. Thus, on the cut line $-1 < x < 1$, formulae (A.324) and (A.325) have to be taken as

$$P_n^m(x) = (-1)^m (1 - x^2)^{m/2} \frac{\mathrm{d}^m}{\mathrm{d}x^m} P_n(x), \tag{A.330}$$

and

$$Q_n^m(x) = (-1)^m (1 - x^2)^{m/2} \frac{\mathrm{d}^m}{\mathrm{d}x^m} Q_n(x). \tag{A.331}$$

We remark that some authors define the associated Legendre functions on the cut line omitting the factor $(-1)^m$.

Further extensions of the associated Legendre functions for a complex degree ν or a complex order μ can be performed by adapting the Schläfli integrals (A.278) and (A.279). They can be also expressed in terms of hypergeometric functions.

b) Properties on the complex plane

The associated Legendre functions P_ν^μ satisfy, for all $z \in \mathbb{C}$ outside the cut line $[-1, 1]$, and for unrestricted degree ν and order μ, the recurrence relations

$$(2\nu + 1) z P_\nu^\mu(z) = (\nu - \mu + 1) P_{\nu+1}^\mu(z) + (\nu + \mu) P_{\nu-1}^\mu(z), \tag{A.332}$$

$$(z^2 - 1)^{1/2} P_\nu^{\mu+1}(z) = (\nu - \mu) z P_\nu^\mu(z) - (\nu + \mu) P_{\nu-1}^\mu(z), \tag{A.333}$$

$$(z^2 - 1) \frac{\mathrm{d}P_\nu^\mu}{\mathrm{d}z}(z) = (\nu + \mu)(\nu - \mu + 1)(z^2 - 1)^{1/2} P_\nu^{\mu-1}(z) - \mu z P_\nu^\mu(z), \tag{A.334}$$

$$(z^2 - 1) \frac{\mathrm{d}P_\nu^\mu}{\mathrm{d}z}(z) = \nu z P_\nu^\mu(z) - (\nu + \mu) P_{\nu-1}^\mu(z), \tag{A.335}$$

$$P_{\nu+1}^\mu(z) = P_{\nu-1}^\mu(z) + (2\nu + 1)(z^2 - 1)^{1/2} P_\nu^{\mu-1}(z), \tag{A.336}$$

$$(z^2 - 1)^{1/2} P_\nu^{\mu+1}(z) = (\nu + \mu)(\nu - \mu + 1)(z^2 - 1)^{1/2} P_\nu^{\mu-1}(z) - 2\mu z P_\nu^\mu(z), \tag{A.337}$$

which hold also for Q_ν^μ and for any linear combination of P_ν^μ and Q_ν^μ. They hold also on the cut line $-1 < x < 1$, when we replace

$$(z^2 - 1)^{1/2} \quad \text{by} \quad (1 - x^2)^{1/2}. \tag{A.338}$$

The associated Legendre functions of order zero are simply the Legendre functions, i.e.,

$$P_\nu^0(z) = P_\nu(z), \tag{A.339}$$

$$Q_\nu^0(z) = Q_\nu(z). \tag{A.340}$$

With respect to the degree ν we have the identities

$$P_\nu^\mu(z) = P_{-\nu-1}^\mu(z), \tag{A.341}$$

$$Q_\nu^\mu(z) = Q_{-\nu-1}^\mu(z). \tag{A.342}$$

c) Properties on the cut line

For an integer degree n and an integer order m, the associated Legendre functions P_n^m satisfy, on the cut line $-1 < x < 1$, the recurrence relations

$$(2n+1)xP_n^m(x) = (n-m+1)P_{n+1}^m(x) + (n+m)P_{n-1}^m(x), \tag{A.343}$$

$$\sqrt{1-x^2}P_n^{m+1}(x) = (n-m)xP_n^m(x) - (n+m)P_{n-1}^m(x), \tag{A.344}$$

$$(x^2-1)\frac{\mathrm{d}P_n^m}{\mathrm{d}x}(x) = (n+m)(n-m+1)\sqrt{1-x^2}P_n^{m-1}(x) - mxP_n^m(x), \tag{A.345}$$

$$(x^2-1)\frac{\mathrm{d}P_n^m}{\mathrm{d}x}(x) = nxP_n^m(x) - (n+m)P_{n-1}^m(x), \tag{A.346}$$

$$P_{n+1}^m(x) = P_{n-1}^m(x) + (2n+1)\sqrt{1-x^2}P_n^{m-1}(x), \tag{A.347}$$

$$\sqrt{1-x^2}P_n^{m+1}(x) = (n+m)(n-m+1)\sqrt{1-x^2}P_n^{m-1}(x) - 2mxP_n^m(x), \tag{A.348}$$

which hold also for Q_n^m and for any linear combination of P_n^m and Q_n^m. The associated Legendre functions P_n^m and Q_n^m on the cut line are represented graphically in Figure A.10 for some integer orders. On the cut line, the associated Legendre functions of order zero are again the Legendre functions, i.e.,

$$P_n^0(x) = P_n(x), \tag{A.349}$$

$$Q_n^0(x) = Q_n(x). \tag{A.350}$$

With respect to the integer degree n we have the identities

$$P_n^m(x) = P_{-n-1}^m(x), \tag{A.351}$$

$$Q_n^m(x) = Q_{-n-1}^m(x). \tag{A.352}$$

If the order m is higher than the degree n, then the associated Legendre function of the first kind P_n^m is zero, namely

$$P_n^m(x) = 0, \qquad m > n, \tag{A.353}$$

which does not apply to the function Q_n^m. For negative arguments we have that

$$P_n^m(-x) = (-1)^{n+m}P_n^m(x), \tag{A.354}$$

For a negative order $m \in \{0, 1, \ldots, n\}$ it holds that

$$P_n^{-m}(x) = (-1)^m\frac{(n-m)!}{(n+m)!}P_n^m(x), \tag{A.355}$$

$$Q_n^{-m}(x) = (-1)^m\frac{(n-m)!}{(n+m)!}Q_n^m(x). \tag{A.356}$$

Additional identities are

$$P_n^n(x) = (-1)^n\frac{(2n)!}{2^n n!}(1-x^2)^{n/2}, \tag{A.357}$$

$$P_{n+1}^n(x) = x(2n+1)P_n^n(x), \tag{A.358}$$

$$P_n^{-n}(x) = \frac{1}{2^n n!}(1-x^2)^{n/2}, \tag{A.359}$$

$$P_{n+1}^{-n}(x) = \frac{(-1)^n}{(2n)!} x P_n^n(x). \tag{A.360}$$

A generating function for the associated Legendre functions of the first kind is

$$\frac{(-1)^m (2m)!(1-x^2)^{m/2} t^m}{2^m m!(1-2tx+t^2)^{m+1/2}} = \sum_{n=m}^{\infty} P_n^m(x) t^n, \qquad |t| < 1. \tag{A.361}$$

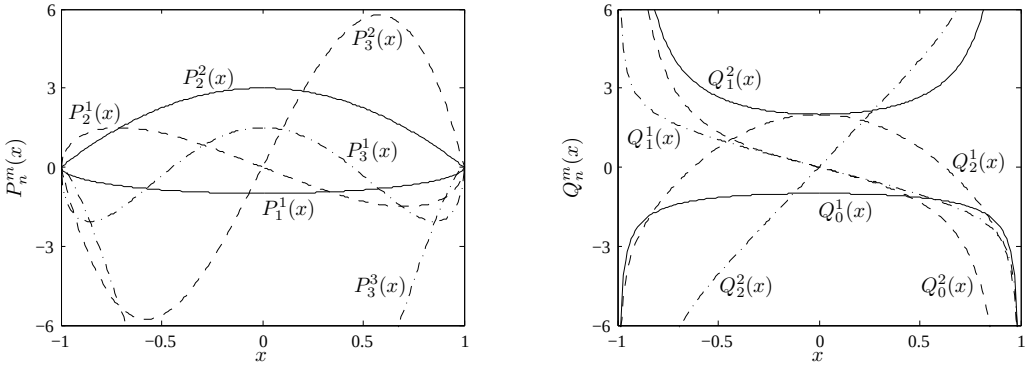

(a) Associated Legendre functions of the first kind $P_n^m(x)$, for $1 \leq n \leq 3$ and $1 \leq m \leq n$

(b) Associated Legendre functions of the second kind $Q_n^m(x)$, for $0 \leq n \leq 2$ and $m \in \{1, 2\}$

FIGURE A.10. Associated Legendre functions on the cut line.

The associated Legendre functions of the first kind are orthogonal in the interval $[-1, 1]$ with respect to degree, and satisfy the relation

$$\int_{-1}^{1} P_n^m(x) P_l^m(x)\, \mathrm{d}x = \frac{2}{(2n+1)} \frac{(n+m)!}{(n-m)!} \delta_{nl}, \qquad m \in \{0, 1, \ldots, n\}, \tag{A.362}$$

where δ_{nl} denotes the delta of Kronecker. They are also orthogonal in the interval $[-1, 1]$ with respect to order when using the weighting function $(1-x^2)^{-1}$, namely

$$\int_{-1}^{1} \frac{P_n^m(x) P_n^k(x)}{(1-x^2)}\, \mathrm{d}x = \frac{(n+m)!}{m(n-m)!} \delta_{mk}, \qquad m, k \in \{0, 1, \ldots, n\}, \tag{A.363}$$

when m and k are not simultaneously zero.

d) Explicit expressions

Some explicit expressions for associated Legendre functions of the first kind, considering respectively $-1 \leq x \leq 1$ and $\cos\theta = x$, for $1 \leq n \leq 3$ and $1 \leq m \leq n$, are

$$P_1^1(x) = -\sqrt{1-x^2}, \qquad P_1^1(\cos\theta) = -\sin\theta, \tag{A.364}$$

$$P_2^1(x) = -3x\sqrt{1-x^2}, \qquad P_2^1(\cos\theta) = -3\cos\theta\sin\theta, \tag{A.365}$$

$$P_2^2(x) = 3(1-x^2), \qquad P_2^2(\cos\theta) = 3\sin^2\theta, \tag{A.366}$$

$$P_3^1(x) = -\frac{3}{2}(5x^2-1)\sqrt{1-x^2}, \qquad P_3^1(\cos\theta) = -\frac{3}{2}(5\cos^2\theta - 1)\sin\theta, \tag{A.367}$$

$$P_3^2(x) = 15x(1-x^2), \qquad P_3^2(\cos\theta) = 15\cos\theta\sin^2\theta, \tag{A.368}$$

$$P_3^3(x) = -15(1-x^2)^{3/2}, \qquad P_3^3(\cos\theta) = -15\sin^3\theta. \tag{A.369}$$

For the associated Legendre functions of the second kind, considering $0 \leq n \leq 2$ and $m \in \{1, 2\}$, we have that

$$Q_0^1(x) = -\frac{1}{\sqrt{1-x^2}}, \tag{A.370}$$

$$Q_0^2(x) = \frac{2x}{1-x^2}, \tag{A.371}$$

$$Q_1^1(x) = -\frac{1}{2}\sqrt{1-x^2}\ln\left(\frac{1+x}{1-x}\right) - \frac{x}{\sqrt{1-x^2}}, \tag{A.372}$$

$$Q_1^2(x) = \frac{2}{1-x^2}, \tag{A.373}$$

$$Q_2^1(x) = -\frac{3x}{2}\sqrt{1-x^2}\ln\left(\frac{1+x}{1-x}\right) - \frac{3x^2-2}{\sqrt{1-x^2}}, \tag{A.374}$$

$$Q_2^2(x) = \frac{3}{2}(1-x^2)\ln\left(\frac{1+x}{1-x}\right) - \frac{x(3x^2-5)}{1-x^2}. \tag{A.375}$$

We remark that to extend formulae (A.364)–(A.369) from x to $z \in \mathbb{C}$, we have to consider the replacement done in (A.338). For the formulae (A.370)–(A.375), additionally the replacement done in (A.276) has to be taken into account.

A.2.10 Spherical harmonics

a) Differential equation and definition

Spherical harmonics, also known as surface harmonics or tesseral and sectoral harmonics, are special functions that appear when solving Laplace's equation using separation of variables in spherical coordinates. They represent the angular portion of the solution, and are formed by products between trigonometric functions and associated Legendre functions (cf. Subsection A.2.9). The spherical harmonics constitute thus an orthonormal basis over the unit sphere. Some of the references for them are Abramowitz & Stegun (1972), Arfken & Weber (2005), Erdélyi (1953), Jackson (1999), Magnus & Oberhettinger (1954), Nédélec (2001), Sommerfeld (1949), and Weisstein (2002). For the spherical harmonics, we follow mainly the notation of Jackson (1999) and Weisstein (2002).

We consider in $\mathbb{R}^3$ the system of spherical coordinates (r, θ, φ), which is described with the convention normally used in physics, i.e., reversing the roles of θ and φ. Thus, we denote by r the radius ($0 \leq r < \infty$), by θ the polar or colatitudinal coordinate ($0 \leq \theta \leq \pi$), and by φ the azimuthal or longitudinal coordinate ($-\pi < \varphi \leq \pi$), as shown in Figure A.11. The spherical coordinates (r, θ, φ) and the cartesian coordinates (x, y, z) are related through

$$r = \sqrt{x^2+y^2+z^2}, \qquad x = r\sin\theta\cos\varphi, \tag{A.376}$$

$$\theta = \arctan\left(\frac{\sqrt{x^2+y^2}}{z}\right), \qquad y = r\sin\theta\sin\varphi, \tag{A.377}$$

$$\varphi = \arctan\left(\frac{y}{x}\right), \qquad z = r\cos\theta. \tag{A.378}$$

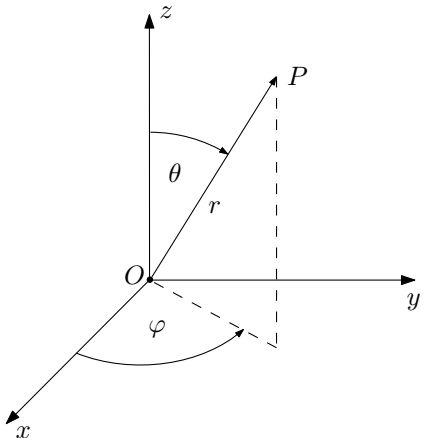

FIGURE A.11. Spherical coordinates.

By considering in $\mathbb{R}^3$ the angular part of Laplace's equation in spherical coordinates, i.e., working on the unit sphere with $r = 1$, we obtain the spherical harmonic differential equation of degree $l = 0, 1, 2, \ldots$, given by

$$\frac{1}{\sin\theta}\frac{\partial}{\partial\theta}\left\{\sin\theta\,\frac{\partial Y}{\partial\theta}(\theta,\varphi)\right\} + \frac{1}{\sin^2\theta}\frac{\partial^2 Y}{\partial\varphi^2}(\theta,\varphi) + l(l+1)Y(\theta,\varphi) = 0. \tag{A.379}$$

The solutions of this differential equation are the spherical harmonics

$$Y_l^m(\theta,\varphi) = \sqrt{\frac{2l+1}{4\pi}\,\frac{(l-m)!}{(l+m)!}}\,P_l^m(\cos\theta)e^{im\varphi}, \tag{A.380}$$

where $m \in \{-l, -(l-1), \ldots, 0, \ldots, (l-1), l\}$ and $P_l^m(x)$ denotes the associated Legendre function of degree l and order m. Some spherical harmonics are illustrated in Figure A.12.

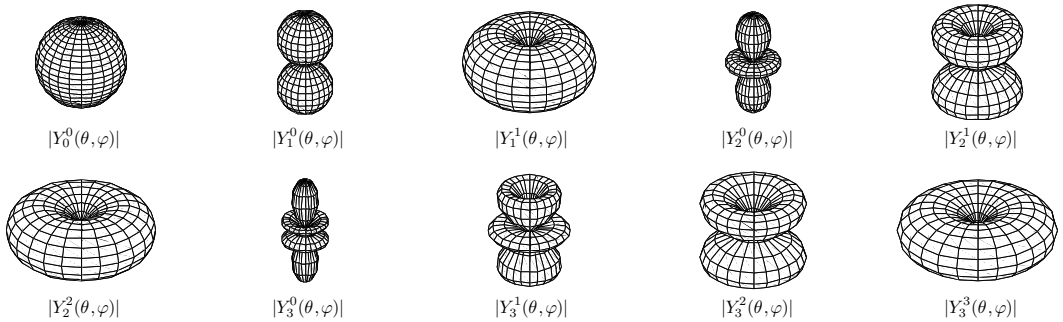

FIGURE A.12. Spherical harmonics in absolute value.

b) Properties

The spherical harmonics form a complete orthogonal set on the surface of the unit sphere in the two indices l, m. Their orthonormality implies that

$$\int_0^{2\pi} \int_0^{\pi} Y_l^m(\theta, \varphi)\, \overline{Y_n^k(\theta, \varphi)} \sin\theta \, \mathrm{d}\theta \, \mathrm{d}\varphi = \delta_{ln}\delta_{mk}, \tag{A.381}$$

where $\overline{z}$ denotes the complex conjugate of z, and δ_{ln} the delta of Kronecker for the coefficients l and n. For a negative order m it holds that

$$Y_l^{-m}(\theta, \varphi) = (-1)^m \overline{Y_l^m(\theta, \varphi)}. \tag{A.382}$$

Spherical harmonics are bounded by

$$|Y_l^m(\theta, \varphi)| \leq \sqrt{\frac{2l+1}{4\pi}}. \tag{A.383}$$

Some particular cases of spherical harmonics are

$$Y_l^l(\theta, \varphi) = \frac{(-1)^l}{2^l l!} \sqrt{\frac{(2l+1)!}{4\pi}}\, \sin^l\theta \, e^{il\varphi}, \tag{A.384}$$

$$Y_l^0(\theta, \varphi) = \sqrt{\frac{2l+1}{4\pi}}\, P_l(\cos\theta), \tag{A.385}$$

$$Y_l^{-l}(\theta, \varphi) = \frac{1}{2^l l!} \sqrt{\frac{(2l+1)!}{4\pi}}\, \sin^l\theta \, e^{-il\varphi}, \tag{A.386}$$

where $P_l(x)$ denotes the Legendre polynomial of degree l.

c) Addition theorem

We consider two different directions (θ_1, φ_1) and (θ_2, φ_2) in the spherical coordinate system on the unit sphere, which are separated by an angle β, as shown in Figure A.13. These angles satisfy the trigonometric identity

$$\cos\beta = \cos\theta_1 \cos\theta_2 + \sin\theta_1 \sin\theta_2 \cos(\varphi_1 - \varphi_2). \tag{A.387}$$

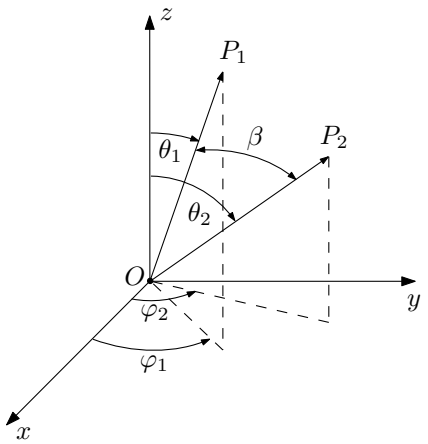

FIGURE A.13. Angles for the addition theorem of spherical harmonics.

The addition theorem for spherical harmonics asserts that

$$P_n(\cos\beta) = \frac{4\pi}{2n+1} \sum_{m=-n}^{n} (-1)^m Y_n^m(\theta_1,\varphi_1)\, Y_n^{-m}(\theta_2,\varphi_2), \tag{A.388}$$

or, equivalently,

$$P_n(\cos\beta) = \frac{4\pi}{2n+1} \sum_{m=-n}^{n} Y_n^m(\theta_1,\varphi_1)\, \overline{Y_n^m(\theta_2,\varphi_2)}. \tag{A.389}$$

In terms of the associated Legendre functions the addition theorem is

$$\begin{aligned} P_n(\cos\beta) &= P_n(\cos\theta_1) P_n(\cos\theta_2) \\ &\quad + 2\sum_{m=1}^{n} \frac{(n-m)!}{(n+m)!} P_n^m(\cos\theta_1) P_n^m(\cos\theta_2) \cos\big(m(\varphi_1-\varphi_2)\big), \end{aligned} \tag{A.390}$$

being the expression (A.387) the particular case of the theorem when $n = 1$.

d) Explicit expressions

Some explicit expressions of spherical harmonics are

$$Y_0^0(\theta,\varphi) = \frac{1}{\sqrt{4\pi}}, \qquad Y_1^{-1}(\theta,\varphi) = \sqrt{\frac{3}{8\pi}}\, \sin\theta\, e^{-i\varphi}, \tag{A.391}$$

$$Y_1^0(\theta,\varphi) = \sqrt{\frac{3}{4\pi}}\, \cos\theta, \qquad Y_1^1(\theta,\varphi) = -\sqrt{\frac{3}{8\pi}}\, \sin\theta\, e^{i\varphi}, \tag{A.392}$$

$$Y_2^{-2}(\theta,\varphi) = \sqrt{\frac{15}{32\pi}}\, \sin^2\theta\, e^{-2i\varphi}, \qquad Y_2^{-1}(\theta,\varphi) = \sqrt{\frac{15}{8\pi}}\, \sin\theta\cos\theta\, e^{-i\varphi}, \tag{A.393}$$

$$Y_2^0(\theta,\varphi) = \sqrt{\frac{5}{16\pi}}\, (3\cos^2\theta - 1), \qquad Y_2^1(\theta,\varphi) = -\sqrt{\frac{15}{8\pi}}\, \sin\theta\cos\theta\, e^{i\varphi}, \tag{A.394}$$

$$Y_2^2(\theta,\varphi) = \sqrt{\frac{15}{32\pi}}\, \sin^2\theta\, e^{2i\varphi}, \qquad Y_3^{-3}(\theta,\varphi) = \sqrt{\frac{35}{64\pi}}\, \sin^3\theta\, e^{-3i\varphi}, \tag{A.395}$$

$$Y_3^{-2}(\theta,\varphi) = \sqrt{\frac{105}{32\pi}}\, \sin^2\theta\cos\theta\, e^{-2i\varphi}, \tag{A.396}$$

$$Y_3^{-1}(\theta,\varphi) = \sqrt{\frac{21}{64\pi}}\, \sin\theta(5\cos^2\theta - 1)\, e^{-i\varphi}, \tag{A.397}$$

$$Y_3^0(\theta,\varphi) = \sqrt{\frac{7}{16\pi}}\, (5\cos^3\theta - 3\cos\theta), \tag{A.398}$$

$$Y_3^1(\theta,\varphi) = -\sqrt{\frac{21}{64\pi}}\, \sin\theta(5\cos^2\theta - 1)\, e^{i\varphi}, \tag{A.399}$$

$$Y_3^2(\theta,\varphi) = -\sqrt{\frac{105}{32\pi}}\, \sin^2\theta\cos\theta\, e^{2i\varphi}, \tag{A.400}$$

$$Y_3^3(\theta,\varphi) = -\sqrt{\frac{35}{64\pi}}\, \sin^3\theta\, e^{3i\varphi}, \tag{A.401}$$

A.3 Functional analysis

Functional analysis is the branch of mathematics, and specifically of analysis, that is concerned with the study of infinite-dimensional vector spaces (mainly function spaces) and operators acting upon them. It is an essential tool in the proper understanding of all kind of problems in pure and applied mathematics, physics, biology, economics, etc. Functional analysis is particularly useful to state the adequate framework for the existence and uniqueness of the solution of these problems, and to characterize its dependence on different parameters of them. Some classical references are Brezis (1999) and Rudin (1973). Other references are Griffel (1985), Reed & Simon (1980), and Werner (1997).

A.3.1 Normed vector spaces

A vector space is a set E for which the operations of vector addition and scalar multiplication are well defined, i.e., such that the addition of any two elements of E (called vectors) belongs to E, and such that the multiplication of any element of E by a scalar of a field $\mathbb{K}$ (either $\mathbb{C}$ or $\mathbb{R}$) belongs also to E. A normed vector space corresponds to a vector space E that is supplied with a norm, i.e., with an application $\|\cdot\|_E : E \to \mathbb{R}_+$ that fulfills for all $u, v \in E$ and $\alpha \in \mathbb{K}$:

$$\|u\|_E = 0 \quad \Leftrightarrow \quad u = 0_E, \tag{A.402}$$

$$\|\alpha u\|_E = |\alpha| \, \|u\|_E, \tag{A.403}$$

$$\|u + v\|_E \leq \|u\|_E + \|v\|_E, \tag{A.404}$$

where 0_E denotes the null element or zero vector of E. A norm induces a distance on the set E that determines how far apart its elements are between each other. The distance $d(u, v)$ between any two elements $u, v \in E$ is then defined by

$$d(u, v) = \|u - v\|_E. \tag{A.405}$$

A norm characterizes the topology on E and thus the notion of convergence on this set.

a) Banach spaces

A Banach space is essentially a normed vector space that is complete with respect to the metric induced by the norm. It receives its name from the eminent Polish mathematician and university professor Stefan Banach (1892–1945), who was one of the founders of functional analysis. A normed vector space $(E, \|\cdot\|_E)$ is said to be complete if every Cauchy sequence in E has a limit in E. A sequence $\{u_n\} \subset E$ is of Cauchy if for all $\varepsilon > 0$ there exists an integer M such that $\|u_n - u_m\|_E \leq \varepsilon$ for all $n, m \geq M$. In other words, it holds in a Banach space that if the elements of a sequence become closer to each other as the sequence progresses, then the sequence is convergent.

b) Hilbert spaces

A Hilbert space H is a Banach space where the norm is defined by an inner product. It is named after the German mathematician David Hilbert (1862–1943), who is recognized as one of the most influential and universal mathematicians of the 19th and early 20th centuries. A Hilbert space is thus an abstract vector space that has geometric properties.

An inner or scalar product is a positive-definite sesquilinear form $(\cdot,\cdot)_H : H \times H \to \mathbb{K}$, which satisfies for all $u, v, w, x \in H$ and $\alpha, \beta \in \mathbb{K}$:

$$(u,u)_H > 0, \quad u \neq 0_H, \tag{A.406}$$

$$(u,v)_H = \overline{(v,u)_H}, \tag{A.407}$$

$$(u+v, w+x)_H = (u,w)_H + (u,x)_H + (v,w)_H + (v,x)_H, \tag{A.408}$$

$$(\alpha u, \beta v)_H = \alpha\overline{\beta}\,(u,v)_H, \tag{A.409}$$

where $\overline{\beta}$ denotes the complex conjugate of β. The property (A.406) implies the positive-definiteness, whereas the sesquilinearity is given by (A.408) and (A.409). In the case that the underlying field is real, i.e., $\mathbb{K} = \mathbb{R}$, the sesquilinearity turns into bilinearity and the inner product becomes symmetric due (A.407). The induced norm $\|\cdot\|_H$ is defined by

$$\|u\|_H = \sqrt{(u,u)_H} \qquad \forall u \in H, \tag{A.410}$$

and it satisfies the Cauchy-Schwartz inequality

$$|(u,v)_H| \leq \|u\|_H \|v\|_H \qquad \forall u, v \in H. \tag{A.411}$$

A.3.2 Linear operators and dual spaces

Let E and F be two Banach spaces with norms $\|\cdot\|_E$ and $\|\cdot\|_F$, respectively. We define a linear operator as an application $L : E \to F$ that satisfies for all $u, v \in E$ and $\alpha, \beta \in \mathbb{K}$:

$$L(\alpha u + \beta v) = \alpha L(u) + \beta L(v). \tag{A.412}$$

The linear operator L is continuous or bounded if there exists a constant C such that

$$\|L(v)\|_F \leq C\|v\|_E \qquad \forall v \in E. \tag{A.413}$$

We denote in particular by $\mathscr{L}(E,F)$ the space of all linear and continuous operators from E to F, which is also a Banach space when it is supplied with the norm

$$\|L\|_{\mathscr{L}(E,F)} = \sup_{v \neq 0_E} \frac{\|L(v)\|_F}{\|v\|_E} = \sup_{\|v\|_E \leq 1} \|L(v)\|_F = \sup_{\|v\|_E = 1} \|L(v)\|_F. \tag{A.414}$$

It holds therefore that

$$\|L(v)\|_F \leq \|L\|_{\mathscr{L}(E,F)} \|v\|_E \qquad \forall v \in E, \ \ \forall L \in \mathscr{L}(E,F). \tag{A.415}$$

The kernel, nucleus, or nullspace of a linear operator $L \in \mathscr{L}(E,F)$ is defined by

$$\mathcal{N}(L) = \{v \in E : \ L(v) = 0_F\}, \tag{A.416}$$

whereas its image or rang is given by

$$\mathcal{R}(L) = \{w \in F : \ w = L(v), \ \ v \in E\}. \tag{A.417}$$

When $F = E$, then we abbreviate $\mathscr{L}(E,E)$ simply by $\mathscr{L}(E)$.

a) Dual spaces

The dual space E' of a Banach space E corresponds to the space $\mathscr{L}(E,\mathbb{K})$ of all linear and continuous functionals from E to the field $\mathbb{K}$. The dual space E' is also a Banach space

when it is supplied with the norm

$$\|L\|_{E'} = \sup_{v \neq 0_E} \frac{|L(v)|}{\|v\|_E} = \sup_{\|v\|_E \leq 1} |L(v)| = \sup_{\|v\|_E = 1} |L(v)|. \tag{A.418}$$

We denote by $\langle \cdot, \cdot \rangle_{E',E} : E' \times E \to \mathbb{K}$ the scalar duality product between both spaces, which is a bilinear form. If $L \in E'$ is given, then the application $\langle L, \cdot \rangle_{E',E} : E \to \mathbb{K}$ is linear and continuous. For $L \in E'$ and $v \in E$, the notation $\langle L, v \rangle_{E',E}$ is thus equivalent to $L(v)$, but can be also understood as $v(L)$. The duality product, analogously as in (A.415), fulfills

$$|\langle L, v \rangle_{E',E}| \leq \|L\|_{E'} \|v\|_E \qquad \forall v \in E, \ \ \forall L \in E'. \tag{A.419}$$

When the underlying field $\mathbb{K}$ is the set of complex numbers $\mathbb{C}$, then the dual space E' is frequently taken as the space $\mathscr{A}(E, \mathbb{K})$ of all antilinear and continuous functionals from E to the field $\mathbb{K}$. In this case the duality product becomes a sesquilinear form, i.e., a form that is linear in one argument and antilinear in the other. An operator $A \in \mathscr{A}(E, \mathbb{K})$ is said to be antilinear or conjugate linear if for all $u, v \in E$ and $\alpha, \beta \in \mathbb{K}$:

$$A(\alpha u + \beta v) = \overline{\alpha} A(u) + \overline{\beta} A(v). \tag{A.420}$$

The topological properties of linear and antilinear operators are the same, and they differ only on the issue of the complex conjugation. Clearly, if $\mathbb{K} = \mathbb{R}$, then the distinction between linearity and antilinearity disappears, and the sesquilinear forms become bilinear. We remark that the roles of linearity and antilinearity can be assigned at will in the duality product, when consistency is preserved. Duality can be thus understood either in a bilinear or in a sesquilinear sense (and even a biantilinear sense could be also used).

We can also define the bidual, double dual, or second dual space E'' of E, i.e., the dual space of E', which is the space $\mathscr{L}(E', \mathbb{K})$ of all linear and continuous functionals from E' to $\mathbb{K}$. In this case we consider the duality product $\langle \cdot, \cdot \rangle_{E',E''} : E' \times E'' \to \mathbb{K}$, which is again a bilinear (or sesquilinear) form. The space E can be then identified with a subspace of E'' if we use a linear mapping $J : E \to E''$ defined by

$$\langle L, J(v) \rangle_{E',E''} = \langle L, v \rangle_{E',E} \qquad \forall v \in E, \ \ \forall L \in E'. \tag{A.421}$$

The subspace $J(E)$ is closed in E'' and J is an isometry, i.e.,

$$\|J(v)\|_{E''} = \|v\|_E \qquad \forall v \in E. \tag{A.422}$$

Thus J is an isometric isomorphism of E onto a closed subspace of E''. Frequently E is identified with $J(E)$, in which case E is regarded as a subspace of E''. The spaces for which $J(E) = E''$ are called reflexive.

b) Orthogonal vector subspaces

Let E be a Banach space, E' its dual space, and $\langle \cdot, \cdot \rangle_{E',E}$ their duality product. We consider the vector subspaces $M \subset E$ and $N \subset E'$. We define the orthogonal vector space $M^\perp$ of M by

$$M^\perp = \{A \in E' : \langle A, v \rangle_{E',E} = 0 \quad \forall v \in M\}, \tag{A.423}$$

which is a closed vector subspace of E'. In the same way we define the orthogonal vector space $N^{\perp}$ of N by

$$N^{\perp} = \{v \in E : \langle A, v\rangle_{E',E} = 0 \quad \forall A \in N\}, \tag{A.424}$$

which is a closed vector subspace of E. If the duality product between $A \in E'$ and $v \in E$ becomes zero, then both elements can be considered as being in some way orthogonal, similarly as the orthogonality concept for the inner product in Hilbert spaces.

c) Riesz's representation theorem for Hilbert spaces

Every Hilbert space H is reflexive, i.e., it can be naturally identified with its double dual space H''. Furthermore, the Riesz representation theorem (cf., e.g. Brezis 1999), named after the Hungarian mathematician Frigyes Riesz (1880–1956), gives a complete and convenient description of the dual space H' of H, which is itself also a Hilbert space. It states that for each $L \in H'$ there exists a unique $u \in H$ such that

$$\langle L, v\rangle_{H',H} = (u, v)_H \qquad \forall v \in H, \tag{A.425}$$

where

$$\|u\|_H = \|L\|_{H'}. \tag{A.426}$$

This theorem implies that every linear and continuous functional L on H can be represented with the help of the inner product $(\cdot,\cdot)_H$. The application $L \mapsto u$ is an isometric isomorphism that identifies H and H'. We note that this identification is done often, but not always, since the simultaneous identification between a subspace of the Hilbert space and its dual does not work and yields absurd results (cf. Brezis 1999).

A.3.3 Adjoint and compact operators

Let E and F be two Banach spaces, whose dual spaces are given respectively by E' and F'. We define the adjoint operator of a linear operator $T \in \mathscr{L}(E, F)$ as the unique linear operator $T^* \in \mathscr{L}(F', E')$, or antilinear operator $T^* \in \mathscr{A}(F', E')$, that satisfies

$$\langle w, Tv\rangle_{F',F} = \langle T^* w, v\rangle_{E',E} \qquad \forall v \in E, \ \ \forall w \in F', \tag{A.427}$$

depending respectively on whether the duality product is bilinear or sesquilinear. Moreover, and depending again on the type of duality, the adjoint operator T^* is such that

$$\|T\|_{\mathscr{L}(E,F)} = \|T^*\|_{\mathscr{L}(F',E')} \qquad \text{or} \qquad \|T\|_{\mathscr{L}(E,F)} = \|T^*\|_{\mathscr{A}(F',E')}. \tag{A.428}$$

The adjoint operator T^* is thus either linear or antilinear. In finite-dimensional normed vector spaces, the linear operator T can be represented by a matrix and, in this case, its linear adjoint corresponds to its transposed matrix, whereas its antilinear adjoint corresponds to its hermitian matrix, i.e., its transposed and conjugated matrix.

In the case of a Hilbert space H, the adjoint of a linear operator $T \in \mathscr{L}(H)$ is the unique antilinear operator $T^* \in \mathscr{A}(H)$ that satisfies

$$(w, Tv)_H = (T^* w, v)_H \qquad \forall v, w \in H, \tag{A.429}$$

which is also such that

$$\|T\|_{\mathscr{L}(H)} = \|T^*\|_{\mathscr{A}(H)}. \tag{A.430}$$

The following properties hold for $S, T \in \mathscr{L}(H)$ and $\alpha \in \mathbb{K}$:

$$(S+T)^* = S^* + T^*, \qquad (\alpha T)^* = \overline{\alpha}\, T^*, \tag{A.431}$$

$$(ST)^* = T^* S^*, \qquad T^{**} = T. \tag{A.432}$$

A linear operator $T \in \mathscr{L}(E, F)$ is said to be compact if and only if for each bounded sequence $\{u_n\} \subset E$, the sequence $\{Tu_n\} \subset F$ admits a convergent subsequence. A compact operator thus maps bounded sets in E into a relatively compact sets in F, i.e., into sets whose closure is compact in F. It holds that any linear combination of compact operators is compact. Furthermore, the operator T is compact if and only if its adjoint operator $T^* \in \mathscr{L}(F', E')$ is also compact. If G denotes another Banach space, then the composition or product $ST \in \mathscr{L}(E, F)$ of two continuous linear operators $S \in \mathscr{L}(E, G)$ and $T \in \mathscr{L}(G, F)$ is compact if one of the two operators S or T is compact.

A.3.4 Imbeddings

Let E and F be two Banach spaces such that $E \subseteq F$. We say that E is continuously imbedded in F, written as $E \hookrightarrow F$, if E is a vector subspace of F and if the identity operator $I : E \to F$ defined by $I(v) = v$ for all $v \in E$ is continuous, i.e., if there exists a constant C such that

$$\|v\|_F \leq C \|v\|_E \qquad \forall v \in E. \tag{A.433}$$

Moreover, the space E is said to be compactly imbedded in F, written as $E \overset{c}{\hookrightarrow} F$, if E is continuously imbedded in F and if the identity operator $I : E \to F$ is a compact operator, i.e., if each bounded sequence in E admits a convergent subsequence in F.

A.3.5 Lax-Milgram's theorem

Lax-Milgram's theorem gives a sufficient condition to ensure the existence and uniqueness for the solution of a linear problem, which makes it a simple and powerful tool to solve partial differential equations of elliptic type. It was first established and proved by Lax & Milgram (1954) and constitutes a particular case of the projection theorem on convex closed sets in Hilbert spaces (cf., e.g., Brezis 1999).

The theorem is stated as follows. Let H be a Hilbert space and H' its dual space. Let $a : H \times H \to \mathbb{K}$ be a sesquilinear form on H, i.e., such that for all $u, v, w, x \in H$ and for all $\alpha, \beta \in \mathbb{K}$:

$$a(u+v, w+x) = a(u,w) + a(u,x) + a(v,w) + a(v,x), \tag{A.434}$$

$$a(\alpha u, \beta v) = \alpha \overline{\beta}\, a(u,v). \tag{A.435}$$

We suppose that the form $a(\cdot,\cdot)$ is continuous and coercive on $H \times H$, i.e., that there exist some constants $M > 0$ and $\alpha > 0$ such that for all $u, v \in H$:

$$|a(u,v)| \leq M \|u\|_H \|v\|_H, \tag{A.436}$$

$$\mathfrak{Re}\{a(u,u)\} \geq \alpha \|u\|_H^2. \tag{A.437}$$

Then, for any $f \in H'$ there exists a unique solution $u \in H$ such that

$$a(u, v) = \langle f, v \rangle_{H',H} \qquad \forall v \in H. \tag{A.438}$$

Moreover, the solution u depends continuously on f:

$$\|u\|_H \leq \frac{1}{\alpha} \|f\|_{H'}. \tag{A.439}$$

Lax-Milgram's theorem allows thus to state a sufficient condition to solve a linear problem of the form

$$Au = f, \tag{A.440}$$

where $A : H \to H'$ is a continuous linear operator and $f \in H'$. Typically (A.440) represents the differential problem, while (A.438) denotes its variational formulation.

A.3.6 Fredholm's alternative

The alternative of Fredholm is a theorem that characterizes the existence and uniqueness of the solution for a compactly perturbed linear problem. It is named after the Swedish mathematician Erik Ivar Fredholm (1866–1927), who established the modern theory of integral equations. The theorem generalizes the existence and uniqueness of the solution for a linear system in a finite-dimensional space. Some references are Brezis (1999), Colton & Kress (1983), Hsiao & Wendland (2008), and Ramm (2001, 2005).

Fredholm's alternative states that if E is a Banach space and if $T \in \mathscr{L}(E)$ is a compact operator, then

1. $\mathcal{N}(I - T)$ is of finite dimension,
2. $\mathcal{R}(I - T)$ is closed, i.e., $\mathcal{R}(I - T) = \mathcal{N}(I - T^*)^\perp$,
3. $\mathcal{N}(I - T) = \{0_E\} \quad \Leftrightarrow \quad \mathcal{R}(I - T) = E$,
4. $\dim \mathcal{N}(I - T) = \dim \mathcal{N}(I - T^*)$.

When solving an equation of the form $u - Tu = f$, the alternative is thus stated as follows. Either for any $f \in E$ the equation $u - Tu = f$ admits a unique solution $u \in E$ that depends continuously on f; or the homogeneous equation $u - Tu = 0_E$ admits n linearly independent solutions $u_1, u_2, \ldots, u_n \in \mathcal{N}(I-T) \subset E$ and, in this case, the inhomogeneous equation $u - Tu = f$ is solvable (not necessarily uniquely) if and only if f satisfies n orthogonality conditions, i.e., $f \in \mathcal{R}(I - T) = \mathcal{N}(I - T^*)^\perp$, which is of finite dimension.

The importance of Fredholm's alternative lies in the fact that it transforms the existence problem for the solution of the inhomogeneous equation $u - Tu = f$, which is quite difficult, into a uniqueness problem that removes the non-trivial solutions for the homogeneous equation $u - Tu = 0_E$, which is easier to accomplish. In other words, this theorem tells us that a compact perturbation of the identity operator is injective if and only if it is surjective. We remark that the alternative still remains valid when we replace $I - T$ by $S - T$, where $S \in \mathscr{L}(E)$ is a continuous and invertible linear operator whose inverse S^{-1} is also continuous. This stems from the fact that an equation of the form $Su - Tu = f$ can then be readily transformed into the equivalent form $u - S^{-1}Tu = S^{-1}f$, where $S^{-1}T$ is compact since T is compact.

Another way to express Fredholm's alternative is by considering the four operator equations

$$u - Tu = f \qquad \text{in } E, \tag{A.441}$$

$$u - Tu = 0_E \qquad \text{in } E, \tag{A.442}$$

$$w - T^*w = g \qquad \text{in } E', \tag{A.443}$$

$$w - T^*w = 0_{E'} \qquad \text{in } E'. \tag{A.444}$$

If $T \in \mathscr{L}(E)$ is a compact operator, then the following alternative holds. Either (A.442) has only the trivial solution $u = 0_E$, and then (A.444) has only the trivial solution $w = 0_{E'}$, and equations (A.441) and (A.443) are uniquely solvable for any right-hand sides $f \in E$ and $g \in E'$; or (A.442) has exactly n linearly independent solutions u_j, $1 \leq j \leq n$, and then (A.444) has also n linearly independent solutions w_j, $1 \leq j \leq n$, and equations (A.441) and (A.443) are solvable if and only if correspondingly

$$\langle w_j, f\rangle_{E',E} = 0 \quad \text{and} \quad \langle g, u_j\rangle_{E',E} = 0, \quad \text{for all } 1 \leq j \leq n. \tag{A.445}$$

If they are solvable, then their solutions are not unique and their general solutions are, respectively,

$$u = u_p + \sum_{j=1}^{n} \alpha_j u_j \qquad \text{and} \qquad w = w_p + \sum_{j=1}^{n} \beta_j w_j, \tag{A.446}$$

where α_j and β_j are arbitrary scalar constants in $\mathbb{K}$, and u_p and w_p are some particular solutions to (A.441) and (A.443), respectively.

Fredholm's alternative can be also interpreted from the point of view of eigenvalues and eigenvectors. It holds that the eigenvalues of a compact operator $T \in \mathscr{L}(E)$ form a discrete set in the complex plane, with zero as the only possible limit, and for each eigenvalue there are only a finite number of linearly independent eigenvectors. Roughly speaking, the eigenvalues $\lambda \in \mathbb{C}$ and eigenvectors $v \in E$, $v \neq 0_E$, of an operator $T \in \mathscr{L}(E)$ are such that $(T - \lambda I)v = 0_E$. The resolvent set is defined as

$$\rho(T) = \{\lambda \in \mathbb{C} \,:\, (T - \lambda I) \text{ is bijective from } E \text{ to } E\}. \tag{A.447}$$

We remark that if $\lambda \in \rho(T)$, then $(T - \lambda I)^{-1} \in \mathscr{L}(E)$. We define the spectrum $\sigma(T)$ of T as the complement of the resolvent set, i.e., $\sigma(T) = \mathbb{C} \setminus \rho(T)$. The spectrum $\sigma(T)$ is a compact set and such that

$$\lambda \in \sigma(T) \quad \Rightarrow \quad |\lambda| \leq \|T\|_{\mathscr{L}(E)}. \tag{A.448}$$

We say that $\lambda \in \mathbb{C}$ is an eigenvalue, written as $\lambda \in \mathcal{EV}(T)$, if $\mathcal{N}(T - \lambda I) \neq \{0_E\}$, where $\mathcal{N}(T - \lambda I)$ is the eigenspace associated with λ. We have that $\mathcal{EV}(T) \subset \sigma(T)$. If $T \in \mathscr{L}(E)$ is a compact operator and E an infinite-dimensional Banach space, then

1. $0 \in \sigma(T)$,
2. $\sigma(T) \setminus \{0\} = \mathcal{EV}(T) \setminus \{0\}$,
3. one of the following holds:
   - $\sigma(T) = \{0\}$,
   - $\sigma(T) \setminus \{0\}$ is finite,

- $\sigma(T) \setminus \{0\}$ is a sequence that tends towards zero.

In other words, the elements of $\sigma(T)\setminus\{0\}$ are isolated points and at most countably infinite. Fredholm's alternative can be thus restated in the following form: a nonzero λ is either an eigenvalue of T, or it lies in the resolvent set $\rho(T)$.

Furthermore, a generalization to Lax-Milgram's theorem can be stated by setting Fredholm's alternative in the framework of variational forms. We consider in this case a Hilbert space H with an inner product $(\cdot,\cdot)_H$ and a dual space H', where the duality product is denoted by $\langle\cdot,\cdot\rangle_{H',H}$. Let $a : H \times H \to \mathbb{C}$ be a continuous sesquilinear form, and we suppose that it satisfies a Gårding inequality of the form

$$\mathfrak{Re}\big\{a(u,u) + (Cu,u)_H\big\} \geq \alpha\|u\|_H^2 \qquad \forall u \in H, \tag{A.449}$$

for some constant $\alpha > 0$ and for some compact linear operator $C : H \to H$. This inequality is named after the Swedish mathematician Lars Gårding, and it generalizes the coercitivity condition (A.437) that is required for the Lax-Milgram theorem. We consider the four variational problems

$$a(u,v) = \langle f, v\rangle_{H',H} \qquad \forall v \in H, \tag{A.450}$$

$$a(u,v) = 0 \qquad \forall v \in H, \tag{A.451}$$

$$\overline{a(v,w)} = \langle g, v\rangle_{H',H} \qquad \forall v \in H, \tag{A.452}$$

$$\overline{a(v,w)} = 0 \qquad \forall v \in H. \tag{A.453}$$

Then there holds the following alternative. Either (A.450) has exactly one solution $u \in H$ for every given $f \in H'$ and (A.452) has exactly one solution $w \in H$ for every given $g \in H'$; or the homogeneous problems (A.451) and (A.453) have finite-dimensional nullspaces of the same dimension $k > 0$, and the non-homogeneous problems (A.450) and (A.452) admit solutions if and only if respectively the orthogonality conditions

$$\langle f, w_j\rangle_{H',H} = 0 \quad \text{and} \quad \langle g, u_j\rangle_{H',H} = 0 \quad \text{for all } 1 \leq j \leq n \tag{A.454}$$

are satisfied, where $\{u_j\}_{j=1}^k$ spans the eigenspace of (A.451) and $\{w_j\}_{j=1}^k$ spans the eigenspace of (A.453), respectively.

A.4 Sobolev spaces

Sobolev spaces are function spaces which play a fundamental role in the modern theory of partial differential equations (PDE). A wider range of solutions of PDE, so-called weak solutions, are naturally found in Sobolev spaces rather than in the classical spaces of continuous functions and with the derivatives understood in the classical sense. Sobolev spaces allow an easy characterization of the regularity of these solutions. They are named after the Russian mathematician Sergei L'vovich Sobolev (1908–1989), who introduced these spaces together with the notion of generalized functions or distributions.

In particular, the solutions of the wave propagation problems treated in this thesis are searched in Sobolev spaces. Other boundary-value problems of PDE may require sometimes adaptations of Sobolev spaces, so-called weighted spaces, which are not discussed here. Complete surveys of Sobolev spaces can be found in Adams (1975), Brezis (1999), Grisvard (1985), Hsiao & Wendland (2008), Lions & Magenes (1972), and Ziemer (1989). For further applications and properties of Sobolev spaces we mention also the references Atkinson & Han (2005), Bony (2001), Chen & Zhou (1992), Nédélec (1977, 2001), Raviart & Thomas (1983), and Steinbach (2008).

We consider a domain Ω in $\mathbb{R}^N$ with a regular boundary $\Gamma = \partial\Omega$. By domain we understand an open nonempty and connected set. What is understood by the regularity of the boundary is specified later on. For the moment let us assume simply that the domain lies locally on only one side of Γ, and that Γ does not have cusps. Thus the situations in Figure A.14 are ruled out.

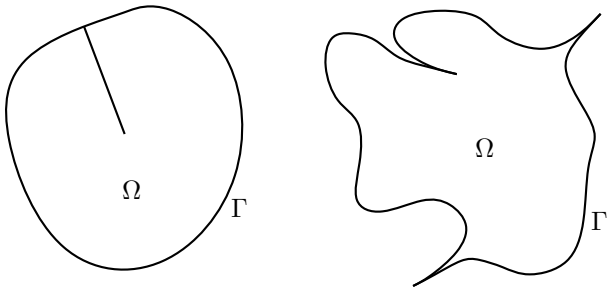

FIGURE A.14. Nonadmissible domains Ω.

Let f be a real-, or more generally, a complex-valued function defined on the domain Ω. Let $\boldsymbol{\alpha} = (\alpha_1, \alpha_2, \ldots, \alpha_N) \in \mathbb{N}_0^N$ be a multi-index of nonnegative integers. We write

$$D^{\boldsymbol{\alpha}} f = \left(\frac{\partial}{\partial x_1}\right)^{\alpha_1} \left(\frac{\partial}{\partial x_2}\right)^{\alpha_2} \cdots \left(\frac{\partial}{\partial x_N}\right)^{\alpha_N} f \tag{A.455}$$

to denote a mixed partial derivative of f of order

$$|\boldsymbol{\alpha}| = \alpha_1 + \alpha_2 + \cdots + \alpha_N. \tag{A.456}$$

A.4.1 Continuous function spaces

We denote by $C^m(\Omega)$ the space of all continuous functions whose derivatives up until order $m \in \mathbb{N}_0$ exist and are continuous in Ω. Thus, for $m = 0$, the space of all the continuous functions defined in Ω is denoted by $C^0(\Omega)$ or simply by $C(\Omega)$. Similarly, $C^\infty(\Omega)$ denotes the space of infinitely differentiable functions in Ω, which is such that

$$C^\infty(\Omega) = \bigcap_{m \in \mathbb{N}_0} C^m(\Omega). \tag{A.457}$$

It clearly holds that $C^\infty(\Omega) \subset C^{m+1}(\Omega) \subset C^m(\Omega)$ for all $m \in \mathbb{N}_0$. We remark that since Ω is open, the functions in $C^m(\Omega)$ need not to be bounded on Ω.

We represent by $C_0^m(\Omega)$ the space of functions in $C^m(\Omega)$ that have a compact support in Ω. By the support of a function we mean the closure of the set of points where the function is different from zero. A set in $\mathbb{R}^N$ is said to be compact if it is closed and bounded. In the same way as before, we denote by $C_0^\infty(\Omega)$ the set of all infinitely differentiable functions which, together with all of their derivatives, have compact support in Ω.

Similarly, one can define $C^m(\overline{\Omega})$ to be the space of functions in $C^m(\Omega)$ which, together with their derivatives of order $\leq m$, have continuous extensions to $\overline{\Omega} = \Omega \cup \Gamma$. If Ω is bounded and $m < \infty$, then $C^m(\overline{\Omega})$ is a Banach space (vid. Section A.3) with the norm

$$\|f\|_{C^m(\overline{\Omega})} = \sum_{|\boldsymbol{\alpha}| \leq m} \sup_{\boldsymbol{x} \in \overline{\Omega}} |D^{\boldsymbol{\alpha}} f(\boldsymbol{x})|. \tag{A.458}$$

If the domain Ω is unbounded, then we consider as $C^m(\overline{\Omega})$ the space of all functions of class C^m that are bounded in $\overline{\Omega}$. This space is a Banach space with the norm (A.458).

A function f that is defined in Ω is said to be Hölder continuous with exponent α, for $0 < \alpha < 1$, if there exists a constant $C > 0$ such that

$$|f(\boldsymbol{x}) - f(\boldsymbol{y})| \leq C\,|\boldsymbol{x} - \boldsymbol{y}|^\alpha \qquad \forall \boldsymbol{x}, \boldsymbol{y} \in \Omega. \tag{A.459}$$

If f fulfills (A.459) for $\alpha = 1$, then the function is said to be Lipschitz continuous. We say that f is locally Hölder or Lipschitz continuous with exponent α in Ω if it is Hölder or Lipschitz continuous with exponent α in every compact subset of Ω, respectively. These names were given after the German mathematicians Otto Ludwig Hölder (1859–1937) and Rudolf Otto Sigismund Lipschitz (1832–1903).

By $C^{m,\alpha}(\Omega)$, $m \in \mathbb{N}_0$, $0 < \alpha \leq 1$, we denote the space of functions in $C^m(\Omega)$ whose derivatives of order m are locally Hölder or Lipschitz continuous with exponent α in Ω. We remark that Hölder continuity may be viewed as a fractional differentiability. For $\alpha = 0$, we set $C^{m,0}(\Omega) = C^m(\Omega)$.

Further, by $C^{m,\alpha}(\overline{\Omega})$ we denote the subspace of $C^m(\overline{\Omega})$ consisting of functions which have m-th order Hölder or Lipschitz continuous derivatives of exponent α in Ω. If Ω is bounded, then we define the Hölder or Lipschitz norm by

$$\|f\|_{C^{m,\alpha}(\overline{\Omega})} = \|f\|_{C^m(\overline{\Omega})} + \sum_{|\boldsymbol{\beta}|=m} \sup_{\substack{\boldsymbol{x},\boldsymbol{y} \in \overline{\Omega} \\ \boldsymbol{x} \neq \boldsymbol{y}}} \frac{|D^{\boldsymbol{\beta}} f(\boldsymbol{x}) - D^{\boldsymbol{\beta}} f(\boldsymbol{y})|}{|\boldsymbol{x} - \boldsymbol{y}|^\alpha}. \tag{A.460}$$

The so-called Hölder space $C^{m,\alpha}(\overline{\Omega})$, equipped with the norm $\|\cdot\|_{C^{m,\alpha}(\overline{\Omega})}$, becomes a Banach space. Again, for an unbounded domain Ω we consider as $C^{m,\alpha}(\overline{\Omega})$ the Banach space of all bounded functions of class C^m. We have for $0 < \beta < \alpha \leq 1$ the inclusions

$$C^{m,\alpha}(\overline{\Omega}) \subset C^{m,\beta}(\overline{\Omega}) \subset C^m(\overline{\Omega}). \tag{A.461}$$

It is also clear that $C^{m,1}(\overline{\Omega}) \not\subset C^{m+1}(\overline{\Omega})$. In general $C^{m+1}(\overline{\Omega}) \not\subset C^{m,1}(\overline{\Omega})$ either, but for some particular domains Ω the inclusion applies, e.g., for convex domains.

Let $m \in \mathbb{N}_0$ and let $0 < \beta < \alpha \leq 1$, then we have the continuous imbeddings

$$C^{m+1}(\overline{\Omega}) \hookrightarrow C^m(\overline{\Omega}), \tag{A.462}$$

$$C^{m,\alpha}(\overline{\Omega}) \hookrightarrow C^m(\overline{\Omega}), \tag{A.463}$$

$$C^{m,\alpha}(\overline{\Omega}) \hookrightarrow C^{m,\beta}(\overline{\Omega}). \tag{A.464}$$

If Ω is bounded, then the imbeddings (A.463) and (A.464) are compact. Furthermore, if Ω is convex, then we have also the continuous imbeddings

$$C^{m+1}(\overline{\Omega}) \hookrightarrow C^{m,1}(\overline{\Omega}), \tag{A.465}$$

$$C^{m+1}(\overline{\Omega}) \hookrightarrow C^{m,\alpha}(\overline{\Omega}). \tag{A.466}$$

If Ω is convex and bounded, then the imbeddings (A.462) and (A.466) are compact.

A.4.2 Lebesgue spaces

The Lebesgue or L^p spaces correspond to classes of Lebesgue measurable functions defined on the domain $\Omega \subset \mathbb{R}^N$. They are defined, for $1 \leq p \leq \infty$, by

$$L^p(\Omega) = \{f : \Omega \to \mathbb{C} \mid \|f\|_{L^p(\Omega)} < \infty\}, \tag{A.467}$$

where the L^p-norm is given by

$$\|f\|_{L^p(\Omega)} = \begin{cases} \left(\displaystyle\int_\Omega |f(\boldsymbol{x})|^p \,\mathrm{d}\boldsymbol{x}\right)^{1/p}, & 1 \leq p < \infty, \\ \operatorname*{ess\,sup}_{\boldsymbol{x}\in\Omega} |f(\boldsymbol{x})|, & p = \infty. \end{cases} \tag{A.468}$$

The appearing integrals have to be understood in the sense of Lebesgue (cf. Royden 1988), which is named after the French mathematician Henri Léon Lebesgue (1875–1941), who became famous for his theory of integration. We say that two functions are equal almost everywhere if they are equal except on a set of measure zero. Functions which are equal almost everywhere in the domain Ω are therefore identified together in $L^p(\Omega)$. The essential supremum is likewise defined in this sense by

$$\operatorname*{ess\,sup}_{\boldsymbol{x}\in\Omega} |f(\boldsymbol{x})| = \inf\{C > 0 : \ |f(\boldsymbol{x})| \leq C \ \text{ almost everywhere in } \Omega\}. \tag{A.469}$$

We remark that L^p spaces, supplied with the L^p-norm, are Banach spaces. A normed vector space is said to be separable if it contains a countable dense subset. For $1 < p < \infty$, we have that the space $L^p(\Omega)$ is separable, reflexive, and its dual space $L^p(\Omega)'$ is identified with $L^q(\Omega)$, where $\frac{1}{p} + \frac{1}{q} = 1$. The space $L^1(\Omega)$ is separable, but not reflexive, and its dual space $L^1(\Omega)'$ is identified with $L^\infty(\Omega)$. The space $L^\infty(\Omega)$ is neither separable nor reflexive,

and its dual space $L^\infty(\Omega)'$ is strictly contained in $L^1(\Omega)$. If

$$f_i \in L^{p_i}(\Omega) \quad (1 \le i \le n) \qquad \text{with} \qquad \frac{1}{p} = \sum_{i=1}^{n} \frac{1}{p_i} \le 1, \quad 1 \le p_i \le \infty, \tag{A.470}$$

then the multiplication of these functions f_i is such that

$$f = f_1 f_2 \cdots f_n \in L^p(\Omega), \tag{A.471}$$

and furthermore

$$\|f\|_{L^p(\Omega)} \le \|f\|_{L^{p_1}(\Omega)} \|f\|_{L^{p_2}(\Omega)} \cdots \|f\|_{L^{p_n}(\Omega)}. \tag{A.472}$$

If $f \in L^p(\Omega) \cap L^q(\Omega)$ with $1 \le p \le q \le \infty$, then $f \in L^r(\Omega)$ for all $p \le r \le q$, and we have moreover the interpolation inequality

$$\|f\|_{L^r(\Omega)} \le \|f\|^{\alpha}_{L^p(\Omega)} \|f\|^{1-\alpha}_{L^q(\Omega)}, \quad \text{where} \quad \frac{1}{r} = \frac{\alpha}{p} + \frac{1-\alpha}{q} \quad (0 \le \alpha \le 1). \tag{A.473}$$

In the particular case when $p = 2$, it holds that $L^2(\Omega)$ is also a Hilbert space with respect to the inner product

$$(f, g)_{L^2(\Omega)} = \int_\Omega f(\boldsymbol{x})\, \overline{g(\boldsymbol{x})}\, \mathrm{d}\boldsymbol{x}, \qquad \forall f, g \in L^2(\Omega). \tag{A.474}$$

Its dual space $L^2(\Omega)'$ is identified with the space $L^2(\Omega)$ itself.

We can likewise define the L^p_{loc} spaces by

$$L^p_{\text{loc}}(\Omega) = \{f : \Omega \to \mathbb{C} \mid f \in L^p(K) \quad \forall K \subset \Omega,\ K \text{ compact}\}, \tag{A.475}$$

which behave locally as L^p spaces, i.e., on each compact subset K of Ω. These locally defined functional spaces can not be supplied with reasonable norms, but nevertheless a Fréchet space structure may be defined for them (cf. Bony 2001). Fréchet spaces are certain topological vector spaces which are locally convex and complete with respect to a translation invariant metric. They receive their name from the French mathematician Maurice Fréchet (1878–1973), who is responsible for introducing the concept of metric spaces.

A.4.3 Sobolev spaces of integer order

We define now the Sobolev spaces $W^{m,p}$, for $1 \le p \le \infty$ and $m \in \mathbb{N}_0$, by

$$W^{m,p}(\Omega) = \{f : \Omega \to \mathbb{C} \mid D^{\boldsymbol{\alpha}} f \in L^p(\Omega) \ \ \forall \boldsymbol{\alpha} \in \mathbb{N}_0^N,\ |\boldsymbol{\alpha}| \le m\}, \tag{A.476}$$

or alternatively, by

$$W^{m,p}(\Omega) = \{f : \Omega \to \mathbb{C} \mid \|f\|_{W^{m,p}(\Omega)} < \infty\}, \tag{A.477}$$

where the $W^{m,p}$-norm is given by

$$\|f\|_{W^{m,p}(\Omega)} = \begin{cases} \displaystyle\left(\sum_{|\boldsymbol{\alpha}| \le m} \|D^{\boldsymbol{\alpha}} f\|^p_{L^p(\Omega)} \right)^{1/p}, & 1 \le p < \infty, \\ \displaystyle\max_{|\boldsymbol{\alpha}| \le m} \|D^{\boldsymbol{\alpha}} f\|_{L^\infty(\Omega)}, & p = \infty. \end{cases} \tag{A.478}$$

The Sobolev spaces $W^{m,p}$ are actually Banach spaces, provided that the derivatives are taken in the sense of distributions (vid. Section A.6). If $m = 0$, then we retrieve

$$W^{0,p}(\Omega) = L^p(\Omega), \qquad 1 \leq p \leq \infty. \tag{A.479}$$

For $p = 2$ the space $W^{m,2}(\Omega)$ becomes a Hilbert space, and is denoted in particular by

$$H^m(\Omega) = W^{m,2}(\Omega). \tag{A.480}$$

The space $H^m(\Omega)$ is supplied with the inner product

$$(f, g)_{H^m(\Omega)} = \sum_{|\boldsymbol{\alpha}| \leq m} \int_\Omega D^{\boldsymbol{\alpha}} f(\boldsymbol{x})\, \overline{D^{\boldsymbol{\alpha}} g(\boldsymbol{x})}\, \mathrm{d}\boldsymbol{x} \qquad \forall f, g \in H^m(\Omega), \tag{A.481}$$

and hence with the norm

$$\|f\|_{H^m(\Omega)} = \left(\sum_{|\boldsymbol{\alpha}| \leq m} \int_\Omega |D^{\boldsymbol{\alpha}} f(\boldsymbol{x})|^2\, \mathrm{d}\boldsymbol{x} \right)^{1/2} \qquad \forall f \in H^m(\Omega). \tag{A.482}$$

We refer to $H^m(\Omega)$ as the Sobolev space of order m. Sobolev spaces of higher order contain elements with a higher degree of smoothness or regularity. We remark that if $f \in H^m(\Omega)$, then $\partial f / \partial x_i \in H^{m-1}(\Omega)$ for $1 \leq i \leq N$.

Due density, we can define now the space $H_0^m(\Omega)$ as the closure of $C_0^m(\Omega)$ under the H^m-norm (A.482), i.e.,

$$H_0^m(\Omega) = \overline{C_0^m(\Omega)}^{\|\cdot\|_{H^m(\Omega)}}. \tag{A.483}$$

We remark that if the domain Ω is regular enough, then the space $H^m(\Omega)$ can be defined alternatively as the completion of $C^\infty(\overline{\Omega})$ with respect to the norm $\|\cdot\|_{H^m(\Omega)}$, which means that for every $f \in H^m(\Omega)$ there exists a sequence $\{f_k\}_{k \in \mathbb{N}} \subset C^\infty(\overline{\Omega})$ such that

$$\lim_{k \to \infty} \|f - f_k\|_{H^m(\Omega)} = 0. \tag{A.484}$$

In the same manner as for the L^p spaces, we can also consider locally defined H^m_{loc} Sobolev spaces, given by

$$H^m_{\mathrm{loc}}(\Omega) = \{f : \Omega \to \mathbb{C} \mid f \in H^m(K) \ \ \forall K \subset \Omega,\ K \text{ compact}\}, \tag{A.485}$$

which behave as H^m spaces on each compact subset K of Ω, and can be treated in the framework of Fréchet spaces.

A.4.4 Sobolev spaces of fractional order

Sobolev spaces can be also defined for non-integer values of m, so-called fractional orders and denoted by s. For this we consider first the particular case when the domain Ω is the full space $\mathbb{R}^N$, in which case the Sobolev spaces of fractional order are defined by means of a Fourier transform (vid. Section A.7). For a real value s we use the norm

$$\|f\|_{H^s(\mathbb{R}^N)} = \left(\int_{\mathbb{R}^N} (1 + |\boldsymbol{\xi}|^2)^s |\widehat{f}(\boldsymbol{\xi})|^2\, \mathrm{d}\boldsymbol{\xi} \right)^{1/2}, \tag{A.486}$$

where $\widehat{f}$ denotes the Fourier transform of f. The weighting factor $(1+|\boldsymbol{\xi}|^2)^{s/2}$ is known as Bessel's potential of order s. The expression (A.486) defines an equivalent norm to (A.482) in $H^m(\mathbb{R}^N)$ if $s=m$, but holds also for non-integer and even negative values of s. If s is real and positive, then the Sobolev spaces of fractional order are defined by

$$H^s(\mathbb{R}^N) = \{f \in L^2(\mathbb{R}^N) : \|f\|_{H^s(\mathbb{R}^N)} < \infty\}, \tag{A.487}$$

which is equivalent to the definition given previously, when $s=m$. If we allow negative values for s, then the definition (A.487) has to be extended to admit as well tempered distributions in $\mathcal{S}'(\mathbb{R}^N)$ (vid. Sections A.6 & A.7). Thus in general, if $s \in \mathbb{R}$, then the Sobolev spaces of fractional order are defined by

$$H^s(\mathbb{R}^N) = \{f \in \mathcal{S}'(\mathbb{R}^N) : \|f\|_{H^s(\mathbb{R}^N)} < \infty\}. \tag{A.488}$$

We observe that the Sobolev space $H^{-s}(\mathbb{R}^N)$ is the dual space of $H^s(\mathbb{R}^N)$.

If we consider now a proper subdomain Ω of $\mathbb{R}^N$, then the Sobolev spaces of fractional order, for $s \geq 0$, are defined by

$$H^s(\Omega) = \{f : \Omega \to \mathbb{C} \mid \exists F \in H^s(\mathbb{R}^N) \text{ such that } F|_\Omega = f\}, \tag{A.489}$$

and have the norm

$$\|f\|_{H^s(\Omega)} = \inf\{\|F\|_{H^s(\mathbb{R}^N)} : F|_\Omega = f\}. \tag{A.490}$$

We remark that if Ω is a pathological domain such as those depicted in Figure A.14, then the new definition (A.489) is not equivalent to the old one for $H^m(\Omega)$ if $s=m$.

Since $C_0^\infty(\Omega) \subset C^\infty(\overline{\Omega})$, where for any $f \in C_0^\infty(\Omega)$ the trivial extension $\widetilde{f}$ by zero outside of Ω is in $C_0^\infty(\mathbb{R}^N)$, we define the space $\widetilde{H}^s(\Omega)$ for $s \geq 0$ to be the completion of $C_0^\infty(\Omega)$ with respect to the norm

$$\|f\|_{\widetilde{H}^s(\Omega)} = \|\widetilde{f}\|_{H^s(\mathbb{R}^N)}. \tag{A.491}$$

This definition implies that

$$\widetilde{H}^s(\Omega) = \{f \in H^s(\mathbb{R}^N) : \operatorname{supp} f \subset \overline{\Omega}\}. \tag{A.492}$$

We remark that the space $\widetilde{H}^s(\Omega)$ is often also denoted as $H^s_{00}(\Omega)$ (cf., e.g., Lions & Magenes 1972). If $\Omega = \mathbb{R}^N$, then the H^s and $\widetilde{H}^s$ spaces coincide, i.e.,

$$\widetilde{H}^s(\mathbb{R}^N) = H^s(\mathbb{R}^N). \tag{A.493}$$

For negative orders we have that $H^{-s}(\Omega)$ is the dual space of $\widetilde{H}^s(\Omega)$, i.e.,

$$H^{-s}(\Omega) = \widetilde{H}^s(\Omega)', \tag{A.494}$$

where the norm is defined by means of the inner product in $L^2(\Omega)$, namely

$$\|f\|_{H^{-s}(\Omega)} = \sup_{0 \neq \varphi \in \widetilde{H}^s(\Omega)} \frac{|(f,\varphi)_{L^2(\Omega)}|}{\|\varphi\|_{\widetilde{H}^s(\Omega)}}, \qquad s > 0. \tag{A.495}$$

In the same way, the space $\widetilde{H}^{-s}(\Omega)$ is the dual space of $H^s(\Omega)$, i.e.,

$$\widetilde{H}^{-s}(\Omega) = H^s(\Omega)', \tag{A.496}$$

and is provided with the norm of the dual space

$$\|f\|_{\widetilde{H}^{-s}(\Omega)} = \sup_{0\neq\psi\in H^s(\Omega)} \frac{|(f,\psi)_{L^2(\Omega)}|}{\|\psi\|_{H^s(\Omega)}}, \qquad s>0. \tag{A.497}$$

It can be shown that the definition (A.492) applies also for $s<0$ if Ω is regular enough. For $s>0$ we obtain the inclusions

$$\widetilde{H}^s(\Omega) \subset H^s(\Omega) \subset L^2(\Omega) \subset \widetilde{H}^{-s}(\Omega) \subset H^{-s}(\Omega). \tag{A.498}$$

It holds in particular for $0 \leq s < \frac{1}{2}$ that $\widetilde{H}^s(\Omega) = H^s(\Omega)$ and $\widetilde{H}^{-s}(\Omega) = H^{-s}(\Omega)$, which is not true anymore for $s \geq \frac{1}{2}$. We have in this chain that $L^2(\Omega)$ is the only Sobolev space that is identified with its dual space, and is therefore called pivot space. It is a standard practice to represent the duality pairings among Sobolev spaces just as inner products in $L^2(\Omega)$, that is, the integral notation is maintained even if the elements are no longer L^2-integrable. In fact, the norm definitions (A.495) and (A.497) for the dual spaces $V' = H^{-s}(\Omega)$ and $\widetilde{H}^{-s}(\Omega)$ for $s>0$ are based on this representation. In this case, if $f \in V'$ but $f \notin L^2(\Omega)$, then we define

$$\langle f,\varphi\rangle_{V',V} = \lim_{n\to\infty}(f_n,\varphi)_{L^2(\Omega)} = \lim_{n\to\infty}\int_\Omega f_n(\boldsymbol{x})\,\overline{\varphi(\boldsymbol{x})}\,\mathrm{d}\boldsymbol{x} \qquad \forall\varphi\in V, \tag{A.499}$$

where V is correspondingly either $\widetilde{H}^s(\Omega)$ or $H^s(\Omega)$, where $\langle\cdot,\cdot\rangle_{V',V}$ denotes the sesquilinear duality product between V' and V, and where $\{f_n\} \subset L^2(\Omega)$ is a sequence such that

$$\lim_{n\to\infty}\|f-f_n\|_{V'} = 0. \tag{A.500}$$

We know that the sequence $\{f_n\}$ exists and that (A.499) makes sense, since $H^{-s}(\Omega)$ is the completion of $L^2(\Omega)$ with respect to the norm of the dual space (A.495). We write thus

$$\langle f,\varphi\rangle_{V',V} = (f,\varphi)_{L^2(\Omega)} \tag{A.501}$$

for the duality pairing $(f,\varphi)\in V'\times V$, where the L^2-inner product on the right-hand side is understood in the sense of (A.499) for $f\notin L^2(\Omega)$.

For $s>t$ it holds also that $H^s(\Omega)\subset H^t(\Omega)$ and $\widetilde{H}^s(\Omega)\subset\widetilde{H}^t(\Omega)$, i.e., as the order of the Sobolev spaces increases, so does the smoothness of their elements. If $s=m+\sigma\geq 0$, for $m\in\mathbb{N}_0$ and $0<\sigma<1$, then the space $\widetilde{H}^s(\Omega)$ can be characterized as the completion of the space $C_0^{m+1}(\Omega)$ with respect to the norm (A.491), namely

$$\widetilde{H}^s(\Omega) = \overline{C_0^{m+1}(\Omega)}^{\|\cdot\|_{H^s(\mathbb{R}^N)}}. \tag{A.502}$$

A closely related space is

$$H_0^s(\Omega) = \overline{C_0^{m+1}(\Omega)}^{\|\cdot\|_{H^s(\Omega)}}, \tag{A.503}$$

which considers the closure of $C_0^{m+1}(\Omega)$, but now under the norm (A.490). It holds that

$$\widetilde{H}^s(\Omega) = H_0^s(\Omega) \qquad \forall s=m+\sigma,\quad m\in\mathbb{N}_0,\quad |\sigma|<\frac{1}{2}, \tag{A.504}$$

and when $s=m+1/2$, then the space $\widetilde{H}^s(\Omega)$ is strictly contained in $H_0^s(\Omega)$.

We observe that the Sobolev space $H^s(\Omega)$ of fractional order $s = m + \sigma$, for $m \in \mathbb{N}_0$ and $0 < \sigma < 1$, can be alternatively defined as

$$H^s(\Omega) = \{f \in L^2(\Omega) : \|f\|_{H^s(\Omega)} < \infty\}, \tag{A.505}$$

by means of the norm

$$\|f\|_{H^s(\Omega)} = \left(\|f\|^2_{H^m(\Omega)} + \sum_{|\boldsymbol{\alpha}|=m} \int_\Omega \int_\Omega \frac{|D^{\boldsymbol{\alpha}} f(\boldsymbol{x}) - D^{\boldsymbol{\alpha}} f(\boldsymbol{y})|^2}{|\boldsymbol{x} - \boldsymbol{y}|^{N+2\sigma}} \, \mathrm{d}\boldsymbol{x} \, \mathrm{d}\boldsymbol{y} \right)^{1/2}, \tag{A.506}$$

where $\| \cdot \|_{H^m(\Omega)}$ is the norm for the Sobolev space of integer order m defined in (A.482). For further details we refer to Hsiao & Wendland (2008).

A.4.5 Trace spaces

Trace spaces are Sobolev spaces for functions defined on the boundary. If $f \in H^s(\Omega)$ is continuous up to the boundary Γ of Ω, then one can say that the value which f takes on Γ is the restriction to Γ (of the extension by continuity to $\overline{\Omega}$) of the function f, which is denoted by $f|_\Gamma$. In general, however, the elements of $H^s(\Omega)$ are defined except for a set of N-dimensional zero measure and it is meaningless therefore to speak of their restrictions to Γ (which has an N-dimensional zero measure). Therefore we use the concept of the trace of a function on Γ, which substitutes and generalizes that of the restriction $f|_\Gamma$ whenever the latter in the classical sense is inapplicable.

We follow the approach found in standard text books of identifying the boundary Γ with $\mathbb{R}^{N-1}$ by means of local parametric representations of Γ. Roughly speaking, we define the trace spaces to be isomorphic to the Sobolev spaces $H^s(\mathbb{R}^{N-1})$.

a) Regularity of the boundary

To characterize properly the regularity of the domain Ω, its boundary Γ is described locally by the graph of a function φ, and the properties of Γ are then specified through the properties of φ. We say that the boundary Γ is of class $C^{m,\alpha}$, for $m \in \mathbb{N}_0$ and $0 \leq \alpha \leq 1$, if for each $\boldsymbol{x} \in \Gamma$ there exists a neighborhood Θ of $\boldsymbol{x}$ in $\mathbb{R}^N$ and a new orthogonal coordinate system $\boldsymbol{y} = (\boldsymbol{y}_s, y_N) \in \mathbb{R}^N$, being $\boldsymbol{y}_s = (y_1, \ldots, y_{N-1}) \in \mathbb{R}^{N-1}$, such that

1. for some $\delta, \varepsilon > 0$ the neighborhood Θ is a hypercylinder in the new coordinates:

$$\Theta = \{\boldsymbol{y} \in \mathbb{R}^N : \, |\boldsymbol{y}_s| < \delta, \;\; |y_N| < \varepsilon\}; \tag{A.507}$$

2. there exists a function φ of class $C^{m,\alpha}$ defined on $Q = \{\boldsymbol{y}_s : |\boldsymbol{y}_s| < \delta\}$ such that

$$|\varphi(\boldsymbol{y}_s)| \leq \frac{\varepsilon}{2} \qquad \forall \boldsymbol{y}_s \in Q, \tag{A.508}$$

$$\Omega \cap \Theta = \{\boldsymbol{y} \in \Theta : \, y_N < \varphi(\boldsymbol{y}_s)\}, \tag{A.509}$$

$$\Gamma \cap \Theta = \{\boldsymbol{y} \in \Theta : \, y_N = \varphi(\boldsymbol{y}_s)\}. \tag{A.510}$$

In other words, in a neighborhood Θ of $\boldsymbol{x}$, the domain Ω is below the graph of φ and consequently the boundary Γ is the graph of φ, as illustrated in Figure A.15. The pair (Θ, φ) is called a local chart of Γ. The relation between the new coordinates $\boldsymbol{y} \in \mathbb{R}^N$ and the old

ones $\boldsymbol{x} \in \mathbb{R}^N$ is given by

$$\boldsymbol{x} = \boldsymbol{b} + \boldsymbol{T}(\boldsymbol{y}), \tag{A.511}$$

where $\boldsymbol{b} \in \mathbb{R}^N$ is a constant translation vector (eventually $\boldsymbol{b} \in \Gamma$), and where $\boldsymbol{T}$ is an orthogonal linear transformation, i.e., an orthogonal $N \times N$ matrix.

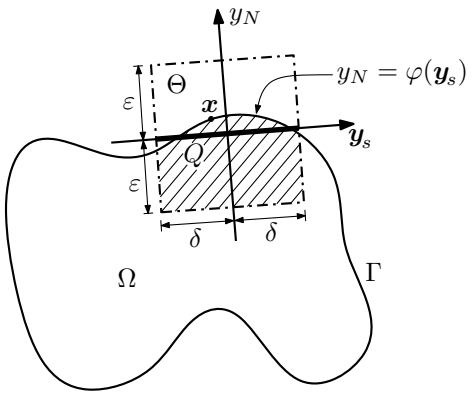

FIGURE A.15. Local chart of Γ.

For $\alpha = 0$, we say simply that Γ is of class C^m. By the regularity of the domain Ω we mean the regularity of its boundary Γ, and thus we may write indistinctly $\Omega \in C^m$ or $\Gamma \in C^m$. The boundary Γ is said to be of class C^∞ if $\Gamma \in \cap_{m=0}^{\infty} C^m$.

In the case when $\Gamma \in C^{0,1}$, the boundary is called a Lipschitz boundary (with a strong Lipschitz property) and Ω is called a (strong) Lipschitz domain, written as $\Omega \in C^{0,1}$. Such a boundary lies locally on only one side of Γ and does not have cusps, but can contain conical points or edges, which are not continuously differentiable. In particular, the domains shown in Figure A.14 are not strong Lipschitz domains. For strong Lipschitz domains a unique unit normal vector can be defined almost everywhere on Γ. These domains are useful for almost all practical purposes and they are regular enough so that the different definitions of Sobolev spaces on them usually coincide.

A boundary $\Gamma \in C^{1,\alpha}$ with $0 < \alpha < 1$ is called a Lyapunov boundary, and it has the property that a unique unit normal vector can be defined everywhere on Γ. It is named after the Russian mathematician and physicist Aleksandr Mikhailovich Lyapunov (1857–1918). In particular, we have the inclusions

$$C^{2,0} \subset C^{1,1} \subset C^{1,\alpha} \subset C^{1,0} \subset C^{0,1}, \tag{A.512}$$

and, more in general,

$$C^{m+1} \subset C^{m,1} \subset C^{m,\alpha} \subset C^m \qquad \forall m \in \mathbb{N}_0, \;\; 0 < \alpha < 1. \tag{A.513}$$

To prove them, let us consider a point $\boldsymbol{x} \in \Gamma$, which is contained in some local chart (Θ, φ) and described as $x_N = \varphi(\boldsymbol{x}_s)$, where $\boldsymbol{x} = (\boldsymbol{x}_s, x_N)$. Then there exists a neighborhood of $\boldsymbol{x}_s$ whose closure is convex and contained in the definition domain Q of the function φ. Hence, from (A.463), (A.464), and (A.465), we obtain the inclusions (A.512) and (A.513).

b) Definition of the trace spaces

Now let $L^2(\Gamma)$ be the completion of $C^0(\Gamma)$, the space of all continuous functions on Γ, with respect to the norm

$$\|f\|_{L^2(\Gamma)} = \left(\int_\Gamma |f(\boldsymbol{x})|^2 \, \mathrm{d}\gamma(\boldsymbol{x}) \right)^{1/2}, \tag{A.514}$$

which is a Hilbert space with the scalar product

$$(f,g)_{L^2(\Gamma)} = \int_\Gamma f(\boldsymbol{x}) \, \overline{g(\boldsymbol{x})} \, \mathrm{d}\gamma(\boldsymbol{x}) \qquad \forall f,g \in L^2(\Gamma). \tag{A.515}$$

For a strong Lipschitz domain $\Omega \in C^{0,1}$ it can be shown that there exists a unique linear mapping $\gamma_0 : H^1(\Omega) \to L^2(\Gamma)$ such that if $f \in C^0(\overline{\Omega})$ then $\gamma_0 f = f|_\Gamma$. For $f \in H^1(\Omega)$ we call $\gamma_0 f$ the trace of f on Γ and the mapping γ_0 the trace operator (of order 0). However, in order to characterize all those elements in $L^2(\Gamma)$ which can be the trace of elements of $H^1(\Omega)$, we introduce also the trace spaces $H^s(\Gamma)$. For $s = 0$ we set $H^0(\Gamma) = L^2(\Gamma)$.

Let the boundary Γ be bounded, in which case there exists a covering of Γ by a finite union of open neighborhoods $\Theta_j \subset \mathbb{R}^N$ in the form of (A.507), for $1 \le j \le p < \infty$, such that Γ is enclosed in the set $\bigcup_{j=1}^p \Theta_j$. Such an open covering of Γ and the collection of all the local parametric representations φ_j of Γ on each neighborhood Θ_j is called a finite atlas. Each function φ_j has a definition domain Q_j and is described by a different orthogonal coordinate system, which is obtained by means of a translation vector $\boldsymbol{b}_j$ and an orthogonal linear transformation $\boldsymbol{T}_j$, as described in (A.511). If the boundary Γ is unbounded, we still suppose that there exists a finite atlas of Γ, i.e., there is a finite amount of local charts that encompasses the unbounded portions of Γ, and therefore the same results apply also to this case. We consider now the parametric representation of Γ through the mappings $\Phi_j : Q_j \to \Gamma$ defined by

$$\boldsymbol{x} = \Phi_j(\boldsymbol{y}_s) = \boldsymbol{b}_j + \boldsymbol{T}_j\big(\boldsymbol{y}_s, \varphi_j(\boldsymbol{y}_s)\big), \qquad \boldsymbol{y}_s \in Q_j, \;\; \boldsymbol{x} \in \Gamma. \tag{A.516}$$

For $\Gamma \in C^{m,\alpha}$, this allows us to define in a first step the trace space $H^s(\Gamma)$, for all s with $0 \le s < m + \alpha$ for non-integer $m + \alpha$ or $0 \le s \le m + \alpha$ for integer $m + \alpha$, by

$$H^s(\Gamma) = \{ f \in L^2(\Gamma) : \; f \circ \Phi_j \in H^s(Q_j), \;\; 1 \le j \le p \}, \tag{A.517}$$

where $\circ$ denotes the composition of two functions. This space is equipped with the norm

$$\|f\|_{H^s(\Gamma)} = \left(\sum_{j=1}^p \|f \circ \Phi_j\|^2_{H^s(Q_j)} \right)^{1/2}, \tag{A.518}$$

and it becomes a Hilbert space with the inner product

$$(f,g)_{H^s(\Gamma)} = \sum_{j=1}^p (f \circ \Phi_j, g \circ \Phi_j)_{H^s(Q_j)} \qquad \forall f,g \in H^s(\Gamma). \tag{A.519}$$

We note that the above restrictions for s are necessary since otherwise the differentiations with respect to $\boldsymbol{y}_s$ required in (A.518) and (A.519) may not be well defined. In an additional step, these definitions, (A.518) and (A.519), can be rewritten in terms of the Sobolev

spaces $H^s(\mathbb{R}^{N-1})$ by using a partition of unity, i.e., a set of positive functions $\lambda_j \in C_0^\infty(\Theta_j)$ such that

$$\sum_{j=1}^{p} \lambda_j(\boldsymbol{x}) = 1 \tag{A.520}$$

in some neighborhood of Γ. For f given on Γ, we define the extended function on $\mathbb{R}^{N-1}$ by

$$(\widetilde{\lambda_j f})(\boldsymbol{y}_s) = \begin{cases} (\lambda_j f)\big(\Phi_j(\boldsymbol{y}_s)\big) & \text{for } \boldsymbol{y}_s \in Q_j, \\ 0 & \text{otherwise.} \end{cases} \tag{A.521}$$

This allows us to redefine the trace space (A.517) as

$$H^s(\Gamma) = \{f \in L^2(\Gamma) : \widetilde{\lambda_j f} \in H^s(\mathbb{R}^{N-1}),\ \ 1 \le j \le p\}. \tag{A.522}$$

The corresponding norm now reads

$$\|f\|_{H^s(\Gamma)} = \left(\sum_{j=1}^{p} \|\widetilde{\lambda_j f}\|^2_{H^s(\mathbb{R}^{N-1})} \right)^{1/2}, \tag{A.523}$$

and is associated with the scalar product

$$(f,g)_{H^s(\Gamma)} = \sum_{j=1}^{p} (\widetilde{\lambda_j f}, \widetilde{\lambda_j g})_{H^s(\mathbb{R}^{N-1})} \qquad \forall f, g \in H^s(\Gamma). \tag{A.524}$$

Since the extended functions $\widetilde{\lambda_j f}$ are defined on $\mathbb{R}^{N-1}$ having compact supports in Q_j, and since in (A.523) and (A.524) we are using $H^s(\mathbb{R}^{N-1})$, we can introduce via L^2-duality the whole scale of Sobolev spaces $H^s(\Gamma)$, for all s with $-m-\alpha < s < m+\alpha$ for non-integer $m+\alpha$ or $-m-\alpha \le s \le m+\alpha$ for integer $m+\alpha$. We have that $H^{-s}(\Gamma)$ is the dual space of $H^s(\Gamma)$, and for $s > 0$ it can be defined as the completion of $L^2(\Gamma)$ with respect to the norm

$$\|f\|_{H^{-s}(\Gamma)} = \sup_{\|\varphi\|_{H^s(\Gamma)}=1} |(\varphi, f)_{L^2(\Gamma)}|. \tag{A.525}$$

The trace spaces can be alternatively defined in terms of boundary norms. We define the space $H^s(\Gamma)$, for $0 < s < 1$, as the completion of $C^0(\Gamma)$ with respect to the norm

$$\|f\|_{H^s(\Gamma)} = \left(\|f\|^2_{L^2(\Gamma)} + \int_\Gamma \int_\Gamma \frac{|f(\boldsymbol{x}) - f(\boldsymbol{y})|^2}{|\boldsymbol{x}-\boldsymbol{y}|^{N-1+2s}} \,\mathrm{d}\boldsymbol{x}\,\mathrm{d}\boldsymbol{y} \right)^{1/2}, \tag{A.526}$$

which means that we can define

$$H^s(\Gamma) = \{f \in L^2(\Gamma) : \|f\|_{H^s(\Gamma)} < \infty\}. \tag{A.527}$$

Again, $H^s(\Gamma)$ is a Hilbert space when equipped with the inner product

$$(f,g)_{H^s(\Gamma)} = (f,g)_{L^2(\Gamma)} + \int_\Gamma \int_\Gamma \frac{\big(f(\boldsymbol{x}) - f(\boldsymbol{y})\big)\overline{\big(g(\boldsymbol{x}) - g(\boldsymbol{y})\big)}}{|\boldsymbol{x}-\boldsymbol{y}|^{N-1+2s}} \,\mathrm{d}\boldsymbol{x}\,\mathrm{d}\boldsymbol{y}. \tag{A.528}$$

To use this definition for $s \ge 1$ is more complicated. Further details can be found in the book of Hsiao & Wendland (2008).

A third alternative to define the trace spaces on Γ is to use extensions of functions defined on Γ to Sobolev spaces defined in Ω. For $s > 0$ we define the Sobolev space

$$H^s(\Gamma) = \{f \in L^2(\Gamma) : \exists\, \widetilde{f} \in H^{s+\frac{1}{2}}(\Omega) \text{ such that } \gamma_0 \widetilde{f} = \widetilde{f}|_\Gamma = f \text{ on } \Gamma\}, \tag{A.529}$$

which is supplied with the norm

$$\|f\|_{H^s(\Gamma)} = \inf_{\gamma_0 \widetilde{f} = f} \|\widetilde{f}\|_{H^{s+1/2}(\Omega)}. \tag{A.530}$$

We observe that this definition for trace spaces can be used without problem for any $s > 0$, and it fulfills in a natural way the trace theorem.

As mentioned in Grisvard (1985), we remark that when a function f is a solution in Ω of an elliptic partial differential equation, then f has traces on the boundary provided it belongs to any Sobolev space, without any restriction to s.

c) Trace theorem

The trace theorem characterizes the conditions for the existence of the so-called trace operator. Let Ω be a domain with a boundary Γ of class $C^{m,1}$ with $m \in \mathbb{N}_0$ and where s is taken such that $\frac{1}{2} < s \leq m + 1$. Under these conditions, the trace theorem states that there exists a linear continuous trace operator γ_0 with

$$\gamma_0 : H^s(\Omega) \longrightarrow H^{s-\frac{1}{2}}(\Gamma), \tag{A.531}$$

which is an extension of

$$\gamma_0 f = f|_\Gamma \quad \text{for } f \in C^0(\overline{\Omega}). \tag{A.532}$$

The theorem characterizes also traces of higher order. For a domain Ω with a boundary Γ of class $C^{m,1}$, we consider $j, m \in \mathbb{N}_0$ and we take s such that $\frac{1}{2} + j < s \leq m + 1$. Then there exists a linear continuous trace operator γ_j with

$$\gamma_j : H^s(\Omega) \longrightarrow H^{s-j-\frac{1}{2}}(\Gamma), \tag{A.533}$$

which is an extension of the normal derivatives of order j

$$\gamma_j f = \frac{\partial^j f}{\partial n^j}|_\Gamma = (\boldsymbol{n} \cdot \nabla)^j f|_\Gamma \quad \text{for } f \in C^\ell(\overline{\Omega}) \quad \text{with } s + j \leq \ell \in \mathbb{N}, \tag{A.534}$$

where $\boldsymbol{n}$ denotes the unit boundary normal vector that points outwards of the domain Ω. Moreover, the trace theorem states that under these conditions all the different definitions of trace spaces are equivalent.

d) The spaces $H^{1/2}(\Gamma)$, $H^{-1/2}(\Gamma)$, and $H^1(\Delta; \Omega)$

Of particular interest in our case are the trace spaces $H^{1/2}(\Gamma)$ and $H^{-1/2}(\Gamma)$. The trace space $H^{1/2}(\Gamma)$ can be defined either by (A.522), (A.527), or (A.529) for $s = \frac{1}{2}$, where the norm is given respectively by (A.523), (A.526), or (A.530). If $\Gamma \in C^{0,1}$, then the three presented alternative definitions for $H^{1/2}(\Gamma)$ coincide. Its dual space $H^{-1/2}(\Gamma)$ is given by the completion of $L^2(\Gamma)$ with respect to the norm of the dual space (A.525).

As mentioned in Raviart (1991), we have that a particularly interesting space to work with traces is

$$H^1(\Delta;\Omega) = \{f \in H^1(\Omega) : \Delta f \in L^2(\Omega)\}, \tag{A.535}$$

provided with the norm

$$\|f\|_{H^1(\Delta;\Omega)} = \left(\|f\|^2_{H^1(\Omega)} + \|\Delta f\|^2_{L^2(\Omega)}\right)^{1/2}, \tag{A.536}$$

since this space is adjusted enough so as to still allow to define the trace of the normal derivative. In fact, for $f \in H^1(\Delta;\Omega)$ and due the trace theorem, we have that

$$\gamma_0 f = f|_\Gamma \in H^{1/2}(\Gamma), \tag{A.537}$$

$$\gamma_1 f = \frac{\partial f}{\partial n}|_\Gamma \in H^{-1/2}(\Gamma). \tag{A.538}$$

e) Trace spaces on an open surface

In some applications we need trace spaces on an open connected part $\Gamma_0 \subset \Gamma$ of a closed boundary Γ. Let us assume that $\Gamma \in C^{m,1}$ with $m \in \mathbb{N}_0$. In the two-dimensional case $\Gamma_0 \subset \Gamma = \partial\Omega$ with $\Omega \in \mathbb{R}^2$, the boundary of Γ_0 is denoted by $\gamma = \partial\Gamma_0$ and consists just of two endpoints $\gamma = \{\boldsymbol{z}_1, \boldsymbol{z}_2\}$. In the three-dimensional case, the boundary $\partial\Gamma_0$ of Γ_0 is a closed curve γ. We assume that s satisfies $|s| \leq m+1$, and thus all the definitions for the trace space $H^s(\Gamma)$ coincide. As before, let us introduce the space of trivial extensions from $\overline{\Gamma}_0$ to Γ of functions f defined on $\overline{\Gamma}_0$ by zero outside of $\overline{\Gamma}_0$, which are denoted by $\widetilde{f}$. Thus we define

$$\widetilde{H}^s(\Gamma_0) = \{f \in H^s(\Gamma) : f|_{\Gamma\setminus\overline{\Gamma}_0} = 0\} = \{f \in H^s(\Gamma) : \operatorname{supp} f \subset \overline{\Gamma}_0\} \tag{A.539}$$

as a subspace of $H^s(\Gamma)$ with the corresponding norm

$$\|f\|_{\widetilde{H}^s(\Gamma_0)} = \|\widetilde{f}\|_{H^s(\Gamma)}. \tag{A.540}$$

By definition, $\widetilde{H}^s(\Gamma_0) \subset H^s(\Gamma)$. For $s \geq 0$ we also introduce the space

$$H^s(\Gamma_0) = \{f = F|_{\Gamma_0} : F \in H^s(\Gamma)\}, \tag{A.541}$$

equipped with the norm

$$\|f\|_{H^s(\Gamma_0)} = \inf_{\substack{F\in H^s(\Gamma)\\ F|_{\Gamma_0}=f}} \|F\|_{H^s(\Gamma)}. \tag{A.542}$$

Clearly $\widetilde{H}^s(\Gamma_0) \subset H^s(\Gamma_0)$. The dual space $H^{-s}(\Gamma_0)$ with respect to the inner product in $L^2(\Gamma_0)$ is well defined by the completion of $L^2(\Gamma_0)$ with respect to the norm

$$\|f\|_{H^{-s}(\Gamma_0)} = \sup_{0\neq\varphi\in\widetilde{H}^s(\Gamma_0)} \frac{|(f,\varphi)_{L^2(\Gamma_0)}|}{\|\varphi\|_{\widetilde{H}^s(\Gamma_0)}}, \qquad s > 0. \tag{A.543}$$

Correspondingly, we also have the dual space $\widetilde{H}^{-s}(\Gamma_0)$ with the norm

$$\|f\|_{\widetilde{H}^{-s}(\Gamma_0)} = \sup_{0\neq\psi\in H^s(\Gamma_0)} \frac{|(f,\psi)_{L^2(\Gamma_0)}|}{\|\psi\|_{H^s(\Gamma_0)}}, \qquad s > 0. \tag{A.544}$$

It holds therefore that

$$H^{-s}(\Gamma_0) = \widetilde{H}^s(\Gamma_0)', \tag{A.545}$$

$$\widetilde{H}^{-s}(\Gamma_0) = H^s(\Gamma_0)'. \tag{A.546}$$

We have for $s > 0$ also the inclusions

$$\widetilde{H}^s(\Gamma_0) \subset H^s(\Gamma_0) \subset L^2(\Gamma_0) \subset \widetilde{H}^{-s}(\Gamma_0) \subset H^{-s}(\Gamma_0). \tag{A.547}$$

Similar as before, if $s < \frac{1}{2}$, then $\widetilde{H}^s(\Gamma_0) = H^s(\Gamma_0)$. For $s > \frac{1}{2}$, we note that $f \in \widetilde{H}^s(\Gamma_0)$ satisfies $f|_\gamma = 0$. Hence, we can introduce the space $H_0^s(\Gamma_0)$ as the completion of $\widetilde{H}^s(\Gamma_0)$ with respect to the norm $\|\cdot\|_{H^s(\Gamma_0)}$. It holds then that $\widetilde{H}^s(\Gamma_0) = H_0^s(\Gamma_0)$ if $s \neq m + \frac{1}{2}$ for $m \in \mathbb{N}_0$, and that $\widetilde{H}^{m+1/2}(\Gamma_0)$ is strictly contained in $H_0^{m+1/2}(\Gamma_0)$.

A.4.6 Imbeddings of Sobolev spaces

It is primarily the imbedding characteristics (vid. Section A.3) of Sobolev spaces that render these spaces so useful in analysis, especially in the study of differential and integral operators. By knowing the mapping properties of such an operator in terms of Sobolev spaces, for example, it can be determined whether the operator is continuous or compact.

In $\mathbb{R}^N$ we have the continuous imbedding

$$H^s(\mathbb{R}^N) \hookrightarrow H^t(\mathbb{R}^N) \qquad \text{for} \quad -\infty < t \leq s < \infty. \tag{A.548}$$

If $m \in \mathbb{N}_0$ and $0 \leq \alpha < 1$, then it holds that

$$H^s(\mathbb{R}^N) \hookrightarrow C^{m,\alpha}(\mathbb{R}^N) \qquad \text{for} \quad s > m + \alpha + \frac{N}{2}, \tag{A.549}$$

which holds also if $s = m + \alpha + \frac{N}{2}$ and $0 < \alpha < 1$.

We consider now a bounded strong Lipschitz domain $\Omega \in C^{0,1}$. Then we have the compact and continuous imbeddings

$$H^s(\Omega) \overset{c}{\hookrightarrow} H^t(\Omega) \qquad \text{for} \quad -\infty < t < s < \infty, \tag{A.550}$$

$$\widetilde{H}^s(\Omega) \overset{c}{\hookrightarrow} \widetilde{H}^t(\Omega) \qquad \text{for} \quad -\infty < t < s < \infty, \tag{A.551}$$

$$H^s(\Omega) \overset{c}{\hookrightarrow} C^{m,\alpha}(\overline{\Omega}) \qquad \text{for} \quad s > m + \alpha - \frac{N}{2}, \;\; 0 \leq \alpha < 1, \;\; m \in \mathbb{N}_0. \tag{A.552}$$

We have also the continuous imbedding

$$H^s(\Omega) \hookrightarrow C^{m,\alpha}(\overline{\Omega}) \qquad \text{for} \quad s = m + \alpha - \frac{N}{2}, \;\; 0 < \alpha < 1, \;\; m \in \mathbb{N}_0. \tag{A.553}$$

Let Γ be a boundary of class $C^{k,1}$, $k \in \mathbb{N}_0$, and let $|t|, |s| \leq k + \frac{1}{2}$. Then we have the compact imbeddings

$$H^s(\Gamma) \overset{c}{\hookrightarrow} H^t(\Gamma) \qquad \text{for} \quad t < s, \tag{A.554}$$

$$H^s(\Gamma) \overset{c}{\hookrightarrow} C^{m,\alpha}(\Gamma) \quad \text{for} \quad s > m + \alpha + \frac{N}{2} - \frac{1}{2}, \;\; 0 \leq \alpha < 1, \;\; m \in \mathbb{N}_0. \tag{A.555}$$

A.5 Vector calculus and elementary differential geometry

Vector calculus, also known as vector analysis, is a field in mathematics that is concerned with multi-variable real or complex analysis of vectors. Vector calculus is concerned with scalar fields, which associate a scalar to every point in space, and vector fields, which associate a vector to every point in space. Differential geometry is a mathematical discipline that uses the methods of differential and integral calculus to study problems in geometry. It has grown into a field that is concerned more generally with geometric structures on differentiable manifolds, being closely related to differential topology and with the geometric aspects of the theory of differential equations.

Our goal is not to give a complete survey, but rather to define roughly operators that arise in these disciplines and use them to state some important integral theorems, which are used throughout this thesis. The main references for our approach on these subjects are Lenoir (2005), Nédélec (2001), and Terrasse & Abboud (2006).

A.5.1 Differential operators on scalar and vector fields

We are herein interested in defining differential operators that act on complex scalar and vector fields in $\mathbb{R}^N$, in particular for $N = 2$ or 3. We define the scalar, inner, or dot product of two vectors $\boldsymbol{a}, \boldsymbol{b} \in \mathbb{C}^N$ by the scalar quantity

$$\boldsymbol{a} \cdot \boldsymbol{b} = \sum_{i=1}^{N} a_i \overline{b}_i, \tag{A.556}$$

where $\overline{z}$ stands for the complex conjugate of $z \in \mathbb{C}$. Some properties of the dot product, for $\boldsymbol{a}, \boldsymbol{b}, \boldsymbol{c} \in \mathbb{C}^N$, are

$$\boldsymbol{a} \cdot \boldsymbol{a} = |\boldsymbol{a}|^2, \tag{A.557}$$

$$\boldsymbol{a} \cdot \boldsymbol{b} = \overline{\boldsymbol{b} \cdot \boldsymbol{a}}, \tag{A.558}$$

$$\boldsymbol{a} \cdot (\boldsymbol{b} + \boldsymbol{c}) = \boldsymbol{a} \cdot \boldsymbol{b} + \boldsymbol{a} \cdot \boldsymbol{c}. \tag{A.559}$$

The vector or cross product of two vectors, on the other hand, is particular to three-dimensional space ($N = 3$). It is defined, for $\boldsymbol{a}, \boldsymbol{b} \in \mathbb{C}^3$, by the vector

$$\boldsymbol{a} \times \boldsymbol{b} = \begin{vmatrix} \hat{\boldsymbol{x}}_1 & \hat{\boldsymbol{x}}_2 & \hat{\boldsymbol{x}}_3 \\ a_1 & a_2 & a_3 \\ b_1 & b_2 & b_3 \end{vmatrix} = (a_2 b_3 - a_3 b_2)\hat{\boldsymbol{x}}_1 + (a_3 b_1 - a_1 b_3)\hat{\boldsymbol{x}}_2 + (a_1 b_2 - a_2 b_1)\hat{\boldsymbol{x}}_3, \tag{A.560}$$

where $\hat{\boldsymbol{x}}_1$, $\hat{\boldsymbol{x}}_2$, and $\hat{\boldsymbol{x}}_3$ are the canonical cartesian unit vectors in $\mathbb{R}^3$. We can define also a cross product in two dimensions ($N = 2$), which yields for $\boldsymbol{a}, \boldsymbol{b} \in \mathbb{C}^2$ the scalar value

$$\boldsymbol{a} \times \boldsymbol{b} = \begin{vmatrix} a_1 & a_2 \\ b_1 & b_2 \end{vmatrix} = a_1 b_2 - a_2 b_1. \tag{A.561}$$

The cross product satisfies, for $\boldsymbol{a}, \boldsymbol{b}, \boldsymbol{c} \in \mathbb{C}^N$ and $\alpha \in \mathbb{C}$, the identities

$$\boldsymbol{a} \times \boldsymbol{a} = \boldsymbol{0}, \tag{A.562}$$

$$\boldsymbol{a} \times \boldsymbol{b} = -\boldsymbol{b} \times \boldsymbol{a}, \tag{A.563}$$

$$\boldsymbol{a} \times (\boldsymbol{b} + \boldsymbol{c}) = \boldsymbol{a} \times \boldsymbol{b} + \boldsymbol{a} \times \boldsymbol{c}, \tag{A.564}$$

$$(\alpha \boldsymbol{a}) \times \boldsymbol{b} = \boldsymbol{a} \times (\alpha \boldsymbol{b}) = \alpha(\boldsymbol{a} \times \boldsymbol{b}). \tag{A.565}$$

In particular when $N = 3$, the dot and cross products satisfy, for $\boldsymbol{a}, \boldsymbol{b}, \boldsymbol{c}, \boldsymbol{d} \in \mathbb{C}^3$,

$$\boldsymbol{a} \cdot (\boldsymbol{b} \times \boldsymbol{c}) = \boldsymbol{b} \cdot (\boldsymbol{c} \times \boldsymbol{a}) = \boldsymbol{c} \cdot (\boldsymbol{a} \times \boldsymbol{b}), \tag{A.566}$$

$$\boldsymbol{a} \times (\boldsymbol{b} \times \boldsymbol{c}) = (\boldsymbol{a} \cdot \boldsymbol{c})\boldsymbol{b} - (\boldsymbol{a} \cdot \boldsymbol{b})\boldsymbol{c}, \tag{A.567}$$

$$(\boldsymbol{a} \times \boldsymbol{b}) \cdot (\boldsymbol{c} \times \boldsymbol{d}) = (\boldsymbol{a} \cdot \boldsymbol{c})(\boldsymbol{b} \cdot \boldsymbol{d}) - (\boldsymbol{a} \cdot \boldsymbol{d})(\boldsymbol{b} \cdot \boldsymbol{c}). \tag{A.568}$$

For $N = 2$ and $\boldsymbol{a}, \boldsymbol{b}, \boldsymbol{c}, \boldsymbol{d} \in \mathbb{C}^2$, it holds that

$$\boldsymbol{a}(\boldsymbol{b} \times \boldsymbol{c}) = \boldsymbol{b}(\boldsymbol{a} \times \boldsymbol{c}) - \boldsymbol{c}(\boldsymbol{a} \times \boldsymbol{b}), \tag{A.569}$$

$$(\boldsymbol{a} \times \boldsymbol{b})(\boldsymbol{c} \times \boldsymbol{d}) = (\boldsymbol{a} \cdot \boldsymbol{c})(\boldsymbol{b} \cdot \boldsymbol{d}) - (\boldsymbol{a} \cdot \boldsymbol{d})(\boldsymbol{b} \cdot \boldsymbol{c}). \tag{A.570}$$

Another vector operation is given by the dyadic, tensor, or outer product of two vectors, which results in a matrix and is defined, for $\boldsymbol{a}, \boldsymbol{b} \in \mathbb{C}^N$, by

$$\boldsymbol{a} \otimes \boldsymbol{b} = \boldsymbol{a}\, \boldsymbol{b}^* = \boldsymbol{a}\, \overline{\boldsymbol{b}}^T, \tag{A.571}$$

where $\boldsymbol{b}^*$ stands for the conjugated transpose of $\boldsymbol{b}$, being $\boldsymbol{b}^T$ the transposed vector. In three dimensions ($N = 3$) it is given by

$$\boldsymbol{a} \otimes \boldsymbol{b} = \begin{bmatrix} a_1 \\ a_2 \\ a_3 \end{bmatrix} \begin{bmatrix} \overline{b}_1 & \overline{b}_2 & \overline{b}_3 \end{bmatrix} = \begin{bmatrix} a_1\overline{b}_1 & a_1\overline{b}_2 & a_1\overline{b}_3 \\ a_2\overline{b}_1 & a_2\overline{b}_2 & a_2\overline{b}_3 \\ a_3\overline{b}_1 & a_3\overline{b}_2 & a_3\overline{b}_3 \end{bmatrix}, \tag{A.572}$$

whereas in two dimensions ($N = 2$) it takes the form of

$$\boldsymbol{a} \otimes \boldsymbol{b} = \begin{bmatrix} a_1 \\ a_2 \end{bmatrix} \begin{bmatrix} \overline{b}_1 & \overline{b}_2 \end{bmatrix} = \begin{bmatrix} a_1\overline{b}_1 & a_1\overline{b}_2 \\ a_2\overline{b}_1 & a_2\overline{b}_2 \end{bmatrix}. \tag{A.573}$$

The dyadic product satisfies, for $\boldsymbol{a}, \boldsymbol{b}, \boldsymbol{c} \in \mathbb{C}^N$ and $\alpha \in \mathbb{C}$, the properties

$$(\alpha \boldsymbol{a}) \otimes \boldsymbol{b} = \boldsymbol{a} \otimes (\alpha \boldsymbol{b}) = \alpha(\boldsymbol{a} \otimes \boldsymbol{b}), \tag{A.574}$$

$$\boldsymbol{a} \otimes (\boldsymbol{b} + \boldsymbol{c}) = \boldsymbol{a} \otimes \boldsymbol{b} + \boldsymbol{a} \otimes \boldsymbol{c}, \tag{A.575}$$

$$(\boldsymbol{a} + \boldsymbol{b}) \otimes \boldsymbol{c} = \boldsymbol{a} \otimes \boldsymbol{c} + \boldsymbol{b} \otimes \boldsymbol{c}. \tag{A.576}$$

It is interesting to observe that the $N \times N$ identity matrix $\boldsymbol{I}$ can be expressed as

$$\boldsymbol{I} = \sum_{i=1}^{N} \hat{\boldsymbol{x}}_i \otimes \hat{\boldsymbol{x}}_i, \tag{A.577}$$

being $\hat{\boldsymbol{x}}_i$, for $1 \leq i \leq N$, the canonical vectors in $\mathbb{R}^N$.

We define the gradient of a scalar field $f : \mathbb{R}^N \to \mathbb{C}$ as the vector field whose components are the partial derivatives of f, i.e.,

$$\operatorname{grad} f = \nabla f = \left(\frac{\partial f}{\partial x_1}, \frac{\partial f}{\partial x_2}, \ldots, \frac{\partial f}{\partial x_N} \right). \tag{A.578}$$

The divergence of a vector field $\boldsymbol{v} : \mathbb{R}^N \to \mathbb{C}^N$ is defined as the scalar field

$$\operatorname{div} \boldsymbol{v} = \nabla \cdot \boldsymbol{v} = \sum_{i=1}^{N} \frac{\partial v_i}{\partial x_i}. \tag{A.579}$$

The common notation $\nabla \cdot \boldsymbol{v}$ for the divergence is a convenient mnemonic, although it constitutes a slight abuse of notation and therefore we rather denote it by $\operatorname{div} \boldsymbol{v}$.

The curl or rotor of a vector field has no general formula that holds for all dimensions. It is particular to three-dimensional space, although generalizations to other dimensions have been performed by using exterior or wedge products. In three dimensions and in cartesian coordinates, the curl of a vector field $\boldsymbol{v} : \mathbb{R}^3 \to \mathbb{C}^3$ is defined as the vector field

$$\operatorname{curl} \boldsymbol{v} = \nabla \times \boldsymbol{v} = \left(\frac{\partial v_3}{\partial x_2} - \frac{\partial v_2}{\partial x_3} \right) \hat{\boldsymbol{x}}_1 + \left(\frac{\partial v_1}{\partial x_3} - \frac{\partial v_3}{\partial x_1} \right) \hat{\boldsymbol{x}}_2 + \left(\frac{\partial v_2}{\partial x_1} - \frac{\partial v_1}{\partial x_2} \right) \hat{\boldsymbol{x}}_3. \tag{A.580}$$

The curl can be also rewritten as a determinant or a matrix operation, namely

$$\operatorname{curl} \boldsymbol{v} = \begin{vmatrix} \hat{\boldsymbol{x}}_1 & \hat{\boldsymbol{x}}_2 & \hat{\boldsymbol{x}}_3 \\ \frac{\partial}{\partial x_1} & \frac{\partial}{\partial x_2} & \frac{\partial}{\partial x_3} \\ v_1 & v_2 & v_3 \end{vmatrix} = \begin{bmatrix} 0 & -\frac{\partial}{\partial x_3} & \frac{\partial}{\partial x_2} \\ \frac{\partial}{\partial x_3} & 0 & -\frac{\partial}{\partial x_1} \\ -\frac{\partial}{\partial x_2} & \frac{\partial}{\partial x_1} & 0 \end{bmatrix} \boldsymbol{v}. \tag{A.581}$$

In two dimensions we can define two different curls, a scalar and a vectorial one, which are respectively given, for $\boldsymbol{v} : \mathbb{R}^2 \to \mathbb{C}^2$ and $f : \mathbb{R}^2 \to \mathbb{C}$, by

$$\operatorname{curl} \boldsymbol{v} = \nabla \times \boldsymbol{v} = \begin{vmatrix} \frac{\partial}{\partial x_1} & \frac{\partial}{\partial x_2} \\ v_1 & v_2 \end{vmatrix} = \frac{\partial v_2}{\partial x_1} - \frac{\partial v_1}{\partial x_2}, \tag{A.582}$$

$$\operatorname{Curl} f = \begin{vmatrix} \hat{\boldsymbol{x}}_1 & \hat{\boldsymbol{x}}_2 \\ \frac{\partial f}{\partial x_1} & \frac{\partial f}{\partial x_2} \end{vmatrix} = \frac{\partial f}{\partial x_2} \hat{\boldsymbol{x}}_1 - \frac{\partial f}{\partial x_1} \hat{\boldsymbol{x}}_2. \tag{A.583}$$

The Laplace operator for a scalar field $f : \mathbb{R}^N \to \mathbb{C}$ is defined by

$$\Delta f = \sum_{i=1}^{N} \frac{\partial^2 f}{\partial x_i^2}, \tag{A.584}$$

whereas the Laplace operator for a vectorial field $\boldsymbol{v} : \mathbb{R}^N \to \mathbb{C}^N$ is given by

$$\Delta \boldsymbol{v} = \sum_{i=1}^{N} \frac{\partial^2 \boldsymbol{v}}{\partial x_i^2}. \tag{A.585}$$

The double-gradient or Hessian matrix of a scalar field $f : \mathbb{R}^N \to \mathbb{C}$ is the square matrix of its second-order partial derivatives, which is defined by

$$\nabla\nabla f = \boldsymbol{H} f = \nabla \otimes \nabla f = \begin{bmatrix} \frac{\partial^2 f}{\partial x_1^2} & \cdots & \frac{\partial^2 f}{\partial x_1 \partial x_N} \\ \vdots & \ddots & \vdots \\ \frac{\partial^2 f}{\partial x_N \partial x_1} & \cdots & \frac{\partial^2 f}{\partial x_N^2} \end{bmatrix}. \tag{A.586}$$

The following vector identities hold for $\boldsymbol{v} : \mathbb{R}^N \to \mathbb{C}^N$ and $f, g : \mathbb{R}^N \to \mathbb{C}$:

$$\nabla(fg) = f\nabla g + g\nabla f, \tag{A.587}$$

$$\operatorname{div}(f\boldsymbol{v}) = f \operatorname{div} \boldsymbol{v} + \nabla f \cdot \boldsymbol{v}, \tag{A.588}$$

$$\operatorname{curl}(f\boldsymbol{v}) = f \operatorname{curl} \boldsymbol{v} + \nabla f \times \boldsymbol{v}, \tag{A.589}$$

In three dimensions, for $\boldsymbol{v}, \boldsymbol{u} : \mathbb{R}^3 \to \mathbb{C}^3$ and $f : \mathbb{R}^3 \to \mathbb{C}$, we have in particular that

$$\Delta\boldsymbol{v} = \nabla \operatorname{div} \boldsymbol{v} - \operatorname{curl} \operatorname{curl} \boldsymbol{v}, \tag{A.590}$$

$$\Delta f = \operatorname{div} \nabla f, \tag{A.591}$$

$$\operatorname{div}(\boldsymbol{u} \times \boldsymbol{v}) = \boldsymbol{v} \cdot \operatorname{curl} \boldsymbol{u} - \boldsymbol{u} \cdot \operatorname{curl} \boldsymbol{v}, \tag{A.592}$$

$$\operatorname{curl}(\boldsymbol{u} \times \boldsymbol{v}) = (\boldsymbol{v} \cdot \nabla)\boldsymbol{u} - (\boldsymbol{u} \cdot \nabla)\boldsymbol{v} - \boldsymbol{v} \operatorname{div} \boldsymbol{u} + \boldsymbol{u} \operatorname{div} \boldsymbol{v}, \tag{A.593}$$

$$\nabla(\boldsymbol{u} \cdot \boldsymbol{v}) = (\boldsymbol{v} \cdot \nabla)\boldsymbol{u} + (\boldsymbol{u} \cdot \nabla)\boldsymbol{v} + \boldsymbol{v} \times \operatorname{curl} \boldsymbol{u} + \boldsymbol{u} \times \operatorname{curl} \boldsymbol{v}, \tag{A.594}$$

$$\operatorname{div} \operatorname{curl} \boldsymbol{v} = 0, \tag{A.595}$$

$$\operatorname{curl} \nabla f = \boldsymbol{0}, \tag{A.596}$$

whereas in two dimensions, for $\boldsymbol{v}, \boldsymbol{u} : \mathbb{R}^2 \to \mathbb{C}^2$ and $f, g : \mathbb{R}^2 \to \mathbb{C}$, it holds that

$$\Delta\boldsymbol{v} = \nabla \operatorname{div} \boldsymbol{v} - \operatorname{Curl} \operatorname{curl} \boldsymbol{v}, \tag{A.597}$$

$$\Delta f = \operatorname{div} \nabla f = -\operatorname{curl} \operatorname{Curl} f, \tag{A.598}$$

$$\operatorname{Curl}(fg) = f \operatorname{Curl} g + g \operatorname{Curl} f, \tag{A.599}$$

$$\operatorname{Curl}(\boldsymbol{u} \cdot \boldsymbol{v}) = \boldsymbol{u}^\perp \operatorname{div} \boldsymbol{v} + \boldsymbol{v}^\perp \operatorname{div} \boldsymbol{u} + (\boldsymbol{v} \times \nabla)\boldsymbol{u} + (\boldsymbol{u} \times \nabla)\boldsymbol{v}, \tag{A.600}$$

$$\operatorname{Curl}(\boldsymbol{u} \times \boldsymbol{v}) = \boldsymbol{u} \operatorname{div} \boldsymbol{v} - \boldsymbol{v} \operatorname{div} \boldsymbol{u} + (\boldsymbol{v} \cdot \nabla)\boldsymbol{u} - \boldsymbol{u} \cdot \nabla)\boldsymbol{v}, \tag{A.601}$$

$$\nabla(\boldsymbol{u} \cdot \boldsymbol{v}) = \boldsymbol{u} \operatorname{div} \boldsymbol{v} + \boldsymbol{v} \operatorname{div} \boldsymbol{u} - (\boldsymbol{v} \times \nabla)\boldsymbol{u}^\perp - (\boldsymbol{u} \times \nabla)\boldsymbol{v}^\perp, \tag{A.602}$$

$$\nabla(\boldsymbol{u} \times \boldsymbol{v}) = \boldsymbol{u} \operatorname{curl} \boldsymbol{v} - \boldsymbol{v} \operatorname{curl} \boldsymbol{u} - (\boldsymbol{v} \times \nabla)\boldsymbol{u} + (\boldsymbol{u} \times \nabla)\boldsymbol{v}, \tag{A.603}$$

$$\operatorname{Curl} f \times \boldsymbol{v} = \nabla f \cdot \boldsymbol{v}, \tag{A.604}$$

$$\operatorname{Curl} f = \nabla f^\perp, \tag{A.605}$$

$$\operatorname{div} \operatorname{Curl} f = 0, \tag{A.606}$$

$$\operatorname{Curl} \operatorname{div} \boldsymbol{v} = \boldsymbol{0}, \tag{A.607}$$

$$\operatorname{curl} \nabla f = 0, \tag{A.608}$$

$$\nabla \operatorname{curl} \boldsymbol{v} = \boldsymbol{0}, \tag{A.609}$$

where $\boldsymbol{v}^\perp = (v_2, -v_1)$ denotes the orthogonal vector to $\boldsymbol{v}$, which fulfills $\boldsymbol{v} \cdot \boldsymbol{v}^\perp = 0$.

A.5.2 Green's integral theorems

The Green's integral theorems constitute a generalization of the known integration-by-parts formula of integral calculus to functions with several variables. As is the case with the Green's function, these theorems are also named after the British mathematician and physicist George Green (1793–1841). They play a crucial role in the development of integral representations and equations for harmonic and scattering problems.

As shown in Figure A.16, we consider an open and bounded domain $\Omega \subset \mathbb{R}^N$, that has a regular (strong Lipschitz) boundary $\Gamma = \partial\Omega$, and where the unit surface normal $\boldsymbol{n}$ points outwards of Ω.

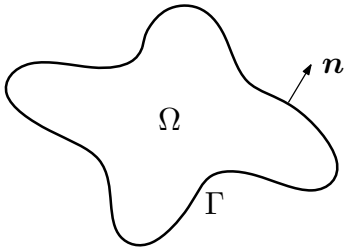

FIGURE A.16. Domain Ω for the Green's integral theorems.

The Gauss-Green theorem states that if $u \in H^1(\Omega)$, then

$$\int_\Omega \frac{\partial u}{\partial x_i}\,\mathrm{d}\boldsymbol{x} = \int_\Gamma u\, n_i\,\mathrm{d}\gamma \qquad (i = 1, \ldots, N), \tag{A.610}$$

which is directly related to the divergence theorem for a vector field (stated below).

The integration-by-parts formula in several variables is given, for $u, v \in H^1(\Omega)$, by

$$\int_\Omega \frac{\partial u}{\partial x_i} v\,\mathrm{d}\boldsymbol{x} = -\int_\Omega u \frac{\partial v}{\partial x_i}\,\mathrm{d}\boldsymbol{x} + \int_\Gamma u\, v\, n_i\,\mathrm{d}\gamma \qquad (i = 1, \ldots, N), \tag{A.611}$$

which is obtained by applying the Gauss-Green theorem (A.610) to $u\,v$.

Green's first integral theorem states, for $u \in H^2(\Omega)$ and $v \in H^1(\Omega)$, that

$$\int_\Omega \Delta u\, v\,\mathrm{d}\boldsymbol{x} = -\int_\Omega \nabla u \cdot \nabla v\,\mathrm{d}\boldsymbol{x} + \int_\Gamma \frac{\partial u}{\partial n}\, v\,\mathrm{d}\gamma, \tag{A.612}$$

obtained by employing (A.611) with $v = \partial u/\partial x_i$. The theorem still remains valid for somewhat less regular functions u, v such that $u, v \in H^1(\Omega)$ and $\Delta u \in L^2(\Omega)$, that is, when $u \in H^1(\Delta;\Omega)$. In this case the integral on Γ in (A.612) has to be understood in general in the sense of the duality product between $H^{-1/2}(\Gamma)$ and $H^{1/2}(\Gamma)$.

Similarly, by combining adequately u and v in (A.612) we obtain Green's second integral theorem, given, for $u, v \in H^2(\Omega)$, by

$$\int_\Omega (u\Delta v - v\Delta u)\,\mathrm{d}\boldsymbol{x} = \int_\Gamma \left(u\frac{\partial v}{\partial n} - v\frac{\partial u}{\partial n}\right)\mathrm{d}\gamma, \tag{A.613}$$

which holds also for $u, v \in H^1(\Omega)$ such that $\Delta u, \Delta v \in L^2(\Omega)$, i.e., for $u, v \in H^1(\Delta;\Omega)$. Again, in the latter case we have to consider in general the integrals on Γ in the sense of the duality product between $H^{-1/2}(\Gamma)$ and $H^{1/2}(\Gamma)$.

A.5.3 Divergence integral theorem

The divergence theorem, also known as Gauss's theorem, is related to the divergence of a vector field. It states that if $\Omega \subset \mathbb{R}^N$ is an open and bounded domain with a regular (strong

Lipschitz) boundary Γ and with a unit surface normal $\boldsymbol{n}$ pointing outwards of Ω as shown in Figure A.16, then we have for all $u \in H^1(\Omega)$ and $\boldsymbol{v} \in H^1(\Omega)^N$ that

$$\int_\Omega \operatorname{div}(u\,\boldsymbol{v})\,\mathrm{d}\boldsymbol{x} = \int_\Omega (\nabla u \cdot \boldsymbol{v} + u \operatorname{div} \boldsymbol{v})\,\mathrm{d}\boldsymbol{x} = \int_\Gamma u\,\boldsymbol{v} \cdot \boldsymbol{n}\,\mathrm{d}\gamma. \tag{A.614}$$

By considering $u = 1$ we obtain the following simpler version of the divergence theorem:

$$\int_\Omega \operatorname{div} \boldsymbol{v}\,\mathrm{d}\boldsymbol{x} = \int_\Gamma \boldsymbol{v} \cdot \boldsymbol{n}\,\mathrm{d}\gamma. \tag{A.615}$$

The divergence theorem can be proven from the integration-by-parts formula (A.611). In three-dimensional space, in particular, the divergence theorem relates a volume integral over Ω (on the left-hand side) with a surface integral on Γ (on the right-hand side). More adjusted functional spaces for the divergence theorem that still allow to define traces on the boundary can be found in the book of Nédélec (2001).

A.5.4 Curl integral theorem

The curl theorem, also known as Stokes' theorem after the Irish mathematician and physicist Sir George Gabriel Stokes (1819–1903), is related with the curl of a vector field and holds in three-dimensional space. There are, though, adaptations for other dimensions.

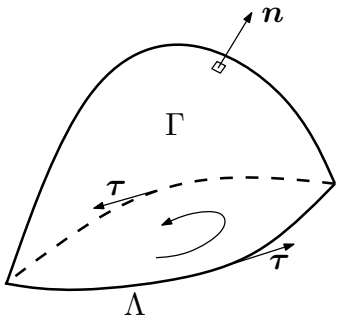

FIGURE A.17. Surface Γ for Stokes' integral theorem.

This integral theorem considers an oriented smooth surface $\Gamma \subset \mathbb{R}^3$ that is bounded by a simple, closed, and smooth boundary curve $\Lambda = \partial\Gamma$. The curve Λ has thus a positive orientation, i.e., it is described counterclockwise according to the direction of the unit tangent $\boldsymbol{\tau}$ when the unit normal $\boldsymbol{n}$ of the surface Γ points towards the viewer, as shown in Figure A.17, following the right-hand rule. The curl theorem states then for $u \in H^1(\Gamma)$ and $\boldsymbol{v} \in H^1(\Gamma)^3$ that

$$\int_\Gamma (\nabla u \times \boldsymbol{v} + u \operatorname{curl} \boldsymbol{v}) \cdot \boldsymbol{n}\,\mathrm{d}\gamma = \int_\Lambda u\,\boldsymbol{v} \cdot \boldsymbol{\tau}\,\mathrm{d}\lambda. \tag{A.616}$$

By considering $u = 1$ we obtain the following simpler version of the curl theorem:

$$\int_\Gamma \operatorname{curl} \boldsymbol{v} \cdot \boldsymbol{n}\,\mathrm{d}\gamma = \int_\Lambda \boldsymbol{v} \cdot \boldsymbol{\tau}\,\mathrm{d}\lambda. \tag{A.617}$$

The curl theorem relates thus a surface integral over Γ with a line integral on Λ. We remark that if the surface Γ is closed, then the line integrals on Λ, located on the right-hand side of (A.616) and (A.617), become zero. As with Green's theorems, more adjusted functional spaces so as to still allow to define traces on the boundary can be also defined for the curl theorem. We refer to the book of Nédélec (2001) for further details.

A.5.5 Other integral theorems

We can derive also other integral theorems from the previous ones, being particularly useful for this purpose the integration-by-parts formula (A.611). Let Ω be a domain in $\mathbb{R}^N$, for $N = 2$ or 3, whose boundary Γ is regular and whose unit normal points outwards of the domain, as shown in Figure A.16.

In three-dimensional space ($N = 3$) and for $\boldsymbol{u}, \boldsymbol{v} \in H^1(\Omega)^3$ it holds that

$$\int_\Omega (\boldsymbol{v} \cdot \operatorname{curl} \boldsymbol{u} - \boldsymbol{u} \cdot \operatorname{curl} \boldsymbol{v}) \, \mathrm{d}\boldsymbol{x} = \int_\Gamma \boldsymbol{u} \cdot (\boldsymbol{v} \times \boldsymbol{n}) \, \mathrm{d}\gamma. \tag{A.618}$$

In two dimensions ($N = 2$), for $u \in H^1(\Omega)$ and $\boldsymbol{v} \in H^1(\Omega)^2$, we have that

$$\int_\Omega (\boldsymbol{v} \cdot \operatorname{Curl} u - u \operatorname{curl} \boldsymbol{v}) \, \mathrm{d}\boldsymbol{x} = \int_\Gamma u \, (\boldsymbol{v} \times \boldsymbol{n}) \, \mathrm{d}\gamma. \tag{A.619}$$

By considering now the Gauss-Green theorem (A.610) and a function $u \in H^2(\Omega)$, we obtain the relation

$$\int_\Omega \frac{\partial^2 u}{\partial x_i \partial x_j} \, \mathrm{d}\boldsymbol{x} = \int_\Gamma \frac{\partial u}{\partial x_j} \, n_i \, \mathrm{d}\gamma = \int_\Gamma \frac{\partial u}{\partial x_i} \, n_j \, \mathrm{d}\gamma \qquad i, j = 1, \ldots, N. \tag{A.620}$$

A.5.6 Elementary differential geometry

When dealing with trace spaces, we need to work sometimes with differential operators on a regular surface Γ that is defined by a system of local charts, as the one shown in Figure A.15. We are interested herein in a short and elementary introduction to this kind of operators, and for simplicity we will avoid the language of differential forms that is usual in differential geometry, although all the operators which we will describe are of such nature.

Let Γ be the regular boundary (e.g., of class C^2) of a domain Ω in $\mathbb{R}^N$, for $N = 2$ or 3, which has a unit normal $\boldsymbol{n}$ that points outwards of Ω, as depicted in Figure A.16. For every point $\boldsymbol{x} \in \mathbb{R}^N$ we denote by $d(\boldsymbol{x}, \Gamma)$ the distance from $\boldsymbol{x}$ to the boundary Γ, given by

$$d(\boldsymbol{x}, \Gamma) = \inf_{\boldsymbol{y} \in \Gamma} |\boldsymbol{x} - \boldsymbol{y}|. \tag{A.621}$$

A collection of points whose distance to the boundary is less than ε is called a tubular neighborhood of Γ. Such a neighborhood Ω_ε is thus defined by

$$\Omega_\varepsilon = \{\boldsymbol{x} \in \mathbb{R}^N : \ d(\boldsymbol{x}, \Gamma) < \varepsilon\} = \Omega_\varepsilon^+ \cup \Gamma \cup \Omega_\varepsilon^-, \tag{A.622}$$

where

$$\Omega_\varepsilon^+ = \{\boldsymbol{x} \in \overline{\Omega}^c : \ d(\boldsymbol{x}, \Gamma) < \varepsilon\} \qquad \text{and} \qquad \Omega_\varepsilon^- = \{\boldsymbol{x} \in \Omega : \ d(\boldsymbol{x}, \Gamma) < \varepsilon\}. \tag{A.623}$$

For ε small enough and when the boundary is regular and oriented, any point $\boldsymbol{x}$ in such a neighborhood Ω_ε has a unique projection $\boldsymbol{x}_\Gamma = \mathcal{P}_\Gamma(\boldsymbol{x})$ on the boundary Γ which satisfies

$$|\boldsymbol{x} - \boldsymbol{x}_\Gamma| = d(\boldsymbol{x}, \Gamma). \tag{A.624}$$

For a regular boundary Γ that admits a tangent plane at the point $\boldsymbol{x}_\Gamma$, the line $\boldsymbol{x} - \boldsymbol{x}_\Gamma$ is directed along the normal of the boundary at this point. Inside Ω_ε the function $d(\boldsymbol{x}, \Gamma)$ is regular. We introduce the vector field

$$\boldsymbol{n}(\boldsymbol{x}) = \begin{cases} \nabla d(\boldsymbol{x}, \Gamma) & \text{if } \boldsymbol{x} \in \Omega_\varepsilon^+, \\ -\nabla d(\boldsymbol{x}, \Gamma) & \text{if } \boldsymbol{x} \in \Omega_\varepsilon^-, \end{cases} \tag{A.625}$$

which extends in a continuous manner the unit normal $\boldsymbol{n}$ on Γ, and is such that

$$\boldsymbol{n}(\boldsymbol{x}) = \boldsymbol{n}(\boldsymbol{x}_\Gamma) \quad \forall \boldsymbol{x} \in \Omega_\varepsilon, \quad \text{where } \boldsymbol{x}_\Gamma = \mathcal{P}_\Gamma(\boldsymbol{x}). \tag{A.626}$$

Any point $\boldsymbol{x}$ in the tubular neighborhood Ω_ε can be parametrically described by

$$\boldsymbol{x} = \boldsymbol{x}(\boldsymbol{x}_\Gamma, s) = \boldsymbol{x}_\Gamma + s\,\boldsymbol{n}(\boldsymbol{x}_\Gamma), \qquad -\varepsilon \le s \le \varepsilon, \tag{A.627}$$

where $\boldsymbol{x}_\Gamma \in \Gamma$ and

$$s = \begin{cases} d(\boldsymbol{x}, \Gamma), & \text{if } \boldsymbol{x} \in \Omega_\varepsilon^+, \\ -d(\boldsymbol{x}, \Gamma), & \text{if } \boldsymbol{x} \in \Omega_\varepsilon^-. \end{cases} \tag{A.628}$$

The tubular neighborhood can be parametrized as

$$\Omega_\varepsilon = \{\boldsymbol{x} = \boldsymbol{x}_\Gamma + s\,\boldsymbol{n}(\boldsymbol{x}_\Gamma) : \quad \boldsymbol{x}_\Gamma \in \Gamma, \quad -\varepsilon < s < \varepsilon\}, \tag{A.629}$$

and similarly

$$\Omega_\varepsilon^+ = \{\boldsymbol{x} = \boldsymbol{x}_\Gamma + s\,\boldsymbol{n}(\boldsymbol{x}_\Gamma) : \quad \boldsymbol{x}_\Gamma \in \Gamma, \quad 0 < s < \varepsilon\}, \tag{A.630}$$

$$\Omega_\varepsilon^- = \{\boldsymbol{x} = \boldsymbol{x}_\Gamma + s\,\boldsymbol{n}(\boldsymbol{x}_\Gamma) : \quad \boldsymbol{x}_\Gamma \in \Gamma, \quad -\varepsilon < s < 0\}. \tag{A.631}$$

For any fixed s such that $-\varepsilon < s < \varepsilon$, we introduce the surface

$$\Gamma_s = \{\boldsymbol{x} = \boldsymbol{x}_\Gamma + s\,\boldsymbol{n}(\boldsymbol{x}_\Gamma) : \quad \boldsymbol{x}_\Gamma \in \Gamma\}. \tag{A.632}$$

The field $\boldsymbol{n}(\boldsymbol{x})$ is always normal to Γ_s. We remark that

$$\boldsymbol{n}(\boldsymbol{x}) = \nabla s(\boldsymbol{x}) \qquad \forall \boldsymbol{x} \in \Omega_\varepsilon. \tag{A.633}$$

The derivative with respect to s of a regular function defined on the tubular neighborhood Ω_ε is confounded with the normal derivative of the function on Γ_s. Let u be a regular scalar function defined on Γ. We denote now by $\tilde{u}$ the lifting of u defined on Ω_ε that is constant along the normal direction, and thus given by

$$\tilde{u}(\boldsymbol{x}) = \tilde{u}\big(\boldsymbol{x}_\Gamma + s\,\boldsymbol{n}(\boldsymbol{x}_\Gamma)\big) = u(\boldsymbol{x}_\Gamma). \tag{A.634}$$

We introduce now some differential operators, which act on functions defined on the surfaces Γ and Γ_s. The tangential gradient $\nabla_\Gamma u$ is defined as

$$\nabla_\Gamma u = \mathrm{grad}_\Gamma u = \nabla \tilde{u}|_\Gamma, \tag{A.635}$$

which is the gradient of $\tilde{u}$ restricted to Γ. In the same way we can define the operator $\nabla_{\Gamma_s} u$. It can be proven that if u is any regular function defined on the tubular neighborhood Ω_ε,

then for any point $\boldsymbol{x} = \boldsymbol{x}_\Gamma + s\,\boldsymbol{n}(\boldsymbol{x}_\Gamma)$, and in particular for $s = 0$, it holds that

$$\nabla u = \nabla_{\Gamma_s} u + \frac{\partial u}{\partial s}\boldsymbol{n}. \tag{A.636}$$

The tangential curl or rotational of the scalar function u is defined as

$$\operatorname{Curl}_\Gamma u = \begin{cases} \operatorname{curl}(\tilde{u}\,\boldsymbol{n})|_\Gamma & \text{if } N = 3, \\ \operatorname{Curl}\tilde{u}|_\Gamma & \text{if } N = 2. \end{cases} \tag{A.637}$$

The field of normals is a gradient, which implies that when $N = 3$, then

$$\operatorname{curl}\boldsymbol{n} = \boldsymbol{0}. \tag{A.638}$$

By using (A.589) we obtain that the tangential curl in three dimensions is also given by

$$\operatorname{Curl}_\Gamma u = \nabla_\Gamma u \times \boldsymbol{n}. \tag{A.639}$$

The definition of a tangential vector field's lifting is not so straightforward as in (A.634) for a scalar field (cf. Nédélec 2001). In this case we have to consider also a curvature operator of the form

$$\mathcal{R}_s = \nabla\boldsymbol{n} = \nabla \otimes \boldsymbol{n}, \tag{A.640}$$

where the gradient of a vector is understood again in the sense of a dyadic or tensor product. The curvature operator $\mathcal{R}_s$ is a symmetric tensor acting on the tangent plane, and its normal derivative is given by

$$\frac{\partial}{\partial s}\mathcal{R}_s = -\mathcal{R}_s^2. \tag{A.641}$$

On the surface Γ (when $s = 0$), we omit the index s. The diffeomorphism from Γ onto Γ_s defined by $\boldsymbol{x} = \boldsymbol{x}_\Gamma + s\,\boldsymbol{n}(\boldsymbol{x}_\Gamma)$ has now $\boldsymbol{x}_\Gamma = \boldsymbol{x} - s\,\boldsymbol{n}(\boldsymbol{x})$ as its inverse, and it satisfies

$$\mathcal{R}(\boldsymbol{x}_\Gamma) - \mathcal{R}_s(\boldsymbol{x}) = s\mathcal{R}_s(\boldsymbol{x})\mathcal{R}(\boldsymbol{x}_\Gamma) = s\mathcal{R}(\boldsymbol{x}_\Gamma)\mathcal{R}_s(\boldsymbol{x}), \tag{A.642}$$

$$\big(I + s\mathcal{R}(\boldsymbol{x}_\Gamma)\big)^{-1} = I - s\mathcal{R}_s(\boldsymbol{x}). \tag{A.643}$$

A regular tangential vector field $\boldsymbol{v}$ defined on Γ has to be extended towards the tubular neighborhood Ω_ε as

$$\tilde{\boldsymbol{v}}(\boldsymbol{x}) = \boldsymbol{v}(\boldsymbol{x}_\Gamma) - s\mathcal{R}_s(\boldsymbol{x})\boldsymbol{v}(\boldsymbol{x}_\Gamma), \tag{A.644}$$

which corresponds to a constant extension along the normal direction, where the tangential components of the vector are rotated proportionally with the distance s. We note that in two dimensions the curvature operator has no effect, but it is important in three dimensions due the degrees of freedom of the tangent planes. The surface divergence of the vector field $\boldsymbol{v}$ is now defined as

$$\operatorname{div}_\Gamma \boldsymbol{v} = \operatorname{div}\tilde{\boldsymbol{v}}|_\Gamma, \tag{A.645}$$

while its surface curl is given by the scalar field

$$\operatorname{curl}_\Gamma \boldsymbol{v} = \begin{cases} (\operatorname{curl}\tilde{\boldsymbol{v}} \cdot \boldsymbol{n})|_\Gamma & \text{if } N = 3, \\ \operatorname{curl}\tilde{\boldsymbol{v}}|_\Gamma & \text{if } N = 2. \end{cases} \tag{A.646}$$

For $N = 3$ it holds that

$$\operatorname{curl}_\Gamma \boldsymbol{v} = \operatorname{div}_\Gamma(\boldsymbol{v} \times \boldsymbol{n}). \tag{A.647}$$

Similarly as in (A.639), we have in the two-dimensional case ($N = 2$) that

$$\operatorname{curl}_\Gamma(u\,\boldsymbol{n}) = \nabla_\Gamma u \times \boldsymbol{n}. \tag{A.648}$$

The Laplace-Beltrami operator or scalar surface Laplacian is defined by

$$\Delta_\Gamma u = \operatorname{div}_\Gamma \nabla_\Gamma u = -\operatorname{curl}_\Gamma \operatorname{Curl}_\Gamma u, \tag{A.649}$$

whereas the Hodge operator or vectorial Laplacian is given by

$$\Delta_\Gamma \boldsymbol{v} = \nabla_\Gamma \operatorname{div}_\Gamma \boldsymbol{v} - \operatorname{Curl}_\Gamma \operatorname{curl}_\Gamma \boldsymbol{v}. \tag{A.650}$$

It holds also that

$$\operatorname{div}_\Gamma \operatorname{Curl}_\Gamma u = 0, \qquad \operatorname{Curl}_\Gamma \operatorname{div}_\Gamma \boldsymbol{v} = \boldsymbol{0}, \tag{A.651}$$

$$\operatorname{curl}_\Gamma \nabla_\Gamma u = 0, \qquad \nabla_\Gamma \operatorname{curl}_\Gamma \boldsymbol{v} = \boldsymbol{0}. \tag{A.652}$$

If Γ is a closed boundary surface, $u \in C^1(\Gamma)$ a scalar function, and $\boldsymbol{v} \in C^1(\Gamma)^{N-1}$ a tangential vector field, then the following Stokes' identities hold:

$$\int_\Gamma \nabla_\Gamma u \cdot \boldsymbol{v}\,\mathrm{d}\gamma = -\int_\Gamma u \operatorname{div}_\Gamma \boldsymbol{v}\,\mathrm{d}\gamma, \tag{A.653}$$

$$\int_\Gamma \operatorname{Curl}_\Gamma u \cdot \boldsymbol{v}\,\mathrm{d}\gamma = \int_\Gamma u \operatorname{curl}_\Gamma \boldsymbol{v}\,\mathrm{d}\gamma. \tag{A.654}$$

Similarly, if $u, v \in C^1(\Gamma)$, then we have also that

$$\int_\Gamma u \operatorname{Curl}_\Gamma v\,\mathrm{d}\gamma = -\int_\Gamma v \operatorname{Curl}_\Gamma u\,\mathrm{d}\gamma. \tag{A.655}$$

For $u \in C^2(\Gamma)$ and $v \in C^1(\Gamma)$ it holds that

$$-\int_\Gamma \Delta_\Gamma u\, v\,\mathrm{d}\gamma = \int_\Gamma \nabla_\Gamma u \cdot \nabla_\Gamma v\,\mathrm{d}\gamma = \int_\Gamma \operatorname{Curl}_\Gamma u \cdot \operatorname{Curl}_\Gamma v\,\mathrm{d}\gamma. \tag{A.656}$$

If $\boldsymbol{u} \in C^2(\Gamma)^{N-1}$ and $\boldsymbol{v} \in C^1(\Gamma)^{N-1}$ are tangential vector fields, then

$$-\int_\Gamma \Delta_\Gamma \boldsymbol{u} \cdot \boldsymbol{v}\,\mathrm{d}\gamma = \int_\Gamma \operatorname{div}_\Gamma \boldsymbol{u} \operatorname{div}_\Gamma \boldsymbol{v}\,\mathrm{d}\gamma + \int_\Gamma \operatorname{curl}_\Gamma \boldsymbol{u} \operatorname{curl}_\Gamma \boldsymbol{v}\,\mathrm{d}\gamma. \tag{A.657}$$

Finally, by considering (A.620) and $u \in C^2(\Gamma)$ we can derive the Stokes' type formulae

$$\int_\Gamma (\nabla_\Gamma u \times \boldsymbol{n})\,\mathrm{d}\gamma = \int_\Gamma \operatorname{Curl}_\Gamma u\,\mathrm{d}\gamma = \boldsymbol{0} \qquad (N = 3), \tag{A.658}$$

$$\int_\Gamma (\nabla_\Gamma u \times \boldsymbol{n})\,\mathrm{d}\gamma = \int_\Gamma \operatorname{curl}_\Gamma (u\,\boldsymbol{n})\,\mathrm{d}\gamma = 0 \qquad (N = 2). \tag{A.659}$$

A.6 Theory of distributions

The theory of generalized functions or distributions was invented in order to give a solid theoretical foundation to the Dirac delta function. The solid foundation of the theory was developed in 1945 by the French mathematician Laurent Schwartz (1915–2002). Today, this theory is fundamental in the study of partial differential equations, and comes naturally into use in the treatment of boundary integral equations. Of special importance is the notion of weak or distributional derivative of an integrable function, which is used in the definition of Sobolev spaces (vid. Section A.4).

The computation of Green's functions is performed naturally in the framework of the theory of distributions, due the appearance of Dirac masses in its definition. It is therefore important to have some notions of its characteristics. A complete survey of the theory of distributions can be found in Gel'fand & Shilov (1964) and Schwartz (1978). Other references for this theory and its applications are Bony (2001), Bremermann (1965), Chen & Zhou (1992), Estrada & Kanwal (2002), Gasquet & Witomski (1999), Griffel (1985), Hsiao & Wendland (2008), and Rudin (1973).

A.6.1 Definition of distribution

Let Ω be a domain in $\mathbb{R}^N$. We denote as test functions in Ω the elements of the space $C_0^\infty(\Omega)$ of indefinitely differentiable functions with compact support in Ω. The support of a function is the closure of the set of points where the function does not vanish. The space $C_0^\infty(\Omega)$ is also denoted by $\mathcal{D}(\Omega)$ and has a Fréchet space structure. We say that a sequence $\{\varphi_n\}$ of test functions converges to φ in $\mathcal{D}(\Omega)$ if there exists a compact set $K \subset \Omega$ such that $\operatorname{supp}(\varphi_n - \varphi) \subset K$ for every n, and if for each multi-index $\boldsymbol{\alpha} \in \mathbb{N}_0^N$,

$$\lim_{n\to\infty} D^{\boldsymbol{\alpha}}\varphi_n(\boldsymbol{x}) = D^{\boldsymbol{\alpha}}\varphi(\boldsymbol{x}), \quad \text{uniformly on } K. \tag{A.660}$$

We define a continuous linear functional T on $\mathcal{D}(\Omega)$ as a mapping from $\mathcal{D}(\Omega)$ to the field $\mathbb{K}$ (either $\mathbb{C}$ or $\mathbb{R}$), denoted by $\langle T, \varphi\rangle$ for $\varphi \in \mathcal{D}(\Omega)$, that satisfies

$$\langle T, \alpha\varphi_1 + \beta\varphi_2\rangle = \alpha\,\langle T, \varphi_1\rangle + \beta\,\langle T, \varphi_2\rangle \qquad \forall\alpha,\beta \in \mathbb{K},\ \ \forall\varphi_1,\varphi_2 \in \mathcal{D}(\Omega), \tag{A.661}$$

and is such that

$$\varphi_n \to 0 \ \text{ in } \ \mathcal{D}(\Omega) \quad \Longrightarrow \quad \langle T, \varphi_n\rangle \to 0 \ \text{ in } \ \mathbb{K}. \tag{A.662}$$

Such a continuous linear functional is called a distribution or generalized function. The space of (Schwartz) distributions is denoted by $\mathcal{D}'(\Omega)$ and corresponds to the dual space of $\mathcal{D}(\Omega)$. Thus, the bilinear form $\langle\cdot,\cdot\rangle : \mathcal{D}'(\Omega) \times \mathcal{D}(\Omega) \to \mathbb{K}$ represents the duality product between both spaces. Strictly speaking, when the underlying field $\mathbb{K}$ is taken as $\mathbb{C}$, then the duality product should be considered as a sesquilinear form and the distributions as antilinear functionals. Nonetheless, for the sake of simplicity this is not usually done, since the results in $\mathcal{D}'(\Omega)$ are the same with the exception of a complex conjugation on the test functions in $\mathcal{D}(\Omega)$. We note that the space $\mathcal{D}'(\Omega)$ has the weak*-topology of the dual space (cf. Rudin 1973). The vector space and convergence operations in $\mathcal{D}'(\Omega)$ can be

summarized, if $T, S, T_n \in \mathcal{D}'(\Omega)$ and $\alpha, \beta \in \mathbb{K}$, by

$$\langle \alpha T + \beta S, \varphi \rangle = \alpha \langle T, \varphi \rangle + \beta \langle S, \varphi \rangle \qquad \forall \varphi \in \mathcal{D}(\Omega), \tag{A.663}$$

and

$$T_n \to T \text{ in } \mathcal{D}'(\Omega) \iff \langle T_n, \varphi \rangle \to \langle T, \varphi \rangle \text{ in } \mathbb{K} \qquad \forall \varphi \in \mathcal{D}(\Omega). \tag{A.664}$$

Distributions may be also multiplied by indefinitely differentiable functions to form new distributions. If $T \in \mathcal{D}'(\Omega)$ and $\eta \in C^\infty(\Omega)$, then the product $\eta\, T \in \mathcal{D}'(\Omega)$ is defined by

$$\langle \eta\, T, \varphi \rangle = \langle T, \eta\, \varphi \rangle \qquad \forall \varphi \in \mathcal{D}(\Omega). \tag{A.665}$$

We remark, however, that the product of two distributions is not well-defined in general.

Every locally integrable function $f \in L^1_{\text{loc}}(\Omega)$ defines a distribution via

$$\langle f, \varphi \rangle = \int_\Omega f(\boldsymbol{x}) \varphi(\boldsymbol{x}) \, \mathrm{d}\boldsymbol{x} \qquad \forall \varphi \in \mathcal{D}(\Omega). \tag{A.666}$$

The distribution f is said to be generated by the function f. A distribution that is generated by a locally integrable function is called a regular distribution. All other distributions are called singular. This suggests the notation

$$\langle T, \varphi \rangle = \int_\Omega T(\boldsymbol{x}) \varphi(\boldsymbol{x}) \, \mathrm{d}\boldsymbol{x} \tag{A.667}$$

for a continuous linear functional T even when T is not an L^1_{loc} function.

A.6.2 Differentiation of distributions

Let us now define the important operation of differentiation on distributions. For any $T \in \mathcal{D}'(\Omega)$, we define $D^{\boldsymbol{\alpha}} T$ to be a linear functional such that

$$\langle D^{\boldsymbol{\alpha}} T, \varphi \rangle = (-1)^{|\boldsymbol{\alpha}|} \langle T, D^{\boldsymbol{\alpha}} \varphi \rangle \qquad \forall \varphi \in \mathcal{D}(\Omega), \tag{A.668}$$

for a given multi-index $\boldsymbol{\alpha} \in \mathbb{N}_0^N$. It is not difficult to see that $D^{\boldsymbol{\alpha}} T$ itself is again a continuous linear functional, i.e., a distribution. When T is a function such that $D^{\boldsymbol{\beta}} T \in L^1_{\text{loc}}(\Omega)$ for all $|\boldsymbol{\beta}| \leq |\boldsymbol{\alpha}|$, then the definition (A.668) amounts to no more than integration by parts. But when T does not admit classical derivatives, then (A.668) still allows to differentiate in the sense of distributions, shifting the burden of differentiability from T to φ. Thus every distribution in $\mathcal{D}'(\Omega)$ possesses derivatives of arbitrary orders. This is particularly useful when dealing with discontinuous functions, since even for them there exist well-defined derivatives in the distributional sense.

We now define the concept of a weak or distributional derivative of a locally integrable function $f \in L^1_{\text{loc}}(\Omega)$. There may or may not exist a function $g_{\boldsymbol{\alpha}} \in L^1_{\text{loc}}(\Omega)$ such that $D^{\boldsymbol{\alpha}} f = g_{\boldsymbol{\alpha}}$ in $\mathcal{D}'(\Omega)$. If such a $g_{\boldsymbol{\alpha}}$ exists, it is unique up to sets of measure zero, it is called the weak or distributional partial derivative of f, and it satisfies

$$\int_\Omega g_{\boldsymbol{\alpha}}(\boldsymbol{x}) \varphi(\boldsymbol{x}) \, \mathrm{d}\boldsymbol{x} = (-1)^{|\boldsymbol{\alpha}|} \int_\Omega f(\boldsymbol{x}) D^{\boldsymbol{\alpha}} \varphi(\boldsymbol{x}) \, \mathrm{d}\boldsymbol{x} \qquad \forall \varphi \in \mathcal{D}(\Omega). \tag{A.669}$$

If f is sufficiently smooth to have a continuous partial derivative $D^{\boldsymbol{\alpha}} f$ in the classical sense, then $D^{\boldsymbol{\alpha}} f$ is also a distributional partial derivative of f. Of course $D^{\boldsymbol{\alpha}} f$ may exist in the distributional sense without existing in the classical sense.

A.6.3 Primitives of distributions

Taking a primitive from a distribution amounts to the same as when dealing with functions. Let us begin with the case $N = 1$ by supposing that $\Omega \subset \mathbb{R}$. In this case, if $T \in \mathcal{D}'(\Omega)$, then a distribution S such that

$$\langle S', \varphi \rangle = \langle T, \varphi \rangle \qquad \forall \varphi \in \mathcal{D}(\Omega) \tag{A.670}$$

is called a primitive or antiderivative of T. Any distribution $T \in \mathcal{D}'(\Omega)$ has a primitive S in $\mathcal{D}'(\Omega)$ which is unique up to an additive constant, i.e., all the primitives of T are of the form $S + C$, where C is some constant.

We have further that any distribution $T \in \mathcal{D}'(\Omega)$, for $N = 1$, has primitives of any order. A primitive of m-th order of T is a distribution $R \in \mathcal{D}'(\Omega)$ such that

$$\langle R^{(m)}, \varphi \rangle = \langle T, \varphi \rangle \qquad \forall \varphi \in \mathcal{D}(\Omega). \tag{A.671}$$

The primitive of m-th order is unique up to an additive polynomial of order $m - 1$.

Furthermore, in the general case when $N \geq 1$, for any $T \in \mathcal{D}'(\Omega)$ there exists a distribution S such that $\partial S / \partial x_j = T$ in $\mathcal{D}'(\Omega)$, being $j \in \{1, \ldots, N\}$. This primitive is unique up to an additive locally integrable function that does not depend upon x_j. Thus every distribution possesses primitives of arbitrary order.

A.6.4 Dirac's delta function

The Dirac delta or impulse function δ, which is not strictly speaking a function, was introduced by the British theoretical physicist Paul Adrien Maurice Dirac (1902–1984) as a technical device in the mathematical formulation of quantum mechanics. The Dirac delta vanishes everywhere except at the origin, where its value is infinite, and so that its integral has a value of one. It is therefore defined by

$$\delta(\boldsymbol{x}) = \begin{cases} \infty & \text{if } \boldsymbol{x} = \mathbf{0}, \\ 0 & \text{if } \boldsymbol{x} \neq \mathbf{0}, \end{cases} \tag{A.672}$$

and has the property

$$\int_{\Omega} \delta(\boldsymbol{x}) \, \mathrm{d}\boldsymbol{x} = 1 \qquad \text{if } \mathbf{0} \in \Omega. \tag{A.673}$$

There exists no function with these properties. However, the Dirac delta is well-defined as a distribution, in which case it associates to each test function φ its value at the origin. Assuming that $\mathbf{0} \in \Omega$, the Dirac delta is defined as the distribution δ that satisfies

$$\int_{\Omega} \delta(\boldsymbol{x}) \varphi(\boldsymbol{x}) \, \mathrm{d}\boldsymbol{x} = \varphi(\mathbf{0}) \qquad \forall \varphi \in \mathcal{D}(\Omega). \tag{A.674}$$

The linear functional δ defined on $\mathcal{D}(\Omega)$ by

$$\langle \delta, \varphi \rangle = \varphi(\mathbf{0}) \tag{A.675}$$

is continuous, and hence clearly a distribution on Ω.

From (A.674) several other properties for the Dirac delta δ can be derived. It is a symmetric distribution, i.e., $\delta(\boldsymbol{x}) = \delta(-\boldsymbol{x})$, and its support is the point $\boldsymbol{x} = \mathbf{0}$. The shifted Dirac mass, $\delta_{\boldsymbol{a}}(\boldsymbol{x}) = \delta(\boldsymbol{x} - \boldsymbol{a})$, has its mass concentrated at the point $\boldsymbol{a} \in \Omega$. It thus picks out the conjugated value of a test function φ at the point $\boldsymbol{a}$, namely

$$\langle \delta_{\boldsymbol{a}}, \varphi \rangle = \langle \delta(\boldsymbol{x} - \boldsymbol{a}), \varphi(\boldsymbol{x}) \rangle = \langle \delta(\boldsymbol{x}), \varphi(\boldsymbol{x} + \boldsymbol{a}) \rangle = \varphi(\boldsymbol{a}) \qquad \forall \varphi \in \mathcal{D}(\Omega). \tag{A.676}$$

A scaling of the Dirac mass by $\lambda \in \mathbb{K}$, $\lambda \neq 0$, yields

$$\langle \delta(\lambda \boldsymbol{x}), \varphi(\boldsymbol{x}) \rangle = |\lambda|^{-N} \langle \delta(\boldsymbol{x}), \varphi(\boldsymbol{x}/\lambda) \rangle = |\lambda|^{-N} \varphi(\mathbf{0}) \qquad \forall \varphi \in \mathcal{D}(\Omega), \tag{A.677}$$

and hence

$$\delta(\lambda \boldsymbol{x}) = |\lambda|^{-N} \delta(\boldsymbol{x}). \tag{A.678}$$

An arbitrary derivative of the dirac Delta function, $D^{\boldsymbol{\alpha}}\delta$, is given by

$$\langle D^{\boldsymbol{\alpha}}\delta, \varphi \rangle = (-1)^{|\boldsymbol{\alpha}|} D^{\boldsymbol{\alpha}} \varphi(\mathbf{0}) \qquad \forall \varphi \in \mathcal{D}(\Omega). \tag{A.679}$$

We remark that the multi-dimensional Dirac mass can be decomposed as a multiplication of one-dimensional Dirac deltas, namely

$$\delta(\boldsymbol{x}) = \prod_{j=1}^{N} \delta(x_j). \tag{A.680}$$

An important fact is that Dirac distributions appear when differentiating functions that have jumps. To see this, we consider, e.g., for $\Omega = \mathbb{R}$, the Heaviside step function

$$H(x) = \begin{cases} 1 & \text{if } x > 0, \\ 0 & \text{if } x < 0, \end{cases} \tag{A.681}$$

which is named after the self-taught English electrical engineer, mathematician, and physicist Oliver Heaviside (1850–1925), who developed this function among several other important contributions. The Heaviside function belongs to $L^1_{\text{loc}}(\mathbb{R})$, and defines thus a regular distribution, namely

$$\langle H, \varphi \rangle = \int_0^\infty \varphi(x) \, \mathrm{d}x \qquad \forall \varphi \in \mathcal{D}(\mathbb{R}). \tag{A.682}$$

The function H is differentiable everywhere with pointwise derivative zero, except at the origin, where it is non-differentiable in the classical sense. The distributional derivative H' of H satisfies

$$\langle H', \varphi \rangle = -\langle H, \varphi' \rangle = -\int_0^\infty \varphi'(x) \, \mathrm{d}x = \varphi(0). \tag{A.683}$$

Therefore we have

$$H'(x) = \delta(x) \qquad \text{in } \mathbb{R}. \tag{A.684}$$

The Dirac delta can be also generalized to consider line or surface mass distributions. For a line or a surface $\Gamma \subset \Omega$, we define the Dirac distribution δ_Γ as

$$\langle \delta_\Gamma, \varphi \rangle = \int_\Gamma \varphi(\boldsymbol{x}) \, \mathrm{d}\gamma(\boldsymbol{x}) \qquad \forall \varphi \in \mathcal{D}(\Omega). \tag{A.685}$$

This type of Dirac distributions appear, e.g., when differentiating over a jump that extends along a line or a surface. Further generalizations of the Dirac distribution that use the language of differential forms can be found in Gel'fand & Shilov (1964).

A.6.5 Principal value and finite parts

Let us study some special singular distributions. For the sake of simplicity we consider $\Omega = \mathbb{R}$, i.e., $N = 1$. In this case, the function $f(x) = 1/x$, defined for $x \neq 0$, is not integrable around the origin. Thus we cannot associate a distribution with f, and we will have the same problem with any rational function having a real pole. The difficulty is that the integrand has a singularity so strong that it must be excised from the domain and the integral has to be defined by a limiting process, the result of which is called an improper integral. This inconvenient, though, can be solved. Although f is not locally integrable, its primitive $F(x) = \ln|x|$ is locally integrable, being its indefinite integral $x \ln|x| - x$. The distribution that helps to solve our problem is simply the derivative of F in the sense of distributions. This distribution is now well-defined and is called the principal value, being denoted by $\mathrm{pv}(1/x)$. We take symmetric limits (ϵ and $-\epsilon$) around the origin and obtain

$$\lim_{\epsilon \to 0^+} \left\{ \int_{-\infty}^{-\epsilon} \frac{\varphi(x)}{x}\,\mathrm{d}x + \int_{\epsilon}^{\infty} \frac{\varphi(x)}{x}\,\mathrm{d}x \right\} = -\int_{-\infty}^{\infty} \ln|x|\,\varphi'(x)\,\mathrm{d}x \qquad \forall \varphi \in \mathcal{D}(\mathbb{R}). \tag{A.686}$$

The distribution $\mathrm{pv}(1/x)$, which is the natural choice for a distribution corresponding to $1/x$, is thus defined by

$$\langle \mathrm{pv}(1/x), \varphi \rangle = -\langle \ln|x|, \varphi' \rangle \qquad \forall \varphi \in \mathcal{D}(\mathbb{R}). \tag{A.687}$$

We can interpret this equation as follows: to evaluate the improper integral $\int_{-\infty}^{\infty} \varphi(x)/x\,\mathrm{d}x$, integrate it by parts as if it were a convergent integral. The result is the convergent integral $\int_{-\infty}^{\infty} \ln|x|\varphi'(x)\,\mathrm{d}x$. The integration by parts is not justified, but this procedure gives the result (A.687) of our rigorous definitions, and can be therefore regarded as a formal procedure to obtain the results of the correct theory. The principal value of $1/x$ satisfies

$$x\ \mathrm{pv}\left(\frac{1}{x}\right) = 1, \tag{A.688}$$

and is characterized by

$$\mathrm{pv}\left(\frac{1}{x}\right) = (\ln|x|)'. \tag{A.689}$$

The converse of (A.688), though, does not apply. A distribution T satisfies $x\,T = 1$ if and only if for some constant C

$$T(x) = \mathrm{pv}\left(\frac{1}{x}\right) + C\,\delta(x). \tag{A.690}$$

In general, if f is a function defined for $x \neq 0$, then we define the (Cauchy) principal value of the integral $\int_{-\infty}^{\infty} f(x)\,\mathrm{d}x$ by

$$\mathrm{pv}\left(\int_{-\infty}^{\infty} f(x)\,\mathrm{d}x\right) = \fint_{-\infty}^{\infty} f(x)\,\mathrm{d}x = \lim_{\epsilon \to 0^+} \int_{|x| \geq \epsilon} f(x)\,\mathrm{d}x, \tag{A.691}$$

whenever the limit exists. As expressed in (A.691), the notation $\fint$ is also used to denote a Cauchy principal value for the integral.

We remark that the concept of principal value applies likewise and more in general to contour integrals in the complex plane. In this case we consider a complex-valued function $f(z)$, for $z \in \mathbb{C}$, with a pole on the integration contour L. The pole is enclosed with a circle of radius ϵ and the portion of the path lying outside this circle is denoted by $L(\epsilon)$. Provided that the function $f(z)$ is integrable over $L(\epsilon)$, the Cauchy principal value is defined now as the limit

$$\mathrm{pv}\left(\int_L f(z)\,\mathrm{d}z\right) = \fint_L f(z)\,\mathrm{d}z = \lim_{\epsilon\to 0}\int_{L(\epsilon)} f(z)\,\mathrm{d}z. \tag{A.692}$$

We can define distributions corresponding to other negative powers of x, but the principal value cannot be used to assign a definite value to $\int_{-\infty}^{\infty}\varphi(x)/x^n\,\mathrm{d}x$, because it does not exist if $n > 1$. In this case the integral is truly divergent. We therefore define negative powers directly as derivatives of $\ln|x|$. For any integer $n > 1$, we define the distribution x^{-n} to be the n-th derivative of

$$F(x) = \frac{(-1)^{n-1}}{(n-1)!}\ln|x|. \tag{A.693}$$

This procedure is known as extracting the finite part of a divergent integral, and is denoted by $\mathrm{fp}(1/x^n)$. It is equivalent to

$$\langle \mathrm{fp}(1/x^n), \varphi\rangle = \frac{(-1)^{n-1}}{(n-1)!}\langle \ln|x|, \varphi^{(n)}\rangle \qquad \forall\varphi \in \mathcal{D}(\mathbb{R}), \tag{A.694}$$

and can be again interpreted as integrating n times by parts until the integral becomes convergent. This formal procedure was invented in 1932 by the French mathematician Jacques Salomon Hadamard (1865–1963), long before the development of the theory of distributions, as a convenient device for dealing with divergent integrals appearing in the theory of wave propagation.

A.7 Fourier transforms

The Fourier transform is a special integral transform that decomposes a function described in the spatial (or temporal) domain into a continuous spectrum of its frequency components. It is named in honor of the French mathematician and physicist Jean Baptiste Joseph Fourier (1768–1830), who initiated the investigation of Fourier series and their application to problems of heat flow. Fourier transforms have many applications, particularly because they allow to treat differential equations as algebraic equations in the spectral domain. Sobolev spaces of fractional order are also defined by means of Fourier transforms (vid. Section A.4).

Fourier transforms are frequently used in the computation of Green's functions in free-space or in half-spaces, since usually explicit expressions of them in the spectral domain can easily be found. It is, however, sometimes quite difficult to find the corresponding spatial counterpart. In this thesis, in particular, we deal widely with Fourier transforms to find Green's functions in the half-space problems. Some references are Bony (2001), Bremermann (1965), Gasquet & Witomski (1999), Griffel (1985), Reed & Simon (1980), and Weisstein (2002). Applications for Fourier transforms in signal analysis and complex variables may be found respectively in Irarrázaval (1999) and Weinberger (1995). For further studies on signals and wavelets we refer to Mallat (2000), and for applications in biomedical imaging, to Ammari (2008). Useful tables of integrals to compute Fourier transforms can be found in Bateman (1954) and Gradshteyn & Ryzhik (2007). Other Fourier transforms of special functions, particularly of Bessel functions and their spherical versions, are listed in Magnus & Oberhettinger (1954).

A.7.1 Definition of Fourier transform

We define the direct or forward Fourier transform $\widehat{f} = \mathcal{F}\{f\}$ of an integrable function $f \in L^1(\mathbb{R}^N)$ as

$$\widehat{f}(\boldsymbol{\xi}) = \frac{1}{(2\pi)^{N/2}} \int_{\mathbb{R}^N} f(\boldsymbol{x})\, e^{-i\boldsymbol{\xi}\cdot\boldsymbol{x}}\, \mathrm{d}\boldsymbol{x}, \qquad \boldsymbol{\xi} \in \mathbb{R}^N, \tag{A.695}$$

and its inverse or backward Fourier transform $f = \mathcal{F}^{-1}\{\widehat{f}\,\}$ by

$$f(\boldsymbol{x}) = \frac{1}{(2\pi)^{N/2}} \int_{\mathbb{R}^N} \widehat{f}(\boldsymbol{\xi})\, e^{i\boldsymbol{\xi}\cdot\boldsymbol{x}}\, \mathrm{d}\boldsymbol{\xi}, \qquad \boldsymbol{x} \in \mathbb{R}^N. \tag{A.696}$$

We remark that there exist several different definitions for the Fourier transform. Some authors do not distribute the $(2\pi)^N$ coefficient that lies before the integrals symmetrically between both transforms as we do, but assign it completely to the inverse Fourier transform. Other authors prefer to consider in the Fourier domain a frequency variable $\boldsymbol{\nu}$ instead of our pulsation variable $\boldsymbol{\xi}$, being their relation $\boldsymbol{\xi} = 2\pi\boldsymbol{\nu}$, and avoiding thus the need of the beforementioned coefficient $(2\pi)^N$. Thus, care has to be taken to identify the definition used by each author, since different Fourier transform pairs result from them.

The Fourier transforms (A.695) and (A.696) can be used also for a more general class of functions f, such as for functions in $L^2(\mathbb{R}^N)$ or even for tempered distributions in the

space $\mathcal{S}'(\mathbb{R}^N)$, the dual of the Schwartz space of rapidly decreasing functions

$$\mathcal{S}(\mathbb{R}^N) = \big\{ f \in C^\infty(\mathbb{R}^N) \mid \boldsymbol{x}^{\boldsymbol{\beta}} D^{\boldsymbol{\alpha}} f \in L^\infty(\mathbb{R}^N) \quad \forall \boldsymbol{\alpha}, \boldsymbol{\beta} \in \mathbb{N}_0^N \big\}, \tag{A.697}$$

where $\boldsymbol{x}^{\boldsymbol{\beta}} = x_1^{\beta_1} x_2^{\beta_2} \cdots x_N^{\beta_N}$ for a multi-index $\boldsymbol{\beta} \in \mathbb{N}_0^N$. The space $\mathcal{S}(\mathbb{R}^N)$ has the important property of being invariant under Fourier transforms, i.e., $\varphi \in \mathcal{S}(\mathbb{R}^N) \Leftrightarrow \widehat{\varphi} \in \mathcal{S}(\mathbb{R}^N)$. We have in particular the inclusion $\mathcal{D}(\mathbb{R}^N) \subset \mathcal{S}(\mathbb{R}^N)$, and thus $\mathcal{S}'(\mathbb{R}^N) \subset \mathcal{D}'(\mathbb{R}^N)$. The convergence in $\mathcal{S}'(\mathbb{R}^N)$ is the same as for distributions (vid. Section A.6), but with respect to test functions in $\mathcal{S}(\mathbb{R}^N)$. In effect, if $T_n, T \in \mathcal{S}'(\mathbb{R}^N)$, then

$$T_n \to T \ \text{ in } \ \mathcal{S}'(\mathbb{R}^N) \quad \Longleftrightarrow \quad \langle T_n, \varphi \rangle \to \langle T, \varphi \rangle \ \text{ in } \ \mathbb{K} \qquad \forall \varphi \in \mathcal{S}(\mathbb{R}^N). \tag{A.698}$$

A distribution $T \in \mathcal{D}'(\mathbb{R}^N)$ is at the same time a tempered distribution, i.e., $T \in \mathcal{S}'(\mathbb{R}^N)$, if and only if T is a continuous linear functional on $\mathcal{D}(\mathbb{R}^N)$ in the topology of $\mathcal{S}(\mathbb{R}^N)$. In particular, every function in $L^p(\mathbb{R}^N)$, $p \geq 1$, is a tempered distribution. Every slowly increasing function $f \in L^1_{\text{loc}}(\mathbb{R}^N)$ such that

$$|f(\boldsymbol{x})| \leq C\Big(1 + |\boldsymbol{x}|^M\Big) \qquad \forall \boldsymbol{x} \in \mathbb{R}^N, \tag{A.699}$$

for some constant $C > 0$ and some integer $M \in \mathbb{N}$, is also a tempered distribution. In general, for any tempered distribution $T \in \mathcal{S}'(\mathbb{R}^N)$, there are integers $n_1, n_2, \ldots, n_p$ and slowly increasing continuous functions $f_1, f_2, \ldots, f_p$ such that

$$T = \sum_{j=1}^{p} f_j^{(n_j)}. \tag{A.700}$$

The direct Fourier transform $\widehat{T} = \mathcal{F}\{T\}$ of a tempered distribution $T \in \mathcal{S}'(\mathbb{R}^N)$ is now defined by

$$\langle \widehat{T}, \varphi \rangle = \langle T, \widehat{\varphi} \rangle \qquad \forall \varphi \in \mathcal{S}(\mathbb{R}^N). \tag{A.701}$$

We have that $\widehat{T}$ is also a tempered distribution, because the Fourier transform is a continuous linear operator on $\mathcal{S}(\mathbb{R}^N)$. Formula (A.701) extends the Fourier transform from $L^1(\mathbb{R}^N)$ or $L^2(\mathbb{R}^N)$ to tempered distributions. The inverse Fourier transform $T = \mathcal{F}^{-1}\{\widehat{T}\}$ of a tempered distribution $\widehat{T} \in \mathcal{S}'(\mathbb{R}^N)$ is defined by

$$\langle T, \widehat{\varphi} \rangle = \langle \widehat{T}, \varphi \rangle \qquad \forall \widehat{\varphi} \in \mathcal{S}(\mathbb{R}^N). \tag{A.702}$$

The Fourier transform is thus a linear, 1-to-1, bicontinuous mapping from $\mathcal{S}'(\mathbb{R}^N)$ to $\mathcal{S}'(\mathbb{R}^N)$. For all $T \in \mathcal{S}'(\mathbb{R}^N)$ we have

$$\mathcal{F}^{-1}\left\{\mathcal{F}\{T\}\right\} = \mathcal{F}\left\{\mathcal{F}^{-1}\{T\}\right\} = T. \tag{A.703}$$

A.7.2 Properties of Fourier transforms

In what follows, we consider arbitrary distributions $S, T \in \mathcal{S}'(\mathbb{R}^N)$, and arbitrary constants $\alpha, \beta \in \mathbb{K}$, $\boldsymbol{a} \in \mathbb{R}^N$, and $b \in \mathbb{R}$. We write

$$T(\boldsymbol{x}) \quad \xrightarrow{\ \mathcal{F}\ } \quad \widehat{T}(\boldsymbol{\xi}) \tag{A.704}$$

to denote that $\widehat{T}(\boldsymbol{\xi})$ is the Fourier transform of $T(\boldsymbol{x})$, i.e., $\widehat{T} = \mathcal{F}\{T\}$. The linearity of the Fourier transform implies that

$$\alpha\, S(\boldsymbol{x}) + \beta\, T(\boldsymbol{x}) \quad \xrightarrow{\mathcal{F}} \quad \alpha\, \widehat{S}(\boldsymbol{\xi}) + \beta\, \widehat{T}(\boldsymbol{\xi}). \tag{A.705}$$

The duality or symmetry property of the Fourier transform means that

$$\widehat{T}(\boldsymbol{x}) \quad \xrightarrow{\mathcal{F}} \quad T(-\boldsymbol{\xi}). \tag{A.706}$$

The reflection property yields

$$T(-\boldsymbol{x}) \quad \xrightarrow{\mathcal{F}} \quad \widehat{T}(-\boldsymbol{\xi}). \tag{A.707}$$

The translation or shifting property states that

$$T(\boldsymbol{x} - \boldsymbol{a}) \quad \xrightarrow{\mathcal{F}} \quad e^{-i\boldsymbol{a}\cdot\boldsymbol{\xi}}\, \widehat{T}(\boldsymbol{\xi}), \tag{A.708}$$

$$e^{i\boldsymbol{a}\cdot\boldsymbol{x}}\, T(\boldsymbol{x}) \quad \xrightarrow{\mathcal{F}} \quad \widehat{T}(\boldsymbol{\xi} - \boldsymbol{a}). \tag{A.709}$$

The scaling property, for $a_1, a_2, \ldots, a_N \neq 0$, yields

$$T\left(\frac{x_1}{a_1}, \frac{x_2}{a_2}, \ldots, \frac{x_N}{a_N}\right) \quad \xrightarrow{\mathcal{F}} \quad |a_1 a_2 \cdots a_N|\, \widehat{T}(a_1\xi_1, a_2\xi_2, \ldots, a_N\xi_N), \tag{A.710}$$

$$T(a_1 x_1, a_2 x_2, \ldots, a_N x_N) \quad \xrightarrow{\mathcal{F}} \quad \frac{1}{|a_1 a_2 \cdots a_N|}\, \widehat{T}\left(\frac{\xi_1}{a_1}, \frac{\xi_2}{a_2}, \ldots, \frac{\xi_N}{a_N}\right), \tag{A.711}$$

and, in particular, for $b \neq 0$,

$$T\left(\frac{\boldsymbol{x}}{b}\right) \quad \xrightarrow{\mathcal{F}} \quad |b|^N\, \widehat{T}(b\,\boldsymbol{\xi}), \tag{A.712}$$

$$T(b\,\boldsymbol{x}) \quad \xrightarrow{\mathcal{F}} \quad \frac{1}{|b|^N}\, \widehat{T}\left(\frac{\boldsymbol{\xi}}{b}\right). \tag{A.713}$$

The modulation property implies that

$$T(\boldsymbol{x})\cos(\boldsymbol{a}\cdot\boldsymbol{x}) \quad \xrightarrow{\mathcal{F}} \quad \frac{1}{2}\Big(\widehat{T}(\boldsymbol{\xi} - \boldsymbol{a}) + \widehat{T}(\boldsymbol{\xi} + \boldsymbol{a})\Big), \tag{A.714}$$

$$\frac{1}{2}\Big(T(\boldsymbol{x} - \boldsymbol{a}) + T(\boldsymbol{x} + \boldsymbol{a})\Big) \quad \xrightarrow{\mathcal{F}} \quad \widehat{T}(\boldsymbol{\xi})\cos(\boldsymbol{a}\cdot\boldsymbol{\xi}). \tag{A.715}$$

The parity property of the Fourier transform involves that

$$T \text{ even} \quad \xrightarrow{\mathcal{F}} \quad \widehat{T} \text{ even}, \tag{A.716}$$

$$T \text{ odd} \quad \xrightarrow{\mathcal{F}} \quad \widehat{T} \text{ odd}, \tag{A.717}$$

$$T \text{ real and even} \quad \xrightarrow{\mathcal{F}} \quad \widehat{T} \text{ real and even}, \tag{A.718}$$

$$T \text{ real and odd} \quad \xrightarrow{\mathcal{F}} \quad \widehat{T} \text{ imaginary and odd}, \tag{A.719}$$

$$T \text{ imaginary and even} \quad \xrightarrow{\mathcal{F}} \quad \widehat{T} \text{ imaginary and even}, \tag{A.720}$$

$$T \text{ imaginary and odd} \quad \xrightarrow{\mathcal{F}} \quad \widehat{T} \text{ real and odd}. \tag{A.721}$$

For the complex conjugation we have that

$$\overline{T(\boldsymbol{x})} \quad \xrightarrow{\mathcal{F}} \quad \overline{\widehat{T}(-\boldsymbol{\xi})}. \tag{A.722}$$

The important derivation property of the Fourier transform, that transforms derivatives into multiplications by monomials, is given by

$$\frac{\partial T}{\partial x_j}(\boldsymbol{x}) \quad \xrightarrow{\mathcal{F}} \quad i\xi_j\,\widehat{T}(\boldsymbol{\xi}), \qquad j \in \{1,2,\ldots,N\}, \tag{A.723}$$

$$D^{\boldsymbol{\alpha}}T(\boldsymbol{x}) \quad \xrightarrow{\mathcal{F}} \quad (i\boldsymbol{\xi})^{\boldsymbol{\alpha}}\,\widehat{T}(\boldsymbol{\xi}), \qquad \boldsymbol{\alpha} \in \mathbb{N}_0^N, \tag{A.724}$$

which holds also for the inverses

$$-ix_j\,T(\boldsymbol{x}) \quad \xrightarrow{\mathcal{F}} \quad \frac{\partial \widehat{T}}{\partial \xi_j}(\boldsymbol{\xi}), \qquad j \in \{1,2,\ldots,N\}, \tag{A.725}$$

$$(-i\boldsymbol{x})^{\boldsymbol{\alpha}}\,T(\boldsymbol{x}) \quad \xrightarrow{\mathcal{F}} \quad D^{\boldsymbol{\alpha}}\widehat{T}(\boldsymbol{\xi}), \qquad \boldsymbol{\alpha} \in \mathbb{N}_0^N. \tag{A.726}$$

The integration property, for $j \in \{1,2,\ldots,N\}$, states that

$$\int_{-\infty}^{x_j} T|_{x_j=y_j}(\boldsymbol{x})\,\mathrm{d}y_j \quad \xrightarrow{\mathcal{F}} \quad \frac{\widehat{T}(\boldsymbol{\xi})}{i\xi_j} + \pi\delta(\xi_j)\widehat{T}|_{\xi_j=0}(\boldsymbol{\xi}), \tag{A.727}$$

and similarly

$$-\frac{T(\boldsymbol{x})}{ix_j} + \pi\delta(x_j)T|_{x_j=0}(\boldsymbol{x}) \quad \xrightarrow{\mathcal{F}} \quad \int_{-\infty}^{\xi_j} \widehat{T}|_{\xi_j=\eta_j}(\boldsymbol{\xi})\,\mathrm{d}\eta_j. \tag{A.728}$$

We say that a distribution $T \in \mathcal{S}'(\mathbb{R}^N)$, is separable if there exist some distributions $T_j \in \mathcal{S}'(\mathbb{R})$, for $j \in \{1,2,\ldots,N\}$, such that

$$T(\boldsymbol{x}) = T_1(x_1)T_2(x_2)\cdots T_N(x_N). \tag{A.729}$$

The separability property of the Fourier transform states that if T is a separable distribution, then so is $\widehat{T}$, i.e.,

$$T_1(x_1)T_2(x_2)\cdots T_N(x_N) \quad \xrightarrow{\mathcal{F}} \quad \widehat{T}_1(\xi_1)\widehat{T}_2(\xi_2)\cdots\widehat{T}_N(\xi_N). \tag{A.730}$$

This means that for separable distributions we can compute independently the partial Fourier transform of each factor, and multiply the results at the end. This property holds also if a distribution is partially separable, i.e., separable for only some of its variables.

We have that if $f \in L^2(\mathbb{R}^N)$, then its Fourier transform $\widehat{f}$ is in $L^2(\mathbb{R}^N)$ too. We have also, for $f, g \in L^1(\mathbb{R}^N)$ or $f, g \in L^2(\mathbb{R}^N)$, that

$$\int_{\mathbb{R}^N} \widehat{f}(\boldsymbol{x})g(\boldsymbol{x})\,\mathrm{d}\boldsymbol{x} = \int_{\mathbb{R}^N} f(\boldsymbol{x})\widehat{g}(\boldsymbol{x})\,\mathrm{d}\boldsymbol{x}. \tag{A.731}$$

Furthermore, if $f, g \in L^2(\mathbb{R}^N)$, then we have Parseval's formula

$$\int_{\mathbb{R}^N} f(\boldsymbol{x})\overline{g(\boldsymbol{x})}\,\mathrm{d}\boldsymbol{x} = \int_{\mathbb{R}^N} \widehat{f}(\boldsymbol{\xi})\overline{\widehat{g}(\boldsymbol{\xi})}\,\mathrm{d}\boldsymbol{\xi}, \tag{A.732}$$

named after the French mathematician Marc-Antoine Parseval des Chênes (1755–1836). In particular, when $f = g$, then (A.732) turns into Plancherel's formula

$$\int_{\mathbb{R}^N} |f(\boldsymbol{x})|^2\,\mathrm{d}\boldsymbol{x} = \int_{\mathbb{R}^N} |\widehat{f}(\boldsymbol{\xi})|^2\,\mathrm{d}\boldsymbol{\xi}, \tag{A.733}$$

which is named after the Swiss mathematician Michel Plancherel (1885–1967).

A.7.3 Convolution

We define the convolution or faltung $f * g$ of two functions f and g from $\mathbb{R}^N$ to $\mathbb{K}$, if it exists, as

$$f(\boldsymbol{x}) * g(\boldsymbol{x}) = \int_{\mathbb{R}^N} f(\boldsymbol{y}) g(\boldsymbol{x} - \boldsymbol{y}) \, \mathrm{d}\boldsymbol{y} = \int_{\mathbb{R}^N} f(\boldsymbol{x} - \boldsymbol{y}) g(\boldsymbol{y}) \, \mathrm{d}\boldsymbol{y}. \tag{A.734}$$

The convolution has the property of regularizing a function by averaging, and is a commutative operation, i.e.,

$$f(\boldsymbol{x}) * g(\boldsymbol{x}) = g(\boldsymbol{x}) * f(\boldsymbol{x}). \tag{A.735}$$

The convolution is well-defined if $f, g \in L^2(\mathbb{R}^N)$. It can be further shown that the convolution $L^p(\mathbb{R}^N) * L^q(\mathbb{R}^N)$ is well-defined for $p, q, r \geq 1$ and such that $\frac{1}{p} + \frac{1}{q} - 1 = \frac{1}{r}$. In this case, if $f \in L^p(\mathbb{R}^N)$ and $g \in L^q(\mathbb{R}^N)$, then $f * g$ is in $L^r(\mathbb{R}^N)$. Moreover, the notion of convolution can be extended to the framework of distributions, in which case the convolutions $\mathcal{D}(\mathbb{R}^N) * \mathcal{D}'(\mathbb{R}^N)$, $\mathcal{S}(\mathbb{R}^N) * \mathcal{S}'(\mathbb{R}^N)$, $\mathcal{E}(\mathbb{R}^N) * \mathcal{E}'(\mathbb{R}^N)$, and even $\mathcal{E}'(\mathbb{R}^N) * \mathcal{S}'(\mathbb{R}^N)$ and $\mathcal{E}'(\mathbb{R}^N) * \mathcal{D}'(\mathbb{R}^N)$ are well-defined. By $\mathcal{E}'(\mathbb{R}^N)$ we denote the subspace of $\mathcal{D}'(\mathbb{R}^N)$ of those distributions that have compact support, which is the dual of $\mathcal{E}(\mathbb{R}^N) = C^\infty(\mathbb{R}^N)$. It can be shown that $\mathcal{E}'(\mathbb{R}^N)$ is also a linear subspace of $\mathcal{S}'(\mathbb{R}^N)$. The inclusions are such that

$$\mathcal{D} \subset \mathcal{E}', \quad \mathcal{S} \subset \mathcal{S}', \quad \mathcal{E} \subset \mathcal{D}', \quad \mathcal{D} \subset \mathcal{S} \subset \mathcal{E}, \quad \text{and} \quad \mathcal{E}' \subset \mathcal{S}' \subset \mathcal{D}'. \tag{A.736}$$

If $T \in \mathcal{D}'(\mathbb{R}^N)$ and $\varphi \in C^\infty(\mathbb{R}^N)$, then the convolution $T * \varphi$ is defined by

$$T(\boldsymbol{x}) * \varphi(\boldsymbol{x}) = \langle T(\boldsymbol{y}), \varphi(\boldsymbol{x} - \boldsymbol{y}) \rangle = \langle T(\boldsymbol{x} - \boldsymbol{y}), \varphi(\boldsymbol{y}) \rangle. \tag{A.737}$$

If $S \in \mathcal{E}'(\mathbb{R}^N)$ and $T \in \mathcal{D}'(\mathbb{R}^N)$, then

$$\psi_T(\boldsymbol{y}) = \langle T(\boldsymbol{x}), \varphi(\boldsymbol{x} + \boldsymbol{y}) \rangle \in C^\infty(\mathbb{R}^N), \tag{A.738}$$

$$\psi_S(\boldsymbol{y}) = \langle S(\boldsymbol{x}), \varphi(\boldsymbol{x} + \boldsymbol{y}) \rangle \in \mathcal{D}(\mathbb{R}^N), \tag{A.739}$$

and therefore the convolution $S * T$ is defined by

$$\langle S(\boldsymbol{x}) * T(\boldsymbol{x}), \varphi(\boldsymbol{x}) \rangle = \big\langle S(\boldsymbol{y}), \langle T(\boldsymbol{x}), \varphi(\boldsymbol{x} + \boldsymbol{y}) \rangle \big\rangle = \big\langle T(\boldsymbol{y}), \langle S(\boldsymbol{x}), \varphi(\boldsymbol{x} + \boldsymbol{y}) \rangle \big\rangle \tag{A.740}$$

for all $\varphi \in \mathcal{D}(\mathbb{R}^N)$.

Let $T \in \mathcal{D}'(\mathbb{R}^N)$ be a distribution. Then the Dirac delta function δ acts like a unit element for the convolution, namely

$$D^{\boldsymbol{\alpha}} \delta * T = T * D^{\boldsymbol{\alpha}} \delta = D^{\boldsymbol{\alpha}} T, \qquad \boldsymbol{\alpha} \in \mathbb{N}_0^N, \tag{A.741}$$

and is, in particular, its neuter element, i.e.,

$$\delta * T = T * \delta = T. \tag{A.742}$$

The δ-function allows also to shift arguments by means of

$$\delta_{\boldsymbol{a}}(\boldsymbol{x}) * T(\boldsymbol{x}) = T(\boldsymbol{x}) * \delta_{\boldsymbol{a}}(\boldsymbol{x}) = T(\boldsymbol{x} - \boldsymbol{a}). \tag{A.743}$$

The convolution has the property of distributing the derivatives among its members. Thus, if $S \in \mathcal{E}'(\mathbb{R}^N)$ and $T \in \mathcal{D}'(\mathbb{R}^N)$, then

$$\frac{\partial}{\partial x_j}\{S * T\} = \frac{\partial S}{\partial x_j} * T = S * \frac{\partial T}{\partial x_j}, \qquad j \in \{1, 2, \ldots, N\}, \tag{A.744}$$

and, more generally,

$$D^{\boldsymbol{\alpha}}\{S * T\} = D^{\boldsymbol{\alpha}} S * T = S * D^{\boldsymbol{\alpha}} T, \qquad \boldsymbol{\alpha} \in \mathbb{N}_0^N. \tag{A.745}$$

An important property of the Fourier transform is that it turns convolutions into multiplications and viceversa. Thus, if $S \in \mathcal{E}'(\mathbb{R}^N)$ and $T \in \mathcal{S}'(\mathbb{R}^N)$, then we have that

$$T(\boldsymbol{x}) * S(\boldsymbol{x}) \quad \xrightarrow{\mathcal{F}} \quad (2\pi)^{N/2}\, \widehat{T}(\boldsymbol{\xi})\widehat{S}(\boldsymbol{\xi}), \tag{A.746}$$

$$(2\pi)^{N/2}\, T(\boldsymbol{x})S(\boldsymbol{x}) \quad \xrightarrow{\mathcal{F}} \quad \widehat{T}(\boldsymbol{\xi}) * \widehat{S}(\boldsymbol{\xi}). \tag{A.747}$$

A.7.4 Some Fourier transform pairs

We consider now some Fourier transform pairs, defined on $\mathbb{R}^N$, that use the definitions (A.695) and (A.696). For the Dirac delta δ holds that

$$\delta(\boldsymbol{x}) \quad \xrightarrow{\mathcal{F}} \quad \frac{1}{(2\pi)^{N/2}}, \tag{A.748}$$

$$\frac{1}{(2\pi)^{N/2}} \quad \xrightarrow{\mathcal{F}} \quad \delta(\boldsymbol{\xi}). \tag{A.749}$$

The complex exponential function, for $\boldsymbol{a} \in \mathbb{R}^N$, satisfies

$$e^{i\boldsymbol{a}\cdot\boldsymbol{x}} \quad \xrightarrow{\mathcal{F}} \quad (2\pi)^{N/2}\delta(\boldsymbol{\xi} - \boldsymbol{a}), \tag{A.750}$$

$$(2\pi)^{N/2}\delta(\boldsymbol{x} + \boldsymbol{a}) \quad \xrightarrow{\mathcal{F}} \quad e^{i\boldsymbol{a}\cdot\boldsymbol{\xi}}. \tag{A.751}$$

For the cosine function we have

$$\cos(\boldsymbol{a}\cdot\boldsymbol{x}) \quad \xrightarrow{\mathcal{F}} \quad \frac{(2\pi)^{N/2}}{2}\big(\delta(\boldsymbol{\xi} - \boldsymbol{a}) + \delta(\boldsymbol{\xi} + \boldsymbol{a})\big), \tag{A.752}$$

$$\frac{(2\pi)^{N/2}}{2}\big(\delta(\boldsymbol{x} + \boldsymbol{a}) + \delta(\boldsymbol{x} - \boldsymbol{a})\big) \quad \xrightarrow{\mathcal{F}} \quad \cos(\boldsymbol{a}\cdot\boldsymbol{\xi}), \tag{A.753}$$

and for the sine function we have

$$\sin(\boldsymbol{a}\cdot\boldsymbol{x}) \quad \xrightarrow{\mathcal{F}} \quad \frac{(2\pi)^{N/2}}{2\,i}\big(\delta(\boldsymbol{\xi} - \boldsymbol{a}) - \delta(\boldsymbol{\xi} + \boldsymbol{a})\big), \tag{A.754}$$

$$\frac{(2\pi)^{N/2}}{2\,i}\big(\delta(\boldsymbol{x} + \boldsymbol{a}) - \delta(\boldsymbol{x} - \boldsymbol{a})\big) \quad \xrightarrow{\mathcal{F}} \quad \sin(\boldsymbol{a}\cdot\boldsymbol{\xi}). \tag{A.755}$$

Powers of monomials, for $n \in \mathbb{N}_0$ and $j \in \{1, 2, \ldots, N\}$, yield

$$x_j^n \quad \xrightarrow{\mathcal{F}} \quad i^n(2\pi)^{N/2}\frac{\partial^n \delta}{\partial \xi_j^n}(\boldsymbol{\xi}), \tag{A.756}$$

$$(-i)^n(2\pi)^{N/2}\frac{\partial^n \delta}{\partial x_j^n}(\boldsymbol{x}) \quad \xrightarrow{\mathcal{F}} \quad \xi_j^n, \tag{A.757}$$

and, for the general case when $\boldsymbol{\alpha} \in \mathbb{N}_0^N$ is a multi-index, yield

$$\boldsymbol{x}^{\boldsymbol{\alpha}} \quad \xrightarrow{\mathcal{F}} \quad i^{|\boldsymbol{\alpha}|}(2\pi)^{N/2} D^{\boldsymbol{\alpha}} \delta(\boldsymbol{\xi}), \tag{A.758}$$

$$(-i)^{|\boldsymbol{\alpha}|}(2\pi)^{N/2} D^{\boldsymbol{\alpha}} \delta(\boldsymbol{x}) \quad \xrightarrow{\mathcal{F}} \quad \boldsymbol{\xi}^{\boldsymbol{\alpha}}. \tag{A.759}$$

A.7.5 Fourier transforms in 1D

The direct Fourier transform $\widehat{f}$ of an integrable function or tempered distribution f in the one-dimensional case, i.e., when $N = 1$, is defined by

$$\widehat{f}(\xi) = \frac{1}{\sqrt{2\pi}} \int_{-\infty}^{\infty} f(x)\, e^{-i\xi x}\, \mathrm{d}x, \qquad \xi \in \mathbb{R}, \tag{A.760}$$

and its inverse Fourier transform by

$$f(x) = \frac{1}{\sqrt{2\pi}} \int_{-\infty}^{\infty} \widehat{f}(\xi)\, e^{i\xi x}\, \mathrm{d}\xi, \qquad x \in \mathbb{R}. \tag{A.761}$$

Several signals, either functions or distributions, are commonly used for the 1D case. Among them we have the Heaviside step function $H(x)$, which is defined in (A.681). We have further the sign function

$$\operatorname{sign}(x) = \begin{cases} 1 & \text{if } x > 0, \\ -1 & \text{if } x < 0. \end{cases} \tag{A.762}$$

The rect function $\sqcap(x)$ is defined by

$$\sqcap(x) = \begin{cases} 1 & \text{if } |x| < \frac{1}{2}, \\ 0 & \text{if } |x| > \frac{1}{2}. \end{cases} \tag{A.763}$$

The triangle function $\wedge(x)$ is given by

$$\wedge(x) = \begin{cases} 1 - |x| & \text{if } |x| \leq 1, \\ 0 & \text{if } |x| > 1. \end{cases} \tag{A.764}$$

We have now the 1D Fourier transform pairs

$$\delta(x) \quad \xrightarrow{\mathcal{F}} \quad \frac{1}{\sqrt{2\pi}}, \tag{A.765}$$

$$\frac{1}{\sqrt{2\pi}} \quad \xrightarrow{\mathcal{F}} \quad \delta(\xi), \tag{A.766}$$

$$\operatorname{sign}(x) \quad \xrightarrow{\mathcal{F}} \quad -i\sqrt{\frac{2}{\pi}}\, \operatorname{pv}\left(\frac{1}{\xi}\right), \tag{A.767}$$

$$H(x) \quad \xrightarrow{\mathcal{F}} \quad \frac{1}{i\sqrt{2\pi}}\, \operatorname{pv}\left(\frac{1}{\xi}\right) + \sqrt{\frac{\pi}{2}}\, \delta(\xi), \tag{A.768}$$

$$x^n \quad \xrightarrow{\mathcal{F}} \quad i^n \sqrt{2\pi}\, \delta^{(n)}(\xi) \qquad (n \geq 1), \tag{A.769}$$

$$\operatorname{pv}\left(\frac{1}{x}\right) \quad \xrightarrow{\mathcal{F}} \quad -i\sqrt{\frac{\pi}{2}}\, \operatorname{sign}(\xi), \tag{A.770}$$

$$\mathrm{fp}\left(\frac{1}{x^n}\right) \quad \xrightarrow{\mathcal{F}} \quad -i\sqrt{\frac{\pi}{2}}\,\frac{(-i\xi)^{n-1}}{(n-1)!}\,\mathrm{sign}(\xi) \qquad (n \geq 1), \tag{A.771}$$

$$\sqcap(x) \quad \xrightarrow{\mathcal{F}} \quad \frac{1}{\sqrt{2\pi}}\,\frac{\sin(\xi/2)}{\xi/2}, \tag{A.772}$$

$$\wedge(x) \quad \xrightarrow{\mathcal{F}} \quad \frac{1}{\sqrt{2\pi}}\left(\frac{\sin(\xi/2)}{\xi/2}\right)^2, \tag{A.773}$$

$$\frac{\sin(\pi x)}{\pi x} \quad \xrightarrow{\mathcal{F}} \quad \frac{1}{\sqrt{2\pi}}\,\sqcap\!\left(\frac{\xi}{2\pi}\right), \tag{A.774}$$

$$e^{-a|x|} \quad \xrightarrow{\mathcal{F}} \quad \sqrt{\frac{2}{\pi}}\,\frac{a}{a^2+\xi^2} \qquad (\mathfrak{Re}\, a > 0), \tag{A.775}$$

$$e^{-ax^2} \quad \xrightarrow{\mathcal{F}} \quad \frac{1}{\sqrt{2a}}\,e^{-\xi^2/4a} \qquad (a > 0), \tag{A.776}$$

$$e^{-ax}H(x) \quad \xrightarrow{\mathcal{F}} \quad \frac{1}{\sqrt{2\pi}\,(a+i\xi)} \qquad (\mathfrak{Re}\, a > 0), \tag{A.777}$$

$$\cos(ax) \quad \xrightarrow{\mathcal{F}} \quad \sqrt{\frac{\pi}{2}}\,\big(\delta(\xi+a)+\delta(\xi-a)\big) \qquad (a \in \mathbb{R}), \tag{A.778}$$

$$\sin(ax) \quad \xrightarrow{\mathcal{F}} \quad i\sqrt{\frac{\pi}{2}}\,\big(\delta(\xi+a)-\delta(\xi-a)\big) \qquad (a \in \mathbb{R}), \tag{A.779}$$

$$\frac{1}{\sqrt{|x|}} \quad \xrightarrow{\mathcal{F}} \quad \frac{1}{\sqrt{|\xi|}}. \tag{A.780}$$

In the sense of homogeneous distributions (cf. Gel'fand & Shilov 1964), we have that

$$\ln\left(\sqrt{x^2+a^2}\right) \quad \xrightarrow{\mathcal{F}} \quad -\sqrt{\frac{\pi}{2}}\,\frac{e^{-|a||\xi|}}{|\xi|} \qquad (a \in \mathbb{R}). \tag{A.781}$$

Some Fourier transforms involving Bessel and Hankel functions (vid. Subsection A.2.4), for $a \in \mathbb{R}$ and $b > 0$, are

$$J_0(x) \quad \xrightarrow{\mathcal{F}} \quad \sqrt{\frac{2}{\pi}}\,\frac{\sqcap(\xi/2)}{\sqrt{1-\xi^2}}, \tag{A.782}$$

$$J_0\left(b\sqrt{x^2+a^2}\right) \quad \xrightarrow{\mathcal{F}} \quad \sqrt{\frac{2}{\pi}}\,\frac{\sqcap(\xi/2b)}{\sqrt{b^2-\xi^2}}\cos\Big(\sqrt{b^2-\xi^2}\,|a|\Big), \tag{A.783}$$

$$\begin{aligned} Y_0\left(b\sqrt{x^2+a^2}\right) \quad \xrightarrow{\mathcal{F}} \quad & \sqrt{\frac{2}{\pi}}\,\frac{\sqcap(\xi/2b)}{\sqrt{b^2-\xi^2}}\sin\Big(\sqrt{b^2-\xi^2}\,|a|\Big) \\ & - \sqrt{\frac{2}{\pi}}\,\frac{e^{-\sqrt{\xi^2-b^2}\,|a|}}{\sqrt{\xi^2-b^2}}\big(1-\sqcap(\xi/2b)\big), \end{aligned} \tag{A.784}$$

$$H_0^{(1)}\left(b\sqrt{x^2+a^2}\right) \quad \xrightarrow{\mathcal{F}} \quad -i\sqrt{\frac{2}{\pi}}\,\frac{e^{-\sqrt{\xi^2-b^2}\,|a|}}{\sqrt{\xi^2-b^2}}, \tag{A.785}$$

where the complex square root in (A.785) is defined in such a way that

$$\sqrt{\xi^2-b^2} = -i\sqrt{b^2-\xi^2}. \tag{A.786}$$

A.7.6 Fourier transforms in 2D

The direct Fourier transform $\widehat{f}$ of an integrable function or tempered distribution f in the two-dimensional case, i.e., when $N = 2$, is defined by

$$\widehat{f}(\xi_1, \xi_2) = \frac{1}{2\pi} \int_{-\infty}^{\infty} \int_{-\infty}^{\infty} f(x_1, x_2)\, e^{-i(\xi_1 x_1 + \xi_2 x_2)}\, \mathrm{d}x_1\, \mathrm{d}x_2, \qquad \xi_1, \xi_2 \in \mathbb{R}, \tag{A.787}$$

and its inverse Fourier transform by

$$f(x_1, x_2) = \frac{1}{2\pi} \int_{-\infty}^{\infty} \int_{-\infty}^{\infty} \widehat{f}(\xi_1, \xi_2)\, e^{i(\xi_1 x_1 + \xi_2 x_2)}\, \mathrm{d}\xi_1\, \mathrm{d}\xi_2, \qquad x_1, x_2 \in \mathbb{R}. \tag{A.788}$$

To express the radial components we use the notation

$$r = |\boldsymbol{x}| = \sqrt{x_1^2 + x_2^2} \qquad \text{and} \qquad \rho = |\boldsymbol{\xi}| = \sqrt{\xi_1^2 + \xi_2^2}. \tag{A.789}$$

It holds that the two-dimensional Fourier transform of a circularly symmetric function is also circularly symmetric and the same is true for the converse. The 2D Fourier transform turns in this case into the Hankel transform of order zero, which is given by

$$\widehat{f}(\rho) = \int_0^{\infty} f(r) J_0(\rho r)\, r\, \mathrm{d}r, \qquad \rho \geq 0, \tag{A.790}$$

and its inverse by

$$f(r) = \int_0^{\infty} \widehat{f}(\rho) J_0(\rho r)\, \rho\, \mathrm{d}\rho, \qquad r \geq 0. \tag{A.791}$$

This relation between both integral transforms stems from the integral representation of the zeroth-order Bessel function (A.112), which implies that

$$J_0(\rho r) = \frac{1}{2\pi} \int_0^{2\pi} e^{i\rho r \cos\psi}\, \mathrm{d}\psi = \frac{1}{2\pi} \int_0^{2\pi} e^{-i\rho r \cos\psi}\, \mathrm{d}\psi. \tag{A.792}$$

If we denote the polar angles by

$$\theta = \arctan\left(\frac{x_2}{x_1}\right) \qquad \text{and} \qquad \psi = \arctan\left(\frac{\xi_2}{\xi_1}\right), \tag{A.793}$$

then we can relate (A.788) and (A.791), due (A.792), by means of

$$\begin{aligned} f(x_1, x_2) = f(r) &= \frac{1}{2\pi} \int_0^{\infty} \int_0^{2\pi} \widehat{f}(\rho)\, \rho\, e^{i\rho r(\cos\theta\cos\psi + \sin\theta\sin\psi)}\, \mathrm{d}\psi\, \mathrm{d}\rho \\ &= \frac{1}{2\pi} \int_0^{\infty} \widehat{f}(\rho)\, \rho \int_0^{2\pi} e^{i\rho r\cos(\psi-\theta)}\, \mathrm{d}\psi\, \mathrm{d}\rho \\ &= \int_0^{\infty} \widehat{f}(\rho) J_0(\rho r)\, \rho\, \mathrm{d}\rho. \end{aligned} \tag{A.794}$$

The relation between (A.787) and (A.790) can be proved using a similar development.

For the 2D case there are also several signals that are commonly used. Among them we have the two-dimensional rect function $\sqcap(x_1, x_2)$, defined by

$$\sqcap(x_1, x_2) = \sqcap(x_1)\sqcap(x_2) = \begin{cases} 1 & \text{if } |x_1| < \frac{1}{2} \text{ and } |x_2| < \frac{1}{2}, \\ 0 & \text{elsewhere,} \end{cases} \tag{A.795}$$

and the circ function, defined by

$$\sqcap(r) = \begin{cases} 1 & \text{if } r < \frac{1}{2}, \\ 0 & \text{elsewhere.} \end{cases} \tag{A.796}$$

We have now the 2D Fourier transform pairs

$$\delta(x_1, x_2) \quad \xrightarrow{\mathcal{F}} \quad \frac{1}{2\pi}, \tag{A.797}$$

$$\frac{1}{2\pi} \quad \xrightarrow{\mathcal{F}} \quad \delta(\xi_1, \xi_2), \tag{A.798}$$

$$\delta(x_1) \quad \xrightarrow{\mathcal{F}} \quad \delta(\xi_2), \tag{A.799}$$

$$\delta(x_2) \quad \xrightarrow{\mathcal{F}} \quad \delta(\xi_1), \tag{A.800}$$

$$\sqcap(x_1, x_2) \quad \xrightarrow{\mathcal{F}} \quad \frac{1}{2\pi} \frac{\sin(\xi_1/2)}{\xi_1/2} \frac{\sin(\xi_2/2)}{\xi_2/2}, \tag{A.801}$$

$$\sqcap(r) \quad \xrightarrow{\mathcal{F}} \quad \frac{J_1(\rho/2)}{2\rho}, \tag{A.802}$$

$$e^{-ar^2} \quad \xrightarrow{\mathcal{F}} \quad \frac{1}{2a}\, e^{-\rho^2/4a} \qquad (a > 0), \tag{A.803}$$

$$\frac{1}{r} \quad \xrightarrow{\mathcal{F}} \quad \frac{1}{\rho}. \tag{A.804}$$

Other interesting 2D Fourier transforms, for $a \in \mathbb{R}$ and $b > 0$, are

$$\frac{1}{\sqrt{r^2 + a^2}} \quad \xrightarrow{\mathcal{F}} \quad \frac{e^{-\rho|a|}}{\rho}, \tag{A.805}$$

$$\frac{\sin\left(b\sqrt{r^2 + a^2}\right)}{\sqrt{r^2 + a^2}} \quad \xrightarrow{\mathcal{F}} \quad \frac{\cos\left(\sqrt{b^2 - \rho^2}\,|a|\right)}{\sqrt{b^2 - \rho^2}} \sqcap\left(\frac{\xi_1}{2b}, \frac{\xi_2}{2b}\right), \tag{A.806}$$

$$\begin{aligned} \frac{\cos\left(b\sqrt{r^2 + a^2}\right)}{\sqrt{r^2 + a^2}} \quad \xrightarrow{\mathcal{F}} \quad & -\frac{\sin\left(\sqrt{b^2 - \rho^2}\,|a|\right)}{\sqrt{b^2 - \rho^2}} \sqcap\left(\frac{\xi_1}{2b}, \frac{\xi_2}{2b}\right) \\ & + \frac{e^{-\sqrt{\rho^2 - b^2}\,|a|}}{\sqrt{\rho^2 - b^2}} \left(1 - \sqcap\left(\frac{\xi_1}{2b}, \frac{\xi_2}{2b}\right)\right), \end{aligned} \tag{A.807}$$

$$\frac{e^{ib\sqrt{r^2 + a^2}}}{\sqrt{r^2 + a^2}} \quad \xrightarrow{\mathcal{F}} \quad \frac{e^{-\sqrt{\rho^2 - b^2}\,|a|}}{\sqrt{\rho^2 - b^2}}, \tag{A.808}$$

where the complex square root in (A.808) is defined in such a way that

$$\sqrt{\rho^2 - b^2} = -i\sqrt{b^2 - \rho^2}. \tag{A.809}$$

We observe that the left-hand side of the expressions (A.806), (A.807), and (A.808) is closely related with the spherical Bessel and Hankel functions j_0, y_0, and $h_0^{(1)}$, respectively. For further details, see Subsection A.2.6.

A.8 Green's functions and fundamental solutions

Green's functions are used to solve inhomogeneous boundary-value problems for differential equations subject to boundary conditions. They receive their name from the British mathematician and physicist George Green (1793–1841), who was the first to study a special case of this type of functions in his research on potential theory, which he developed in a famous essay (Green 1828).

The concept of a Green's function is essential throughout this thesis, so it becomes important to understand properly their significance. Our main references for these functions, treated in the sense of distributions, are Griffel (1985) and Terrasse & Abboud (2006). A more classical treatment of Green's functions in the context of mathematical physics can be found, e.g., in Bateman (1932), Courant & Hilbert (1966), and Morse & Feshbach (1953). There exist also several books that are almost entirely dedicated to Green's functions, like Barton (1989), DeSanto (1992), Duffy (2001), and Greenberg (1971). An exhaustive amount of them are likewise listed in Polyanin (2002).

The Green's function of a boundary-value problem for a linear differential equation is the fundamental solution of this equation satisfying homogeneous boundary conditions. It is thus the kernel of the integral operator that is the inverse of the differential operator generated by the given differential equation and the homogeneous boundary conditions. The Green's function yields therefore solutions for the inhomogeneous boundary-value problem. Finding the Green's function reduces the study of the properties for the differential operator to the study of similar properties for the corresponding integral operator.

A.8.1 Fundamental solutions

Technically, a fundamental solution for a partial differential operator $\mathcal{L}$, linear, with constant coefficients, and defined on the space of distributions $\mathcal{D}'(\mathbb{R}^N)$, is a distribution E that satisfies

$$\mathcal{L}E = \delta \qquad \text{in } \mathcal{D}'(\mathbb{R}^N), \tag{A.810}$$

where δ is the Dirac delta or impulse function, centered at the origin. The main interest of such a fundamental solution lies in the fact that if the convolution has a sense, then the solution of

$$\mathcal{L}u = f \qquad \text{in } \mathcal{D}'(\mathbb{R}^N), \tag{A.811}$$

for a known data function f, is given by

$$u = E * f. \tag{A.812}$$

In fact, due the linearity of $\mathcal{L}$, since E is a fundamental solution, and since δ is the neutral element of the convolution, we have

$$\mathcal{L}u = \mathcal{L}\{E * f\} = \mathcal{L}E * f = \delta * f = f. \tag{A.813}$$

By adding to the fundamental solution non-trivial solutions for the homogeneous problem, new fundamental solutions can be obtained. The fundamental solution for a well-posed problem is unique, if additional conditions are specified for the behavior of the solution, e.g., the decaying behavior at infinity, being these conditions often determined through

physical considerations. In the construction of the fundamental solution it is permissible to use any methods to find the solutions of the equation, provided that the result is then justified by rigorous arguments.

We remark also that from the fundamental solution other solutions can be derived when, in the sense of distributions, derivatives of the Dirac delta function δ appear on the right-hand side. For example, the solution of

$$\mathcal{L}F = \frac{\partial \delta}{\partial x_i} \qquad \text{in } \mathcal{D}'(\mathbb{R}^N) \tag{A.814}$$

is given by

$$F = E * \frac{\partial \delta}{\partial x_i} = \frac{\partial E}{\partial x_i} * \delta = \frac{\partial E}{\partial x_i}. \tag{A.815}$$

A.8.2 Green's functions

In the case of the Green's function, the fundamental solution considers also homogeneous boundary conditions, and the Dirac delta function is no longer centered at the origin, but at a fixed source point. Thus, a Green's function of a partial differential operator $\mathcal{L}_{\boldsymbol{y}}$ with homogeneous boundary conditions, linear, with constant coefficients, acting on the variable $\boldsymbol{y}$, and defined on the space of distributions $\mathcal{D}'(\mathbb{R}^N)$, is a distribution G such that

$$\mathcal{L}_{\boldsymbol{y}}\{G(\boldsymbol{x}, \boldsymbol{y})\} = \delta_{\boldsymbol{x}}(\boldsymbol{y}) \qquad \text{in } \mathcal{D}'(\mathbb{R}^N), \tag{A.816}$$

where $\delta_{\boldsymbol{x}}$ is the Dirac delta or impulse function with the Dirac mass centered at the source point $\boldsymbol{x}$, i.e., $\delta_{\boldsymbol{x}}(\boldsymbol{y}) = \delta(\boldsymbol{y} - \boldsymbol{x})$. The Green's function represents thus the impulse response of the operator $\mathcal{L}_{\boldsymbol{y}}$ with respect to the source point $\boldsymbol{x}$, being therefore the nucleus or kernel of the inverse operator of $\mathcal{L}_{\boldsymbol{y}}$, denoted by $\mathcal{L}_{\boldsymbol{y}}^{-1}$, which corresponds to an integral operator, and $G(\boldsymbol{x}, \boldsymbol{y}) = \mathcal{L}_{\boldsymbol{y}}^{-1}\{\delta_{\boldsymbol{x}}(\boldsymbol{y})\}$. The Green's function, differently as the fundamental solution, is searched in some particular domain $\Omega \subset \mathbb{R}^N$ and satisfies some boundary conditions, but for simplicity we consider here just $\Omega = \mathbb{R}^N$.

The solution of the inhomogeneous partial differential boundary-value problem

$$\mathcal{L}_{\boldsymbol{x}}\{u(\boldsymbol{x})\} = f(\boldsymbol{x}) \qquad \text{in } \mathcal{D}'(\mathbb{R}^N), \tag{A.817}$$

is in this case given, if the convolution has a sense, by

$$u(\boldsymbol{x}) = G(\boldsymbol{x}, \boldsymbol{y}) * f(\boldsymbol{y}), \tag{A.818}$$

where G is the Green's function of the operator $\mathcal{L}_{\boldsymbol{x}}$, which is symmetric, i.e.,

$$G(\boldsymbol{x}, \boldsymbol{y}) = G(\boldsymbol{y}, \boldsymbol{x}). \tag{A.819}$$

Again, as for the fundamental solution, we have

$$\begin{aligned} \mathcal{L}_{\boldsymbol{x}}\{u(\boldsymbol{x})\} &= \mathcal{L}_{\boldsymbol{x}}\{G(\boldsymbol{x}, \boldsymbol{y}) * f(\boldsymbol{y})\} = \mathcal{L}_{\boldsymbol{x}}\{G(\boldsymbol{x}, \boldsymbol{y})\} * f(\boldsymbol{y}) \\ &= \delta_{\boldsymbol{x}}(\boldsymbol{y}) * f(\boldsymbol{y}) = f(\boldsymbol{x}). \end{aligned} \tag{A.820}$$

We observe that the free- or full-space Green's function, i.e., without boundary conditions, is linked to the fundamental solution through the relation

$$G(\boldsymbol{x}, \boldsymbol{y}) = E(\boldsymbol{x} - \boldsymbol{y}) = E(\boldsymbol{y} - \boldsymbol{x}). \tag{A.821}$$

A.8.3 Some free-space Green's functions

We consider now some examples of free-space Green's functions of our interest. The free-space Green's function for the Laplace equation satisfies in the sense of distributions

$$\Delta_{\boldsymbol{y}} G(\boldsymbol{x},\boldsymbol{y}) = \delta_{\boldsymbol{x}}(\boldsymbol{y}) \qquad \text{in } \mathcal{D}'(\mathbb{R}^N), \tag{A.822}$$

and is given by (Polyanin 2002)

$$G(\boldsymbol{x},\boldsymbol{y}) = \begin{cases} \dfrac{|y-x|}{2} & \text{for } N=1, \\ \dfrac{1}{2\pi}\ln|\boldsymbol{y}-\boldsymbol{x}| & \text{for } N=2, \\ -\dfrac{1}{4\pi|\boldsymbol{y}-\boldsymbol{x}|} & \text{for } N=3, \\ -\dfrac{\Gamma\left(\frac{N}{2}\right)}{2\pi^{N/2}(N-2)|\boldsymbol{y}-\boldsymbol{x}|^{N-2}} & \text{for } N\geq 4, \end{cases} \tag{A.823}$$

where Γ denotes the gamma function (vid. Subsection A.2.2).

The free-space Green's function of outgoing-wave behavior for the Helmholtz equation, on the other hand, satisfies in the sense of distributions

$$\Delta_{\boldsymbol{y}} G(\boldsymbol{x},\boldsymbol{y}) + k^2 G(\boldsymbol{x},\boldsymbol{y}) = \delta_{\boldsymbol{x}}(\boldsymbol{y}) \qquad \text{in } \mathcal{D}'(\mathbb{R}^N), \tag{A.824}$$

and has to be supplied with the Sommerfeld radiation condition

$$\lim_{|\boldsymbol{y}|\to\infty} |\boldsymbol{y}|^{\frac{N-1}{2}} \left(\frac{\partial G}{\partial |\boldsymbol{y}|}(\boldsymbol{x},\boldsymbol{y}) - ikG(\boldsymbol{x},\boldsymbol{y}) \right) = 0, \tag{A.825}$$

where $k \in \mathbb{C}$ corresponds to the wave number. By adapting the expressions listed in Polyanin (2002) we acquire in this case that

$$G(\boldsymbol{x},\boldsymbol{y}) = \begin{cases} -\dfrac{i}{2k}\, e^{ik|y-x|} & \text{for } N=1, \\ -\dfrac{i}{4} H_0^{(1)}\big(k|\boldsymbol{y}-\boldsymbol{x}|\big) & \text{for } N=2, \\ -\dfrac{e^{ik|\boldsymbol{y}-\boldsymbol{x}|}}{4\pi|\boldsymbol{y}-\boldsymbol{x}|} & \text{for } N=3, \\ -\dfrac{i}{4}\left(\dfrac{k}{2\pi|\boldsymbol{y}-\boldsymbol{x}|}\right)^{\frac{N-2}{2}} H^{(1)}_{\frac{N-2}{2}}\big(k|\boldsymbol{y}-\boldsymbol{x}|\big) & \text{for } N\geq 4, \end{cases} \tag{A.826}$$

where $H_\nu^{(1)}$ denotes the Hankel function of the first kind of order ν (vid. Subsection A.2.4).

A.9 Wave propagation

Wave propagation is a complex physical phenomenon, whose mathematical description is in general not easy to accomplish. Some generalities concerning wave propagation and its mathematical modeling are presented below. Some references are Nédélec (2001), Jackson (1999), Kuttruff (2007), Wilcox (1975), Strauss (1992), and Evans (1998). An interesting survey of several research areas in wave propagation can be found in Keller (1979). A thorough discussion on the amount of samples per wavelength required in the discretization procedure and on some other related aspects is given in Marburg (2008).

A.9.1 Generalities on waves

A wave is a disturbance that propagates with time through a certain medium transferring energy progressively from point to point. The medium through which the wave travels may experience some local oscillations around fixed positions as the wave passes, but the particles in the medium do not travel with the wave, and are thus not displaced permanently. The medium could even be the vacuum as in the case of electromagnetic waves. The disturbance may take any of a number of shapes, from a finite width pulse to an infinitely long sine wave. Several kinds of waves exist, e.g., mechanical (sound, elastic, seismic, and ocean surface waves), electromagnetic (visible light, radio waves, X-rays), temperature, or gravitational waves.

Waves are characterized by crests and troughs, either perpendicular or parallel to the wave's motion. Waves in which the propagating disturbance is perpendicular to its motion are called transverse waves (waves on a string or electromagnetic waves), while waves in which it is parallel are called longitudinal waves (sound or pressure waves). Transverse waves can be polarized. Unpolarized waves can oscillate in any direction in the plane perpendicular to the direction of travel, while polarized waves oscillate in only one direction perpendicular to the line of travel.

All waves have a common behavior under a number of standard situations. They all can experience the phenomena of rectilinear propagation, interference, reflection, refraction, diffraction, and scattering. Rectilinear propagation states that waves in a homogeneous medium move or spread out in straight lines. Interference is the superposition of two or more waves resulting in a new wave pattern. The principle of linear superposition of waves states that the resultant displacement at a given point is equal to the sum of the displacements of different waves at that point. Reflection is an abrupt change in direction of a wave at an interface between two dissimilar media so that the wave returns into the medium from which it originated. Refraction is the change in direction of a wave due to a change in its velocity when entering a new medium with different refractive index. Diffraction is the bending of waves when they meet one (or more) partial obstacles, which deform the shape of the wavefronts as they pass. Scattering or dispersion is the process whereby waves are forced to deviate from a straight trajectory into many directions by one or more localized non-uniformities (called scatterers) in the medium through which they pass. Scattering is therefore a form of reflection in which a portion of the incident waves is redistributed into many directions by a scatterer.

A.9.2 Wave modeling

Waves are modeled physically and mathematically as solutions of a wave equation. Each kind of waves has its own wave equation and associated auxiliary conditions, e.g., boundary conditions, that can be applied. The most studied wave equation is probably the scalar wave equation of linear acoustics, which describes the propagation of sound in a homogeneous medium in the space $\mathbb{R}^N$ ($N = 1$, 2, or 3). It takes the form of the hyperbolic partial differential equation

$$\frac{\partial^2 p}{\partial t^2} - c^2 \Delta p = 0, \qquad \boldsymbol{x} \in \mathbb{R}^N, \;\; t \in \mathbb{R}_+, \tag{A.827}$$

where c is the speed of sound and $p = p(\boldsymbol{x}, t)$ is the induced pressure. By Δ we denote the Laplace operator

$$\Delta p = \sum_{j=1}^{N} \frac{\partial^2 p}{\partial x_j^2}, \tag{A.828}$$

named in honor of the French mathematician and astronomer Pierre-Simon, marquis de Laplace (1749–1827), whose work was pivotal to the development of mathematical astronomy. He formulated Laplace's equation and invented the Laplace transform, which appears in many branches of mathematical physics, a field that he took a leading role in forming.

After a mathematical trick attributed to the French mathematician, mechanician, physicist, and philosopher Jean le Rond d'Alembert (1717–1783), in a space of dimension $N = 1$ all regular solutions of (A.827) are of the form

$$p(x, t) = f(x - c\,t) + g(x + c\,t), \tag{A.829}$$

where f and g are arbitrary functions. This expression shows that if the functions f and g have compact support, then the solution propagates at a finite speed equal to c. Finite speed propagation is one of the essential characteristics of hyperbolic equations.

A time-harmonic solution of the wave equation (A.827) is a function of the form

$$p(\boldsymbol{x}, t) = \mathfrak{Re}\big\{u(\boldsymbol{x})e^{-i\omega t}\big\}, \tag{A.830}$$

where u is the amplitude of the pressure and i denotes the complex imaginary unit, which represents the square root of -1. The quantity ω is called the pulsation or angular frequency of the harmonic wave. Here the time convention $e^{-i\omega t}$ has been taken, which determines the sign of ingoing and outgoing waves, and thus also of the outgoing radiation condition when dealing with unbounded domains. After applying this separation of variables to (A.827), the function u becomes a solution of the Helmholtz equation

$$\Delta u + k^2 u = 0, \qquad k = \frac{\omega}{c}. \tag{A.831}$$

The number k is called wave number. The quantity $f = \omega/2\pi$ is called frequency and the length $\lambda = c/f = 2\pi/k$ is called wavelength. This equation carries the name of the German physician and physicist Hermann Ludwig Ferdinand von Helmholtz (1821–1894), for his contributions to mathematical acoustics and electromagnetism. When the frequency (or the

wave number) is zero, then we obtain the Laplace equation

$$\Delta u = 0, \qquad \omega = 0. \tag{A.832}$$

The Helmholtz equation has a very special family of solutions called plane waves. Up to a multiplicative factor, they are the complex-valued functions of the form

$$u(\boldsymbol{x}) = e^{i\boldsymbol{k}\cdot\boldsymbol{x}}, \qquad (\boldsymbol{k}\cdot\boldsymbol{k}) = k^2. \tag{A.833}$$

They correspond to wavefronts that travel with velocity c in the direction given by the wave propagation vector $\boldsymbol{k}$. The vector $\boldsymbol{k}$ can be real, in which case $k = |\boldsymbol{k}|$ and these solutions are of modulus 1. When the vector $\boldsymbol{k}$ is complex, then the solutions are exponentially decreasing in a half-space determined by the imaginary part of the vector $\boldsymbol{k}$ and exponentially increasing in the other half-space, i.e., where they explode. They are called plane waves because $e^{i(\boldsymbol{k}\cdot\boldsymbol{x}-\omega t)}$ is constant on the planes $(\boldsymbol{k}\cdot\boldsymbol{x}-\omega t) =$ constant.

A.9.3 Discretization requirements

Wave propagation problems dealing with geometries that are too complex to solve analytically are nowadays solved with the help of computers, by using appropriate numerical methods and discretization procedures. For this purpose, the considered geometry is discretized using a finite mesh to describe it. In computational linear time-harmonic wave propagation modeling, it is widely accepted that the appropriate refinement and configuration of this discretized mesh, i.e., the placement of its discretization nodes, should be related to the wavelength. The commonly applied rule of thumb is to use a fixed number of nodes per wavelength. In many cases, this number of nodes per wavelength varies typically between three and ten, although it is advised to use at least five or even six of them. Obviously, this number is closely related to a certain desired accuracy. Often the error is of an acceptable magnitude, which depends on the user and on certain technical requirements. A sine-wave discretization for different numbers of nodes per wavelength for an equidistant node distribution is depicted in Figure A.18.

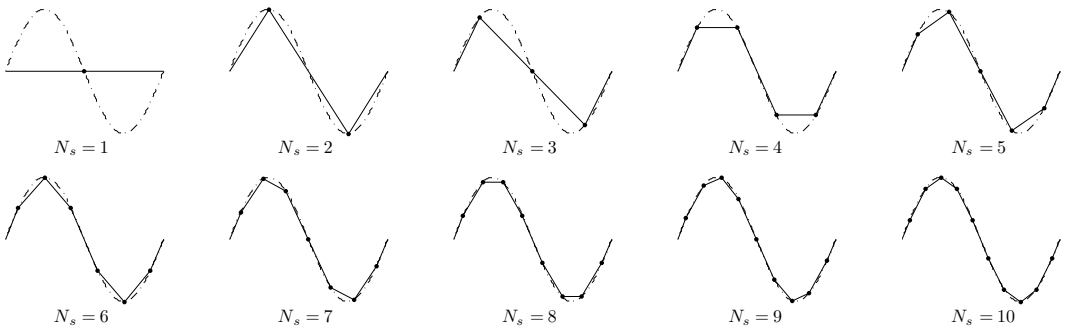

FIGURE A.18. Sine-wave discretization for different numbers of nodes per wavelength.

The idea of using a fixed number of nodes per wavelength is most likely a consequence of the Nyquist-Shannon sampling theorem, also known as Nyquist's sampling theorem, Shannon's sampling theorem, or simply as the sampling theorem. It is named after the Swedish electronic engineer Harry Nyquist (1889–1976) and the American electronic engineer and mathematician Claude Elwood Shannon (1916–2001), who laid the foundations that led to the development of information theory. Some references for this theorem are the extensive survey articles of Jerry (1977, 1979) and Unser (2000), and the books of Gasquet & Witomski (1999) and Irarrázaval (1999). The Nyquist-Shannon sampling theorem is of fundamental importance in wave propagation and in vibration analysis for experimental measurements and frequency detection. It states that at least two points per wavelength (or period of an oscillating function) are necessary to detect the corresponding frequency. However, a simple detection cannot be sufficient to approximate the function, as stated in Marburg (2008), who refers to several other authors and performs an extensive analysis on the discretization requirements for wave propagation problems, considering different types of finite elements. It is mentioned there that two points per wavelength are strictly sufficient, but would still not lead to an accurate reconstruction of the function, and it is therefore advised to take rather an amount of six to ten nodes per wavelength. In particular for boundary element methods, the common rule is to use six constant or linear boundary elements per wavelength. The concluding remarks recommend the use of discontinuous boundary elements with nodes located at the zeros of Legendre polynomials (vid. Subsection A.2.8), provided that the involved problem is essentially related to the inversion of the double layer potential operator. It is also mentioned that in the case of mixed problems and when the hypersingular operator is used, then probably other optimal locations for the nodes will be found.

A.10 Linear water-wave theory

The linear water-wave theory is concerned with the propagation of waves on the surface of the water, considered as small perturbations so that they can be linearly described. The study of these waves has many applications, including naval architecture, ocean engineering, and geophysical hydrodynamics. For example, it is required for predicting the behavior of floating structures (immersed totally or partially), such as ships, submarines, and tension-leg platforms, and for describing flows over bottom topography. Furthermore, the investigation of wave patterns of ships and other vehicles in forward motion is closely related to the calculation of the wave-making resistance and other hydrodynamic characteristics that are used in marine design. Another area of application is the mathematical modeling of unsteady waves resulting from such phenomena as underwater earthquakes, blasts, etc. We are herein interested in the derivation of the governing differential equations of these waves, obtained on the basis of general dynamics of an inviscid incompressible fluid (water is the standard example of such a fluid), and their linearization.

We are particularly devoted to waves arising in two closely related phenomena, which are radiation of waves by oscillating immersed bodies and scattering of incoming progressive waves by an obstacle (a floating body or variable bottom topography). Mathematically these phenomena give rise to a boundary-value problem that is usually referred to as the water-wave problem. The difficulty of this problem stems from several facts. First, it is essential that the water domain is infinite. Second, there is a spectral parameter (it is related to the radian frequency of waves) in a boundary condition on a semi-infinite part of the boundary (referred to as the free surface of water). Above all, the free surface may consist of more than one component as occurs for a surface-piercing toroidal body.

Good and complete references for the linear theory of water waves are Kuznetsov, Maz'ya & Vainberg (2002) and Wehausen & Laitone (1960), which are closely followed herein, in particular the former. Other references on this topic are Hazard & Lenoir (1998), Howe (2007), John (1949, 1950), Lamb (1916), Linton & McIver (2001), Mei (1983), Mei, Stiassnie & Yue (2005), Stoker (1957), and Wehausen (1971).

Water waves, also known as gravity waves, ocean surface waves, or simply surface waves, are created normally by a gravitational force in the presence of a free surface along which the pressure is constant. There are two ways to describe these waves mathematically. It is possible to trace the paths of individual particles (a Lagrangian description), but in this thesis an alternative form of equations (usually referred to as Eulerian) is adopted. The first description receives its name from the Italian-French mathematician and astronomer Joseph Louis Lagrange (1736–1813), who made important contributions to classical and celestial mechanics and to number theory. The second description is named after the already mentioned great Swissborn Russian mathematician and physicist Leonhard Euler (1707–1783). The motion is determined by the velocity field in the domain occupied by water at every moment of the time t.

Water is assumed to occupy a certain domain Ω bounded by one or more moving or fixed surfaces that separate water from some other medium. Actually we consider boundaries of two types: the above-mentioned free surface separating water from the atmosphere, and rigid surfaces including the bottom and surfaces of bodies floating in and/or beneath the free surface.

It is convenient to use rectangular coordinates $\boldsymbol{x} = (x_1, x_2, x_3) \in \mathbb{R}^3$ with the origin in the free surface at rest (which coincides with the mean free surface), and with the x_3 axis directed opposite to the acceleration caused by gravity. For the sake of brevity we will write $\boldsymbol{x}_s$ instead of (x_1, x_2). Two-dimensional problems can be treated simultaneously by considering the variables $(x_s, x_3) \in \mathbb{R}^2$, i.e., taking a scalar x_s instead of the vectorial $\boldsymbol{x}_s$, and renaming eventually x_3 by x_2. Two-dimensional problems form an important class of problems considering water motions that are the same in every plane orthogonal to a certain direction. As usual, $\nabla u = (\partial u/\partial x_1, \partial u/\partial x_2, \partial u/\partial x_3)$, and the horizontal component of ∇ will be denoted by ∇_s, that is, $\nabla_s u = (\partial u/\partial x_1, \partial u/\partial x_2, 0)$.

A.10.1 Equations of motion and boundary conditions

In the Eulerian formulation one seeks the velocity vector $\boldsymbol{v}$, the pressure p, and the fluid density ρ as functions of $\boldsymbol{x} \in \overline{\Omega}$ and $t \geq t_0$, where t_0 denotes a certain initial moment. Assuming the fluid to be inviscid without surface tension, one obtains the equations of motion from conservation laws. The conservation of mass implies the continuity equation

$$\frac{\partial \rho}{\partial t} + \nabla \cdot (\rho \boldsymbol{v}) = 0 \qquad \text{in } \Omega. \tag{A.834}$$

Under the assumption that the fluid is incompressible (which is usual in the water-wave theory), the last equation becomes

$$\nabla \cdot \boldsymbol{v} = 0 \qquad \text{in } \Omega. \tag{A.835}$$

The conservation of momentum in inviscid fluid leads to the so-called Euler equations. Taking into account the gravity force, one can write these three (or two) equations in the vector form

$$\frac{\partial \boldsymbol{v}}{\partial t} + \boldsymbol{v} \cdot \nabla \boldsymbol{v} = -\frac{1}{\rho} \nabla p + \boldsymbol{g} \qquad \text{in } \Omega. \tag{A.836}$$

Here $\boldsymbol{g}$ is the vector of the gravity force having zero horizontal components and the vertical one equal to $-g$, where g denotes the acceleration caused by gravity.

An irrotational character of motion is another usual assumption in the theory, i.e.,

$$\nabla \times \boldsymbol{v} = 0 \qquad \text{in } \Omega. \tag{A.837}$$

Note that one can prove that the motion is irrotational if it has this property at the initial moment. The last equation guarantees the existence of a velocity potential ϕ so that

$$\boldsymbol{v} = \nabla \phi \qquad \text{in } \overline{\Omega}. \tag{A.838}$$

This is obvious for simply connected domains, otherwise (for example, when one considers a two-dimensional problem for a totally immersed body), the so-called no-flow condition should be taken into account (vid. (A.843) below).

From (A.835) and (A.838) one obtains the Laplace equation

$$\Delta\phi = 0 \qquad \text{in } \Omega. \tag{A.839}$$

This greatly facilitates the theory but, in general, solutions of (A.839) do not manifest wave character. Waves are created by the boundary conditions on the free surface.

Let $x_3 = \eta(\boldsymbol{x}_s, t)$ be the equation of the free surface valid for $\boldsymbol{x}_s \in \Gamma$, where Γ is a union of some domains (generally depending on t) in $\mathbb{R}^{N-1}$, with $N = 2, 3$. The pressure is prescribed to be equal to the constant atmospheric pressure p_0 on $x_3 = \eta(\boldsymbol{x}_s, t)$, and the surface tension is neglected. From (A.837) and (A.838) one immediately obtains Bernoulli's equation

$$\frac{\partial\phi}{\partial t} + \frac{|\nabla\phi|^2}{2} = -\frac{p}{\rho} - gx_3 + C \qquad \text{in } \overline{\Omega}, \tag{A.840}$$

where C is a function of t alone. Indeed, applying ∇ to both sides in (A.840) and using (A.837) and (A.838), one obtains $\nabla C = 0$. Then, by changing ϕ by a suitable additive function of t, one can convert C into a constant having, for example, the value

$$C = \frac{p_0}{\rho}. \tag{A.841}$$

Now (A.840) gives the dynamic boundary condition on the free surface

$$g\eta + \frac{\partial\phi}{\partial t} + \frac{|\nabla\phi|^2}{2} = 0 \qquad \text{for } x_3 = \eta(\boldsymbol{x}_s, t), \quad \boldsymbol{x}_s \in \Gamma. \tag{A.842}$$

Another boundary condition holds on every "physical" surface $\mathcal{S}$ bounding the fluid domain Ω and expressing the kinematic property that there is no transfer of matter across $\mathcal{S}$. Let $s(\boldsymbol{x}_s, x_3, t) = 0$ be the equation of $\mathcal{S}$, then

$$\frac{\mathrm{d}s}{\mathrm{d}t} = \boldsymbol{v}\cdot\nabla s + \frac{\partial s}{\partial t} = 0 \qquad \text{on } \mathcal{S}. \tag{A.843}$$

Under assumption (A.838) this takes the form of

$$\frac{\partial\phi}{\partial n} = -\frac{1}{|\nabla s|}\frac{\partial s}{\partial t} = v_n \qquad \text{on } \mathcal{S}, \tag{A.844}$$

where v_n denotes the normal velocity of $\mathcal{S}$. Thus the kinematic boundary condition (A.844) means that the normal velocity of particles is continuous across a physical boundary.

On the fixed part of $\mathcal{S}$, (A.844) takes the form of

$$\frac{\partial\phi}{\partial n} = 0. \tag{A.845}$$

On the free surface, condition (A.843), written as follows,

$$\frac{\partial\eta}{\partial t} + \nabla_s\phi\cdot\nabla_s\eta - \frac{\partial\phi}{\partial x_3} = 0 \qquad \text{for } x_3 = \eta(\boldsymbol{x}_s, t), \quad \boldsymbol{x}_s \in \Gamma, \tag{A.846}$$

complements the dynamic condition (A.842). Thus, in the present approach, two non-linear conditions (A.842) and (A.846) on the unknown boundary are responsible for waves, which constitutes the main characteristic feature of water-surface wave theory.

This brief account of governing equations can be summarized as follows. In the water-wave problem one seeks the velocity potential $\phi(\boldsymbol{x}_s, x_3, t)$ and the free surface elevation $\eta(\boldsymbol{x}_s, t)$ satisfying (A.839), (A.842), (A.844), and (A.846). The initial values of ϕ and η should also be prescribed, as well as the conditions at infinity (for unbounded Ω) to complete the problem, which is known as the Cauchy-Poisson problem.

A.10.2 Energy and its flow

Let Ω_0 be a subdomain of Ω, bounded by a "geometric" surface $\partial\Omega_0$ that may not be related to physical obstacles, and that is permitted to vary in time independently of moving water unlike the "physical" surfaces described below. Let $s_0(\boldsymbol{x}_s, x_3, t) = 0$ be the equation of $\partial\Omega_0$. The total energy contained in Ω_0 consists of kinetic and potential components, and is given by

$$E = \rho \int_{\Omega_0} \left(g x_3 + \frac{|\nabla\phi|^2}{2} \right) \mathrm{d}\boldsymbol{x}. \tag{A.847}$$

The first term related to the vertical displacement of a water particle corresponds to the potential energy, whereas the second one gives the kinetic energy that is proportional to the velocity squared. Using (A.840) and (A.841), one can write this in the form of

$$E = -\int_{\Omega_0} \left(\rho \frac{\partial\phi}{\partial t} + p - p_0 \right) \mathrm{d}\boldsymbol{x}. \tag{A.848}$$

Differentiating (A.848) with respect to t we get (John 1949, Lamb 1916)

$$\frac{\mathrm{d}E}{\mathrm{d}t} = \rho \int_{\Omega_0} \nabla\phi \cdot \nabla \frac{\partial\phi}{\partial t} \, \mathrm{d}\boldsymbol{x} + \int_{\partial\Omega_0} \frac{1}{|\nabla s_0|} \frac{\partial s_0}{\partial t} \left(\rho \frac{\partial\phi}{\partial t} + p - p_0 \right) \mathrm{d}\gamma(\boldsymbol{x}). \tag{A.849}$$

Green's first integral theorem (A.612) applied to the first integral of (A.849) leads to

$$\frac{\mathrm{d}E}{\mathrm{d}t} = \int_{\partial\Omega_0} \left\{ \rho \frac{\partial\phi}{\partial t} \left(\frac{\partial\phi}{\partial n} - v_n \right) - (p - p_0) v_n \right\} \mathrm{d}\gamma(\boldsymbol{x}), \tag{A.850}$$

where (A.839) is taken into account and v_n denotes the normal velocity of $\partial\Omega_0$. Hence the integrand in (A.850) is the rate of energy flow from Ω_0 through $\partial\Omega_0$ taken per units of time and area. The velocity of energy propagation is known as the group velocity. Further details can be found for this topic in Wehausen & Laitone (1960).

If a portion of $\partial\Omega_0$ is a fixed geometric surface, then $v_n = 0$ on this portion. The rate of energy flow is given by $-\rho(\partial\phi/\partial t)(\partial\phi/\partial n)$.

If a portion of $\partial\Omega_0$ is a "physical" boundary that is not penetrable by water particles, then (A.844) shows that the integrand in (A.850) is equal to $(p_0 - p)v_n$. Therefore, there is no energy flow through this portion of $\partial\Omega_0$ if either of two factors vanishes. In particular, this is true for the free surface ($p = p_0$) and for the bottom ($v_n = 0$).

A.10.3 Linearized unsteady problem

The presented problem is quite general, and it is very complicated to find an explicit solution for these equations. The difficulties arising from the fact that ϕ is a solution of the potential equation determined by non-linear boundary conditions on a variable boundary are considerable. A large number of papers has been published and great progress has been

achieved in the mathematical treatment of non-linear water-wave problems. However, all rigorous results in this direction are concerned with water waves in the absence of floating bodies, although some numerical results treating different aspects of the non-linear problem have been achieved.

To be in a position to describe water waves in the presence of bodies, the equations should be approximated by more tractable ones. The usual and rather reasonable simplification consists in a linearization of the problem under certain assumptions concerning the motion of a floating body. An example of such assumptions (there are other ones leading to the same conclusions) suggests that a body's motion near the equilibrium position is so small that it produces only waves having a small amplitude and a small wavelength. There are three characteristic geometric parameters: a typical value of the wave height H, a typical wavelength L, and the water depth D. They give three characteristic quotients: H/L, H/D, and L/D. The relative importance of these quotients is different in different situations. Nevertheless, it was found that if

$$\frac{H}{D} \ll 1 \qquad \text{and} \qquad \frac{H}{L}\left(\frac{L}{D}\right)^3 \ll 1, \tag{A.851}$$

then the linearization can be justified by some heuristic considerations. The last parameter $(H/L)(L/D)^3 = (H/D)(L/D^2)$ is usually referred to as Ursell's number.

The linearized theory leads to results that are in a rather good agreement with experiments and observations. Furthermore, there is mathematical evidence that the linearized problem provides an approximation to the non-linear one. For the Cauchy-Poisson problem describing waves in a water layer caused by prescribed initial conditions, the linear approximation is justified rigorously. More precisely, under the assumption that the undisturbed water occupies a layer of constant depth, the following are proved. The non-linear problem is solvable for sufficiently small values of the linearization parameter. As this parameter tends to zero, solutions of the non-linear problem do converge to the solution of the linearized problem in the norm of some suitable function space.

A formal perturbation procedure leading to a sequence o linear problems can be developed as follows. Let us assume that the velocity potential ϕ and the free surface elevation η admit expansions with respect to a certain small parameter ϵ:

$$\phi(\boldsymbol{x}_s, x_3, t) = \epsilon\phi^{(1)}(\boldsymbol{x}_s, x_3, t) + \epsilon^2\phi^{(2)}(\boldsymbol{x}_s, x_3, t) + \epsilon^3\phi^{(3)}(\boldsymbol{x}_s, x_3, t) + \dots, \tag{A.852}$$

$$\eta(\boldsymbol{x}_s, t) = \eta^{(0)}(\boldsymbol{x}_s, t) + \epsilon\eta^{(1)}(\boldsymbol{x}_s, t) + \epsilon^2\eta^{(2)}(\boldsymbol{x}_s, t) + \dots, \tag{A.853}$$

where $\phi^{(1)}$, $\phi^{(2)}$, …, $\eta^{(0)}$, $\eta^{(1)}$, …, and all their derivatives are bounded. Consequently, the velocities of water particles are supposed to be small (proportional to ϵ), and $\epsilon = 0$ corresponds to water permanently at rest.

Substituting (A.852) into (A.839) gives

$$\Delta\phi^{(k)} = 0 \qquad \text{in } \Omega, \quad k = 1, 2, \dots. \tag{A.854}$$

Furthermore, $\eta^{(0)}$ describing the free surface at rest cannot depend on t. When the expansions for ϕ and η are substituted into the Bernoulli boundary condition (A.842) and

grouped according to powers of ϵ, one obtains

$$\eta^{(0)} = 0 \qquad \text{for } \boldsymbol{x}_s \in \Gamma. \tag{A.855}$$

This and Taylor's expansion of $\phi(\boldsymbol{x}_s, \eta(\boldsymbol{x}_s, t), t)$ in powers of ϵ yield the following for orders higher than zero:

$$\frac{\partial \phi^{(1)}}{\partial t} + g\eta^{(1)} = 0 \qquad \text{for } x_3 = 0, \ \ \boldsymbol{x}_s \in \Gamma, \tag{A.856}$$

$$\frac{\partial \phi^{(2)}}{\partial t} + g\eta^{(2)} = -\eta^{(1)} \frac{\partial^2 \phi^{(1)}}{\partial t \partial x_3} - \frac{|\nabla \phi^{(1)}|^2}{2} \qquad \text{for } x_3 = 0, \ \ \boldsymbol{x}_s \in \Gamma, \tag{A.857}$$

and so on, i.e., all these conditions hold on the mean position of the free surface at rest.

Similarly, the kinematic condition (A.846) leads to

$$\frac{\partial \phi^{(1)}}{\partial x_3} - \frac{\partial \eta^{(1)}}{\partial t} = 0 \qquad \text{for } x_3 = 0, \ \ \boldsymbol{x}_s \in \Gamma, \tag{A.858}$$

$$\frac{\partial \phi^{(2)}}{\partial x_3} - \frac{\partial \eta^{(2)}}{\partial t} = -\eta^{(1)} \frac{\partial^2 \phi^{(1)}}{\partial x_3^2} + \nabla_s \phi^{(1)} \cdot \nabla \eta^{(1)} \qquad \text{for } x_3 = 0, \ \ \boldsymbol{x}_s \in \Gamma, \tag{A.859}$$

and so on. Eliminating $\eta^{(1)}$ between (A.856) and (A.858), one finds the classical first-order linear free-surface condition

$$\frac{\partial^2 \phi^{(1)}}{\partial t^2} + g \frac{\partial \phi^{(1)}}{\partial x_3} = 0 \qquad \text{for } x_3 = 0, \ \ \boldsymbol{x}_s \in \Gamma. \tag{A.860}$$

In the same way, for $x_3 = 0$ and $\boldsymbol{x}_s \in \Gamma$, one obtains from (A.857) and (A.859) that

$$\frac{\partial^2 \phi^{(2)}}{\partial t^2} + g \frac{\partial \phi^{(2)}}{\partial x_3} = -\frac{\partial \phi^{(1)}}{\partial t} \nabla_s^2 \phi^{(1)} - \frac{1}{g^2} \frac{\partial}{\partial t} \left\{ \frac{\partial \phi^{(1)}}{\partial t} \frac{\partial^3 \phi^{(1)}}{\partial t^3} + |\nabla_s \phi^{(1)}|^2 \right\}. \tag{A.861}$$

Further free-surface conditions can be obtained for terms in (A.852) having higher orders in ϵ. All these conditions have the same operator in the left-hand side, and the right-hand term depends non-linearly on terms of smaller orders. It is worth mentioning that all of the high-order problems are formulated in the same domain Ω occupied by the water at rest. In particular, the free-surface boundary conditions are imposed at $\{x_3 = 0, \, \boldsymbol{x}_s \in \Gamma\}$.

A.10.4 Boundary condition on an immersed rigid surface

First, we note that the homogeneous Neumann condition (A.845) is linear on fixed surfaces. Hence, this condition is true for $\phi^{(k)}$, $k = 1, 2, \ldots$. The situation reverses for the inhomogeneous Neumann condition (A.844) on a moving surface $\mathcal{S}$, which can be subjected, for example, to a prescribed motion or freely floating. The problem of a body freely floating near its equilibrium position will not be treated here, and we restrict ourselves to the linearization of (A.844) for $\mathcal{S} = S(t, \epsilon)$ undergoing a given small amplitude motion near an equilibrium position S, i.e., when $S(t, \epsilon)$ tends to S as $\epsilon \to 0$.

It is convenient to carry out the linearization locally. Let us consider a neighborhood of $(\boldsymbol{x}_s^{(0)}, x_3^{(0)}) \in S$, where the surface is given explicitly in local cartesian coordinates $(\boldsymbol{\xi}_s, \xi_3)$, being in the three-dimensional case $\boldsymbol{\xi}_s = (\xi_1, \xi_2)$, and having an origin at $(\boldsymbol{x}_s^{(0)}, x_3^{(0)})$ and the ξ_3 axis directed into water normally to S. Let $\xi_3 = \zeta^{(0)}(\boldsymbol{\xi}_s)$ be the

equation of S, and $S(t,\epsilon)$ be given by $\xi_3 = \zeta(\boldsymbol{\xi}_s, t, \epsilon)$, where

$$\zeta(\boldsymbol{\xi}_s, t, \epsilon) = \zeta^{(0)}(\boldsymbol{\xi}_s) + \epsilon\zeta^{(1)}(\boldsymbol{\xi}_s, t) + \epsilon^2\zeta^{(2)}(\boldsymbol{\xi}_s, t) + \dots . \tag{A.862}$$

After substituting (A.852) and $s = \xi_3 - \zeta(\boldsymbol{\xi}_s, t, \epsilon)$ into (A.843), we use (A.838), (A.862), and Taylor's expansion in the same way as, e.g., in (A.856). This gives the first-order equation

$$\frac{\partial\phi^{(1)}}{\partial\xi_3}(\boldsymbol{\xi}_s, \zeta^{(0)}, t) - \nabla_s\phi^{(1)}(\boldsymbol{\xi}_s, \zeta^{(0)}, t)\cdot\nabla_s\zeta^{(0)}(\boldsymbol{\xi}_s) = \frac{\partial\zeta^{(1)}}{\partial t}(\boldsymbol{\xi}_s, t), \tag{A.863}$$

which implies the linearized boundary condition

$$\frac{\partial\phi^{(1)}}{\partial n} = v_n^{(1)} \qquad \text{on } \mathcal{S}, \tag{A.864}$$

where

$$v_n^{(1)} = \frac{\partial\zeta^{(1)}/\partial t}{\sqrt{(1+|\nabla_s\zeta^{(0)}|^2)}} \tag{A.865}$$

is the first-order approximation of the normal velocity of $S(t,\epsilon)$.

The second-order boundary condition on S has the form

$$\frac{\partial\phi^{(2)}}{\partial n} = \frac{\partial\zeta^{(2)}/\partial t}{\sqrt{(1+|\nabla_s\zeta^{(0)}|^2)}} - \zeta^{(1)}\frac{\partial^2\phi^{(1)}}{\partial n^2} - \sqrt{\frac{1+|\nabla_s\zeta^{(1)}|^2}{1+|\nabla_s\zeta^{(0)}|^2}}\,\frac{\partial\phi^{(1)}}{\partial n^{(1)}}, \tag{A.866}$$

where $\partial\phi^{(1)}/\partial n^{(1)}$ is the derivative in the direction of normal $\xi_3 = \zeta^{(1)}(\boldsymbol{\xi}_s, t)$ calculated on S. In addition, further conditions on S of the Neumann type can be obtained for terms of higher order in ϵ.

Thus, all $\phi^{(k)}$ satisfy the same linear boundary-value problem with different right-hand side terms in conditions on the free surface at rest and on the equilibrium surfaces of immersed bodies. These right-hand side terms depend on solutions obtained on previous steps. Solving these problems successively, beginning with problems (A.854), (A.860), and (A.864) complemented by some initial conditions, one can, generally speaking, find a solution to the non-linear problem in the form of (A.852) and (A.853). However, this procedure is not justified mathematically up to the present time. Therefore, we restrict ourselves to the first-order approximation, which on its own right gives rise to an extensive mathematical theory.

We summarize now the boundary-value problem for the first-order velocity potential $\phi^{(1)}(\boldsymbol{x}_s, x_3, t)$. It is defined in Ω occupied by water at rest with a boundary consisting of the free surface Γ, the bottom B, and the wetted surface of immersed bodies S, and it must satisfy

$$\Delta\phi^{(1)} = 0 \qquad \text{in } \Omega, \tag{A.867}$$

$$\frac{\partial^2\phi^{(1)}}{\partial t^2} + g\frac{\partial\phi^{(1)}}{\partial x_3} = 0 \qquad \text{for } x_3 = 0, \ \ \boldsymbol{x}_s \in \Gamma, \tag{A.868}$$

$$\frac{\partial\phi^{(1)}}{\partial n} = v_n^{(1)} \qquad \text{on } S, \tag{A.869}$$

$$\frac{\partial \phi^{(1)}}{\partial n} = 0 \qquad \text{on } B, \tag{A.870}$$

$$\phi^{(1)}(\boldsymbol{x}_s, 0, 0) = \phi_0(\boldsymbol{x}_s) \qquad \text{and} \qquad \frac{\partial \phi^{(1)}}{\partial t}(\boldsymbol{x}_s, 0, 0) = -g\eta_0(\boldsymbol{x}_s), \tag{A.871}$$

where ϕ_0, $v_n^{(1)}$, and η_0 are given functions, and $\eta_0(\boldsymbol{x}_s) = \eta^{(1)}(\boldsymbol{x}_s, 0)$ (see (A.856)). Then

$$\eta^{(1)}(\boldsymbol{x}_s, t) = -\frac{1}{g}\frac{\partial \phi^{(1)}}{\partial t}(\boldsymbol{x}_s, 0, t) \tag{A.872}$$

gives the first-order approximation for the elevation of the free surface.

A.10.5 Linear time-harmonic waves

We are interested in the study of the steady-state problem of radiation and scattering of water waves by bodies floating in and/or beneath the free surface, assuming all motions to be simple harmonic in the time. The corresponding radian frequency is denoted by ω. Thus, the right-hand side term in (A.864) is

$$v_n^{(1)} = \mathfrak{Re}\{e^{-i\omega t} f\} \qquad \text{on } S, \tag{A.873}$$

where f is a complex function independent of t, and the first-order velocity potential $\phi^{(1)}$ can then be written in the form

$$\phi^{(1)}(\boldsymbol{x}_s, x_3, t) = \mathfrak{Re}\{e^{-i\omega t} u(\boldsymbol{x}_s, x_3)\}. \tag{A.874}$$

The latter assumption is justified by the so-called limiting amplitude principle, which is concerned with large-time behavior of a solution to the initial-boundary-value problem having (A.873) as the right-hand side term. According to this principle, such a solution tends to the potential (A.874) as $t \to \infty$, and u satisfies a steady-state problem. The limiting amplitude principle has general applicability in the theory of wave motions. Thus the problem of our interest describes waves developing at large time from time-periodic disturbances.

A complex function u in (A.874) is also referred to as velocity potential (but in this case with respect to time-harmonic dependence). We recall that u is defined in the fixed domain Ω occupied by water at rest outside any bodies present. The boundary $\partial\Omega$ consists of three disjoint sets: (i) S, which is the union of the wetted surfaces of bodies in equilibrium; (ii) Γ, denoting the free surface at rest that is the part of $x_3 = 0$ outside all the bodies; and (iii) B, which denotes the bottom positioned below $\Gamma \cup S$. Sometimes Ω is considered unbounded below and corresponding to infinitely deep water. This is the case in this thesis and it involves that $\partial\Omega = \Gamma \cup S$.

Substituting thus (A.873) and (A.874) into (A.867)–(A.870) gives the boundary-value problem for u:

$$\Delta u = 0 \qquad \text{in } \Omega, \tag{A.875}$$

$$\frac{\partial u}{\partial x_3} - \nu u = 0 \qquad \text{on } \Gamma, \tag{A.876}$$

$$\frac{\partial u}{\partial n} = f \qquad \text{on } S, \tag{A.877}$$

$$\frac{\partial u}{\partial n} = 0 \qquad \text{on } B, \tag{A.878}$$

where $\nu = \omega^2/g$. We suppose that the normal $\boldsymbol{n}$ to a surface is always directed outwards of the water domain Ω.

For deep water ($B = \emptyset$), condition (A.878) should be replaced by something like

$$\sup_{(\boldsymbol{x}_s, x_3)\in\Omega} |u(\boldsymbol{x}_s, x_3)| < \infty. \tag{A.879}$$

This condition has no direct hydrodynamic meaning, apart from stating that the solution has to remain bounded in Ω. It implies the natural asymptotic behavior for the velocity field given by

$$|\nabla u| \longrightarrow 0 \qquad \text{as} \qquad x_3 \longrightarrow -\infty, \tag{A.880}$$

that is, the water motion decays with depth. Conditions at infinity that are similar to the last two conditions are usually imposed in the boundary-value problems for the Laplacian in domains exterior to a compact set in $\mathbb{R}^2$ and $\mathbb{R}^3$. A natural requirement that a solution to (A.875)–(A.879) should be unique also imposes a certain restriction on the behavior of u as $|\boldsymbol{x}_s| \to \infty$. We will return again to this topic below.

Let us consider now some simple examples of waves existing in the absence of bodies. The corresponding potentials can be easily obtained by separation of variables.

For a layer Ω of constant depth d, we consider the free surface $\Gamma = \{\boldsymbol{x}_s \in \mathbb{R}^2, x_3 = 0\}$ and the bottom $B = \{\boldsymbol{x}_s \in \mathbb{R}^2, x_3 = -d\}$. A plane progressive wave propagating in the direction of a wave vector $\boldsymbol{k}_s = (k_1, k_2)$ has the velocity potential

$$\mathfrak{Re}\big\{A \exp(i\boldsymbol{k}_s \cdot \boldsymbol{x}_s - i\omega t)\big\} \cosh\{k_s(x_3 + d)\}. \tag{A.881}$$

Here A is an arbitrary complex constant, $k_s = |\boldsymbol{k}_s|$, and the following relationship,

$$\nu = \frac{\omega^2}{g} = k_s \tanh(k_s d), \tag{A.882}$$

holds between ω and k_s. Tending d to infinity, we note that k_s becomes equal to ν and, instead of (A.881), we have

$$\mathfrak{Re}\big\{A \exp(i\boldsymbol{k}_s \cdot \boldsymbol{x}_s - i\omega t)\big\}\, e^{\nu x_3} \tag{A.883}$$

for the velocity potential of a plane progressive wave in deep water.

A sum of two potentials (A.881) corresponding to identical progressive waves propagating in opposite directions gives a standing wave. Putting the term $\exp(\nu x_3)$ instead of $\cosh\{k_s(x_3 + d)\}$ in (A.881) and omitting $\tanh(k_s d)$ in (A.882), one gets the potential of a progressive wave in deep water.

A standing cylindrical wave in a water layer of depth d has the potential

$$w_{\text{st}}(\boldsymbol{x}_s, x_3) \cos(\omega t), \tag{A.884}$$

where

$$w_{\text{st}}(\boldsymbol{x}_s, x_3) = C_1 \cosh\{k_s(x_3 + d)\} J_0(k_s|\boldsymbol{x}_s|), \tag{A.885}$$

and where k_s is defined by (A.882), C_1 is a real constant, and J_0 denotes the Bessel function of order zero (vid. Subsection A.2.4). The same manipulation as above gives the standing wave in deep water.

A cylindrical wave having an arbitrary phase at infinity may be obtained as a combination of w_{st} and a similar potential with J_0 replaced by Y_0, the Neumann function of order zero. This allows one to construct a potential of outgoing waves as

$$\mathfrak{Re}\big\{e^{-i\omega t} w_{\text{out}}(\boldsymbol{x}_s, x_3)\big\}, \tag{A.886}$$

where

$$w_{\text{out}}(\boldsymbol{x}_s, x_3) = C_2 \cosh\{k_s(x_3 + d)\} H_0^{(1)}(k_s|\boldsymbol{x}_s|), \tag{A.887}$$

and where k_s is defined by (A.882), C_2 is a complex constant, and $H_0^{(1)}$ denotes the zeroth order Hankel function of the first kind. The outgoing behavior of this wave becomes clear from the asymptotic formula

$$H_0^{(1)}(k_s|\boldsymbol{x}_s|) = \sqrt{\frac{2}{\pi k_s|\boldsymbol{x}_s|}}\, e^{i(k_s|\boldsymbol{x}_s| - \pi/4)}\big(1 + \mathcal{O}(|\boldsymbol{x}_s|^{-1})\big) \qquad \text{as } |\boldsymbol{x}_s| \to \infty, \tag{A.888}$$

where $\mathcal{O}(\cdot)$ denotes the highest order of the remaining terms at infinity. Therefore, the wave w_{out} behaves at large distances like a radially outgoing progressive wave, but it is singular on the axis $|\boldsymbol{x}_s| = 0$. This is natural from a physical point of view, because outgoing waves should be radiated by a certain disturbance. In the case under consideration, the wave is produced by sources distributed with a suitable density over $\{|\boldsymbol{x}_s| = 0,\ -d < x_3 < 0\}$. Replacing $H_0^{(1)}$ in (A.887) by the zeroth order Hankel function of the second kind, $H_0^{(2)}$, one obtains an incoming wave.

A.10.6 Radiation conditions

The examples of waves existing in the absence of bodies, e.g., plane progressive and cylindrical waves, demonstrate that problem (A.875)–(A.878) should be complemented by an appropriate condition as $|\boldsymbol{x}_s| \to \infty$ to avoid non-uniqueness of the solution, which follows from the fact that there are infinitely many solutions in the form of (A.881). On the other hand, the energy dissipates when waves are radiated or scattered, i.e., there exists a flow of energy to infinity. On the contrary, there is no such flow for standing waves and no net flow for progressive waves. Since we are interested in describing radiation and scattering phenomena, a condition should be introduced to eliminate waves having no flow of energy to infinity. For this purpose a mathematical expression is used that is known as a radiation condition. To formulate this condition, we have to specify the geometry of the water domain at infinity.

Let Ω be an N-dimensional domain ($N = 2, 3$), which at infinity coincides with the layer $\{\boldsymbol{x}_s \in \mathbb{R}^{N-1},\ -d < x_3 < 0\}$, where $0 < d \leq \infty$. We say that u satisfies the radiation

condition of the Sommerfeld type if

$$\frac{\partial u}{\partial|\boldsymbol{x}_s|} - ik_s u = \sigma(x_3)\mathcal{O}(|\boldsymbol{x}_s|^{(2-N)/2}) \qquad \text{as } |\boldsymbol{x}_s| \to \infty, \text{ uniformly in } x_3, \theta. \quad \text{(A.889)}$$

Here $\sigma(x_3) = (1+|x_3|)^{-N+1}$ if $d = \infty$, $\sigma(x_3) = 1$ if $d < \infty$, k_s is defined by (A.882) for $d < \infty$, and $k_s = \nu$ for $d = \infty$, and $\theta \in [0, 2\pi)$ is the polar angle in the plane $\{x_3 = 0\}$. Uniformity in θ should be imposed only for the three-dimensional problem ($N = 3$).

Let us show that (A.889) guarantees dissipation of energy. For the sake of simplicity we assume that $d < \infty$. By $\mathcal{C}_r$ we denote a cylindrical surface $\Omega \cap \{|\boldsymbol{x}_s| = r\}$ contained inside Ω. By (A.850) the average energy flow to infinity through $\mathcal{C}_r$ over one period of oscillations is equal to

$$F_r = -\frac{\rho\omega}{2\pi}\int_0^{2\pi/\omega}\int_{\mathcal{C}_r} \frac{\partial\phi}{\partial t}\,\frac{\partial\phi}{\partial|\boldsymbol{x}_s|}\,\mathrm{d}\gamma\,\mathrm{d}t. \quad \text{(A.890)}$$

Substituting (A.874) and taking into account that

$$\int_0^{2\pi/\omega} e^{\pm 2i\omega t}\,\mathrm{d}t = 0, \quad \text{(A.891)}$$

one finds that

$$\begin{aligned} F_r &= -\frac{\rho\omega^2}{8\pi}\int_0^{2\pi/\omega}\int_{\mathcal{C}_r} (ie^{i\omega t}\bar{u} - ie^{-i\omega t}u)\left(e^{-i\omega t}\frac{\partial u}{\partial|\boldsymbol{x}_s|} + e^{i\omega t}\frac{\partial\bar{u}}{\partial|\boldsymbol{x}_s|}\right)\mathrm{d}\gamma\,\mathrm{d}t \\ &= -\frac{\rho\omega}{4\pi}\int_{\mathcal{C}_r}\left(i\bar{u}\frac{\partial u}{\partial|\boldsymbol{x}_s|} - iu\frac{\partial\bar{u}}{\partial|\boldsymbol{x}_s|}\right)\mathrm{d}\gamma = \frac{\rho\omega}{2}\,\mathfrak{Im}\int_{\mathcal{C}_r}\bar{u}\frac{\partial u}{\partial|\boldsymbol{x}_s|}\,\mathrm{d}\gamma. \end{aligned} \quad \text{(A.892)}$$

This can be written as

$$F_r = \frac{\rho\omega}{4k_s}\left\{\int_{\mathcal{C}_r}\left(\left|\frac{\partial u}{\partial|\boldsymbol{x}_s|}\right|^2 + k_s^2|u|^2\right)\mathrm{d}\gamma - \int_{\mathcal{C}_r}\left|\frac{\partial u}{\partial|\boldsymbol{x}_s|} - ik_s u\right|^2\mathrm{d}\gamma\right\}. \quad \text{(A.893)}$$

Moreover, F_r does not depend on r when the obstacle surface S lies inside the cylinder $\{|\boldsymbol{x}_s| = r\}$, which can be proved as follows.

By Ω_r and Γ_r we denote $\Omega \cap \{|\boldsymbol{x}_s| < r\}$ and $\Gamma \cap \{|\boldsymbol{x}_s| < r\}$, respectively. Let us multiply (A.875) by $\bar{u}$ and integrate the result over Ω_r. By applying then Green's theorem we obtain

$$\int_{\Omega_r}|\nabla u|^2\,\mathrm{d}\boldsymbol{x}_s\,\mathrm{d}x_3 = \int_{\partial\Omega_r}\bar{u}\frac{\partial u}{\partial n}\,\mathrm{d}\gamma, \quad \text{(A.894)}$$

where the normal $\boldsymbol{n}$ is directed outside of Ω_r. Using (A.876) and (A.878) we get

$$\int_{\Omega_r}|\nabla u|^2\,\mathrm{d}\boldsymbol{x}_s\,\mathrm{d}x_3 = \nu\int_{\Gamma_r}|u|^2\,\mathrm{d}\boldsymbol{x}_s + \int_{\mathcal{C}_r}\bar{u}\frac{\partial u}{\partial|\boldsymbol{x}_s|}\,\mathrm{d}\gamma - \int_S\bar{u}\frac{\partial u}{\partial n}\,\mathrm{d}\gamma. \quad \text{(A.895)}$$

Comparing this with (A.892) we find that

$$F_r = \frac{\rho\omega}{2}\,\mathfrak{Im}\int_S\bar{u}\frac{\partial u}{\partial|\boldsymbol{x}_s|}\,\mathrm{d}\gamma \quad \text{(A.896)}$$

is independent of r.

This fact yields that $F_r \geq 0$ because (A.889) implies that the last integral in (A.893) tends to zero as $r \to \infty$.

The crucial point in the proof that $F_r \geq 0$ is the equality (A.893), which suggests that (A.889) can be replaced by a weaker radiation condition of the Rellich type

$$\int_{\mathcal{C}_r} \left| \frac{\partial u}{\partial |\boldsymbol{x}_s|} - ik_s u \right|^2 \mathrm{d}\gamma = \mathcal{O}(1) \qquad \text{as} \quad r \to \infty. \tag{A.897}$$

Actually, (A.889) and (A.897) are equivalent.

So, problem (A.875)–(A.878) has to be complemented by either (A.889) or (A.897). In various papers this problem appears under different names: the floating body problem, the sea-keeping problem, the wave-body interaction problem, the water-wave radiation (scattering) problem, and so on.

A.11 Linear acoustic theory

The linear acoustic theory is concerned with the propagation of sound waves considered as small perturbations in a fluid or gas. Consequently the equations of acoustics are obtained by linearization of the equations for the motion of fluids. The two main media for the propagation and scattering of sound waves are air and water (underwater acoustics). A third important medium with properties close to those of water is the human body, i.e., biological tissue (ultrasound). We are herein interested in obtaining the differential equations that govern the acoustic wave propagation, whose linearization yields the scalar wave equation of acoustics. By considering simple-harmonic waves for the wave equation, we obtain finally the Helmholtz equation. When the frequency is zero, this equation turns into the Poisson or the Laplace equation. The corresponding boundary conditions are also developed, in particular the impedance boundary condition. A good and complete reference for the linear acoustic theory is the article by Morse & Ingard (1961), which is closely followed herein. Other references are DeSanto (1992), Elmore & Heald (1969), Howe (2007), Kinsler, Frey, Coppens & Sanders (1999), Kress (2002), and Strutt (1877).

Acoustic motion is, almost by definition, a perturbation. The slow compressions and expansions of materials, studied in thermodynamics, are not thought of as acoustical phenomena, nor is the steady flow of air usually called sound. It is only when the compression is irregular enough so that overall thermodynamic equilibrium may not be maintained, or when the steady flow is deflected by some obstacles so that wave motion is produced, that we consider part of the motion to be acoustical. In other words, we think of sound as a by-product, wanted or unwanted, of slower, more regular mechanical processes. And, whether the generating process be the motion of a violin bow or the rush of gas from a turbo-jet, the part of motion we call sound usually carries but a minute fraction of the energy present in the primary process, which is not considered to be acoustical.

This definition of acoustical motion as being the small, irregular part of some larger, more regular motion of matter, gives rise to difficulties when we try to develop a consistent mathematical representation of its behavior. When the irregularities are large enough, for example, there is no clear-cut way of separating the acoustical from the non-acoustical part of the motion. In fact, only in the cases where the non-steady motions are first-order perturbations of some larger, steady-state motion can one hope to make a self-consistent definition which separates acoustic from non-acoustic motion and, even here, there are ambiguities in the case of some types of near field. Thus it is not surprising that the earliest work in acoustic theory, and even now a vast quantity, has to do with situations where the acoustical part of the motion is small enough so that linear approximations can be used. These are our cases of interest in this thesis. Strictly speaking, the equations to be discussed here are valid only when the acoustical component of the motion is "sufficiently" small, but it is only in this limit that we can unequivocably separate the total motion into its acoustical and its non-acoustical parts.

Still another limitation of the validity of acoustical theory is imposed by the atomicity of matter. The thermal motions of individual molecules, for instance, are not usually

representable by the equations of sound. These equations are meant to represent the average behavior of large assemblies of molecules. Thus, for instance, when we speak of an element of volume we implicitly assume that its dimensions, while being smaller than any wavelength of acoustical motion present, are large compared to inter-molecular spacings.

A.11.1 Differential equations

a) Basic equations of motion

Considering the fluid as a continuous medium, two points of view can be adopted in describing its motion. In the first, the Lagrangian motion, the history of each individual fluid element, or particle, is recorded in terms of its position $\boldsymbol{x}$ as a function of the time t. Each particle is identified by means of a parameter, which is usually chosen to be the position vector $\boldsymbol{x}_0$ of the element at $t = 0$. The Lagrangian description of fluid motion is expressed by the set of functions $\boldsymbol{x} = \boldsymbol{x}(\boldsymbol{x}_0, t)$.

In the second, or Eulerian, description, on the other hand, the fluid motion is described in terms of a velocity field $\boldsymbol{V}(\boldsymbol{x}, t)$ in which the position $\boldsymbol{x}$ and the time t are independent variables. The variation of $\boldsymbol{V}$ with time, or of any other fluid property in this description, refers thus to a fixed point in space rather than to a specific fluid element, as is the case with the Lagrangian description.

If a field quantity is denoted by Ψ_L in the Lagrangian and by Ψ_E in the Eulerian description, then the relation between the time derivatives in the two descriptions is

$$\frac{\mathrm{d}\Psi_L}{\mathrm{d}t} = \frac{\partial \Psi_E}{\partial t} + (\boldsymbol{V} \cdot \nabla)\Psi_E. \tag{A.898}$$

We remark that in the case of linear acoustics for a homogeneous medium at rest we need not be concerned about the difference between $(\mathrm{d}\Psi_L/\mathrm{d}t)$ and $(\partial\Psi_E/\partial t)$, since the term $(\boldsymbol{V} \cdot \nabla)\Psi_E$ is then of second order. However, in a moving or inhomogeneous medium the distinction must be maintained even in the linear approximation.

We shall ordinarily use the Eulerian description and, if we ever need the Lagrangian time derivative, we shall express it as the right-hand side of (A.898), omitting the subscripts. We express herein the fluid motion in terms of the three velocity components V_i of the velocity vector $\boldsymbol{V}$. We denote further the velocity amplitude as $V = |\boldsymbol{V}|$. In addition, the state of the fluid is described in terms of two independent thermodynamic variables such as pressure and temperature or density and entropy. We assume that thermodynamic equilibrium is maintained within each volume element. Thus in all we have five field variables: the three velocity components and the two independent thermodynamic variables. In order to determine these functions of $\boldsymbol{x}$ and t we need five equations. These turn out to be conservation laws: conservation of mass (one equation), conservation of momentum (three equations), and conservation of energy (one equation).

If the density of the fluid is denoted by ϱ and $i, j \in \{1, 2, 3\}$, then the mass flow in the fluid can be expressed by the vector components

$$\varrho V_i \tag{A.899}$$

and the total momentum flux by the tensor

$$t_{ij} = P_{ij} + \varrho V_i V_j, \tag{A.900}$$

in which the first term is the contribution from the thermal motion and the second term the contribution from the gross motion of the fluid. The term P_{ij} is the fluid stress tensor

$$P_{ij} = (P - \varepsilon \nabla \cdot \boldsymbol{V})\delta_{ij} - 2\eta U_{ij} = P\delta_{ij} - D_{ij}, \tag{A.901}$$

where P is the total pressure in the fluid, δ_{ij} is the delta of Kronecker, D_{ij} is the viscous stress tensor, ε and η are two coefficients of viscosity, and

$$U_{ij} = \frac{1}{2}\left(\frac{\partial V_i}{\partial x_j} + \frac{\partial V_j}{\partial x_i}\right) \tag{A.902}$$

is the shear-strain tensor. In this notation the bulk viscosity would be $3\varepsilon + 2\eta$, and if this were zero (as Stokes assumed for an ideal gas), then η would equal $-3\varepsilon/2$. However, acoustical measurement shows that bulk viscosity is not usually zero (in some cases it may be considerably larger than η) so it will be assumed that ε and η are independent parameters of the fluid. In addition, we define the energy density of the fluid as

$$h = \frac{1}{2}\varrho V^2 + \varrho E, \tag{A.903}$$

the sum of its kinetic energy and the internal energy (E denotes the internal energy per unit mass), and the energy flow vector as

$$I_i = hV_i + \sum_j P_{ij}V_j - K\frac{\partial T}{\partial x_i}, \tag{A.904}$$

in which T is the temperature, K is the thermal conductivity constant, and $\partial T/\partial x_i$ is the temperature gradient in the location of interest. Thus $-K(\partial T/\partial x_i)$ corresponds to the heat flow vector. The term $\sum_j P_{ij}V_j$ contains the work done by the pressure as well as the dissipation caused by the viscous stresses.

The basic equations of motion for the fluid, representing the conservation of mass, momentum, and energy, can thus be written in the forms

$$\frac{\partial \varrho}{\partial t} + \sum_i \frac{\partial(\varrho V_i)}{\partial x_i} = Q(\boldsymbol{x}, t), \tag{A.905}$$

$$\frac{\partial(\varrho V_i)}{\partial t} + \sum_j \frac{\partial t_{ij}}{\partial x_j} = F_i(\boldsymbol{x}, t), \tag{A.906}$$

$$\frac{\partial h}{\partial t} + \sum_i \frac{\partial I_i}{\partial x_i} = H(\boldsymbol{x}, t), \tag{A.907}$$

where Q, F_i, and H are source terms representing the time rate of introduction of mass, momentum, and heat energy into the fluid, per unit volume. The energy equation (A.907) can be rewritten in the somewhat different form

$$\varrho\frac{\mathrm{d}E}{\mathrm{d}t} = \varrho\left(\frac{\partial E}{\partial t} + \boldsymbol{V}\cdot\nabla E\right) = K\Delta T + D - P\nabla\cdot\boldsymbol{V} + H, \tag{A.908}$$

which represents the fact that a given element of fluid has its internal energy changed either by heat flow, or by viscous dissipation

$$D = \sum_{ij} D_{ij} U_{ij} = \varepsilon \sum_{j} U_{jj}^2 + 2\eta \sum_{ij} U_{ij}^2, \tag{A.909}$$

or by direct change of volume, or else by direct injection of heat from outside the system. This last form of energy equation can be obtained directly from the first law of thermodynamics

$$\frac{\mathrm{d}E}{\mathrm{d}t} = T\frac{\mathrm{d}S}{\mathrm{d}t} + \frac{P}{\varrho^2}\frac{\mathrm{d}\varrho}{\mathrm{d}t}, \tag{A.910}$$

if, for the rate of entropy production per unit mass $\mathrm{d}S/\mathrm{d}t$, we introduce

$$T\frac{\mathrm{d}S}{\mathrm{d}t} = \frac{K}{\varrho}\Delta T + \frac{D}{\varrho} + \frac{H}{\varrho}, \tag{A.911}$$

and, for the density change $\mathrm{d}\varrho/\mathrm{d}t$ we use

$$\frac{\mathrm{d}\varrho}{\mathrm{d}t} = \frac{\partial \varrho}{\partial t} + \boldsymbol{V}\cdot\nabla\varrho = -\varrho\nabla\cdot\boldsymbol{V}. \tag{A.912}$$

If we wish to change from one pair of thermodynamic variables to another we usually make use of the equation of state of the gas

$$P = P(\varrho, T). \tag{A.913}$$

For a perfect gas, it is given by

$$P = R\varrho T, \tag{A.914}$$

being $R = 8.314472$ [J/°K/mol] the (ideal) gas constant.

b) Wave equation

Returning to equations (A.905) to (A.907), by elimination of $\partial^2(\varrho V_i)/\partial x_i \partial t$ from the first two, we obtain

$$\frac{\partial^2 \varrho}{\partial t^2} - c_0^2 \Delta\varrho = \frac{\partial Q}{\partial t} - \sum_i \frac{\partial F_i}{\partial x_i} + \Delta(P - c_0^2\varrho) + \sum_{ij}\left(\frac{\partial^2 D_{ij}}{\partial x_i \partial x_j} + \frac{\partial^2(\varrho V_i V_j)}{\partial x_i \partial x_j}\right). \tag{A.915}$$

We have subtracted the term $c_0^2\Delta\varrho$ from both sides of the equation, where c_0 is the space average of the velocity of sound (c_0 can depend on t). The right-hand terms will vanish for a homogeneous, lossless, and source-free medium at rest, in which case we obtain for the density ϱ the familiar wave equation

$$\Delta\varrho - \frac{1}{c_0^2}\frac{\partial^2 \varrho}{\partial t^2} = 0. \tag{A.916}$$

Under all other circumstances the right-hand side of (A.915) will not vanish, but will represent some sort of sound source, either produced by external forces or injections of fluid or by inhomogeneities, motions, or losses in the fluid itself.

The first term, representing the injection of fluid, gives rise to a monopole wave. For air-flow sirens and pulsed-jet engines, for example, it represents the major source term. The second term, corresponding to body forces on the fluid, gives rise to dipole waves. Even

when this term is independent of time it may have an effect on sound transmission, as, e.g., in the case of the force of gravity.

The third term represents several effects. The variation of pressure is produced both by a density and an entropy variation. If the fluid changes are isentropic, then the third term corresponds to the scattering or refraction of sound by variations in temperature or composition of the medium. It may also correspond to a source of sound, in the case of a fluctuating temperature in a turbulent medium. If the motion is not isentropic, then the term $\Delta(P - c_0^2\varrho)$ also contains contributions from entropy fluctuations in the medium. These effects will include losses produced by heat conduction and also the generation of sound by heat sources.

The fourth term, the double divergence of D_{ij}, represents the effects of viscous losses and/or the generation of sound by oscillating viscous stresses in a moving medium. If the coefficients of viscosity should vary from point to point, one would have also the effect of scattering from such inhomogeneities, but these are usually quite negligible. Finally, the fifth term, the double divergence of the term $\varrho V_i V_j$, represents the scattering or the generation of sound caused by the motion of the medium. If the two previous terms are thought of as stresses produced by thermal motion, this last term can be considered as representing the Reynolds stress of the gross motion. It is the major source of sound in turbulent flow and produces quadrupole radiation.

c) Linear approximation

After having summarized the possible effects in fluid motion, we shall now consider the problem of linearisation of the equations (A.905) to (A.907) and the interpretation of its results. These equations are non-linear in the variables ϱ and V_i. Not only are there terms where the product ϱV_i occurs explicitly, but also terms such as h and I_i implicitly depend on ϱ and V_i in a non-linear way. Furthermore, the momentum flux t_{ij} is not usually linearly related to the other field variables. In the first place the gross motion of the fluid, if there is one, contributes a stress $\varrho V_i V_j$ and in the second place there is a non-linear relationship between the pressure P and the other thermodynamic variables. For example, in an isentropic motion we have $(P/P_0) = (\varrho/\varrho_0)^\gamma$, and for a non-isentropic motion we have

$$\frac{P}{P_0} = \left(\frac{\varrho}{\varrho_0}\right)^\gamma e^{(S-S_0)/C_v}. \tag{A.917}$$

A Taylor expansion of this last equation around the equilibrium state (ϱ_0, S_0) yields

$$P - P_0 = c^2(\varrho - \varrho_0) + \frac{P_0}{C_v}(S - S_0) + \frac{1}{2}(\gamma - 1)c^2(\varrho - \varrho_0)^2 + \frac{P_0}{2C_v^2}(S - S_0)^2 + \dots \tag{A.918}$$

where C_p and C_v are respectively the specific heats at constant pressure and constant volume, $\gamma = C_p/C_v$, and $c^2 = \gamma P_0/\varrho_0$. Thus, only when the deviation of P from the equilibrium value P_0 is small enough is the linear relation

$$P \approx P_0 + c^2(\varrho - \varrho_0) + \frac{P_0}{C_v}(S - S_0) \tag{A.919}$$

a good approximation. As we already mentioned, in acoustics we are usually concerned with the effects of some small, time-dependent deviations from some equilibrium state of the system. When the equilibrium state is homogeneous and static, the perturbation can easily be separated off and the resulting first order equations are relatively simple. But when the equilibrium state involves inhomogeneities or steady flows the separation is less straightforward. Even here, however, if the inhomogeneities are confined to a finite region of space, the equilibrium state outside this region being homogeneous and static, then the separating out of the acoustic motions in the outer region is not difficult.

In any case, we assume that the medium in the equilibrium state is described by the field quantities $\boldsymbol{V}_0 = \boldsymbol{v}$, P_0, ϱ_0, T_0, and S_0, for example, and define the acoustic velocity, pressure, density, temperature, and entropy as the differences between the actual values and the equilibrium values

$$\begin{aligned} \boldsymbol{u} = \boldsymbol{V} - \boldsymbol{V}_0 = \boldsymbol{V} - \boldsymbol{v}, \qquad & p = P - P_0, \qquad \delta = \varrho - \varrho_0, \\ \theta = T - T_0, \qquad & \sigma = S - S_0. \end{aligned} \tag{A.920}$$

If $\boldsymbol{u}$, p, etc., are small enough we can obtain reasonably accurate equations, involving these acoustic variables to the first order, in terms of the equilibrium values (not necessarily to the first order). If we have already solved for the equilibrium state, the equilibrium values $\boldsymbol{V}_0 = \boldsymbol{v}$, P_0, etc., may be regarded as known parameters, being $\boldsymbol{u}$, p, etc., the unknowns. Thus the first order relationship between the acoustic pressure, density, and entropy arising from (A.918) is

$$p \approx c^2 \delta + \frac{P_0}{C_v} \sigma. \tag{A.921}$$

Our procedure will thus be to replace the quantities ϱ, $\boldsymbol{V}$, T, etc., in equations (A.905) to (A.908) by $(\varrho_0 + \delta)$, $(\boldsymbol{v} + \boldsymbol{u})$, $(T_0 + \theta)$, etc., and to keep only terms in first order of the acoustic quantities δ, $\boldsymbol{u}$, θ, etc. The terms containing only ϱ_0, $\boldsymbol{v}$, T_0 (which we call inhomogeneous terms) need not be considered when we are computing the propagation of sound. On the other hand, in the study of the generation of sound these inhomogeneous terms are often the source terms.

In general, the linear approximations thus obtained will be valid if the mean acoustic velocity amplitude $u = |\boldsymbol{u}|$ is small compared to the wave velocity c. There are exceptions however. In the problem of the diffraction of sound by a semi-infinite screen, for example, the acoustic velocity becomes very large in the regions close to the edge of the screen. In such regions non-linear effects are to be expected.

The linearized forms for the equations of mass, momentum, and energy conservation, and the equation of state (perfect gas), for a moving, inhomogeneous medium, are

$$\frac{\partial \delta}{\partial t} + \delta \sum_i \frac{\partial v_i}{\partial x_i} + \varrho_0 \sum_i \frac{\partial u_i}{\partial x_i} + \sum_i u_i \frac{\partial \varrho_0}{\partial x_i} \approx Q, \tag{A.922}$$

$$\frac{\partial}{\partial t}\left(\varrho_0 u_i + \delta v_i\right) + \sum_j \frac{\partial}{\partial x_j}\left\{\varrho_0 (u_i v_j + u_j v_i) + \delta v_i v_j + p_{ij}\right\} \approx F_i, \tag{A.923}$$

$$\varrho_0 T_0 \left(\frac{\partial \sigma}{\partial t} + \boldsymbol{u} \cdot \nabla S_0 \right) + \frac{p}{R} \frac{\mathrm{d}S_0}{\mathrm{d}t} \approx K \Delta\theta + 4\eta \sum_{ij} u_{ij} v_{ij} + H, \tag{A.924}$$

$$p \approx R\varrho_0 \theta + R T_0 \delta = c^2 \delta + \frac{P_0}{C_v} \sigma, \tag{A.925}$$

where

$$\frac{\mathrm{d}}{\mathrm{d}t} = \frac{\partial}{\partial t} + (\boldsymbol{V} \cdot \nabla), \tag{A.926}$$

$$u_{ij} = \frac{1}{2} \left(\frac{\partial u_i}{\partial x_j} + \frac{\partial u_j}{\partial x_i} \right), \tag{A.927}$$

and

$$p_{ij} = p\delta_{ij} - d_{ij}, \tag{A.928}$$

$$d_{ij} = \varepsilon \, \mathrm{div}(\boldsymbol{u}) \delta_{ij} + 2\eta u_{ij}, \tag{A.929}$$

are acoustic counterparts of the quantities defined earlier. The source terms Q, $\boldsymbol{F}$, and H are the non-equilibrium parts of the fluid injection, body force, and heat injection. The equilibrium part of Q, for example, has been canceled against $(\partial \varrho_0 / \partial t) + \mathrm{div}(\varrho_0 \boldsymbol{v})$ from the left-hand side of (A.905).

These results are so general as to be impractical to use without further specialization. For example, one has to assume that $\mathrm{div}(\boldsymbol{v}) = 0$ (usually a quite allowable assumption) before one can obtain the linear form of the general wave equation

$$\left(\frac{\partial}{\partial t} + \boldsymbol{v} \cdot \nabla \right)^2 \delta - \Delta p \approx \frac{\partial Q}{\partial t} - \nabla \cdot \boldsymbol{F} + \nabla \cdot \mathfrak{D} \cdot \nabla, \tag{A.930}$$

where the last term is the double divergence of the tensor $\mathfrak{D}$, which has elements d_{ij}. In order to obtain a wave equation in terms of acoustic pressure p alone, we must determine δ and d_{ij} in terms of p. To do this in the most general case is not a particularly rewarding exercise, it is much more useful to do it for a number of specific situations which are of practical interest.

But, before we go to special cases, it is necessary to say a few words about the meaning of such quadratic quantities as acoustic intensity, acoustic energy, density, and the like. For example, the energy flow vector

$$\boldsymbol{I} = \left(\frac{1}{2} \varrho V^2 + \varrho E \right) \boldsymbol{V} + \mathfrak{P} \cdot \boldsymbol{V} - K \nabla T, \tag{A.931}$$

where $\mathfrak{P}$ is the fluid stress tensor, with elements P_{ij}. The natural definition of the acoustic energy flow would be

$$\boldsymbol{i} = (\boldsymbol{I})_{\text{with sound}} - (\boldsymbol{I})_{\text{without sound}} = \boldsymbol{I} - \boldsymbol{I}_0, \tag{A.932}$$

with corresponding expressions for the acoustic energy density, $w = h - h_0$, and mass flow vector, $(\varrho \boldsymbol{V})_{\text{with sound}} - (\varrho_0 \boldsymbol{V}_0)$. Similarly with the momentum flow tensor, from which the acoustic radiation pressure tensor is obtained, i.e.,

$$m_{ij} = (P_{ij} + \varrho V_i V_j)_{\text{with sound}} - (P_{ij} + \varrho V_i V_j)_{\text{without sound}}. \tag{A.933}$$

These quantities clearly will contain second order terms in the acoustic variables, therefore their rigorous calculation would require acoustic equations which are correct to the second order. As with equation (A.930), it is not very useful to perform this calculation in the most general case. It is sufficient to point out here that the acoustic energy flow, etc., correct to second order, can indeed be expressed in terms of products of the first order acoustic variables.

In the general acoustic equations (A.922) to (A.925) we have included the source terms Q, $\boldsymbol{F}$, and H, corresponding to the rate of transfer of mass, momentum, and heat energy from external sources. The sound field produced by these sources can be expressed in terms of volume integrals over these source functions. As mentioned above, we have not included terms, such as $\varrho V_i V_j$ or ΔP_0, which do not include acoustic variables. The justification for this omission is that these terms balance each other locally in the equations of motion, for example fluctuations in velocities are balanced by local pressure fluctuations, and the like. These fluctuations produce sound (i.e., acoustic radiation), but in the region where the fluctuations occur (the near field), the acoustic radiation is small compared to the fluctuations themselves. However, the acoustic radiation produced produced by the fluctuations extends outside the region of fluctuation, into regions where the fluid is otherwise homogeneous and at rest (the far field), and here it can more easily be computed (and, experimentally, more easily measured).

Thus, in the study of the generation of sound by fluctuations in the fluid itself, it is essential to retain in the source terms the terms which do not contain the acoustic variables themselves. Within the region of fluctuation, the differentiation between sound and equilibrium motion is quite artificial (the local fluid motion could be regarded as part of the acoustic near field), and in many cases it is more straightforward to use the original equations (A.905) to (A.908) and (A.915) in their integral form, where the net effect of the sources appears as an integral over the region of fluctuation.

d) Acoustic equations for a fluid at rest

We discuss herein the special forms taken on by equations (A.922) to (A.933) when the equilibrium state of the fluid involves only a few of the various possible effects discussed above. At first we will assume that, in the equilibrium state, the fluid is at rest and that the acoustic changes in density are isentropic ($\sigma = 0$). In this case the relation between the acoustic pressure p and the acoustic density δ, from equation (A.921), is simply

$$p = c^2 \delta, \qquad c^2 = \frac{\gamma P}{\varrho}. \tag{A.934}$$

From here on we will omit the subscript 0 from the symbols for equilibrium values in situations like that of equation (A.934), where the difference between P and P_0 or ϱ and ϱ_0 would make only a second-order difference in the equations. We also will use the symbol $=$ instead of $\approx$, since from now on we commit ourselves to the linear equations. The wave equation (A.930) then reduces to the familiar

$$\Delta p - \frac{1}{c^2} \frac{\partial^2 p}{\partial t^2} = 0. \tag{A.935}$$

Once the pressure has been computed, the other acoustic variables follow from the equations defined previously:

$$\text{Velocity} \qquad \boldsymbol{u} = -\frac{1}{\varrho}\int \nabla p \, \mathrm{d}t, \tag{A.936}$$

$$\text{Displacement} \qquad \boldsymbol{d} = \int \boldsymbol{u} \, \mathrm{d}t, \tag{A.937}$$

$$\text{Temperature} \qquad \theta = (\gamma - 1)\frac{T}{\varrho c^2} p, \qquad \left(\gamma = \frac{C_p}{C_v}\right) \tag{A.938}$$

$$\text{Density} \qquad \delta = \frac{p}{c^2}. \tag{A.939}$$

All these variables satisfy a homogeneous wave equation such as (A.935).

Waves with simple-harmonic time dependence are of the form

$$p = p_0 e^{-i\omega t}, \qquad \omega = kc, \tag{A.940}$$

where p_0 does not depend on t, and where i denotes the complex imaginary unit, ω the pulsation, and k the wave number. These are single-frequency waves and have a time factor $e^{-i\omega t}$. For these waves, the acoustic variables of velocity and displacement are given, in particular, by

$$\text{Velocity} \qquad \boldsymbol{u} = -\frac{1}{ik\varrho c}\nabla p, \tag{A.941}$$

$$\text{Displacement} \qquad \boldsymbol{d} = -\frac{1}{k^2 \varrho c^2}\nabla p. \tag{A.942}$$

For a plane sound wave, which has the general form

$$p = f(c\,t - \boldsymbol{n}\cdot\boldsymbol{x}), \tag{A.943}$$

being $\boldsymbol{n}$ a unit vector normal to the wave front, the acoustic velocity is

$$\boldsymbol{u} = \frac{\boldsymbol{n}}{\varrho c} f(c\,t - \boldsymbol{n}\cdot\boldsymbol{x}). \tag{A.944}$$

The quantity ϱc is called the characteristic acoustic impedance of the medium. Since $\mathrm{div}(\boldsymbol{d})$ is the relative volume change of the medium, we can use equation (A.934) to obtain another relation between $\boldsymbol{d}$ and p, namely

$$p = -\varrho c^2 \,\mathrm{div}(\boldsymbol{d}), \tag{A.945}$$

which states that the isentropic compressibility of the fluid is equal to $1/(\varrho c^2)$.

The sound energy flow vector (the sound intensity) is

$$\boldsymbol{i} = p\boldsymbol{u} = \varrho c u^2 \boldsymbol{n} = \frac{p^2}{\varrho c}\boldsymbol{n}. \tag{A.946}$$

It is tempting to consider this equation as self-evident, but it should be remembered that $\boldsymbol{i}$ is a second-order quantity, which must be evaluated from equation (A.932). In the special

case of a homogeneous medium at rest, the other second-order terms cancel out and equation (A.946) is indeed correct to second order. In a moving medium, the result is not so simple.

The situation is also not so straightforward in regard to the mass flow vector. One might assume that it equals $\delta\boldsymbol{u}$, but this would result in a non-zero, time-average, mass flow for a plane wave, an erroneous result. In this case, the additional second-order terms in the basic equations do contribute, making the mass flow vector zero in the second-order approximation.

On the other hand, the magnitude of the acoustic momentum flux is correctly given by the expression ϱu^2 to the second order. The rate of momentum transfer is equal to the radiation pressure on a perfect absorber.

Generally we are interested in the time average of these quantities. For single-frequency waves (time factor $e^{-i\omega t}$), these are

$$\boldsymbol{i} = \frac{1}{2}\,\mathfrak{Re}\{p\bar{\boldsymbol{u}}\}, \tag{A.947}$$

where $\bar{\boldsymbol{u}}$ denotes the complex conjugate of $\boldsymbol{u}$. For a plane wave, like (A.943), we have

$$\boldsymbol{i} = \frac{1}{2}\varrho c u^2 \boldsymbol{n} = \frac{\boldsymbol{n}}{2\varrho c}|p|^2. \tag{A.948}$$

The acoustic density is

$$w = \frac{1}{2}\varrho u^2 + \frac{1}{2\varrho c^2}|p|^2, \tag{A.949}$$

where the first term is the kinetic energy density and the second term the potential energy density. In a plane wave these are equal. We note that the magnitude of the acoustic radiation pressure is thus equal to the acoustic energy density.

The simple wave equation (A.935) is modified when there are body forces or inhomogeneities present, even though there is no motion of the fluid in the equilibrium state, as two examples will suffice to show. For example, the force of gravity has a direct effect on the wave motion, in addition to the indirect effect produced by the change in density with height. In this case, the body force $\boldsymbol{F}$ is equal to $\varrho\,\boldsymbol{g}$, where $\boldsymbol{g}$ is the acceleration of gravity, being $g = |\boldsymbol{g}|$, and thus the term $\mathrm{div}(\boldsymbol{F})$ in equation (A.930) becomes $\boldsymbol{g}\cdot\nabla\varrho + \varrho\nabla\cdot\boldsymbol{g}$, where the magnitude of the second term is to that of the first as the wavelength is to the radius of the Earth, so the second term can usually be neglected. Therefore the wave equation in the presence of the force of gravity is

$$\frac{\partial^2 p}{\partial t^2} = c^2\Delta p + \boldsymbol{g}\cdot\nabla p. \tag{A.950}$$

The added term has the effect of making the medium anisotropic. For a simple-harmonic, plane wave $\exp(ik\boldsymbol{n}\cdot\boldsymbol{x} - i\omega t)$, if $\boldsymbol{n}$ is perpendicular to $\boldsymbol{g}$, then $k = \omega/c$, but if $\boldsymbol{n}$ is parallel to $\boldsymbol{g}$, the propagation constant k is

$$k_g = i\frac{g}{2c^2} + \frac{\omega}{c}\sqrt{1 - \frac{g^2}{4c^2\omega^2}}. \tag{A.951}$$

We note that a wave propagating downward (in the direction of the acceleration of gravity $\boldsymbol{g}$) is attenuated at a rate $e^{-\alpha x_3}$, where $\alpha = (g/2c^2)$, independent of frequency, and its phase velocity is $c/\sqrt{1-(g^2/4c^2\omega^2)}$. If the frequency of the wave is less than $(g/4\pi c)$, there will be no wave motion downward.

A similar anisotropy occurs when the anisotropy is not produced by a body force, but is caused by an inhomogeneity in one of the characteristics of the medium. In a solid or liquid medium the elasticity or the density may vary from point to point (as is caused by a salinity gradient in sea-water, for instance). If the medium is a gas, the inhomogeneity must manifest itself by changes in temperature and/or entropy density. For a source-free medium at rest, equation (A.930) shows that $(\partial^2\delta/\partial t^2) = \Delta p$, but this equation reduces to the usual wave equation (A.935) only when the equilibrium entropy density is uniform and the acoustical motions are isentropic. If the equilibrium entropy density S_0 is not uniform the wave equation is modified, even though the acoustic motion is still isentropic.

If the acoustic disturbance is isentropic, then $(\mathrm{d}S/\mathrm{d}t) = (\partial S/\partial t) + \boldsymbol{u}\cdot\nabla S = 0$, and if the equilibrium entropy density S_0 is a function of position but not of time, then

$$\frac{\partial\sigma}{\partial t} + \boldsymbol{u}\cdot\nabla S_0 = 0. \tag{A.952}$$

Referring to equations (A.921) and (A.936), we obtain

$$\frac{\partial\delta}{\partial t} = \frac{1}{c^2}\frac{\partial p}{\partial t} - \frac{\varrho}{C_p}\frac{\partial\sigma}{\partial t} = \frac{1}{c^2}\frac{\partial p}{\partial t} + \frac{\varrho}{C_p}\boldsymbol{u}\cdot\nabla S_0, \tag{A.953}$$

and thus

$$\frac{\partial^2\delta}{\partial t^2} = \frac{1}{c^2}\frac{\partial^2 p}{\partial t^2} - \frac{1}{C_p}\nabla p\cdot\nabla S_0, \tag{A.954}$$

which, when inserted into equation (A.930) for a source-free medium at rest finally produces the equation

$$\frac{1}{c^2}\frac{\partial^2 p}{\partial t^2} = \Delta p + \frac{1}{C_p}\nabla p\cdot\nabla S_0, \tag{A.955}$$

which has the same form as equation (A.950) representing the effect of gravity. Thus an entropy gradient in the equilibrium state will produce anisotropy in sound propagation. As with the solutions for equation (A.950), sound will be attenuated in the direction of entropy increase, will be amplified in the direction of decreasing S_0. However, a much larger effect arises from the fact that a change in entropy will produce a change in c from point to point, so that the coefficient of $(\partial^2 p/\partial t^2)$ in equation (A.955) will depend on position.

Further effects of fluid motion, transport phenomena, and internal energy losses can be appreciated in Morse & Ingard (1961).

e) Simple-harmonic waves

Simple-harmonic waves are used when the sources and fields have a single frequency, or else, when the total field has been analyzed into its frequency components and we are studying one of these components. These waves acquire thus the form of equation (A.940). Here all aspects of the wave have a common time factor $e^{-i\omega t}$ and the space part of the pressure or density wave (vid. equations (A.915) and (A.930)) satisfies the inhomogeneous

Helmholtz equation in the variable $\boldsymbol{x}$, namely

$$\Delta\Psi + k^2\Psi = q(\boldsymbol{x}), \qquad k = \frac{\omega}{c}, \tag{A.956}$$

where Ψ may be the density ϱ, in which case q represents $-(1/c_0^2)$ times the quantities on the right-hand side of equation (A.915), with time factor $e^{-i\omega t}$ divided out, or else, if we are using the linear approximations, Ψ may be the acoustic pressure p, in which case q may be some of the terms on the right-hand side of equation (A.930). Some of these quantities are truly inhomogeneous terms, being completely specified functions of the spatial coordinates $\boldsymbol{x}$, other terms are linear in the unknown Ψ or its derivatives, and still other terms are quadratic in Ψ and its derivatives (the quadratic terms are neglected in our present discussion). From Ψ, of course, we can obtain the other properties of the wave, its fluid velocity, displacement, temperature, etc., by means of the relations given in equations (A.936) to (A.939).

The Helmholtz equation (A.956) can be solved for any wave number k. If we assume, in the equilibrium state, that the fluid is at rest and that the acoustic changes in density are isentropic, then we obtain the familiar homogeneous Helmholtz equation

$$\Delta\Psi + k^2\Psi = 0. \tag{A.957}$$

A particular case of this equation is when the frequency f is zero, being $f = \omega/2\pi$, in which case the Laplace equation appears, namely

$$\Delta\Psi = 0, \qquad k = 0. \tag{A.958}$$

Similarly, if the frequency is zero for the inhomogeneous Helmholtz equation (A.956), then we obtain the Poisson equation

$$\Delta\Psi = q(\boldsymbol{x}), \qquad k = 0. \tag{A.959}$$

A.11.2 Boundary conditions

a) Reaction of the surface to sound

We discuss now the behavior of sound in the neighborhood of a boundary surface, and see whether we can express this behavior in terms of boundary conditions on the acoustic field. It turns out that in many cases the sorts of boundary conditions familiar in the classical theory of boundary-value problems, such as that the ratio of value to normal gradient of pressure is specified at every point on the boundary, is at least approximately valid.

At first sight it may seem surprising that the ratio of pressure to its normal gradient, which to first order equals the ratio of pressure to normal velocity at the surface, could be specified, even approximately, at each point of the surface, independently of the configuration of the incident wave (vid. equation (A.936)). Of course, if the wall is perfectly rigid so that the value of the ratio is infinite everywhere, then the assumption that this ratio is independent of the nature of the incident wave is not so surprising. But many actual boundary surfaces are not very rigid, and in many problems in theoretical acoustics the effect of the yielding of the boundary to the sound pressure is the essential part of the problem. When the boundary does yield, for the classical boundary conditions to be valid would imply that

the ratio of incident pressure to normal displacement of the boundary would be a characteristic of each point of the surface by itself, independent of what happens at any other point of the surface. To see what this implies, regarding the acoustic nature of the boundary surface, and when it is likely to be valid, let us discuss the simple case of the incidence of a plane wave of sound on a plane boundary surface.

Suppose the boundary is the x_2-x_3 plane, with the boundary material occupying the region of positive x_1 and the fluid carrying the incident sound wave occupying the region of negative x_1, to the left of the boundary plane. Suppose also that the incident wave has frequency $f = \omega/2\pi$ and that its direction of propagation is at the angle of incidence ϕ to the x_1 axis, the direction normal to the boundary. The incident wave, therefore, has a pressure and fluid velocity distribution, within the fluid (vid. equation (A.944)), given by

$$p = p_i \exp(ikx_1 \cos\phi + ikx_2 \sin\phi - i\omega t), \tag{A.960}$$

$$\boldsymbol{u} = \frac{p}{\varrho c}(\boldsymbol{a}_1 \cos\phi + \boldsymbol{a}_2 \sin\phi), \qquad k = \frac{\omega}{c} = \frac{2\pi}{\lambda}, \tag{A.961}$$

where ϱ is the fluid density, c is the velocity of sound waves, and λ the wavelength of the wave in the fluid in the region $x_1 < 0$.

At $x_1 = 0$ the wave is modified because the boundary surface does not move in response to the pressure in the same way that the free fluid does. In general, the presence of the acoustic pressure p produces motion of the surface, but the degree of motion depends on the nature of the boundary material and its structure. If the fluid viscosity is small, we can safely assume that the tangential component of fluid velocity close to the surface need not be equal to the tangential velocity of the boundary itself, thus a discontinuity in tangential velocity is allowed at the boundary. But there must be continuity in normal velocity through the boundary surface, and there must also be continuity in pressure across the surface.

If the surface is porous, so that the fluid can penetrate into the surface material, then there can be an average fluid velocity into the surface without motion of the boundary material itself. If the pores do not interconnect, then it would be true that the mean normal velocity of penetration of the fluid into the pores would bear a simple ratio to the pressure at the surface, independent of the pressure and velocity of the wave at other points on the surface. In this case we could expect the ratio between pressure and normal velocity at the surface to be a point property of the surface, perhaps dependent on the frequency of the incident wave, but independent of its configuration.

b) Acoustic impedance

The ratio between pressure and velocity normal to a boundary surface is called the normal acoustic impedance z_n of the surface. When it is a point property of the surface, independent of the configuration of the incident wave (and we have indicated that this is the case in practice for many porous surfaces), then the classical type of boundary condition is applicable. For a wave of frequency $f = \omega/2\pi$, the normal fluid velocity just outside the surface is equal to $(1/i\omega\varrho)$ times the normal gradient of the pressure there. Thus the

ratio of pressure to its normal gradient at a point of the surface would equal the value of the normal impedance of the surface at the point, divided by $ik\varrho c$, where $k = \omega/c = 2\pi/\lambda$, and where ϱc is the characteristic impedance of the fluid medium (vid. equation (A.944)):

$$\frac{p}{\partial p/\partial n} = \frac{z_n}{ik\varrho c} = \frac{\zeta}{ik} = \frac{1}{ik}(\chi - i\xi), \tag{A.962}$$

where ζ is the dimensionless specific impedance of the surface, and χ and ξ are its resistive and reactive components. If z_n is a point property of the surface, then classical boundary conditions can be used for single-frequency incident waves.

For example, for the conditions of equations (A.960) and (A.961), the ratio between the reflected amplitude p_r and the incident amplitude p_i in in the region $x_1 < 0$, being the total wave

$$p = \left(p_i e^{ikx_1\cos\phi} + p_r e^{-ikx_1\cos\phi}\right) e^{ikx_2\sin\phi - i\omega t}, \tag{A.963}$$

is easily shown from equation (A.962) to be

$$R = \frac{p_r}{p_i} = \frac{-1 + \zeta\cos\phi}{1 + \zeta\cos\phi} = -\frac{(1 - \chi\cos\phi) + i\xi\cos\phi}{(1 + \chi\cos\phi) - i\xi\cos\phi}, \tag{A.964}$$

and the ratio of reflected to incident intensity is

$$|R|^2 = 1 - \alpha = \frac{(1 - \chi\cos\phi)^2 + \xi^2\cos^2\phi}{(1 + \chi\cos\phi)^2 + \xi^2\cos^2\phi}, \tag{A.965}$$

where α is called the absorption coefficient of the surface. If χ and ξ are point properties of the surface, independent of the configuration of the incident wave (independent, in this case, of the angle of incidence ϕ), then the problem is solved. The fraction α of energy absorbed by the surface can be computed from equation (A.965) as a function of the incident angle ϕ, considering χ and ξ to be independent of ϕ. For example, if the specific resistance χ is larger than unity, then the absorption coefficient has a maximum for an angle of incidence $\phi = \arccos(1/\chi)$, dropping to zero at grazing incidence, $\phi = 90°$.

But if $z_n = \varrho c\zeta$ is not a point function of position on the boundary surface, then the problem is not really solved, for the value of z_n will depend on the configuration of the motion of the boundary surface itself, and to obtain the appropriate values of χ and ξ to use in equation (A.965), we will have to investigate the behavior of the sound wave inside the boundary material, an investigation we do not need to undertake when z_n is a point function of position and the classical boundary conditions of equation (A.962) can be used.

c) Exceptions to the classical boundary conditions

To appreciate the nature of difficulties which can arise, let us continue to discuss the simple example of the equations (A.960) and (A.961), that of a plane wave incident on a plane boundary, for the case where we do have to consider the wave motion inside the boundary. To keep the example simple, we suppose the material forming the boundary to fill the region $x_1 > 0$ uniformly. We will also suppose that the material is homogeneous to the extent that we can talk about a mean displacement and velocity of the material. The wave properties of the material may not be isotropic, however, we shall assume that the wave velocity in the x_1 direction is c_n and that in a direction parallel to the boundary plane

it is c_t, where both these quantities may be complex and also frequency dependent. In other words, pressure waves are possible in the material, the wave equation and the relation between pressure and material velocity,

$$c_n^2 \frac{\partial^2 p}{\partial x_1^2} + c_t^2 \left(\frac{\partial^2 p}{\partial x_2^2} + \frac{\partial^2 p}{\partial x_3^2} \right) + \omega^2 p = 0, \tag{A.966}$$

$$u_1 = \frac{1}{i\omega \varrho_n} \frac{\partial p}{\partial x_1}, \qquad u_2 = \frac{1}{i\omega \varrho_t} \frac{\partial p}{\partial x_2}, \qquad u_3 = \frac{1}{i\omega \varrho_t} \frac{\partial p}{\partial x_3}, \tag{A.967}$$

serving to define the quantities c_n, c_t, ϱ_n and ϱ_t.

If the pressure inside the boundary ($x_1 > 0$) is to satisfy this wave equation and also to fit the wave form of equation (A.963) at $x_1 = 0$, then the pressure and velocity waves inside the material must be

$$p = p_t \exp \left(ik_n x_1 \sqrt{1 - \left(\frac{c_t}{c} \right)^2 \sin^2 \phi} + ikx_2 \sin \phi - i\omega t \right), \tag{A.968}$$

$$\boldsymbol{u} = \frac{p}{\varrho_n c_n} \boldsymbol{a}_1 \sqrt{1 - \left(\frac{c_t}{c} \right)^2 \sin^2 \phi} + \frac{p}{\varrho_t c_t} \boldsymbol{a}_2 \frac{c_t}{c} \sin \phi, \tag{A.969}$$

where $k_n = \omega / c_n$, $k = \omega / c$, and c is the sound velocity in the fluid outside the boundary ($x_1 < 0$). Equating p and u_1 at $x_1 = 0$ with those from equation (A.963), we find for the ratio of reflected to incident pressures, outside the boundary surface, that

$$R = \frac{p_r}{p_i} = \frac{-\sqrt{1 - (c_t/c)^2 \sin^2 \phi} + (\varrho_n c_n / \varrho c) \cos \phi}{\sqrt{1 - (c_t/c)^2 \sin^2 \phi} + (\varrho_n c_n / \varrho c) \cos \phi}. \tag{A.970}$$

The absorption coefficient α is $1 - |R|^2$, as before.

Comparison with equation (A.964) shows that the specific surface impedance in this instance is

$$\zeta(\phi) = \frac{\varrho_n c_n}{\varrho c} \left\{ 1 - \left(\frac{c_t}{c} \right)^2 \sin^2 \phi \right\}^{-1/2}, \tag{A.971}$$

which is not independent of ϕ unless c_t, the transverse velocity in the boundary material, is negligibly small compared to c, the wave velocity in the fluid outside the boundary. Unless c_t is small compared to c, the impedance of the surface is not a point property of the surface, independent of the configuration of the incident wave (in the example, independent of ϕ), and to find its value for any specific configuration of incident wave we must work out the corresponding wave configuration inside the boundary material.

From the point of view of the theoretical acoustician, therefore, there are two general types of boundary-value problems which are encountered. The first type is where the boundary material is such that its normal acoustic impedance is a point property of the surface, independent of the configuration of the incident wave. For this type the ratio of pressure to normal gradient of pressure at each point of the boundary is uniquely specified for each frequency, and the well-known methods of the classical theory of boundary-value problems can be employed. The second type is where it is not possible to consider the surface impedance to be independent of the configuration of the incident wave. In these

types of problems it is not possible to substitute a surface impedance for an analysis of the wave inside the boundary, here the internal wave must be studied in detail and its reaction to the incident external wave must be calculated for each configuration of incident wave. These types of problems are usually much more difficult to solve than are the first type.

For further effects on the boundary conditions by the relative motion of fluid and boundary, and for viscous and conduction losses near the boundary we refer to the article by Morse & Ingard (1961).

B. FULL-PLANE IMPEDANCE LAPLACE PROBLEM

B.1 Introduction

In this appendix we study the perturbed full-plane or free-plane impedance Laplace problem, also known as the exterior impedance Laplace problem in 2D, using integral equation techniques and the boundary element method.

We consider the problem of the Laplace equation in two dimensions on the exterior of a bounded obstacle. The Laplace equation for an exterior domain, using typically either Dirichlet or Neumann boundary conditions, is a good example to illustrate the complexity of the integral equation techniques. For a more general treatment and in order to allow a better comparison with the development performed before for half-spaces, we consider in particular an impedance boundary condition. The perturbed full-plane impedance Laplace problem is not strictly speaking a wave scattering problem, but it can be regarded as a limit case of such a problem when the frequency tends towards zero (vid. Appendix C). It can be also regarded as a surface wave problem around a bounded two-dimensional obstacle. The three-dimensional case is treated thoroughly in Appendix D.

For the problem treated herein we follow mainly Nédélec (1977, 1979, 2001) and Raviart (1991). Further related books and doctorate theses are Chen & Zhou (1992), Evans (1998), Giroire (1987), Hsiao & Wendland (2008), Kellogg (1929), Kress (1989), Muskhelishvili (1953), Rjasanow & Steinbach (2007), and Steinbach (2008). Some articles that consider the Laplace equation with an impedance boundary condition are Ahner & Wiener (1991), Lanzani & Shen (2004), and Medková (1998). Wendland, Stephan & Hsiao (1979) treat the mixed boundary-value problem. Interesting theoretical details on transmission problems can be found in Costabel & Stephan (1985). The boundary element calculations are performed in Bendali & Devys (1986). The coupling of boundary integral equations and finite element methods is done in Johnson & Nédélec (1980). The use of cracked domains is studied by Medková & Krutitskii (2005), and the inverse problem by Fasino & Inglese (1999) and Lin & Fang (2005). Applications of the Laplace problem can be found, among others, for electrostatics (Jackson 1999), for conductivity in biomedical imaging (Ammari 2008), and for incompressible plane potential flows (Spurk 1997).

The Laplace equation does not allow the propagation of volume waves inside the considered domain, but the addition of an impedance boundary condition permits the propagation of surface waves along the boundary of the obstacle. The main difficulty in the numerical treatment and resolution of these problems is the fact that the exterior domain is unbounded. We treat this issue by using integral equation techniques and the boundary element method. The idea behind these techniques is to use Green's integral theorems to transform the problem and express it on the boundary of the obstacle, which is bounded. These methods require thus only the calculation of boundary values, rather than values throughout the unbounded exterior domain. They are in a significant manner more efficient in terms of computational resources for problems where the surface versus volume ratio is small. The drawback of these techniques is a more complex mathematical treatment and the requirement of knowing the Green's function of the system. It is the Green's function

which stores the information of the system's physics throughout the exterior domain and which allows to collapse the problem to hold only on the boundary. The dimension of a problem expressed in a volume is therefore reduced towards a surface, i.e., one dimension less, which is what makes these methods so interesting to consider.

This appendix is structured in 13 sections, including this introduction. The direct perturbation problem of the Laplace equation in a two-dimensional exterior domain with an impedance boundary condition is presented in Section B.2. The Green's function and its far-field expression are computed respectively in Sections B.3 and B.4. Extending the direct perturbation problem towards a transmission problem, as done in Section B.5, allows its resolution by using integral equation techniques, which is discussed in Section B.6. These techniques allow also to represent the far field of the solution, as shown in Section B.7. A particular problem that takes as domain the exterior of a circle is solved analytically in Section B.8. The appropriate function spaces and some existence and uniqueness results for the solution of the problem are presented in Section B.9. By means of the variational formulation developed in Section B.10, the obtained integral equation is discretized using the boundary element method, which is described in Section B.11. The boundary element calculations required to build the matrix of the linear system resulting from the numerical discretization are explained in Section B.12. Finally, in Section B.13 a benchmark problem based on the exterior circle problem is solved numerically.

B.2 Direct perturbation problem

We consider an exterior open and connected domain $\Omega_e \subset \mathbb{R}^2$ that lies outside a bounded obstacle Ω_i and whose boundary $\Gamma = \partial\Omega_e = \partial\Omega_i$ is regular (e.g., of class C^2), as shown in Figure B.1. As a perturbation problem, we decompose the total field u_T as $u_T = u_W + u$, where u_W represents the known field without obstacle, and where u denotes the perturbed field due its presence, which has bounded energy. The direct perturbation problem of interest is to find the perturbed field u that satisfies the Laplace equation in Ω_e, an impedance boundary condition on Γ, and a decaying condition at infinity. We consider that the origin is located in Ω_i and that the unit normal $\boldsymbol{n}$ is taken always outwardly oriented of Ω_e, i.e., pointing inwards of Ω_i.

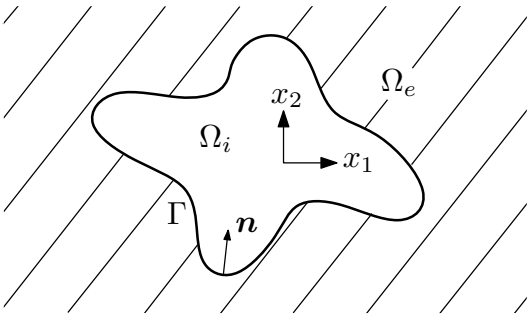

FIGURE B.1. Perturbed full-plane impedance Laplace problem domain.

The total field u_T satisfies the Laplace equation

$$\Delta u_T = 0 \qquad \text{in } \Omega_e, \tag{B.1}$$

which is also satisfied by the fields u_W and u, due linearity. For the perturbed field u we take also the inhomogeneous impedance boundary condition

$$-\frac{\partial u}{\partial n} + Zu = f_z \qquad \text{on } \Gamma, \tag{B.2}$$

where Z is the impedance on the boundary, and where the impedance data function f_z is assumed to be known. If $Z = 0$ or $Z = \infty$, then we retrieve respectively the classical Neumann or Dirichlet boundary conditions. In general, we consider a complex-valued impedance $Z(\boldsymbol{x})$ depending on the position $\boldsymbol{x}$. The function $f_z(\boldsymbol{x})$ may depend on Z and u_W, but is independent of u. If a homogeneous impedance boundary condition is desired for the total field u_T, then due linearity we can express the function f_z as

$$f_z = \frac{\partial u_W}{\partial n} - Zu_W \qquad \text{on } \Gamma. \tag{B.3}$$

The Laplace equation (B.1) admits different kinds of non-trivial solutions u_W, when we consider the domain Ω_e as the unperturbed full-plane $\mathbb{R}^2$. One kind of solutions are the harmonic polynomials

$$u_W(\boldsymbol{x}) = \mathfrak{Re}\{P(z)\}, \tag{B.4}$$

where $P(z)$ denotes a polynomial in the complex variable $z = x_1 + ix_2$. There exist in $\mathbb{R}^2$ likewise non-polynomial solutions of the form

$$u_W(\boldsymbol{x}) = \mathfrak{Re}\{\phi(z)\}, \tag{B.5}$$

where $\phi(z)$ is an entire function in the variable z, e.g., the exponential function e^z. From Liouville's theorem in complex variable theory (cf. Bak & Newman 1997), we know that the growth at infinity of such a function ϕ is bigger than for any polynomial. Any such function can be taken as the known field without perturbation u_W, which holds in particular for all the constant and linear functions in $\mathbb{R}^2$.

For the perturbed field u in the exterior domain Ω_e, though, these functions represent undesired non-physical solutions, which have to be avoided in order to ensure uniqueness of the solution u. To eliminate them, it suffices to impose for u an asymptotic decaying behavior at infinity that excludes the polynomials. This decaying condition involves finite energy throughout Ω_e and can be interpreted as an additional boundary condition at infinity. In our case it is given, for a great value of $|\boldsymbol{x}|$, by

$$u(\boldsymbol{x}) = \mathcal{O}\left(\frac{1}{|\boldsymbol{x}|}\right) \qquad \text{and} \qquad |\nabla u(\boldsymbol{x})| = \mathcal{O}\left(\frac{1}{|\boldsymbol{x}|^2}\right). \tag{B.6}$$

where $\mathcal{O}(\cdot)$ describes the asymptotic upper bound in terms of simpler functions, known as the big $\mathcal{O}$. The asymptotic decaying condition (B.6) can be expressed equivalently, for some constants $C > 0$, by

$$|u(\boldsymbol{x})| \leq \frac{C}{|\boldsymbol{x}|} \qquad \text{and} \qquad |\nabla u(\boldsymbol{x})| \leq \frac{C}{|\boldsymbol{x}|^2} \qquad \text{as } |\boldsymbol{x}| \to \infty. \tag{B.7}$$

In fact, the decaying condition can be even stated as

$$u(\boldsymbol{x}) = \mathcal{O}\left(\frac{1}{|\boldsymbol{x}|^{\alpha}}\right) \qquad \text{and} \qquad |\nabla u(\boldsymbol{x})| = \mathcal{O}\left(\frac{1}{|\boldsymbol{x}|^{1+\alpha}}\right) \qquad \text{for } \; 0 < \alpha \leq 1, \tag{B.8}$$

or as the more weaker and general formulation

$$\lim_{R\to\infty} \int_{S_R} \frac{|u|^2}{R}\, \mathrm{d}\gamma = 0 \qquad \text{and} \qquad \lim_{R\to\infty} \int_{S_R} R\, |\nabla u|^2\, \mathrm{d}\gamma = 0, \tag{B.9}$$

where $S_R = \{\boldsymbol{x} \in \mathbb{R}^2 : |\boldsymbol{x}| = R\}$ is the circle of radius R and where the boundary differential element in polar coordinates is given by $\mathrm{d}\gamma = R\, \mathrm{d}\theta$. A different way to express the decaying condition, which is used, e.g., by Costabel & Stephan (1985), is to specify some constants $a, b \in \mathbb{C}$ such that

$$|u(\boldsymbol{x})| = a + \frac{b}{2\pi} \ln |\boldsymbol{x}| + \mathcal{O}\left(\frac{1}{|\boldsymbol{x}|}\right) \qquad \text{and} \qquad |\nabla u(\boldsymbol{x})| = \frac{b}{2\pi|\boldsymbol{x}|} + \mathcal{O}\left(\frac{1}{|\boldsymbol{x}|^2}\right). \tag{B.10}$$

For simplicity, in our development we consider just $a = b = 0$.

The perturbed full-plane impedance Laplace problem can be finally stated as

$$\begin{cases} \text{Find } u : \Omega_e \to \mathbb{C} \text{ such that} & \\ \Delta u = 0 & \text{in } \; \Omega_e, \\ -\dfrac{\partial u}{\partial n} + Zu = f_z & \text{on } \; \Gamma, \\ |u(\boldsymbol{x})| \leq \dfrac{C}{|\boldsymbol{x}|} & \text{as } \; |\boldsymbol{x}| \to \infty, \\ |\nabla u(\boldsymbol{x})| \leq \dfrac{C}{|\boldsymbol{x}|^2} & \text{as } \; |\boldsymbol{x}| \to \infty. \end{cases} \tag{B.11}$$

B.3 Green's function

The Green's function represents the response of the unperturbed system (without an obstacle) to a Dirac mass. It corresponds to a function G, which depends on a fixed source point $\boldsymbol{x} \in \mathbb{R}^2$ and an observation point $\boldsymbol{y} \in \mathbb{R}^2$. The Green's function is computed in the sense of distributions for the variable $\boldsymbol{y}$ in the full-plane $\mathbb{R}^2$ by placing at the right-hand side of the Laplace equation a Dirac mass $\delta_{\boldsymbol{x}}$, centered at the point $\boldsymbol{x}$. It is therefore a solution $G(\boldsymbol{x}, \cdot) : \mathbb{R}^2 \to \mathbb{C}$ for the radiation problem of a point source, namely

$$\Delta_{\boldsymbol{y}} G(\boldsymbol{x}, \boldsymbol{y}) = \delta_{\boldsymbol{x}}(\boldsymbol{y}) \qquad \text{in } \; \mathcal{D}'(\mathbb{R}^2). \tag{B.12}$$

Due to the radial symmetry of the problem (B.12), it is natural to look for solutions in the form $G = G(r)$, where $r = |\boldsymbol{y} - \boldsymbol{x}|$. By considering only the radial component, the Laplace equation in $\mathbb{R}^2$ becomes

$$\frac{1}{r} \frac{\mathrm{d}}{\mathrm{d}r} \left(r \frac{\mathrm{d}G}{\mathrm{d}r} \right) = 0, \qquad r > 0. \tag{B.13}$$

The general solution of (B.13) is of the form

$$G(r) = C_1 \ln r + C_2, \tag{B.14}$$

for some constants C_1 and C_2. The choice of C_2 is arbitrary, while C_1 is fixed by the presence of the Dirac mass in (B.12). To determine C_1, we have to perform thus a computation in the sense of distributions (cf. Gel'fand & Shilov 1964), using the fact that G is harmonic for $r \neq 0$. For a test function $\varphi \in \mathcal{D}(\mathbb{R}^2)$, we have by definition that

$$\langle \Delta_{\boldsymbol{y}} G, \varphi \rangle = \langle G, \Delta\varphi \rangle = \int_{\mathbb{R}^2} G\, \Delta\varphi \, \mathrm{d}\boldsymbol{y} = \lim_{\varepsilon \to 0} \int_{r \geq \varepsilon} G\, \Delta\varphi \, \mathrm{d}\boldsymbol{y}. \tag{B.15}$$

We apply here Green's second integral theorem (A.613), choosing as bounded domain the circular shell $\varepsilon \leq r \leq a$, where a is large enough so that the test function $\varphi(\boldsymbol{y})$, of bounded support, vanishes identically for $r \geq a$. Then

$$\int_{r \geq \varepsilon} G\, \Delta\varphi \, \mathrm{d}\boldsymbol{y} = \int_{r \geq \varepsilon} \Delta_{\boldsymbol{y}} G\, \varphi \, \mathrm{d}\boldsymbol{y} - \int_{r=\varepsilon} G \frac{\partial \varphi}{\partial r} \, \mathrm{d}\gamma + \int_{r=\varepsilon} \frac{\partial G}{\partial r_{\boldsymbol{y}}} \varphi \, \mathrm{d}\gamma, \tag{B.16}$$

where $\mathrm{d}\gamma$ is the line element on the circle $r = \varepsilon$. Now

$$\int_{r \geq \varepsilon} \Delta_{\boldsymbol{y}} G\, \varphi \, \mathrm{d}\boldsymbol{y} = 0, \tag{B.17}$$

since outside the ball $r \leq \varepsilon$ the function G is harmonic. As for the other terms, by replacing (B.14), we obtain that

$$\int_{r=\varepsilon} G \frac{\partial \varphi}{\partial r} \, \mathrm{d}\gamma = (C_1 \ln \varepsilon + C_2) \int_{r=\varepsilon} \frac{\partial \varphi}{\partial r} \, \mathrm{d}\gamma = \mathcal{O}(\varepsilon \ln \varepsilon), \tag{B.18}$$

and

$$\int_{r=\varepsilon} \frac{\partial G}{\partial r_{\boldsymbol{y}}} \varphi \, \mathrm{d}\gamma = \frac{C_1}{\varepsilon} \int_{r=\varepsilon} \varphi \, \mathrm{d}\gamma = 2\pi C_1 S_\varepsilon(\varphi), \tag{B.19}$$

where $S_\varepsilon(\varphi)$ is the mean value of $\varphi(\boldsymbol{y})$ on the circle of radius ε and centered at $\boldsymbol{x}$. In the limit as $\varepsilon \to 0$, we obtain that $S_\varepsilon(\varphi) \to \varphi(\boldsymbol{x})$, so that

$$\langle \Delta_{\boldsymbol{y}} G, \varphi \rangle = \lim_{\varepsilon \to 0} \int_{r \geq \varepsilon} G\, \Delta\varphi \, \mathrm{d}\boldsymbol{y} = 2\pi C_1 \varphi(\boldsymbol{x}) = 2\pi C_1 \langle \delta_{\boldsymbol{x}}, \varphi \rangle. \tag{B.20}$$

Thus if $C_1 = 1/2\pi$, then (B.12) is fulfilled. When we consider not only radial solutions, then the general solution of (B.12) is given by

$$G(\boldsymbol{x}, \boldsymbol{y}) = \frac{1}{2\pi} \ln |\boldsymbol{y} - \boldsymbol{x}| + \phi(\boldsymbol{x}, \boldsymbol{y}), \tag{B.21}$$

where $\phi(\boldsymbol{x}, \boldsymbol{y})$ is any harmonic function in the variable $\boldsymbol{y}$, i.e., such that $\Delta_{\boldsymbol{y}} \phi = 0$ in $\mathbb{R}^2$, which means that ϕ acquires the form of (B.4) or (B.5).

If we impose additionally, for a fixed $\boldsymbol{x}$, the asymptotic decaying condition

$$|\nabla_{\boldsymbol{y}} G(\boldsymbol{x}, \boldsymbol{y})| = \mathcal{O}\left(\frac{1}{|\boldsymbol{y}|}\right) \qquad \text{as} \quad |\boldsymbol{y}| \longrightarrow \infty, \tag{B.22}$$

then we eliminate any polynomial (or bigger) growth at infinity, but we admit constant and logarithmic growth. By choosing arbitrarily that any constant has to be zero, we obtain finally that our Green's function satisfying (B.12) and (B.22) is given by

$$G(\boldsymbol{x}, \boldsymbol{y}) = \frac{1}{2\pi} \ln |\boldsymbol{y} - \boldsymbol{x}|, \tag{B.23}$$

being its gradient

$$\nabla_{\boldsymbol{y}} G(\boldsymbol{x},\boldsymbol{y}) = \frac{\boldsymbol{y}-\boldsymbol{x}}{2\pi|\boldsymbol{y}-\boldsymbol{x}|^2}. \tag{B.24}$$

We can likewise define a gradient with respect to the $\boldsymbol{x}$ variable by

$$\nabla_{\boldsymbol{x}} G(\boldsymbol{x},\boldsymbol{y}) = \frac{\boldsymbol{x}-\boldsymbol{y}}{2\pi|\boldsymbol{x}-\boldsymbol{y}|^2}, \tag{B.25}$$

and a double-gradient matrix by

$$\nabla_{\boldsymbol{x}}\nabla_{\boldsymbol{y}} G(\boldsymbol{x},\boldsymbol{y}) = \begin{bmatrix} \dfrac{\partial^2 G}{\partial x_1 \partial y_1} & \dfrac{\partial^2 G}{\partial x_1 \partial y_2} \\ \dfrac{\partial^2 G}{\partial x_2 \partial y_1} & \dfrac{\partial^2 G}{\partial x_2 \partial y_2} \end{bmatrix} = -\frac{\boldsymbol{I}}{2\pi|\boldsymbol{x}-\boldsymbol{y}|^2} + \frac{(\boldsymbol{x}-\boldsymbol{y})\otimes(\boldsymbol{x}-\boldsymbol{y})}{\pi|\boldsymbol{x}-\boldsymbol{y}|^4}, \tag{B.26}$$

where $\boldsymbol{I}$ denotes a 2×2 identity matrix and where $\otimes$ denotes the dyadic or outer product of two vectors, which results in a matrix and is defined in (A.573).

We note that the Green's function (B.23) is symmetric in the sense that

$$G(\boldsymbol{x},\boldsymbol{y}) = G(\boldsymbol{y},\boldsymbol{x}), \tag{B.27}$$

and it fulfills similarly

$$\nabla_{\boldsymbol{y}} G(\boldsymbol{x},\boldsymbol{y}) = \nabla_{\boldsymbol{y}} G(\boldsymbol{y},\boldsymbol{x}) = -\nabla_{\boldsymbol{x}} G(\boldsymbol{x},\boldsymbol{y}) = -\nabla_{\boldsymbol{x}} G(\boldsymbol{y},\boldsymbol{x}), \tag{B.28}$$

and

$$\nabla_{\boldsymbol{x}}\nabla_{\boldsymbol{y}} G(\boldsymbol{x},\boldsymbol{y}) = \nabla_{\boldsymbol{y}}\nabla_{\boldsymbol{x}} G(\boldsymbol{x},\boldsymbol{y}) = \nabla_{\boldsymbol{x}}\nabla_{\boldsymbol{y}} G(\boldsymbol{y},\boldsymbol{x}) = \nabla_{\boldsymbol{y}}\nabla_{\boldsymbol{x}} G(\boldsymbol{y},\boldsymbol{x}). \tag{B.29}$$

B.4 Far field of the Green's function

The far field of the Green's function describes its asymptotic behavior at infinity, i.e., when $|\boldsymbol{x}| \to \infty$ and assuming that $\boldsymbol{y}$ is fixed. For this purpose, we search the terms of highest order at infinity by expanding the logarithm according to

$$\begin{aligned} \ln|\boldsymbol{x}-\boldsymbol{y}| &= \frac{1}{2}\ln\left(|\boldsymbol{x}|^2\right) + \frac{1}{2}\ln\left(\frac{|\boldsymbol{x}-\boldsymbol{y}|^2}{|\boldsymbol{x}|^2}\right) \\ &= \ln|\boldsymbol{x}| + \frac{1}{2}\ln\left(1 - 2\,\frac{\boldsymbol{y}\cdot\boldsymbol{x}}{|\boldsymbol{x}|^2} + \frac{|\boldsymbol{y}|^2}{|\boldsymbol{x}|^2}\right). \end{aligned} \tag{B.30}$$

Using a Taylor expansion of the logarithm around one yields

$$\ln|\boldsymbol{x}-\boldsymbol{y}| = \ln|\boldsymbol{x}| - \frac{\boldsymbol{y}\cdot\boldsymbol{x}}{|\boldsymbol{x}|^2} + \mathcal{O}\left(\frac{1}{|\boldsymbol{x}|^2}\right). \tag{B.31}$$

We express the point $\boldsymbol{x}$ as $\boldsymbol{x} = |\boldsymbol{x}|\,\hat{\boldsymbol{x}}$, being $\hat{\boldsymbol{x}}$ a unitary vector. The far field of the Green's function, as $|\boldsymbol{x}| \to \infty$, is thus given by

$$G^{ff}(\boldsymbol{x},\boldsymbol{y}) = \frac{1}{2\pi}\ln|\boldsymbol{x}| - \frac{\boldsymbol{y}\cdot\hat{\boldsymbol{x}}}{2\pi|\boldsymbol{x}|}. \tag{B.32}$$

Similarly, as $|\boldsymbol{x}| \to \infty$, we have for its gradient with respect to $\boldsymbol{y}$, that

$$\nabla_{\boldsymbol{y}} G^{ff}(\boldsymbol{x},\boldsymbol{y}) = -\frac{\hat{\boldsymbol{x}}}{2\pi|\boldsymbol{x}|}, \tag{B.33}$$

for its gradient with respect to $\boldsymbol{x}$, that

$$\nabla_{\boldsymbol{x}} G^{ff}(\boldsymbol{x},\boldsymbol{y}) = \frac{\hat{\boldsymbol{x}}}{2\pi|\boldsymbol{x}|}, \tag{B.34}$$

and for its double-gradient matrix, that

$$\nabla_{\boldsymbol{x}}\nabla_{\boldsymbol{y}} G^{ff}(\boldsymbol{x},\boldsymbol{y}) = -\frac{\boldsymbol{I}}{2\pi|\boldsymbol{x}|^2} + \frac{\hat{\boldsymbol{x}}\otimes\hat{\boldsymbol{x}}}{\pi|\boldsymbol{x}|^2}. \tag{B.35}$$

B.5 Transmission problem

We are interested in expressing the solution u of the direct perturbation problem (B.11) by means of an integral representation formula over the boundary Γ. To study this kind of representations, the differential problem defined on Ω_e is extended as a transmission problem defined now on the whole plane $\mathbb{R}^2$ by combining (B.11) with a corresponding interior problem defined on Ω_i. For the transmission problem, which specifies jump conditions over the boundary Γ, a general integral representation can be developed, and the particular integral representations of interest are then established by the specific choice of the corresponding interior problem.

A transmission problem is then a differential problem for which the jump conditions of the solution field, rather than boundary conditions, are specified on the boundary Γ. As shown in Figure B.1, we consider the exterior domain Ω_e and the interior domain Ω_i, taking the unit normal $\boldsymbol{n}$ pointing towards Ω_i. We search now a solution u defined in $\Omega_e \cup \Omega_i$, and use the notation $u_e = u|_{\Omega_e}$ and $u_i = u|_{\Omega_i}$. We define the jumps of the traces of u on both sides of the boundary Γ as

$$[u] = u_e - u_i \qquad \text{and} \qquad \left[\frac{\partial u}{\partial n}\right] = \frac{\partial u_e}{\partial n} - \frac{\partial u_i}{\partial n}. \tag{B.36}$$

The transmission problem is now given by

$$\begin{cases} \text{Find } u : \Omega_e \cup \Omega_i \to \mathbb{C} \text{ such that} \\ \Delta u = 0 & \text{in } \Omega_e \cup \Omega_i, \\ [u] = \mu & \text{on } \Gamma, \\ \left[\dfrac{\partial u}{\partial n}\right] = \nu & \text{on } \Gamma, \\ \text{+ Decaying condition as } |\boldsymbol{x}| \to \infty, \end{cases} \tag{B.37}$$

where $\mu, \nu : \Gamma \to \mathbb{C}$ are known functions. The decaying condition is still (B.7), and it is required to ensure uniqueness of the solution.

B.6 Integral representations and equations

B.6.1 Integral representation

To develop for the solution u an integral representation formula over the boundary Γ, we define by $\Omega_{R,\varepsilon}$ the domain $\Omega_e \cup \Omega_i$ without the ball B_ε of radius $\varepsilon > 0$ centered at the

point $\boldsymbol{x} \in \Omega_e \cup \Omega_i$, and truncated at infinity by the ball B_R of radius $R > 0$ centered at the origin. We consider that the ball B_ε is entirely contained either in Ω_e or in Ω_i, depending on the location of its center $\boldsymbol{x}$. Therefore, as shown in Figure B.2, we have that

$$\Omega_{R,\varepsilon} = \big((\Omega_e \cup \Omega_i) \cap B_R\big) \setminus \overline{B_\varepsilon}, \tag{B.38}$$

where

$$B_R = \{\boldsymbol{y} \in \mathbb{R}^2 : |\boldsymbol{y}| < R\} \qquad \text{and} \qquad B_\varepsilon = \{\boldsymbol{y} \in \mathbb{R}^2 : |\boldsymbol{y} - \boldsymbol{x}| < \varepsilon\}. \tag{B.39}$$

We consider similarly the boundaries of the balls

$$S_R = \{\boldsymbol{y} \in \mathbb{R}^2 : |\boldsymbol{y}| = R\} \qquad \text{and} \qquad S_\varepsilon = \{\boldsymbol{y} \in \mathbb{R}^2 : |\boldsymbol{y} - \boldsymbol{x}| = \varepsilon\}. \tag{B.40}$$

The idea is to retrieve the domain $\Omega_e \cup \Omega_i$ at the end when the limits $R \to \infty$ and $\varepsilon \to 0$ are taken for the truncated domain $\Omega_{R,\varepsilon}$.

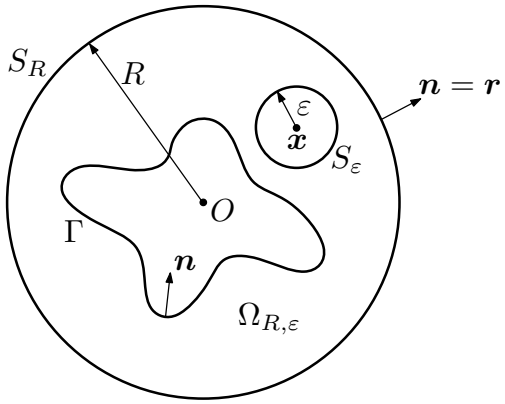

FIGURE B.2. Truncated domain $\Omega_{R,\varepsilon}$ for $\boldsymbol{x} \in \Omega_e \cup \Omega_i$.

We apply now Green's second integral theorem (A.613) to the functions u and $G(\boldsymbol{x}, \cdot)$ in the bounded domain $\Omega_{R,\varepsilon}$, yielding

$$\begin{aligned}
0 &= \int_{\Omega_{R,\varepsilon}} \big(u(\boldsymbol{y})\Delta_{\boldsymbol{y}} G(\boldsymbol{x},\boldsymbol{y}) - G(\boldsymbol{x},\boldsymbol{y})\Delta u(\boldsymbol{y})\big)\mathrm{d}\boldsymbol{y} \\
&= \int_{S_R} \left(u(\boldsymbol{y})\frac{\partial G}{\partial r_{\boldsymbol{y}}}(\boldsymbol{x},\boldsymbol{y}) - G(\boldsymbol{x},\boldsymbol{y})\frac{\partial u}{\partial r}(\boldsymbol{y})\right)\mathrm{d}\gamma(\boldsymbol{y}) \\
&- \int_{S_\varepsilon} \left(u(\boldsymbol{y})\frac{\partial G}{\partial r_{\boldsymbol{y}}}(\boldsymbol{x},\boldsymbol{y}) - G(\boldsymbol{x},\boldsymbol{y})\frac{\partial u}{\partial r}(\boldsymbol{y})\right)\mathrm{d}\gamma(\boldsymbol{y}) \\
&+ \int_{\Gamma} \left([u](\boldsymbol{y})\frac{\partial G}{\partial n_{\boldsymbol{y}}}(\boldsymbol{x},\boldsymbol{y}) - G(\boldsymbol{x},\boldsymbol{y})\left[\frac{\partial u}{\partial n}\right](\boldsymbol{y})\right)\mathrm{d}\gamma(\boldsymbol{y}).
\end{aligned} \tag{B.41}$$

For R large enough, the integral on S_R tends to zero, since

$$\left|\int_{S_R} u(\boldsymbol{y})\frac{\partial G}{\partial r_{\boldsymbol{y}}}(\boldsymbol{x},\boldsymbol{y})\,\mathrm{d}\gamma(\boldsymbol{y})\right| \leq \frac{C}{R}, \tag{B.42}$$

and

$$\left| \int_{S_R} G(\boldsymbol{x},\boldsymbol{y}) \frac{\partial u}{\partial r}(\boldsymbol{y})\, \mathrm{d}\gamma(\boldsymbol{y}) \right| \leq \frac{C}{R} \ln R, \tag{B.43}$$

for some constants $C > 0$, due the asymptotic decaying behavior at infinity (B.7). If the function u is regular enough in the ball B_ε, then the second term of the integral on S_ε, when $\varepsilon \to 0$ and due (B.23), is bounded by

$$\left| \int_{S_\varepsilon} G(\boldsymbol{x},\boldsymbol{y}) \frac{\partial u}{\partial r}(\boldsymbol{y})\, \mathrm{d}\gamma(\boldsymbol{y}) \right| \leq \varepsilon \ln \varepsilon \sup_{\boldsymbol{y}\in B_\varepsilon} \left| \frac{\partial u}{\partial r}(\boldsymbol{y}) \right|, \tag{B.44}$$

and tends to zero. The regularity of u can be specified afterwards once the integral representation has been determined and generalized by means of density arguments. The first integral term on S_ε can be decomposed as

$$\begin{aligned} \int_{S_\varepsilon} u(\boldsymbol{y}) \frac{\partial G}{\partial r_{\boldsymbol{y}}}(\boldsymbol{x},\boldsymbol{y})\, \mathrm{d}\gamma(\boldsymbol{y}) &= u(\boldsymbol{x}) \int_{S_\varepsilon} \frac{\partial G}{\partial r_{\boldsymbol{y}}}(\boldsymbol{x},\boldsymbol{y})\, \mathrm{d}\gamma(\boldsymbol{y}) \\ &\quad + \int_{S_\varepsilon} \frac{\partial G}{\partial r_{\boldsymbol{y}}}(\boldsymbol{x},\boldsymbol{y}) \big(u(\boldsymbol{y}) - u(\boldsymbol{x})\big)\, \mathrm{d}\gamma(\boldsymbol{y}), \end{aligned} \tag{B.45}$$

For the first term in the right-hand side of (B.45), by replacing (B.24), we have that

$$\int_{S_\varepsilon} \frac{\partial G}{\partial r_{\boldsymbol{y}}}(\boldsymbol{x},\boldsymbol{y})\, \mathrm{d}\gamma(\boldsymbol{y}) = 1, \tag{B.46}$$

while the second term is bounded by

$$\left| \int_{S_\varepsilon} \big(u(\boldsymbol{y}) - u(\boldsymbol{x})\big) \frac{\partial G}{\partial r_{\boldsymbol{y}}}(\boldsymbol{x},\boldsymbol{y})\, \mathrm{d}\gamma(\boldsymbol{y}) \right| \leq \sup_{\boldsymbol{y}\in B_\varepsilon} |u(\boldsymbol{y}) - u(\boldsymbol{x})|, \tag{B.47}$$

which tends towards zero when $\varepsilon \to 0$.

In conclusion, when the limits $R \to \infty$ and $\varepsilon \to 0$ are taken in (B.41), then the following integral representation formula holds for the solution u of the transmission problem:

$$u(\boldsymbol{x}) = \int_\Gamma \left([u](\boldsymbol{y}) \frac{\partial G}{\partial n_{\boldsymbol{y}}}(\boldsymbol{x},\boldsymbol{y}) - G(\boldsymbol{x},\boldsymbol{y}) \left[\frac{\partial u}{\partial n}\right](\boldsymbol{y}) \right) \mathrm{d}\gamma(\boldsymbol{y}), \qquad \boldsymbol{x} \in \Omega_e \cup \Omega_i. \tag{B.48}$$

We observe thus that if the values of the jump of u and of its normal derivative are known on Γ, then the transmission problem (B.37) is readily solved and its solution given explicitly by (B.48), which, in terms of μ and ν, becomes

$$u(\boldsymbol{x}) = \int_\Gamma \left(\mu(\boldsymbol{y}) \frac{\partial G}{\partial n_{\boldsymbol{y}}}(\boldsymbol{x},\boldsymbol{y}) - G(\boldsymbol{x},\boldsymbol{y}) \nu(\boldsymbol{y}) \right) \mathrm{d}\gamma(\boldsymbol{y}), \qquad \boldsymbol{x} \in \Omega_e \cup \Omega_i. \tag{B.49}$$

To determine the values of the jumps, an adequate integral equation has to be developed, i.e., an equation whose unknowns are the traces of the solution on Γ.

An alternative way to demonstrate the integral representation (B.48) is to proceed in the sense of distributions. We consider in this case a test function $\varphi \in \mathcal{D}(\mathbb{R}^2)$ and use Green's second integral theorem (A.613) to obtain that

$$\langle \Delta u, \varphi \rangle = \langle u, \Delta \varphi \rangle = \int_{\Omega_e} u \Delta \varphi\, \mathrm{d}\boldsymbol{x} = \int_\Gamma \left([u] \frac{\partial \varphi}{\partial n} - \left[\frac{\partial u}{\partial n}\right] \varphi \right) \mathrm{d}\gamma. \tag{B.50}$$

For any function f, e.g., continuous over Γ, we define the distributions $f\delta_\Gamma$ and $\frac{\partial}{\partial n}(f\delta_\Gamma)$ of $\mathcal{D}'(\mathbb{R}^2)$ respectively by

$$\langle f\delta_\Gamma, \varphi\rangle = \int_\Gamma f\varphi \,\mathrm{d}\gamma \qquad \text{and} \qquad \left\langle \frac{\partial}{\partial n}(f\delta_\Gamma), \varphi \right\rangle = -\int_\Gamma f\frac{\partial \varphi}{\partial n}\,\mathrm{d}\gamma. \tag{B.51}$$

From a physical or mechanical point of view, the distribution $f\delta_\Gamma$ can be considered as a distribution of sources with density f over Γ, while $\frac{\partial}{\partial n}(f\delta_\Gamma)$ is a distribution of dipoles oriented according to the unit normal $\boldsymbol{n}$ and of density f over Γ. Using the notation (B.51) we have thus from (B.50) in the sense of distributions that

$$\Delta u = -\frac{\partial}{\partial n}\big([u]\delta_\Gamma\big) - \left[\frac{\partial u}{\partial n}\right]\delta_\Gamma \qquad \text{in } \mathbb{R}^2. \tag{B.52}$$

Hence Δu can be interpreted as the sum of a distribution of sources and of a distribution of dipoles over Γ. Since the Green's function (B.23) is the fundamental solution of the Laplace operator Δ, we have that a solution in $\mathcal{D}'(\mathbb{R}^2)$ of the equation (B.52) is given by

$$u = G * \left(-\frac{\partial}{\partial n}\big([u]\delta_\Gamma\big) - \left[\frac{\partial u}{\partial n}\right]\delta_\Gamma\right). \tag{B.53}$$

This illustrates clearly how the solution u is obtained as a convolution with the Green's function. Furthermore, the asymptotic decaying condition (B.7) implies that the solution (B.53) is unique. To obtain (B.48) it remains only to make (B.53) explicit. The term

$$\left\{G * \left[\frac{\partial u}{\partial n}\right]\delta_\Gamma\right\}(\boldsymbol{x}) = \int_\Gamma G(\boldsymbol{x},\boldsymbol{y})\left[\frac{\partial u}{\partial n}\right](\boldsymbol{y})\,\mathrm{d}\gamma(\boldsymbol{y}) \tag{B.54}$$

is called single layer potential, associated with the distribution of sources $[\partial u/\partial n]\delta_\Gamma$, while

$$\left\{G * \frac{\partial}{\partial n}\big([u]\delta_\Gamma\big)\right\}(\boldsymbol{x}) = -\int_\Gamma \frac{\partial G}{\partial n_{\boldsymbol{y}}}(\boldsymbol{x},\boldsymbol{y})[u](\boldsymbol{y})\,\mathrm{d}\gamma(\boldsymbol{y}) \tag{B.55}$$

represents a double layer potential, associated with the distribution of dipoles $\frac{\partial}{\partial n}([u]\delta_\Gamma)$. Combining (B.54) and (B.55) yields finally the desired integral representation (B.48).

We note that to obtain the gradient of the integral representation (B.48) we can pass directly the derivatives inside the integral, since there are no singularities if $\boldsymbol{x} \in \Omega_e \cup \Omega_i$. Therefore we have that

$$\nabla u(\boldsymbol{x}) = \int_\Gamma \left([u](\boldsymbol{y})\nabla_{\boldsymbol{x}}\frac{\partial G}{\partial n_{\boldsymbol{y}}}(\boldsymbol{x},\boldsymbol{y}) - \nabla_{\boldsymbol{x}} G(\boldsymbol{x},\boldsymbol{y})\left[\frac{\partial u}{\partial n}\right](\boldsymbol{y})\right)\mathrm{d}\gamma(\boldsymbol{y}). \tag{B.56}$$

We remark also that the asymptotic decaying behavior (B.7) and Green's first integral theorem (A.612) imply that

$$\int_\Gamma \frac{\partial u_e}{\partial n}\,\mathrm{d}\gamma = \int_\Gamma \frac{\partial u_i}{\partial n}\,\mathrm{d}\gamma = 0, \tag{B.57}$$

since

$$\int_\Gamma \frac{\partial u_e}{\partial n}\,\mathrm{d}\gamma = \int_{\Omega_e \cap B_R} \Delta u_e \,\mathrm{d}\boldsymbol{x} - \int_{S_R} \frac{\partial u_e}{\partial r}\,\mathrm{d}\gamma = -\int_{S_R} \frac{\partial u_e}{\partial r}\,\mathrm{d}\gamma \xrightarrow[R\to\infty]{} 0, \tag{B.58}$$

and

$$\int_\Gamma \frac{\partial u_i}{\partial n}\,\mathrm{d}\gamma = -\int_{\Omega_i} \Delta u_i\,\mathrm{d}\boldsymbol{x} = 0. \tag{B.59}$$

Reciprocally, by using the integral representation formula (B.48) it can be verified that this hypothesis (B.57) implies the asymptotic decaying behavior (B.7).

B.6.2 Integral equations

To determine the values of the traces that conform the jumps for the transmission problem (B.37), an integral equation has to be developed. For this purpose we place the source point $\boldsymbol{x}$ on the boundary Γ, as shown in Figure B.3, and apply the same procedure as before for the integral representation (B.48), treating differently in (B.41) only the integrals on S_ε. The integrals on S_R still behave well and tend towards zero as $R \to \infty$. The Ball B_ε, though, is split in half into the two pieces $\Omega_e \cap B_\varepsilon$ and $\Omega_i \cap B_\varepsilon$, which are asymptotically separated by the tangent of the boundary if Γ is regular. Thus the associated integrals on S_ε give rise to a term $-(u_e(\boldsymbol{x})+u_i(\boldsymbol{x}))/2$ instead of just $-u(\boldsymbol{x})$ as before. We must notice that in this case, the integrands associated with the boundary Γ admit an integrable singularity at the point $\boldsymbol{x}$. The desired integral equation related with (B.48) is then given by

$$\frac{u_e(\boldsymbol{x}) + u_i(\boldsymbol{x})}{2} = \int_\Gamma \left([u](\boldsymbol{y}) \frac{\partial G}{\partial n_{\boldsymbol{y}}}(\boldsymbol{x},\boldsymbol{y}) - G(\boldsymbol{x},\boldsymbol{y}) \left[\frac{\partial u}{\partial n}\right](\boldsymbol{y}) \right) \mathrm{d}\gamma(\boldsymbol{y}), \quad \boldsymbol{x} \in \Gamma. \tag{B.60}$$

By choosing adequately the boundary condition of the interior problem, and by considering also the boundary condition of the exterior problem and the jump definitions (B.36), this integral equation can be expressed in terms of only one unknown function on Γ. Thus, solving the problem (B.11) is equivalent to solve (B.60) and then replace the obtained solution in (B.48).

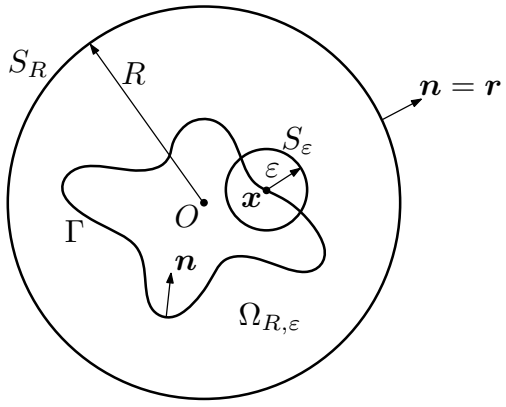

FIGURE B.3. Truncated domain $\Omega_{R,\varepsilon}$ for $\boldsymbol{x} \in \Gamma$.

We remark that the integral equation (B.60) has to be understood in the sense of a mean between the traces of the solution u on both sides of Γ, as illustrated in Figure B.4. It gives information only for the jumps, but not for the solution of the problem. The true value of the solution on the boundary Γ for the exterior and the interior problems is always given

by the limit case as $\boldsymbol{x}$ tends towards Γ respectively from Ω_e and Ω_i of the representation formula (B.48).

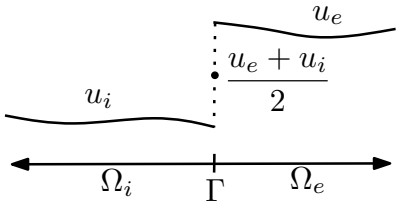

FIGURE B.4. Jump over Γ of the solution u.

The integral equation holds only when the boundary Γ is regular (e.g., of class C^2). Otherwise, taking the limit $\varepsilon \to 0$ can no longer be well-defined and the result is false in general. In particular, if the boundary Γ has an angular point at $\boldsymbol{x} \in \Gamma$, as shown in Figure B.5 and where θ represents the angle in radians ($0 < \theta < 2\pi$) of the tangents of the boundary on that particular point $\boldsymbol{x}$ measured over Ω_e, then the left-hand side of the integral equation (B.60) is modified on that point according to the portion of the ball B_ε that remains inside Ω_e, namely

$$\frac{\theta}{2\pi}u_e(\boldsymbol{x})+\left(1-\frac{\theta}{2\pi}\right)u_i(\boldsymbol{x}) = \int_\Gamma \left([u](\boldsymbol{y})\frac{\partial G}{\partial n_{\boldsymbol{y}}}(\boldsymbol{x},\boldsymbol{y}) - G(\boldsymbol{x},\boldsymbol{y})\left[\frac{\partial u}{\partial n}\right](\boldsymbol{y})\right)\mathrm{d}\gamma(\boldsymbol{y}). \quad \text{(B.61)}$$

The solution u usually presents singularities on those points where Γ fails to be regular.

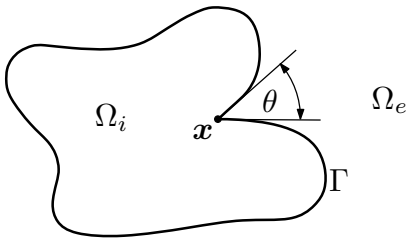

FIGURE B.5. Angular point $\boldsymbol{x}$ of the boundary Γ.

Another integral equation can be also derived for the normal derivative of the solution u on the boundary Γ, by studying the jump properties of the single and double layer potentials. Its derivation is more complicated than for (B.60), being the specific details explicited below in the subsection of boundary layer potentials. If the boundary is regular at $\boldsymbol{x} \in \Gamma$, then we obtain

$$\frac{1}{2}\frac{\partial u_e}{\partial n}(\boldsymbol{x}) + \frac{1}{2}\frac{\partial u_i}{\partial n}(\boldsymbol{x}) = \int_\Gamma \left([u](\boldsymbol{y})\frac{\partial^2 G}{\partial n_{\boldsymbol{x}}\partial n_{\boldsymbol{y}}}(\boldsymbol{x},\boldsymbol{y}) - \frac{\partial G}{\partial n_{\boldsymbol{x}}}(\boldsymbol{x},\boldsymbol{y})\left[\frac{\partial u}{\partial n}\right](\boldsymbol{y})\right)\mathrm{d}\gamma(\boldsymbol{y}). \quad \text{(B.62)}$$

This integral equation is modified in the same way as (B.61) if $\boldsymbol{x}$ is an angular point.

B.6.3 Integral kernels

The integral kernels G, $\partial G/\partial n_{\boldsymbol{y}}$, and $\partial G/\partial n_{\boldsymbol{x}}$ are weakly singular, and thus integrable, whereas the kernel $\partial^2 G/\partial n_{\boldsymbol{x}}\partial n_{\boldsymbol{y}}$ has a strong singularity at the point $\boldsymbol{x}$, which is not integrable and therefore referred to as a hypersingular kernel.

In general, a kernel $K(\boldsymbol{x},\boldsymbol{y})$ of an integral operator of the form

$$T\varphi(\boldsymbol{x}) = \int_\Gamma K(\boldsymbol{x},\boldsymbol{y})\varphi(\boldsymbol{y})\,\mathrm{d}\gamma(\boldsymbol{y}), \qquad \boldsymbol{x}\in\Gamma\subset\mathbb{R}^N, \tag{B.63}$$

is said to be weakly singular if it is defined and continuous for $\boldsymbol{x}\neq\boldsymbol{y}$, and if there exist some constants $C>0$ and $0<\lambda<N-1$ such that

$$|K(\boldsymbol{x},\boldsymbol{y})| \leq \frac{C}{|\boldsymbol{x}-\boldsymbol{y}|^\lambda} \qquad \forall \boldsymbol{x},\boldsymbol{y}\in\Gamma, \tag{B.64}$$

in which case the integral operator (B.63) is improper, but integrable, i.e., such that

$$\int_\Gamma |K(\boldsymbol{x},\boldsymbol{y})|\,\mathrm{d}\gamma(\boldsymbol{y}) < \infty. \tag{B.65}$$

If $K(\boldsymbol{x},\boldsymbol{y})$ requires $\lambda\geq N-1$ in (B.64), then the kernel is said to be hypersingular.

The kernel G defined in (B.23) is logarithmic and thus fulfills (B.64) for any $\lambda>0$. The kernels $\partial G/\partial n_{\boldsymbol{y}}$ and $\partial G/\partial n_{\boldsymbol{x}}$ are less singular along Γ than they appear at first sight, due the regularizing effect of the normal derivatives. They are given respectively by

$$\frac{\partial G}{\partial n_{\boldsymbol{y}}}(\boldsymbol{x},\boldsymbol{y}) = \frac{(\boldsymbol{y}-\boldsymbol{x})\cdot\boldsymbol{n}_{\boldsymbol{y}}}{2\pi|\boldsymbol{y}-\boldsymbol{x}|^2} \qquad \text{and} \qquad \frac{\partial G}{\partial n_{\boldsymbol{x}}}(\boldsymbol{x},\boldsymbol{y}) = \frac{(\boldsymbol{x}-\boldsymbol{y})\cdot\boldsymbol{n}_{\boldsymbol{x}}}{2\pi|\boldsymbol{x}-\boldsymbol{y}|^2}. \tag{B.66}$$

Let us consider first the kernel $\partial G/\partial n_{\boldsymbol{y}}$. A regular boundary Γ can be described in the neighborhood of a point $\boldsymbol{y}$ as the graph of a regular function φ that takes variables on the tangent line at $\boldsymbol{y}$. We write $\eta_2=\varphi(\eta_1)$, being the origin of the coordinate system (η_1,η_2) located at $\boldsymbol{y}$, where η_2 is aligned with $\boldsymbol{n}_{\boldsymbol{y}}$, and where η_1 lies on the tangent line at $\boldsymbol{y}$, as shown in Figure B.6. It holds thus that $\varphi(0)=0$ and $\varphi'(0)=0$. A Taylor expansion around the origin yields

$$\eta_2 = \varphi(0)+\varphi'(0)\eta_1+\mathcal{O}(|\eta_1|^2) = \mathcal{O}(|\eta_1|^2), \tag{B.67}$$

and therefore

$$(\boldsymbol{x}-\boldsymbol{y})\cdot\boldsymbol{n}_{\boldsymbol{y}} = \eta_2 = \varphi(\eta_1) = \mathcal{O}(|\eta_1|^2). \tag{B.68}$$

Since, on the other hand, we have

$$|\boldsymbol{y}-\boldsymbol{x}|^2 = |\eta_1|^2+|\eta_2|^2 = \mathcal{O}(|\eta_1|^2), \tag{B.69}$$

consequently we obtain that

$$(\boldsymbol{y}-\boldsymbol{x})\cdot\boldsymbol{n}_{\boldsymbol{y}} = \mathcal{O}(|\boldsymbol{y}-\boldsymbol{x}|^2). \tag{B.70}$$

By inversing the roles, the same holds also when considering $\boldsymbol{n}_{\boldsymbol{x}}$ instead of $\boldsymbol{n}_{\boldsymbol{y}}$, i.e.,

$$(\boldsymbol{x}-\boldsymbol{y})\cdot\boldsymbol{n}_{\boldsymbol{x}} = \mathcal{O}(|\boldsymbol{x}-\boldsymbol{y}|^2). \tag{B.71}$$

This means that

$$\frac{\partial G}{\partial n_{\boldsymbol{y}}}(\boldsymbol{x},\boldsymbol{y}) = \mathcal{O}(1) \qquad \text{and} \qquad \frac{\partial G}{\partial n_{\boldsymbol{x}}}(\boldsymbol{x},\boldsymbol{y}) = \mathcal{O}(1). \tag{B.72}$$

The singularities of the kernels $\partial G/\partial n_{\boldsymbol{y}}$ and $\partial G/\partial n_{\boldsymbol{x}}$ along Γ are thus only apparent and can be repaired by redefining the value of these kernels at $\boldsymbol{y} = \boldsymbol{x}$.

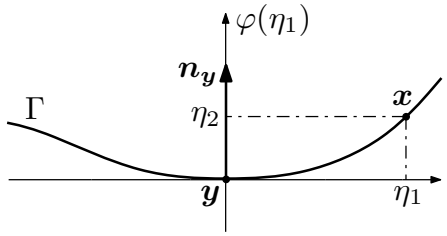

FIGURE B.6. Graph of the function φ on the tangent line of Γ.

The kernel $\partial^2 G/\partial n_{\boldsymbol{x}}\partial n_{\boldsymbol{y}}$, on the other hand, is strongly singular along Γ. It adopts the expression

$$\frac{\partial^2 G}{\partial n_{\boldsymbol{x}}\partial n_{\boldsymbol{y}}}(\boldsymbol{x},\boldsymbol{y}) = -\frac{\boldsymbol{n_x}\cdot\boldsymbol{n_y}}{2\pi|\boldsymbol{y}-\boldsymbol{x}|^2} - \frac{\big((\boldsymbol{x}-\boldsymbol{y})\cdot\boldsymbol{n_x}\big)\big((\boldsymbol{y}-\boldsymbol{x})\cdot\boldsymbol{n_y}\big)}{\pi|\boldsymbol{y}-\boldsymbol{x}|^4}. \tag{B.73}$$

The regularizing effect of the normal derivatives applies only to its second term, but not to the first, since

$$\boldsymbol{n_x}\cdot\boldsymbol{n_y} = \mathcal{O}(1). \tag{B.74}$$

Hence the kernel (B.73) is clearly hypersingular, with $\lambda = 2$, and it holds that

$$\frac{\partial^2 G}{\partial n_{\boldsymbol{x}}\partial n_{\boldsymbol{y}}}(\boldsymbol{x},\boldsymbol{y}) = \mathcal{O}\bigg(\frac{1}{|\boldsymbol{y}-\boldsymbol{x}|^2}\bigg). \tag{B.75}$$

This kernel is no longer integrable and the associated integral operator has to be thus interpreted in some appropriate sense as a divergent integral (cf., e.g., Hsiao & Wendland 2008, Lenoir 2005, Nédélec 2001).

B.6.4 Boundary layer potentials

We regard now the jump properties on the boundary Γ of the boundary layer potentials that have appeared in our calculations. For the development of the integral representation (B.49) we already made acquaintance with the single and double layer potentials, which we define now more precisely for $\boldsymbol{x} \in \Omega_e \cup \Omega_i$ as the integral operators

$$\mathcal{S}\nu(\boldsymbol{x}) = \int_\Gamma G(\boldsymbol{x},\boldsymbol{y})\nu(\boldsymbol{y})\,\mathrm{d}\gamma(\boldsymbol{y}), \tag{B.76}$$

$$\mathcal{D}\mu(\boldsymbol{x}) = \int_\Gamma \frac{\partial G}{\partial n_{\boldsymbol{y}}}(\boldsymbol{x},\boldsymbol{y})\mu(\boldsymbol{y})\,\mathrm{d}\gamma(\boldsymbol{y}). \tag{B.77}$$

The integral representation (B.49) can be now stated in terms of the layer potentials as

$$u = \mathcal{D}\mu - \mathcal{S}\nu. \tag{B.78}$$

We remark that for any functions $\nu, \mu : \Gamma \to \mathbb{C}$ that are regular enough, the single and double layer potentials satisfy the Laplace equation, namely

$$\Delta \mathcal{S}\nu = 0 \qquad \text{in } \Omega_e \cup \Omega_i, \tag{B.79}$$

$$\Delta \mathcal{D}\mu = 0 \qquad \text{in } \Omega_e \cup \Omega_i. \tag{B.80}$$

For the integral equations (B.60) and (B.62), which are defined for $\boldsymbol{x} \in \Gamma$, we require the four boundary integral operators:

$$S\nu(\boldsymbol{x}) = \int_\Gamma G(\boldsymbol{x}, \boldsymbol{y})\nu(\boldsymbol{y})\, \mathrm{d}\gamma(\boldsymbol{y}), \tag{B.81}$$

$$D\mu(\boldsymbol{x}) = \int_\Gamma \frac{\partial G}{\partial n_{\boldsymbol{y}}}(\boldsymbol{x}, \boldsymbol{y})\mu(\boldsymbol{y})\, \mathrm{d}\gamma(\boldsymbol{y}), \tag{B.82}$$

$$D^*\nu(\boldsymbol{x}) = \int_\Gamma \frac{\partial G}{\partial n_{\boldsymbol{x}}}(\boldsymbol{x}, \boldsymbol{y})\nu(\boldsymbol{y})\, \mathrm{d}\gamma(\boldsymbol{y}), \tag{B.83}$$

$$N\mu(\boldsymbol{x}) = \int_\Gamma \frac{\partial^2 G}{\partial n_{\boldsymbol{x}} \partial n_{\boldsymbol{y}}}(\boldsymbol{x}, \boldsymbol{y})\mu(\boldsymbol{y})\, \mathrm{d}\gamma(\boldsymbol{y}). \tag{B.84}$$

The operator D^* is in fact the adjoint of the operator D. As we already mentioned, the kernel of the integral operator N defined in (B.84) is not integrable, yet we write it formally as an improper integral. An appropriate sense for this integral will be given below. The integral equations (B.60) and (B.62) can be now stated in terms of the integral operators as

$$\frac{1}{2}(u_e + u_i) = D\mu - S\nu, \tag{B.85}$$

$$\frac{1}{2}\left(\frac{\partial u_e}{\partial n} + \frac{\partial u_i}{\partial n}\right) = N\mu - D^*\nu. \tag{B.86}$$

These integral equations can be easily derived from the jump properties of the single and double layer potentials. The single layer potential (B.76) is continuous and its normal derivative has a jump of size $-\nu$ across Γ, i.e.,

$$\mathcal{S}\nu|_{\Omega_e} = S\nu = \mathcal{S}\nu|_{\Omega_i}, \tag{B.87}$$

$$\frac{\partial}{\partial n}\mathcal{S}\nu|_{\Omega_e} = \left(-\frac{1}{2} + D^*\right)\nu, \tag{B.88}$$

$$\frac{\partial}{\partial n}\mathcal{S}\nu|_{\Omega_i} = \left(\frac{1}{2} + D^*\right)\nu. \tag{B.89}$$

The double layer potential (B.77), on the other hand, has a jump of size μ across Γ and its normal derivative is continuous, namely

$$\mathcal{D}\mu|_{\Omega_e} = \left(\frac{1}{2} + D\right)\mu, \tag{B.90}$$

$$\mathcal{D}\mu|_{\Omega_i} = \left(-\frac{1}{2} + D\right)\mu, \tag{B.91}$$

$$\frac{\partial}{\partial n}\mathcal{D}\mu|_{\Omega_e} = N\mu = \frac{\partial}{\partial n}\mathcal{D}\mu|_{\Omega_i}. \tag{B.92}$$

The integral equation (B.85) is obtained directly either from (B.87) and (B.90), or from (B.87) and (B.91), by considering the appropriate trace of (B.78) and by defining the functions μ and ν as in (B.37). These three jump properties are easily proven by regarding the details of the proof for (B.60).

Similarly, the integral equation (B.86) for the normal derivative is obtained directly either from (B.88) and (B.92), or from (B.89) and (B.92), by considering the appropriate trace of the normal derivative of (B.78) and by defining again the functions μ and ν as in (B.37). The proof of these other three jump properties is done below.

a) Jump of the normal derivative of the single layer potential

Let us then study first the proof of (B.88) and (B.89). The traces of the normal derivative of the single layer potential are given by

$$\frac{\partial}{\partial n}\mathcal{S}\nu(\boldsymbol{x})|_{\Omega_e} = \lim_{\Omega_e \ni \boldsymbol{z}\to\boldsymbol{x}} \nabla\mathcal{S}\nu(\boldsymbol{z})\cdot\boldsymbol{n}_{\boldsymbol{x}}, \tag{B.93}$$

$$\frac{\partial}{\partial n}\mathcal{S}\nu(\boldsymbol{x})|_{\Omega_i} = \lim_{\Omega_i \ni \boldsymbol{z}\to\boldsymbol{x}} \nabla\mathcal{S}\nu(\boldsymbol{z})\cdot\boldsymbol{n}_{\boldsymbol{x}}. \tag{B.94}$$

Now we have that

$$\nabla\mathcal{S}\nu(\boldsymbol{z})\cdot\boldsymbol{n}_{\boldsymbol{x}} = \int_\Gamma \boldsymbol{n}_{\boldsymbol{x}}\cdot\nabla_{\boldsymbol{z}}G(\boldsymbol{z},\boldsymbol{y})\nu(\boldsymbol{y})\,\mathrm{d}\gamma(\boldsymbol{y}). \tag{B.95}$$

For $\varepsilon > 0$ we denote $\Gamma_\varepsilon = \Gamma \cap B_\varepsilon$, i.e., the portion of Γ contained inside the ball B_ε of radius ε and centered at $\boldsymbol{x}$. By decomposing the integral we obtain that

$$\nabla\mathcal{S}\nu(\boldsymbol{z})\cdot\boldsymbol{n}_{\boldsymbol{x}} = \int_{\Gamma\setminus\Gamma_\varepsilon} \boldsymbol{n}_{\boldsymbol{x}}\cdot\nabla_{\boldsymbol{z}}G(\boldsymbol{z},\boldsymbol{y})\nu(\boldsymbol{y})\,\mathrm{d}\gamma(\boldsymbol{y}) + \int_{\Gamma_\varepsilon} \boldsymbol{n}_{\boldsymbol{x}}\cdot\nabla_{\boldsymbol{z}}G(\boldsymbol{z},\boldsymbol{y})\nu(\boldsymbol{y})\,\mathrm{d}\gamma(\boldsymbol{y}). \tag{B.96}$$

For the first integral in (B.96) we can take without problems the limit $\boldsymbol{z}\to\boldsymbol{x}$, since for a fixed ε the integral is regular in $\boldsymbol{x}$. Since the singularity of the resulting kernel $\partial G/\partial n_{\boldsymbol{x}}$ is integrable, Lebesgue's dominated convergence theorem (cf. Royden 1988) implies that

$$\lim_{\varepsilon\to 0}\int_{\Gamma\setminus\Gamma_\varepsilon}\frac{\partial G}{\partial n_{\boldsymbol{x}}}(\boldsymbol{x},\boldsymbol{y})\nu(\boldsymbol{y})\,\mathrm{d}\gamma(\boldsymbol{y}) = \int_\Gamma \frac{\partial G}{\partial n_{\boldsymbol{x}}}(\boldsymbol{x},\boldsymbol{y})\nu(\boldsymbol{y})\,\mathrm{d}\gamma(\boldsymbol{y}) = D^*\nu(\boldsymbol{x}). \tag{B.97}$$

Let us treat now the second integral in (B.96), which is again decomposed in different integrals in such a way that

$$\begin{aligned}\int_{\Gamma_\varepsilon} \boldsymbol{n}_{\boldsymbol{x}}\cdot\nabla_{\boldsymbol{z}}G(\boldsymbol{z},\boldsymbol{y})\nu(\boldsymbol{y})\,\mathrm{d}\gamma(\boldsymbol{y}) &= \int_{\Gamma_\varepsilon}(\boldsymbol{n}_{\boldsymbol{x}}-\boldsymbol{n}_{\boldsymbol{y}})\cdot\nabla_{\boldsymbol{z}}G(\boldsymbol{z},\boldsymbol{y})\nu(\boldsymbol{y})\,\mathrm{d}\gamma(\boldsymbol{y})\\ &+\int_{\Gamma_\varepsilon}\boldsymbol{n}_{\boldsymbol{y}}\cdot\nabla_{\boldsymbol{z}}G(\boldsymbol{z},\boldsymbol{y})\big(\nu(\boldsymbol{y})-\nu(\boldsymbol{x})\big)\,\mathrm{d}\gamma(\boldsymbol{y}) + \nu(\boldsymbol{x})\int_{\Gamma_\varepsilon}\boldsymbol{n}_{\boldsymbol{y}}\cdot\nabla_{\boldsymbol{z}}G(\boldsymbol{z},\boldsymbol{y})\,\mathrm{d}\gamma(\boldsymbol{y}).\end{aligned} \tag{B.98}$$

When ε is small, and since Γ is supposed to be regular, therefore Γ_ε resembles a straight line segment of length 2ε. Thus we have that

$$\lim_{\varepsilon\to 0}\int_{\Gamma_\varepsilon}(\boldsymbol{n}_{\boldsymbol{x}}-\boldsymbol{n}_{\boldsymbol{y}})\cdot\nabla_{\boldsymbol{z}}G(\boldsymbol{z},\boldsymbol{y})\nu(\boldsymbol{y})\,\mathrm{d}\gamma(\boldsymbol{y}) = 0. \tag{B.99}$$

If ν is regular enough, then we have also that

$$\lim_{\varepsilon \to 0} \int_{\Gamma_\varepsilon} \boldsymbol{n_y} \cdot \nabla_{\boldsymbol{z}} G(\boldsymbol{z}, \boldsymbol{y}) \big(\nu(\boldsymbol{y}) - \nu(\boldsymbol{x})\big) \, \mathrm{d}\gamma(\boldsymbol{y}) = 0. \tag{B.100}$$

For the remaining term in (B.98) we consider the angle θ under which the almost straight line segment Γ_ε is seen from point $\boldsymbol{z}$ (cf. Figure B.7). If we denote $\boldsymbol{R} = \boldsymbol{y} - \boldsymbol{z}$ and $R = |\boldsymbol{R}|$, and consider an oriented boundary differential element $\mathrm{d}\boldsymbol{\gamma} = \boldsymbol{n_y} \mathrm{d}\gamma(\boldsymbol{y})$ seen from point $\boldsymbol{z}$, then we can express the angle differential element by

$$\mathrm{d}\theta = \frac{\boldsymbol{R}}{R^2} \cdot \mathrm{d}\boldsymbol{\gamma} = \frac{\boldsymbol{R} \cdot \boldsymbol{n_y}}{R^2} \, \mathrm{d}\gamma(\boldsymbol{y}) = 2\pi \, \boldsymbol{n_y} \cdot \nabla_{\boldsymbol{y}} G(\boldsymbol{z}, \boldsymbol{y}) \, \mathrm{d}\gamma(\boldsymbol{y}). \tag{B.101}$$

Integrating over the segment Γ_ε and considering (B.28) yields the angle θ, namely

$$\theta = \int_{\Gamma_\varepsilon} \mathrm{d}\theta = 2\pi \int_{\Gamma_\varepsilon} \boldsymbol{n_y} \cdot \nabla_{\boldsymbol{y}} G(\boldsymbol{z}, \boldsymbol{y}) \, \mathrm{d}\gamma(\boldsymbol{y}) = -2\pi \int_{\Gamma_\varepsilon} \boldsymbol{n_y} \cdot \nabla_{\boldsymbol{z}} G(\boldsymbol{z}, \boldsymbol{y}) \, \mathrm{d}\gamma(\boldsymbol{y}), \tag{B.102}$$

where $-\pi \leq \theta \leq \pi$. The angle θ is positive when the vectors $\boldsymbol{R}$ and $\boldsymbol{n_y}$ point towards the same side of Γ_ε, and negative when they oppose each other. Thus if $\boldsymbol{z}$ is very close to $\boldsymbol{x}$ and if ε is small enough so that Γ_ε behaves as a straight line segment, then

$$\int_{\Gamma_\varepsilon} \boldsymbol{n_y} \cdot \nabla_{\boldsymbol{z}} G(\boldsymbol{z}, \boldsymbol{y}) \, \mathrm{d}\gamma(\boldsymbol{y}) \approx \begin{cases} -1/2 & \text{if } \boldsymbol{z} \in \Omega_e, \\ 1/2 & \text{if } \boldsymbol{z} \in \Omega_i. \end{cases} \tag{B.103}$$

Hence we obtain the desired jump formulae (B.88) and (B.89).

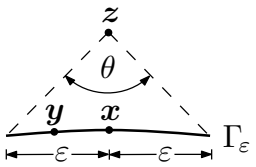

FIGURE B.7. Angle under which Γ_ε is seen from point $\boldsymbol{z}$.

b) Continuity of the normal derivative of the double layer potential

We are now interested in proving the continuity of the normal derivative of the double layer potential across Γ, as expressed in (B.92). This will allow us at the same time to define an appropriate sense for the improper integral (B.84). This integral is divergent in a classical sense, but it can be nonetheless properly defined in a weak or distributional sense by considering it as a linear functional acting on a test function $\varphi \in \mathcal{D}(\mathbb{R}^2)$. By considering (B.80) and Green's first integral theorem (A.612), we can express our values of interest in a weak sense as

$$\left\langle \frac{\partial}{\partial n} \mathcal{D}\mu|_{\Omega_e}, \, \varphi \right\rangle = \int_\Gamma \frac{\partial}{\partial n} \mathcal{D}\mu(\boldsymbol{x})|_{\Omega_e} \, \varphi(\boldsymbol{x}) \, \mathrm{d}\gamma(\boldsymbol{x}) = \int_{\Omega_e} \nabla \mathcal{D}\mu(\boldsymbol{x}) \cdot \nabla \varphi(\boldsymbol{x}) \, \mathrm{d}\boldsymbol{x}, \tag{B.104}$$

$$\left\langle \frac{\partial}{\partial n} \mathcal{D}\mu|_{\Omega_i}, \, \varphi \right\rangle = \int_\Gamma \frac{\partial}{\partial n} \mathcal{D}\mu(\boldsymbol{x})|_{\Omega_i} \, \varphi(\boldsymbol{x}) \, \mathrm{d}\gamma(\boldsymbol{x}) = -\int_{\Omega_i} \nabla \mathcal{D}\mu(\boldsymbol{x}) \cdot \nabla \varphi(\boldsymbol{x}) \, \mathrm{d}\boldsymbol{x}. \tag{B.105}$$

From (A.588) and (B.28) we obtain the relation

$$\frac{\partial G}{\partial n_{\boldsymbol{y}}}(\boldsymbol{x},\boldsymbol{y}) = \boldsymbol{n}_{\boldsymbol{y}} \cdot \nabla_{\boldsymbol{y}} G(\boldsymbol{x},\boldsymbol{y}) = -\boldsymbol{n}_{\boldsymbol{y}} \cdot \nabla_{\boldsymbol{x}} G(\boldsymbol{x},\boldsymbol{y}) = -\operatorname{div}_{\boldsymbol{x}}\big(G(\boldsymbol{x},\boldsymbol{y})\boldsymbol{n}_{\boldsymbol{y}}\big). \tag{B.106}$$

Thus for the double layer potential (B.77) we have that

$$\mathcal{D}\mu(\boldsymbol{x}) = -\operatorname{div}\int_{\Gamma} G(\boldsymbol{x},\boldsymbol{y})\mu(\boldsymbol{y})\boldsymbol{n}_{\boldsymbol{y}}\,\mathrm{d}\gamma(\boldsymbol{y}) = -\operatorname{div}\mathcal{S}(\mu\,\boldsymbol{n}_{\boldsymbol{y}})(\boldsymbol{x}), \tag{B.107}$$

being its gradient given by

$$\nabla\mathcal{D}\mu(\boldsymbol{x}) = -\nabla\operatorname{div}\int_{\Gamma} G(\boldsymbol{x},\boldsymbol{y})\mu(\boldsymbol{y})\boldsymbol{n}_{\boldsymbol{y}}\,\mathrm{d}\gamma(\boldsymbol{y}). \tag{B.108}$$

From (A.589) we have that

$$\operatorname{curl}_{\boldsymbol{x}}\big(G(\boldsymbol{x},\boldsymbol{y})\boldsymbol{n}_{\boldsymbol{y}}\big) = \nabla_{\boldsymbol{x}} G(\boldsymbol{x},\boldsymbol{y}) \times \boldsymbol{n}_{\boldsymbol{y}}. \tag{B.109}$$

Hence, by considering (A.597), (B.80), and (B.109) in (B.108), we obtain that

$$\nabla\mathcal{D}\mu(\boldsymbol{x}) = \operatorname{Curl}\int_{\Gamma}\big(\boldsymbol{n}_{\boldsymbol{y}} \times \nabla_{\boldsymbol{x}} G(\boldsymbol{x},\boldsymbol{y})\big)\mu(\boldsymbol{y})\,\mathrm{d}\gamma(\boldsymbol{y}). \tag{B.110}$$

From (B.28) and (A.659) we have that

$$\begin{aligned}\int_{\Gamma}\big(\boldsymbol{n}_{\boldsymbol{y}} \times \nabla_{\boldsymbol{x}} G(\boldsymbol{x},\boldsymbol{y})\big)\mu(\boldsymbol{y})\,\mathrm{d}\gamma(\boldsymbol{y}) &= -\int_{\Gamma}\boldsymbol{n}_{\boldsymbol{y}} \times \big(\nabla_{\boldsymbol{y}} G(\boldsymbol{x},\boldsymbol{y})\mu(\boldsymbol{y})\big)\,\mathrm{d}\gamma(\boldsymbol{y}) \\ &= \int_{\Gamma}\boldsymbol{n}_{\boldsymbol{y}} \times \big(G(\boldsymbol{x},\boldsymbol{y})\nabla\mu(\boldsymbol{y})\big)\,\mathrm{d}\gamma(\boldsymbol{y}),\end{aligned} \tag{B.111}$$

and consequently

$$\nabla\mathcal{D}\mu(\boldsymbol{x}) = \operatorname{Curl}\int_{\Gamma} G(\boldsymbol{x},\boldsymbol{y})\big(\boldsymbol{n}_{\boldsymbol{y}} \times \nabla\mu(\boldsymbol{y})\big)\,\mathrm{d}\gamma(\boldsymbol{y}). \tag{B.112}$$

Now, considering (A.608) and (A.619), and replacing (B.112) in (B.104), implies that

$$\int_{\Omega_e}\nabla\mathcal{D}\mu(\boldsymbol{x})\cdot\nabla\varphi(\boldsymbol{x})\,\mathrm{d}\boldsymbol{x} = -\int_{\Gamma}\int_{\Gamma} G(\boldsymbol{x},\boldsymbol{y})\big(\nabla\mu(\boldsymbol{y}) \times \boldsymbol{n}_{\boldsymbol{y}}\big)\big(\nabla\varphi(\boldsymbol{x}) \times \boldsymbol{n}_{\boldsymbol{x}}\big)\,\mathrm{d}\gamma(\boldsymbol{y})\,\mathrm{d}\gamma(\boldsymbol{x}). \tag{B.113}$$

Analogously, when replacing in (B.105) we have that

$$\int_{\Omega_i}\nabla\mathcal{D}\mu(\boldsymbol{x})\cdot\nabla\varphi(\boldsymbol{x})\,\mathrm{d}\boldsymbol{x} = \int_{\Gamma}\int_{\Gamma} G(\boldsymbol{x},\boldsymbol{y})\big(\nabla\mu(\boldsymbol{y}) \times \boldsymbol{n}_{\boldsymbol{y}}\big)\big(\nabla\varphi(\boldsymbol{x}) \times \boldsymbol{n}_{\boldsymbol{x}}\big)\,\mathrm{d}\gamma(\boldsymbol{y})\,\mathrm{d}\gamma(\boldsymbol{x}). \tag{B.114}$$

Hence, from (B.104), (B.105), (B.113), and (B.114) we conclude the proof of (B.92). The integral operator (B.84) is thus properly defined in a weak sense for $\varphi \in \mathcal{D}(\mathbb{R}^2)$ by

$$\langle N\mu(\boldsymbol{x}),\,\varphi\rangle = -\int_{\Gamma}\int_{\Gamma} G(\boldsymbol{x},\boldsymbol{y})\big(\nabla\mu(\boldsymbol{y}) \times \boldsymbol{n}_{\boldsymbol{y}}\big)\big(\nabla\varphi(\boldsymbol{x}) \times \boldsymbol{n}_{\boldsymbol{x}}\big)\,\mathrm{d}\gamma(\boldsymbol{y})\,\mathrm{d}\gamma(\boldsymbol{x}). \tag{B.115}$$

B.6.5 Calderón projectors

The surface layer potentials (B.81)–(B.84) are linked together by means of the so-called Calderón relations, which receive their name from the Argentine mathematician Alberto Pedro Calderón (1920–1998), who is best known for his work on the theory of partial differential equations and singular integral operators. The exterior and interior traces of a

function u defined by (B.78) can be characterized, due (B.85) and (B.86), by

$$\begin{pmatrix} u_e \\ \dfrac{\partial u_e}{\partial n} \end{pmatrix} = \begin{pmatrix} \dfrac{I}{2} + D & -S \\ N & \dfrac{I}{2} - D^* \end{pmatrix} \begin{pmatrix} \mu \\ \nu \end{pmatrix} = \left(\frac{I}{2} + H \right) \begin{pmatrix} \mu \\ \nu \end{pmatrix}, \tag{B.116}$$

$$\begin{pmatrix} u_i \\ \dfrac{\partial u_i}{\partial n} \end{pmatrix} = \begin{pmatrix} -\dfrac{I}{2} + D & -S \\ N & -\dfrac{I}{2} - D^* \end{pmatrix} \begin{pmatrix} \mu \\ \nu \end{pmatrix} = \left(-\frac{I}{2} + H \right) \begin{pmatrix} \mu \\ \nu \end{pmatrix}, \tag{B.117}$$

where

$$H = \begin{pmatrix} D & -S \\ N & -D^* \end{pmatrix}, \tag{B.118}$$

and where the vector $(\mu, \nu)^T$ is known as the Cauchy data on Γ. We define the exterior and interior Calderón projectors respectively by the operators

$$C_e = \frac{I}{2} + H \qquad \text{and} \qquad C_i = \frac{I}{2} - H, \tag{B.119}$$

which satisfy

$$C_e^2 = C_e, \qquad C_i^2 = C_i, \qquad C_e + C_i = I. \tag{B.120}$$

The identities (B.120) are equivalent to the set of relations

$$H^2 = \frac{I}{4}, \tag{B.121}$$

or more explicitly

$$DS = SD^*, \qquad D^2 - SN = \frac{I}{4}, \tag{B.122}$$

$$ND = D^*N, \qquad D^{*2} - NS = \frac{I}{4}. \tag{B.123}$$

Calderón projectors and relations synthesize in another way the structure of the integral equations, and are used more for theoretical purposes (e.g., matrix preconditioning).

B.6.6 Alternatives for integral representations and equations

By taking into account the transmission problem (B.37), its integral representation formula (B.48), and its integral equations (B.60) and (B.62), several particular alternatives for integral representations and equations of the exterior problem (B.11) can be developed. The way to perform this is to extend properly the exterior problem towards the interior domain Ω_i, either by specifying explicitly this extension or by defining an associated interior problem, so as to become the desired jump properties across Γ. The extension has to satisfy the Laplace equation (B.1) in Ω_i and a boundary condition that corresponds adequately to the impedance boundary condition (B.2). The obtained system of integral representations and equations allows finally to solve the exterior problem (B.11), by using the solution of the integral equation in the integral representation formula.

a) Extension by zero

An extension by zero towards the interior domain Ω_i implies that

$$u_i = 0 \qquad \text{in } \Omega_i. \tag{B.124}$$

The jumps over Γ are characterized in this case by

$$[u] = u_e = \mu, \tag{B.125}$$

$$\left[\frac{\partial u}{\partial n}\right] = \frac{\partial u_e}{\partial n} = Zu_e - f_z = Z\mu - f_z, \tag{B.126}$$

where $\mu : \Gamma \to \mathbb{C}$ is a function to be determined.

An integral representation formula of the solution, for $\boldsymbol{x} \in \Omega_e \cup \Omega_i$, is given by

$$u(\boldsymbol{x}) = \int_\Gamma \left(\frac{\partial G}{\partial n_{\boldsymbol{y}}}(\boldsymbol{x},\boldsymbol{y}) - Z(\boldsymbol{y})G(\boldsymbol{x},\boldsymbol{y})\right)\mu(\boldsymbol{y})\,\mathrm{d}\gamma(\boldsymbol{y}) + \int_\Gamma G(\boldsymbol{x},\boldsymbol{y})f_z(\boldsymbol{y})\,\mathrm{d}\gamma(\boldsymbol{y}). \tag{B.127}$$

Since

$$\frac{1}{2}\big(u_e(\boldsymbol{x}) + u_i(\boldsymbol{x})\big) = \frac{\mu(\boldsymbol{x})}{2}, \qquad \boldsymbol{x} \in \Gamma, \tag{B.128}$$

we obtain, for $\boldsymbol{x} \in \Gamma$, the Fredholm integral equation of the second kind

$$\frac{\mu(\boldsymbol{x})}{2} + \int_\Gamma \left(Z(\boldsymbol{y})G(\boldsymbol{x},\boldsymbol{y}) - \frac{\partial G}{\partial n_{\boldsymbol{y}}}(\boldsymbol{x},\boldsymbol{y})\right)\mu(\boldsymbol{y})\,\mathrm{d}\gamma(\boldsymbol{y}) = \int_\Gamma G(\boldsymbol{x},\boldsymbol{y})f_z(\boldsymbol{y})\,\mathrm{d}\gamma(\boldsymbol{y}), \tag{B.129}$$

which has to be solved for the unknown μ. In terms of boundary layer potentials, the integral representation and the integral equation can be respectively expressed by

$$u = \mathcal{D}(\mu) - \mathcal{S}(Z\mu) + \mathcal{S}(f_z) \qquad \text{in } \Omega_e \cup \Omega_i, \tag{B.130}$$

$$\frac{\mu}{2} + S(Z\mu) - D(\mu) = S(f_z) \qquad \text{on } \Gamma. \tag{B.131}$$

Alternatively, since

$$\frac{1}{2}\left(\frac{\partial u_e}{\partial n}(\boldsymbol{x}) + \frac{\partial u_i}{\partial n}(\boldsymbol{x})\right) = \frac{Z(\boldsymbol{x})}{2}\mu(\boldsymbol{x}) - \frac{f_z(\boldsymbol{x})}{2}, \qquad \boldsymbol{x} \in \Gamma, \tag{B.132}$$

we obtain also, for $\boldsymbol{x} \in \Gamma$, the Fredholm integral equation of the second kind

$$\frac{Z(\boldsymbol{x})}{2}\mu(\boldsymbol{x}) + \int_\Gamma \left(-\frac{\partial^2 G}{\partial n_{\boldsymbol{x}}\partial n_{\boldsymbol{y}}}(\boldsymbol{x},\boldsymbol{y}) + Z(\boldsymbol{y})\frac{\partial G}{\partial n_{\boldsymbol{x}}}(\boldsymbol{x},\boldsymbol{y})\right)\mu(\boldsymbol{y})\,\mathrm{d}\gamma(\boldsymbol{y}) = \frac{f_z(\boldsymbol{x})}{2} + \int_\Gamma \frac{\partial G}{\partial n_{\boldsymbol{x}}}(\boldsymbol{x},\boldsymbol{y})f_z(\boldsymbol{y})\,\mathrm{d}\gamma(\boldsymbol{y}), \tag{B.133}$$

which in terms of boundary layer potentials becomes

$$\frac{Z}{2}\mu - N(\mu) + D^*(Z\mu) = \frac{f_z}{2} + D^*(f_z) \qquad \text{on } \Gamma. \tag{B.134}$$

b) Continuous impedance

We associate to (B.11) the interior problem

$$\begin{cases} \text{Find } u_i : \Omega_i \to \mathbb{C} \text{ such that} & \\ \Delta u_i = 0 & \text{in } \Omega_i, \\ -\dfrac{\partial u_i}{\partial n} + Z u_i = f_z & \text{on } \Gamma. \end{cases} \tag{B.135}$$

The jumps over Γ are characterized in this case by

$$[u] = u_e - u_i = \mu, \tag{B.136}$$

$$\left[\frac{\partial u}{\partial n}\right] = \frac{\partial u_e}{\partial n} - \frac{\partial u_i}{\partial n} = Z(u_e - u_i) = Z\mu, \tag{B.137}$$

where $\mu : \Gamma \to \mathbb{C}$ is a function to be determined. In particular it holds that the jump of the impedance is zero, namely

$$\left[-\frac{\partial u}{\partial n} + Zu\right] = \left(-\frac{\partial u_e}{\partial n} + Z u_e\right) - \left(-\frac{\partial u_i}{\partial n} + Z u_i\right) = 0. \tag{B.138}$$

An integral representation formula of the solution, for $\boldsymbol{x} \in \Omega_e \cup \Omega_i$, is given by

$$u(\boldsymbol{x}) = \int_\Gamma \left(\frac{\partial G}{\partial n_{\boldsymbol{y}}}(\boldsymbol{x}, \boldsymbol{y}) - Z(\boldsymbol{y}) G(\boldsymbol{x}, \boldsymbol{y})\right) \mu(\boldsymbol{y}) \, \mathrm{d}\gamma(\boldsymbol{y}). \tag{B.139}$$

Since

$$-\frac{1}{2}\left(\frac{\partial u_e}{\partial n}(\boldsymbol{x}) + \frac{\partial u_i}{\partial n}(\boldsymbol{x})\right) + \frac{Z(\boldsymbol{x})}{2}\big(u_e(\boldsymbol{x}) + u_i(\boldsymbol{x})\big) = f_z(\boldsymbol{x}), \qquad \boldsymbol{x} \in \Gamma, \tag{B.140}$$

we obtain, for $\boldsymbol{x} \in \Gamma$, the Fredholm integral equation of the first kind

$$\begin{aligned} \int_\Gamma \left(-\frac{\partial^2 G}{\partial n_{\boldsymbol{x}} \partial n_{\boldsymbol{y}}}(\boldsymbol{x}, \boldsymbol{y}) + Z(\boldsymbol{y}) \frac{\partial G}{\partial n_{\boldsymbol{x}}}(\boldsymbol{x}, \boldsymbol{y})\right) \mu(\boldsymbol{y}) \, \mathrm{d}\gamma(\boldsymbol{y}) & \\ + Z(\boldsymbol{x}) \int_\Gamma \left(\frac{\partial G}{\partial n_{\boldsymbol{y}}}(\boldsymbol{x}, \boldsymbol{y}) - Z(\boldsymbol{y}) G(\boldsymbol{x}, \boldsymbol{y})\right) \mu(\boldsymbol{y}) \, \mathrm{d}\gamma(\boldsymbol{y}) = f_z(\boldsymbol{x}), & \end{aligned} \tag{B.141}$$

which has to be solved for the unknown μ. In terms of boundary layer potentials, the integral representation and the integral equation can be respectively expressed by

$$u = \mathcal{D}(\mu) - \mathcal{S}(Z\mu) \qquad \text{in } \Omega_e \cup \Omega_i, \tag{B.142}$$

$$-N(\mu) + D^*(Z\mu) + ZD(\mu) - ZS(Z\mu) = f_z \qquad \text{on } \Gamma. \tag{B.143}$$

c) Continuous value

We associate to (B.11) the interior problem

$$\begin{cases} \text{Find } u_i : \Omega_i \to \mathbb{C} \text{ such that} & \\ \Delta u_i = 0 & \text{in } \Omega_i, \\ -\dfrac{\partial u_e}{\partial n} + Z u_i = f_z & \text{on } \Gamma. \end{cases} \tag{B.144}$$

The jumps over Γ are characterized in this case by

$$[u] = u_e - u_i = \frac{1}{Z}\left(\frac{\partial u_e}{\partial n} - f_z\right) - \frac{1}{Z}\left(\frac{\partial u_e}{\partial n} - f_z\right) = 0, \tag{B.145}$$

$$\left[\frac{\partial u}{\partial n}\right] = \frac{\partial u_e}{\partial n} - \frac{\partial u_i}{\partial n} = \nu, \tag{B.146}$$

where $\nu : \Gamma \to \mathbb{C}$ is a function to be determined.

An integral representation formula of the solution, for $\boldsymbol{x} \in \Omega_e \cup \Omega_i$, is given by the single layer potential

$$u(\boldsymbol{x}) = -\int_\Gamma G(\boldsymbol{x}, \boldsymbol{y})\nu(\boldsymbol{y})\,\mathrm{d}\gamma(\boldsymbol{y}). \tag{B.147}$$

Since

$$-\frac{1}{2}\left(\frac{\partial u_e}{\partial n}(\boldsymbol{x}) + \frac{\partial u_i}{\partial n}(\boldsymbol{x})\right) + \frac{Z(\boldsymbol{x})}{2}\big(u_e(\boldsymbol{x}) + u_i(\boldsymbol{x})\big) = \frac{\nu(\boldsymbol{x})}{2} + f_z(\boldsymbol{x}), \quad \boldsymbol{x} \in \Gamma, \tag{B.148}$$

we obtain, for $\boldsymbol{x} \in \Gamma$, the Fredholm integral equation of the second kind

$$\frac{\nu(\boldsymbol{x})}{2} + \int_\Gamma \left(Z(\boldsymbol{x})G(\boldsymbol{x}, \boldsymbol{y}) - \frac{\partial G}{\partial n_{\boldsymbol{x}}}(\boldsymbol{x}, \boldsymbol{y})\right)\nu(\boldsymbol{y})\,\mathrm{d}\gamma(\boldsymbol{y}) = -f_z(\boldsymbol{x}), \tag{B.149}$$

which has to be solved for the unknown ν. In terms of boundary layer potentials, the integral representation and the integral equation can be respectively expressed by

$$u = -\mathcal{S}(\nu) \qquad \text{in } \Omega_e \cup \Omega_i, \tag{B.150}$$

$$\frac{\nu}{2} + ZS(\nu) - D^*(\nu) = -f_z \qquad \text{on } \Gamma. \tag{B.151}$$

d) Continuous normal derivative

We associate to (B.11) the interior problem

$$\begin{cases} \text{Find } u_i : \Omega_i \to \mathbb{C} \text{ such that} \\ \Delta u_i = 0 & \text{in } \Omega_i, \\ -\dfrac{\partial u_i}{\partial n} + Z u_e = f_z & \text{on } \Gamma. \end{cases} \tag{B.152}$$

The jumps over Γ are characterized in this case by

$$[u] = u_e - u_i = \mu, \tag{B.153}$$

$$\left[\frac{\partial u}{\partial n}\right] = \frac{\partial u_e}{\partial n} - \frac{\partial u_i}{\partial n} = \big(Z u_e - f_z\big) - \big(Z u_e - f_z\big) = 0, \tag{B.154}$$

where $\mu : \Gamma \to \mathbb{C}$ is a function to be determined.

An integral representation formula of the solution, for $\boldsymbol{x} \in \Omega_e \cup \Omega_i$, is given by the double layer potential

$$u(\boldsymbol{x}) = \int_\Gamma \frac{\partial G}{\partial n_{\boldsymbol{y}}}(\boldsymbol{x}, \boldsymbol{y})\mu(\boldsymbol{y})\,\mathrm{d}\gamma(\boldsymbol{y}). \tag{B.155}$$

Since when $\boldsymbol{x} \in \Gamma$,

$$-\frac{1}{2}\left(\frac{\partial u_e}{\partial n}(\boldsymbol{x}) + \frac{\partial u_i}{\partial n}(\boldsymbol{x})\right) + \frac{Z(\boldsymbol{x})}{2}\big(u_e(\boldsymbol{x}) + u_i(\boldsymbol{x})\big) = -\frac{Z(\boldsymbol{x})}{2}\mu(\boldsymbol{x}) + f_z(\boldsymbol{x}), \quad \text{(B.156)}$$

we obtain, for $\boldsymbol{x} \in \Gamma$, the Fredholm integral equation of the second kind

$$\frac{Z(\boldsymbol{x})}{2}\mu(\boldsymbol{x}) + \int_\Gamma \left(-\frac{\partial^2 G}{\partial n_{\boldsymbol{x}} \partial n_{\boldsymbol{y}}}(\boldsymbol{x},\boldsymbol{y}) + Z(\boldsymbol{x})\frac{\partial G}{\partial n_{\boldsymbol{y}}}(\boldsymbol{x},\boldsymbol{y})\right)\mu(\boldsymbol{y})\,\mathrm{d}\gamma(\boldsymbol{y}) = f_z(\boldsymbol{x}), \quad \text{(B.157)}$$

which has to be solved for the unknown μ. In terms of boundary layer potentials, the integral representation and the integral equation can be respectively expressed by

$$u = \mathcal{D}(\mu) \qquad \text{in } \ \Omega_e \cup \Omega_i, \quad \text{(B.158)}$$

$$\frac{Z}{2}\mu - N(\mu) + ZD(\mu) = f_z \qquad \text{on } \ \Gamma. \quad \text{(B.159)}$$

B.6.7 Adjoint integral equations

Due Fredholm's alternative, there is a close relation between the solution of an integral equation and the one of its adjoint counterpart. The so-called adjoint integral equation is obtained by taking the adjoint of the integral operators that appear in the integral equation, disregarding the source terms at the right-hand side. For a function $\varphi : \Gamma \subset \mathbb{R}^N \to \mathbb{C}$, the linear adjoint of an integral operator of the form

$$T\varphi(\boldsymbol{x}) = \int_\Gamma K(\boldsymbol{x},\boldsymbol{y})\varphi(\boldsymbol{y})\,\mathrm{d}\gamma(\boldsymbol{y}), \qquad \boldsymbol{x} \in \Gamma, \quad \text{(B.160)}$$

is given by the integral operator

$$T^*\varphi(\boldsymbol{x}) = \int_\Gamma K(\boldsymbol{y},\boldsymbol{x})\varphi(\boldsymbol{y})\,\mathrm{d}\gamma(\boldsymbol{y}), \qquad \boldsymbol{x} \in \Gamma. \quad \text{(B.161)}$$

It is not difficult to see that the boundary layer potentials S and N are self-adjoint due their symmetric kernels, and that D and D^* are mutually adjoint, i.e.,

$$S^* = S, \qquad N^* = N, \qquad \text{and} \qquad D^* = D. \quad \text{(B.162)}$$

When we include also the impedance, then it holds that

$$\big(S(Z\varphi)\big)^* = ZS(\varphi), \qquad \big(D^*(Z\varphi)\big)^* = ZD(\varphi), \qquad \big(ZS(Z\varphi)\big)^* = ZS(Z\varphi). \quad \text{(B.163)}$$

It can be seen now that the integral equations (B.131) of the first extension by zero and (B.151) of the continuous value are mutually adjoint. The same holds for the integral equations (B.134) of the second extension by zero and (B.159) of the continuous normal derivative, which are also mutually adjoint. The integral equation (B.143) of the continuous impedance, on the other hand, is self-adjoint.

B.7 Far field of the solution

The asymptotic behavior at infinity of the solution u of (B.11) is described by the far field. It is denoted by u^{ff} and is characterized by

$$u(\boldsymbol{x}) \sim u^{ff}(\boldsymbol{x}) \qquad \text{as } \ |\boldsymbol{x}| \to \infty. \quad \text{(B.164)}$$

Its expression can be deduced by replacing the far field of the Green's function G^{ff} and its derivatives in the integral representation formula (B.48), which yields

$$u^{ff}(\boldsymbol{x}) = \int_\Gamma \left([u](\boldsymbol{y}) \frac{\partial G^{ff}}{\partial n_{\boldsymbol{y}}}(\boldsymbol{x}, \boldsymbol{y}) - G^{ff}(\boldsymbol{x}, \boldsymbol{y}) \left[\frac{\partial u}{\partial n} \right](\boldsymbol{y}) \right) \mathrm{d}\gamma(\boldsymbol{y}). \tag{B.165}$$

By replacing now (B.32) and (B.33) in (B.165), we obtain that

$$\begin{aligned} u^{ff}(\boldsymbol{x}) = & -\frac{1}{2\pi|\boldsymbol{x}|} \int_\Gamma \left(\hat{\boldsymbol{x}} \cdot \boldsymbol{n}_{\boldsymbol{y}} \, [u](\boldsymbol{y}) - \hat{\boldsymbol{x}} \cdot \boldsymbol{y} \left[\frac{\partial u}{\partial n} \right](\boldsymbol{y}) \right) \mathrm{d}\gamma(\boldsymbol{y}) \\ & - \frac{1}{2\pi} \ln|\boldsymbol{x}| \int_\Gamma \left[\frac{\partial u}{\partial n} \right](\boldsymbol{y}) \, \mathrm{d}\gamma(\boldsymbol{y}). \end{aligned} \tag{B.166}$$

Due (B.57) the second integral in (B.166) is zero. Thus the far field of the solution u is

$$u^{ff}(\boldsymbol{x}) = -\frac{1}{2\pi|\boldsymbol{x}|} \int_\Gamma \left(\hat{\boldsymbol{x}} \cdot \boldsymbol{n}_{\boldsymbol{y}} \, [u](\boldsymbol{y}) - \hat{\boldsymbol{x}} \cdot \boldsymbol{y} \left[\frac{\partial u}{\partial n} \right](\boldsymbol{y}) \right) \mathrm{d}\gamma(\boldsymbol{y}). \tag{B.167}$$

The asymptotic behavior of the solution u at infinity is therefore given by

$$u(\boldsymbol{x}) = \frac{1}{|\boldsymbol{x}|} \left\{ u_\infty(\hat{\boldsymbol{x}}) + \mathcal{O}\left(\frac{1}{|\boldsymbol{x}|} \right) \right\}, \qquad |\boldsymbol{x}| \to \infty, \tag{B.168}$$

uniformly in all directions $\hat{\boldsymbol{x}}$ on the unit circle, where

$$u_\infty(\hat{\boldsymbol{x}}) = -\frac{1}{2\pi} \int_\Gamma \left(\hat{\boldsymbol{x}} \cdot \boldsymbol{n}_{\boldsymbol{y}} \, [u](\boldsymbol{y}) - \hat{\boldsymbol{x}} \cdot \boldsymbol{y} \left[\frac{\partial u}{\partial n} \right](\boldsymbol{y}) \right) \mathrm{d}\gamma(\boldsymbol{y}) \tag{B.169}$$

is called the far-field pattern of u. It can be expressed in decibels (dB) by means of the asymptotic cross section

$$Q_s(\hat{\boldsymbol{x}}) \ \ [\mathrm{dB}] = 20 \log_{10} \left(\frac{|u_\infty(\hat{\boldsymbol{x}})|}{|u_0|} \right), \tag{B.170}$$

where the reference level u_0 may typically depend on u_W, but for simplicity we take $u_0 = 1$.

We remark that the far-field behavior (B.168) of the solution is in accordance with the decaying condition (B.7), which justifies its choice.

B.8 Exterior circle problem

To understand better the resolution of the direct perturbation problem (B.11), we study now the particular case when the domain $\Omega_e \subset \mathbb{R}^2$ is taken as the exterior of a circle of radius $R > 0$. The interior of the circle is then given by $\Omega_i = \{\boldsymbol{x} \in \mathbb{R}^2 : |\boldsymbol{x}| < R\}$ and its boundary by $\Gamma = \partial\Omega_e$, as shown in Figure B.8. We place the origin at the center of Ω_i and we consider that the unit normal $\boldsymbol{n}$ is taken outwardly oriented of Ω_e, i.e., $\boldsymbol{n} = -\boldsymbol{r}$.

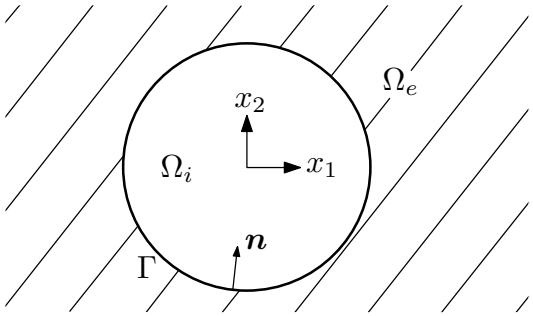

FIGURE B.8. Exterior of the circle.

The exterior circle problem is then stated as

$$\begin{cases} \text{Find } u : \Omega_e \to \mathbb{C} \text{ such that} \\ \Delta u = 0 \qquad\qquad \text{in } \ \Omega_e, \\ \dfrac{\partial u}{\partial r} + Zu = f_z \qquad \text{on } \ \Gamma, \\ \text{+ Decaying condition as } |\boldsymbol{x}| \to \infty, \end{cases} \tag{B.171}$$

where we consider a constant impedance $Z \in \mathbb{C}$ and where the asymptotic decaying condition is as usual given by (B.7).

Due the particular chosen geometry, the solution u of (B.171) can be easily found analytically by using the method of variable separation, i.e., by supposing that

$$u(\boldsymbol{x}) = u(r, \theta) = h(r)g(\theta), \tag{B.172}$$

where $r \geq 0$ and $-\pi < \theta \leq \pi$ are the polar coordinates in $\mathbb{R}^2$, characterized by

$$r = \sqrt{x_1^2 + x_2^2} \qquad \text{and} \qquad \theta = \arctan\left(\frac{x_2}{x_1}\right). \tag{B.173}$$

If the Laplace equation in (B.171) is expressed using polar coordinates, then

$$\Delta u = \frac{\partial^2 u}{\partial r^2} + \frac{1}{r}\frac{\partial u}{\partial r} + \frac{1}{r^2}\frac{\partial^2 u}{\partial \theta^2} = 0. \tag{B.174}$$

By replacing now (B.172) in (B.174) we obtain

$$h''(r)g(\theta) + \frac{1}{r}h'(r)g(\theta) + \frac{1}{r^2}h(r)g''(\theta) = 0. \tag{B.175}$$

Multiplying by r^2, dividing by gh, and rearranging according to each variable yields

$$r^2\frac{h''(r)}{h(r)} + r\frac{h'(r)}{h(r)} = -\frac{g''(\theta)}{g(\theta)}. \tag{B.176}$$

Since both sides in equation (B.176) involve different variables, therefore they are equal to a constant, denoted for convenience by n^2, and we have that

$$r^2\frac{h''(r)}{h(r)} + r\frac{h'(r)}{h(r)} = -\frac{g''(\theta)}{g(\theta)} = n^2. \tag{B.177}$$

From (B.177) we obtain the two ordinary differential equations

$$g''(\theta) + n^2 g(\theta) = 0, \tag{B.178}$$

$$r^2 h''(r) + r h'(r) - n^2 h(r) = 0. \tag{B.179}$$

The solutions for (B.178) have the general form

$$g(\theta) = a_n \cos(n\theta) + b_n \sin(n\theta), \qquad n \in \mathbb{N}_0, \tag{B.180}$$

where $a_n, b_n \in \mathbb{C}$ are arbitrary constants. The requirement that $n \in \mathbb{N}_0$ stems from the periodicity condition

$$g(\theta) = g(\theta + 2\pi n) \qquad \forall n \in \mathbb{Z}, \tag{B.181}$$

where we segregate positive and negative values for n. The solutions for (B.179), on the other hand, have the general form

$$h(r) = c_n r^{-n} + d_n r^n, \qquad n > 0, \tag{B.182}$$

and for the particular case $n = 0$, as already done in (B.14), it holds that

$$h(r) = c_0 + d_0 \ln r, \tag{B.183}$$

where $c_n, d_n \in \mathbb{C}$ are again arbitrary constants. The general solution for the Laplace equation considers the linear combination of all the solutions in the form of (B.172), namely

$$u(r,\theta) = a_0(c_0 + d_0 \ln r) + \sum_{n=1}^{\infty} \big(c_n r^{-n} + d_n r^n\big)\big(a_n \cos(n\theta) + b_n \sin(n\theta)\big). \tag{B.184}$$

The decaying condition (B.7) implies that

$$c_0 = d_0 = d_n = 0, \qquad n \in \mathbb{N}. \tag{B.185}$$

Thus the general solution (B.184) turns into

$$u(r,\theta) = \sum_{n=1}^{\infty} r^{-n}\big(a_n e^{in\theta} + b_n e^{-in\theta}\big), \tag{B.186}$$

where all the undetermined constants have been merged into a_n and b_n, due their arbitrariness. The radial derivative of (B.186) is given by

$$\frac{\partial u}{\partial r}(r,\theta) = -\sum_{n=1}^{\infty} n r^{-(n+1)}\big(a_n e^{in\theta} + b_n e^{-in\theta}\big). \tag{B.187}$$

The constants a_n and b_n in (B.186) are determined through the impedance boundary condition on Γ. For this purpose, we expand the impedance data function f_z as a Fourier series:

$$f_z(\theta) = \sum_{n=-\infty}^{\infty} f_n e^{in\theta}, \qquad -\pi < \theta \leq \pi, \tag{B.188}$$

where

$$f_n = \frac{1}{2\pi} \int_{-\pi}^{\pi} f_z(\theta) e^{-in\theta}\, \mathrm{d}\theta, \qquad n \in \mathbb{Z}. \tag{B.189}$$

The impedance boundary condition considers $r = R$ and thus takes the form

$$\sum_{n=1}^{\infty} \left(\frac{ZR - n}{R^{n+1}} \right) \left(a_n e^{in\theta} + b_n e^{-in\theta} \right) = f_z(\theta) = \sum_{n=-\infty}^{\infty} f_n e^{in\theta}. \tag{B.190}$$

We observe that the constants a_n and b_n can be uniquely determined only if $f_0 = 0$ and if $ZR \neq n$, for $n \in \mathbb{N}$ and $n \geq 1$. The first condition, which is usually referred to as a compatibility condition, is necessary to ensure the existence of the solution u, and can be restated as

$$\int_{\Gamma} f_z \, \mathrm{d}\gamma = 0. \tag{B.191}$$

The second condition is more related with the loss of the solution's uniqueness. Therefore, if we suppose, for $n \in \mathbb{N}$ and $n \geq 1$, that $ZR \neq n$ and (B.191) hold, then

$$a_n = \frac{R^{n+1} f_n}{ZR - n} \qquad \text{and} \qquad b_n = \frac{R^{n+1} f_{-n}}{ZR - n}. \tag{B.192}$$

The unique solution for the exterior circle problem (B.171) is then given by

$$u(r, \theta) = \sum_{n=1}^{\infty} \left(\frac{R^{n+1}}{ZR - n} \right) r^{-n} \left(f_n e^{in\theta} + f_{-n} e^{-in\theta} \right). \tag{B.193}$$

If we consider now the case when $ZR = m$, for some particular integer $m \geq 1$, then the solution u is not unique. The constants a_m and b_m are then no longer defined by (B.192), and can be chosen in an arbitrary manner. For the existence of a solution in this case, however, we require, together with the compatibility condition (B.191), also the orthogonality conditions $f_m = f_{-m} = 0$, which are equivalent to

$$\int_{-\pi}^{\pi} f_z(\theta) e^{im\theta} \, \mathrm{d}\theta = \int_{-\pi}^{\pi} f_z(\theta) e^{-im\theta} \, \mathrm{d}\theta = 0. \tag{B.194}$$

Instead of (B.193), the solution of (B.171) is now given by the infinite family of functions

$$u(r, \theta) = \sum_{1 \leq n \neq m} \left(\frac{R^{n+1}}{ZR - n} \right) r^{-n} \left(f_n e^{in\theta} + f_{-n} e^{-in\theta} \right) + \alpha \frac{e^{im\theta}}{r^m} + \beta \frac{e^{-im\theta}}{r^m}, \tag{B.195}$$

where $\alpha, \beta \in \mathbb{C}$ are arbitrary and where their associated terms have the form of surface waves, i.e., waves that propagate along Γ and decrease towards the interior of Ω_e. Thus, if the compatibility condition (B.191) is satisfied, then the exterior circle problem (B.171) admits a unique solution u, except on a countable set of values for ZR. And even in this last case there exists a solution, although not unique, if two orthogonality conditions are additionally satisfied. This behavior for the existence and uniqueness of the solution is typical of the Fredholm alternative, which applies when solving problems that involve compact perturbations of invertible operators.

We remark that when a non-constant impedance $Z(\theta)$ is taken, then the compatibility condition (B.191) is no longer required for the existence of the solution u, a fact that can be inferred from (B.190) by considering the Fourier series terms of the impedance. An analytic formula for the solution is more difficult to obtain in this case, but it holds again that this solution will exist and be unique, except possibly for some at most countable set

of values where the uniqueness is lost and where additional orthogonality conditions have to be satisfied, which depend on $Z(\theta)$.

B.9 Existence and uniqueness

B.9.1 Function spaces

To state a precise mathematical formulation of the herein treated problems, we have to define properly the involved function spaces. For the associated interior problems defined on the bounded set Ω_i we use the classical Sobolev space (vid. Section A.4)

$$H^1(\Omega_i) = \left\{v : \ v \in L^2(\Omega_i), \ \nabla v \in L^2(\Omega_i)^2\right\}, \tag{B.196}$$

which is a Hilbert space and has the norm

$$\|v\|_{H^1(\Omega_i)} = \left(\|v\|^2_{L^2(\Omega_i)} + \|\nabla v\|^2_{L^2(\Omega_i)^2}\right)^{1/2}. \tag{B.197}$$

For the exterior problem defined on the unbounded domain Ω_e, on the other hand, we introduce the weighted Sobolev space (cf., e.g., Raviart 1991)

$$W^1(\Omega_e) = \left\{v : \ \frac{v}{\sqrt{1+r^2}\,\ln(2+r^2)} \in L^2(\Omega_e), \ \frac{\partial v}{\partial x_i} \in L^2(\Omega_e) \ \ \forall i \in \{1,2\}\right\}, \tag{B.198}$$

where $r = |\boldsymbol{x}|$. If $W^1(\Omega_e)$ is provided with the norm

$$\|v\|_{W^1(\Omega_e)} = \left(\left\|\frac{v}{\sqrt{1+r^2}\,\ln(2+r^2)}\right\|^2_{L^2(\Omega_e)} + \|\nabla v\|^2_{L^2(\Omega_e)^2}\right)^{1/2}, \tag{B.199}$$

then it becomes a Hilbert space. The restriction to any bounded open set $B \subset \Omega_e$ of the functions of $W^1(\Omega_e)$ belongs to $H^1(B)$, i.e., we have the inclusion $W^1(\Omega_e) \subset H^1_{\text{loc}}(\Omega_e)$, and the functions in these two spaces differ only by their behavior at infinity. We remark that the space $W^1(\Omega_e)$ contains the constant functions and all the functions of $H^1_{\text{loc}}(\Omega_e)$ that satisfy the decaying condition (B.7). The justification for the use of these function spaces lies in the variational formulation of the differential problem, and they remain valid even when considering a source term with the same decaying behavior in the right-hand side of the Laplace equation, i.e., when working with the Poisson equation.

When dealing with Sobolev spaces, even a strong Lipschitz boundary $\Gamma \in C^{0,1}$ is admissible. In this case, and due the trace theorem (A.531), if $v \in H^1(\Omega_i)$ or $v \in W^1(\Omega_e)$, then the trace of v fulfills

$$\gamma_0 v = v|_\Gamma \in H^{1/2}(\Gamma). \tag{B.200}$$

Moreover, the trace of the normal derivative can be also defined, and it holds that

$$\gamma_1 v = \frac{\partial v}{\partial n}|_\Gamma \in H^{-1/2}(\Gamma), \tag{B.201}$$

since $\Delta v = 0 \in L^2(\Omega_i \cup \Omega_e)$. This way we do not need to work with the more cumbersome spaces $H^1(\Delta;\Omega_i)$ and $W^1(\Delta;\Omega_e)$, being the former defined in (A.535) and the latter in an analogous manner, but for (B.198).

B.9.2 Regularity of the integral operators

The boundary integral operators (B.81), (B.82), (B.83), and (B.84) can be characterized as linear and continuous applications such that

$$S : H^{-1/2+s}(\Gamma) \longrightarrow H^{1/2+s}(\Gamma), \qquad D : H^{1/2+s}(\Gamma) \longrightarrow H^{3/2+s}(\Gamma), \tag{B.202}$$

$$D^* : H^{-1/2+s}(\Gamma) \longrightarrow H^{1/2+s}(\Gamma), \qquad N : H^{1/2+s}(\Gamma) \longrightarrow H^{-1/2+s}(\Gamma). \tag{B.203}$$

This result holds for any $s \in \mathbb{R}$ if the boundary Γ is of class C^∞, which can be derived from the theory of singular integral operators with pseudo-homogeneous kernels (cf., e.g., Nédélec 2001). Due the compact injection (A.554), it holds also that the operators

$$D : H^{1/2+s}(\Gamma) \longrightarrow H^{1/2+s}(\Gamma) \qquad \text{and} \qquad D^* : H^{-1/2+s}(\Gamma) \longrightarrow H^{-1/2+s}(\Gamma) \tag{B.204}$$

are compact. For a strong Lipschitz boundary $\Gamma \in C^{0,1}$, on the other hand, these results hold only when $|s| < 1$ (cf. Costabel 1988). In the case of more regular boundaries, the range for s increases, but remains finite. For our purposes we use $s = 0$, namely

$$S : H^{-1/2}(\Gamma) \longrightarrow H^{1/2}(\Gamma), \qquad D : H^{1/2}(\Gamma) \longrightarrow H^{1/2}(\Gamma), \tag{B.205}$$

$$D^* : H^{-1/2}(\Gamma) \longrightarrow H^{-1/2}(\Gamma), \qquad N : H^{1/2}(\Gamma) \longrightarrow H^{-1/2}(\Gamma), \tag{B.206}$$

which are all linear and continuous operators, and where the operators D and D^* are compact. Similarly, we can characterize the single and double layer potentials defined respectively in (B.76) and (B.77) as linear and continuous integral operators such that

$$\mathcal{S} : H^{-1/2}(\Gamma) \longrightarrow W^1(\Omega_e \cup \Omega_i) \qquad \text{and} \qquad \mathcal{D} : H^{1/2}(\Gamma) \longrightarrow W^1(\Omega_e \cup \Omega_i). \tag{B.207}$$

B.9.3 Application to the integral equations

It is not difficult to see that if $\mu \in H^{1/2}(\Gamma)$ and $\nu \in H^{-1/2}(\Gamma)$ are given, then the transmission problem (B.37) admits a unique solution $u \in W^1(\Omega_e \cup \Omega_i)$, as a consequence of the integral representation formula (B.49). For the direct perturbation problem (B.11), though, this is not always the case, as was appreciated in the exterior circle problem (B.171). Nonetheless, if the Fredholm alternative applies, then we know that the existence and uniqueness of the problem can be ensured almost always, i.e., except on a countable set of values for the impedance.

We consider an impedance $Z \in L^\infty(\Gamma)$ and an impedance data function $f_z \in H^{-1/2}(\Gamma)$. In both cases all the continuous functions on Γ are included. We remark that the product of a function $f \in L^\infty(\Gamma)$ by a function $g \in H^{1/2}(\Gamma)$ most likely does not appertain to $H^{1/2}(\Gamma)$, but is rather such that $fg \in H^{1/2-\epsilon}(\Gamma)$ for some $\epsilon > 0$. What we can state for sure in this case is that $fg \in L^2(\Gamma)$, since $H^{1/2}(\Gamma) \subset L^2(\Gamma)$ and the product of a function in $L^\infty(\Gamma)$ by a function in $L^2(\Gamma)$ is in $L^2(\Gamma)$, as stated in (A.471). It holds similarly that if $f \in L^\infty(\Gamma)$ and $g \in H^1(\Gamma)$, then $fg \in H^1(\Gamma)$.

a) First extension by zero

Let us study the first integral equation of the extension-by-zero alternative (B.129), which is given in terms of boundary layer potentials, for $\mu \in H^{1/2}(\Gamma)$, by

$$\frac{\mu}{2} + S(Z\mu) - D(\mu) = S(f_z) \qquad \text{in } \ H^{1/2}(\Gamma). \tag{B.208}$$

The following mapping properties hold:

$$\mu \in H^{1/2}(\Gamma) \ \longmapsto \ \frac{\mu}{2} \in H^{1/2}(\Gamma), \tag{B.209}$$

$$Z\mu \in L^2(\Gamma) \ \longmapsto \ S(Z\mu) \in H^1(\Gamma) \overset{c}{\hookrightarrow} H^{1/2}(\Gamma), \tag{B.210}$$

$$\mu \in H^{1/2}(\Gamma) \ \longmapsto \ D(\mu) \in H^{3/2}(\Gamma) \overset{c}{\hookrightarrow} H^{1/2}(\Gamma), \tag{B.211}$$

$$f_z \in H^{-1/2}(\Gamma) \ \longmapsto \ S(f_z) \in H^{1/2}(\Gamma). \tag{B.212}$$

We observe that (B.209) is the identity operator (disregarding the multiplicative constant), and that (B.210) and (B.211) are compact, due the imbeddings of Sobolev spaces. Thus the integral equation (B.208) has the form of (A.441) and the Fredholm alternative holds.

b) Second extension by zero

The second integral equation of the extension-by-zero alternative (B.133) is given in terms of boundary layer potentials, for $\mu \in H^{1/2}(\Gamma)$, by

$$\frac{Z}{2}\mu - N(\mu) + D^*(Z\mu) = \frac{f_z}{2} + D^*(f_z) \qquad \text{in } \ H^{-1/2}(\Gamma). \tag{B.213}$$

In this case we have the mapping properties:

$$\mu \in H^{1/2}(\Gamma) \ \longmapsto \ \frac{Z}{2}\mu \in L^2(\Gamma) \overset{c}{\hookrightarrow} H^{-1/2}(\Gamma), \tag{B.214}$$

$$\mu \in H^{1/2}(\Gamma) \ \longmapsto \ N(\mu) \in H^{-1/2}(\Gamma), \tag{B.215}$$

$$Z\mu \in L^2(\Gamma) \ \longmapsto \ D^*(Z\mu) \in H^1(\Gamma) \overset{c}{\hookrightarrow} H^{-1/2}(\Gamma), \tag{B.216}$$

$$f_z \in H^{-1/2}(\Gamma) \ \longmapsto \ \frac{f_z}{2} \in H^{-1/2}(\Gamma), \tag{B.217}$$

$$f_z \in H^{-1/2}(\Gamma) \ \longmapsto \ D^*(f_z) \in H^{1/2}(\Gamma) \overset{c}{\hookrightarrow} H^{-1/2}(\Gamma). \tag{B.218}$$

We see that the operators (B.214) and (B.216) are compact, whereas (B.215) represents the term of leading order and plays the role of the identity. In fact, by applying the operator S on the integral equation (B.213) and due the second Calderón identity in (B.122), the resulting operator SN can be decomposed as an identity and a compact operator. Thus again the Fredholm alternative holds.

c) Continuous impedance

The integral equation of the continuous-impedance alternative (B.141) is given in terms of boundary layer potentials, for $\mu \in H^{1/2}(\Gamma)$, by

$$-N(\mu) + D^*(Z\mu) + ZD(\mu) - ZS(Z\mu) = f_z \qquad \text{in } \ H^{-1/2}(\Gamma). \tag{B.219}$$

We have the mapping properties:

$$\mu \in H^{1/2}(\Gamma) \;\longmapsto\; N(\mu) \in H^{-1/2}(\Gamma), \tag{B.220}$$

$$Z\mu \in L^2(\Gamma) \;\longmapsto\; D^*(Z\mu) \in H^1(\Gamma) \overset{c}{\hookrightarrow} H^{-1/2}(\Gamma), \tag{B.221}$$

$$\mu \in H^{1/2}(\Gamma) \;\longmapsto\; ZD(\mu) \in H^1(\Gamma) \overset{c}{\hookrightarrow} H^{-1/2}(\Gamma), \tag{B.222}$$

$$Z\mu \in L^2(\Gamma) \;\longmapsto\; ZS(Z\mu) \in H^1(\Gamma) \overset{c}{\hookrightarrow} H^{-1/2}(\Gamma), \tag{B.223}$$

$$f_z \in H^{-1/2}(\Gamma) \;\longmapsto\; f_z \in H^{-1/2}(\Gamma). \tag{B.224}$$

The operators (B.221), (B.222), and (B.223) are compact, whereas (B.220) plays the role of the identity. Thus the Fredholm alternative applies.

d) Continuous value

The integral equation of the continuous-value alternative (B.149) is given in terms of boundary layer potentials, for $\nu \in H^{-1/2}(\Gamma)$, by

$$\frac{\nu}{2} + ZS(\nu) - D^*(\nu) = -f_z \qquad \text{in } H^{-1/2}(\Gamma). \tag{B.225}$$

We have the mapping properties:

$$\nu \in H^{-1/2}(\Gamma) \;\longmapsto\; \frac{\nu}{2} \in H^{-1/2}(\Gamma), \tag{B.226}$$

$$\nu \in H^{-1/2}(\Gamma) \;\longmapsto\; ZS(\nu) \in L^2(\Gamma) \overset{c}{\hookrightarrow} H^{-1/2}(\Gamma), \tag{B.227}$$

$$\nu \in H^{-1/2}(\Gamma) \;\longmapsto\; D^*(\nu) \in H^{1/2}(\Gamma) \overset{c}{\hookrightarrow} H^{-1/2}(\Gamma), \tag{B.228}$$

$$f_z \in H^{-1/2}(\Gamma) \;\longmapsto\; -f_z \in H^{-1/2}(\Gamma). \tag{B.229}$$

We observe that (B.226) is the identity operator, whereas (B.227) and (B.228) are compact. Thus the Fredholm alternative holds.

e) Continuous normal derivative

The integral equation of the continuous-normal-derivative alternative (B.157) is given in terms of boundary layer potentials, for $\mu \in H^{1/2}(\Gamma)$, by

$$\frac{Z}{2}\mu - N(\mu) + ZD(\mu) = f_z \qquad \text{in } H^{-1/2}(\Gamma). \tag{B.230}$$

We have the following mapping properties:

$$\mu \in H^{1/2}(\Gamma) \;\longmapsto\; \frac{Z}{2}\mu \in L^2(\Gamma) \overset{c}{\hookrightarrow} H^{-1/2}(\Gamma), \tag{B.231}$$

$$\mu \in H^{1/2}(\Gamma) \;\longmapsto\; N(\mu) \in H^{-1/2}(\Gamma), \tag{B.232}$$

$$\mu \in H^{1/2}(\Gamma) \;\longmapsto\; ZD(\mu) \in H^1(\Gamma) \overset{c}{\hookrightarrow} H^{-1/2}(\Gamma), \tag{B.233}$$

$$f_z \in H^{-1/2}(\Gamma) \;\longmapsto\; f_z \in H^{-1/2}(\Gamma). \tag{B.234}$$

The operators (B.231) and (B.233) are compact, whereas (B.232) plays the role of the identity. Thus the Fredholm alternative again applies.

B.9.4 Consequences of Fredholm's alternative

Since the Fredholm alternative applies to each integral equation, therefore it applies also to the exterior differential problem (B.11) due the integral representation formula. The existence of the exterior problem's solution is thus determined by its uniqueness, and the impedances $Z \in \mathbb{C}$ for which the uniqueness is lost constitute a countable set, which we call the impedance spectrum of the exterior problem and denote it by σ_Z. The existence and uniqueness of the solution is therefore ensured almost everywhere. The same holds obviously for the solution of the integral equation, whose impedance spectrum we denote by ς_Z. Since each integral equation is derived from the exterior problem, it holds that $\sigma_Z \subset \varsigma_Z$. The converse, though, is not necessarily true and depends on each particular integral equation. In any way, the set $\varsigma_Z \setminus \sigma_Z$ is at most countable.

Fredholm's alternative applies as much to the integral equation itself as to its adjoint counterpart, and equally to their homogeneous versions. Moreover, each integral equation solves at the same time an exterior and an interior differential problem. The loss of uniqueness of the integral equation's solution appears when the impedance Z is an eigenvalue of some associated interior problem, either of the homogeneous integral equation or of its adjoint counterpart. Such an impedance Z is contained in ς_Z.

The integral equation (B.131) is associated with the extension by zero (B.124), for which no eigenvalues appear. Nevertheless, its adjoint integral equation (B.151) of the continuous value is associated with the interior problem (B.144), whose solution is unique for all $Z \neq 0$.

The integral equation (B.134) is also associated with the extension by zero (B.124), for which no eigenvalues appear. Nonetheless, its adjoint integral equation (B.159) of the continuous normal derivative is associated with the interior problem (B.152), whose solution is unique for all Z, without restriction.

The integral equation (B.143) of the continuous impedance is self-adjoint and is associated with the interior problem (B.135), which has a countable quantity of eigenvalues Z.

Let us consider now the transmission problem generated by the homogeneous exterior problem

$$\begin{cases} \text{Find } u_e : \Omega_e \to \mathbb{C} \text{ such that} \\ \Delta u_e = 0 & \text{in } \Omega_e, \\ -\dfrac{\partial u_e}{\partial n} + Z u_e = 0 & \text{on } \Gamma, \\ \text{+ Decaying condition as } |\boldsymbol{x}| \to \infty, \end{cases} \tag{B.235}$$

and the associated homogeneous interior problem

$$\begin{cases} \text{Find } u_i : \Omega_i \to \mathbb{C} \text{ such that} \\ \Delta u_i = 0 & \text{in } \Omega_i, \\ \dfrac{\partial u_i}{\partial n} + Z u_i = 0 & \text{on } \Gamma, \end{cases} \tag{B.236}$$

where the asymptotic decaying condition is as usual given by (B.7), and where the unit normal $\boldsymbol{n}$ always points outwards of Ω_e. Its jumps are characterized by

$$[u] = u_e - u_i = \frac{1}{Z}\left(\frac{\partial u_e}{\partial n} + \frac{\partial u_i}{\partial n}\right), \tag{B.237}$$

$$\left[\frac{\partial u}{\partial n}\right] = \frac{\partial u_e}{\partial n} - \frac{\partial u_i}{\partial n} = Z\big(u_e + u_i\big). \tag{B.238}$$

It holds that the integral equations for this transmission problem composed by (B.235) and (B.236) have either the same left-hand side or are mutually adjoint to all other possible alternatives of integral equations that can be built for the exterior problem (B.11), and in particular to all the alternatives that were mentioned in the last subsection. The eigenvalues Z of the homogeneous interior problem (B.236) are thus also contained in ς_Z. To see this, let us construct the corresponding integral equations. By adding the Calderón relations (B.116) and (B.117) for the jumps (B.237) and (B.238), we obtain a system of integral equations that only relates these jumps, namely

$$\frac{1}{2}\begin{pmatrix} u_e + u_i \\ \dfrac{\partial u_e}{\partial n} + \dfrac{\partial u_i}{\partial n} \end{pmatrix} = \begin{pmatrix} D & -S \\ N & -D^* \end{pmatrix} \begin{pmatrix} [u] \\ \left[\dfrac{\partial u}{\partial n}\right] \end{pmatrix} = \begin{pmatrix} \dfrac{1}{2Z}\left[\dfrac{\partial u}{\partial n}\right] \\ \dfrac{Z}{2}[u] \end{pmatrix}. \tag{B.239}$$

We observe that even if the problems (B.235) and (B.236) are homogeneous, any possible jump condition can be assigned to them. The resulting system of integral equations can then be always combined in such a way that it has the same left-hand side or is mutually adjoint to any integral equation derived for the exterior problem (B.11).

In the case of the extension by zero we use the jumps (B.125) and (B.126). By replacing them in (B.239), we obtain the integral equations

$$\frac{\mu}{2} + S(Z\mu) - D(\mu) = S(f_z) + \frac{f_z}{2Z} \qquad \text{in } \ H^{1/2}(\Gamma), \tag{B.240}$$

$$\frac{Z}{2}\mu - N(\mu) + D^*(Z\mu) = D^*(f_z) \qquad \text{in } \ H^{-1/2}(\Gamma). \tag{B.241}$$

It can be clearly observed that the equations (B.240) and (B.241) have the same left-hand side as (B.208) and (B.213), respectively.

For the continuous impedance we use the jumps (B.136) and (B.137). By replacing them in (B.239), multiplying the first row by Z, and subtracting it from the second row, we obtain the integral equation

$$-N(\mu) + D^*(Z\mu) + ZD(\mu) - ZS(Z\mu) = 0 \qquad \text{in } \ H^{-1/2}(\Gamma). \tag{B.242}$$

This integral equation has the same left-hand side as (B.219).

In the case of the continuous value we consider the jumps (B.145) and (B.146). By replacing them in (B.239) and subtracting the second row from the first, we obtain the integral equation

$$\frac{\nu}{2} + ZS(\nu) - D^*(\nu) = 0 \qquad \text{in } \ H^{-1/2}(\Gamma). \tag{B.243}$$

Again, this integral equation has the same left-hand side as (B.225).

For the continuous normal derivative we use the jumps (B.153) and (B.154). By replacing them in (B.239), multiplying the first row by Z and adding the second row to the first, we obtain the integral equation

$$\frac{Z}{2}\mu - N(\mu) + ZD(\mu) = 0 \qquad \text{in } \; H^{-1/2}(\Gamma). \tag{B.244}$$

This integral equation has the same left-hand side as (B.230).

We remark that additional alternatives for integral representations and equations based on non-homogeneous versions of the problem (B.236) can be also derived for the exterior impedance problem (cf. Ha-Duong 1987).

The determination of the impedance spectrum σ_Z of the exterior problem (B.11) is not so easy, but can be achieved for simple geometries where an analytic solution is known.

In conclusion, the exterior problem (B.11) admits a unique solution u if $Z \notin \sigma_Z$, and each integral equation admits a unique solution, either μ or ν, if $Z \notin \varsigma_Z$.

B.9.5 Compatibility condition

As we appreciated for the exterior circle problem, if a constant impedance $Z \in \mathbb{C}$ is considered, then the impedance data function f_z has to satisfy some sort of compatibility condition like

$$\int_\Gamma f_z \, \mathrm{d}\gamma = 0, \tag{B.245}$$

which is required for the existence of a solution u of the exterior problem (B.11). To understand this better, we assume that u is the solution of (B.11) and that f_z satisfies (B.245). If we consider a constant $f_0 \in \mathbb{C}$ and a constant impedance $Z \neq 0$, then

$$\widetilde{u} = u + \frac{f_0}{Z} \tag{B.246}$$

satisfies the Laplace equation

$$\Delta\widetilde{u} = \Delta\left(u + \frac{f_0}{Z}\right) = 0 \qquad \text{in } \; \Omega_e, \tag{B.247}$$

and the impedance boundary condition

$$-\frac{\partial\widetilde{u}}{\partial n} + Z\widetilde{u} = -\frac{\partial u}{\partial n} + Zu + f_0 = f_z + f_0 = \widetilde{f}_z \qquad \text{on } \; \Gamma, \tag{B.248}$$

where

$$\int_\Gamma \widetilde{f}_z \, \mathrm{d}\gamma = f_0. \tag{B.249}$$

Nonetheless, we observe that the function $\widetilde{u}$ does not fulfill the decaying condition (B.7) if $f_0 \neq 0$ and is thus not admissible as a solution for the exterior problem with the impedance data function $\widetilde{f}_z$.

If we consider now a Neumann boundary condition ($Z = 0$), then the compatibility condition (B.245) is obtained by replacing the data function f_z in (B.57).

In any case, it is the decaying condition (B.7) that generates the need of the compatibility condition (B.245). If we disregard the latter, then the exterior problem (B.11) still admits a solution that not necessarily satisfies the decaying condition.

B.10 Variational formulation

To solve a particular integral equation we convert it to its variational or weak formulation, i.e., we solve it with respect to certain test functions in a bilinear (or sesquilinear) form. Basically, the integral equation is multiplied by the (conjugated) test function and then the equation is integrated over the boundary of the domain. The test functions are taken in the same function space as the solution of the integral equation.

a) First extension by zero

The variational formulation for the first integral equation (B.208) of the extension-by-zero alternative searches $\mu \in H^{1/2}(\Gamma)$ such that $\forall \varphi \in H^{1/2}(\Gamma)$

$$\left\langle \frac{\mu}{2} + S(Z\mu) - D(\mu), \varphi \right\rangle = \big\langle S(f_z), \varphi \big\rangle, \tag{B.250}$$

which in terms of integrals is expressed as

$$\begin{aligned} \int_\Gamma \int_\Gamma \left(Z(\boldsymbol{y}) G(\boldsymbol{x}, \boldsymbol{y}) - \frac{\partial G}{\partial n_{\boldsymbol{y}}}(\boldsymbol{x}, \boldsymbol{y}) \right) \mu(\boldsymbol{y}) \varphi(\boldsymbol{x}) \,\mathrm{d}\gamma(\boldsymbol{y}) \,\mathrm{d}\gamma(\boldsymbol{x}) \\ + \frac{1}{2} \int_\Gamma \mu(\boldsymbol{x}) \varphi(\boldsymbol{x}) \,\mathrm{d}\gamma(\boldsymbol{x}) = \int_\Gamma \int_\Gamma G(\boldsymbol{x}, \boldsymbol{y}) f_z(\boldsymbol{y}) \varphi(\boldsymbol{x}) \,\mathrm{d}\gamma(\boldsymbol{y}) \,\mathrm{d}\gamma(\boldsymbol{x}). \end{aligned} \tag{B.251}$$

b) Second extension by zero

The variational formulation for the second integral equation (B.213) of the extension-by-zero alternative searches $\mu \in H^{1/2}(\Gamma)$ such that $\forall \varphi \in H^{1/2}(\Gamma)$

$$\left\langle \frac{Z}{2}\mu - N(\mu) + D^*(Z\mu), \varphi \right\rangle = \left\langle \frac{f_z}{2} + D^*(f_z), \varphi \right\rangle, \tag{B.252}$$

which in terms of integrals is expressed as

$$\begin{aligned} \int_\Gamma \int_\Gamma G(\boldsymbol{x}, \boldsymbol{y}) \big(\nabla \mu(\boldsymbol{y}) \times \boldsymbol{n}_{\boldsymbol{y}} \big) \big(\nabla \varphi(\boldsymbol{x}) \times \boldsymbol{n}_{\boldsymbol{x}} \big) \,\mathrm{d}\gamma(\boldsymbol{y}) \,\mathrm{d}\gamma(\boldsymbol{x}) \\ + \int_\Gamma \int_\Gamma Z(\boldsymbol{y}) \frac{\partial G}{\partial n_{\boldsymbol{x}}}(\boldsymbol{x}, \boldsymbol{y}) \mu(\boldsymbol{y}) \varphi(\boldsymbol{x}) \,\mathrm{d}\gamma(\boldsymbol{y}) \,\mathrm{d}\gamma(\boldsymbol{x}) + \frac{1}{2} \int_\Gamma Z(\boldsymbol{x}) \mu(\boldsymbol{x}) \varphi(\boldsymbol{x}) \,\mathrm{d}\gamma(\boldsymbol{x}) \\ = \frac{1}{2} \int_\Gamma f_z(\boldsymbol{x}) \varphi(\boldsymbol{x}) \,\mathrm{d}\gamma(\boldsymbol{x}) + \int_\Gamma \int_\Gamma \frac{\partial G}{\partial n_{\boldsymbol{x}}}(\boldsymbol{x}, \boldsymbol{y}) f_z(\boldsymbol{y}) \varphi(\boldsymbol{x}) \,\mathrm{d}\gamma(\boldsymbol{y}) \,\mathrm{d}\gamma(\boldsymbol{x}). \end{aligned} \tag{B.253}$$

c) Continuous impedance

The variational formulation for the integral equation (B.219) of the alternative of the continuous-impedance searches $\mu \in H^{1/2}(\Gamma)$ such that $\forall \varphi \in H^{1/2}(\Gamma)$

$$\big\langle -N(\mu) + D^*(Z\mu) + ZD(\mu) - ZS(Z\mu), \varphi \big\rangle = \big\langle f_z, \varphi \big\rangle, \tag{B.254}$$

which in terms of integrals is expressed as

$$\int_\Gamma\int_\Gamma G(\boldsymbol{x},\boldsymbol{y})\Big[\big(\nabla\mu(\boldsymbol{y})\times\boldsymbol{n}_{\boldsymbol{y}}\big)\big(\nabla\varphi(\boldsymbol{x})\times\boldsymbol{n}_{\boldsymbol{x}}\big)-Z(\boldsymbol{x})Z(\boldsymbol{y})\mu(\boldsymbol{y})\varphi(\boldsymbol{x})\Big]\,\mathrm{d}\gamma(\boldsymbol{y})\,\mathrm{d}\gamma(\boldsymbol{x})$$
$$+\int_\Gamma\int_\Gamma\left(Z(\boldsymbol{y})\frac{\partial G}{\partial n_{\boldsymbol{x}}}(\boldsymbol{x},\boldsymbol{y})+Z(\boldsymbol{x})\frac{\partial G}{\partial n_{\boldsymbol{y}}}(\boldsymbol{x},\boldsymbol{y})\right)\mu(\boldsymbol{y})\varphi(\boldsymbol{x})\,\mathrm{d}\gamma(\boldsymbol{y})\,\mathrm{d}\gamma(\boldsymbol{x})$$
$$=\int_\Gamma f_z(\boldsymbol{x})\varphi(\boldsymbol{x})\,\mathrm{d}\gamma(\boldsymbol{x}). \tag{B.255}$$

d) Continuous value

The variational formulation for the integral equation (B.225) of the continuous-value alternative searches $\nu\in H^{-1/2}(\Gamma)$ such that $\forall\psi\in H^{-1/2}(\Gamma)$

$$\left\langle\frac{\nu}{2}+ZS(\nu)-D^*(\nu),\psi\right\rangle=\big\langle-f_z,\psi\big\rangle, \tag{B.256}$$

which in terms of integrals is expressed as

$$\int_\Gamma\int_\Gamma\left(Z(\boldsymbol{x})G(\boldsymbol{x},\boldsymbol{y})-\frac{\partial G}{\partial n_{\boldsymbol{x}}}(\boldsymbol{x},\boldsymbol{y})\right)\nu(\boldsymbol{y})\psi(\boldsymbol{x})\,\mathrm{d}\gamma(\boldsymbol{y})\,\mathrm{d}\gamma(\boldsymbol{x})$$
$$+\frac{1}{2}\int_\Gamma\nu(\boldsymbol{x})\psi(\boldsymbol{x})\,\mathrm{d}\gamma(\boldsymbol{x})=-\int_\Gamma f_z(\boldsymbol{x})\psi(\boldsymbol{x})\,\mathrm{d}\gamma(\boldsymbol{x}). \tag{B.257}$$

e) Continuous normal derivative

The variational formulation for the integral equation (B.230) of the continuous-normal-derivative alternative searches $\mu\in H^{1/2}(\Gamma)$ such that $\forall\varphi\in H^{1/2}(\Gamma)$

$$\left\langle\frac{Z}{2}\mu-N(\mu)+ZD(\mu),\varphi\right\rangle=\big\langle f_z,\varphi\big\rangle, \tag{B.258}$$

which in terms of integrals is expressed as

$$\int_\Gamma\int_\Gamma G(\boldsymbol{x},\boldsymbol{y})\big(\nabla\mu(\boldsymbol{y})\times\boldsymbol{n}_{\boldsymbol{y}}\big)\big(\nabla\varphi(\boldsymbol{x})\times\boldsymbol{n}_{\boldsymbol{x}}\big)\,\mathrm{d}\gamma(\boldsymbol{y})\,\mathrm{d}\gamma(\boldsymbol{x})$$
$$+\int_\Gamma\int_\Gamma Z(\boldsymbol{x})\frac{\partial G}{\partial n_{\boldsymbol{y}}}(\boldsymbol{x},\boldsymbol{y})\mu(\boldsymbol{y})\varphi(\boldsymbol{x})\,\mathrm{d}\gamma(\boldsymbol{y})\,\mathrm{d}\gamma(\boldsymbol{x})+\frac{1}{2}\int_\Gamma Z(\boldsymbol{x})\mu(\boldsymbol{x})\varphi(\boldsymbol{x})\,\mathrm{d}\gamma(\boldsymbol{x})$$
$$=\int_\Gamma f_z(\boldsymbol{x})\varphi(\boldsymbol{x})\,\mathrm{d}\gamma(\boldsymbol{x}). \tag{B.259}$$

B.11 Numerical discretization

B.11.1 Discretized function spaces

The exterior problem (B.11) is solved numerically with the boundary element method by employing a Galerkin scheme on the variational formulation of an integral equation. We use on the boundary curve Γ Lagrange finite elements of type either $\mathbb{P}_1$ or $\mathbb{P}_0$. As shown in Figure B.9, the curve Γ is approximated by the discretized curve Γ^h, composed by I rectilinear segments T_j, sequentially ordered in clockwise direction for $1\leq j\leq I$, such that their length $|T_j|$ is less or equal than h, and with their endpoints on top of Γ.

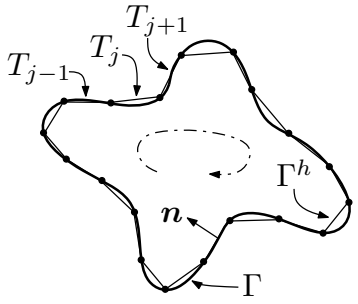

FIGURE B.9. Curve Γ^h, discretization of Γ.

The function space $H^{1/2}(\Gamma)$ is approximated using the conformal space of continuous piecewise linear polynomials with complex coefficients

$$Q_h = \big\{\varphi_h \in C^0(\Gamma^h) \,:\, \varphi_h|_{T_j} \in \mathbb{P}_1(\mathbb{C}),\;\; 1 \leq j \leq I\big\}. \tag{B.260}$$

The space Q_h has a finite dimension I, and we describe it using the standard base functions for finite elements of type $\mathbb{P}_1$, denoted by $\{\chi_j\}_{j=1}^I$, shown in Figure B.10, and expressed as

$$\chi_j(\boldsymbol{x}) = \begin{cases} \dfrac{|\boldsymbol{x} - \boldsymbol{r}_{j-1}|}{|T_{j-1}|} & \text{if } \boldsymbol{x} \in T_{j-1}, \\ \dfrac{|\boldsymbol{r}_{j+1} - \boldsymbol{x}|}{|T_j|} & \text{if } \boldsymbol{x} \in T_j, \\ 0 & \text{if } \boldsymbol{x} \notin T_{j-1} \cup T_j, \end{cases} \tag{B.261}$$

where segment T_{j-1} has as endpoints $\boldsymbol{r}_{j-1}$ and $\boldsymbol{r}_j$, while the endpoints of segment T_j are given by $\boldsymbol{r}_j$ and $\boldsymbol{r}_{j+1}$.

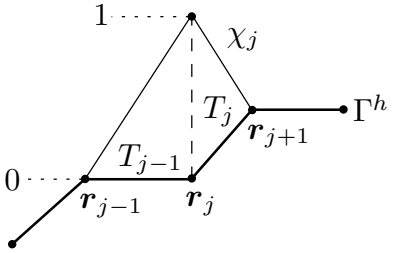

FIGURE B.10. Base function χ_j for finite elements of type $\mathbb{P}_1$.

The function space $H^{-1/2}(\Gamma)$, on the other hand, is approximated using the conformal space of piecewise constant polynomials with complex coefficients

$$P_h = \big\{\psi_h : \Gamma^h \to \mathbb{C} \mid\; \psi_h|_{T_j} \in \mathbb{P}_0(\mathbb{C}),\;\; 1 \leq j \leq I\big\}. \tag{B.262}$$

The space P_h has a finite dimension I, and is described using the standard base functions for finite elements of type $\mathbb{P}_0$, denoted by $\{\kappa_j\}_{j=1}^I$, shown in Figure B.11, and expressed as

$$\kappa_j(\boldsymbol{x}) = \begin{cases} 1 & \text{if } \boldsymbol{x} \in T_j, \\ 0 & \text{if } \boldsymbol{x} \notin T_j. \end{cases} \tag{B.263}$$

Again, we denote by $\boldsymbol{r}_j$ and $\boldsymbol{r}_{j+1}$ the endpoints of segment T_j.

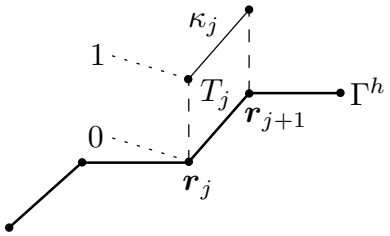

FIGURE B.11. Base function κ_j for finite elements of type $\mathbb{P}_0$.

In virtue of this discretization, any function $\varphi_h \in Q_h$ or $\psi_h \in P_h$ can be expressed as a linear combination of the elements of the base, namely

$$\varphi_h(\boldsymbol{x}) = \sum_{j=1}^{I} \varphi_j \, \chi_j(\boldsymbol{x}) \qquad \text{and} \qquad \psi_h(\boldsymbol{x}) = \sum_{j=1}^{I} \psi_j \, \kappa_j(\boldsymbol{x}) \qquad \text{for } \boldsymbol{x} \in \Gamma^h, \tag{B.264}$$

where $\varphi_j, \psi_j \in \mathbb{C}$ for $1 \leq j \leq I$. The solutions $\mu \in H^{1/2}(\Gamma)$ and $\nu \in H^{-1/2}(\Gamma)$ of the variational formulations can be therefore approximated respectively by

$$\mu_h(\boldsymbol{x}) = \sum_{j=1}^{I} \mu_j \, \chi_j(\boldsymbol{x}) \qquad \text{and} \qquad \nu_h(\boldsymbol{x}) = \sum_{j=1}^{I} \nu_j \, \kappa_j(\boldsymbol{x}) \qquad \text{for } \boldsymbol{x} \in \Gamma^h, \tag{B.265}$$

where $\mu_j, \nu_j \in \mathbb{C}$ for $1 \leq j \leq I$. The function f_z can be also approximated by

$$f_z^h(\boldsymbol{x}) = \sum_{j=1}^{I} f_j \, \chi_j(\boldsymbol{x}) \qquad \text{for } \boldsymbol{x} \in \Gamma^h, \quad \text{with } f_j = f_z(\boldsymbol{r}_j), \tag{B.266}$$

or

$$f_z^h(\boldsymbol{x}) = \sum_{j=1}^{I} f_j \, \kappa_j(\boldsymbol{x}) \qquad \text{for } \boldsymbol{x} \in \Gamma^h, \quad \text{with } f_j = \frac{f_z(\boldsymbol{r}_j) + f_z(\boldsymbol{r}_{j+1})}{2}, \tag{B.267}$$

depending on whether the original integral equation is stated in $H^{1/2}(\Gamma)$ or in $H^{-1/2}(\Gamma)$.

B.11.2 Discretized integral equations

a) First extension by zero

To see how the boundary element method operates, we apply it to the first integral equation of the extension-by-zero alternative, i.e., to the variational formulation (B.250). We characterize all the discrete approximations by the index h, including also the impedance and the boundary layer potentials. The numerical approximation of (B.250) leads to the

discretized problem that searches $\mu_h \in Q_h$ such that $\forall \varphi_h \in Q_h$

$$\int_{\Gamma^h}\int_{\Gamma^h}\left(Z_h(\boldsymbol{y})G(\boldsymbol{x},\boldsymbol{y}) - \frac{\partial G}{\partial n_{\boldsymbol{y}}}(\boldsymbol{x},\boldsymbol{y})\right)\mu_h(\boldsymbol{y})\varphi_h(\boldsymbol{x})\,\mathrm{d}\gamma(\boldsymbol{y})\,\mathrm{d}\gamma(\boldsymbol{x}) + \frac{1}{2}\int_{\Gamma^h}\mu_h(\boldsymbol{x})\varphi_h(\boldsymbol{x})\,\mathrm{d}\gamma(\boldsymbol{x}) = \int_{\Gamma^h}\int_{\Gamma^h} G(\boldsymbol{x},\boldsymbol{y})f_z^h(\boldsymbol{y})\varphi_h(\boldsymbol{x})\,\mathrm{d}\gamma(\boldsymbol{y})\,\mathrm{d}\gamma(\boldsymbol{x}), \quad \text{(B.268)}$$

which in terms of boundary layer potentials becomes

$$\left\langle \frac{\mu_h}{2} + S_h(Z_h\mu_h) - D_h(\mu_h), \varphi_h \right\rangle = \left\langle S_h(f_z^h), \varphi_h \right\rangle. \quad \text{(B.269)}$$

Considering the decomposition of μ_h in terms of the base $\{\chi_j\}$ and taking as test functions the same base functions, $\varphi_h = \chi_i$ for $1 \leq i \leq I$, yields the discrete linear system

$$\sum_{j=1}^{I}\mu_j\left(\frac{1}{2}\langle\chi_j,\chi_i\rangle + \langle S_h(Z_h\chi_j),\chi_i\rangle - \langle D_h(\chi_j),\chi_i\rangle\right) = \sum_{j=1}^{I} f_j\,\langle S_h(\chi_j),\chi_i\rangle. \quad \text{(B.270)}$$

This constitutes a system of linear equations that can be expressed as a linear matrix system:

$$\begin{cases} \text{Find } \boldsymbol{\mu} \in \mathbb{C}^I \text{ such that} \\ \boldsymbol{M}\boldsymbol{\mu} = \boldsymbol{b}. \end{cases} \quad \text{(B.271)}$$

The elements m_{ij} of the matrix $\boldsymbol{M}$ are given by

$$m_{ij} = \frac{1}{2}\langle\chi_j,\chi_i\rangle + \langle S_h(Z_h\chi_j),\chi_i\rangle - \langle D_h(\chi_j),\chi_i\rangle \qquad \text{for } 1 \leq i,j \leq I, \quad \text{(B.272)}$$

and the elements b_i of the vector $\boldsymbol{b}$ by

$$b_i = \left\langle S_h(f_z^h),\chi_i\right\rangle = \sum_{j=1}^{I} f_j\,\langle S_h(\chi_j),\chi_i\rangle \qquad \text{for } 1 \leq i \leq I. \quad \text{(B.273)}$$

The discretized solution u_h, which approximates u, is finally obtained by discretizing the integral representation formula (B.127) for $\boldsymbol{x} \in \Omega_e \cup \Omega_i$ according to

$$u_h(\boldsymbol{x}) = \int_{\Gamma^h}\left(\frac{\partial G}{\partial n_{\boldsymbol{y}}}(\boldsymbol{x},\boldsymbol{y}) - Z_h(\boldsymbol{y})G(\boldsymbol{x},\boldsymbol{y})\right)\mu_h(\boldsymbol{y})\,\mathrm{d}\gamma(\boldsymbol{y}) + \int_{\Gamma^h} G(\boldsymbol{x},\boldsymbol{y})f_z^h(\boldsymbol{y})\,\mathrm{d}\gamma(\boldsymbol{y}), \quad \text{(B.274)}$$

or, in terms of boundary layer potentials, according to

$$u_h = \mathcal{D}_h(\mu_h) - \mathcal{S}_h(Z_h\mu_h) + \mathcal{S}_h(f_z^h). \quad \text{(B.275)}$$

More specifically, the solution is computed by

$$u_h = \sum_{j=1}^{I}\mu_j\big(\mathcal{D}_h(\chi_j) - \mathcal{S}_h(Z_h\chi_j)\big) + \sum_{j=1}^{I} f_j\,\mathcal{S}_h(\chi_j). \quad \text{(B.276)}$$

By proceeding in the same way, the discretization of all the other alternatives of integral equations can be also expressed as a linear matrix system like (B.271). The resulting matrix $\boldsymbol{M}$ is in general complex, full, non-symmetric, and with dimensions $I \times I$. The right-hand side vector $\boldsymbol{b}$ is complex and of size I. The boundary element calculations required to compute numerically the elements of $\boldsymbol{M}$ and $\boldsymbol{b}$ have to be performed carefully,

since the integrals that appear become singular when the involved segments are adjacent or coincident, due the singularity of the Green's function at its source point.

b) Second extension by zero

In the case of the second integral equation of the extension-by-zero alternative, i.e., of the variational formulation (B.252), the elements m_{ij} that constitute the matrix $\boldsymbol{M}$ of the linear system (B.271) are given by

$$m_{ij} = \frac{1}{2}\langle Z_h\chi_j, \chi_i\rangle - \langle N_h(\chi_j), \chi_i\rangle + \langle D_h^*(Z_h\chi_j), \chi_i\rangle \qquad \text{for } 1 \le i, j \le I, \tag{B.277}$$

whereas the elements b_i of the vector $\boldsymbol{b}$ are expressed as

$$b_i = \sum_{j=1}^{I} f_j \left(\frac{1}{2}\langle \chi_j, \chi_i\rangle + \langle D_h^*(Z_h\chi_j), \chi_i\rangle\right) \qquad \text{for } 1 \le i \le I. \tag{B.278}$$

The discretized solution u_h is again computed by (B.276).

c) Continuous impedance

In the case of the continuous-impedance alternative, i.e., of the variational formulation (B.254), the elements m_{ij} that constitute the matrix $\boldsymbol{M}$ of the linear system (B.271) are given, for $1 \le i, j \le I$, by

$$m_{ij} = -\langle N_h(\chi_j), \chi_i\rangle + \langle D_h^*(Z_h\chi_j), \chi_i\rangle + \langle Z_h D_h(\chi_j), \chi_i\rangle - \langle Z_h S_h(Z_h\chi_j), \chi_i\rangle, \tag{B.279}$$

whereas the elements b_i of the vector $\boldsymbol{b}$ are expressed as

$$b_i = \sum_{j=1}^{I} f_j \langle \chi_j, \chi_i\rangle \qquad \text{for } 1 \le i \le I. \tag{B.280}$$

It can be observed that for this particular alternative the matrix $\boldsymbol{M}$ turns out to be symmetric, since the integral equation is self-adjoint. The discretized solution u_h, due (B.142), is then computed by

$$u_h = \sum_{j=1}^{I} \mu_j\big(\mathcal{D}_h(\chi_j) - \mathcal{S}_h(Z_h\chi_j)\big). \tag{B.281}$$

d) Continuous value

In the case of the alternative of the continuous-value, i.e., of the variational formulation (B.256), the elements m_{ij} that constitute the matrix $\boldsymbol{M}$, now of the linear system

$$\begin{cases} \text{Find } \boldsymbol{\nu} \in \mathbb{C}^I \text{ such that} \\ \boldsymbol{M}\boldsymbol{\nu} = \boldsymbol{b}, \end{cases} \tag{B.282}$$

are given by

$$m_{ij} = \frac{1}{2}\langle \kappa_j, \kappa_i\rangle + \langle Z_h S_h(\kappa_j), \kappa_i\rangle - \langle D_h^*(\kappa_j), \kappa_i\rangle \qquad \text{for } 1 \le i, j \le I, \tag{B.283}$$

whereas the elements b_i of the vector $\boldsymbol{b}$ are expressed as

$$b_i = -\sum_{j=1}^{I} f_j \, \langle \kappa_j, \kappa_i \rangle \qquad \text{for } \; 1 \leq i \leq I. \tag{B.284}$$

The discretized solution u_h, due (B.150), is then computed by

$$u_h = -\sum_{j=1}^{I} \nu_j \, \mathcal{S}_h(\kappa_j). \tag{B.285}$$

e) Continuous normal derivative

In the case of the continuous-normal-derivative alternative, i.e., of the variational formulation (B.258), the elements m_{ij} that conform the matrix $\boldsymbol{M}$ of the linear system (B.271) are given by

$$m_{ij} = \frac{1}{2}\langle Z_h \chi_j, \chi_i \rangle - \langle N_h(\chi_j), \chi_i \rangle + \langle Z_h D_h(\chi_j), \chi_i \rangle \qquad \text{for } \; 1 \leq i, j \leq I, \tag{B.286}$$

whereas the elements b_i of the vector $\boldsymbol{b}$ are expressed as

$$b_i = \sum_{j=1}^{I} f_j \, \langle \chi_j, \chi_i \rangle \qquad \text{for } \; 1 \leq i \leq I. \tag{B.287}$$

The discretized solution u_h, due (B.158), is then computed by

$$u_h = \sum_{j=1}^{I} \mu_j \, \mathcal{D}_h(\chi_j). \tag{B.288}$$

B.12 Boundary element calculations

B.12.1 Geometry

The boundary element calculations build the elements of the matrix $\boldsymbol{M}$ resulting from the discretization of the integral equation, i.e., from (B.271) or (B.282). They permit thus to compute numerically expressions like (B.272). To evaluate the appearing singular integrals, we use the semi-numerical methods described in the report of Bendali & Devys (1986).

Let us consider the elemental interactions between two straight segments T_K and T_L of a discrete closed curve Γ^h, which is composed by rectilinear segments and described in clockwise direction. The unit normal points always inwards of the domain encompassed by the curve Γ^h (vid. Figure B.9).

We denote the segments more simply just as $K = T_K$ and $L = T_L$. As depicted in Figure B.12, the following notation is used:

- $|K|$ denotes the length of segment K.
- $|L|$ denotes the length of segment L.
- $\boldsymbol{\tau}_K, \boldsymbol{\tau}_L$ denote the unit tangents of segments K and L.
- $\boldsymbol{n}_K, \boldsymbol{n}_L$ denote the unit normals of segments K and L.
- $\boldsymbol{r}_1^K, \boldsymbol{r}_2^K$ denote the endpoints of segment K.

- $\boldsymbol{r}_1^L, \boldsymbol{r}_2^L$ denote the endpoints of segment L.
- $\boldsymbol{r}(\boldsymbol{x})$ denotes a variable location on segment K (dependent on variable $\boldsymbol{x}$).
- $\boldsymbol{r}(\boldsymbol{y})$ denotes a variable location on segment L (dependent on variable $\boldsymbol{y}$).

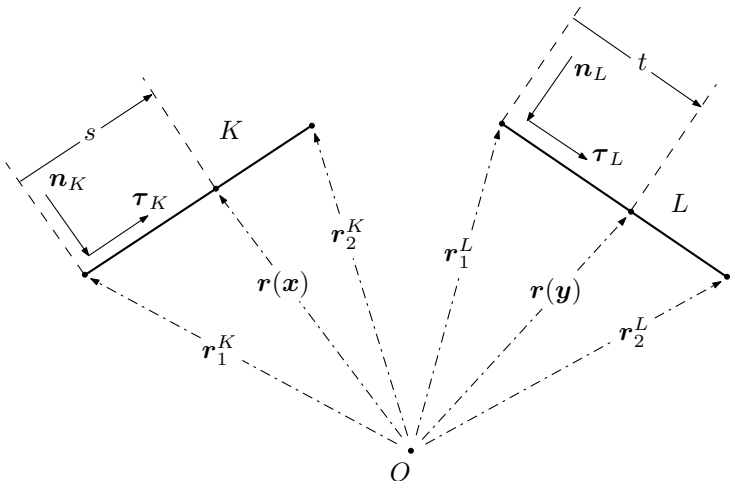

FIGURE B.12. Geometric characteristics of the segments K and L.

Segment K is parametrically described by

$$\boldsymbol{r}(\boldsymbol{x}) = \boldsymbol{r}_1^K + s\,\boldsymbol{\tau}_K, \qquad 0 \le s \le |K|. \tag{B.289}$$

In the same manner, segment L is parametrically described by

$$\boldsymbol{r}(\boldsymbol{y}) = \boldsymbol{r}_1^L + t\,\boldsymbol{\tau}_L, \qquad 0 \le t \le |L|. \tag{B.290}$$

Thus the parameters s and t can be expressed as

$$s = \big(\boldsymbol{r}(\boldsymbol{x}) - \boldsymbol{r}_1^K\big) \cdot \boldsymbol{\tau}_K, \tag{B.291}$$

$$t = \big(\boldsymbol{r}(\boldsymbol{y}) - \boldsymbol{r}_1^L\big) \cdot \boldsymbol{\tau}_L. \tag{B.292}$$

The lengths of the segments are given by

$$|K| = \big|\boldsymbol{r}_2^K - \boldsymbol{r}_1^K\big|, \tag{B.293}$$

$$|L| = \big|\boldsymbol{r}_2^L - \boldsymbol{r}_1^L\big|. \tag{B.294}$$

The unit tangents of the segments, $\boldsymbol{\tau}_K = (\tau_1^K, \tau_2^K)$ and $\boldsymbol{\tau}_L = (\tau_1^L, \tau_2^L)$, are calculated as

$$\boldsymbol{\tau}_K = \frac{\boldsymbol{r}_2^K - \boldsymbol{r}_1^K}{|K|}, \tag{B.295}$$

$$\boldsymbol{\tau}_L = \frac{\boldsymbol{r}_2^L - \boldsymbol{r}_1^L}{|L|}. \tag{B.296}$$

The unit normals of the segments, $\boldsymbol{n}_K = (n_1^K, n_2^K)$ and $\boldsymbol{n}_L = (n_1^L, n_2^L)$, are perpendicular to the tangents and can be thus calculated as

$$(n_1^K, n_2^K) = (\tau_2^K, -\tau_1^K), \tag{B.297}$$

$$(n_1^L, n_2^L) = (\tau_2^L, -\tau_1^L). \tag{B.298}$$

For the elemental interactions between a point $\boldsymbol{x}$ on segment K and a point $\boldsymbol{y}$ on segment L, the following notation is also used:

- $\boldsymbol{R}$ denotes the vector pointing from the point $\boldsymbol{x}$ towards the point $\boldsymbol{y}$.
- R denotes the distance between the points $\boldsymbol{x}$ and $\boldsymbol{y}$.

These values are given by

$$\boldsymbol{R} = \boldsymbol{r}(\boldsymbol{y}) - \boldsymbol{r}(\boldsymbol{x}), \tag{B.299}$$

$$R = |\boldsymbol{R}| = |\boldsymbol{y} - \boldsymbol{x}|. \tag{B.300}$$

For the singular integral calculations, when considering the point $\boldsymbol{x}$ as a parameter, the following notation is also used (vid. Figure B.13):

- $\boldsymbol{R}_1^L, \boldsymbol{R}_2^L$ denote the vectors pointing from $\boldsymbol{x}$ towards the endpoints of segment L.
- R_1^L, R_2^L denote the distances from $\boldsymbol{x}$ to the endpoints of segment L.
- d_L denotes the signed distance from $\boldsymbol{x}$ to the line that contains segment L.
- θ_L denotes the angle formed by the vectors $\boldsymbol{R}_1^L$ and $\boldsymbol{R}_2^L$ ($-\pi \leq \theta_L \leq \pi$).

Thus on segment L the following holds:

$$\boldsymbol{R}_1^L = \boldsymbol{r}_1^L - \boldsymbol{r}(\boldsymbol{x}), \qquad R_1^L = |\boldsymbol{R}_1^L|, \tag{B.301}$$

$$\boldsymbol{R}_2^L = \boldsymbol{r}_2^L - \boldsymbol{r}(\boldsymbol{x}), \qquad R_2^L = |\boldsymbol{R}_2^L|. \tag{B.302}$$

Likewise as before, we have that

$$\boldsymbol{R} = \boldsymbol{R}_1^L + t\,\boldsymbol{\tau}_L, \qquad 0 \leq t \leq |L|, \tag{B.303}$$

$$t = \left(\boldsymbol{R} - \boldsymbol{R}_1^L\right) \cdot \boldsymbol{\tau}_L. \tag{B.304}$$

The signed distance d_L is constant on L and is characterized by

$$d_L = \boldsymbol{R} \cdot \boldsymbol{n}_L = \boldsymbol{R}_1^L \cdot \boldsymbol{n}_L = \boldsymbol{R}_2^L \cdot \boldsymbol{n}_L. \tag{B.305}$$

Finally the signed angle θ_L is given by

$$\theta_L = \arccos\left(\frac{\boldsymbol{R}_1^L \cdot \boldsymbol{R}_2^L}{R_1^L\, R_2^L}\right) \operatorname{sign}(d_L), \qquad -\pi \leq \theta_L \leq \pi. \tag{B.306}$$

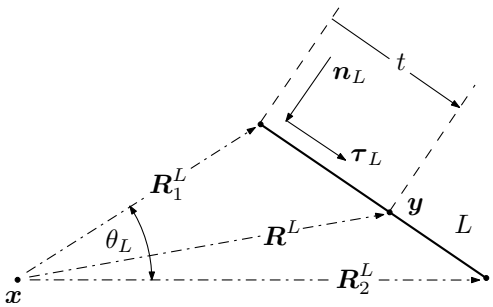

FIGURE B.13. Geometric characteristics of the singular integral calculations.

B.12.2 Boundary element integrals

The boundary element integrals are the basic integrals needed to perform the boundary element calculations. In our case, by considering $a, b \in \{0, 1\}$, they can be expressed as

$$ZA_{a,b} = \int_K \int_L \left(\frac{s}{|K|}\right)^a \left(\frac{t}{|L|}\right)^b G(\boldsymbol{x}, \boldsymbol{y}) \, \mathrm{d}L(\boldsymbol{y}) \, \mathrm{d}K(\boldsymbol{x}), \tag{B.307}$$

$$ZB_{a,b} = \int_K \int_L \left(\frac{s}{|K|}\right)^a \left(\frac{t}{|L|}\right)^b \frac{\partial G}{\partial n_{\boldsymbol{y}}}(\boldsymbol{x}, \boldsymbol{y}) \, \mathrm{d}L(\boldsymbol{y}) \, \mathrm{d}K(\boldsymbol{x}), \tag{B.308}$$

$$ZC_{a,b} = \int_K \int_L \left(\frac{s}{|K|}\right)^a \left(\frac{t}{|L|}\right)^b \frac{\partial G}{\partial n_{\boldsymbol{x}}}(\boldsymbol{x}, \boldsymbol{y}) \, \mathrm{d}L(\boldsymbol{y}) \, \mathrm{d}K(\boldsymbol{x}), \tag{B.309}$$

where the parameters s and t depend respectively on the variables $\boldsymbol{x}$ and $\boldsymbol{y}$, as stated in (B.291) and (B.292). When the segments have to be specified, i.e., if $K = T_i$ and $L = T_j$, then we use respectively also the notation $ZA^{i,j}_{a,b}$, $ZB^{i,j}_{a,b}$, or $ZC^{i,j}_{a,b}$, e.g.,

$$ZA^{i,j}_{a,b} = \int_{T_i} \int_{T_j} \left(\frac{s}{|K|}\right)^a \left(\frac{t}{|L|}\right)^b G(\boldsymbol{x}, \boldsymbol{y}) \, \mathrm{d}\gamma(\boldsymbol{y}) \, \mathrm{d}\gamma(\boldsymbol{x}). \tag{B.310}$$

It should be observed that (B.309) can be expressed in terms of (B.308):

$$ZC^{i,j}_{a,b} = ZB^{j,i}_{b,a}, \tag{B.311}$$

since the involved operators are self-adjoint. It occurs therefore that all the integrals that stem from the numerical discretization can be expressed in terms of the two basic boundary element integrals (B.307) and (B.308).

For this to hold true, the impedance is discretized as a piecewise constant function Z_h, which on each segment T_j adopts a constant value $Z_j \in \mathbb{C}$, e.g.,

$$Z_h|_{T_j} = Z_j = \frac{1}{2}\big(Z(\boldsymbol{r}_j) + Z(\boldsymbol{r}_{j+1})\big). \tag{B.312}$$

Now we can compute all the integrals of interest. We begin with the ones that are related with the finite elements of type $\mathbb{P}_0$, which are easier. It can be observed that

$$\langle \kappa_j, \kappa_i \rangle = \int_{\Gamma^h} \kappa_j(\boldsymbol{x}) \kappa_i(\boldsymbol{x}) \, \mathrm{d}\gamma(\boldsymbol{x}) = \begin{cases} |T_i| & \text{if } \ j = i, \\ 0 & \text{if } \ j \neq i. \end{cases} \tag{B.313}$$

We have likewise that

$$\langle Z_h S_h(\kappa_j), \kappa_i \rangle = \int_{\Gamma^h} \int_{\Gamma^h} Z_h(\boldsymbol{x}) G(\boldsymbol{x}, \boldsymbol{y}) \kappa_j(\boldsymbol{y}) \kappa_i(\boldsymbol{x}) \, \mathrm{d}\gamma(\boldsymbol{y}) \, \mathrm{d}\gamma(\boldsymbol{x}) = Z_i ZA^{i,j}_{0,0}. \tag{B.314}$$

It holds similarly that

$$\langle D^*_h(\kappa_j), \kappa_i \rangle = \int_{\Gamma^h} \int_{\Gamma^h} \frac{\partial G}{\partial n_{\boldsymbol{x}}}(\boldsymbol{x}, \boldsymbol{y}) \kappa_j(\boldsymbol{y}) \kappa_i(\boldsymbol{x}) \, \mathrm{d}\gamma(\boldsymbol{y}) \, \mathrm{d}\gamma(\boldsymbol{x}) = ZB^{j,i}_{0,0}. \tag{B.315}$$

We consider now the integrals for the finite elements of type $\mathbb{P}_1$. We have that

$$\langle \chi_j, \chi_i \rangle = \int_{\Gamma^h} \chi_j(\boldsymbol{x})\chi_i(\boldsymbol{x})\,\mathrm{d}\gamma(\boldsymbol{x}) = \begin{cases} |T_{i-1}|/6 & \text{if } j = i-1, \\ \big(|T_{i-1}| + |T_i|\big)/3 & \text{if } j = i, \\ |T_i|/6 & \text{if } j = i+1, \\ 0 & \text{if } j \notin \{i-1, i, i+1\}. \end{cases} \tag{B.316}$$

In the same way, it occurs that

$$\langle Z_h\chi_j, \chi_i \rangle = \begin{cases} Z_{i-1}|T_{i-1}|/6 & \text{if } j = i-1, \\ \big(Z_{i-1}|T_{i-1}| + Z_i|T_i|\big)/3 & \text{if } j = i, \\ Z_i|T_i|/6 & \text{if } j = i+1, \\ 0 & \text{if } j \notin \{i-1, i, i+1\}. \end{cases} \tag{B.317}$$

We have also that

$$\begin{aligned} \langle S_h(\chi_j), \chi_i \rangle &= \int_{\Gamma^h}\int_{\Gamma^h} G(\boldsymbol{x},\boldsymbol{y})\chi_j(\boldsymbol{y})\chi_i(\boldsymbol{x})\,\mathrm{d}\gamma(\boldsymbol{y})\,\mathrm{d}\gamma(\boldsymbol{x}) \\ &= ZA_{1,1}^{i-1,j-1} + ZA_{0,1}^{i,j-1} - ZA_{1,1}^{i,j-1} + ZA_{1,0}^{i-1,j} - ZA_{1,1}^{i-1,j} \\ &\quad + ZA_{0,0}^{i,j} - ZA_{0,1}^{i,j} - ZA_{1,0}^{i,j} + ZA_{1,1}^{i,j}. \end{aligned} \tag{B.318}$$

Additionally it holds that

$$\begin{aligned} \langle S_h(Z_h\chi_j), \chi_i \rangle &= \int_{\Gamma^h}\int_{\Gamma^h} Z_h(\boldsymbol{y})G(\boldsymbol{x},\boldsymbol{y})\chi_j(\boldsymbol{y})\chi_i(\boldsymbol{x})\,\mathrm{d}\gamma(\boldsymbol{y})\,\mathrm{d}\gamma(\boldsymbol{x}) \\ &= Z_{j-1}\big(ZA_{1,1}^{i-1,j-1} + ZA_{0,1}^{i,j-1} - ZA_{1,1}^{i,j-1}\big) \\ &\quad + Z_j\big(ZA_{1,0}^{i-1,j} - ZA_{1,1}^{i-1,j} + ZA_{0,0}^{i,j} - ZA_{0,1}^{i,j} - ZA_{1,0}^{i,j} + ZA_{1,1}^{i,j}\big). \end{aligned} \tag{B.319}$$

Furthermore we see that

$$\begin{aligned} \langle Z_h S_h(Z_h\chi_j), \chi_i \rangle &= \int_{\Gamma^h}\int_{\Gamma^h} Z_h(\boldsymbol{x})Z_h(\boldsymbol{y})G(\boldsymbol{x},\boldsymbol{y})\chi_j(\boldsymbol{y})\chi_i(\boldsymbol{x})\,\mathrm{d}\gamma(\boldsymbol{y})\,\mathrm{d}\gamma(\boldsymbol{x}) \\ &= Z_{i-1}Z_{j-1}ZA_{1,1}^{i-1,j-1} + Z_iZ_{j-1}\big(ZA_{0,1}^{i,j-1} - ZA_{1,1}^{i,j-1}\big) \\ &\quad + Z_{i-1}Z_j\big(ZA_{1,0}^{i-1,j} - ZA_{1,1}^{i-1,j}\big) + Z_iZ_j\big(ZA_{0,0}^{i,j} - ZA_{0,1}^{i,j} - ZA_{1,0}^{i,j} + ZA_{1,1}^{i,j}\big). \end{aligned} \tag{B.320}$$

Likewise it occurs that

$$\begin{aligned} \langle D_h(\chi_j), \chi_i \rangle &= \int_{\Gamma^h}\int_{\Gamma^h} \frac{\partial G}{\partial n_{\boldsymbol{y}}}(\boldsymbol{x},\boldsymbol{y})\chi_j(\boldsymbol{y})\chi_i(\boldsymbol{x})\,\mathrm{d}\gamma(\boldsymbol{y})\,\mathrm{d}\gamma(\boldsymbol{x}) \\ &= ZB_{1,1}^{i-1,j-1} + ZB_{0,1}^{i,j-1} - ZB_{1,1}^{i,j-1} + ZB_{1,0}^{i-1,j} - ZB_{1,1}^{i-1,j} \\ &\quad + ZB_{0,0}^{i,j} - ZB_{0,1}^{i,j} - ZB_{1,0}^{i,j} + ZB_{1,1}^{i,j}. \end{aligned} \tag{B.321}$$

It holds moreover that

$$\begin{aligned} \langle Z_h D_h(\chi_j), \chi_i \rangle &= \int_{\Gamma^h}\int_{\Gamma^h} Z_h(\boldsymbol{x})\frac{\partial G}{\partial n_{\boldsymbol{y}}}(\boldsymbol{x},\boldsymbol{y})\chi_j(\boldsymbol{y})\chi_i(\boldsymbol{x})\,\mathrm{d}\gamma(\boldsymbol{y})\,\mathrm{d}\gamma(\boldsymbol{x}) \\ &= Z_{i-1}\big(ZB_{1,1}^{i-1,j-1} + ZB_{1,0}^{i-1,j} - ZB_{1,1}^{i-1,j}\big) \\ &\quad + Z_i\big(ZB_{0,1}^{i,j-1} - ZB_{1,1}^{i,j-1} + ZB_{0,0}^{i,j} - ZB_{0,1}^{i,j} - ZB_{1,0}^{i,j} + ZB_{1,1}^{i,j}\big). \end{aligned} \tag{B.322}$$

We have also that

$$\begin{aligned}\langle D_h^*(\chi_j),\chi_i\rangle &= \int_{\Gamma^h}\int_{\Gamma^h}\frac{\partial G}{\partial n_{\boldsymbol{x}}}(\boldsymbol{x},\boldsymbol{y})\chi_j(\boldsymbol{y})\chi_i(\boldsymbol{x})\,\mathrm{d}\gamma(\boldsymbol{y})\,\mathrm{d}\gamma(\boldsymbol{x})\\ &= ZB_{1,1}^{j-1,i-1}+ZB_{1,0}^{j-1,i}-ZB_{1,1}^{j-1,i}+ZB_{0,1}^{j,i-1}-ZB_{1,1}^{j,i-1}\\ &\quad+ZB_{0,0}^{j,i}-ZB_{1,0}^{j,i}-ZB_{0,1}^{j,i}+ZB_{1,1}^{j,i}. \end{aligned}\tag{B.323}$$

Similarly it occurs that

$$\begin{aligned}\langle D_h^*(Z_h\chi_j),\chi_i\rangle &= \int_{\Gamma^h}\int_{\Gamma^h}Z_h(\boldsymbol{y})\frac{\partial G}{\partial n_{\boldsymbol{x}}}(\boldsymbol{x},\boldsymbol{y})\chi_j(\boldsymbol{y})\chi_i(\boldsymbol{x})\,\mathrm{d}\gamma(\boldsymbol{y})\,\mathrm{d}\gamma(\boldsymbol{x})\\ &= Z_{j-1}\big(ZB_{1,1}^{j-1,i-1}+ZB_{1,0}^{j-1,i}-ZB_{1,1}^{j-1,i}\big)\\ &\quad+Z_j\big(ZB_{0,1}^{j,i-1}-ZB_{1,1}^{j,i-1}+ZB_{0,0}^{j,i}-ZB_{1,0}^{j,i}-ZB_{0,1}^{j,i}+ZB_{1,1}^{j,i}\big). \end{aligned}\tag{B.324}$$

And finally, for the hypersingular term we have that

$$\begin{aligned}\langle N_h(\chi_j),\chi_i\rangle &= -\int_{\Gamma^h}\int_{\Gamma^h}G(\boldsymbol{x},\boldsymbol{y})\big(\nabla\chi_j(\boldsymbol{y})\times\boldsymbol{n}_{\boldsymbol{y}}\big)\big(\nabla\chi_i(\boldsymbol{x})\times\boldsymbol{n}_{\boldsymbol{x}}\big)\,\mathrm{d}\gamma(\boldsymbol{y})\,\mathrm{d}\gamma(\boldsymbol{x})\\ &= -ZA_{0,0}^{i-1,j-1}\frac{(\boldsymbol{\tau}_{j-1}\times\boldsymbol{n}_{j-1})}{|T_{j-1}|}\frac{(\boldsymbol{\tau}_{i-1}\times\boldsymbol{n}_{i-1})}{|T_{i-1}|}+ZA_{0,0}^{i,j-1}\frac{(\boldsymbol{\tau}_{j-1}\times\boldsymbol{n}_{j-1})}{|T_{j-1}|}\frac{(\boldsymbol{\tau}_{i}\times\boldsymbol{n}_{i})}{|T_{i}|}\\ &\quad+ZA_{0,0}^{i-1,j}\frac{(\boldsymbol{\tau}_{j}\times\boldsymbol{n}_{j})}{|T_{j}|}\frac{(\boldsymbol{\tau}_{i-1}\times\boldsymbol{n}_{i-1})}{|T_{i-1}|}-ZA_{0,0}^{i,j}\frac{(\boldsymbol{\tau}_{j}\times\boldsymbol{n}_{j})}{|T_{j}|}\frac{(\boldsymbol{\tau}_{i}\times\boldsymbol{n}_{i})}{|T_{i}|}. \end{aligned}\tag{B.325}$$

We remark that these formulae hold when the segments T_{i-1} and T_i, as well as the segments T_{j-1} and T_j, exist and are adjacent.

It remains now to compute the integrals (B.307) and (B.308), which are calculated in two steps with a semi-numerical integration, i.e., the singular parts are calculated analytically and the other parts numerically. First the internal integral for $\boldsymbol{y}$ is computed, then the external one for $\boldsymbol{x}$. This can be expressed as

$$ZA_{a,b}=\int_K\left(\frac{s}{|K|}\right)^a ZF_b(\boldsymbol{x})\,\mathrm{d}K(\boldsymbol{x}),\tag{B.326}$$

$$ZF_b(\boldsymbol{x})=\int_L\left(\frac{t}{|L|}\right)^b G(\boldsymbol{x},\boldsymbol{y})\,\mathrm{d}L(\boldsymbol{y}),\tag{B.327}$$

and

$$ZB_{a,b}=\int_K\left(\frac{s}{|K|}\right)^a ZG_b(\boldsymbol{x})\,\mathrm{d}K(\boldsymbol{x}),\tag{B.328}$$

$$ZG_b(\boldsymbol{x})=\int_L\left(\frac{t}{|L|}\right)^b \frac{\partial G}{\partial n_{\boldsymbol{y}}}(\boldsymbol{x},\boldsymbol{y})\,\mathrm{d}L(\boldsymbol{y}).\tag{B.329}$$

This kind of integrals can be also used to compute the terms associated with the discretized solution u_h. Using an analogous notation as in (B.310), we have that

$$\mathcal{S}_h(\kappa_j)=\int_{\Gamma^h}G(\boldsymbol{x},\boldsymbol{y})\kappa_j(\boldsymbol{y})\,\mathrm{d}\gamma(\boldsymbol{y})=ZF_0^j(\boldsymbol{x}).\tag{B.330}$$

Similarly it holds that

$$\mathcal{S}_h(\chi_j) = \int_{\Gamma^h} G(\boldsymbol{x},\boldsymbol{y})\chi_j(\boldsymbol{y})\,\mathrm{d}\gamma(\boldsymbol{y}) = ZF_1^{j-1}(\boldsymbol{x}) + ZF_0^j(\boldsymbol{x}) - ZF_1^j(\boldsymbol{x}), \tag{B.331}$$

and

$$\begin{aligned}\mathcal{S}_h(Z_h\chi_j) &= \int_{\Gamma^h} Z_h(\boldsymbol{y})G(\boldsymbol{x},\boldsymbol{y})\chi_j(\boldsymbol{y})\,\mathrm{d}\gamma(\boldsymbol{y}) \\ &= Z_{j-1}ZF_1^{j-1}(\boldsymbol{x}) + Z_j\big(ZF_0^j(\boldsymbol{x}) - ZF_1^j(\boldsymbol{x})\big).\end{aligned} \tag{B.332}$$

The remaining term is computed as

$$\mathcal{D}_h(\chi_j) = \int_{\Gamma^h} \frac{\partial G}{\partial n_{\boldsymbol{y}}}(\boldsymbol{x},\boldsymbol{y})\chi_j(\boldsymbol{y})\,\mathrm{d}\gamma(\boldsymbol{y}) = ZG_1^{j-1}(\boldsymbol{x}) + ZG_0^j(\boldsymbol{x}) - ZG_1^j(\boldsymbol{x}). \tag{B.333}$$

B.12.3 Numerical integration for the non-singular integrals

The numerical integration of the non-singular integrals of the boundary element calculations is performed by a two-point Gauss quadrature formula (cf., e.g., Abramowitz & Stegun 1972). The points considered on each segment are denoted as

$$\boldsymbol{x}_1 = \alpha_1\boldsymbol{r}_1^K + \alpha_2\boldsymbol{r}_2^K, \qquad \boldsymbol{x}_2 = \alpha_2\boldsymbol{r}_1^K + \alpha_1\boldsymbol{r}_2^K, \tag{B.334}$$

$$\boldsymbol{y}_1 = \alpha_1\boldsymbol{r}_1^L + \alpha_2\boldsymbol{r}_2^L, \qquad \boldsymbol{y}_2 = \alpha_2\boldsymbol{r}_1^L + \alpha_1\boldsymbol{r}_2^L, \tag{B.335}$$

where

$$\alpha_1 = \frac{1}{2}\left(1 + \frac{1}{\sqrt{3}}\right) \qquad \text{and} \qquad \alpha_2 = \frac{1}{2}\left(1 - \frac{1}{\sqrt{3}}\right). \tag{B.336}$$

When considering a function $\varphi : L \to \mathbb{C}$, this formula is given by

$$\int_{\boldsymbol{r}_1^L}^{\boldsymbol{r}_2^L} \left(\frac{t}{|L|}\right)^b \varphi(\boldsymbol{y})\,\mathrm{d}L(\boldsymbol{y}) \approx \frac{|L|}{2}\Big(\alpha_2^b\varphi(\boldsymbol{y}_1) + \alpha_1^b\varphi(\boldsymbol{y}_2)\Big). \tag{B.337}$$

An equivalent formula is used when considering a function $\phi : K \to \mathbb{C}$, given by

$$\int_{\boldsymbol{r}_1^K}^{\boldsymbol{r}_2^K} \left(\frac{s}{|K|}\right)^a \phi(\boldsymbol{x})\,\mathrm{d}K(\boldsymbol{x}) \approx \frac{|K|}{2}\Big(\alpha_2^a\phi(\boldsymbol{x}_1) + \alpha_1^a\phi(\boldsymbol{x}_2)\Big). \tag{B.338}$$

The Gauss quadrature formula can be extended straightforwardly to a function of two variables, $\Phi : K \times L \to \mathbb{C}$, using both formulas shown above. Therefore

$$\begin{aligned}\int_{\boldsymbol{r}_1^K}^{\boldsymbol{r}_2^K}\int_{\boldsymbol{r}_1^L}^{\boldsymbol{r}_2^L} \left(\frac{s}{|K|}\right)^a \left(\frac{t}{|L|}\right)^b \Phi(\boldsymbol{x},\boldsymbol{y})\,\mathrm{d}L(\boldsymbol{y})\mathrm{d}K(\boldsymbol{x}) \approx \frac{|K|\,|L|}{4}\Bigg(&\alpha_2^{a+b}\Phi(\boldsymbol{x}_1,\boldsymbol{y}_1) \\ &+ \alpha_2^a\alpha_1^b\Phi(\boldsymbol{x}_1,\boldsymbol{y}_2) + \alpha_1^a\alpha_2^b\Phi(\boldsymbol{x}_2,\boldsymbol{y}_1) + \alpha_1^{a+b}\Phi(\boldsymbol{x}_2,\boldsymbol{y}_2)\Bigg).\end{aligned} \tag{B.339}$$

The points on which the non-singular integrals have to be evaluated to perform the numerical integration are depicted in Figure B.14.

We have that the integrals on K, (B.326) and (B.328), are non-singular and thus evaluated numerically with the two-point Gauss quadrature formula (B.338).

For the integrals on L, (B.327) and (B.329), two different cases have to be taken into account. If the segments K and L are not close together, e.g., neither adjacent nor equal,

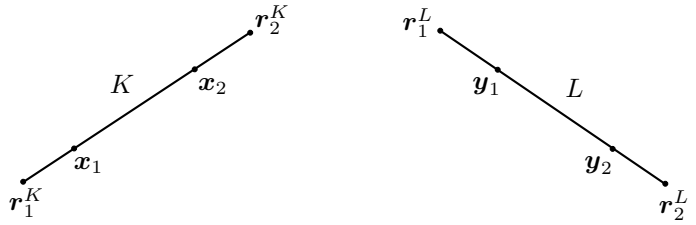

FIGURE B.14. Evaluation points for the numerical integration.

then (B.327) and (B.329) can also be numerically integrated using the formula (B.337), i.e., in the whole, the integrals $ZA_{a,b}$ and $ZB_{a,b}$ are calculated employing (B.339).

For the computation of the discretized solution u_h, the quadrature formula (B.337) is taken into account if $\boldsymbol{x} \notin \Gamma^h$. Otherwise we use the analytical formulae for singular integrals that are below.

The quadrature formula (B.337) is likewise used in the computation of the far field, namely for the discretization of the far-field pattern (B.169).

B.12.4 Analytical integration for the singular integrals

If the segments K and L are close together, then the integrals (B.327) and (B.329) are calculated analytically, treating $\boldsymbol{x}$ as a given parameter. They are specifically given by

$$ZF_0(\boldsymbol{x}) = \int_L \frac{\ln R}{2\pi}\,\mathrm{d}L(\boldsymbol{y}), \tag{B.340}$$

$$ZF_1(\boldsymbol{x}) = \int_L t\,\frac{\ln R}{2\pi|L|}\,\mathrm{d}L(\boldsymbol{y}), \tag{B.341}$$

and

$$ZG_0(\boldsymbol{x}) = \int_L \frac{\boldsymbol{R}\cdot\boldsymbol{n}_L}{2\pi R^2}\,\mathrm{d}L(\boldsymbol{y}), \tag{B.342}$$

$$ZG_1(\boldsymbol{x}) = \int_L t\,\frac{\boldsymbol{R}\cdot\boldsymbol{n}_L}{2\pi R^2|L|}\,\mathrm{d}L(\boldsymbol{y}). \tag{B.343}$$

a) Computation of $ZG_0(\boldsymbol{x})$

The integral (B.342) is closely related with Gauss's divergence theorem. If we consider an oriented surface differential element $\mathrm{d}\boldsymbol{\gamma} = \boldsymbol{n}_L \mathrm{d}L(\boldsymbol{y})$ seen from point $\boldsymbol{x}$, then we can express the angle differential element by

$$\mathrm{d}\theta = \frac{\boldsymbol{R}}{R^2}\cdot\mathrm{d}\boldsymbol{\gamma} = \frac{\boldsymbol{R}\cdot\boldsymbol{n}_L}{R^2}\,\mathrm{d}L(\boldsymbol{y}) = 2\pi\frac{\partial G}{\partial n_{\boldsymbol{y}}}(\boldsymbol{x},\boldsymbol{y})\,\mathrm{d}L(\boldsymbol{y}). \tag{B.344}$$

Integrating over segment L yields the angle θ_L, as expressed in (B.306), namely

$$\theta_L = \int_L \mathrm{d}\theta \qquad (-\pi \le \theta_L \le \pi). \tag{B.345}$$

The angle θ_L is positive when the vectors $\boldsymbol{R}$ and $\boldsymbol{n}_L$ point towards the same side of L. Thus integral (B.342) is obtained by integrating (B.344), which yields

$$ZG_0(\boldsymbol{x}) = \int_L \frac{\boldsymbol{R}\cdot\boldsymbol{n}_L}{2\pi R^2}\,\mathrm{d}L(\boldsymbol{y}) = \frac{\theta_L}{2\pi}. \tag{B.346}$$

b) Computation of $ZF_1(\boldsymbol{x})$

For the integral (B.341) we have that

$$\begin{aligned} ZF_1(\boldsymbol{x}) &= \frac{1}{2\pi|L|}\int_L \ln(R)\left(\boldsymbol{R}-\boldsymbol{R}_1^L\right)\cdot\boldsymbol{\tau}_L\,\mathrm{d}L(\boldsymbol{y}) \\ &= \frac{1}{2\pi|L|}\int_L R\,\ln(R)\,\frac{\boldsymbol{R}}{R}\cdot\boldsymbol{\tau}_L\,\mathrm{d}L(\boldsymbol{y}) - \frac{\boldsymbol{R}_1^L\cdot\boldsymbol{\tau}_L}{|L|}\,ZF_0(\boldsymbol{x}). \end{aligned} \tag{B.347}$$

If we denote the primitive of $R\,\ln R$ that vanishes for $R=0$ by

$$v(R) = \frac{R^2}{2}\left(\ln R - \frac{1}{2}\right), \tag{B.348}$$

then (B.347) can be rewritten as

$$ZF_1(\boldsymbol{x}) = \frac{1}{2\pi|L|}\int_L \frac{\partial v}{\partial t}\,\mathrm{d}L(\boldsymbol{y}) - \frac{\boldsymbol{R}_1^L\cdot\boldsymbol{\tau}_L}{|L|}\,ZF_0(\boldsymbol{x}), \tag{B.349}$$

and therefore $ZF_1(\boldsymbol{x})$ can be finally calculated as

$$ZF_1(\boldsymbol{x}) = \frac{v(R_2^L)-v(R_1^L)}{2\pi|L|} - \frac{\boldsymbol{R}_1^L\cdot\boldsymbol{\tau}_L}{|L|}\,ZF_0(\boldsymbol{x}). \tag{B.350}$$

c) Computation of $ZF_0(\boldsymbol{x})$

We consider now a function $w = w(R)$ that is bounded in the vicinity of zero and is such that

$$\Delta w = \frac{1}{R}\frac{\mathrm{d}}{\mathrm{d}R}\left(R\,\frac{\mathrm{d}w}{\mathrm{d}R}\right) = \ln R. \tag{B.351}$$

Hence, taking a primitive that vanishes at zero, it holds that

$$\frac{\mathrm{d}w}{\mathrm{d}R} = \frac{R}{2}\left(\ln R - \frac{1}{2}\right). \tag{B.352}$$

We turn now to the local orthonormal variables t and n, where

$$\boldsymbol{R} = \boldsymbol{R}_1^L + t\,\boldsymbol{\tau}_L + n\,\boldsymbol{n}_L. \tag{B.353}$$

Since the Laplace operator Δ is invariant under orthonormal variable changes, we have from (B.351) that

$$ZF_0(\boldsymbol{x}) = \frac{1}{2\pi}\int_L \left(\frac{\partial^2 w}{\partial t^2} + \frac{\partial^2 w}{\partial n^2}\right)\mathrm{d}L(\boldsymbol{y}). \tag{B.354}$$

By considering (B.352) we obtain that

$$\nabla w = \frac{\mathrm{d}w}{\mathrm{d}R}\frac{\boldsymbol{R}}{R} = \frac{1}{2}\left(\ln R - \frac{1}{2}\right)\boldsymbol{R}, \tag{B.355}$$

$$\frac{\partial w}{\partial t} = \nabla w \cdot \boldsymbol{\tau}_L = \frac{1}{2}\left(\ln R - \frac{1}{2}\right)\boldsymbol{R}\cdot\boldsymbol{\tau}_L, \tag{B.356}$$

$$\frac{\partial w}{\partial n} = \nabla w \cdot \boldsymbol{n}_L = \frac{1}{2}\left(\ln R - \frac{1}{2}\right)\boldsymbol{R}\cdot\boldsymbol{n}_L, \tag{B.357}$$

$$\frac{\partial^2 w}{\partial n^2} = \frac{1}{2}\boldsymbol{R}\cdot\boldsymbol{n}_L\frac{\partial}{\partial n}\ln R + \frac{1}{2}\left(\ln R - \frac{1}{2}\right). \tag{B.358}$$

The first integral in (B.354) is therefore given by

$$\frac{1}{2\pi}\int_L \frac{\partial^2 w}{\partial t^2}\,\mathrm{d}L(\boldsymbol{y}) = \frac{1}{4\pi}\left(\ln R_2^L - \frac{1}{2}\right)\boldsymbol{R}_2^L\cdot\boldsymbol{\tau}_L - \frac{1}{4\pi}\left(\ln R_1^L - \frac{1}{2}\right)\boldsymbol{R}_1^L\cdot\boldsymbol{\tau}_L, \tag{B.359}$$

while for the second one, due (B.305), it holds that

$$\frac{1}{2\pi}\int_L \frac{\partial^2 w}{\partial n^2}\,\mathrm{d}L(\boldsymbol{y}) = \frac{d_L}{2}ZG_0(\boldsymbol{x}) + \frac{1}{2}ZF_0(\boldsymbol{x}) - \frac{|L|}{8\pi}. \tag{B.360}$$

From (B.346), (B.354), (B.359), and (B.360), we obtain the desired expression

$$ZF_0(\boldsymbol{x}) = \frac{1}{2\pi}\Big(\boldsymbol{R}_2^L\cdot\boldsymbol{\tau}_L\ln R_2^L - \boldsymbol{R}_1^L\cdot\boldsymbol{\tau}_L\ln R_1^L - |L| + d_L\theta_L\Big). \tag{B.361}$$

d) Computation of $ZG_1(\boldsymbol{x})$

The integral (B.343) is found straightforwardly by replacing (B.304), yielding

$$\begin{aligned} ZG_1(\boldsymbol{x}) &= \int_L \frac{\boldsymbol{R}\cdot\boldsymbol{n}_L}{2\pi R^2|L|}\left(\boldsymbol{R}-\boldsymbol{R}_1^L\right)\cdot\boldsymbol{\tau}_L\,\mathrm{d}L(\boldsymbol{y}) \\ &= \int_L \frac{\boldsymbol{R}\cdot\boldsymbol{n}_L}{2\pi R^2|L|}\,\boldsymbol{R}\cdot\boldsymbol{\tau}_L\,\mathrm{d}L(\boldsymbol{y}) - \frac{\boldsymbol{R}_1^L\cdot\boldsymbol{\tau}_L}{|L|}\,ZG_0(\boldsymbol{x}). \end{aligned} \tag{B.362}$$

Due (B.305) we have then

$$ZG_1(\boldsymbol{x}) = \frac{\ln(R_2^L/R_1^L)}{2\pi|L|}\,\boldsymbol{R}_1^L\cdot\boldsymbol{n}_L - \frac{\boldsymbol{R}_1^L\cdot\boldsymbol{\tau}_L}{|L|}\,ZG_0(\boldsymbol{x}). \tag{B.363}$$

e) Final computation of the singular integrals

In conclusion, the singular integrals (B.327) and (B.329) are computed using the formulae (B.346), (B.350), (B.361), and (B.363).

It should be observed that $ZB_{a,b} = 0$ when the segments coincide, i.e., when $K = L$, since in this case $d_L = 0$, and thus (B.346) and (B.363) become zero.

B.13 Benchmark problem

As benchmark problem we consider the exterior circle problem (B.171), whose domain is shown in Figure B.8. The exact solution of this problem is stated in (B.193), and the idea is to retrieve it numerically with the integral equation techniques and the boundary element method described throughout this chapter.

For the computational implementation and the numerical resolution of the benchmark problem, we consider only the first integral equation of the extension-by-zero alternative (B.129), which is given in terms of boundary layer potentials by (B.208). The linear system (B.271) resulting from the discretization (B.269) of its variational formulation (B.250) is solved computationally with finite boundary elements of type $\mathbb{P}_1$ by using subroutines programmed in Fortran 90, by generating the mesh Γ^h of the boundary with the free software Gmsh 2.4, and by representing graphically the results in Matlab 7.5 (R2007b).

We consider a radius $R = 1$ and a constant impedance $Z = 0.8$. The discretized boundary curve Γ^h has $I = 120$ segments and a discretization step $h = 0.05235$, being

$$h = \max_{1 \le j \le I} |T_j|. \tag{B.364}$$

We observe that $h \approx 2\pi/I$. As the known field without obstacle we take

$$u_W(r, \theta) = \frac{e^{i\theta}}{r} = \frac{x_1 + ix_2}{x_1^2 + x_2^2}, \tag{B.365}$$

which implies that the impedance data function is given by

$$f_z(\theta) = -\frac{\partial u_W}{\partial r}(R, \theta) - Z u_W(R, \theta) = -\frac{e^{i\theta}}{R^2}(ZR - 1). \tag{B.366}$$

The exact solution of the problem and its trace on the boundary are thus given by

$$u(\boldsymbol{x}) = -u_W(r, \theta) = -\frac{e^{i\theta}}{r} \qquad \text{and} \qquad \mu(\theta) = -u_W(R, \theta) = -\frac{e^{i\theta}}{R}. \tag{B.367}$$

The numerically calculated trace of the solution μ_h of the benchmark problem, which was computed by using the boundary element method, is depicted in Figure B.15. In the same manner, the numerical solution u_h is illustrated in Figures B.16 and B.17. It can be observed that the numerical solution is quite close to the exact one.

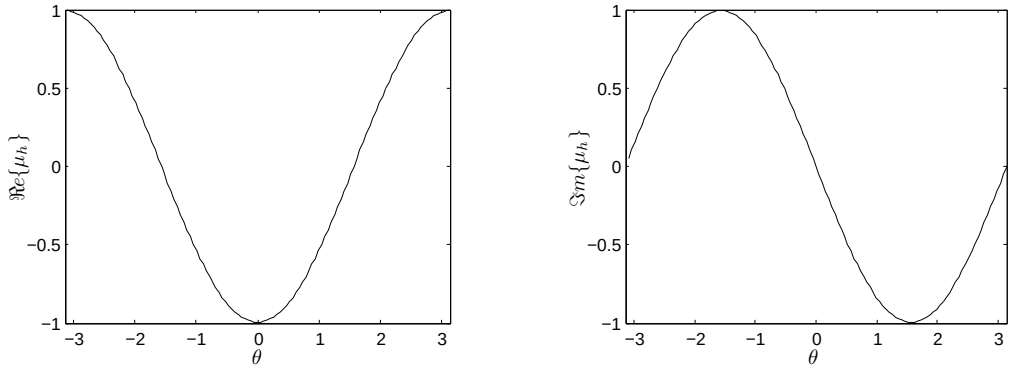

(a) Real part (b) Imaginary part

FIGURE B.15. Numerically computed trace of the solution μ_h.

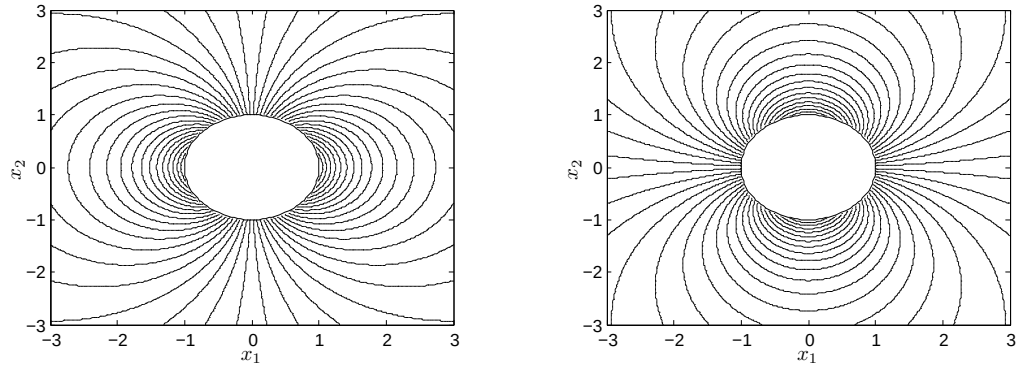

(a) Real part (b) Imaginary part

FIGURE B.16. Contour plot of the numerically computed solution u_h.

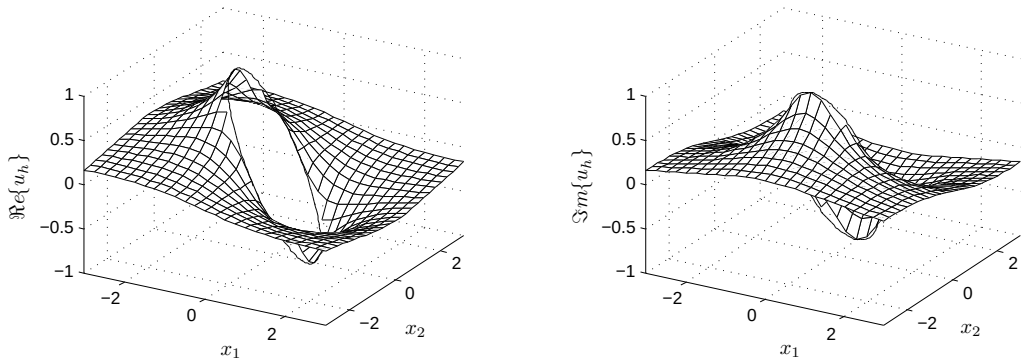

(a) Real part (b) Imaginary part

FIGURE B.17. Oblique view of the numerically computed solution u_h.

We define the relative error of the trace of the solution as

$$E_2(h,\Gamma^h) = \frac{\|\Pi_h\mu - \mu_h\|_{L^2(\Gamma^h)}}{\|\Pi_h\mu\|_{L^2(\Gamma^h)}}, \tag{B.368}$$

where $\Pi_h\mu$ denotes the Lagrange interpolating function of the exact solution's trace μ, i.e.,

$$\Pi_h\mu(\boldsymbol{x}) = \sum_{j=1}^{I} \mu(\boldsymbol{r}_j)\,\chi_j(\boldsymbol{x}) \quad \text{and} \quad \mu_h(\boldsymbol{x}) = \sum_{j=1}^{I} \mu_j\,\chi_j(\boldsymbol{x}) \quad \text{for } \boldsymbol{x}\in\Gamma^h. \tag{B.369}$$

It holds therefore that

$$\|\Pi_h\mu - \mu_h\|^2_{L^2(\Gamma^h)} = (\tilde{\boldsymbol{\mu}} - \boldsymbol{\mu})^*\boldsymbol{A}\,(\tilde{\boldsymbol{\mu}} - \boldsymbol{\mu}) \qquad \text{and} \qquad \|\Pi_h\mu\|^2_{L^2(\Gamma^h)} = \tilde{\boldsymbol{\mu}}^*\boldsymbol{A}\,\tilde{\boldsymbol{\mu}}, \tag{B.370}$$

where $\mu(\boldsymbol{r}_j)$ and μ_j are respectively the elements of vectors $\tilde{\boldsymbol{\mu}}$ and $\boldsymbol{\mu}$, for $1 \le j \le I$, and where the elements a_{ij} of the matrix $\boldsymbol{A}$ are specified in (B.316) and given by

$$a_{ij} = \langle \chi_j, \chi_i \rangle \qquad \text{for } 1 \le i,j \le I. \tag{B.371}$$

In our case, for a step $h = 0.05235$, we obtained a relative error of $E_2(h,\Gamma^h) = 0.004571$.

Similarly as for the trace, we define the relative error of the solution as

$$E_\infty(h,\Omega_L)=\frac{\|u-u_h\|_{L^\infty(\Omega_L)}}{\|u\|_{L^\infty(\Omega_L)}}, \tag{B.372}$$

being $\Omega_L=\{\boldsymbol{x}\in\Omega_e:\ \|\boldsymbol{x}\|_\infty<L\}$ for $L>0$, and where

$$\|u-u_h\|_{L^\infty(\Omega_L)}=\max_{\boldsymbol{x}\in\Omega_L}|u(\boldsymbol{x})-u_h(\boldsymbol{x})| \quad \text{and} \quad \|u\|_{L^\infty(\Omega_L)}=\max_{\boldsymbol{x}\in\Omega_L}|u(\boldsymbol{x})|. \tag{B.373}$$

We consider $L=3$ and approximate Ω_L by a triangular finite element mesh of refinement h near the boundary. For $h=0.05235$, the relative error that we obtained for the solution was $E_\infty(h,\Omega_L)=0.004870$.

The results for different mesh refinements, i.e., for different numbers of segments I and discretization steps h for Γ^h, are listed in Table B.1. These results are illustrated graphically in Figure B.18. It can be observed that the relative errors are approximately of order h^2.

TABLE B.1. Relative errors for different mesh refinements.

I	h	$E_2(h,\Gamma^h)$	$E_\infty(h,\Omega_L)$
12	0.5176	$4.330\cdot10^{-1}$	$4.330\cdot10^{-1}$
40	0.1569	$4.100\cdot10^{-2}$	$4.100\cdot10^{-2}$
80	0.07852	$1.027\cdot10^{-2}$	$1.082\cdot10^{-2}$
120	0.05235	$4.571\cdot10^{-3}$	$4.870\cdot10^{-3}$
240	0.02618	$1.143\cdot10^{-3}$	$1.239\cdot10^{-3}$
500	0.01257	$2.633\cdot10^{-4}$	$2.879\cdot10^{-4}$
1000	0.006283	$6.581\cdot10^{-5}$	$7.222\cdot10^{-5}$

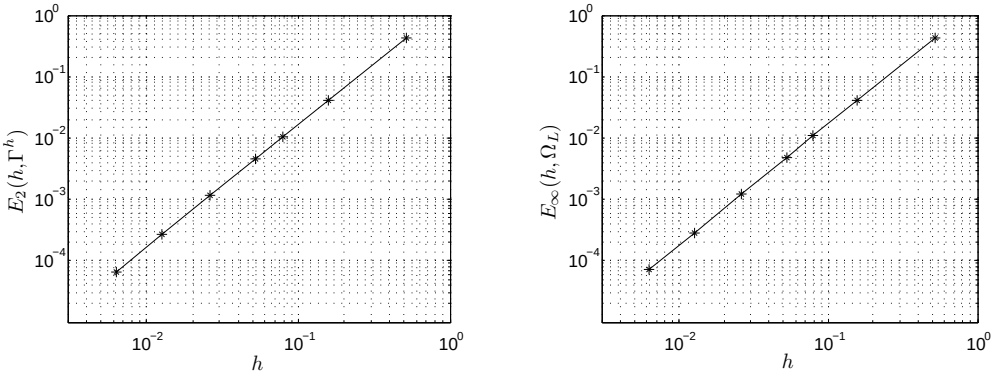

(a) Relative error $E_2(h,\Gamma^h)$ (b) Relative error $E_\infty(h,\Omega_L)$

FIGURE B.18. Logarithmic plots of the relative errors versus the discretization step.

C. FULL-PLANE IMPEDANCE HELMHOLTZ PROBLEM

C.1 Introduction

In this appendix we study the perturbed full-plane or free-plane impedance Helmholtz problem, also known as the exterior impedance Helmholtz problem in 2D, using integral equation techniques and the boundary element method.

We consider the problem of the Helmholtz equation in two dimensions on the exterior of a bounded obstacle with an impedance boundary condition. The perturbed full-plane impedance Helmholtz problem is a wave scattering problem around a bounded two-dimensional obstacle. In acoustic obstacle scattering the impedance boundary-value problem appears when we suppose that the normal velocity is proportional to the excess pressure on the boundary of the impenetrable obstacle. The special case of frequency zero for the volume waves has been treated already in Appendix B, since then we deal with the Laplace equation. The three-dimensional Helmholtz problem is treated thoroughly in Appendix E.

The main references for the problem treated herein are Kress (2002), Lenoir (2005), Nédélec (2001), and Terrasse & Abboud (2006). Additional related books and doctorate theses are the ones of Chen & Zhou (1992), Colton & Kress (1983), Ha-Duong (1987), Hsiao & Wendland (2008), Rjasanow & Steinbach (2007), and Steinbach (2008). Articles that take the Helmholtz equation with an impedance boundary condition into account are Angell & Kleinman (1982), Angell & Kress (1984), Angell, Kleinman & Hettlich (1990), Cakoni, Colton & Monk (2001), and Krutitskii (2002, 2003*a*,*b*). Interesting theoretical details on transmission problems can be found in Costabel & Stephan (1985). For more information on resonances of volume waves we refer to Poisson & Joly (1991). Eigenvalues for the far-field operator are computed in Colton & Kress (1995). The boundary element calculations are performed in the report of Bendali & Devys (1986) and in the article of Bendali & Souilah (1994). Hypersingular integral equations are considered by Feistauer, Hsiao & Kleinman (1996) and Kress (1995). The use of cracked domains is studied by Kress & Lee (2003), and the inverse problem in the articles of Cakoni et al. (2001) and Smith (1985). An optimal control problem is treated by Kirsch (1981). Applications for the Helmholtz problem can be found, among others, for acoustics (Morse & Ingard 1961) and for ultrasound imaging (Ammari 2008).

The Helmholtz equation allows the propagation of volume waves inside the considered domain, and when supplied with an impedance boundary condition it allows also the propagation of surface waves along the domain's boundary. The main difficulty in the numerical treatment and resolution of our problem is the fact that the exterior domain is unbounded. We solve it therefore with integral equation techniques and the boundary element method, which require the knowledge of the Green's function.

This appendix is structured in 14 sections, including this introduction. The direct scattering problem of the Helmholtz equation in a two-dimensional exterior domain with an impedance boundary condition is presented in Section C.2. The Green's function and its

far-field expression are computed respectively in Sections C.3 and C.4. Extending the direct scattering problem towards a transmission problem, as done in Section C.5, allows its resolution by using integral equation techniques, which is discussed in Section C.6. These techniques allow also to represent the far field of the solution, as shown in Section C.7. A particular problem that takes as domain the exterior of a circle is solved analytically in Section C.8. The appropriate function spaces and some existence and uniqueness results for the solution of the problem are presented in Section C.9. The dissipative problem is studied in Section C.10. By means of the variational formulation developed in Section C.11, the obtained integral equation is discretized using the boundary element method, which is described in Section C.12. The boundary element calculations required to build the matrix of the linear system resulting from the numerical discretization are explained in Section C.13. Finally, in Section C.14 a benchmark problem based on the exterior circle problem is solved numerically.

C.2 Direct scattering problem

We consider the direct scattering problem of linear time-harmonic acoustic waves on an exterior domain $\Omega_e \subset \mathbb{R}^2$, lying outside a bounded obstacle Ω_i and having a regular boundary $\Gamma = \partial\Omega_e = \partial\Omega_i$, as shown in Figure C.1. The time convention $e^{-i\omega t}$ is taken and the incident field u_I is known. The goal is to find the scattered field u as a solution to the Helmholtz equation in Ω_e, satisfying an outgoing radiation condition, and such that the total field u_T, decomposed as $u_T = u_I + u$, satisfies a homogeneous impedance boundary condition on the regular boundary Γ (e.g., of class C^2). The unit normal $\boldsymbol{n}$ is taken outwardly oriented of Ω_e. A given wave number $k > 0$ is considered, which depends on the pulsation ω and the speed of wave propagation c through the ratio $k = \omega/c$.

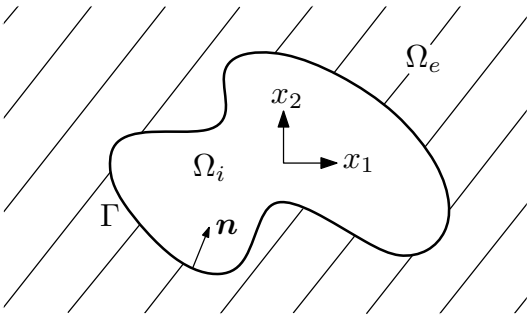

FIGURE C.1. Perturbed full-plane impedance Helmholtz problem domain.

The total field u_T satisfies thus the Helmholtz equation

$$\Delta u_T + k^2 u_T = 0 \qquad \text{in } \Omega_e, \tag{C.1}$$

which is also satisfied by the incident field u_I and the scattered field u, due linearity. For the total field u_T we take the homogeneous impedance boundary condition

$$-\frac{\partial u_T}{\partial n} + Z u_T = 0 \qquad \text{on } \Gamma, \tag{C.2}$$

where Z is the impedance on the boundary. If $Z = 0$ or $Z = \infty$, then we retrieve respectively the classical Neumann or Dirichlet boundary conditions. In general, we consider a complex-valued impedance $Z(\boldsymbol{x})$ that depends on the position $\boldsymbol{x}$ and that may depend also on the pulsation ω. The scattered field u satisfies the non-homogeneous impedance boundary condition

$$-\frac{\partial u}{\partial n} + Z u = f_z \qquad \text{on } \Gamma, \tag{C.3}$$

where the impedance data function f_z is given by

$$f_z = \frac{\partial u_I}{\partial n} - Z u_I \qquad \text{on } \Gamma. \tag{C.4}$$

The solutions of the Helmholtz equation (C.1) in the full-plane $\mathbb{R}^2$ are the so-called plane waves, which we take as the known incident field u_I. Up to an arbitrary multiplicative factor, they are given by

$$u_I(\boldsymbol{x}) = e^{i\boldsymbol{k}\cdot\boldsymbol{x}}, \qquad (\boldsymbol{k}\cdot\boldsymbol{k}) = k^2, \tag{C.5}$$

where the wave propagation vector $\boldsymbol{k}$ is taken such that $\boldsymbol{k} \in \mathbb{R}^2$ to obtain physically admissible waves which do not explode towards infinity. By considering a parametrization through the angle of incidence θ_I, for $0 \leq \theta_I < 2\pi$, we can express the wave propagation vector as $\boldsymbol{k} = (-k\cos\theta_I, -k\sin\theta_I)$. The plane waves can be thus also represented as

$$u_I(\boldsymbol{x}) = e^{-ik(x_1\cos\theta_I + x_2\sin\theta_I)}. \tag{C.6}$$

An outgoing radiation condition is also imposed for the scattered field u, which specifies its decaying behavior at infinity and eliminates the non-physical solutions, e.g., plane waves and ingoing waves from infinity. It is known as the Sommerfeld radiation condition and receives its name from the German theoretical physicist Arnold Johannes Wilhelm Sommerfeld (1868–1951). This radiation condition allows only outgoing waves, i.e., waves moving away from the obstacle, and therefore characterizes an outward energy flux. It is also closely related with causality and fixes the positive sense of time (cf. Terrasse & Abboud 2006). The described outgoing waves have bounded energy and are thus physically admissible. The Sommerfeld radiation condition is stated either as

$$\frac{\partial u}{\partial r} - iku = \mathcal{O}\left(\frac{1}{r}\right) \tag{C.7}$$

for $r = |\boldsymbol{x}|$, or, for some constant $C > 0$, by

$$\left|\frac{\partial u}{\partial r} - iku\right| \leq \frac{C}{r} \qquad \text{as } r \to \infty. \tag{C.8}$$

Alternatively it can be also expressed as

$$\lim_{r\to\infty} \sqrt{r}\left(\frac{\partial u}{\partial r} - iku\right) = 0, \tag{C.9}$$

or even as

$$\frac{\partial u}{\partial r} - iku = \mathcal{O}\left(\frac{1}{r^\alpha}\right) \qquad \text{for } \frac{1}{2} < \alpha < \frac{3}{2}. \tag{C.10}$$

Likewise, a weaker and more general formulation of this radiation condition is

$$\lim_{R\to\infty} \int_{S_R} \left|\frac{\partial u}{\partial r} - iku\right|^2 \mathrm{d}\gamma = 0, \tag{C.11}$$

where $S_R = \{\boldsymbol{x} \in \mathbb{R}^2 : |\boldsymbol{x}| = R\}$ is the circle of radius R that is centered at the origin. If the opposite sign is taken, then we obtain a radiation condition for ingoing waves, namely

$$\lim_{r\to\infty} \sqrt{r}\left(\frac{\partial u}{\partial r} + iku\right) = 0. \tag{C.12}$$

It describes ingoing waves of unbounded energy coming from infinity, which are not physically admissible and therefore not appropriate for our scattering problem. We remark that the correct sign for the ingoing and outgoing radiation conditions is determined exclusively by the chosen time convention. If we used the time convention $e^{i\omega t}$ instead of $e^{-i\omega t}$, then (C.12) would have been the outgoing radiation condition and (C.9) the ingoing one.

The perturbed full-plane impedance Helmholtz problem can be finally stated as

$$\begin{cases} \text{Find } u : \Omega_e \to \mathbb{C} \text{ such that} \\ \Delta u + k^2 u = 0 & \text{in } \Omega_e, \\ -\dfrac{\partial u}{\partial n} + Zu = f_z & \text{on } \Gamma, \\ \left|\dfrac{\partial u}{\partial r} - iku\right| \leq \dfrac{C}{r} & \text{as } r \to \infty. \end{cases} \tag{C.13}$$

C.3 Green's function

The Green's function represents the response of the unperturbed system (without an obstacle) to a Dirac mass. It corresponds to a function G, which depends on a fixed source point $\boldsymbol{x} \in \mathbb{R}^2$ and an observation point $\boldsymbol{y} \in \mathbb{R}^2$. The Green's function is computed in the sense of distributions for the variable $\boldsymbol{y}$ in the full-plane $\mathbb{R}^2$ by placing at the right-hand side of the Helmholtz equation a Dirac mass $\delta_{\boldsymbol{x}}$, centered at the point $\boldsymbol{x}$. It is therefore a solution $G(\boldsymbol{x}, \cdot) : \mathbb{R}^2 \to \mathbb{C}$ for the radiation problem of a point source, namely

$$\Delta_{\boldsymbol{y}} G(\boldsymbol{x}, \boldsymbol{y}) + k^2 G(\boldsymbol{x}, \boldsymbol{y}) = \delta_{\boldsymbol{x}}(\boldsymbol{y}) \qquad \text{in } \mathcal{D}'(\mathbb{R}^2). \tag{C.14}$$

The solution of this equation is not unique, and therefore its behavior at infinity has to be specified. For this purpose we impose on the Green's function also the outgoing radiation condition (C.8).

Due to the radial symmetry of the problem (C.14), it is natural to look for solutions in the form $G = G(r)$, where $r = |\boldsymbol{y} - \boldsymbol{x}|$. By considering only the radial component, the

Helmholtz equation in $\mathbb{R}^2$ becomes

$$\frac{1}{r}\frac{\mathrm{d}}{\mathrm{d}r}\left(r\frac{\mathrm{d}G}{\mathrm{d}r}\right)+k^2G=0, \qquad r>0. \tag{C.15}$$

Replacing now $z=kr$ and considering $\psi(z)=G(r)$ yields $\frac{\mathrm{d}G}{\mathrm{d}r}=k\frac{\mathrm{d}\psi}{\mathrm{d}z}$ and consequently

$$\frac{k^2}{z}\left(z\frac{\mathrm{d}^2\psi}{\mathrm{d}z^2}+\frac{\mathrm{d}\psi}{\mathrm{d}z}\right)+k^2\psi=0, \tag{C.16}$$

which is equivalent to the zeroth order Bessel differential equation (vid. Subsection A.2.4)

$$z^2\frac{\mathrm{d}^2\psi}{\mathrm{d}z^2}+z\frac{\mathrm{d}\psi}{\mathrm{d}z}+z^2\psi=0. \tag{C.17}$$

Independent solutions for this equation are the zeroth order Bessel functions of the first and second kinds, $J_0(z)$ and $Y_0(z)$, and equally the zeroth order Hankel functions of the first and second kinds, $H_0^{(1)}(z)$ and $H_0^{(2)}(z)$. The latter satisfy respectively the outgoing and ingoing radiation conditions and behave for small arguments, as $z\to 0$, like

$$H_0^{(1)}(z)\sim\frac{2i}{\pi}\ln(z), \qquad H_0^{(2)}(z)\sim-\frac{2i}{\pi}\ln(z). \tag{C.18}$$

For large arguments, as $|z|\to\infty$, they behave like

$$H_0^{(1)}(z)\sim\sqrt{\frac{2}{\pi z}}e^{i\left(z-\frac{\pi}{4}\right)}, \qquad H_0^{(2)}(z)\sim\sqrt{\frac{2}{\pi z}}e^{-i\left(z-\frac{\pi}{4}\right)}. \tag{C.19}$$

Thus the solution of (C.17) is given by

$$\psi(z)=\alpha H_0^{(1)}(z)+\beta H_0^{(2)}(z), \qquad \alpha,\beta\in\mathbb{C}, \tag{C.20}$$

and consequently

$$G(r)=\alpha H_0^{(1)}(kr)+\beta H_0^{(2)}(kr), \qquad \alpha,\beta\in\mathbb{C}. \tag{C.21}$$

An outgoing wave behavior for the Green's function implies that $\beta=0$, due (C.8). We know from (C.18) that the singularity of the Green's function is of logarithmic type. The multiplicative constant α can be thus determined in the same way as for the Green's function of the Laplace equation in (B.20) by means of a computation in the sense of distributions for (C.14). The unique radial outgoing fundamental solution of the Helmholtz equation turns out to be

$$G(r)=-\frac{i}{4}H_0^{(1)}(kr). \tag{C.22}$$

The Green's function for outgoing waves is then finally given by

$$G(\boldsymbol{x},\boldsymbol{y})=-\frac{i}{4}H_0^{(1)}\big(k|\boldsymbol{y}-\boldsymbol{x}|\big). \tag{C.23}$$

We remark that the Green's function for ingoing waves would have been

$$G(\boldsymbol{x},\boldsymbol{y})=\frac{i}{4}H_0^{(2)}\big(k|\boldsymbol{y}-\boldsymbol{x}|\big). \tag{C.24}$$

To compute the derivatives of the Green's function we require some additional properties of Hankel functions. It holds that

$$\frac{\mathrm{d}}{\mathrm{d}z}H_0^{(1)}(z) = -H_1^{(1)}(z), \qquad \frac{\mathrm{d}}{\mathrm{d}z}H_0^{(2)}(z) = -H_1^{(2)}(z), \tag{C.25}$$

and

$$\frac{\mathrm{d}}{\mathrm{d}z}H_1^{(1)}(z) = H_0^{(1)}(z) - \frac{1}{z}H_1^{(1)}(z), \qquad \frac{\mathrm{d}}{\mathrm{d}z}H_1^{(2)}(z) = H_0^{(2)}(z) - \frac{1}{z}H_1^{(2)}(z), \tag{C.26}$$

where $H_1^{(1)}(z)$ and $H_1^{(2)}(z)$ denote the first order Hankel functions of the first and second kinds, respectively. For small arguments, as $z \to 0$, they behave like

$$H_1^{(1)}(z) \sim -\frac{2i}{\pi z}, \qquad H_1^{(2)}(z) \sim \frac{2i}{\pi z}, \tag{C.27}$$

and for large arguments, as $|z| \to \infty$, they behave like

$$H_1^{(1)}(z) \sim \sqrt{\frac{2}{\pi z}}e^{i\left(z-\frac{3\pi}{4}\right)}, \qquad H_1^{(2)}(z) \sim \sqrt{\frac{2}{\pi z}}e^{-i\left(z-\frac{3\pi}{4}\right)}. \tag{C.28}$$

The gradient of the Green's function (C.23) is therefore given by

$$\nabla_{\boldsymbol{y}} G(\boldsymbol{x},\boldsymbol{y}) = \frac{ik}{4}H_1^{(1)}\big(k|\boldsymbol{y}-\boldsymbol{x}|\big)\frac{\boldsymbol{y}-\boldsymbol{x}}{|\boldsymbol{y}-\boldsymbol{x}|}, \tag{C.29}$$

and the gradient with respect to the $\boldsymbol{x}$ variable by

$$\nabla_{\boldsymbol{x}} G(\boldsymbol{x},\boldsymbol{y}) = \frac{ik}{4}H_1^{(1)}\big(k|\boldsymbol{x}-\boldsymbol{y}|\big)\frac{\boldsymbol{x}-\boldsymbol{y}}{|\boldsymbol{x}-\boldsymbol{y}|}. \tag{C.30}$$

The double-gradient matrix is given by

$$\begin{aligned}\nabla_{\boldsymbol{x}}\nabla_{\boldsymbol{y}} G(\boldsymbol{x},\boldsymbol{y}) = \frac{ik}{4}H_1^{(1)}\big(k|\boldsymbol{x}-\boldsymbol{y}|\big)\left(-\frac{\boldsymbol{I}}{|\boldsymbol{x}-\boldsymbol{y}|} + 2\frac{(\boldsymbol{x}-\boldsymbol{y})\otimes(\boldsymbol{x}-\boldsymbol{y})}{|\boldsymbol{x}-\boldsymbol{y}|^3}\right)\\ - \frac{ik^2}{4}H_0^{(1)}\big(k|\boldsymbol{x}-\boldsymbol{y}|\big)\frac{(\boldsymbol{x}-\boldsymbol{y})\otimes(\boldsymbol{x}-\boldsymbol{y})}{|\boldsymbol{x}-\boldsymbol{y}|^2},\end{aligned} \tag{C.31}$$

where $\boldsymbol{I}$ denotes a 2×2 identity matrix and where $\otimes$ denotes the dyadic or outer product of two vectors, which results in a matrix and is defined in (A.573).

We note that the Green's function (C.23) is symmetric in the sense that

$$G(\boldsymbol{x},\boldsymbol{y}) = G(\boldsymbol{y},\boldsymbol{x}), \tag{C.32}$$

and it fulfills similarly

$$\nabla_{\boldsymbol{y}} G(\boldsymbol{x},\boldsymbol{y}) = \nabla_{\boldsymbol{y}} G(\boldsymbol{y},\boldsymbol{x}) = -\nabla_{\boldsymbol{x}} G(\boldsymbol{x},\boldsymbol{y}) = -\nabla_{\boldsymbol{x}} G(\boldsymbol{y},\boldsymbol{x}), \tag{C.33}$$

and

$$\nabla_{\boldsymbol{x}}\nabla_{\boldsymbol{y}} G(\boldsymbol{x},\boldsymbol{y}) = \nabla_{\boldsymbol{y}}\nabla_{\boldsymbol{x}} G(\boldsymbol{x},\boldsymbol{y}) = \nabla_{\boldsymbol{x}}\nabla_{\boldsymbol{y}} G(\boldsymbol{y},\boldsymbol{x}) = \nabla_{\boldsymbol{y}}\nabla_{\boldsymbol{x}} G(\boldsymbol{y},\boldsymbol{x}). \tag{C.34}$$

Furthermore, due the exponential decrease of the Hankel functions at infinity, we observe that the expression (C.23) of the Green's function for outgoing waves is still valid if a complex wave number $k \in \mathbb{C}$ such that $\mathfrak{Im}\{k\} > 0$ is used, which holds also for its derivatives (C.29), (C.30), and (C.31). In the case of ingoing waves, the expression (C.24)

and its derivatives are valid if a complex wave number $k \in \mathbb{C}$ now such that $\mathfrak{Im}\{k\} < 0$ is taken into account.

On the account of performing the numerical evaluation of the Hankel functions, for real and complex arguments, we mention the polynomial approximations described in Abramowitz & Stegun (1972) and Newman (1984*a*), and the algorithms developed by Amos (1986, 1990*c*, 1995) and Morris (1993).

C.4 Far field of the Green's function

The far field of the Green's function describes its asymptotic behavior at infinity, i.e., when $|\boldsymbol{x}| \to \infty$ and assuming that $\boldsymbol{y}$ is fixed. In this case and due (C.19), we have that

$$H_0^{(1)}\big(k|\boldsymbol{x}-\boldsymbol{y}|\big) \sim e^{-i\pi/4}\sqrt{\frac{2}{\pi k}}\frac{e^{ik|\boldsymbol{x}-\boldsymbol{y}|}}{\sqrt{|\boldsymbol{x}-\boldsymbol{y}|}}. \tag{C.35}$$

By using a Taylor expansion we obtain that

$$|\boldsymbol{x}-\boldsymbol{y}| = |\boldsymbol{x}|\left(1 - 2\,\frac{\boldsymbol{y}\cdot\boldsymbol{x}}{|\boldsymbol{x}|^2} + \frac{|\boldsymbol{y}|^2}{|\boldsymbol{x}|^2}\right)^{1/2} = |\boldsymbol{x}| - \frac{\boldsymbol{y}\cdot\boldsymbol{x}}{|\boldsymbol{x}|} + \mathcal{O}\left(\frac{1}{|\boldsymbol{x}|}\right). \tag{C.36}$$

A similar expansion yields

$$\frac{1}{\sqrt{|\boldsymbol{x}-\boldsymbol{y}|}} = \frac{1}{\sqrt{|\boldsymbol{x}|}} + \mathcal{O}\left(\frac{1}{|\boldsymbol{x}|^{3/2}}\right), \tag{C.37}$$

and we have also that

$$e^{ik|\boldsymbol{x}-\boldsymbol{y}|} = e^{ik|\boldsymbol{x}|}e^{-ik\boldsymbol{y}\cdot\boldsymbol{x}/|\boldsymbol{x}|}\left(1 + \mathcal{O}\left(\frac{1}{|\boldsymbol{x}|}\right)\right). \tag{C.38}$$

We express the point $\boldsymbol{x}$ as $\boldsymbol{x} = |\boldsymbol{x}|\,\hat{\boldsymbol{x}}$, being $\hat{\boldsymbol{x}}$ a unitary vector. The far field of the Green's function, as $|\boldsymbol{x}| \to \infty$, is thus given by

$$G^{ff}(\boldsymbol{x},\boldsymbol{y}) = -\frac{e^{i\pi/4}}{\sqrt{8\pi k}}\frac{e^{ik|\boldsymbol{x}|}}{\sqrt{|\boldsymbol{x}|}}e^{-ik\hat{\boldsymbol{x}}\cdot\boldsymbol{y}}. \tag{C.39}$$

Similarly, as $|\boldsymbol{x}| \to \infty$, we have for its gradient with respect to $\boldsymbol{y}$, that

$$\nabla_{\boldsymbol{y}} G^{ff}(\boldsymbol{x},\boldsymbol{y}) = i\,e^{i\pi/4}\sqrt{\frac{k}{8\pi}}\frac{e^{ik|\boldsymbol{x}|}}{\sqrt{|\boldsymbol{x}|}}e^{-ik\hat{\boldsymbol{x}}\cdot\boldsymbol{y}}\,\hat{\boldsymbol{x}}, \tag{C.40}$$

for its gradient with respect to $\boldsymbol{x}$, that

$$\nabla_{\boldsymbol{x}} G^{ff}(\boldsymbol{x},\boldsymbol{y}) = -i\,e^{i\pi/4}\sqrt{\frac{k}{8\pi}}\frac{e^{ik|\boldsymbol{x}|}}{\sqrt{|\boldsymbol{x}|}}e^{-ik\hat{\boldsymbol{x}}\cdot\boldsymbol{y}}\,\hat{\boldsymbol{x}}, \tag{C.41}$$

and for its double-gradient matrix, that

$$\nabla_{\boldsymbol{x}}\nabla_{\boldsymbol{y}} G^{ff}(\boldsymbol{x},\boldsymbol{y}) = -e^{i\pi/4}\sqrt{\frac{k^3}{8\pi}}\frac{e^{ik|\boldsymbol{x}|}}{\sqrt{|\boldsymbol{x}|}}e^{-ik\hat{\boldsymbol{x}}\cdot\boldsymbol{y}}\,(\hat{\boldsymbol{x}}\otimes\hat{\boldsymbol{x}}). \tag{C.42}$$

We remark that these far fields are still valid if a complex wave number $k \in \mathbb{C}$ such that $\mathfrak{Im}\{k\} > 0$ is used, in which case the appearing complex square root is taken in such a way that its real part is nonnegative.

C.5 Transmission problem

We are interested in expressing the solution u of the direct scattering problem (C.13) by means of an integral representation formula over the boundary Γ. To study this kind of representations, the differential problem defined on Ω_e is extended as a transmission problem defined now on the whole plane $\mathbb{R}^2$ by combining (C.13) with a corresponding interior problem defined on Ω_i. For the transmission problem, which specifies jump conditions over the boundary Γ, a general integral representation can be developed, and the particular integral representations of interest are then established by the specific choice of the corresponding interior problem.

A transmission problem is then a differential problem for which the jump conditions of the solution field, rather than boundary conditions, are specified on the boundary Γ. As shown in Figure C.1, we consider the exterior domain Ω_e and the interior domain Ω_i, taking the unit normal $\boldsymbol{n}$ pointing towards Ω_i. We search now a solution u defined in $\Omega_e \cup \Omega_i$, and use the notation $u_e = u|_{\Omega_e}$ and $u_i = u|_{\Omega_i}$. We define the jumps of the traces of u on both sides of the boundary Γ as

$$[u] = u_e - u_i \qquad \text{and} \qquad \left[\frac{\partial u}{\partial n}\right] = \frac{\partial u_e}{\partial n} - \frac{\partial u_i}{\partial n}. \tag{C.43}$$

The transmission problem is now given by

$$\begin{cases} \text{Find } u : \Omega_e \cup \Omega_i \to \mathbb{C} \text{ such that} \\ \Delta u + k^2 u = 0 \qquad \text{in } \ \Omega_e \cup \Omega_i, \\ [u] = \mu \qquad\qquad \text{on } \ \Gamma, \\ \left[\dfrac{\partial u}{\partial n}\right] = \nu \qquad \text{on } \ \Gamma, \\ \text{+ Outgoing radiation condition as } |\boldsymbol{x}| \to \infty, \end{cases} \tag{C.44}$$

where $\mu, \nu : \Gamma \to \mathbb{C}$ are known functions. The outgoing radiation condition is still (C.8), and it is required to ensure uniqueness of the solution.

C.6 Integral representations and equations

C.6.1 Integral representation

To develop for the solution u an integral representation formula over the boundary Γ, we define by $\Omega_{R,\varepsilon}$ the domain $\Omega_e \cup \Omega_i$ without the ball B_ε of radius $\varepsilon > 0$ centered at the point $\boldsymbol{x} \in \Omega_e \cup \Omega_i$, and truncated at infinity by the ball B_R of radius $R > 0$ centered at the origin. We consider that the ball B_ε is entirely contained either in Ω_e or in Ω_i, depending

on the location of its center $\boldsymbol{x}$. Therefore, as shown in Figure C.2, we have that

$$\Omega_{R,\varepsilon} = \big((\Omega_e \cup \Omega_i) \cap B_R\big) \setminus \overline{B_\varepsilon} \qquad \text{and} \qquad \Omega_R = (\Omega_e \cup \Omega_i) \cap B_R, \tag{C.45}$$

where

$$B_R = \{\boldsymbol{y} \in \mathbb{R}^2 : \, |\boldsymbol{y}| < R\} \qquad \text{and} \qquad B_\varepsilon = \{\boldsymbol{y} \in \mathbb{R}^2 : \, |\boldsymbol{y} - \boldsymbol{x}| < \varepsilon\}. \tag{C.46}$$

We consider similarly the boundaries of the balls

$$S_R = \{\boldsymbol{y} \in \mathbb{R}^2 : \, |\boldsymbol{y}| = R\} \qquad \text{and} \qquad S_\varepsilon = \{\boldsymbol{y} \in \mathbb{R}^2 : \, |\boldsymbol{y} - \boldsymbol{x}| = \varepsilon\}. \tag{C.47}$$

The idea is to retrieve the domain $\Omega_e \cup \Omega_i$ at the end when the limits $R \to \infty$ and $\varepsilon \to 0$ are taken for the truncated domains $\Omega_{R,\varepsilon}$ and Ω_R.

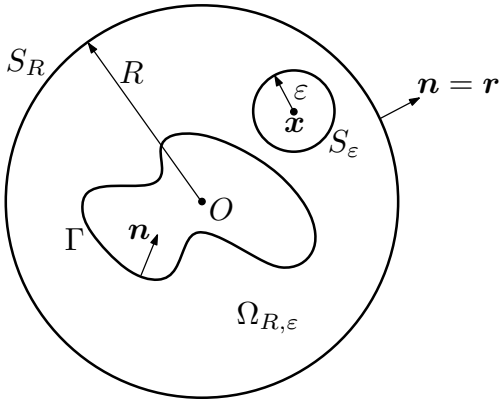

FIGURE C.2. Truncated domain $\Omega_{R,\varepsilon}$ for $\boldsymbol{x} \in \Omega_e \cup \Omega_i$.

Let us analyze first the asymptotic decaying behavior of the solution u, which satisfies the Helmholtz equation and the Sommerfeld radiation condition. For more generality, we assume here that the wave number k ($\neq 0$) is complex and such that $\mathfrak{Im}\{k\} \geq 0$. We consider the weakest form of the radiation condition, namely (C.11), and develop

$$\int_{S_R} \left| \frac{\partial u}{\partial r} - iku \right|^2 \mathrm{d}\gamma = \int_{S_R} \left[\left| \frac{\partial u}{\partial r} \right|^2 + |k|^2 |u|^2 + 2\, \mathfrak{Im} \left\{ ku \frac{\partial \bar{u}}{\partial r} \right\} \right] \mathrm{d}\gamma. \tag{C.48}$$

From the divergence theorem (A.614) applied on the truncated domain Ω_R and considering the complex conjugated Helmholtz equation we have

$$\begin{aligned} k \int_{S_R} u \frac{\partial \bar{u}}{\partial r} \, \mathrm{d}\gamma + k \int_\Gamma u \frac{\partial \bar{u}}{\partial n} \, \mathrm{d}\gamma &= k \int_{\Omega_R} \mathrm{div}(u \nabla \bar{u}) \, \mathrm{d}\boldsymbol{x} \\ &= k \int_{\Omega_R} |\nabla u|^2 \, \mathrm{d}\boldsymbol{x} - k\bar{k}^2 \int_{\Omega_R} |u|^2 \, \mathrm{d}\boldsymbol{x}. \end{aligned} \tag{C.49}$$

Replacing the imaginary part of (C.49) in (C.48) and taking the limit as $R \to \infty$, yields

$$\lim_{R\to\infty}\left[\int_{S_R}\left(\left|\frac{\partial u}{\partial r}\right|^2+|k|^2|u|^2\right)\mathrm{d}\gamma+2\,\mathfrak{Im}\{k\}\int_{\Omega_R}\left(|\nabla u|^2+|k|^2|u|^2\right)\mathrm{d}\boldsymbol{x}\right]$$
$$=2\,\mathfrak{Im}\left\{k\int_\Gamma u\frac{\partial\bar{u}}{\partial n}\,\mathrm{d}\gamma\right\}. \tag{C.50}$$

Since the right-hand side is finite and since the left-hand side is nonnegative, we see that

$$\int_{S_R}|u|^2\,\mathrm{d}\gamma=\mathcal{O}(1)\qquad\text{and}\qquad\int_{S_R}\left|\frac{\partial u}{\partial r}\right|^2\mathrm{d}\gamma=\mathcal{O}(1)\qquad\text{as}\;\;R\to\infty, \tag{C.51}$$

and therefore it holds for a great value of $r=|\boldsymbol{x}|$ that

$$u=\mathcal{O}\left(\frac{1}{\sqrt{r}}\right)\qquad\text{and}\qquad|\nabla u|=\mathcal{O}\left(\frac{1}{\sqrt{r}}\right). \tag{C.52}$$

We apply now Green's second integral theorem (A.613) to the functions u and $G(\boldsymbol{x},\cdot)$ in the bounded domain $\Omega_{R,\varepsilon}$, by subtracting their respective Helmholtz equations, yielding

$$\begin{aligned}0&=\int_{\Omega_{R,\varepsilon}}\big(u(\boldsymbol{y})\Delta_{\boldsymbol{y}}G(\boldsymbol{x},\boldsymbol{y})-G(\boldsymbol{x},\boldsymbol{y})\Delta u(\boldsymbol{y})\big)\mathrm{d}\boldsymbol{y}\\&=\int_{S_R}\left(u(\boldsymbol{y})\frac{\partial G}{\partial r_{\boldsymbol{y}}}(\boldsymbol{x},\boldsymbol{y})-G(\boldsymbol{x},\boldsymbol{y})\frac{\partial u}{\partial r}(\boldsymbol{y})\right)\mathrm{d}\gamma(\boldsymbol{y})\\&-\int_{S_\varepsilon}\left(u(\boldsymbol{y})\frac{\partial G}{\partial r_{\boldsymbol{y}}}(\boldsymbol{x},\boldsymbol{y})-G(\boldsymbol{x},\boldsymbol{y})\frac{\partial u}{\partial r}(\boldsymbol{y})\right)\mathrm{d}\gamma(\boldsymbol{y})\\&+\int_\Gamma\left([u](\boldsymbol{y})\frac{\partial G}{\partial n_{\boldsymbol{y}}}(\boldsymbol{x},\boldsymbol{y})-G(\boldsymbol{x},\boldsymbol{y})\left[\frac{\partial u}{\partial n}\right](\boldsymbol{y})\right)\mathrm{d}\gamma(\boldsymbol{y}).\end{aligned} \tag{C.53}$$

The integral on S_R can be rewritten as

$$\int_{S_R}\left[u(\boldsymbol{y})\left(\frac{\partial G}{\partial r_{\boldsymbol{y}}}(\boldsymbol{x},\boldsymbol{y})-ikG(\boldsymbol{x},\boldsymbol{y})\right)-G(\boldsymbol{x},\boldsymbol{y})\left(\frac{\partial u}{\partial r}(\boldsymbol{y})-iku(\boldsymbol{y})\right)\right]\mathrm{d}\gamma(\boldsymbol{y}), \tag{C.54}$$

which for R large enough and due the radiation condition (C.8) tends to zero, since

$$\left|\int_{S_R}u(\boldsymbol{y})\left(\frac{\partial G}{\partial r_{\boldsymbol{y}}}(\boldsymbol{x},\boldsymbol{y})-ikG(\boldsymbol{x},\boldsymbol{y})\right)\mathrm{d}\gamma(\boldsymbol{y})\right|\le\frac{C}{\sqrt{R}}, \tag{C.55}$$

and

$$\left|\int_{S_R}G(\boldsymbol{x},\boldsymbol{y})\left(\frac{\partial u}{\partial r}(\boldsymbol{y})-iku(\boldsymbol{y})\right)\mathrm{d}\gamma(\boldsymbol{y})\right|\le\frac{C}{\sqrt{R}}, \tag{C.56}$$

for some constants $C>0$. If the function u is regular enough in the ball B_ε, then the second term of the integral on S_ε, when $\varepsilon\to 0$ and due (C.23), is bounded by

$$\left|\int_{S_\varepsilon}G(\boldsymbol{x},\boldsymbol{y})\frac{\partial u}{\partial r}(\boldsymbol{y})\,\mathrm{d}\gamma(\boldsymbol{y})\right|\le\frac{\pi\varepsilon}{2}\left|H_0^{(1)}(k\varepsilon)\right|\sup_{\boldsymbol{y}\in B_\varepsilon}\left|\frac{\partial u}{\partial r}(\boldsymbol{y})\right|, \tag{C.57}$$

and tends to zero due (C.18). The regularity of u can be specified afterwards once the integral representation has been determined and generalized by means of density arguments.

The first integral term on S_ε can be decomposed as

$$\int_{S_\varepsilon} u(\boldsymbol{y})\frac{\partial G}{\partial r_{\boldsymbol{y}}}(\boldsymbol{x},\boldsymbol{y})\,\mathrm{d}\gamma(\boldsymbol{y}) = u(\boldsymbol{x})\int_{S_\varepsilon}\frac{\partial G}{\partial r_{\boldsymbol{y}}}(\boldsymbol{x},\boldsymbol{y})\,\mathrm{d}\gamma(\boldsymbol{y}) + \int_{S_\varepsilon}\frac{\partial G}{\partial r_{\boldsymbol{y}}}(\boldsymbol{x},\boldsymbol{y})\big(u(\boldsymbol{y})-u(\boldsymbol{x})\big)\,\mathrm{d}\gamma(\boldsymbol{y}), \tag{C.58}$$

For the first term in the right-hand side of (C.58), by replacing (C.29), we have that

$$\int_{S_\varepsilon}\frac{\partial G}{\partial r_{\boldsymbol{y}}}(\boldsymbol{x},\boldsymbol{y})\,\mathrm{d}\gamma(\boldsymbol{y}) = \frac{ik\pi\varepsilon}{2}H_1^{(1)}(k\varepsilon) \quad\xrightarrow[\varepsilon\to 0]{}\quad 1, \tag{C.59}$$

which tends towards one due (C.27), while the second term is bounded by

$$\left|\int_{S_\varepsilon}\big(u(\boldsymbol{y})-u(\boldsymbol{x})\big)\frac{\partial G}{\partial r_{\boldsymbol{y}}}(\boldsymbol{x},\boldsymbol{y})\,\mathrm{d}\gamma(\boldsymbol{y})\right| \le \frac{k\pi\varepsilon}{2}\left|H_1^{(1)}(k\varepsilon)\right| \sup_{\boldsymbol{y}\in B_\varepsilon}|u(\boldsymbol{y})-u(\boldsymbol{x})|, \tag{C.60}$$

which tends towards zero when $\varepsilon\to 0$.

In conclusion, when the limits $R\to\infty$ and $\varepsilon\to 0$ are taken in (C.53), then the following integral representation formula holds for the solution u of the transmission problem:

$$u(\boldsymbol{x}) = \int_\Gamma\left([u](\boldsymbol{y})\frac{\partial G}{\partial n_{\boldsymbol{y}}}(\boldsymbol{x},\boldsymbol{y}) - G(\boldsymbol{x},\boldsymbol{y})\left[\frac{\partial u}{\partial n}\right](\boldsymbol{y})\right)\mathrm{d}\gamma(\boldsymbol{y}), \qquad \boldsymbol{x}\in\Omega_e\cup\Omega_i. \tag{C.61}$$

We observe thus that if the values of the jump of u and of its normal derivative are known on Γ, then the transmission problem (C.44) is readily solved and its solution given explicitly by (C.61), which, in terms of μ and ν, becomes

$$u(\boldsymbol{x}) = \int_\Gamma\left(\mu(\boldsymbol{y})\frac{\partial G}{\partial n_{\boldsymbol{y}}}(\boldsymbol{x},\boldsymbol{y}) - G(\boldsymbol{x},\boldsymbol{y})\nu(\boldsymbol{y})\right)\mathrm{d}\gamma(\boldsymbol{y}), \qquad \boldsymbol{x}\in\Omega_e\cup\Omega_i. \tag{C.62}$$

To determine the values of the jumps, an adequate integral equation has to be developed, i.e., an equation whose unknowns are the traces of the solution on Γ.

An alternative way to demonstrate the integral representation (C.61) is to proceed in the sense of distributions, in the same way as done in Section B.6. Again we obtain the single layer potential

$$\left\{G * \left[\frac{\partial u}{\partial n}\right]\delta_\Gamma\right\}(\boldsymbol{x}) = \int_\Gamma G(\boldsymbol{x},\boldsymbol{y})\left[\frac{\partial u}{\partial n}\right](\boldsymbol{y})\,\mathrm{d}\gamma(\boldsymbol{y}) \tag{C.63}$$

associated with the distribution of sources $[\partial u/\partial n]\delta_\Gamma$, and the double layer potential

$$\left\{G * \frac{\partial}{\partial n}\big([u]\delta_\Gamma\big)\right\}(\boldsymbol{x}) = -\int_\Gamma\frac{\partial G}{\partial n_{\boldsymbol{y}}}(\boldsymbol{x},\boldsymbol{y})[u](\boldsymbol{y})\,\mathrm{d}\gamma(\boldsymbol{y}) \tag{C.64}$$

associated with the distribution of dipoles $\frac{\partial}{\partial n}([u]\delta_\Gamma)$. Combining properly (C.63) and (C.64) yields the desired integral representation (C.61).

We note that to obtain the gradient of the integral representation (C.61) we can pass directly the derivatives inside the integral, since there are no singularities if $\boldsymbol{x}\in\Omega_e\cup\Omega_i$. Therefore we have that

$$\nabla u(\boldsymbol{x}) = \int_\Gamma\left([u](\boldsymbol{y})\nabla_{\boldsymbol{x}}\frac{\partial G}{\partial n_{\boldsymbol{y}}}(\boldsymbol{x},\boldsymbol{y}) - \nabla_{\boldsymbol{x}}G(\boldsymbol{x},\boldsymbol{y})\left[\frac{\partial u}{\partial n}\right](\boldsymbol{y})\right)\mathrm{d}\gamma(\boldsymbol{y}). \tag{C.65}$$

C.6.2 Integral equations

To determine the values of the traces that conform the jumps for the transmission problem (C.44), an integral equation has to be developed. For this purpose we place the source point $\boldsymbol{x}$ on the boundary Γ and apply the same procedure as before for the integral representation (C.61), treating differently in (C.53) only the integrals on S_ε. The integrals on S_R still behave well and tend towards zero as $R \to \infty$. The Ball B_ε, though, is split in half into the two pieces $\Omega_e \cap B_\varepsilon$ and $\Omega_i \cap B_\varepsilon$, which are asymptotically separated by the tangent of the boundary if Γ is regular. Thus the associated integrals on S_ε give rise to a term $-(u_e(\boldsymbol{x}) + u_i(\boldsymbol{x}))/2$ instead of just $-u(\boldsymbol{x})$ as before. We must notice that in this case, the integrands associated with the boundary Γ admit an integrable singularity at the point $\boldsymbol{x}$. The desired integral equation related with (C.61) is then given by

$$\frac{u_e(\boldsymbol{x}) + u_i(\boldsymbol{x})}{2} = \int_\Gamma \left([u](\boldsymbol{y}) \frac{\partial G}{\partial n_{\boldsymbol{y}}}(\boldsymbol{x}, \boldsymbol{y}) - G(\boldsymbol{x}, \boldsymbol{y}) \left[\frac{\partial u}{\partial n} \right](\boldsymbol{y}) \right) \mathrm{d}\gamma(\boldsymbol{y}), \quad \boldsymbol{x} \in \Gamma. \quad \text{(C.66)}$$

By choosing adequately the boundary condition of the interior problem, and by considering also the boundary condition of the exterior problem and the jump definitions (C.43), this integral equation can be expressed in terms of only one unknown function on Γ. Thus, solving the problem (C.13) is equivalent to solve (C.66) and then replace the obtained solution in (C.61).

The integral equation holds only when the boundary Γ is regular (e.g., of class C^2). Otherwise, taking the limit $\varepsilon \to 0$ can no longer be well-defined and the result is false in general. In particular, if the boundary Γ has an angular point at $\boldsymbol{x} \in \Gamma$, then the left-hand side of the integral equation (C.66) is modified on that point according to the portion of the angle that remains inside Ω_e, in the same way as in (B.61).

Another integral equation can be also derived for the normal derivative of the solution u on the boundary Γ, by studying the jump properties of the single and double layer potentials. It is performed in the same manner as for the Laplace equation. If the boundary is regular at $\boldsymbol{x} \in \Gamma$, then it holds that

$$\frac{1}{2} \frac{\partial u_e}{\partial n}(\boldsymbol{x}) + \frac{1}{2} \frac{\partial u_i}{\partial n}(\boldsymbol{x}) = \int_\Gamma \left([u](\boldsymbol{y}) \frac{\partial^2 G}{\partial n_{\boldsymbol{x}} \partial n_{\boldsymbol{y}}}(\boldsymbol{x}, \boldsymbol{y}) - \frac{\partial G}{\partial n_{\boldsymbol{x}}}(\boldsymbol{x}, \boldsymbol{y}) \left[\frac{\partial u}{\partial n} \right](\boldsymbol{y}) \right) \mathrm{d}\gamma(\boldsymbol{y}). \quad \text{(C.67)}$$

This integral equation is modified correspondingly if $\boldsymbol{x}$ is an angular point.

C.6.3 Integral kernels

In the same manner as for the Laplace equation, the integral kernels G, $\partial G / \partial n_{\boldsymbol{y}}$, and $\partial G / \partial n_{\boldsymbol{x}}$ are weakly singular, and thus integrable, whereas the kernel $\partial^2 G / \partial n_{\boldsymbol{x}} \partial n_{\boldsymbol{y}}$ is not integrable and therefore hypersingular.

The kernel G defined in (C.23) has the same logarithmic singularity as the Laplace equation, namely

$$G(\boldsymbol{x}, \boldsymbol{y}) \sim \frac{1}{2\pi} \ln |\boldsymbol{x} - \boldsymbol{y}| \qquad \text{as } \boldsymbol{x} \to \boldsymbol{y}. \quad \text{(C.68)}$$

It fulfills therefore (B.64) for any $\lambda > 0$. The kernels $\partial G / \partial n_{\boldsymbol{y}}$ and $\partial G / \partial n_{\boldsymbol{x}}$ are less singular along Γ than they appear at first sight, due the regularizing effect of the normal

derivatives. They are given respectively by

$$\frac{\partial G}{\partial n_{\boldsymbol{y}}}(\boldsymbol{x},\boldsymbol{y}) = \frac{ik}{4} H_1^{(1)}\big(k|\boldsymbol{y}-\boldsymbol{x}|\big)\frac{(\boldsymbol{y}-\boldsymbol{x})\cdot\boldsymbol{n}_{\boldsymbol{y}}}{|\boldsymbol{y}-\boldsymbol{x}|}, \tag{C.69}$$

and

$$\frac{\partial G}{\partial n_{\boldsymbol{x}}}(\boldsymbol{x},\boldsymbol{y}) = \frac{ik}{4} H_1^{(1)}\big(k|\boldsymbol{x}-\boldsymbol{y}|\big)\frac{(\boldsymbol{x}-\boldsymbol{y})\cdot\boldsymbol{n}_{\boldsymbol{x}}}{|\boldsymbol{x}-\boldsymbol{y}|}, \tag{C.70}$$

and their singularities, as $\boldsymbol{x} \to \boldsymbol{y}$ for $\boldsymbol{x}, \boldsymbol{y} \in \Gamma$, adopt the form

$$\frac{\partial G}{\partial n_{\boldsymbol{y}}}(\boldsymbol{x},\boldsymbol{y}) \sim \frac{(\boldsymbol{y}-\boldsymbol{x})\cdot\boldsymbol{n}_{\boldsymbol{y}}}{2\pi|\boldsymbol{y}-\boldsymbol{x}|^2} \qquad \text{and} \qquad \frac{\partial G}{\partial n_{\boldsymbol{x}}}(\boldsymbol{x},\boldsymbol{y}) \sim \frac{(\boldsymbol{x}-\boldsymbol{y})\cdot\boldsymbol{n}_{\boldsymbol{x}}}{2\pi|\boldsymbol{x}-\boldsymbol{y}|^2}. \tag{C.71}$$

Since the singularities are the same as for the Laplace equation, the estimates (B.70) and (B.71) continue to hold. Therefore we have that

$$\frac{\partial G}{\partial n_{\boldsymbol{y}}}(\boldsymbol{x},\boldsymbol{y}) = \mathcal{O}(1) \qquad \text{and} \qquad \frac{\partial G}{\partial n_{\boldsymbol{x}}}(\boldsymbol{x},\boldsymbol{y}) = \mathcal{O}(1). \tag{C.72}$$

The singularities of the kernels $\partial G/\partial n_{\boldsymbol{y}}$ and $\partial G/\partial n_{\boldsymbol{x}}$ along Γ are thus only apparent and can be repaired by redefining the value of these kernels at $\boldsymbol{y} = \boldsymbol{x}$.

The kernel $\partial^2 G/\partial n_{\boldsymbol{x}}\partial n_{\boldsymbol{y}}$, on the other hand, adopts the form

$$\begin{aligned}\frac{\partial^2 G}{\partial n_{\boldsymbol{x}}\partial n_{\boldsymbol{y}}}(\boldsymbol{x},\boldsymbol{y}) = \frac{ik}{4} H_1^{(1)}\big(k|\boldsymbol{x}-\boldsymbol{y}|\big)\left(-\frac{\boldsymbol{n}_{\boldsymbol{x}}\cdot\boldsymbol{n}_{\boldsymbol{y}}}{|\boldsymbol{x}-\boldsymbol{y}|} - 2\frac{\big((\boldsymbol{x}-\boldsymbol{y})\cdot\boldsymbol{n}_{\boldsymbol{x}}\big)\big((\boldsymbol{y}-\boldsymbol{x})\cdot\boldsymbol{n}_{\boldsymbol{y}}\big)}{|\boldsymbol{x}-\boldsymbol{y}|^3}\right)\\ + \frac{ik^2}{4} H_0^{(1)}\big(k|\boldsymbol{x}-\boldsymbol{y}|\big)\frac{\big((\boldsymbol{x}-\boldsymbol{y})\cdot\boldsymbol{n}_{\boldsymbol{x}}\big)\big((\boldsymbol{y}-\boldsymbol{x})\cdot\boldsymbol{n}_{\boldsymbol{y}}\big)}{|\boldsymbol{x}-\boldsymbol{y}|^2}.\end{aligned} \tag{C.73}$$

Its singularity, when $\boldsymbol{x} \to \boldsymbol{y}$ for $\boldsymbol{x}, \boldsymbol{y} \in \Gamma$, expresses itself as

$$\frac{\partial^2 G}{\partial n_{\boldsymbol{x}}\partial n_{\boldsymbol{y}}}(\boldsymbol{x},\boldsymbol{y}) \sim -\frac{\boldsymbol{n}_{\boldsymbol{x}}\cdot\boldsymbol{n}_{\boldsymbol{y}}}{2\pi|\boldsymbol{y}-\boldsymbol{x}|^2} - \frac{\big((\boldsymbol{x}-\boldsymbol{y})\cdot\boldsymbol{n}_{\boldsymbol{x}}\big)\big((\boldsymbol{y}-\boldsymbol{x})\cdot\boldsymbol{n}_{\boldsymbol{y}}\big)}{\pi|\boldsymbol{y}-\boldsymbol{x}|^4}. \tag{C.74}$$

The regularizing effect of the normal derivatives applies only to its second term, but not to the first. Hence this kernel is hypersingular, with $\lambda = 2$, and it holds that

$$\frac{\partial^2 G}{\partial n_{\boldsymbol{x}}\partial n_{\boldsymbol{y}}}(\boldsymbol{x},\boldsymbol{y}) = \mathcal{O}\left(\frac{1}{|\boldsymbol{y}-\boldsymbol{x}|^2}\right). \tag{C.75}$$

The kernel is no longer integrable and the associated integral operator has to be thus interpreted in some appropriate sense as a divergent integral (cf., e.g., Hsiao & Wendland 2008, Lenoir 2005, Nédélec 2001).

C.6.4 Boundary layer potentials

We regard now the jump properties on the boundary Γ of the boundary layer potentials that have appeared in our calculations. For the development of the integral representation (C.62) we already made acquaintance with the single and double layer potentials, which we define now more precisely for $\boldsymbol{x} \in \Omega_e \cup \Omega_i$ as the integral operators

$$\mathcal{S}\nu(\boldsymbol{x}) = \int_\Gamma G(\boldsymbol{x},\boldsymbol{y})\nu(\boldsymbol{y})\,\mathrm{d}\gamma(\boldsymbol{y}), \tag{C.76}$$

$$\mathcal{D}\mu(\boldsymbol{x}) = \int_\Gamma \frac{\partial G}{\partial n_{\boldsymbol{y}}}(\boldsymbol{x},\boldsymbol{y})\mu(\boldsymbol{y})\,\mathrm{d}\gamma(\boldsymbol{y}). \tag{C.77}$$

The integral representation (C.62) can be now stated in terms of the layer potentials as

$$u = \mathcal{D}\mu - \mathcal{S}\nu. \tag{C.78}$$

We remark that for any functions $\nu, \mu : \Gamma \to \mathbb{C}$ that are regular enough, the single and double layer potentials satisfy the Helmholtz equation, namely

$$(\Delta + k^2)\,\mathcal{S}\nu = 0 \qquad \text{in } \Omega_e \cup \Omega_i, \tag{C.79}$$

$$(\Delta + k^2)\,\mathcal{D}\mu = 0 \qquad \text{in } \Omega_e \cup \Omega_i. \tag{C.80}$$

For the integral equations (C.66) and (C.67), which are defined for $\boldsymbol{x} \in \Gamma$, we require the four boundary integral operators:

$$S\nu(\boldsymbol{x}) = \int_\Gamma G(\boldsymbol{x},\boldsymbol{y})\nu(\boldsymbol{y})\,\mathrm{d}\gamma(\boldsymbol{y}), \tag{C.81}$$

$$D\mu(\boldsymbol{x}) = \int_\Gamma \frac{\partial G}{\partial n_{\boldsymbol{y}}}(\boldsymbol{x},\boldsymbol{y})\mu(\boldsymbol{y})\,\mathrm{d}\gamma(\boldsymbol{y}), \tag{C.82}$$

$$D^*\nu(\boldsymbol{x}) = \int_\Gamma \frac{\partial G}{\partial n_{\boldsymbol{x}}}(\boldsymbol{x},\boldsymbol{y})\nu(\boldsymbol{y})\,\mathrm{d}\gamma(\boldsymbol{y}), \tag{C.83}$$

$$N\mu(\boldsymbol{x}) = \int_\Gamma \frac{\partial^2 G}{\partial n_{\boldsymbol{x}}\partial n_{\boldsymbol{y}}}(\boldsymbol{x},\boldsymbol{y})\mu(\boldsymbol{y})\,\mathrm{d}\gamma(\boldsymbol{y}). \tag{C.84}$$

The operator D^* is in fact the adjoint of the operator D. As we already mentioned, the kernel of the integral operator N defined in (C.84) is not integrable, yet we write it formally as an improper integral. An appropriate sense for this integral will be given below. The integral equations (C.66) and (C.67) can be now stated in terms of the integral operators as

$$\frac{1}{2}(u_e + u_i) = D\mu - S\nu, \tag{C.85}$$

$$\frac{1}{2}\left(\frac{\partial u_e}{\partial n} + \frac{\partial u_i}{\partial n}\right) = N\mu - D^*\nu. \tag{C.86}$$

These integral equations can be easily derived from the jump properties of the single and double layer potentials. The single layer potential (C.76) is continuous and its normal derivative has a jump of size $-\nu$ across Γ, i.e.,

$$\mathcal{S}\nu|_{\Omega_e} = S\nu = \mathcal{S}\nu|_{\Omega_i}, \tag{C.87}$$

$$\frac{\partial}{\partial n}\mathcal{S}\nu|_{\Omega_e} = \left(-\frac{1}{2} + D^*\right)\nu, \tag{C.88}$$

$$\frac{\partial}{\partial n}\mathcal{S}\nu|_{\Omega_i} = \left(\frac{1}{2} + D^*\right)\nu. \tag{C.89}$$

The double layer potential (C.77), on the other hand, has a jump of size μ across Γ and its normal derivative is continuous, namely

$$\mathcal{D}\mu|_{\Omega_e} = \left(\frac{1}{2} + D\right)\mu, \tag{C.90}$$

$$\mathcal{D}\mu|_{\Omega_i} = \left(-\frac{1}{2} + D\right)\mu, \tag{C.91}$$

$$\frac{\partial}{\partial n}\mathcal{D}\mu|_{\Omega_e} = N\mu = \frac{\partial}{\partial n}\mathcal{D}\mu|_{\Omega_i}. \tag{C.92}$$

The integral equation (C.85) is obtained directly either from (C.87) and (C.90), or from (C.87) and (C.91), by considering the appropriate trace of (C.78) and by defining the functions μ and ν as in (C.44). These three jump properties are easily proven by regarding the details of the proof for (C.66).

Similarly, the integral equation (C.86) for the normal derivative is obtained directly either from (C.88) and (C.92), or from (C.89) and (C.92), by considering the appropriate trace of the normal derivative of (C.78) and by defining again the functions μ and ν as in (C.44). The proof of the jump properties (C.88) and (C.89) is the same as for the Laplace equation, since the same singularities are involved, whereas the proof of (C.92) is similar, but with some differences, and is therefore replicated below.

a) Continuity of the normal derivative of the double layer potential

Differently as in the proof for the Laplace equation, in this case an additional term appears for the operator N, since it is the Helmholtz equation (C.80) that has to be considered in (B.104) and (B.105), yielding now for a test function $\varphi \in \mathcal{D}(\mathbb{R}^2)$ that

$$\left\langle \frac{\partial}{\partial n}\mathcal{D}\mu|_{\Omega_e},\, \varphi \right\rangle = \int_{\Omega_e} \nabla\mathcal{D}\mu(\boldsymbol{x}) \cdot \nabla\varphi(\boldsymbol{x})\,\mathrm{d}\boldsymbol{x} - k^2 \int_{\Omega_e} \mathcal{D}\mu(\boldsymbol{x})\,\varphi(\boldsymbol{x})\,\mathrm{d}\boldsymbol{x}, \tag{C.93}$$

$$\left\langle \frac{\partial}{\partial n}\mathcal{D}\mu|_{\Omega_i},\, \varphi \right\rangle = -\int_{\Omega_i} \nabla\mathcal{D}\mu(\boldsymbol{x}) \cdot \nabla\varphi(\boldsymbol{x})\,\mathrm{d}\boldsymbol{x} + k^2 \int_{\Omega_i} \mathcal{D}\mu(\boldsymbol{x})\,\varphi(\boldsymbol{x})\,\mathrm{d}\boldsymbol{x}. \tag{C.94}$$

From (A.588) and (C.33) we obtain the relation

$$\frac{\partial G}{\partial n_{\boldsymbol{y}}}(\boldsymbol{x},\boldsymbol{y}) = \boldsymbol{n}_{\boldsymbol{y}} \cdot \nabla_{\boldsymbol{y}} G(\boldsymbol{x},\boldsymbol{y}) = -\boldsymbol{n}_{\boldsymbol{y}} \cdot \nabla_{\boldsymbol{x}} G(\boldsymbol{x},\boldsymbol{y}) = -\operatorname{div}_{\boldsymbol{x}}\big(G(\boldsymbol{x},\boldsymbol{y})\boldsymbol{n}_{\boldsymbol{y}}\big). \tag{C.95}$$

Thus for the double layer potential (C.77) we have that

$$\mathcal{D}\mu(\boldsymbol{x}) = -\operatorname{div}\int_\Gamma G(\boldsymbol{x},\boldsymbol{y})\mu(\boldsymbol{y})\boldsymbol{n}_{\boldsymbol{y}}\,\mathrm{d}\gamma(\boldsymbol{y}) = -\operatorname{div}\mathcal{S}(\mu\,\boldsymbol{n}_{\boldsymbol{y}})(\boldsymbol{x}), \tag{C.96}$$

being its gradient given by

$$\nabla\mathcal{D}\mu(\boldsymbol{x}) = -\nabla\operatorname{div}\int_\Gamma G(\boldsymbol{x},\boldsymbol{y})\mu(\boldsymbol{y})\boldsymbol{n}_{\boldsymbol{y}}\,\mathrm{d}\gamma(\boldsymbol{y}). \tag{C.97}$$

From (A.589) we have that

$$\operatorname{curl}_{\boldsymbol{x}}\big(G(\boldsymbol{x},\boldsymbol{y})\boldsymbol{n}_{\boldsymbol{y}}\big) = \nabla_{\boldsymbol{x}} G(\boldsymbol{x},\boldsymbol{y}) \times \boldsymbol{n}_{\boldsymbol{y}}. \tag{C.98}$$

Hence, by considering (A.597), (C.80), and (C.98) in (C.97), we obtain that

$$\nabla\mathcal{D}\mu(\boldsymbol{x}) = \mathrm{Curl}\int_\Gamma \big(\boldsymbol{n_y}\times\nabla_{\boldsymbol{x}}G(\boldsymbol{x},\boldsymbol{y})\big)\mu(\boldsymbol{y})\,\mathrm{d}\gamma(\boldsymbol{y}) + k^2\int_\Gamma G(\boldsymbol{x},\boldsymbol{y})\mu(\boldsymbol{y})\boldsymbol{n_y}\,\mathrm{d}\gamma(\boldsymbol{y}). \quad \text{(C.99)}$$

From (C.33) and (A.659) we have that

$$\begin{aligned}\int_\Gamma \big(\boldsymbol{n_y}\times\nabla_{\boldsymbol{x}}G(\boldsymbol{x},\boldsymbol{y})\big)\mu(\boldsymbol{y})\,\mathrm{d}\gamma(\boldsymbol{y}) &= -\int_\Gamma \boldsymbol{n_y}\times\big(\nabla_{\boldsymbol{y}}G(\boldsymbol{x},\boldsymbol{y})\mu(\boldsymbol{y})\big)\,\mathrm{d}\gamma(\boldsymbol{y})\\ &= \int_\Gamma \boldsymbol{n_y}\times\big(G(\boldsymbol{x},\boldsymbol{y})\nabla\mu(\boldsymbol{y})\big)\,\mathrm{d}\gamma(\boldsymbol{y}), \qquad \text{(C.100)}\end{aligned}$$

and consequently

$$\nabla\mathcal{D}\mu(\boldsymbol{x}) = \mathrm{Curl}\int_\Gamma G(\boldsymbol{x},\boldsymbol{y})\big(\boldsymbol{n_y}\times\nabla\mu(\boldsymbol{y})\big)\,\mathrm{d}\gamma(\boldsymbol{y}) + k^2\int_\Gamma G(\boldsymbol{x},\boldsymbol{y})\mu(\boldsymbol{y})\boldsymbol{n_y}\,\mathrm{d}\gamma(\boldsymbol{y}). \quad \text{(C.101)}$$

Now, the first expression in (C.93), due (A.608), (A.619), and (C.101), is given by

$$\begin{aligned}\int_{\Omega_e}\nabla\mathcal{D}\mu(\boldsymbol{x})\cdot\nabla\varphi(\boldsymbol{x})\,\mathrm{d}\boldsymbol{x} = &-\int_\Gamma\int_\Gamma G(\boldsymbol{x},\boldsymbol{y})\big(\nabla\mu(\boldsymbol{y})\times\boldsymbol{n_y}\big)\big(\nabla\varphi(\boldsymbol{x})\times\boldsymbol{n_x}\big)\,\mathrm{d}\gamma(\boldsymbol{y})\,\mathrm{d}\gamma(\boldsymbol{x})\\ &+ k^2\int_{\Omega_e}\left(\int_\Gamma G(\boldsymbol{x},\boldsymbol{y})\mu(\boldsymbol{y})\boldsymbol{n_y}\,\mathrm{d}\gamma(\boldsymbol{y})\right)\cdot\nabla\varphi(\boldsymbol{x})\,\mathrm{d}\boldsymbol{x}. \quad \text{(C.102)}\end{aligned}$$

Applying (A.614) on the second term of (C.102) and considering (C.96), yields

$$\begin{aligned}\int_{\Omega_e}\nabla\mathcal{D}\mu(\boldsymbol{x})\cdot\nabla\varphi(\boldsymbol{x})\,\mathrm{d}\boldsymbol{x} = &-\int_\Gamma\int_\Gamma G(\boldsymbol{x},\boldsymbol{y})\big(\nabla\mu(\boldsymbol{y})\times\boldsymbol{n_y}\big)\big(\nabla\varphi(\boldsymbol{x})\times\boldsymbol{n_x}\big)\,\mathrm{d}\gamma(\boldsymbol{y})\,\mathrm{d}\gamma(\boldsymbol{x})\\ &+ k^2\int_{\Omega_e}\mathcal{D}\mu(\boldsymbol{x})\,\varphi(\boldsymbol{x})\,\mathrm{d}\boldsymbol{x} + \int_\Gamma\int_\Gamma G(\boldsymbol{x},\boldsymbol{y})\mu(\boldsymbol{y})\varphi(\boldsymbol{x})(\boldsymbol{n_y}\cdot\boldsymbol{n_x})\,\mathrm{d}\gamma(\boldsymbol{y})\,\mathrm{d}\gamma(\boldsymbol{x}). \quad \text{(C.103)}\end{aligned}$$

By replacing (C.103) in (C.93) we obtain finally that

$$\begin{aligned}\left\langle\frac{\partial}{\partial n}\mathcal{D}\mu|_{\Omega_e},\,\varphi\right\rangle = &-\int_\Gamma\int_\Gamma G(\boldsymbol{x},\boldsymbol{y})\big(\nabla\mu(\boldsymbol{y})\times\boldsymbol{n_y}\big)\big(\nabla\varphi(\boldsymbol{x})\times\boldsymbol{n_x}\big)\,\mathrm{d}\gamma(\boldsymbol{y})\,\mathrm{d}\gamma(\boldsymbol{x})\\ &+ k^2\int_\Gamma\int_\Gamma G(\boldsymbol{x},\boldsymbol{y})\mu(\boldsymbol{y})\varphi(\boldsymbol{x})(\boldsymbol{n_y}\cdot\boldsymbol{n_x})\,\mathrm{d}\gamma(\boldsymbol{y})\,\mathrm{d}\gamma(\boldsymbol{x}). \qquad \text{(C.104)}\end{aligned}$$

The analogous development for (C.94) yields

$$\begin{aligned}\left\langle\frac{\partial}{\partial n}\mathcal{D}\mu|_{\Omega_i},\,\varphi\right\rangle = &-\int_\Gamma\int_\Gamma G(\boldsymbol{x},\boldsymbol{y})\big(\nabla\mu(\boldsymbol{y})\times\boldsymbol{n_y}\big)\big(\nabla\varphi(\boldsymbol{x})\times\boldsymbol{n_x}\big)\,\mathrm{d}\gamma(\boldsymbol{y})\,\mathrm{d}\gamma(\boldsymbol{x})\\ &+ k^2\int_\Gamma\int_\Gamma G(\boldsymbol{x},\boldsymbol{y})\mu(\boldsymbol{y})\varphi(\boldsymbol{x})(\boldsymbol{n_y}\cdot\boldsymbol{n_x})\,\mathrm{d}\gamma(\boldsymbol{y})\,\mathrm{d}\gamma(\boldsymbol{x}). \qquad \text{(C.105)}\end{aligned}$$

This concludes the proof of (C.92), and shows that the integral operator (C.84) is properly defined in a weak sense for $\varphi\in\mathcal{D}(\mathbb{R}^2)$, instead of (B.115), by

$$\begin{aligned}\langle N\mu(\boldsymbol{x}),\,\varphi\rangle = &-\int_\Gamma\int_\Gamma G(\boldsymbol{x},\boldsymbol{y})\big(\nabla\mu(\boldsymbol{y})\times\boldsymbol{n_y}\big)\big(\nabla\varphi(\boldsymbol{x})\times\boldsymbol{n_x}\big)\,\mathrm{d}\gamma(\boldsymbol{y})\,\mathrm{d}\gamma(\boldsymbol{x})\\ &+ k^2\int_\Gamma\int_\Gamma G(\boldsymbol{x},\boldsymbol{y})\mu(\boldsymbol{y})\varphi(\boldsymbol{x})(\boldsymbol{n_y}\cdot\boldsymbol{n_x})\,\mathrm{d}\gamma(\boldsymbol{y})\,\mathrm{d}\gamma(\boldsymbol{x}). \qquad \text{(C.106)}\end{aligned}$$

C.6.5 Alternatives for integral representations and equations

By taking into account the transmission problem (C.44), its integral representation formula (C.61), and its integral equations (C.66) and (C.67), several particular alternatives for integral representations and equations of the exterior problem (C.13) can be developed. The way to perform this is to extend properly the exterior problem towards the interior domain Ω_i, either by specifying explicitly this extension or by defining an associated interior problem, so as to become the desired jump properties across Γ. The extension has to satisfy the Helmholtz equation (C.1) in Ω_i and a boundary condition that corresponds adequately to the impedance boundary condition (C.3). The obtained system of integral representations and equations allows finally to solve the exterior problem (C.13), by using the solution of the integral equation in the integral representation formula.

a) Extension by zero

An extension by zero towards the interior domain Ω_i implies that

$$u_i = 0 \qquad \text{in } \Omega_i. \tag{C.107}$$

The jumps over Γ are characterized in this case by

$$[u] = u_e = \mu, \tag{C.108}$$

$$\left[\frac{\partial u}{\partial n}\right] = \frac{\partial u_e}{\partial n} = Zu_e - f_z = Z\mu - f_z, \tag{C.109}$$

where $\mu : \Gamma \to \mathbb{C}$ is a function to be determined.

An integral representation formula of the solution, for $\boldsymbol{x} \in \Omega_e \cup \Omega_i$, is given by

$$u(\boldsymbol{x}) = \int_\Gamma \left(\frac{\partial G}{\partial n_{\boldsymbol{y}}}(\boldsymbol{x},\boldsymbol{y}) - Z(\boldsymbol{y})G(\boldsymbol{x},\boldsymbol{y})\right)\mu(\boldsymbol{y})\,\mathrm{d}\gamma(\boldsymbol{y}) + \int_\Gamma G(\boldsymbol{x},\boldsymbol{y})f_z(\boldsymbol{y})\,\mathrm{d}\gamma(\boldsymbol{y}). \tag{C.110}$$

Since

$$\frac{1}{2}\big(u_e(\boldsymbol{x}) + u_i(\boldsymbol{x})\big) = \frac{\mu(\boldsymbol{x})}{2}, \qquad \boldsymbol{x} \in \Gamma, \tag{C.111}$$

we obtain, for $\boldsymbol{x} \in \Gamma$, the Fredholm integral equation of the second kind

$$\frac{\mu(\boldsymbol{x})}{2} + \int_\Gamma \left(Z(\boldsymbol{y})G(\boldsymbol{x},\boldsymbol{y}) - \frac{\partial G}{\partial n_{\boldsymbol{y}}}(\boldsymbol{x},\boldsymbol{y})\right)\mu(\boldsymbol{y})\,\mathrm{d}\gamma(\boldsymbol{y}) = \int_\Gamma G(\boldsymbol{x},\boldsymbol{y})f_z(\boldsymbol{y})\,\mathrm{d}\gamma(\boldsymbol{y}), \tag{C.112}$$

which has to be solved for the unknown μ. In terms of boundary layer potentials, the integral representation and the integral equation can be respectively expressed by

$$u = \mathcal{D}(\mu) - \mathcal{S}(Z\mu) + \mathcal{S}(f_z) \qquad \text{in } \Omega_e \cup \Omega_i, \tag{C.113}$$

$$\frac{\mu}{2} + S(Z\mu) - D(\mu) = S(f_z) \qquad \text{on } \Gamma. \tag{C.114}$$

Alternatively, since

$$\frac{1}{2}\left(\frac{\partial u_e}{\partial n}(\boldsymbol{x}) + \frac{\partial u_i}{\partial n}(\boldsymbol{x})\right) = \frac{Z(\boldsymbol{x})}{2}\mu(\boldsymbol{x}) - \frac{f_z(\boldsymbol{x})}{2}, \qquad \boldsymbol{x} \in \Gamma, \tag{C.115}$$

we obtain also, for $\boldsymbol{x} \in \Gamma$, the Fredholm integral equation of the second kind

$$\frac{Z(\boldsymbol{x})}{2}\mu(\boldsymbol{x}) + \int_\Gamma \left(-\frac{\partial^2 G}{\partial n_{\boldsymbol{x}} \partial n_{\boldsymbol{y}}}(\boldsymbol{x},\boldsymbol{y}) + Z(\boldsymbol{y})\frac{\partial G}{\partial n_{\boldsymbol{x}}}(\boldsymbol{x},\boldsymbol{y}) \right) \mu(\boldsymbol{y})\, \mathrm{d}\gamma(\boldsymbol{y}) = \frac{f_z(\boldsymbol{x})}{2} + \int_\Gamma \frac{\partial G}{\partial n_{\boldsymbol{x}}}(\boldsymbol{x},\boldsymbol{y}) f_z(\boldsymbol{y})\, \mathrm{d}\gamma(\boldsymbol{y}), \tag{C.116}$$

which in terms of boundary layer potentials becomes

$$\frac{Z}{2}\mu - N(\mu) + D^*(Z\mu) = \frac{f_z}{2} + D^*(f_z) \qquad \text{on } \Gamma. \tag{C.117}$$

b) Continuous impedance

We associate to (C.13) the interior problem

$$\begin{cases} \text{Find } u_i : \Omega_i \to \mathbb{C} \text{ such that} \\ \Delta u_i + k^2 u_i = 0 & \text{in } \Omega_i, \\ -\dfrac{\partial u_i}{\partial n} + Z u_i = f_z & \text{on } \Gamma. \end{cases} \tag{C.118}$$

The jumps over Γ are characterized in this case by

$$[u] = u_e - u_i = \mu, \tag{C.119}$$

$$\left[\frac{\partial u}{\partial n}\right] = \frac{\partial u_e}{\partial n} - \frac{\partial u_i}{\partial n} = Z(u_e - u_i) = Z\mu, \tag{C.120}$$

where $\mu : \Gamma \to \mathbb{C}$ is a function to be determined. In particular it holds that the jump of the impedance is zero, namely

$$\left[-\frac{\partial u}{\partial n} + Zu\right] = \left(-\frac{\partial u_e}{\partial n} + Z u_e\right) - \left(-\frac{\partial u_i}{\partial n} + Z u_i\right) = 0. \tag{C.121}$$

An integral representation formula of the solution, for $\boldsymbol{x} \in \Omega_e \cup \Omega_i$, is given by

$$u(\boldsymbol{x}) = \int_\Gamma \left(\frac{\partial G}{\partial n_{\boldsymbol{y}}}(\boldsymbol{x},\boldsymbol{y}) - Z(\boldsymbol{y}) G(\boldsymbol{x},\boldsymbol{y}) \right) \mu(\boldsymbol{y})\, \mathrm{d}\gamma(\boldsymbol{y}). \tag{C.122}$$

Since

$$-\frac{1}{2}\left(\frac{\partial u_e}{\partial n}(\boldsymbol{x}) + \frac{\partial u_i}{\partial n}(\boldsymbol{x}) \right) + \frac{Z(\boldsymbol{x})}{2}\big(u_e(\boldsymbol{x}) + u_i(\boldsymbol{x})\big) = f_z(\boldsymbol{x}), \qquad \boldsymbol{x} \in \Gamma, \tag{C.123}$$

we obtain, for $\boldsymbol{x} \in \Gamma$, the Fredholm integral equation of the first kind

$$\int_\Gamma \left(-\frac{\partial^2 G}{\partial n_{\boldsymbol{x}} \partial n_{\boldsymbol{y}}}(\boldsymbol{x},\boldsymbol{y}) + Z(\boldsymbol{y})\frac{\partial G}{\partial n_{\boldsymbol{x}}}(\boldsymbol{x},\boldsymbol{y}) \right) \mu(\boldsymbol{y})\, \mathrm{d}\gamma(\boldsymbol{y}) + Z(\boldsymbol{x}) \int_\Gamma \left(\frac{\partial G}{\partial n_{\boldsymbol{y}}}(\boldsymbol{x},\boldsymbol{y}) - Z(\boldsymbol{y}) G(\boldsymbol{x},\boldsymbol{y}) \right) \mu(\boldsymbol{y})\, \mathrm{d}\gamma(\boldsymbol{y}) = f_z(\boldsymbol{x}), \tag{C.124}$$

which has to be solved for the unknown μ. In terms of boundary layer potentials, the integral representation and the integral equation can be respectively expressed by

$$u = \mathcal{D}(\mu) - \mathcal{S}(Z\mu) \qquad \text{in } \Omega_e \cup \Omega_i, \tag{C.125}$$

$$-N(\mu) + D^*(Z\mu) + ZD(\mu) - ZS(Z\mu) = f_z \quad \text{on } \Gamma. \tag{C.126}$$

We observe that the integral equation (C.126) is self-adjoint.

c) Continuous value

We associate to (C.13) the interior problem

$$\begin{cases} \text{Find } u_i : \Omega_i \to \mathbb{C} \text{ such that} \\ \Delta u_i + k^2 u_i = 0 & \text{in } \Omega_i, \\ -\dfrac{\partial u_e}{\partial n} + Z u_i = f_z & \text{on } \Gamma. \end{cases} \tag{C.127}$$

The jumps over Γ are characterized in this case by

$$[u] = u_e - u_i = \frac{1}{Z}\left(\frac{\partial u_e}{\partial n} - f_z\right) - \frac{1}{Z}\left(\frac{\partial u_e}{\partial n} - f_z\right) = 0, \tag{C.128}$$

$$\left[\frac{\partial u}{\partial n}\right] = \frac{\partial u_e}{\partial n} - \frac{\partial u_i}{\partial n} = \nu, \tag{C.129}$$

where $\nu : \Gamma \to \mathbb{C}$ is a function to be determined.

An integral representation formula of the solution, for $\boldsymbol{x} \in \Omega_e \cup \Omega_i$, is given by the single layer potential

$$u(\boldsymbol{x}) = -\int_\Gamma G(\boldsymbol{x}, \boldsymbol{y})\nu(\boldsymbol{y})\, \mathrm{d}\gamma(\boldsymbol{y}). \tag{C.130}$$

Since

$$-\frac{1}{2}\left(\frac{\partial u_e}{\partial n}(\boldsymbol{x}) + \frac{\partial u_i}{\partial n}(\boldsymbol{x})\right) + \frac{Z(\boldsymbol{x})}{2}\big(u_e(\boldsymbol{x}) + u_i(\boldsymbol{x})\big) = \frac{\nu(\boldsymbol{x})}{2} + f_z(\boldsymbol{x}), \quad \boldsymbol{x} \in \Gamma, \tag{C.131}$$

we obtain, for $\boldsymbol{x} \in \Gamma$, the Fredholm integral equation of the second kind

$$-\frac{\nu(\boldsymbol{x})}{2} + \int_\Gamma \left(\frac{\partial G}{\partial n_{\boldsymbol{x}}}(\boldsymbol{x}, \boldsymbol{y}) - Z(\boldsymbol{x})G(\boldsymbol{x}, \boldsymbol{y})\right)\nu(\boldsymbol{y})\, \mathrm{d}\gamma(\boldsymbol{y}) = f_z(\boldsymbol{x}), \tag{C.132}$$

which has to be solved for the unknown ν. In terms of boundary layer potentials, the integral representation and the integral equation can be respectively expressed by

$$u = -\mathcal{S}(\nu) \qquad \text{in } \Omega_e \cup \Omega_i, \tag{C.133}$$

$$\frac{\nu}{2} + ZS(\nu) - D^*(\nu) = -f_z \qquad \text{on } \Gamma. \tag{C.134}$$

We observe that the integral equation (C.134) is mutually adjoint with (C.114).

d) Continuous normal derivative

We associate to (C.13) the interior problem

$$\begin{cases} \text{Find } u_i : \Omega_i \to \mathbb{C} \text{ such that} \\ \Delta u_i + k^2 u_i = 0 & \text{in } \Omega_i, \\ -\dfrac{\partial u_i}{\partial n} + Z u_e = f_z & \text{on } \Gamma. \end{cases} \tag{C.135}$$

The jumps over Γ are characterized in this case by

$$[u] = u_e - u_i = \mu, \tag{C.136}$$

$$\left[\frac{\partial u}{\partial n}\right] = \frac{\partial u_e}{\partial n} - \frac{\partial u_i}{\partial n} = \big(Zu_e - f_z\big) - \big(Zu_e - f_z\big) = 0, \tag{C.137}$$

where $\mu : \Gamma \to \mathbb{C}$ is a function to be determined.

An integral representation formula of the solution, for $\boldsymbol{x} \in \Omega_e \cup \Omega_i$, is given by the double layer potential

$$u(\boldsymbol{x}) = \int_\Gamma \frac{\partial G}{\partial n_{\boldsymbol{y}}}(\boldsymbol{x}, \boldsymbol{y})\mu(\boldsymbol{y})\,\mathrm{d}\gamma(\boldsymbol{y}). \tag{C.138}$$

Since when $\boldsymbol{x} \in \Gamma$,

$$-\frac{1}{2}\left(\frac{\partial u_e}{\partial n}(\boldsymbol{x}) + \frac{\partial u_i}{\partial n}(\boldsymbol{x})\right) + \frac{Z(\boldsymbol{x})}{2}\big(u_e(\boldsymbol{x}) + u_i(\boldsymbol{x})\big) = -\frac{Z(\boldsymbol{x})}{2}\mu(\boldsymbol{x}) + f_z(\boldsymbol{x}), \tag{C.139}$$

we obtain, for $\boldsymbol{x} \in \Gamma$, the Fredholm integral equation of the second kind

$$\frac{Z(\boldsymbol{x})}{2}\mu(\boldsymbol{x}) + \int_\Gamma \left(-\frac{\partial^2 G}{\partial n_{\boldsymbol{x}} \partial n_{\boldsymbol{y}}}(\boldsymbol{x}, \boldsymbol{y}) + Z(\boldsymbol{x})\frac{\partial G}{\partial n_{\boldsymbol{y}}}(\boldsymbol{x}, \boldsymbol{y})\right)\mu(\boldsymbol{y})\,\mathrm{d}\gamma(\boldsymbol{y}) = f_z(\boldsymbol{x}), \tag{C.140}$$

which has to be solved for the unknown μ. In terms of boundary layer potentials, the integral representation and the integral equation can be respectively expressed by

$$u = \mathcal{D}(\mu) \qquad \text{in } \Omega_e \cup \Omega_i, \tag{C.141}$$

$$\frac{Z}{2}\mu - N(\mu) + ZD(\mu) = f_z \qquad \text{on } \Gamma. \tag{C.142}$$

We observe that the integral equation (C.142) is mutually adjoint with (C.117).

C.7 Far field of the solution

The asymptotic behavior at infinity of the solution u of (C.13) is described by the far field u^{ff}. Its expression can be deduced by replacing the far field of the Green's function G^{ff} and its derivatives in the integral representation formula (C.61), which yields

$$u^{ff}(\boldsymbol{x}) = \int_\Gamma \left([u](\boldsymbol{y})\frac{\partial G^{ff}}{\partial n_{\boldsymbol{y}}}(\boldsymbol{x}, \boldsymbol{y}) - G^{ff}(\boldsymbol{x}, \boldsymbol{y})\left[\frac{\partial u}{\partial n}\right](\boldsymbol{y})\right)\mathrm{d}\gamma(\boldsymbol{y}). \tag{C.143}$$

By replacing now (C.39) and (C.40) in (C.143), we have that the far field of the solution is

$$u^{ff}(\boldsymbol{x}) = \frac{e^{ik|\boldsymbol{x}|}}{\sqrt{|\boldsymbol{x}|}}\frac{e^{i\pi/4}}{\sqrt{8\pi k}}\int_\Gamma e^{-ik\hat{\boldsymbol{x}}\cdot\boldsymbol{y}}\left(ik\hat{\boldsymbol{x}}\cdot\boldsymbol{n}_{\boldsymbol{y}}\,[u](\boldsymbol{y}) + \left[\frac{\partial u}{\partial n}\right](\boldsymbol{y})\right)\mathrm{d}\gamma(\boldsymbol{y}). \tag{C.144}$$

The asymptotic behavior of the solution u at infinity is therefore given by

$$u(\boldsymbol{x}) = \frac{e^{ik|\boldsymbol{x}|}}{\sqrt{|\boldsymbol{x}|}}\left\{u_\infty(\hat{\boldsymbol{x}}) + \mathcal{O}\left(\frac{1}{|\boldsymbol{x}|}\right)\right\}, \qquad |\boldsymbol{x}| \to \infty, \tag{C.145}$$

uniformly in all directions $\hat{\boldsymbol{x}}$ on the unit circle, where

$$u_\infty(\hat{\boldsymbol{x}}) = \frac{e^{i\pi/4}}{\sqrt{8\pi k}}\int_\Gamma e^{-ik\hat{\boldsymbol{x}}\cdot\boldsymbol{y}}\left(ik\hat{\boldsymbol{x}}\cdot\boldsymbol{n}_{\boldsymbol{y}}\,[u](\boldsymbol{y}) + \left[\frac{\partial u}{\partial n}\right](\boldsymbol{y})\right)\mathrm{d}\gamma(\boldsymbol{y}) \tag{C.146}$$

is called the far-field pattern of u. It can be expressed in decibels (dB) by means of the scattering cross section

$$Q_s(\hat{\boldsymbol{x}}) \ \ [\text{dB}] = 20 \log_{10}\left(\frac{|u_\infty(\hat{\boldsymbol{x}})|}{|u_0|}\right), \tag{C.147}$$

where the reference level u_0 is typically taken as $u_0 = u_I$ when the incident field is given by a plane wave of the form (C.5), i.e., $|u_0| = 1$.

We remark that the far-field behavior (C.145) of the solution is in accordance with the Sommerfeld radiation condition (C.8), which justifies its choice.

C.8 Exterior circle problem

To understand better the resolution of the direct scattering problem (C.13), we study now the particular case when the domain $\Omega_e \subset \mathbb{R}^2$ is taken as the exterior of a circle of radius $R > 0$. The interior of the circle is then given by $\Omega_i = \{\boldsymbol{x} \in \mathbb{R}^2 : |\boldsymbol{x}| < R\}$ and its boundary by $\Gamma = \partial\Omega_e$, as shown in Figure C.3. We place the origin at the center of Ω_i and we consider that the unit normal $\boldsymbol{n}$ is taken outwardly oriented of Ω_e, i.e., $\boldsymbol{n} = -\boldsymbol{r}$.

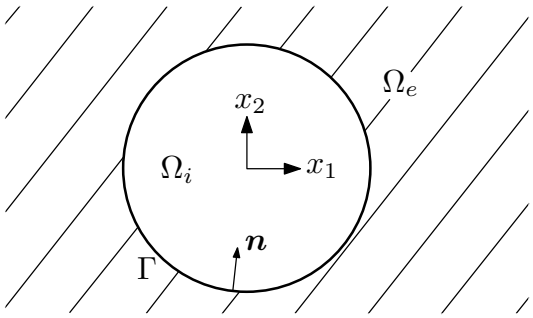

FIGURE C.3. Exterior of the circle.

The exterior circle problem is then stated as

$$\begin{cases} \text{Find } u : \Omega_e \to \mathbb{C} \text{ such that} \\ \Delta u + k^2 u = 0 \qquad \text{in } \ \Omega_e, \\ \dfrac{\partial u}{\partial r} + Zu = f_z \qquad \text{on } \ \Gamma, \\ \text{+ Outgoing radiation condition as } |\boldsymbol{x}| \to \infty, \end{cases} \tag{C.148}$$

where we consider a constant impedance $Z \in \mathbb{C}$, a wave number $k > 0$, and where the radiation condition is as usual given by (C.8). As the incident field u_I we consider a plane wave in the form of (C.5), in which case the impedance data function f_z is given by

$$f_z = -\frac{\partial u_I}{\partial r} - Zu_I \qquad \text{on } \ \Gamma. \tag{C.149}$$

Due the particular chosen geometry, the solution u of (C.148) can be easily found analytically by using the method of variable separation, i.e., by supposing that

$$u(\boldsymbol{x}) = u(r, \theta) = h(r)g(\theta), \tag{C.150}$$

where $r \geq 0$ and $-\pi < \theta \leq \pi$ are the polar coordinates in $\mathbb{R}^2$. If the Helmholtz equation in (C.148) is expressed using polar coordinates, then

$$\Delta u + k^2 u = \frac{\partial^2 u}{\partial r^2} + \frac{1}{r}\frac{\partial u}{\partial r} + \frac{1}{r^2}\frac{\partial^2 u}{\partial \theta^2} + k^2 u = 0. \tag{C.151}$$

By replacing now (C.150) in (C.151) we obtain

$$h''(r)g(\theta) + \frac{1}{r}h'(r)g(\theta) + \frac{1}{r^2}h(r)g''(\theta) + k^2 h(r)g(\theta) = 0. \tag{C.152}$$

Multiplying by r^2, dividing by gh, and rearranging according to each variable yields

$$r^2\frac{h''(r)}{h(r)} + r\frac{h'(r)}{h(r)} + k^2 r^2 = -\frac{g''(\theta)}{g(\theta)}. \tag{C.153}$$

Since both sides in equation (C.153) involve different variables, therefore they are equal to a constant, denoted for convenience by n^2, and we have that

$$r^2\frac{h''(r)}{h(r)} + r\frac{h'(r)}{h(r)} + k^2 r^2 = -\frac{g''(\theta)}{g(\theta)} = n^2. \tag{C.154}$$

From (C.154) we obtain the two ordinary differential equations

$$g''(\theta) + n^2 g(\theta) = 0, \tag{C.155}$$

$$r^2 h''(r) + r h'(r) + (k^2 r^2 - n^2)h(r) = 0. \tag{C.156}$$

The solutions for (C.155) have the general form

$$g(\theta) = a_n \cos(n\theta) + b_n \sin(n\theta), \qquad n \in \mathbb{N}_0, \tag{C.157}$$

where $a_n, b_n \in \mathbb{C}$ are arbitrary constants. The requirement that $n \in \mathbb{N}_0$ stems from the periodicity condition

$$g(\theta) = g(\theta + 2\pi n) \qquad \forall n \in \mathbb{Z}, \tag{C.158}$$

where we segregate positive and negative values for n. By considering for (C.156) the change of variables $z = kr$ and expressing $\psi(z) = h(r)$, we obtain the Bessel differential equation of order n, namely

$$z^2\psi''(z) + z\psi'(z) + (z^2 - n^2)\psi(z) = 0. \tag{C.159}$$

The independent solutions of (C.159) are $H_n^{(1)}(z)$ and $H_n^{(2)}(z)$, the Hankel functions of order n, and therefore the solutions of (C.156) have the general form

$$h(r) = c_n H_n^{(1)}(kr) + d_n H_n^{(2)}(kr), \qquad n \geq 0, \tag{C.160}$$

where $c_n, d_n \in \mathbb{C}$ are again arbitrary constants. The general solution for the Helmholtz equation considers the linear combination of all the solutions in the form of (C.150), namely

$$u(r, \theta) = \sum_{n=0}^{\infty} \big(c_n H_n^{(1)}(kr) + d_n H_n^{(2)}(kr)\big)\big(a_n \cos(n\theta) + b_n \sin(n\theta)\big). \tag{C.161}$$

The radiation condition (C.8) implies that

$$d_n = 0, \qquad n \in \mathbb{N}_0. \tag{C.162}$$

Thus the general solution (C.161) turns into

$$u(r,\theta) = \sum_{n=0}^{\infty} H_n^{(1)}(kr)\big(a_n e^{in\theta} + b_n e^{-in\theta}\big), \tag{C.163}$$

where all the undetermined constants have been merged into a_n and b_n, due their arbitrariness. Due the recurrence relation (A.121), the radial derivative of (C.163) is given by

$$\frac{\partial u}{\partial r}(r,\theta) = \sum_{n=0}^{\infty} \Big(\frac{n}{r} H_n^{(1)}(kr) - kH_{n+1}^{(1)}(kr)\Big)\big(a_n e^{in\theta} + b_n e^{-in\theta}\big). \tag{C.164}$$

The constants a_n and b_n in (C.163) are determined through the impedance boundary condition on Γ. For this purpose, we expand the impedance data function f_z as a Fourier series:

$$f_z(\theta) = \sum_{n=-\infty}^{\infty} f_n e^{in\theta}, \qquad -\pi < \theta \le \pi, \tag{C.165}$$

where

$$f_n = \frac{1}{2\pi}\int_{-\pi}^{\pi} f_z(\theta) e^{-in\theta}\,\mathrm{d}\theta, \qquad n \in \mathbb{Z}. \tag{C.166}$$

In particular, for a plane wave in the form of (C.5) we have the Jacobi-Anger expansion

$$u_I(\boldsymbol{x}) = e^{i\boldsymbol{k}\cdot\boldsymbol{x}} = e^{-ikr\cos(\theta-\theta_P)} = \sum_{n=-\infty}^{\infty} i^n J_n(kr) e^{in(\theta-\theta_P)}, \tag{C.167}$$

where J_n is the Bessel function of order n, where $\theta_P = \theta_I + \pi$ is the propagation angle of the plane wave, and where

$$\boldsymbol{k} = \begin{pmatrix} k_1 \\ k_2 \end{pmatrix} = k\begin{pmatrix} \cos\theta_P \\ \sin\theta_P \end{pmatrix}, \qquad \boldsymbol{x} = \begin{pmatrix} x_1 \\ x_2 \end{pmatrix} = r\begin{pmatrix} \cos\theta \\ \sin\theta \end{pmatrix}. \tag{C.168}$$

For a plane wave, the impedance data function (C.149) can be thus expressed as

$$f_z(\theta) = -\sum_{n=-\infty}^{\infty} i^n \left(\Big(Z + \frac{n}{R}\Big) J_n(kR) - kJ_{n+1}(kR)\right) e^{in(\theta-\theta_P)}, \tag{C.169}$$

which implies that

$$f_n = -i^n \left(\Big(Z + \frac{n}{R}\Big) J_n(kR) - kJ_{n+1}(kR)\right) e^{-in\theta_P}, \qquad n \in \mathbb{Z}. \tag{C.170}$$

The impedance boundary condition takes therefore the form

$$\sum_{n=0}^{\infty} \left(\Big(Z + \frac{n}{R}\Big) H_n^{(1)}(kR) - kH_{n+1}^{(1)}(kR)\right)\big(a_n e^{in\theta} + b_n e^{-in\theta}\big) = \sum_{n=-\infty}^{\infty} f_n e^{in\theta}. \tag{C.171}$$

We observe that the constants a_n and b_n can be uniquely determined only if

$$\Big(Z + \frac{n}{R}\Big) H_n^{(1)}(kR) - kH_{n+1}^{(1)}(kR) \neq 0 \qquad \text{for } \ n \in \mathbb{N}_0. \tag{C.172}$$

If this condition is not fulfilled, then the solution is no longer unique. The values $k, Z \in \mathbb{C}$ for which this occurs form a countable set. In particular, for a fixed k, the impedances Z which do not fulfill (C.172) can be explicitly characterized by

$$Z = k\frac{H_{n+1}^{(1)}(kR)}{H_n^{(1)}(kR)} - \frac{n}{R} \qquad \text{for } \ n \in \mathbb{N}_0. \tag{C.173}$$

The wave numbers k which do not fulfill (C.172), for a fixed Z, can only be characterized implicitly through the relation

$$\Big(Z + \frac{n}{R}\Big)H_n^{(1)}(kR) - kH_{n+1}^{(1)}(kR) = 0 \qquad \text{for } \ n \in \mathbb{N}_0. \tag{C.174}$$

If we suppose now that (C.172) takes place, then

$$a_0 = b_0 = \frac{f_0}{2ZH_0^{(1)}(kR) - 2kH_1^{(1)}(kR)}, \tag{C.175}$$

$$a_n = \frac{Rf_n}{(ZR+n)H_n^{(1)}(kR) - kRH_{n+1}^{(1)}(kR)} \qquad (n \geq 1), \tag{C.176}$$

$$b_n = \frac{Rf_{-n}}{(ZR+n)H_n^{(1)}(kR) - kRH_{n+1}^{(1)}(kR)} \qquad (n \geq 1). \tag{C.177}$$

In the case of a plane wave we consider for f_n and f_{-n} the expression (C.170). The unique solution for the exterior circle problem (C.148) is then given by

$$u(r,\theta) = \frac{H_0^{(1)}(kr)f_0}{ZH_0^{(1)}(kR) - kH_1^{(1)}(kR)} + \sum_{n=1}^{\infty} \frac{RH_n^{(1)}(kr)\big(f_n e^{in\theta} + f_{-n}e^{-in\theta}\big)}{(ZR+n)H_n^{(1)}(kR) - kRH_{n+1}^{(1)}(kR)}. \tag{C.178}$$

We remark that there is no need here for an additional compatibility condition like (B.191).

If the condition (C.172) does not hold for some particular $m \in \mathbb{N}_0$, then the solution u is not unique. The constants a_m and b_m are then no longer defined by (C.176) and (C.176), and can be chosen in an arbitrary manner. For the existence of a solution in this case, however, we require also the orthogonality conditions $f_m = f_{-m} = 0$. Instead of (C.178), the solution of (C.148) is now given by the infinite family of functions

$$u(r,\theta) = \sum_{n=1}^{\infty} \frac{RH_n^{(1)}(kr)\big(f_n e^{in\theta} + f_{-n}e^{-in\theta}\big)}{(ZR+n)H_n^{(1)}(kR) - kRH_{n+1}^{(1)}(kR)} + \alpha H_0^{(1)}(kr) \qquad (m=0), \tag{C.179}$$

$$\begin{aligned} u(r,\theta) = {} & \frac{H_0^{(1)}(kr)f_0}{ZH_0^{(1)}(kR) - kH_1^{(1)}(kR)} + \sum_{1 \leq n \neq m} \frac{RH_n^{(1)}(kr)\big(f_n e^{in\theta} + f_{-n}e^{-in\theta}\big)}{(ZR+n)H_n^{(1)}(kR) - kRH_{n+1}^{(1)}(kR)} \\ & + H_m^{(1)}(kr)\big(\alpha e^{im\theta} + \beta e^{-im\theta}\big) \qquad (m \geq 1), \end{aligned} \tag{C.180}$$

where $\alpha, \beta \in \mathbb{C}$ are arbitrary and where their associated terms have the form of volume waves, i.e., waves that propagate inside Ω_e. The exterior circle problem (C.148) admits thus a unique solution u, except on a countable set of values for k and Z which do not fulfill the condition (C.172). And even in this last case there exists a solution, although not unique, if two orthogonality conditions are additionally satisfied. This behavior for

the existence and uniqueness of the solution is typical of the Fredholm alternative, which applies when solving problems that involve compact perturbations of invertible operators.

C.9 Existence and uniqueness

C.9.1 Function spaces

To state a precise mathematical formulation of the herein treated problems, we have to define properly the involved function spaces. For the associated interior problems defined on the bounded set Ω_i we use the classical Sobolev space (vid. Section A.4)

$$H^1(\Omega_i) = \left\{v :\ v \in L^2(\Omega_i),\ \nabla v \in L^2(\Omega_i)^2\right\}, \tag{C.181}$$

which is a Hilbert space and has the norm

$$\|v\|_{H^1(\Omega_i)} = \left(\|v\|^2_{L^2(\Omega_i)} + \|\nabla v\|^2_{L^2(\Omega_i)^2}\right)^{1/2}. \tag{C.182}$$

For the exterior problem defined on the unbounded domain Ω_e, on the other hand, we introduce the weighted Sobolev space (cf., e.g., Nédélec 2001)

$$\begin{aligned} W^1(\Omega_e) = \Bigg\{ v : & \frac{v}{\sqrt{1+r^2}\,\ln(2+r^2)} \in L^2(\Omega_e), \\ & \frac{\nabla v}{\sqrt{1+r^2}\,\ln(2+r^2)} \in L^2(\Omega_e)^2,\ \frac{\partial v}{\partial r} - ikv \in L^2(\Omega_e) \Bigg\}, \end{aligned} \tag{C.183}$$

where $r = |\boldsymbol{x}|$. If $W^1(\Omega_e)$ is provided with the norm

$$\begin{aligned} \|v\|_{W^1(\Omega_e)} = \Bigg(& \left\| \frac{v}{\sqrt{1+r^2}\,\ln(2+r^2)} \right\|^2_{L^2(\Omega_e)} \\ & + \left\| \frac{\nabla v}{\sqrt{1+r^2}\,\ln(2+r^2)} \right\|^2_{L^2(\Omega_e)^2} + \left\| \frac{\partial v}{\partial r} - ikv \right\|^2_{L^2(\Omega_e)} \Bigg)^{1/2}, \end{aligned} \tag{C.184}$$

then it becomes a Hilbert space. The restriction to any bounded open set $B \subset \Omega_e$ of the functions of $W^1(\Omega_e)$ belongs to $H^1(B)$, i.e., we have the inclusion $W^1(\Omega_e) \subset H^1_{\text{loc}}(\Omega_e)$, and the functions in these two spaces differ only by their behavior at infinity. We remark that the space $W^1(\Omega_e)$ contains the constant functions and all the functions of $H^1_{\text{loc}}(\Omega_e)$ that satisfy the radiation condition (C.8).

When dealing with Sobolev spaces, even a strong Lipschitz boundary $\Gamma \in C^{0,1}$ is admissible. In this case, and due the trace theorem (A.531), if $v \in H^1(\Omega_i)$ or $v \in W^1(\Omega_e)$, then the trace of v fulfills

$$\gamma_0 v = v|_\Gamma \in H^{1/2}(\Gamma). \tag{C.185}$$

Moreover, the trace of the normal derivative can be also defined, and it holds that

$$\gamma_1 v = \frac{\partial v}{\partial n}|_\Gamma \in H^{-1/2}(\Gamma). \tag{C.186}$$

C.9.2 Regularity of the integral operators

The boundary integral operators (C.81), (C.82), (C.83), and (C.84) can be characterized as linear and continuous applications such that

$$S : H^{-1/2+s}(\Gamma) \longrightarrow H^{1/2+s}(\Gamma), \qquad D : H^{1/2+s}(\Gamma) \longrightarrow H^{3/2+s}(\Gamma), \tag{C.187}$$

$$D^* : H^{-1/2+s}(\Gamma) \longrightarrow H^{1/2+s}(\Gamma), \qquad N : H^{1/2+s}(\Gamma) \longrightarrow H^{-1/2+s}(\Gamma). \tag{C.188}$$

This result holds for any $s \in \mathbb{R}$ if the boundary Γ is of class C^∞, which can be derived from the theory of singular integral operators with pseudo-homogeneous kernels (cf., e.g., Nédélec 2001). Due the compact injection (A.554), it holds also that the operators

$$D : H^{1/2+s}(\Gamma) \longrightarrow H^{1/2+s}(\Gamma) \qquad \text{and} \qquad D^* : H^{-1/2+s}(\Gamma) \longrightarrow H^{-1/2+s}(\Gamma) \tag{C.189}$$

are compact. For a strong Lipschitz boundary $\Gamma \in C^{0,1}$, on the other hand, these results hold only when $|s| < 1$ (cf. Costabel 1988). In the case of more regular boundaries, the range for s increases, but remains finite. For our purposes we use $s = 0$, namely

$$S : H^{-1/2}(\Gamma) \longrightarrow H^{1/2}(\Gamma), \qquad D : H^{1/2}(\Gamma) \longrightarrow H^{1/2}(\Gamma), \tag{C.190}$$

$$D^* : H^{-1/2}(\Gamma) \longrightarrow H^{-1/2}(\Gamma), \qquad N : H^{1/2}(\Gamma) \longrightarrow H^{-1/2}(\Gamma), \tag{C.191}$$

which are all linear and continuous operators, and where the operators D and D^* are compact. Similarly, we can characterize the single and double layer potentials defined respectively in (C.76) and (C.77) as linear and continuous integral operators such that

$$\mathcal{S} : H^{-1/2}(\Gamma) \longrightarrow W^1(\Omega_e \cup \Omega_i) \qquad \text{and} \qquad \mathcal{D} : H^{1/2}(\Gamma) \longrightarrow W^1(\Omega_e \cup \Omega_i). \tag{C.192}$$

C.9.3 Application to the integral equations

It is not difficult to see that if $\mu \in H^{1/2}(\Gamma)$ and $\nu \in H^{-1/2}(\Gamma)$ are given, then the transmission problem (C.44) admits a unique solution $u \in W^1(\Omega_e \cup \Omega_i)$, as a consequence of the integral representation formula (C.62). For the direct scattering problem (C.13), though, this is not always the case, as was appreciated in the exterior circle problem (C.148). Nonetheless, if the Fredholm alternative applies, then we know that the existence and uniqueness of the problem can be ensured almost always, i.e., except on a countable set of values for the wave number and for the impedance.

We consider an impedance $Z \in L^\infty(\Gamma)$ and an impedance data function $f_z \in H^{-1/2}(\Gamma)$. In both cases all the continuous functions on Γ are included.

a) First extension by zero

Let us consider the first integral equation of the extension-by-zero alternative (C.112), which is given in terms of boundary layer potentials, for $\mu \in H^{1/2}(\Gamma)$, by

$$\frac{\mu}{2} + S(Z\mu) - D(\mu) = S(f_z) \qquad \text{in } H^{1/2}(\Gamma). \tag{C.193}$$

Due the imbedding properties of Sobolev spaces and in the same way as for the full-plane impedance Laplace problem, it holds that the left-hand side of the integral equation corresponds to an identity and two compact operators, and thus Fredholm's alternative applies.

b) Second extension by zero

The second integral equation of the extension-by-zero alternative (C.116) is given in terms of boundary layer potentials, for $\mu \in H^{1/2}(\Gamma)$, by

$$\frac{Z}{2}\mu - N(\mu) + D^*(Z\mu) = \frac{f_z}{2} + D^*(f_z) \qquad \text{in } H^{-1/2}(\Gamma). \tag{C.194}$$

The operator N plays the role of the identity and the other terms on the left-hand side are compact, thus Fredholm's alternative holds.

c) Continuous impedance

The integral equation of the continuous-impedance alternative (C.124) is given in terms of boundary layer potentials, for $\mu \in H^{1/2}(\Gamma)$, by

$$-N(\mu) + D^*(Z\mu) + ZD(\mu) - ZS(Z\mu) = f_z \qquad \text{in } H^{-1/2}(\Gamma). \tag{C.195}$$

Again, the operator N plays the role of the identity and the remaining terms on the left-hand side are compact, thus Fredholm's alternative applies.

d) Continuous value

The integral equation of the continuous-value alternative (C.132) is given in terms of boundary layer potentials, for $\nu \in H^{-1/2}(\Gamma)$, by

$$\frac{\nu}{2} + ZS(\nu) - D^*(\nu) = -f_z \qquad \text{in } H^{-1/2}(\Gamma). \tag{C.196}$$

On the left-hand side we have an identity operator and the remaining operators are compact, thus Fredholm's alternative holds.

e) Continuous normal derivative

The integral equation of the continuous-normal-derivative alternative (C.140) is given in terms of boundary layer potentials, for $\mu \in H^{1/2}(\Gamma)$, by

$$\frac{Z}{2}\mu - N(\mu) + ZD(\mu) = f_z \qquad \text{in } H^{-1/2}(\Gamma). \tag{C.197}$$

As before, Fredholm's alternative again applies, since on the left-hand side we have the operator N and two compact operators.

C.9.4 Consequences of Fredholm's alternative

Since the Fredholm alternative applies to each integral equation, therefore it applies also to the exterior differential problem (C.13) due the integral representation formula. The existence of the exterior problem's solution is thus determined by its uniqueness, and the wave numbers $k \in \mathbb{C}$ and impedances $Z \in \mathbb{C}$ for which the uniqueness is lost constitute a countable set, which we call respectively wave number spectrum and impedance spectrum of the exterior problem and denote them by σ_k and σ_Z. The spectrum σ_k considers a fixed Z and, conversely, the spectrum σ_Z considers a fixed k. The existence and uniqueness of the solution is therefore ensured almost everywhere. The same holds obviously for the solution of the integral equation, whose wave number spectrum and impedance spectrum we denote respectively by ς_k and ς_Z. Since each integral equation is derived from the exterior problem,

it holds that $\sigma_k \subset \varsigma_k$ and $\sigma_Z \subset \varsigma_Z$. The converse, though, is not necessarily true and depends on each particular integral equation. In any way, the sets $\varsigma_k \setminus \sigma_k$ and $\varsigma_Z \setminus \sigma_Z$ are at most countable.

Fredholm's alternative applies as much to the integral equation itself as to its adjoint counterpart, and equally to their homogeneous versions. Moreover, each integral equation solves at the same time an exterior and an interior differential problem. The loss of uniqueness of the integral equation's solution appears when the wave number k and the impedance Z are eigenvalues of some associated interior problem, either of the homogeneous integral equation or of its adjoint counterpart. Such a wave number k or impedance Z are contained respectively in ς_k or ς_Z.

The integral equation (C.114) is associated with the extension by zero (C.107), for which no eigenvalues appear. Nevertheless, its adjoint integral equation (C.134) of the continuous value is associated with the interior problem (C.127), which has a countable amount of eigenvalues k, but behaves otherwise well for all $Z \neq 0$.

The integral equation (C.117) is also associated with the extension by zero (C.107), for which no eigenvalues appear. Nonetheless, its adjoint integral equation (C.142) of the continuous normal derivative is associated with the interior problem (C.135), which has a countable amount of eigenvalues k, but behaves well for all Z, without restriction.

The integral equation (C.126) of the continuous impedance is self-adjoint and is associated with the interior problem (C.118), which has a countable quantity of eigenvalues k and Z.

Let us consider now the transmission problem generated by the homogeneous exterior problem

$$\begin{cases} \text{Find } u_e : \Omega_e \to \mathbb{C} \text{ such that} \\ \Delta u_e + k^2 u_e = 0 \qquad \text{in } \Omega_e, \\ -\dfrac{\partial u_e}{\partial n} + Z u_e = 0 \qquad \text{on } \Gamma, \\ \text{+ Outgoing radiation condition as } |\boldsymbol{x}| \to \infty, \end{cases} \tag{C.198}$$

and the associated homogeneous interior problem

$$\begin{cases} \text{Find } u_i : \Omega_i \to \mathbb{C} \text{ such that} \\ \Delta u_i + k^2 u_i = 0 \qquad \text{in } \Omega_i, \\ \dfrac{\partial u_i}{\partial n} + Z u_i = 0 \qquad \text{on } \Gamma, \end{cases} \tag{C.199}$$

where the radiation condition is as usual given by (C.8), and where the unit normal $\boldsymbol{n}$ always points outwards of Ω_e.

As for the Laplace equation, it holds again that the integral equations for this transmission problem have either the same left-hand side or are mutually adjoint to all other possible alternatives of integral equations that can be built for the exterior problem (C.13), and in particular to all the alternatives that were mentioned in the last subsection. The

eigenvalues k and Z of the homogeneous interior problem (C.199) are thus also contained respectively in ς_k and ς_Z.

We remark that additional alternatives for integral representations and equations based on non-homogeneous versions of the problem (C.199) can be also derived for the exterior impedance problem (cf. Ha-Duong 1987).

The determination of the wave number spectrum σ_k and the impedance spectrum σ_Z of the exterior problem (C.13) is not so easy, but can be achieved for simple geometries where an analytic solution is known.

In conclusion, the exterior problem (C.13) admits a unique solution u if $k \notin \sigma_k$, and $Z \notin \sigma_Z$, and each integral equation admits a unique solution, either μ or ν, if $k \notin \varsigma_k$ and $Z \notin \varsigma_Z$.

C.10 Dissipative problem

The dissipative problem considers waves that lose their amplitude as they travel through the medium. These waves dissipate their energy as they propagate and are modeled by a complex wave number $k \in \mathbb{C}$ whose imaginary part is strictly positive, i.e., $\mathfrak{Im}\{k\} > 0$. This choice ensures that the Green's function (C.23) decreases exponentially at infinity. Due the dissipative nature of the medium, it is no longer suited to take plane waves in the form of (C.5) as the incident field u_I. Instead, we have to take a source of volume waves at a finite distance from the obstacle. For example, we can consider a point source located at $\boldsymbol{z} \in \Omega_e$, in which case the incident field is given, up to a multiplicative constant, by

$$u_I(\boldsymbol{x}) = G(\boldsymbol{x}, \boldsymbol{z}) = -\frac{i}{4} H_0^{(1)}\big(k|\boldsymbol{x} - \boldsymbol{z}|\big). \tag{C.200}$$

This incident field u_I satisfies the Helmholtz equation with a source term in the right-hand side, namely

$$\Delta u_I + k^2 u_I = \delta_{\boldsymbol{z}} \qquad \text{in } \mathcal{D}'(\Omega_e), \tag{C.201}$$

which holds also for the total field u_T but not for the scattered field u, in which case the Helmholtz equation remains homogeneous. For a general source distribution g_s, whose support is contained in Ω_e, the incident field can be expressed by

$$u_I(\boldsymbol{x}) = G(\boldsymbol{x}, \boldsymbol{z}) * g_s(\boldsymbol{z}) = \int_{\Omega_e} G(\boldsymbol{x}, \boldsymbol{z})\, g_s(\boldsymbol{z})\, \mathrm{d}\boldsymbol{z}. \tag{C.202}$$

This incident field u_I satisfies now

$$\Delta u_I + k^2 u_I = g_s \qquad \text{in } \mathcal{D}'(\Omega_e), \tag{C.203}$$

which holds again also for the total field u_T but not for the scattered field u.

The dissipative nature of the medium implies also that a radiation condition like (C.8) is no longer required. The ingoing waves are readily ruled out, since they verify $\mathfrak{Im}\{k\} < 0$.

The dissipative scattering problem can be therefore stated as

$$\left\{\begin{array}{l} \text{Find } u:\Omega_e\to\mathbb{C} \text{ such that} \\ \Delta u + k^2 u = 0 \qquad\qquad \text{in } \Omega_e, \\ -\dfrac{\partial u}{\partial n} + Zu = f_z \qquad \text{on } \Gamma, \end{array}\right. \tag{C.204}$$

where the impedance data function f_z is again given by

$$f_z = \frac{\partial u_I}{\partial n} - Z u_I \qquad \text{on } \Gamma. \tag{C.205}$$

The solution is now such that $u \in H^1(\Omega_e)$ (cf., e.g., Hazard & Lenoir 1998, Lenoir 2005), therefore, instead of (C.55) and (C.56), we obtain that

$$\left| \int_{S_R} \left(u(\boldsymbol{y}) \frac{\partial G}{\partial r_{\boldsymbol{y}}}(\boldsymbol{x},\boldsymbol{y}) - G(\boldsymbol{x},\boldsymbol{y}) \frac{\partial u}{\partial r}(\boldsymbol{y}) \right) \mathrm{d}\gamma(\boldsymbol{y}) \right| \leq \frac{C}{\sqrt{R}}\, e^{-R\,\mathfrak{Im}\{k\}}. \tag{C.206}$$

It is not difficult to see that all the other developments performed for the non-dissipative case are also valid when considering dissipation. The only difference is that now a complex wave number k such that $\mathfrak{Im}\{k\} > 0$ has to be taken everywhere into account and that the outgoing radiation condition is no longer needed.

C.11 Variational formulation

To solve a particular integral equation we convert it to its variational or weak formulation, i.e., we solve it with respect to certain test functions in a bilinear (or sesquilinear) form. Basically, the integral equation is multiplied by the (conjugated) test function and then the equation is integrated over the boundary of the domain. The test functions are taken in the same function space as the solution of the integral equation.

a) First extension by zero

The variational formulation for the first integral equation (C.193) of the extension-by-zero alternative searches $\mu \in H^{1/2}(\Gamma)$ such that $\forall \varphi \in H^{1/2}(\Gamma)$

$$\left\langle \frac{\mu}{2} + S(Z\mu) - D(\mu), \varphi \right\rangle = \left\langle S(f_z), \varphi \right\rangle. \tag{C.207}$$

b) Second extension by zero

The variational formulation for the second integral equation (C.194) of the extension-by-zero alternative searches $\mu \in H^{1/2}(\Gamma)$ such that $\forall \varphi \in H^{1/2}(\Gamma)$

$$\left\langle \frac{Z}{2}\mu - N(\mu) + D^*(Z\mu), \varphi \right\rangle = \left\langle \frac{f_z}{2} + D^*(f_z), \varphi \right\rangle. \tag{C.208}$$

c) Continuous impedance

The variational formulation for the integral equation (C.195) of the alternative of the continuous-impedance searches $\mu \in H^{1/2}(\Gamma)$ such that $\forall \varphi \in H^{1/2}(\Gamma)$

$$\left\langle -N(\mu) + D^*(Z\mu) + ZD(\mu) - ZS(Z\mu), \varphi \right\rangle = \left\langle f_z, \varphi \right\rangle. \tag{C.209}$$

d) Continuous value

The variational formulation for the integral equation (C.196) of the continuous-value alternative searches $\nu \in H^{-1/2}(\Gamma)$ such that $\forall \psi \in H^{-1/2}(\Gamma)$

$$\left\langle \frac{\nu}{2} + ZS(\nu) - D^*(\nu), \psi \right\rangle = \big\langle -f_z, \psi \big\rangle. \tag{C.210}$$

e) Continuous normal derivative

The variational formulation for the integral equation (C.197) of the continuous-normal-derivative alternative searches $\mu \in H^{1/2}(\Gamma)$ such that $\forall \varphi \in H^{1/2}(\Gamma)$

$$\left\langle \frac{Z}{2}\mu - N(\mu) + ZD(\mu), \varphi \right\rangle = \big\langle f_z, \varphi \big\rangle. \tag{C.211}$$

C.12 Numerical discretization

C.12.1 Discretized function spaces

The exterior problem (C.13) is solved numerically with the boundary element method by employing a Galerkin scheme on the variational formulation of an integral equation. We use on the boundary curve Γ Lagrange finite elements of type either $\mathbb{P}_1$ or $\mathbb{P}_0$. As shown in Figure C.4, the curve Γ is approximated by the discretized curve Γ^h, composed by I rectilinear segments T_j, sequentially ordered in clockwise direction for $1 \leq j \leq I$, such that their length $|T_j|$ is less or equal than h, and with their endpoints on top of Γ.

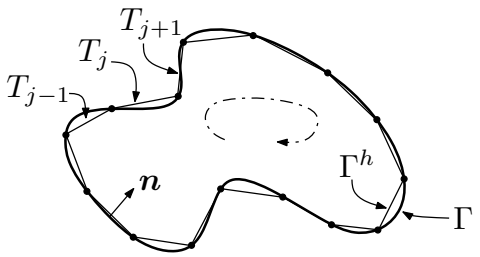

FIGURE C.4. Curve Γ^h, discretization of Γ.

The function space $H^{1/2}(\Gamma)$ is approximated using the conformal space of continuous piecewise linear polynomials with complex coefficients

$$Q_h = \big\{ \varphi_h \in C^0(\Gamma^h) \,:\, \varphi_h|_{T_j} \in \mathbb{P}_1(\mathbb{C}), \;\; 1 \leq j \leq I \big\}. \tag{C.212}$$

The space Q_h has a finite dimension I, and we describe it using the standard base functions for finite elements of type $\mathbb{P}_1$, which we denote by $\{\chi_j\}_{j=1}^I$ as in (B.261) and where $\boldsymbol{r}_j$ and $\boldsymbol{r}_{j+1}$ represent the endpoints of segment T_j.

The function space $H^{-1/2}(\Gamma)$, on the other hand, is approximated using the conformal space of piecewise constant polynomials with complex coefficients

$$P_h = \big\{ \psi_h : \Gamma^h \to \mathbb{C} \mid \; \psi_h|_{T_j} \in \mathbb{P}_0(\mathbb{C}), \;\; 1 \leq j \leq I \big\}. \tag{C.213}$$

The space P_h has a finite dimension I, and is described using the standard base functions for finite elements of type $\mathbb{P}_0$, which we denote by $\{\kappa_j\}_{j=1}^I$ as in (B.263).

In virtue of this discretization, any function $\varphi_h \in Q_h$ or $\psi_h \in P_h$ can be expressed as a linear combination of the elements of the base, namely

$$\varphi_h(\boldsymbol{x}) = \sum_{j=1}^{I} \varphi_j \, \chi_j(\boldsymbol{x}) \qquad \text{and} \qquad \psi_h(\boldsymbol{x}) = \sum_{j=1}^{I} \psi_j \, \kappa_j(\boldsymbol{x}) \qquad \text{for } \boldsymbol{x} \in \Gamma^h, \tag{C.214}$$

where $\varphi_j, \psi_j \in \mathbb{C}$ for $1 \leq j \leq I$. The solutions $\mu \in H^{1/2}(\Gamma)$ and $\nu \in H^{-1/2}(\Gamma)$ of the variational formulations can be therefore approximated respectively by

$$\mu_h(\boldsymbol{x}) = \sum_{j=1}^{I} \mu_j \, \chi_j(\boldsymbol{x}) \qquad \text{and} \qquad \nu_h(\boldsymbol{x}) = \sum_{j=1}^{I} \nu_j \, \kappa_j(\boldsymbol{x}) \qquad \text{for } \boldsymbol{x} \in \Gamma^h, \tag{C.215}$$

where $\mu_j, \nu_j \in \mathbb{C}$ for $1 \leq j \leq I$. The function f_z can be also approximated by

$$f_z^h(\boldsymbol{x}) = \sum_{j=1}^{I} f_j \, \chi_j(\boldsymbol{x}) \qquad \text{for } \boldsymbol{x} \in \Gamma^h, \quad \text{with } f_j = f_z(\boldsymbol{r}_j), \tag{C.216}$$

or

$$f_z^h(\boldsymbol{x}) = \sum_{j=1}^{I} f_j \, \kappa_j(\boldsymbol{x}) \qquad \text{for } \boldsymbol{x} \in \Gamma^h, \quad \text{with } f_j = \frac{f_z(\boldsymbol{r}_j) + f_z(\boldsymbol{r}_{j+1})}{2}, \tag{C.217}$$

depending on whether the original integral equation is stated in $H^{1/2}(\Gamma)$ or in $H^{-1/2}(\Gamma)$.

C.12.2 Discretized integral equations

a) First extension by zero

To see how the boundary element method operates, we apply it to the first integral equation of the extension-by-zero alternative, i.e., to the variational formulation (C.207). We characterize all the discrete approximations by the index h, including also the impedance and the boundary layer potentials. The numerical approximation of (C.207) leads to the discretized problem that searches $\mu_h \in Q_h$ such that $\forall \varphi_h \in Q_h$

$$\left\langle \frac{\mu_h}{2} + S_h(Z_h \mu_h) - D_h(\mu_h), \varphi_h \right\rangle = \left\langle S_h(f_z^h), \varphi_h \right\rangle. \tag{C.218}$$

Considering the decomposition of μ_h in terms of the base $\{\chi_j\}$ and taking as test functions the same base functions, $\varphi_h = \chi_i$ for $1 \leq i \leq I$, yields the discrete linear system

$$\sum_{j=1}^{I} \mu_j \left(\frac{1}{2} \langle \chi_j, \chi_i \rangle + \langle S_h(Z_h \chi_j), \chi_i \rangle - \langle D_h(\chi_j), \chi_i \rangle \right) = \sum_{j=1}^{I} f_j \, \langle S_h(\chi_j), \chi_i \rangle. \tag{C.219}$$

This constitutes a system of linear equations that can be expressed as a linear matrix system:

$$\begin{cases} \text{Find } \boldsymbol{\mu} \in \mathbb{C}^I \text{ such that} \\ \boldsymbol{M}\boldsymbol{\mu} = \boldsymbol{b}. \end{cases} \tag{C.220}$$

The elements m_{ij} of the matrix $\boldsymbol{M}$ are given by

$$m_{ij} = \frac{1}{2}\langle \chi_j, \chi_i \rangle + \langle S_h(Z_h \chi_j), \chi_i \rangle - \langle D_h(\chi_j), \chi_i \rangle \qquad \text{for } 1 \leq i, j \leq I, \tag{C.221}$$

and the elements b_i of the vector $\boldsymbol{b}$ by

$$b_i = \big\langle S_h(f_z^h), \chi_i \big\rangle = \sum_{j=1}^{I} f_j \, \langle S_h(\chi_j), \chi_i \rangle \qquad \text{for } 1 \leq i \leq I. \tag{C.222}$$

The discretized solution u_h, which approximates u, is finally obtained by discretizing the integral representation formula (C.110) according to

$$u_h = \mathcal{D}_h(\mu_h) - \mathcal{S}_h(Z_h \mu_h) + \mathcal{S}_h(f_z^h), \tag{C.223}$$

which, more specifically, can be expressed as

$$u_h = \sum_{j=1}^{I} \mu_j \big(\mathcal{D}_h(\chi_j) - \mathcal{S}_h(Z_h \chi_j) \big) + \sum_{j=1}^{I} f_j \, \mathcal{S}_h(\chi_j). \tag{C.224}$$

By proceeding in the same way, the discretization of all the other alternatives of integral equations can be also expressed as a linear matrix system like (C.220). The resulting matrix $\boldsymbol{M}$ is in general complex, full, non-symmetric, and with dimensions $I \times I$. The right-hand side vector $\boldsymbol{b}$ is complex and of size I. The boundary element calculations required to compute numerically the elements of $\boldsymbol{M}$ and $\boldsymbol{b}$ have to be performed carefully, since the integrals that appear become singular when the involved segments are adjacent or coincident, due the singularity of the Green's function at its source point.

b) Second extension by zero

In the case of the second integral equation of the extension-by-zero alternative, i.e., of the variational formulation (C.208), the elements m_{ij} that constitute the matrix $\boldsymbol{M}$ of the linear system (C.220) are given by

$$m_{ij} = \frac{1}{2}\langle Z_h \chi_j, \chi_i \rangle - \langle N_h(\chi_j), \chi_i \rangle + \langle D_h^*(Z_h \chi_j), \chi_i \rangle \qquad \text{for } 1 \leq i, j \leq I, \tag{C.225}$$

whereas the elements b_i of the vector $\boldsymbol{b}$ are expressed as

$$b_i = \sum_{j=1}^{I} f_j \left(\frac{1}{2}\langle \chi_j, \chi_i \rangle + \langle D_h^*(Z_h \chi_j), \chi_i \rangle \right) \qquad \text{for } 1 \leq i \leq I. \tag{C.226}$$

The discretized solution u_h is again computed by (C.224).

c) Continuous impedance

In the case of the continuous-impedance alternative, i.e., of the variational formulation (C.209), the elements m_{ij} that constitute the matrix $\boldsymbol{M}$ of the linear system (C.220) are given, for $1 \leq i, j \leq I$, by

$$m_{ij} = -\langle N_h(\chi_j), \chi_i \rangle + \langle D_h^*(Z_h \chi_j), \chi_i \rangle + \langle Z_h D_h(\chi_j), \chi_i \rangle - \langle Z_h S_h(Z_h \chi_j), \chi_i \rangle, \tag{C.227}$$

whereas the elements b_i of the vector $\boldsymbol{b}$ are expressed as

$$b_i = \sum_{j=1}^{I} f_j \, \langle \chi_j, \chi_i \rangle \qquad \text{for } \; 1 \leq i \leq I. \tag{C.228}$$

It can be observed that for this particular alternative the matrix $\boldsymbol{M}$ turns out to be symmetric, since the integral equation is self-adjoint. The discretized solution u_h, due (C.125), is then computed by

$$u_h = \sum_{j=1}^{I} \mu_j \big(\mathcal{D}_h(\chi_j) - \mathcal{S}_h(Z_h \chi_j) \big). \tag{C.229}$$

d) Continuous value

In the case of the continuous-value alternative, that is, of the variational formulation (C.210), the elements m_{ij} that constitute the matrix $\boldsymbol{M}$, now of the linear system

$$\begin{cases} \text{Find } \boldsymbol{\nu} \in \mathbb{C}^I \text{ such that} \\ \boldsymbol{M\nu} = \boldsymbol{b}, \end{cases} \tag{C.230}$$

are given by

$$m_{ij} = \frac{1}{2} \langle \kappa_j, \kappa_i \rangle + \langle Z_h S_h(\kappa_j), \kappa_i \rangle - \langle D_h^*(\kappa_j), \kappa_i \rangle \qquad \text{for } \; 1 \leq i, j \leq I, \tag{C.231}$$

whereas the elements b_i of the vector $\boldsymbol{b}$ are expressed as

$$b_i = -\sum_{j=1}^{I} f_j \, \langle \kappa_j, \kappa_i \rangle \qquad \text{for } \; 1 \leq i \leq I. \tag{C.232}$$

The discretized solution u_h, due (B.150), is then computed by

$$u_h = -\sum_{j=1}^{I} \nu_j \, \mathcal{S}_h(\kappa_j). \tag{C.233}$$

e) Continuous normal derivative

In the case of the continuous-normal-derivative alternative, i.e., of the variational formulation (C.211), the elements m_{ij} that conform the matrix $\boldsymbol{M}$ of the linear system (C.220) are given by

$$m_{ij} = \frac{1}{2} \langle Z_h \chi_j, \chi_i \rangle - \langle N_h(\chi_j), \chi_i \rangle + \langle Z_h D_h(\chi_j), \chi_i \rangle \qquad \text{for } \; 1 \leq i, j \leq I, \tag{C.234}$$

whereas the elements b_i of the vector $\boldsymbol{b}$ are expressed as

$$b_i = \sum_{j=1}^{I} f_j \, \langle \chi_j, \chi_i \rangle \qquad \text{for } \; 1 \leq i \leq I. \tag{C.235}$$

The discretized solution u_h, due (C.141), is then computed by

$$u_h = \sum_{j=1}^{I} \mu_j \, \mathcal{D}_h(\chi_j). \tag{C.236}$$

C.13 Boundary element calculations

The boundary element calculations build the elements of the matrix $\boldsymbol{M}$ resulting from the discretization of the integral equation, i.e., from (C.220) or (C.230). They permit thus to compute numerically expressions like (C.221). To evaluate the appearing singular integrals, we use the semi-numerical methods described in the report of Bendali & Devys (1986).

We use the same notation as in Section B.12, and the required boundary element integrals, for $a, b \in \{0, 1\}$, are again

$$ZA_{a,b} = \int_K \int_L \left(\frac{s}{|K|}\right)^a \left(\frac{t}{|L|}\right)^b G(\boldsymbol{x}, \boldsymbol{y}) \, \mathrm{d}L(\boldsymbol{y}) \, \mathrm{d}K(\boldsymbol{x}), \tag{C.237}$$

$$ZB_{a,b} = \int_K \int_L \left(\frac{s}{|K|}\right)^a \left(\frac{t}{|L|}\right)^b \frac{\partial G}{\partial n_{\boldsymbol{y}}}(\boldsymbol{x}, \boldsymbol{y}) \, \mathrm{d}L(\boldsymbol{y}) \, \mathrm{d}K(\boldsymbol{x}). \tag{C.238}$$

All the integrals that stem from the numerical discretization can be expressed in terms of these two basic boundary element integrals. The impedance is again discretized as a piecewise constant function Z_h, which on each segment T_j adopts a constant value $Z_j \in \mathbb{C}$. The integrals of interest are the same as for the Laplace equation, except for the hypersingular term, which is now given by

$$\begin{aligned}
\langle N_h(\chi_j), \chi_i \rangle &= -\int_{\Gamma^h} \int_{\Gamma^h} G(\boldsymbol{x}, \boldsymbol{y}) \big(\nabla \chi_j(\boldsymbol{y}) \times \boldsymbol{n}_{\boldsymbol{y}}\big) \big(\nabla \chi_i(\boldsymbol{x}) \times \boldsymbol{n}_{\boldsymbol{x}}\big) \, \mathrm{d}\gamma(\boldsymbol{y}) \, \mathrm{d}\gamma(\boldsymbol{x}) \\
&\quad + k^2 \int_{\Gamma^h} \int_{\Gamma^h} G(\boldsymbol{x}, \boldsymbol{y}) \chi_j(\boldsymbol{y}) \chi_i(\boldsymbol{x}) (\boldsymbol{n}_{\boldsymbol{y}} \cdot \boldsymbol{n}_{\boldsymbol{x}}) \, \mathrm{d}\gamma(\boldsymbol{y}) \, \mathrm{d}\gamma(\boldsymbol{x}) \\
&= -ZA_{0,0}^{i-1,j-1} \frac{(\boldsymbol{\tau}_{j-1} \times \boldsymbol{n}_{j-1})}{|T_{j-1}|} \frac{(\boldsymbol{\tau}_{i-1} \times \boldsymbol{n}_{i-1})}{|T_{i-1}|} + ZA_{0,0}^{i,j-1} \frac{(\boldsymbol{\tau}_{j-1} \times \boldsymbol{n}_{j-1})}{|T_{j-1}|} \frac{(\boldsymbol{\tau}_i \times \boldsymbol{n}_i)}{|T_i|} \\
&\quad + ZA_{0,0}^{i-1,j} \frac{(\boldsymbol{\tau}_j \times \boldsymbol{n}_j)}{|T_j|} \frac{(\boldsymbol{\tau}_{i-1} \times \boldsymbol{n}_{i-1})}{|T_{i-1}|} - ZA_{0,0}^{i,j} \frac{(\boldsymbol{\tau}_j \times \boldsymbol{n}_j)}{|T_j|} \frac{(\boldsymbol{\tau}_i \times \boldsymbol{n}_i)}{|T_i|} \\
&\quad + k^2 \Big(ZA_{1,1}^{i-1,j-1} (\boldsymbol{n}_{j-1} \cdot \boldsymbol{n}_{i-1}) + \big(ZA_{0,0}^{i,j} - ZA_{0,1}^{i,j} - ZA_{1,0}^{i,j} + ZA_{1,1}^{i,j}\big)(\boldsymbol{n}_j \cdot \boldsymbol{n}_i) \\
&\quad + \big(ZA_{0,1}^{i,j-1} - ZA_{1,1}^{i,j-1}\big)(\boldsymbol{n}_{j-1} \cdot \boldsymbol{n}_i) + \big(ZA_{1,0}^{i-1,j} - ZA_{1,1}^{i-1,j}\big)(\boldsymbol{n}_j \cdot \boldsymbol{n}_{i-1}) \Big).
\end{aligned} \tag{C.239}$$

To compute the boundary element integrals (C.237) and (C.238), we isolate the singular part of the Green's function G according to

$$G(R) \approx \frac{\ln(R)}{2\pi} + \phi(R) \qquad \text{if } |kR| \leq \frac{3}{4}, \tag{C.240}$$

where $\phi(R)$ is a non-singular function, which due (A.99) and (A.100) is given by

$$\begin{aligned}
\phi(R) &\approx \frac{\ln(k)}{2\pi} + J_0(kR) \left\{ -\frac{i}{4} + \frac{\gamma - \ln(2)}{2\pi} \right\} \\
&\quad + \frac{1}{2\pi} \left\{ \left(\frac{kR}{2}\right)^2 - \frac{3}{8} \left(\frac{kR}{2}\right)^4 + \frac{11}{216} \left(\frac{kR}{2}\right)^6 - \frac{25}{6912} \left(\frac{kR}{2}\right)^8 \right\}.
\end{aligned} \tag{C.241}$$

For the derivative $G'(R)$ we have similarly that

$$G'(R) \approx \frac{1}{2\pi R} + \phi'(R) \qquad \text{if } |kR| \leq \frac{3}{4}, \tag{C.242}$$

where $\phi'(R)$ is also a non-singular function, which due (A.101) and (A.102) is given by

$$\begin{aligned}\phi'(R) \approx & -\frac{k}{2\pi} J_1(kR) \left\{ -\frac{i\pi}{2} + \ln\left(\frac{kR}{2}\right) + \gamma \right\} \\ & - \frac{k}{4\pi} \left\{ -\frac{kR}{2} + \frac{5}{4}\left(\frac{kR}{2}\right)^3 - \frac{5}{18}\left(\frac{kR}{2}\right)^5 + \frac{47}{1728}\left(\frac{kR}{2}\right)^7 \right\}. \end{aligned} \tag{C.243}$$

We observe that

$$\frac{\partial G}{\partial n_{\boldsymbol{y}}}(\boldsymbol{x}, \boldsymbol{y}) = G'(R)\, \frac{\boldsymbol{R}}{R} \cdot \boldsymbol{n}_{\boldsymbol{y}}. \tag{C.244}$$

It is not difficult to see that the singular part corresponds to the Green's function of the Laplace equation, and therefore the associated integrals are computed in the same way, if the corresponding segments are close enough. Otherwise, and in the same way for the integrals associated with $\phi(R)$ and $\phi'(R)$, which are non-singular, a two-point Gauss quadrature formula is used. All the other computations are performed in the same manner as in Section B.12 for the Laplace equation.

C.14 Benchmark problem

As benchmark problem we consider the exterior circle problem (C.148), whose domain is shown in Figure C.3. The exact solution of this problem is stated in (C.178), and the idea is to retrieve it numerically with the integral equation techniques and the boundary element method described throughout this chapter.

For the computational implementation and the numerical resolution of the benchmark problem, we consider only the first integral equation of the extension-by-zero alternative (C.112), which is given in terms of boundary layer potentials by (C.193). The linear system (C.220) resulting from the discretization (C.218) of its variational formulation (C.207) is solved computationally with finite boundary elements of type $\mathbb{P}_1$ by using subroutines programmed in Fortran 90, by generating the mesh Γ^h of the boundary with the free software Gmsh 2.4, and by representing graphically the results in Matlab 7.5 (R2007b).

We consider a radius $R = 1$, a wave number $k = 3$, and a constant impedance $Z = 0.8$. The discretized boundary curve Γ^h consists of $I = 120$ segments and has a discretization step $h = 0.05235$, being

$$h = \max_{1 \leq j \leq I} |T_j|. \tag{C.245}$$

We observe that $h \approx 2\pi/I$. As incident field u_I we consider a plane wave in the form of (C.5) with a wave propagation vector $\boldsymbol{k} = (1, 0)$, i.e., such that the angle of incidence in (C.6) is given by $\theta_I = \pi$.

From (C.178), we can approximate the exact solution as the truncated series

$$u(r,\theta) = \frac{H_0^{(1)}(kr) f_0}{ZH_0^{(1)}(kR) - kH_1^{(1)}(kR)} + \sum_{n=1}^{40} \frac{RH_n^{(1)}(kr)\big(f_n e^{in\theta} + f_{-n} e^{-in\theta}\big)}{(ZR+n)H_n^{(1)}(kR) - kRH_{n+1}^{(1)}(kR)}, \quad \text{(C.246)}$$

being its trace on the boundary of the circle approximated by

$$\mu(\theta) = \frac{H_0^{(1)}(kR) f_0}{ZH_0^{(1)}(kR) - kH_1^{(1)}(kR)} + \sum_{n=1}^{40} \frac{RH_n^{(1)}(kR)\big(f_n e^{in\theta} + f_{-n} e^{-in\theta}\big)}{(ZR+n)H_n^{(1)}(kR) - kRH_{n+1}^{(1)}(kR)}. \quad \text{(C.247)}$$

The terms f_n related to the impedance data function are specified in (C.170).

The numerically calculated trace of the solution μ_h of the benchmark problem, which was computed by using the boundary element method, is depicted in Figure C.5. In the same manner, the numerical solution u_h is illustrated in Figures C.6 and C.7. It can be observed that the numerical solution is quite close to the exact one.

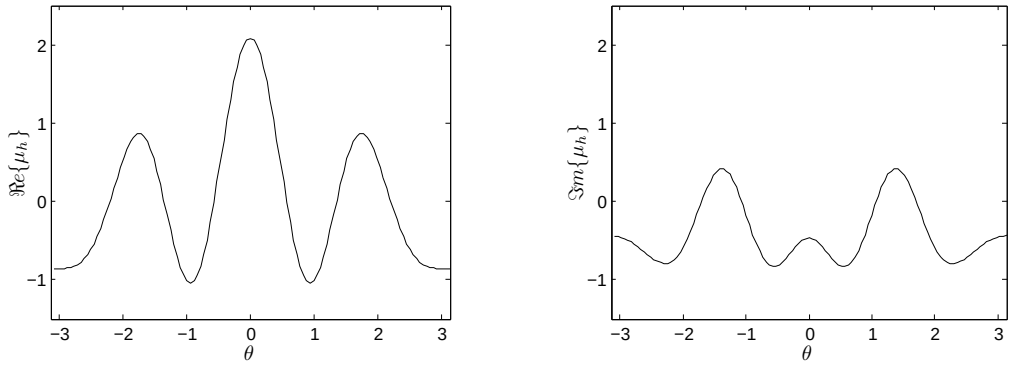

(a) Real part (b) Imaginary part

FIGURE C.5. Numerically computed trace of the solution μ_h.

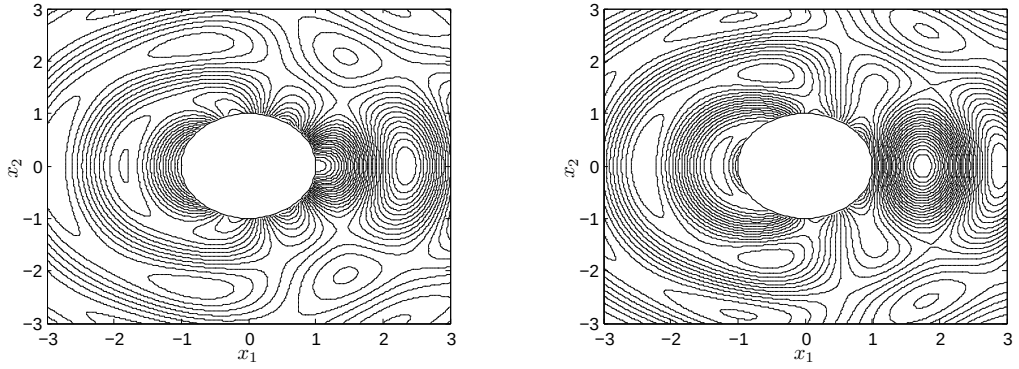

(a) Real part (b) Imaginary part

FIGURE C.6. Contour plot of the numerically computed solution u_h.

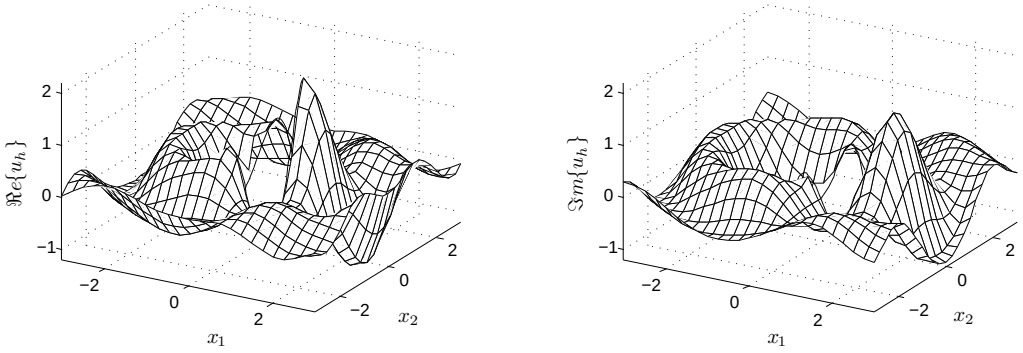

(a) Real part (b) Imaginary part

FIGURE C.7. Oblique view of the numerically computed solution u_h.

On behalf of the far field, two scattering cross sections are shown in Figure C.8. The bistatic radiation diagram represents the far-field pattern of the solution for a particular incident field in all observation directions. The monostatic radiation diagram, on the other hand, depicts the backscattering of incident fields from all directions, i.e., the far-field pattern in the same observation direction as for each incident field.

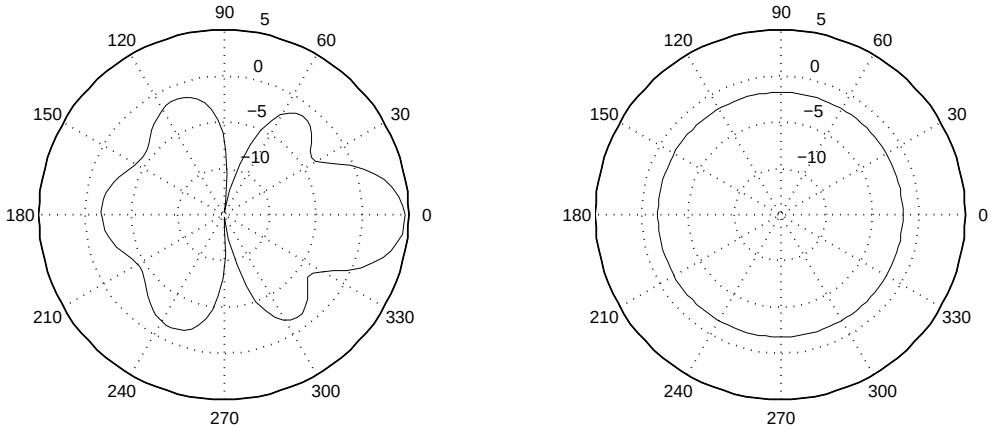

(a) Bistatic radiation diagram for $\theta_I = \pi$ (b) Monostatic radiation diagram

FIGURE C.8. Scattering cross sections in [dB].

Likewise as in (B.368), we define the relative error of the trace of the solution as

$$E_2(h, \Gamma^h) = \frac{\|\Pi_h \mu - \mu_h\|_{L^2(\Gamma^h)}}{\|\Pi_h \mu\|_{L^2(\Gamma^h)}}, \tag{C.248}$$

where $\Pi_h\mu$ denotes the Lagrange interpolating function of the exact solution's trace μ, i.e.,

$$\Pi_h\mu(\boldsymbol{x}) = \sum_{j=1}^{I} \mu(\boldsymbol{r}_j)\,\chi_j(\boldsymbol{x}) \quad \text{and} \quad \mu_h(\boldsymbol{x}) = \sum_{j=1}^{I} \mu_j\,\chi_j(\boldsymbol{x}) \quad \text{for } \boldsymbol{x} \in \Gamma^h. \tag{C.249}$$

In our case, for a step $h = 0.05235$, we obtained a relative error of $E_2(h, \Gamma^h) = 0.04185$.

As in (B.372), we define the relative error of the solution as

$$E_\infty(h, \Omega_L) = \frac{\|u - u_h\|_{L^\infty(\Omega_L)}}{\|u\|_{L^\infty(\Omega_L)}}, \tag{C.250}$$

being $\Omega_L = \{\boldsymbol{x} \in \Omega_e : \|\boldsymbol{x}\|_\infty < L\}$ for $L > 0$. We consider $L = 3$ and approximate Ω_L by a triangular finite element mesh of refinement h near the boundary. For $h = 0.05235$, the relative error that we obtained for the solution was $E_\infty(h, \Omega_L) = 0.03906$.

The results for different mesh refinements, i.e., for different numbers of segments I and discretization steps h, are listed in Table C.1. These results are illustrated graphically in Figure C.9. It can be observed that the relative errors are approximately of order h.

TABLE C.1. Relative errors for different mesh refinements.

I	h	$E_2(h, \Gamma^h)$	$E_\infty(h, \Omega_L)$
12	0.5176	$5.563 \cdot 10^{-1}$	$4.604 \cdot 10^{-1}$
40	0.1569	$1.344 \cdot 10^{-1}$	$1.270 \cdot 10^{-1}$
80	0.07852	$6.383 \cdot 10^{-2}$	$5.979 \cdot 10^{-2}$
120	0.05235	$4.185 \cdot 10^{-2}$	$3.906 \cdot 10^{-2}$
240	0.02618	$2.058 \cdot 10^{-2}$	$1.914 \cdot 10^{-2}$
500	0.01257	$9.794 \cdot 10^{-3}$	$9.091 \cdot 10^{-3}$
1000	0.006283	$4.878 \cdot 10^{-3}$	$4.524 \cdot 10^{-3}$

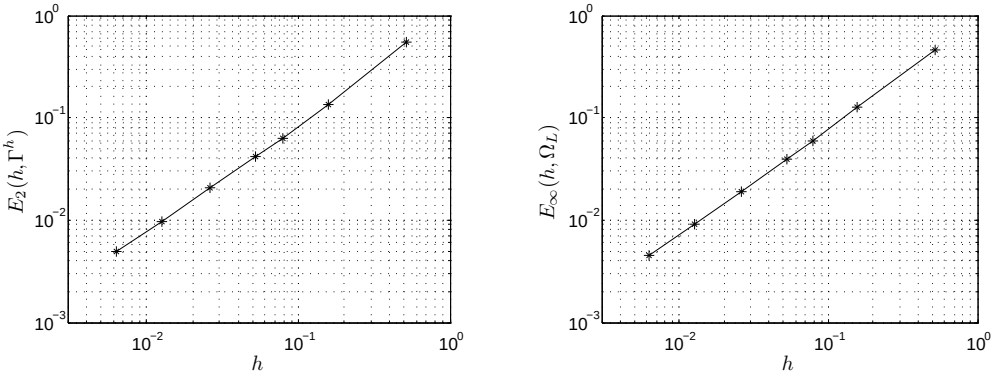

(a) Relative error $E_2(h, \Gamma^h)$ (b) Relative error $E_\infty(h, \Omega_L)$

FIGURE C.9. Logarithmic plots of the relative errors versus the discretization step.

D. FULL-SPACE IMPEDANCE LAPLACE PROBLEM

D.1 Introduction

In this appendix we study the perturbed full-space or free-space impedance Laplace problem, also known as the exterior impedance Laplace problem in 3D, using integral equation techniques and the boundary element method.

We consider the problem of the Laplace equation in three dimensions on the exterior of a bounded obstacle with an impedance boundary condition. The perturbed full-space impedance Laplace problem is not strictly speaking a wave scattering problem, but it can be regarded as a limit case of such a problem when the frequency tends towards zero (vid. Appendix E). It can be also regarded as a surface wave problem around a bounded three-dimensional obstacle. The two-dimensional problem has been already treated thoroughly in Appendix B.

For the problem treated herein we follow mainly Nédélec (1977, 1979, 2001) and Raviart (1991). Further related books and doctorate theses are Chen & Zhou (1992), Evans (1998), Giroire (1987), Hsiao & Wendland (2008), Johnson (1987), Kellogg (1929), Kress (1989), Rjasanow & Steinbach (2007), and Steinbach (2008). Some articles that deal specifically with the Laplace equation with an impedance boundary condition are Ahner & Wiener (1991), Lanzani & Shen (2004), and Medková (1998). The mixed boundary-value problem is treated by Wendland, Stephan & Hsiao (1979). Interesting theoretical details on transmission problems can be found in Costabel & Stephan (1985). The boundary element calculations can be found in Bendali & Devys (1986). The use of cracked domains is studied by Medková & Krutitskii (2005), and the inverse problem by Fasino & Inglese (1999) and Lin & Fang (2005). Applications of the Laplace problem can be found, among others, for electrostatics (Jackson 1999), for conductivity in biomedical imaging (Ammari 2008), and for incompressible three-dimensional potential flows (Spurk 1997).

The Laplace equation does not allow the propagation of volume waves inside the considered domain, but the addition of an impedance boundary condition permits the propagation of surface waves along the boundary of the obstacle. The main difficulty in the numerical treatment and resolution of our problem is the fact that the exterior domain is unbounded. We solve it therefore with integral equation techniques and the boundary element method, which require the knowledge of the Green's function.

This appendix is structured in 13 sections, including this introduction. The differential problem of the Laplace equation in a three-dimensional exterior domain with an impedance boundary condition is presented in Section D.2. The Green's function and its far-field expression are computed respectively in Sections D.3 and D.4. Extending the differential problem towards a transmission problem, as done in Section D.5, allows its resolution by using integral equation techniques, which is discussed in Section D.6. These techniques allow also to represent the far field of the solution, as shown in Section D.7. A particular problem that takes as domain the exterior of a sphere is solved analytically in Section D.8. The appropriate function spaces and some existence and uniqueness results for the solution

of the problem are presented in Section D.9. By means of the variational formulation developed in Section D.10, the obtained integral equation is discretized using the boundary element method, which is described in Section D.11. The boundary element calculations required to build the matrix of the linear system resulting from the numerical discretization are explained in Section D.12. Finally, in Section D.13 a benchmark problem based on the exterior sphere problem is solved numerically.

D.2 Direct perturbation problem

We consider an exterior open and connected domain $\Omega_e \subset \mathbb{R}^3$ that lies outside a bounded obstacle Ω_i and whose boundary $\Gamma = \partial\Omega_e = \partial\Omega_i$ is regular (e.g., of class C^2), as shown in Figure D.1. As a perturbation problem, we decompose the total field u_T as $u_T = u_W + u$, where u_W represents the known field without obstacle, and where u denotes the perturbed field due its presence, which has bounded energy. The direct perturbation problem of interest is to find the perturbed field u that satisfies the Laplace equation in Ω_e, an impedance boundary condition on Γ, and a decaying condition at infinity. We consider that the origin is located in Ω_i and that the unit normal $\boldsymbol{n}$ is taken always outwardly oriented of Ω_e, i.e., pointing inwards of Ω_i.

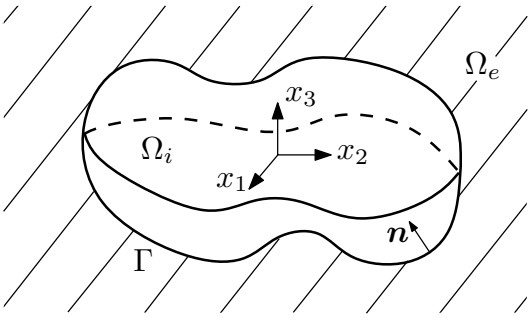

FIGURE D.1. Perturbed full-space impedance Laplace problem domain.

The total field u_T satisfies the Laplace equation

$$\Delta u_T = 0 \qquad \text{in } \Omega_e, \tag{D.1}$$

which is also satisfied by the fields u_W and u, due linearity. For the perturbed field u we take also the inhomogeneous impedance boundary condition

$$-\frac{\partial u}{\partial n} + Zu = f_z \qquad \text{on } \Gamma, \tag{D.2}$$

where Z is the impedance on the boundary, and where the impedance data function f_z is assumed to be known. If $Z = 0$ or $Z = \infty$, then we retrieve respectively the classical Neumann or Dirichlet boundary conditions. In general, we consider a complex-valued impedance $Z(\boldsymbol{x})$ depending on the position $\boldsymbol{x}$. The function $f_z(\boldsymbol{x})$ may depend on Z and u_w, but is independent of u.

The Laplace equation (D.1) admits different kinds of non-trivial solutions u_W, when we consider the domain Ω_e as the unperturbed full-space $\mathbb{R}^3$. One kind of solutions are the harmonic polynomials in $\mathbb{R}^3$. There exist likewise other harmonic non-polynomial functions that satisfy the Laplace equation in $\mathbb{R}^3$, but which have a bigger growth at infinity than any polynomial, e.g., the exponential functions

$$u_W(\boldsymbol{x}) = e^{\boldsymbol{a}\cdot\boldsymbol{x}}, \qquad \text{where } \ \boldsymbol{a} \in \mathbb{C}^3 \ \text{ and } \ a_1^2 + a_2^2 + a_3^2 = 0. \tag{D.3}$$

Any such function can be taken as the known field without perturbation u_W, which holds in particular for all the constant and linear functions in $\mathbb{R}^3$.

For the perturbed field u in the exterior domain Ω_e, though, these functions represent undesired non-physical solutions, which have to be avoided in order to ensure uniqueness of the solution u. To eliminate them, it suffices to impose for u an asymptotic decaying behavior at infinity that excludes the polynomials. This decaying condition involves finite energy throughout Ω_e and can be interpreted as an additional boundary condition at infinity. In our case it is given, for a great value of $|\boldsymbol{x}|$, by

$$u(\boldsymbol{x}) = \mathcal{O}\left(\frac{1}{|\boldsymbol{x}|}\right) \qquad \text{and} \qquad |\nabla u(\boldsymbol{x})| = \mathcal{O}\left(\frac{1}{|\boldsymbol{x}|^2}\right). \tag{D.4}$$

It can be expressed equivalently, for some constants $C > 0$, by

$$|u(\boldsymbol{x})| \leq \frac{C}{|\boldsymbol{x}|} \qquad \text{and} \qquad |\nabla u(\boldsymbol{x})| \leq \frac{C}{|\boldsymbol{x}|^2} \qquad \text{as } \ |\boldsymbol{x}| \to \infty. \tag{D.5}$$

In fact, the decaying condition can be even stated as

$$u(\boldsymbol{x}) = \mathcal{O}\left(\frac{1}{|\boldsymbol{x}|^{\alpha}}\right) \qquad \text{and} \qquad |\nabla u(\boldsymbol{x})| = \mathcal{O}\left(\frac{1}{|\boldsymbol{x}|^{1+\alpha}}\right) \qquad \text{for } \ 0 < \alpha \leq 1, \tag{D.6}$$

or as the more weaker and general formulation

$$\lim_{R\to\infty} \int_{S_R} \frac{|u|^2}{R^2}\, \mathrm{d}\gamma = 0 \qquad \text{and} \qquad \lim_{R\to\infty} \int_{S_R} |\nabla u|^2\, \mathrm{d}\gamma = 0, \tag{D.7}$$

where $S_R = \{\boldsymbol{x} \in \mathbb{R}^3 : |\boldsymbol{x}| = R\}$ is the sphere of radius R and where the boundary differential element in spherical coordinates is given by $\mathrm{d}\gamma = R^2 \sin\theta\, \mathrm{d}\theta\, \mathrm{d}\varphi$.

The perturbed full-space impedance Laplace problem can be finally stated as

$$\begin{cases} \text{Find } u : \Omega_e \to \mathbb{C} \text{ such that} \\ \Delta u = 0 & \text{in } \ \Omega_e, \\ -\dfrac{\partial u}{\partial n} + Zu = f_z & \text{on } \ \Gamma, \\ |u(\boldsymbol{x})| \leq \dfrac{C}{|\boldsymbol{x}|} & \text{as } \ |\boldsymbol{x}| \to \infty, \\ |\nabla u(\boldsymbol{x})| \leq \dfrac{C}{|\boldsymbol{x}|^2} & \text{as } \ |\boldsymbol{x}| \to \infty. \end{cases} \tag{D.8}$$

D.3 Green's function

The Green's function represents the response of the unperturbed system (without an obstacle) to a Dirac mass. It corresponds to a function G, which depends on a fixed source point $\boldsymbol{x} \in \mathbb{R}^3$ and an observation point $\boldsymbol{y} \in \mathbb{R}^3$. The Green's function is computed in the sense of distributions for the variable $\boldsymbol{y}$ in the full-space $\mathbb{R}^3$ by placing at the right-hand side of the Laplace equation a Dirac mass $\delta_{\boldsymbol{x}}$, centered at the point $\boldsymbol{x}$. It is therefore a solution $G(\boldsymbol{x}, \cdot) : \mathbb{R}^3 \to \mathbb{C}$ for the radiation problem of a point source, namely

$$\Delta_{\boldsymbol{y}} G(\boldsymbol{x}, \boldsymbol{y}) = \delta_{\boldsymbol{x}}(\boldsymbol{y}) \qquad \text{in } \mathcal{D}'(\mathbb{R}^3). \tag{D.9}$$

Due to the radial symmetry of the problem (D.9), it is natural to look for solutions in the form $G = G(r)$, where $r = |\boldsymbol{y} - \boldsymbol{x}|$. By considering only the radial component, the Laplace equation in $\mathbb{R}^3$ becomes

$$\frac{1}{r^2}\frac{\mathrm{d}}{\mathrm{d}r}\left(r^2 \frac{\mathrm{d}G}{\mathrm{d}r}\right) = 0, \qquad r > 0. \tag{D.10}$$

The general solution of (D.10) is of the form

$$G(r) = \frac{C_1}{r} + C_2, \tag{D.11}$$

for some constants C_1 and C_2. The choice of C_2 is arbitrary, while C_1 is fixed by the presence of the Dirac mass in (D.9). To determine C_1, we have to perform thus a computation in the sense of distributions (cf. Gel'fand & Shilov 1964), using the fact that G is harmonic for $r \neq 0$. For a test function $\varphi \in \mathcal{D}(\mathbb{R}^3)$, we have by definition that

$$\langle \Delta_{\boldsymbol{y}} G, \varphi \rangle = \langle G, \Delta\varphi \rangle = \int_{\mathbb{R}^3} G\, \Delta\varphi \, \mathrm{d}\boldsymbol{y} = \lim_{\varepsilon \to 0} \int_{r \geq \varepsilon} G\, \Delta\varphi \, \mathrm{d}\boldsymbol{y}. \tag{D.12}$$

We apply here Green's second integral theorem (A.613), choosing as bounded domain the spherical shell $\varepsilon \leq r \leq a$, where a is large enough so that the test function $\varphi(\boldsymbol{y})$, of bounded support, vanishes identically for $r \geq a$. Then

$$\int_{r \geq \varepsilon} G\, \Delta\varphi \, \mathrm{d}\boldsymbol{y} = \int_{r \geq \varepsilon} \Delta_{\boldsymbol{y}} G\, \varphi \, \mathrm{d}\boldsymbol{y} - \int_{r=\varepsilon} G \frac{\partial \varphi}{\partial r} \, \mathrm{d}\gamma + \int_{r=\varepsilon} \frac{\partial G}{\partial r_{\boldsymbol{y}}} \varphi \, \mathrm{d}\gamma, \tag{D.13}$$

where $\mathrm{d}\gamma$ is the line element on the sphere $r = \varepsilon$. Now

$$\int_{r \geq \varepsilon} \Delta_{\boldsymbol{y}} G\, \varphi \, \mathrm{d}\boldsymbol{y} = 0, \tag{D.14}$$

since outside the ball $r \leq \varepsilon$ the function G is harmonic. As for the other terms, by replacing (D.11), we obtain that

$$\int_{r=\varepsilon} G \frac{\partial \varphi}{\partial r} \, \mathrm{d}\gamma = \left(\frac{C_1}{\varepsilon} + C_2\right) \int_{r=\varepsilon} \frac{\partial \varphi}{\partial r} \, \mathrm{d}\gamma = \mathcal{O}(\varepsilon), \tag{D.15}$$

and

$$\int_{r=\varepsilon} \frac{\partial G}{\partial r_{\boldsymbol{y}}} \varphi \, \mathrm{d}\gamma = -\frac{C_1}{\varepsilon^2} \int_{r=\varepsilon} \varphi \, \mathrm{d}\gamma = -4\pi C_1 S_\varepsilon(\varphi), \tag{D.16}$$

where $S_\varepsilon(\varphi)$ is the mean value of $\varphi(\boldsymbol{y})$ on the sphere of radius ε and centered at $\boldsymbol{x}$. In the limit as $\varepsilon \to 0$, we obtain that $S_\varepsilon(\varphi) \to \varphi(\boldsymbol{x})$, so that

$$\langle \Delta_{\boldsymbol{y}} G, \varphi \rangle = \lim_{\varepsilon \to 0} \int_{r \geq \varepsilon} G \, \Delta\varphi \, \mathrm{d}\boldsymbol{y} = -4\pi C_1 \varphi(\boldsymbol{x}) = -4\pi C_1 \langle \delta_{\boldsymbol{x}}, \varphi \rangle. \tag{D.17}$$

Thus if $C_1 = -1/4\pi$, then (D.9) is fulfilled. When we consider not only radial solutions, then the general solution of (D.9) is given by

$$G(\boldsymbol{x}, \boldsymbol{y}) = -\frac{1}{4\pi |\boldsymbol{y} - \boldsymbol{x}|} + \phi(\boldsymbol{x}, \boldsymbol{y}), \tag{D.18}$$

where $\phi(\boldsymbol{x}, \boldsymbol{y})$ is any harmonic function in the variable $\boldsymbol{y}$, i.e., such that $\Delta_{\boldsymbol{y}} \phi = 0$ in $\mathbb{R}^3$, e.g., an harmonic polynomial in $\mathbb{R}^3$ or a function of the form of (D.3).

If we impose additionally, for a fixed $\boldsymbol{x}$, the asymptotic decaying condition

$$|\nabla_{\boldsymbol{y}} G(\boldsymbol{x}, \boldsymbol{y})| = \mathcal{O}\left(\frac{1}{|\boldsymbol{y}|^2}\right) \qquad \text{as} \quad |\boldsymbol{y}| \longrightarrow \infty, \tag{D.19}$$

then we eliminate any polynomial (or bigger) growth at infinity, including constant and logarithmic growth. The Green's function satisfying (D.9) and (D.19) is finally given by

$$G(\boldsymbol{x}, \boldsymbol{y}) = -\frac{1}{4\pi |\boldsymbol{y} - \boldsymbol{x}|}, \tag{D.20}$$

being its gradient

$$\nabla_{\boldsymbol{y}} G(\boldsymbol{x}, \boldsymbol{y}) = \frac{\boldsymbol{y} - \boldsymbol{x}}{4\pi |\boldsymbol{y} - \boldsymbol{x}|^3}. \tag{D.21}$$

We can likewise define a gradient with respect to the $\boldsymbol{x}$ variable by

$$\nabla_{\boldsymbol{x}} G(\boldsymbol{x}, \boldsymbol{y}) = \frac{\boldsymbol{x} - \boldsymbol{y}}{4\pi |\boldsymbol{x} - \boldsymbol{y}|^3}, \tag{D.22}$$

and a double-gradient matrix by

$$\nabla_{\boldsymbol{x}} \nabla_{\boldsymbol{y}} G(\boldsymbol{x}, \boldsymbol{y}) = -\frac{\boldsymbol{I}}{4\pi |\boldsymbol{x} - \boldsymbol{y}|^3} + \frac{3(\boldsymbol{x} - \boldsymbol{y}) \otimes (\boldsymbol{x} - \boldsymbol{y})}{4\pi |\boldsymbol{x} - \boldsymbol{y}|^5}, \tag{D.23}$$

where $\boldsymbol{I}$ denotes a 3×3 identity matrix and where $\otimes$ denotes the dyadic or outer product of two vectors, which results in a matrix and is defined in (A.572).

We note that the Green's function (D.20) is symmetric in the sense that

$$G(\boldsymbol{x}, \boldsymbol{y}) = G(\boldsymbol{y}, \boldsymbol{x}), \tag{D.24}$$

and it fulfills similarly

$$\nabla_{\boldsymbol{y}} G(\boldsymbol{x}, \boldsymbol{y}) = \nabla_{\boldsymbol{y}} G(\boldsymbol{y}, \boldsymbol{x}) = -\nabla_{\boldsymbol{x}} G(\boldsymbol{x}, \boldsymbol{y}) = -\nabla_{\boldsymbol{x}} G(\boldsymbol{y}, \boldsymbol{x}), \tag{D.25}$$

and

$$\nabla_{\boldsymbol{x}} \nabla_{\boldsymbol{y}} G(\boldsymbol{x}, \boldsymbol{y}) = \nabla_{\boldsymbol{y}} \nabla_{\boldsymbol{x}} G(\boldsymbol{x}, \boldsymbol{y}) = \nabla_{\boldsymbol{x}} \nabla_{\boldsymbol{y}} G(\boldsymbol{y}, \boldsymbol{x}) = \nabla_{\boldsymbol{y}} \nabla_{\boldsymbol{x}} G(\boldsymbol{y}, \boldsymbol{x}). \tag{D.26}$$

D.4 Far field of the Green's function

The far field of the Green's function describes its asymptotic behavior at infinity, i.e., when $|\boldsymbol{x}| \to \infty$ and assuming that $\boldsymbol{y}$ is fixed. For this purpose, we search the terms of

highest order at infinity by expanding with respect to the variable $\boldsymbol{x}$ the expressions

$$|\boldsymbol{x}-\boldsymbol{y}|^2 = |\boldsymbol{x}|^2\left(1-\frac{2\boldsymbol{x}\cdot\boldsymbol{y}}{|\boldsymbol{x}|^2}+\frac{|\boldsymbol{y}|^2}{|\boldsymbol{x}|^2}\right), \tag{D.27}$$

$$|\boldsymbol{x}-\boldsymbol{y}| = |\boldsymbol{x}|\left(1-\frac{\boldsymbol{x}\cdot\boldsymbol{y}}{|\boldsymbol{x}|^2}+\mathcal{O}\left(\frac{1}{|\boldsymbol{x}|^2}\right)\right), \tag{D.28}$$

$$\frac{1}{|\boldsymbol{x}-\boldsymbol{y}|} = \frac{1}{|\boldsymbol{x}|}\left(1+\frac{\boldsymbol{x}\cdot\boldsymbol{y}}{|\boldsymbol{x}|^2}+\mathcal{O}\left(\frac{1}{|\boldsymbol{x}|^2}\right)\right). \tag{D.29}$$

We express the point $\boldsymbol{x}$ as $\boldsymbol{x} = |\boldsymbol{x}|\hat{\boldsymbol{x}}$, being $\hat{\boldsymbol{x}}$ a unitary vector. The far field of the Green's function, as $|\boldsymbol{x}| \to \infty$, is thus given by

$$G^{ff}(\boldsymbol{x},\boldsymbol{y}) = -\frac{1}{4\pi|\boldsymbol{x}|}-\frac{\boldsymbol{y}\cdot\hat{\boldsymbol{x}}}{4\pi|\boldsymbol{x}|^2}. \tag{D.30}$$

Similarly, as $|\boldsymbol{x}| \to \infty$, we have for its gradient with respect to $\boldsymbol{y}$, that

$$\nabla_{\boldsymbol{y}} G^{ff}(\boldsymbol{x},\boldsymbol{y}) = -\frac{\hat{\boldsymbol{x}}}{4\pi|\boldsymbol{x}|^2}, \tag{D.31}$$

for its gradient with respect to $\boldsymbol{x}$, that

$$\nabla_{\boldsymbol{x}} G^{ff}(\boldsymbol{x},\boldsymbol{y}) = \frac{\hat{\boldsymbol{x}}}{4\pi|\boldsymbol{x}|^2}, \tag{D.32}$$

and for its double-gradient matrix, that

$$\nabla_{\boldsymbol{x}}\nabla_{\boldsymbol{y}} G^{ff}(\boldsymbol{x},\boldsymbol{y}) = -\frac{\boldsymbol{I}}{4\pi|\boldsymbol{x}|^3}+\frac{3(\hat{\boldsymbol{x}}\otimes\hat{\boldsymbol{x}})}{4\pi|\boldsymbol{x}|^3}. \tag{D.33}$$

D.5 Transmission problem

We are interested in expressing the solution u of the direct perturbation problem (D.8) by means of an integral representation formula over the boundary Γ. To study this kind of representations, the differential problem defined on Ω_e is extended as a transmission problem defined now on the whole space $\mathbb{R}^3$ by combining (D.8) with a corresponding interior problem defined on Ω_i. For the transmission problem, which specifies jump conditions over the boundary Γ, a general integral representation can be developed, and the particular integral representations of interest are then established by the specific choice of the corresponding interior problem.

A transmission problem is then a differential problem for which the jump conditions of the solution field, rather than boundary conditions, are specified on the boundary Γ. As shown in Figure D.1, we consider the exterior domain Ω_e and the interior domain Ω_i, taking the unit normal $\boldsymbol{n}$ pointing towards Ω_i. We search now a solution u defined in $\Omega_e \cup \Omega_i$, and use the notation $u_e = u|_{\Omega_e}$ and $u_i = u|_{\Omega_i}$. We define the jumps of the traces of u on both sides of the boundary Γ as

$$[u] = u_e - u_i \qquad \text{and} \qquad \left[\frac{\partial u}{\partial n}\right] = \frac{\partial u_e}{\partial n}-\frac{\partial u_i}{\partial n}. \tag{D.34}$$

The transmission problem is now given by

$$\begin{cases} \text{Find } u : \Omega_e \cup \Omega_i \to \mathbb{C} \text{ such that} \\ \Delta u = 0 \qquad\qquad \text{in } \ \Omega_e \cup \Omega_i, \\ [u] = \mu \qquad\qquad \text{on } \ \Gamma, \\ \left[\dfrac{\partial u}{\partial n}\right] = \nu \qquad \text{on } \ \Gamma, \\ \text{+ Decaying condition as } |\boldsymbol{x}| \to \infty, \end{cases} \tag{D.35}$$

where $\mu, \nu : \Gamma \to \mathbb{C}$ are known functions. The decaying condition is still (D.5), and it is required to ensure uniqueness of the solution.

D.6 Integral representations and equations

D.6.1 Integral representation

To develop for the solution u an integral representation formula over the boundary Γ, we define by $\Omega_{R,\varepsilon}$ the domain $\Omega_e \cup \Omega_i$ without the ball B_ε of radius $\varepsilon > 0$ centered at the point $\boldsymbol{x} \in \Omega_e \cup \Omega_i$, and truncated at infinity by the ball B_R of radius $R > 0$ centered at the origin. We consider that the ball B_ε is entirely contained either in Ω_e or in Ω_i, depending on the location of its center $\boldsymbol{x}$. Therefore, as shown in Figure D.2, we have that

$$\Omega_{R,\varepsilon} = \big((\Omega_e \cup \Omega_i) \cap B_R\big) \setminus \overline{B_\varepsilon}, \tag{D.36}$$

where

$$B_R = \{\boldsymbol{y} \in \mathbb{R}^3 : \ |\boldsymbol{y}| < R\} \qquad \text{and} \qquad B_\varepsilon = \{\boldsymbol{y} \in \mathbb{R}^3 : \ |\boldsymbol{y} - \boldsymbol{x}| < \varepsilon\}. \tag{D.37}$$

We consider similarly the boundaries of the balls

$$S_R = \{\boldsymbol{y} \in \mathbb{R}^3 : \ |\boldsymbol{y}| = R\} \qquad \text{and} \qquad S_\varepsilon = \{\boldsymbol{y} \in \mathbb{R}^3 : \ |\boldsymbol{y} - \boldsymbol{x}| = \varepsilon\}. \tag{D.38}$$

The idea is to retrieve the domain $\Omega_e \cup \Omega_i$ at the end when the limits $R \to \infty$ and $\varepsilon \to 0$ are taken for the truncated domain $\Omega_{R,\varepsilon}$.

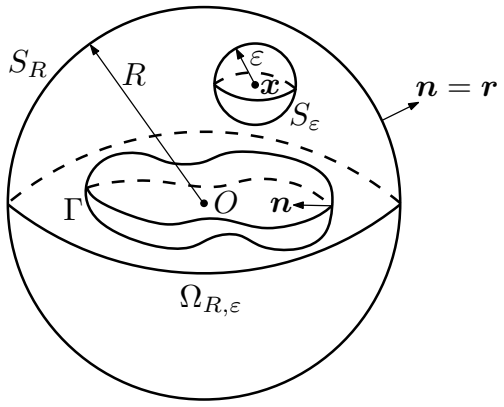

FIGURE D.2. Truncated domain $\Omega_{R,\varepsilon}$ for $\boldsymbol{x} \in \Omega_e \cup \Omega_i$.

We apply now Green's second integral theorem (A.613) to the functions u and $G(\boldsymbol{x},\cdot)$ in the bounded domain $\Omega_{R,\varepsilon}$, yielding

$$\begin{aligned}
0 &= \int_{\Omega_{R,\varepsilon}} \big(u(\boldsymbol{y})\Delta_{\boldsymbol{y}} G(\boldsymbol{x},\boldsymbol{y}) - G(\boldsymbol{x},\boldsymbol{y})\Delta u(\boldsymbol{y})\big)\mathrm{d}\boldsymbol{y} \\
&= \int_{S_R} \left(u(\boldsymbol{y})\frac{\partial G}{\partial r_{\boldsymbol{y}}}(\boldsymbol{x},\boldsymbol{y}) - G(\boldsymbol{x},\boldsymbol{y})\frac{\partial u}{\partial r}(\boldsymbol{y})\right)\mathrm{d}\gamma(\boldsymbol{y}) \\
&- \int_{S_\varepsilon} \left(u(\boldsymbol{y})\frac{\partial G}{\partial r_{\boldsymbol{y}}}(\boldsymbol{x},\boldsymbol{y}) - G(\boldsymbol{x},\boldsymbol{y})\frac{\partial u}{\partial r}(\boldsymbol{y})\right)\mathrm{d}\gamma(\boldsymbol{y}) \\
&+ \int_{\Gamma} \left([u](\boldsymbol{y})\frac{\partial G}{\partial n_{\boldsymbol{y}}}(\boldsymbol{x},\boldsymbol{y}) - G(\boldsymbol{x},\boldsymbol{y})\left[\frac{\partial u}{\partial n}\right](\boldsymbol{y})\right)\mathrm{d}\gamma(\boldsymbol{y}). \qquad \text{(D.39)}
\end{aligned}$$

For R large enough, the integral on S_R tends to zero, since

$$\left|\int_{S_R} u(\boldsymbol{y})\frac{\partial G}{\partial r_{\boldsymbol{y}}}(\boldsymbol{x},\boldsymbol{y})\,\mathrm{d}\gamma(\boldsymbol{y})\right| \leq \frac{C}{R}, \qquad \text{(D.40)}$$

and

$$\left|\int_{S_R} G(\boldsymbol{x},\boldsymbol{y})\frac{\partial u}{\partial r}(\boldsymbol{y})\,\mathrm{d}\gamma(\boldsymbol{y})\right| \leq \frac{C}{R}, \qquad \text{(D.41)}$$

for some constants $C > 0$, due the asymptotic decaying behavior at infinity (D.5). If the function u is regular enough in the ball B_ε, then the second term of the integral on S_ε, when $\varepsilon \to 0$ and due (D.20), is bounded by

$$\left|\int_{S_\varepsilon} G(\boldsymbol{x},\boldsymbol{y})\frac{\partial u}{\partial r}(\boldsymbol{y})\,\mathrm{d}\gamma(\boldsymbol{y})\right| \leq \varepsilon \sup_{\boldsymbol{y}\in B_\varepsilon}\left|\frac{\partial u}{\partial r}(\boldsymbol{y})\right|, \qquad \text{(D.42)}$$

and tends to zero. The regularity of u can be specified afterwards once the integral representation has been determined and generalized by means of density arguments. The first integral term on S_ε can be decomposed as

$$\begin{aligned}
\int_{S_\varepsilon} u(\boldsymbol{y})\frac{\partial G}{\partial r_{\boldsymbol{y}}}(\boldsymbol{x},\boldsymbol{y})\,\mathrm{d}\gamma(\boldsymbol{y}) &= u(\boldsymbol{x})\int_{S_\varepsilon}\frac{\partial G}{\partial r_{\boldsymbol{y}}}(\boldsymbol{x},\boldsymbol{y})\,\mathrm{d}\gamma(\boldsymbol{y}) \\
&+ \int_{S_\varepsilon}\frac{\partial G}{\partial r_{\boldsymbol{y}}}(\boldsymbol{x},\boldsymbol{y})\big(u(\boldsymbol{y}) - u(\boldsymbol{x})\big)\,\mathrm{d}\gamma(\boldsymbol{y}), \qquad \text{(D.43)}
\end{aligned}$$

For the first term in the right-hand side of (D.43), by replacing (D.21), we have that

$$\int_{S_\varepsilon}\frac{\partial G}{\partial r_{\boldsymbol{y}}}(\boldsymbol{x},\boldsymbol{y})\,\mathrm{d}\gamma(\boldsymbol{y}) = 1, \qquad \text{(D.44)}$$

while the second term is bounded by

$$\left|\int_{S_\varepsilon}\big(u(\boldsymbol{y}) - u(\boldsymbol{x})\big)\frac{\partial G}{\partial r_{\boldsymbol{y}}}(\boldsymbol{x},\boldsymbol{y})\,\mathrm{d}\gamma(\boldsymbol{y})\right| \leq \sup_{\boldsymbol{y}\in B_\varepsilon}|u(\boldsymbol{y}) - u(\boldsymbol{x})|, \qquad \text{(D.45)}$$

which tends towards zero when $\varepsilon \to 0$.

In conclusion, when the limits $R \to \infty$ and $\varepsilon \to 0$ are taken in (D.39), then the following integral representation formula holds for the solution u of the transmission problem:

$$u(\boldsymbol{x}) = \int_{\Gamma}\left([u](\boldsymbol{y})\frac{\partial G}{\partial n_{\boldsymbol{y}}}(\boldsymbol{x},\boldsymbol{y}) - G(\boldsymbol{x},\boldsymbol{y})\left[\frac{\partial u}{\partial n}\right](\boldsymbol{y})\right)\mathrm{d}\gamma(\boldsymbol{y}), \qquad \boldsymbol{x}\in\Omega_e\cup\Omega_i. \qquad \text{(D.46)}$$

We observe thus that if the values of the jump of u and of its normal derivative are known on Γ, then the transmission problem (D.35) is readily solved and its solution given explicitly by (D.46), which, in terms of μ and ν, becomes

$$u(\boldsymbol{x}) = \int_\Gamma \left(\mu(\boldsymbol{y}) \frac{\partial G}{\partial n_{\boldsymbol{y}}}(\boldsymbol{x}, \boldsymbol{y}) - G(\boldsymbol{x}, \boldsymbol{y}) \nu(\boldsymbol{y}) \right) \mathrm{d}\gamma(\boldsymbol{y}), \qquad \boldsymbol{x} \in \Omega_e \cup \Omega_i. \tag{D.47}$$

To determine the values of the jumps, an adequate integral equation has to be developed, i.e., an equation whose unknowns are the traces of the solution on Γ.

An alternative way to demonstrate the integral representation (D.46) is to proceed in the sense of distributions, in the same way as done in Section B.6. Again we obtain the single layer potential

$$\left\{ G * \left[\frac{\partial u}{\partial n} \right] \delta_\Gamma \right\} (\boldsymbol{x}) = \int_\Gamma G(\boldsymbol{x}, \boldsymbol{y}) \left[\frac{\partial u}{\partial n} \right] (\boldsymbol{y}) \, \mathrm{d}\gamma(\boldsymbol{y}) \tag{D.48}$$

associated with the distribution of sources $[\partial u / \partial n] \delta_\Gamma$, and the double layer potential

$$\left\{ G * \frac{\partial}{\partial n} \big([u] \delta_\Gamma \big) \right\} (\boldsymbol{x}) = - \int_\Gamma \frac{\partial G}{\partial n_{\boldsymbol{y}}}(\boldsymbol{x}, \boldsymbol{y}) [u](\boldsymbol{y}) \, \mathrm{d}\gamma(\boldsymbol{y}) \tag{D.49}$$

associated with the distribution of dipoles $\frac{\partial}{\partial n}([u]\delta_\Gamma)$. Combining properly (D.48) and (D.49) yields the desired integral representation (D.46).

We note that to obtain the gradient of the integral representation (D.46) we can pass directly the derivatives inside the integral, since there are no singularities if $\boldsymbol{x} \in \Omega_e \cup \Omega_i$. Therefore we have that

$$\nabla u(\boldsymbol{x}) = \int_\Gamma \left([u](\boldsymbol{y}) \nabla_{\boldsymbol{x}} \frac{\partial G}{\partial n_{\boldsymbol{y}}}(\boldsymbol{x}, \boldsymbol{y}) - \nabla_{\boldsymbol{x}} G(\boldsymbol{x}, \boldsymbol{y}) \left[\frac{\partial u}{\partial n} \right] (\boldsymbol{y}) \right) \mathrm{d}\gamma(\boldsymbol{y}). \tag{D.50}$$

We remark also that Green's first integral theorem (A.612) implies for the solution u_i of the interior problem that

$$\int_\Gamma \frac{\partial u_i}{\partial n} \, \mathrm{d}\gamma = - \int_{\Omega_i} \Delta u_i \, \mathrm{d}\boldsymbol{x} = 0. \tag{D.51}$$

Nonetheless a three-dimensional equivalent of (B.58) does no longer apply, since this integral converges to a constant as $R \to \infty$, which is not necessarily zero.

D.6.2 Integral equation

To determine the values of the traces that conform the jumps for the transmission problem (D.35), an integral equation has to be developed. For this purpose we place the source point $\boldsymbol{x}$ on the boundary Γ and apply the same procedure as before for the integral representation (D.46), treating differently in (D.39) only the integrals on S_ε. The integrals on S_R still behave well and tend towards zero as $R \to \infty$. The Ball B_ε, though, is split in half into the two pieces $\Omega_e \cap B_\varepsilon$ and $\Omega_i \cap B_\varepsilon$, which are asymptotically separated by the tangent of the boundary if Γ is regular. Thus the associated integrals on S_ε give rise to a term $-(u_e(\boldsymbol{x}) + u_i(\boldsymbol{x}))/2$ instead of just $-u(\boldsymbol{x})$ as before. We must notice that in this case, the integrands associated with the boundary Γ admit an integrable singularity at the

point $\boldsymbol{x}$. The desired integral equation related with (D.46) is then given by

$$\frac{u_e(\boldsymbol{x})+u_i(\boldsymbol{x})}{2}=\int_\Gamma\left([u](\boldsymbol{y})\frac{\partial G}{\partial n_{\boldsymbol{y}}}(\boldsymbol{x},\boldsymbol{y})-G(\boldsymbol{x},\boldsymbol{y})\left[\frac{\partial u}{\partial n}\right](\boldsymbol{y})\right)\mathrm{d}\gamma(\boldsymbol{y}),\quad \boldsymbol{x}\in\Gamma. \quad \text{(D.52)}$$

By choosing adequately the boundary condition of the interior problem, and by considering also the boundary condition of the exterior problem and the jump definitions (D.34), this integral equation can be expressed in terms of only one unknown function on Γ. Thus, solving the problem (D.8) is equivalent to solve (D.52) and then replace the obtained solution in (D.46).

The integral equation holds only when the boundary Γ is regular (e.g., of class C^2). Otherwise, taking the limit $\varepsilon\to 0$ can no longer be well-defined and the result is false in general. In particular, if the boundary Γ has an angular point at $\boldsymbol{x}\in\Gamma$, then the left-hand side of the integral equation (D.52) is modified on that point according to the portion of the ball B_ε that remains inside Ω_e, analogously as was done for the two-dimensional case in (B.61), but now for solid angles.

Another integral equation can be also derived for the normal derivative of the solution u on the boundary Γ, by studying the jump properties of the single and double layer potentials. Its derivation is more complicated than for (D.52), being the specific details explicited in the subsection of boundary layer potentials. If the boundary is regular at $\boldsymbol{x}\in\Gamma$, then we obtain

$$\frac{1}{2}\frac{\partial u_e}{\partial n}(\boldsymbol{x})+\frac{1}{2}\frac{\partial u_i}{\partial n}(\boldsymbol{x})=\int_\Gamma\left([u](\boldsymbol{y})\frac{\partial^2 G}{\partial n_{\boldsymbol{x}}\partial n_{\boldsymbol{y}}}(\boldsymbol{x},\boldsymbol{y})-\frac{\partial G}{\partial n_{\boldsymbol{x}}}(\boldsymbol{x},\boldsymbol{y})\left[\frac{\partial u}{\partial n}\right](\boldsymbol{y})\right)\mathrm{d}\gamma(\boldsymbol{y}). \quad \text{(D.53)}$$

This integral equation is modified correspondingly if $\boldsymbol{x}$ is an angular point.

D.6.3 Integral kernels

In the same manner as in the two-dimensional case, the integral kernels G, $\partial G/\partial n_{\boldsymbol{y}}$, and $\partial G/\partial n_{\boldsymbol{x}}$ are weakly singular, and thus integrable, whereas the kernel $\partial^2 G/\partial n_{\boldsymbol{x}}\partial n_{\boldsymbol{y}}$ is not integrable and therefore hypersingular.

The kernel G defined in (D.20) fulfills evidently (B.64) with $\lambda=1$. On the other hand, the kernels $\partial G/\partial n_{\boldsymbol{y}}$ and $\partial G/\partial n_{\boldsymbol{x}}$ are less singular along Γ than they appear at first sight, due the regularizing effect of the normal derivatives. They are given respectively by

$$\frac{\partial G}{\partial n_{\boldsymbol{y}}}(\boldsymbol{x},\boldsymbol{y})=\frac{(\boldsymbol{y}-\boldsymbol{x})\cdot\boldsymbol{n}_{\boldsymbol{y}}}{4\pi|\boldsymbol{y}-\boldsymbol{x}|^3}\qquad\text{and}\qquad\frac{\partial G}{\partial n_{\boldsymbol{x}}}(\boldsymbol{x},\boldsymbol{y})=\frac{(\boldsymbol{x}-\boldsymbol{y})\cdot\boldsymbol{n}_{\boldsymbol{x}}}{4\pi|\boldsymbol{x}-\boldsymbol{y}|^3}. \quad \text{(D.54)}$$

It can be shown that the estimates (B.70) and (B.71) hold also in three dimensions, by using the same reasoning as in the two-dimensional case for the graph of a regular function φ that takes variables now on the tangent plane. Therefore we have that

$$\frac{\partial G}{\partial n_{\boldsymbol{y}}}(\boldsymbol{x},\boldsymbol{y})=\mathcal{O}\left(\frac{1}{|\boldsymbol{y}-\boldsymbol{x}|}\right)\qquad\text{and}\qquad\frac{\partial G}{\partial n_{\boldsymbol{x}}}(\boldsymbol{x},\boldsymbol{y})=\mathcal{O}\left(\frac{1}{|\boldsymbol{x}-\boldsymbol{y}|}\right), \quad \text{(D.55)}$$

and hence these kernels satisfy (B.64) with $\lambda=1$.

The kernel $\partial^2 G/\partial n_{\boldsymbol{x}} \partial n_{\boldsymbol{y}}$, on the other hand, adopts the form

$$\frac{\partial^2 G}{\partial n_{\boldsymbol{x}} \partial n_{\boldsymbol{y}}}(\boldsymbol{x}, \boldsymbol{y}) = -\frac{\boldsymbol{n}_{\boldsymbol{x}} \cdot \boldsymbol{n}_{\boldsymbol{y}}}{4\pi |\boldsymbol{y} - \boldsymbol{x}|^3} - \frac{3\big((\boldsymbol{x} - \boldsymbol{y}) \cdot \boldsymbol{n}_{\boldsymbol{x}}\big)\big((\boldsymbol{y} - \boldsymbol{x}) \cdot \boldsymbol{n}_{\boldsymbol{y}}\big)}{4\pi |\boldsymbol{y} - \boldsymbol{x}|^5}. \tag{D.56}$$

The regularizing effect of the normal derivatives applies only to its second term, but not to the first. Hence this kernel is hypersingular, with $\lambda = 3$, and it holds that

$$\frac{\partial^2 G}{\partial n_{\boldsymbol{x}} \partial n_{\boldsymbol{y}}}(\boldsymbol{x}, \boldsymbol{y}) = \mathcal{O}\bigg(\frac{1}{|\boldsymbol{y} - \boldsymbol{x}|^3}\bigg). \tag{D.57}$$

The kernel is no longer integrable and the associated integral operator has to be thus interpreted in some appropriate sense as a divergent integral (cf., e.g., Hsiao & Wendland 2008, Lenoir 2005, Nédélec 2001).

D.6.4 Boundary layer potentials

We regard now the jump properties on the boundary Γ of the boundary layer potentials that have appeared in our calculations. For the development of the integral representation (D.47) we already made acquaintance with the single and double layer potentials, which we define now more precisely for $\boldsymbol{x} \in \Omega_e \cup \Omega_i$ as the integral operators

$$\mathcal{S}\nu(\boldsymbol{x}) = \int_\Gamma G(\boldsymbol{x}, \boldsymbol{y}) \nu(\boldsymbol{y}) \, \mathrm{d}\gamma(\boldsymbol{y}), \tag{D.58}$$

$$\mathcal{D}\mu(\boldsymbol{x}) = \int_\Gamma \frac{\partial G}{\partial n_{\boldsymbol{y}}}(\boldsymbol{x}, \boldsymbol{y}) \mu(\boldsymbol{y}) \, \mathrm{d}\gamma(\boldsymbol{y}). \tag{D.59}$$

The integral representation (D.47) can be now stated in terms of the layer potentials as

$$u = \mathcal{D}\mu - \mathcal{S}\nu. \tag{D.60}$$

We remark that for any functions $\nu, \mu : \Gamma \to \mathbb{C}$ that are regular enough, the single and double layer potentials satisfy the Laplace equation, namely

$$\Delta \mathcal{S}\nu = 0 \qquad \text{in } \Omega_e \cup \Omega_i, \tag{D.61}$$

$$\Delta \mathcal{D}\mu = 0 \qquad \text{in } \Omega_e \cup \Omega_i. \tag{D.62}$$

For the integral equations (D.52) and (D.53), which are defined for $\boldsymbol{x} \in \Gamma$, we require the four boundary integral operators:

$$S\nu(\boldsymbol{x}) = \int_\Gamma G(\boldsymbol{x}, \boldsymbol{y}) \nu(\boldsymbol{y}) \, \mathrm{d}\gamma(\boldsymbol{y}), \tag{D.63}$$

$$D\mu(\boldsymbol{x}) = \int_\Gamma \frac{\partial G}{\partial n_{\boldsymbol{y}}}(\boldsymbol{x}, \boldsymbol{y}) \mu(\boldsymbol{y}) \, \mathrm{d}\gamma(\boldsymbol{y}), \tag{D.64}$$

$$D^*\nu(\boldsymbol{x}) = \int_\Gamma \frac{\partial G}{\partial n_{\boldsymbol{x}}}(\boldsymbol{x}, \boldsymbol{y}) \nu(\boldsymbol{y}) \, \mathrm{d}\gamma(\boldsymbol{y}), \tag{D.65}$$

$$N\mu(\boldsymbol{x}) = \int_\Gamma \frac{\partial^2 G}{\partial n_{\boldsymbol{x}} \partial n_{\boldsymbol{y}}}(\boldsymbol{x}, \boldsymbol{y}) \mu(\boldsymbol{y}) \, \mathrm{d}\gamma(\boldsymbol{y}). \tag{D.66}$$

The operator D^* is in fact the adjoint of the operator D. As we already mentioned, the kernel of the integral operator N defined in (D.66) is not integrable, yet we write it formally

as an improper integral. An appropriate sense for this integral will be given below. The integral equations (D.52) and (D.53) can be now stated in terms of the integral operators as

$$\frac{1}{2}(u_e + u_i) = D\mu - S\nu, \tag{D.67}$$

$$\frac{1}{2}\left(\frac{\partial u_e}{\partial n} + \frac{\partial u_i}{\partial n}\right) = N\mu - D^*\nu. \tag{D.68}$$

These integral equations can be easily derived from the jump properties of the single and double layer potentials. The single layer potential (D.58) is continuous and its normal derivative has a jump of size $-\nu$ across Γ, i.e.,

$$\mathcal{S}\nu|_{\Omega_e} = S\nu = \mathcal{S}\nu|_{\Omega_i}, \tag{D.69}$$

$$\frac{\partial}{\partial n}\mathcal{S}\nu|_{\Omega_e} = \left(-\frac{1}{2} + D^*\right)\nu, \tag{D.70}$$

$$\frac{\partial}{\partial n}\mathcal{S}\nu|_{\Omega_i} = \left(\frac{1}{2} + D^*\right)\nu. \tag{D.71}$$

The double layer potential (D.59), on the other hand, has a jump of size μ across Γ and its normal derivative is continuous, namely

$$\mathcal{D}\mu|_{\Omega_e} = \left(\frac{1}{2} + D\right)\mu, \tag{D.72}$$

$$\mathcal{D}\mu|_{\Omega_i} = \left(-\frac{1}{2} + D\right)\mu, \tag{D.73}$$

$$\frac{\partial}{\partial n}\mathcal{D}\mu|_{\Omega_e} = N\mu = \frac{\partial}{\partial n}\mathcal{D}\mu|_{\Omega_i}. \tag{D.74}$$

The integral equation (D.67) is obtained directly either from (D.69) and (D.72), or from (D.69) and (D.73), by considering the appropriate trace of (D.60) and by defining the functions μ and ν as in (D.35). These three jump properties are easily proven by regarding the details of the proof for (D.52).

Similarly, the integral equation (D.68) for the normal derivative is obtained directly either from (D.70) and (D.74), or from (D.71) and (D.74), by considering the appropriate trace of the normal derivative of (D.60) and by defining again the functions μ and ν as in (D.35). The proof of these other three jump properties is done below.

a) Jump of the normal derivative of the single layer potential

Let us then study first the proof of (D.70) and (D.71). The traces of the normal derivative of the single layer potential are given by

$$\frac{\partial}{\partial n}\mathcal{S}\nu(\boldsymbol{x})|_{\Omega_e} = \lim_{\Omega_e \ni \boldsymbol{z} \to \boldsymbol{x}} \nabla \mathcal{S}\nu(\boldsymbol{z}) \cdot \boldsymbol{n}_{\boldsymbol{x}}, \tag{D.75}$$

$$\frac{\partial}{\partial n}\mathcal{S}\nu(\boldsymbol{x})|_{\Omega_i} = \lim_{\Omega_i \ni \boldsymbol{z} \to \boldsymbol{x}} \nabla \mathcal{S}\nu(\boldsymbol{z}) \cdot \boldsymbol{n}_{\boldsymbol{x}}. \tag{D.76}$$

Now we have that

$$\nabla \mathcal{S}\nu(\boldsymbol{z}) \cdot \boldsymbol{n}_{\boldsymbol{x}} = \int_{\Gamma} \boldsymbol{n}_{\boldsymbol{x}} \cdot \nabla_{\boldsymbol{z}} G(\boldsymbol{z}, \boldsymbol{y}) \nu(\boldsymbol{y}) \, \mathrm{d}\gamma(\boldsymbol{y}). \tag{D.77}$$

For $\varepsilon > 0$ we denote $\Gamma_\varepsilon = \Gamma \cap B_\varepsilon$, i.e., the portion of Γ contained inside the ball B_ε of radius ε and centered at $\boldsymbol{x}$. By decomposing the integral we obtain that

$$\nabla \mathcal{S}\nu(\boldsymbol{z}) \cdot \boldsymbol{n}_{\boldsymbol{x}} = \int_{\Gamma \setminus \Gamma_\varepsilon} \boldsymbol{n}_{\boldsymbol{x}} \cdot \nabla_{\boldsymbol{z}} G(\boldsymbol{z}, \boldsymbol{y}) \nu(\boldsymbol{y}) \, \mathrm{d}\gamma(\boldsymbol{y}) + \int_{\Gamma_\varepsilon} \boldsymbol{n}_{\boldsymbol{x}} \cdot \nabla_{\boldsymbol{z}} G(\boldsymbol{z}, \boldsymbol{y}) \nu(\boldsymbol{y}) \, \mathrm{d}\gamma(\boldsymbol{y}). \tag{D.78}$$

For the first integral in (D.78) we can take without problems the limit $\boldsymbol{z} \to \boldsymbol{x}$, since for a fixed ε the integral is regular in $\boldsymbol{x}$. Since the singularity of the resulting kernel $\partial G / \partial n_{\boldsymbol{x}}$ is integrable, Lebesgue's dominated convergence theorem (cf. Royden 1988) implies that

$$\lim_{\varepsilon \to 0} \int_{\Gamma \setminus \Gamma_\varepsilon} \frac{\partial G}{\partial n_{\boldsymbol{x}}}(\boldsymbol{x}, \boldsymbol{y}) \nu(\boldsymbol{y}) \, \mathrm{d}\gamma(\boldsymbol{y}) = \int_{\Gamma} \frac{\partial G}{\partial n_{\boldsymbol{x}}}(\boldsymbol{x}, \boldsymbol{y}) \nu(\boldsymbol{y}) \, \mathrm{d}\gamma(\boldsymbol{y}) = D^* \nu(\boldsymbol{x}). \tag{D.79}$$

Let us treat now the second integral in (D.78), which is again decomposed in different integrals in such a way that

$$\begin{aligned} \int_{\Gamma_\varepsilon} \boldsymbol{n}_{\boldsymbol{x}} \cdot \nabla_{\boldsymbol{z}} G(\boldsymbol{z}, \boldsymbol{y}) \nu(\boldsymbol{y}) \, \mathrm{d}\gamma(\boldsymbol{y}) &= \int_{\Gamma_\varepsilon} (\boldsymbol{n}_{\boldsymbol{x}} - \boldsymbol{n}_{\boldsymbol{y}}) \cdot \nabla_{\boldsymbol{z}} G(\boldsymbol{z}, \boldsymbol{y}) \nu(\boldsymbol{y}) \, \mathrm{d}\gamma(\boldsymbol{y}) \\ &+ \int_{\Gamma_\varepsilon} \boldsymbol{n}_{\boldsymbol{y}} \cdot \nabla_{\boldsymbol{z}} G(\boldsymbol{z}, \boldsymbol{y}) \big(\nu(\boldsymbol{y}) - \nu(\boldsymbol{x})\big) \, \mathrm{d}\gamma(\boldsymbol{y}) + \nu(\boldsymbol{x}) \int_{\Gamma_\varepsilon} \boldsymbol{n}_{\boldsymbol{y}} \cdot \nabla_{\boldsymbol{z}} G(\boldsymbol{z}, \boldsymbol{y}) \, \mathrm{d}\gamma(\boldsymbol{y}). \end{aligned} \tag{D.80}$$

When ε is small, and since Γ is supposed to be regular, therefore Γ_ε resembles a flat disc of radius ε. Thus we have that

$$\lim_{\varepsilon \to 0} \int_{\Gamma_\varepsilon} (\boldsymbol{n}_{\boldsymbol{x}} - \boldsymbol{n}_{\boldsymbol{y}}) \cdot \nabla_{\boldsymbol{z}} G(\boldsymbol{z}, \boldsymbol{y}) \nu(\boldsymbol{y}) \, \mathrm{d}\gamma(\boldsymbol{y}) = 0. \tag{D.81}$$

If ν is regular enough, then we have also that

$$\lim_{\varepsilon \to 0} \int_{\Gamma_\varepsilon} \boldsymbol{n}_{\boldsymbol{y}} \cdot \nabla_{\boldsymbol{z}} G(\boldsymbol{z}, \boldsymbol{y}) \big(\nu(\boldsymbol{y}) - \nu(\boldsymbol{x})\big) \, \mathrm{d}\gamma(\boldsymbol{y}) = 0. \tag{D.82}$$

For the remaining term in (D.80) we consider the solid angle Θ under which the almost flat disc Γ_ε is seen from point $\boldsymbol{z}$ (cf. Figure D.3). If we denote $\boldsymbol{R} = \boldsymbol{y} - \boldsymbol{z}$ and $R = |\boldsymbol{R}|$, and consider an oriented surface differential element $\mathrm{d}\boldsymbol{\gamma} = \boldsymbol{n}_{\boldsymbol{y}} \mathrm{d}\gamma(\boldsymbol{y})$ seen from point $\boldsymbol{z}$, then we can express the solid angle differential element by (cf. Terrasse & Abboud 2006)

$$\mathrm{d}\Theta = \frac{\boldsymbol{R}}{R^3} \cdot \mathrm{d}\boldsymbol{\gamma} = \frac{\boldsymbol{R} \cdot \boldsymbol{n}_{\boldsymbol{y}}}{R^3} \, \mathrm{d}\gamma(\boldsymbol{y}) = 4\pi \, \boldsymbol{n}_{\boldsymbol{y}} \cdot \nabla_{\boldsymbol{y}} G(\boldsymbol{z}, \boldsymbol{y}) \, \mathrm{d}\gamma(\boldsymbol{y}). \tag{D.83}$$

Integrating over the disc Γ_ε and considering (D.25) yields the solid angle Θ, namely

$$\Theta = \int_{\Gamma_\varepsilon} \mathrm{d}\Theta = 4\pi \int_{\Gamma_\varepsilon} \boldsymbol{n}_{\boldsymbol{y}} \cdot \nabla_{\boldsymbol{y}} G(\boldsymbol{z}, \boldsymbol{y}) \, \mathrm{d}\gamma(\boldsymbol{y}) = -4\pi \int_{\Gamma_\varepsilon} \boldsymbol{n}_{\boldsymbol{y}} \cdot \nabla_{\boldsymbol{z}} G(\boldsymbol{z}, \boldsymbol{y}) \, \mathrm{d}\gamma(\boldsymbol{y}), \tag{D.84}$$

where $-2\pi \leq \Theta \leq 2\pi$. The solid angle Θ is positive when the vectors $\boldsymbol{R}$ and $\boldsymbol{n}_{\boldsymbol{y}}$ point towards the same side of Γ_ε, and negative when they oppose each other. Thus if $\boldsymbol{z}$ is very close to $\boldsymbol{x}$ and if ε is small enough so that Γ_ε behaves as a flat disc, then

$$\int_{\Gamma_\varepsilon} \boldsymbol{n}_{\boldsymbol{y}} \cdot \nabla_{\boldsymbol{z}} G(\boldsymbol{z}, \boldsymbol{y}) \, \mathrm{d}\gamma(\boldsymbol{y}) \approx \begin{cases} -1/2 & \text{if } \boldsymbol{z} \in \Omega_e, \\ 1/2 & \text{if } \boldsymbol{z} \in \Omega_i. \end{cases} \tag{D.85}$$

Hence we obtain the desired jump formulae (D.70) and (D.71).

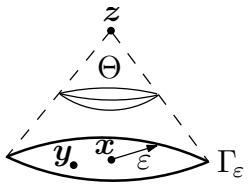

FIGURE D.3. Solid angle under which Γ_ε is seen from point $\boldsymbol{z}$.

b) Continuity of the normal derivative of the double layer potential

We are now interested in proving the continuity of the normal derivative of the double layer potential across Γ, as expressed in (D.74). This will allow us at the same time to define an appropriate sense for the improper integral (D.66). This integral is divergent in a classical sense, but it can be nonetheless properly defined in a weak or distributional sense by considering it as a linear functional acting on a test function $\varphi \in \mathcal{D}(\mathbb{R}^3)$. By considering (D.62) and Green's first integral theorem (A.612), we can express our values of interest in a weak sense as

$$\left\langle \frac{\partial}{\partial n}\mathcal{D}\mu|_{\Omega_e},\, \varphi \right\rangle = \int_\Gamma \frac{\partial}{\partial n}\mathcal{D}\mu(\boldsymbol{x})|_{\Omega_e}\, \varphi(\boldsymbol{x})\, \mathrm{d}\gamma(\boldsymbol{x}) = \int_{\Omega_e} \nabla\mathcal{D}\mu(\boldsymbol{x}) \cdot \nabla\varphi(\boldsymbol{x})\, \mathrm{d}\boldsymbol{x}, \tag{D.86}$$

$$\left\langle \frac{\partial}{\partial n}\mathcal{D}\mu|_{\Omega_i},\, \varphi \right\rangle = \int_\Gamma \frac{\partial}{\partial n}\mathcal{D}\mu(\boldsymbol{x})|_{\Omega_i}\, \varphi(\boldsymbol{x})\, \mathrm{d}\gamma(\boldsymbol{x}) = -\int_{\Omega_i} \nabla\mathcal{D}\mu(\boldsymbol{x}) \cdot \nabla\varphi(\boldsymbol{x})\, \mathrm{d}\boldsymbol{x}. \tag{D.87}$$

From (A.588) and (D.25) we obtain the relation

$$\frac{\partial G}{\partial n_{\boldsymbol{y}}}(\boldsymbol{x},\boldsymbol{y}) = \boldsymbol{n}_{\boldsymbol{y}} \cdot \nabla_{\boldsymbol{y}} G(\boldsymbol{x},\boldsymbol{y}) = -\boldsymbol{n}_{\boldsymbol{y}} \cdot \nabla_{\boldsymbol{x}} G(\boldsymbol{x},\boldsymbol{y}) = -\operatorname{div}_{\boldsymbol{x}}\big(G(\boldsymbol{x},\boldsymbol{y})\boldsymbol{n}_{\boldsymbol{y}}\big). \tag{D.88}$$

Thus for the double layer potential (D.59) we have that

$$\mathcal{D}\mu(\boldsymbol{x}) = -\operatorname{div}\int_\Gamma G(\boldsymbol{x},\boldsymbol{y})\mu(\boldsymbol{y})\boldsymbol{n}_{\boldsymbol{y}}\, \mathrm{d}\gamma(\boldsymbol{y}) = -\operatorname{div}\mathcal{S}(\mu\,\boldsymbol{n}_{\boldsymbol{y}})(\boldsymbol{x}), \tag{D.89}$$

being its gradient given by

$$\nabla\mathcal{D}\mu(\boldsymbol{x}) = -\nabla\operatorname{div}\int_\Gamma G(\boldsymbol{x},\boldsymbol{y})\mu(\boldsymbol{y})\boldsymbol{n}_{\boldsymbol{y}}\, \mathrm{d}\gamma(\boldsymbol{y}). \tag{D.90}$$

From (A.589) we have that

$$\operatorname{curl}_{\boldsymbol{x}}\big(G(\boldsymbol{x},\boldsymbol{y})\boldsymbol{n}_{\boldsymbol{y}}\big) = \nabla_{\boldsymbol{x}} G(\boldsymbol{x},\boldsymbol{y}) \times \boldsymbol{n}_{\boldsymbol{y}}. \tag{D.91}$$

Hence, by considering (A.590), (D.62), and (D.91) in (D.90), we obtain that

$$\nabla\mathcal{D}\mu(\boldsymbol{x}) = \operatorname{curl}\int_\Gamma \big(\boldsymbol{n}_{\boldsymbol{y}} \times \nabla_{\boldsymbol{x}} G(\boldsymbol{x},\boldsymbol{y})\big)\mu(\boldsymbol{y})\, \mathrm{d}\gamma(\boldsymbol{y}). \tag{D.92}$$

From (D.25) and (A.658) we have that

$$\int_\Gamma \big(\boldsymbol{n_y} \times \nabla_{\boldsymbol{x}} G(\boldsymbol{x},\boldsymbol{y})\big)\mu(\boldsymbol{y})\,\mathrm{d}\gamma(\boldsymbol{y}) = -\int_\Gamma \boldsymbol{n_y} \times \big(\nabla_{\boldsymbol{y}} G(\boldsymbol{x},\boldsymbol{y})\mu(\boldsymbol{y})\big)\,\mathrm{d}\gamma(\boldsymbol{y})$$
$$= \int_\Gamma \boldsymbol{n_y} \times \big(G(\boldsymbol{x},\boldsymbol{y})\nabla\mu(\boldsymbol{y})\big)\,\mathrm{d}\gamma(\boldsymbol{y}), \tag{D.93}$$

and consequently

$$\nabla\mathcal{D}\mu(\boldsymbol{x}) = \mathrm{curl}\int_\Gamma G(\boldsymbol{x},\boldsymbol{y})\big(\boldsymbol{n_y} \times \nabla\mu(\boldsymbol{y})\big)\,\mathrm{d}\gamma(\boldsymbol{y}). \tag{D.94}$$

Now, considering (A.596) and (A.618), and replacing (D.94) in (D.86), implies that

$$\int_{\Omega_e} \nabla\mathcal{D}\mu(\boldsymbol{x})\cdot\nabla\varphi(\boldsymbol{x})\,\mathrm{d}\boldsymbol{x} = -\int_\Gamma\int_\Gamma G(\boldsymbol{x},\boldsymbol{y})\big(\nabla\mu(\boldsymbol{y})\times\boldsymbol{n_y}\big)\cdot\big(\nabla\varphi(\boldsymbol{x})\times\boldsymbol{n_x}\big)\,\mathrm{d}\gamma(\boldsymbol{y})\,\mathrm{d}\gamma(\boldsymbol{x}). \tag{D.95}$$

Analogously, when replacing in (D.87) we have that

$$\int_{\Omega_i} \nabla\mathcal{D}\mu(\boldsymbol{x})\cdot\nabla\varphi(\boldsymbol{x})\,\mathrm{d}\boldsymbol{x} = \int_\Gamma\int_\Gamma G(\boldsymbol{x},\boldsymbol{y})\big(\nabla\mu(\boldsymbol{y})\times\boldsymbol{n_y}\big)\cdot\big(\nabla\varphi(\boldsymbol{x})\times\boldsymbol{n_x}\big)\,\mathrm{d}\gamma(\boldsymbol{y})\,\mathrm{d}\gamma(\boldsymbol{x}). \tag{D.96}$$

Hence, from (D.86), (D.87), (D.95), and (D.96) we conclude the proof of (D.74). The integral operator (D.66) is thus properly defined in a weak sense for $\varphi \in \mathcal{D}(\mathbb{R}^3)$ by

$$\langle N\mu(\boldsymbol{x}),\,\varphi\rangle = -\int_\Gamma\int_\Gamma G(\boldsymbol{x},\boldsymbol{y})\big(\nabla\mu(\boldsymbol{y})\times\boldsymbol{n_y}\big)\cdot\big(\nabla\varphi(\boldsymbol{x})\times\boldsymbol{n_x}\big)\,\mathrm{d}\gamma(\boldsymbol{y})\,\mathrm{d}\gamma(\boldsymbol{x}). \tag{D.97}$$

D.6.5 Alternatives for integral representations and equations

By taking into account the transmission problem (D.35), its integral representation formula (D.46), and its integral equations (D.52) and (D.53), several particular alternatives for integral representations and equations of the exterior problem (D.8) can be developed. The way to perform this is to extend properly the exterior problem towards the interior domain Ω_i, either by specifying explicitly this extension or by defining an associated interior problem, so as to become the desired jump properties across Γ. The extension has to satisfy the Laplace equation (D.1) in Ω_i and a boundary condition that corresponds adequately to the impedance boundary condition (D.2). The obtained system of integral representations and equations allows finally to solve the exterior problem (D.8), by using the solution of the integral equation in the integral representation formula.

a) Extension by zero

An extension by zero towards the interior domain Ω_i implies that

$$u_i = 0 \qquad \text{in } \Omega_i. \tag{D.98}$$

The jumps over Γ are characterized in this case by

$$[u] = u_e = \mu, \tag{D.99}$$

$$\left[\frac{\partial u}{\partial n}\right] = \frac{\partial u_e}{\partial n} = Zu_e - f_z = Z\mu - f_z, \tag{D.100}$$

where $\mu : \Gamma \to \mathbb{C}$ is a function to be determined.

An integral representation formula of the solution, for $\boldsymbol{x} \in \Omega_e \cup \Omega_i$, is given by

$$u(\boldsymbol{x}) = \int_\Gamma \left(\frac{\partial G}{\partial n_{\boldsymbol{y}}}(\boldsymbol{x}, \boldsymbol{y}) - Z(\boldsymbol{y}) G(\boldsymbol{x}, \boldsymbol{y}) \right) \mu(\boldsymbol{y}) \, \mathrm{d}\gamma(\boldsymbol{y}) + \int_\Gamma G(\boldsymbol{x}, \boldsymbol{y}) f_z(\boldsymbol{y}) \, \mathrm{d}\gamma(\boldsymbol{y}). \quad \text{(D.101)}$$

Since

$$\frac{1}{2}\big(u_e(\boldsymbol{x}) + u_i(\boldsymbol{x})\big) = \frac{\mu(\boldsymbol{x})}{2}, \qquad \boldsymbol{x} \in \Gamma, \quad \text{(D.102)}$$

we obtain, for $\boldsymbol{x} \in \Gamma$, the Fredholm integral equation of the second kind

$$\frac{\mu(\boldsymbol{x})}{2} + \int_\Gamma \left(Z(\boldsymbol{y}) G(\boldsymbol{x}, \boldsymbol{y}) - \frac{\partial G}{\partial n_{\boldsymbol{y}}}(\boldsymbol{x}, \boldsymbol{y}) \right) \mu(\boldsymbol{y}) \, \mathrm{d}\gamma(\boldsymbol{y}) = \int_\Gamma G(\boldsymbol{x}, \boldsymbol{y}) f_z(\boldsymbol{y}) \, \mathrm{d}\gamma(\boldsymbol{y}), \quad \text{(D.103)}$$

which has to be solved for the unknown μ. In terms of boundary layer potentials, the integral representation and the integral equation can be respectively expressed by

$$u = \mathcal{D}(\mu) - \mathcal{S}(Z\mu) + \mathcal{S}(f_z) \qquad \text{in } \Omega_e \cup \Omega_i, \quad \text{(D.104)}$$

$$\frac{\mu}{2} + S(Z\mu) - D(\mu) = S(f_z) \qquad \text{on } \Gamma. \quad \text{(D.105)}$$

Alternatively, since

$$\frac{1}{2}\left(\frac{\partial u_e}{\partial n}(\boldsymbol{x}) + \frac{\partial u_i}{\partial n}(\boldsymbol{x}) \right) = \frac{Z(\boldsymbol{x})}{2}\mu(\boldsymbol{x}) - \frac{f_z(\boldsymbol{x})}{2}, \qquad \boldsymbol{x} \in \Gamma, \quad \text{(D.106)}$$

we obtain also, for $\boldsymbol{x} \in \Gamma$, the Fredholm integral equation of the second kind

$$\frac{Z(\boldsymbol{x})}{2}\mu(\boldsymbol{x}) + \int_\Gamma \left(-\frac{\partial^2 G}{\partial n_{\boldsymbol{x}} \partial n_{\boldsymbol{y}}}(\boldsymbol{x}, \boldsymbol{y}) + Z(\boldsymbol{y}) \frac{\partial G}{\partial n_{\boldsymbol{x}}}(\boldsymbol{x}, \boldsymbol{y}) \right) \mu(\boldsymbol{y}) \, \mathrm{d}\gamma(\boldsymbol{y}) = \frac{f_z(\boldsymbol{x})}{2} + \int_\Gamma \frac{\partial G}{\partial n_{\boldsymbol{x}}}(\boldsymbol{x}, \boldsymbol{y}) f_z(\boldsymbol{y}) \, \mathrm{d}\gamma(\boldsymbol{y}), \quad \text{(D.107)}$$

which in terms of boundary layer potentials becomes

$$\frac{Z}{2}\mu - N(\mu) + D^*(Z\mu) = \frac{f_z}{2} + D^*(f_z) \qquad \text{on } \Gamma. \quad \text{(D.108)}$$

b) Continuous impedance

We associate to (D.8) the interior problem

$$\begin{cases} \text{Find } u_i : \Omega_i \to \mathbb{C} \text{ such that} \\ \Delta u_i = 0 & \text{in } \Omega_i, \\ -\dfrac{\partial u_i}{\partial n} + Z u_i = f_z & \text{on } \Gamma. \end{cases} \quad \text{(D.109)}$$

The jumps over Γ are characterized in this case by

$$[u] = u_e - u_i = \mu, \quad \text{(D.110)}$$

$$\left[\frac{\partial u}{\partial n} \right] = \frac{\partial u_e}{\partial n} - \frac{\partial u_i}{\partial n} = Z(u_e - u_i) = Z\mu, \quad \text{(D.111)}$$

where $\mu : \Gamma \to \mathbb{C}$ is a function to be determined. In particular it holds that the jump of the impedance is zero, namely

$$\left[-\frac{\partial u}{\partial n} + Zu\right] = \left(-\frac{\partial u_e}{\partial n} + Zu_e\right) - \left(-\frac{\partial u_i}{\partial n} + Zu_i\right) = 0. \tag{D.112}$$

An integral representation formula of the solution, for $\boldsymbol{x} \in \Omega_e \cup \Omega_i$, is given by

$$u(\boldsymbol{x}) = \int_\Gamma \left(\frac{\partial G}{\partial n_{\boldsymbol{y}}}(\boldsymbol{x}, \boldsymbol{y}) - Z(\boldsymbol{y})G(\boldsymbol{x}, \boldsymbol{y})\right) \mu(\boldsymbol{y})\, \mathrm{d}\gamma(\boldsymbol{y}). \tag{D.113}$$

Since

$$-\frac{1}{2}\left(\frac{\partial u_e}{\partial n}(\boldsymbol{x}) + \frac{\partial u_i}{\partial n}(\boldsymbol{x})\right) + \frac{Z(\boldsymbol{x})}{2}\big(u_e(\boldsymbol{x}) + u_i(\boldsymbol{x})\big) = f_z(\boldsymbol{x}), \qquad \boldsymbol{x} \in \Gamma, \tag{D.114}$$

we obtain, for $\boldsymbol{x} \in \Gamma$, the Fredholm integral equation of the first kind

$$\begin{aligned}\int_\Gamma \left(-\frac{\partial^2 G}{\partial n_{\boldsymbol{x}} \partial n_{\boldsymbol{y}}}(\boldsymbol{x}, \boldsymbol{y}) + Z(\boldsymbol{y})\frac{\partial G}{\partial n_{\boldsymbol{x}}}(\boldsymbol{x}, \boldsymbol{y})\right) \mu(\boldsymbol{y})\, \mathrm{d}\gamma(\boldsymbol{y}) \\ + Z(\boldsymbol{x}) \int_\Gamma \left(\frac{\partial G}{\partial n_{\boldsymbol{y}}}(\boldsymbol{x}, \boldsymbol{y}) - Z(\boldsymbol{y})G(\boldsymbol{x}, \boldsymbol{y})\right) \mu(\boldsymbol{y})\, \mathrm{d}\gamma(\boldsymbol{y}) = f_z(\boldsymbol{x}),\end{aligned} \tag{D.115}$$

which has to be solved for the unknown μ. In terms of boundary layer potentials, the integral representation and the integral equation can be respectively expressed by

$$u = \mathcal{D}(\mu) - \mathcal{S}(Z\mu) \qquad \text{in } \Omega_e \cup \Omega_i, \tag{D.116}$$

$$-N(\mu) + D^*(Z\mu) + ZD(\mu) - ZS(Z\mu) = f_z \quad \text{on } \Gamma. \tag{D.117}$$

We observe that the integral equation (D.117) is self-adjoint.

c) Continuous value

We associate to (D.8) the interior problem

$$\begin{cases} \text{Find } u_i : \Omega_i \to \mathbb{C} \text{ such that} \\ \Delta u_i = 0 & \text{in } \Omega_i, \\ -\dfrac{\partial u_e}{\partial n} + Zu_i = f_z & \text{on } \Gamma. \end{cases} \tag{D.118}$$

The jumps over Γ are characterized in this case by

$$[u] = u_e - u_i = \frac{1}{Z}\left(\frac{\partial u_e}{\partial n} - f_z\right) - \frac{1}{Z}\left(\frac{\partial u_e}{\partial n} - f_z\right) = 0, \tag{D.119}$$

$$\left[\frac{\partial u}{\partial n}\right] = \frac{\partial u_e}{\partial n} - \frac{\partial u_i}{\partial n} = \nu, \tag{D.120}$$

where $\nu : \Gamma \to \mathbb{C}$ is a function to be determined.

An integral representation formula of the solution, for $\boldsymbol{x} \in \Omega_e \cup \Omega_i$, is given by the single layer potential

$$u(\boldsymbol{x}) = -\int_\Gamma G(\boldsymbol{x}, \boldsymbol{y})\nu(\boldsymbol{y})\, \mathrm{d}\gamma(\boldsymbol{y}). \tag{D.121}$$

Since

$$-\frac{1}{2}\left(\frac{\partial u_e}{\partial n}(\boldsymbol{x})+\frac{\partial u_i}{\partial n}(\boldsymbol{x})\right)+\frac{Z(\boldsymbol{x})}{2}\big(u_e(\boldsymbol{x})+u_i(\boldsymbol{x})\big)=\frac{\nu(\boldsymbol{x})}{2}+f_z(\boldsymbol{x}),\quad \boldsymbol{x}\in\Gamma, \tag{D.122}$$

we obtain, for $\boldsymbol{x}\in\Gamma$, the Fredholm integral equation of the second kind

$$-\frac{\nu(\boldsymbol{x})}{2}+\int_\Gamma\left(\frac{\partial G}{\partial n_{\boldsymbol{x}}}(\boldsymbol{x},\boldsymbol{y})-Z(\boldsymbol{x})G(\boldsymbol{x},\boldsymbol{y})\right)\nu(\boldsymbol{y})\,\mathrm{d}\gamma(\boldsymbol{y})=f_z(\boldsymbol{x}), \tag{D.123}$$

which has to be solved for the unknown ν. In terms of boundary layer potentials, the integral representation and the integral equation can be respectively expressed by

$$u=-\mathcal{S}(\nu) \qquad \text{in } \Omega_e\cup\Omega_i, \tag{D.124}$$

$$\frac{\nu}{2}+ZS(\nu)-D^*(\nu)=-f_z \qquad \text{on } \Gamma. \tag{D.125}$$

We observe that the integral equation (D.125) is mutually adjoint with (D.105).

d) Continuous normal derivative

We associate to (D.8) the interior problem

$$\begin{cases} \text{Find } u_i:\Omega_i\to\mathbb{C} \text{ such that} \\ \Delta u_i=0 & \text{in } \Omega_i, \\ -\dfrac{\partial u_i}{\partial n}+Zu_e=f_z & \text{on } \Gamma. \end{cases} \tag{D.126}$$

The jumps over Γ are characterized in this case by

$$[u]=u_e-u_i=\mu, \tag{D.127}$$

$$\left[\frac{\partial u}{\partial n}\right]=\frac{\partial u_e}{\partial n}-\frac{\partial u_i}{\partial n}=\big(Zu_e-f_z\big)-\big(Zu_e-f_z\big)=0, \tag{D.128}$$

where $\mu:\Gamma\to\mathbb{C}$ is a function to be determined.

An integral representation formula of the solution, for $\boldsymbol{x}\in\Omega_e\cup\Omega_i$, is given by the double layer potential

$$u(\boldsymbol{x})=\int_\Gamma\frac{\partial G}{\partial n_{\boldsymbol{y}}}(\boldsymbol{x},\boldsymbol{y})\mu(\boldsymbol{y})\,\mathrm{d}\gamma(\boldsymbol{y}). \tag{D.129}$$

Since when $\boldsymbol{x}\in\Gamma$,

$$-\frac{1}{2}\left(\frac{\partial u_e}{\partial n}(\boldsymbol{x})+\frac{\partial u_i}{\partial n}(\boldsymbol{x})\right)+\frac{Z(\boldsymbol{x})}{2}\big(u_e(\boldsymbol{x})+u_i(\boldsymbol{x})\big)=-\frac{Z(\boldsymbol{x})}{2}\mu(\boldsymbol{x})+f_z(\boldsymbol{x}), \tag{D.130}$$

we obtain, for $\boldsymbol{x}\in\Gamma$, the Fredholm integral equation of the second kind

$$\frac{Z(\boldsymbol{x})}{2}\mu(\boldsymbol{x})+\int_\Gamma\left(-\frac{\partial^2 G}{\partial n_{\boldsymbol{x}}\partial n_{\boldsymbol{y}}}(\boldsymbol{x},\boldsymbol{y})+Z(\boldsymbol{x})\frac{\partial G}{\partial n_{\boldsymbol{y}}}(\boldsymbol{x},\boldsymbol{y})\right)\mu(\boldsymbol{y})\,\mathrm{d}\gamma(\boldsymbol{y})=f_z(\boldsymbol{x}), \tag{D.131}$$

which has to be solved for the unknown μ. In terms of boundary layer potentials, the integral representation and the integral equation can be respectively expressed by

$$u=\mathcal{D}(\mu) \qquad \text{in } \Omega_e\cup\Omega_i, \tag{D.132}$$

$$\frac{Z}{2}\mu - N(\mu) + ZD(\mu) = f_z \qquad \text{on } \Gamma. \tag{D.133}$$

We observe that the integral equation (D.133) is mutually adjoint with (D.108).

D.7 Far field of the solution

The asymptotic behavior at infinity of the solution u of (D.8) is described by the far field u^{ff}. Its expression can be deduced by replacing the far field of the Green's function G^{ff} and its derivatives in the integral representation formula (D.46), which yields

$$u^{ff}(\boldsymbol{x}) = \int_\Gamma \left([u](\boldsymbol{y}) \frac{\partial G^{ff}}{\partial n_{\boldsymbol{y}}}(\boldsymbol{x}, \boldsymbol{y}) - G^{ff}(\boldsymbol{x}, \boldsymbol{y}) \left[\frac{\partial u}{\partial n}\right](\boldsymbol{y}) \right) \mathrm{d}\gamma(\boldsymbol{y}). \tag{D.134}$$

By replacing now (D.30) and (D.31) in (D.134), we have that the far field of the solution is

$$\begin{aligned} u^{ff}(\boldsymbol{x}) = & -\frac{1}{4\pi|\boldsymbol{x}|^2} \int_\Gamma \left(\hat{\boldsymbol{x}} \cdot \boldsymbol{n}_{\boldsymbol{y}} \, [u](\boldsymbol{y}) - \hat{\boldsymbol{x}} \cdot \boldsymbol{y} \left[\frac{\partial u}{\partial n}\right](\boldsymbol{y}) \right) \mathrm{d}\gamma(\boldsymbol{y}) \\ & + \frac{1}{4\pi|\boldsymbol{x}|} \int_\Gamma \left[\frac{\partial u}{\partial n}\right](\boldsymbol{y}) \, \mathrm{d}\gamma(\boldsymbol{y}). \end{aligned} \tag{D.135}$$

The asymptotic behavior of the solution u at infinity is therefore given by

$$u(\boldsymbol{x}) = \frac{C}{|\boldsymbol{x}|} + \frac{u_\infty(\hat{\boldsymbol{x}})}{|\boldsymbol{x}|^2} + \mathcal{O}\left(\frac{1}{|\boldsymbol{x}|^3}\right), \qquad |\boldsymbol{x}| \to \infty, \tag{D.136}$$

uniformly in all directions $\hat{\boldsymbol{x}}$ on the unit sphere, where C is a constant, given by

$$C = \frac{1}{4\pi} \int_\Gamma \left[\frac{\partial u}{\partial n}\right](\boldsymbol{y}) \, \mathrm{d}\gamma(\boldsymbol{y}), \tag{D.137}$$

and where

$$u_\infty(\hat{\boldsymbol{x}}) = -\frac{1}{4\pi} \int_\Gamma \left(\hat{\boldsymbol{x}} \cdot \boldsymbol{n}_{\boldsymbol{y}} \, [u](\boldsymbol{y}) - \hat{\boldsymbol{x}} \cdot \boldsymbol{y} \left[\frac{\partial u}{\partial n}\right](\boldsymbol{y}) \right) \mathrm{d}\gamma(\boldsymbol{y}) \tag{D.138}$$

is called the far-field pattern of u. It can be expressed in decibels (dB) by means of the asymptotic cross section

$$Q_s(\hat{\boldsymbol{x}}) \ \ [\text{dB}] = 20 \log_{10}\left(\frac{|u_\infty(\hat{\boldsymbol{x}})|}{|u_0|}\right), \tag{D.139}$$

where the reference level u_0 may typically depend on u_W, but for simplicity we take $u_0 = 1$.

We remark that the far-field behavior (D.136) of the solution is in accordance with the decaying condition (D.5), which justifies its choice.

D.8 Exterior sphere problem

To understand better the resolution of the direct perturbation problem (D.8), we study now the particular case when the domain $\Omega_e \subset \mathbb{R}^3$ is taken as the exterior of a sphere of radius $R > 0$. The interior of the sphere is then given by $\Omega_i = \{\boldsymbol{x} \in \mathbb{R}^3 : |\boldsymbol{x}| < R\}$ and its boundary by $\Gamma = \partial\Omega_e$, as shown in Figure D.4. We place the origin at the center of Ω_i and we consider that the unit normal $\boldsymbol{n}$ is taken outwardly oriented of Ω_e, i.e., $\boldsymbol{n} = -\boldsymbol{r}$.

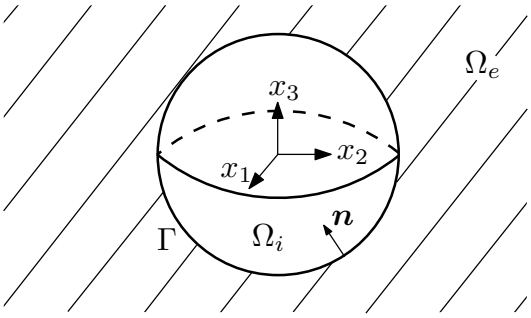

FIGURE D.4. Exterior of the sphere.

The exterior sphere problem is then stated as

$$\begin{cases} \text{Find } u : \Omega_e \to \mathbb{C} \text{ such that} \\ \Delta u = 0 & \text{in } \Omega_e, \\ \dfrac{\partial u}{\partial r} + Zu = f_z & \text{on } \Gamma, \\ \text{+ Decaying condition as } |\boldsymbol{x}| \to \infty, \end{cases} \tag{D.140}$$

where we consider a constant impedance $Z \in \mathbb{C}$ and where the asymptotic decaying condition is as usual given by (D.5).

Due the particular chosen geometry, the solution u of (D.140) can be easily found analytically by using the method of variable separation, i.e., by supposing that

$$u(\boldsymbol{x}) = u(r, \theta, \varphi) = \frac{h(r)}{r} g(\theta) f(\varphi), \tag{D.141}$$

where the radius $r \geq 0$, the polar angle $0 \leq \theta \leq \pi$, and the azimuthal angle $-\pi < \varphi \leq \pi$ denote the spherical coordinates in $\mathbb{R}^3$, which are characterized by

$$r = \sqrt{x_1^2 + x_2^2 + x_3^2}\,, \qquad \theta = \arctan\left(\frac{\sqrt{x^2 + y^2}}{z}\right), \qquad \varphi = \arctan\left(\frac{y}{x}\right). \tag{D.142}$$

If the Laplace equation in (D.140) is expressed using spherical coordinates, then

$$\Delta u = \frac{1}{r}\frac{\partial^2}{\partial r^2}(ru) + \frac{1}{r^2 \sin\theta}\frac{\partial}{\partial \theta}\left(\sin\theta \frac{\partial u}{\partial \theta}\right) + \frac{1}{r^2 \sin^2\theta}\frac{\partial^2 u}{\partial \varphi^2} = 0. \tag{D.143}$$

By replacing now (D.141) in (D.143) we obtain

$$\frac{h''(r)}{r} g(\theta) f(\varphi) + \frac{h(r) f(\varphi)}{r^3 \sin\theta}\frac{\mathrm{d}}{\mathrm{d}\theta}\left(\sin\theta \frac{\mathrm{d}g}{\mathrm{d}\theta}(\theta)\right) + \frac{h(r) g(\theta) f''(\varphi)}{r^3 \sin^2\theta} = 0. \tag{D.144}$$

Multiplying by $r^3 \sin^2\theta$, dividing by hgf, and rearranging yields

$$r^2 \sin^2\theta \left[\frac{h''(r)}{h(r)} + \frac{1}{g(\theta) r^2 \sin\theta}\frac{\mathrm{d}}{\mathrm{d}\theta}\left(\sin\theta \frac{\mathrm{d}g}{\mathrm{d}\theta}(\theta)\right)\right] + \frac{f''(\varphi)}{f(\varphi)} = 0. \tag{D.145}$$

The dependence on φ has now been isolated in the last term. Consequently this term must be equal to a constant, which for convenience we denote by $-m^2$, i.e.,

$$\frac{f''(\varphi)}{f(\varphi)} = -m^2. \tag{D.146}$$

The solution of (D.146), up to a multiplicative constant, is of the form

$$f(\varphi) = e^{\pm im\varphi}. \tag{D.147}$$

For $f(\varphi)$ to be single-valued, m must be an integer if the full azimuthal range is allowed. By similar considerations we find the following separate equations for $g(\theta)$ and $h(r)$:

$$\frac{1}{\sin\theta}\frac{\mathrm{d}}{\mathrm{d}\theta}\left(\sin\theta\frac{\mathrm{d}g}{\mathrm{d}\theta}(\theta)\right) + \left(l(l+1) - \frac{m^2}{\sin^2\theta}\right) g(\theta) = 0, \tag{D.148}$$

$$r^2 h''(r) - l(l+1)h(r) = 0, \tag{D.149}$$

where $l(l+1)$ is another conveniently denoted real constant. The solution $h(r)$ of the radial equation (D.149) is easily found to be

$$h(r) = a_l\, r^{l-1} + b_l\, r^{-l}, \tag{D.150}$$

where $a_l, b_l \in \mathbb{C}$ are arbitrary constants and where l is still undetermined. For the equation of the polar angle θ we consider the change of variables $x = \cos\theta$. In this case (D.148) turns into

$$\frac{\mathrm{d}}{\mathrm{d}x}\left((1-x^2)\frac{\mathrm{d}g}{\mathrm{d}x}(x)\right) + \left(l(l+1) - \frac{m^2}{1-x^2}\right) g(x) = 0, \tag{D.151}$$

which corresponds to the generalized or associated Legendre differential equation (A.323), whose solutions on the interval $-1 \leq x \leq 1$ are the associated Legendre functions P_l^m and Q_l^m, which are characterized respectively by (A.330) and (A.331). If the solution is to be single-valued, finite, and continuous in $-1 \leq x \leq 1$, then we have to exclude the solutions Q_l^m, take l as a positive integer or zero, and admit for the integer m only the values $-l, -(l-1), \ldots, 0, \ldots, (l-1), l$. The solution of (D.148), up to an arbitrary multiplicative constant, is therefore given by

$$g(\theta) = P_l^m(\cos\theta). \tag{D.152}$$

It is practical to combine the angular factors $g(\theta)$ and $f(\varphi)$ into orthonormal functions over the unit sphere, the so-called spherical harmonics $Y_l^m(\theta, \varphi)$, which are defined in (A.380). The general solution for the Laplace equation considers the linear combination of all the solutions in the form (D.141), namely

$$u(r, \theta, \varphi) = \sum_{l=0}^{\infty} \sum_{m=-l}^{l} \left(A_{lm}\, r^l + B_{lm}\, r^{-(l+1)}\right) Y_l^m(\theta, \varphi), \tag{D.153}$$

for some undetermined arbitrary constants $A_{lm}, B_{lm} \in \mathbb{C}$. The decaying condition (D.5) implies that

$$A_{lm} = 0, \quad -l \leq m \leq l, \quad l \geq 0. \tag{D.154}$$

Thus the general solution (D.153) turns into

$$u(r,\theta,\varphi) = \sum_{l=0}^{\infty} \sum_{m=-l}^{l} B_{lm}\, r^{-(l+1)}\, Y_l^m(\theta,\varphi), \tag{D.155}$$

and its radial derivative is given by

$$\frac{\partial u}{\partial r}(r,\theta,\varphi) = -\sum_{l=0}^{\infty} \sum_{m=-l}^{l} (l+1) B_{lm}\, r^{-(l+2)}\, Y_l^m(\theta,\varphi). \tag{D.156}$$

The constants B_{lm} in (D.155) are determined through the impedance boundary condition on Γ. For this purpose, we expand the impedance data function f_z into spherical harmonics:

$$f_z(\theta,\varphi) = \sum_{l=0}^{\infty} \sum_{m=-l}^{l} f_{lm}\, Y_l^m(\theta,\varphi), \qquad 0 \le \theta \le \pi, \;\; -\pi < \varphi \le \pi, \tag{D.157}$$

where

$$f_{lm} = \int_{-\pi}^{\pi} \int_{0}^{\pi} f_z(\theta,\varphi)\, \overline{Y_l^m(\theta,\varphi)}\, \sin\theta \,\mathrm{d}\theta \,\mathrm{d}\varphi, \quad m \in \mathbb{Z}, \;\; -l \le m \le l. \tag{D.158}$$

The impedance boundary condition considers $r = R$ and thus takes the form

$$\sum_{l=0}^{\infty} \sum_{m=-l}^{l} \left(\frac{ZR - (l+1)}{R^{l+2}} \right) B_{lm}\, Y_l^m(\theta,\varphi) = f_z(\theta,\varphi) = \sum_{l=0}^{\infty} \sum_{m=-l}^{l} f_{lm}\, Y_l^m(\theta,\varphi). \tag{D.159}$$

We observe that the constants B_{lm} can be uniquely determined only if $ZR \neq (l+1)$ for $l \in \mathbb{N}_0$. If this condition is not fulfilled, then the solution is no longer unique. Therefore, if we suppose that $ZR \neq (l+1)$ for $l \in \mathbb{N}_0$, then

$$B_{lm} = \frac{R^{l+2} f_{lm}}{ZR - (l+1)}. \tag{D.160}$$

The unique solution for the exterior sphere problem (D.140) is then given by

$$u(r,\theta,\varphi) = \sum_{l=0}^{\infty} \sum_{m=-l}^{l} \left(\frac{R^{l+2} f_{lm}}{ZR - (l+1)} \right) r^{-(l+1)}\, Y_l^m(\theta,\varphi). \tag{D.161}$$

We remark that there is no need here for an additional compatibility condition like (B.191).

If we consider now the case when $ZR = (n+1)$, for some particular integer $n \in \mathbb{N}_0$, then the solution u is not unique. The constants B_{nm} for $-n \le m \le n$ are then no longer defined by (D.160), and can be chosen in an arbitrary manner. For the existence of a solution in this case, however, we require also the orthogonality conditions $f_{nm} = 0$ for $-n \le m \le n$, which are equivalent to

$$\int_{-\pi}^{\pi} \int_{0}^{\pi} f_z(\theta,\varphi)\, \overline{Y_n^m(\theta,\varphi)}\, \sin\theta \,\mathrm{d}\theta \,\mathrm{d}\varphi = 0, \quad -n \le m \le n. \tag{D.162}$$

Instead of (D.161), the solution of (D.140) is now given by the infinite family of functions

$$u(r,\theta,\varphi) = \sum_{0 \le l \ne n} \sum_{m=-l}^{l} \left(\frac{R^{l+2} f_{lm}}{ZR - (l+1)} \right) r^{-(l+1)} Y_l^m(\theta,\varphi) + \sum_{m=-n}^{n} \frac{\alpha_m}{r^{n+1}}\, Y_n^m(\theta,\varphi), \tag{D.163}$$

where $\alpha_m \in \mathbb{C}$ for $-n \leq m \leq n$ are arbitrary and where their associated terms have the form of surface waves, i.e., waves that propagate along Γ and decrease towards the interior of Ω_e. The exterior sphere problem (D.140) admits thus a unique solution u, except on a countable set of values for ZR. And even in this last case there exists a solution, although not unique, if $2n+1$ orthogonality conditions are additionally satisfied. This behavior for the existence and uniqueness of the solution is typical of the Fredholm alternative, which applies when solving problems that involve compact perturbations of invertible operators.

D.9 Existence and uniqueness

D.9.1 Function spaces

To state a precise mathematical formulation of the herein treated problems, we have to define properly the involved function spaces. For the associated interior problems defined on the bounded set Ω_i we use the classical Sobolev space (vid. Section A.4)

$$H^1(\Omega_i) = \left\{ v : \; v \in L^2(\Omega_i), \; \nabla v \in L^2(\Omega_i)^3 \right\}, \tag{D.164}$$

which is a Hilbert space and has the norm

$$\|v\|_{H^1(\Omega_i)} = \left(\|v\|^2_{L^2(\Omega_i)} + \|\nabla v\|^2_{L^2(\Omega_i)^3} \right)^{1/2}. \tag{D.165}$$

For the exterior problem defined on the unbounded domain Ω_e, on the other hand, we introduce the weighted Sobolev space (cf. Nédélec 2001)

$$W^1(\Omega_e) = \left\{ v : \; \frac{v}{(1+r^2)^{1/2}} \in L^2(\Omega_e), \; \frac{\partial v}{\partial x_i} \in L^2(\Omega_e) \;\; \forall i \in \{1,2,3\} \right\}, \tag{D.166}$$

where $r = |\boldsymbol{x}|$. If $W^1(\Omega_e)$ is provided with the norm

$$\|v\|_{W^1(\Omega_e)} = \left(\left\| \frac{v}{(1+r^2)^{1/2}} \right\|^2_{L^2(\Omega_e)} + \|\nabla v\|^2_{L^2(\Omega_e)^3} \right)^{1/2}, \tag{D.167}$$

then it becomes a Hilbert space. The restriction to any bounded open set $B \subset \Omega_e$ of the functions of $W^1(\Omega_e)$ belongs to $H^1(B)$, i.e., we have the inclusion $W^1(\Omega_e) \subset H^1_{\text{loc}}(\Omega_e)$, and the functions in these two spaces differ only by their behavior at infinity. We remark that the space $W^1(\Omega_e)$ contains the constant functions and all the functions of $H^1_{\text{loc}}(\Omega_e)$ that satisfy the decaying condition (D.5).

When dealing with Sobolev spaces, even a strong Lipschitz boundary $\Gamma \in C^{0,1}$ is admissible. In this case, and due the trace theorem (A.531), if $v \in H^1(\Omega_i)$ or $v \in W^1(\Omega_e)$, then the trace of v fulfills

$$\gamma_0 v = v|_\Gamma \in H^{1/2}(\Gamma). \tag{D.168}$$

Moreover, the trace of the normal derivative can be also defined, and it holds that

$$\gamma_1 v = \frac{\partial v}{\partial n}|_\Gamma \in H^{-1/2}(\Gamma). \tag{D.169}$$

D.9.2 Regularity of the integral operators

The boundary integral operators (D.63), (D.64), (D.65), and (D.66) can be characterized as linear and continuous applications such that

$$S : H^{-1/2+s}(\Gamma) \longrightarrow H^{1/2+s}(\Gamma), \qquad D : H^{1/2+s}(\Gamma) \longrightarrow H^{3/2+s}(\Gamma), \tag{D.170}$$

$$D^* : H^{-1/2+s}(\Gamma) \longrightarrow H^{1/2+s}(\Gamma), \qquad N : H^{1/2+s}(\Gamma) \longrightarrow H^{-1/2+s}(\Gamma). \tag{D.171}$$

This result holds for any $s \in \mathbb{R}$ if the boundary Γ is of class C^∞, which can be derived from the theory of singular integral operators with pseudo-homogeneous kernels (cf., e.g., Nédélec 2001). Due the compact injection (A.554), it holds also that the operators

$$D : H^{1/2+s}(\Gamma) \longrightarrow H^{1/2+s}(\Gamma) \qquad \text{and} \qquad D^* : H^{-1/2+s}(\Gamma) \longrightarrow H^{-1/2+s}(\Gamma) \tag{D.172}$$

are compact. For a strong Lipschitz boundary $\Gamma \in C^{0,1}$, on the other hand, these results hold only when $|s| < 1$ (cf. Costabel 1988). In the case of more regular boundaries, the range for s increases, but remains finite. For our purposes we use $s = 0$, namely

$$S : H^{-1/2}(\Gamma) \longrightarrow H^{1/2}(\Gamma), \qquad D : H^{1/2}(\Gamma) \longrightarrow H^{1/2}(\Gamma), \tag{D.173}$$

$$D^* : H^{-1/2}(\Gamma) \longrightarrow H^{-1/2}(\Gamma), \qquad N : H^{1/2}(\Gamma) \longrightarrow H^{-1/2}(\Gamma), \tag{D.174}$$

which are all linear and continuous operators, and where the operators D and D^* are compact. Similarly, we can characterize the single and double layer potentials defined respectively in (D.58) and (D.59) as linear and continuous integral operators such that

$$\mathcal{S} : H^{-1/2}(\Gamma) \longrightarrow W^1(\Omega_e \cup \Omega_i) \qquad \text{and} \qquad \mathcal{D} : H^{1/2}(\Gamma) \longrightarrow W^1(\Omega_e \cup \Omega_i). \tag{D.175}$$

D.9.3 Application to the integral equations

It is not difficult to see that if $\mu \in H^{1/2}(\Gamma)$ and $\nu \in H^{-1/2}(\Gamma)$ are given, then the transmission problem (D.35) admits a unique solution $u \in W^1(\Omega_e \cup \Omega_i)$, as a consequence of the integral representation formula (D.47). For the direct perturbation problem (D.8), though, this is not always the case, as was appreciated in the exterior sphere problem (D.140). Nonetheless, if the Fredholm alternative applies, then we know that the existence and uniqueness of the problem can be ensured almost always, i.e., except on a countable set of values for the impedance.

We consider an impedance $Z \in L^\infty(\Gamma)$ and an impedance data function $f_z \in H^{-1/2}(\Gamma)$. In both cases all the continuous functions on Γ are included.

a) First extension by zero

Let us consider the first integral equation of the extension-by-zero alternative (D.103), which is given in terms of boundary layer potentials, for $\mu \in H^{1/2}(\Gamma)$, by

$$\frac{\mu}{2} + S(Z\mu) - D(\mu) = S(f_z) \qquad \text{in } H^{1/2}(\Gamma). \tag{D.176}$$

Due the imbedding properties of Sobolev spaces and in the same way as for the full-plane impedance Laplace problem, it holds that the left-hand side of the integral equation corresponds to an identity and two compact operators, and thus Fredholm's alternative applies.

b) Second extension by zero

The second integral equation of the extension-by-zero alternative (D.107) is given in terms of boundary layer potentials, for $\mu \in H^{1/2}(\Gamma)$, by

$$\frac{Z}{2}\mu - N(\mu) + D^*(Z\mu) = \frac{f_z}{2} + D^*(f_z) \qquad \text{in } H^{-1/2}(\Gamma). \tag{D.177}$$

The operator N plays the role of the identity and the other terms on the left-hand side are compact, thus Fredholm's alternative holds.

c) Continuous impedance

The integral equation of the continuous-impedance alternative (D.115) is given in terms of boundary layer potentials, for $\mu \in H^{1/2}(\Gamma)$, by

$$-N(\mu) + D^*(Z\mu) + ZD(\mu) - ZS(Z\mu) = f_z \qquad \text{in } H^{-1/2}(\Gamma). \tag{D.178}$$

Again, the operator N plays the role of the identity and the remaining terms on the left-hand side are compact, thus Fredholm's alternative applies.

d) Continuous value

The integral equation of the continuous-value alternative (D.123) is given in terms of boundary layer potentials, for $\nu \in H^{-1/2}(\Gamma)$, by

$$\frac{\nu}{2} + ZS(\nu) - D^*(\nu) = -f_z \qquad \text{in } H^{-1/2}(\Gamma). \tag{D.179}$$

On the left-hand side we have an identity operator and the remaining operators are compact, thus Fredholm's alternative holds.

e) Continuous normal derivative

The integral equation of the continuous-normal-derivative alternative (D.131) is given in terms of boundary layer potentials, for $\mu \in H^{1/2}(\Gamma)$, by

$$\frac{Z}{2}\mu - N(\mu) + ZD(\mu) = f_z \qquad \text{in } H^{-1/2}(\Gamma). \tag{D.180}$$

As before, Fredholm's alternative again applies, since on the left-hand side we have the operator N and two compact operators.

D.9.4 Consequences of Fredholm's alternative

Since the Fredholm alternative applies to each integral equation, therefore it applies also to the exterior differential problem (D.8) due the integral representation formula. The existence of the exterior problem's solution is thus determined by its uniqueness, and the impedances $Z \in \mathbb{C}$ for which the uniqueness is lost constitute a countable set, which we call the impedance spectrum of the exterior problem and denote it by σ_Z. The existence and uniqueness of the solution is therefore ensured almost everywhere. The same holds obviously for the solution of the integral equation, whose impedance spectrum we denote by ς_Z. Since each integral equation is derived from the exterior problem, it holds that $\sigma_Z \subset \varsigma_Z$. The converse, though, is not necessarily true and depends on each particular integral equation. In any way, the set $\varsigma_Z \setminus \sigma_Z$ is at most countable.

Fredholm's alternative applies as much to the integral equation itself as to its adjoint counterpart, and equally to their homogeneous versions. Moreover, each integral equation solves at the same time an exterior and an interior differential problem. The loss of uniqueness of the integral equation's solution appears when the impedance Z is an eigenvalue of some associated interior problem, either of the homogeneous integral equation or of its adjoint counterpart. Such an impedance Z is contained in ς_Z.

The integral equation (D.105) is associated with the extension by zero (D.98), for which no eigenvalues appear. Nevertheless, its adjoint integral equation (D.125) of the continuous value is associated with the interior problem (D.118), whose solution is unique for all $Z \neq 0$.

The integral equation (D.108) is also associated with the extension by zero (D.98), for which no eigenvalues appear. Nonetheless, its adjoint integral equation (D.133) of the continuous normal derivative is associated with the interior problem (D.126), whose solution is unique for all Z, without restriction.

The integral equation (D.117) of the continuous impedance is self-adjoint and is associated with the interior problem (D.109), which has a countable quantity of eigenvalues Z.

Let us consider now the transmission problem generated by the homogeneous exterior problem

$$\begin{cases} \text{Find } u_e : \Omega_e \to \mathbb{C} \text{ such that} \\ \Delta u_e = 0 & \text{in } \Omega_e, \\ -\dfrac{\partial u_e}{\partial n} + Z u_e = 0 & \text{on } \Gamma, \\ \text{+ Decaying condition as } |\boldsymbol{x}| \to \infty, \end{cases} \tag{D.181}$$

and the associated homogeneous interior problem

$$\begin{cases} \text{Find } u_i : \Omega_i \to \mathbb{C} \text{ such that} \\ \Delta u_i = 0 & \text{in } \Omega_i, \\ \dfrac{\partial u_i}{\partial n} + Z u_i = 0 & \text{on } \Gamma, \end{cases} \tag{D.182}$$

where the asymptotic decaying condition is as usual given by (D.5), and where the unit normal $\boldsymbol{n}$ always points outwards of Ω_e.

As in the two-dimensional case, it holds again that the integral equations for this transmission problem have either the same left-hand side or are mutually adjoint to all other possible alternatives of integral equations that can be built for the exterior problem (D.8), and in particular to all the alternatives that were mentioned in the last subsection. The eigenvalues Z of the homogeneous interior problem (D.182) are thus also contained in ς_Z.

We remark that additional alternatives for integral representations and equations based on non-homogeneous versions of the problem (D.182) can be also derived for the exterior impedance problem (cf. Ha-Duong 1987).

The determination of the impedance spectrum σ_Z of the exterior problem (D.8) is not so easy, but can be achieved for simple geometries where an analytic solution is known.

In conclusion, the exterior problem (D.8) admits a unique solution u if $Z \notin \sigma_Z$, and each integral equation admits a unique solution, either μ or ν, if $Z \notin \varsigma_Z$.

D.10 Variational formulation

To solve a particular integral equation we convert it to its variational or weak formulation, i.e., we solve it with respect to certain test functions in a bilinear (or sesquilinear) form. Basically, the integral equation is multiplied by the (conjugated) test function and then the equation is integrated over the boundary of the domain. The test functions are taken in the same function space as the solution of the integral equation.

a) First extension by zero

The variational formulation for the first integral equation (D.176) of the extension-by-zero alternative searches $\mu \in H^{1/2}(\Gamma)$ such that $\forall \varphi \in H^{1/2}(\Gamma)$

$$\left\langle \frac{\mu}{2} + S(Z\mu) - D(\mu), \varphi \right\rangle = \big\langle S(f_z), \varphi \big\rangle. \tag{D.183}$$

b) Second extension by zero

The variational formulation for the second integral equation (D.177) of the extension-by-zero alternative searches $\mu \in H^{1/2}(\Gamma)$ such that $\forall \varphi \in H^{1/2}(\Gamma)$

$$\left\langle \frac{Z}{2}\mu - N(\mu) + D^*(Z\mu), \varphi \right\rangle = \left\langle \frac{f_z}{2} + D^*(f_z), \varphi \right\rangle. \tag{D.184}$$

c) Continuous impedance

The variational formulation for the integral equation (D.178) of the alternative of the continuous-impedance searches $\mu \in H^{1/2}(\Gamma)$ such that $\forall \varphi \in H^{1/2}(\Gamma)$

$$\big\langle -N(\mu) + D^*(Z\mu) + ZD(\mu) - ZS(Z\mu), \varphi \big\rangle = \big\langle f_z, \varphi \big\rangle. \tag{D.185}$$

d) Continuous value

The variational formulation for the integral equation (D.179) of the continuous-value alternative searches $\nu \in H^{-1/2}(\Gamma)$ such that $\forall \psi \in H^{-1/2}(\Gamma)$

$$\left\langle \frac{\nu}{2} + ZS(\nu) - D^*(\nu), \psi \right\rangle = \big\langle -f_z, \psi \big\rangle. \tag{D.186}$$

e) Continuous normal derivative

The variational formulation for the integral equation (D.180) of the continuous-normal-derivative alternative searches $\mu \in H^{1/2}(\Gamma)$ such that $\forall \varphi \in H^{1/2}(\Gamma)$

$$\left\langle \frac{Z}{2}\mu - N(\mu) + ZD(\mu), \varphi \right\rangle = \big\langle f_z, \varphi \big\rangle. \tag{D.187}$$

D.11 Numerical discretization

D.11.1 Discretized function spaces

The exterior problem (D.8) is solved numerically with the boundary element method by employing a Galerkin scheme on the variational formulation of an integral equation. We use on the boundary surface Γ Lagrange finite elements of type either $\mathbb{P}_1$ or $\mathbb{P}_0$. The surface Γ is approximated by the triangular mesh Γ^h, composed by T flat triangles T_j, for $1 \leq j \leq T$, and I nodes $\boldsymbol{r}_i \in \mathbb{R}^3$, $1 \leq i \leq I$. The triangles have a diameter less or equal than h, and their vertices or corners, i.e., the nodes $\boldsymbol{r}_i$, are on top of Γ, as shown in Figure D.5. The diameter of a triangle K is given by

$$\operatorname{diam}(K) = \sup_{\boldsymbol{x},\boldsymbol{y}\in K} |\boldsymbol{y} - \boldsymbol{x}|. \tag{D.188}$$

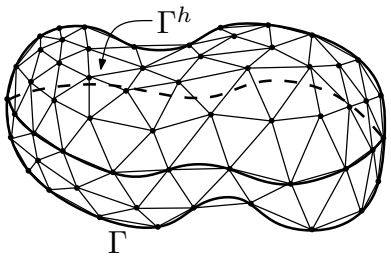

FIGURE D.5. Mesh Γ^h, discretization of Γ.

The function space $H^{1/2}(\Gamma)$ is approximated using the conformal space of continuous piecewise linear polynomials with complex coefficients

$$Q_h = \big\{\varphi_h \in C^0(\Gamma^h) \,:\, \varphi_h|_{T_j} \in \mathbb{P}_1(\mathbb{C}),\;\; 1 \leq j \leq T\big\}. \tag{D.189}$$

The space Q_h has a finite dimension I, and we describe it using the standard base functions for finite elements of type $\mathbb{P}_1$, denoted by $\{\chi_j\}_{j=1}^I$ and illustrated in Figure D.6. The base function χ_j is associated with the node $\boldsymbol{r}_j$ and has its support $\operatorname{supp}\chi_j$ on the triangles that have $\boldsymbol{r}_j$ as one of their vertices. On $\boldsymbol{r}_j$ it has a value of one and on the opposed edges of the triangles its value is zero, being linearly interpolated in between and zero otherwise.

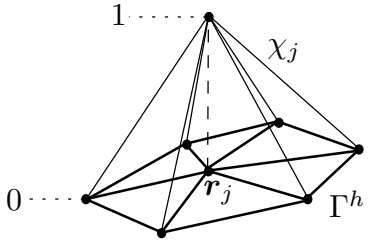

FIGURE D.6. Base function χ_j for finite elements of type $\mathbb{P}_1$.

The function space $H^{-1/2}(\Gamma)$, on the other hand, is approximated using the conformal space of piecewise constant polynomials with complex coefficients

$$P_h = \big\{\psi_h : \Gamma^h \to \mathbb{C} \mid \ \psi_h|_{T_j} \in \mathbb{P}_0(\mathbb{C}), \ \ 1 \le j \le T\big\}. \tag{D.190}$$

The space P_h has a finite dimension T, and is described using the standard base functions for finite elements of type $\mathbb{P}_0$, denoted by $\{\kappa_j\}_{j=1}^T$, shown in Figure D.7, and expressed as

$$\kappa_j(\boldsymbol{x}) = \begin{cases} 1 & \text{if } \ \boldsymbol{x} \in T_j, \\ 0 & \text{if } \ \boldsymbol{x} \notin T_j. \end{cases} \tag{D.191}$$

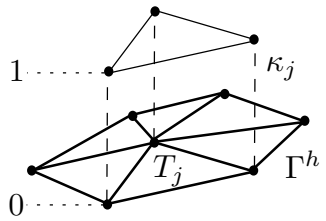

FIGURE D.7. Base function κ_j for finite elements of type $\mathbb{P}_0$.

In virtue of this discretization, any function $\varphi_h \in Q_h$ or $\psi_h \in P_h$ can be expressed as a linear combination of the elements of the base, namely

$$\varphi_h(\boldsymbol{x}) = \sum_{j=1}^{I} \varphi_j \, \chi_j(\boldsymbol{x}) \qquad \text{and} \qquad \psi_h(\boldsymbol{x}) = \sum_{j=1}^{T} \psi_j \, \kappa_j(\boldsymbol{x}) \qquad \text{for } \ \boldsymbol{x} \in \Gamma^h, \tag{D.192}$$

where $\varphi_j, \psi_j \in \mathbb{C}$. The solutions $\mu \in H^{1/2}(\Gamma)$ and $\nu \in H^{-1/2}(\Gamma)$ of the variational formulations can be therefore approximated respectively by

$$\mu_h(\boldsymbol{x}) = \sum_{j=1}^{I} \mu_j \, \chi_j(\boldsymbol{x}) \qquad \text{and} \qquad \nu_h(\boldsymbol{x}) = \sum_{j=1}^{T} \nu_j \, \kappa_j(\boldsymbol{x}) \qquad \text{for } \ \boldsymbol{x} \in \Gamma^h, \tag{D.193}$$

where $\mu_j, \nu_j \in \mathbb{C}$. The function f_z can be also approximated by

$$f_z^h(\boldsymbol{x}) = \sum_{j=1}^{I} f_j \, \chi_j(\boldsymbol{x}) \qquad \text{for } \ \boldsymbol{x} \in \Gamma^h, \quad \text{with } \ f_j = f_z(\boldsymbol{r}_j), \tag{D.194}$$

or

$$f_z^h(\boldsymbol{x}) = \sum_{j=1}^{T} f_j \, \kappa_j(\boldsymbol{x}) \qquad \text{for } \ \boldsymbol{x} \in \Gamma^h, \quad \text{with } \ f_j = \frac{f_z(\boldsymbol{r}_1^j) + f_z(\boldsymbol{r}_2^j) + f_z(\boldsymbol{r}_3^j)}{3}, \tag{D.195}$$

depending on whether the original integral equation is stated in $H^{1/2}(\Gamma)$ or in $H^{-1/2}(\Gamma)$. We denote by $\boldsymbol{r}_d^j$, for $d \in \{1, 2, 3\}$, the three vertices of triangle T_j.

D.11.2 Discretized integral equations

a) First extension by zero

To see how the boundary element method operates, we apply it to the first integral equation of the extension-by-zero alternative, i.e., to the variational formulation (D.183). We characterize all the discrete approximations by the index h, including also the impedance and the boundary layer potentials. The numerical approximation of (D.183) leads to the discretized problem that searches $\mu_h \in Q_h$ such that $\forall \varphi_h \in Q_h$

$$\left\langle \frac{\mu_h}{2} + S_h(Z_h\mu_h) - D_h(\mu_h), \varphi_h \right\rangle = \left\langle S_h(f_z^h), \varphi_h \right\rangle. \tag{D.196}$$

Considering the decomposition of μ_h in terms of the base $\{\chi_j\}$ and taking as test functions the same base functions, $\varphi_h = \chi_i$ for $1 \leq i \leq I$, yields the discrete linear system

$$\sum_{j=1}^{I} \mu_j \left(\frac{1}{2}\langle \chi_j, \chi_i \rangle + \langle S_h(Z_h\chi_j), \chi_i \rangle - \langle D_h(\chi_j), \chi_i \rangle \right) = \sum_{j=1}^{I} f_j \, \langle S_h(\chi_j), \chi_i \rangle. \tag{D.197}$$

This constitutes a system of linear equations that can be expressed as a linear matrix system:

$$\begin{cases} \text{Find } \boldsymbol{\mu} \in \mathbb{C}^I \text{ such that} \\ \boldsymbol{M}\boldsymbol{\mu} = \boldsymbol{b}. \end{cases} \tag{D.198}$$

The elements m_{ij} of the matrix $\boldsymbol{M}$ are given by

$$m_{ij} = \frac{1}{2}\langle \chi_j, \chi_i \rangle + \langle S_h(Z_h\chi_j), \chi_i \rangle - \langle D_h(\chi_j), \chi_i \rangle \qquad \text{for } \; 1 \leq i, j \leq I, \tag{D.199}$$

and the elements b_i of the vector $\boldsymbol{b}$ by

$$b_i = \left\langle S_h(f_z^h), \chi_i \right\rangle = \sum_{j=1}^{I} f_j \, \langle S_h(\chi_j), \chi_i \rangle \qquad \text{for } \; 1 \leq i \leq I. \tag{D.200}$$

The discretized solution u_h, which approximates u, is finally obtained by discretizing the integral representation formula (D.104) according to

$$u_h = \mathcal{D}_h(\mu_h) - \mathcal{S}_h(Z_h\mu_h) + \mathcal{S}_h(f_z^h), \tag{D.201}$$

which, more specifically, can be expressed as

$$u_h = \sum_{j=1}^{I} \mu_j \big(\mathcal{D}_h(\chi_j) - \mathcal{S}_h(Z_h\chi_j) \big) + \sum_{j=1}^{I} f_j \, \mathcal{S}_h(\chi_j). \tag{D.202}$$

By proceeding in the same way, the discretization of all the other alternatives of integral equations can be also expressed as a linear matrix system like (D.198). The resulting matrix $\boldsymbol{M}$ is in general complex, full, non-symmetric, and with dimensions $I \times I$ for elements of type $\mathbb{P}_1$ and $T \times T$ for elements of type $\mathbb{P}_0$. The right-hand side vector $\boldsymbol{b}$ is complex and of size either I or T. The boundary element calculations required to compute numerically the elements of $\boldsymbol{M}$ and $\boldsymbol{b}$ have to be performed carefully, since the integrals that appear become singular when the involved triangles are coincident, or when they have a common vertex or edge, due the singularity of the Green's function at its source point.

b) Second extension by zero

In the case of the second integral equation of the extension-by-zero alternative, i.e., of the variational formulation (D.184), the elements m_{ij} that constitute the matrix $\boldsymbol{M}$ of the linear system (D.198) are given by

$$m_{ij} = \frac{1}{2}\langle Z_h\chi_j, \chi_i\rangle - \langle N_h(\chi_j), \chi_i\rangle + \langle D_h^*(Z_h\chi_j), \chi_i\rangle \qquad \text{for } 1 \le i, j \le I, \tag{D.203}$$

whereas the elements b_i of the vector $\boldsymbol{b}$ are expressed as

$$b_i = \sum_{j=1}^{I} f_j \left(\frac{1}{2}\langle \chi_j, \chi_i\rangle + \langle D_h^*(Z_h\chi_j), \chi_i\rangle\right) \qquad \text{for } 1 \le i \le I. \tag{D.204}$$

The discretized solution u_h is again computed by (D.202).

c) Continuous impedance

In the case of the continuous-impedance alternative, i.e., of the variational formulation (D.185), the elements m_{ij} that constitute the matrix $\boldsymbol{M}$ of the linear system (D.198) are given, for $1 \le i, j \le I$, by

$$m_{ij} = -\langle N_h(\chi_j), \chi_i\rangle + \langle D_h^*(Z_h\chi_j), \chi_i\rangle + \langle Z_h D_h(\chi_j), \chi_i\rangle - \langle Z_h S_h(Z_h\chi_j), \chi_i\rangle, \tag{D.205}$$

whereas the elements b_i of the vector $\boldsymbol{b}$ are expressed as

$$b_i = \sum_{j=1}^{I} f_j \langle \chi_j, \chi_i\rangle \qquad \text{for } 1 \le i \le I. \tag{D.206}$$

It can be observed that for this particular alternative the matrix $\boldsymbol{M}$ turns out to be symmetric, since the integral equation is self-adjoint. The discretized solution u_h, due (D.116), is then computed by

$$u_h = \sum_{j=1}^{I} \mu_j \big(\mathcal{D}_h(\chi_j) - \mathcal{S}_h(Z_h\chi_j)\big). \tag{D.207}$$

d) Continuous value

In the case of the continuous-value alternative, that is, of the variational formulation (D.186), the elements m_{ij} that constitute the matrix $\boldsymbol{M}$, now of the linear system

$$\begin{cases} \text{Find } \boldsymbol{\nu} \in \mathbb{C}^T \text{ such that} \\ \boldsymbol{M\nu} = \boldsymbol{b}, \end{cases} \tag{D.208}$$

are given by

$$m_{ij} = \frac{1}{2}\langle \kappa_j, \kappa_i\rangle + \langle Z_h S_h(\kappa_j), \kappa_i\rangle - \langle D_h^*(\kappa_j), \kappa_i\rangle \qquad \text{for } 1 \le i, j \le T, \tag{D.209}$$

whereas the elements b_i of the vector $\boldsymbol{b}$ are expressed as

$$b_i = -\sum_{j=1}^{T} f_j \langle \kappa_j, \kappa_i\rangle \qquad \text{for } 1 \le i \le T. \tag{D.210}$$

The discretized solution u_h, due (D.124), is then computed by

$$u_h = -\sum_{j=1}^{T} \nu_j \, \mathcal{S}_h(\kappa_j). \tag{D.211}$$

e) Continuous normal derivative

In the case of the continuous-normal-derivative alternative, i.e., of the variational formulation (D.187), the elements m_{ij} that conform the matrix $\boldsymbol{M}$ of the linear system (D.198) are given by

$$m_{ij} = \frac{1}{2}\langle Z_h \chi_j, \chi_i\rangle - \langle N_h(\chi_j), \chi_i\rangle + \langle Z_h D_h(\chi_j), \chi_i\rangle \qquad \text{for } 1 \le i, j \le I, \tag{D.212}$$

whereas the elements b_i of the vector $\boldsymbol{b}$ are expressed as

$$b_i = \sum_{j=1}^{I} f_j \, \langle \chi_j, \chi_i\rangle \qquad \text{for } 1 \le i \le I. \tag{D.213}$$

The discretized solution u_h, due (D.132), is then computed by

$$u_h = \sum_{j=1}^{I} \mu_j \, \mathcal{D}_h(\chi_j). \tag{D.214}$$

D.12 Boundary element calculations

D.12.1 Geometry

The boundary element calculations build the elements of the matrix $\boldsymbol{M}$ resulting from the discretization of the integral equation, i.e., from (D.198) or (D.208). They permit thus to compute numerically expressions like (D.199). To evaluate the appearing singular integrals, we use the semi-numerical methods described in the report of Bendali & Devys (1986).

We consider the elemental interactions between two triangles T_K and T_L of a mesh Γ^h. The unit normal points always inwards of the domain encompassed by the mesh Γ^h.

We denote the triangles more simply just as $K = T_K$ and $L = T_L$. As depicted in Figure D.8, the following notation is used:

- $|K|$ denotes the area of triangle K.
- $|L|$ denotes the area of triangle L.
- $\boldsymbol{r}_1^K, \boldsymbol{r}_2^K, \boldsymbol{r}_3^K$ denote the ordered vertices or corners of triangle K.
- $\boldsymbol{r}_1^L, \boldsymbol{r}_2^L, \boldsymbol{r}_3^L$ denote the ordered vertices or corners of triangle L.
- $\boldsymbol{n}_K, \boldsymbol{n}_L$ denote the unit normals of triangles K and L (oriented with the vertices).

The vertices of the triangles are obtained by renumbering locally the nodes $\boldsymbol{r}_i$, $1 \le i \le I$.

Furthermore, as shown in Figure D.9, we also use the notation:

- h_1^K, h_2^K, h_3^K denote the heights of triangle K.
- h_1^L, h_2^L, h_3^L denote the heights of triangle L.
- $\boldsymbol{\tau}_1^K, \boldsymbol{\tau}_2^K, \boldsymbol{\tau}_3^K$ denote the unit edge tangents of triangle K.

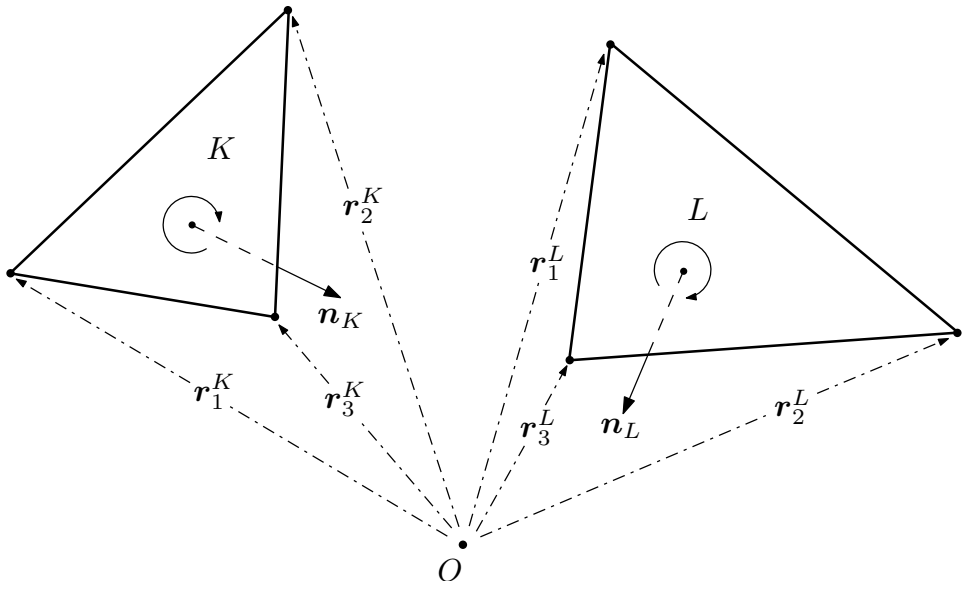

FIGURE D.8. Vertices and unit normals of triangles K and L.

- $\boldsymbol{\tau}_1^L, \boldsymbol{\tau}_2^L, \boldsymbol{\tau}_3^L$ denote the unit edge tangents of triangle L.
- $\boldsymbol{\nu}_1^K, \boldsymbol{\nu}_2^K, \boldsymbol{\nu}_3^K$ denote the unit edge normals of triangle K.
- $\boldsymbol{\nu}_1^L, \boldsymbol{\nu}_2^L, \boldsymbol{\nu}_3^L$ denote the unit edge normals of triangle L.

The unit edge tangents and normals are located on the same plane as the respective triangle.

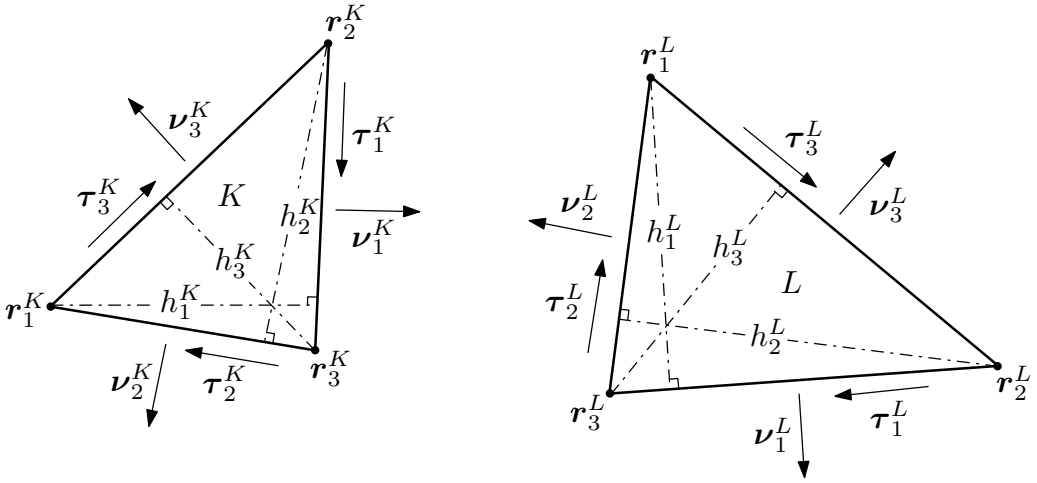

FIGURE D.9. Heights and unit edge normals and tangents of triangles K and L.

For the parametric description of the triangles, shown in Figure D.10, we take into account the notation:

- $\boldsymbol{r}(\boldsymbol{x})$ denotes a variable location on triangle K (dependent on variable $\boldsymbol{x}$).
- $\boldsymbol{r}(\boldsymbol{y})$ denotes a variable location on triangle L (dependent on variable $\boldsymbol{y}$).

- $\boldsymbol{r}_c^K, \boldsymbol{r}_d^L$ denote the vertices of triangles K and L, being $c, d \in \{1, 2, 3\}$.

Triangle K can be parametrically described by

$$\boldsymbol{r}(\boldsymbol{x}) = \boldsymbol{r}_c^K + s_c \boldsymbol{\nu}_c^K + p_c \boldsymbol{\tau}_c^K, \qquad 0 \leq s_c \leq h_c^K, \qquad c \in \{1, 2, 3\}, \tag{D.215}$$

where

$$-\frac{s_1}{h_1^K}(\boldsymbol{r}_1^K - \boldsymbol{r}_2^K) \cdot \boldsymbol{\tau}_1^K \leq p_1 \leq \frac{s_1}{h_1^K}(\boldsymbol{r}_3^K - \boldsymbol{r}_1^K) \cdot \boldsymbol{\tau}_1^K, \tag{D.216}$$

$$-\frac{s_2}{h_2^K}(\boldsymbol{r}_2^K - \boldsymbol{r}_3^K) \cdot \boldsymbol{\tau}_2^K \leq p_2 \leq \frac{s_2}{h_2^K}(\boldsymbol{r}_1^K - \boldsymbol{r}_2^K) \cdot \boldsymbol{\tau}_2^K, \tag{D.217}$$

$$-\frac{s_3}{h_3^K}(\boldsymbol{r}_3^K - \boldsymbol{r}_1^K) \cdot \boldsymbol{\tau}_3^K \leq p_3 \leq \frac{s_3}{h_3^K}(\boldsymbol{r}_2^K - \boldsymbol{r}_3^K) \cdot \boldsymbol{\tau}_3^K. \tag{D.218}$$

Similarly, triangle L can be parametrically described by

$$\boldsymbol{r}(\boldsymbol{y}) = \boldsymbol{r}_d^L + t_d \boldsymbol{\nu}_d^L + q_d \boldsymbol{\tau}_d^L, \qquad 0 \leq t_d \leq h_d^L, \qquad d \in \{1, 2, 3\}, \tag{D.219}$$

where

$$-\frac{t_1}{h_1^L}(\boldsymbol{r}_1^L - \boldsymbol{r}_2^L) \cdot \boldsymbol{\tau}_1^L \leq q_1 \leq \frac{t_1}{h_1^L}(\boldsymbol{r}_3^L - \boldsymbol{r}_1^L) \cdot \boldsymbol{\tau}_1^L, \tag{D.220}$$

$$-\frac{t_2}{h_2^L}(\boldsymbol{r}_2^L - \boldsymbol{r}_3^L) \cdot \boldsymbol{\tau}_2^L \leq q_2 \leq \frac{t_2}{h_2^L}(\boldsymbol{r}_1^L - \boldsymbol{r}_2^L) \cdot \boldsymbol{\tau}_2^L, \tag{D.221}$$

$$-\frac{t_3}{h_3^L}(\boldsymbol{r}_3^L - \boldsymbol{r}_1^L) \cdot \boldsymbol{\tau}_3^L \leq q_3 \leq \frac{t_3}{h_3^L}(\boldsymbol{r}_2^L - \boldsymbol{r}_3^L) \cdot \boldsymbol{\tau}_3^L. \tag{D.222}$$

Thus the parameters p_c, s_c, q_d, and t_d can be expressed as

$$p_c = \big(\boldsymbol{r}(\boldsymbol{x}) - \boldsymbol{r}_c^K\big) \cdot \boldsymbol{\tau}_c^K, \qquad c \in \{1, 2, 3\}, \tag{D.223}$$

$$s_c = \big(\boldsymbol{r}(\boldsymbol{x}) - \boldsymbol{r}_c^K\big) \cdot \boldsymbol{\nu}_c^K, \qquad c \in \{1, 2, 3\}, \tag{D.224}$$

$$q_d = \big(\boldsymbol{r}(\boldsymbol{y}) - \boldsymbol{r}_d^L\big) \cdot \boldsymbol{\tau}_d^L, \qquad d \in \{1, 2, 3\}. \tag{D.225}$$

$$t_d = \big(\boldsymbol{r}(\boldsymbol{y}) - \boldsymbol{r}_d^L\big) \cdot \boldsymbol{\nu}_d^L, \qquad d \in \{1, 2, 3\}. \tag{D.226}$$

The areas of the triangles K and L are given by

$$|K| = \frac{1}{2} h_1^K |\boldsymbol{r}_3^K - \boldsymbol{r}_2^K| = \frac{1}{2} h_2^K |\boldsymbol{r}_3^K - \boldsymbol{r}_1^K| = \frac{1}{2} h_3^K |\boldsymbol{r}_2^K - \boldsymbol{r}_1^K|, \tag{D.227}$$

$$|L| = \frac{1}{2} h_1^L |\boldsymbol{r}_3^L - \boldsymbol{r}_2^L| = \frac{1}{2} h_2^L |\boldsymbol{r}_3^L - \boldsymbol{r}_1^L| = \frac{1}{2} h_3^L |\boldsymbol{r}_2^L - \boldsymbol{r}_1^L|. \tag{D.228}$$

The unit normals $\boldsymbol{n}_K$ and $\boldsymbol{n}_L$ can be computed as

$$\boldsymbol{n}_K = \frac{\boldsymbol{\tau}_1^K \times \boldsymbol{\tau}_2^K}{|\boldsymbol{\tau}_1^K \times \boldsymbol{\tau}_2^K|} = \frac{\boldsymbol{\tau}_2^K \times \boldsymbol{\tau}_3^K}{|\boldsymbol{\tau}_2^K \times \boldsymbol{\tau}_3^K|} = \frac{\boldsymbol{\tau}_3^K \times \boldsymbol{\tau}_1^K}{|\boldsymbol{\tau}_3^K \times \boldsymbol{\tau}_1^K|}, \tag{D.229}$$

$$\boldsymbol{n}_L = \frac{\boldsymbol{\tau}_1^L \times \boldsymbol{\tau}_2^L}{|\boldsymbol{\tau}_1^L \times \boldsymbol{\tau}_2^L|} = \frac{\boldsymbol{\tau}_2^L \times \boldsymbol{\tau}_3^L}{|\boldsymbol{\tau}_2^L \times \boldsymbol{\tau}_3^L|} = \frac{\boldsymbol{\tau}_3^L \times \boldsymbol{\tau}_1^L}{|\boldsymbol{\tau}_3^L \times \boldsymbol{\tau}_1^L|}. \tag{D.230}$$

For the unit edge tangents $\boldsymbol{\tau}_c^K$ and $\boldsymbol{\tau}_d^L$ we have that

$$\boldsymbol{\tau}_1^K = \frac{\boldsymbol{r}_3^K - \boldsymbol{r}_2^K}{|\boldsymbol{r}_3^K - \boldsymbol{r}_2^K|}, \qquad \boldsymbol{\tau}_2^K = \frac{\boldsymbol{r}_1^K - \boldsymbol{r}_3^K}{|\boldsymbol{r}_1^K - \boldsymbol{r}_3^K|}, \qquad \boldsymbol{\tau}_3^K = \frac{\boldsymbol{r}_2^K - \boldsymbol{r}_1^K}{|\boldsymbol{r}_2^K - \boldsymbol{r}_1^K|}, \tag{D.231}$$

$$\boldsymbol{\tau}_1^L = \frac{\boldsymbol{r}_3^L - \boldsymbol{r}_2^L}{|\boldsymbol{r}_3^L - \boldsymbol{r}_2^L|}, \qquad \boldsymbol{\tau}_2^L = \frac{\boldsymbol{r}_1^L - \boldsymbol{r}_3^L}{|\boldsymbol{r}_1^L - \boldsymbol{r}_3^L|}, \qquad \boldsymbol{\tau}_3^L = \frac{\boldsymbol{r}_2^L - \boldsymbol{r}_1^L}{|\boldsymbol{r}_2^L - \boldsymbol{r}_1^L|}, \tag{D.232}$$

and for the unit edge normals $\boldsymbol{\nu}_c^K$ and $\boldsymbol{\nu}_d^L$, that

$$\boldsymbol{\nu}_c^K = \boldsymbol{\tau}_c^K \times \boldsymbol{n}_K, \qquad c \in \{1,2,3\}, \tag{D.233}$$

$$\boldsymbol{\nu}_d^L = \boldsymbol{\tau}_d^L \times \boldsymbol{n}_L, \qquad d \in \{1,2,3\}. \tag{D.234}$$

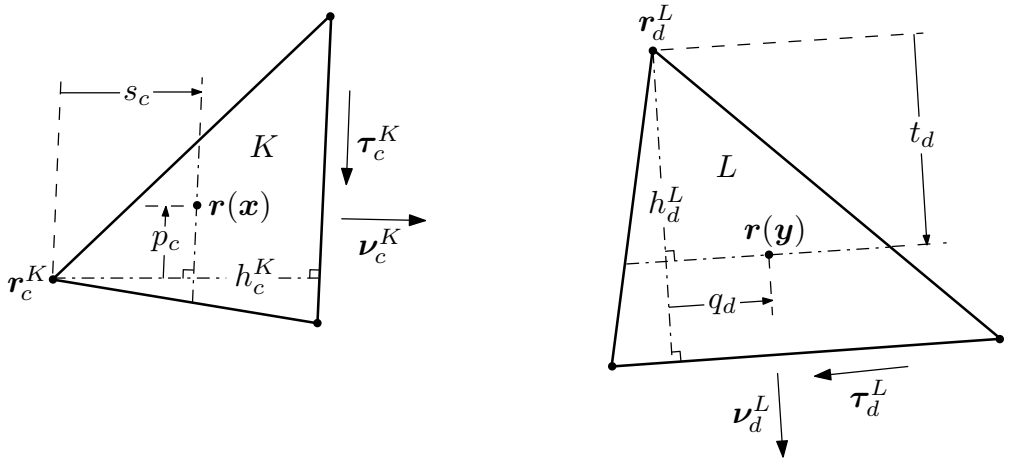

FIGURE D.10. Parametric description of triangles K and L.

The triangles K and L can be also parametrically described using barycentric coordinates λ_c^K and λ_d^L, i.e.,

$$\boldsymbol{r}(\boldsymbol{x}) = \sum_{c=1}^{3} \lambda_c^K \boldsymbol{r}_c^K, \qquad \sum_{c=1}^{3} \lambda_c^K = 1, \qquad 0 \leq \lambda_c^K \leq 1, \tag{D.235}$$

$$\boldsymbol{r}(\boldsymbol{y}) = \sum_{d=1}^{3} \lambda_d^L \boldsymbol{r}_d^L, \qquad \sum_{d=1}^{3} \lambda_d^L = 1, \qquad 0 \leq \lambda_d^L \leq 1. \tag{D.236}$$

For the elemental interactions between a point $\boldsymbol{x}$ on triangle K and a point $\boldsymbol{y}$ on triangle L, the following notation is also used:

- $\boldsymbol{R}$ denotes the vector pointing from the point $\boldsymbol{x}$ towards the point $\boldsymbol{y}$.
- R denotes the distance between the points $\boldsymbol{x}$ and $\boldsymbol{y}$.

These values are given by

$$\boldsymbol{R} = \boldsymbol{r}(\boldsymbol{y}) - \boldsymbol{r}(\boldsymbol{x}), \tag{D.237}$$

$$R = |\boldsymbol{R}| = |\boldsymbol{y} - \boldsymbol{x}|. \tag{D.238}$$

For the singular integral calculations, when considering the point $\boldsymbol{x}$ as a parameter, the following notation is also used (vid. Figure D.11):

- $\boldsymbol{R}_1^L, \boldsymbol{R}_2^L, \boldsymbol{R}_3^L$ denote the vectors pointing from $\boldsymbol{x}$ towards the vertices of triangle L.

- R_1^L, R_2^L, R_3^L denote the distances from $\boldsymbol{x}$ to the vertices of triangle L.
- C_1^L, C_2^L, C_3^L denote the edges or sides of triangle L.
- d_L denotes the signed distance from $\boldsymbol{x}$ to the plane that contains triangle L.
- Θ_L denotes the solid angle formed by the vectors $\boldsymbol{R}_1^L$, $\boldsymbol{R}_2^L$, and $\boldsymbol{R}_3^L$, through which triangle L is seen from point $\boldsymbol{x}$ ($-2\pi \leq \Theta_L \leq 2\pi$).

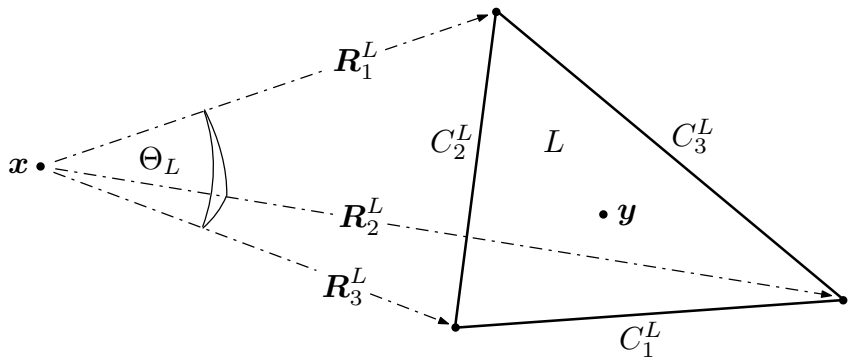

FIGURE D.11. Geometric characteristics for the singular integral calculations.

Thus on triangle L the following holds:

$$\boldsymbol{R}_d^L = \boldsymbol{r}_d^L - \boldsymbol{r}(\boldsymbol{x}), \qquad R_d^L = |\boldsymbol{R}_d^L|, \qquad d \in \{1,2,3\}. \tag{D.239}$$

Likewise as before, we have for $d \in \{1,2,3\}$ that

$$\boldsymbol{R} = \boldsymbol{R}_d^L + t_d\, \boldsymbol{\nu}_d^L + q_d\, \boldsymbol{\tau}_d^L, \tag{D.240}$$

$$t_d = \big(\boldsymbol{R} - \boldsymbol{R}_d^L\big) \cdot \boldsymbol{\nu}_d^L, \tag{D.241}$$

$$q_d = \big(\boldsymbol{R} - \boldsymbol{R}_d^L\big) \cdot \boldsymbol{\tau}_d^L. \tag{D.242}$$

In particular, the edges C_d^L are parametrically described by

$$\boldsymbol{R} = \boldsymbol{R}_d^L + h_d^L\, \boldsymbol{\nu}_d^L + q_d\, \boldsymbol{\tau}_d^L. \tag{D.243}$$

The signed distance d_L is constant on L and is characterized by

$$d_L = \boldsymbol{R} \cdot \boldsymbol{n}_L = \boldsymbol{R}_1^L \cdot \boldsymbol{n}_L = \boldsymbol{R}_2^L \cdot \boldsymbol{n}_L = \boldsymbol{R}_3^L \cdot \boldsymbol{n}_L. \tag{D.244}$$

Finally, the solid angle Θ_L can be computed by using the formula described in the article of Van Oosterom & Strackee (1983):

$$\tan\left(\frac{\Theta_L}{2}\right) = \frac{\big[\boldsymbol{R}_1^L \boldsymbol{R}_2^L \boldsymbol{R}_3^L\big]}{R_1^L R_2^L R_3^L + (\boldsymbol{R}_1^L \cdot \boldsymbol{R}_2^L) R_3^L + (\boldsymbol{R}_1^L \cdot \boldsymbol{R}_3^L) R_2^L + (\boldsymbol{R}_2^L \cdot \boldsymbol{R}_3^L) R_1^L}, \tag{D.245}$$

where $-2\pi \leq \Theta_L \leq 2\pi$ and where the triple scalar product

$$\big[\boldsymbol{R}_1^L \boldsymbol{R}_2^L \boldsymbol{R}_3^L\big] = \boldsymbol{R}_1^L \cdot (\boldsymbol{R}_2^L \times \boldsymbol{R}_3^L) = \boldsymbol{R}_2^L \cdot (\boldsymbol{R}_3^L \times \boldsymbol{R}_1^L) = \boldsymbol{R}_3^L \cdot (\boldsymbol{R}_1^L \times \boldsymbol{R}_2^L) \tag{D.246}$$

represents the signed volume of the parallelepiped spanned by the vectors $\boldsymbol{R}_1^L$, $\boldsymbol{R}_2^L$, and $\boldsymbol{R}_3^L$.

D.12.2 Boundary element integrals

The boundary element integrals are the basic integrals needed to perform the boundary element calculations. In our case, by considering $a, b \in \{0, 1\}$ and $c, d \in \{1, 2, 3\}$, they can be expressed as

$$ZA_{a,b}^{c,d} = \int_K \int_L \left(\frac{s_c}{h_c^K}\right)^a \left(\frac{t_d}{h_d^L}\right)^b G(\boldsymbol{x}, \boldsymbol{y}) \, \mathrm{d}L(\boldsymbol{y}) \, \mathrm{d}K(\boldsymbol{x}), \tag{D.247}$$

$$ZB_{a,b}^{c,d} = \int_K \int_L \left(\frac{s_c}{h_c^K}\right)^a \left(\frac{t_d}{h_d^L}\right)^b \frac{\partial G}{\partial n_{\boldsymbol{y}}}(\boldsymbol{x}, \boldsymbol{y}) \, \mathrm{d}L(\boldsymbol{y}) \, \mathrm{d}K(\boldsymbol{x}), \tag{D.248}$$

$$ZC_{a,b}^{c,d} = \int_K \int_L \left(\frac{s_c}{h_c^K}\right)^a \left(\frac{t_d}{h_d^L}\right)^b \frac{\partial G}{\partial n_{\boldsymbol{x}}}(\boldsymbol{x}, \boldsymbol{y}) \, \mathrm{d}L(\boldsymbol{y}) \, \mathrm{d}K(\boldsymbol{x}), \tag{D.249}$$

where the parameters s_c and t_d depend respectively on the variables $\boldsymbol{x}$ and $\boldsymbol{y}$, as stated in (D.224) and (D.226). When the triangles have to be specified, i.e., if $K = T_i$ and $L = T_j$, then we state it respectively as $ZA_{a,b}^{c,d}(T_i, T_j)$, $ZB_{a,b}^{c,d}(T_i, T_j)$, or $ZC_{a,b}^{c,d}(T_i, T_j)$, e.g.,

$$ZA_{a,b}^{c,d}(T_i, T_j) = \int_{T_i} \int_{T_j} \left(\frac{s_c}{h_c^K}\right)^a \left(\frac{t_d}{h_d^L}\right)^b G(\boldsymbol{x}, \boldsymbol{y}) \, \mathrm{d}\gamma(\boldsymbol{y}) \, \mathrm{d}\gamma(\boldsymbol{x}). \tag{D.250}$$

It should be observed that (D.249) can be expressed in terms of (D.248):

$$ZC_{a,b}^{c,d}(T_i, T_j) = ZB_{b,a}^{d,c}(T_j, T_i), \tag{D.251}$$

since the involved operators are self-adjoint. It occurs therefore that all the integrals that stem from the numerical discretization can be expressed in terms of the two basic boundary element integrals (D.247) and (D.248).

For this to hold true, the impedance is discretized as a piecewise constant function Z_h, which on each triangle T_j adopts a constant value $Z_j \in \mathbb{C}$, e.g.,

$$Z_h|_{T_j} = Z_j = \frac{1}{3}\Big(Z\big(\boldsymbol{r}_1^{T_j}\big) + Z\big(\boldsymbol{r}_2^{T_j}\big) + Z\big(\boldsymbol{r}_3^{T_j}\big)\Big). \tag{D.252}$$

Now we can compute all the integrals of interest. We begin with the ones that are related with the finite elements of type $\mathbb{P}_0$, which are easier. It can be observed that

$$\langle \kappa_j, \kappa_i \rangle = \int_{\Gamma^h} \kappa_j(\boldsymbol{x}) \kappa_i(\boldsymbol{x}) \, \mathrm{d}\gamma(\boldsymbol{x}) = \begin{cases} |T_i| & \text{if } j = i, \\ 0 & \text{if } j \neq i. \end{cases} \tag{D.253}$$

We have likewise that

$$\begin{aligned} \langle Z_h S_h(\kappa_j), \kappa_i \rangle &= \int_{\Gamma^h} \int_{\Gamma^h} Z_h(\boldsymbol{x}) G(\boldsymbol{x}, \boldsymbol{y}) \kappa_j(\boldsymbol{y}) \kappa_i(\boldsymbol{x}) \, \mathrm{d}\gamma(\boldsymbol{y}) \, \mathrm{d}\gamma(\boldsymbol{x}) \\ &= Z_i ZA_{0,0}^{c,d}(T_i, T_j), \end{aligned} \tag{D.254}$$

which is independent of $c, d \in \{1, 2, 3\}$. It holds similarly that

$$\langle D_h^*(\kappa_j), \kappa_i \rangle = \int_{\Gamma^h} \int_{\Gamma^h} \frac{\partial G}{\partial n_{\boldsymbol{x}}}(\boldsymbol{x}, \boldsymbol{y}) \kappa_j(\boldsymbol{y}) \kappa_i(\boldsymbol{x}) \, \mathrm{d}\gamma(\boldsymbol{y}) \, \mathrm{d}\gamma(\boldsymbol{x}) = ZB_{0,0}^{d,c}(T_j, T_i), \tag{D.255}$$

which is again independent of $c, d \in \{1, 2, 3\}$. We consider now the integrals for the finite elements of type $\mathbb{P}_1$. By taking as zero the sum over an empty set, we have that

$$\langle \chi_j, \chi_i \rangle = \int_{\Gamma^h} \chi_j(\boldsymbol{x}) \chi_i(\boldsymbol{x}) \, \mathrm{d}\gamma(\boldsymbol{x}) = \begin{cases} \displaystyle\sum_{K \ni \boldsymbol{r}_i} \frac{|K|}{6} & \text{if } \ j = i, \\ \displaystyle\sum_{K \ni \boldsymbol{r}_i, \boldsymbol{r}_j} \frac{|K|}{12} & \text{if } \ i \neq j. \end{cases} \tag{D.256}$$

In the same way, it occurs that

$$\langle Z_h \chi_j, \chi_i \rangle = \begin{cases} \displaystyle\sum_{K \ni \boldsymbol{r}_i} \frac{Z_K |K|}{6} & \text{if } \ j = i, \\ \displaystyle\sum_{K \ni \boldsymbol{r}_i, \boldsymbol{r}_j} \frac{Z_K |K|}{12} & \text{if } \ i \neq j. \end{cases} \tag{D.257}$$

We have also that

$$\begin{aligned} \langle S_h(\chi_j), \chi_i \rangle &= \int_{\Gamma^h} \int_{\Gamma^h} G(\boldsymbol{x}, \boldsymbol{y}) \chi_j(\boldsymbol{y}) \chi_i(\boldsymbol{x}) \, \mathrm{d}\gamma(\boldsymbol{y}) \, \mathrm{d}\gamma(\boldsymbol{x}) \\ &= \sum_{K \ni \boldsymbol{r}_i} \sum_{L \ni \boldsymbol{r}_j} \left(ZA_{0,0}^{c_i^K, d_j^L} - ZA_{0,1}^{c_i^K, d_j^L} - ZA_{1,0}^{c_i^K, d_j^L} + ZA_{1,1}^{c_i^K, d_j^L} \right), \end{aligned} \tag{D.258}$$

where the local subindexes c_i^K and d_j^L are always such that

$$\boldsymbol{r}_{c_i^K}^K = \boldsymbol{r}_i \qquad \text{and} \qquad \boldsymbol{r}_{d_j^L}^L = \boldsymbol{r}_j, \tag{D.259}$$

and where we use the more simplified notation

$$ZA_{a,b}^{c_i^K, d_j^L} = ZA_{a,b}^{c_i^K, d_j^L}(K, L). \tag{D.260}$$

Additionally it holds that

$$\begin{aligned} \langle S_h(Z_h \chi_j), \chi_i \rangle &= \int_{\Gamma^h} \int_{\Gamma^h} Z_h(\boldsymbol{y}) G(\boldsymbol{x}, \boldsymbol{y}) \chi_j(\boldsymbol{y}) \chi_i(\boldsymbol{x}) \, \mathrm{d}\gamma(\boldsymbol{y}) \, \mathrm{d}\gamma(\boldsymbol{x}) \\ &= \sum_{K \ni \boldsymbol{r}_i} \sum_{L \ni \boldsymbol{r}_j} Z_L \left(ZA_{0,0}^{c_i^K, d_j^L} - ZA_{0,1}^{c_i^K, d_j^L} - ZA_{1,0}^{c_i^K, d_j^L} + ZA_{1,1}^{c_i^K, d_j^L} \right). \end{aligned} \tag{D.261}$$

Furthermore we see that

$$\begin{aligned} \langle Z_h S_h(Z_h \chi_j), \chi_i \rangle &= \int_{\Gamma^h} \int_{\Gamma^h} Z_h(\boldsymbol{x}) Z_h(\boldsymbol{y}) G(\boldsymbol{x}, \boldsymbol{y}) \chi_j(\boldsymbol{y}) \chi_i(\boldsymbol{x}) \, \mathrm{d}\gamma(\boldsymbol{y}) \, \mathrm{d}\gamma(\boldsymbol{x}) \\ &= \sum_{K \ni \boldsymbol{r}_i} \sum_{L \ni \boldsymbol{r}_j} Z_K Z_L \left(ZA_{0,0}^{c_i^K, d_j^L} - ZA_{0,1}^{c_i^K, d_j^L} - ZA_{1,0}^{c_i^K, d_j^L} + ZA_{1,1}^{c_i^K, d_j^L} \right). \end{aligned} \tag{D.262}$$

Likewise it occurs that

$$\begin{aligned} \langle D_h(\chi_j), \chi_i \rangle &= \int_{\Gamma^h} \int_{\Gamma^h} \frac{\partial G}{\partial n_{\boldsymbol{y}}}(\boldsymbol{x}, \boldsymbol{y}) \chi_j(\boldsymbol{y}) \chi_i(\boldsymbol{x}) \, \mathrm{d}\gamma(\boldsymbol{y}) \, \mathrm{d}\gamma(\boldsymbol{x}) \\ &= \sum_{K \ni \boldsymbol{r}_i} \sum_{L \ni \boldsymbol{r}_j} \left(ZB_{0,0}^{c_i^K, d_j^L} - ZB_{0,1}^{c_i^K, d_j^L} - ZB_{1,0}^{c_i^K, d_j^L} + ZB_{1,1}^{c_i^K, d_j^L} \right). \end{aligned} \tag{D.263}$$

It holds moreover that

$$\langle Z_h D_h(\chi_j), \chi_i \rangle = \int_{\Gamma^h} \int_{\Gamma^h} Z_h(\boldsymbol{x}) \frac{\partial G}{\partial n_{\boldsymbol{y}}}(\boldsymbol{x}, \boldsymbol{y}) \chi_j(\boldsymbol{y}) \chi_i(\boldsymbol{x}) \, \mathrm{d}\gamma(\boldsymbol{y}) \, \mathrm{d}\gamma(\boldsymbol{x})$$
$$= \sum_{K \ni \boldsymbol{r}_i} \sum_{L \ni \boldsymbol{r}_j} Z_K \left(ZB_{0,0}^{c_i^K, d_j^L} - ZB_{0,1}^{c_i^K, d_j^L} - ZB_{1,0}^{c_i^K, d_j^L} + ZB_{1,1}^{c_i^K, d_j^L} \right). \quad \text{(D.264)}$$

We have also that

$$\langle D_h^*(\chi_j), \chi_i \rangle = \int_{\Gamma^h} \int_{\Gamma^h} \frac{\partial G}{\partial n_{\boldsymbol{x}}}(\boldsymbol{x}, \boldsymbol{y}) \chi_j(\boldsymbol{y}) \chi_i(\boldsymbol{x}) \, \mathrm{d}\gamma(\boldsymbol{y}) \, \mathrm{d}\gamma(\boldsymbol{x})$$
$$= \sum_{K \ni \boldsymbol{r}_i} \sum_{L \ni \boldsymbol{r}_j} \left(ZB_{0,0}^{d_j^L, c_i^K} - ZB_{1,0}^{d_j^L, c_i^K} - ZB_{0,1}^{d_j^L, c_i^K} + ZB_{1,1}^{d_j^L, c_i^K} \right), \quad \text{(D.265)}$$

where the change in index order is understood as

$$ZB_{b,a}^{d_j^L, c_i^K} = ZB_{b,a}^{d_j^L, c_i^K}(L, K). \quad \text{(D.266)}$$

Similarly it occurs that

$$\langle D_h^*(Z_h \chi_j), \chi_i \rangle = \int_{\Gamma^h} \int_{\Gamma^h} Z_h(\boldsymbol{y}) \frac{\partial G}{\partial n_{\boldsymbol{x}}}(\boldsymbol{x}, \boldsymbol{y}) \chi_j(\boldsymbol{y}) \chi_i(\boldsymbol{x}) \, \mathrm{d}\gamma(\boldsymbol{y}) \, \mathrm{d}\gamma(\boldsymbol{x})$$
$$= \sum_{K \ni \boldsymbol{r}_i} \sum_{L \ni \boldsymbol{r}_j} Z_L \left(ZB_{0,0}^{d_j^L, c_i^K} - ZB_{1,0}^{d_j^L, c_i^K} - ZB_{0,1}^{d_j^L, c_i^K} + ZB_{1,1}^{d_j^L, c_i^K} \right). \quad \text{(D.267)}$$

And finally, for the hypersingular term we have that

$$\langle N_h(\chi_j), \chi_i \rangle = - \int_{\Gamma^h} \int_{\Gamma^h} G(\boldsymbol{x}, \boldsymbol{y}) \big(\nabla \chi_j(\boldsymbol{y}) \times \boldsymbol{n}_{\boldsymbol{y}} \big) \cdot \big(\nabla \chi_i(\boldsymbol{x}) \times \boldsymbol{n}_{\boldsymbol{x}} \big) \, \mathrm{d}\gamma(\boldsymbol{y}) \, \mathrm{d}\gamma(\boldsymbol{x})$$
$$= - \sum_{K \ni \boldsymbol{r}_i} \sum_{L \ni \boldsymbol{r}_j} \frac{ZA_{0,0}^{c_i^K, d_j^L}}{h_{c_i^K}^K h_{d_j^L}^L} \big(\boldsymbol{\nu}_{c_i^K}^K \times \boldsymbol{n}_K \big) \cdot \big(\boldsymbol{\nu}_{d_j^L}^L \times \boldsymbol{n}_L \big). \quad \text{(D.268)}$$

It remains now to compute the integrals (D.247) and (D.248), which are calculated in two steps with a semi-numerical integration, i.e., the singular parts are calculated analytically and the other parts numerically. First the internal integral for $\boldsymbol{y}$ is computed, then the external one for $\boldsymbol{x}$. This can be expressed as

$$ZA_{a,b}^{c,d} = \int_K \left(\frac{s_c}{h_c^K} \right)^a ZF_b^d(\boldsymbol{x}) \, \mathrm{d}K(\boldsymbol{x}), \quad \text{(D.269)}$$

$$ZF_b^d(\boldsymbol{x}) = \int_L \left(\frac{t_d}{h_d^L} \right)^b G(\boldsymbol{x}, \boldsymbol{y}) \, \mathrm{d}L(\boldsymbol{y}), \quad \text{(D.270)}$$

and

$$ZB_{a,b}^{c,d} = \int_K \left(\frac{s_c}{h_c^K} \right)^a ZG_b^d(\boldsymbol{x}) \, \mathrm{d}K(\boldsymbol{x}), \quad \text{(D.271)}$$

$$ZG_b^d(\boldsymbol{x}) = \int_L \left(\frac{t_d}{h_d^L} \right)^b \frac{\partial G}{\partial n_{\boldsymbol{y}}}(\boldsymbol{x}, \boldsymbol{y}) \, \mathrm{d}L(\boldsymbol{y}). \quad \text{(D.272)}$$

This kind of integrals can be also used to compute the terms associated with the discretized solution u_h. Using an analogous notation as in (D.250), we have that

$$\mathcal{S}_h(\kappa_j) = \int_{\Gamma^h} G(\boldsymbol{x},\boldsymbol{y})\kappa_j(\boldsymbol{y})\,\mathrm{d}\gamma(\boldsymbol{y}) = ZF_0^d(T_j)(\boldsymbol{x}), \tag{D.273}$$

which is independent of $d \in \{1,2,3\}$. Similarly it holds that

$$\mathcal{S}_h(\chi_j) = \int_{\Gamma^h} G(\boldsymbol{x},\boldsymbol{y})\chi_j(\boldsymbol{y})\,\mathrm{d}\gamma(\boldsymbol{y}) = \sum_{L\ni\boldsymbol{r}_j}\left(ZF_0^{d_j^L}(L)(\boldsymbol{x}) - ZF_1^{d_j^L}(L)(\boldsymbol{x})\right), \tag{D.274}$$

and

$$\mathcal{S}_h(Z_h\chi_j) = \int_{\Gamma^h} Z_h(\boldsymbol{y})G(\boldsymbol{x},\boldsymbol{y})\chi_j(\boldsymbol{y})\,\mathrm{d}\gamma(\boldsymbol{y}) = \sum_{L\ni\boldsymbol{r}_j} Z_L\left(ZF_0^{d_j^L}(L)(\boldsymbol{x}) - ZF_1^{d_j^L}(L)(\boldsymbol{x})\right). \tag{D.275}$$

The remaining term is computed as

$$\mathcal{D}_h(\chi_j) = \int_{\Gamma^h} \frac{\partial G}{\partial n_{\boldsymbol{y}}}(\boldsymbol{x},\boldsymbol{y})\chi_j(\boldsymbol{y})\,\mathrm{d}\gamma(\boldsymbol{y}) = \sum_{L\ni\boldsymbol{r}_j}\left(ZG_0^{d_j^L}(L)(\boldsymbol{x}) - ZG_1^{d_j^L}(L)(\boldsymbol{x})\right). \tag{D.276}$$

D.12.3 Numerical integration for the non-singular integrals

For the numerical integration of the non-singular integrals of the boundary element calculations we use three-point and six-point Gauss-Lobatto quadrature formulae (cf., e.g. Cowper 1973, Dunavant 1985). We describe the triangles K and L by means of barycentric coordinates as done in (D.235) and (D.236).

a) Three-point Gauss-Lobatto quadrature formulae

As shown in Figure D.12, for the three-point Gauss-Lobatto quadrature we consider, respectively on the triangles K and L, the points

$$\boldsymbol{x}_1 = \frac{2}{3}\boldsymbol{r}_1^K + \frac{1}{6}\boldsymbol{r}_2^K + \frac{1}{6}\boldsymbol{r}_3^K, \qquad \boldsymbol{y}_1 = \frac{2}{3}\boldsymbol{r}_1^L + \frac{1}{6}\boldsymbol{r}_2^L + \frac{1}{6}\boldsymbol{r}_3^L, \tag{D.277}$$

$$\boldsymbol{x}_2 = \frac{1}{6}\boldsymbol{r}_1^K + \frac{2}{3}\boldsymbol{r}_2^K + \frac{1}{6}\boldsymbol{r}_3^K, \qquad \boldsymbol{y}_2 = \frac{1}{6}\boldsymbol{r}_1^L + \frac{2}{3}\boldsymbol{r}_2^L + \frac{1}{6}\boldsymbol{r}_3^L, \tag{D.278}$$

$$\boldsymbol{x}_3 = \frac{1}{6}\boldsymbol{r}_1^K + \frac{1}{6}\boldsymbol{r}_2^K + \frac{2}{3}\boldsymbol{r}_3^K, \qquad \boldsymbol{y}_3 = \frac{1}{6}\boldsymbol{r}_1^L + \frac{1}{6}\boldsymbol{r}_2^L + \frac{2}{3}\boldsymbol{r}_3^L. \tag{D.279}$$

When considering a function $\varphi : L \to \mathbb{C}$, the quadrature formula is given by

$$\int_L \left(\frac{t_d}{h_d^L}\right)^b \varphi(\boldsymbol{y})\,\mathrm{d}L(\boldsymbol{y}) \approx \frac{|L|}{3}\sum_{q=1}^{3}\left\{\frac{\left(\boldsymbol{y}_q - \boldsymbol{r}_d^L\right)\cdot\boldsymbol{\nu}_d^L}{h_d^L}\right\}^b \varphi(\boldsymbol{y}_q). \tag{D.280}$$

An equivalent formula is used when considering a function $\phi : K \to \mathbb{C}$, given by

$$\int_K \left(\frac{s_c}{h_c^K}\right)^a \phi(\boldsymbol{x})\,\mathrm{d}K(\boldsymbol{x}) \approx \frac{|K|}{3}\sum_{p=1}^{3}\left\{\frac{\left(\boldsymbol{x}_p - \boldsymbol{r}_c^K\right)\cdot\boldsymbol{\nu}_c^K}{h_c^K}\right\}^a \phi(\boldsymbol{x}_p). \tag{D.281}$$

The Gauss-Lobatto quadrature formula can be extended straightforwardly to a function of two variables, $\Phi : K \times L \to \mathbb{C}$, using both formulas shown above. Therefore

$$\int_K \int_L \left(\frac{s_c}{h_c^K}\right)^a \left(\frac{t_d}{h_d^L}\right)^b \Phi(\boldsymbol{x},\boldsymbol{y})\,\mathrm{d}L(\boldsymbol{y})\mathrm{d}K(\boldsymbol{x}) \approx \frac{|K|\,|L|}{9}\sum_{p=1}^{3}\sum_{q=1}^{3}\left\{\frac{\left(\boldsymbol{x}_p-\boldsymbol{r}_c^K\right)\cdot\boldsymbol{\nu}_c^K}{h_c^K}\right\}^a\left\{\frac{\left(\boldsymbol{y}_q-\boldsymbol{r}_d^L\right)\cdot\boldsymbol{\nu}_d^L}{h_d^L}\right\}^b\Phi(\boldsymbol{x}_p,\boldsymbol{y}_q). \quad \text{(D.282)}$$

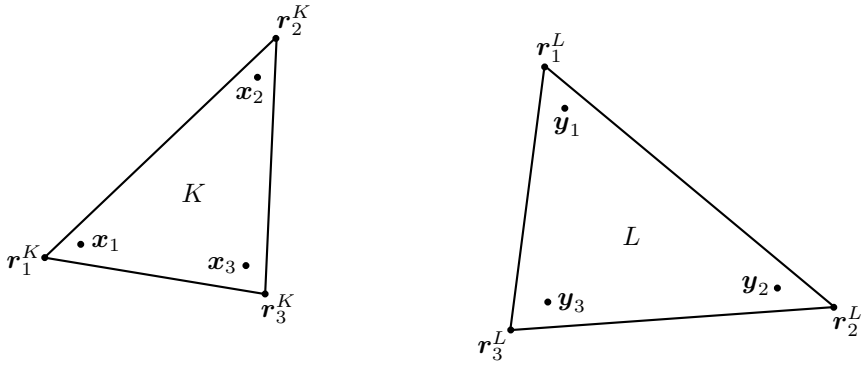

FIGURE D.12. Evaluation points for the three-point Gauss-Lobatto quadrature formulae.

b) Six-point Gauss-Lobatto quadrature formulae

For the six-point Gauss-Lobatto quadrature we consider respectively on the triangles K and L, as depicted in Figure D.13, the points

$$\boldsymbol{x}_1 = \alpha_1\boldsymbol{r}_1^K + \alpha_2\boldsymbol{r}_2^K + \alpha_2\boldsymbol{r}_3^K, \qquad \boldsymbol{y}_1 = \alpha_1\boldsymbol{r}_1^L + \alpha_2\boldsymbol{r}_2^L + \alpha_2\boldsymbol{r}_3^L, \quad \text{(D.283)}$$

$$\boldsymbol{x}_2 = \alpha_2\boldsymbol{r}_1^K + \alpha_1\boldsymbol{r}_2^K + \alpha_2\boldsymbol{r}_3^K, \qquad \boldsymbol{y}_2 = \alpha_2\boldsymbol{r}_1^L + \alpha_1\boldsymbol{r}_2^L + \alpha_2\boldsymbol{r}_3^L, \quad \text{(D.284)}$$

$$\boldsymbol{x}_3 = \alpha_2\boldsymbol{r}_1^K + \alpha_2\boldsymbol{r}_2^K + \alpha_1\boldsymbol{r}_3^K, \qquad \boldsymbol{y}_3 = \alpha_2\boldsymbol{r}_1^L + \alpha_2\boldsymbol{r}_2^L + \alpha_1\boldsymbol{r}_3^L, \quad \text{(D.285)}$$

$$\tilde{\boldsymbol{x}}_1 = \beta_1\boldsymbol{r}_1^K + \beta_2\boldsymbol{r}_2^K + \beta_2\boldsymbol{r}_3^K, \qquad \tilde{\boldsymbol{y}}_1 = \beta_1\boldsymbol{r}_1^L + \beta_2\boldsymbol{r}_2^L + \beta_2\boldsymbol{r}_3^L, \quad \text{(D.286)}$$

$$\tilde{\boldsymbol{x}}_2 = \beta_2\boldsymbol{r}_1^K + \beta_1\boldsymbol{r}_2^K + \beta_2\boldsymbol{r}_3^K, \qquad \tilde{\boldsymbol{y}}_2 = \beta_2\boldsymbol{r}_1^L + \beta_1\boldsymbol{r}_2^L + \beta_2\boldsymbol{r}_3^L, \quad \text{(D.287)}$$

$$\tilde{\boldsymbol{x}}_3 = \beta_2\boldsymbol{r}_1^K + \beta_2\boldsymbol{r}_2^K + \beta_1\boldsymbol{r}_3^K, \qquad \tilde{\boldsymbol{y}}_3 = \beta_2\boldsymbol{r}_1^L + \beta_2\boldsymbol{r}_2^L + \beta_1\boldsymbol{r}_3^L, \quad \text{(D.288)}$$

where

$$\alpha_1 = 0.816847572980459, \qquad \alpha_2 = 0.091576213509771, \quad \text{(D.289)}$$

$$\beta_1 = 0.108103018168070, \qquad \beta_2 = 0.445948490915965. \quad \text{(D.290)}$$

The weights are given by

$$\alpha_w = 0.109951743655322, \qquad \beta_w = 0.223381589678011. \quad \text{(D.291)}$$

When considering a function $\varphi : L \to \mathbb{C}$, the quadrature formula is given by

$$\int_L \left(\frac{t_d}{h_d^L}\right)^b \varphi(\boldsymbol{y})\,\mathrm{d}L(\boldsymbol{y}) \approx \alpha_w |L| \sum_{q=1}^{3} \left\{\frac{\left(\boldsymbol{y}_q - \boldsymbol{r}_d^L\right)\cdot \boldsymbol{\nu}_d^L}{h_d^L}\right\}^b \varphi(\boldsymbol{y}_q) + \beta_w |L| \sum_{q=1}^{3} \left\{\frac{\left(\tilde{\boldsymbol{y}}_q - \boldsymbol{r}_d^L\right)\cdot \boldsymbol{\nu}_d^L}{h_d^L}\right\}^b \varphi(\tilde{\boldsymbol{y}}_q). \tag{D.292}$$

An equivalent formula is used when considering a function $\phi : K \to \mathbb{C}$, given by

$$\int_K \left(\frac{s_c}{h_c^K}\right)^a \phi(\boldsymbol{x})\,\mathrm{d}K(\boldsymbol{x}) \approx \alpha_w |K| \sum_{p=1}^{3} \left\{\frac{\left(\boldsymbol{x}_p - \boldsymbol{r}_c^K\right)\cdot \boldsymbol{\nu}_c^K}{h_c^K}\right\}^a \phi(\boldsymbol{x}_p) + \beta_w |K| \sum_{p=1}^{3} \left\{\frac{\left(\tilde{\boldsymbol{x}}_p - \boldsymbol{r}_c^K\right)\cdot \boldsymbol{\nu}_c^K}{h_c^K}\right\}^a \phi(\tilde{\boldsymbol{x}}_p). \tag{D.293}$$

The Gauss-Lobatto quadrature formula can be extended straightforwardly to a function of two variables, $\Phi : K \times L \to \mathbb{C}$, using both formulas shown above. Therefore

$$\begin{aligned}
&\int_K \int_L \left(\frac{s_c}{h_c^K}\right)^a \left(\frac{t_d}{h_d^L}\right)^b \Phi(\boldsymbol{x},\boldsymbol{y})\,\mathrm{d}L(\boldsymbol{y})\mathrm{d}K(\boldsymbol{x}) \\
&\quad\approx \alpha_w^2 |K|\,|L| \sum_{p=1}^{3}\sum_{q=1}^{3} \left\{\frac{\left(\boldsymbol{x}_p - \boldsymbol{r}_c^K\right)\cdot \boldsymbol{\nu}_c^K}{h_c^K}\right\}^a \left\{\frac{\left(\boldsymbol{y}_q - \boldsymbol{r}_d^L\right)\cdot \boldsymbol{\nu}_d^L}{h_d^L}\right\}^b \Phi(\boldsymbol{x}_p,\boldsymbol{y}_q) \\
&\quad+ \beta_w^2 |K|\,|L| \sum_{p=1}^{3}\sum_{q=1}^{3} \left\{\frac{\left(\tilde{\boldsymbol{x}}_p - \boldsymbol{r}_c^K\right)\cdot \boldsymbol{\nu}_c^K}{h_c^K}\right\}^a \left\{\frac{\left(\tilde{\boldsymbol{y}}_q - \boldsymbol{r}_d^L\right)\cdot \boldsymbol{\nu}_d^L}{h_d^L}\right\}^b \Phi(\tilde{\boldsymbol{x}}_p,\tilde{\boldsymbol{y}}_q) \\
&\quad+ \alpha_w\beta_w |K|\,|L| \sum_{p=1}^{3}\sum_{q=1}^{3} \left\{\frac{\left(\tilde{\boldsymbol{x}}_p - \boldsymbol{r}_c^K\right)\cdot \boldsymbol{\nu}_c^K}{h_c^K}\right\}^a \left\{\frac{\left(\boldsymbol{y}_q - \boldsymbol{r}_d^L\right)\cdot \boldsymbol{\nu}_d^L}{h_d^L}\right\}^b \Phi(\tilde{\boldsymbol{x}}_p,\boldsymbol{y}_q) \\
&\quad+ \alpha_w\beta_w |K|\,|L| \sum_{p=1}^{3}\sum_{q=1}^{3} \left\{\frac{\left(\boldsymbol{x}_p - \boldsymbol{r}_c^K\right)\cdot \boldsymbol{\nu}_c^K}{h_c^K}\right\}^a \left\{\frac{\left(\tilde{\boldsymbol{y}}_q - \boldsymbol{r}_d^L\right)\cdot \boldsymbol{\nu}_d^L}{h_d^L}\right\}^b \Phi(\boldsymbol{x}_p,\tilde{\boldsymbol{y}}_q).
\end{aligned} \tag{D.294}$$

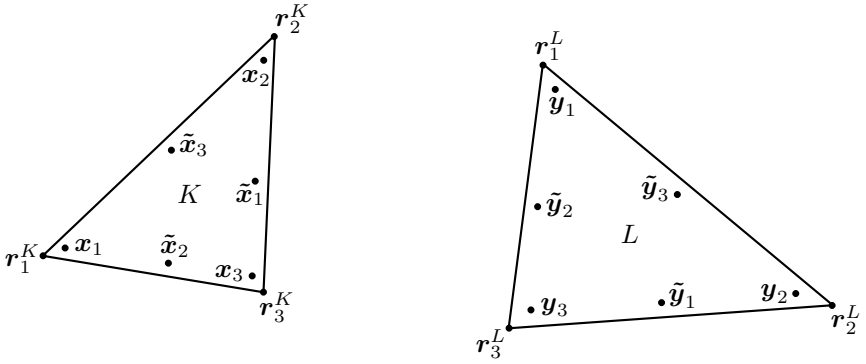

FIGURE D.13. Evaluation points for the six-point Gauss-Lobatto quadrature formulae.

c) Overall numerical integration

For the overall numerical integration we consider two different cases to achieve enough accuracy in the computations and to minimize the calculation time.

If the triangles K and L are not adjacent nor equal, then the integrals on K, (D.269) and (D.271), and the integrals on L, (D.270) and (D.272), are computed respectively using three-point Gauss-Lobatto quadrature formulae, i.e., (D.281) and (D.280), since in this case they are non-singular. Thus, in the whole, the integrals $ZA_{a,b}^{c,d}$ and $ZB_{a,b}^{c,d}$ are calculated employing (D.282).

On the other hand, if the triangles K and L have at least a common vertex, then the integrals on K are evaluated using the six-point Gauss-Lobatto quadrature formula (D.293), while the integrals on L, which become singular, are evaluated using the analytical formulae described next.

D.12.4 Analytical integration for the singular integrals

If the triangles K and L are close together, then the integrals (D.270) and (D.272) are calculated analytically, treating $\boldsymbol{x}$ as a given parameter. They are specifically given by

$$ZF_0^d(\boldsymbol{x}) = -\int_L \frac{1}{4\pi R}\,\mathrm{d}L(\boldsymbol{y}), \tag{D.295}$$

$$ZF_1^d(\boldsymbol{x}) = -\int_L \frac{t_d}{4\pi R\, h_d^L}\,\mathrm{d}L(\boldsymbol{y}), \tag{D.296}$$

and

$$ZG_0^d(\boldsymbol{x}) = \int_L \frac{\boldsymbol{R}\cdot\boldsymbol{n}_L}{4\pi R^3}\,\mathrm{d}L(\boldsymbol{y}), \tag{D.297}$$

$$ZG_1^d(\boldsymbol{x}) = \int_L t_d\,\frac{\boldsymbol{R}\cdot\boldsymbol{n}_L}{4\pi R^3\, h_d^L}\,\mathrm{d}L(\boldsymbol{y}). \tag{D.298}$$

a) Computation of $ZG_0^d(\boldsymbol{x})$

The integral (D.297) is closely related with Gauss's divergence theorem. If we consider an oriented surface differential element $\mathrm{d}\boldsymbol{\gamma} = \boldsymbol{n}_L \mathrm{d}L(\boldsymbol{y})$ seen from point $\boldsymbol{x}$, then we can express the solid angle differential element by (cf. Terrasse & Abboud 2006)

$$\mathrm{d}\Theta = \frac{\boldsymbol{R}}{R^3}\cdot\mathrm{d}\boldsymbol{\gamma} = \frac{\boldsymbol{R}\cdot\boldsymbol{n}_L}{R^3}\,\mathrm{d}L(\boldsymbol{y}) = 4\pi\frac{\partial G}{\partial n_{\boldsymbol{y}}}(\boldsymbol{x},\boldsymbol{y})\,\mathrm{d}L(\boldsymbol{y}). \tag{D.299}$$

Integrating over triangle L yields the solid angle Θ_L, as expressed in (D.245), namely

$$\Theta_L = \int_L \mathrm{d}\Theta \qquad (-2\pi \le \Theta_L \le 2\pi). \tag{D.300}$$

The solid angle Θ_L is positive when the vectors $\boldsymbol{R}$ and $\boldsymbol{n}_L$ point towards the same side of L. Thus integral (D.297) is obtained by integrating (D.299), which yields

$$ZG_0^d(\boldsymbol{x}) = \int_L \frac{\boldsymbol{R}\cdot\boldsymbol{n}_L}{4\pi R^3}\,\mathrm{d}L(\boldsymbol{y}) = \frac{\Theta_L}{4\pi}. \tag{D.301}$$

b) Computation of $ZF_0^d(\boldsymbol{x})$

For the integral (D.295) we consider before some vectorial identities and properties. We have that

$$\Delta R = \frac{1}{R^2}\frac{\partial}{\partial R}\left(R^2\frac{\partial R}{\partial R}\right) = \frac{2}{R}. \tag{D.302}$$

On the other hand, by using the relation (A.590) with the vector $R\,\boldsymbol{n}_L$ and performing afterwards a dot product with $\boldsymbol{n}_L$ yields

$$\Delta R = \frac{\partial^2 R}{\partial n^2} - \operatorname{curl}\operatorname{curl}(R\,\boldsymbol{n}_L)\cdot\boldsymbol{n}_L. \tag{D.303}$$

Since

$$\nabla R = \frac{\boldsymbol{R}}{R} \qquad \text{and} \qquad \nabla\nabla R = \frac{\mathbf{1}\otimes\mathbf{1}}{R} - \frac{\boldsymbol{R}\otimes\boldsymbol{R}}{R^3}, \tag{D.304}$$

therefore we obtain that

$$\frac{\partial R}{\partial n} = \frac{\boldsymbol{R}\cdot\boldsymbol{n}_L}{R} \qquad \text{and} \qquad \frac{\partial^2 R}{\partial n^2} = \frac{1}{R} - \frac{(\boldsymbol{R}\cdot\boldsymbol{n}_L)^2}{R^3}. \tag{D.305}$$

Hence, considering (D.302), (D.303), and (D.305), yields

$$\frac{1}{R} = -\frac{(\boldsymbol{R}\cdot\boldsymbol{n}_L)^2}{R^3} - \operatorname{curl}\operatorname{curl}(R\,\boldsymbol{n}_L)\cdot\boldsymbol{n}_L. \tag{D.306}$$

This way the integral (D.295) can be rewritten as

$$ZF_0^d(\boldsymbol{x}) = \int_L \frac{(\boldsymbol{R}\cdot\boldsymbol{n}_L)^2}{4\pi R^3}\,\mathrm{d}L(\boldsymbol{y}) + \frac{1}{4\pi}\int_L \operatorname{curl}\operatorname{curl}(R\,\boldsymbol{n}_L)\cdot\boldsymbol{n}_L\,\mathrm{d}L(\boldsymbol{y}). \tag{D.307}$$

Considering (D.244) and (D.301) for the first integral, and applying to the second one the curl theorem (A.617), yields

$$ZF_0^d(\boldsymbol{x}) = \frac{d_L\Theta_L}{4\pi} + \frac{1}{4\pi}\sum_{m=1}^{3}\int_{C_m^L} \operatorname{curl}(R\,\boldsymbol{n}_L)\cdot\boldsymbol{\tau}_m^L\,\mathrm{d}C(\boldsymbol{y}). \tag{D.308}$$

We have additionally, from (A.566), (A.589), and (D.234), that

$$\operatorname{curl}(R\,\boldsymbol{n}_L)\cdot\boldsymbol{\tau}_m^L = (\nabla R\times\boldsymbol{n}_L)\cdot\boldsymbol{\tau}_m^L = -\frac{\boldsymbol{R}}{R}\cdot(\boldsymbol{\tau}_m^L\times\boldsymbol{n}_L) = -\frac{\boldsymbol{R}\cdot\boldsymbol{\nu}_m^L}{R}. \tag{D.309}$$

Since $\boldsymbol{R}\cdot\boldsymbol{\nu}_m^L$ is constant on C_m^L, we can compute it as

$$\boldsymbol{R}\cdot\boldsymbol{\nu}_m^L = (\boldsymbol{R}_m^L + h_m^L\boldsymbol{\nu}_m^L)\cdot\boldsymbol{\nu}_m^L. \tag{D.310}$$

Hence (D.308) turns into

$$ZF_0^d(\boldsymbol{x}) = \frac{d_L\Theta_L}{4\pi} - \frac{1}{4\pi}\sum_{m=1}^{3}(\boldsymbol{R}_m^L + h_m^L\boldsymbol{\nu}_m^L)\cdot\boldsymbol{\nu}_m^L\int_{C_m^L}\frac{1}{R}\,\mathrm{d}C(\boldsymbol{y}), \tag{D.311}$$

where only the computation of the integral on C_m^L remains to be done.

c) Computation of $ZF_1^d(\boldsymbol{x})$

The integral (D.296) is somewhat simpler to treat. By replacing (D.241) inside this integral we obtain

$$\begin{aligned} ZF_1^d(\boldsymbol{x}) &= -\frac{1}{4\pi h_d^L}\int_L \frac{1}{R}\left(\boldsymbol{R}-\boldsymbol{R}_d^L\right)\cdot\boldsymbol{\nu}_d^L\,\mathrm{d}L(\boldsymbol{y}) \\ &= -\frac{1}{4\pi h_d^L}\int_L \frac{\boldsymbol{R}}{R}\cdot\boldsymbol{\nu}_d^L\,\mathrm{d}L(\boldsymbol{y}) - \frac{\boldsymbol{R}_d^L\cdot\boldsymbol{\nu}_d^L}{h_d^L}\,ZF_0^d(\boldsymbol{x}). \end{aligned} \tag{D.312}$$

It holds now that

$$\frac{\boldsymbol{R}}{R} = \nabla R = \frac{\partial R}{\partial n}\boldsymbol{n}_L + \nabla_L R, \tag{D.313}$$

where ∇_L denotes the surface gradient with respect to the parametrization of the plane of the triangle L. From (D.312) we obtain therefore

$$ZF_1^d(\boldsymbol{x}) = -\frac{\boldsymbol{\nu}_d^L}{4\pi h_d^L}\cdot\left(\int_L \frac{\partial R}{\partial n}\boldsymbol{n}_L\,\mathrm{d}L(\boldsymbol{y}) + \int_L \nabla_L R\,\mathrm{d}L(\boldsymbol{y})\right) - \frac{\boldsymbol{R}_d^L\cdot\boldsymbol{\nu}_d^L}{h_d^L}\,ZF_0^d(\boldsymbol{x}). \tag{D.314}$$

For the first integral in (D.314) we consider (D.244) and (D.305), which yields

$$\int_L \frac{\partial R}{\partial n}\boldsymbol{n}_L\,\mathrm{d}L(\boldsymbol{y}) = d_L\boldsymbol{n}_L\int_L \frac{1}{R}\,\mathrm{d}L(\boldsymbol{y}) = -4\pi d_L\boldsymbol{n}_L ZF_0^d(\boldsymbol{x}). \tag{D.315}$$

For the second integral in (D.314) we apply the Gauss-Green theorem (A.610) on the plane of the triangle L, which implies that

$$\int_L \nabla_L R\,\mathrm{d}L(\boldsymbol{y}) = \sum_{m=1}^{3}\boldsymbol{\nu}_m^L\int_{C_m^L} R\,\mathrm{d}C(\boldsymbol{y}). \tag{D.316}$$

Hence, by considering (D.315) and (D.316) in (D.314), we obtain

$$ZF_1^d(\boldsymbol{x}) = -\frac{\boldsymbol{\nu}_d^L}{4\pi h_d^L}\cdot\sum_{m=1}^{3}\boldsymbol{\nu}_m^L\int_{C_m^L} R\,\mathrm{d}C(\boldsymbol{y}) + \frac{\boldsymbol{\nu}_d^L}{h_d^L}\cdot\left(d_L\boldsymbol{n}_L - \boldsymbol{R}_d^L\right)ZF_0^d(\boldsymbol{x}), \tag{D.317}$$

where only the computation of the integral on C_m^L remains to be done.

d) Computation of $ZG_1^d(\boldsymbol{x})$

By replacing (D.241) and (D.244) inside the integral (D.298), we obtain

$$\begin{aligned} ZG_1^d(\boldsymbol{x}) &= \int_L \frac{\boldsymbol{R}\cdot\boldsymbol{n}_L}{4\pi R^3\,h_d^L}\left(\boldsymbol{R}-\boldsymbol{R}_d^L\right)\cdot\boldsymbol{\nu}_d^L\,\mathrm{d}L(\boldsymbol{y}) \\ &= \frac{d_L\boldsymbol{\nu}_d^L}{4\pi h_d^L}\cdot\int_L \frac{\boldsymbol{R}}{R^3}\,\mathrm{d}L(\boldsymbol{y}) - \frac{\boldsymbol{R}_d^L\cdot\boldsymbol{\nu}_d^L}{h_d^L}\,ZG_0^d(\boldsymbol{x}). \end{aligned} \tag{D.318}$$

Similarly as before, it holds that

$$-\frac{\boldsymbol{R}}{R^3} = \nabla\frac{1}{R} = \frac{\partial}{\partial n}\frac{1}{R}\,\boldsymbol{n}_L + \nabla_L\frac{1}{R}, \tag{D.319}$$

where ∇_L denotes again the surface gradient with respect to the parametrization of the plane of the triangle L. From (D.318) we obtain therefore

$$ZG_1^d(\boldsymbol{x}) = -\frac{d_L \boldsymbol{\nu}_d^L}{4\pi h_d^L} \cdot \left(\int_L \frac{\partial}{\partial n} \frac{1}{R} \, \boldsymbol{n}_L \, \mathrm{d}L(\boldsymbol{y}) + \int_L \nabla_L \frac{1}{R} \, \mathrm{d}L(\boldsymbol{y}) \right) - \frac{\boldsymbol{R}_d^L \cdot \boldsymbol{\nu}_d^L}{h_d^L} \, ZG_0^d(\boldsymbol{x}). \quad \text{(D.320)}$$

For the first integral in (D.320) we consider (D.301), which yields

$$\int_L \frac{\partial}{\partial n} \frac{1}{R} \, \boldsymbol{n}_L \, \mathrm{d}L(\boldsymbol{y}) = -\boldsymbol{n}_L \int_L \frac{\boldsymbol{R} \cdot \boldsymbol{n}_L}{R^3} \, \mathrm{d}L(\boldsymbol{y}) = -4\pi \boldsymbol{n}_L ZG_0^d(\boldsymbol{x}). \quad \text{(D.321)}$$

For the second integral in (D.320), as before, we apply the Gauss-Green theorem (A.610) on the plane of the triangle L, which implies that

$$\int_L \nabla_L \frac{1}{R} \, \mathrm{d}L(\boldsymbol{y}) = \sum_{m=1}^{3} \boldsymbol{\nu}_m^L \int_{C_m^L} \frac{1}{R} \, \mathrm{d}C(\boldsymbol{y}). \quad \text{(D.322)}$$

Hence, by considering (D.321) and (D.322) in (D.320), we obtain

$$ZG_1^d(\boldsymbol{x}) = -\frac{d_L \boldsymbol{\nu}_d^L}{4\pi h_d^L} \cdot \sum_{m=1}^{3} \boldsymbol{\nu}_m^L \int_{C_m^L} \frac{1}{R} \, \mathrm{d}C(\boldsymbol{y}) + \frac{\boldsymbol{\nu}_d^L}{h_d^L} \cdot \left(d_L \boldsymbol{n}_L - \boldsymbol{R}_d^L \right) ZG_0^d(\boldsymbol{x}), \quad \text{(D.323)}$$

where only the computation of the integral on C_m^L remains to be done.

e) Computation of the integrals on each edge C_m^L

The integrals on each edge C_m^L that remain to be computed are

$$\int_{C_m^L} \frac{1}{R} \, \mathrm{d}C(\boldsymbol{y}) \qquad \text{and} \qquad \int_{C_m^L} R \, \mathrm{d}C(\boldsymbol{y}). \quad \text{(D.324)}$$

To simplify the notation, we drop the indexes and denote the edge segment C_m^L just as C. Similarly, and as depicted in Figure D.14, we use also the notation:

- $|C|$ denotes the length of segment C.
- $\boldsymbol{R}_0, \boldsymbol{R}_1$ denote the endpoints of segment C, belonging to $\{\boldsymbol{R}_1^L, \boldsymbol{R}_2^L, \boldsymbol{R}_3^L\}$.
- $\boldsymbol{\tau}$ denotes the unit tangent of segment C, coinciding with $\boldsymbol{\tau}_m^L$.
- $\boldsymbol{\sigma}$ denotes the unit vector orthogonal to C that lies in the same plane as $\boldsymbol{x}$ and C.

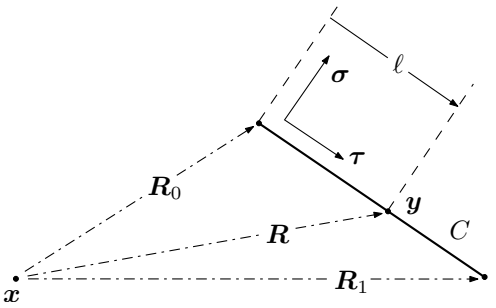

FIGURE D.14. Geometric characteristics for the calculation of the integrals on the edges.

We consider that the segment C is parametrically described by

$$\boldsymbol{R} = \boldsymbol{R}_0 + \ell\boldsymbol{\tau}, \qquad 0 \leq \ell \leq |C|, \tag{D.325}$$

and thus the parameter ℓ can be expressed as

$$\ell = (\boldsymbol{R} - \boldsymbol{R}_0) \cdot \boldsymbol{\tau} = |\boldsymbol{R} - \boldsymbol{R}_0|. \tag{D.326}$$

We have furthermore that

$$|C| = |\boldsymbol{R}_1 - \boldsymbol{R}_0| \qquad \text{and} \qquad \boldsymbol{R}_1 = \boldsymbol{R}_0 + |C|\boldsymbol{\tau}. \tag{D.327}$$

The unit vector $\boldsymbol{\sigma}$ that is orthogonal to C is given by

$$\boldsymbol{\sigma} = (\boldsymbol{R}_0 \times \boldsymbol{\tau}) \times \boldsymbol{\tau}. \tag{D.328}$$

Since we parametrized by ℓ, therefore all derivatives are taken with respect to this variable. It holds in particular that

$$RR' = \boldsymbol{R} \cdot \frac{\partial \boldsymbol{R}}{\partial \ell} = \boldsymbol{R} \cdot \boldsymbol{\tau}, \tag{D.329}$$

and hence

$$R(R + \boldsymbol{R} \cdot \boldsymbol{\tau})' = \boldsymbol{R} \cdot \boldsymbol{\tau} + R. \tag{D.330}$$

Consequently, by rearranging (D.330) we obtain

$$\frac{(R + \boldsymbol{R} \cdot \boldsymbol{\tau})'}{R + \boldsymbol{R} \cdot \boldsymbol{\tau}} = \frac{1}{R}. \tag{D.331}$$

Thus the first of the desired integrals in (D.324) is given by

$$\int_C \frac{1}{R}\,\mathrm{d}\ell = \ln\left(\frac{R_1 + \boldsymbol{R}_1 \cdot \boldsymbol{\tau}}{R_0 + \boldsymbol{R}_0 \cdot \boldsymbol{\tau}}\right). \tag{D.332}$$

We have also, from (D.329), that

$$\ell R' = \frac{\boldsymbol{R}}{R} \cdot (\ell\boldsymbol{\tau}) = R - \boldsymbol{R}_0 \cdot \frac{\boldsymbol{R}}{R}. \tag{D.333}$$

Expressing $\boldsymbol{R}_0, \boldsymbol{R}$ in terms of $\boldsymbol{\sigma}$ and $\boldsymbol{\tau}$ yields

$$\boldsymbol{R}_0 = (\boldsymbol{R}_0 \cdot \boldsymbol{\sigma})\boldsymbol{\sigma} + (\boldsymbol{R}_0 \cdot \boldsymbol{\tau})\boldsymbol{\tau}, \tag{D.334}$$

$$\boldsymbol{R} = (\boldsymbol{R}_0 \cdot \boldsymbol{\sigma})\boldsymbol{\sigma} + (\boldsymbol{R} \cdot \boldsymbol{\tau})\boldsymbol{\tau}, \tag{D.335}$$

$$\boldsymbol{R}_0 \cdot \boldsymbol{R} = (\boldsymbol{R}_0 \cdot \boldsymbol{\sigma})^2 + (\boldsymbol{R}_0 \cdot \boldsymbol{\tau})(\boldsymbol{R} \cdot \boldsymbol{\tau}), \tag{D.336}$$

and therefore, considering also (D.329), we obtain

$$\ell R' = R - \boldsymbol{R}_0 \cdot \frac{\boldsymbol{R}}{R} = R - \frac{1}{R}(\boldsymbol{R}_0 \cdot \boldsymbol{\sigma})^2 - (\boldsymbol{R}_0 \cdot \boldsymbol{\tau})R'. \tag{D.337}$$

By integrating we have that

$$\int_0^{|C|} \ell R'\,\mathrm{d}\ell = \int_C R\,\mathrm{d}\ell - (\boldsymbol{R}_0 \cdot \boldsymbol{\sigma})^2 \int_C \frac{1}{R}\,\mathrm{d}\ell - (\boldsymbol{R}_0 \cdot \boldsymbol{\tau})(R_1 - R_0). \tag{D.338}$$

An integration by parts on the left-hand side of (D.338) and a rearrangement of the terms yields finally the second of the desired integrals in (D.324), which is given by

$$\int_C R\,\mathrm{d}\ell = \frac{1}{2}\left(|C|R_1 + (\boldsymbol{R}_0 \cdot \boldsymbol{\sigma})^2 \int_C \frac{1}{R}\,\mathrm{d}\ell + (\boldsymbol{R}_0 \cdot \boldsymbol{\tau})(R_1 - R_0)\right). \tag{D.339}$$

We remark that from (D.336) we can express

$$(\boldsymbol{R}_0 \cdot \boldsymbol{\sigma})^2 = \boldsymbol{R}_0 \cdot \boldsymbol{R}_0 - (\boldsymbol{R}_0 \cdot \boldsymbol{\tau})^2. \tag{D.340}$$

f) Final computation of the singular integrals

In conclusion, the singular integrals (D.270) and (D.272) are computed using the formulae (D.301), (D.311), (D.317), and (D.323), where the integrals on the edges are calculated using (D.332) and (D.339).

It should be observed that $ZB_{a,b}^{c,d} = 0$ when the triangles coincide, i.e., when $K = L$, since in this case $d_L = 0$, and thus (D.301) and (D.323) become zero.

D.13 Benchmark problem

As benchmark problem we consider the exterior sphere problem (D.140), whose domain is shown in Figure D.4. The exact solution of this problem is stated in (D.161), and the idea is to retrieve it numerically with the integral equation techniques and the boundary element method described throughout this chapter.

For the computational implementation and the numerical resolution of the benchmark problem, we consider only the first integral equation of the extension-by-zero alternative (D.103), which is given in terms of boundary layer potentials by (D.176). The linear system (D.198) resulting from the discretization (D.196) of its variational formulation (D.183) is solved computationally with finite boundary elements of type $\mathbb{P}_1$ by using subroutines programmed in Fortran 90, by generating the mesh Γ^h of the boundary with the free software Gmsh 2.4, and by representing graphically the results in Matlab 7.5 (R2007b).

We consider a radius $R = 1$ and a constant impedance $Z = 0.8$. The discretized boundary surface Γ^h has $I = 702$ nodes, $T = 1400$ triangles, and a step $h = 0.2136$, being

$$h = \max_{1 \le j \le T} \operatorname{diam}(T_j). \tag{D.341}$$

As the known field without obstacle we take

$$u_W(r, \theta, \varphi) = \frac{\sin\theta\, e^{i\varphi} + \cos\theta}{r^2} = \frac{x_1 + i x_2 + x_3}{(x_1^2 + x_2^2 + x_3^2)^{3/2}}, \tag{D.342}$$

which implies that the impedance data function is given by

$$f_z(\theta, \varphi) = -\frac{\partial u_W}{\partial r}(R, \theta, \varphi) - Z u_W(R, \theta, \varphi) = -\frac{ZR - 2}{R^3}(\sin\theta\, e^{i\varphi} + \cos\theta). \tag{D.343}$$

The exact solution of the problem and its trace on the boundary are thus given by

$$u(\boldsymbol{x}) = -u_W(r, \theta, \varphi) = -\frac{\sin\theta\, e^{i\varphi} + \cos\theta}{r^2}, \tag{D.344}$$

$$\mu(\theta, \varphi) = -u_W(R, \theta, \varphi) = -\frac{\sin\theta\, e^{i\varphi} + \cos\theta}{R^2}. \tag{D.345}$$

The numerically calculated trace of the solution μ_h of the benchmark problem, which was computed by using the boundary element method, is depicted in Figure D.15. In the

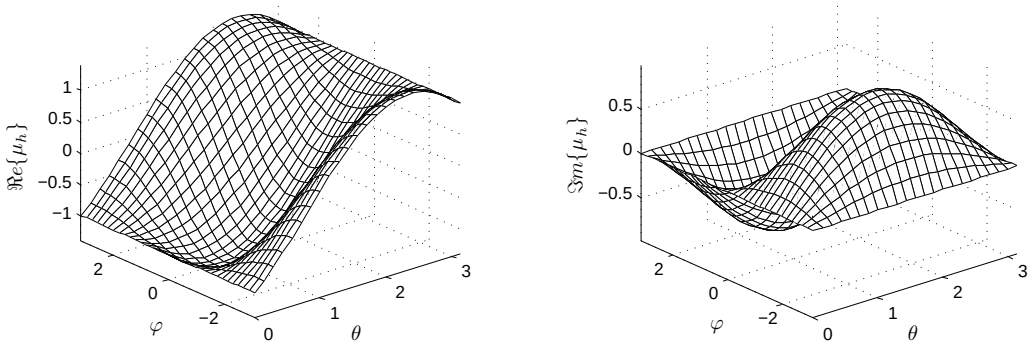

(a) Real part (b) Imaginary part

FIGURE D.15. Numerically computed trace of the solution μ_h.

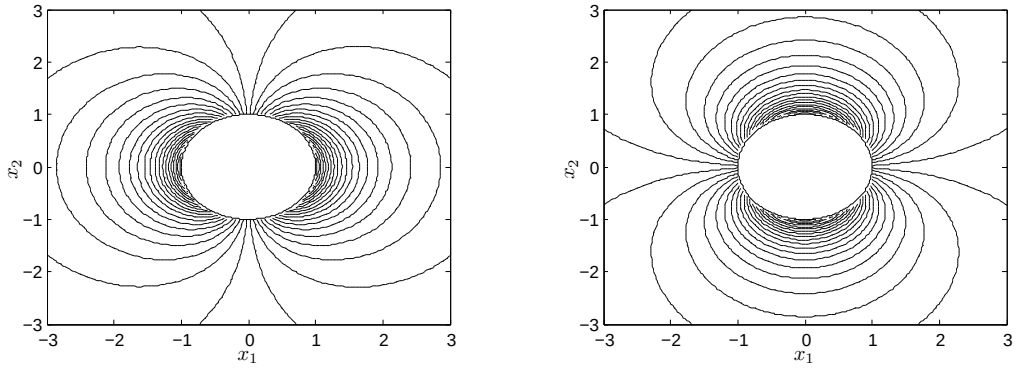

(a) Real part (b) Imaginary part

FIGURE D.16. Contour plot of the numerically computed solution u_h for $\theta = \pi/2$.

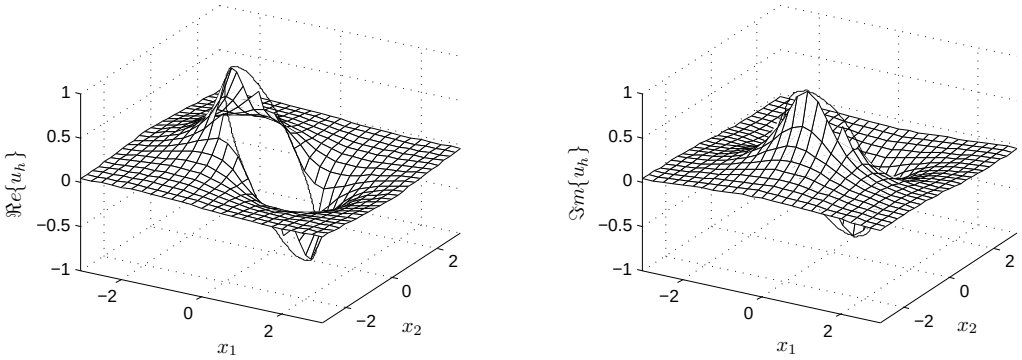

(a) Real part (b) Imaginary part

FIGURE D.17. Oblique view of the numerically computed solution u_h for $\theta = \pi/2$.

same manner, the numerical solution u_h is illustrated in Figures D.16 and D.17 for an angle $\theta = \pi/2$. It can be observed that the numerical solution is close to the exact one.

We define the relative error of the trace of the solution as

$$E_2(h, \Gamma^h) = \frac{\|\Pi_h \mu - \mu_h\|_{L^2(\Gamma^h)}}{\|\Pi_h \mu\|_{L^2(\Gamma^h)}}, \tag{D.346}$$

where $\Pi_h \mu$ denotes the Lagrange interpolating function of the exact solution's trace μ, i.e.,

$$\Pi_h \mu(\boldsymbol{x}) = \sum_{j=1}^{I} \mu(\boldsymbol{r}_j)\, \chi_j(\boldsymbol{x}) \quad \text{and} \quad \mu_h(\boldsymbol{x}) = \sum_{j=1}^{I} \mu_j\, \chi_j(\boldsymbol{x}) \quad \text{for } \boldsymbol{x} \in \Gamma^h. \tag{D.347}$$

It holds therefore that

$$\|\Pi_h \mu - \mu_h\|^2_{L^2(\Gamma^h)} = (\tilde{\boldsymbol{\mu}} - \boldsymbol{\mu})^* \boldsymbol{A}\, (\tilde{\boldsymbol{\mu}} - \boldsymbol{\mu}) \qquad \text{and} \qquad \|\Pi_h \mu\|^2_{L^2(\Gamma^h)} = \tilde{\boldsymbol{\mu}}^* \boldsymbol{A}\, \tilde{\boldsymbol{\mu}}, \tag{D.348}$$

where $\mu(\boldsymbol{r}_j)$ and μ_j are respectively the elements of vectors $\tilde{\boldsymbol{\mu}}$ and $\boldsymbol{\mu}$, for $1 \leq j \leq I$, and where the elements a_{ij} of the matrix $\boldsymbol{A}$ are specified in (D.256) and given by

$$a_{ij} = \langle \chi_j, \chi_i \rangle \qquad \text{for } 1 \leq i, j \leq I. \tag{D.349}$$

In our case, for a step $h = 0.2136$, we obtained a relative error of $E_2(h, \Gamma^h) = 0.01302$.

Similarly as for the trace, we define the relative error of the solution as

$$E_\infty(h, \Omega_L) = \frac{\|u - u_h\|_{L^\infty(\Omega_L)}}{\|u\|_{L^\infty(\Omega_L)}}, \tag{D.350}$$

being $\Omega_L = \{\boldsymbol{x} \in \Omega_e : \|\boldsymbol{x}\|_\infty < L\}$ for $L > 0$, and where

$$\|u - u_h\|_{L^\infty(\Omega_L)} = \max_{\boldsymbol{x} \in \Omega_L} |u(\boldsymbol{x}) - u_h(\boldsymbol{x})| \quad \text{and} \quad \|u\|_{L^\infty(\Omega_L)} = \max_{\boldsymbol{x} \in \Omega_L} |u(\boldsymbol{x})|. \tag{D.351}$$

We consider $L = 3$ and approximate Ω_L by a triangular finite element mesh of refinement h near the boundary. For $h = 0.2136$, the relative error that we obtained for the solution was $E_\infty(h, \Omega_L) = 0.02142$.

The results for different mesh refinements, i.e., for different numbers of triangles T, nodes I, and discretization steps h for Γ^h, are listed in Table D.1. These results are illustrated graphically in Figure D.18. It can be observed that the relative errors are approximately of order h^2.

TABLE D.1. Relative errors for different mesh refinements.

T	I	h	$E_2(h, \Gamma^h)$	$E_\infty(h, \Omega_L)$
32	18	1.0000	$5.112 \cdot 10^{-1}$	$5.162 \cdot 10^{-1}$
90	47	0.7071	$2.163 \cdot 10^{-1}$	$2.277 \cdot 10^{-1}$
336	170	0.4334	$5.664 \cdot 10^{-2}$	$7.218 \cdot 10^{-2}$
930	467	0.2419	$1.965 \cdot 10^{-2}$	$2.653 \cdot 10^{-2}$
1400	702	0.2136	$1.302 \cdot 10^{-2}$	$2.142 \cdot 10^{-2}$
2448	1226	0.1676	$6.995 \cdot 10^{-3}$	$1.086 \cdot 10^{-2}$

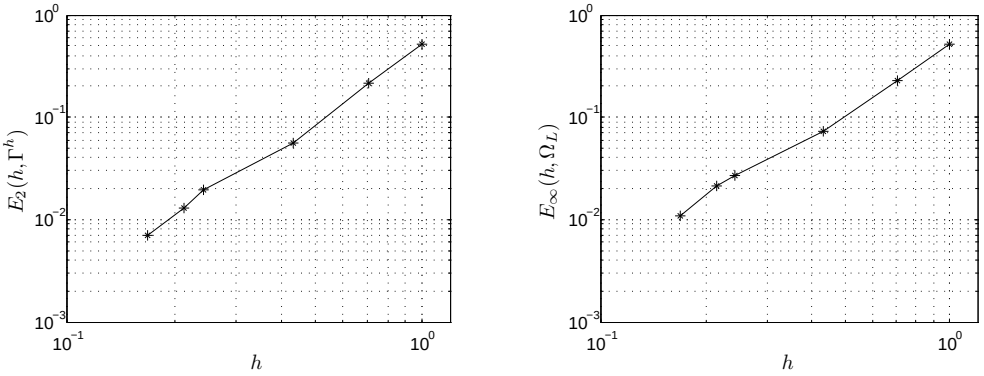

(a) Relative error $E_2(h, \Gamma^h)$ (b) Relative error $E_\infty(h, \Omega_L)$

FIGURE D.18. Logarithmic plots of the relative errors versus the discretization step.

E. FULL-SPACE IMPEDANCE HELMHOLTZ PROBLEM

E.1 Introduction

In this appendix we study the perturbed full-space or free-space impedance Helmholtz problem, also known as the exterior impedance Helmholtz problem in 3D, using integral equation techniques and the boundary element method.

We consider the problem of the Helmholtz equation in three dimensions on the exterior of a bounded obstacle with an impedance boundary condition. The perturbed full-plane impedance Helmholtz problem is a wave scattering problem around a bounded three-dimensional obstacle. In acoustic obstacle scattering the impedance boundary-value problem appears when we suppose that the normal velocity is proportional to the excess pressure on the boundary of the impenetrable obstacle. The special case of frequency zero for the volume waves has been treated already in Appendix D, since then we deal with the Laplace equation. The two-dimensional Helmholtz problem was treated thoroughly in Appendix C.

The main references for the problem treated herein are Kress (2002), Lenoir (2005), Nédélec (2001), and Terrasse & Abboud (2006). Additional related books and doctorate theses are the ones of Chen & Zhou (1992), Colton & Kress (1983), Ha-Duong (1987), Hsiao & Wendland (2008), Kirsch & Grinberg (2008), Rjasanow & Steinbach (2007), and Steinbach (2008). Articles where the Helmholtz equation with an impedance boundary condition is taken into account are Ahner (1978), Angell & Kleinman (1982), Angell & Kress (1984), Angell, Kleinman & Hettlich (1990), Dassios & Kamvyssas (1997), Krutitskii (2003*a*,*b*), and Lin (1987). Theoretical details on transmission problems are given in Costabel & Stephan (1985). The inverse problem is studied in Colton & Kirsch (1981). The boundary element calculations can be found in the report of Bendali & Devys (1986) and in the article by Bendali & Souilah (1994). Applications for the impedance Helmholtz problem can be found, among others, for acoustics (Morse & Ingard 1961) and for ultrasound imaging (Ammari 2008).

The Helmholtz equation allows the propagation of volume waves inside the considered domain, and when supplied with an impedance boundary condition it allows also the propagation of surface waves along the domain's boundary. The main difficulty in the numerical treatment and resolution of our problem is the fact that the exterior domain is unbounded. We solve it therefore with integral equation techniques and the boundary element method, which require the knowledge of the Green's function.

This appendix is structured in 14 sections, including this introduction. The direct scattering problem of the Helmholtz equation in a three-dimensional exterior domain with an impedance boundary condition is presented in Section E.2. The Green's function and its far-field expression are computed respectively in Sections E.3 and E.4. Extending the direct scattering problem towards a transmission problem, as done in Section E.5, allows its resolution by using integral equation techniques, which is discussed in Section E.6. These techniques allow also to represent the far field of the solution, as shown in Section E.7. A particular problem that takes as domain the exterior of a sphere is solved analytically in

Section E.8. The appropriate function spaces and some existence and uniqueness results for the solution of the problem are presented in Section E.9. The dissipative problem is studied in Section E.10. By means of the variational formulation developed in Section E.11, the obtained integral equation is discretized using the boundary element method, which is described in Section E.12. The boundary element calculations required to build the matrix of the linear system resulting from the numerical discretization are explained in Section E.13. Finally, in Section E.14 a benchmark problem based on the exterior sphere problem is solved numerically.

E.2 Direct scattering problem

We consider the direct scattering problem of linear time-harmonic acoustic waves on an exterior domain $\Omega_e \subset \mathbb{R}^3$, lying outside a bounded obstacle Ω_i and having a regular boundary $\Gamma = \partial\Omega_e = \partial\Omega_i$, as shown in Figure E.1. The time convention $e^{-i\omega t}$ is taken and the incident field u_I is known. The goal is to find the scattered field u as a solution to the Helmholtz equation in Ω_e, satisfying an outgoing radiation condition, and such that the total field u_T, decomposed as $u_T = u_I + u$, satisfies a homogeneous impedance boundary condition on the regular boundary Γ (e.g., of class C^2). The unit normal $\boldsymbol{n}$ is taken outwardly oriented of Ω_e. A given wave number $k > 0$ is considered, which depends on the pulsation ω and the speed of wave propagation c through the ratio $k = \omega/c$.

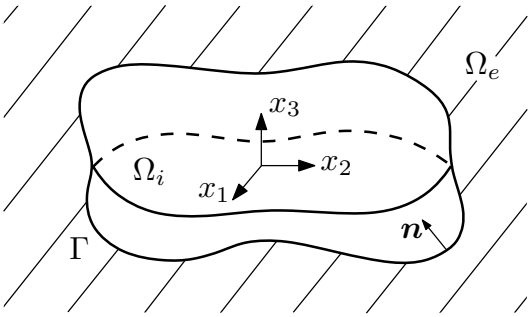

FIGURE E.1. Perturbed full-space impedance Helmholtz problem domain.

The total field u_T satisfies thus the Helmholtz equation

$$\Delta u_T + k^2 u_T = 0 \qquad \text{in } \Omega_e, \tag{E.1}$$

which is also satisfied by the incident field u_I and the scattered field u, due linearity. For the total field u_T we take the homogeneous impedance boundary condition

$$-\frac{\partial u_T}{\partial n} + Z u_T = 0 \qquad \text{on } \Gamma, \tag{E.2}$$

where Z is the impedance on the boundary. If $Z = 0$ or $Z = \infty$, then we retrieve respectively the classical Neumann or Dirichlet boundary conditions. In general, we consider a complex-valued impedance $Z(\boldsymbol{x})$ that depends on the position $\boldsymbol{x}$ and that may depend also on the pulsation ω. The scattered field u satisfies the non-homogeneous impedance

boundary condition

$$-\frac{\partial u}{\partial n} + Zu = f_z \qquad \text{on } \Gamma, \tag{E.3}$$

where the impedance data function f_z is given by

$$f_z = \frac{\partial u_I}{\partial n} - Zu_I \qquad \text{on } \Gamma. \tag{E.4}$$

The solutions of the Helmholtz equation (E.1) in the full-space $\mathbb{R}^3$ are the so-called plane waves, which we take as the known incident field u_I. Up to an arbitrary multiplicative factor, they are given by

$$u_I(\boldsymbol{x}) = e^{i\boldsymbol{k}\cdot\boldsymbol{x}}, \qquad (\boldsymbol{k}\cdot\boldsymbol{k}) = k^2, \tag{E.5}$$

where the wave propagation vector $\boldsymbol{k}$ is taken such that $\boldsymbol{k} \in \mathbb{R}^3$ to obtain physically admissible waves which do not explode towards infinity. By considering a parametrization through the angles of incidence θ_I and φ_I for $0 \leq \theta_I \leq \pi$ and $-\pi < \varphi_I \leq \pi$, we can express the wave propagation vector as $\boldsymbol{k} = (-k\sin\theta_I\cos\varphi_I, -k\sin\theta_I\sin\varphi_I, -k\cos\theta_I)$. The plane waves can be thus also represented as

$$u_I(\boldsymbol{x}) = e^{-ik(x_1\sin\theta_I\cos\varphi_I + x_2\sin\theta_I\sin\varphi_I + x_3\cos\theta_I)}. \tag{E.6}$$

An outgoing radiation condition is also imposed for the scattered field u, which specifies its decaying behavior at infinity and eliminates the non-physical solutions. It is known as a Sommerfeld radiation condition and is stated either as

$$\frac{\partial u}{\partial r} - iku = \mathcal{O}\left(\frac{1}{r^2}\right) \tag{E.7}$$

for $r = |\boldsymbol{x}|$, or, for some constant $C > 0$, by

$$\left|\frac{\partial u}{\partial r} - iku\right| \leq \frac{C}{r^2} \qquad \text{as } r \to \infty. \tag{E.8}$$

Alternatively it can be also expressed as

$$\lim_{r\to\infty} r\left(\frac{\partial u}{\partial r} - iku\right) = 0, \tag{E.9}$$

or even as

$$\frac{\partial u}{\partial r} - iku = \mathcal{O}\left(\frac{1}{r^\alpha}\right) \qquad \text{for } 1 < \alpha < 3. \tag{E.10}$$

Likewise, a weaker and more general formulation of this radiation condition is

$$\lim_{R\to\infty} \int_{S_R} \left|\frac{\partial u}{\partial r} - iku\right|^2 \mathrm{d}\gamma = 0, \tag{E.11}$$

where $S_R = \{\boldsymbol{x} \in \mathbb{R}^3 : |\boldsymbol{x}| = R\}$ is the sphere of radius R that is centered at the origin. We remark that an ingoing radiation condition would have the opposite sign, namely

$$\lim_{r\to\infty} r\left(\frac{\partial u}{\partial r} + iku\right) = 0. \tag{E.12}$$

The perturbed full-space impedance Helmholtz problem can be finally stated as

$$\begin{cases} \text{Find } u : \Omega_e \to \mathbb{C} \text{ such that} \\ \Delta u + k^2 u = 0 & \text{in } \Omega_e, \\ -\dfrac{\partial u}{\partial n} + Zu = f_z & \text{on } \Gamma, \\ \left| \dfrac{\partial u}{\partial r} - iku \right| \leq \dfrac{C}{r^2} & \text{as } r \to \infty. \end{cases} \tag{E.13}$$

E.3 Green's function

The Green's function represents the response of the unperturbed system (without an obstacle) to a Dirac mass. It corresponds to a function G, which depends on a fixed source point $\boldsymbol{x} \in \mathbb{R}^3$ and an observation point $\boldsymbol{y} \in \mathbb{R}^3$. The Green's function is computed in the sense of distributions for the variable $\boldsymbol{y}$ in the full-space $\mathbb{R}^3$ by placing at the right-hand side of the Helmholtz equation a Dirac mass $\delta_{\boldsymbol{x}}$, centered at the point $\boldsymbol{x}$. It is therefore a solution $G(\boldsymbol{x}, \cdot) : \mathbb{R}^3 \to \mathbb{C}$ for the radiation problem of a point source, namely

$$\Delta_{\boldsymbol{y}} G(\boldsymbol{x}, \boldsymbol{y}) + k^2 G(\boldsymbol{x}, \boldsymbol{y}) = \delta_{\boldsymbol{x}}(\boldsymbol{y}) \qquad \text{in } \mathcal{D}'(\mathbb{R}^3). \tag{E.14}$$

The solution of this equation is not unique, and therefore its behavior at infinity has to be specified. For this purpose we impose on the Green's function also the outgoing radiation condition (E.8).

Due to the radial symmetry of the problem (E.14), it is natural to look for solutions in the form $G = G(r)$, where $r = |\boldsymbol{y} - \boldsymbol{x}|$. By considering only the radial component, the Helmholtz equation in $\mathbb{R}^3$ becomes

$$\frac{1}{r^2} \frac{\mathrm{d}}{\mathrm{d}r} \left(r^2 \frac{\mathrm{d}G}{\mathrm{d}r} \right) + k^2 G = 0, \qquad r > 0. \tag{E.15}$$

Replacing now $z = kr$ and considering $\psi(z) = G(r)$ yields $\frac{\mathrm{d}G}{\mathrm{d}r} = k \frac{\mathrm{d}\psi}{\mathrm{d}z}$ and consequently

$$k^2 \frac{\mathrm{d}^2 \psi}{\mathrm{d}z^2} + \frac{2k^2}{z} \frac{\mathrm{d}\psi}{\mathrm{d}z} + k^2 \psi = 0, \tag{E.16}$$

which is equivalent to the zeroth order spherical Bessel differential equation (vid. Subsection A.2.6)

$$z^2 \frac{\mathrm{d}^2 \psi}{\mathrm{d}z^2} + 2z \frac{\mathrm{d}\psi}{\mathrm{d}z} + z^2 \psi = 0. \tag{E.17}$$

Independent solutions for this equation are the zeroth order spherical Bessel functions of the first and second kinds, $j_0(z)$ and $y_0(z)$, and equally the zeroth order spherical Hankel functions of the first and second kinds, $h_0^{(1)}(z)$ and $h_0^{(2)}(z)$. The latter satisfy respectively the outgoing and ingoing radiation conditions and are expressed by

$$h_0^{(1)}(z) = -\frac{i}{z} e^{iz}, \qquad h_0^{(2)}(z) = \frac{i}{z} e^{-iz}. \tag{E.18}$$

Thus the solution of (E.17) is given by

$$\psi(z) = \alpha \frac{e^{iz}}{z} + \beta \frac{e^{-iz}}{z}, \qquad \alpha, \beta \in \mathbb{C}, \tag{E.19}$$

and consequently

$$G(r) = \alpha \frac{e^{ikr}}{r} + \beta \frac{e^{-ikr}}{r}, \qquad \alpha, \beta \in \mathbb{C}, \tag{E.20}$$

where α and β are different than before, but still arbitrary. An outgoing wave behavior for the Green's function implies that $\beta = 0$, due (E.8). We observe from (E.18) that the singularity of the Green's function has the form $1/z$. The multiplicative constant α can be thus determined in the same way as for the Green's function of the Laplace equation in (D.17) by means of a computation in the sense of distributions for (E.14). The unique radial outgoing fundamental solution of the Helmholtz equation turns out to be

$$G(r) = -\frac{e^{ikr}}{4\pi r} = -\frac{ik}{4\pi} h_0^{(1)}(kr). \tag{E.21}$$

The Green's function for outgoing waves is then finally given by

$$G(\boldsymbol{x}, \boldsymbol{y}) = -\frac{e^{ik|\boldsymbol{y}-\boldsymbol{x}|}}{4\pi|\boldsymbol{y}-\boldsymbol{x}|} = -\frac{ik}{4\pi} h_0^{(1)}\big(k|\boldsymbol{y}-\boldsymbol{x}|\big). \tag{E.22}$$

We remark that the Green's function for ingoing waves would have been

$$G(\boldsymbol{x}, \boldsymbol{y}) = \frac{e^{-ik|\boldsymbol{y}-\boldsymbol{x}|}}{4\pi|\boldsymbol{y}-\boldsymbol{x}|} = -\frac{ik}{4\pi} h_0^{(2)}\big(k|\boldsymbol{y}-\boldsymbol{x}|\big). \tag{E.23}$$

To compute the derivatives of the Green's function we require some additional properties of spherical Hankel functions. It holds that

$$\frac{\mathrm{d}}{\mathrm{d}z} h_0^{(1)}(z) = -h_1^{(1)}(z), \qquad \frac{\mathrm{d}}{\mathrm{d}z} h_0^{(2)}(z) = -h_1^{(2)}(z), \tag{E.24}$$

and

$$\frac{\mathrm{d}}{\mathrm{d}z} h_1^{(1)}(z) = h_0^{(1)}(z) - \frac{2}{z} h_1^{(1)}(z), \qquad \frac{\mathrm{d}}{\mathrm{d}z} h_1^{(2)}(z) = h_0^{(2)}(z) - \frac{2}{z} h_1^{(2)}(z), \tag{E.25}$$

where $h_1^{(1)}(z)$ and $h_1^{(2)}(z)$ denote the first order spherical Hankel functions of the first and second kinds, respectively, which are expressed as

$$h_1^{(1)}(z) = \left(-\frac{1}{z} - \frac{i}{z^2}\right) e^{iz}, \qquad h_1^{(2)}(z) = \left(-\frac{1}{z} + \frac{i}{z^2}\right) e^{-iz}. \tag{E.26}$$

The gradient of the Green's function (E.22) is therefore given by

$$\nabla_{\boldsymbol{y}} G(\boldsymbol{x}, \boldsymbol{y}) = \frac{e^{ik|\boldsymbol{y}-\boldsymbol{x}|}}{4\pi}\big(1 - ik|\boldsymbol{y}-\boldsymbol{x}|\big)\frac{\boldsymbol{y}-\boldsymbol{x}}{|\boldsymbol{y}-\boldsymbol{x}|^3} = \frac{ik^2}{4\pi} h_1^{(1)}\big(k|\boldsymbol{y}-\boldsymbol{x}|\big)\frac{\boldsymbol{y}-\boldsymbol{x}}{|\boldsymbol{y}-\boldsymbol{x}|}, \tag{E.27}$$

and the gradient with respect to the $\boldsymbol{x}$ variable by

$$\nabla_{\boldsymbol{x}} G(\boldsymbol{x}, \boldsymbol{y}) = \frac{e^{ik|\boldsymbol{x}-\boldsymbol{y}|}}{4\pi}\big(1 - ik|\boldsymbol{x}-\boldsymbol{y}|\big)\frac{\boldsymbol{x}-\boldsymbol{y}}{|\boldsymbol{x}-\boldsymbol{y}|^3} = \frac{ik^2}{4\pi} h_1^{(1)}\big(k|\boldsymbol{x}-\boldsymbol{y}|\big)\frac{\boldsymbol{x}-\boldsymbol{y}}{|\boldsymbol{x}-\boldsymbol{y}|}. \tag{E.28}$$

The double-gradient matrix is given by

$$\begin{aligned}\nabla_{\boldsymbol{x}}\nabla_{\boldsymbol{y}} G(\boldsymbol{x}, \boldsymbol{y}) = {} & \frac{ik^2}{4\pi} h_1^{(1)}\big(k|\boldsymbol{x}-\boldsymbol{y}|\big)\left(-\frac{\boldsymbol{I}}{|\boldsymbol{x}-\boldsymbol{y}|} + 3\frac{(\boldsymbol{x}-\boldsymbol{y})\otimes(\boldsymbol{x}-\boldsymbol{y})}{|\boldsymbol{x}-\boldsymbol{y}|^3}\right) \\ & - \frac{ik^3}{4\pi} h_0^{(1)}\big(k|\boldsymbol{x}-\boldsymbol{y}|\big)\frac{(\boldsymbol{x}-\boldsymbol{y})\otimes(\boldsymbol{x}-\boldsymbol{y})}{|\boldsymbol{x}-\boldsymbol{y}|^2},\end{aligned} \tag{E.29}$$

where $\boldsymbol{I}$ denotes a 3×3 identity matrix and where $\otimes$ denotes the dyadic or outer product of two vectors, which results in a matrix and is defined in (A.572).

We note that the Green's function (E.22) is symmetric in the sense that

$$G(\boldsymbol{x}, \boldsymbol{y}) = G(\boldsymbol{y}, \boldsymbol{x}), \tag{E.30}$$

and it fulfills similarly

$$\nabla_{\boldsymbol{y}} G(\boldsymbol{x}, \boldsymbol{y}) = \nabla_{\boldsymbol{y}} G(\boldsymbol{y}, \boldsymbol{x}) = -\nabla_{\boldsymbol{x}} G(\boldsymbol{x}, \boldsymbol{y}) = -\nabla_{\boldsymbol{x}} G(\boldsymbol{y}, \boldsymbol{x}), \tag{E.31}$$

and

$$\nabla_{\boldsymbol{x}} \nabla_{\boldsymbol{y}} G(\boldsymbol{x}, \boldsymbol{y}) = \nabla_{\boldsymbol{y}} \nabla_{\boldsymbol{x}} G(\boldsymbol{x}, \boldsymbol{y}) = \nabla_{\boldsymbol{x}} \nabla_{\boldsymbol{y}} G(\boldsymbol{y}, \boldsymbol{x}) = \nabla_{\boldsymbol{y}} \nabla_{\boldsymbol{x}} G(\boldsymbol{y}, \boldsymbol{x}). \tag{E.32}$$

Furthermore, due the exponential decrease of the spherical Hankel functions at infinity, we observe that the expression (E.22) of the Green's function for outgoing waves is still valid if a complex wave number $k \in \mathbb{C}$ such that $\mathfrak{Im}\{k\} > 0$ is used, which holds also for its derivatives (E.27), (E.28), and (E.29). In the case of ingoing waves, the expression (E.23) and its derivatives are valid if a complex wave number $k \in \mathbb{C}$ now such that $\mathfrak{Im}\{k\} < 0$ is taken into account.

E.4 Far field of the Green's function

The far field of the Green's function describes its asymptotic behavior at infinity, i.e., when $|\boldsymbol{x}| \to \infty$ and assuming that $\boldsymbol{y}$ is fixed. By using a Taylor expansion we obtain that

$$|\boldsymbol{x} - \boldsymbol{y}| = |\boldsymbol{x}| \left(1 - 2 \, \frac{\boldsymbol{y} \cdot \boldsymbol{x}}{|\boldsymbol{x}|^2} + \frac{|\boldsymbol{y}|^2}{|\boldsymbol{x}|^2} \right)^{1/2} = |\boldsymbol{x}| - \frac{\boldsymbol{y} \cdot \boldsymbol{x}}{|\boldsymbol{x}|} + \mathcal{O}\left(\frac{1}{|\boldsymbol{x}|} \right). \tag{E.33}$$

A similar expansion yields

$$\frac{1}{|\boldsymbol{x} - \boldsymbol{y}|} = \frac{1}{|\boldsymbol{x}|} + \mathcal{O}\left(\frac{1}{|\boldsymbol{x}|^2} \right), \tag{E.34}$$

and we have also that

$$e^{ik|\boldsymbol{x}-\boldsymbol{y}|} = e^{ik|\boldsymbol{x}|} e^{-ik\boldsymbol{y}\cdot\boldsymbol{x}/|\boldsymbol{x}|} \left(1 + \mathcal{O}\left(\frac{1}{|\boldsymbol{x}|} \right) \right). \tag{E.35}$$

We express the point $\boldsymbol{x}$ as $\boldsymbol{x} = |\boldsymbol{x}| \, \hat{\boldsymbol{x}}$, being $\hat{\boldsymbol{x}}$ a unitary vector. The far field of the Green's function, as $|\boldsymbol{x}| \to \infty$, is thus given by

$$G^{ff}(\boldsymbol{x}, \boldsymbol{y}) = -\frac{e^{ik|\boldsymbol{x}|}}{4\pi|\boldsymbol{x}|} e^{-ik\hat{\boldsymbol{x}}\cdot\boldsymbol{y}}. \tag{E.36}$$

Similarly, as $|\boldsymbol{x}| \to \infty$, we have for its gradient with respect to $\boldsymbol{y}$, that

$$\nabla_{\boldsymbol{y}} G^{ff}(\boldsymbol{x}, \boldsymbol{y}) = \frac{ike^{ik|\boldsymbol{x}|}}{4\pi|\boldsymbol{x}|} e^{-ik\hat{\boldsymbol{x}}\cdot\boldsymbol{y}} \, \hat{\boldsymbol{x}}, \tag{E.37}$$

for its gradient with respect to $\boldsymbol{x}$, that

$$\nabla_{\boldsymbol{x}} G^{ff}(\boldsymbol{x}, \boldsymbol{y}) = -\frac{ike^{ik|\boldsymbol{x}|}}{4\pi|\boldsymbol{x}|} e^{-ik\hat{\boldsymbol{x}}\cdot\boldsymbol{y}} \, \hat{\boldsymbol{x}}, \tag{E.38}$$

and for its double-gradient matrix, that

$$\nabla_{\boldsymbol{x}}\nabla_{\boldsymbol{y}}G^{ff}(\boldsymbol{x},\boldsymbol{y}) = -\frac{k^2 e^{ik|\boldsymbol{x}|}}{4\pi|\boldsymbol{x}|}e^{-ik\hat{\boldsymbol{x}}\cdot\boldsymbol{y}}\,(\hat{\boldsymbol{x}}\otimes\hat{\boldsymbol{x}}). \tag{E.39}$$

We remark that these far fields are still valid if a complex wave number $k \in \mathbb{C}$ such that $\mathfrak{Im}\{k\} > 0$ is used.

E.5 Transmission problem

We are interested in expressing the solution u of the direct scattering problem (E.13) by means of an integral representation formula over the boundary Γ. To study this kind of representations, the differential problem defined on Ω_e is extended as a transmission problem defined now on the whole space $\mathbb{R}^3$ by combining (E.13) with a corresponding interior problem defined on Ω_i. For the transmission problem, which specifies jump conditions over the boundary Γ, a general integral representation can be developed, and the particular integral representations of interest are then established by the specific choice of the corresponding interior problem.

A transmission problem is then a differential problem for which the jump conditions of the solution field, rather than boundary conditions, are specified on the boundary Γ. As shown in Figure E.1, we consider the exterior domain Ω_e and the interior domain Ω_i, taking the unit normal $\boldsymbol{n}$ pointing towards Ω_i. We search now a solution u defined in $\Omega_e \cup \Omega_i$, and use the notation $u_e = u|_{\Omega_e}$ and $u_i = u|_{\Omega_i}$. We define the jumps of the traces of u on both sides of the boundary Γ as

$$[u] = u_e - u_i \qquad \text{and} \qquad \left[\frac{\partial u}{\partial n}\right] = \frac{\partial u_e}{\partial n} - \frac{\partial u_i}{\partial n}. \tag{E.40}$$

The transmission problem is now given by

$$\begin{cases} \text{Find } u : \Omega_e \cup \Omega_i \to \mathbb{C} \text{ such that} \\ \Delta u + k^2 u = 0 \qquad \text{in } \ \Omega_e \cup \Omega_i, \\ [u] = \mu \qquad\qquad\ \text{on } \ \Gamma, \\ \left[\dfrac{\partial u}{\partial n}\right] = \nu \qquad\ \text{on } \ \Gamma, \\ \text{+ Outgoing radiation condition as } |\boldsymbol{x}| \to \infty, \end{cases} \tag{E.41}$$

where $\mu, \nu : \Gamma \to \mathbb{C}$ are known functions. The outgoing radiation condition is still (E.8), and it is required to ensure uniqueness of the solution.

E.6 Integral representations and equations

E.6.1 Integral representation

To develop for the solution u an integral representation formula over the boundary Γ, we define by $\Omega_{R,\varepsilon}$ the domain $\Omega_e \cup \Omega_i$ without the ball B_ε of radius $\varepsilon > 0$ centered at the point $\boldsymbol{x} \in \Omega_e \cup \Omega_i$, and truncated at infinity by the ball B_R of radius $R > 0$ centered at the

origin. We consider that the ball B_ε is entirely contained either in Ω_e or in Ω_i, depending on the location of its center $\boldsymbol{x}$. Therefore, as shown in Figure E.2, we have that

$$\Omega_{R,\varepsilon} = \big((\Omega_e \cup \Omega_i) \cap B_R\big) \setminus \overline{B_\varepsilon} \qquad \text{and} \qquad \Omega_R = (\Omega_e \cup \Omega_i) \cap B_R, \tag{E.42}$$

where

$$B_R = \{\boldsymbol{y} \in \mathbb{R}^3 : |\boldsymbol{y}| < R\} \qquad \text{and} \qquad B_\varepsilon = \{\boldsymbol{y} \in \mathbb{R}^3 : |\boldsymbol{y} - \boldsymbol{x}| < \varepsilon\}. \tag{E.43}$$

We consider similarly the boundaries of the balls

$$S_R = \{\boldsymbol{y} \in \mathbb{R}^3 : |\boldsymbol{y}| = R\} \qquad \text{and} \qquad S_\varepsilon = \{\boldsymbol{y} \in \mathbb{R}^3 : |\boldsymbol{y} - \boldsymbol{x}| = \varepsilon\}. \tag{E.44}$$

The idea is to retrieve the domain $\Omega_e \cup \Omega_i$ at the end when the limits $R \to \infty$ and $\varepsilon \to 0$ are taken for the truncated domains $\Omega_{R,\varepsilon}$ and Ω_R.

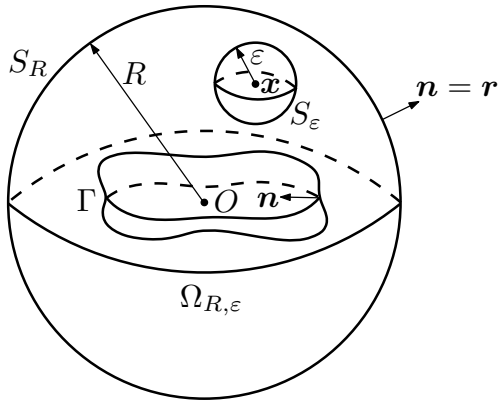

FIGURE E.2. Truncated domain $\Omega_{R,\varepsilon}$ for $\boldsymbol{x} \in \Omega_e \cup \Omega_i$.

Let us analyze first the asymptotic decaying behavior of the solution u, which satisfies the Helmholtz equation and the Sommerfeld radiation condition. For more generality, we assume here that the wave number k ($\neq 0$) is complex and such that $\mathfrak{Im}\{k\} \geq 0$. We consider the weakest form of the radiation condition, namely (E.11), and develop

$$\int_{S_R} \left| \frac{\partial u}{\partial r} - iku \right|^2 \mathrm{d}\gamma = \int_{S_R} \left[\left| \frac{\partial u}{\partial r} \right|^2 + |k|^2 |u|^2 + 2\,\mathfrak{Im}\left\{ ku \frac{\partial \bar{u}}{\partial r} \right\} \right] \mathrm{d}\gamma. \tag{E.45}$$

From the divergence theorem (A.614) applied on the truncated domain Ω_R and considering the complex conjugated Helmholtz equation we have

$$\begin{aligned} k \int_{S_R} u \frac{\partial \bar{u}}{\partial r}\, \mathrm{d}\gamma + k \int_\Gamma u \frac{\partial \bar{u}}{\partial n}\, \mathrm{d}\gamma &= k \int_{\Omega_R} \mathrm{div}(u \nabla \bar{u})\, \mathrm{d}\boldsymbol{x} \\ &= k \int_{\Omega_R} |\nabla u|^2\, \mathrm{d}\boldsymbol{x} - k\bar{k}^2 \int_{\Omega_R} |u|^2\, \mathrm{d}\boldsymbol{x}. \end{aligned} \tag{E.46}$$

Replacing the imaginary part of (E.46) in (E.45) and taking the limit as $R \to \infty$, yields

$$\lim_{R\to\infty}\left[\int_{S_R}\left(\left|\frac{\partial u}{\partial r}\right|^2+|k|^2|u|^2\right)\mathrm{d}\gamma+2\,\mathfrak{Im}\{k\}\int_{\Omega_R}\left(|\nabla u|^2+|k|^2|u|^2\right)\mathrm{d}\boldsymbol{x}\right]$$
$$=2\,\mathfrak{Im}\left\{k\int_\Gamma u\frac{\partial\bar{u}}{\partial n}\,\mathrm{d}\gamma\right\}. \tag{E.47}$$

Since the right-hand side is finite and since the left-hand side is nonnegative, we see that

$$\int_{S_R}|u|^2\,\mathrm{d}\gamma=\mathcal{O}(1)\qquad\text{and}\qquad\int_{S_R}\left|\frac{\partial u}{\partial r}\right|^2\mathrm{d}\gamma=\mathcal{O}(1)\qquad\text{as}\;\;R\to\infty, \tag{E.48}$$

and therefore it holds for a great value of $r=|\boldsymbol{x}|$ that

$$u=\mathcal{O}\left(\frac{1}{r}\right)\qquad\text{and}\qquad|\nabla u|=\mathcal{O}\left(\frac{1}{r}\right). \tag{E.49}$$

We apply now Green's second integral theorem (A.613) to the functions u and $G(\boldsymbol{x},\cdot)$ in the bounded domain $\Omega_{R,\varepsilon}$, by subtracting their respective Helmholtz equations, yielding

$$\begin{aligned}0&=\int_{\Omega_{R,\varepsilon}}\big(u(\boldsymbol{y})\Delta_{\boldsymbol{y}}G(\boldsymbol{x},\boldsymbol{y})-G(\boldsymbol{x},\boldsymbol{y})\Delta u(\boldsymbol{y})\big)\mathrm{d}\boldsymbol{y}\\&=\int_{S_R}\left(u(\boldsymbol{y})\frac{\partial G}{\partial r_{\boldsymbol{y}}}(\boldsymbol{x},\boldsymbol{y})-G(\boldsymbol{x},\boldsymbol{y})\frac{\partial u}{\partial r}(\boldsymbol{y})\right)\mathrm{d}\gamma(\boldsymbol{y})\\&-\int_{S_\varepsilon}\left(u(\boldsymbol{y})\frac{\partial G}{\partial r_{\boldsymbol{y}}}(\boldsymbol{x},\boldsymbol{y})-G(\boldsymbol{x},\boldsymbol{y})\frac{\partial u}{\partial r}(\boldsymbol{y})\right)\mathrm{d}\gamma(\boldsymbol{y})\\&+\int_\Gamma\left([u](\boldsymbol{y})\frac{\partial G}{\partial n_{\boldsymbol{y}}}(\boldsymbol{x},\boldsymbol{y})-G(\boldsymbol{x},\boldsymbol{y})\left[\frac{\partial u}{\partial n}\right](\boldsymbol{y})\right)\mathrm{d}\gamma(\boldsymbol{y}).\end{aligned} \tag{E.50}$$

The integral on S_R can be rewritten as

$$\int_{S_R}\left[u(\boldsymbol{y})\left(\frac{\partial G}{\partial r_{\boldsymbol{y}}}(\boldsymbol{x},\boldsymbol{y})-ikG(\boldsymbol{x},\boldsymbol{y})\right)-G(\boldsymbol{x},\boldsymbol{y})\left(\frac{\partial u}{\partial r}(\boldsymbol{y})-iku(\boldsymbol{y})\right)\right]\mathrm{d}\gamma(\boldsymbol{y}), \tag{E.51}$$

which for R large enough and due the radiation condition (E.8) tends to zero, since

$$\left|\int_{S_R}u(\boldsymbol{y})\left(\frac{\partial G}{\partial r_{\boldsymbol{y}}}(\boldsymbol{x},\boldsymbol{y})-ikG(\boldsymbol{x},\boldsymbol{y})\right)\mathrm{d}\gamma(\boldsymbol{y})\right|\le\frac{C}{R}, \tag{E.52}$$

and

$$\left|\int_{S_R}G(\boldsymbol{x},\boldsymbol{y})\left(\frac{\partial u}{\partial r}(\boldsymbol{y})-iku(\boldsymbol{y})\right)\mathrm{d}\gamma(\boldsymbol{y})\right|\le\frac{C}{R}, \tag{E.53}$$

for some constants $C>0$. If the function u is regular enough in the ball B_ε, then the second term of the integral on S_ε, when $\varepsilon\to 0$ and due (E.22), is bounded by

$$\left|\int_{S_\varepsilon}G(\boldsymbol{x},\boldsymbol{y})\frac{\partial u}{\partial r}(\boldsymbol{y})\,\mathrm{d}\gamma(\boldsymbol{y})\right|\le\varepsilon\,|e^{ik\varepsilon}|\sup_{\boldsymbol{y}\in B_\varepsilon}\left|\frac{\partial u}{\partial r}(\boldsymbol{y})\right|, \tag{E.54}$$

and tends to zero. The regularity of u can be specified afterwards once the integral representation has been determined and generalized by means of density arguments. The first

integral term on S_ε can be decomposed as

$$\int_{S_\varepsilon} u(\boldsymbol{y}) \frac{\partial G}{\partial r_{\boldsymbol{y}}}(\boldsymbol{x},\boldsymbol{y})\,\mathrm{d}\gamma(\boldsymbol{y}) = u(\boldsymbol{x}) \int_{S_\varepsilon} \frac{\partial G}{\partial r_{\boldsymbol{y}}}(\boldsymbol{x},\boldsymbol{y})\,\mathrm{d}\gamma(\boldsymbol{y}) + \int_{S_\varepsilon} \frac{\partial G}{\partial r_{\boldsymbol{y}}}(\boldsymbol{x},\boldsymbol{y})\big(u(\boldsymbol{y}) - u(\boldsymbol{x})\big)\,\mathrm{d}\gamma(\boldsymbol{y}), \tag{E.55}$$

For the first term in the right-hand side of (E.55), by replacing (E.27), we have that

$$\int_{S_\varepsilon} \frac{\partial G}{\partial r_{\boldsymbol{y}}}(\boldsymbol{x},\boldsymbol{y})\,\mathrm{d}\gamma(\boldsymbol{y}) = (1 - ik\varepsilon)\, e^{ik\varepsilon} \quad \xrightarrow[\varepsilon\to 0]{} \quad 1, \tag{E.56}$$

which tends towards one, while the second term is bounded by

$$\left| \int_{S_\varepsilon} \big(u(\boldsymbol{y}) - u(\boldsymbol{x})\big) \frac{\partial G}{\partial r_{\boldsymbol{y}}}(\boldsymbol{x},\boldsymbol{y})\,\mathrm{d}\gamma(\boldsymbol{y}) \right| \leq |1 - ik\varepsilon|\, |e^{ik\varepsilon}| \sup_{\boldsymbol{y}\in B_\varepsilon} |u(\boldsymbol{y}) - u(\boldsymbol{x})|, \tag{E.57}$$

which tends towards zero when $\varepsilon \to 0$.

In conclusion, when the limits $R \to \infty$ and $\varepsilon \to 0$ are taken in (E.50), then the following integral representation formula holds for the solution u of the transmission problem:

$$u(\boldsymbol{x}) = \int_\Gamma \left([u](\boldsymbol{y}) \frac{\partial G}{\partial n_{\boldsymbol{y}}}(\boldsymbol{x},\boldsymbol{y}) - G(\boldsymbol{x},\boldsymbol{y}) \left[\frac{\partial u}{\partial n}\right](\boldsymbol{y}) \right) \mathrm{d}\gamma(\boldsymbol{y}), \qquad \boldsymbol{x} \in \Omega_e \cup \Omega_i. \tag{E.58}$$

We observe thus that if the values of the jump of u and of its normal derivative are known on Γ, then the transmission problem (E.41) is readily solved and its solution given explicitly by (E.58), which, in terms of μ and ν, becomes

$$u(\boldsymbol{x}) = \int_\Gamma \left(\mu(\boldsymbol{y}) \frac{\partial G}{\partial n_{\boldsymbol{y}}}(\boldsymbol{x},\boldsymbol{y}) - G(\boldsymbol{x},\boldsymbol{y}) \nu(\boldsymbol{y}) \right) \mathrm{d}\gamma(\boldsymbol{y}), \qquad \boldsymbol{x} \in \Omega_e \cup \Omega_i. \tag{E.59}$$

To determine the values of the jumps, an adequate integral equation has to be developed, i.e., an equation whose unknowns are the traces of the solution on Γ.

An alternative way to demonstrate the integral representation (E.58) is to proceed in the sense of distributions, in the same way as done in Section B.6. Again we obtain the single layer potential

$$\left\{ G * \left[\frac{\partial u}{\partial n}\right] \delta_\Gamma \right\}(\boldsymbol{x}) = \int_\Gamma G(\boldsymbol{x},\boldsymbol{y}) \left[\frac{\partial u}{\partial n}\right](\boldsymbol{y})\,\mathrm{d}\gamma(\boldsymbol{y}) \tag{E.60}$$

associated with the distribution of sources $[\partial u/\partial n]\delta_\Gamma$, and the double layer potential

$$\left\{ G * \frac{\partial}{\partial n}\big([u]\delta_\Gamma\big) \right\}(\boldsymbol{x}) = -\int_\Gamma \frac{\partial G}{\partial n_{\boldsymbol{y}}}(\boldsymbol{x},\boldsymbol{y}) [u](\boldsymbol{y})\,\mathrm{d}\gamma(\boldsymbol{y}) \tag{E.61}$$

associated with the distribution of dipoles $\frac{\partial}{\partial n}([u]\delta_\Gamma)$. Combining properly (E.60) and (E.61) yields the desired integral representation (E.58).

We note that to obtain the gradient of the integral representation (E.58) we can pass directly the derivatives inside the integral, since there are no singularities if $\boldsymbol{x} \in \Omega_e \cup \Omega_i$. Therefore we have that

$$\nabla u(\boldsymbol{x}) = \int_\Gamma \left([u](\boldsymbol{y}) \nabla_{\boldsymbol{x}} \frac{\partial G}{\partial n_{\boldsymbol{y}}}(\boldsymbol{x},\boldsymbol{y}) - \nabla_{\boldsymbol{x}} G(\boldsymbol{x},\boldsymbol{y}) \left[\frac{\partial u}{\partial n}\right](\boldsymbol{y}) \right) \mathrm{d}\gamma(\boldsymbol{y}). \tag{E.62}$$

E.6.2 Integral equations

To determine the values of the traces that conform the jumps for the transmission problem (E.41), an integral equation has to be developed. For this purpose we place the source point $\boldsymbol{x}$ on the boundary Γ and apply the same procedure as before for the integral representation (E.58), treating differently in (E.50) only the integrals on S_ε. The integrals on S_R still behave well and tend towards zero as $R \to \infty$. The Ball B_ε, though, is split in half into the two pieces $\Omega_e \cap B_\varepsilon$ and $\Omega_i \cap B_\varepsilon$, which are asymptotically separated by the tangent of the boundary if Γ is regular. Thus the associated integrals on S_ε give rise to a term $-(u_e(\boldsymbol{x}) + u_i(\boldsymbol{x}))/2$ instead of just $-u(\boldsymbol{x})$ as before. We must notice that in this case, the integrands associated with the boundary Γ admit an integrable singularity at the point $\boldsymbol{x}$. The desired integral equation related with (E.58) is then given by

$$\frac{u_e(\boldsymbol{x}) + u_i(\boldsymbol{x})}{2} = \int_\Gamma \left([u](\boldsymbol{y}) \frac{\partial G}{\partial n_{\boldsymbol{y}}}(\boldsymbol{x}, \boldsymbol{y}) - G(\boldsymbol{x}, \boldsymbol{y}) \left[\frac{\partial u}{\partial n} \right] (\boldsymbol{y}) \right) \mathrm{d}\gamma(\boldsymbol{y}), \quad \boldsymbol{x} \in \Gamma. \quad \text{(E.63)}$$

By choosing adequately the boundary condition of the interior problem, and by considering also the boundary condition of the exterior problem and the jump definitions (E.40), this integral equation can be expressed in terms of only one unknown function on Γ. Thus, solving the problem (E.13) is equivalent to solve (E.63) and then replace the obtained solution in (E.58).

The integral equation holds only when the boundary Γ is regular (e.g., of class C^2). Otherwise, taking the limit $\varepsilon \to 0$ can no longer be well-defined and the result is false in general. In particular, if the boundary Γ has an angular point at $\boldsymbol{x} \in \Gamma$, then the left-hand side of the integral equation (E.63) is modified on that point according to the portion of the ball B_ε that remains inside Ω_e, analogously as was done for the two-dimensional case in (B.61), but now for solid angles.

Another integral equation can be also derived for the normal derivative of the solution u on the boundary Γ, by studying the jump properties of the single and double layer potentials. It is performed in the same manner as for the Laplace equation. If the boundary is regular at $\boldsymbol{x} \in \Gamma$, then it holds that

$$\frac{1}{2} \frac{\partial u_e}{\partial n}(\boldsymbol{x}) + \frac{1}{2} \frac{\partial u_i}{\partial n}(\boldsymbol{x}) = \int_\Gamma \left([u](\boldsymbol{y}) \frac{\partial^2 G}{\partial n_{\boldsymbol{x}} \partial n_{\boldsymbol{y}}}(\boldsymbol{x}, \boldsymbol{y}) - \frac{\partial G}{\partial n_{\boldsymbol{x}}}(\boldsymbol{x}, \boldsymbol{y}) \left[\frac{\partial u}{\partial n} \right] (\boldsymbol{y}) \right) \mathrm{d}\gamma(\boldsymbol{y}). \quad \text{(E.64)}$$

This integral equation is modified correspondingly if $\boldsymbol{x}$ is an angular point.

E.6.3 Integral kernels

In the same manner as for the Laplace equation, the integral kernels G, $\partial G / \partial n_{\boldsymbol{y}}$, and $\partial G / \partial n_{\boldsymbol{x}}$ are weakly singular, and thus integrable, whereas the kernel $\partial^2 G / \partial n_{\boldsymbol{x}} \partial n_{\boldsymbol{y}}$ is not integrable and therefore hypersingular.

The kernel G defined in (E.22) has the same singularity as the Laplace equation, namely

$$G(\boldsymbol{x}, \boldsymbol{y}) \sim -\frac{1}{4\pi |\boldsymbol{x} - \boldsymbol{y}|} \qquad \text{as } \boldsymbol{x} \to \boldsymbol{y}. \quad \text{(E.65)}$$

It fulfills therefore (B.64) with $\lambda = 1$. The kernels $\partial G/\partial n_{\boldsymbol{y}}$ and $\partial G/\partial n_{\boldsymbol{x}}$ are less singular along Γ than they appear at first sight, due the regularizing effect of the normal derivatives. They are given respectively by

$$\frac{\partial G}{\partial n_{\boldsymbol{y}}}(\boldsymbol{x},\boldsymbol{y}) = \frac{e^{ik|\boldsymbol{y}-\boldsymbol{x}|}}{4\pi}\big(1-ik|\boldsymbol{y}-\boldsymbol{x}|\big)\frac{(\boldsymbol{y}-\boldsymbol{x})\cdot\boldsymbol{n}_{\boldsymbol{y}}}{|\boldsymbol{y}-\boldsymbol{x}|^3}, \tag{E.66}$$

and

$$\frac{\partial G}{\partial n_{\boldsymbol{x}}}(\boldsymbol{x},\boldsymbol{y}) = \frac{e^{ik|\boldsymbol{y}-\boldsymbol{x}|}}{4\pi}\big(1-ik|\boldsymbol{y}-\boldsymbol{x}|\big)\frac{(\boldsymbol{x}-\boldsymbol{y})\cdot\boldsymbol{n}_{\boldsymbol{x}}}{|\boldsymbol{y}-\boldsymbol{x}|^3}, \tag{E.67}$$

and their singularities, as $\boldsymbol{x}\to\boldsymbol{y}$ for $\boldsymbol{x},\boldsymbol{y}\in\Gamma$, adopt the form

$$\frac{\partial G}{\partial n_{\boldsymbol{y}}}(\boldsymbol{x},\boldsymbol{y}) \sim \frac{(\boldsymbol{y}-\boldsymbol{x})\cdot\boldsymbol{n}_{\boldsymbol{y}}}{4\pi|\boldsymbol{y}-\boldsymbol{x}|^3} \qquad \text{and} \qquad \frac{\partial G}{\partial n_{\boldsymbol{x}}}(\boldsymbol{x},\boldsymbol{y}) \sim \frac{(\boldsymbol{x}-\boldsymbol{y})\cdot\boldsymbol{n}_{\boldsymbol{x}}}{4\pi|\boldsymbol{x}-\boldsymbol{y}|^3}. \tag{E.68}$$

The appearing singularities are the same as for the Laplace equation and it can be shown that for the singularity the estimates (B.70) and (B.71) hold also in three dimensions, by using the same reasoning as in the two-dimensional case for the graph of a regular function φ that takes variables now on the tangent plane. Therefore we have that

$$\frac{\partial G}{\partial n_{\boldsymbol{y}}}(\boldsymbol{x},\boldsymbol{y}) = \mathcal{O}\bigg(\frac{1}{|\boldsymbol{y}-\boldsymbol{x}|}\bigg) \qquad \text{and} \qquad \frac{\partial G}{\partial n_{\boldsymbol{x}}}(\boldsymbol{x},\boldsymbol{y}) = \mathcal{O}\bigg(\frac{1}{|\boldsymbol{x}-\boldsymbol{y}|}\bigg), \tag{E.69}$$

and hence these kernels satisfy (B.64) with $\lambda = 1$.

The kernel $\partial^2 G/\partial n_{\boldsymbol{x}}\partial n_{\boldsymbol{y}}$, on the other hand, adopts the form

$$\begin{aligned}\frac{\partial^2 G}{\partial n_{\boldsymbol{x}}\partial n_{\boldsymbol{y}}}(\boldsymbol{x},\boldsymbol{y}) = \frac{ik^2}{4\pi}h_1^{(1)}\big(k|\boldsymbol{x}-\boldsymbol{y}|\big)\left(-\frac{\boldsymbol{n}_{\boldsymbol{x}}\cdot\boldsymbol{n}_{\boldsymbol{y}}}{|\boldsymbol{x}-\boldsymbol{y}|} - 3\frac{\big((\boldsymbol{x}-\boldsymbol{y})\cdot\boldsymbol{n}_{\boldsymbol{x}}\big)\big((\boldsymbol{y}-\boldsymbol{x})\cdot\boldsymbol{n}_{\boldsymbol{y}}\big)}{|\boldsymbol{x}-\boldsymbol{y}|^3}\right)\\ + \frac{ik^3}{4\pi}h_0^{(1)}\big(k|\boldsymbol{x}-\boldsymbol{y}|\big)\frac{\big((\boldsymbol{x}-\boldsymbol{y})\cdot\boldsymbol{n}_{\boldsymbol{x}}\big)\big((\boldsymbol{y}-\boldsymbol{x})\cdot\boldsymbol{n}_{\boldsymbol{y}}\big)}{|\boldsymbol{x}-\boldsymbol{y}|^2}.\end{aligned} \tag{E.70}$$

Its singularity, when $\boldsymbol{x}\to\boldsymbol{y}$ for $\boldsymbol{x},\boldsymbol{y}\in\Gamma$, expresses itself as

$$\frac{\partial^2 G}{\partial n_{\boldsymbol{x}}\partial n_{\boldsymbol{y}}}(\boldsymbol{x},\boldsymbol{y}) \sim -\frac{\boldsymbol{n}_{\boldsymbol{x}}\cdot\boldsymbol{n}_{\boldsymbol{y}}}{4\pi|\boldsymbol{y}-\boldsymbol{x}|^3} - \frac{3\big((\boldsymbol{x}-\boldsymbol{y})\cdot\boldsymbol{n}_{\boldsymbol{x}}\big)\big((\boldsymbol{y}-\boldsymbol{x})\cdot\boldsymbol{n}_{\boldsymbol{y}}\big)}{4\pi|\boldsymbol{y}-\boldsymbol{x}|^5}. \tag{E.71}$$

The regularizing effect of the normal derivatives applies only to its second term, but not to the first. Hence this kernel is hypersingular, with $\lambda = 3$, and it holds that

$$\frac{\partial^2 G}{\partial n_{\boldsymbol{x}}\partial n_{\boldsymbol{y}}}(\boldsymbol{x},\boldsymbol{y}) = \mathcal{O}\bigg(\frac{1}{|\boldsymbol{y}-\boldsymbol{x}|^3}\bigg). \tag{E.72}$$

The kernel is no longer integrable and the associated integral operator has to be thus interpreted in some appropriate sense as a divergent integral (cf., e.g., Hsiao & Wendland 2008, Lenoir 2005, Nédélec 2001).

E.6.4 Boundary layer potentials

We regard now the jump properties on the boundary Γ of the boundary layer potentials that have appeared in our calculations. For the development of the integral representation (E.59) we already made acquaintance with the single and double layer potentials,

which we define now more precisely for $\boldsymbol{x} \in \Omega_e \cup \Omega_i$ as the integral operators

$$\mathcal{S}\nu(\boldsymbol{x}) = \int_\Gamma G(\boldsymbol{x}, \boldsymbol{y})\nu(\boldsymbol{y})\,\mathrm{d}\gamma(\boldsymbol{y}), \tag{E.73}$$

$$\mathcal{D}\mu(\boldsymbol{x}) = \int_\Gamma \frac{\partial G}{\partial n_{\boldsymbol{y}}}(\boldsymbol{x}, \boldsymbol{y})\mu(\boldsymbol{y})\,\mathrm{d}\gamma(\boldsymbol{y}). \tag{E.74}$$

The integral representation (E.59) can be now stated in terms of the layer potentials as

$$u = \mathcal{D}\mu - \mathcal{S}\nu. \tag{E.75}$$

We remark that for any functions $\nu, \mu : \Gamma \to \mathbb{C}$ that are regular enough, the single and double layer potentials satisfy the Helmholtz equation, namely

$$(\Delta + k^2)\,\mathcal{S}\nu = 0 \qquad \text{in } \Omega_e \cup \Omega_i, \tag{E.76}$$

$$(\Delta + k^2)\,\mathcal{D}\mu = 0 \qquad \text{in } \Omega_e \cup \Omega_i. \tag{E.77}$$

For the integral equations (E.63) and (E.64), which are defined for $\boldsymbol{x} \in \Gamma$, we require the four boundary integral operators:

$$S\nu(\boldsymbol{x}) = \int_\Gamma G(\boldsymbol{x}, \boldsymbol{y})\nu(\boldsymbol{y})\,\mathrm{d}\gamma(\boldsymbol{y}), \tag{E.78}$$

$$D\mu(\boldsymbol{x}) = \int_\Gamma \frac{\partial G}{\partial n_{\boldsymbol{y}}}(\boldsymbol{x}, \boldsymbol{y})\mu(\boldsymbol{y})\,\mathrm{d}\gamma(\boldsymbol{y}), \tag{E.79}$$

$$D^*\nu(\boldsymbol{x}) = \int_\Gamma \frac{\partial G}{\partial n_{\boldsymbol{x}}}(\boldsymbol{x}, \boldsymbol{y})\nu(\boldsymbol{y})\,\mathrm{d}\gamma(\boldsymbol{y}), \tag{E.80}$$

$$N\mu(\boldsymbol{x}) = \int_\Gamma \frac{\partial^2 G}{\partial n_{\boldsymbol{x}} \partial n_{\boldsymbol{y}}}(\boldsymbol{x}, \boldsymbol{y})\mu(\boldsymbol{y})\,\mathrm{d}\gamma(\boldsymbol{y}). \tag{E.81}$$

The operator D^* is in fact the adjoint of the operator D. As we already mentioned, the kernel of the integral operator N defined in (E.81) is not integrable, yet we write it formally as an improper integral. An appropriate sense for this integral will be given below. The integral equations (E.63) and (E.64) can be now stated in terms of the integral operators as

$$\frac{1}{2}(u_e + u_i) = D\mu - S\nu, \tag{E.82}$$

$$\frac{1}{2}\left(\frac{\partial u_e}{\partial n} + \frac{\partial u_i}{\partial n}\right) = N\mu - D^*\nu. \tag{E.83}$$

These integral equations can be easily derived from the jump properties of the single and double layer potentials. The single layer potential (E.73) is continuous and its normal derivative has a jump of size $-\nu$ across Γ, i.e.,

$$\mathcal{S}\nu|_{\Omega_e} = S\nu = \mathcal{S}\nu|_{\Omega_i}, \tag{E.84}$$

$$\frac{\partial}{\partial n}\mathcal{S}\nu|_{\Omega_e} = \left(-\frac{1}{2} + D^*\right)\nu, \tag{E.85}$$

$$\frac{\partial}{\partial n}\mathcal{S}\nu|_{\Omega_i} = \left(\frac{1}{2} + D^*\right)\nu. \tag{E.86}$$

The double layer potential (E.74), on the other hand, has a jump of size μ across Γ and its normal derivative is continuous, namely

$$\mathcal{D}\mu|_{\Omega_e} = \left(\frac{1}{2} + D\right)\mu, \tag{E.87}$$

$$\mathcal{D}\mu|_{\Omega_i} = \left(-\frac{1}{2} + D\right)\mu, \tag{E.88}$$

$$\frac{\partial}{\partial n}\mathcal{D}\mu|_{\Omega_e} = N\mu = \frac{\partial}{\partial n}\mathcal{D}\mu|_{\Omega_i}. \tag{E.89}$$

The integral equation (E.82) is obtained directly either from (E.84) and (E.87), or from (E.84) and (E.88), by considering the appropriate trace of (E.75) and by defining the functions μ and ν as in (E.41). These three jump properties are easily proven by regarding the details of the proof for (E.63).

Similarly, the integral equation (E.83) for the normal derivative is obtained directly either from (E.85) and (E.89), or from (E.86) and (E.89), by considering the appropriate trace of the normal derivative of (E.75) and by defining again the functions μ and ν as in (E.41). The proof of the jump properties (E.85) and (E.86) is the same as for the Laplace equation, since the same singularities are involved, whereas the proof of (E.89) is similar, but with some differences, and is therefore replicated below.

a) Continuity of the normal derivative of the double layer potential

Differently as in the proof for the Laplace equation, in this case an additional term appears for the operator N, since it is the Helmholtz equation (E.77) that has to be considered in (D.86) and (D.87), yielding now for a test function $\varphi \in \mathcal{D}(\mathbb{R}^3)$ that

$$\left\langle \frac{\partial}{\partial n}\mathcal{D}\mu|_{\Omega_e},\, \varphi \right\rangle = \int_{\Omega_e} \nabla\mathcal{D}\mu(\boldsymbol{x}) \cdot \nabla\varphi(\boldsymbol{x})\,\mathrm{d}\boldsymbol{x} - k^2 \int_{\Omega_e} \mathcal{D}\mu(\boldsymbol{x})\,\varphi(\boldsymbol{x})\,\mathrm{d}\boldsymbol{x}, \tag{E.90}$$

$$\left\langle \frac{\partial}{\partial n}\mathcal{D}\mu|_{\Omega_i},\, \varphi \right\rangle = -\int_{\Omega_i} \nabla\mathcal{D}\mu(\boldsymbol{x}) \cdot \nabla\varphi(\boldsymbol{x})\,\mathrm{d}\boldsymbol{x} + k^2 \int_{\Omega_i} \mathcal{D}\mu(\boldsymbol{x})\,\varphi(\boldsymbol{x})\,\mathrm{d}\boldsymbol{x}. \tag{E.91}$$

From (A.588) and (E.31) we obtain the relation

$$\frac{\partial G}{\partial n_{\boldsymbol{y}}}(\boldsymbol{x},\boldsymbol{y}) = \boldsymbol{n_y} \cdot \nabla_{\boldsymbol{y}} G(\boldsymbol{x},\boldsymbol{y}) = -\boldsymbol{n_y} \cdot \nabla_{\boldsymbol{x}} G(\boldsymbol{x},\boldsymbol{y}) = -\operatorname{div}_{\boldsymbol{x}}\big(G(\boldsymbol{x},\boldsymbol{y})\boldsymbol{n_y}\big). \tag{E.92}$$

Thus for the double layer potential (E.74) we have that

$$\mathcal{D}\mu(\boldsymbol{x}) = -\operatorname{div}\int_\Gamma G(\boldsymbol{x},\boldsymbol{y})\mu(\boldsymbol{y})\boldsymbol{n_y}\,\mathrm{d}\gamma(\boldsymbol{y}) = -\operatorname{div}\mathcal{S}(\mu\,\boldsymbol{n_y})(\boldsymbol{x}), \tag{E.93}$$

being its gradient given by

$$\nabla\mathcal{D}\mu(\boldsymbol{x}) = -\nabla\operatorname{div}\int_\Gamma G(\boldsymbol{x},\boldsymbol{y})\mu(\boldsymbol{y})\boldsymbol{n_y}\,\mathrm{d}\gamma(\boldsymbol{y}). \tag{E.94}$$

From (A.589) we have that

$$\operatorname{curl}_{\boldsymbol{x}}\big(G(\boldsymbol{x},\boldsymbol{y})\boldsymbol{n}_{\boldsymbol{y}}\big) = \nabla_{\boldsymbol{x}} G(\boldsymbol{x},\boldsymbol{y}) \times \boldsymbol{n}_{\boldsymbol{y}}. \tag{E.95}$$

Hence, by considering (A.590), (E.77), and (E.95) in (E.94), we obtain that

$$\nabla \mathcal{D}\mu(\boldsymbol{x}) = \operatorname{curl} \int_\Gamma \big(\boldsymbol{n}_{\boldsymbol{y}} \times \nabla_{\boldsymbol{x}} G(\boldsymbol{x},\boldsymbol{y})\big)\mu(\boldsymbol{y})\,\mathrm{d}\gamma(\boldsymbol{y}) + k^2 \int_\Gamma G(\boldsymbol{x},\boldsymbol{y})\mu(\boldsymbol{y})\boldsymbol{n}_{\boldsymbol{y}}\,\mathrm{d}\gamma(\boldsymbol{y}). \tag{E.96}$$

From (E.31) and (A.658) we have that

$$\begin{aligned}\int_\Gamma \big(\boldsymbol{n}_{\boldsymbol{y}} \times \nabla_{\boldsymbol{x}} G(\boldsymbol{x},\boldsymbol{y})\big)\mu(\boldsymbol{y})\,\mathrm{d}\gamma(\boldsymbol{y}) &= -\int_\Gamma \boldsymbol{n}_{\boldsymbol{y}} \times \big(\nabla_{\boldsymbol{y}} G(\boldsymbol{x},\boldsymbol{y})\mu(\boldsymbol{y})\big)\,\mathrm{d}\gamma(\boldsymbol{y}) \\ &= \int_\Gamma \boldsymbol{n}_{\boldsymbol{y}} \times \big(G(\boldsymbol{x},\boldsymbol{y})\nabla\mu(\boldsymbol{y})\big)\,\mathrm{d}\gamma(\boldsymbol{y}),\end{aligned} \tag{E.97}$$

and consequently

$$\nabla \mathcal{D}\mu(\boldsymbol{x}) = \operatorname{curl} \int_\Gamma G(\boldsymbol{x},\boldsymbol{y})\big(\boldsymbol{n}_{\boldsymbol{y}} \times \nabla\mu(\boldsymbol{y})\big)\,\mathrm{d}\gamma(\boldsymbol{y}) + k^2 \int_\Gamma G(\boldsymbol{x},\boldsymbol{y})\mu(\boldsymbol{y})\boldsymbol{n}_{\boldsymbol{y}}\,\mathrm{d}\gamma(\boldsymbol{y}). \tag{E.98}$$

Now, the first expression in (E.90), due (A.596), (A.618), and (E.98), is given by

$$\begin{aligned}\int_{\Omega_e} \nabla \mathcal{D}\mu(\boldsymbol{x}) \cdot \nabla\varphi(\boldsymbol{x})\,\mathrm{d}\boldsymbol{x} = &-\int_\Gamma \int_\Gamma G(\boldsymbol{x},\boldsymbol{y})\big(\nabla\mu(\boldsymbol{y}) \times \boldsymbol{n}_{\boldsymbol{y}}\big) \cdot \big(\nabla\varphi(\boldsymbol{x}) \times \boldsymbol{n}_{\boldsymbol{x}}\big)\,\mathrm{d}\gamma(\boldsymbol{y})\,\mathrm{d}\gamma(\boldsymbol{x}) \\ &+ k^2 \int_{\Omega_e} \left(\int_\Gamma G(\boldsymbol{x},\boldsymbol{y})\mu(\boldsymbol{y})\boldsymbol{n}_{\boldsymbol{y}}\,\mathrm{d}\gamma(\boldsymbol{y})\right) \cdot \nabla\varphi(\boldsymbol{x})\,\mathrm{d}\boldsymbol{x}.\end{aligned} \tag{E.99}$$

Applying (A.614) on the second term of (E.99) and considering (E.93), yields

$$\begin{aligned}\int_{\Omega_e} \nabla \mathcal{D}\mu(\boldsymbol{x}) \cdot \nabla\varphi(\boldsymbol{x})\,\mathrm{d}\boldsymbol{x} = &-\int_\Gamma \int_\Gamma G(\boldsymbol{x},\boldsymbol{y})\big(\nabla\mu(\boldsymbol{y}) \times \boldsymbol{n}_{\boldsymbol{y}}\big) \cdot \big(\nabla\varphi(\boldsymbol{x}) \times \boldsymbol{n}_{\boldsymbol{x}}\big)\,\mathrm{d}\gamma(\boldsymbol{y})\mathrm{d}\gamma(\boldsymbol{x}) \\ &+ k^2 \int_{\Omega_e} \mathcal{D}\mu(\boldsymbol{x})\,\varphi(\boldsymbol{x})\,\mathrm{d}\boldsymbol{x} + \int_\Gamma \int_\Gamma G(\boldsymbol{x},\boldsymbol{y})\mu(\boldsymbol{y})\varphi(\boldsymbol{x})(\boldsymbol{n}_{\boldsymbol{y}} \cdot \boldsymbol{n}_{\boldsymbol{x}})\,\mathrm{d}\gamma(\boldsymbol{y})\,\mathrm{d}\gamma(\boldsymbol{x}).\end{aligned} \tag{E.100}$$

By replacing (E.100) in (E.90) we obtain finally that

$$\begin{aligned}\left\langle \frac{\partial}{\partial n}\mathcal{D}\mu|_{\Omega_e},\, \varphi \right\rangle = &-\int_\Gamma \int_\Gamma G(\boldsymbol{x},\boldsymbol{y})\big(\nabla\mu(\boldsymbol{y}) \times \boldsymbol{n}_{\boldsymbol{y}}\big) \cdot \big(\nabla\varphi(\boldsymbol{x}) \times \boldsymbol{n}_{\boldsymbol{x}}\big)\,\mathrm{d}\gamma(\boldsymbol{y})\,\mathrm{d}\gamma(\boldsymbol{x}) \\ &+ k^2 \int_\Gamma \int_\Gamma G(\boldsymbol{x},\boldsymbol{y})\mu(\boldsymbol{y})\varphi(\boldsymbol{x})(\boldsymbol{n}_{\boldsymbol{y}} \cdot \boldsymbol{n}_{\boldsymbol{x}})\,\mathrm{d}\gamma(\boldsymbol{y})\,\mathrm{d}\gamma(\boldsymbol{x}).\end{aligned} \tag{E.101}$$

The analogous development for (E.91) yields

$$\begin{aligned}\left\langle \frac{\partial}{\partial n}\mathcal{D}\mu|_{\Omega_i},\, \varphi \right\rangle = &-\int_\Gamma \int_\Gamma G(\boldsymbol{x},\boldsymbol{y})\big(\nabla\mu(\boldsymbol{y}) \times \boldsymbol{n}_{\boldsymbol{y}}\big) \cdot \big(\nabla\varphi(\boldsymbol{x}) \times \boldsymbol{n}_{\boldsymbol{x}}\big)\,\mathrm{d}\gamma(\boldsymbol{y})\,\mathrm{d}\gamma(\boldsymbol{x}) \\ &+ k^2 \int_\Gamma \int_\Gamma G(\boldsymbol{x},\boldsymbol{y})\mu(\boldsymbol{y})\varphi(\boldsymbol{x})(\boldsymbol{n}_{\boldsymbol{y}} \cdot \boldsymbol{n}_{\boldsymbol{x}})\,\mathrm{d}\gamma(\boldsymbol{y})\,\mathrm{d}\gamma(\boldsymbol{x}).\end{aligned} \tag{E.102}$$

This concludes the proof of (E.89), and shows that the integral operator (E.81) is properly defined in a weak sense for $\varphi \in \mathcal{D}(\mathbb{R}^3)$, instead of (D.97), by

$$\langle N\mu(\boldsymbol{x}),\, \varphi\rangle = -\int_\Gamma\int_\Gamma G(\boldsymbol{x},\boldsymbol{y})\big(\nabla\mu(\boldsymbol{y})\times\boldsymbol{n}_{\boldsymbol{y}}\big)\cdot\big(\nabla\varphi(\boldsymbol{x})\times\boldsymbol{n}_{\boldsymbol{x}}\big)\,\mathrm{d}\gamma(\boldsymbol{y})\,\mathrm{d}\gamma(\boldsymbol{x}) + k^2\int_\Gamma\int_\Gamma G(\boldsymbol{x},\boldsymbol{y})\mu(\boldsymbol{y})\varphi(\boldsymbol{x})(\boldsymbol{n}_{\boldsymbol{y}}\cdot\boldsymbol{n}_{\boldsymbol{x}})\,\mathrm{d}\gamma(\boldsymbol{y})\,\mathrm{d}\gamma(\boldsymbol{x}). \tag{E.103}$$

E.6.5 Alternatives for integral representations and equations

By taking into account the transmission problem (E.41), its integral representation formula (E.58), and its integral equations (E.63) and (E.64), several particular alternatives for integral representations and equations of the exterior problem (E.13) can be developed. The way to perform this is to extend properly the exterior problem towards the interior domain Ω_i, either by specifying explicitly this extension or by defining an associated interior problem, so as to become the desired jump properties across Γ. The extension has to satisfy the Helmholtz equation (E.1) in Ω_i and a boundary condition that corresponds adequately to the impedance boundary condition (E.3). The obtained system of integral representations and equations allows finally to solve the exterior problem (E.13), by using the solution of the integral equation in the integral representation formula.

a) Extension by zero

An extension by zero towards the interior domain Ω_i implies that

$$u_i = 0 \qquad \text{in } \Omega_i. \tag{E.104}$$

The jumps over Γ are characterized in this case by

$$[u] = u_e = \mu, \tag{E.105}$$

$$\left[\frac{\partial u}{\partial n}\right] = \frac{\partial u_e}{\partial n} = Zu_e - f_z = Z\mu - f_z, \tag{E.106}$$

where $\mu : \Gamma \to \mathbb{C}$ is a function to be determined.

An integral representation formula of the solution, for $\boldsymbol{x} \in \Omega_e \cup \Omega_i$, is given by

$$u(\boldsymbol{x}) = \int_\Gamma \left(\frac{\partial G}{\partial n_{\boldsymbol{y}}}(\boldsymbol{x},\boldsymbol{y}) - Z(\boldsymbol{y})G(\boldsymbol{x},\boldsymbol{y})\right)\mu(\boldsymbol{y})\,\mathrm{d}\gamma(\boldsymbol{y}) + \int_\Gamma G(\boldsymbol{x},\boldsymbol{y})f_z(\boldsymbol{y})\,\mathrm{d}\gamma(\boldsymbol{y}). \tag{E.107}$$

Since

$$\frac{1}{2}\big(u_e(\boldsymbol{x}) + u_i(\boldsymbol{x})\big) = \frac{\mu(\boldsymbol{x})}{2}, \qquad \boldsymbol{x} \in \Gamma, \tag{E.108}$$

we obtain, for $\boldsymbol{x} \in \Gamma$, the Fredholm integral equation of the second kind

$$\frac{\mu(\boldsymbol{x})}{2} + \int_\Gamma \left(Z(\boldsymbol{y})G(\boldsymbol{x},\boldsymbol{y}) - \frac{\partial G}{\partial n_{\boldsymbol{y}}}(\boldsymbol{x},\boldsymbol{y})\right)\mu(\boldsymbol{y})\,\mathrm{d}\gamma(\boldsymbol{y}) = \int_\Gamma G(\boldsymbol{x},\boldsymbol{y})f_z(\boldsymbol{y})\,\mathrm{d}\gamma(\boldsymbol{y}), \tag{E.109}$$

which has to be solved for the unknown μ. In terms of boundary layer potentials, the integral representation and the integral equation can be respectively expressed by

$$u = \mathcal{D}(\mu) - \mathcal{S}(Z\mu) + \mathcal{S}(f_z) \qquad \text{in } \Omega_e \cup \Omega_i, \tag{E.110}$$

$$\frac{\mu}{2} + S(Z\mu) - D(\mu) = S(f_z) \qquad \text{on } \Gamma. \tag{E.111}$$

Alternatively, since

$$\frac{1}{2}\left(\frac{\partial u_e}{\partial n}(\boldsymbol{x}) + \frac{\partial u_i}{\partial n}(\boldsymbol{x})\right) = \frac{Z(\boldsymbol{x})}{2}\mu(\boldsymbol{x}) - \frac{f_z(\boldsymbol{x})}{2}, \qquad \boldsymbol{x} \in \Gamma, \tag{E.112}$$

we obtain also, for $\boldsymbol{x} \in \Gamma$, the Fredholm integral equation of the second kind

$$\begin{aligned}\frac{Z(\boldsymbol{x})}{2}\mu(\boldsymbol{x}) + \int_\Gamma \left(-\frac{\partial^2 G}{\partial n_{\boldsymbol{x}} \partial n_{\boldsymbol{y}}}(\boldsymbol{x},\boldsymbol{y}) + Z(\boldsymbol{y})\frac{\partial G}{\partial n_{\boldsymbol{x}}}(\boldsymbol{x},\boldsymbol{y})\right)\mu(\boldsymbol{y})\,\mathrm{d}\gamma(\boldsymbol{y}) \\ = \frac{f_z(\boldsymbol{x})}{2} + \int_\Gamma \frac{\partial G}{\partial n_{\boldsymbol{x}}}(\boldsymbol{x},\boldsymbol{y}) f_z(\boldsymbol{y})\,\mathrm{d}\gamma(\boldsymbol{y}),\end{aligned} \tag{E.113}$$

which in terms of boundary layer potentials becomes

$$\frac{Z}{2}\mu - N(\mu) + D^*(Z\mu) = \frac{f_z}{2} + D^*(f_z) \qquad \text{on } \Gamma. \tag{E.114}$$

b) Continuous impedance

We associate to (E.13) the interior problem

$$\begin{cases} \text{Find } u_i : \Omega_i \to \mathbb{C} \text{ such that} \\ \Delta u_i + k^2 u_i = 0 \qquad \text{in } \Omega_i, \\ -\dfrac{\partial u_i}{\partial n} + Z u_i = f_z \qquad \text{on } \Gamma. \end{cases} \tag{E.115}$$

The jumps over Γ are characterized in this case by

$$[u] = u_e - u_i = \mu, \tag{E.116}$$

$$\left[\frac{\partial u}{\partial n}\right] = \frac{\partial u_e}{\partial n} - \frac{\partial u_i}{\partial n} = Z(u_e - u_i) = Z\mu, \tag{E.117}$$

where $\mu : \Gamma \to \mathbb{C}$ is a function to be determined. In particular it holds that the jump of the impedance is zero, namely

$$\left[-\frac{\partial u}{\partial n} + Zu\right] = \left(-\frac{\partial u_e}{\partial n} + Z u_e\right) - \left(-\frac{\partial u_i}{\partial n} + Z u_i\right) = 0. \tag{E.118}$$

An integral representation formula of the solution, for $\boldsymbol{x} \in \Omega_e \cup \Omega_i$, is given by

$$u(\boldsymbol{x}) = \int_\Gamma \left(\frac{\partial G}{\partial n_{\boldsymbol{y}}}(\boldsymbol{x},\boldsymbol{y}) - Z(\boldsymbol{y})G(\boldsymbol{x},\boldsymbol{y})\right)\mu(\boldsymbol{y})\,\mathrm{d}\gamma(\boldsymbol{y}). \tag{E.119}$$

Since

$$-\frac{1}{2}\left(\frac{\partial u_e}{\partial n}(\boldsymbol{x}) + \frac{\partial u_i}{\partial n}(\boldsymbol{x})\right) + \frac{Z(\boldsymbol{x})}{2}\big(u_e(\boldsymbol{x}) + u_i(\boldsymbol{x})\big) = f_z(\boldsymbol{x}), \qquad \boldsymbol{x} \in \Gamma, \tag{E.120}$$

we obtain, for $\boldsymbol{x} \in \Gamma$, the Fredholm integral equation of the first kind

$$\int_\Gamma \left(-\frac{\partial^2 G}{\partial n_{\boldsymbol{x}} \partial n_{\boldsymbol{y}}}(\boldsymbol{x},\boldsymbol{y}) + Z(\boldsymbol{y}) \frac{\partial G}{\partial n_{\boldsymbol{x}}}(\boldsymbol{x},\boldsymbol{y}) \right) \mu(\boldsymbol{y}) \, \mathrm{d}\gamma(\boldsymbol{y}) + Z(\boldsymbol{x}) \int_\Gamma \left(\frac{\partial G}{\partial n_{\boldsymbol{y}}}(\boldsymbol{x},\boldsymbol{y}) - Z(\boldsymbol{y}) G(\boldsymbol{x},\boldsymbol{y}) \right) \mu(\boldsymbol{y}) \, \mathrm{d}\gamma(\boldsymbol{y}) = f_z(\boldsymbol{x}), \quad \text{(E.121)}$$

which has to be solved for the unknown μ. In terms of boundary layer potentials, the integral representation and the integral equation can be respectively expressed by

$$u = \mathcal{D}(\mu) - \mathcal{S}(Z\mu) \qquad \text{in } \Omega_e \cup \Omega_i, \quad \text{(E.122)}$$

$$-N(\mu) + D^*(Z\mu) + ZD(\mu) - ZS(Z\mu) = f_z \qquad \text{on } \Gamma. \quad \text{(E.123)}$$

We observe that the integral equation (E.123) is self-adjoint.

c) Continuous value

We associate to (E.13) the interior problem

$$\begin{cases} \text{Find } u_i : \Omega_i \to \mathbb{C} \text{ such that} \\ \Delta u_i + k^2 u_i = 0 & \text{in } \Omega_i, \\ -\dfrac{\partial u_e}{\partial n} + Z u_i = f_z & \text{on } \Gamma. \end{cases} \quad \text{(E.124)}$$

The jumps over Γ are characterized in this case by

$$[u] = u_e - u_i = \frac{1}{Z}\left(\frac{\partial u_e}{\partial n} - f_z \right) - \frac{1}{Z}\left(\frac{\partial u_e}{\partial n} - f_z \right) = 0, \quad \text{(E.125)}$$

$$\left[\frac{\partial u}{\partial n} \right] = \frac{\partial u_e}{\partial n} - \frac{\partial u_i}{\partial n} = \nu, \quad \text{(E.126)}$$

where $\nu : \Gamma \to \mathbb{C}$ is a function to be determined.

An integral representation formula of the solution, for $\boldsymbol{x} \in \Omega_e \cup \Omega_i$, is given by the single layer potential

$$u(\boldsymbol{x}) = -\int_\Gamma G(\boldsymbol{x},\boldsymbol{y}) \nu(\boldsymbol{y}) \, \mathrm{d}\gamma(\boldsymbol{y}). \quad \text{(E.127)}$$

Since

$$-\frac{1}{2}\left(\frac{\partial u_e}{\partial n}(\boldsymbol{x}) + \frac{\partial u_i}{\partial n}(\boldsymbol{x}) \right) + \frac{Z(\boldsymbol{x})}{2}\big(u_e(\boldsymbol{x}) + u_i(\boldsymbol{x}) \big) = \frac{\nu(\boldsymbol{x})}{2} + f_z(\boldsymbol{x}), \quad \boldsymbol{x} \in \Gamma, \quad \text{(E.128)}$$

we obtain, for $\boldsymbol{x} \in \Gamma$, the Fredholm integral equation of the second kind

$$-\frac{\nu(\boldsymbol{x})}{2} + \int_\Gamma \left(\frac{\partial G}{\partial n_{\boldsymbol{x}}}(\boldsymbol{x},\boldsymbol{y}) - Z(\boldsymbol{x}) G(\boldsymbol{x},\boldsymbol{y}) \right) \nu(\boldsymbol{y}) \, \mathrm{d}\gamma(\boldsymbol{y}) = f_z(\boldsymbol{x}), \quad \text{(E.129)}$$

which has to be solved for the unknown ν. In terms of boundary layer potentials, the integral representation and the integral equation can be respectively expressed by

$$u = -\mathcal{S}(\nu) \qquad \text{in } \Omega_e \cup \Omega_i, \quad \text{(E.130)}$$

$$\frac{\nu}{2} + ZS(\nu) - D^*(\nu) = -f_z \qquad \text{on } \Gamma. \quad \text{(E.131)}$$

We observe that the integral equation (E.131) is mutually adjoint with (E.111).

d) Continuous normal derivative

We associate to (E.13) the interior problem

$$\begin{cases} \text{Find } u_i : \Omega_i \to \mathbb{C} \text{ such that} \\ \Delta u_i + k^2 u_i = 0 & \text{in } \Omega_i, \\ -\dfrac{\partial u_i}{\partial n} + Z u_e = f_z & \text{on } \Gamma. \end{cases} \tag{E.132}$$

The jumps over Γ are characterized in this case by

$$[u] = u_e - u_i = \mu, \tag{E.133}$$

$$\left[\frac{\partial u}{\partial n}\right] = \frac{\partial u_e}{\partial n} - \frac{\partial u_i}{\partial n} = \big(Z u_e - f_z\big) - \big(Z u_e - f_z\big) = 0, \tag{E.134}$$

where $\mu : \Gamma \to \mathbb{C}$ is a function to be determined.

An integral representation formula of the solution, for $\boldsymbol{x} \in \Omega_e \cup \Omega_i$, is given by the double layer potential

$$u(\boldsymbol{x}) = \int_\Gamma \frac{\partial G}{\partial n_{\boldsymbol{y}}}(\boldsymbol{x}, \boldsymbol{y}) \mu(\boldsymbol{y}) \, \mathrm{d}\gamma(\boldsymbol{y}). \tag{E.135}$$

Since when $\boldsymbol{x} \in \Gamma$,

$$-\frac{1}{2}\left(\frac{\partial u_e}{\partial n}(\boldsymbol{x}) + \frac{\partial u_i}{\partial n}(\boldsymbol{x})\right) + \frac{Z(\boldsymbol{x})}{2}\big(u_e(\boldsymbol{x}) + u_i(\boldsymbol{x})\big) = -\frac{Z(\boldsymbol{x})}{2}\mu(\boldsymbol{x}) + f_z(\boldsymbol{x}), \tag{E.136}$$

we obtain, for $\boldsymbol{x} \in \Gamma$, the Fredholm integral equation of the second kind

$$\frac{Z(\boldsymbol{x})}{2}\mu(\boldsymbol{x}) + \int_\Gamma \left(-\frac{\partial^2 G}{\partial n_{\boldsymbol{x}} \partial n_{\boldsymbol{y}}}(\boldsymbol{x}, \boldsymbol{y}) + Z(\boldsymbol{x}) \frac{\partial G}{\partial n_{\boldsymbol{y}}}(\boldsymbol{x}, \boldsymbol{y})\right) \mu(\boldsymbol{y}) \, \mathrm{d}\gamma(\boldsymbol{y}) = f_z(\boldsymbol{x}), \tag{E.137}$$

which has to be solved for the unknown μ. In terms of boundary layer potentials, the integral representation and the integral equation can be respectively expressed by

$$u = \mathcal{D}(\mu) \qquad \text{in } \Omega_e \cup \Omega_i, \tag{E.138}$$

$$\frac{Z}{2}\mu - N(\mu) + Z D(\mu) = f_z \qquad \text{on } \Gamma. \tag{E.139}$$

We observe that the integral equation (E.139) is mutually adjoint with (E.114).

E.7 Far field of the solution

The asymptotic behavior at infinity of the solution u of (E.13) is described by the far field u^{ff}. Its expression can be deduced by replacing the far field of the Green's function G^{ff} and its derivatives in the integral representation formula (E.58), which yields

$$u^{ff}(\boldsymbol{x}) = \int_\Gamma \left([u](\boldsymbol{y}) \frac{\partial G^{ff}}{\partial n_{\boldsymbol{y}}}(\boldsymbol{x}, \boldsymbol{y}) - G^{ff}(\boldsymbol{x}, \boldsymbol{y}) \left[\frac{\partial u}{\partial n}\right](\boldsymbol{y})\right) \mathrm{d}\gamma(\boldsymbol{y}). \tag{E.140}$$

By replacing now (E.36) and (E.37) in (E.140), we have that the far field of the solution is

$$u^{ff}(\boldsymbol{x}) = \frac{e^{ik|\boldsymbol{x}|}}{4\pi|\boldsymbol{x}|} \int_\Gamma e^{-ik\hat{\boldsymbol{x}}\cdot\boldsymbol{y}} \left(ik\hat{\boldsymbol{x}} \cdot \boldsymbol{n}_{\boldsymbol{y}} \, [u](\boldsymbol{y}) + \left[\frac{\partial u}{\partial n}\right](\boldsymbol{y})\right) \mathrm{d}\gamma(\boldsymbol{y}). \tag{E.141}$$

The asymptotic behavior of the solution u at infinity is therefore given by

$$u(\boldsymbol{x}) = \frac{e^{ik|\boldsymbol{x}|}}{|\boldsymbol{x}|}\left\{u_\infty(\hat{\boldsymbol{x}}) + \mathcal{O}\left(\frac{1}{|\boldsymbol{x}|}\right)\right\}, \qquad |\boldsymbol{x}| \to \infty, \tag{E.142}$$

uniformly in all directions $\hat{\boldsymbol{x}}$ on the unit sphere, where

$$u_\infty(\hat{\boldsymbol{x}}) = \frac{1}{4\pi}\int_\Gamma e^{-ik\hat{\boldsymbol{x}}\cdot\boldsymbol{y}}\left(ik\hat{\boldsymbol{x}}\cdot\boldsymbol{n}_{\boldsymbol{y}}\,[u](\boldsymbol{y}) + \left[\frac{\partial u}{\partial n}\right](\boldsymbol{y})\right)\mathrm{d}\gamma(\boldsymbol{y}) \tag{E.143}$$

is called the far-field pattern of u. It can be expressed in decibels (dB) by means of the scattering cross section

$$Q_s(\hat{\boldsymbol{x}}) \;\; [\text{dB}] = 20\log_{10}\left(\frac{|u_\infty(\hat{\boldsymbol{x}})|}{|u_0|}\right), \tag{E.144}$$

where the reference level u_0 is typically taken as $u_0 = u_I$ when the incident field is given by a plane wave of the form (E.5), i.e., $|u_0| = 1$.

We remark that the far-field behavior (E.142) of the solution is in accordance with the Sommerfeld radiation condition (E.8), which justifies its choice.

E.8 Exterior sphere problem

To understand better the resolution of the direct scattering problem (E.13), we study now the particular case when the domain $\Omega_e \subset \mathbb{R}^3$ is taken as the exterior of a sphere of radius $R > 0$. The interior of the sphere is then given by $\Omega_i = \{\boldsymbol{x} \in \mathbb{R}^3 : |\boldsymbol{x}| < R\}$ and its boundary by $\Gamma = \partial\Omega_e$, as shown in Figure E.3. We place the origin at the center of Ω_i and we consider that the unit normal $\boldsymbol{n}$ is taken outwardly oriented of Ω_e, i.e., $\boldsymbol{n} = -\boldsymbol{r}$.

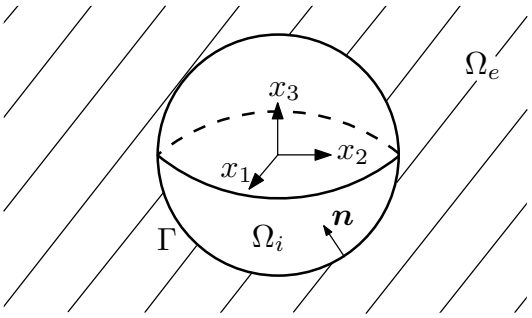

FIGURE E.3. Exterior of the sphere.

The exterior sphere problem is then stated as

$$\begin{cases} \text{Find } u : \Omega_e \to \mathbb{C} \text{ such that} \\ \Delta u + k^2 u = 0 \qquad \text{in } \Omega_e, \\ \dfrac{\partial u}{\partial r} + Zu = f_z \qquad \text{on } \Gamma, \\ \text{+ Outgoing Radiation condition as } |\boldsymbol{x}| \to \infty, \end{cases} \tag{E.145}$$

where we consider a constant impedance $Z \in \mathbb{C}$, a wave number $k > 0$, and where the radiation condition is as usual given by (E.8). As the incident field u_I we consider a plane wave in the form of (E.5), in which case the impedance data function f_z is given by

$$f_z = -\frac{\partial u_I}{\partial r} - Z u_I \qquad \text{on } \Gamma. \tag{E.146}$$

Due the particular chosen geometry, the solution u of (E.145) can be easily found analytically by using the method of variable separation, i.e., by supposing that

$$u(\boldsymbol{x}) = u(r, \theta, \varphi) = h(r)g(\theta)f(\varphi), \tag{E.147}$$

where the radius $r \geq 0$, the polar angle $0 \leq \theta \leq \pi$, and the azimuthal angle $-\pi < \varphi \leq \pi$ denote the spherical coordinates in $\mathbb{R}^3$. If the Helmholtz equation in (E.145) is expressed using spherical coordinates, then

$$\Delta u + k^2 u = \frac{1}{r}\frac{\partial^2}{\partial r^2}(ru) + \frac{1}{r^2 \sin\theta}\frac{\partial}{\partial\theta}\left(\sin\theta \frac{\partial u}{\partial\theta}\right) + \frac{1}{r^2\sin^2\theta}\frac{\partial^2 u}{\partial\varphi^2} + k^2 u = 0. \tag{E.148}$$

By replacing now (E.147) in (E.148) we obtain

$$\begin{aligned} h''(r)g(\theta)f(\varphi) + \frac{2}{r}h'(r)g(\theta)f(\varphi) + \frac{h(r)f(\varphi)}{r^2\sin\theta}\frac{\mathrm{d}}{\mathrm{d}\theta}\left(\sin\theta\frac{\mathrm{d}g}{\mathrm{d}\theta}(\theta)\right) \\ + \frac{h(r)g(\theta)f''(\varphi)}{r^2\sin^2\theta} + k^2 h(r)g(\theta)f(\varphi) = 0. \end{aligned} \tag{E.149}$$

Multiplying by $r^2\sin^2\theta$, dividing by hgf, and rearranging yields

$$r^2\sin^2\theta\left[\frac{h''(r)}{h(r)} + \frac{2}{r}\frac{h'(r)}{h(r)} + \frac{1}{g(\theta)r^2\sin\theta}\frac{\mathrm{d}}{\mathrm{d}\theta}\left(\sin\theta\frac{\mathrm{d}g}{\mathrm{d}\theta}(\theta)\right) + k^2\right] + \frac{f''(\varphi)}{f(\varphi)} = 0. \tag{E.150}$$

The dependence on φ has now been isolated in the last term. Consequently this term must be equal to a constant, which for convenience we denote by $-m^2$, i.e.,

$$\frac{f''(\varphi)}{f(\varphi)} = -m^2. \tag{E.151}$$

The solution of (E.151), up to a multiplicative constant, is of the form

$$f(\varphi) = e^{\pm im\varphi}. \tag{E.152}$$

For $f(\varphi)$ to be single-valued, m must be an integer if the full azimuthal range is allowed. By similar considerations we find the following separate equations for $g(\theta)$ and $h(r)$:

$$\frac{1}{\sin\theta}\frac{\mathrm{d}}{\mathrm{d}\theta}\left(\sin\theta\frac{\mathrm{d}g}{\mathrm{d}\theta}(\theta)\right) + \left(l(l+1) - \frac{m^2}{\sin^2\theta}\right)g(\theta) = 0, \tag{E.153}$$

$$r^2 h''(r) + 2rh'(r) + \big(k^2r^2 - l(l+1)\big)h(r) = 0, \tag{E.154}$$

where $l(l+1)$ is another conveniently denoted real constant. For the equation of the polar angle θ we consider the change of variables $x = \cos\theta$. In this case (E.153) turns into

$$\frac{\mathrm{d}}{\mathrm{d}x}\left((1-x^2)\frac{\mathrm{d}g}{\mathrm{d}x}(x)\right) + \left(l(l+1) - \frac{m^2}{1-x^2}\right)g(x) = 0, \tag{E.155}$$

which corresponds to the generalized or associated Legendre differential equation (A.323), whose solutions on the interval $-1 \leq x \leq 1$ are the associated Legendre functions P_l^m and Q_l^m, which are characterized respectively by (A.330) and (A.331). If the solution is to be single-valued, finite, and continuous in $-1 \leq x \leq 1$, then we have to exclude the solutions Q_l^m, take l as a positive integer or zero, and admit for the integer m only the values $-l, -(l-1), \ldots, 0, \ldots, (l-1), l$. The solution of (E.153), up to an arbitrary multiplicative constant, is therefore given by

$$g(\theta) = P_l^m(\cos\theta). \tag{E.156}$$

As for the Laplace equation, we combine the angular factors $g(\theta)$ and $f(\varphi)$ into the spherical harmonics $Y_l^m(\theta, \varphi)$, which are defined in (A.380). For the radial equation (E.154) we consider the change of variables $z = kr$ and express $\psi(z) = h(r)$, which yields the spherical Bessel differential equation of order l, namely

$$z^2\psi''(z) + 2z\psi'(z) + \big(z^2 - l(l+1)\big)\psi(z) = 0. \tag{E.157}$$

The independent solutions of (E.157) are $h_l^{(1)}(z)$ and $h_l^{(2)}(z)$, the spherical Hankel functions of order l, and therefore the solutions of (E.154) have the general form

$$h(r) = a_l\, h_l^{(1)}(kr) + b_l\, h_l^{(2)}(kr), \qquad l \geq 0, \tag{E.158}$$

where $a_l, b_l \in \mathbb{C}$ are arbitrary constants. The general solution for the Helmholtz equation considers the linear combination of all the solutions in the form (E.147), namely

$$u(r, \theta, \varphi) = \sum_{l=0}^{\infty} \sum_{m=-l}^{l} \big(A_{lm}\, h_l^{(1)}(kr) + B_{lm}\, h_l^{(2)}(kr)\big)\, Y_l^m(\theta, \varphi), \tag{E.159}$$

for some undetermined arbitrary constants $A_{lm}, B_{lm} \in \mathbb{C}$. The radiation condition (E.8) implies that

$$B_{lm} = 0, \quad -l \leq m \leq l, \quad l \geq 0. \tag{E.160}$$

Thus the general solution (E.159) turns into

$$u(r, \theta, \varphi) = \sum_{l=0}^{\infty} \sum_{m=-l}^{l} A_{lm}\, h_l^{(1)}(kr)\, Y_l^m(\theta, \varphi). \tag{E.161}$$

Due the recurrence relation (A.216), the radial derivative of (E.161) is given by

$$\frac{\partial u}{\partial r}(r, \theta, \varphi) = \sum_{l=0}^{\infty} \sum_{m=-l}^{l} A_{lm} \left(\frac{l}{r} h_l^{(1)}(kr) - k h_{l+1}^{(1)}(kr) \right) Y_l^m(\theta, \varphi). \tag{E.162}$$

The constants A_{lm} in (E.161) are determined through the impedance boundary condition on Γ. For this purpose, we expand the impedance data function f_z into spherical harmonics:

$$f_z(\theta, \varphi) = \sum_{l=0}^{\infty} \sum_{m=-l}^{l} f_{lm}\, Y_l^m(\theta, \varphi), \qquad 0 \leq \theta \leq \pi, \;\; -\pi < \varphi \leq \pi, \tag{E.163}$$

where

$$f_{lm} = \int_{-\pi}^{\pi} \int_{0}^{\pi} f_z(\theta, \varphi)\, \overline{Y_l^m(\theta, \varphi)} \sin\theta \, \mathrm{d}\theta \, \mathrm{d}\varphi, \quad m \in \mathbb{Z}, \;\; -l \leq m \leq l. \tag{E.164}$$

In particular, for a plane wave in the form of (E.5) we have the Jacobi-Anger expansion

$$u_I(\boldsymbol{x}) = e^{i\boldsymbol{k}\cdot\boldsymbol{x}} = 4\pi \sum_{l=0}^{\infty} i^l j_l(kr) \sum_{m=-l}^{l} \overline{Y_l^m(\theta_P, \varphi_P)}\, Y_l^m(\theta, \varphi), \tag{E.165}$$

where j_l is the spherical Bessel function of order l, and where $\theta_P = \pi - \theta_I$ and $\varphi_P = \varphi_I - \pi$ are the propagation angles of the plane wave, i.e., of the wave vector $\boldsymbol{k}$. We observe that the expression (E.165) can be also written in a more compact manner by using the addition theorem (A.389) and eventually also the relation (A.385). For a plane wave, the impedance data function (E.146) can be thus expressed as

$$f_z(\theta) = -4\pi \sum_{l=0}^{\infty} i^l \left(\left(Z + \frac{l}{R} \right) j_l(kR) - k j_{l+1}(kR) \right) \sum_{m=-l}^{l} \overline{Y_l^m(\theta_P, \varphi_P)}\, Y_l^m(\theta, \varphi), \tag{E.166}$$

which implies that

$$f_{lm} = -4\pi i^l \left(\left(Z + \frac{l}{R} \right) j_l(kR) - k j_{l+1}(kR) \right) \overline{Y_l^m(\theta_P, \varphi_P)}. \tag{E.167}$$

The impedance boundary condition takes therefore the form

$$\sum_{l=0}^{\infty} \sum_{m=-l}^{l} A_{lm} \left(\left(Z + \frac{l}{R} \right) h_l^{(1)}(kR) - k h_{l+1}^{(1)}(kR) \right) Y_l^m(\theta, \varphi) = \sum_{l=0}^{\infty} \sum_{m=-l}^{l} f_{lm}\, Y_l^m(\theta, \varphi). \tag{E.168}$$

We observe that the constants A_{lm} can be uniquely determined only if

$$\left(Z + \frac{l}{R} \right) h_l^{(1)}(kR) - k h_{l+1}^{(1)}(kR) \neq 0 \qquad \text{for } \; l \in \mathbb{N}_0. \tag{E.169}$$

If this condition is not fulfilled, then the solution is no longer unique. The values $k, Z \in \mathbb{C}$ for which this occurs form a countable set. In particular, for a fixed k, the impedances Z which do not fulfill (E.169) can be explicitly characterized by

$$Z = k \frac{h_{l+1}^{(1)}(kR)}{h_l^{(1)}(kR)} - \frac{l}{R} \qquad \text{for } \; l \in \mathbb{N}_0. \tag{E.170}$$

The wave numbers k which do not fulfill (E.169), for a fixed Z, can only be characterized implicitly through the relation

$$\left(Z + \frac{l}{R} \right) h_l^{(1)}(kR) - k h_{l+1}^{(1)}(kR) = 0 \qquad \text{for } \; l \in \mathbb{N}_0. \tag{E.171}$$

If we suppose now that (E.169) takes place, then

$$A_{lm} = \frac{R f_{lm}}{(ZR + l)\, h_l^{(1)}(kR) - kR\, h_{l+1}^{(1)}(kR)}. \tag{E.172}$$

In the case of a plane wave we consider for f_{lm} the expression (E.167). The unique solution for the exterior sphere problem (E.145) is then given by

$$u(r, \theta, \varphi) = \sum_{l=0}^{\infty} \sum_{m=-l}^{l} \frac{R f_{lm}\, h_l^{(1)}(kr)\, Y_l^m(\theta, \varphi)}{(ZR + l)\, h_l^{(1)}(kR) - kR\, h_{l+1}^{(1)}(kR)}. \tag{E.173}$$

We remark that there is no need here for an additional compatibility condition like (B.191).

If the condition (E.169) does not hold for some particular $n \in \mathbb{N}_0$, then the solution u is not unique. The constants A_{nm} are then no longer defined by (E.172), and can be chosen in an arbitrary manner. For the existence of a solution in this case, however, we require also the orthogonality conditions $f_{nm} = 0$ for $-n \leq m \leq n$. Instead of (E.173), the solution of (E.145) is now given by the infinite family of functions

$$u(r,\theta,\varphi) = \sum_{0\leq l\neq n} \sum_{m=-l}^{l} \frac{R f_{lm}\, h_l^{(1)}(kr)\, Y_l^m(\theta,\varphi)}{(ZR+l)\, h_l^{(1)}(kR) - kR\, h_{l+1}^{(1)}(kR)} + \sum_{m=-n}^{n} \alpha_m\, h_n^{(1)}(kr)\, Y_n^m(\theta,\varphi), \tag{E.174}$$

where $\alpha_m \in \mathbb{C}$ for $-n \leq m \leq n$ are arbitrary and where their associated terms have the form of volume waves, i.e., waves that propagate inside Ω_e. The exterior sphere problem (E.145) admits thus a unique solution u, except on a countable set of values for k and Z which do not fulfill the condition (E.169). And even in this last case there exists a solution, although not unique, if $2n+1$ orthogonality conditions are additionally satisfied. This behavior for the existence and uniqueness of the solution is typical of the Fredholm alternative, which applies when solving problems that involve compact perturbations of invertible operators.

E.9 Existence and uniqueness

E.9.1 Function spaces

To state a precise mathematical formulation of the herein treated problems, we have to define properly the involved function spaces. For the associated interior problems defined on the bounded set Ω_i we use the classical Sobolev space (vid. Section A.4)

$$H^1(\Omega_i) = \big\{v :\ v \in L^2(\Omega_i),\ \nabla v \in L^2(\Omega_i)^3\big\}, \tag{E.175}$$

which is a Hilbert space and has the norm

$$\|v\|_{H^1(\Omega_i)} = \Big(\|v\|^2_{L^2(\Omega_i)} + \|\nabla v\|^2_{L^2(\Omega_i)^3}\Big)^{1/2}. \tag{E.176}$$

For the exterior problem defined on the unbounded domain Ω_e, on the other hand, we introduce the weighted Sobolev space (cf. Nédélec 2001)

$$W^1(\Omega_e) = \left\{v :\ \frac{v}{(1+r^2)^{1/2}} \in L^2(\Omega_e),\ \frac{\nabla v}{(1+r^2)^{1/2}} \in L^2(\Omega_e)^3,\ \frac{\partial v}{\partial r} - ikv \in L^2(\Omega_e)\right\}, \tag{E.177}$$

where $r = |\boldsymbol{x}|$. If $W^1(\Omega_e)$ is provided with the norm

$$\|v\|_{W^1(\Omega_e)} = \left(\left\| \frac{v}{(1+r^2)^{1/2}} \right\|^2_{L^2(\Omega_e)} + \left\| \frac{\nabla v}{(1+r^2)^{1/2}} \right\|^2_{L^2(\Omega_e)^3} + \left\| \frac{\partial v}{\partial r} - ikv \right\|^2_{L^2(\Omega_e)} \right)^{1/2}, \tag{E.178}$$

then it becomes a Hilbert space. The restriction to any bounded open set $B \subset \Omega_e$ of the functions of $W^1(\Omega_e)$ belongs to $H^1(B)$, i.e., we have the inclusion $W^1(\Omega_e) \subset H^1_{\text{loc}}(\Omega_e)$, and the functions in these two spaces differ only by their behavior at infinity. We remark

that the space $W^1(\Omega_e)$ contains the constant functions and all the functions of $H^1_{\text{loc}}(\Omega_e)$ that satisfy the radiation condition (E.8).

When dealing with Sobolev spaces, even a strong Lipschitz boundary $\Gamma \in C^{0,1}$ is admissible. In this case, and due the trace theorem (A.531), if $v \in H^1(\Omega_i)$ or $v \in W^1(\Omega_e)$, then the trace of v fulfills

$$\gamma_0 v = v|_\Gamma \in H^{1/2}(\Gamma). \tag{E.179}$$

Moreover, the trace of the normal derivative can be also defined, and it holds that

$$\gamma_1 v = \frac{\partial v}{\partial n}|_\Gamma \in H^{-1/2}(\Gamma). \tag{E.180}$$

E.9.2 Regularity of the integral operators

The boundary integral operators (E.78), (E.79), (E.80), and (E.81) can be characterized as linear and continuous applications such that

$$S : H^{-1/2+s}(\Gamma) \longrightarrow H^{1/2+s}(\Gamma), \qquad D : H^{1/2+s}(\Gamma) \longrightarrow H^{3/2+s}(\Gamma), \tag{E.181}$$

$$D^* : H^{-1/2+s}(\Gamma) \longrightarrow H^{1/2+s}(\Gamma), \qquad N : H^{1/2+s}(\Gamma) \longrightarrow H^{-1/2+s}(\Gamma). \tag{E.182}$$

This result holds for any $s \in \mathbb{R}$ if the boundary Γ is of class C^∞, which can be derived from the theory of singular integral operators with pseudo-homogeneous kernels (cf., e.g., Nédélec 2001). Due the compact injection (A.554), it holds also that the operators

$$D : H^{1/2+s}(\Gamma) \longrightarrow H^{1/2+s}(\Gamma) \qquad \text{and} \qquad D^* : H^{-1/2+s}(\Gamma) \longrightarrow H^{-1/2+s}(\Gamma) \tag{E.183}$$

are compact. For a strong Lipschitz boundary $\Gamma \in C^{0,1}$, on the other hand, these results hold only when $|s| < 1$ (cf. Costabel 1988). In the case of more regular boundaries, the range for s increases, but remains finite. For our purposes we use $s = 0$, namely

$$S : H^{-1/2}(\Gamma) \longrightarrow H^{1/2}(\Gamma), \qquad D : H^{1/2}(\Gamma) \longrightarrow H^{1/2}(\Gamma), \tag{E.184}$$

$$D^* : H^{-1/2}(\Gamma) \longrightarrow H^{-1/2}(\Gamma), \qquad N : H^{1/2}(\Gamma) \longrightarrow H^{-1/2}(\Gamma), \tag{E.185}$$

which are all linear and continuous operators, and where the operators D and D^* are compact. Similarly, we can characterize the single and double layer potentials defined respectively in (E.73) and (E.74) as linear and continuous integral operators such that

$$\mathcal{S} : H^{-1/2}(\Gamma) \longrightarrow W^1(\Omega_e \cup \Omega_i) \qquad \text{and} \qquad \mathcal{D} : H^{1/2}(\Gamma) \longrightarrow W^1(\Omega_e \cup \Omega_i). \tag{E.186}$$

E.9.3 Application to the integral equations

It is not difficult to see that if $\mu \in H^{1/2}(\Gamma)$ and $\nu \in H^{-1/2}(\Gamma)$ are given, then the transmission problem (E.41) admits a unique solution $u \in W^1(\Omega_e \cup \Omega_i)$, as a consequence of the integral representation formula (E.59). For the direct scattering problem (E.13), though, this is not always the case, as was appreciated in the exterior sphere problem (E.145). Nonetheless, if the Fredholm alternative applies, then we know that the existence and uniqueness of the problem can be ensured almost always, i.e., except on a countable set of values for the wave number and for the impedance.

We consider an impedance $Z \in L^\infty(\Gamma)$ and an impedance data function $f_z \in H^{-1/2}(\Gamma)$. In both cases all the continuous functions on Γ are included.

a) First extension by zero

Let us consider the first integral equation of the extension-by-zero alternative (E.109), which is given in terms of boundary layer potentials, for $\mu \in H^{1/2}(\Gamma)$, by

$$\frac{\mu}{2} + S(Z\mu) - D(\mu) = S(f_z) \qquad \text{in } \; H^{1/2}(\Gamma). \tag{E.187}$$

Due the imbedding properties of Sobolev spaces and in the same way as for the full-plane impedance Laplace problem, it holds that the left-hand side of the integral equation corresponds to an identity and two compact operators, and thus Fredholm's alternative applies.

b) Second extension by zero

The second integral equation of the extension-by-zero alternative (E.113) is given in terms of boundary layer potentials, for $\mu \in H^{1/2}(\Gamma)$, by

$$\frac{Z}{2}\mu - N(\mu) + D^*(Z\mu) = \frac{f_z}{2} + D^*(f_z) \qquad \text{in } \; H^{-1/2}(\Gamma). \tag{E.188}$$

The operator N plays the role of the identity and the other terms on the left-hand side are compact, thus Fredholm's alternative holds.

c) Continuous impedance

The integral equation of the continuous-impedance alternative (E.121) is given in terms of boundary layer potentials, for $\mu \in H^{1/2}(\Gamma)$, by

$$-N(\mu) + D^*(Z\mu) + ZD(\mu) - ZS(Z\mu) = f_z \qquad \text{in } \; H^{-1/2}(\Gamma). \tag{E.189}$$

Again, the operator N plays the role of the identity and the remaining terms on the left-hand side are compact, thus Fredholm's alternative applies.

d) Continuous value

The integral equation of the continuous-value alternative (E.129) is given in terms of boundary layer potentials, for $\nu \in H^{-1/2}(\Gamma)$, by

$$\frac{\nu}{2} + ZS(\nu) - D^*(\nu) = -f_z \qquad \text{in } \; H^{-1/2}(\Gamma). \tag{E.190}$$

On the left-hand side we have an identity operator and the remaining operators are compact, thus Fredholm's alternative holds.

e) Continuous normal derivative

The integral equation of the continuous-normal-derivative alternative (E.137) is given in terms of boundary layer potentials, for $\mu \in H^{1/2}(\Gamma)$, by

$$\frac{Z}{2}\mu - N(\mu) + ZD(\mu) = f_z \qquad \text{in } \; H^{-1/2}(\Gamma). \tag{E.191}$$

As before, Fredholm's alternative again applies, since on the left-hand side we have the operator N and two compact operators.

E.9.4 Consequences of Fredholm's alternative

Since the Fredholm alternative applies to each integral equation, therefore it applies also to the exterior differential problem (E.13) due the integral representation formula. The existence of the exterior problem's solution is thus determined by its uniqueness, and the wave numbers $k \in \mathbb{C}$ and impedances $Z \in \mathbb{C}$ for which the uniqueness is lost constitute a countable set, which we call respectively wave number spectrum and impedance spectrum of the exterior problem and denote them by σ_k and σ_Z. The spectrum σ_k considers a fixed Z and, conversely, the spectrum σ_Z considers a fixed k. The existence and uniqueness of the solution is therefore ensured almost everywhere. The same holds obviously for the solution of the integral equation, whose wave number spectrum and impedance spectrum we denote respectively by ς_k and ς_Z. Since each integral equation is derived from the exterior problem, it holds that $\sigma_k \subset \varsigma_k$ and $\sigma_Z \subset \varsigma_Z$. The converse, though, is not necessarily true and depends on each particular integral equation. In any way, the sets $\varsigma_k \setminus \sigma_k$ and $\varsigma_Z \setminus \sigma_Z$ are at most countable.

Fredholm's alternative applies as much to the integral equation itself as to its adjoint counterpart, and equally to their homogeneous versions. Moreover, each integral equation solves at the same time an exterior and an interior differential problem. The loss of uniqueness of the integral equation's solution appears when the wave number k and the impedance Z are eigenvalues of some associated interior problem, either of the homogeneous integral equation or of its adjoint counterpart. Such a wave number k or impedance Z are contained respectively in ς_k or ς_Z.

The integral equation (E.111) is associated with the extension by zero (E.104), for which no eigenvalues appear. Nevertheless, its adjoint integral equation (E.131) of the continuous value is associated with the interior problem (E.124), which has a countable amount of eigenvalues k, but behaves otherwise well for all $Z \neq 0$.

The integral equation (E.114) is also associated with the extension by zero (E.104), for which no eigenvalues appear. Nonetheless, its adjoint integral equation (E.139) of the continuous normal derivative is associated with the interior problem (E.132), which has a countable amount of eigenvalues k, but behaves well for all Z, without restriction.

The integral equation (E.123) of the continuous impedance is self-adjoint and is associated with the interior problem (E.115), which has a countable quantity of eigenvalues k and Z.

Let us consider now the transmission problem generated by the homogeneous exterior problem

$$\begin{cases} \text{Find } u_e : \Omega_e \to \mathbb{C} \text{ such that} \\ \Delta u_e + k^2 u_e = 0 \qquad \text{in } \Omega_e, \\ -\dfrac{\partial u_e}{\partial n} + Z u_e = 0 \qquad \text{on } \Gamma, \\ \text{+ Outgoing radiation condition as } |\boldsymbol{x}| \to \infty, \end{cases} \tag{E.192}$$

and the associated homogeneous interior problem

$$\begin{cases} \text{Find } u_i : \Omega_i \to \mathbb{C} \text{ such that} \\ \Delta u_i + k^2 u_i = 0 \qquad \text{in } \Omega_i, \\ \dfrac{\partial u_i}{\partial n} + Z u_i = 0 \qquad \text{on } \Gamma, \end{cases} \tag{E.193}$$

where the radiation condition is as usual given by (E.8), and where the unit normal $\boldsymbol{n}$ always points outwards of Ω_e.

As in the two-dimensional case, it holds again that the integral equations for this transmission problem have either the same left-hand side or are mutually adjoint to all other possible alternatives of integral equations that can be built for the exterior problem (E.13), and in particular to all the alternatives that were mentioned in the last subsection. The eigenvalues k and Z of the homogeneous interior problem (E.193) are thus also contained respectively in ς_k and ς_Z.

We remark that additional alternatives for integral representations and equations based on non-homogeneous versions of the problem (E.193) can be also derived for the exterior impedance problem (cf. Ha-Duong 1987).

The determination of the wave number spectrum σ_k and the impedance spectrum σ_Z of the exterior problem (E.13) is not so easy, but can be achieved for simple geometries where an analytic solution is known.

In conclusion, the exterior problem (E.13) admits a unique solution u if $k \notin \sigma_k$, and $Z \notin \sigma_Z$, and each integral equation admits a unique solution, either μ or ν, if $k \notin \varsigma_k$ and $Z \notin \varsigma_Z$.

E.10 Dissipative problem

The dissipative problem considers waves that lose their amplitude as they travel through the medium. These waves dissipate their energy as they propagate and are modeled by a complex wave number $k \in \mathbb{C}$ whose imaginary part is strictly positive, i.e., $\mathfrak{Im}\{k\} > 0$. This choice ensures that the Green's function (E.22) decreases exponentially at infinity. Due the dissipative nature of the medium, it is no longer suited to take plane waves in the form of (E.5) as the incident field u_I. Instead, we have to take a source of volume waves at a finite distance from the obstacle. For example, we can consider a point source located at $\boldsymbol{z} \in \Omega_e$, in which case the incident field is given, up to a multiplicative constant, by

$$u_I(\boldsymbol{x}) = G(\boldsymbol{x}, \boldsymbol{z}) = -\frac{e^{ik|\boldsymbol{x}-\boldsymbol{z}|}}{4\pi|\boldsymbol{x}-\boldsymbol{z}|} = -\frac{ik}{4\pi} h_0^{(1)}\big(k|\boldsymbol{x}-\boldsymbol{z}|\big). \tag{E.194}$$

This incident field u_I satisfies the Helmholtz equation with a source term in the right-hand side, namely

$$\Delta u_I + k^2 u_I = \delta_{\boldsymbol{z}} \qquad \text{in } \mathcal{D}'(\Omega_e), \tag{E.195}$$

which holds also for the total field u_T but not for the scattered field u, in which case the Helmholtz equation remains homogeneous. For a general source distribution g_s, whose

support is contained in Ω_e, the incident field can be expressed by

$$u_I(\boldsymbol{x}) = G(\boldsymbol{x},\boldsymbol{z}) * g_s(\boldsymbol{z}) = \int_{\Omega_e} G(\boldsymbol{x},\boldsymbol{z})\, g_s(\boldsymbol{z})\, \mathrm{d}\boldsymbol{z}. \tag{E.196}$$

This incident field u_I satisfies now

$$\Delta u_I + k^2 u_I = g_s \qquad \text{in } \mathcal{D}'(\Omega_e), \tag{E.197}$$

which holds again also for the total field u_T but not for the scattered field u.

The dissipative nature of the medium implies also that a radiation condition like (E.8) is no longer required. The ingoing waves are ruled out, since they verify $\mathfrak{Im}\{k\} < 0$. The dissipative scattering problem can be therefore stated as

$$\left\{ \begin{array}{l} \text{Find } u : \Omega_e \to \mathbb{C} \text{ such that} \\ \Delta u + k^2 u = 0 \qquad\qquad \text{in } \Omega_e, \\ -\dfrac{\partial u}{\partial n} + Zu = f_z \qquad \text{on } \Gamma, \end{array} \right. \tag{E.198}$$

where the impedance data function f_z is again given by

$$f_z = \frac{\partial u_I}{\partial n} - Z u_I \qquad \text{on } \Gamma. \tag{E.199}$$

The solution is now such that $u \in H^1(\Omega_e)$ (cf., e.g., Hazard & Lenoir 1998, Lenoir 2005), therefore, instead of (E.52) and (E.53), we obtain that

$$\left| \int_{S_R} \left(u(\boldsymbol{y}) \frac{\partial G}{\partial r_{\boldsymbol{y}}}(\boldsymbol{x},\boldsymbol{y}) - G(\boldsymbol{x},\boldsymbol{y}) \frac{\partial u}{\partial r}(\boldsymbol{y}) \right) \mathrm{d}\gamma(\boldsymbol{y}) \right| \leq \frac{C}{R}\, e^{-R\,\mathfrak{Im}\{k\}}. \tag{E.200}$$

It is not difficult to see that all the other developments performed for the non-dissipative case are also valid when considering dissipation. The only difference is that now a complex wave number k such that $\mathfrak{Im}\{k\} > 0$ has to be taken everywhere into account and that the outgoing radiation condition is no longer needed.

E.11 Variational formulation

To solve a particular integral equation we convert it to its variational or weak formulation, i.e., we solve it with respect to certain test functions in a bilinear (or sesquilinear) form. Basically, the integral equation is multiplied by the (conjugated) test function and then the equation is integrated over the boundary of the domain. The test functions are taken in the same function space as the solution of the integral equation.

a) First extension by zero

The variational formulation for the first integral equation (E.187) of the extension-by-zero alternative searches $\mu \in H^{1/2}(\Gamma)$ such that $\forall \varphi \in H^{1/2}(\Gamma)$

$$\left\langle \frac{\mu}{2} + S(Z\mu) - D(\mu), \varphi \right\rangle = \left\langle S(f_z), \varphi \right\rangle. \tag{E.201}$$

b) Second extension by zero

The variational formulation for the second integral equation (E.188) of the extension-by-zero alternative searches $\mu \in H^{1/2}(\Gamma)$ such that $\forall \varphi \in H^{1/2}(\Gamma)$

$$\left\langle \frac{Z}{2}\mu - N(\mu) + D^*(Z\mu), \varphi \right\rangle = \left\langle \frac{f_z}{2} + D^*(f_z), \varphi \right\rangle. \tag{E.202}$$

c) Continuous impedance

The variational formulation for the integral equation (E.189) of the alternative of the continuous-impedance searches $\mu \in H^{1/2}(\Gamma)$ such that $\forall \varphi \in H^{1/2}(\Gamma)$

$$\big\langle -N(\mu) + D^*(Z\mu) + ZD(\mu) - ZS(Z\mu), \varphi \big\rangle = \big\langle f_z, \varphi \big\rangle. \tag{E.203}$$

d) Continuous value

The variational formulation for the integral equation (E.190) of the continuous-value alternative searches $\nu \in H^{-1/2}(\Gamma)$ such that $\forall \psi \in H^{-1/2}(\Gamma)$

$$\left\langle \frac{\nu}{2} + ZS(\nu) - D^*(\nu), \psi \right\rangle = \big\langle -f_z, \psi \big\rangle. \tag{E.204}$$

e) Continuous normal derivative

The variational formulation for the integral equation (E.191) of the continuous-normal-derivative alternative searches $\mu \in H^{1/2}(\Gamma)$ such that $\forall \varphi \in H^{1/2}(\Gamma)$

$$\left\langle \frac{Z}{2}\mu - N(\mu) + ZD(\mu), \varphi \right\rangle = \big\langle f_z, \varphi \big\rangle. \tag{E.205}$$

E.12 Numerical discretization

E.12.1 Discretized function spaces

The exterior problem (E.13) is solved numerically with the boundary element method by employing a Galerkin scheme on the variational formulation of an integral equation. We use on the boundary surface Γ Lagrange finite elements of type either $\mathbb{P}_1$ or $\mathbb{P}_0$. The surface Γ is approximated by the triangular mesh Γ^h, composed by T flat triangles T_j, $1 \leq j \leq T$, and I nodes $\boldsymbol{r}_i \in \mathbb{R}^3$, $1 \leq i \leq I$. The triangles have a diameter less or equal than h, and their vertices or corners, i.e., the nodes $\boldsymbol{r}_i$, are on top of Γ, as shown in Figure E.4. The diameter of a triangle K is given by

$$\operatorname{diam}(K) = \sup_{\boldsymbol{x},\boldsymbol{y} \in K} |\boldsymbol{y} - \boldsymbol{x}|. \tag{E.206}$$

The function space $H^{1/2}(\Gamma)$ is approximated using the conformal space of continuous piecewise linear polynomials with complex coefficients

$$Q_h = \big\{ \varphi_h \in C^0(\Gamma^h) \,:\, \varphi_h|_{T_j} \in \mathbb{P}_1(\mathbb{C}), \;\; 1 \leq j \leq T \big\}. \tag{E.207}$$

The space Q_h has a finite dimension I, and we describe it using the standard base functions for finite elements of type $\mathbb{P}_1$, which we denote by $\{\chi_j\}_{j=1}^I$. The base function χ_j is

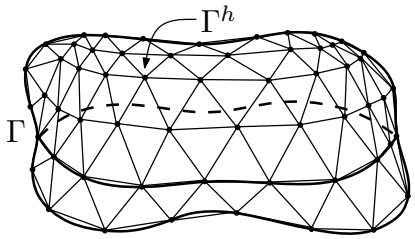

FIGURE E.4. Mesh Γ^h, discretization of Γ.

associated with the node $\boldsymbol{r}_j$ and has its support $\operatorname{supp}\chi_j$ on the triangles that have $\boldsymbol{r}_j$ as one of their vertices. On $\boldsymbol{r}_j$ it has a value of one and on the opposed edges of the triangles its value is zero, being linearly interpolated in between and zero otherwise.

The function space $H^{-1/2}(\Gamma)$, on the other hand, is approximated using the conformal space of piecewise constant polynomials with complex coefficients

$$P_h = \big\{\psi_h : \Gamma^h \to \mathbb{C} \mid \ \psi_h|_{T_j} \in \mathbb{P}_0(\mathbb{C}), \ \ 1 \leq j \leq T\big\}. \tag{E.208}$$

The space P_h has a finite dimension T, and is described using the standard base functions for finite elements of type $\mathbb{P}_0$, which we denote by $\{\kappa_j\}_{j=1}^T$.

In virtue of this discretization, any function $\varphi_h \in Q_h$ or $\psi_h \in P_h$ can be expressed as a linear combination of the elements of the base, namely

$$\varphi_h(\boldsymbol{x}) = \sum_{j=1}^{I} \varphi_j \, \chi_j(\boldsymbol{x}) \qquad \text{and} \qquad \psi_h(\boldsymbol{x}) = \sum_{j=1}^{T} \psi_j \, \kappa_j(\boldsymbol{x}) \qquad \text{for } \ \boldsymbol{x} \in \Gamma^h, \tag{E.209}$$

where $\varphi_j, \psi_j \in \mathbb{C}$. The solutions $\mu \in H^{1/2}(\Gamma)$ and $\nu \in H^{-1/2}(\Gamma)$ of the variational formulations can be therefore approximated respectively by

$$\mu_h(\boldsymbol{x}) = \sum_{j=1}^{I} \mu_j \, \chi_j(\boldsymbol{x}) \qquad \text{and} \qquad \nu_h(\boldsymbol{x}) = \sum_{j=1}^{T} \nu_j \, \kappa_j(\boldsymbol{x}) \qquad \text{for } \ \boldsymbol{x} \in \Gamma^h, \tag{E.210}$$

where $\mu_j, \nu_j \in \mathbb{C}$. The function f_z can be also approximated by

$$f_z^h(\boldsymbol{x}) = \sum_{j=1}^{I} f_j \, \chi_j(\boldsymbol{x}) \qquad \text{for } \ \boldsymbol{x} \in \Gamma^h, \quad \text{with } \ f_j = f_z(\boldsymbol{r}_j), \tag{E.211}$$

or

$$f_z^h(\boldsymbol{x}) = \sum_{j=1}^{T} f_j \, \kappa_j(\boldsymbol{x}) \qquad \text{for } \ \boldsymbol{x} \in \Gamma^h, \quad \text{with } \ f_j = \frac{f_z(\boldsymbol{r}_1^j) + f_z(\boldsymbol{r}_2^j) + f_z(\boldsymbol{r}_3^j)}{3}, \tag{E.212}$$

depending on whether the original integral equation is stated in $H^{1/2}(\Gamma)$ or in $H^{-1/2}(\Gamma)$. We denote by $\boldsymbol{r}_d^j$, for $d \in \{1, 2, 3\}$, the three vertices of triangle T_j.

E.12.2 Discretized integral equations

a) First extension by zero

To see how the boundary element method operates, we apply it to the first integral equation of the extension-by-zero alternative, i.e., to the variational formulation (E.201). We characterize all the discrete approximations by the index h, including also the impedance and the boundary layer potentials. The numerical approximation of (E.201) leads to the discretized problem that searches $\mu_h \in Q_h$ such that $\forall \varphi_h \in Q_h$

$$\left\langle \frac{\mu_h}{2} + S_h(Z_h\mu_h) - D_h(\mu_h), \varphi_h \right\rangle = \left\langle S_h(f_z^h), \varphi_h \right\rangle. \tag{E.213}$$

Considering the decomposition of μ_h in terms of the base $\{\chi_j\}$ and taking as test functions the same base functions, $\varphi_h = \chi_i$ for $1 \leq i \leq I$, yields the discrete linear system

$$\sum_{j=1}^{I} \mu_j \left(\frac{1}{2}\langle \chi_j, \chi_i \rangle + \langle S_h(Z_h\chi_j), \chi_i \rangle - \langle D_h(\chi_j), \chi_i \rangle \right) = \sum_{j=1}^{I} f_j \, \langle S_h(\chi_j), \chi_i \rangle. \tag{E.214}$$

This constitutes a system of linear equations that can be expressed as a linear matrix system:

$$\begin{cases} \text{Find } \boldsymbol{\mu} \in \mathbb{C}^I \text{ such that} \\ \boldsymbol{M}\boldsymbol{\mu} = \boldsymbol{b}. \end{cases} \tag{E.215}$$

The elements m_{ij} of the matrix $\boldsymbol{M}$ are given by

$$m_{ij} = \frac{1}{2}\langle \chi_j, \chi_i \rangle + \langle S_h(Z_h\chi_j), \chi_i \rangle - \langle D_h(\chi_j), \chi_i \rangle \qquad \text{for } \; 1 \leq i, j \leq I, \tag{E.216}$$

and the elements b_i of the vector $\boldsymbol{b}$ by

$$b_i = \left\langle S_h(f_z^h), \chi_i \right\rangle = \sum_{j=1}^{I} f_j \, \langle S_h(\chi_j), \chi_i \rangle \qquad \text{for } \; 1 \leq i \leq I. \tag{E.217}$$

The discretized solution u_h, which approximates u, is finally obtained by discretizing the integral representation formula (E.110) according to

$$u_h = \mathcal{D}_h(\mu_h) - \mathcal{S}_h(Z_h\mu_h) + \mathcal{S}_h(f_z^h), \tag{E.218}$$

which, more specifically, can be expressed as

$$u_h = \sum_{j=1}^{I} \mu_j \big(\mathcal{D}_h(\chi_j) - \mathcal{S}_h(Z_h\chi_j) \big) + \sum_{j=1}^{I} f_j \, \mathcal{S}_h(\chi_j). \tag{E.219}$$

By proceeding in the same way, the discretization of all the other alternatives of integral equations can be also expressed as a linear matrix system like (E.215). The resulting matrix $\boldsymbol{M}$ is in general complex, full, non-symmetric, and with dimensions $I \times I$ for elements of type $\mathbb{P}_1$ and $T \times T$ for elements of type $\mathbb{P}_0$. The right-hand side vector $\boldsymbol{b}$ is complex and of size either I or T. The boundary element calculations required to compute numerically the elements of $\boldsymbol{M}$ and $\boldsymbol{b}$ have to be performed carefully, since the integrals that appear become singular when the involved triangles are coincident, or when they have a common vertex or edge, due the singularity of the Green's function at its source point.

b) Second extension by zero

In the case of the second integral equation of the extension-by-zero alternative, i.e., of the variational formulation (E.202), the elements m_{ij} that constitute the matrix $\boldsymbol{M}$ of the linear system (E.215) are given by

$$m_{ij} = \frac{1}{2}\langle Z_h\chi_j, \chi_i\rangle - \langle N_h(\chi_j), \chi_i\rangle + \langle D_h^*(Z_h\chi_j), \chi_i\rangle \qquad \text{for } 1 \le i, j \le I, \tag{E.220}$$

whereas the elements b_i of the vector $\boldsymbol{b}$ are expressed as

$$b_i = \sum_{j=1}^{I} f_j \left(\frac{1}{2}\langle \chi_j, \chi_i\rangle + \langle D_h^*(Z_h\chi_j), \chi_i\rangle\right) \qquad \text{for } 1 \le i \le I. \tag{E.221}$$

The discretized solution u_h is again computed by (E.219).

c) Continuous impedance

In the case of the continuous-impedance alternative, i.e., of the variational formulation (E.203), the elements m_{ij} that constitute the matrix $\boldsymbol{M}$ of the linear system (E.215) are given, for $1 \le i, j \le I$, by

$$m_{ij} = -\langle N_h(\chi_j), \chi_i\rangle + \langle D_h^*(Z_h\chi_j), \chi_i\rangle + \langle Z_h D_h(\chi_j), \chi_i\rangle - \langle Z_h S_h(Z_h\chi_j), \chi_i\rangle, \tag{E.222}$$

whereas the elements b_i of the vector $\boldsymbol{b}$ are expressed as

$$b_i = \sum_{j=1}^{I} f_j \langle \chi_j, \chi_i\rangle \qquad \text{for } 1 \le i \le I. \tag{E.223}$$

It can be observed that for this particular alternative the matrix $\boldsymbol{M}$ turns out to be symmetric, since the integral equation is self-adjoint. The discretized solution u_h, due (E.122), is then computed by

$$u_h = \sum_{j=1}^{I} \mu_j\big(\mathcal{D}_h(\chi_j) - \mathcal{S}_h(Z_h\chi_j)\big). \tag{E.224}$$

d) Continuous value

In the case of the continuous-value alternative, that is, of the variational formulation (E.204), the elements m_{ij} that constitute the matrix $\boldsymbol{M}$, now of the linear system

$$\begin{cases} \text{Find } \boldsymbol{\nu} \in \mathbb{C}^T \text{ such that} \\ \boldsymbol{M\nu} = \boldsymbol{b}, \end{cases} \tag{E.225}$$

are given by

$$m_{ij} = \frac{1}{2}\langle \kappa_j, \kappa_i\rangle + \langle Z_h S_h(\kappa_j), \kappa_i\rangle - \langle D_h^*(\kappa_j), \kappa_i\rangle \qquad \text{for } 1 \le i, j \le T, \tag{E.226}$$

whereas the elements b_i of the vector $\boldsymbol{b}$ are expressed as

$$b_i = -\sum_{j=1}^{T} f_j \langle \kappa_j, \kappa_i\rangle \qquad \text{for } 1 \le i \le T. \tag{E.227}$$

The discretized solution u_h, due (E.130), is then computed by

$$u_h = -\sum_{j=1}^{T} \nu_j \, \mathcal{S}_h(\kappa_j). \tag{E.228}$$

e) Continuous normal derivative

In the case of the continuous-normal-derivative alternative, i.e., of the variational formulation (E.205), the elements m_{ij} that conform the matrix $\boldsymbol{M}$ of the linear system (E.215) are given by

$$m_{ij} = \frac{1}{2}\langle Z_h \chi_j, \chi_i\rangle - \langle N_h(\chi_j), \chi_i\rangle + \langle Z_h D_h(\chi_j), \chi_i\rangle \qquad \text{for } 1 \le i, j \le I, \tag{E.229}$$

whereas the elements b_i of the vector $\boldsymbol{b}$ are expressed as

$$b_i = \sum_{j=1}^{I} f_j \, \langle \chi_j, \chi_i\rangle \qquad \text{for } 1 \le i \le I. \tag{E.230}$$

The discretized solution u_h, due (E.138), is then computed by

$$u_h = \sum_{j=1}^{I} \mu_j \, \mathcal{D}_h(\chi_j). \tag{E.231}$$

E.13 Boundary element calculations

The boundary element calculations build the elements of the matrix $\boldsymbol{M}$ resulting from the discretization of the integral equation, i.e., from (E.215) or (E.225). They permit thus to compute numerically expressions like (E.216). To evaluate the appearing singular integrals, we use the semi-numerical methods described in the report of Bendali & Devys (1986).

We use the same notation as in Section D.12, and the required boundary element integrals, for $a, b \in \{0, 1\}$ and $c, d \in \{1, 2, 3\}$, are again

$$ZA_{a,b}^{c,d} = \int_K \int_L \left(\frac{s_c}{h_c^K}\right)^a \left(\frac{t_d}{h_d^L}\right)^b G(\boldsymbol{x}, \boldsymbol{y}) \, \mathrm{d}L(\boldsymbol{y}) \, \mathrm{d}K(\boldsymbol{x}), \tag{E.232}$$

$$ZB_{a,b}^{c,d} = \int_K \int_L \left(\frac{s_c}{h_c^K}\right)^a \left(\frac{t_d}{h_d^L}\right)^b \frac{\partial G}{\partial n_{\boldsymbol{y}}}(\boldsymbol{x}, \boldsymbol{y}) \, \mathrm{d}L(\boldsymbol{y}) \, \mathrm{d}K(\boldsymbol{x}), \tag{E.233}$$

All the integrals that stem from the numerical discretization can be expressed in terms of these two basic boundary element integrals. The impedance is again discretized as a piecewise constant function Z_h, which on each triangle T_j adopts a constant value $Z_j \in \mathbb{C}$. The integrals of interest are the same as for the Laplace equation, except for the hypersingular

term, which is now given by

$$\begin{aligned}\langle N_h(\chi_j),\chi_i\rangle &= -\int_{\Gamma^h}\int_{\Gamma^h} G(\boldsymbol{x},\boldsymbol{y})\big(\nabla\chi_j(\boldsymbol{y})\times\boldsymbol{n}_{\boldsymbol{y}}\big)\cdot\big(\nabla\chi_i(\boldsymbol{x})\times\boldsymbol{n}_{\boldsymbol{x}}\big)\,\mathrm{d}\gamma(\boldsymbol{y})\,\mathrm{d}\gamma(\boldsymbol{x})\\ &\quad + k^2\int_{\Gamma^h}\int_{\Gamma^h} G(\boldsymbol{x},\boldsymbol{y})\chi_j(\boldsymbol{y})\chi_i(\boldsymbol{x})(\boldsymbol{n}_{\boldsymbol{y}}\cdot\boldsymbol{n}_{\boldsymbol{x}})\,\mathrm{d}\gamma(\boldsymbol{y})\,\mathrm{d}\gamma(\boldsymbol{x})\\ &= -\sum_{K\ni\boldsymbol{r}_i}\sum_{L\ni\boldsymbol{r}_j}\frac{ZA_{0,0}^{c_i^K,d_j^L}}{h^K_{c_i^K}h^L_{d_j^L}}\big(\boldsymbol{\nu}^K_{c_i^K}\times\boldsymbol{n}_K\big)\cdot\big(\boldsymbol{\nu}^L_{d_j^L}\times\boldsymbol{n}_L\big)\\ &\quad + k^2\sum_{K\ni\boldsymbol{r}_i}\sum_{L\ni\boldsymbol{r}_j}\Big(ZA_{0,0}^{c_i^K,d_j^L}-ZA_{0,1}^{c_i^K,d_j^L}-ZA_{1,0}^{c_i^K,d_j^L}+ZA_{1,1}^{c_i^K,d_j^L}\Big)(\boldsymbol{n}_L\cdot\boldsymbol{n}_K).\end{aligned}\tag{E.234}$$

To compute the boundary element integrals (E.232) and (E.233), we isolate the singular part of the Green's function G according to

$$G(R) = -\frac{1}{4\pi R}+\phi(R),\tag{E.235}$$

where $\phi(R)$ is a non-singular function, which is given by

$$\phi(R)=\frac{1-e^{ikR}}{4\pi R}.\tag{E.236}$$

For the derivative $G'(R)$ we have similarly that

$$G'(R)=\frac{1}{4\pi R^2}+\phi'(R),\tag{E.237}$$

where $\phi'(R)$ is also a non-singular function, which is given by

$$\phi'(R)=-\frac{1-(1-ikR)e^{ikR}}{4\pi R^2}.\tag{E.238}$$

We observe that

$$\frac{\partial G}{\partial n_{\boldsymbol{y}}}(\boldsymbol{x},\boldsymbol{y})=G'(R)\,\frac{\boldsymbol{R}}{R}\cdot\boldsymbol{n}_{\boldsymbol{y}}.\tag{E.239}$$

It is not difficult to see that the singular part corresponds to the Green's function of the Laplace equation, and therefore the associated integrals are computed in the same way. For the integrals associated with $\phi(R)$ and $\phi'(R)$, which are non-singular, a three-point Gauss-Lobatto quadrature formula is used. All the other computations are performed in the same manner as in Section D.12 for the Laplace equation.

E.14 Benchmark problem

As benchmark problem we consider the exterior sphere problem (E.145), whose domain is shown in Figure E.3. The exact solution of this problem is stated in (E.173), and the idea is to retrieve it numerically with the integral equation techniques and the boundary element method described throughout this chapter.

For the computational implementation and the numerical resolution of the benchmark problem, we consider only the first integral equation of the extension-by-zero alternative (E.109), which is given in terms of boundary layer potentials by (E.187). The

linear system (E.215) resulting from the discretization (E.213) of its variational formulation (E.201) is solved computationally with finite boundary elements of type $\mathbb{P}_1$ by using subroutines programmed in Fortran 90, by generating the mesh Γ^h of the boundary with the free software Gmsh 2.4, and by representing graphically the results in Matlab 7.5 (R2007b).

We consider a radius $R = 1$, a wave number $k = 3$, and a constant impedance $Z = 0.8$. The discretized boundary surface Γ^h has $I = 702$ nodes, $T = 1400$ triangles, and a discretization step $h = 0.2136$, being

$$h = \max_{1 \leq j \leq T} \operatorname{diam}(T_j). \tag{E.240}$$

As incident field u_I we consider a plane wave in the form of (E.5) with a wave propagation vector $\boldsymbol{k} = (0, 1, 0)$, i.e., such that the angles of incidence in (E.6) are given by $\theta_I = \pi/2$ and $\varphi_I = -\pi/2$.

From (E.173) and (E.167), we can approximate the exact solution as the truncated series

$$u(r, \theta, \varphi) = -4\pi \sum_{l=0}^{40} i^l \frac{(ZR + l)\, j_l(kR) - kR\, j_{l+1}(kR)}{(ZR + l)\, h_l^{(1)}(kR) - kR\, h_{l+1}^{(1)}(kR)} h_l^{(1)}(kr) \Upsilon_l(\theta, \varphi), \tag{E.241}$$

where

$$\Upsilon_l(\theta, \varphi) = \sum_{m=-l}^{l} Y_l^m(\theta, \varphi) \overline{Y_l^m(\theta_P, \varphi_P)} = \frac{2l+1}{4\pi} \Bigg(P_l(\cos\theta) P_l(\cos\theta_P) + 2 \sum_{m=1}^{l} \frac{(l-m)!}{(l+m)!} P_l^m(\cos\theta) P_l^m(\cos\theta_P) \cos\big(m(\varphi - \varphi_P)\big) \Bigg), \tag{E.242}$$

and where the trace on the boundary of the sphere is approximated by

$$\mu(\theta, \varphi) = -4\pi \sum_{l=0}^{40} i^l \frac{(ZR + l)\, j_l(kR) - kR\, j_{l+1}(kR)}{(ZR + l)\, h_l^{(1)}(kR) - kR\, h_{l+1}^{(1)}(kR)} h_l^{(1)}(kR) \Upsilon_l(\theta, \varphi). \tag{E.243}$$

The numerically calculated trace of the solution μ_h of the benchmark problem, which was computed by using the boundary element method, is depicted in Figure E.5. In the same manner, the numerical solution u_h is illustrated in Figures E.6 and E.7 for an angle $\theta = \pi/2$. It can be observed that the numerical solution is close to the exact one.

On behalf of the far field, two scattering cross sections are shown in Figure E.8. The bistatic radiation diagram represents the far-field pattern of the solution for a particular incident field in all observation directions. The monostatic radiation diagram, on the other hand, depicts the backscattering of incident fields from all directions, i.e., the far-field pattern in the same observation direction as for each incident field.

Likewise as in (D.346), we define the relative error of the trace of the solution as

$$E_2(h, \Gamma^h) = \frac{\|\Pi_h \mu - \mu_h\|_{L^2(\Gamma^h)}}{\|\Pi_h \mu\|_{L^2(\Gamma^h)}}, \tag{E.244}$$

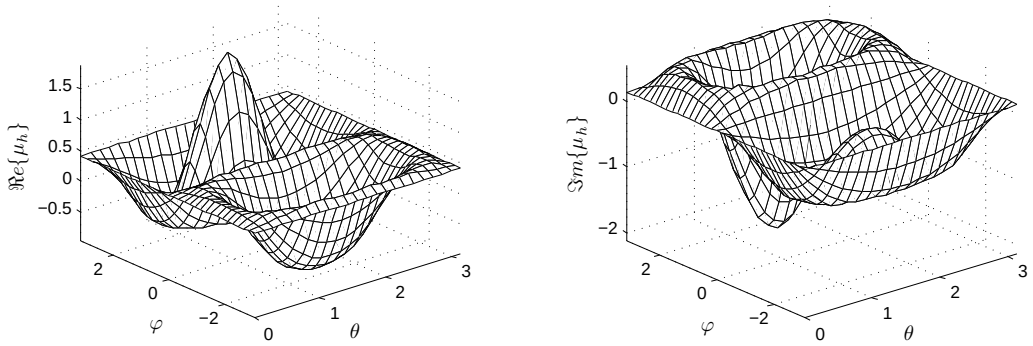

(a) Real part (b) Imaginary part

FIGURE E.5. Numerically computed trace of the solution μ_h.

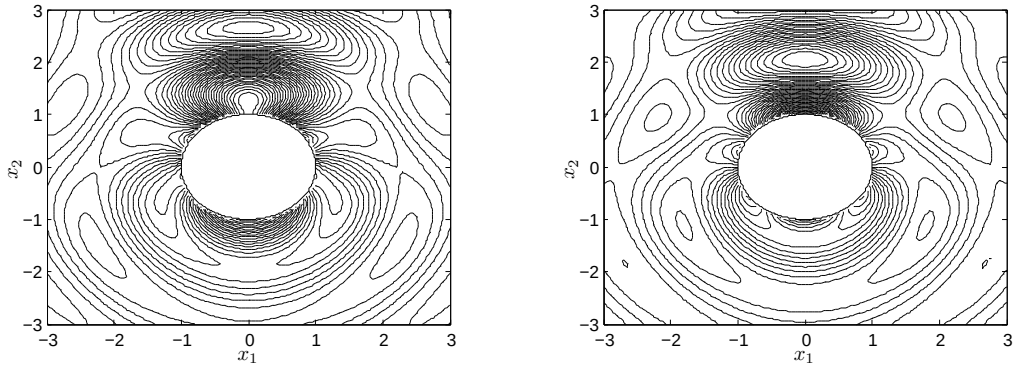

(a) Real part (b) Imaginary part

FIGURE E.6. Contour plot of the numerically computed solution u_h for $\theta = \pi/2$.

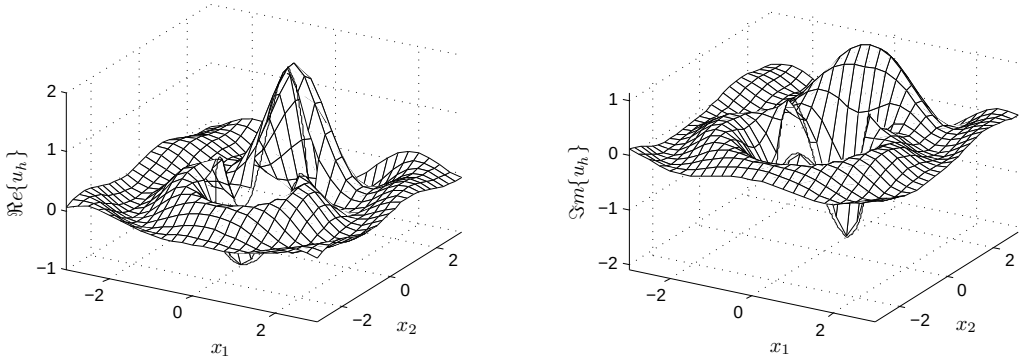

(a) Real part (b) Imaginary part

FIGURE E.7. Oblique view of the numerically computed solution u_h for $\theta = \pi/2$.

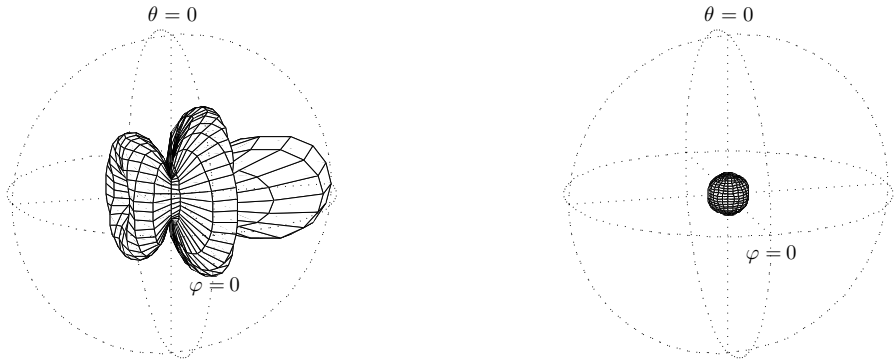

(a) Bistatic radiation diagram for $\theta_I = \frac{\pi}{2}$, $\varphi_I = -\frac{\pi}{2}$ (b) Monostatic radiation diagram

FIGURE E.8. Scattering cross sections ranging from -14 to 6 [dB].

where $\Pi_h \mu$ denotes the Lagrange interpolating function of the exact solution's trace μ, i.e.,

$$\Pi_h \mu(\boldsymbol{x}) = \sum_{j=1}^{I} \mu(\boldsymbol{r}_j)\, \chi_j(\boldsymbol{x}) \quad \text{and} \quad \mu_h(\boldsymbol{x}) = \sum_{j=1}^{I} \mu_j\, \chi_j(\boldsymbol{x}) \quad \text{for } \boldsymbol{x} \in \Gamma^h. \tag{E.245}$$

In our case, for a step $h = 0.2136$, we obtained a relative error of $E_2(h, \Gamma^h) = 0.01400$.

As in (D.350), we define the relative error of the solution as

$$E_\infty(h, \Omega_L) = \frac{\|u - u_h\|_{L^\infty(\Omega_L)}}{\|u\|_{L^\infty(\Omega_L)}}, \tag{E.246}$$

being $\Omega_L = \{\boldsymbol{x} \in \Omega_e : \|\boldsymbol{x}\|_\infty < L\}$ for $L > 0$. We consider $L = 3$ and approximate Ω_L by a triangular finite element mesh of refinement h near the boundary. For $h = 0.2136$, the relative error that we obtained for the solution was $E_\infty(h, \Omega_L) = 0.01667$.

The results for different mesh refinements, i.e., for different numbers of triangles T, nodes I, and discretization steps h for Γ^h, are listed in Table E.1. These results are illustrated graphically in Figure E.9. It can be observed that the relative errors are approximately of order h^2.

TABLE E.1. Relative errors for different mesh refinements.

T	I	h	$E_2(h, \Gamma^h)$	$E_\infty(h, \Omega_L)$
32	18	1.0000	$4.286 \cdot 10^{-1}$	$5.753 \cdot 10^{-1}$
90	47	0.7071	$1.954 \cdot 10^{-1}$	$1.986 \cdot 10^{-1}$
336	170	0.4334	$5.821 \cdot 10^{-2}$	$6.207 \cdot 10^{-2}$
930	467	0.2419	$2.020 \cdot 10^{-2}$	$2.148 \cdot 10^{-2}$
1400	702	0.2136	$1.400 \cdot 10^{-2}$	$1.667 \cdot 10^{-2}$
2448	1226	0.1676	$7.892 \cdot 10^{-3}$	$8.745 \cdot 10^{-3}$

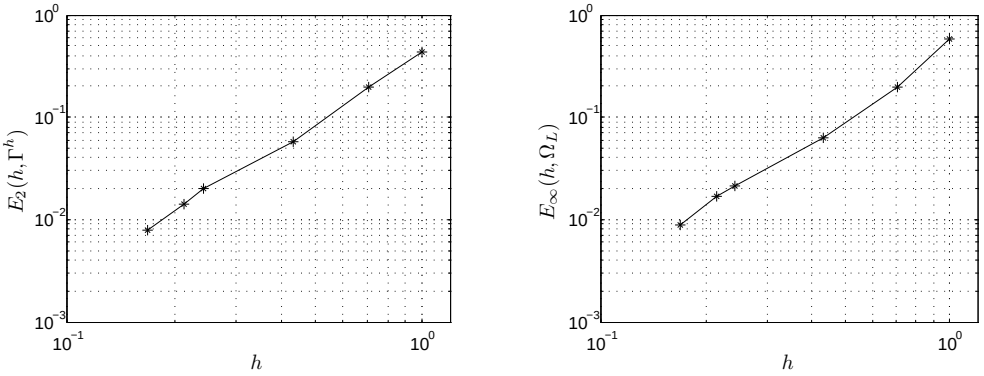

(a) Relative error $E_2(h, \Gamma^h)$ (b) Relative error $E_\infty(h, \Omega_L)$

FIGURE E.9. Logarithmic plots of the relative errors versus the discretization step.